

20th Edition



**PROCEEDINGS OF
INTERNATIONAL CONFERENCE OF
HYDRAULICS, PNEUMATICS, TOOLS,
SEALING ELEMENTS, FINE MECHANICS,
SPECIFIC ELECTRONIC EQUIPMENT &
MECHATRONICS**

HERVEX 2012



November 2012
20th Edition

INTERNATIONAL CONFERENCE AND EXHIBITION

HERVEX 2012

Hydraulics ; Pneumatics ; Sealing systems
Fine mechanics ; Tools ; Mecatronics
Dedicated electronic devices and equipment

SIMPOSYUM EXHIBITION BROKERAGE

CALIMANESTI - CACIULATA, 7 - 9 NOVEMBER 2012

ORGANIZERS



HYDRAULICS AND PNEUMATICS RESEARCH INSTITUTE
BUCHAREST, ROMANIA



CHAMBER OF COMMERCE AND INDUSTRY VALCEA, ROMANIA

PARTNERS



DEVELOPMENT AND ASSESSMENT INSTITUTE IN WASTE WATER
TECHNOLOGY, AACHEN, GERMANY



WROCLAW UNIVERSITY OF TECHNOLOGY, POLAND.



"POLITEHNICA" UNIVERSITY OF BUCHAREST, ROMANIA



"GHEORGHE ASACHI" TECHNICAL UNIVERSITY OF IASI, ROMANIA



TECHNICAL UNIVERSITY OF CLUJ-NAPOCA, ROMANIA



"POLITEHNICA" UNIVERSITY OF TIMISOARA, ROMANIA

MEDIA PARTNERS



CONFERENCE HELD UNDER THE PATRONAGE OF

Comité Européen des Transmissions Oléohydrauliques et
Pneumatiques **CETOP**



Published by - Hydraulics and Pneumatics Research Institute, Bucharest, Romania
- Chamber of Commerce and Industry Valcea, Romania

HERVEX 2012



INTERNATIONAL CONFERENCE AND EXHIBITION

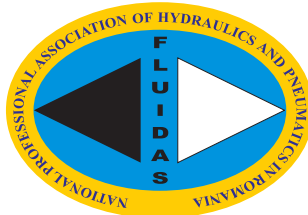
HERVEX 2012

IS SUPPORTED BY:

NATIONAL AUTHORITY FOR SCIENTIFIC RESEARCH FROM ROMANIA



**NATIONAL PROFESSIONAL ASSOCIATION OF HYDRAULICS AND
PNEUMATICS IN ROMANIA - "FLUIDAS"**



COMMITTEES

HONORARY COMMITTEE

Etienne PIOT – President of European Fluid Power Committee - CETOP

John SAVAGE – Vice President CETOP – Education / BFPA Chairman Education and
Training, England

Henryk CHROSTOWSKI - Wroclaw University of Technology, POLAND

Hubertus MURRENHOF - Institute for Fluid Power Drives and Controls at
Aachen University , GERMANY

ORGANIZING COMMITTEE

COORDINATED BY

Dipl.Eng. Gheorghe RIZOIU - General Manager of Chamber of Commerce and Industry Valcea,
Romania

Dr. Ing. Corneliu CRISTESCU - Hydraulics and Pneumatics Research Institute in Bucharest, Romania

Assoc.Prof. PhD.Eng. Erol MURAD - “POLITEHNICA” University of Bucharest, Romania

Prof. PhD. Eng. Dan OPRUTA – Technical University of Cluj, Romania

Assoc.Prof. PhD.Eng. Constantin CHIRITA - Technical University “Gheorghe Asachi”- Iasi,
Romania

Prof. PhD. Eng. Ilare BORDEAȘU - Politehnica University from Timisoara, Romania

PhD. Eng. Elmar DORGELOH – Manager of Development and Assessment Institute in Waste Water
Technology at RWTH Aachen University, Germany

PhD. Eng. Krzysztof KEDZIA - Wroclaw University of Technology, POLAND

MEMBERS

PhD.Eng. Mohamed HAJJAM – University of Poitiers - IUT Angoulême France

Prof. PhD.Eng. Nicolae ALEXANDRESCU - “POLITEHNICA” University of Bucharest, Romania

Eng. Ionel ANDREI - Romanian Ministry of Education, Research and Innovation

Assoc.Prof. PhD.Eng. Constantin RANEA - General Secretary - National Authority for Scientific
Research from Romania (NASR)

Dipl.Eng. Radu ALEXANDRU - FESTO S.R.L.

Prof. PhD.Eng. Valeriu BANU - S.M.C. Romania

PhD.Eng. Zygmunt DOMAGALA – Wroclaw University of Technology, POLAND

PhD.Eng. Amadio BOLTZANI - ASSOFLUID – Italy

PhD.Eng. Gabriela MATACHE - Hydraulics and Pneumatics Research Institute in Bucharest, Romania

Dipl.Eng. Marius BURLANESCU - S.C. HERVIL Ramnicu Valcea, Romania

Prof. PhD.Eng. Doru CALARASU - Technical University “Gheorghe Asachi”- Iasi, Romania

Dipl.Eng. Ioan CAMPEAN - S.C. HIDROSIB S.A. Sibiu, Romania

PhD.Eng. Tudor CRACIUNOIU - S.C. ICTCM S.A. Bucharest, Romania

Dipl.Eng. Mircea DANCIU - PARKER HANNIFIN Corporation Romania

Prof. PhD.Eng. Gheorghe GHEORGHE - General Manager - National Institute of Research and Development in Mechatronics and Measurement Technique (INCDMTM), Bucharest, Romania

Prof. PhD.Eng. Vasile JAVGUREANU - Technical University of Chisinau Moldova

PhD.Eng. Ioan LEPADATU - Hydraulics and Pneumatics Research Institute in Bucharest, Romania

Dipl.Eng. Leopold LUPUSANSCHI- S.C. CEROB S.R.L. Bucharest, Romania

Prof. PhD.Eng. Pavel MACH – Technical University of Praga, Czech

PhD.Eng. Daniel MARIN- S.C. General Fluid S.A. Bucharest, Romania

PhD.Eng. Adrian MIREA – SC ROMFLUID SA, Bucharest, Romania

Dipl.Eng. Ioan MOLDOVEANU - Festo S.R.L., Bucharest, Romania

PhD.Eng. Andrei Drumea - “POLITEHNICA” University of Bucharest, Romania

Prof. PhD.Eng. Johann NICOLICI - Technical University of Viena, Austria

Dipl.Eng. Cristian Sen - SUSZI - INDUSTRIAL SRL Constanta, Romania

Prof. PhD.Eng. Petru PATRUT - Technical University of Civil Engineering of Bucharest, Romania

PhD.Eng. Ion PIRNA - General Manager - National Institute Of Research - Development for Machines and Installations Designed to Agriculture and Food Industry – INMA, Bucharest- Romania

PhD.Eng. Mircea PRICOP- S.C. HESPER S.A. Bucharest- Romania

Dipl.Eng. Petru BREAZ - HIDRAULICA U.M. PLOPENI – Plopeni, Romania

Prof. PhD.Eng. Liviu VAIDA - Technical University of Cluj, Romania

Prof. PhD.Eng. Nicolae VASILIU - “POLITEHNICA” University of Bucharest, Romania

Dipl.Eng. Nicolae TASU - HANSA FLEX Romania

Prof. PhD.Eng. Paul SVASTA - “POLITEHNICA” University of Bucharest, Romania

Phd.Eng. Catalin DUMITRESCU - Hydraulics and Pneumatics Research Institute in Bucharest, Romania

Prof. PhD.Eng. Kallita WLODZIMIERZ – Faculty of Rezejow – Poland

Assoc.Prof. PhD. Marian KRÁLIK - University of Technology in Bratislava - Slovakia

EXECUTIVE COMMITTEE

Dipl.Eng. Valentin CISMARU - President of Chamber of Commerce and Industry Valcea, Romania
PhD.Eng. Petrin DRUMEA – Manager - Hydraulics and Pneumatics Research Institute in Bucharest, Romania
PhD. Eng. Elmar DORGELOH – Manager of Development and Assessment Institute in Waste Water Technology at RWTH Aachen University, Germany
Assoc.Prof. PhD.Eng. Constantin CHIRITA - Technical University “Gheorghe Asachi”- Iasi, Romania
Prof. PhD.Eng. Alexandru MARIN – “POLITEHNICA” University of Bucharest, Romania
PhD.Eng. Adrian MIREA – General Secretary – Association FLUIDAS, Bucharest - Romania
Dipl.Eng. Gheorghe RIZOIU - General Manager of Chamber of Commerce and Industry Valcea, Romania
PhD.Eng. Corneliu CRISTESCU - Hydraulics and Pneumatics Research Institute in Bucharest, Romania
PhD.Eng. Zygmunt DOMAGALA - Wroclaw University of Technology, Poland
Prof. PhD. Eng. Liviu VAIDA – Technical University of Cluj Napoca, Romania
PhD. Eng. Gabriela MATAACHE - Hydraulics and Pneumatics Research Institute in Bucharest, Romania

SECRETARY

Valentin MIROIU - Hydraulics and Pneumatics Research Institute in Bucharest, Romania
PhD.Eng. Iulian DUTU - Hydraulics and Pneumatics Research Institute in Bucharest, Romania
Lorena MATEESCU - Chamber of Commerce and Industry Valcea, Romania

EXHIBITION ORGANIZING COMMITTEE

Lorena MATEESCU - Chamber of Commerce and Industry Valcea, Romania
PhD.Eng. Ioan LEPADATU - Hydraulics and Pneumatics Research Institute in Bucharest, Romania

SPECIALIZED REVIEWER COMMITTEE

PhD.Eng. Heinrich Theissen - Institute for Fluid Power Drives and Controls, Aachen University - Germania
PhD.Eng. Petrin DRUMEA - Manager - Hydraulics and Pneumatics Research Institute in Bucharest, Romania
Assoc.Prof. PhD.Eng. Constantin RANEA - General Secretary - National Authority for Scientific Research from Romania (NASR)
Prof. PhD.Eng. Nicolae ALEXANDRESCU - Politehnica University of Bucharest, Romania
Prof. PhD.Eng. Paul SVASTA - Politehnica“POLITEHNICA” of Bucharest, Romania

PhD. Eng. Costinel POPESCU - Hydraulics and Pneumatics Research Institute in Bucharest, Romania

PhD. Eng. Krzysztof KEDZIA - Wroclaw University of Technology, Poland

PhD.Eng. Mohamed HAJJAM - University of Poitiers - IUT Angoulême, France

Prof. PhD.Eng. Vasile JAVGUREANU - Technical University of Chisinau, Moldova

Prof. PhD.Eng. Pavel MACH - Technical University of Praga, Czech

Prof. PhD.Eng. Johann NICOLICS - Technical University of Viena, Austria

MANAGER OF PUBLICATION

- PhD.Eng. Petrin DRUMEA - Manager - Hydraulics and Pneumatics Research Institute in Bucharest, Romania

EDITORIAL STAFF

Chief Editor

- PhD. Eng. Gabriela MATACHE - Hydraulics and Pneumatics Research Institute in Bucharest, Romania

Executive Editors

- Ana-Maria POPESCU - Hydraulics and Pneumatics Research Institute in Bucharest, Romania

- Valentin MIROIU - Hydraulics and Pneumatics Research Institute in Bucharest, Romania

CONTENTS

SECTION I: INDUSTRIAL HYDRAULICS AND MECHATRONICS

<ul style="list-style-type: none"> • MODERN TRENDS OF SUSTAINABILITY RELATED RESEARCH IN FLUID POWER 	
Hubertus Murrenhoff – Executive Director of Institute for Fluid Power Drives and Controls – IFAS, Aachen, GERMANY	15 - 55
<ul style="list-style-type: none"> • HYDRAULIC SWITCHING CONTROL – OBJECTIVES, CONCEPTS, CHALLENGES AND POTENTIAL APPLICATIONS 	
Rudolf Scheidl, Helmut Kogler, Bernd Winkler- Institute of Machine Design and Hydraulic Drives, AUSTRIA	56 - 67
<ul style="list-style-type: none"> • MAINTENANCE OF FLUID POWER EQUIPMENTS 	
Corneliu Cristescu, Krzysztof Kedzia, Catalin Dumitrescu, Radu Radoi - Hydraulics and Pneumatics Research Institute in Bucharest, ROMANIA / Wroclaw University of Technology, POLAND	68 - 76
<ul style="list-style-type: none"> • SOME ASPECTS OF THE NEW MODEL OF ROBOT ACTUATION – MERO 	
Ion Ion, Alexandru Marin, Laura-Florenta Boanta, Cristian Simion, Cornel Dinu – “POLITEHNICA” University of Bucharest, ROMANIA	77 - 86
<ul style="list-style-type: none"> • REHABILITATION AND TESTING OF AXIAL PISTON AND ADJUSTABLE FLOW HIGH-WEAR PUMPS 	
Petrica Krevey, Radu Sauciuc, Genoveva Vranceanu - Hydraulics and Pneumatics Research Institute in Bucharest, ROMANIA	87 – 93
<ul style="list-style-type: none"> • THE VISION-BASED MECHATRONIC SYSTEMS USED IN PRODUCTION QUALITY CONTROL OF HYDRAULIC COMPONENTS 	
Anca Atanasescu, Sorin Sorea, Alexandru Constantinescu – National Institute of Research and Development in Mechatronics and Measurement Technique in Bucharest-ROMANIA	94 – 102
<ul style="list-style-type: none"> • NUMERICAL SIMULATION OF THE SERVO MECHANISM FOR ADJUSTING THE CAPACITY OF THE RADIAL PISTON PUMPS 	
Cătălin Dumitrescu, Liliana Dumitrescu, Ioan Iepădatu - Hydraulics and Pneumatics Research Institute in Bucharest, ROMANIA	103 – 108
<ul style="list-style-type: none"> • DESIGN AND DEVELOPMENT OF MECHATRONIC SYSTEM WITH TELEMONITORING AND PREDICTIVE TELEMaintenance CONTROL 	
Anghel Constantin , Sergiu Dumitru - National Institute of Research and Development in Mechatronics and Measurement Technique in Bucharest-ROMANIA	109 – 116
<ul style="list-style-type: none"> • MECHATRONIC SYSTEM FOR WINDING ROLLED WIRE 	
Ioana Ilie, Marian Blejan, Constantin Ranea - Hydraulics and Pneumatics Research Institute in Bucharest, ROMANIA / “POLITEHNICA” University of Bucharest, ROMANIA	117 – 120
<ul style="list-style-type: none"> • SCIENTIFIC STRATEGIES AND METHODS OF ADAPTRONICS APPROACH, AS KEY TECHNOLOGY FOR FUTURE 	
Gheorghe Gheorghe - National Institute of Research and Development in Mechatronics and Measurement Technique in Bucharest-ROMANIA	121 – 130
<ul style="list-style-type: none"> • FLOW ASPECTS THROUGH HYDRAULIC RESISTANCES 	
Ioana Sfârlea, Florin Bode, Dan Opruța – Technical University of Cluj-Napoca, ROMANIA	131 - 134
<ul style="list-style-type: none"> • THE CONSTRUCTIVE-FUNCTIONAL STRUCTURE OF THE MODEL SLOW RUNNING ROTATIONAL HYDRAULIC MOTOR 	
Laura Grama, Liviu Vaida - Technical University of Cluj-Napoca, ROMANIA	135 - 139
<ul style="list-style-type: none"> • ROTATIONAL SPEED MATHEMATICAL MODEL OF THE ALTERNATING FLOW DRIVEN THREE-PHASE HYDRAULIC MOTORS 	
Ioan-Lucian Marcu, Daniel-Vasile Banyai, Liviu Vaida - Technical University of Cluj-Napoca, ROMANIA	140 – 145
<ul style="list-style-type: none"> • MEANS AND METHODS FOR TESTING ADJUSTABLE HYDROSTATIC PUMPS 	
Teodor-Costinel Popescu, Ioan Lepadat - Hydraulics and Pneumatics Research Institute in Bucharest, ROMANIA	146 - 152

- **NEW CONTRIBUTIONS TO THE STUDY OF DESTRUCTION BY CAVITATION OF TWO BIPHASIC (AUSTENITE + FERRITE) STAINLESS STEEL FOR THE MANUFACTURE OF BLADES AND ROTOR HYDRAULIC MACHINES**

Ilare BORDEAȘU, Constantin BORDEAȘU, Brandusa GHIBAN, Ain Dan JURCHELA, Octavian OANĂ, Adrian KARABENCIOV – “POLITEHNICA” University of Timisoara, ROMANIA

153 - 159

- **MAINTENANCE AND TESTING OF THE HYDRAULIC SERVOVALVES**

Radu Radoi, Ioan Balan, Iulian Dutu - Hydraulics and Pneumatics Research Institute in Bucharest, ROMANIA

160 - 165

SECTION II: MOBILE HYDRAULICS AND TRIBOLOGY

- **WHAT TO DO WITH A HYBRID DRIVE SYSTEM?**

Krzysztof Kedzia - Wroclaw University of Technology, POLAND

166 – 174

- **TRIBOLOGICAL RESEARCHES REGARDING THE INCREASING OF PERFORMANCES OF THE FLUID POWER EQUIPMENTS**

Corneliu CRISTESCU, Petrin DRUMEA, Constantin Ranea - Hydraulics and Pneumatics Research Institute in Bucharest, ROMANIA / “POLITEHNICA” University of Bucharest, ROMANIA

175 – 184

- **HYDRAULICS FOR MOBILE VEHICLES. NEW DRIVE SCHEMES**

Mihail Petrache, Sava Anghel, Alina Popescu – LYRA PROD IMPEX Company / Hydraulics and Pneumatics Research Institute in Bucharest, ROMANIA

185 – 190

- **LIFTING PLATFORM WITH POTENTIAL ENERGY RECOVERY SYSTEM**

Catalin Dumitrescu, Corneliu Cristescu, Florin Georgescu, Liliana Dumitrescu - Hydraulics and Pneumatics Research Institute in Bucharest, ROMANIA

191 - 194

- **HYDRAULIC DRIVING SYSTEMS FOR MOBILE EQUIPMENTS DESTINED FOR ASPHALT POURING**

Victor Balasoiiu, Mircea Popoviciu, Ilare Bordeasu - “POLITEHNICA” University of Timisoara, ROMANIA

195 – 202

- **RESEARCH ON FRICTION LOSSES IN THE TENSIONING DEVICES UNDER LOAD**

Andrei Grama, Constantin Chiriță, Mihai Afrăsinei, Vasile Damaschin – Technical University “Gheorghe Asachi” of Iasi, ROMANIA

203 – 209

- **TRANSFER FUNCTION OF A PRESSURE TRANSDUCER WITH DRAWER**

I. Nicolae, M. Cotrumba - Ovidius University of Constanta, ROMANIA

210 – 214

- **LIFTING EQUIPMENT WITH RECOVERY SYSTEM OF POTENTIAL ENERGY**

Stefan Alexandrescu, Corneliu Cristescu, Gheorghe Sovaiala, Alexandru Marinescu, Ioan Pavel - Hydraulics and Pneumatics Research Institute in Bucharest, ROMANIA

215 – 222

- **NUMERICAL SIMULATIONS FOR A HYDRAULIC SYSTEM WITH SECONDARY CONTROL**

Vasile Huian, Doru Călarasu, Constantin Chiriță, Mihai Afrăsinei - Technical University “Gheorghe Asachi” of Iasi, ROMANIA

223 – 228

- **DIGITAL CONTROL MODULES FOR HYDRONIC EQUIPMENTS**

Iulian Dutu, Radoi Radu, Despina Duminica - Hydraulics and Pneumatics Research Institute in Bucharest, ROMANIA / “POLITEHNICA” University of Bucharest, ROMANIA

229 – 234

- **INCREASING THE ENERGETIC EFFICIENCY OF PET BUNDLING PRESS USING HIDROSTATIC ENERGY RECOVERING SYSTEMS**

Ionel Nita, Corneliu Cristescu, Alexandra Liana Visan, Alexandru Marinescu - Hydraulics and Pneumatics Research Institute in Bucharest, ROMANIA

235 – 241

- **HYBRID SYSTEM FOR ENERGY RECOVERY AT BREAKING**

Alexandru Vasile, Andrei Drumea, Cristina MARGHESCU, Paul SVASTA, Andreea BRODEALA - “POLITEHNICA” University of Bucharest, ROMANIA

242 – 247

- **MOBILE SKID SIMULATOR FOR TRAINING OF CAR DRIVERS**

Radu Radoi, Ioan Balan, Marian Blejan - Hydraulics and Pneumatics Research Institute in Bucharest, ROMANIA

248 – 252

- **THEORETICAL AND EXPERIMENTAL RESEARCH OF RECIPROCATING ROD SEALS**

Monica Crudu, Aurelian Fatu, Mohamed Hajjam, Corneliu Cristescu - University of Poitiers, FRANCE / Hydraulics and Pneumatics Research Institute in Bucharest, ROMANIA

253 – 260

• **MODELING AND SIMULATION OF HYDRAULIC AND MECHANICAL SYSTEM OF COMPACT UTILITY LOADER**

Shinok Lee, Mingi Cho, Daeyoung Shin, Gangwon Lee - Institute of Industrial Technology, KOREA

261 – 269

SECTION III: HYDRAULICS SYSTEMS

• **HYDRAULIC SCHEMES FOR IMPACT DEVICES. A CONTROL SYSTEM FOR IMPACT MECHANISMS USING A ROTATABLE DISTRIBUTION VALVE – PART1**

Claudia Kozma, Liviu Vaida - Technical University of Cluj-Napoca, ROMANIA

270 – 280

• **HYDRAULIC SCHEMES FOR IMPACT DEVICES. A CONTROL SYSTEM FOR IMPACT MECHANISMS USING A ROTATABLE DISTRIBUTION VALVE – PART2**

Claudia Kozma, Liviu Vaida - Technical University of Cluj-Napoca, ROMANIA

281 – 284

• **STRENGTHENING SURFACE LAYERS OF COMPONENTS**

Marian Kralik – University of Technology in Bratislava, SLOVAKIA

285 – 290

• **CAMIRO LONG LIFE NEW HYDRAULIC EQUIPMENT TECHNOLOGY FOR DRILLING FLUIDS AND SALT WATER INJECTION PUMP**

Miron M. Procop, Oana-Miruna Procop, Rodica Procop - CAMIRO ENGINEERING Company Constanta, ROMANIA

291 – 294

• **SOME ASPECTS OF THE DRIVE WITH THE MASSES UNBALANCED VIBRATING**

Stoica Dorel, Voicu Gheorghe, Carmen Rusanescu - "POLITEHNICA" University of Bucharest, ROMANIA

295 – 300

• **CONSIDERATIONS ABOUT THE SELECTION OF THE HAMMER MILLS OF LOW CAPACITY**

Mihaela Duțu, Ladislau David, Ion Dinu, Carmen Rusănescu - "POLITEHNICA" University of Bucharest, ROMANIA

301 – 304

• **A NEW SOLUTION FOR WATER JET CUTTING MACHINE TOOL**

Rareș Petruș, Cornel Ciupan, Emilia Ciupan - Technical University of Cluj-Napoca, ROMANIA

305 – 308

• **RESEARCHES TO IMPROVE WORKING PROCESS OF ACTIVE WORKING PARTS, HYDRAULIC ACTUATED, FROM CONSTRUCTION OF THE EQUIPMENT "EXPLANT 500"**

Constantin Cota, Elena Nagy, Nicolae Cioica - National Institute of Research - Development for Machines and Installations Designed to Agriculture and Food Industry – Bucharest- ROMANIA

309 – 314

• **THE CONTROL OF THE ABRASIVE WATER JET PROCESSING USING A NEURONAL NETWORK MODEL**

Emilia Ciupan, Cornel Ciupan, Rareș Petruș - Technical University of Cluj-Napoca, ROMANIA

315 – 319

• **EXPERIMENTAL RESEARCH BY MEASURING THE PULLING FORCE OPERATING PRESSURE USING THE DATA ACQUISITION BOARD**

Constantin Chiriță, Andrei Grama, Mihai Afrăsinei, Vasile Damaschin - Technical University "Gheorghe Asachi" of Iasi, ROMANIA

320 – 326

• **RISK ASSESSING WITH FMEA ANALYSIS AND FUZZY LOGIC**

Despina Duminica, Mihai Avram, Iulian Dutu - "POLITEHNICA" University of Bucharest, ROMANIA / Hydraulics and Pneumatics Research Institute in Bucharest, ROMANIA

327 – 334

• **THE STUDY OF ELASTIC-PLASTIC PROPERTIES OF THE COMPOSITE PLATING MACROINDENTATION**

Vasile Javagureanu, Pavel Gordelenco - Technical University of Moldova - MOLDOVA

335 – 340

• **PLOTTING THE CLARIFYING CURVES AND DETERMINATION OF THE SPECIFIC AMOUNT OF SETTLED MATERIAL DURING THE INITIAL PERIOD TO SEDIMENTATION IN STATIONARY COLUMN OF AQUEOUS SUSPENSIONS OF SOLIDS**

Viorel Safta, Mirel Dilea, Gabriel Constantin-"POLITEHNICA" University of Bucharest, ROMANIA

341 – 346

• **THE MEASUREMENT WITH PNEUMATIC TRANSDUCERS OF THE CERAMIC PRODUCTS CONTRACTION AT DRYING**

Murad Erol, Haraga Georgeta, Dumitrescu Catalin, Liliana Dumitrescu - "POLITEHNICA" University of Bucharest, ROMANIA/ Hydraulics and Pneumatics Research Institute in Bucharest, ROMANIA

347 – 351

• **DIRECT / INDIRECT ADAPTIVE ROBUST CONTROL FOR LINEAR HYDRAULIC ACTUATOR**

Daniel-Vasile Banyai, Ioan-Lucian Marcu, Liviu Vaida - Technical University of Cluj-Napoca, ROMANIA 352 – 358

• **THE CALORIC EFFECTS IN ONE SERIAL SONIC INSTALLATION**

BAL Carmen, BAL Nicolaie - Technical University of Cluj-Napoca, ROMANIA 359 – 363

• **SOME ELASTOPLASTIC DEFORMATION AND FAILURE GALVANIC ELECTROLYTIC IRON COVER**

Vasile Javgureanu, Pavel Gordelenco - Technical University of Moldova - MOLDOVA 364 – 368

• **DESIGN OF THE SYSTEM DRIVE TO THE PNEUMO-VEHICLE WITH PNEUMATIC LINEAR ENGINE IN 2 CYLINDERS**

Constantin Bungău, Tudor Mitran, Tiberiu Vesselenyi, Dan Crăciun- University of Oradea, ROMANIA 369 – 375

SECTION IV: ENVIRONMENT, ECOLOGY AND RENEWABLE ENERGY

• **NOTES ON THE ENERGETIC TRANSFER IN HYDROSTATIC SYSTEMS**

Eugen Dobanda - "POLITEHNICA" University of Timisoara, ROMANIA 376 – 382

• **EXPERIMENTAL RESEARCH TO VALIDATE SIMULATION MODEL OF HYDRAULIC MOTOR HYDRAULIC TRANSMISSION FOR LOW POWER WIND TURBINES**

Constantin Chirită, Mihai Afrăsinei, Vasile Damaschin, Andrei Grama - Technical University "Gheorghe Asachi" of Iasi, ROMANIA 383 – 391

• **CERCETĂRI SI TEHNOLOGII PENTRU REDUCEREA CONSUMULUI DE CARBURANT AL AUTOVEHICULELOR DE TRANSPORT MARFĂ SI PERSOANE**

Zorin Bercea, Liviu Vaida - Technical University of Cluj-Napoca, ROMANIA 392 – 402

• **EXPERIMENTAL RESEARCH TO VALIDATE SIMULATION MODEL OF CONSTANT SPEED AT LOW POWER AXIS WIND TURBINE**

Mihai Afrăsinei, Constantin Chirită, Vasile Damaschin, Andrei Grama - Technical University "Gheorghe Asachi" of Iasi, ROMANIA 403 – 410

• **STATE OF THE ART BIOMASS COMBINED HEAT AND POWER TECHNOLOGY**

Curac Ioan, Craciun Bogdan Ionut Creta Ioan - Technical University of Cluj-Napoca, ROMANIA 411 – 417

• **FACTORI CARE INFLUENTEAZĂ SEMNIFICATIV CONSUMUL DE CARBURANTI ÎN TRANSPORTUL AUTO**

Zorin Bercea, Liviu Vaida - Technical University of Cluj-Napoca, ROMANIA 418 – 425

• **INFLUENCE OF CRIMPING ANGLE ON HEAT TRANSFER FOR HEAT EXCHANGERS**

Oana Giurgiu, Dan Opruta, Angela Plesa - Technical University of Cluj-Napoca, ROMANIA 426 – 429

• **SOLAR POWER INSTALLATION HOT WATER TO HOUSING FAMILY TYPE**

Carmen Rusanescu, Adriana Gruia, Mihaela Dutu, Stoica Dorel – "POLITEHNICA" University of Bucharest, ROMANIA 430 – 433

• **STUDY ON THE WORKING PRINCIPLE OF A HYDRAULIC ENERGY DISSIPATION DEVICE**

Gavril Axinti, Florin Nedelcu, Fanel Scheaua- "Dunarea de Jos" University from Galati, ROMANIA 434 – 439

• **HEAT GENERATORS WITH TLUD GASIFIER FOR GENERATING ENERGY FROM BIOMASS WITH A NEGATIVE BALANCE OF CO₂**

Erol Murad, Florian Dragomir – "POLITEHNICA" University of Bucharest, ROMANIA 440 – 447

• **PNEUMATIC MEASURING OF THE BIOMASS CONSUMPTION FOR TLUD GENERATOR**

Erol Murad, Georgeta Haraga, Cătălin Dumitrescu, Liliana Dumitrescu - "POLITEHNICA" University of Bucharest, ROMANIA / Hydraulics and Pneumatics Research Institute in Bucharest, ROMANIA 448 – 453

• **MONITORING OF ENVIRONMENTAL FACTORS AT VEGETABLE OILS PRODUCING UNITS**

Gabriela Simion, Alina Colan, Mihaela Dutu - "POLITEHNICA" University of Bucharest, ROMANIA 454 – 459

- **EXPERIMENTAL RESEARCH TO VALIDATE THE SIMULATION MODEL HYDRAULIC TRANSMISSION FOR WIND TURBINES SMALL ADAPTIVE PRESSURE CONTROL ON CALCULATION ERRORS**

Vasile Damaschin, Mihai Afrăsinei, Constantin Chirită, Andrei Grama - Technical University "Gheorghe Asachi" of Iasi, ROMANIA 460 – 468

- **CONSIDERATIONS FOR OPTIMIZING THE CROPS IN AGRICULTURAL FARMS FROM THE MARKET ECONOMY IN ROMANIA**

Oana David, Ladislau David, Mihaela Duțu - "POLITEHNICA" University of Bucharest, ROMANIA 469 – 472

- **BIODEGRADABLE OILS – METHODS FOR DETERMINING THE PERFORMANCES OF BIODEGRADABLE OILS**

Alina Popescu, Sava Anghel, Adrian Pantiru, Alexandru Marinescu, Mihail Petrache - Hydraulics and Pneumatics Research Institute in Bucharest, ROMANIA / LYRA PROD IMPEX Company 473 – 477

- **HYDRAULIC INSTALLATION WITH ENERGETIC AUTONOMY FOR LAKES AERATION**

Adrian Ciocanea, Sanda Budea - "POLITEHNICA" University of Bucharest, ROMANIA 478 – 484

SECTION V: EDUCATION AND TRAINING IN FLUID POWER

- **EDUCATION & QUALIFICATIONS IN FLUID POWER**

John Savage – CETOP / National Fluid Power Centre, UNITED KINGDOM 485 – 506

- **NEW SMC DIDACTIC EQUIPMENTS – SUPPORT FOR PERFORMANCE IN EDUCATION**

Valeriu Banu, Dragos Gheorghe – SMC ROMANIA 507 – 523

- **NEW INSTRUMENT FOR LUBRICANTS BEHAVIOR EDUCATION AND TRAINING**

Alexandru Radulescu, Irina Radulescu - "POLITEHNICA" University of Bucharest, ROMANIA / Mechanical Engineering and Research Institute – ICTCM, ROMANIA 524 – 529

- **RELATII PUBLICE SI COMUNICARE IN FOLOSUL ACTIVITATILOR DE CERCETARE-DEZVOLTARE-INOVARE**

Radu Jecu – Centre of Technological Information – CENTIREM, Bucharest, ROMANIA 530 – 532

- **STOCK EXCHANGE OF NEW INVENTIONS**

Petrin Drumea, Niculae Ioniță, Costinel Popescu, Catalin Dumitrescu - Hydraulics and Pneumatics Research Institute in Bucharest, ROMANIA 533 – 542

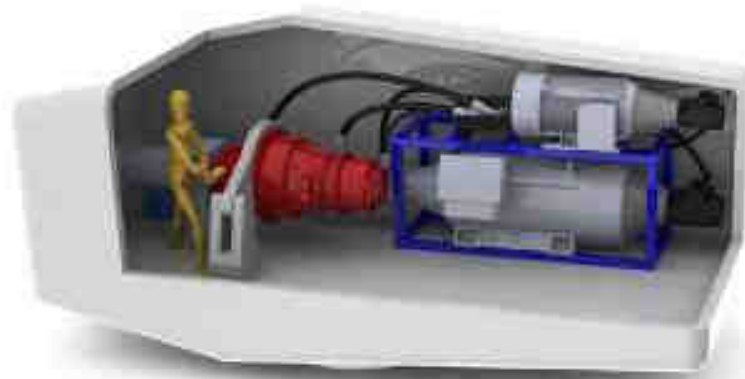
- **EDUCATION IN DEVELOPMENT OF ELECTRONIC MODULES USING FREE AND OPEN SOURCE SOFTWARE TOOLS**

Andrei Drumea, Alexandru Vasile – „POLITEHNICA” University of Bucharest, ROMANIA 543 – 548

- **ELEMENTS OF STRATEGY AND INNOVATION POLICIES IN THE FIELD OF FLUID POWER – INTRODUCTION**

Henryk Chrostowski, Zygmunt Popczyk – Wrocław University of Technology, POLAND 549 – 581

Modern Trends of Sustainability Related Research in Fluid Power



RWTHAACHEN
UNIVERSITY

IFAS

Institute for
Fluid Power
Drives and
Controls

Univ.-Prof. Dr.-Ing. Hubertus Murrenhoff

Institutsdirektor / *Executive Director*

Institut für fluidtechnische Antriebe und Steuerungen (IFAS)

Institute for Fluid Power Drives and Controls (IFAS) - RWTH Aachen University

E-mail: mh@ifas.rwth-aachen.de

Outline

- Introduction
- Tribology
 - A: Analysis of fluids
 - B: Axial piston pumps
- Hybrid Drives
 - A: Hybrid for drive trains
 - B: Boom energy regeneration system
- Hydrostatic Drives for Wind Turbines
- Conclusion and Outlook

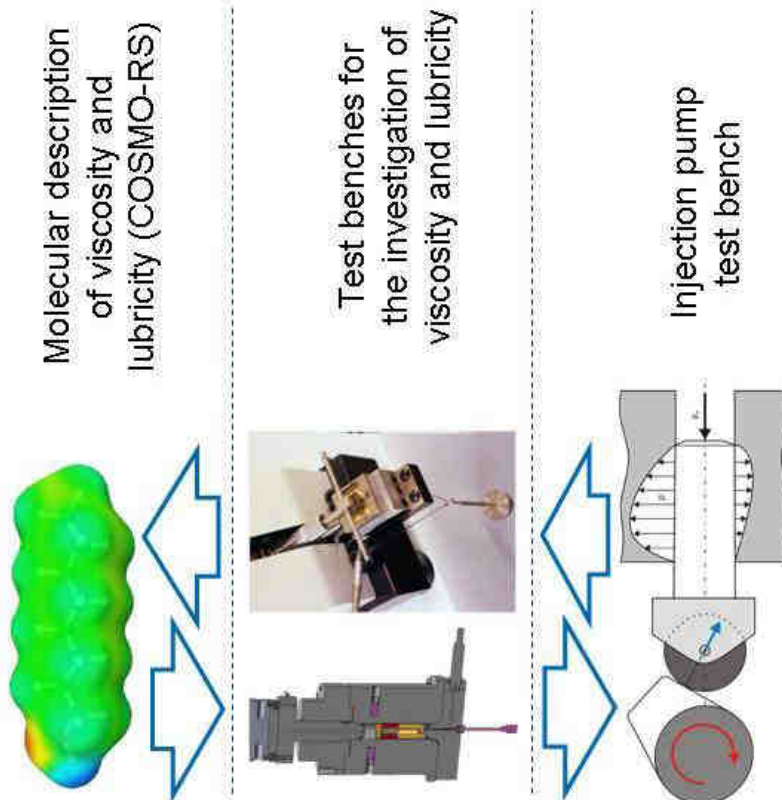


Introduction

- Sustainability is priority No. 1 on a planet with 7 billion people
- Why: limited resources and emissions are leading to depletion, pollution and global warming endangering our environment
- How can fluid power contribute to this No. 1 goal? Some examples are treated in the lecture:
- New fluids from renewable feedstock
- Minimizing losses of hydrostatic displacement units
- Increasing energy efficiency of hydrostatic circuits with energy recuperation
 - a) hybrid drive trains
 - b) boom energy recuperation
- Efficient and intelligent hydrostatic drives for wind turbines
- All examples are part of actual research activities



Tribology and Fluid Analysis



- Test bench design for measurement of
 - Viscosity
 - Bulk modulus
- Lubricity test rig (HFRR) for new fluids
 - First results
 - Potential use of biobased fluids as additive

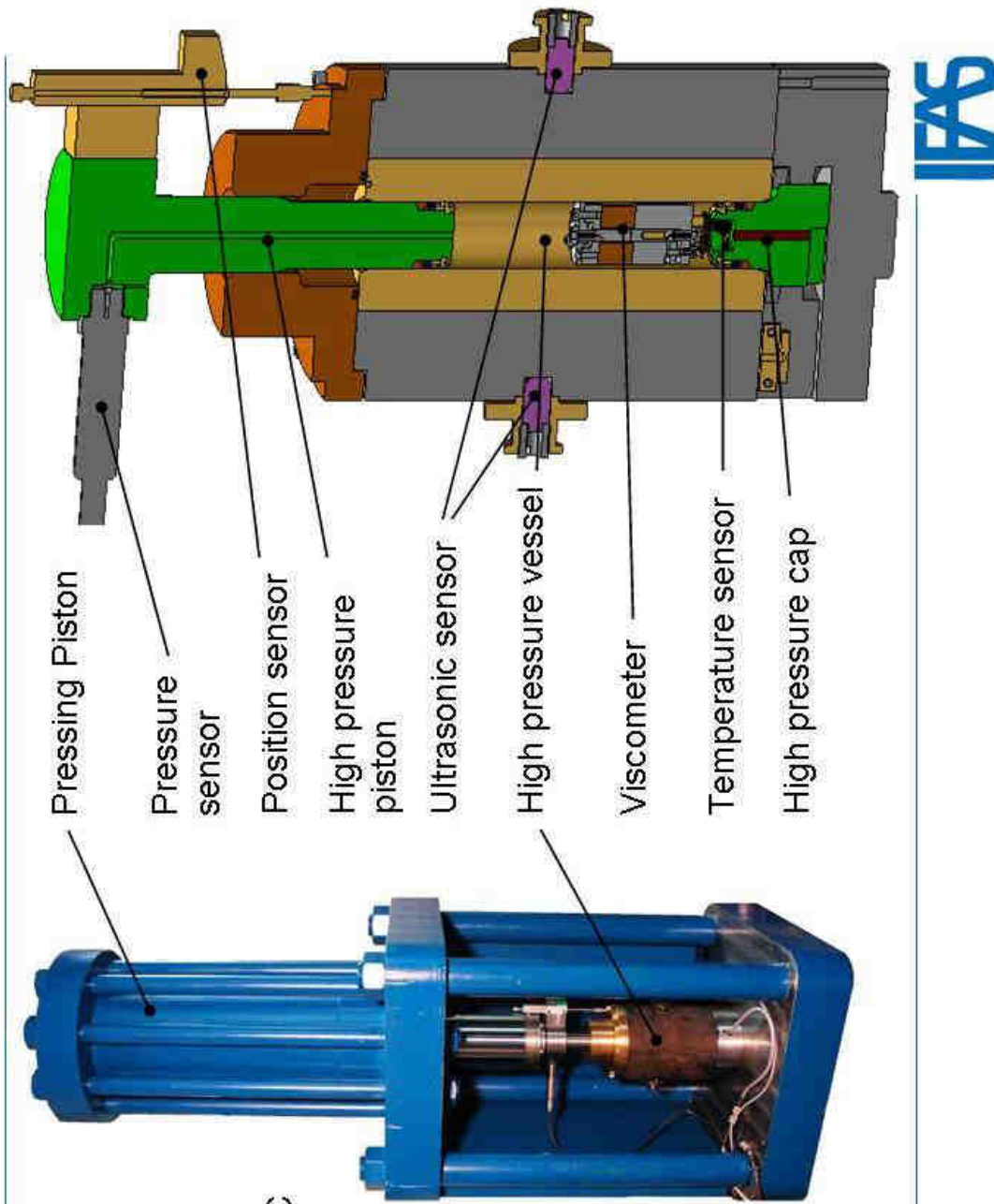
High Pressure Test Rig for 500 MPa

Measured variable:

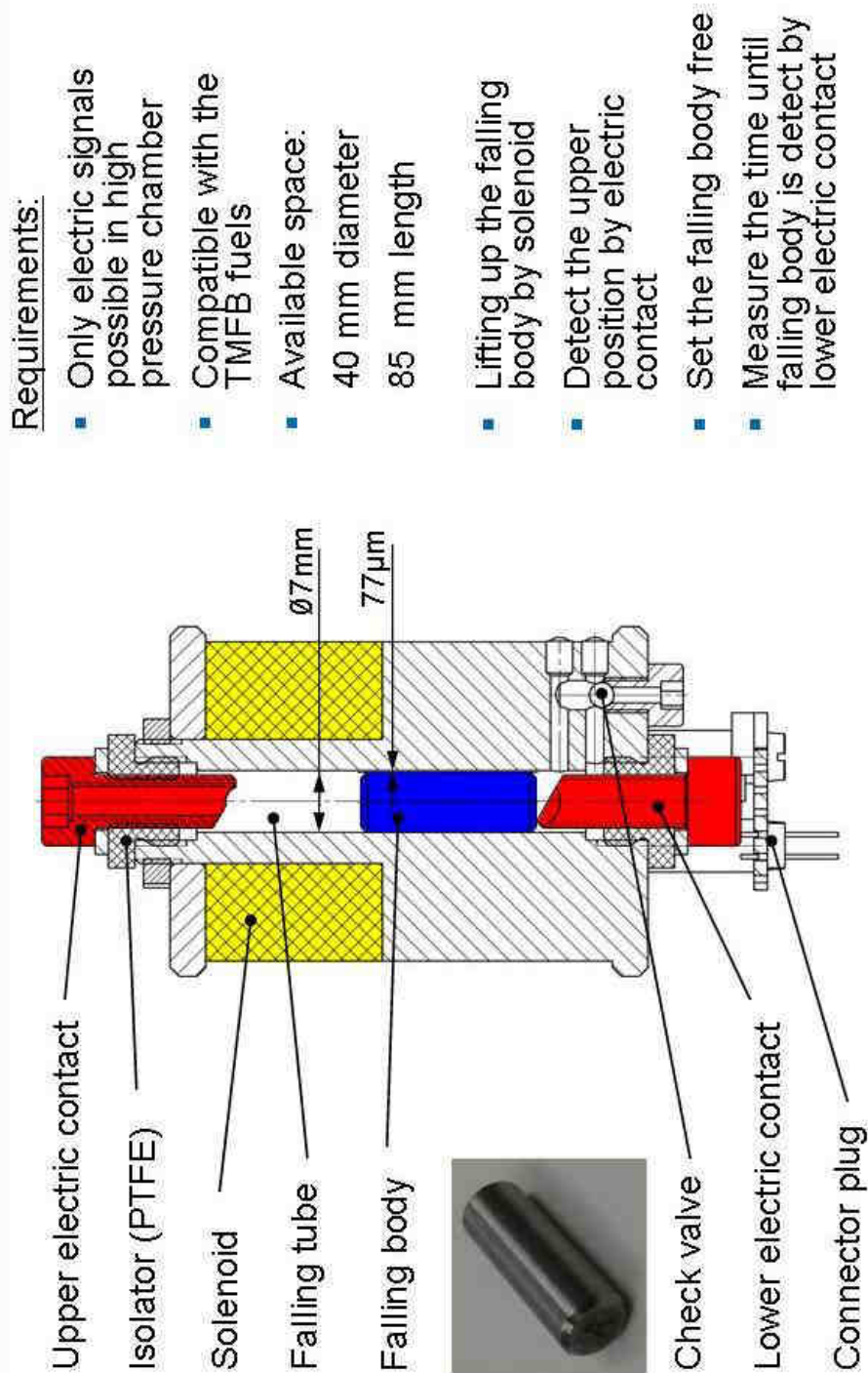
- bulk modulus
- viscosity

Pressure: 0 ... 500 MPa

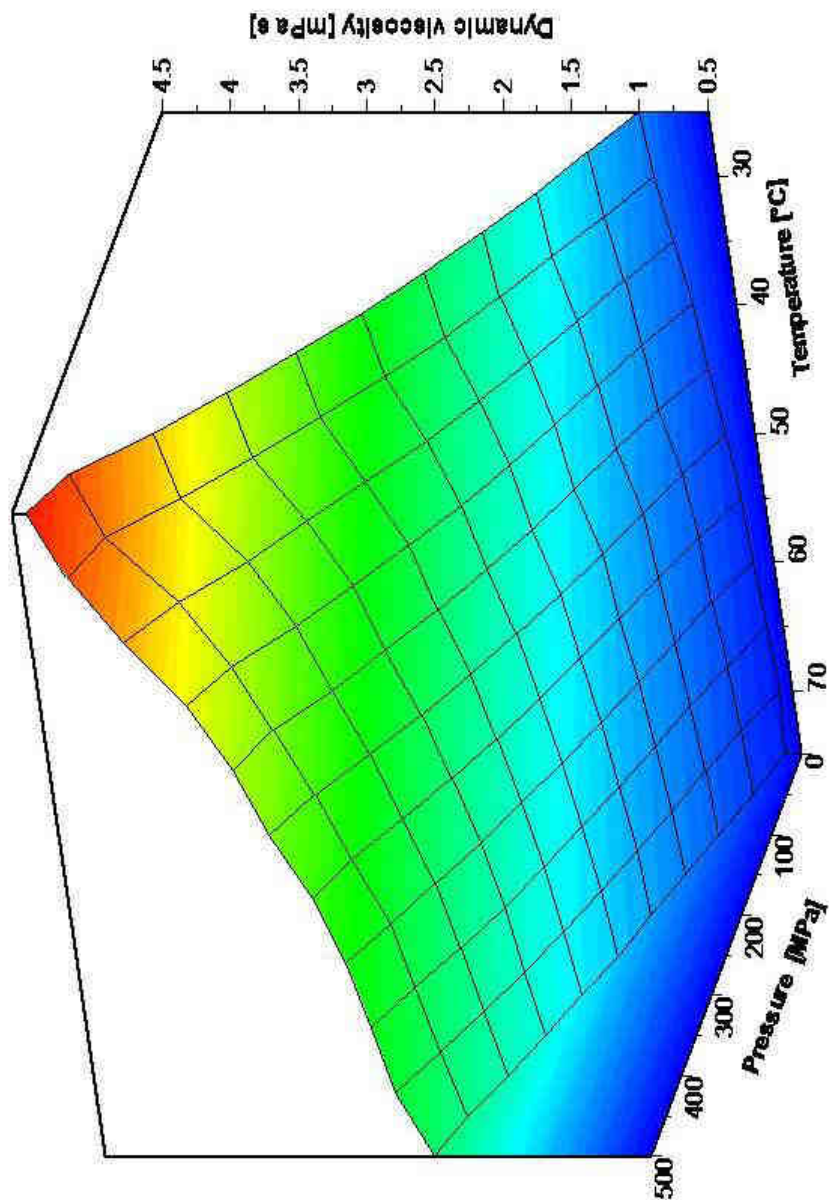
Temperature: 20 ... 120°C



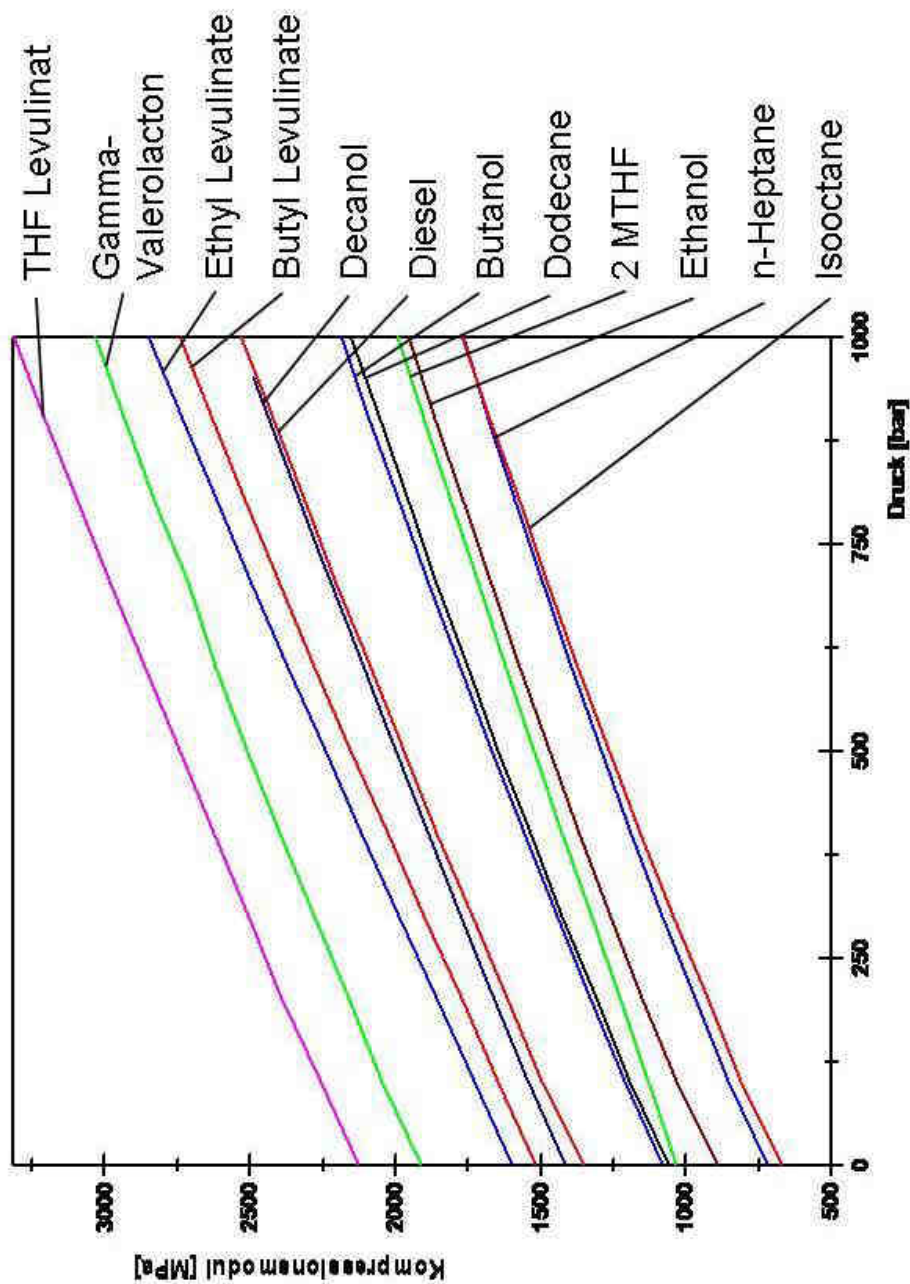
Falling body viscometer for the pressure chamber



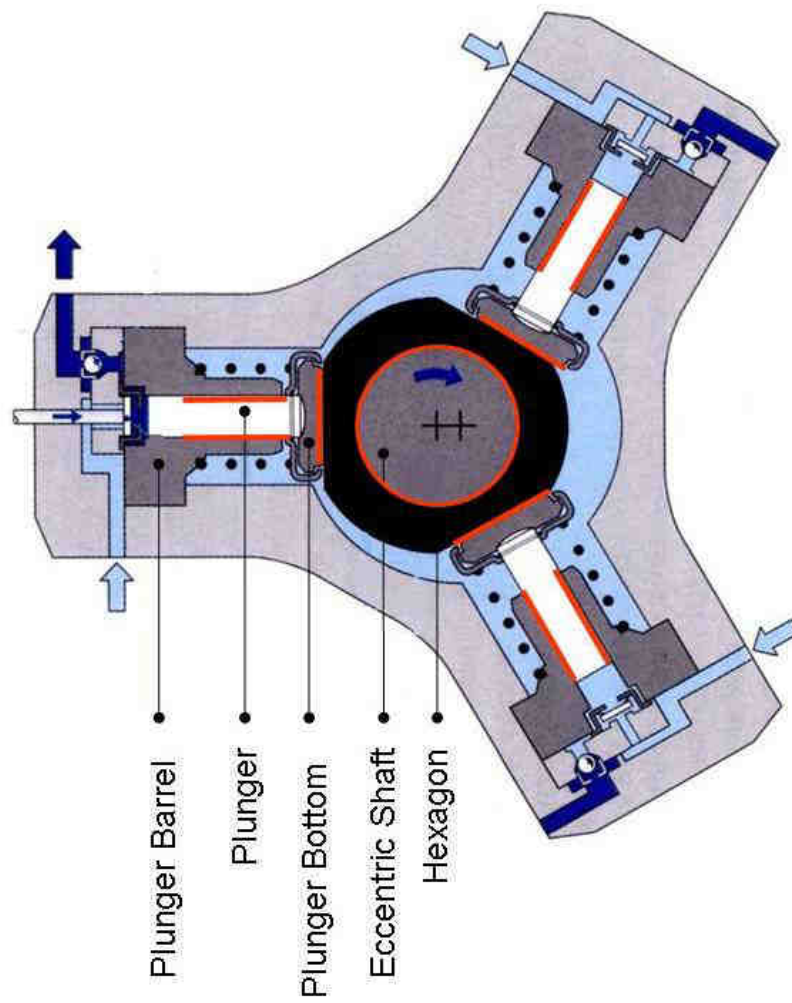
Measurement results for viscosity of ethanol



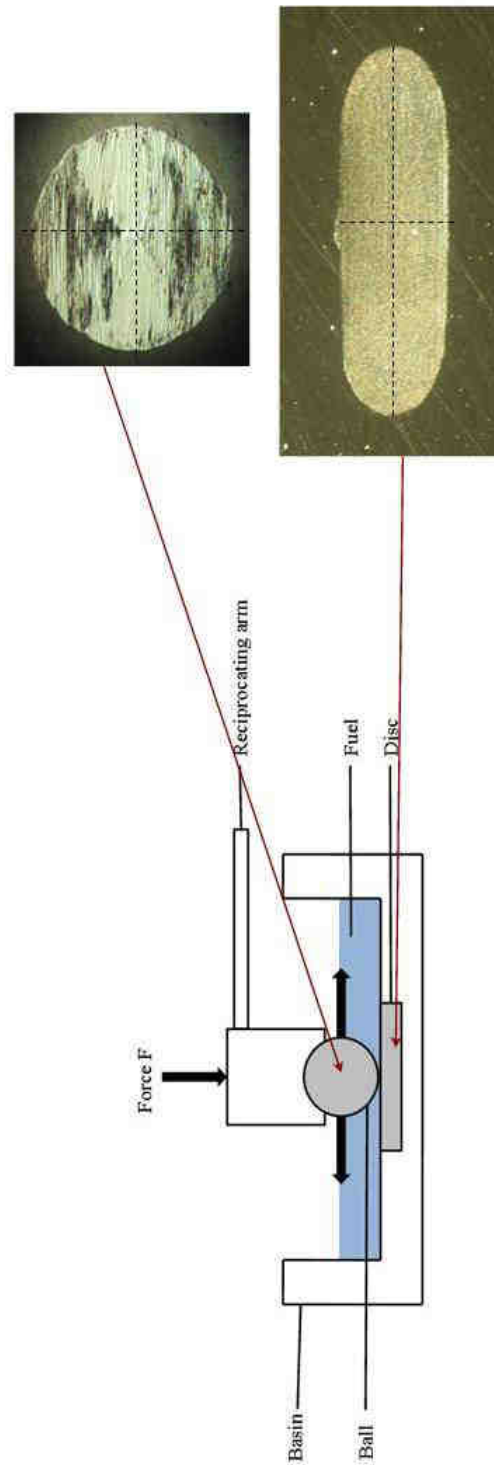
Measurement results for bulk modulus



Tribological Contacts in Injection Pumps (CR)

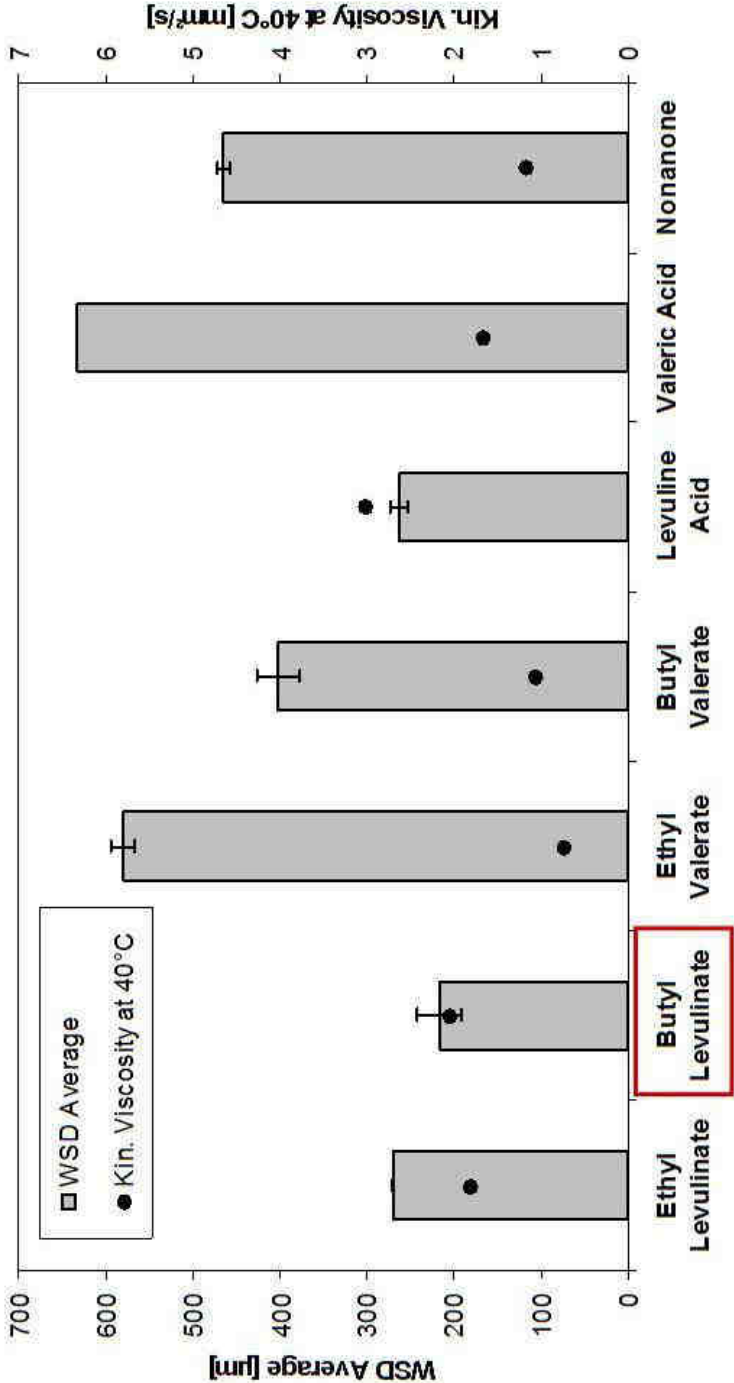
**IAS**

High Frequency Reciprocating Rig (HFRR)

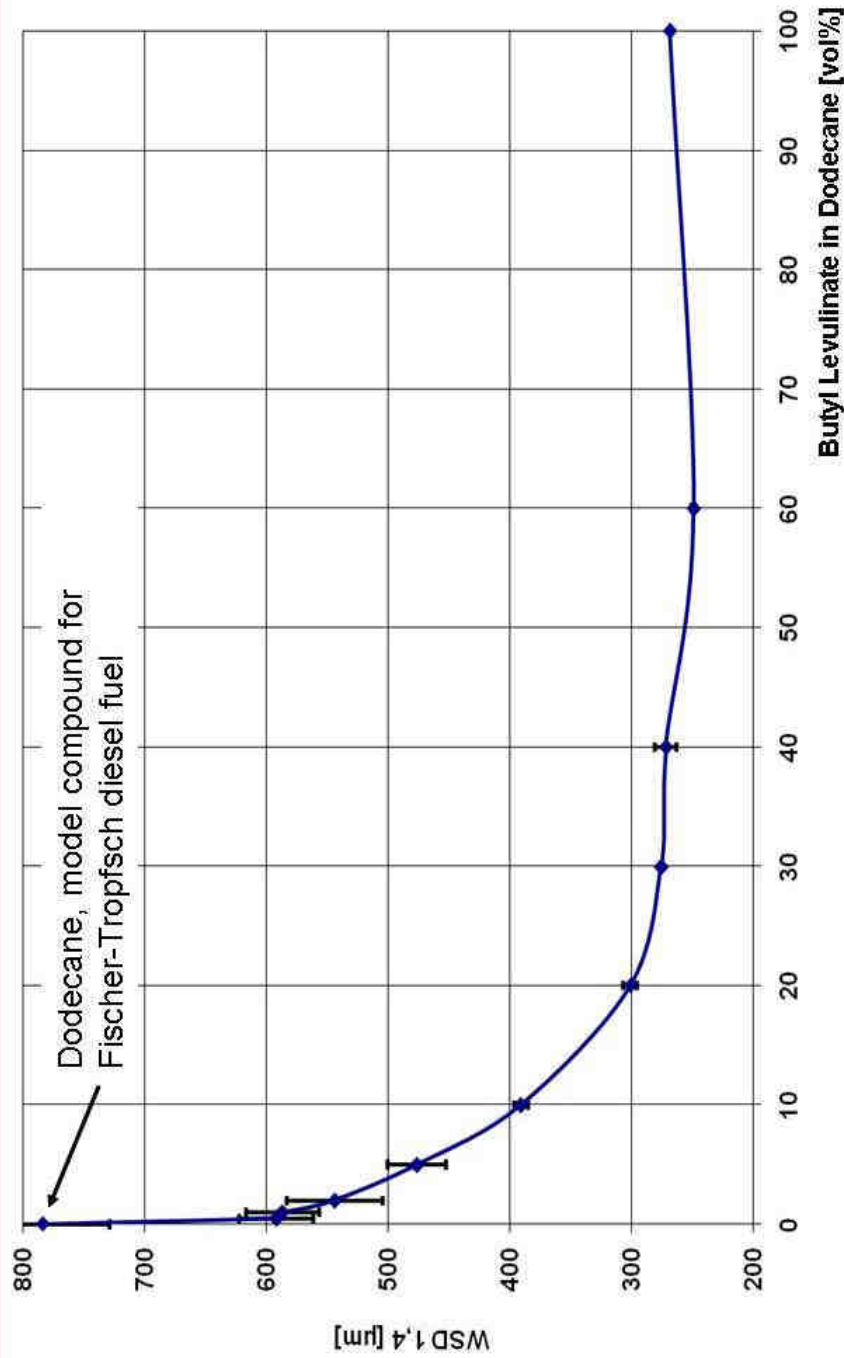


ASTM and DIN for Diesel fuel:
WSD < 460 μm \rightarrow acceptable
WSD > 460 μm \rightarrow lubricity additives must be added
WSD < 230 μm \rightarrow can potentially be used as lubricity additive

Lubricity of TMFB candidates

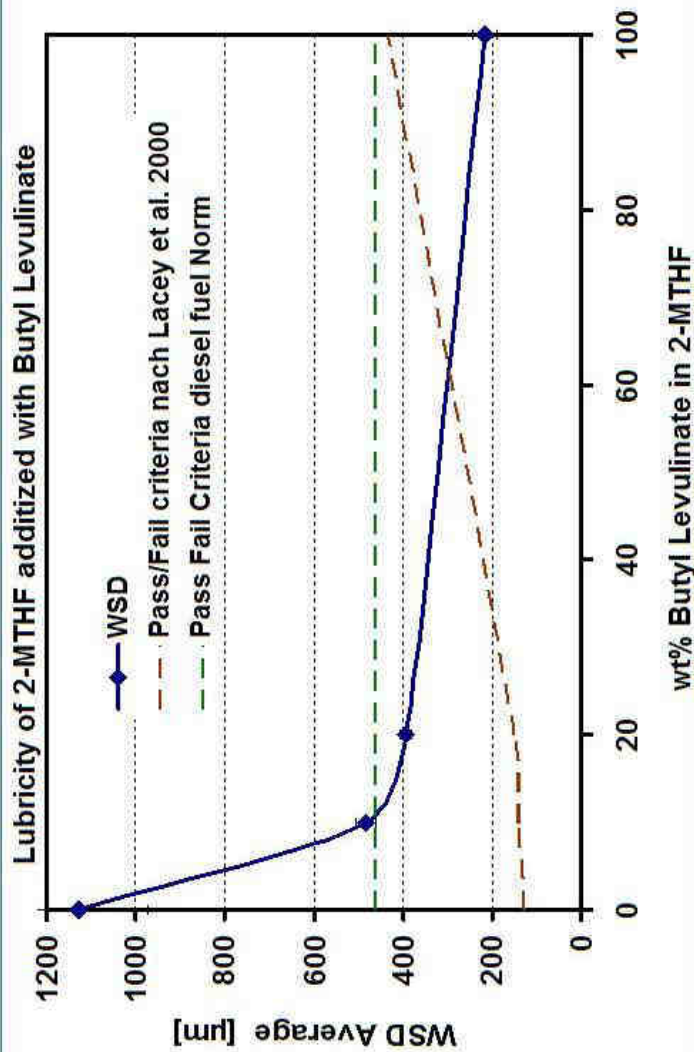


Potential of biofuels as lubricity additive (HFRR)



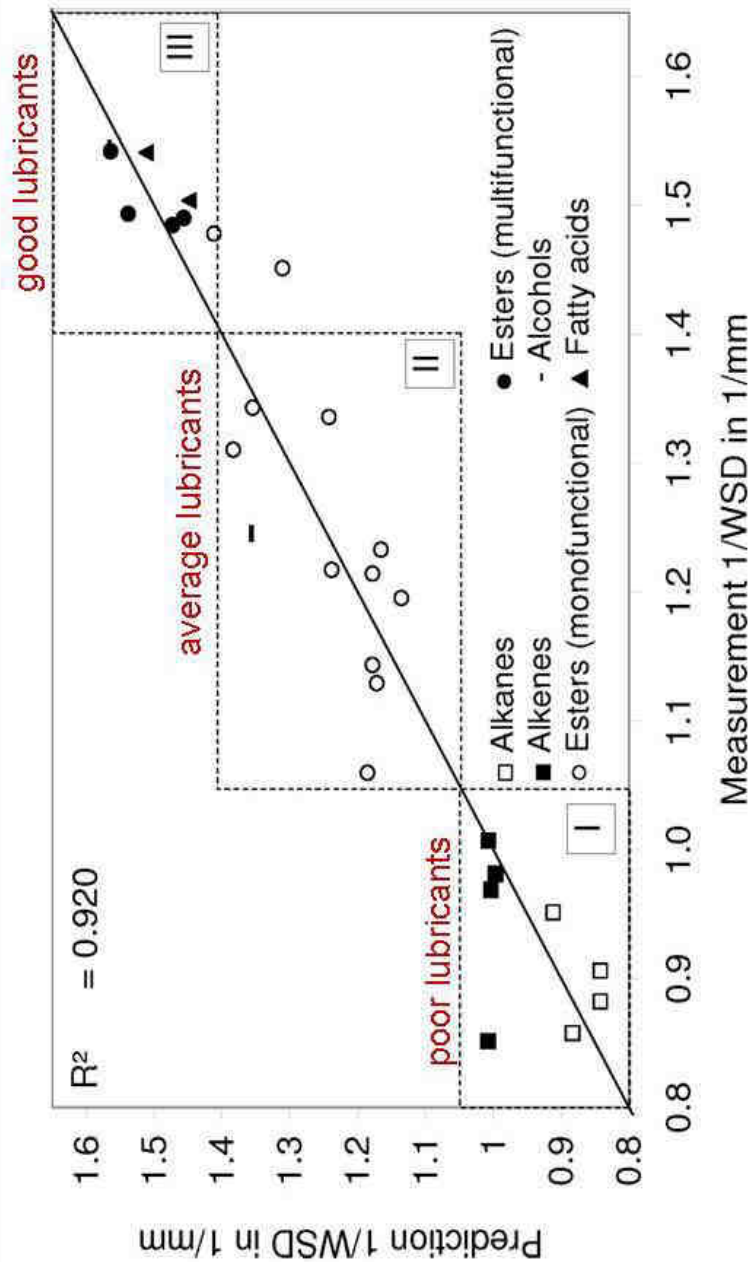
IFAS

Lubricity and viscosity of 2-Methyl tetrahydrofurane (2-MTHF)



Key Results: With 20% blending of Butyl Levulinate 2-MTHF meets the Norm but not the corrected pass/fail of Lacey et al.
The HFRR results for 2-MTHF blends have to be verified with full scale test benches.
Constructive or material solutions can be proposed.

COSMO-RS based pre-selection tool for lubricity



The model can be used as a pre-selection tool for a large number of possible fuel compounds



Outline

- Introduction
- Tribology
 - A: Analysis of fluids
 - B: Axial piston pumps
- Hybrid Drives
 - A: Hybrid for drive trains
 - B: Boom energy regeneration system
- Hydrostatic Drives for Wind Turbines
- Conclusion and Outlook



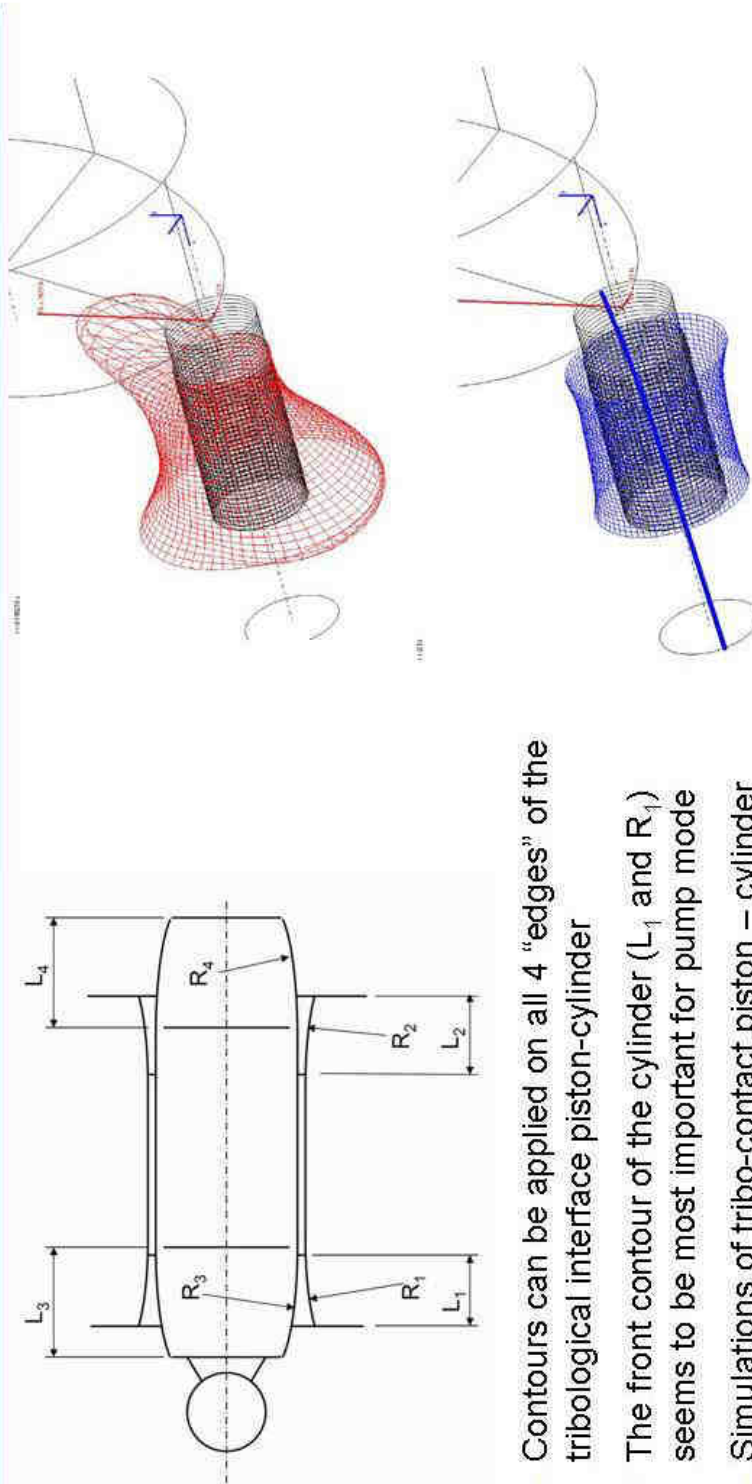
B: Axial piston pump

- Avoiding brass and bronze in axial piston machines has advantages:
 - Ageing of oil is slowed down
 - Environmental protection
 - Reduction of costs
 - Reduction of wear and increase of life-time of the components
 - ...

- Avoiding these non-ferrous metals brings disadvantages as well:
 - Running-in phase no longer possible, a contouring at the piston-cylinder contact has to be machined before assembling the pump
 - Pistons or cylinders should be coated to avoid seizing



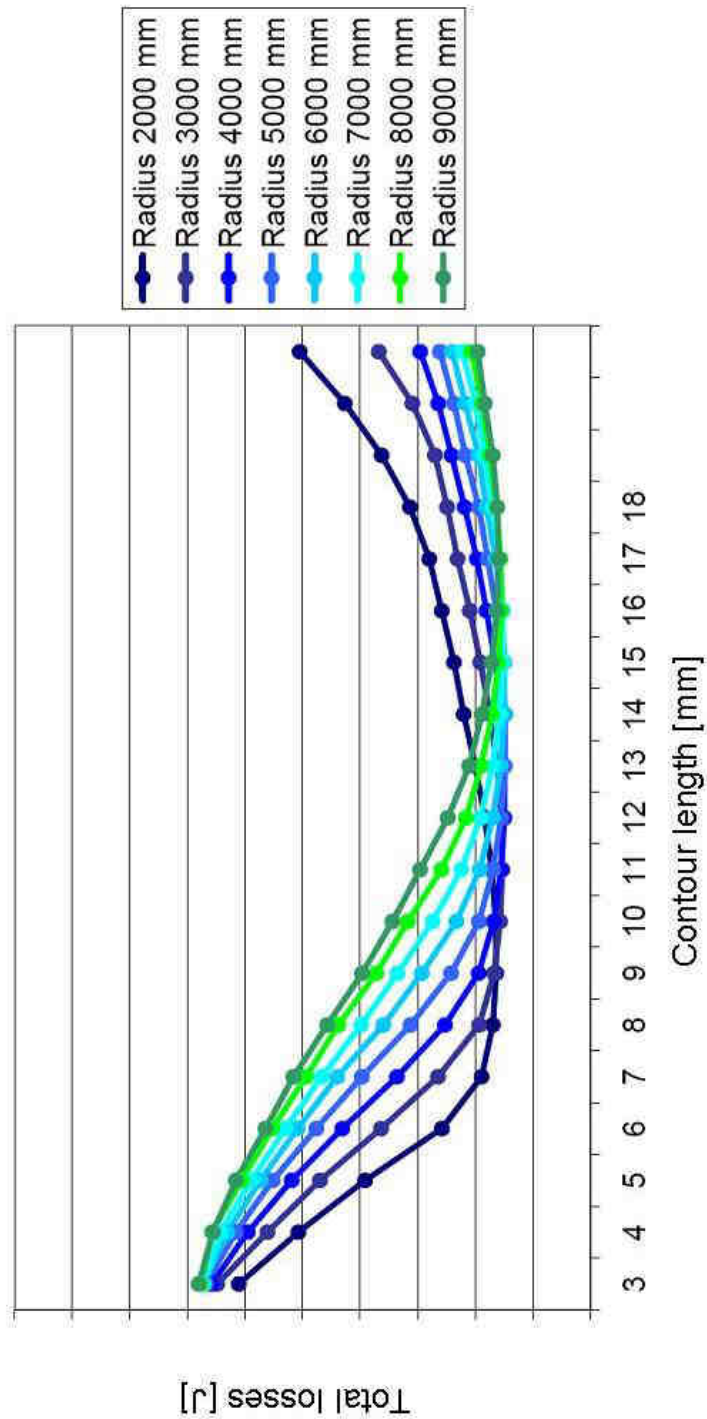
Contouring of cylinders



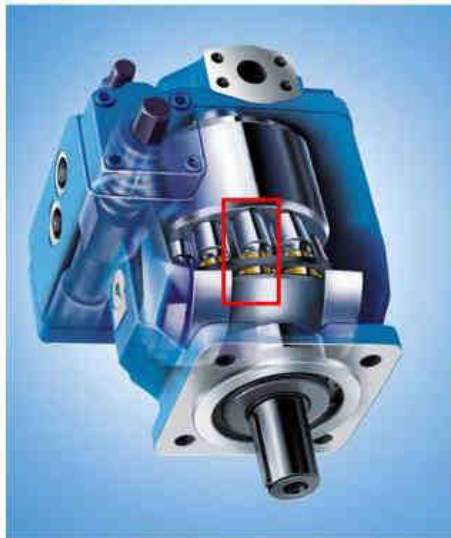
- Contours can be applied on all 4 "edges" of the tribological interface piston-cylinder
- The front contour of the cylinder (L_1 and R_1) seems to be most important for pump mode
- Simulations of tribo-contact piston – cylinder reveal suitable contouring of cylinder
- Cylinder made of tempered steel

Contouring of cylinders

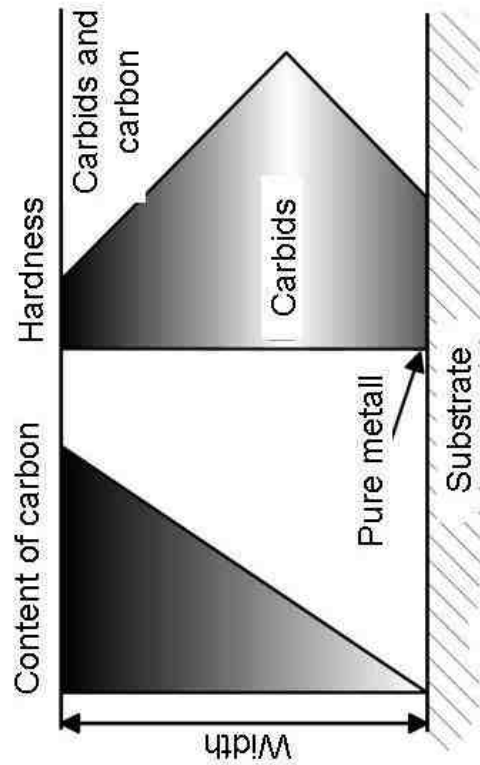
Variation of front contour of cylinder



Coating of pistons and slippers

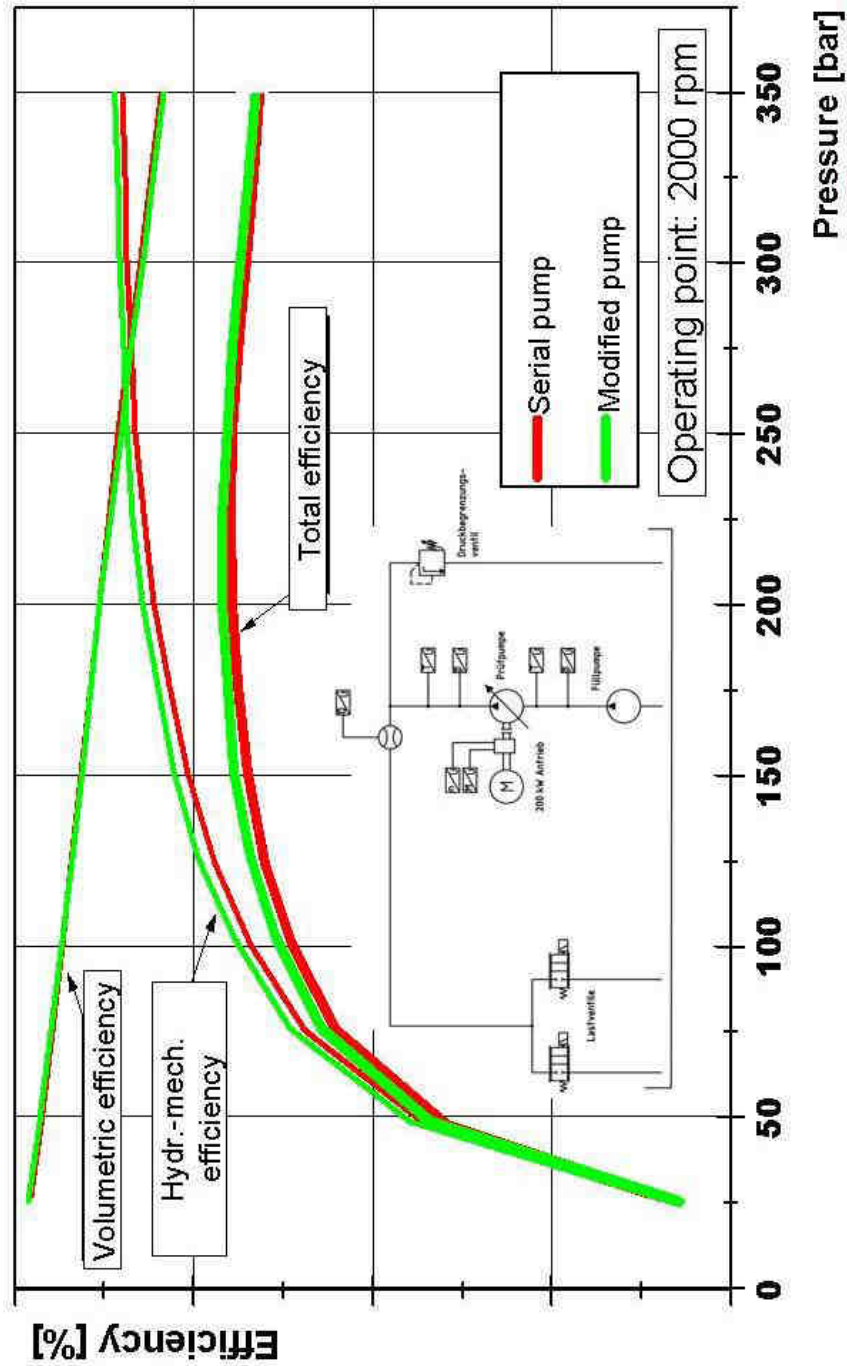


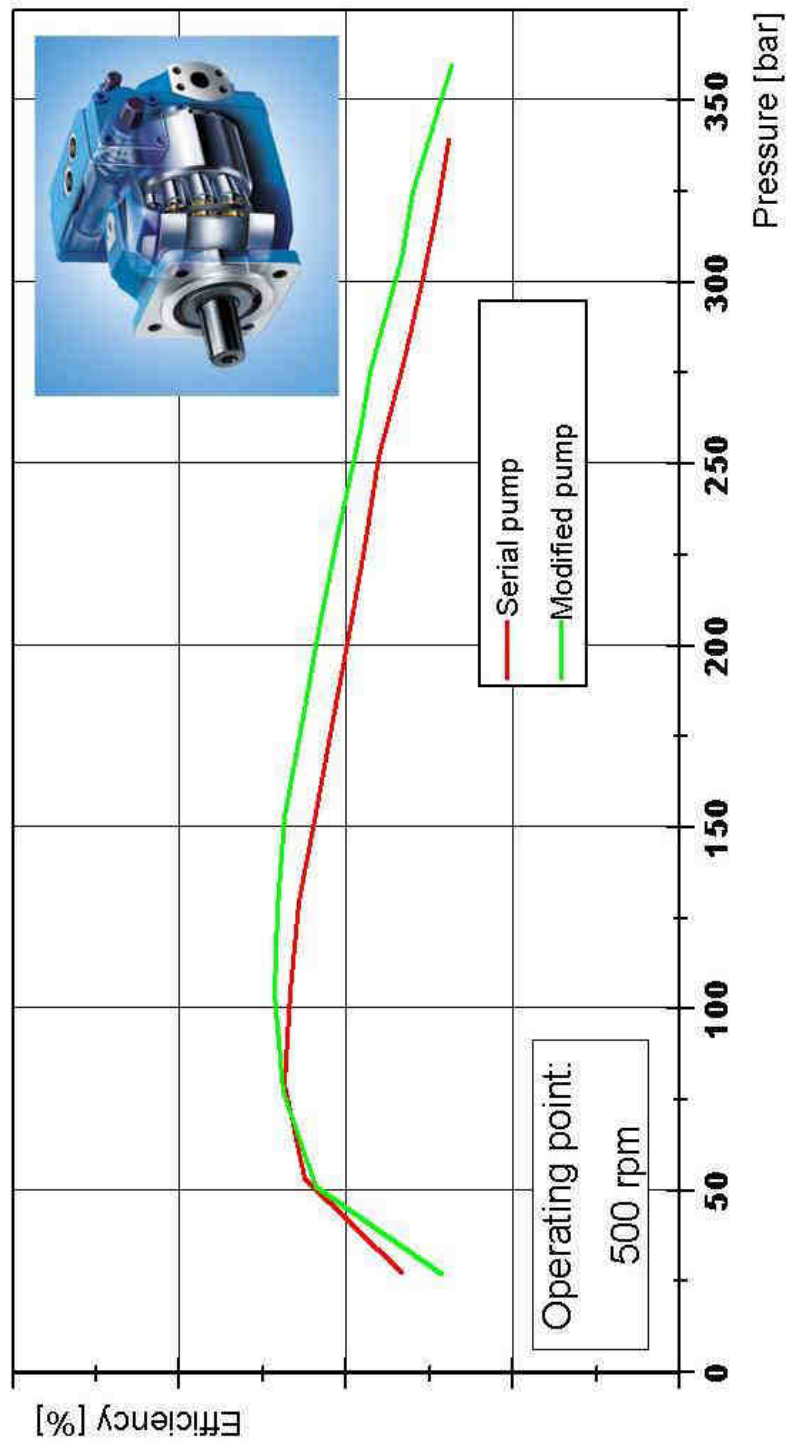
- For pump mode, pistons are not contoured
- Pistons are coated with Zirkonium Carbide (ZrC)
- Slippers made of tempered steel are in use
- Slippers are also coated
- Each tribo-contact consists of a PVD-coating running on tempered steel



IAS

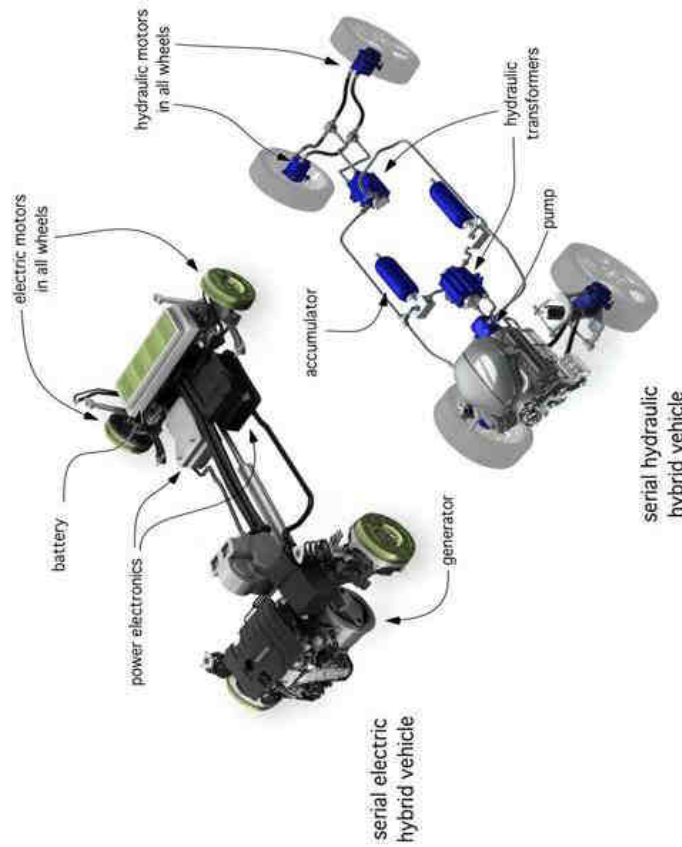
Efficiency tests of modified pump without brass



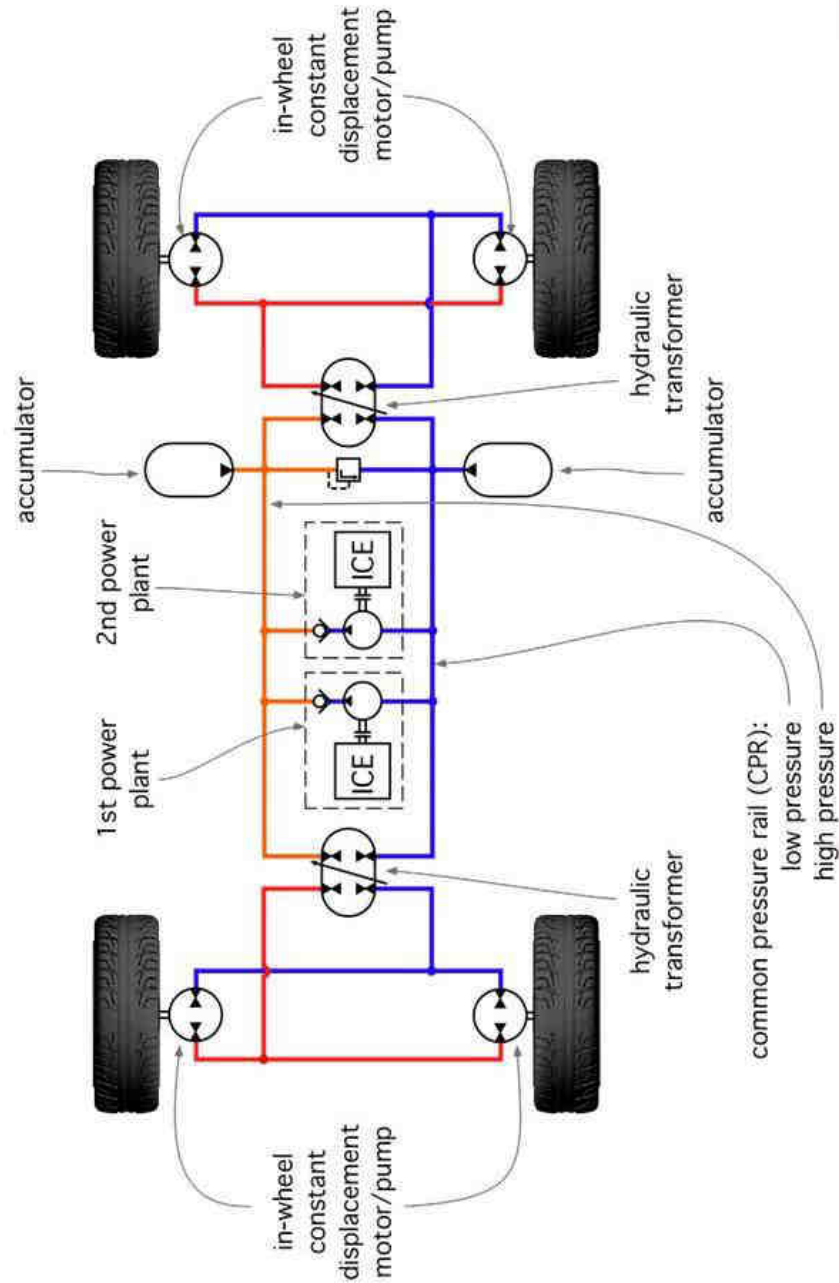
Efficiency tests for low speed

A: Hybrid for drive trains (Innas – Achten)

- Energy saving and CO₂ reduction major challenge
- System vs. component optimization
- Mechanical drive train with high efficiency leads to opposed ICE operating points
- Electric as well as hydraulic drive trains with accumulator disconnect ICE and wheels
- Hydraulic transformer allows pressure boost above rail pressure and energy recuperation during braking
- ICE runs in start-stop operation mode and always in an optimal efficiency range



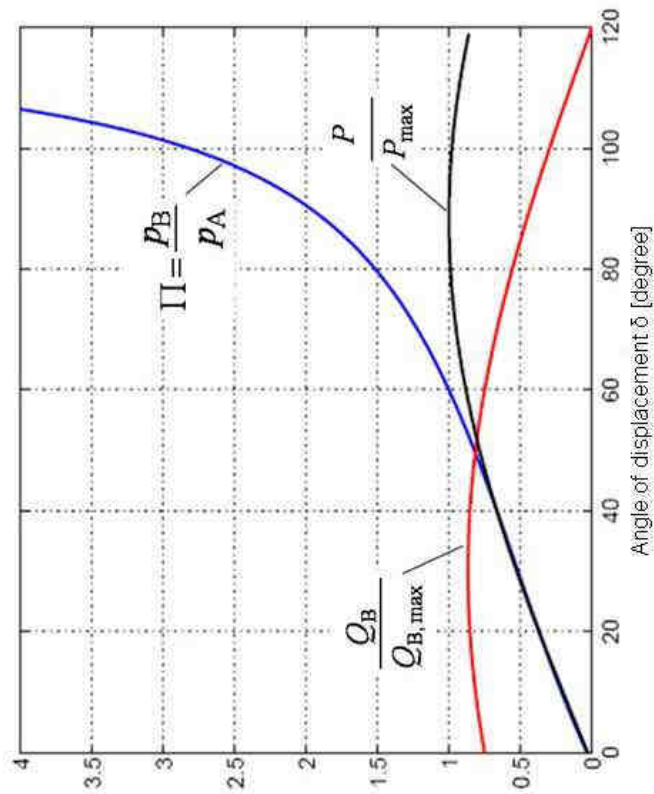
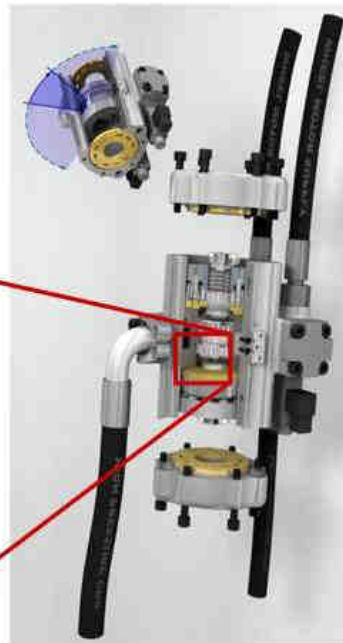
Hybrid car – hydraulic concept



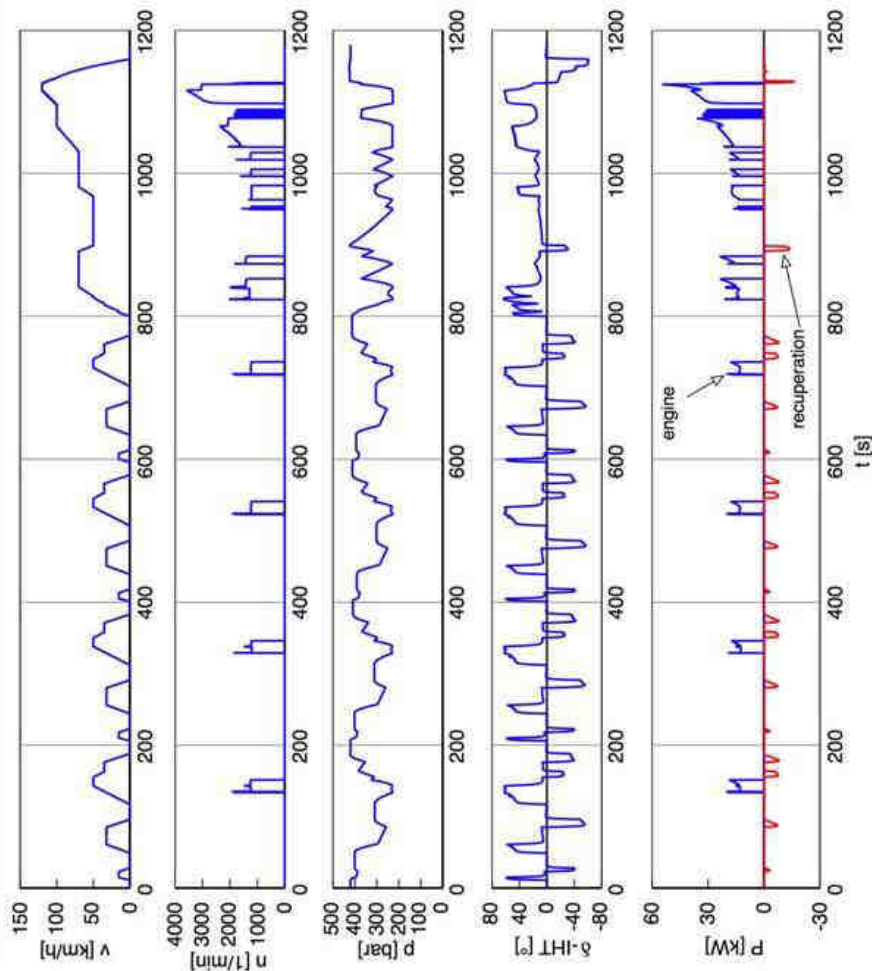
Innas Hydraulic Transformer (IHT)



Floating Cup
principle



NEDC cycle performance and results

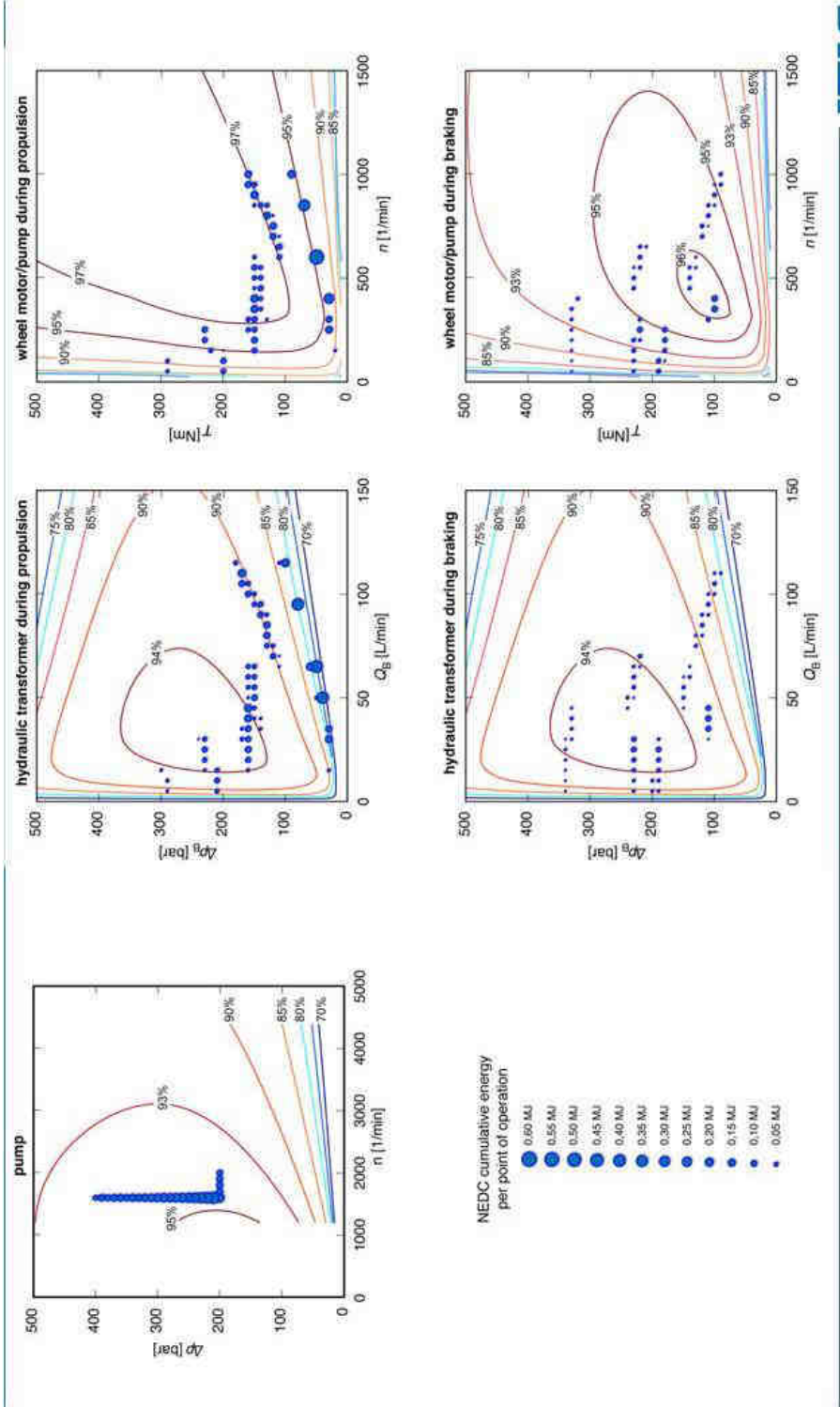


- Engine shut off > 80%
- Recuperation of braking energy
- High efficiency pumps and motors by Floating Cup principle
- Pressure boost above rail pressure by transformers
- ICE forced to run at high efficiency

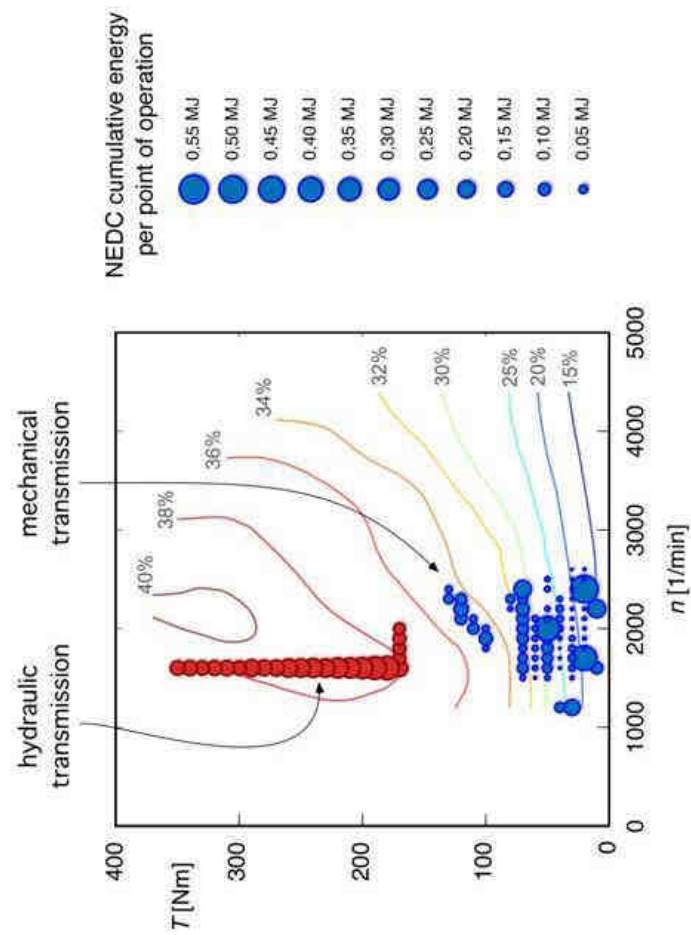
→ by simulation more than 50% reduction in fuel consumption and CO₂ emissions possible



Operating points – hydraulic components



Operating points – internal combustion engine



Outline

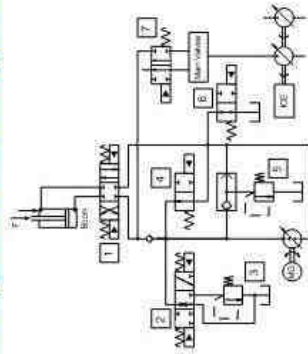
- Introduction
- Tribology
 - A: Analysis of fluids
 - B: Axial piston pumps
- Hybrid Drives
 - A: Hybrid for drive trains
 - B: Boom energy regeneration system
- Hydrostatic Drives for Wind Turbines
- Conclusion and Outlook



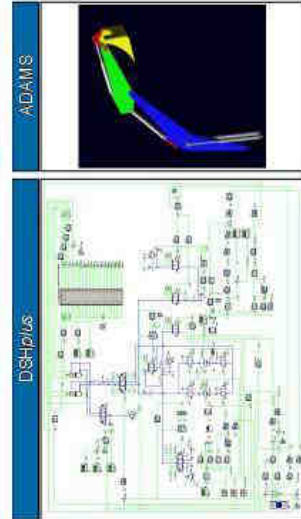
B: Boom energy regeneration system

- Challenge: Fuel reduction and CO₂ savings
 - Regeneration of potential energy
 - Systematic design search and method development

System design



Simulations

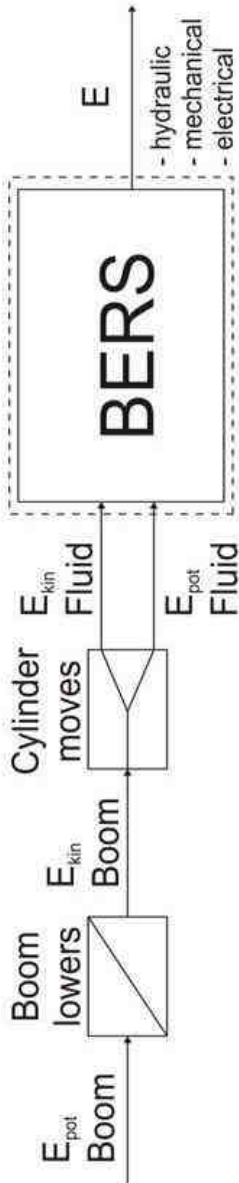


Test bench



Energy regeneration – systematic research

- Research of BERS using construction methods by Pahl / Beitz
 - Function structures of BERS



- Morphological Box with solutions

- Hydraulic
- Mechanic
- Electric

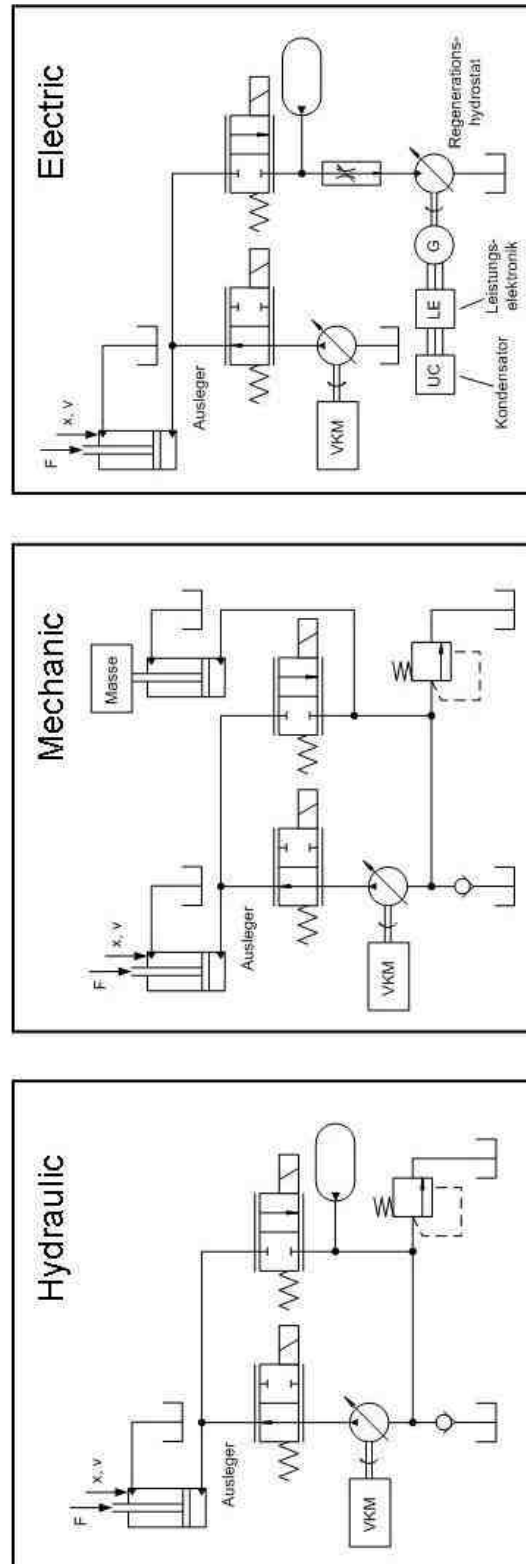
solutions	1	2	3	4	5	6
gathering ($E_{pot} + E_{kin}$) transforming ($\rightarrow E_{kin}$)	hydraulic cylinder	hydraulic motor	gear box			
transforming ($E_{kin} \rightarrow E_{pot}$, $E_{kin} \rightarrow E_{kin}$)	hydraulic cylinder	hydraulic motor	gear box			
storing ($E_{pot} / E_{kin} / E_{kin}$)	hydraulic accumulator	hydraulic accumulator	hydraulic accumulator	hydraulic accumulator	hydraulic accumulator	hydraulic accumulator



Energy regeneration – system design

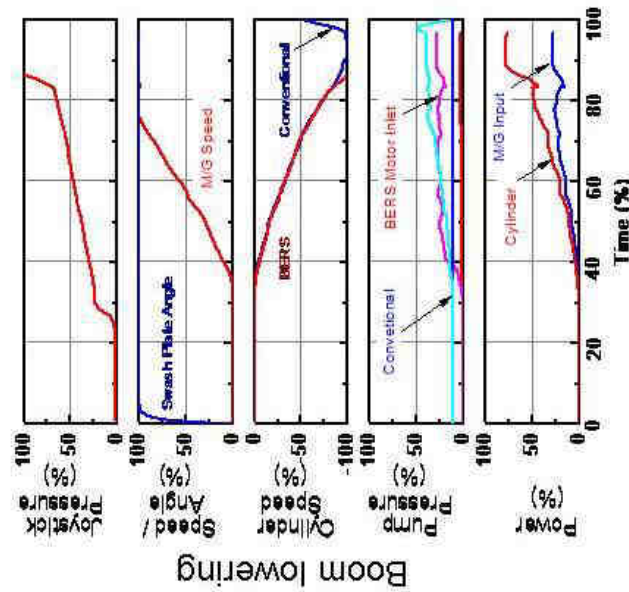
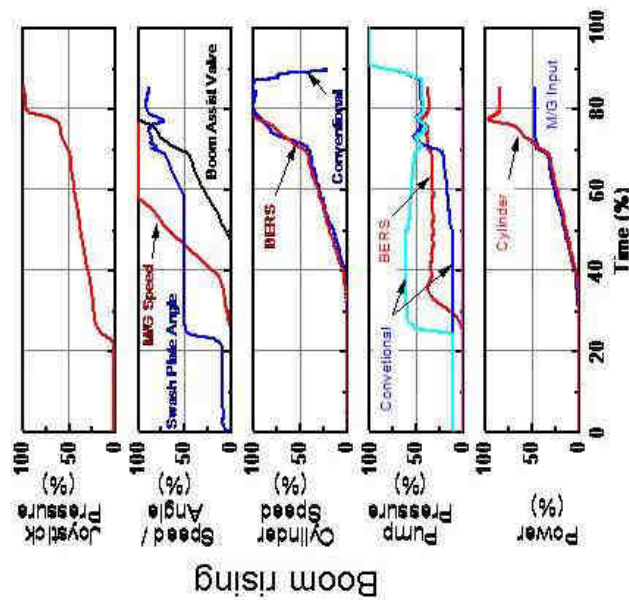
- Development of different concepts for the Boom Energy Regeneration System
 - Hydraulic Systems
 - Mechanical Systems
 - Electrical Systems
 - Compound Systems

Exemplary systems



Energy regeneration – simulation results

- New system has the same operating behaviour as the standard excavator
 - ➔ operator does not feel any differences
- Increased efficiency compared to standard excavator for boom rising and lowering
 - ➔ About 54 % of the potential energy of the boom can be regenerated

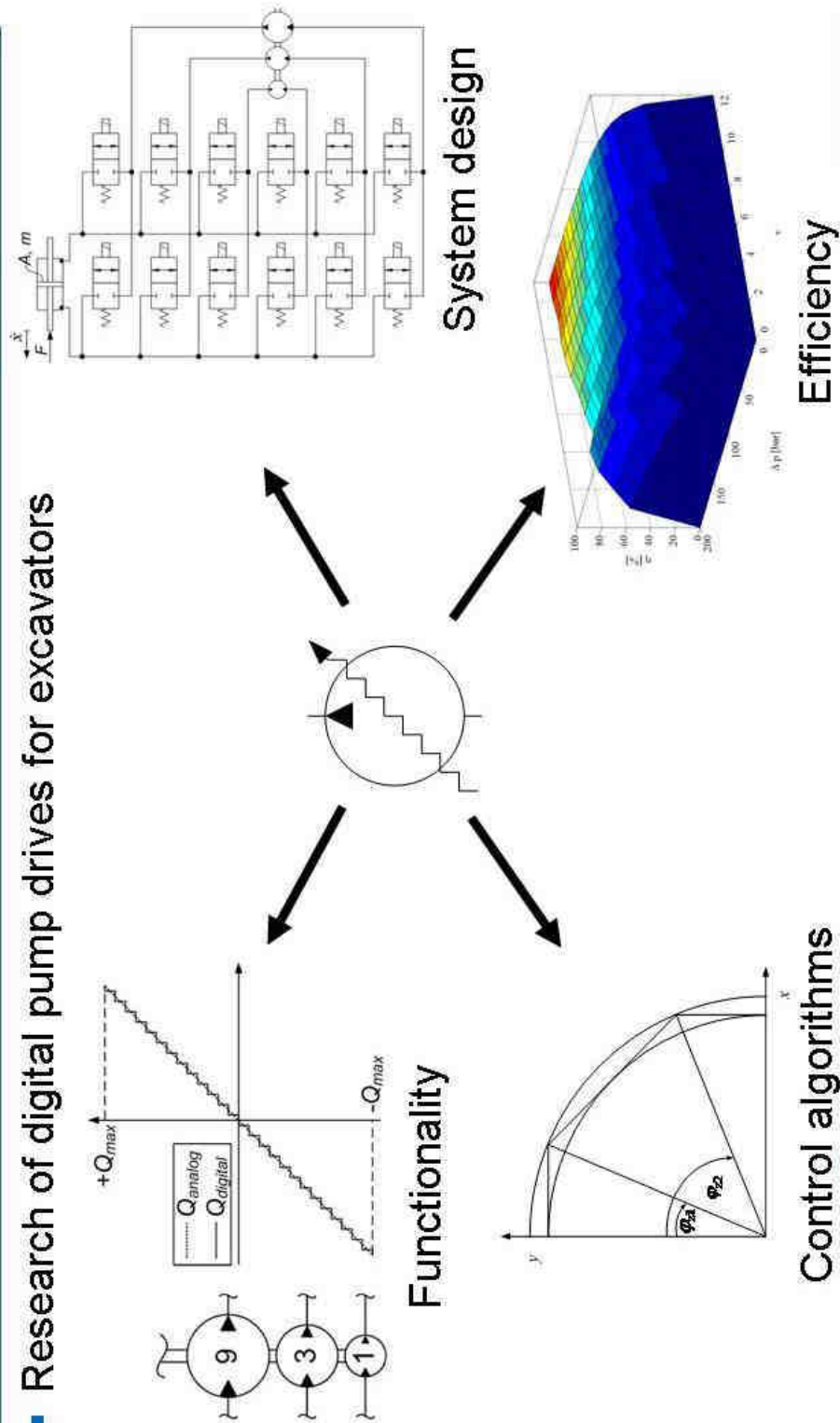


by Kang et al., Doosan



Digital hydraulics – component design

■ Research of digital pump drives for excavators



Outline

- Introduction
- Tribology
 - A: Analysis of fluids
 - B: Axial piston pumps
- Hybrid Drives
 - A: Hybrid for drive trains
 - B: Boom energy regeneration system
- Hydrostatic Drives for Wind Turbines
- Conclusion and Outlook



Project description

„Development of a hydrostatic drive train for Wind Energy Plants on- and offshore“

■ Partner & funding



Bundesministerium
für Umwelt, Naturschutz
und Reaktorsicherheit

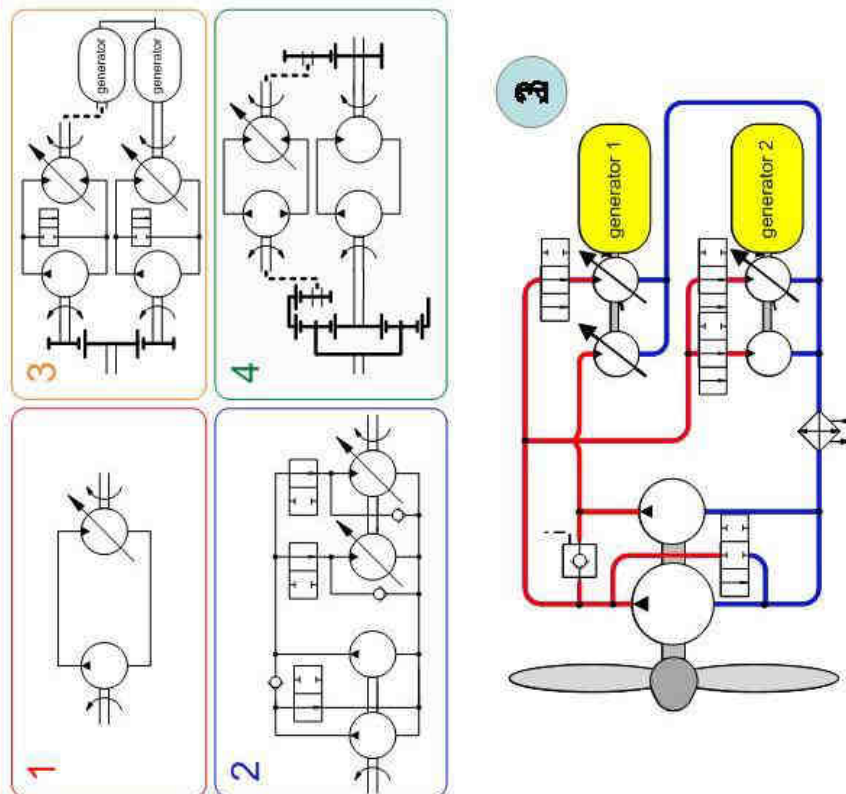


■ Work packages at IFAS

- Development of a hydrostatic drive train for wind energy plants
- Development of an 1-MW-test bench
- Simulation and measurement of the efficiency



Configuration of the transmission



- Different concepts generated in a morphological box
- Evaluation and optimization in simulations

Components

- 2 pumps (13.2 & 52.8 l/rev)
- 3 variable displacement motors
- 1 constant motor
- 2 generators
- Three different modes of operation

Simulation result

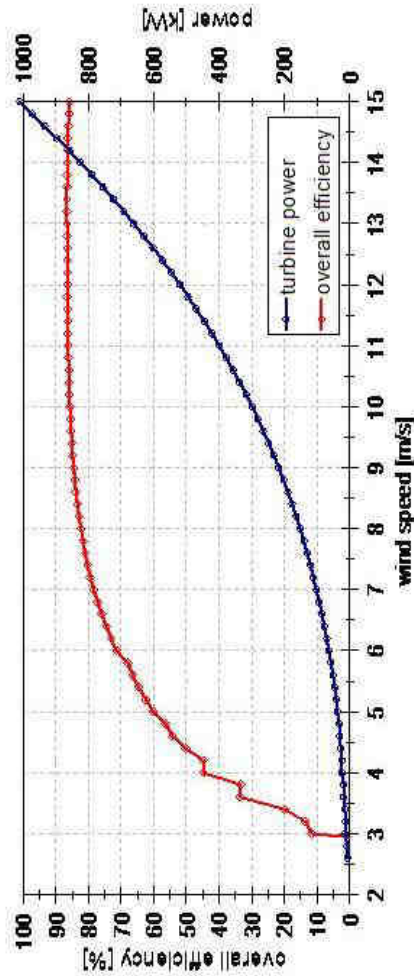
Boundary conditions

- 1-MW-turbine model loads the drive train
- Existing efficiency data of components had to be scaled



Simulated operating points

- 63 simulation runs
- Wind speed
2,6 – 15 m/s



Schmitz, J., Vatheuer, N., Murrenhoff, H., Development of a Hydrostatic Transmission for Wind Turbines, Proceedings of 7.IFK, Aachen, 2010



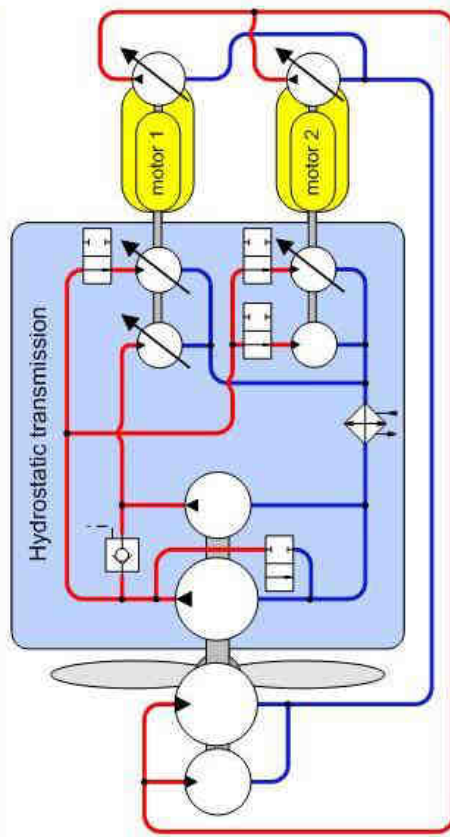
Test bench design

Challenges

- Drive with high torque at low speed
- Applying dynamic loads
- Minimize installed electrical power

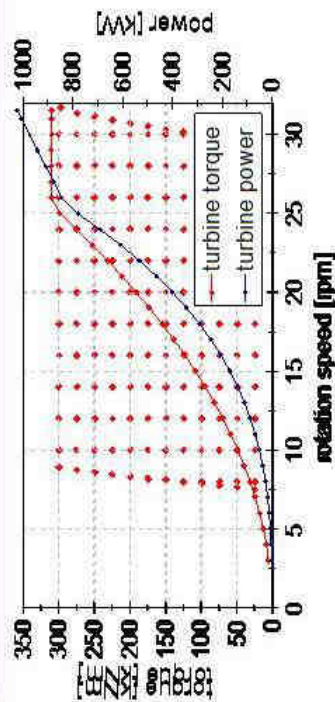
Test bench layout

- Hydrostatic power feed-back
- Generators replaced by electrical motors and axial piston pumps
- Turbine is simulated by radial piston motor
- Drive is controlled by variable displacement pumps



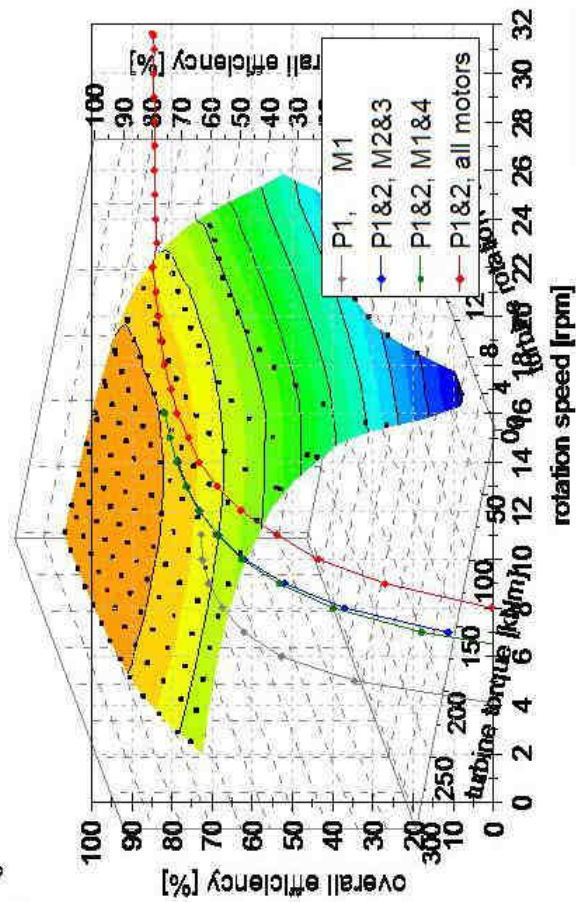
IAS

Measurement results



Procedure of measurements

- Test bench drive impressed the torque
- Transmission controller controls the rotation speed



- Overall efficiency with all pumps and motors switched on
- Overall efficiency in WEP operating points



Outline

- Introduction
- Tribology
 - A: Analysis of fluids
 - B: Axial piston pumps
- Hybrid Drives
 - A: Hybrid for drive trains
 - B: Boom energy regeneration system
- Hydrostatic Drives for Wind Turbines
- Conclusion and Outlook



Conclusion and Outlook

- By research examples an insight was provided where fluid power can contribute to save natural resources and increase efficiency
 - TMFB fluids are suitable for energetic use and some even as additives
 - Incremental innovations help existing piston pump designs to minimize losses
 - System approach is important for the design of drive trains and work hydraulics including the combustion engine
 - Huge potential for fluid power drives with switchable units in wind turbines
-
- Advancing fluid power components and systems remains a rewarding challenge for the future towards the stated goals
 - The innovation process for fluid power requires excellently educated engineers and scientists
 - Satisfying these requirements by universities and companies will lay the foundation for continuing growth of our branch

HYDRAULIC SWITCHING CONTROL – OBJECTIVES, CONCEPTS, CHALLENGES AND POTENTIAL APPLICATIONS

Rudolf SCHEIDL¹, Helmut KOGLER¹, Bernd WINKLER²

¹ Johannes Kepler University Linz, Rudolf.scheidl@jku.at.

² Linz Center of Mechatronics, Bernd.winkler@lcm.at

Abstract: *Hydraulic switching control operates via the switching of valves. Numerous principles exist, some of which are already routinely applied, some others have been studied, but many more are possible. A successful realization of many switching techniques requires fairly advanced hydraulic components, foremost fast switching valves, fast check valves and compact accumulators which can resist high load cycles, and a sound understanding of the relevant processes by advanced modelling, simulation, and experimental analysis. Switching control can bring the following advantages: lower costs, higher robustness, better standardization, easier control due to better repeatability and less hysteresis; better energetic efficiency by the application of energy saving converter principles; generation of very fast motion for relatively high loads. Some elementary switching principles and switching converter principles are described in this paper. The authors expect an early industrial application of novel switching techniques in heavy duty and in agricultural machines.*

Keywords: *Hydraulic switching control, switching converters, buck converter, electric hydraulic analogy.*

1 Introduction

The idea to employ switching systems for realizing some sort of hydraulic transformers is an old idea as the hydraulic ram of Montgolfier from 1796 and Pollard's work on pulsating hydraulic power transmission (1964) [1] show. The major motivation for the current attempts to realize hydraulic switching control is the success of switching control in modern electric drive technology.

Hydraulic switching control is a sub-domain of digital hydraulics, which is characterized by performing control only by the use of components with discrete states (see [2]). In hydraulic switching control these discrete state components are switching valves. Control input parameters are some timing characteristics of these valves which can be: the pulse-width of a pulse width modulated valve switching, the duration of individual pulses, switching frequencies, or the phase shifts of switching pulses of different valves, to mention just a few.

The basic motivations for switching control are:

- To use the simple component switching valve instead of the more complex servo or proportional valves, to achieve one or several of the following goals: lower costs, higher robustness, better standardization
- Easier control: better repeatability, less hysteresis
- Better energetic efficiency by the application of energy saving converter principles
- Generation of very fast motion for relatively high loads

Like in power electronics, the variety of possible switching concepts is very large and there is not just one optimal solution for many applications but rather a few optimal for a small class of applications. Some concepts evaluated so far are:

- Non energy saving concepts: Elementary switching control concepts [3], the LCM ‘Digi-Actuator’ [4], combinations of pulse code and switching control concepts [5].
- Energy saving switching control principles: the Gall&Senn principle [6], buck- [7], resonance- [8], wave- [9], motor-converters [10, 11].

Some hydraulic switching principles are routinely applied since decades in the following applications: ABS break systems, variable valve timing for compressor valves [12], clutch actuation of gears in passenger cars [13], on-line gap adjustment of continuous casting segments [14, 15]. All these drivers require relatively low power and flow rate, respectively. Fast switching valves for such power ratings can be realized much easier than for higher flow rates and also pulsation and noise excitation levels are relatively low. The application of switching control to high power drives is facing the following main challenges:

- Appropriately powerful fast switching and check valves, and fast, compact, and reliable accumulators.
- The sound understanding and the mastering of pulsating phenomena and of acoustic noise.
- Control algorithms for switching control, which not only provide a proper control of the intended motions, force, or pressure but which also cope with the challenges of switching control, in particular with pulsation.

Switching control is also a useful technology for other than mechanical actuation. Not only modern diesel fuel injection, in particular common rail systems, apply switching principles but also the cooling of rollers employs this technology to realize the so called thermal crown in steel and aluminium rolling [16, 17].

There is no limitation of the application of such switching control concepts in principle. Currently, the only reasonable question is which applications are best suited for an early application of these technologies. This is not just a technical matter but depends even more on the disposition of end users to take the front runner role. To convince potential end users a single advantage, like just being more efficient, may be a too weak argument, there must rather be several advantages. In the next chapter some switching control concepts are presented. In chapter 3 areas of early applications of hydraulic switching control are discussed. An outlook on the further development of switching control will be given in chapter 4.

2 Switching control concepts

2.1 Electric – hydraulic analogy and duality

Hydraulic and electric machines are power converters with one mechanical port, a shaft or a rod. Electrical machines employ a dynamical principle for torque or force generation, respectively. This corresponds to hydrodynamic machines, like turbines or centrifugal pumps. Hydrostatic machines, however, employ a static principle which is dual to the dynamic principles. In the dynamic principles machines, torque or force depend on the flow variable, i.e. on the electric current or on the flow rate, respectively; in hydrostatic principles machines torque or force depend on the pressure. We limit this investigation to hydrostatic machines. The duality of static and dynamic machines has significant consequences for switching control.

A very elementary circuit for switching control of an electrical motor is shown in Figure 1a. The current i of the electric motor which is driven by a PWM voltage signal has a small fluctuation due to the flattening effect of the motor inductance. The angular speed's (ω) fluctuation is even smaller, because the inertia of the rotor and of attached moving mechanical parts have a flattening effect too. Both flattening effects are very expressed due to the high switching frequencies of modern drives, which are in the order of 10^4 Hz. That leads to a quite constant speed.

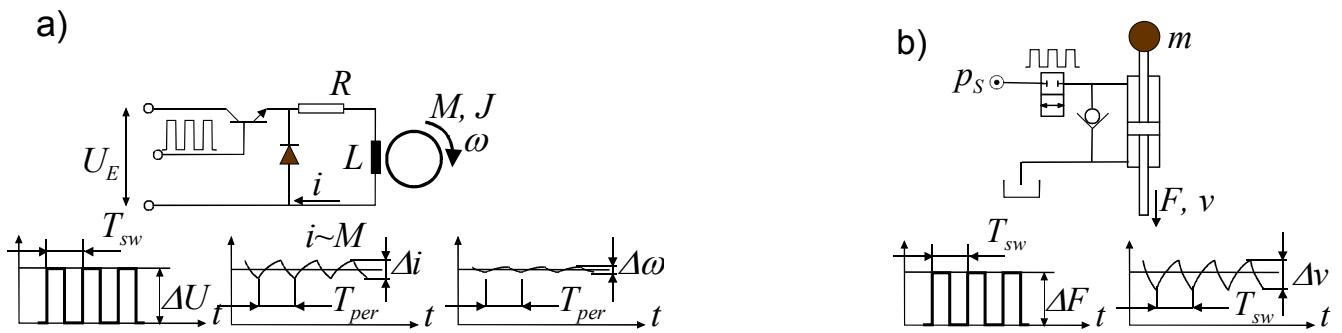


Figure 1: Elementary switching control circuits of a) an electrical motor, b) a hydraulic actuator

Hydraulic elementary switching control, as shown in Figure 1b, intrinsically generates higher speed fluctuations because the acceleration corresponds to the hydraulic force F which is approximately a rectangular signal. This requires extra devices to get rid of the strong pressure pulsation due to switching, particularly if the mechanical inertia of the system to be actuated is relatively small.

A further main difference between electrical and hydraulic switching systems is the high capacity of hydraulic systems. In Figure 1b, for instance, that capacity stems from oil compressibility in the chambers of the cylinder and in the connecting lines. One hardly can get rid of this capacity, which causes energetic losses in combination with the resistance of the valve at higher switching frequencies. There is some resonance effect resulting in an energy optimal switching frequency (see [18]). In electrical switching systems parasitic capacities are a negligible problem unless switching frequencies are extremely high.

On the components level a strong analogy exists between electrical and hydraulic switching systems. This concerns mainly the key component valve, the performance of which is a limiting factor for advancements in switching control. The availability of fast electric 'valves' is a major reason why electrical engineering leads the way. The progress there, for instance with respect to switching frequency or power range, was guided by advancements in power semiconductor technology.

2.2 Elementary switching control principles

In elementary switching control just one or more valves are put in front of a hydraulic cylinder or motor, respectively. There are no other components, like pulsation attenuation devices or transmission lines, which exhibit a significant dynamics at the actual operating condition, between valves and the actuator. The simplest circuit is shown in Figure 2, comprising just two 2-2 way valves. Switching frequency is a major operation parameter for the performance of such a system since high frequencies flatten pressure and velocity pulsation significantly.

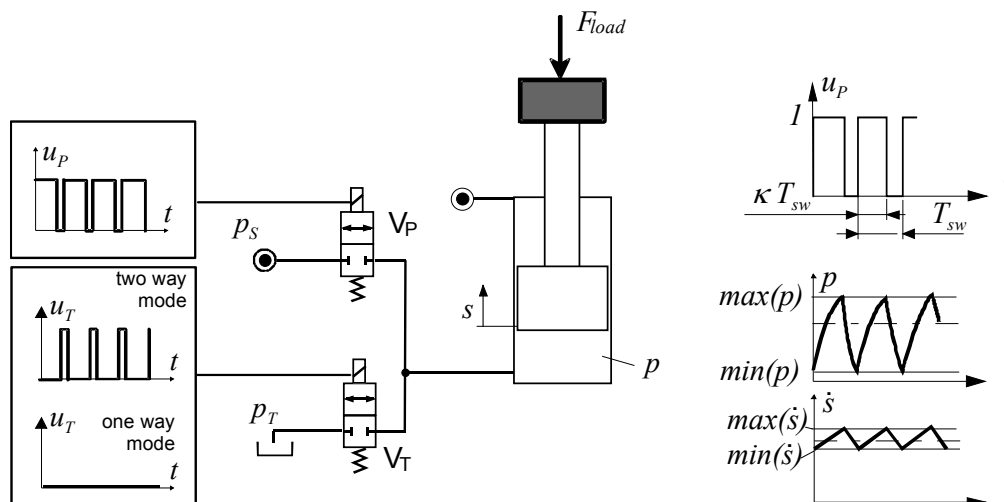


Figure 2: Elementary switching control schematic (left) and typical signals in one way mode of operation (right)

One way mode

In the so called one way mode of operation, only one switching valve is actuated. To lift the load F_{load} , valve V_P is actuated, e.g. employing PWM control with a frequency $\omega/2\pi = 1/T_{SW}$ and a duty cycle κ , to lower the load V_T is activated. The one way mode switching cannot provide better efficiency than resistance control with continuously operating valves. If there is no flow from the tank line to the cylinder in a load lifting operation, continuous or switching control give the same energetic efficiency η .

$$\eta = \frac{F_{load}}{p_s A} = \frac{p}{p_s} \quad (1)$$

The fluctuation in chamber pressure p and in piston velocity \dot{x} depends on several parameters. In [19] the following approximate value for the nondimensional pressure fluctuation $\psi_{fl} = (\max(p) - \min(p))/p_s$ is derived under the assumptions of constant supply pressures p_s , p_T , a very fast switching, and that the nonlinear state equation can be linearized around the mean values of pressure and speed and at position $x_0 = \xi_0 s_{max}$.

$$\psi_{fl} = \frac{(1-\kappa)\kappa (g c_\omega - f_{load} \bar{a}_\omega) 2\pi}{b + \xi_0} \frac{c_\omega}{\varepsilon} \quad (2)$$

The meaning of the nondimensional quantities in this result is given by the following set of relations

$$\begin{aligned} p &= \psi p_s; \quad \xi = \frac{s}{s_{max}}; \quad t = \tau / \omega; \quad v = \frac{d\xi}{d\tau}; \quad \varepsilon = \frac{p_s}{E}; \quad b = \frac{V_0}{A s_{max}}; \quad c_\omega = \frac{p_s A}{m s_{max} \omega^2} \\ a_\omega &= \frac{Q_N}{A s_{max} \omega} \sqrt{\frac{p_s}{p_N}}; \quad f_{load} = \frac{F_{load}}{m s_{max} \omega^2}; \quad g = a_\omega \left(\sqrt{1 - \psi_m} + \frac{\psi_m}{\sqrt{1 - \psi_m}} \right) \\ \bar{a}_\omega &= \frac{a_\omega}{2\sqrt{1 - \psi_m}}; \quad v_m = \frac{g c_\omega - f_{load} \bar{a}_\omega}{c_\omega} \kappa; \quad \psi_m = \frac{f_{load}}{c_\omega} \end{aligned} \quad (3)$$

The fluctuation of the nondimensional speed v around its mean value v_m is of order $O(1/\omega^2)$. ψ_m is the nondimensional pressure mean value. p_s is the system pressure, s the piston position, s_{max} the cylinder stroke, t is the physical, τ the nondimensional time, V_0 is the dead volume of the cylinder chamber at $s = 0$, m the moved mass, A the piston area, Q_N the nominal flow rates of both valves (at nominal pressure loss p_N). An analysis of Eqs. (2), (3) shows that pressure fluctuation can be reduced by a high switching frequency ω , by a valve with a low nominal flow rate Q_N , and by a high dead volume V_0 . Q_N , however, is determined by the required speed of the system, higher V_0 limits the stiffness of the system which may deteriorate the control performance of a closed loop drive. Therefore, the only independent parameter to improve fluctuation is switching frequency.

Large drives which are running relatively low maximum speed require smaller ω to stay below a certain pressure fluctuation level than high speed, short stroke drives.

Two way mode

In this mode pressure and tank valves are switched alternately. Under certain conditions this may yield better or worse efficiency than the one way mode of operation. A better efficiency is obtained if the oscillation of the load m are such that in phases when V_T is switched on oil is sucked from the tank line, a worse efficiency in opposite case.

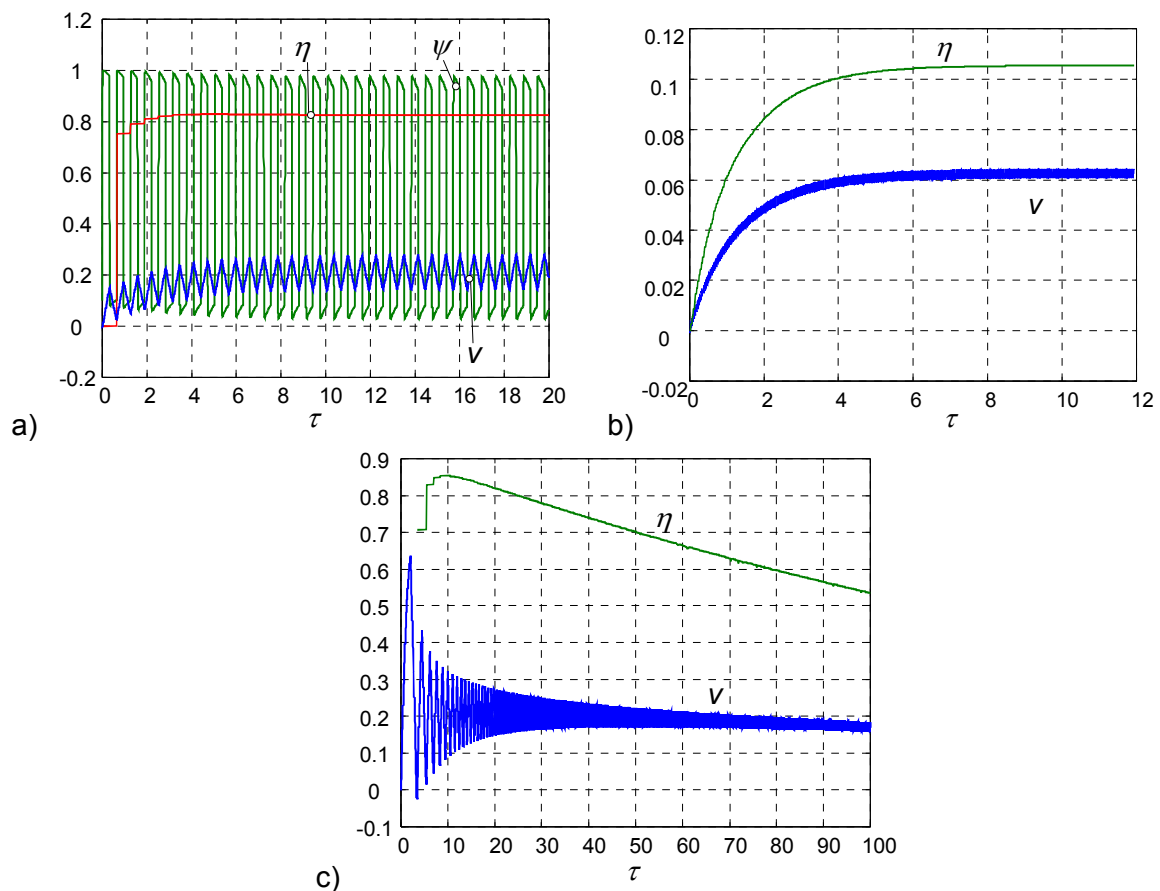


Figure 3: 1 Results of a numeric computation of an elementary switching system in dual mode; switching frequency is: a) identical to natural frequency of the system; b) twenty times the natural frequency; c) wobbled between one tenth and five times the natural frequency; values of the other parameters: $a_\omega = 1$; $c_\omega = 1$; $f_{load} = 0.5$; $\kappa = 0.5$; $(b + \xi_0) = 1$.

Figure 3 shows results of numerical simulations of an elementary switching system according to Figure 2 in two way mode at different switching frequencies. High efficiency is obtained if this frequency is below and up to the natural frequency of the hydraulic drive's free oscillation, determined by the load inertia m and the compliance of the hydraulic cylinder. Going much beyond that frequency reduces fluctuation but efficiency drops and may even fall below that of resistance control because part of the flow from the pressure line is transferred to the tank line. This can be avoided with check valves as has been proposed in [6]. The major drawback of this type of switching control is that a good efficiency is bound to high pressure fluctuation, because only if pressure p reaches nearly system and tank levels in each switching cycle, a good efficiency can be obtained. This requires the frequency not to go much beyond the natural frequency of the system and, therefore, also the speed fluctuation will be high in many cases.

The considerations presented so far were based on the assumptions that

- the supply lines have constant pressure and are not disturbed by the strongly pulsating flows going to or coming from the switching system
- the line between the valves and the actuator are ideal, thus do not exhibit significant impedances.

Particularly for very high frequencies this requires adequate components, e.g. fast response accumulators, and special care in the design of the hydraulic system.

2.3 Switching converters

Converters use some intermediate system between the switching valves and the actuator to resolve the trade-off problem of elementary switching control mentioned before. Figure 4 shows schematics of four switching converters.

Wave Converter

This converter type was investigated in [9, 20]. By resonant switching standing waves are generated in a properly designed pipe network. This network acts as a filter that annihilates lower order pulsation (several low order Fourier Spectrum components) such that at the exit port only very small pressure or flow rate oscillations occur. The output pressure is proportional to the pulse width κ .

The resonance condition requires the length L of the first order twin pipe to have half wavelength. For a switching frequency of 100 Hz L is approx. 6 m. This length condition is the main drawback for a practical implementation unless switching frequencies > 500 Hz are possible.

Resonance Converter

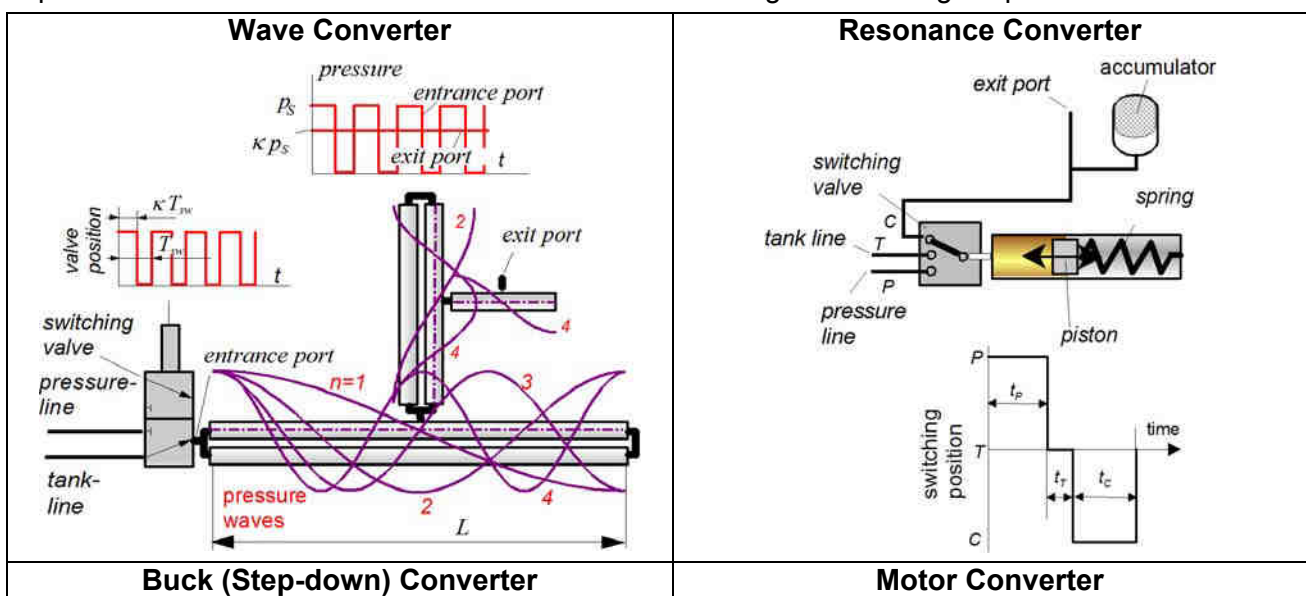
It employs an oscillating mass in form of some piston which is supported by a spring. By switching the cylinder chamber alternately to pressure-, tank-, and exit-line the piston oscillates and hydraulic fluid is transmitted to the consumer. The system operates close to the resonance frequency of the spring mass system utilizing the frequency response characteristics close to the resonance point for flow rate control. More information and results are given in [8, 21]. This system can be made fairly compact for switching frequencies beyond 100 Hz. It is a step-down and step-up converter, thus even output pressures exceeding the system pressure can be realized. The optimal timing of the consecutive switching of the valves is critical for efficiency.

Buck Converter

This is a very simple system and corresponds directly to most electrical switching power supply devices. More can be found in [7, 22]. It is a step-down converter but can also recuperate energy from the hydraulic system. The inductance pipe's length depends on the switching frequency, the higher the shorter this pipe.

Motor Converter

It follows same principles as the buck converter, only the inductance element is not the fluid inertia of a pipe but the rotary inertia of a pump-motor unit (see, e.g. [7, 8]). The advantage is that this inertia can be controlled independently from the capacitance and resistance of the system. The disadvantages of this concept are the costs and weight of the pump-motor unit and the hydraulic capacitance in such units which is a source for losses at higher switching frequencies.



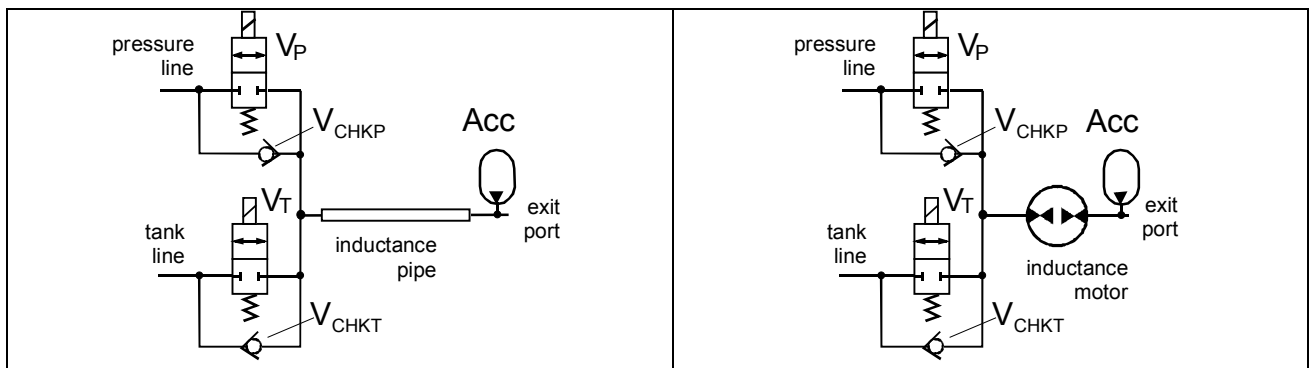


Figure 4: Four types of switching converters

2.4 Exemplary results of the hydraulic buck converter (HBC)

An extensive study of the HBC, its principles, modelling, components design, and control, can be found in the thesis [22], some results concerning its application to mobile robots in [23, 24, 25], and the application of several HBCs in parallel to avoid the accumulator (Acc in Figure 4) in [26]. Figure 5 presents some steady state performance results of a low power HBC prototype. This converter can also recuperate energy which yields a substantial energy improvement over a resistance control concept.

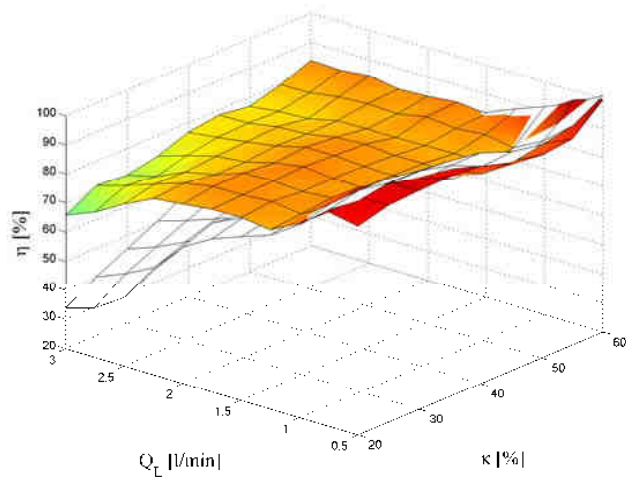


Figure 5: HBC prototype and its steady state efficiency results; (system data: inductance pipe: length: 1.2 m, diameter 3 mm, oil: Shell Tellus 15 cSt @ 40°C; switching valves: LCM FSVi ($Q_N=10$ l/min @ 5 bar); switching frequency: 100 Hz; accumulators: piston accumulators, developed by the authors; find all data in [22] and [24]).

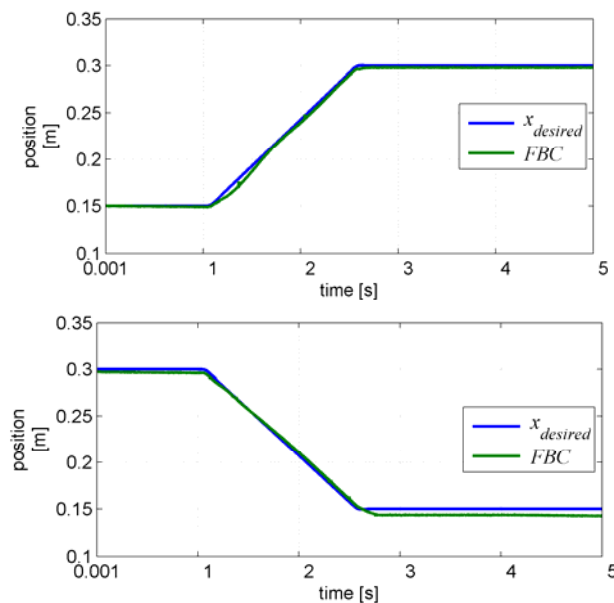
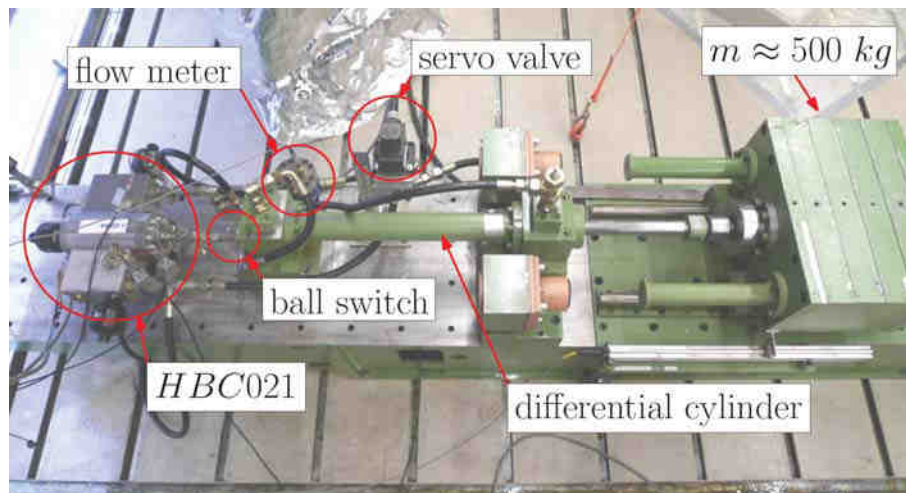


Figure 6: HBC (as shown in Figure 5) in motion control, lifting and lowering a load (Cylinder: 63 mm x 45 mm piston/rod size, stroke $x_{max} = 600 \text{ mm}$); applied control concept: flatness based controller (details in [22]).

Assessment of the HBC:

Pros: This is a simple system which can reduce energy consumption considerably; energy recuperation is possible.

Cons: The size of the inductance pipe may be a problem, unless higher switching frequencies are possible; winding of the inductance pipe to a coil deteriorates efficiency; the accumulator is a highly loaded system and makes the system soft; this requires some sophisticated control to achieve a good dynamical performance; arrangement of several HBCs in parallel and running them in a phase shifted operation is a means to skip the accumulator and improves dynamical performance; performance can become as good as with fast servo-valves, yet with much lower energy consumption (see [26] for details). Such multiple converter concepts facilitate also a simple standardization, since power rating can be easily adjusted by an appropriate number of converter units. A schematic of such multiple converters is shown in Figure 7.

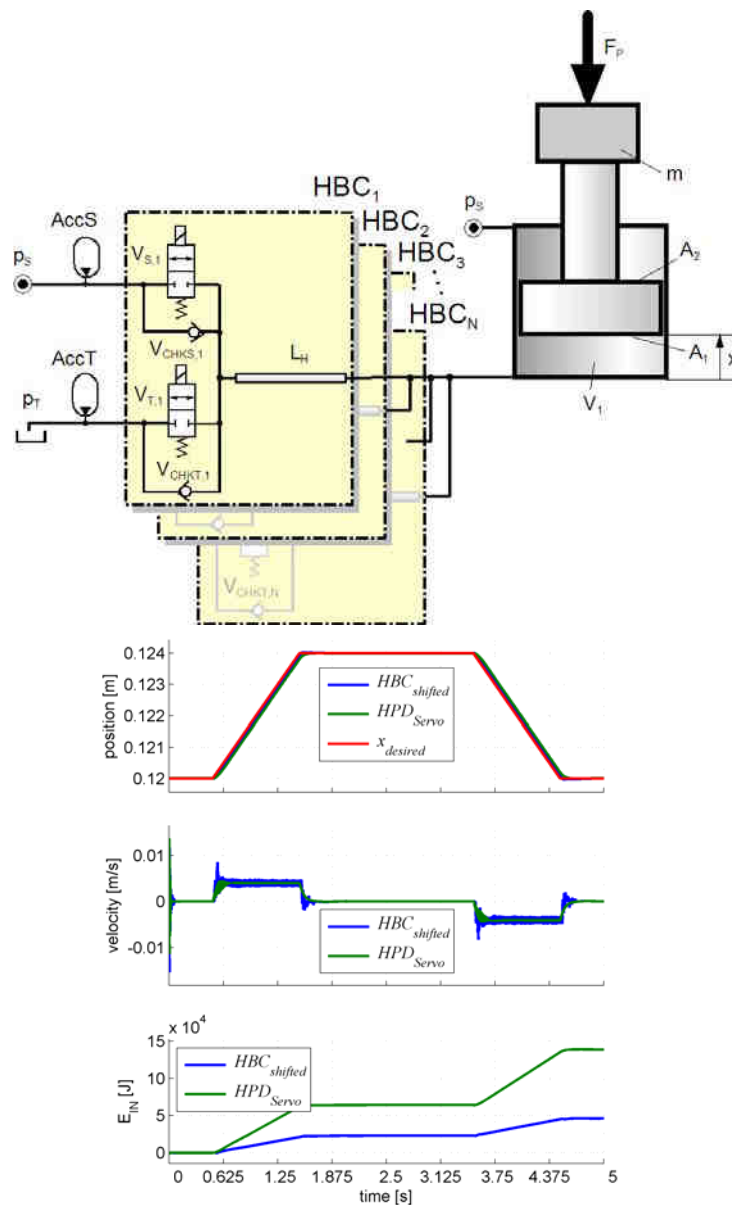


Figure 7: Schematic of a multiple (N) HBC system driving one cylinder and computed performance comparison with a servo drive for the case of a ramp like motion (for details see [26]), some data: The cylinder areas are 1.2 and 0.6 m² and the dead volume in the piston chamber is 150 l, which is sufficient for a good pressure attenuation in case of a phase shifted HBC configuration. A typical velocity for positioning the piston is 4 mm/s, which requires a flow rate of about 300 l/min in this case. Such large flow rates cannot be reasonably handled by a single hydraulic buck converter with state of the art switching valves. Thus, the presented simulations consider 6 HBCs in parallel, which operate at a switching frequency of 50 Hz. The pipe inductance of one individual HBC is about 2.5 m with a hydraulic diameter of 10 mm.

3 Favourable domains of early applications of switching control

Practical implementation of hydraulic switching control is a challenging undertaking despite its long history as a basic idea. It is a fairly new technology, if it has to meet today's requirements on hydraulic drives, since it needs also very advanced components and system understanding. Implementation in advanced machinery or plants requires some risk taking. The question is, which branches and areas of applications are most favourable for switching control. The authors see the following domains:

- **Metal production systems:** they require high forces, high dynamics and high precision, the conditions are often very crude, the systems, particularly in steel production, very extended. Servo-hydraulic drives show excellent performance in terms of dynamics and precision; their drawbacks are: high oil cleanliness requirements, which puts high burden on system installation and maintenance, wear of valve metering edges, drift problems concerning valve zero position, and high energetic losses, for instance due to the leakage of zero lap or under lapped servo valves, and high costs.

Digital hydraulics and switching hydraulics are a promising alternative, to avoid some of the mentioned deficiencies of servo-drives. This requires switching valves with a fast dynamic response, and appropriate control concepts.

Energy saving is not yet a topic of utmost importance. But there is a gradual increase of awareness of customers and, may be, stronger legislative regulations in the one or other field. In steel production, for instance, the political pressure to reduce CO₂ consumption and the fact that the core processes, like blast furnaces or steel making by basic oxygen furnaces are already highly optimized processes put some pressure on other energy consuming processes, like the many mechanical drives and actuators, even though their relative share of total energy consumption is very low.
- **Agricultural machinery:** there is an ongoing trend of mechatronization; this affects also drives and actuators; in [27] the example automatic level control system of a pick-up employing hydraulic actuation is presented; agricultural machines technologies must be low cost, capable of standing the often hard operating conditions, and very service friendly. Switching valves are definitely much more robust than servo or proportional valves and cheaper. An important aspect is also standardization of components leading to a smaller range of product variants which is a major condition for low cost production; this is highly supported by switching control since impedance forming is done by other means but the valve's nominal flow rate or the spool position.

Energy saving is definitely an aspect of high relevance in future; firstly, to save fuel costs, but secondly, to enable higher actuation functionality under the given power limitations of the tractor's engine or the power transmissions. Currently, there are initiatives (for instance, [28]) to install high voltage power supply systems to overcome power limitations of mechanical and hydraulic transmissions between tractors and implements and to improve efficiency. This should be a strong motivation to think about new concepts for hydraulic drives for such machinery.
- **Tool machines:** Hydraulic servo drives have been a dominant technology in tool machines till the upcoming of modern speed variable electrical drives. Hydraulic drives have lost ground and are mainly limited to such drives where either very high forces or high compactness are required. There is a trend toward hybrid drives, combining speed variable electrical motors with a hydrostatic transmission (see, e.g., [29, 30]) for high load applications. The hydrostatic transmission provides force amplification but can also provide, for instance, gear shift, load holding, and fast emergency stop. In such symbiotic drives switching, if needed, fast switching, are basic operations. Particularly in the latter case, typical components and hydraulic processes of hydraulic switching control become relevant. In [31] a hydraulic micro positioning drive for tool machine applications is mentioned. Even though this particular case employs servo valve technology for control, switching control is an interesting alternative in terms of cost, compactness, and robustness. In particular compact actuators will gain more importance for increasing the functionality of tool machines under the condition of already very complex systems which leave little room for additional components. For the success of hydraulic actuation in this field new solutions for the complete hydraulic system must be found. The objectives are to get an overall compact and modular actuation system for functions with high forces, little room space, ultimate response, and high robustness. Hybrid combinations with electrical drives are also a direction of novel advantageous drive solutions which would benefit from advanced digital hydraulic components.

4 Conclusions

Hydraulic switching control is an alternative to existing analog control techniques with several advantages. In contrast to many other hydraulic innovations it requires a whole bunch of innovations for a successful realization: principles, components, and a new system design approach which considers the coupling between dynamical processes, hydraulic pulsation, mechanical oscillation acoustic noise and the design of the system. If a critical mass of such innovative elements exists and can be obtained from several vendors, a rush of digital hydraulic systems will occur. This and the energy saving options will enable new functionality for several machine systems at fairly low cost and with adequate performance. Also electro-hydraulic hybrid drives and actuators will benefit from advancements of hydraulic switching control, both on the components and on the system level.

Acknowledgement

This work was sponsored by the Austrian Center of Competence in Mechatronics (ACCM) which is a COMET K2 center and is funded by the Austrian Federal Government, the Federal State Upper Austria, and its Scientific Partners.

REFERENCES

- [1] F. H. Pollard, "Research Investigation of Hydraulic Pulsation Concepts". First Quarterly Progress Report (RAC-933-1), Republic Aviation Corporation, Farmingdal, L.I., N.Y., June 1963.
- [2] M. Linjama, "Digital Fluid Power – State of the Art." Proc. of the Twelfth Scandinavian International Conference on Fluid Power, Volume 2(4), SICFP'11, May 18-20, 2011, Tampere, Finland.
- [3] R. Scheidl, G. Hametner, "The role of resonance in elementary hydraulic switching control", Proc. Instn. Mech. Engrs. Vol. 217 Part I: J. Systems and Control Engineering, 2003, pp. 469-480.
- [4] A. Plöckinger, R. Scheidl, B. Winker, "Combined PWM- and Hysteresis Switching Control For A Digital Hydraulic Actuator", The Third Workshop on Digital Fluid Power, DFP'10, October 13-14, 2010, Tampere, Finland.
- [5] M. Huova, A. Plöckinger, "Improving resolution of digital hydraulic valve system by utilizing fast switching valves". The Third Workshop on Digital Fluid Power, DFP10, October, 2010, Tampere, Finland.
- [6] H. Gall and K. Senn, „Freilaufventile - Ansteuerungskonzept zur Energieeinsparung bei hydraulischen Linearantrieben“, Öhydraulik und Pneumatik, 38/1994, Nr. 1-2.
- [7] R. Scheidl, B. Manhartgruber, H. Kogler, B. Winkler, M. Mairhofer, "The Hydraulic Buck Converter - Concept and Experimental Results". Proc. 6th IFK, 6. International Fluid Power Conference, Dresden, 31.3.-2.4. 2008.
- [8] R. Scheidl, G. Riha, "Energy Efficient Switching Control by a Hydraulic 'Resonance-Converter'". In C.R. Burrows, K., A. Edge (Eds.): Proc. Workshop on Power Transmission and Motion Control (PTMC'99), Sept. 8-11, Bath, 1999, pp. 267-273.
- [9] R. Scheidl, D. Schindler, G. Riha, W. Leitner, "Basics for the Energy-Efficient Control of Hydraulic Drives by Switching Techniques". In J. Lückel (ed.): Proc. 3rd Conference on Mechatronics and Robotics, Oct. 4-6, Paderborn, Teubner, Stuttgart, 1995.
- [10] J. Dantlgraber. "Hydro-Transformer". European patent application (PCT) Intern. Publication No. WO 00/08339, 2000.
- [11] F. Wanga, L. Gua, Y. Chena, "A continuously variable hydraulic pressure converter based on high-speed on-off valves", Mechatronics, Vol. 21(8), 2011, pp. 1298–1308
- [12] D. M. Deffenbaugh et al., "Advanced Reciprocating Compression Technology". Final Report SwRI, Project No. 18.11052, DOE Award No. DE-FC26-04NT4226, U.S. Department of Energy, December 2005.
- [13] K. Murakami, T. Wakahara, I. Fukunaga, H. Sakai, "The Hydraulic Control System for a New Electronic 4WD System". JSAE Review, Volume 17, Number 4, October 1996 , pp. 447-447.
- [14] R. Brandstetter, „Untersuchung von Antriebskonzepten für die automatische Gießdickenverstellung bei Stranggießanlegen mit segmentierter Strangführung“, Master thesis, Johannes Kepler University Linz, June 1996.

- [15] "SMART Segment & DynaGap SoftReduction",
<http://www.industry.siemens.com/datapool/industry/industrysolutions/metals/simetal/en/SMART-Segment-Dyna-Gap-Soft-Reduction-en.pdf>
- [16] GRIP Engineering AG. Spray Bars for Steel Rolling Mills. Product brochure. 2006.
- [17] N. Chakraborti, B. Siva Kuamr, V. Satish Babu, S. Moitra, A. Mukhopadhyay, "Optimizing Surface Profiles during Hot Rolling: A Genetic Algorithms Based Multi-objective Optimization". Dagstuhl Seminar Proceedings 04461, Practical Approaches to Multi-Objective Optimization,
<http://drops.dagstuhl.de/opus/volltexte/2005/245>.
- [18] R. Scheidl, G. Hametner, "The role of resonance in elementary hydraulic switching control". Proc. Instn. Mech. Engrs. Vol. 217 Part I: J. Systems and Control Engineering, 2003, pp. 469-480.
- [19] M. Garstenauer, B. Manhartgruber, R. Scheidl, "Switching Type Control of Hydraulic Drives - A Promising Perspective for Advanced Actuation in Agricultural Machinery", New Fluid Power Applications and Components, Society of Automotive Engineers, Warrendale, pp. 37-47, 9-2000.
- [20] Schindler D., "Numerische und experimentelle Untersuchungen über pulsierende Strömungen in Rohren und Ventilen als Grundlage für die Entwicklung energieeffizienter Schalttechniken in der Ölhydraulik", PhD thesis, Johannes Kepler University Linz, 1995.
- [21] G. Riha, „Beiträge zur Entwicklung eines energiesparenden hydraulischen Schaltkonverters“, PhD thesis Johannes Kepler University Linz, 1998.
- [22] H. Kogler, "The Hydraulic Buck Converter - Conceptual Study and Experiments", PhD thesis, Johannes Kepler University Linz, 2012.
- [23] E. Guglielmino, C. Semini, H. Kogler, R. Scheidl, D.G. Caldwell, "Power Hydraulics - Switched Mode Control of Hydraulic Actuation", Proc. 2010 IEEE/RSJ International Conference on Intelligent Robots and Systems (IROS 2010), Oct. 18-22, 2010, Taipei, Taiwan.
- [24] H. Kogler, R. Scheidl, M. Ehrentraut, E. Guglielmino, C. Semini, D.G. Caldwell, "A Compact Hydraulic Switching Converter for Robotic Applications", Proc. Bath/ ASME Symposium on Fluid Power and Motion Control - FPMC2010,, Sept. 15-17 2010, Bath, UK, pp. 56-68.
- [25] E. Guglielmino, C. Semini, Y. Yang, D.G. Caldwell, R. Scheidl, H. Kogler, "Energy Efficient Fluid Power in Autonomous Legged Robots", Proc. 2009 ASME Dynamic Systems and Control Conference, Renaissance Hollywood Hotel, October 12-14, 2009, Hollywood, California.
- [26] H. Kogler, R. Scheidl, "The hydraulic buck converter exploiting the load capacitance". Proc. 8th International Fluid Power Conference (8. IFK), March 26 – 28, 2012, Dresden, Germany, Vol. 2(3), pp. 297 – 309.
- [27] B. Winkler, R. Scheidl, "Automatic Level Control in Agricultural Machinery". In Proceedings of the 2nd International FPNI PhD Symposium on Fluid Power, Modena, Italy, 2002.
- [28] M. Geißler, Th. Herlitzius, "Mobile Working Machine With An Electrical 4-Wheel Drive". Seminar MobilTron 2011 - Mannheim, September 28 – 29, 2011.
- [29] T. Neubert, „Drehzahlveränderbarer Verstellpumpenantrieb in Kunststoff – Spritzgießmaschinen“, Ölhydraulik und Pneumatik Nr.45, 10/2001.
- [30] P. Ladner, K. Ladner, R. Scheidl, H. Strasser, "Investigation of a closed electro-hydraulic hybrid drive". In Proceedings of the 11th Scandinavian International Conference on Fluid Power, SICFP'09, IJune 2-4, 2009, Linköping, Sweden.
- [31] B. Winkler, R. Haas, "A Hydraulic Micro-Positioning System for Industrial Mill Centers. Proceedings of 13th Mechatronics Forum International Conference", September 17-19, 2012, Linz, Austria, pp. 855 – 862.

MAINTENANCE OF FLUID POWER EQUIPMENTS

Dr. Eng. Corneliu CRISTESCU¹, Dr. Eng. Krzysztof KEDZIA²,

Dr. Eng. Catalin DUMITRESCU¹, Dr. Eng. Radu RADOI¹

¹ Hydraulics and Pneumatics Research Institute INOE 2000-IHP, Bucharest, ROMANIA,
cristescu.ihp@fluidas.ro

² Politechnika Wroclawska, Instytut Konstrukcji i Eksploatacji Maszyn, Wroclaw, POLAND,
krzysztof.kedzia@pwr.wroc.pl

Abstract: *The paper presents certain considerations regarding the activity of maintenance of the fluid power equipments and systems, including the equipment required for performing tests for checking and retesting the performance levels of the fluid power equipments, after they have been subjected to improvements or repairs.*

It is also presented a case study, where, after an important technical intervention at a hydrostatic pump, it was required to be performed tests on the stand, both for checking and attesting performances after repair and for its adjustment, followed by the presentation of the scientific results achieved.

Keywords: *maintenance, fluid power, hydraulic equipments, testing*

1. Introduction

It is well known that the use in optimum conditions of the fluid power equipments depends a lot on the right selection and adjustment of the hydraulic components, especially of the safety elements [1]. The maintenance activities play a significant role, together with a hydraulic fluid with a low content of impurities as well. The fluid filtering fineness used at a hydraulic installation it is essential and strictly determined by the filtering fineness, imposed by the hydraulic element requiring the lowest filtering class, for ex. 0-1-5 NAS Classes), [2]. At the running of the hydraulic equipment it is required to detect the flaws from their very initial stage, before causing malfunctions to the equipment, sometimes this meaning even during the maintenance, revision and repair operations.

The maintenance encloses operations of revision, inspection, supply, lubrication and periodical interventions, performed in order to prolong the lifespan of the hydraulic equipment. There are certain specific maintenance procedures, during the first period of work and also during the normal working period, which must be strictly applied.

The maintenance is a planned activity, which takes into account the operational mode of the equipment, the stress level and the environmental conditions. The maintenance operations include general works applied to all the hydraulic installations and, also, specific works, for the installation, in general, or different component of interest.

The volume and frequency of the maintenance works depend on the requirements regarding reliability, being determined by the degree of failure admitted for various utilizations.

Generally, in maintenance works, an important role is played by the checkup of the oil temperature and level of the contents of impurities, all these being performed with adequate apparatus. The overheating and high level of noise, generated by certain component parts, is obvious signs that it is necessary to make a revision or even some general repair.

The revision and repair activities sometimes lead to important interventions upon the hydraulic components, implying the replacement of certain parts or elements from the general structure, which can lead to a change in the working performance of these components.

The general objective of the revision and repair is to prevent malfunction and prolong the lifespan of the hydraulic equipment [3].

The maintenance of the hydraulic installations represent an assembly of activities which aim to maintain in good operational conditions the equipment by means of the following works: Planned repairs; Maintenance; Accidental repairs (not planned);

Monitoring the behaviour during use of the equipment. The supply with spare parts and materials required for repairs and maintenance; The elaboration of the technical documentation for repairs and maintenance; and The modernization of the equipment.

2. Troubleshooting and repairing of the hydraulic installations

2.1. The diagnostic of the flaws at hydraulic installations

The diagnosis of the flaws from a hydraulic installation is conditioned by the assimilation of the general knowledge regarding the hydraulic drives as well as of the knowledge in detail of the operational scheme of the faulty installation.

The diagnose starts from the effect found, generated by one or more factors. The diagnose process is a complex one, which takes into account associated effects and in correlation with the effect found, on the basis of some logical hypothesis, leads to the initial cause of the occurrence. When diagnosing flaws, must be updated the sources of noise and abnormal temperatures, cause, generally, the flaws occurring in the hydraulic installations are followed by these two phenomena. Hence the flaw is spotted, for determining its cause, can be performed measurements for noise, pressure and flows. For this, starting from the designing stage of the hydraulic installation, it is required to be provided special couplings for manometers and flow meters.

The flaw tracking is made by successive checkings of the hydraulic component parts analyzed. It is not possible to use an order of checking, applicable in all cases.

In the first stage, the checkups are made only by means of manometers which provide qualitative information regarding the found flaw. For obtaining quantitative information, it is necessary to perform flow measurements as well, requiring a more complex test and diagnose apparatus, developed by well known companies like PARKER [5] and HYDAC [6] etc., Fig.1 and Fig. 2.



Fig. 1 Testing and diagnostic
Sensocontrol from PARKER



Fig. 2 HMG 510 Portable Data
Recorder from HYDAC

The analysis of the flaws is alleviated, if the return lines to the tank and drainage are made of transparent plastic tubing. In this way, may be noticed the leaks and the fluid return, and it is possible to evaluate accurately the working correctness of the delivery elements and the losses by drainage. It is also useful to collect general information about the operational mode, maintenance volume, previous flaws and repairs.

2.2. The characteristic flaws of the hydraulic installations

Generally, at a hydraulic installation are distinguished two types of flaws:

- Flaws found at the periodical checkups and which at the moment when found, did not resulted to have been damaged any component;
- Flaws found as a result of the deterioration of a component system.

From the first category of flaws, characteristic to the hydraulic power installations, the most common are the following: Improper external seal; Overheating of the operational fluid or certain components; Abnormal noise appeared at a certain component or at the whole installation.

2.2.1 The improper external or internal seals

The faulty external seals on the pressure circuits are easy to be found, whenever noticing hydraulic fluid leaks. For example, the improper seal of the circuit of admission-aspiration of the pump, in the case of depressurization, cannot be found directly, but by its effects, the uneven mode of operation of the pump, pump s overheating, foaming hydraulic fluid and noise. This flaw is found by measuring the depression at the pump entry. Its decrease from the value set during the normal work, indicate the aspiration of fake air. Generally, the lack of a proper external and internal seal may come from flaws of the sealing systems of the hydraulic components and couplings from the installation.

2.2.2. The overheating of the hydraulic fluid

This flaw is detected by means of a thermometer placed usually on the oil reservoir, or by hand touch for temperatures up to 50⁰ C. When this value is exceeded it is signaled that something had happened in the proper operation and it is required an examination of the entire installation.

The excessive heating of the hydraulic fluid may be generated by the incorrect supply of the pump, by the pump s wear, the debiting for a long time through a drossel or stroke, a malfunction of the cooling installation

Another source of heating may be pump s wear. This can be caused by a normal wear phenomenon after a long time of work or it is caused by improper use of the pump with fluid contaminated with impurities, or in an inadequate mode of admission aspiration which produced the premature wear of the pump.

2.2.3. The increase of the noise level in the installation

Another frequently met flaw is the increase of noise over the admitted limit. The potential sources, generating over noise, in a hydraulic installation are: the incorrect supply of the pump, vibrations generated by the defected couplings of the bodies in motion, the noises produced by the pressure valves or vibrations of the pressure pipes which have no adequate fixation, in relation with wavelength of the system oscillations.

2.3. Troubleshooting

The correct diagnose of the flaws and causes as well as the good quality remediation, provide the proper work of the installation in the initial conditions of performance, preventing the reoccurrence of the same flaw or of a derived one and in the case of replacing an aggregate, it confers reliability equal with that of the replaced one.

As general rule regarding the interventions in the hydraulic installations, is that of following the requirements regarding the purity of the operational fluid. If the rules are not properly observed, this may very probably lead to the malfunction of the hydraulic installation.

After occurring a major flaw it is required the checkup of the content of impurities from the hydraulic fluid. If it is exceeded the admitted limit of impurities, the installation needs washing and cleaning thoroughly.

For determining the impurity class of the hydraulic fluid used at the hydraulic installations, prestigious firms developed the necessary apparatus, which can detect fast the content of impurities and to which class or category it belongs in an ISO or NAS class. For example, PARKER, [7], developed a system of monitoring and analyze of the impurities, LCM 20 Contamination Monitor, shown in Fig. 3 a and b, which can analyze separately a sample of fluid, or may be connected on line in derivation or directly in the hydraulic installation. At the end of the testing, this apparatus generates a document with the number of particles found for each category of sizes and to which class it belongs.



a) Front view



b) back view

Fig. 3 LCM 20 Contamination Monitor from PARKER

In the case of repairing some hydraulic pumps and motors, the repair is, generally, made by replacing the component parts and subassemblies with some original ones and more rarely by manufacturing and metallization and rectifications of the parts.

After repairing the hydraulic pumps and motors, these must be checked and tested on an adequate stand, on which to be possible to check their technical performances as well as the lack of the abnormal noise and overheating. The stand must also offer conditions for the adjustment of the control devices with which are these equipped (pressure, flow, power compensators etc.) for adjusting them in accordance with the needs.

3. The repairing and testing of a pump with axial pistons

Within a complex technological installation, the drive of some mechanical systems is made by means of a hydraulic drive installation, where the main source of fluid under pressure is supplied by pumps with axial pistons, provided with pressure compensator.

The technological complex is older, but lately it has been modernized, the main components replaced, the old hydrostatic pumps with the new pumps with axial pistons PV 092 produced by PARKER

During the actual stage of revision, for shortening its time, a pump with axial pistons has been replaced with a new one, identical with the former, the old pump being subsequently repaired. After about a month of work the new pump started to produce overheat and the noise during work became abnormal, fact which determined the responsible factors to disassemble it from the installation and replace the new pump with the old one which works acceptably. The client complained about the impossibility of adjusting the pressure level of the regulator-compensator and the displacement geometrical volume of the pump.

The new pump was brought at INOE 2000-IHP, which undertook the action of diagnose, troubleshooting and testing. Because at the date when the pump was disassembled, the color of the fluid from the tank of the installation was dark, were taken samples of hydraulic oil and made tests for finding the impurities contained in the fluid, by means of a PARKER apparatus. The result was surprising, cause the quantity and size of the impurities was from class 12 NAS 1638, equivalent with 22/21/18 to ISO 4406, which was far over the accepted limit of about 7 NAS Class. The oil it, also, contained water. According to the producer's catalogue PARKER, the filtering requirements for the hydraulic oil is in general of class 19/13 to ISO 4406, equivalent with class 8 NAS 1368 and for component parts with higher lifespan it is of 16/13 to ISO 4046, equivalent with class 5 NAS 1638. Taking into account these facts, it was very obvious that the conditions of work of the new pump were not appropriate, were even dangerous for a new pump with minimum adjustments and little use. Therefore, was recommended, to the beneficiary company, to replace completely the hydraulic oil from tank.

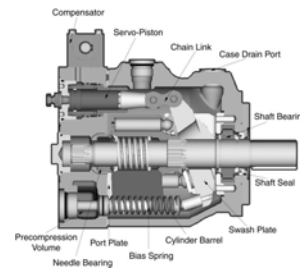
3.1. The diagnose of the hydrostatic pump

The hydrostatic pump with axial pistons, which was investigated, is a pump with pressure compensators type PV 092, Fig. 4, manufactured by PARKER [6]. The main technical data of the

pump are as follows: Pump code PV 092; Pump type with axial pistons; Displacement 92 cm³/rot; Max pressure 350 bar; Nominal pressure 280 bar; Max rev. 3000 rot min.



a) Pump view



b) pump inside body

Fig. 4 The hydrostatic pump with axial pistons

After disassembling and examining the pump, were found the following: the component parts are not much damaged; the port plate is in a good condition; the pressure plate presents scratches of 5-10 μm , insignificant for work; the Assembly pistons plate with bronze coating is good, but the crimping of a piston is deteriorated, cause a semicircular piece broke.

Very probably the break produced cause of a material flaw (blows, inclusions) or the existence of certain internal tensions.

From the way, it looks the break occurred during disassembly cause neither the detached parts nor the adjacent parts have scratches or traces

The lost motion from the crimping of the pistons are a bit bigger than normal being possible to produce in certain conditions some noise even after a longer operation. On the pump casing were noticed rust stains, probably cause there is water in the oil, but the consequences were not very serious. At a careful examination, on the shaft cannot be seen any blue areas which to put into evidence the occurrence of a high temperature and an overheating of the pump. The bearing with cylindrical balls type NU NJ 2209 E YVL ($d_i = 45 \text{ mm}$; $D_e = 85 \text{ mm}$; $l = 23 \text{ mm}$) has an axial loose of 0.8 mm quasi-normal which could generate some beats if the pump s coupling cannot provide the coaxial connection between motor and pump. The interior ring of the bearing has an axial loose between it and the shut safety ring *Seeger of 0.3 mm, which can generate some sort of banging during work. The pressure compensator was completely dismantled but was not found any deterioration of parts or spring breaks etc. It was found that it was attempted to regulate pressure at a different level, but the method for performing that action was not properly known by the operator thus being unable to perform it.

3.2. The repair of the detected flaws

After diagnosing the pump, for repairing the flaws, were proposed and performed the following operations for improving the pump condition

1. Purchase a complete kit of axial pistons from the manufacturing company and assemble it in the pump body;
2. Adjust decrease the axial loose of the interior ring of the bearing with balls by inserting a flat ring which ensures a second support for the interior ring thicker with 0,2 0,3 mm;
3. If it is necessary the bearing with balls will be replaced too, with another with a lower loose between the rings;
4. The testing of the pump on the stand, watching carefully the eventual occurrence of over noise and overheating during work as well as the possibilities of adjustment of the pressure compensator depending on the desired pressure value and the possibility of performing an adjustment variation of the pump's displacement, depending on the pre-set flow.

After drawing the conclusions at testing, it is decided if the pump **may be or not** recommended to be assembled in the hydraulic installation.

After repairing it, the pump with axial pistons and pressure compensator was mounted on the stand for testing the pumps with variable flow, stand from the Lab for testing hydraulic apparatus for high pressure from IHP.

The testing of the pump had focused on the following objectives:

- For testing the workability and adjustability, the pump was mounted on a stand, according to the scheme of testing, Fig. 5.



The testing of the pump consisted in performing different flow, adjustments by means of the special device provided for modifying the pump's displacement RC, as well as other various pressure adjustments at the pressure compensator PC. Were tested the adjustment of the revolution by adjusting the electric motor's supply frequency.

The stand for testing the pumps with variable displacement, from INOE 2000 IHP, shown in Fig. 6, materializes the testing scheme from Fig. 5.



a) overall view of the stand



b) pump on the stand



c) Flow transducer, manometer, throttle and pressure limiter



d) data acquisition system for the fluid flow

Fig. 6. Stand views

3.3.3 The operation mode for testing the pump

The operation performed on the testing stand consisted in the following:

After starting the pump's motor, Fig. 6b, with the throttle DR completely open for each max. pressure value set adjusted at the compensator PC, the throttle was gradually close, until the compensator passed the pump on null, flow = 0. For each pressure value desired and read on the manometer M, Fig. 6c, included in the range of pressure values, from 0 to the max set value, was noted the corresponding flow value, detected by the flow transducer TD and indicated by the electronic measurement system from Fig.6 d. The results were listed in the tables 2, from below.

3.3.4 The adjustment of the pump flow

The adjustment of the pump flow was made by readjusting the displacement of the pump, from the screw, especially provided, and by modifying the frequency of the electric current supply of the motor.

The flow variation by turning on the screw of the displacement RC:

The flow variation was made at a revolution of 1000 rot/min, corresponding to a frequency read on the electric panel of 33,333 Hz, by turning on the screw adjusting displacement, this being placed on the pump body for changing the angle of inclination of the pump disk. This allowed obtaining a max flow of about 92 l/min, of some intermediary flow values and of a very low flow close to 0.

The flow variation by means of varying the supply frequency:

In addition to the initial requirements, during testing the pump, was aimed to reach a variation of the pump flow at min pressure, close to 0, for a revolution of 1000 rot per min corresponding to a frequency of 33,333 Hz, when the flow value was of about 90 92 l/min, as well as for a revolution of about 1500 rot/min corresponding to a frequency of 49.86 Hz, when the flow value was of 134-136 l/min.

3.3.5 The adjustment of pressure at the pressure compensator

The pump which was tested, equipped with a pressure compensator/ regulator, was subjected to special tests for proving the possibility of adjusting the pressure compensator, observing by means of different adjustments its modality of response namely the flow variation at the pressure increase. In this respect were performed the following tests:

The adjustment of the max operational pressure at the compensator.

For this, was taken into account the real constructive solution which allows a number of rotations at the adjustment screw, about 9,5, for covering the entire adjustment range. After 2.3 shifts, starts the adjustment of the max. desired pressure, at which the pressure compensator tips and determines the pump to decrease the flow to almost a null one. The tipping pressure increases, when the number of shifts increased at the adjustment screw, according to the table 1, from below:

Table 1

Nr. of shifts at the adjustment screw	2,75	3,25	3,5	4,0
The tipping pressure PC bar]	20	75	100	150

Variation of the flow and pressure on pump static characteristic

In table 2, from down, are shown the flow and pressure variations for different set values at the pressure compensator CP, till the tipping of the pump and making it have null flow.

Table 2

ADJUSTMENT OF THE PRESSURE COMPENSATOR (PC)									
ADJUSTMENT PC at 15 – 16 bar									
Pressure[bar]	5	10	12	15	16	-	-	-	-
Flow [l/min]	52,5	52	51	46,3	0	-	-	-	-
Adjustment PC at 65 – 70 bar									
Pressure[bar]	-	10	20	30	40	50	60	65	70
Flow [l/min]	-	52	49,7	49	48,4	47,5	47	45	0
Adjustment PC at 140 – 145 bar									
Pressure bar]	-	10	20	50	80	100	120	14	145
Flow [min]	-	52	51	49,9	48,4	47,2	46	43	0

3.3.6 Watch noise and temperature values during operation

The testing on the stand of the pump, took place during summer at the following temperatures: the environmental temperature 33 – 38.0 °C; the oil temperature 54.5 -57.5 °C and pump temperatures 33-6.5 °C.

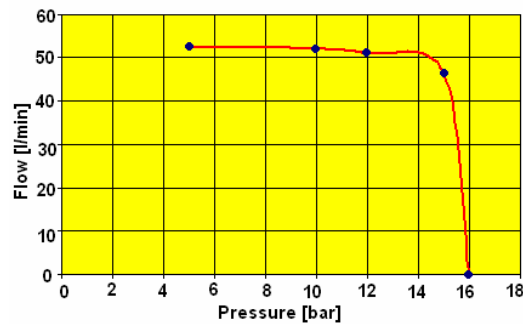
Noise and temperature during operation

During the tests, was carefully followed the noise and found that was in normal limits.

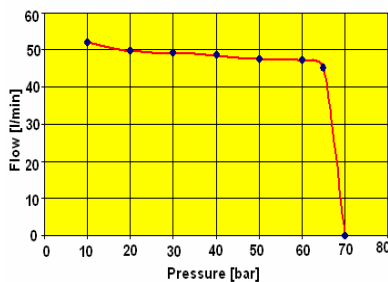
The temperature measured on the pump body, increased during experimentation, but not so much, this being a result of the high temp. from the laboratory and of the oil, this getting higher cause of the small amount existent in the tank, the oil being recalculated more often.

3.3.7 Finding the static characteristics of the pump with pressure compensator

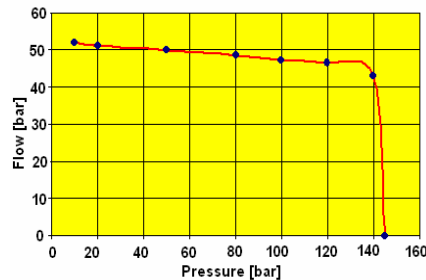
As a result of the experimental measurements, performed for the 3 levels set at the pressure compensator, were detected the static characteristics of the pump with axial pistons, equipped with pressure compensator, these static characteristics are represented in Fig.7 a, b, c.



a) adjusting at 15-16 bar



b) adjusting at 65-70 bar



c) adjusting at 140-145 bar

Fig.7. The static characteristics of the pump with pressure compensator

4. Conclusions and remarks

From the information presented above, it may be noticed the significant role of an adequate maintenance of the hydraulic installations, for ensuring a long lifespan. This comes out from the theoretical approach from the beginning and from the real case studied in the second part. It was concluded that the tested pump has a normal behavior, having the possibility of adjusting the displacement and the pressure compensator as well, these being proven by means of the performed tests. The pump was found adequate for being assembled at the hydraulic installation with the condition of a careful assemblage and of a proper maintenance, being recommended to use good quality hydraulic oil, with the required characteristics, according to the manufacturer's recommendations.

REFERENCES

- [1] N. Vasiliu, D. Vasiliu, "Fluid Power Systems", Vol.I. Technical Publishing House, Bucharest, 2005
- [2]. *** PARKER: Catalogue Industrial Hydraulics HZ11-2500/UK, March 2002
- [3]. Marin V., Moscovici, Rd., Teneslav, D. "Hydraulic drive systems with automatic adjustment. Practical problems, design, execution, exploitation". Technical Publishing, Bucharest, 1981.
- [4]. Drumea, P., Cristescu, C., "Tribology researches on increasing the lifetime of hydraulic components and systems". In: PROCEEDINGS of the International Scientific-Technical Conference **HYDRAULICS AND PNEUMATICS**-2012, 16-18th of May 2012, **Wroclaw**, Poland.
- [5] ***PARKER, Senso-Control, <http://www.rotec.net/pdf/senso%20control.pdf>
- [6] ***HYDAC, HMG 500: <http://www.hydac.com/de-en/products/measurement-display-and-analysis-tools/measuring-instruments/handheld-measuring-instruments/hmg-500.html>
- [7] *** PARKER, LCM20, <http://www.ezihose.com/pdfs/catalogues/LaserCM.pdf>

SOME ASPECTS OF THE NEW MODEL OF ROBOT ACTUATION

MERO

Ion ION¹, Alexandru MARIN², Aurelian VASILE¹, Laura-Florentina BOANȚĂ², Cristian SIMION¹,
Cornel DINU³

¹ Manufacturing of Machine Technology Department, e-mail: ioni51@yahoo.com, vasile_aurelian@yahoo.com

² Hydraulics, Hydraulic Machines and Environmental Engineering Department, e-mail: alexandru.marin@upb.ro, ³ Aeronautic Systems Engineering Department, e-mail: cornel_dinu@yahoo.com
University POLITEHNICA of Bucharest, ROMANIA

Abstract: *In the recent years, walking vehicles have been studied because the industrial plants, the mechanized agriculture and other fields increasingly require that the robots possessed a walking mechanism to replace the humans. The modular walking robots are used to unconventional displacement of the technological loads over the unarranged terrains. The walking robots moving on a terrain, strewn with many obstacles, which can be convex or concave, there is a danger that the position of these robots are not stable. At the Polytechnic University of Bucharest has been developed a walking modular robot to handle farming tools. This paper describes such a walking modular robot. The mechanical structure of the walking robot can be represented as a complex system of bodies assembled by kinematic pairs.*

*Using hydraulic actuators can generally drive systems of this size and weight more efficiently. This walking robot has three two-legged modules. Every leg has three freedom degrees and a tactile sensor to measure the contact, which consists of lower and upper levels. The body of the **MERO** (**ME**chanism **RO**bot) walking robot carries a gyroscopic bearing sensor to measure the pitch and roll angles of the platform.*

The legs are powered by hydraulic drives and are equipped with positions sensors. They are to control a walking robot in the adaptability to a natural ground.

This paper describes such a walking modular robot. The mechanical structure of the walking robot can be represented as a complex system of bodies assembled by kinematic pairs.

Keywords: *robot, walking robot, robot control, shift mechanism.*

1. Introduction

In agriculture and forestry, due to the specific characteristic conditions created by vegetation and state of the ground, as well as in order to protect the environment, caterpillar or wheeled machines used nowadays for performing the activities in these domains have a limited mobility and usually destroy and/or damage the environment, vegetation and young trees in their movements from one place to another. The artificial compaction is the consequence of an exaggerated, unreasonable traffic in the field for farming, transport, hydrological and other similar activities. The negative effects of the compaction, irrespective of its nature and causes, are multiple. Thus, the water retention capacity and especially permeability are decreased, worsening the ground water state and, generally, the soil humidity. Aeration is reduced and at the same time, it often increases considerably the resistance to penetration of the tools used for tilling, digging, excavating etc. Concerning the ground compaction, two main problems are posed. On the soils that are not compacted but where specific equipments will be used for various processing works, special measures are required with a view to prevent their compaction. In this respect, bearing in mind the nowadays mechanization conditions, the needed measures should be taken to avoid the aforesaid. Walking robots better protect the environment, as their contact to the ground is discrete, which considerably diminishes the area underwent to crushing; the robot's weight can be optimally distributed all over the leaning surface, by controlling the forces. Altering the distance to the ground, the robot can pass over young trees or other vegetation, growing in the passage area.

Avoiding hurdles such as logs or tree trunks is a considerable advantage. Likewise, the movement on an unarranged terrain, represents another advantage of the walking robot, as against the other types of vehicles.

Compared to the wheeled or caterpillar robot, the walking robot is a mechatronic system, its practical use requiring both the computer-assisted surveillance and the thorough checking by the movement systems. During this century, the locomotion using feet as a movement system, was reckoned an inefficient movement means. Nevertheless, if we take into account the infrastructure's costs to artificially create the roads for wheeled robot or own roads for the caterpillar robot, arguments for these two robot types, diminish, in some of the cases.

Walking's main feature is the very fact that the movement is not affected by the ground's configuration. More and more applications requiring movement on a natural, unarranged terrain, made the feet-movement solution become more and more attractive.

Here they are, the main features justifying the superiority of the walking robot as compared to the wheeled or caterpillared ones:

- capability to move on unarranged grounds;
- by changing its height (ground clearance) the walking robot can step over certain hurdles;
- the possibility to change the configuration of the walking robot's shift system;
- feet's contact to the ground is discontinuous (it is accomplished only in the leaning phase), when a foot has the opportunity to select the contact point, while descending on the ground, contingent of the latter's surface;
- the possibility to move on a soft ground, which is sometimes more difficult for the wheeled or the caterpillar robot;
- the walking robot's active suspension, accomplished by setting proximity and force sensors in the outermost part of feets, enables the movement on uneven ground, under stable circumstances;
- the specific energy consumption is smaller with the movement on natural unarranged grounds as against other types of mobile robots;
- better preservation of the ground, that the robot moves on, especially in case it is made use of in specific farming or forestry activities;

2. Building of experimental MERO modular walking robot

The new modular walking robot MERO [4],[3]. design by the authors, is a multi-functional mechatronic system designed to carry out planned movements aimed at accomplishing several scheduled target.

The walking robot operates and completes tasks by permanently inter-acting with the environment where there are known or unknown physical objects and obstacles. Its environmental interactions may be technological (by mechanical effort or contact) or contextual ones (route identification, obstacle avoidance, etc).

The New Modular Mobil Walking Robot MERO represents a special category of robots, characterized by having the power source embarked on the platform. This weight of this source is an important part of the total charge that the walking machine can be transported. That is the reason why the walking system must be designed so that the mechanical work necessary for displacement, or the highest power necessary for act it, should be minimal.

The major power consumption of a walking machine is divided into three different categories:

- the energy consumed for generating forces required to sustained the body in gravitational field; in other word, this is the energy consumed to compensate the potential energy variation;
- the energy consumed by leg mechanism actuators, for the walking robot displacement in acceleration and deceleration phases;
- the energy lost by friction forces and moments in kinematic pairs.

The modular walking robot weight can be distributed optimally on the support areas by controlling the forces and the variation of the distance from the soil level, allowing robots to walk over young trees or other plants growing along the passage area [4],[3]. The easiness in obstacle avoidance - tree stumps, logs, felled trees is another advantage of walking robot use.

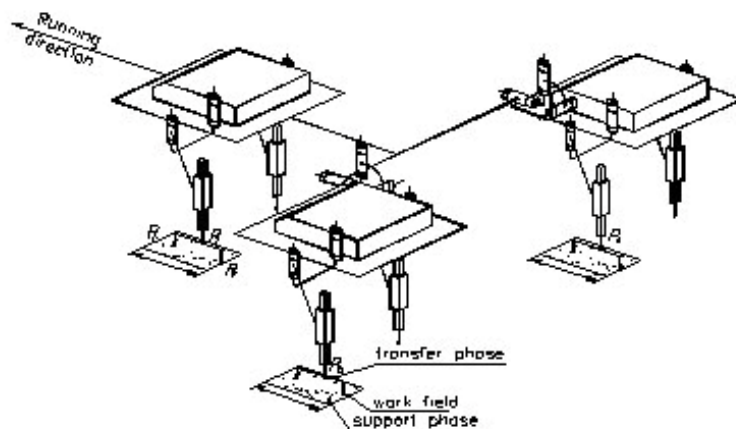


Fig.1 The structure of the leg – RRP

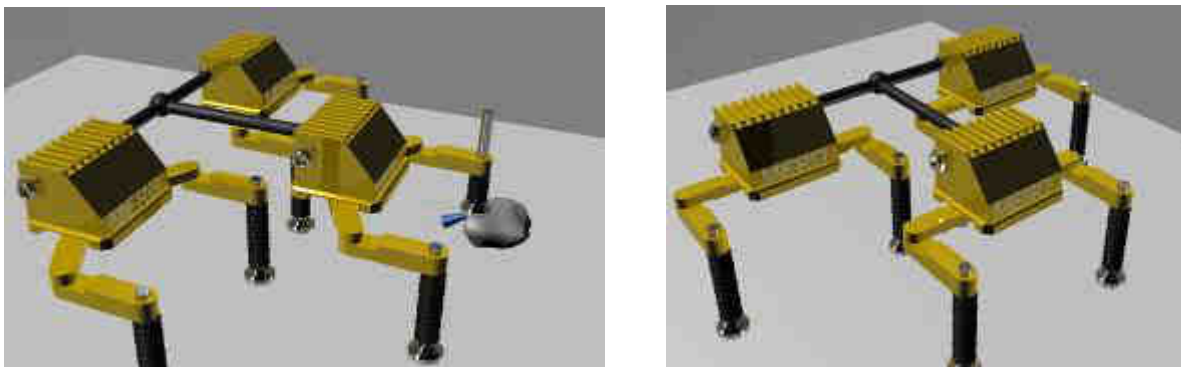


Fig.2 The new modular walking robot MERO-computer graphics model (under construction)

The new modular walking robot MERO will have up of the following parts:

- a) the mechanical system made up of one, two or three modules articulated and shaped according to the requirements of the movement on an uneven ground, the robot's shift system is thus built that it may accomplish many toes' trajectories, which can alter by each step.
- b) the actuating system of feet have a hydraulic or electric drive;
- c) the distribution system is controlled by 18 servo-valves or servo-motors, according to the robot's configuration;
- d) the energy feeding system;
- e) the system of data acquiring on the shift the system's configuration and the environment;
- f). the control panel processing signals received from the driving and the acquiring systems.

2.1 The hydraulic powered system of the MERO modular walking robot

During its brief evolution over the past three decades, the robotics has provided but very few new remarkable solutions to the building of the hydraulic, electric or pneumatic systems for activating mechanism operating. To control the movement of the oscillatory linear and rotary engines, the robotics took over and implemented the latest novelties in the above said field. The performances by the activation systems, condition the acceptance of a basic kinematic structure for the walking robot's movement as for the leading control algorithms. The invention of the walking robots and their capability to move on irregular terrain and their kinematic and dynamic performances, and last but not least, that meet autonomy requirements, imposed new standards as regards size, weight, performance, accuracy and quality for all the mechanical, hydraulic and electronic equipment. Making a minute analysis of the operational capabilities related to the available power sources that can be set in on the walking robots platforms with all the advantages and disadvantages one knows or admits and by taking into account the fact that the modular walking robot, the authors has

developed, is by far more than an experiment, we opted for hydraulic system. The hydraulic powered system distinguishes it self by robustness, a small ration between the weight of its compounds and its nominal power and it

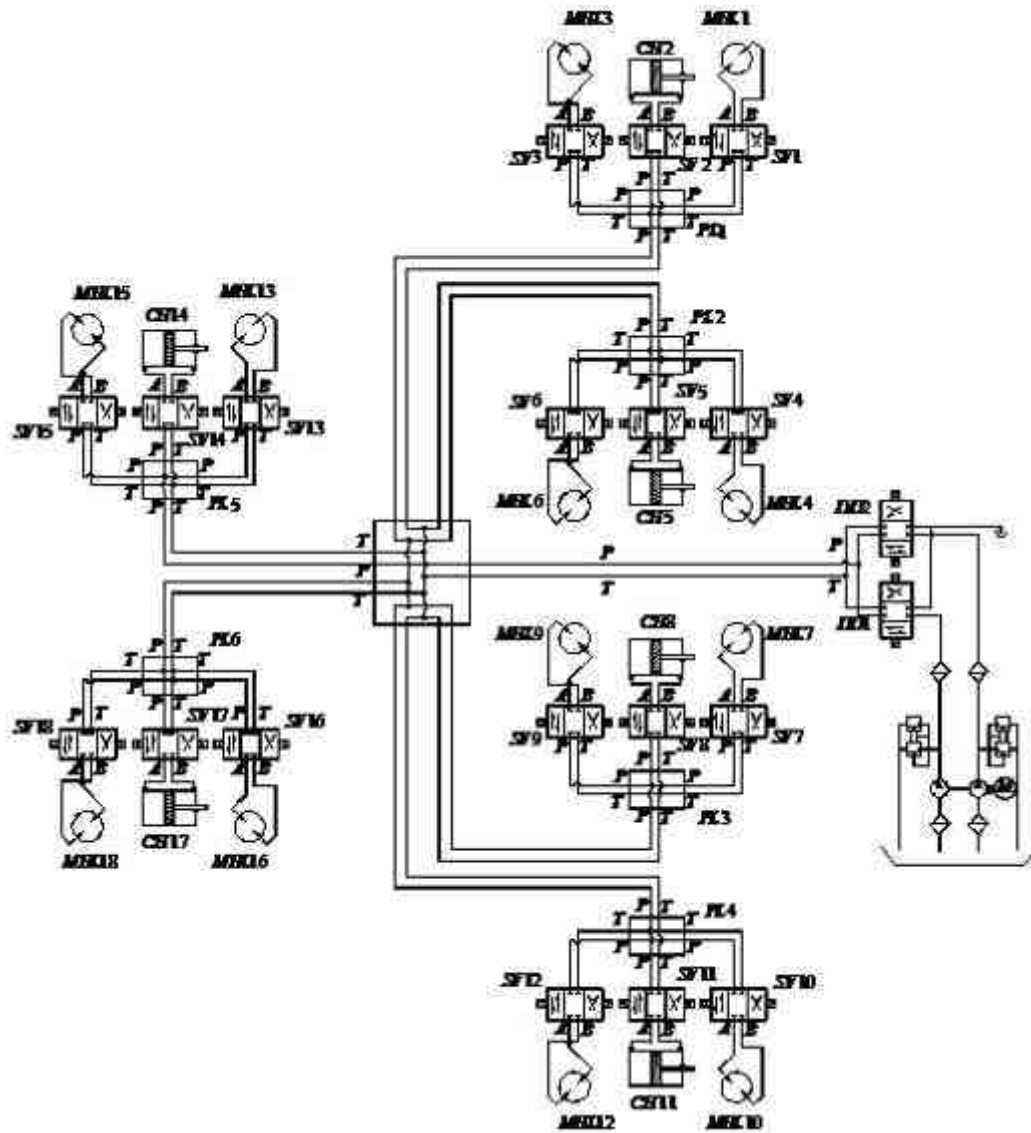


Fig.3 Model of the conventional hydraulic powered system

offers exquisite adjustment capabilities provided that it occurs high regime pressures. The fluid in the R_z tank is absorbed by the $PDC1$ and $PDC2$ pumps and it is sent through the $F1$ and $F2$ filters, to the $DD1$ and $DD2$ respectively discrete distributors which according to the cyclograms, send it to the $SV1, \dots, SV18$ (12) servo-valves. Depending on the signal applied to the servo-valves (Δ_i), in accordance with the walking program, they distribute to the hydraulic motors CH_i, MH_j ($i=3, j=6$) the fluid having a $Q = f(\Delta_i)$ flow capacity. (fig.3)

Contingent on the shifts by the piston rods of the hydraulic motor, imposed by the kinematic parameters of the leading scoops of the leg, according to the simultaneous or successive walking program, the flow capacity required by activating is carried out by the two $PDC1$ and $PDC2$ pumps, as shown in the cyclograms.

The structural complexity of the hydraulic circuits, the intimate knowledge of the phenomena, which change during the time and of their mechanism, claims a mathematical pattern to present as clearly and truthfully as possible - the conduct by the driving system of the modular walking robot.

2.2 Stability of walking robot's movement

Part of the characteristic parameters of the walking robot may change widely enough when using it as transportation means. For instance, an additional load on board, changes the barycenter's position and the inertia moments of the module's platform. Environmental factors such as the wind or other elements may bias the robot, and their influence is barely predictable. Such disturbances may cause considerable deviations in the robot's real movement, than expected. Drawing up and using efficient methods of finding out the causes of such deviations, as well as of avoiding such causes, represent an appropriate way of enhancing the walking robot's proficiency, and this at lower power costs.

Working out and complete enough mathematical pattern for studying the movement of a walking robot, is interesting, both as regards the structure of its control system and verifying the simplifying principles and hypotheses, that the control program's algorithms rely on.. The static stability issue is solved by calculating the positions of each foot against the axes system, jointed to the platform, and whose origin is in the latter's barycenter.

The above depicted walking robot encompasses the following devices:

- 1) the calculating system, sending signals to the drive's control of the driving pairs in the leg mechanisms;
- 2) the block acquiring data on the movement system's configuration and the environment;
- 3) leg operation system;
- 4) power supply block.

The calculating system's comand device, carries out the following operations:

- it shapes the walking's stereotypes, and the required corrections, in accordance with the configuration of the ground, that the robot is moving on;
- it sets up walking's static stability limits and ensures the robot's stability conditions, by appropriately placing the support points, as against the platform;
- it stabilizes the platform's horizontal position contingent of the ground's configuration (provided no further requirements are made);
- it keeps the platform's given height, above the ground's level (unless other requirements exist);
- it interprets the operator's orders.

The data acquiring system is made up of the following parts:

- the position sensor measuring the pair's variables, namely the relative positions of the kinematic elements adjacent to the driving pairs;
- the feet's tactile transducers signaling the feet's contact with the support area;
- the force cell measuring the reaction forces between ground and feet;
- the verticality sensors measuring the platform's deviations from the horizontal positioning unless any further conditions;
- the measuring systems of the platform's height as compared to the ground's surface;
- the measuring devices in the transfer phase of the feet's height as against the ground's level.

The walking robot has a 3-leveled control system. The first level plays the part of a control signal broadcaster to the drive motors set up in the legs' joints, and ensures the robot's movement to a prescribed direction and at a given speed. Language of this level is that of the differential equations.

The second level controls the walking, namely it tunes the legs' movements and provides the required data to achieve the walking. The algorithms of the walking types describe activity at this level.

The third control level defines the walking type, speed and it orientation. An operator, at this level can also ensure control. He can use the control panel to achieve the connection to the robot in order to define the walking type and to send special orders, defining the movement speed vector.

2.3 Distribution of forces in the mechanisms of the robot walking displacement

The walking robots moving on a terrain, strewn with many obstacles, which can be convex or concave, there is a danger that the position of these robots are not stable.

One of conditions imposed on the motion of walking machines is the stability. The movement of the legged robots can be divided in two modes:

- under condition of the static stability;
- under condition of the dynamical stability.

The main difference between robots which walked under the static stability and under the dynamical stability conditions originates from the fact that during statically walking, the vertical projection of the gravity center of the robot must lies into the supporting polygon, where as during the dynamical walking, this condition can be not satisfied.

The problem of quasi-statical stability analysis in condition of arbitrary step when the accelerations of points of component elements are much smaller than gravity acceleration is identical with the problem of stability analysis when the robot does not walk. The inertial forces are neglected and the walking can be controlled in a kinematics way.

For the new version MERO modular walking robot consists of three modules below shows the procedure for determining the reaction forces. (Fig.4)

Feet are modeled by points in the centers of gravity of their surfaces. The land is shaped by moving robot plane passing through the supports.

Stability modular walking robots, bipedal three modules, is discussed during the journey, when it focuses only on three legs.

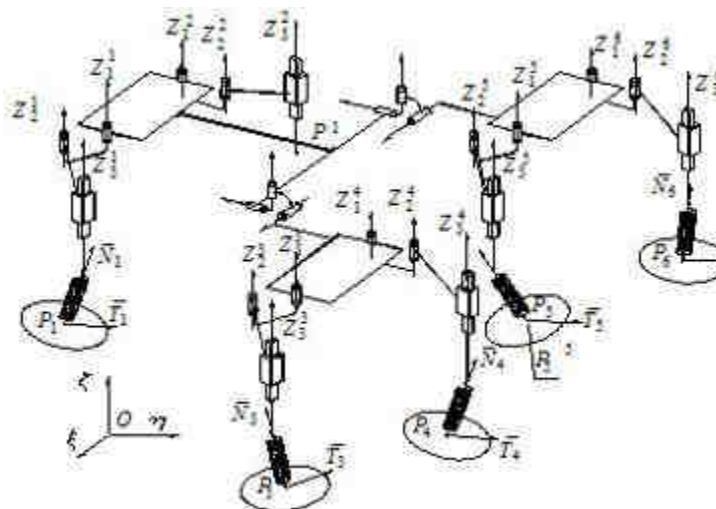
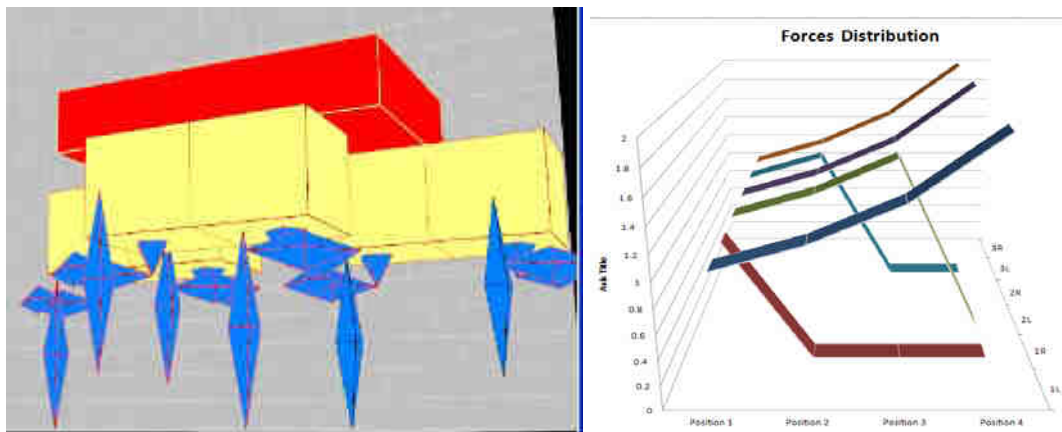


Fig. 4 The reaction forces at points of contact leg with the ground



Equations which is defined planes land, and passing through points P1, P4 and P6 (Fig. 1) are:

$$l_1(x - x_{P1}) + m_1(y - y_{P1}) + n_1(z - z_{P1}) = 0;$$

$$l_4(x - x_{P4}) + m_4(y - y_{P4}) + n_4(z - z_{P4}) = 0;$$

$$l_6(x - x_{P6}) + m_6(y - y_{P6}) + n_6(z - z_{P6}) = 0, \quad (1)$$

where: l_i , m_i și n_i , $i = 1, 4, 6$, are coefficients of the normals to planes executives support. On the structure of the robot act reinforced a system of forces, ie forces and weight of the load components. Torsorul this system is the point of reduction A of components

$$\vec{F} = F_x \vec{i} + F_y \vec{j} + F_z \vec{k} \text{ și } \vec{M} = M_x \vec{i} + M_y \vec{j} + M_z \vec{k}, \text{ where: } F_x, F_y, F_z, M_x, M_y, M_z$$

projections on the axes are fixed system components (the resulting net force and moment)

The reaction forces of the supports P^1 , P^4 și P^6 are: $\vec{R}_i = \vec{N}_i + \vec{T}_i$, $i = 1, 4, 6$,

Where, the normal components \vec{N}_i of support planes are perpendicular and tangential components (frictional forces) \vec{T}_i are contained in planes of support

The equations of equilibrium of forces and moments are:

$$\begin{aligned} F_x + N_1 l_1 + T_1 u_1 + N_4 l_4 + T_4 u_4 + N_6 l_6 + T_6 u_6 &= 0; \\ F_y + N_1 m_1 + T_1 v_1 + N_4 m_4 + T_4 v_4 + N_6 m_6 + T_6 v_6 &= 0; \\ F_z + N_1 n_1 + T_1 w_1 + N_4 n_4 + T_4 w_4 + N_6 n_6 + T_6 w_6 &= 0; \end{aligned} \quad (2)$$

$$\begin{bmatrix} 0 & -z_A & y_A \\ z_A & 0 & -x_A \\ -y_A & x_A & 0 \end{bmatrix} \begin{bmatrix} F_{1x} \\ F_{1y} \\ F_{1z} \end{bmatrix} + \begin{bmatrix} M_{1x} \\ M_{1y} \\ M_{1z} \end{bmatrix} + \mathbf{M}_1 \mathbf{R}_1 + \mathbf{M}_4 \mathbf{R}_4 + \mathbf{M}_6 \mathbf{R}_6 = 0, \quad (3)$$

where: u_i , v_i , w_i directors of the straight lines are the coefficients of the support components of the tangential reaction forces of the supports,

$$\mathbf{M}_i = \begin{bmatrix} 0 & -z_{Pi} & y_{Pi} \\ z_{Pi} & 0 & -x_{Pi} \\ -y_{Pi} & x_{Pi} & 0 \end{bmatrix} \quad \mathbf{R}_i = \begin{bmatrix} N_{ix} + T_{ix} \\ N_{iy} + T_{iy} \\ N_{iz} + T_{iz} \end{bmatrix}, \quad i = 1, 4, 6.$$

These lines are contained in the underlying support planes, so

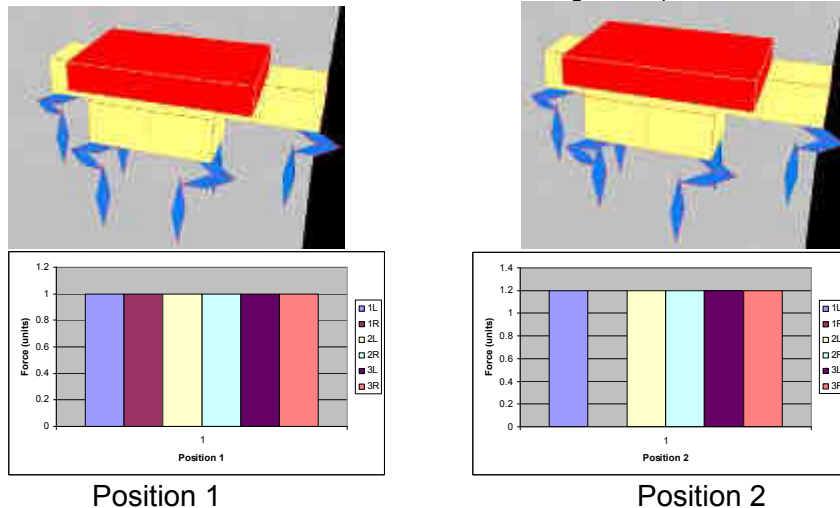
$$l_i u_i + m_i v_i + n_i w_i = 0, \quad (4)$$

$$u_i^2 + v_i^2 + w_i^2 = 1, \quad i = 1, 4, 6. \quad (5)$$

System of equations (1), (2), (3) și (4) resolve uncertainties in relation to N_1 , N_4 , N_6 , T_{1x} , T_{1y} , T_{4z} , T_{4x} , T_{4y} , T_{4z} , T_{6x} , T_{6y} , T_{6z} .

If one or more of the conditions $\sqrt{T_{ix}^2 + T_{iy}^2 + T_{iz}^2} < \mu N_i$, $i = 1, 4, 6$,

is not satisfied at some point, the robot moves by sliding to a position where all inequalities above are verified (μ is the coefficient of friction between feet and ground).



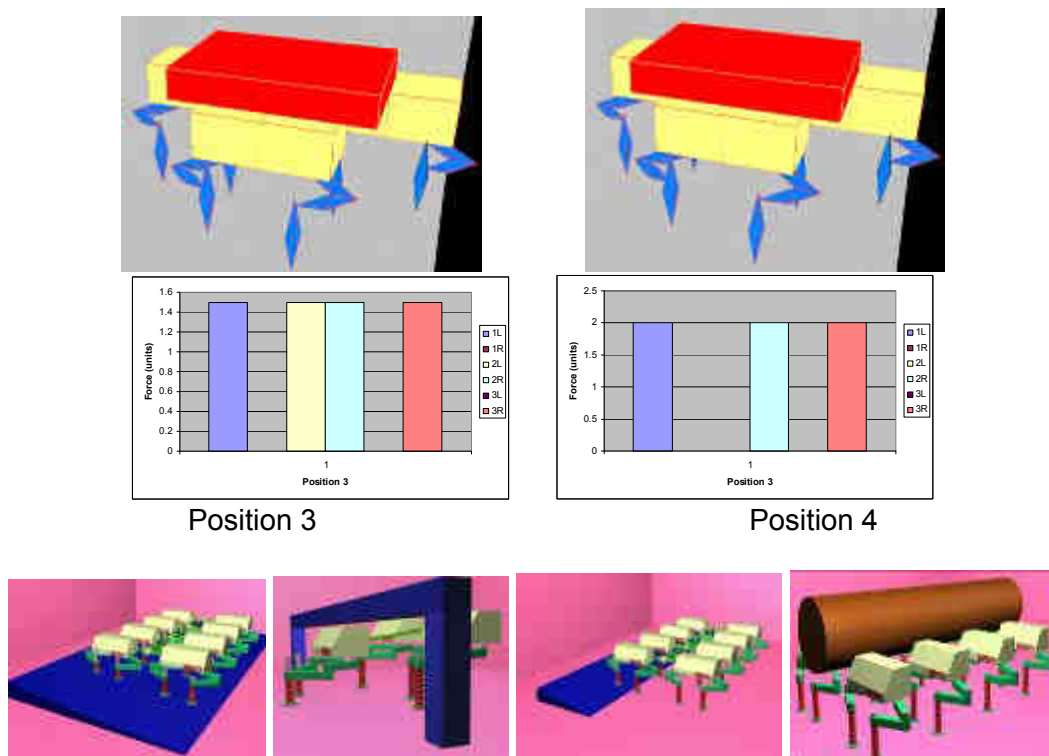


Fig.. 5 Computer graphics simulation the types gaits of the new modular walking robots MERO

2.4 Results and conclusion

The application described here was developed with the purpose of easing the simulation and providing a better understanding of different walk strategies of the new MERO modular robots (crab-like leg RRP) in different configurations. Two main configurations were taken into consideration: RRP - 3 module assembly, one module in the front and two modules in the back, in a triangle shape.

There are two distinct windows that start when the application is launched: The control window (Fig.6) and the visual window (Fig. 7).

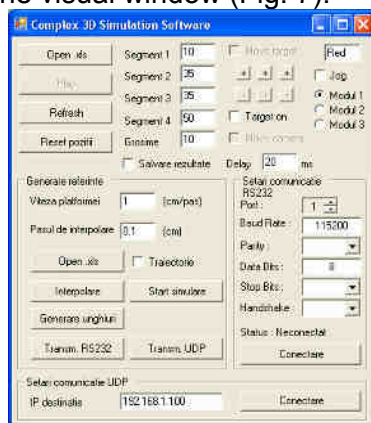


Fig.. 6 Control Window

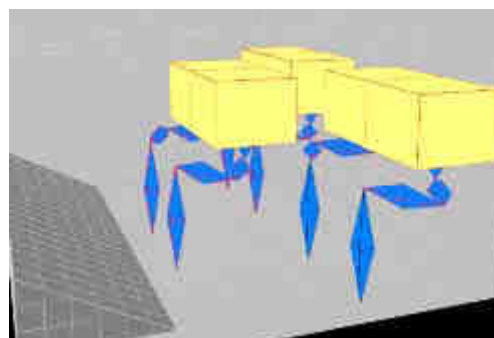


Fig.. 7 Visual Window

The control window supplies the user with every tool needed to simulate different aspects of the robot, visible in the visual window. The application allows zooming, axes rotation and free rotation inside the visual window in order to highlight different. There are three modes of working with this application.

The first one and the simplest is the "Jog" mode. By enabling this mode the user can then select which module he wants to jog and can do so by moving sliders that correspond to each degree of freedom of every joint of the selected robot.

The second mode allows loading an .xls (Microsoft Excel) file containing on each row a set of joint angles or distances in case of a translational joint. The file is analyzed by the application and simulated in the visual window line by line, the robot moving in the way described by the file. There are also functions of interpolating the points given in the file and saving the resulted trajectories of the robot's leg in a different file.

This simulation is done by applying direct cinematic and drawing each of the robot's segment according to the file input. The user can also modify the lengths of each of the robot's segments by modifying the values in the text-boxes on the control window. The last work mode of the application is somewhat the reversed of the previous one. The loaded file contains a trajectory for each leg of the robot.

These calculated values can be then transmitted to the real robot through Ethernet UDP frames or by RS232/RS485 in a proprietary protocol designed for MERO robots. As future feature, the application will also capture the movement of the real robot and compare it with the simulated one in terms of response and trajectory accuracy. An other feature that is being considered is a forth work mode that implies the initial robot's configuration and an unarranged virtual terrain, the application being used to find the best way to overcome the obstacles by choosing one or a combination of two or more previously loaded and learned walk strategies.

REFERENCES

- [1] G., Figliolini, P., Rea, (2006) "Gaits analysis of six-legged Walking Robot when a leg failure occurs", Proceedings of 9th International Conference on Climbing and Walking Robots and support Technologies for Mobile Machines, September 12-14, Brussels, Belgium pp. 276-283,
- [2] Ion I., Simionescu, A., Curaj, A. Vasile (2011), MERO Modular Walking Robots, Solution for Displacing Technological Equipments on Irregular Terrains Proceedings of the 13th World Congress in Mechanism and Machine Science, Guanajuato, México, 19-25 June, 2011
- [3] Ion I., Vladareanu L., Simionescu I. and Vasile A., "The Gait Analysis for Modular Walking Robot MERO Walks on the Slope", ISI Proceedings of the 9th WSEAS International Conference on Automation & Information: Theory and Advanced Technology (ICAI '08), Published by WSEAS Press pag. 222-229, ISBN: 978-960-6766-77-0, (2008)
- [4] Ion I., Marin A., Curaj A., Vladareanu L., Design and Motion Synthesis of Modular Walking Robot MERO, ISMCR 2007 – Technical Challenges in Robotics for the Changing World Proceedings of the 16th International Symposium on Measurement and Control in Robotics, Warsaw, Poland, June 21-23, 2007. pp 146-154 ISSN 83-9211728-7-6
- [5] Ion I., Ion Simionescu Adrian Curaj, Vladareanu Luige, Aurelian Vasile Distribution of reaction forces during movement walking robots FIELD ROBOTICS; Proceedings of the 14th International Conference on Climbing and Walking Robots and the Support Technologies for Mobile Machines, University Pierre et Marie Curie UPMC Paris France 6-8 September 2011; World Scientific Publishing Co Pte. Ltd. - British Library Cataloguing – in – Publication Data. pp: 62-69 ISBN-13 978-981-4374-27-9; ISBN-10 981-4374-27-X.-
- [6] Ion I., Curaj Adrian, Marin Alexandru, Doicin Cristian, Vasile Aurelian. "Simulations strategies walking Mechatronic System MERO" ISRA '10: Proceedings of the 9th WSEAS International Conference on Applications on signal processing, robotics and automation. Mathematics and Computers in Science and Engineering A series of reference Books and Textbooks: pp. 283-287 Recent Advances in signal Processing, Robotics and Automation : 163-170 2010 University of Cambridge, UK, February 20-22, 2010 Anglia, ISSN: 1790-5117 ISBN: 978-960-474-157-1
- [7] A., Roennau., G Heppner., T Kerscher., R Dillmann., (2010), "A behavior-based gait inspired by a walking stick insect" Proceedings of the 13th International Conference on Climbing and Walking robots and

the Support Technologies for Mobile Machines CLAWAR 2010, 31 August – 3 September 2010, Nagoya Japan,

[8] S.M Song. and J.K. Waldron, “(1987). An analytical approach for gait study and its application on wave gaits”, the International Journal of Robotics Research, **6**, 60-71,

[9] W., Lewinger, R., Quinn, “Neurobiologically-based control system for an adaptively walking hexapod” Proceedings of the 13th International Conference on Climbing and Walking robots and the Support Technologies for Mobile Machines CLAWAR 2010, 31 August – 3 September 2010, Nagoya Japan,

[10] K.J., Waldron (1991) Force and Motion Management in Legged Locomotion, Proceedings of the 24th IEEE Conference on Decision and Control, Fort Lauderdale, pp.12-17

REHABILITATION AND TESTING OF AXIAL PISTON AND ADJUSTABLE FLOW HIGH-WEAR PUMPS

Dipl.Eng. Petrica KREVEY, Dipl.Eng. Radu SAUCIUC, Dipl.Eng. Genoveva VRÂNCEANU

¹ INOE 2000-IHP, e-mail address: krevey.ihp@fluidas.ro, sauciuc.ihp@fluidas.ro, vrinceanu.ihp@fluidas.ro

Abstract: *Rehabilitation of hydraulic elements within the generator circuit of axial piston pumps with adjustable flow leads to obtaining kinematic and functional parameters very close to the original, which is one way of restoring the nominal parameters of this type of pump.*

The method of replacing a new set of active elements within the generator circuit is more expensive and agreed to a lower percentage by customers.

Keywords: Rehabilitation, testing, wearing, efficiency

1. Introduction

Wearing of some elements of flow control mechanism and of active and control elements within the flow and pressure generator circuit affects the functional parameters namely by reducing volumetric efficiency, increasing operating temperature and reducing nominal working pressure.

By replacing a full set of active elements (pistons, skates, skate drive plate, bearing, distribution board), there can be obtained functional parameters identical to those of a new pump.

2. Rehabilitation and testing of piston pumps

Rehabilitation of hydraulic elements implies the takeover of clearance and deviations in shape of these elements, within the generator circuit, resulting from recoverable wearing, using compensators, and so kinematic and functional parameters to stay as close as possible to the original.

The purpose is, in each case separately, to remedy wearing by refurbishing as few as possible elements within the generator circuit with minimum expenditure, in view of obtaining functional parameters as close as possible to the initial parameters of a new pump. To this purpose INOE 2000-IHP has developed by self endowment a stand for testing functional parameters (see fig.1) In case of testing a new pump PV180R1K1T1NMRC with axial pistons and adjustable flow with pressure regulator PVCMERCM9-type PARKER, the following are taken into account:

a) TECHNICAL CHARACTERISTICS OF THE PRODUCT

- Capacity: 180 cm³/rev;
- Nominal pressure: 320 bar;
- Nominal speed: 1.450 rev/min

b) TECHNICAL DOCUMENTATION THAT WAS THE BASIS OF THE TESTS

- Procedure : STANDARD
- Catalogue sheets and leaflets.

c) TECHNICAL MEANS USED DURING THE TESTS

3.1. Working fluid environment:

- working fluid: Hydraulic oil H46, viscosity $\nu = 33 \pm 3 \text{ mm}^2/\text{s}$ at $t = 50 \pm 5^\circ\text{C}$
- fineness of filtration: 25 μm ;
- temperature of working fluid: $37 \pm 5^\circ\text{C}$;

3.2. The apparatus used:

- flow transducer, precision $\pm 0.1\%$; $Q=15\dots300\text{ l/min}$; $p_n=400\text{ bar}$; EVS 3100; HYDAC;
- pressure manometer, precision class 1; range $0\dots400\text{ bar}$; HANSA –FLEX;
- throttle valve on the pump discharge route; HK V 257 5-3/4; Dn 20; $Q= 84\text{ l/min}$; $p_n= 400\text{ bar}$;
- throttle valve on the pump draining route; HK V 257 5-1/2; Dn 15; $Q= 47\text{ l/min}$; $p_n= 400\text{ bar}$.

3.3 Annexes for tests:

- couplings, nipples, plugs, enclosures, etc.

d) TESTING SCHEMATIC DIAGRAM

The testing schematic diagram is shown in Figure 1.

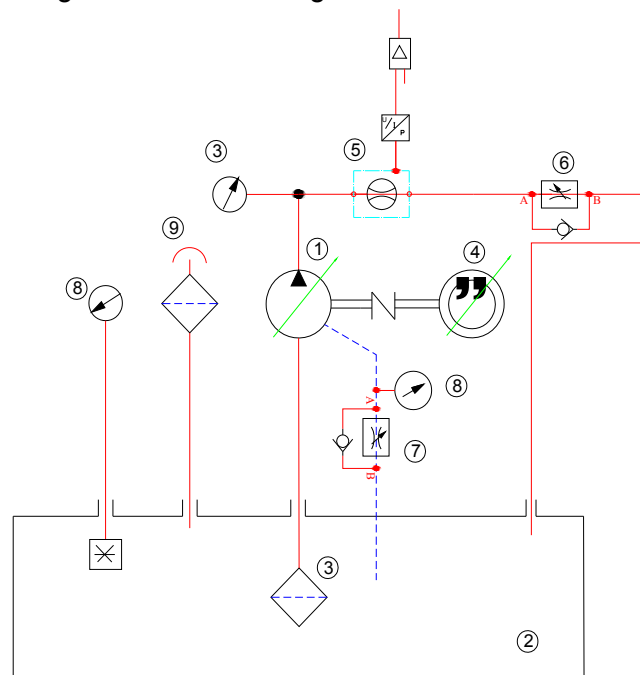


Fig. 1.

- | | |
|---|--|
| 1 – Variable flow pump (to be tested) | 6 – throttle valve on discharge route Dn 20 |
| 2 – oil filter on the suction (suction nozzle) | 7- throttle valve on draining route Dn 15 |
| 3 – anti-vibration manometer $0\dots400\text{ bar}$ | 8 – manometer on the drainage $0\dots5\text{ bar}$ |
| 4 – Three-phase asynchronous electric engine of 18Kw ; $n=1460\text{ rev/min}$. | 9 – filling and ventilation filter |
| 5 – flow transducer $15\dots300\text{ l/min}$ | |

From measurements made according to Table 1, after rehabilitation of several hydraulic elements within the generator circuit there was observed that when testing the pump its volumetric efficiency at idle speed is within the values prescribed by manufacturer.

Table 1

Item	Discharge flow Q [l/min]	Drainage flow Q [l/min]	Rotation n [rev/min]	Effective pressure, discharge p _e [par]	Effective pressure, drainage p _e [bar]	Obs.
MEASURED DATA						
1.	27.8	1	980	3	0	
2.	27.3		980	20		
3.	26.8		980	40		
4.	26.3		980	60		
5.	25.8		970	80		
6.	25.3		960	100		
7.	24.9		950	120		
8.	24.4		950	140		
9.	23.8		950	160		
10.	23.2		920	180		
11.	22.7		900	200		
12.	22.1	10	840	310	2	
CALCULATED DATA						
Item.	Displacement calculated [cm ³ /rev] V _{g0} = Q ₀ /n ₀ (without load)	Displacement calculated at maximum load V _{gs} =Q _s /n _s [cm ³ /rev]	Volumetric efficiency $\eta_v = \frac{V_{gs}}{V_{go}}$		-	-
1.	27.8/980=28.3 cm ³ /rev	22.1/840=26.3 cm ³ /rev	(26.3/28.3)=0.93*			

* Maximum theoretical displacement of the pump tested
 V_{gt} = 180 cm³/rev

The appreciation of rehabilitation operations is made by evaluating the pump volumetric efficiency according to Table 2.

Table 2

Item.	Testing	Results		Obs.
		Provided	Achieved	
1.	Volumetric efficiency at no load	0.97-0.96	0.95	It is included in the technical norms
2.	Volumetric efficiency under the maximum load	0.96*	0.93	It has a variation with the increase of pressure

* Pumps Catalogue PARKER (see fig.2)

PV180

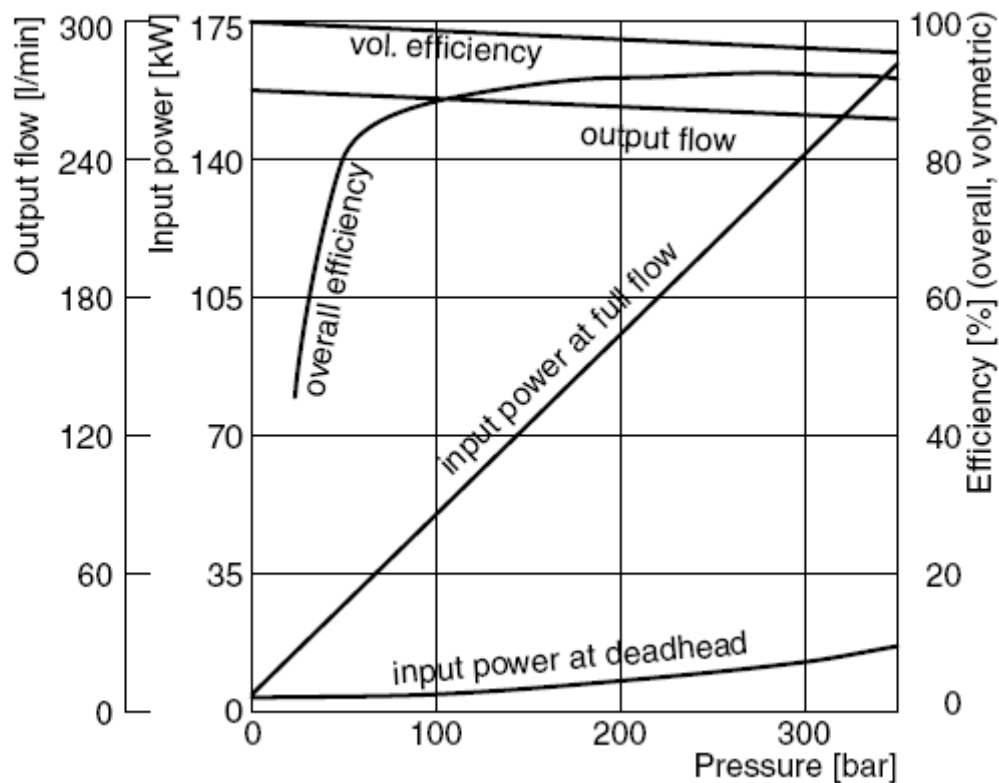


Fig. 2.

When testing the pump under load there was found a slight decrease of volumetric efficiency compared to the one prescribed by manufacturer.

Obtaining the functional parameters depends also on rigorous setting of control and adjustment elements, in this case the pressure regulator, to obtain a static feature similar to that of the manufacturer (see fig.3)

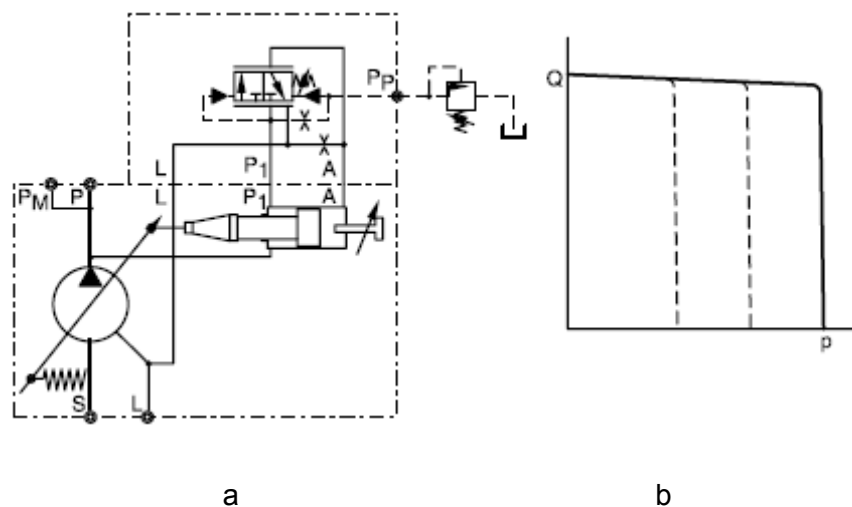


Figure 3.

Drainage losses were within the losses prescribed by manufacturer (10 ... 18 l / min) at test pressure of 310 bar (see diagram in fig.4).

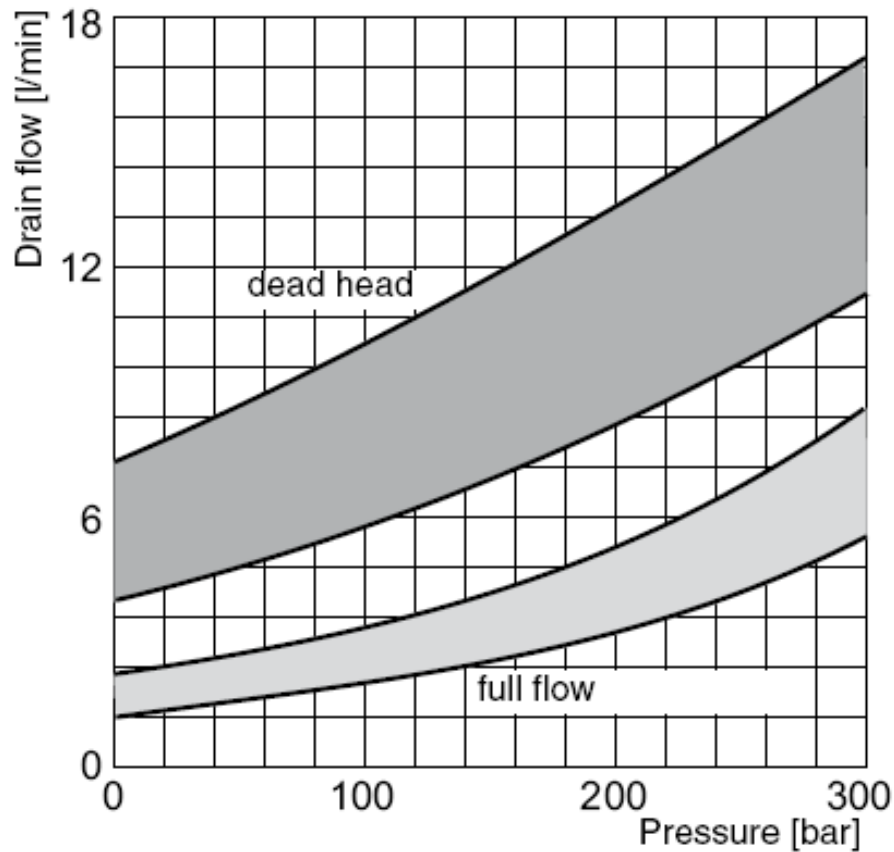


Figure 4.

Since the electric engine used for the test is of 18 kW, and there is the possibility to vary the speed with a frequency converter of 22 kW, there was drawn the static characteristic of the pump equipped with pressure regulator.

The stand for testing whose hydraulic schematic diagram is shown in fig. 1 and made by INOE 2000-IHP is shown in fig. 5, the pump mounted on the stand - in fig.6, and the tested pump is presented in fig. 7.



Fig. 5 Testing stand



Fig. 6 The pump mounted on the stand



Fig. 7 Tested pump

Deviations obtained after rehabilitation can be seen in the static characteristic of the pump equipped with pressure regulator, raised after rehabilitation (Fig. 8), line (a), compared to the manufacturer's static characteristic, line (b).

Steep fall in flow in the case of the manufacturer's schematic diagram is caused by the fact that on achieving the pressure set at the pressure regulator, the pump tilted by minimum flow (~ 0).

If the case of the pump tested after rehabilitation at INOE-IHP, reducing pump flow was performed gradually, using the throttle valve 6 (see fig.1), starting from pressure of 100 bar, pressure at which the feature gradient is identical to that of the manufacturer.

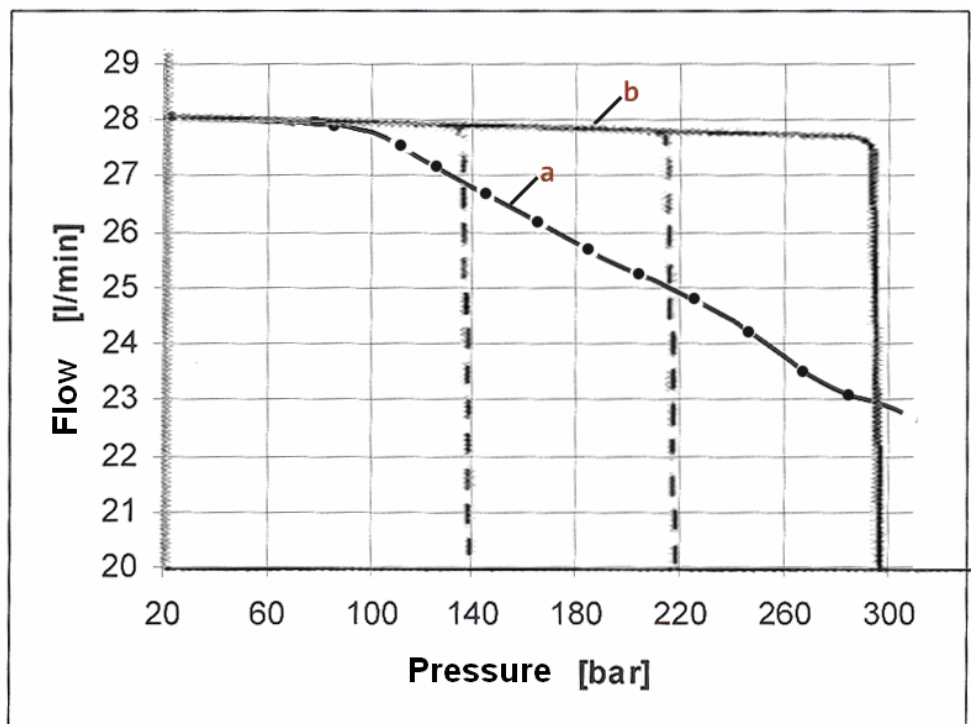


Fig.8 The static characteristic of the pump equipped with pressure regulator

3. Conclusions

- After rehabilitation of this axial piston and adjustable flow pump, kinematic and functional characteristics are kept within acceptable limits;
- Depending on the number of components replaced in rehabilitation there can be noticed the achievement of parameters (flow, pressure) nearest or even equivalent to those of a new pump;
- Drainage flow and pressure is fitting in the diagram of the catalogue (see fig.3);
- The pressure regulator will be set at the customer, according to requested working pressure;
- Volumetric efficiency at no load is kept within the catalogue data;
- Volumetric efficiency under load decreases with increasing pressure.

REFERENCES

- [1] N. Vasiliu, D. Vasiliu, "Fluid Power Systems", Vol.I. Technical Publishing House, Bucharest, 2005.
- [2]*** *Catalog PARKER HANIFIN (USA)*

THE VISION-BASED MECHATRONIC SYSTEMS USED IN PRODUCTION QUALITY CONTROL OF HYDRAULIC COMPONENTS

Sorin SOREA, Anca ATANASESCU, Alexandru CONSTANTINESCU

INCDMTM Bucharest, cefin@cefin.ro

Abstract:

A topical issue in economic theory and practice is total quality management, which requires the involvement of all organizational and functional structures to ensure adequate quality of products and services.

In support of this concept, vision-based mechatronic systems can be integrated as top products in the activities of control and inspection of parts, sub-assemblies and products in the final stage of assembly.

The paper presents two equipment designed by INCDMTM Bucharest related to the quality control process using vision-based mechatronic systems, with direct applicability in industry, particularly in hydraulics.

Keywords: *mechatronic, vision, control, hydraulics*

1. Introduction

In the context of latest constraints encountered in industry (rapidly evolving technologies, market changes, migration of staff) which compels the company to engage in flexible and efficient organization of production factors, the ability to continuously improve product quality becomes a goal and a means to ensure competitiveness and performance on the Community market.

The prosperity of an enterprise is ensured by the high quality of its products and services compared with that of its competitors, the customers' confidence in its products and services being a major competitive advantage. The quality control of products or services generally provides performance improvement in any enterprise, by improving resource efficiency, reducing costs by the elimination of losses caused by lack of quality.

A topical issue in economic theory and practice is total quality management, which requires the involvement of all organizational and functional structures to ensure adequate quality of products and services.

In support of this concept, the vision-based mechatronic systems can be integrated as top products in the activities of control and inspection of parts, sub-assemblies and products in the final stage of assembly.

Any action of control and information obtained by these means of control and inspection is included in the reporting system. Subsequently, they are processed, analyzed, determining actions accordingly.

We present below some of the achievements of our institute regarding the use of vision-based mechatronic systems for quality control process, with direct reference to industrial applications, particularly in hydraulics.

However, summarising, clarifications are required with respect to the criteria for using these vision-based mechatronic systems in diverse industrial control applications.

2. General characterization of the vision-based mechatronic systems

Nowadays, vision-based mechatronic systems are expanding, since there are there are two application categories where they apply:

- applications using PC based equipment with CCD or CMOS cameras;

- applications based on smart cameras, smart image sensors or compact/ embedded image systems.

There are three market segments based on the characteristics of vision control systems (see Figure 1.)



Figure 1.

The three segments are based on the seven criteria of segmentation, as follows (Figure 2):

	Image Sensors	Smart Cameras Smart Image Sensors	Embedded Image Systems.
Integration level	Integrated	Integrated	Less integrated
Price	Lowest Price	The highest price	The highest price
Flexibility / programmability	Low	High	High
I / O	Simple	Complex	Complex
Processing power	Low	Higher	Higher
Memory	Low	Average	High
Resolution	Low	High	High

Figure 2

The comparison of the three segments brings into discussion performance criteria, system architecture and cost effectiveness (see Figure 3):

Performance criteria		
Advantages Image Sensors 1	Smart Cameras Smart Image Sensors 2	Embedded Image Systems. 3
Lowest price Ease of Use	Maintenance - lower than "3" Direct access to image	Can use more than one camera

Integrated lighting Integration level - lower than "3"	processor (as opposed to "3") Flexibility and programmability greater than "1" Capacity to handle more advanced applications than "1"	May use different types of cameras Enhanced CPU performance for image processing Capacity to handle more advanced applications than "1"
Disadvantages		
Image Sensors 1	Smart Cameras Smart Image Sensors 2	Embedded Image Systems. 3
Programmability - Low (may use a limited number of simple functions) Configurability - Low	More difficult to use than "1" More expensive than "1"	More difficult to use than "1" and "2" More expensive than "1"

Figure 3.

Summarize these criteria in the following table:

Table 1

	Optoelectronic systems based on PC	Sensors / smart cameras
Flexibility	Excellent	Poor
Ruggedness	Poor	Excellent
Size	Multi-component/ Camera can be very small	Unitary Not necessarily small camera
Functions	Extensible	Limited
Performance	Extensible	Limited
Ease of use	Requires computer	Does not require a computer
Configuration	Expandable	Fixed
Power	Extensible	Limited
Scalability	Excellent	Poor

2. Control application using a PC based vision equipment

The first equipment that will be presented refers to a stand for inline inter-operational controlling of mechanical parts. The part is a "primary shaft" and the equipment was implemented on the production line of a local manufacturer.

On this stand there are carried out the neutrality control of the gasket seat surface following the super-finishing operation and the feature control of a Ø10mm bolt hole following the operations of washing and deburring.

The control stand consists of an enclosure with two independent control posts namely:

1. one "primary shaft" control post for checking the neutrality specification of the gasket seat surface (pos.1 -Figure 4);
2. a post for checking the Ø10mm bolt hole, following the washing and deburring operations (pos.2 - Figure 4).



Figure 4

The first control post (Figure 5) is composed of:

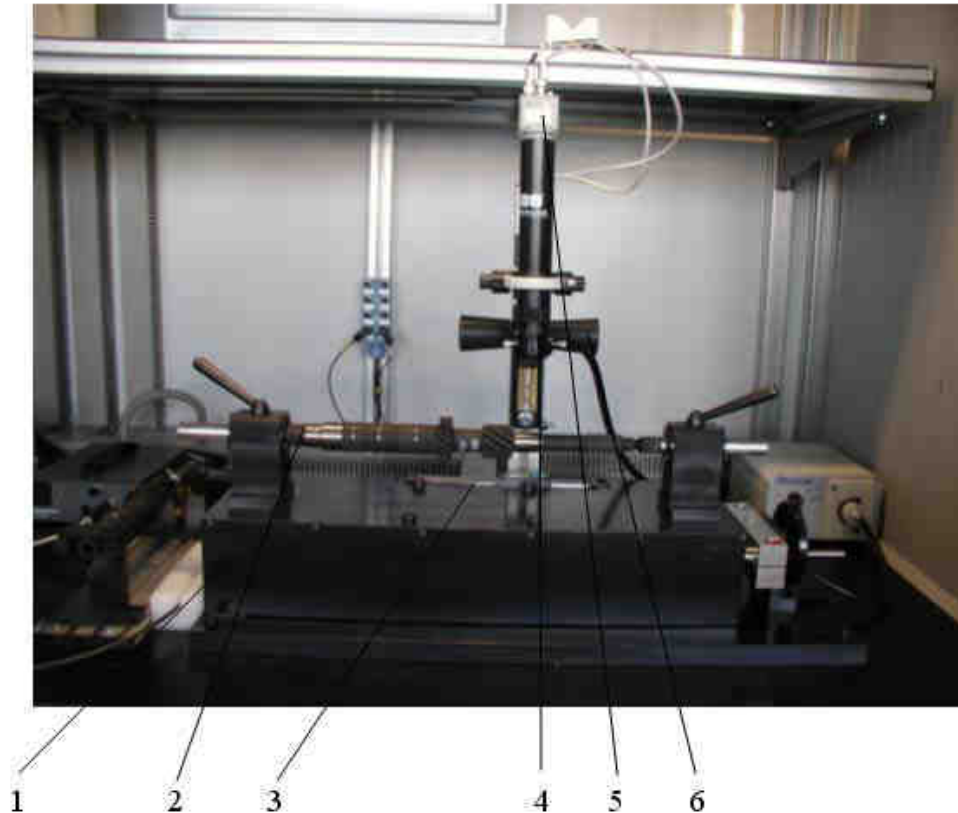


Fig.5

A1) Single axis translation stage for “primary shaft” positioning. On this table, the “primary shaft” is caught and fixed between its peaks. The displacement of the stage and consequently the movement of the “primary shaft” in relation to the fixed control booth, i.e. the optical axis of the image acquisition system, is measured using a horizontal linear transducer endowed with precision digital display.

B1) The image acquisition optoelectronic subsystem consisting of a manual zoom optical system, with 4.5x - 0.7x primary magnifications and a color 1/2" CCD camera. The optoelectronic subsystem is mounted on a vertical column and manually displaced vertically by means of two mechanisms that ensure: one a rough positioning and the other a precise positioning to set up the image.

The image acquired by a frame-grabber installed in an industrial PC is visualized and stored in real time using a specialized software developed in our institute as well. Also the image is displayed in real time on a 19 " industrial monitor within the control stand.

C1) The specialized software developed for this application. The main features are:

- image acquisition and viewing,
- generation of the electronic targeting reticle. It is used to determine the relative position of the table in relation to the optical axis of the image acquisition optoelectronic system,
- storing (saving) images of checked shafts.

The software is implemented on an industrial computer that provides Ethernet connection.

The second checkpoint (Figure 6), which verifies the Ø10mm bore hole following the operations of washing and deburring consists of:

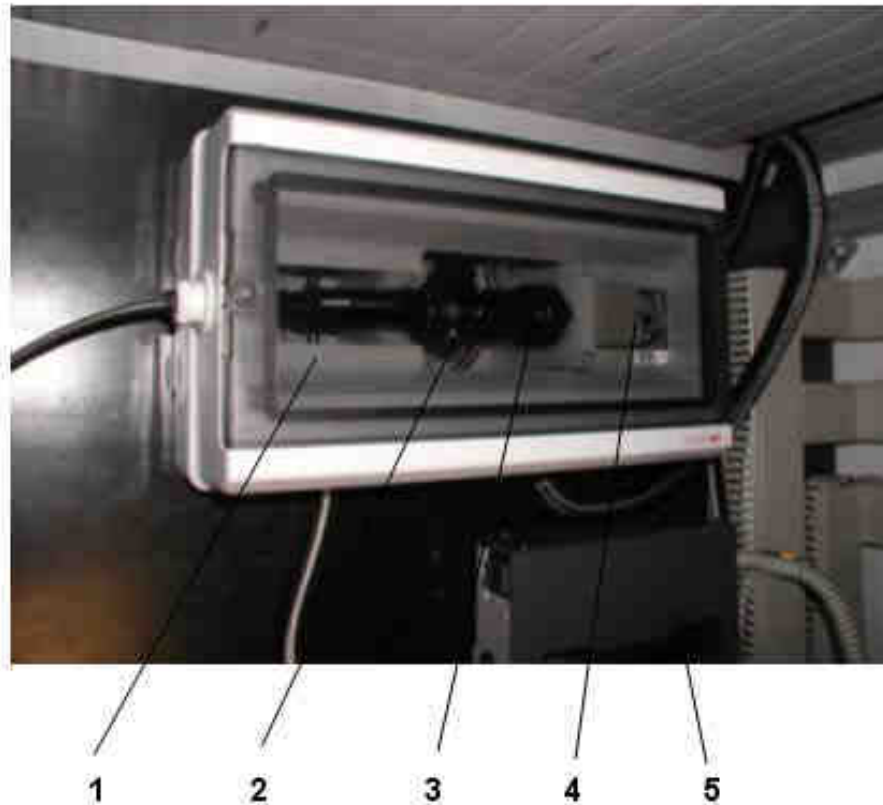


Figure 6.

A2) V-shaped prisms type setting device

The relative position of the prisms may change along the direction of the “primary shaft” axis to optimally position the shaft on the prism. One of the prisms is provided with a fixing device with a screw meant to fasten the part into the control position.

B2) Endoscopy kit installed in a protective enclosure, consisting of :

- flexible endoscope,
- CCD camera adapter ,
- color ½ " CCD camera
- variable light source.

The image of the Ø10mm bore hole is viewed on the same 19" industrial monitor. Switching between the two posts to receive the control image is done by the operator from the control panel.

The second checkpoint uses the same specialized software used in the first checkpoint as described above, with the main functions:

- image acquisition and viewing for the Ø10mm bore hole
- saving images of the Ø10mm bore hole

The stand described above is used to exert random inter-phase control.

The stand is not automatized at this stage.

3. Application based on a smart image sensor

In the quality control applications where mechatronic systems are used successfully, mistake-proofing systems of the vision type are also worth noticing. This is a quality management concept developed in Japan to prevent human error which may occur on the production lines. Mistake-proofing systems are designed to prevent people from committing mistakes, intentionally or accidentally. Mistake-proofing systems, also known as poka-yoke, are normally used to stop the system and warn the operator that something has gone wrong.

In our institute a flexible Mistake-proofing monitoring cell was designed using smart image sensors among other classical sensors.

The flexible cell has been designed as a modular system intended to assist the human operator in an assembling post on a production line characterized by : parts moving at a high rate, high diversity of parts to be assembled, high similarity between versions of the parts to be assembled, frequent changes of manufacturing series.

Practically, in the same assembling workstation, the human operator has to perform similar operations which involve different subsets for different versions of the manufactured product. Because of high rate and similarity of versions, error probability is very high, the operator may misplace a subset, which may prove inappropriate. Usually, the error is detected much later on the manufacturing line, or even during a later stage, which requires removing the product from the line, disassembling it, recalibrating and adjusting it and so on, with major consequences on manufacturing costs.

The mistake-proofing flexible monitoring cell consists of three functional modules identified as being typical in most cases:

- Identification module intended to recognize the version of the part in the assembly station;
- Monitoring module intended to signal specific operations for the identified version and to track down actions taken by the operator in order to validate or signal correct / incorrect actions;
- Command and control module intended to acquire data from all sensors in the post, to command the actuators and signal elements, to interface with the operator and to communicate with the higher level (at the level of production line).

The smart image sensor is integrated in a system on a conveyor belt located at the beginning of an assembly line and is designed to evaluate the conformity of the workpiece located on the belt to the variety selected to be assembled in that workstation.

For this application we used an object recognition smart sensor from IFM, of the Efector Dualis Contour Sensor type.

This smart sensor integrates the optical objective, the LED lighting and the evaluation system into a robust, industrial case.

The fact that the smart image sensor includes both the optical imaging system and the computer and communication system recommends it to be used in real-time on high rate assembly lines.

An commonly example in industrial applications from various fields is detecting the conformity of the presence of a threaded hole in a part on the assembly line (Fig. 7). Thread absence from metal parts can cause oil leakage and eventually engine failure. A smart sensor of the Pixel Counter type detects inconsistencies in threaded surfaces so that defective parts can be removed prior to assembling. This smart image sensor, programmable, provides pass or fail control verdicts.

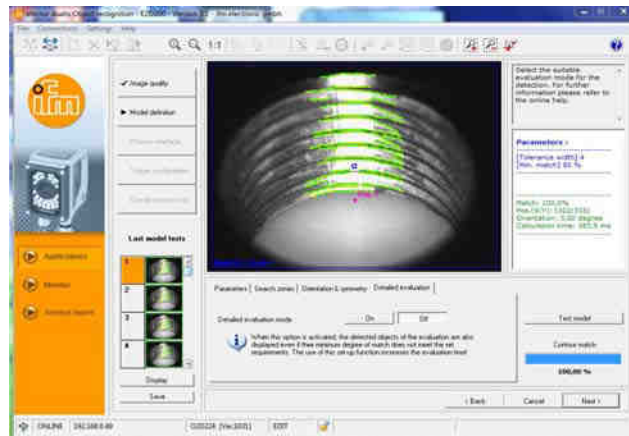


Figure 7

Another application specific to hydraulic industry is presented in Figure 8.

This application identifies the presence of a gasket on a compensator body in a gear pump to be assembled.(Figure 8).



Figure 8

An IFM Contour Sensor is programmed to verify if the operator has set the gasket before having set the compensator. In this case, the smart image sensor, provides pass or fail verdicts too (Figure 9a - 9b).

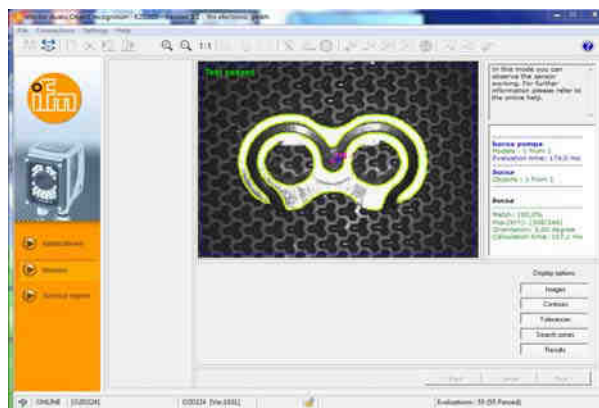


Figure 9a. Image for a "Pass" verdict

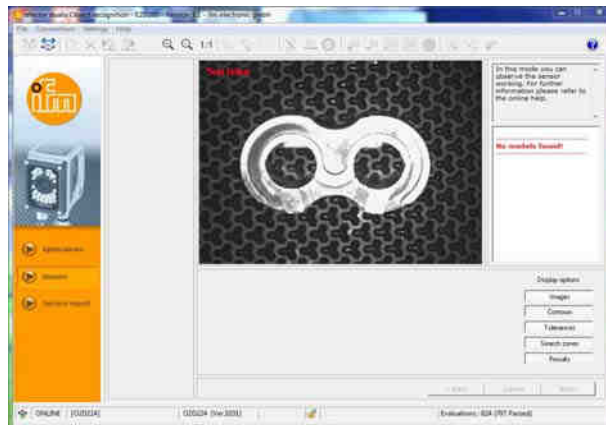


Figure 9b. Image for a “Fail” verdict

4. Conclusions

The vision-based mechatronic systems can solve industrial control problems which until now were impossible to be solved using conventional sensors and technologies.

The advantages induced by the implementation of this technology can generate a significant qualitative leap, these vision systems enabling 100% quality inspection of an automatic production lines.

This has huge benefits because the full checking of quality and compliance of the products can save significant sums. The faulty products can be eliminated since the early stages, that otherwise would have passed through further processing and would generate other costs.

The ability of the vision-based mechatronic systems to “give eyes” to the industrial equipment and production control, allows their use in the various operations of :

- Guidance of robots so they no longer need to get pre-arranged parts and get the ability to avoid collisions,
- Automatic sorting according to different visual parameters of the product,
- Tracking and managing the product serialization
- Control and inspection to determine the conformity of form, appearance, color, geometric size etc.
- Check the presence (or absence) of parts or elements in a part
- Assembly error checking.

REFERENCES

- [1] Vision Systems Design, Magazine - up to date
- [2] Photonics Spectra, Magazine - up to date
- [3] <http://www.ifm.ro> IFM - catalog, prospects, web page
- [4] <http://www.cognex.com> - catalog, prospects, web page
- [5] <http://www.keithley.com> - catalog, prospects, web page
- [6] <http://www.sick.com> - catalog, prospects, web page

NUMERICAL SIMULATION OF THE SERVO MECHANISM FOR ADJUSTING THE CAPACITY OF THE RADIAL PISTON PUMPS

Liliana DUMITRESCU¹, Cătălin DUMITRESCU¹ Ioan LEPĂDATU¹

¹ INOE 2000 - IHP e-mail address: lilianad.ihp@fluidas.ro

Abstract: *The paper presents the simulation of static and dynamic behavior of system capacity control radial piston pumps using the program AMESim.*

Keywords: *simulation, pumps, rung signal, sinusoidal signal*

1. Introduction

To analyze the static and dynamic behavior of the control system capacity of radial piston pumps, was used a powerful and performant graphical program, AMES / Imagine. For the composition of the simulation models were used standardized symbols specific hydraulic elements existing in the library program. AMESim is a simulation environment built on multiport considerations. The exchange of information between the components is bidirectional and thus made fewer lines of communication. At the same time the simulation environment shapes almost exactly real models of the dynamic systems simulated. Another important feature of the program is the automatic choice of the method of integration of the systems of equations that can be adapted during simulation according to the characteristics of equations. From the user point of view, the program is a suggestive graphical interface that displays the evolution of the whole system during the simulation process.

2. Structure for simulation of servo

In fig. 1 is shown the structure for simulation of servo positioning. It is then specified the correspondence between the components of the simulation model and the physical model elements [1]. The analyzed system is the real mechatronic control system eccentricity / flow, which is composed of:

- Electro-hydraulic proportional distributor 4/3 with center closed - Item 8;
- Supply group with oil under pressure - Item 3, 4 and 2;
- Tank - Item 1;
- Position transducer - Item 13;
- Compensator - Item 16;
- Linear hydraulic motor + inertial load + viscous frictions - Item 14, 15, 11, 10 and 12;
- Signal generator - Item 7.

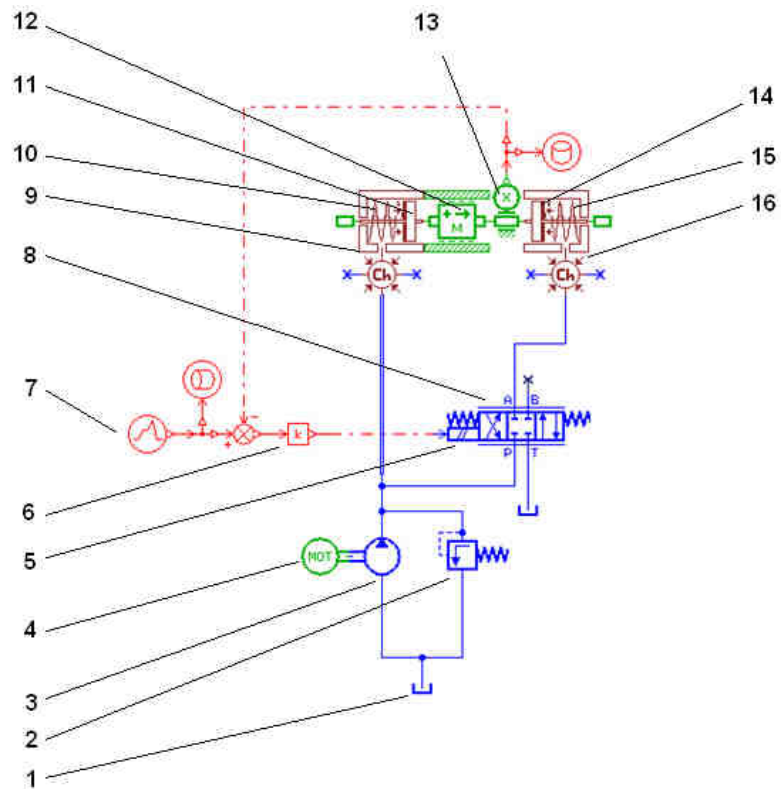
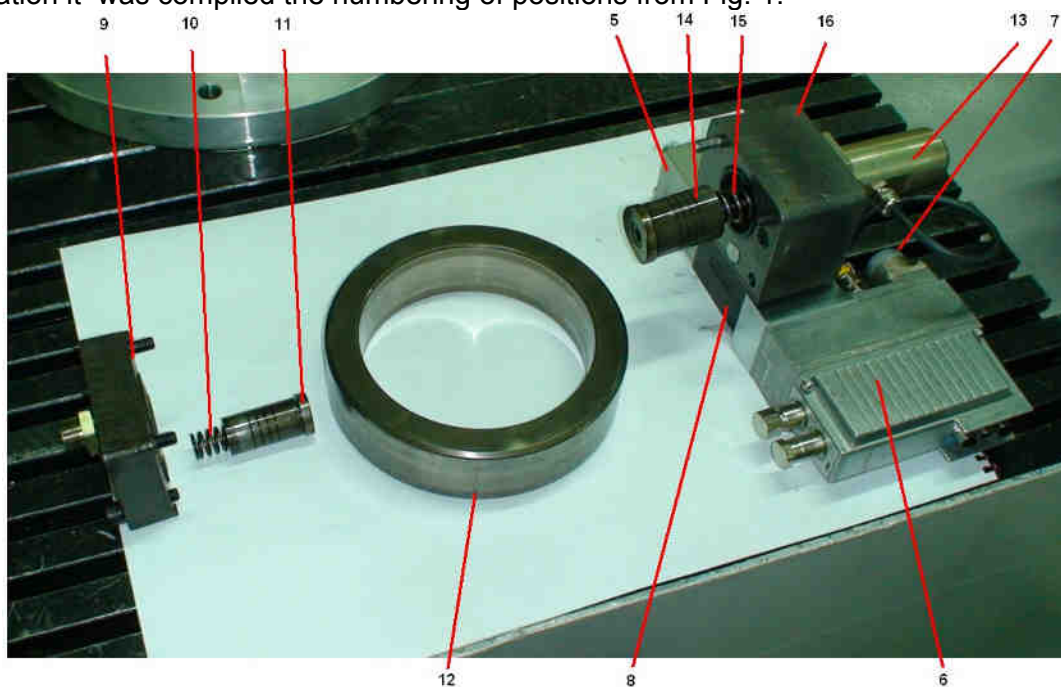


Fig.1 The network for simulation of the servo control of radial piston pump capacity

Their correspondence with the real control system eccentricity is shown in Fig. 2. For an easy identification it was complied the numbering of positions from Fig. 1.



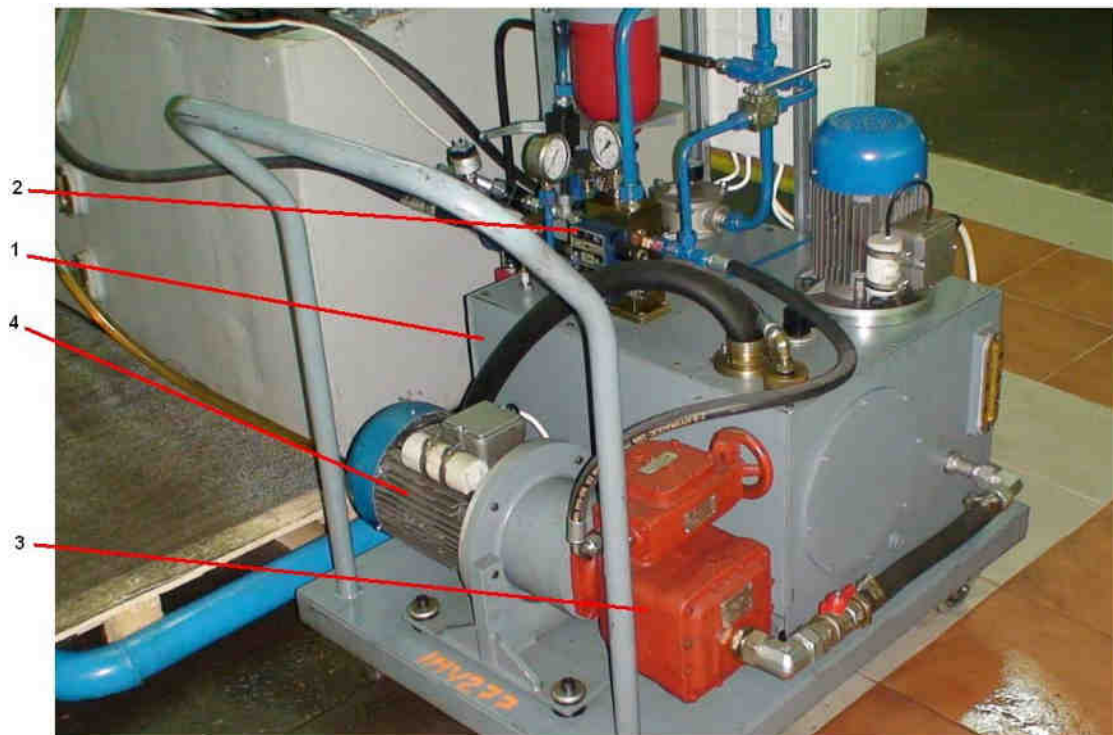


Fig. 2. Physical structure of the positioning system for adjusting the eccentricity

In these pictures are distinguished in the following:

- | | |
|--------------------------------------|------------------------------------|
| 1. tank; | 9. small piston chamber; |
| 2. pressure limiting valve; | 10. small piston spring; |
| 3. Volumetric pump | 11. piston with small area; |
| 4. electric motor; | 12. inertial mass (sliding ring); |
| 5. electromechanical converter; | 13. inductive position transducer; |
| 6. electronic compensator; | 14. piston with large area; |
| 7. the command prescription channel; | 15. piston spring with large area; |
| 8. proportional distributor body; | 16. large piston chamber. |

3. Static and dynamic characteristics of the system

To determine the static and dynamic characteristics of the system, it was controlled by triangular electrical signals voltage step and sinusoidal type in the field (0 ... 10) V DC. Frequency signal, type ramp was chosen small enough to generate a quasi-static regime. The were obtained features from simulation which are presented in Fig. 3...7, the monitored parameter at the (output of the) system output being eccentricity, whose values, when used as an experimental model pump is:

$$e = (\varphi \dots 5) \text{ mm.}$$

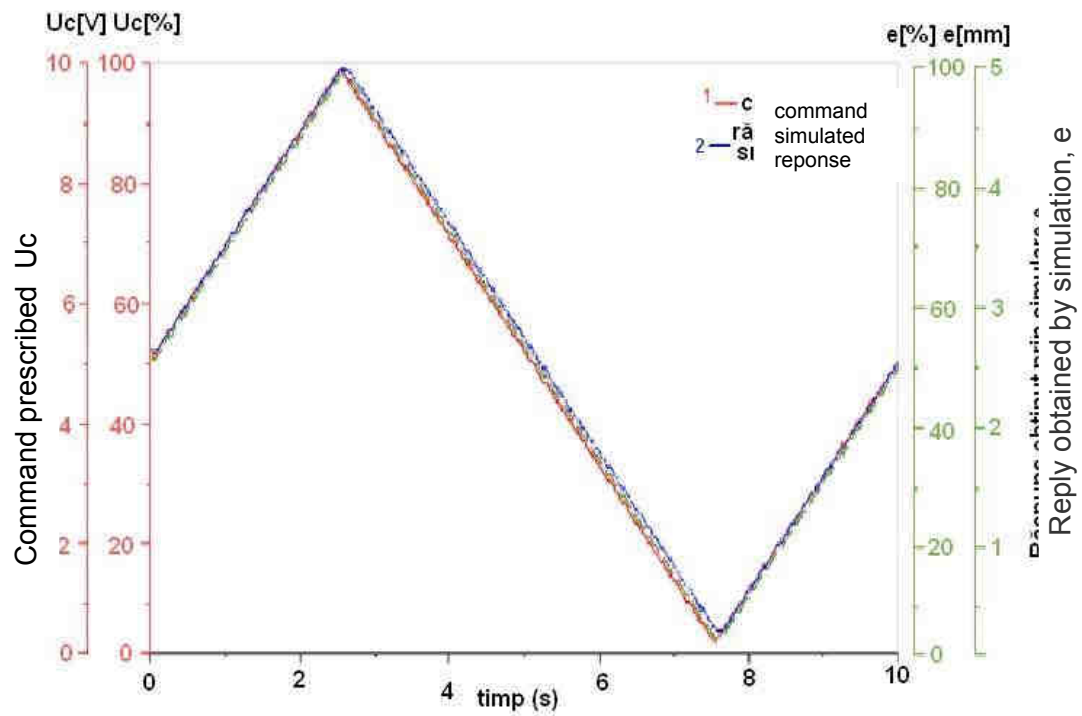


Fig. 3. System response to the ramp signal, frequency 0.1 Hz

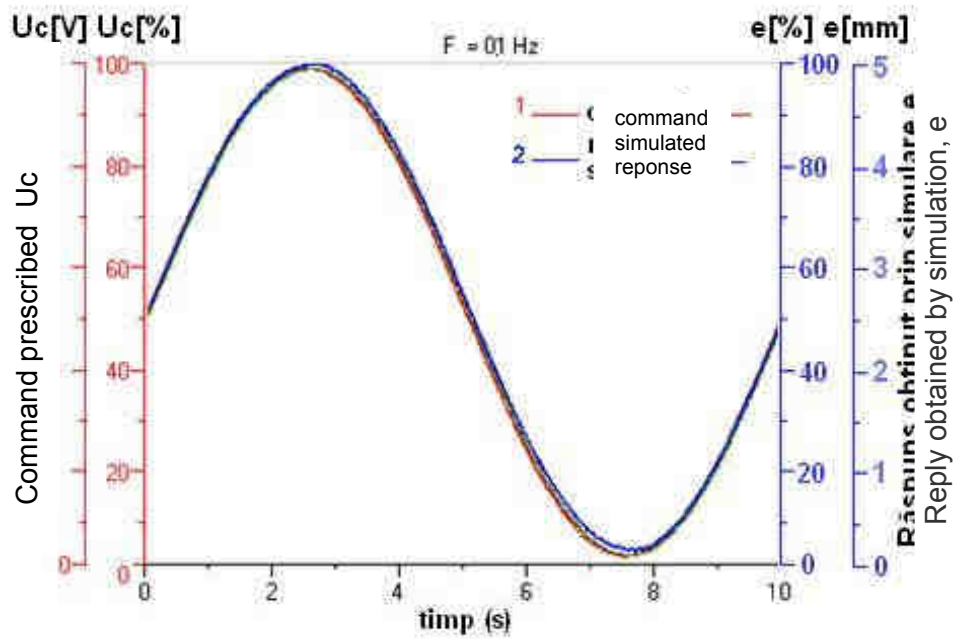


Fig. 4. System response to sinusoidal signal, frequency 0.1 Hz

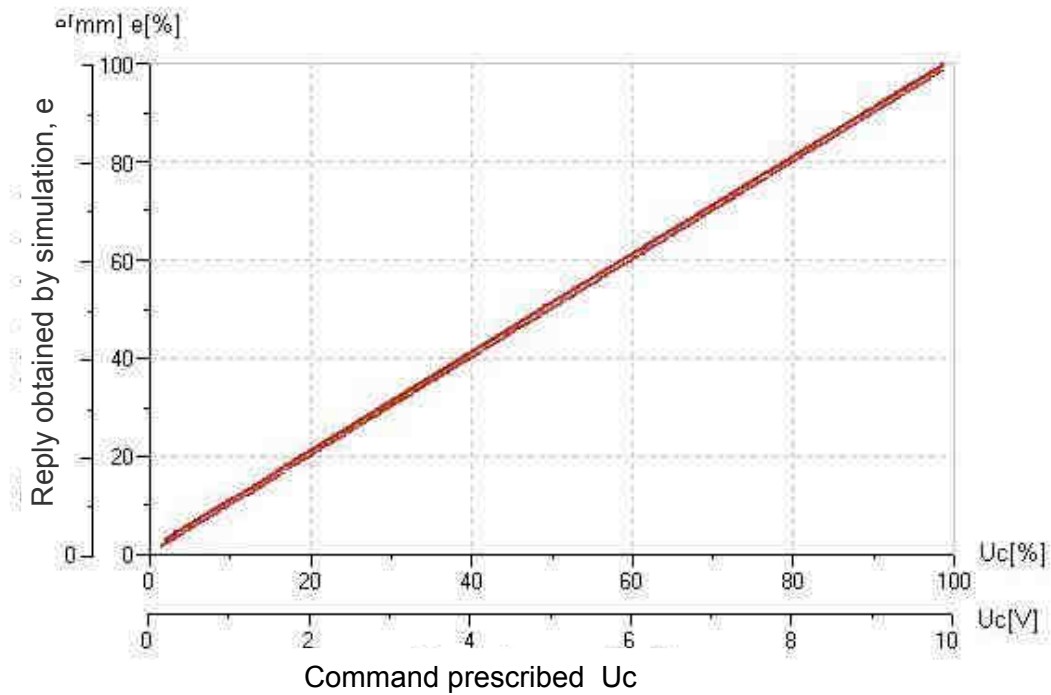


Fig. 5. Static characteristic, frequency of 0.05 Hz

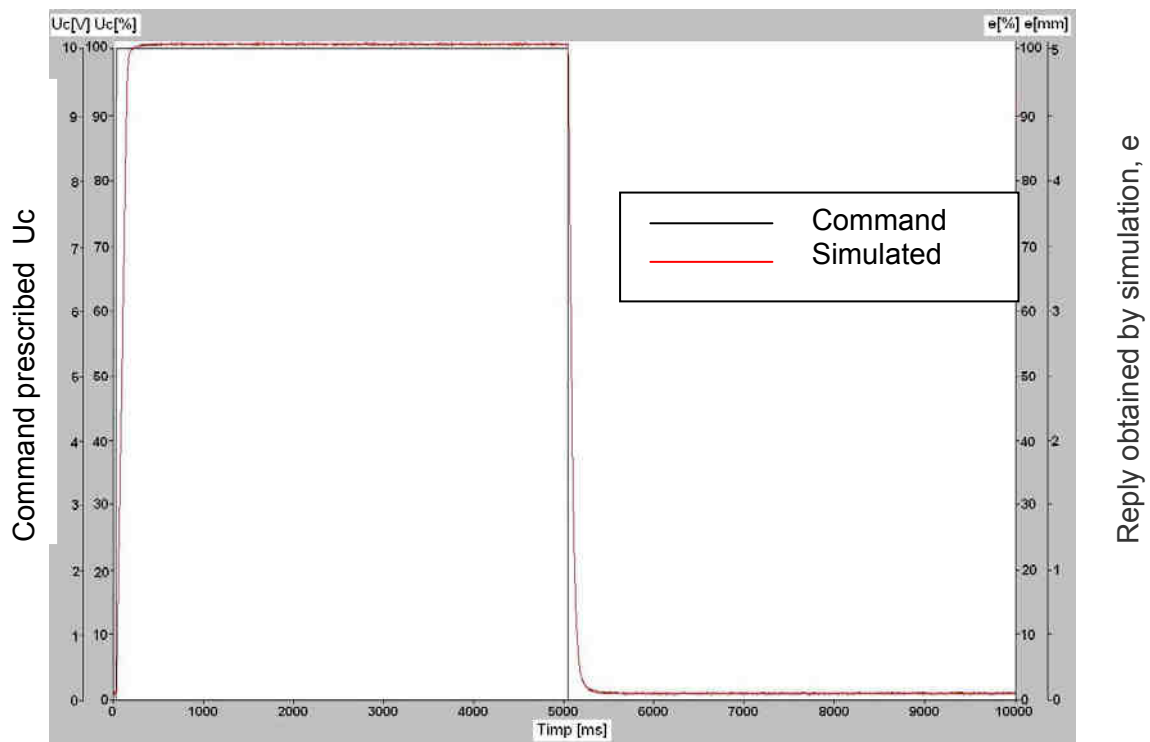


Fig. 6. Response to the signal rung

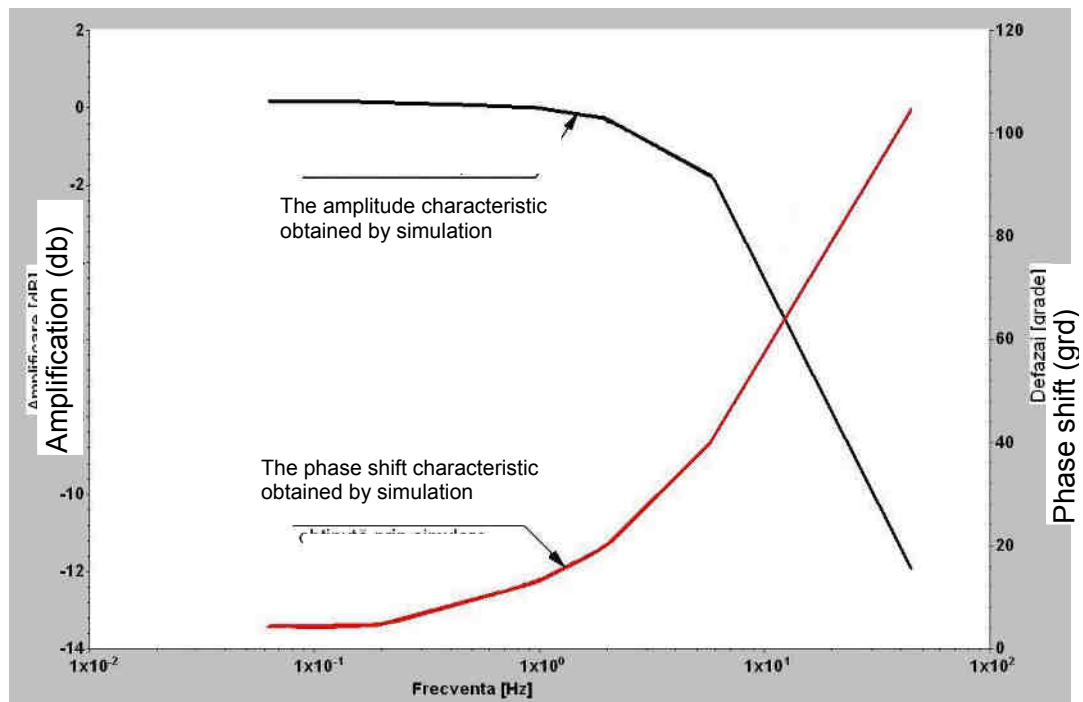


Fig. 7. Bode diagram

4. Conclusions

All features obtained using AMESim program, have very small deviations between the command and simulation which means that the obtained results simulate with a very good accuracy functioning of the control eccentricity system.

Considered the reference, the results obtained by numerical simulation will be validated experimentally. Experimental research results and comparison with the simulated results will be presented in another article.

REFERENCES

- [1] I. Lepădatu, "Theoretical and applied research on mechatronic systems adjusting the flow of hydraulic rotary generators by eccentricity", U.P.B. Doctoral Thesis, 2010.

DESIGN AND DEVELOPMENT OF MECHATRONIC SYSTEM WITH TELEMONITORING AND PREDICTIVE TELEMaintenance CONTROL

Anghel CONSTANTIN¹, Sergiu DUMITRU²

¹ National Institute of Research and Development in Mechatronics and Measurement Technique
e-mail: ¹anghel@incdmtm.ro, ²sdumitru@incdmtm.ro

Abstract: *The Internet provides a low cost way to connect a computer anywhere in the world. Any computer that can connect to a local Internet Service Provider (ISP) can communicate with any other industrial equipment with access to the Internet. With the Internet proliferation, more and more facilities have to remote monitoring and telemaintenance control. This came with the introduction of the networking administration and protocols. The use of these technologies for Predictive Maintenance professionals can be critical to the success of the Predictive Maintenance program at an industrial plant.*

Keywords: *Mechatronics Design, Industrial Telemonitoring, Predictive Maintenance*

1. Introduction

Lately witnessing shows an unprecedented growth interactivity in hierarchical relationships of the industrial end users and providers. In the previous stages of computerization, companies have used IT to streamline internal working's of the organization. These steps coincided with major trends in management, who planned outsourcing, reengineering and downsizing site. Last manifestation of these trends has been the implementation of often complex integrated information systems, aiming at automating internal processes and tracking operative suppliers. Using the Internet should be a different logic, whose central axis is not only a more efficient individual companies, but it merged with the maintenance and service environment.

Competitive advantage comes not only from the ability to implement technological applications that allow acceleration of internal processes or automate them but especially the ability to broadcast system efficiencies of enterprise customers and its suppliers. Major axes of enhancing the collaboration with other business partners consist of the ability to communicate, establish permanent links, to facilitate rapid completion of monitoring and service in the industrial mechatronic field. This can be done without reengineering the enterprise, being sufficient an analysis of their organizational boundaries, followed by the finding a place in the enterprise network, market and state. Mechatronic systems, either stationary or mobile, joint or tentacular arm, wheeled carts, simple or complex types of structures are currently used in various fields, especially in hazardous environments or dangerous for humans, such as : handling of toxic substances. Under these circumstances, even the location of the defect detection in the drive and run basic robot becomes a problem. Defects in robotic structures may be caused by external environmental conditions (operating environment) or internal conditions (structure, sensors, actuators and scheduling management).

All the situations described above can be controlled via a monitoring system (self-diagnosis), which will detect any changes and analyze and control the robot according to a suitable algorithm. Monitoring system, depending on its complexity, may adopt the following management strategies (from simple to complex): Only Fault detection and isolation possibly suggesting actions and/or the avoidance of defective parts, robot motion further provided that conditions stability and safety for minor defects; further movement.

2. Tele-Maintenance Definition

Tele-maintenance is a compound word whose first term refers to the prefix "Tele", meaning from distance. "**Tele**" might also derive from "teleprocessing" that is the use of telecommunications equipment and systems by a computer or a computer service involving input/output at locations remote from the computer itself [1]. The communication process is defined as the information flow from a source point to a receiver point and telecommunication is a communication over long distances [1]. "Tele" could also derive from the neologism "telematica" that is a synonym of teleprocessing. According to the definition, in fact, "Telematica" or "telematic process" is a combination both of telecommunication and of data processing.

Data processing is any operation or combination of operations on data, including everything that happens to data from the time they are observed or collected to the time they are destroyed. It is also known as information processing.

"**Maintenance**", the second term of "Tele-maintenance", is the combination of all technical and administrative actions, including supervision actions, intended to retain an item in, or restore it to, a state in which it can perform a required function [IEC 50 (191)]. Tele-maintenance, therefore, is the combination of all technical and administrative actions, including supervision actions, intended to retain an item in, or restore it to, a state in which it can perform a required function [IEC 50 (191)]. Actions are carried out in a remote site and are supported partially or totally by teleprocessing/telematica (telecommunication plus data processing).

Tele-maintenance is a general term that can be better qualified by more specific terms utilised to indicate only specific teleprocesses such as:

Tele-monitoring is the supervision of equipment/plant correct working in a remote site by continuous or cyclic check of parameters. Tele-monitoring enables the operator to continually monitor the performance of the system from a central point. The information can be stored and returned very quickly to enable future development of the system. Where the system operates outside prearranged limit values the operator can respond very quickly. In the Gas Industry the term "monitoring" is prevalingly associated to the check of process parameters (pressure, flow rates, temperature, gas quality), of correct working of equipment (valves, compressors), and of alarm detection (intrusion systems). Synonyms: remote monitoring, remote reading.

Tele-metering is the transmission of readings of instruments to a remote location by means of wires, radio waves or other means (Ref. 2). In the Gas Industry the term "metering" is prevalingly associated to the supply measurements (m³ at contractual conditions). Synonyms: telemetry, remote metering, remote meter reading, automatic meter reading (AMR), remote reading, gas meter-reading system.

Tele-control is the control of any device by communication (Ref. 3). It is characterised by actions carried out by means of devices to direct and regulate a process or a sequence of events in a remote site.

Tele-control enables plant to be operated from a central point directly or indirectly via the operator. It allows also switching from a damaged to an efficient equipment if redundancy exists. In the Gas Industry the Tele-control is mainly used to vary the set up of the network in relation to operational needs (valves adjustment by means of actuators, actions on the anti-intrusion systems). Synonyms: remote control.

Tele-diagnosis is the set of structured measurements aimed at locating and explaining detectable errors or faults of equipment/plant placed in remote site. The diagnosis might be also realised with expert systems. The diagnosis can be carried out in the remote site with transmission of results to the headquarters or vice versa.

Tele-assistance are the activities led by an expert team in the headquarters, and carried out in the remote site by unskilled personnel.

Tele-repair is the restoration of unserviceable parts, components or assemblies in a remote site. It is peculiar to the software maintenance. The software installed on the remote sites is emulated in the headquarters, it is checked, modified and re-installed.

Tele-servicing is the supply of crafts, tools, materials and spare parts or supply of services by third parties on remote sites as consequence of a client request.

2. Difference Between Preventive and Predictive Maintenance [2]

Predictive maintenance tends to include direct measurement of the item. Example, mechatronic system for the measuring of the dimensional parameters. While **Preventive Maintenance** includes the periodical evaluation of the transducers and calibration status. The manufacturing company is telling you that the life span of the transducers is 3 years and calibration procedure must be initiated every 7 days. So just before expiring 3 years you have decided to replace the transducers with a new and scheduled for maintenance every 7 days for calibration. This is called **Preventive Maintenance**. Business developments also led to the development of the maintenance technology. The organization of the conduct of maintenance activities are aspects of location of the company, field of activity, characteristics of the means of production, etc. .. Systemic approach involves considering the following types of maintenance organization, which according to the resources and objectives, are designed to ensure optimal availability of technical systems, the Figure 2.1:

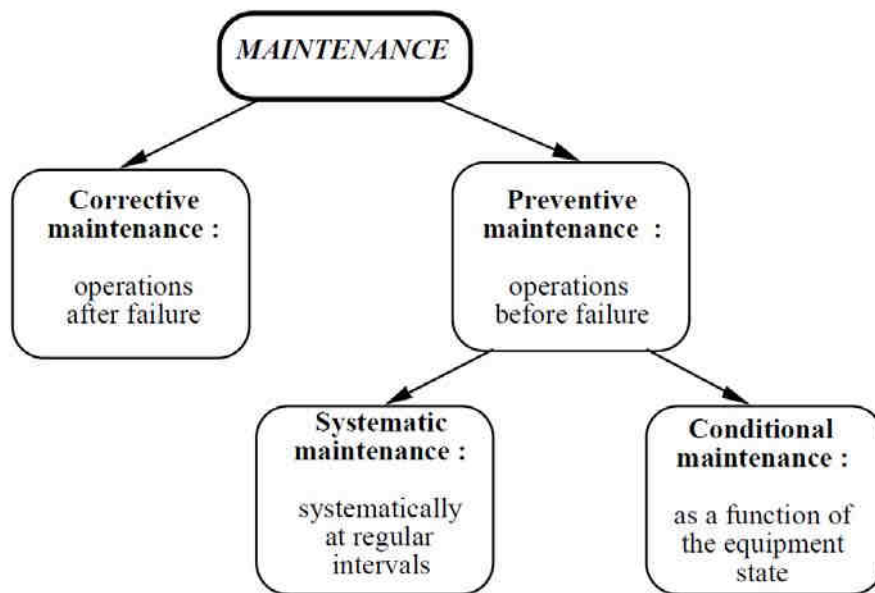


Figure 2.1 - Systemic approach of maintenance [4]

Prior to highlight the benefits of good maintenance activities performed, we show what are the main categories of losses in case of its neglect.

3. COMPLEX MECHATRONIC SYSTEM FOR MEASURING REVERSE MODULE ON AUTOMOTIVE INDUSTRY

The work refers to the modernization of an existing complex measurement systems in order to add functions and maintenance remote monitoring.

Complex measurement system performs dimensional inspection and marking function for one subassembly of an automotive system.

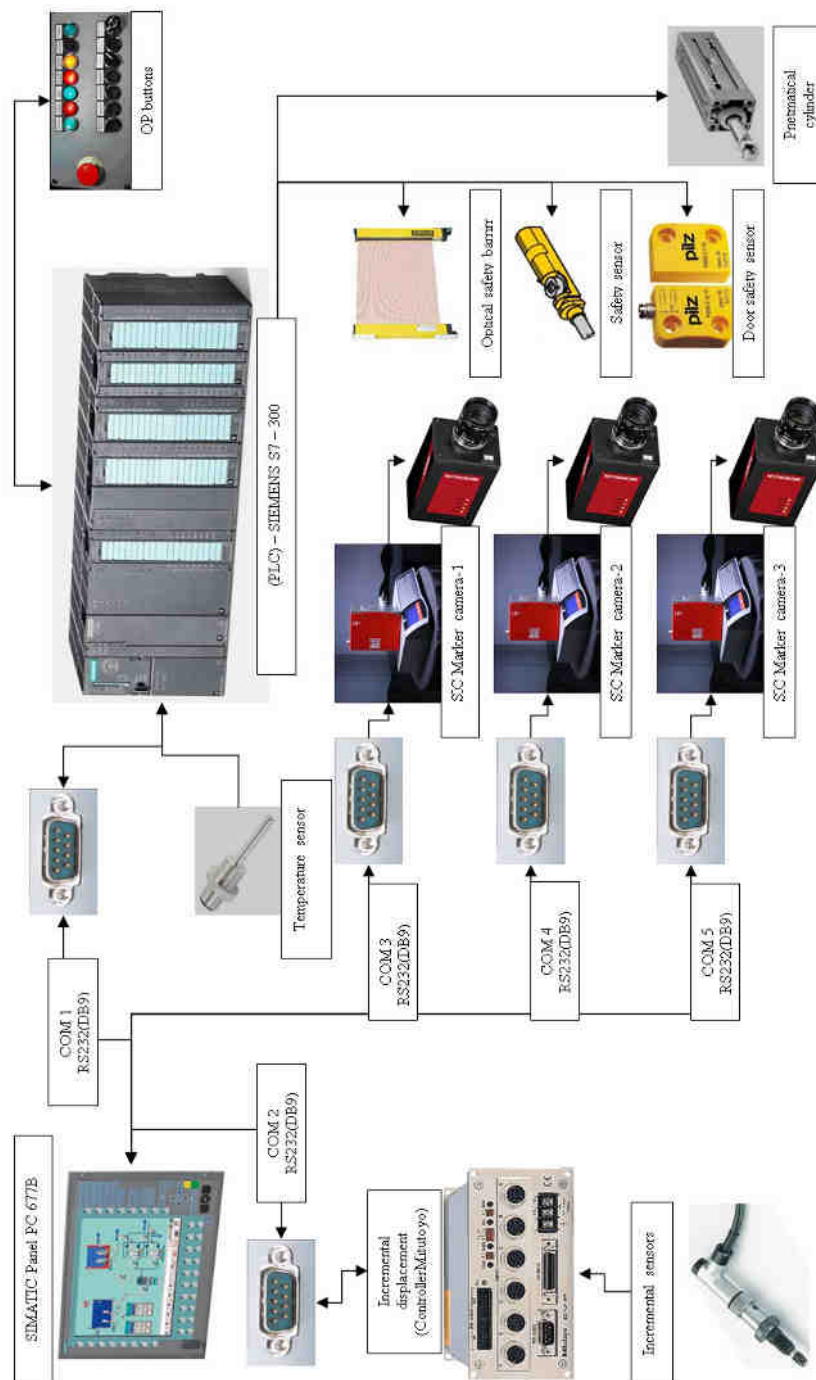


Figure 3.1 – The bloc diagram of the mechatronic system

The project proposes to examine existing technologies already implemented in the system and research aimed at identifying progress in the field, internationally and at home, and trends manifested in the design, evaluation and implementation of an annex for monitoring and remote control.

4. EQUIPMENT ARCHITECTURE

General block diagram of the equipment is shown in the following figure and it shows where the main functional modules and their relationship for a general characterization of how the achievement of key functions is done.

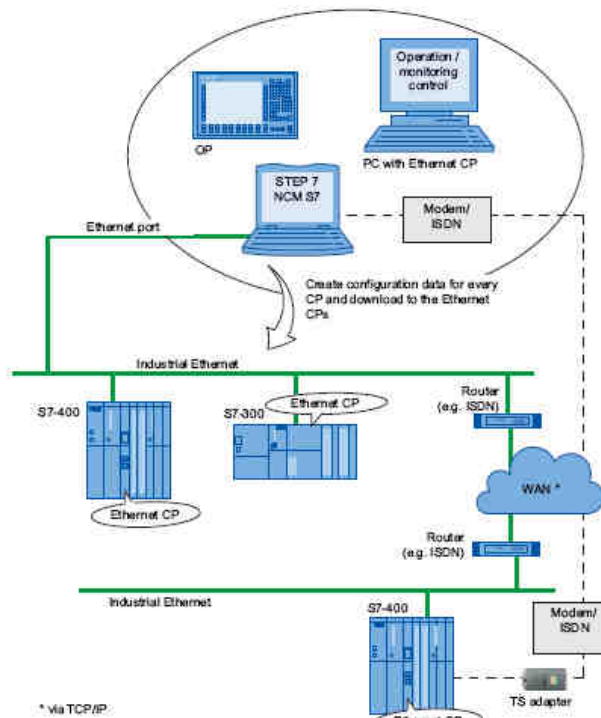


Figure 4.1 - SINAUT ST7cc control center system
Stations

5. SYSTEM DESCRIPTION

The machine plant showed in the Figure 5.1 allows the measurement of two sets of odds ITS modules and marking return if the values obtained is within the limits allowed. To do this, the system consists of three complex control points, with the following functions:

- at the first workstation cylindricity deviations are measured;
- at the second workstation spherical deviations are measured;
- at the third workstation it is evaluated if the previous measurement values are allowed and is impressed as a code matrix containing the series on each of the three components of the module (body, lid and sleeve) and as characters indicating the measured values.

The components of the system is showed in Figure 5.1:

1. Central unit: industrial PC – Siemens
2. IR protection safety barrier
3. Mechatronic intelligent point1 - head of complex dimensional control

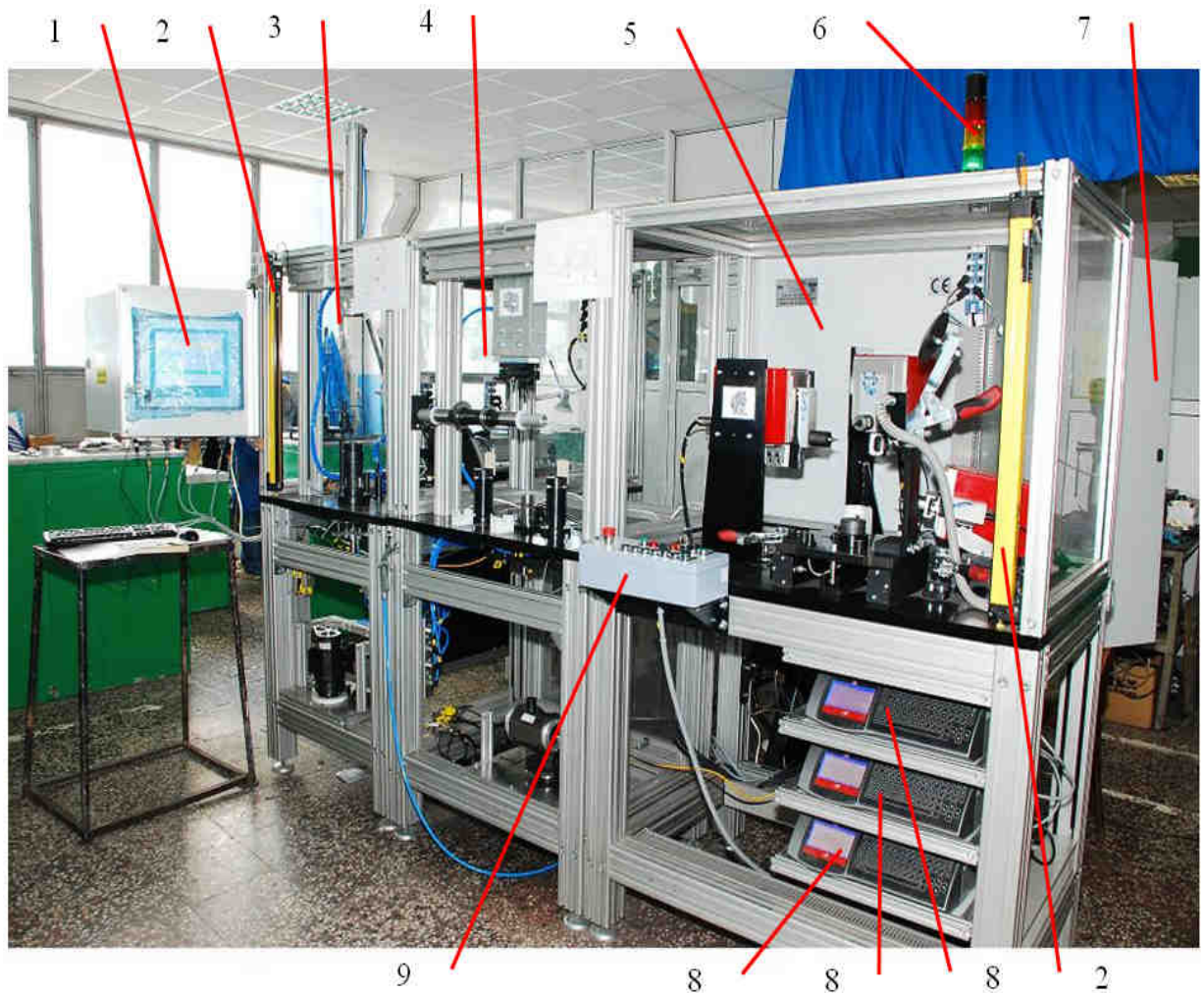


Figure 5.1 – The mechatronic system

4. Mechatronic intelligent measuring point 2 – axial dimensional control
5. Mechatronic intelligent point3 – Marker printer (matrix code)
6. Lighting column for signalling
7. Automation cabinet (PLC)
8. The marking central unit
9. Operator command box

Depending on the measurement results the piece is marked with a marking system equipped with video cameras for confirmation.

This complex mechatronic system is a dimensional control system equipped with a PLC that controls temperature sensors, optical barriers, position sensors for the drive system, sensors for closed doors and realizes the interaction between user and the dimensional control system through the operator panel.

For processing and transmitting data and system status, the system was completed with specialized equipment for data transmission through the network compatible with the industry standards.

Optical barriers and door sensors are used to provide user protection according to the rules imposed by EU Directives

For internet networking connection I use the Module IWLAN / PB PN IO – which can be installed on a standard DIN rail and antenna can be mounted using a connector. The module features are: protection type IP20, a jack 9-pin D-sub for connecting to PROFIBUS, a interface R-SMA antenna connection, the possibility of connecting an external link and LED status indicators.



Figure 5.2 - SIMATIC NET S7-300/400 - Industrial Ethernet

6. Data collection problems

The mechatronic system described above receives control signals through the network communication while in process data acquired by the sensors are all directed to controller via the network. With this topology, additional delays occur due to data transfer. These network delays can be classified in terms of the direction of data transfers as:

- Sensor delays – these delays are present in the direct path of the command.
- Delay times can be grouped, for ease of the analysis as a single time constant, called "control delay". Both delays introduced by the network can be smaller or larger than the sampling period T .

In the first case the process can be conducted under optimal conditions (assuming no lost packets).

In the second case, major problems of discontinuity of the management process may lead to unsatisfactory developments process.

From practically maintenance and telecontrol based on the main procedure showed in Figure 6.1 are proposed following steps [4]:

- To establish the dynamic characteristics of process-driven evaluation, including actuators and transducers in order to choose the sampling period and performance network-testing to be used in the monitoring of functionality.
- To establish the system parameters to be monitored
- To establish the maintenance protocol and priority.

As a result of implementation of the above steps three distinct situations of telemaintenance processes were identified.

Predictive indicators for systems parameters – including the measuring errors tendency and distribution

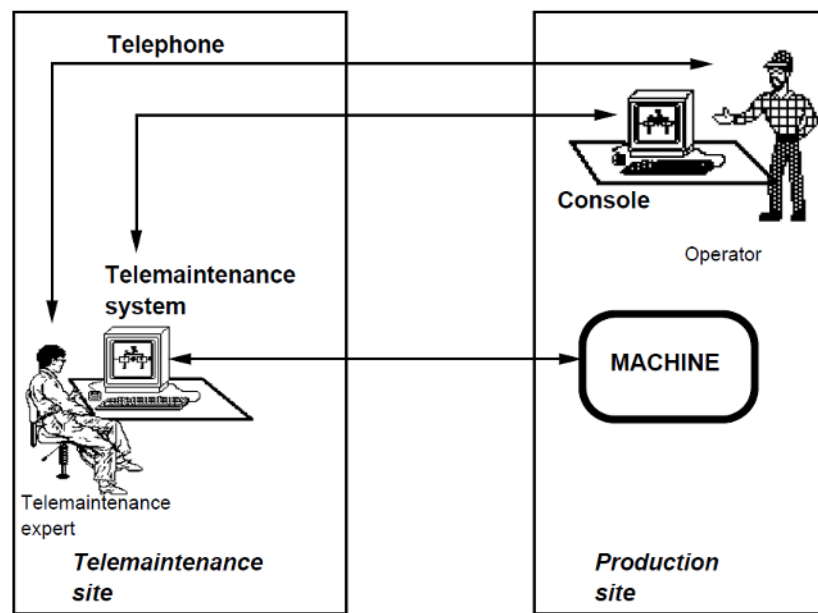


Figure 6.1 – The practically telemaintenance service [4]

7. Conclusions

Currently the telemaintenance systems are being developed and progressively installed on industrial sites. They are particularly interesting in the fields constituting some risks for the human beings, those fields where human intervention and/or the production stops are very expensive. Many operational systems are also found in "intelligent" mechatronic systems and in large remote telecontrolling mechatronic systems.

According to the competence and/or to the function of the operator at the production site, he may also have access to certain functions of the telemaintenance computing system, and may collaborate with the expert by telephone and a console (Figure 6.1). This last case is the subject of research. The operator who is on the production site is likely to perform some maintenance actions on the machine following expert instructions. Nevertheless, for certain repairs, the expert will probably need to go to the production site, or to send a specialist.

It is obvious that the telemaintenance system is integrated into man-machine system in which the characteristics and the tasks of the telemaintenance expert will have a direct influence on the successfully result of the project concerning the telemaintenance system design.

The designer of such telemaintenance systems will need to consider such notions.

REFERENCES

- [1] Battista L. - Pone E. - Theodorakis P. (2001) "Tele-Maintenance and Pipelines"; OMC 2001 - Offshore Mediterranean Conference; Session 13: Pipelines: Design, Installation, Operation and Maintenance; Paper N° 105/13A; pages 10; Ravenna - Italy; March 28-30, 2001.
- [2] http://en.wikipedia.org/wiki/Preventive_maintenance#Difference_Between_Preventive_and_Predictive_Maintenance
- [3] <http://support.automation.siemens.com>
- [4] Christophe KOLSKI, Patrick MILLOT, HUMAN PROBLEMATICS OF TELEMaintenance AND DECISION AID CRITERIA FOR TELEMaintenance SYSTEM DESIGN, Part of this paper was presented at Annual Industrial Ergonomics and Safety Conference, Denver, Colorado, 10-14 June 1992 (Kolski and Millot, 1992).

MECHATRONIC SYSTEM FOR WINDING ROLLED WIRE

PhD. Student Eng. Ioana ILIE¹, PhD. Eng. Marian BLEJAN¹,

Assoc. Prof. PhD.Eng. Constantin RANEA²

¹Hydraulics and Pneumatics Research Institute –INOE 2000-IHP Bucharest, ilie.ihp@fluidas.ro

² “POLITEHNICA” University of Bucharest, ROMANIA, constantin.ranea@ancs.ro

1. Introduction

The mechatronic system for winding rolled wire ensures wire stringing on spool coil by coil, by controlling movements of the debugger head, adapting itself to changes in spool rotational speed; spool rotational speed is dictated by the rolling process parameters and also the wire load of the spool, that is diameter of the coil being wound.

The mechatronic system presented contains an electro-hydraulic linear axis consisting of a bilateral rod hydraulic cylinder, on its liner being located the debugger head, controlled with a proportional flow distributor, transducers monitoring spool rotational speed and the speed of the debugger head, electronics necessary for interfacing the execution elements and transducers with the programmable controller (the PLC), the PLC running a software application that implements the functionality of the mechatronic system, and also two data communication lines, one serial RS485 line with MODBUS protocol implemented and one Ethernet line, that allows connection to TCP / IP networks, on which MODBUS protocol is implemented.

2. Presentation of the mechatronic system

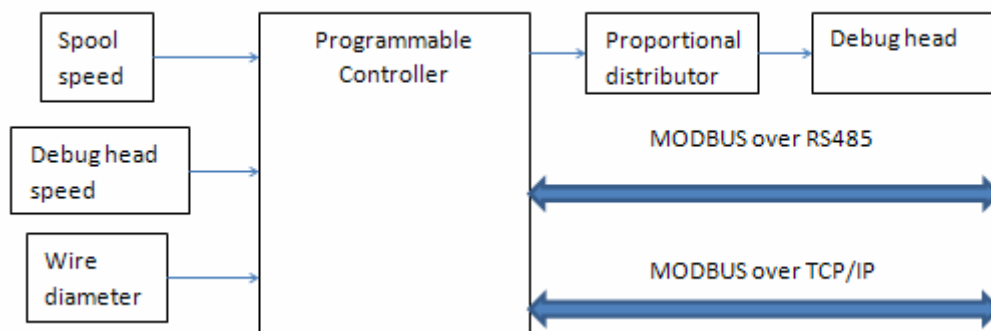


Figure 1. Functional block diagram of the mechatronic system

In fig. 1 is shown the functional block diagram of the mechatronic system. The value of spool rotational speed is measured with spool rotational speed transducer, incremental encoder type, providing pulse electrical signal, 500 pulses per complete rotation of the spool. This transducer, along with the frequency meter software implemented in the programmable controller, allows calculation of spool rotational speed, value that will be used by the running algorithm, implemented in the PLC, to calculate the desired speed of the debugger head.

The actual speed value of the debugger head is measured with the transducer for debugger head speed, type wired incremental encoder, providing an electrical signal type pulse every 0.1 mm. This transducer, along with the frequency meter software implemented in the

programmable controller, allows calculation of actual speed of movement of the debugger head.

Another important parameter required for achieving synchronization between debugger head movement and spool rotational speed is the wire diameter value, which is entered by the operator via the local console of the PLC or, by means of the communication lines RS485 and TCP/IP, this parameter is entered by using the programming software of the PLC running on a computer within a network.

The proportional distributor controls flow through the bilateral rod hydraulic cylinder, cylinder which drives the debugger head; the electric control proportional to the flow is calculated by the PLC via an automated Proportional-Integrative regulator, which compares the desired speed value, value calculated as the product between wire diameter value and spool rotation speed value, with the debugger head speed value, actual speed value measured using the wired incremental encoder.

Interfaces with data communication networks, namely the master-slave network implemented on RS485 communication line and the TCP/IP network implemented on Ethernet line, allow monitoring and parameterization of the mechatronic system through a programming software application of the PLC, software running on a networked PC.



Figure 2. Winder of the rolling mill

In fig. 3 (a, b) is shown the operating software of the PLC in a "ladder diagrams" format. The software implements the start-up of the engine inside the hydraulic unit without load, following that after reaching the operating rotational speed of the engine to be directed entry into load, i.e. incurrence of hydraulic pressure. The software also implements measurement of the spool rotational speed and the value of the movement speed of the debugger head using two frequency meters. Values of the two frequencies are scaled and compared by an automated regulator which implements a control algorithm type Proportional-Integrative; the value present at the output of the automated regulator is applied to the proportional distributor controlling the flow in hydraulic cylinder, flow whose value is proportional to this command. The debugger head, mounted on the hydraulic cylinder liner is equipped with two proximity sensors providing the PLC the information that either of the two ends of spool was reached; the operating software of the PLC uses this information to switch the active field of the proportional distributor, directing hydraulic oil distribution via the path P-> A, B-> T or via the path P->B; A->T, thus determining the displacement direction of hydraulic cylinder.

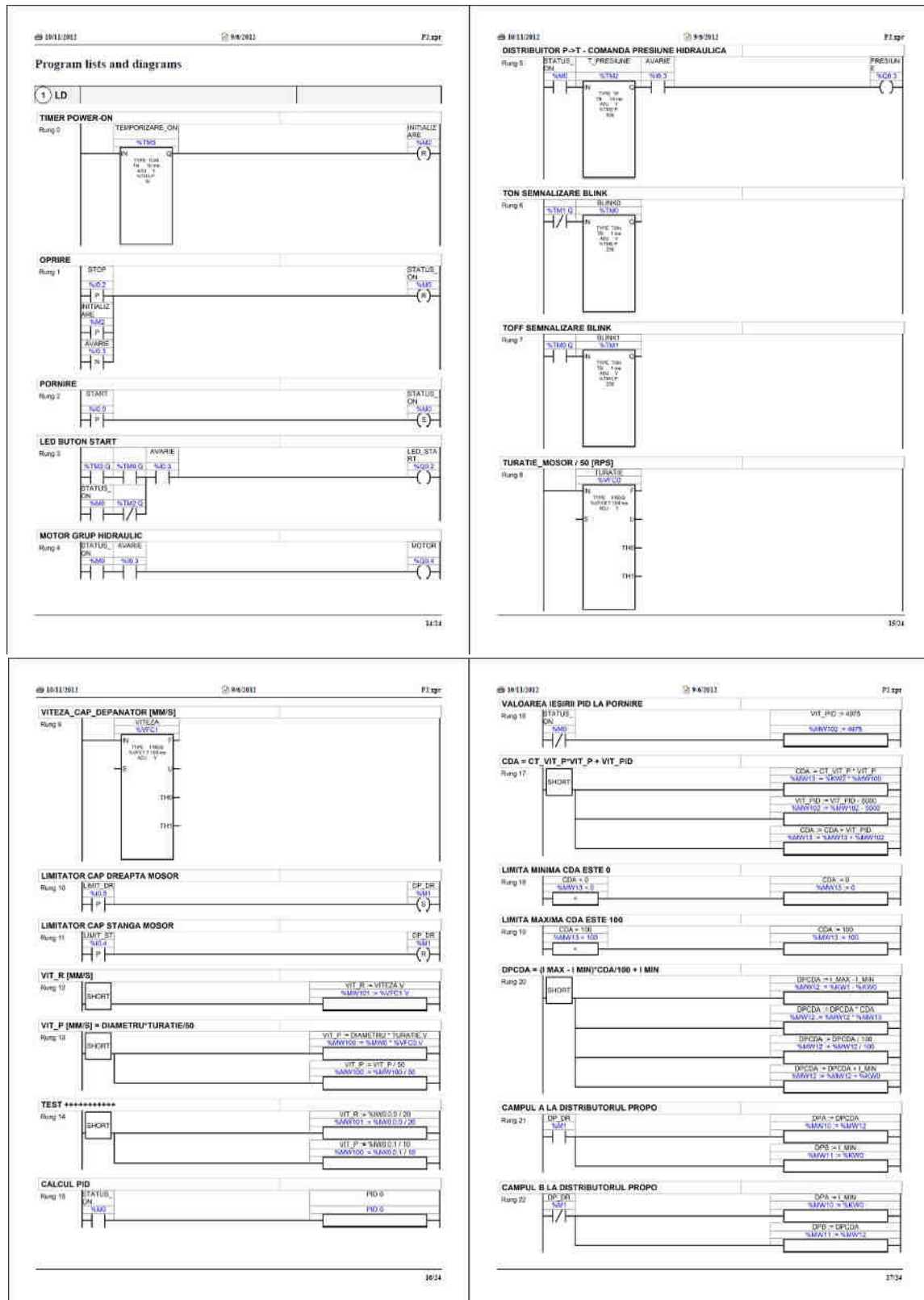


Figure 3. Listing of the PLC operating software in a "ladder diagrams" format

3. Conclusions and original contributions

The current solution for actuating the debugger head of the rolling mill winder requires synchronization in open loop of spool rotational speed with debugger speed; the approach proposed in this material requires monitoring of the spool rotation speed value and the value of the debugger speed, actuation of debugger head being carried out in closed speed loop, the speed being calculated based on the diameter of the wire being wound and spool rotational speed value; this approach reduces by at least an order of magnitude the positioning errors of debugger head compared to its actuation in open loop. Another advantage of the proposed solution is the integration of debugger actuation in an IT system, by providing it with data communication lines, enabling centralized monitoring and parameterization of this system and also logging of events occurring in its operation and functioning.

Original contributions made by the authors refer to achieving a speed control loop of a hydraulic cylinder using a general purpose PLC, use of a transducer type wired incremental encoder to monitor the value of the hydraulic cylinder drive speed and integration of these components into a complex mechatronic system which can be interfaced with the IT system of the beneficiary by means of the two data communication lines.

REFERENCES

1. Marian Blejan, Petrin Drumea, Ioana Ilie – "Mechatronic module for monitoring the hydraulic parameters of industrial equipment", International Conference 6th Workshop on European Scientific and Industrial Collaboration on promoting Advanced Technologies in Manufacturing WESIC'08 Bucharest, 25-26 September 2008
2. Marian Blejan, Bogdan Lupu – "Data Acquisition and Control Unit for Electro Hydraulic Applications", ISSE 2009 Conference, Brno, Czech Republic on May 13-17, 2009
3. Marian BLEJAN, Ioana ILIE and Mircea COMES - "A mechatronics approach to hydraulic drive for applications in robotics", ISBN 978-1-84626-xxx-x Proceedings of 2010 International Conference on Optimisation of the Robots and Manipulators, Calimanesti, Romania, 28-30 May, 2010
4. Marian Blejan, Petrin Drumea, Mircea Comes - "Integration of the Hydraulic Linear Axes in a Computerized System" 3rd International Conference on Innovations, Recent Trends and Challenges in Mechatronics, Mechanical Engineering and New High-Tech Products Development, 22 - 23 September 2011, Bucharest, Romania – MECAHITECH 2011
5. PhD. Eng. Marian BLEJAN, Prof. PhD. Eng. Petrin DRUMEA, Prof. PhD. Eng. Mircea COMES - "MULTI-TIER APPLICATIONS FOR MONITORING AND CONTROLLING OF HYDRAULIC AXES" - Proceedings of 2011 International Salon of Hydraulics and Pneumatics - HERVEX, 9-11 Nov. Calimanesti-Caciulata, Romania. ISSN 1454-8003

SCIENTIFIC STRATEGIES AND METHODS OF ADAPTRONICS APPROACH, AS KEY TECHNOLOGY FOR FUTURE

GHEORGHE I. GHEORGHE¹

¹ INCDMTM, incdmtm@incdmtm.ro

Abstract: *This paper deals with strategies and scientific methods of approaching of Adaptronics as key technology for the future, which will facilitate systems and high-tech micro-systems performance and know-how, and the relevance of most businesses of higher competitiveness.*

Approach of Adaptronics was possible only because of **Mechatronics** and **Integronics** innovative developments, **becoming active technology vector, structural and practical in most industries and hyper-intelligent products and systems**, in technological purposes for evolutionary development of intelligent cybernetic manufacturing.

Keywords: adaptronics, mechatronics, integronics, hyper-intelligent systems, key technology for the future

1. Introduction

Scientific strategy for design - realization - implementation of Adaptronics as part of the key technology for the future facilitates performance and know-how for systems and high-tech micro-nano-systems engineering and relevance to most businesses.

Therefore, **Adaptronics and Adaptronics application**, follows as advanced technology, as an intelligent innovative and multidisciplinary technology that brings together synergistically scientific discoveries news related to fundamental and applied knowledge in **integronics and mechatronics science, intelligent structural mechanics science, intelligent materials science, intelligent architectural science of sensors and actuators, intelligent measurement and integrated control science, as well as computer and informatics science**.

Adaptronic strategy follows as high-tech products, new and highly competitive products and systems that facilitate both performance and creation and evolution of know-how, adds active structural and applicable technological vector for technological purposes of change, improvement and sustainable development and developer vector for changing operating method of environment requirements and influencing and monitoring of all structures of any kind.

Moreover, the success of Adaptronics and adaptronic strategy is guaranteed by cooperating between many different scientific and technical disciplines, between technology and industry and between research-innovation and industrial application and commercial innovation, on national and international markets, supporting intensive technology transfer, information and knowledge to a competitive and with a high level of labour employment.

In brief, **Adaptronics and Adaptronic strategy** create and form an important international platform for key technology for the future, new adaptronic active technologies, structurally applicable in developing innovative products and systems, a new operating mode for change, a new construction of structures of any kind, a new approach to monitoring and influencing, a new form of energy recovery, a new real modelling of real-time control of phenomena and their effects, and a new implementation of competitive and highly competitive products and systems as a direct response to the more growing and changing needs.

The research and approach of this paper in the scientific strategies of adaptronics field, refers to the intelligent domain of mechatronics, integronics and adaptronics regarding intelligent systems for measuring, verifying, control integrated in intelligent manufacturing processes (ex. automotive industry and metrology).

2. ADAPTRONICS design

2.1. Optimization and Adaptability of mechatronic and integronic technologies and systems

By **optimization and adaptability of mechatronic and integronic systems and technologies** is synthesized the first concept of **adaptronic design**, through which is realized the modelling and simulation of parameterized applications and appropriate for structures and functions in order to meet measurable objectives and quantified requirements and corresponding to processes for all problems and solutions.

The **typical design variables** are expressed in properties that define stiffness, by the typical control variables **are represented gain factors** and actuator/sensor **system-specific properties**, while **goals are related to structural mass** and control subsystems, of desired power, of full time response values, etc.

In terms of **techniques for solving optimization problems** is often used an **overall strategy** appropriate to deal with problems coupled structurally and of optimal control, such as:

- addressing fully coupled problem and solving problems simultaneously;
- using a decomposed or assembled approach, where an optimal structural design with constraints for achieving a good performance is performed first, followed by the design of optimal control with optimal constraints for consideration of structural requirements and followed possibly by a optimal structural design;
- heuristic decomposition method;
- mathematical techniques with and without optimization algorithms;
- etc.

The new concept mentioned, also calls for a **package of software** related to **simulation of mechatronic and integronic systems, optimized and adjusted**, which can be considered as representative, but not complete.

Many parts of the software package, participate in this new concept, for the **dynamic and static analysis** of optimized and adapted systems to determine frequencies and their own states, for multi-structural and multi-functional assemblies to reduce patterns, and for modal or condensed representations, including certain models of sub-systems.

Thus, in the software package, are observed programmes that are used in enhancing and adapting technical and technological systems, such as ANSYS, MATLAB, SIMULINK, etc.

By combining design software packages with industrial and commercial software packages, is offered a wide range of data acquisition and processing capabilities combined with graphical user interfaces in an engineering perspective on the future adaptronic system.

2.2 Technological and constructive adaptive fusion of mechatronic and integronic systems for industrial and commercial use

Through the **technology and constructive fusion adaptive to mechatronic and integronic systems** is synthesized the second **adaptronic construction concept**, which is made and assembled as a synergistic combination of technical and technological solutions in mechanical engineering, electronics and information and respectively it is carried the material, structural and functional integration, of mechatronic and integronic components and sub-systems in a systemic mini-structural multi-functional and multi-adaptive compact whole.

With this new adaptronic concept, it is built a new inter-disciplinary mix compendium of several areas of engineering and intelligent manufacturing that supports the information revolution that marked the "intelligent switch" from post-industrialized society to information society.

This adaptronic concept uses the replacement of functional, structural and technological variables with new, optimized or upgraded variables, to complement other design variables, real-time response, efficiency, selection, metrological and technological parameterization, prevention defects, continuous evaluation of the adaptronic systems effects, etc.

In this context, **the aggregate of variables considered**, expresses in fact, the defining and behaviour of components and sub-systems resulted from applying the new adaptronic concept, characterizing the properties, the new functional and structural links, intelligent control of structural chain and of sensor-actuator system, any constraints occurring in the system and other phenomena caused directly or indirectly by any work environment of adaptronic system.

Adaptronic concept of technological and constructive fusion, adapted to mechatronic and integronic systems, synthesizes the full technical, technological, functional and decisional potential integrated in intelligent assemblies and always adaptive to new working and environment conditions, both by self-changing or self-implementing as:

- Innovative mechatronic and micro-mechatronic adaptronic ensemble (Figure 1)
- Innovative integronic and micro-integronic adaptronic ensemble (Figure 2)
- Innovative sensor/actuator and micro-nano sensor/actuator adaptronic ensemble (Figure 3)
- Innovative robotics and micro-nano-robotic adaptronic ensemble (Figure 4)
- Innovative mechatronic adaptronic integronic human adaptive ensemble (Figure 5)
- Adaptronic innovative ensemble (Figure 6)

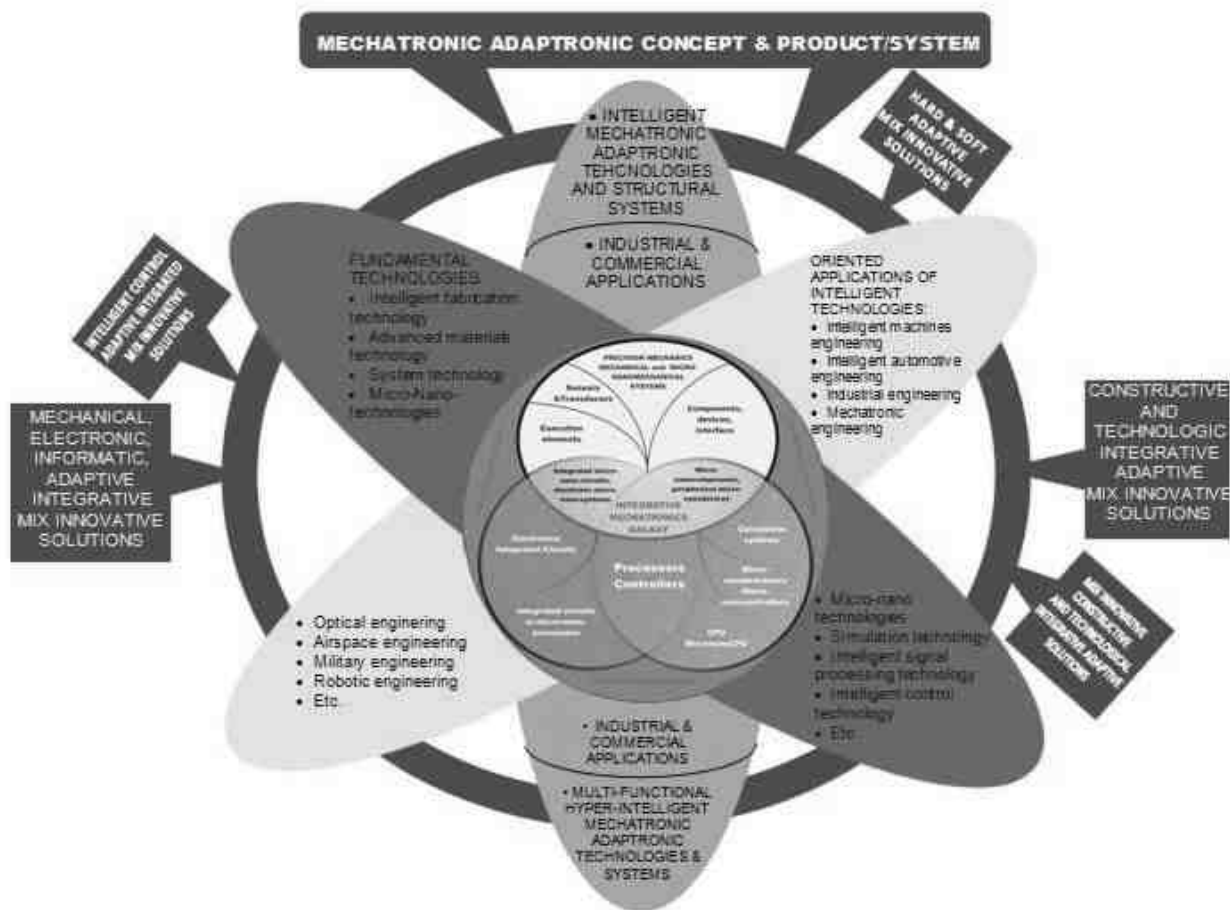


Figure 1. Innovative integronic and micro-integronic mechatronic ensemble

According to the figure mentioned: innovative mechatronic and micro-nano-mechatronic adaptronic ensemble (Jacobs, 1997), as advanced and high-tech domain and as intelligent engineering, fusions synergistically and merging structural / material / technical / technological / operational and decisional the advanced mechatronics and micro-nano-mechatronics with adaptive mix-innovative solutions and constructive adaptive technology, mechanical, electronic and computer, hardware and software and intelligent control, this assembly uses innovative technology integrating core of intelligent manufacturing, advanced materials, systems, micro-nanotechnologies, simulation and modelling, intelligent signal processing, intelligent control, and so

INTEGRONIC ADAPTRONIC CONCEPT & PRODUCT/SYSTEM

INTEGRONICS
MICRO-INTEGRONICS
NANO-INTEGRONICS

FUNDAMENTAL TECHNOLOGIES

- Intelligent simulation technology
- Advanced materials technology
- System technology

ORIENTED APPLICATIONS OF INTELLIGENT ADVANCED TECHNOLOGIES:

- Industrial engineering
- Intelligent machines engineering
- Intelligent automotive engineering
- Integrative engineering
- Optical engineering

INTEGRATIVE ADAPTIVE CONSTRUCTIVE & TECHNOLOGICAL MIX INNOVATIVE SOLUTIONS

INTEGRONIC ADAPTRONIC MULTI-FUNCTIONAL HYPER-INTELLIGENT TECHNOLOGIES & SYSTEMS

INDUSTRIAL & COMMERCIAL APPLICATIONS

INTEGRONIC ADAPTRONIC TECHNOLOGIES AND STRUCTURAL SYSTEMS

EXTERNAL SOLUTIONS:

- HARD / SOFT ADAPTIVE MIX INNOVATIVE SOLUTIONS**
- INTELLIGENT ADAPTIVE MECHANICAL, ELECTRONIC, INFORMATIC, INTEGRONIC MIX INNOVATIVE SOLUTIONS**
- EXPERT & DIAGNOSTIC INTEGRATIVE MIX INNOVATIVE SOLUTIONS**
- HOLONIC DECISIONAL MIX INNOVATIVE SOLUTIONS**
- INTELLIGENT CONTROL, INTELLIGENT ADAPTIVE MIX INNOVATIVE SOLUTIONS**
- INTELLIGENT ADAPTIVE CONSTRUCTIVE & TECHNOLOGICAL MIX INNOVATIVE SOLUTIONS**

According to the figure mentioned: innovative integronic and micro-nano-integrionic adaptronic ensemble (Flemming, 1997) as advanced and high-tech field and as intelligent and hyper-intelligent engineering, merges and integrates synergistic - material / structural / technical / technological / functional / coordinator / decision and transport Information , the high-tech domain of Integrronics and Micro-Nano-Integrronics with mix-innovative solutions constructive adaptive and technological, integrative, mechanical, electronic and informatics integronic intelligent, integrative hard and software, integrated intelligent control, integrated expert diagnosis, this synergy and integration use innovative fundamental smart technologies of advanced materials, fabrication intelligent systems, micro-nanotechnologies, simulation, intelligent processing, signal, intelligent control, and so on, the results of this synergy of advanced high-tech areas are systems and intelligent technology multi-functional structured hyper-intelligent adaptronic integronic, applications of these results are identified in industrial engineering, smart cars, adaptronics, optics, aerospace, military, micro-nano-robotics, adaptronics, and so on; applications of results for the innovative domain integronic and micro-nano-integrionic adaptronic - systems and intelligent technology multi-functional structural and micro-nano-integrionic hyper-intelligent adaptronic integronic are found in industrial and commercial environments, the information society now and in the future.

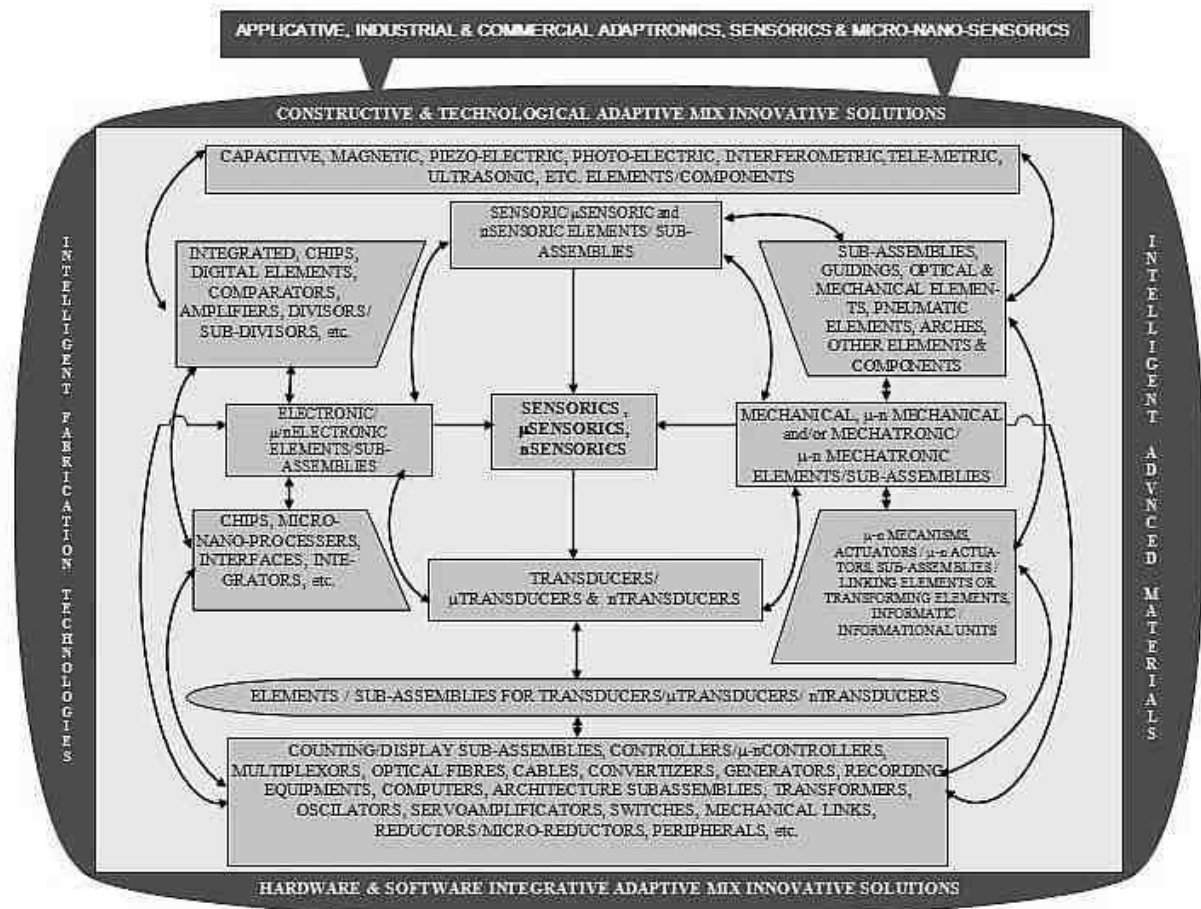


Figure 3. Innovative sensor/actuator and micro-nano sensor actuator adaptronic ensemble

According to the figure mentioned: Innovative sensor/actuator and micro-nano sensor / actuator adaptronic ensemble, as intelligent and high-tech domain and as advanced engineering, fusions architectural and combinative - structural / material / technical / technological / decision making and informational, advanced domain of sensorics and actuators and micro - nano-sensorics and micro-nano-actuators, the solutions mix - constructive and technological innovative adaptive and mix solutions - innovative integrative adaptive hardware and software, this architectural fusion and combination use integrated intelligent manufacturing technologies and advanced smart materials, the results of these mergers is architectures integrating sensory system matrix and assembled actuator subsystem implementations in products and systems for intelligent manufacturing processes in the economy and industry applications of these results are found in many industrial and commercial environments.



126

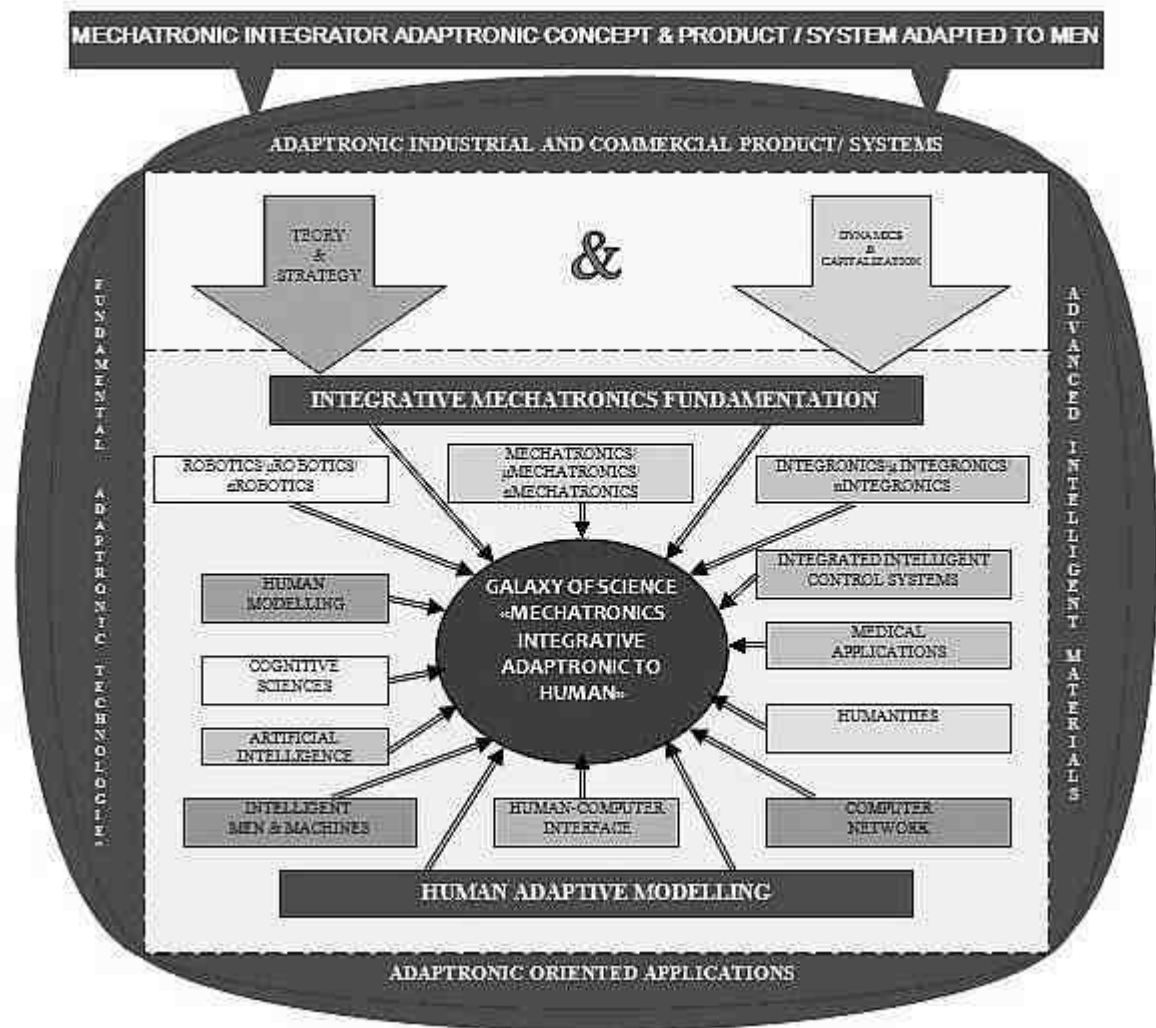


Figure 5. Innovative mechatronic adaptronic integronic human adaptive ensemble

According to the figure mentioned: Innovative mechatronic adaptronic integronic human adaptive ensemble (Gheorghe et. al, 2012), as intelligent high-tech domain and as advanced intelligent engineering, fusions structural, functional, decisional and informational, high-tech domain of mechatronic integronic adaptronic products human adaptive with solutions mix - constructive and innovative adaptive and technology adaptive and solutions mix - innovative adaptive hardware and software technologies; this fusion structural - functional - decision - information using intelligent manufacturing technologies and micro-nano-manufacturing technologies and intelligent materials and advanced intelligent smart micro-nano advanced materials; results of this mix fusion are mechatronic products and systems adaptronic integronic adaptive to man with industrial uses, multiplication and implementations in manufacturing, processing and commercial applications; applications of these results can be found in the economy, industry and society, with direct effects on economic life - social, now and in the future.

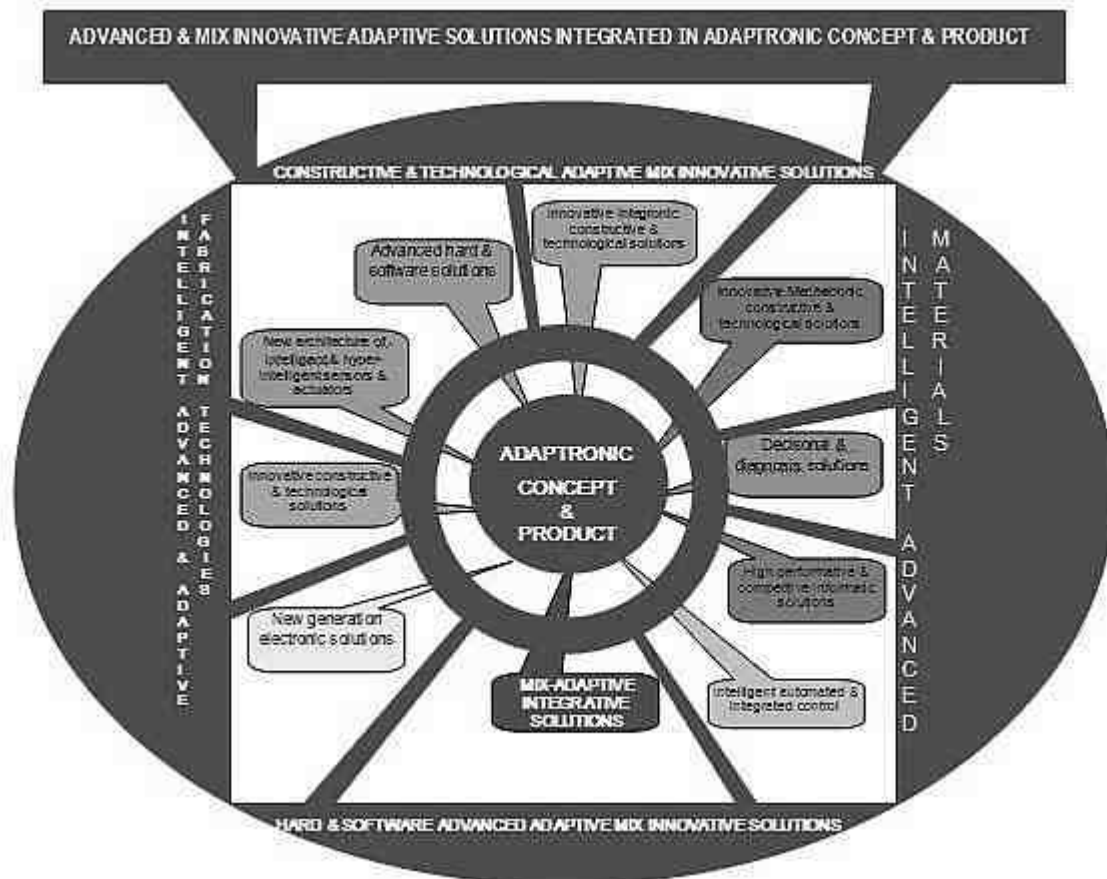


Figure 6. Adaptronic innovative ensemble

According to the figure mentioned: adaptronic innovative ensemble (Gheorghe et. al, 2011), as intelligent and hyper-intelligent advanced field, as sophisticated and high-tech field as intelligent and hyper-intelligent engineering, fusions synergistically and combinative, technical and technological, structural and functional, decisional and informational advanced sophistication domain of adaptronics built on integrative fields of mechatronics and integronics with mix-innovative solutions technological and constructive integrative adaptive, adaptive mix - intelligent integronic innovative solutions, adaptive mix innovative adaptive intelligent mechatronic solutions, solutions mix - innovative mechanical / electronic and adaptive integrative, solutions mix - innovative smart integronic adaptive, mix solutions - innovative adaptive and intelligent control solutions integrated mix of innovative hardware and software performance and highly competitive, this synergistic fusion and high combination of adaptronic use basic technologies such as intelligent manufacturing technologies, structural mechanics, systems, micro-nanotechnology, sensors and actuators architectures, advanced materials, signal processing, intelligent control, and so on, the results of this merger are highly combinative adaptronic structural and multi-functional products and intelligent hyper-intelligent adaptronic systems, applications of these results are identified and used in engineering-smart cars, smart advanced materials, smart car, medical, mechanical, mechatronic, integronics, optical communications, robotics, and so on; these applications are numerous in industrial and commercial environments, now and in the future information society.

3. ADAPTRONICS – key technology for the future

Adaptronics – key technology for the future, is based since 2000, on **Mechatronics and Integrative Mechatronics and Integronics**, when it was designed and implemented as **advanced high-tech field**. **Adaptronics** - is an **innovative intelligent and multi-interdisciplinary technology** that brings together synergistically inter-disciplinary scientific discoveries news related to fundamental and applied knowledge in the science of structural

mechanics, materials science, sensors and actuators architectural science, the science of measurement and intelligent control as well as computer and information science. **Adaptronics as key future technology** facilitates both the **performance and the know-how of mechatronic and integronic, micro and micro-nano-integrionic nano-mechatronic systems and micro-systems and development of products and systems and competitive products**, being found more and more effective in relevance to most businesses. Thus, Adaptronics is reflected both as a new technology for the future as well as products and systems for new, intelligent informatic products. **Adaptronic design and application were possible** only because of innovative developments of Mechatronics, Integrative Mechatronics and Integrronics potential providing future improvements and significant upgrades of technologies and systems for the advanced high-tech field. **Currently, Adaptronics - as new concept for the future** - is the best science and the best new area for national and international markets and industries particularly: aerospace, automotive industry, railway technology industry, shipping industry, medical technology industry, acoustic industry, industrial measurement technology and automatic intelligent control integrated mechatronic measurement industry, mechanical industry, process industry, engineering industry manipulation and automation of production. In the scientific development of the **descriptor: <<Adaptronics>>** is added the **structural active and applicable technological vector** in most industries and **system innovative vector of products, intelligent materials, intelligent sensors and actuators and measurement control and regulation functions, all in changing, improvement and evolutionary development technological purposes**. Therefore, **Adaptronics – as vector for developing new in the high-tech advanced domain** by adapting complex scientific, conceptual / structural / functional and decisional structures, products, systems and technologies, can be **used to change the operating environment requirements to actively control vibration, noise and distortion, to recover energy from vibrating systems and mechanical inertia and influence and monitor** all structures of any kind. In addition, **Adaptronics** will allow the **new design of mechanical and integronic systems and a new potential for improving and upgrading the technical performance** of products and systems as well as of the extended profile of products and systems. **Adaptronics - a new science, was designed and developed** for the first time in the world in **Germany** by Fraunhofer, since **2000** and **gradually more European countries** have began to modernize and develop this advanced high-tech field and **especially countries that have developed and applied mechatronics, Integrative Mechatronics and Integrronics**, among these countries being **Romania** by the **National Institute of Research - Development in Mechatronics and Measurement Technique - INCDMTM Bucharest**, which has already created an **<<Adaptronics Centre>>** since 2010. In this respect, INCDMTM, **works since 2010 in the development and implementation of "Adaptronics"**, with more involvement in intelligent measuring engineering and particularly in intelligent mechatronic and integronic measurement and integrated control system in the intelligent car industry, by designing adaptronic systems and equipment in new and with much improved structural and functional architecture, and with much improved technical performance and technology. Therefore, **there is the belief that this new " adaptronic technology " is of major importance** for the implementation of competitive and hyper-intelligent products, and **is necessary to meet** growing and changing requirements of modern and improved new systems and products, at the same time with developing the smallest and largest possible and more efficient flexibility. In fact, the success of **"Adaptronics" is guaranteed** by the cooperation between many different scientific and technical disciplines and expertise in science, technology and industry and **is understood by** a leading research unit and oriented towards applications as is INCDMTM in Romania.

The further expansion of "Adaptronics" in INCDMTM and Romania, in Europe and in the world market, will focus on the integrative dialogue between research - development - innovation and industrial and commercial application.

Currently, **Adaptronics** - as an inter-multi-disciplinary science, is dynamically expanding, including significant national and international markets, branch industries and in particular mechanical process industry, mechatronic and integronic industry, aerospace industry, medical technology industry, automobile industry, etc.

As innovative science, **Adaptronics** intensively supports and transfers technology, information and knowledge, leads to competitive growth and increased level of employment.

As science vector, **Adaptronics** creates and forms a major "international key adaptronic platform technology for the future."

As an integrative synthesis, structural **Adaptronics is an active technology** - applicable in most branches of industry, **it is an opening of completely new possibilities** for the development of innovative products and basic innovative systems, **it is a new change in operating mode, it is a new construction** of structures of any kind, **is a new approach** to monitoring and influencing, **it is a new form of energy recovery** from mechanical energy and inertia, **is a new active control modelling of real phenomena** and their effects, **it is a new design** of mechanical systems, **it is a potential of new products and systems** to improve performance and extend their profiles, **it is a new implementation** of competitive and highly competitive products and systems, **it is a direct response** to the ever growing and changing demands, **it is the lowest time lowest** for adaptronic development, **it is the optimal cooperation** between multi-and inter-disciplinary experts in science and industry and **it is a complex interaction** between research - innovation and transfer and commercial application. However, **Adaptronics, develops the latest solutions for systems with adaptronic components as well as the latest trends in the advanced high-tech field.**

4. Conclusions

Adaptronics, as a scientific strategy and an integrative multi-inter science, is used as a cutting edge opening new possibilities for design, construction and implementation of innovative adaptronic products and systems, a new approach to monitoring complex interactions and cooperation in the value chain of research - innovation - technology transfer - industrial and commercial application.

REFERENCES

- [1] G. Gheorghe, I. Stiharu, "NanoEngineering", Cefin Publishing House, Bucharest, 2011
- [2] G. Gheorghe, S. Istrateanu, "Adaptronic microtechnologies nanometer micromechatronic regarding nanosystems for micro and nano positioning displacements", 8th International DAAAM Baltic Industrial Engineering, Tallin, Estonia, 2012
- [3] E. Flemming "Tactile sense in minimal invasive surgery: the tamic-project. mst news", vol 19, VDI / VDE, p.13
- [4] R. Jacobs "Control model of human stance using fuzzy logic", Cybern Biol. 77 (1), pp. 63-70
- [5] A. Trasher "Safe adaptive neuro-fuzzy control of neural prostheses using reinforcement learning", pp. (CD-ROM version) 18 / IEEE Conf IEEE EBMS Amsterdam, PT

FLOW ASPECTS THROUGH HYDRAULIC RESISTANCES

Ioana Carmen SFÂRLEA¹, Florin BODE², Dan OPRUȚA³

¹ Technical University of Cluj-Napoca, Department of Mechanical Engineering, Ioana.Sfarlea@termo.utcluj.ro

² Florin.Bode@termo.utcluj.ro

³ Dan.Opruta@termo.utcluj.ro

Abstract: *The paper presents a flow analysis through hydraulic resistances with cylindrical spool and sleeve with circular orifices. A comparative flow study was performed on two models with the same geometric characteristics, having different command openings. From this point of view velocity and pressure fields distribution was considered. The analyzed aspects were flow regime and cavitation phenomenon appearance.*

Keywords: *hydraulic resistance, velocity field, pressure field, cavitation*

1. Introduction

Hydraulic systems have emerged and developed rapidly, mainly due to the need to adjust the high and very high forces with a high precision, while they allow position and speed control for the default load. The paper refers to hydraulic resistances with cylindrical spool, these being most often used in proportional hydraulic equipment, namely to the ones having sleeve with orifices. This type of hydraulic resistances allows a better flow control, due to the fact that although the command spool's opening is larger, the flow section remains small.

The objective of the study is to optimize the geometric configuration of the orifices in the sleeve, in order to achieve turbulent flow regime, low values for hydrodynamic forces and, if possible, to avoid cavitation in small command openings. Regarding this, CFD (Computational Fluid Dynamics) numerical analysis helps by visualizing the flow and the phenomena that occurs during flow, without actually completing the model.

The paper presents a comparative analysis of flow in two hydraulic resistance models with cylindrical spool and sleeve with circular orifices. For the first model a sleeve with 6 circular orifices was chosen, having a 6 mm diameter (figure 1) and a 0,45 mm command opening, while the second has a 4 circular orifice sleeve, of the same diameter (6 mm), but with a 0,30 mm command opening (figure 2). Small command openings were chosen because this condition involves the effects of hydrodynamic forces that disrupt the dynamic behavior of hydraulic equipment, but also because of possibility of cavitation appearance, due to low pressure values

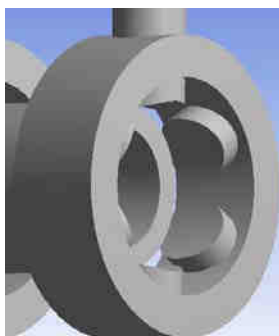


Figure 1 Model 1

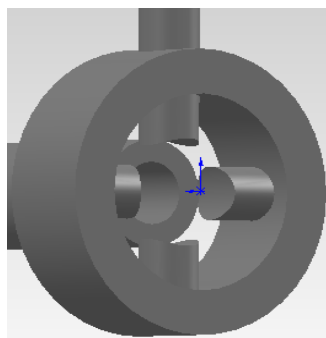


Figure 2 Model 2

The designed geometric models were imported into Ansys Design Modeler where the fluid layer mesh was created, for the both. Models' mesh grid contains aproximatly 2,4 millions tetraheadral elements. Due to high velocity gradients obtained in the command opening areas, the discretization grid is refined, for a better prediction of the flow, becoming more sparse as we move away from the minimum cross section (figure 3)

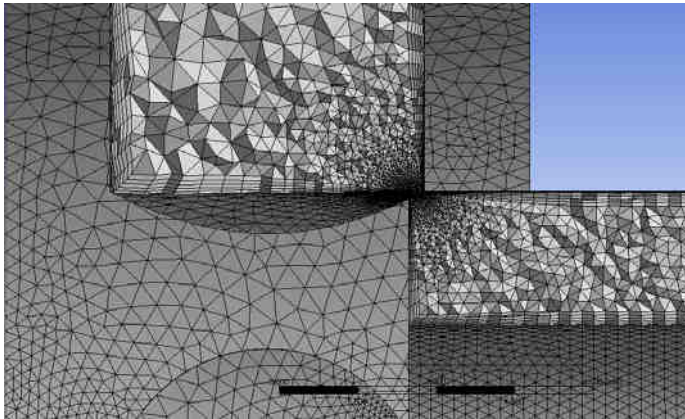


Figure 3 3-D Mesh detail

In terms of imposed boundary conditions, account was taken of the incoming fluid's velocity, i.e. 6 m/s, which led to a flow rate of ~ 10 l/min, and, for the fluid, hydraulic oil was considered with 867 kg/m³ density and $\nu = 45cSt$ kinematic viscosity. The turbulence model chosen for these simulations was k- ϵ RNG (Renormalization Group). This model derives from the k- ϵ turbulence model, enhanced by adding a term in the ϵ equation, thus significantly increasing the work accuracy and by implementing renormalization theory that allows obtaining satisfactory results for smaller Reynolds numbers

2. Numerical analysis

Regarding the flow regime, research is based on the need of a turbulent flow regime and a constant flow coefficient (α) that has a value as close to 1. This close to 1 value of the flow coefficient is based on the fact that it includes in its value all the hydraulic resistances. According to the flow rate equation of a diaphragmatic resistance (eq.1):

$$Q = \alpha \cdot A \cdot \sqrt{\frac{2\Delta p}{\rho}} \quad (1),$$

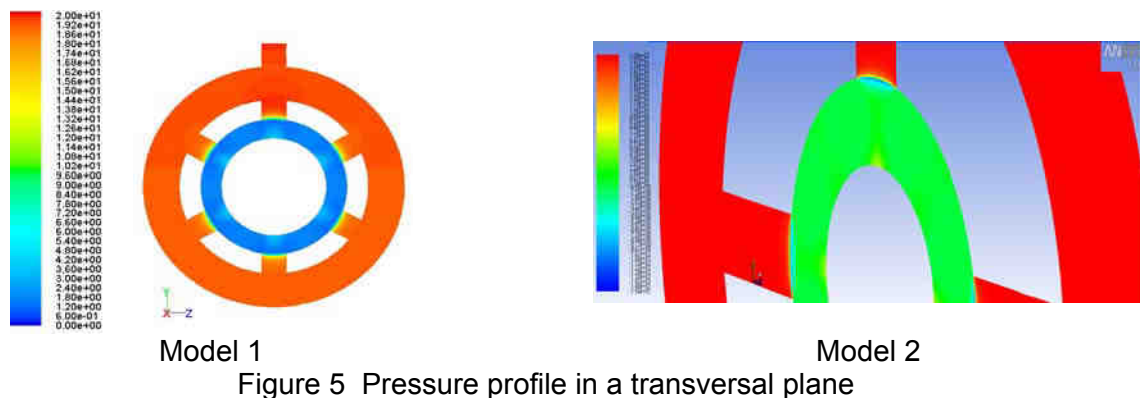
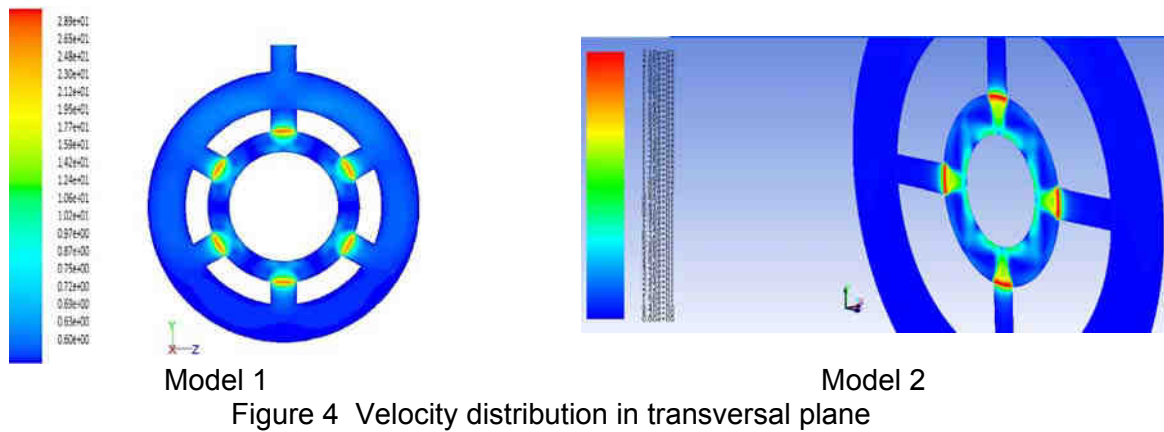
in order to ensure the flow rate proportionality with the command opening, a necessary condition in proportional hydraulics, both the flow coefficient α and pressure drop need to be constant. α has a constant value only in turbulent flow regime. In these circumstances the flow coefficient is independent on the Reynolds number, but it will be highly dependent on the pressure drop. Laminar flow regime should be avoided because in this regime the flow coefficient depends on the working fluid's temperature.

To calculate Re we need the following data:

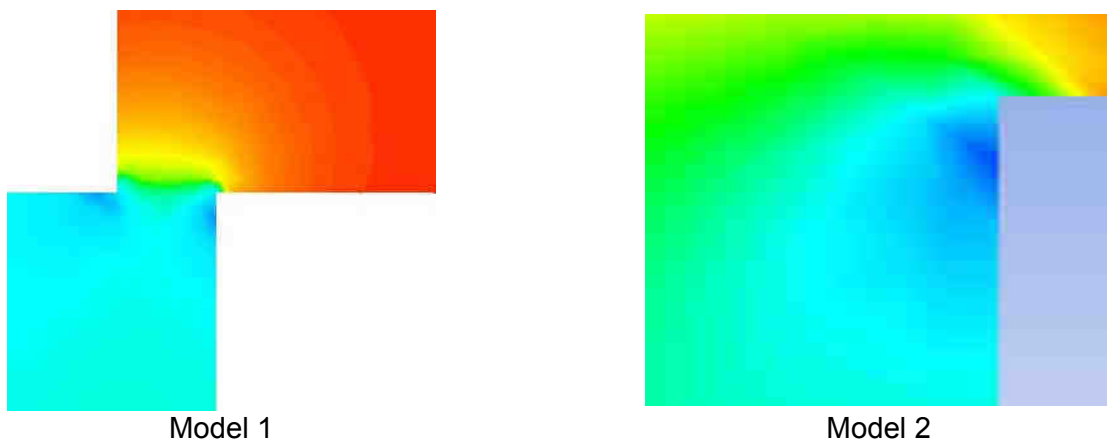
	Model 1	Model 2	MU
Command opening	$0.45 \cdot 10^{-3}$	$0.3 \cdot 10^{-3}$	m
Area	$0.96 \cdot 10^{-6}$	$0.53 \cdot 10^{-6}$	m ²
Flow rate	$169,6 \cdot 10^{-6}$	$169,6 \cdot 10^{-6}$	m ³ /s
Hydraulic diameter	$0.6 \cdot 10^{-3}$	$0.4 \cdot 10^{-3}$	m
Minimum cross-section velocity	176.6	320	m/s
Reynolds number	14128	11377	

The calculations for both geometries show that the flow regime is a turbulent one, so the flow coefficient has a constant value.

In figure 4 the velocity field distribution for both models are shown. Note that, due to decrease of the flow cross section, the flow velocity in these areas increase. Simulation results coincide with the results obtained by calculation. Thus for the first model, with command opening of 0.45 mm, 6 holes sleeve, top speed is about 29 m/s, while for the second model, with command opening of 0.3 mm and only 4 holes in the sleeve, the maximum speed is about 80 m/s.



In figure 5 are presented the pressure fields, observing that in the minimum section area, the value of pressure decreases, in both cases, so much that the area is considered possible cavitation. This can be corrected by modifying input parameters, but also by changing the edge spool's geometry. Figure 6 shows the same distribution of pressure, but in another plane, this time a transversal one. According to the chart's colors, in dark blue we can see the zones where the cavitation phenomenon may occur.



3. Conclusions

This paper has presented a comparison between the results obtained by numerical simulation of flow through two hydraulic resistance models with cylindrical spool and sleeve with circular. The command openings were 0,45 mm for the first model and 0,30 mm for the second. Same tendency is observed of velocity increase in the area of interest, respectively pressure decrease, in the same area, below the vaporization limit, which entail cavitation phenomenon

The Reynolds numbers for both models have values over 10000, which leads to a turbulent flow, as we need. The necessity for a turbulent flow regime emerges from the requirement of a constant flow coefficient, one that doesn't depend on the working fluid's temperature.

It was observed that as the flow section decreases, velocity gradient is increasing, fact confirmed by Bernoulli's equation. Also at the same flow rate, higher values of velocity were registered for the model with 4 holes in the sleeve (80 m / s) than the 6 holes (29 m / s).

ACKNOWLEDGMENT: This paper was supported by the project "Improvement of the doctoral studies quality in engineering science for development of the knowledge based society-QDOC" contract no. POSDRU/107/1.5/S/78534, project co-funded by the European Social Fund through the Sectorial Operational Program Human Resources 2007-2013.

REFERENCES

- [1] Holman, J. – Heat Transfer, McGraw-Hill, 2002
- [2] Deacu, D. Banabic ș.a. – Tehnica Hidraulicii Proportională, Editura Dacia, Cluj-Napoca, 1989
- [3] R. Farmer, R. Pike, G. Cheng, „CFD analysis of complex flow”, Computers and Chemical Engineering 29, 2005; p. 2386-2403
- [4] W. Rodi, „Turbulence models and their application in hydraulics” IAHR, Olanda, 1984; p. 9-46
- [5] Ansys 12.0 Theory Guide
- [6] Dumitrescu. C, s.a – Stand for testing high-pressure hydraulic equipment, Proceedings of 2011 International Salon of Hydraulics and Pneumatics - HERVEX

THE CONSTRUCTIVE-FUNCTIONAL STRUCTURE OF THE MODEL SLOW RUNNING ROTATIONAL HYDRAULIC MOTOR

Laura GRAMA¹, Liviu VAIDA²

¹ Technical University of Cluj-Napoca, laura.grama@termo.utcluj.ro

² liviu.vaida@termo.utcluj.ro

Abstract: *In this paper it is approached the theoretical study of axial piston volumic hydraulic motors, with fixed unit volume from the family F1 (manufactured by the S.C. Hidraulica Plopieni licensed after Rexroth) equipped with a mecano-electro-hydraulic structure control*

Keywords: *volumic motors, axial pistons, mecano-electro-hydraulic control*

1. Introduction

Hydraulic equipments which are used in mechanical engineering generally require the completion of static and dynamic behaviour correlated with application requirements that are used. You can highlight a few:

- Trend of increasing work pressures allowing considerable reductions gauge pumps and motors and thus provides an improved dynamic behaviour. Limiting this trend is due to the high precision of the execution component parts (high cost performance) and quality seals.
- Repeatability regulation entails the use of performance sensors and the introduction of non-conventional control algorithms which don't require high computing power.
- Removing large volumes, parasitic components using command and control motors directly to reduce as much time constants of formation pressure load.
- The tendency of mecanotricising of this equipments along with the associated information flow separation (made almost exclusively by electronic means) of the primary energy.

On principle, rotary hydraulic motors made of a fluid transformation of hydraulic energy provided by a pump into mechanical energy through a limited number of mechanisms (piston, vane and gear) where necessary control of torque and speed.

This study includes simulated hydraulic motor behavior in the modified configuration and aims to estimate's performance and at the same time finding solutions to correct specific elements to improve some performance.

To eliminate the effect of influencing factors were not used in the calculation relations existing in literature were determined based on simplifying assumptions. The only assumption taken into account establishing the numerical model was that of constancy modulus of hydraulic oil used in relation to temperature and pressure. Coefficients involved in relationships were determined based on experimental data from literature on physical performance fluids.

To determine the mathematical model of hydraulic motor functioning structure-mechanical electro-hydraulic control means addressing the following issues:

- Setting the behaviour of the mechanical structure of the whole hydraulic motor - control system
- Setting the dynamic behavior of mechanical-electrical control

- Determination of the hydraulic motor control structure

2. Defining functional motor sizes

The motor that is the subject of study in this paper, is part of the axial piston with piston port block tilting its angular position defining the unit volume of the motor.

The motor is shown in Figure 1.1. This type of hydraulic motor is one of the most used control and hydraulic systems due to reduced gauge, reversibility and relatively low moment of inertia of the moving part. It is part of the high speed hydraulic motors.

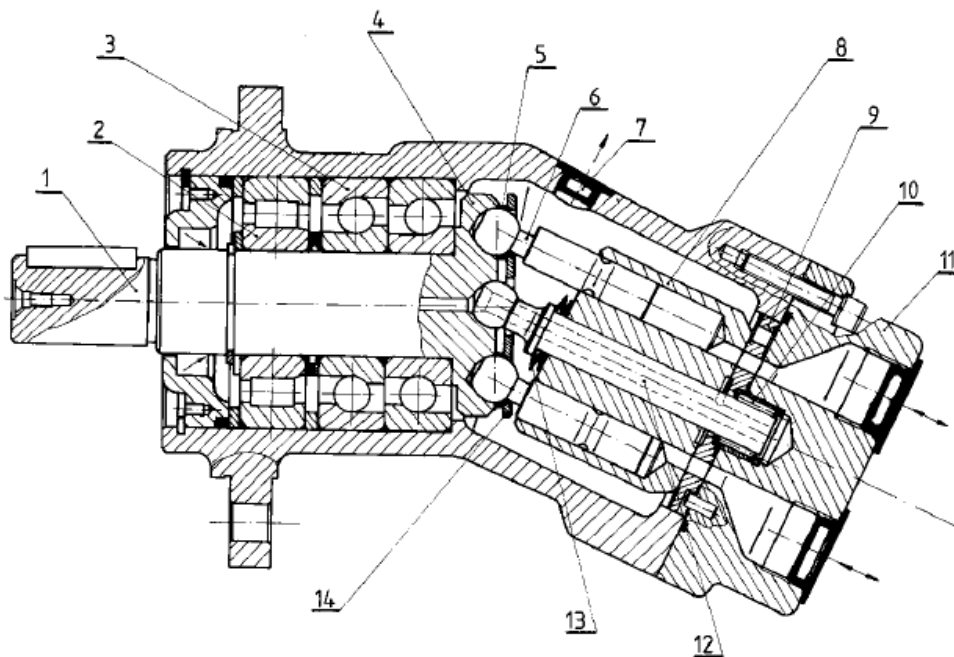


Fig. 1.1. Axial piston motor and tilted block: 1 - shaft, 2 - radial cylindrical roller bearing, 3 - angular ball bearing, 4 - piston disc drive, 5 - spherical bush, 6 - rod; 7 - housing, 8 - cylinder block 9 - Distribution board, 10 - needle roller bearing, 11 - cover joints; 12 - tree guide cylinder block; 13 - spring disc; 14 - connecting rod retaining plate

Block piston port is rotated by the motor shaft. The pistons are arranged round the block, with axes parallel to the axis of rotation. Reciprocating movement thereof is determined by a disk whose axis is inclined to the axis of rotation of the piston block port. The pistons are fixed hydrostatic drive with a skates rod crank mechanism. Separation of the piston and connecting rod disc is hampered by their crimping process.

Successive power piston is achieved through a fixed distribution plate, which is the hydrostatic bearing while between it and block port pistons. Due to block port relationship and contact its piston plate spherical distribution profile, the maximum operating pressure is limited to a continuous functioning of $350 \div 420$ bar.

Energetic and cavitation performances of these motorrrs are very good. Volumetric efficiency and total efficiency have high values ($\eta_v = 0.93 \div 0.97$, $\eta_t = 0.84 \div 0.93$)

These motors are compact and is recommended for use in closed circuit especially in hydraulic systems of mobile equipments. This type of motor is manufactured in the adjustable version.

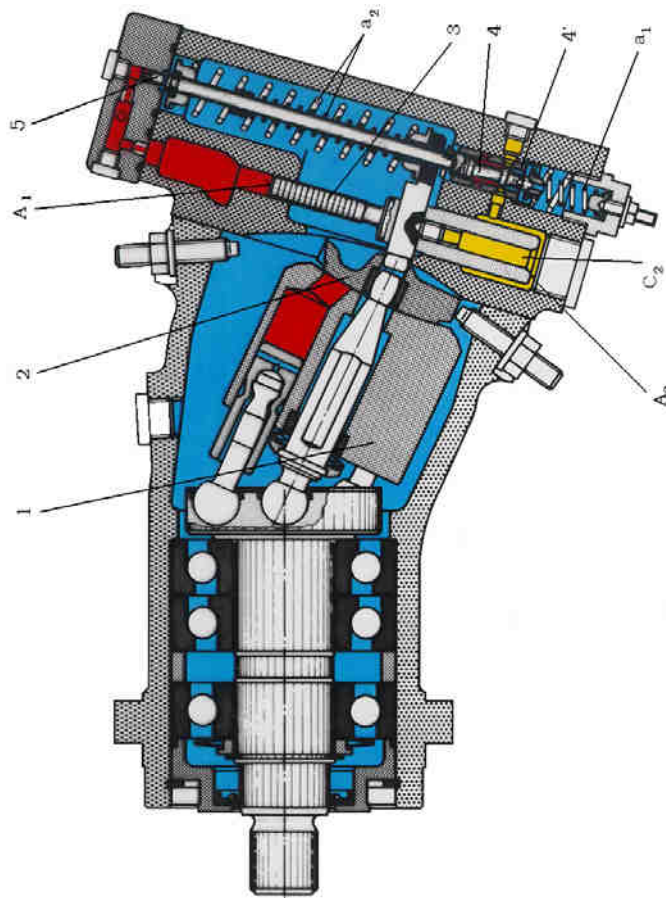


Fig. 1.2 Adjustable motor constructive assembly F6

This distribution board with this block 2 and piston port 1 will be moved by positioning engine 3 (with area ratio $K = A_2/A_1$). Control valve, consisting of tray 4 and sleeve 4', is a type A "semipunte", covering "zero" (actually working with one edge control C2 connecting the engine room positioning and power supply and motor, which is present supply pressure p_s). Such pressure (which acts continuously on area A1 piston positioning motor and area 5) must have certain values that can overcome the resistance of the spring pre-set and can move a1 compartment 4 the control valve. C2 Through this movement and camera positioning engine to be operated at supply pressure p_s , and the fact that $A_2 > A_1$ engine positioning moves the purposes of reducing the tilt angle, α , while compressing the package a2 spring, which will balance the forces on the valve chest, causing his return to the normal position. If the pressure is below p_s corresponding prestressing spring package dispenser drawer a2 4, A2 area will ensure the tank motor positioning, the maximum engine capacity, so for a given flow, speed is minimal.

Hydraulic diagram of this motor is shown in Figure 1.3.

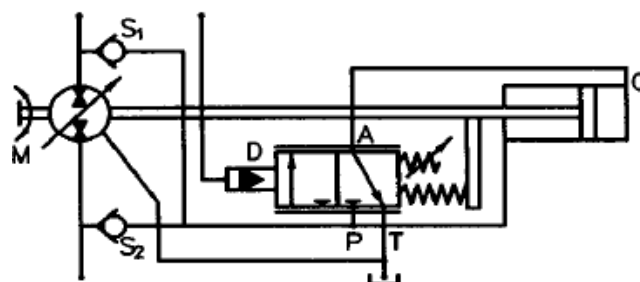


Fig. 1.3 Scheme F6 hydraulic drive motor with hydraulic prescription

2. Proposed design of axial piston hydraulic motor

Starting from the premise that, when working heavy loads at low speeds, it is needed "slow" volume motors that are stable when operating at low speeds and provides high yields moments, we designed a constructive version of axial piston hydraulic motor, which is shown in Figure 1.4

This model was intended as a constructive adjust motor speed to achieve without dissipation of energy by regulating the power flow, but be able to transmit the motor shaft a great time throughout the revolution range.

Slow axial piston hydraulic motors consists of piston 5 which is blocked by its cover 8. Bet on port block slides axial piston pistons 4, linked by rods and ball joints of tilting disc 3 (gear driven). Bore pistons are supplied pressure source or tank made via rotary distributor 6. This solution makes rotating disc to perform a movement around spherical ball joint that connects the piston port block 5.

Rotation of the rotary distributor 6 is accomplished by the electric motor 7 (which can be DC or stepper).

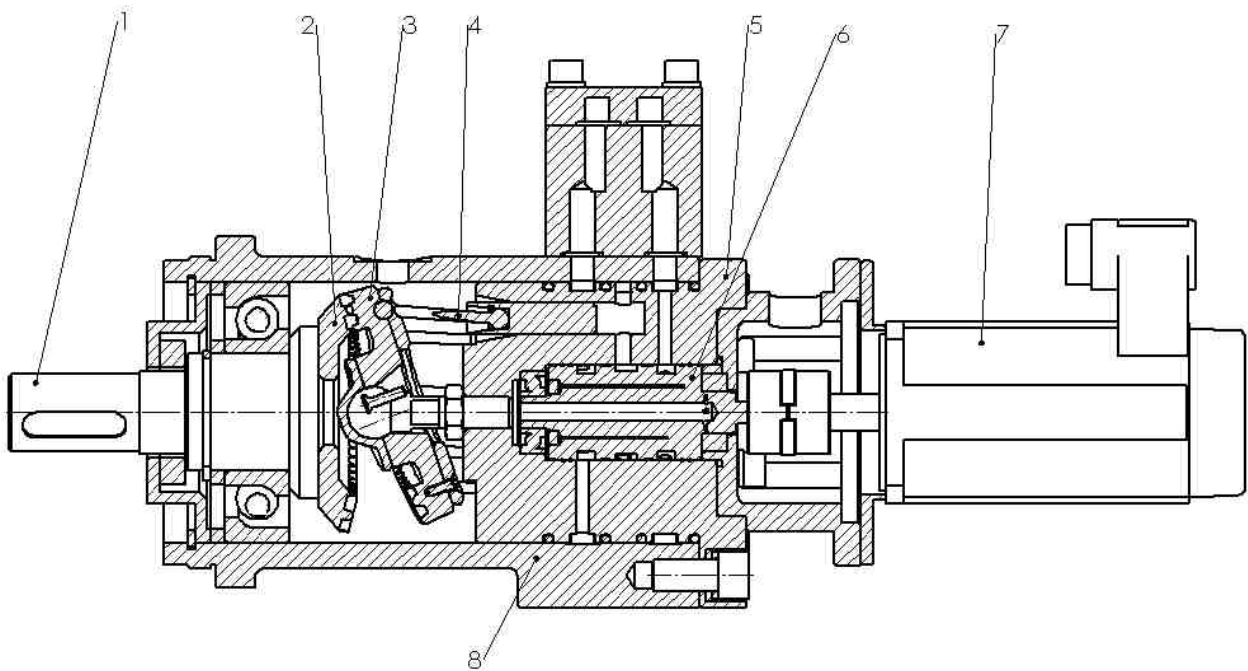


Fig. 2.1 Slow hydraulic motor: 1 - output shaft, 2 - toothed wheel driven, 3 - driving sprocket (tilting disc), 4 - piston 5 - block port pistons, 6 - distributor, 7 - electric motor, 8 – housing

Output shaft is coupled with a tilting disc gear coupled with front teeth that because of ball movement have permanently tilting disc clutch about $\frac{1}{3}$ of the number of teeth.

The two wheels differ in the number of teeth via an unit.

A full rotation of the rotary distributor (one complete oscillation of the disc tilt (3) output shaft rotates at an angle equivalent of a tooth. Example if the gears have 90 and 91 teeth, the angle of rotation of the output shaft is $\varphi = \frac{360}{90} = 4^\circ$ (or $\frac{2\pi}{90} = 0,07rad$).

Hydraulic motor rotates the output shaft only if rotary distributor is trained, making a rigid position feedback.

This solution makes sense not matter rotation (same output shaft rotational rotary dealer) and not change the debit hole.

Thus the output shaft synchronous movement aims spherical tilting disc, making the time required by the driven mechanism

3. Conclusions

In this paper it is presented a constructive solution for designing a hydraulic motor rotating slowly, starting from the basic structure of axial piston hydraulic motors. Hydraulic motor by rotating output shaft, ensures synchronization with the input shaft, resulting in a rigid position feedback.

REFERENCES

- [1]. www.assofluid.it
- [2]. Liviu, Deacu., Hidraulica maşinilor unelte, Litgrafia Institutului politehnic Cluj-Napoca, 1983
- [3]. Liviu, Vaida., Comanda proporţională a pompelor reglabile, PhD. Thesis, Cluj-Napoca, 1999
- [4]. <http://www.scribd.com/document/115818152/Rigiditatea-hidraulica>
- [5]. Daniel Vasile, BANYAI., Metode noi în sinteza maşinilor hidraulice, cu volum unitar variabil şi reglare electro-hidraulică, PhD Thesis, Cluj-Napoca, 2011
- [6]. Daniel Vasile BANYAI, Liviu VAIDA, Ioan-Lucian MARCU, Dan OPRUȚA., The positioning force of the inclined plate for variable displacement pumps, Acta tehnica napocensis, 2009
- [7]. Mihai, Muşat, Gina Stoica., Transmisii mecanice cu reductoare într-o treaptă, Indrumar de proiectare, 2004

ROTATIONAL SPEED MATHEMATICAL MODEL OF THE ALTERNATING FLOW DRIVEN THREE-PHASE HYDRAULIC MOTORS

Ioan-Lucian MARCU¹, Daniel- Vasile BANYAI², Ioan-Liviu VAIDA³

¹ Technical University of Cluj-Napoca, Lucian.Marcu@termo.utcluj.ro

² Daniel.Banyai@termo.utcluj.ro

³ Liviu.Vaida@termo.utcluj.ro

Abstract: *there is detailed presented the way of calculation of the speed of the rotation three-phase hydraulic motor with alternant flows function of the generator driving speed, the constructive parameters of the whole system, considering the elasticity of the phase pipes and the oil column compressibility under pressure. As a result of the mathematical relations determination, there are presented for the both interconnecting schemes comparative diagrams between the curves of the obtained theoretical speeds and the curves obtained by experimental results interpretation, which are validating the elaborated mathematical model.*

Keywords: *alternating flow, three-phase hydraulic motor, rotational speed*

1. Introduction

Alternating flow driven systems involves a new approach of the driving systems using pressurized liquids, because we have here, in the entire system, along the pipes, an energy transmissions without volumetric flow transportation between the energy converters, hydraulic generator and hydraulic motor. [2], [4], [5]

The classical solutions of hydraulic systems imply a unidirectional flow of the fluid through pipes between the energy converters. The hydraulic transmission using alternating flows is based on the bidirectional displacement of a predefined volume of fluid through the connection pipes between the alternating flow and pressure energy generator and the motor. Within these systems, the active stroke of the hydraulic motor pistons, is produced by the pressurized fluid flow from the generator, while, for the retraction stroke there is necessary a supplementary connection (in a star or delta configuration) to a pressure generator, working in opposite phase with respect to the first one. [3]

Generally, an alternating flow driven hydraulic transmission consists in a alternating flows and pressures generator and a motor, the connection between them being realized with a number of pipes equal with the number of phases, the pipes being filled with fluid at a certain (pre-established) pressure. During the functioning of the system the pressure and the flow within each pipe varies in a sinusoidal way, around an average value.

In order to have a proper functioning it is compulsory that the average pressure from each pipe to have the same value and to have a constant value in time. Therefore, to obtain the correct functionality we create from the beginning either a pressure in each phase, higher than the amplitude maximum value, or this pressure is modifying itself during the functioning. This result is obtained by using both a series of hydraulic resistances rigorously calculated which interconnect all the phases and a hydraulic accumulator connected to them. The resistances must eliminate the maximum average pressure rising value in one second when the diminution of the flow amplitude from a phase does not exceeds 1%. The accumulator presence makes the pressure in a connection to be all the time approximately constant, it being able to take over the oil surplus from the dilatations and in the same time to complete the eventually oil losses. [7]

2. General considerations regarding the alternating flow of the three-phase hydraulic gerator

If we consider a axial piston hydraulic generator, represented in figure1, the instantaneous variation of the piston volume and volumetric flow can be determinate as follows: [1]

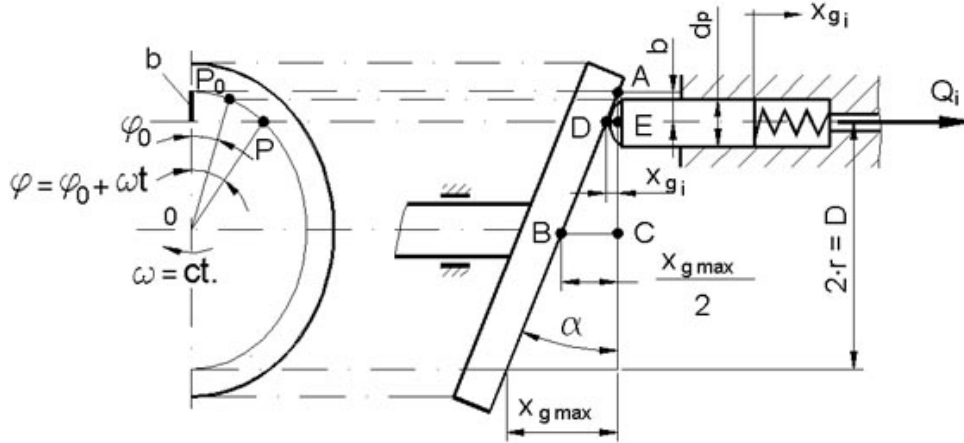


Figure 1. Schematical representation of an alternating flow generator [1]

The instantaneous variation of the piston stroke is defined as:

$$x_{gi} = \frac{x_{g \max}}{2} \cdot [1 - \cos(\varphi_0 + \omega t)] \quad 1$$

The instantaneous variation of the piston volume is:

$$V_i = \frac{x_{g \max} \cdot \pi \cdot d_p^2}{8} \cdot [1 - \cos(\varphi_0 + \omega t)] \quad 2$$

Considering the previous relations the instantaneous variation of the volumetric flow is:

$$Q_i = \frac{dV_i}{d(\varphi_0 + \omega t)} = \frac{\pi \cdot d_p^2 \cdot x_{g \max}}{8} \cdot \sin(\varphi_0 + \omega t) \quad 3$$

The movement of the hydraulic motor pistons will be always determinate by the phase piston which will take in one moment the highest volumetric flow. Form figure 2 we observe that for each phase there it is an $\frac{2\pi}{3}$ section in which the instantaneous flow is higher than in the other two phases.

For the first phase, the instantaneous flow Q_{i1} , is corresponding to the $\frac{\pi}{6}$ and $\frac{5\pi}{6}$ period.

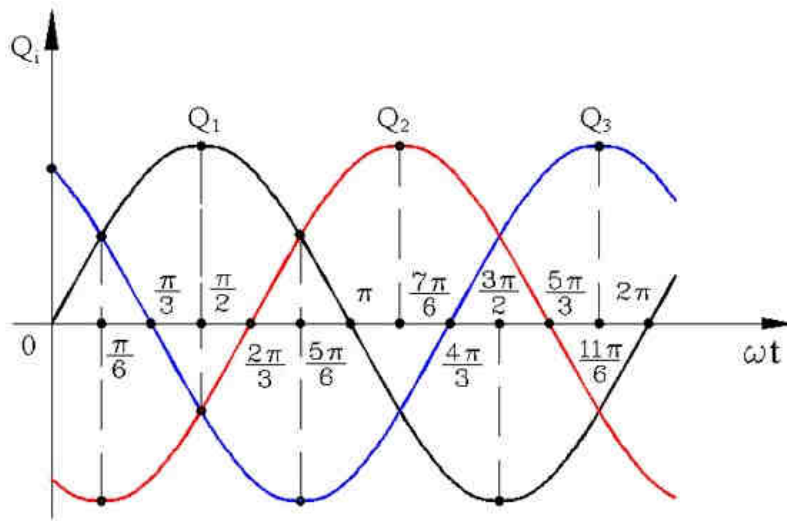


Figure 2. Instantaneous volumetric flow evolution.

Considering the constructive characteristics of the hydraulic generator and motor, and using the medium flow formula, we can calculate the rotational speed of the output shaft of the hydraulic motor as follows. [2], [6]

The instantaneous volumetric flow is defined as:

$$Q_i = \omega_g \cdot \frac{x_g}{2} \cdot S_g \cdot \sin(\omega t + \varphi_0) \quad 4$$

in which x_g is the generator piston stroke, S_g is the generator piston surface, and ω_g is the angular frequency of the generator.

The medium value of the volumetric flow for a phase of the hydraulic generator, for an active angle $\varphi_g = \varphi_{g2} - \varphi_{g1}$, is defined using the equation:

$$Q_{imed_g} = \frac{1}{\varphi_{g2} - \varphi_{g1}} \cdot \int_{\varphi_{g1}}^{\varphi_{g2}} Q_{ig} \cdot d\varphi_g \quad 5$$

Considering the $\frac{\pi}{6}$ and $\frac{5\pi}{6}$ interval, for the first phase, figure 2, we obtain the medium value of the volumetric flow as:

$$Q_{imed_g} = \frac{1}{\frac{5\pi}{6} - \frac{\pi}{6}} \cdot \int_{\frac{\pi}{6}}^{\frac{5\pi}{6}} \omega_g \cdot \frac{x_g}{2} \cdot S_g \cdot \sin \varphi_g \cdot d\varphi_g$$

and resolving that, we obtain:

$$Q_{imed_g} = 0,413 \cdot \omega_g \cdot x_g \cdot S_g \quad 6$$

3. Rotational speed determination of the alternating flow driven three-phase hydraulic motors

A schematically representation of the alternating flow driven hydraulic motor is presented in figure 3.

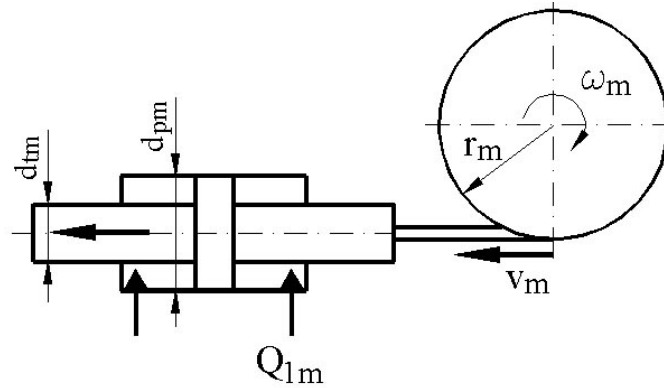


Figure 3. The movement of the phase piston of the hydraulic motor.

According to figure 3 linear speed of the hydraulic motor piston v_m can be calculated with the next relation:

$$v_m = \omega_m \cdot r_m \quad 7$$

in which ω_m is the angular speed of the hydraulic motor and r_m is the action radius of the phase piston.

Knowing that $\omega = \frac{\pi \cdot n}{30}$, in which n is the rotational speed, then we obtain:

$$v_m = \frac{\pi \cdot n_m}{30} \cdot r_m$$

Considering the continuity equation, the speed of the motor piston is:

$$v_m = \frac{Q_{1m}}{S_m} \quad 8$$

If the volumetric flow of the generator is totally used by the hydraulic motor (ideal case) then the rotational speed of the motor is:

$$n_m = \frac{Q_{1med}}{S_m \cdot r_m} \cdot \frac{30}{\pi} \quad 9$$

For the first phase of the alternating flow driven system we obtain:

$$n_m = \frac{3\sqrt{3}}{4\pi} \cdot \frac{n_g \cdot x_g \cdot S_g}{r_m \cdot S_m} \quad 10$$

Considering the active surface of the motor piston as:

$$S_m = \frac{\pi}{4} \cdot (d_{pm}^2 - d_{tm}^2)$$

and for the hydraulic generator:

$$S_g = \frac{\pi \cdot d_{pg}^2}{4}$$

in which d_{pm} is the motor piston diameter, d_{tm} is the motor piston rod diameter and d_{pg} is the generator piston diameter, and also assuming that $K_g = x_g \cdot S_g$ and $K_m = r_m \cdot S_m$ being constructive constants for the hydraulic generator and the hydraulic motor, then the equation defining the ideal rotational speed of the alternating flow drives motor is:

$$n_m = \frac{3\sqrt{3}}{4\pi} \cdot \frac{K_g}{K_m} \cdot n_g \quad 11$$

Equation 11 indicates a similar evolution of the rotational speed of the hydraulic motor like in the conventional hydraulic systems, depending on the hydraulic generator rotational speed and constructive parameters.

Figure 4 present a numerical simulation of the rotational speed of the alternating flow driven hydraulic motor, using the equation 11.

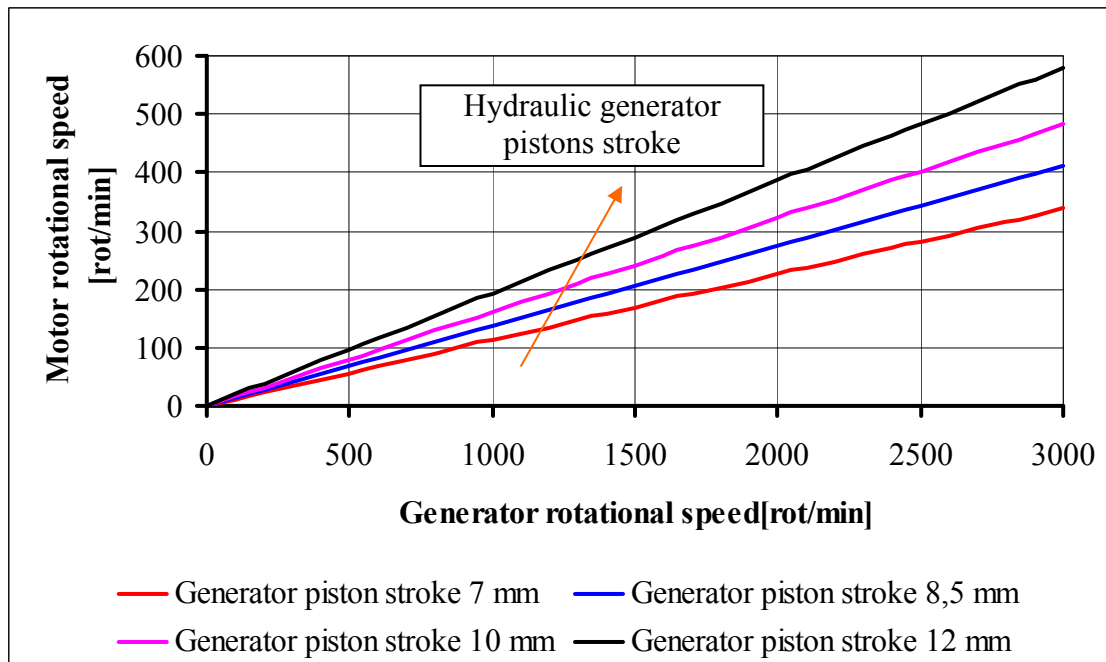


Figure 4. Ideal case evolution of the motor-generator rotational speeds.

The mathematical model was developed considering the two energy converters, hydraulic generator and hydraulic motor, at short distance between them, and also the fluid column being incompressible. In these conditions the volumetric flow provided by the generator is totally used by the hydraulic motor.

4. Conclusions and future developments

If the constructive characteristics of the hydraulic converters are kept constants, then, for the same rotational speed of the hydraulic generator n_g , the numerical constant of the equation 11 aim at 1 with the increase of phase numbers, which means a decrease of the active interval of each phase piston of the hydraulic generator.

Considering the increasing of the hydraulic generator piston strokes from 7 mm to 12 mm, the ratio of the rotational speeds hydraulic generator - hydraulic motor is modifying from 8,88 : 1 at 5,18 : 1.

In the real case the transmission medium is a elastic one, and also the connection pipes. Considering that, the mathematical model must be improved by using the elasticity constant of the fluid and of the pipes materials, depending on the pressure level and the length of interconnection pipes.

REFERENCES

- [1] Deacu, L., Pop, I., "Hidraulica masinilor-unelte", Lito. IPCN, Cluj-Napoca, 1983.
- [2] Marcu, I. L., "Researches and contributions regarding the functional improvements of the alternating flow driven hydraulic systems", PhD Thesis, Technical University of Cluj-Napoca, 2004.
- [3] Marcu, I.L., Pop, I. "Interconnection possibilities for the working volumes of the alternating hydraulic motors" Proc. of the 6th International Conference on Hydraulic Machinery and Hydrodynamics - HMMH2004 in Trans. of Mechanics, Tom 49 (63), Timisoara, October 2004, ISSN 1224-6077, pp. 365-370.
- [4] Pop, I., Marcu, I.L., Khader, M., Denes Pop, I., "Conventional Hydraulics", Ed. U.T.PRES, Cluj-Napoca, 1999.
- [5] Pop, I., "Sonic Theory Treatise", Ed. Performantica, Iasi, 2006.
- [6] Pop, I. et al, "Sonics Applications. Experimental Results", Ed. Performantica, Iasi, 2007.
- [7] Saceanu, V. "In improvements in the functioning of the state-of-the-art multiphase sonic transmissions, by using hydraulic resistances between the phases as well as hydraulic accumulators", Scientific bulletin of the "Politehnica" University of Timisoara, Transaction of Mechanics, Tom 49 (63), Special Issue, October 2004, ISSN 1224-6077, pp. 531-536.

MEANS AND METHODS FOR TESTING ADJUSTABLE HYDROSTATIC PUMPS

Teodor Costinel POPESCU¹, Ioan LEPĂDATU¹

¹ Hydraulics and Pneumatics Research Institute (INOE 2000- IHP), Bucharest, popescu.ihp@fluidas.ro

Abstract: *This paper aims at dissemination of experimental research work conducted at IHP Bucharest, in order to determine the actual performance of hydrostatic adjustable pumps. To this end laboratory tests were conducted on a radial piston pump MOOG type, which can automatically vary the flow rate by adjusting the eccentricity of the stator ring. The paper presents the experimental modern means used for this purpose, the type of experimental tests, results and their interpretation.*

Keywords: *hydrostatic adjustable pump, experimental tests*

1. Introduction

On the adjustable hydrostatic pump tests were conducted under static and dynamic mode [1], [2]. Technique used for the dynamic tests was based on flow measurement by the indirect method, which consists of measuring the differential pressure across a diaphragm mounted on the pump discharge pipe. In this way, the two pressure transducers mounted in the downstream and upstream of the diaphragm measure almost instantaneously pressures and thus, very fast, is known the flow rate value.

2. Presentation of the test stand

Functional schematic diagram of the stand, figure 1, contains: radial piston pump tested PPR, driven by the AC electric motor ME, with power of 37 kW and 1465 rev/min; electropump EP, providing overcharging of aspiration of the pump tested; the filter F, for protection to contamination of the aspirated oil; diaphragm DM and pressure transducers TP1, TP2, which measure the flow discharged by the pump; transducer TPr for measuring the discharge pressure of the pump tested, proportional pressure valve SPP with a role in protection and simulation of the load; throttle DR, for load adjustment at the pump tested; the electric control hydraulic distributor D which in position "0" allows adjustment of valve SPP, in position "b" allows the pump discharge, and in position "a" allows load adjustment by means of throttle DR and calibration of the flow measuring diaphragm by means of the turbine flowmeter TD.

The stand also contains a data acquisition system SAD, type *NATIONAL INSTRUMENTS, Bus-Powered M Series Multifunction DAQ for USB - 16-Bit, up to 400 kS/s, up to 32 Analog Inputs, Isolation*, interface between pressure transducers, type *DRUK SYSCOM 18, cod PTX 1400-400, Pn=400 bar, G1/4"* (TP1, TP2, TPr), flow transducer type *HYDAC, cod EVS 3100-1PTX 1400-400, 60l/min* (TD), and temperature transducer type *DRUK SYSCOM 18, cod PT 100-50...+400°C, G1/2"* (TT), on the one hand, command for adjustment of capacity of the pump tested V_c and acquisition of information about capacity achieved V_r , on the other hand, the command for pressure control of the tested pump discharge P_c and acquisition of information about the achieved discharge pressure P_r ; a computer system PC, type *NATIONAL INSTRUMENTS, cod NI PXI-1031* with an installed data acquisition and processing software type *NI LabVIEW*; a stabilized voltage source STS; a random function generator GFA. For accuracy of measurements, noise of the acquired signals was filtered by means of a "low-passing" filter, with a cutting frequency of 100 Hz.

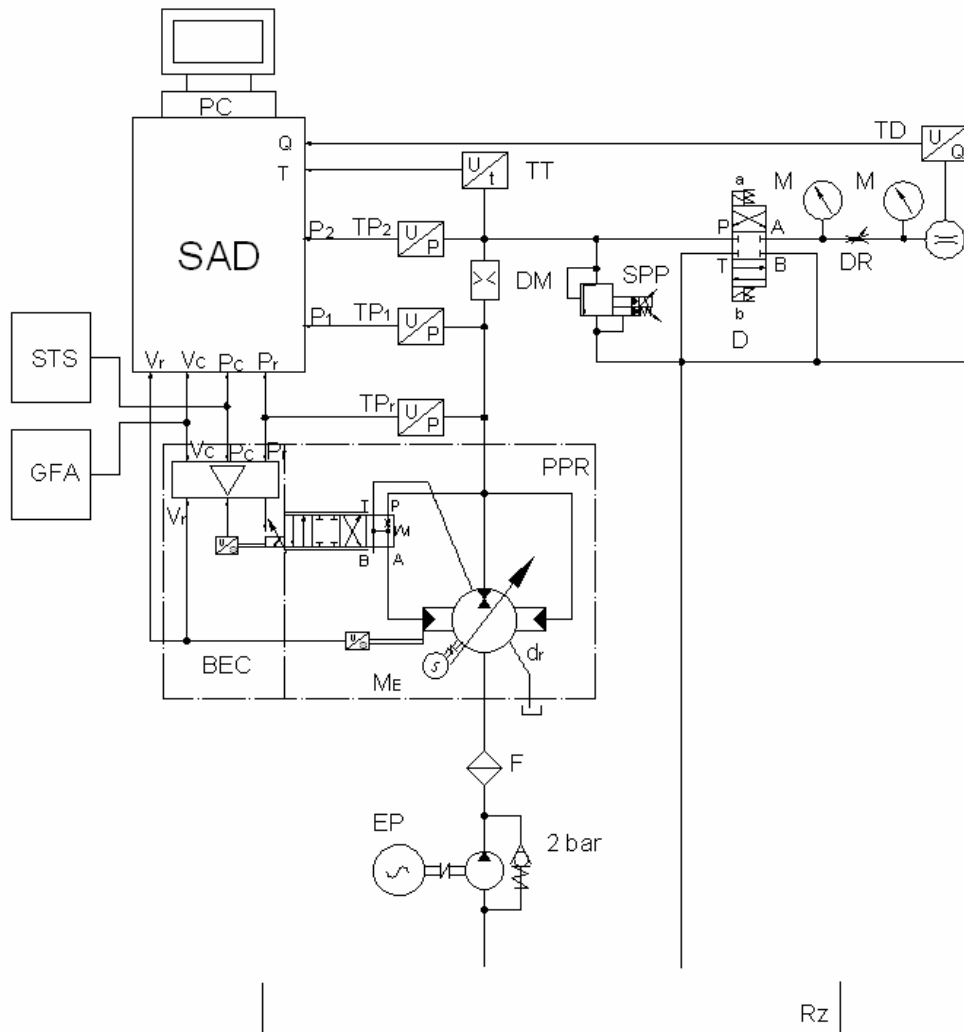


Fig. 1- Functional diagram of the test stand for the pump PPR.

3. Calibration of flow measurement diaphragm

Under dynamic mode flow was measured with the measuring diaphragm located right on the discharge of the pump DM (acc. Figure 1). For calibration of the diaphragm, the flow was measured accurately with a turbine flow meter "Turboquant". The calibration feature of the diaphragm was raised, namely the functional dependence of the flow, as measured by the turbine transducer, on the pressure drop at the diaphragm, measured with the pressure transducers TP1 and TP2. Coordinates of the points on the interpolated calibration feature of the diaphragm are shown in Tables 1 ... 3.

Table 1- Diaphragm calibration results: 0.000-1.723 bar; 0.000-19.393 l/min.

ΔP , bar	0.000	0.260	0.380	0.520	0.740	1.090	1.330	1.723
Q l/min	0.000	6.856	8.594	10.633	12.757	15.547	17.228	19.393

Table 2- Diaphragm calibration results: 6.740-9.012 bar; 38.916-49.987 l/min.

ΔP , bar	2.116	2.592	3.069	3.597	4.125	4.774	5.423	6.082
Q l/min	21.554	23.860	25.936	28.169	30.262	32.252	34.624	36.783

Table 3- Diaphragm calibration results: 6.740-9.012 bar; 38.916-49.987 l/min.

ΔP , bar	6.740	7.558	8.435	8.510	9.012
Q l/min	38.916	41.495	43.955	44.113	49.987

4. Experimental measurements under static mode

To determine the behavior of the pump under static mode there were applied control signals U_c within the range 0 - 10 V, ascending and descending, sinusoidal and ramp-shaped, with frequencies of 1 Hz, 0.7 Hz, 0.35 Hz and 0.1 Hz. All measurements were made at pressure $p = 20$ bar and oil temperature $T_{oil} = 40 \pm 5^\circ\text{C}$.

4.1. Response to ascending / descending ramp

Measurements were made for control signals with maximum amplitude (10Vd.c.) and frequencies of 1 Hz, 0.7 Hz, 0.35 Hz and 0.1 Hz. For frequencies of 1 Hz results are shown in the diagrams of Fig. 2.

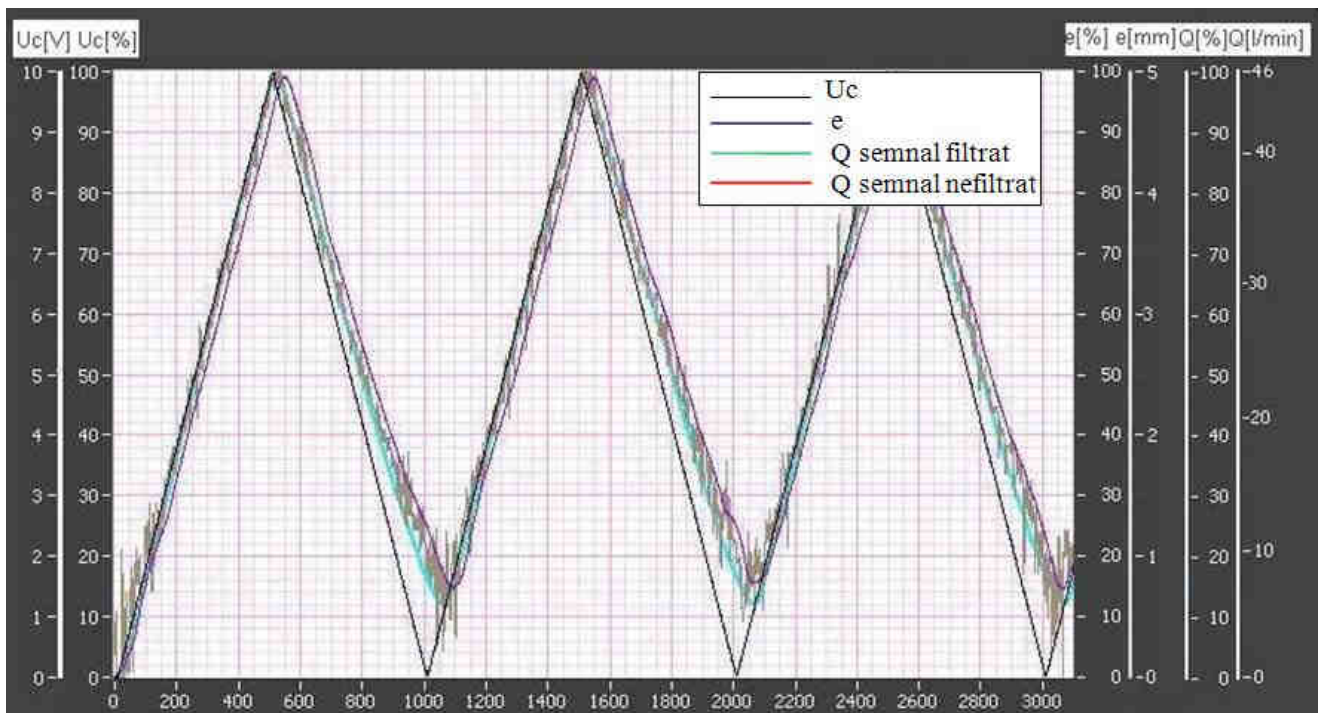


Fig. 2 –Variation over time of flow Q, l/min and eccentricity e, mm, to ramp signal with frequency of 1 Hz.

4.2. Response to low frequency sinusoidal signal

Measurements were made for control signals with maximum amplitude (10Vd.c.) and frequencies of 1 Hz, 0.7 Hz, 0.35 Hz and 0.1 Hz. For frequencies of 0.1 Hz results are shown in the diagrams of Fig. 3.

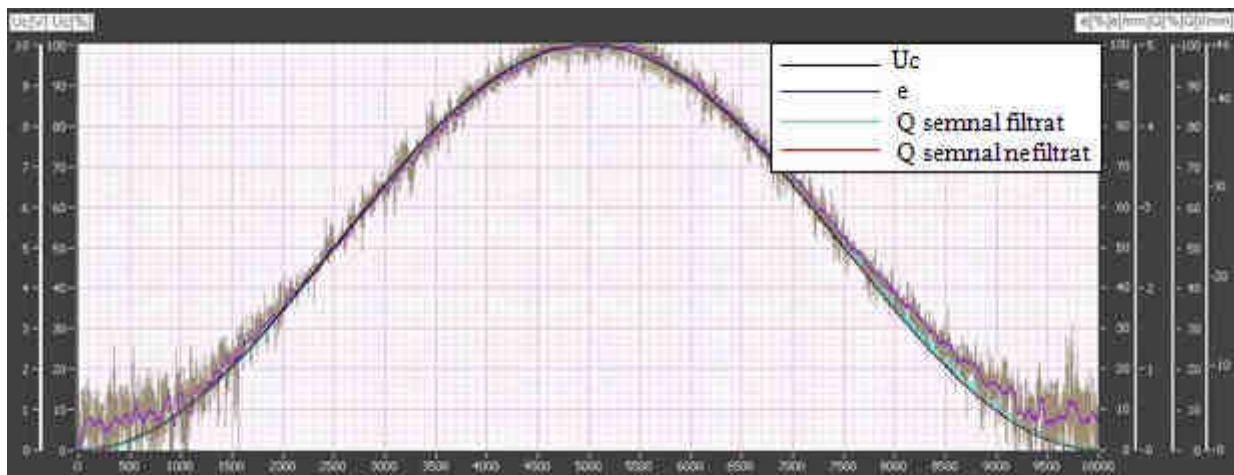


Fig. 3 –Variation over time of flow Q , l/min and eccentricity e , mm , to sinusoidal signal with frequency of 0.1 Hz.

4.3. Pump static characteristic

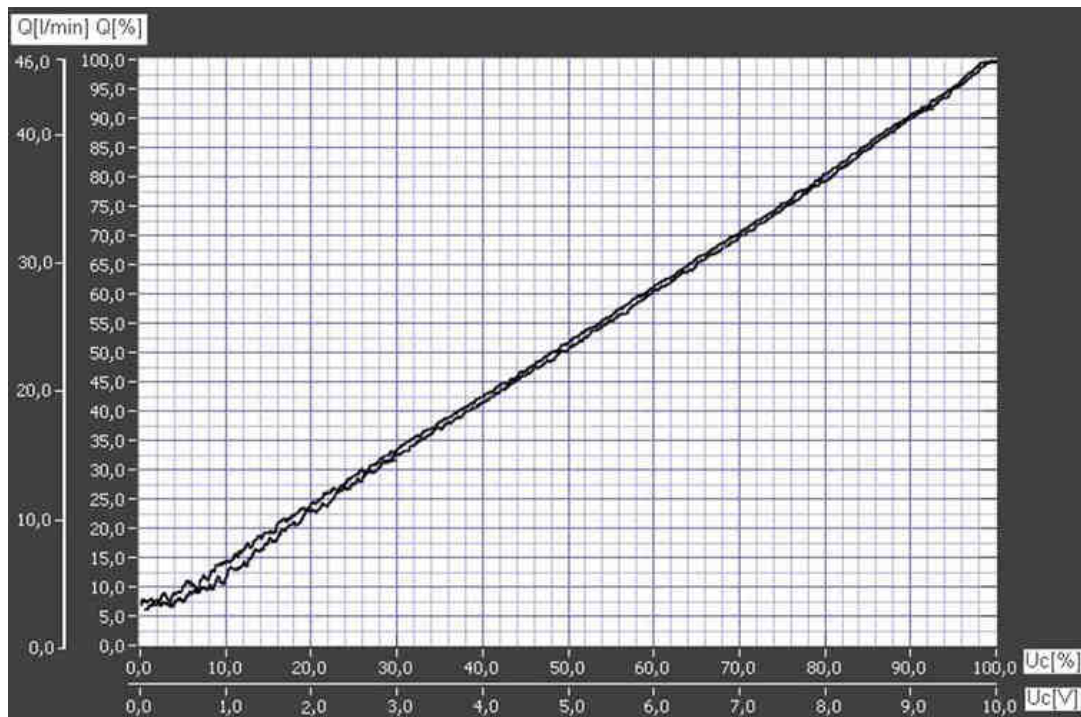


Fig. 4 – Pump static characteristic, flow Q , l/min depending on the prescribed command, voltage U_c , V , to ramp signal with frequency of 0.005 Hz.

Dependence of the prescribed command on the flow achieved by the pump was determined for ascending/ descending ramp-shaped control signal and frequencies between 0.1 Hz and 0.005 Hz. It appears that the hysteresis decreases with decreasing frequency, a phenomenon explained by the fact that the quantities progress being slower, on their decreasing variance there is more time for the transitional regimes, relaxation of materials (especially in springs), etc. to diminish their effects. For the frequency of 0.005 Hz the static control characteristic of the pump is shown in Fig.4.

5. Experimental measurements under dynamic mode

5.1. Response to step signal of the flow discharged by pump

Determination of the response to step signal was performed to multiple amplitudes, respectively 100% (10 V), 75% (7.5 V) and 50% (5V) to see how response times depend on this parameter. At each of amplitudes the system was excited also with a train of step signals of different frequency, respectively 0.1 Hz, 0.5 Hz and 1 Hz, to see if the response is maintained to frequency change.

Response of the positioning system of the stator ring of the radial piston adjustable pump to step signals that have values less than 25% and 50% of the maximum value does not differ essentially, in aspect and performance (over adjustment, delay time, stabilization time) from the response to the maximum value signals, of 10Vd.c.

Figure 5 presents the variation over time of the pump flow to step control signal, with amplitude of 100% (10V) and frequency of 0.1 Hz. From this test results: *delay time* = 116 ms, *stabilization time* = 193 ms, *over adjustment* = zero.

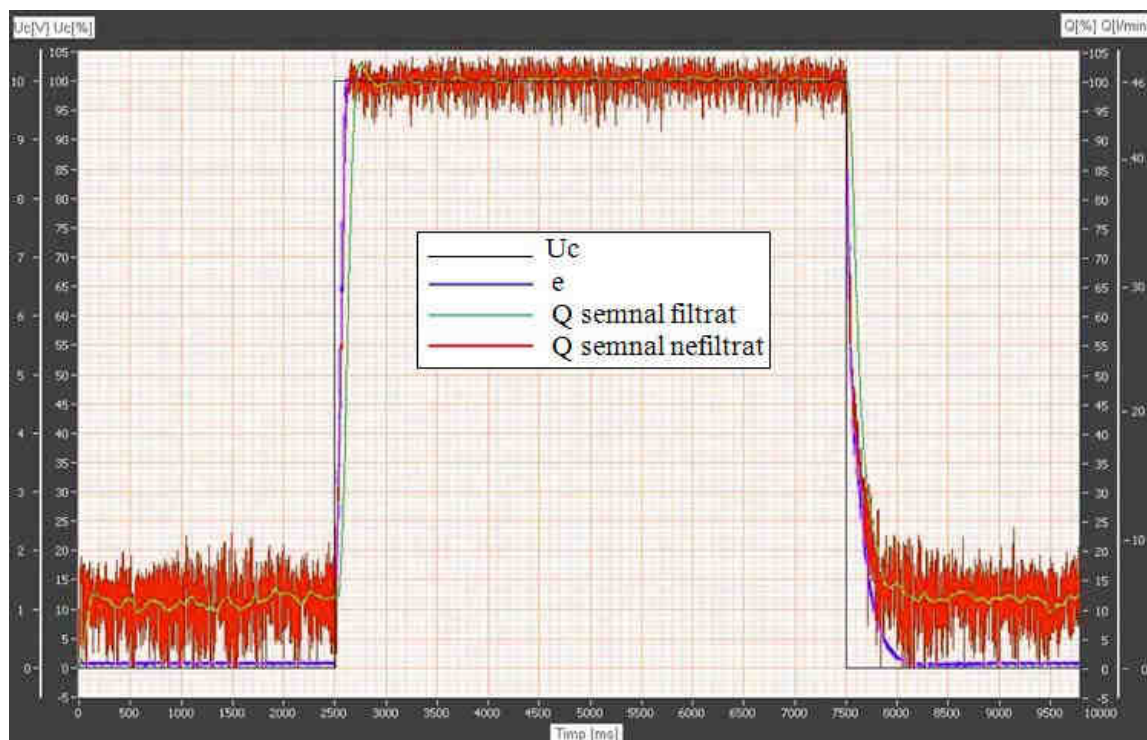


Fig. 5 – Response over time of pump flow Q , l/min to step control signal, with amplitude of 100% (10V) and frequency of 0.1Hz.

5.2. Response to sinusoidal signal of the flow discharged by pump

To determine the response of the pump adjusted flow there were applied control signals with different values of frequency (0.5 Hz, 6 Hz and 10 Hz) and amplitude (100%, 75%). Fig.6 presents the response to sinusoidal signal with amplitude of 100% (10Vd.c.) and frequency of 6 Hz.

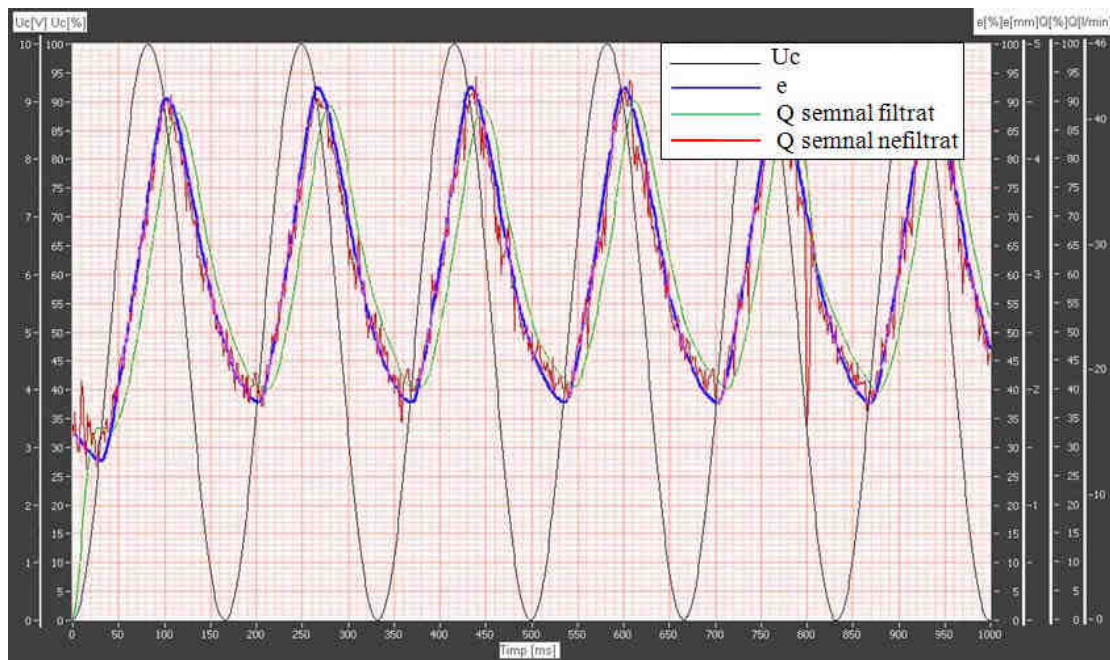


Fig. 6 – Response over time of pump flow Q , l/min to sinusoidal control signal, with amplitude of 100% (10V) and frequency of 6 Hz.

Response of the positioning system to sinusoidal control signals of various frequencies shows that the amplitude of the response decreases, and the phase difference between "control" and "response" increases when the frequency of control signal decreases. Based on these responses there was mapped the Bode diagram.

5.3. Response in frequency

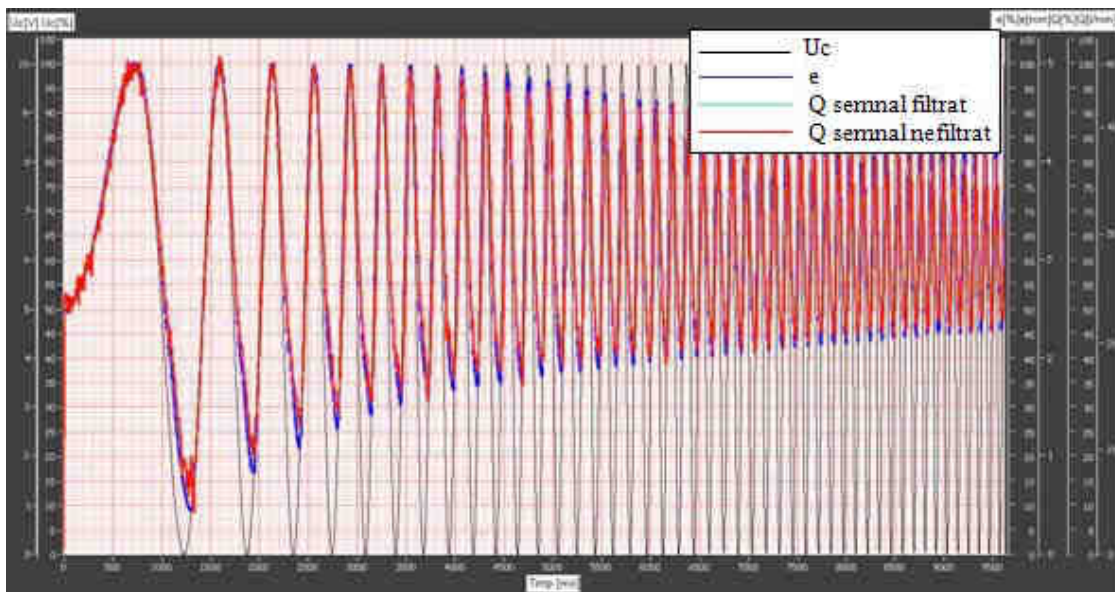


Fig. 7 – Response in frequency of pump flow Q , l/min to sinusoidal control signal, with amplitude of 100% (10V) and frequency of 0.1-20 Hz.

To determine the limit frequency at which the pump performs flow adjustability there was applied a sinusoidal control signal with maximum amplitude (10Vd.c.) and with ascending frequency, starting from 0.1 Hz to 20 Hz for 10 sec. The evolution over time of the flow adjusted by the pump represents the response in frequency of the positioning system developed, shown in Fig.7.

It was noted that when increasing the frequency first minimum flow rates decrease and then the maximum ones; the phenomenon is due to the two springs of the small pistons (large and small spring), components of the positioning system of the pump stator ring, which adjusts the amount of eccentricity e , mm .

5.4. Bode Diagram

Dynamic performance of the radial piston pump, fitted with mechatronic servomechanism for positioning of the stator ring, is highlighted by: attenuation of the response amplitude characteristic, depending on frequency of the control signal; characteristic of phase shift (delay) of response from command, depending on frequency of the control signal. Together, the two characteristics form the Bode diagram, shown in Fig.8. Amplitude and phase shift measurements were made for eight points of frequency: 0.1 Hz, 0.2 Hz, 0.5 Hz, 1 Hz, 2 Hz, 5 Hz, 10 Hz, 20 Hz. From the Bode diagram it results that the amplitude attenuation of 3 dB, i.e. a 30% reduction of the response amplitude, occurs at a frequency of 2.4 Hz of the control signal. At this frequency the phase displacement is 35° .

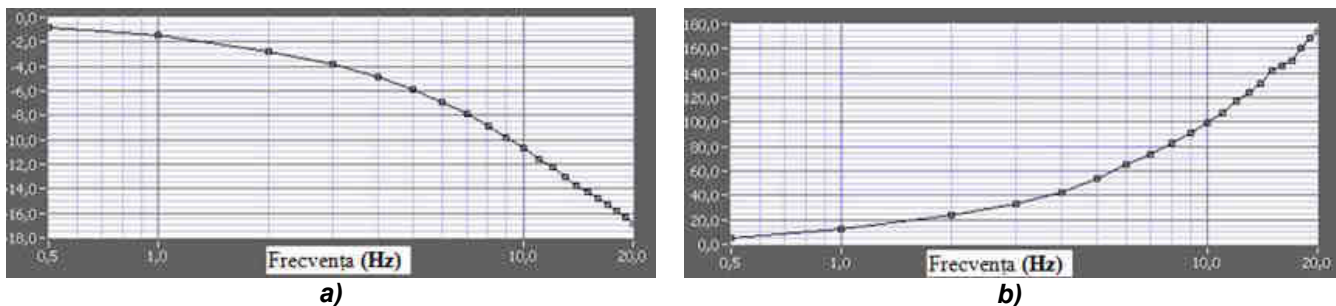


Fig. 8 – a) Bode diagram: Attenuation, dB-Frequency, Hz; b) Phase displacement, deg- Frequency, Hz.

Conclusions

- The article presents a minimal structure of a modern stand, on which can be carried out tests under static and dynamic mode for volumetric rotary machines, namely hydrostatic pumps and motors, fixed or adjustable.
- Performance of this stand has been highlighted by testing a radial piston pump, MOOG production, with capacity adjustable by means of a mechatronic system for positioning the stator ring between 0-32 cm³/rev.
- The following performance of the pump resulted: a good proportionality between the control signal U_c , V and the flow displaced at constant rotational speed, l/min (from static characteristics); *delay time* = 116 ms, *stabilization time* = 193 ms, *over adjustment* = zero (from response to step signal); *attenuation* = 30%, *phase shift* = 35° (from Bode diagram).

REFERENCES

- [1] T.C. Popescu, D.D. Ion Guță, C. Calinoiu, "Modern instruments for analysis of hydrostatic transmissions", U.P.B. Sci. Bull., Series D, Vol 72, Iss 4, 2010.
- [2] I. Lepădatu, "Theoretical and applied research on mechatronic systems adjusting the flow of hydraulic rotary generators by eccentricity", U.P.B. Doctoral Thesis, 2010.

NEW CONTRIBUTIONS TO THE STUDY OF DESTRUCTION BY CAVITATION OF TWO BIPHASIC (AUSTENITE + FERRITE) STAINLESS STEEL FOR THE MANUFACTURE OF BLADES AND ROTOR HYDRAULIC MACHINES

Ilare BORDEAȘU, Constantin BORDEAȘU, Brandusa GHIBAN, Ain Dan JURCHELA,
Octavian OANĂ, Adrian KARABENCIOV

“POLITEHNICA” University of Timisoara, ROMANIA

Summary: New research in the field of hydraulic turbines and pumps follow knowing how to respond to destruction by cavitation erosion composition of steels used in the manufacture of rotor blades. Research in this direction fall and the results presented in the paper. Thus, we analyze and discuss aspects of the degradation products on two stainless steel with biphasic structure (austenite and ferrite, to varying degrees) using photographic images of the microstructure, mechanical strength and deformability properties and comparison with standard steel based OH12NDL parameters and characteristic curves of cavitation erosion. Analyzed steels have similar contents of chromium, nickel and 0.05% carbon and it provides higher availability, reduced risk to weld cracking. The results and conclusions obtained are useful for designers and technologists specialized in materials for the generation of stainless steel, able to increase the life of highly stressed parts cavitation. Cavitation tests are made T1magnetostrictive vibrator device with nickel tube from Cavitation Laboratory in the University Politehnica Timisoara.

Keywords: microstructure, mechanical properties, chemical composition, resistance to cavitation, erosion of cavitation, vibrator device

1. INTRODUCTION

Destruction of materials by cavitation erosion remains a constant concern of scientists and especially hydromechanical equipment manufacturers, ships and boats, because of changes to geometry bodies in contact with the fluid cavity, with implications for performance and service life of equipment. Technological solutions, increase the life of the components of these machines, especially hydraulic turbine which operates as cavitation, has forced researchers to focus their studies to analyze the material in terms of resistance to destruction by erosion and cavitation phenomena occurring in the material structure. This course is required by many factors influencing cavitation erosion: the structural component, chemical constitution, technology development workpiece, heat treatment, chemical, mechanical, etc. Therefore, the results presented are outdated and out of step with the new orientations of professionals in the field to study the morphology of the damage caused by cavitation erosion, a steel for cars.

2. MATERIALS INVESTIGATED

The materials studied are part of stainless steel, for casting blades and rotor hydraulic turbines and other components operating in developed cavitation regime. The made which were taken the samples for determination of mechanical, metallographic analysis and cavitation erosion tests are in the material base of the Cavitation Laboratory, University Politehnica Timisoara and received in 1980 from the former Resita Mechanical Factory, under a cooperation agreement.

Because, the two steels are not produced by standard rules, for identifiers, in this paper are denoted by O1 and O2.

Chemical composition determined Expertise Center Special Materials are presented in Table 1 and the values of the main mechanical properties with influence of the cavitation

resistance are summarized in Table 2. In these tables are shown and data characterizing OH12NDL steel (denoted by OE *), considered standard for turbines in Romania, due to good cavitation qualities, proven in operation aggregates from Gates Iron I and II [1, 3, 5]

Table 1. Chemical composition of stainless steels investigated

Oțel	Chemical composition, %gr								
	C	Si	Mn	P	S	Cr	Ni	Mo sau Cu	Fe
O1	0.05	0.99	2.5	0.03	0.012	20.62	8.71	-	rest
O2	0.05	1.73	2.48	0.04	0.015	20.88	8.00	2.66 Mo	rest
OE*	0.1	0.3	0.4	0.09	0.03	12.8	1.25	0.9 Cu	rest

*-Steel OH12NDL standard for hydraulic turbines in Romania, considered good resistance to cavitation erosion

Table 2. Values of the mechanical properties

Oțel	The tensile strength, R _m , MPa	Yield strength, R _{p0.2} , MPa	Elongation at break, A, %
O1	635	270	40
O2	590	270	40
OE*	650	400	-

With chart Schaffler / bibliography thesis Juchela and Karabenciov, works hilarity / based on equivalents of chromium (22.105% to 26.135% for steel and steel O1 O2) and nickel (11.46% to 10.74% for steel and steel O1 O2) with relations (1), were determined structural constitutions approximate data in Table 3.

$$Cr_{ech.} = \%Cr + \%Mo + 1.5 \times \%Si + 0.5 \times \%Cb \quad (1)$$

$$Ni_{ech.} = \%Ni + 30 \times \%C + 0.5 \times \%Mn$$

Table 3. Microstructural constitution

Steel	The proportion of phase, %		
	Martensite	Austenite	Ferrite
O1	-	80	20
O2	-	45	55
OE*	88%	-	12

3.EQUIPMENT AND METHOD FOR TESTING CAVITATION

Cavitation erosion tests were performed on T1 magnetostrictive vibrator device [1], Figure 1, using a vibratory cavitation test [2].

Operating parameters of the device are:

- Power: 500 W
- Vibration frequency: 7000 Hz ÷ 0.3%
- Double vibration amplitude: 94 μm

- Sample diameter: 12 mm
- Power supply: 220 V/50 Hz
- Sample type: vibrator
- Liquid medium: double-distilled water, whose temperature was kept constant throughout the tests at 21 ± 1 °C.
- Total duration of the attack: 165 minutes

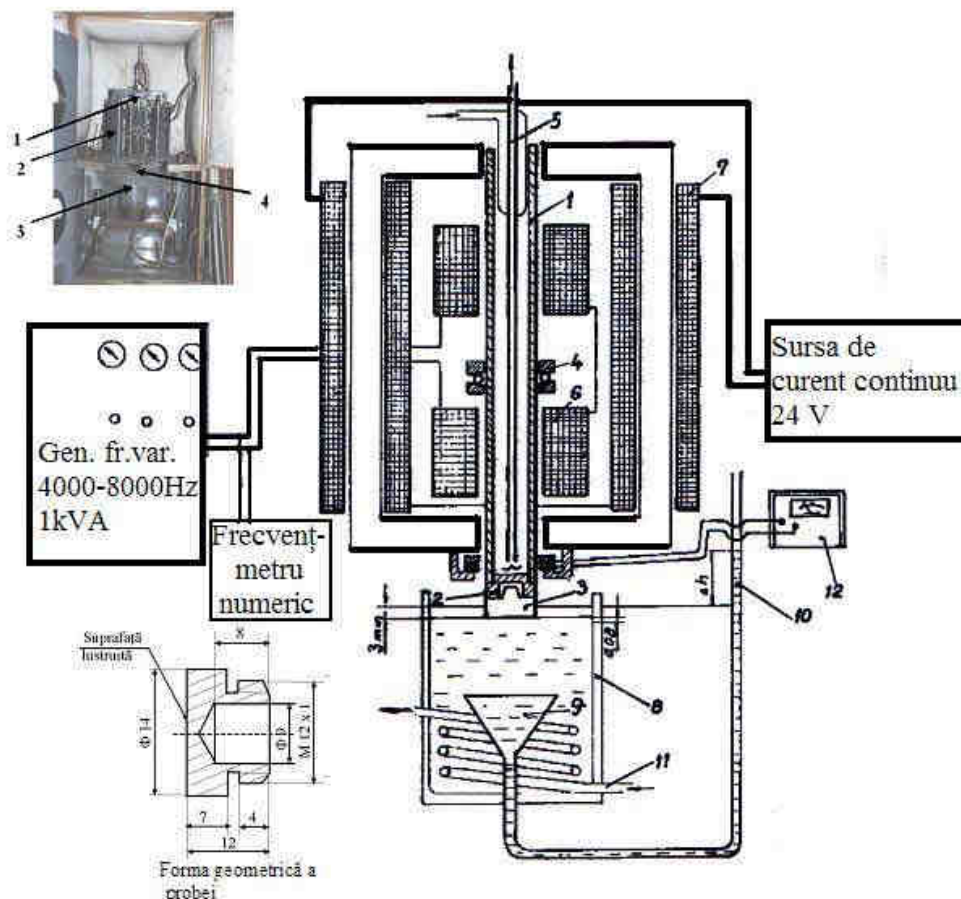


Fig. 1 Vibrator magnetostrictive device with nickel tube T1
1. Nickel tube; 2. The coils of continuous current and alternating current;
3. sample for test; 4. bowl of water

Experimental procedures complied with the standard ASTM [6]

3. EXPERIMENTAL RESULTS

3.1 Characteristic curves and parameters

Figure 2 displays the characteristic curves, which give the average erosion depth variations cumulative MDE (t) and its velocity MDER (t) during cavitation attack.

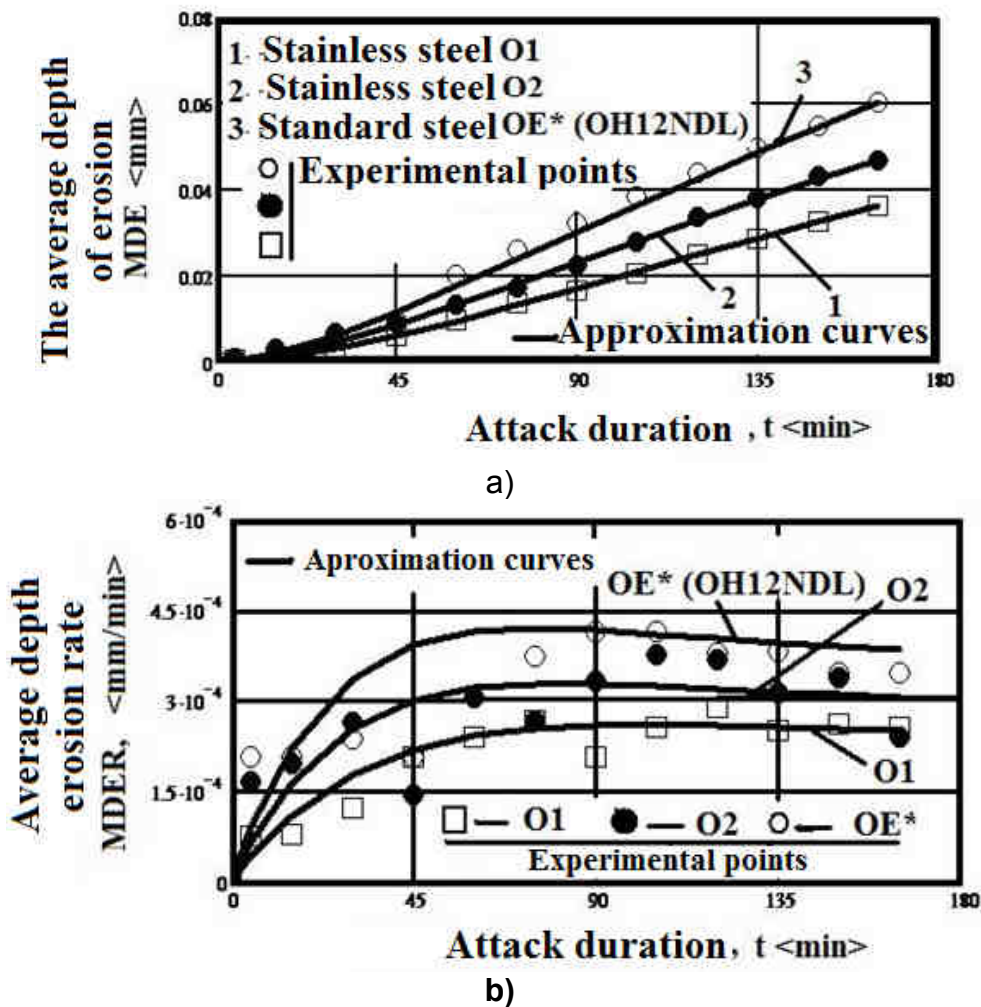


Fig. 2 cavitation erosion curves

a) Variation of penetration depth of erosion, b) change in mean depth of penetration rate of erosion

In Table 4 are shown resistance to cavitation $1/MDER$ determined value value to reverse that tends to stabilize mean depth of erosion rate

Table 4. Cavitation resistance value at the end of cavitation attack

Steel	$1/MDER, \text{min/mm}$	
O1	$3.989 \cdot 10^3$	1.537
O2	$3.271 \cdot 10^3$	1.26
OE*	$2.595 \cdot 10^3$	1

By analyzing the curves in Figure 2 cup dispersion of experimental points and their shape compared to standard steel is found that they have constant behavior during cavitation attack and high resistance steel standard. This finding shows that steel structures can generate the most resistant structural constituents (martensite) can be replaced with proportions between austenite and ferrite well established allies.

The data in Table 4 show that the cavitation resistance of both stainless steel as the ratio of $1/MDER$ parameters compared to standard steel OE * (OH12NDL) tends to an increase of about 1.26-1.537. This conclusion is advantageous hydraulic turbine builders and exploiters because of low carbon content avoid cracking and pre-warming, the necessary process for predominant martensitic steels structure, such as OE *.

3.2 Analysis of morphology degradation

Metallographic optical microscope analysis aimed at highlighting the microstructural characteristics of materials and development of degradation caused by vibratory cavitation. The microphotographs, for the two stainless steel, are shown in Figures 3, images are taken perpendicular to the sample surface, in Figure 4, before the attack cavitation.

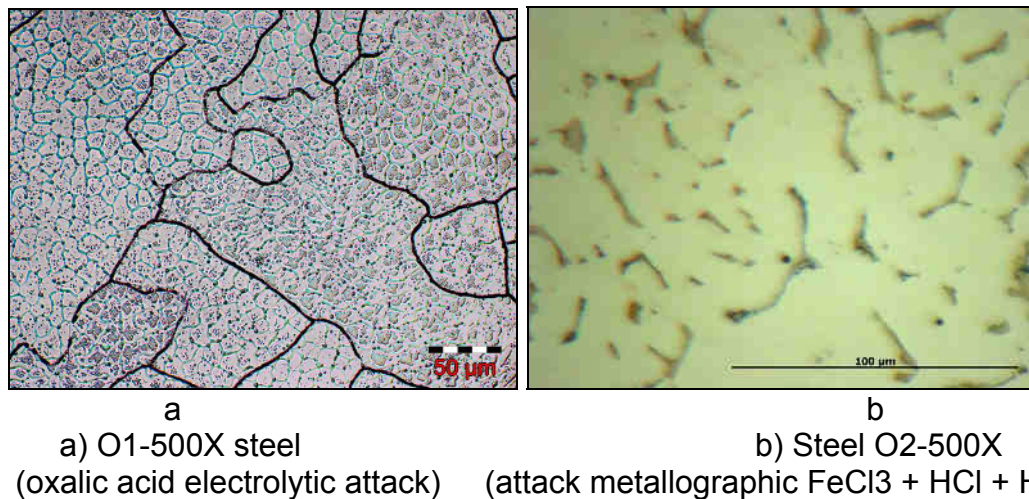


Fig. 4 Metallographic structures

Metallographic structures have been highlighted by reagent FeCl₃ + HCl + H₂O and 5% oxalic acid attack is up to 10 seconds.

If O1 steel is observed to have a biphasic structure of ferrite and austenite, with large grains to form, within them, of a structure under grains extremely fine, beneficial mechanical behavior but also to corrosion by cavitation.

If O2 steel, highlights a structure of solid solution α .

Macroscopic analysis of stainless steels investigated aimed at highlighting appearance subject cavitation and maximum penetration depth measurement cavitation metallic materials. Maximum depth of penetration was possible after cutting cavitation in axial plane, perpendicular to the eroded surface for 165 minutes and metallographic preparation. To look stereomicrostructural to evaluate cavitation three diameters were measured after different directions determined percentage of area affected by cavitation results using the sample mean diameter and the diameter of the section affected by cavitation, Table 5.

Table 5. Determination of percentage area affected by cavitation

Stainless steel	Average diameter of the sample, μm	Average diameter of the section affected by cavitation, μm	Percentage the section affected by cavitation, %
O1	13560	8374	38,14
O2	13718	8456	41.26

From Figure 3 it is observed that stainless steel O1, the cavities evenly distributed within the area affected by cavitation. Area affected by erosion is the rate of 38.14%. Maximum depth of penetration of cavitation is about 335 μm (fig.3b).

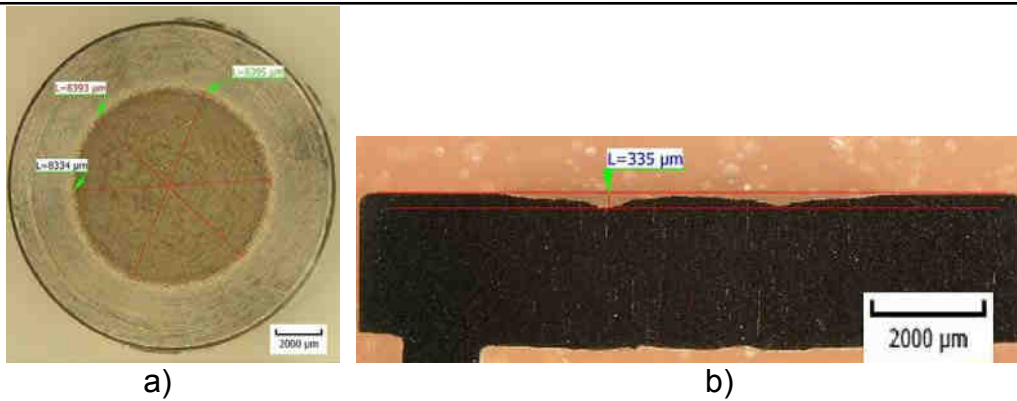


Fig.3. O1 macroscopic appearance of stainless steel at end attack cavitation: to look stereomicrostructural (8X) b-maximum penetration depth measured perpendicular eroded surface (10X);

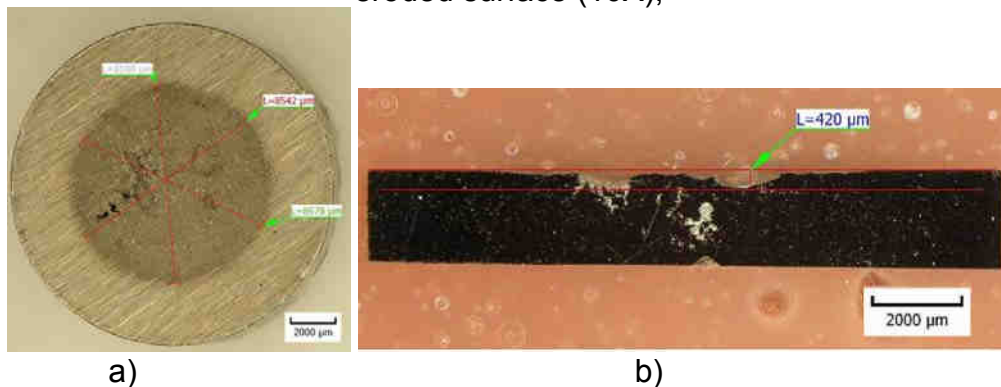


Fig.4. O2 macroscopic appearance of stainless steel at end attack cavitation: to look stereomicrostructural (8X) b-maximum penetration depth measured perpendicular eroded surface (10X);

In stainless steel surface affected by cavitation O2 is well defined, with large caverns and area affected by cavitation of 41.26% (Fig. 4.a) and the maximum penetration depth of 420 μm (Fig. 4.b).

SEM images shown in Figure 5 a and b, aim to highlight how structural damage was done to the two steels.

Photomicrograph of fig.5.a, O1 steel, highlights a cavity surface equal proportions of fine and large cavity with intergranular cracks, propagation by slip cleavage highlighting lines and breaking the fragile nature of intergranular propagation and highlighting areas by cleavage fracture propagation.

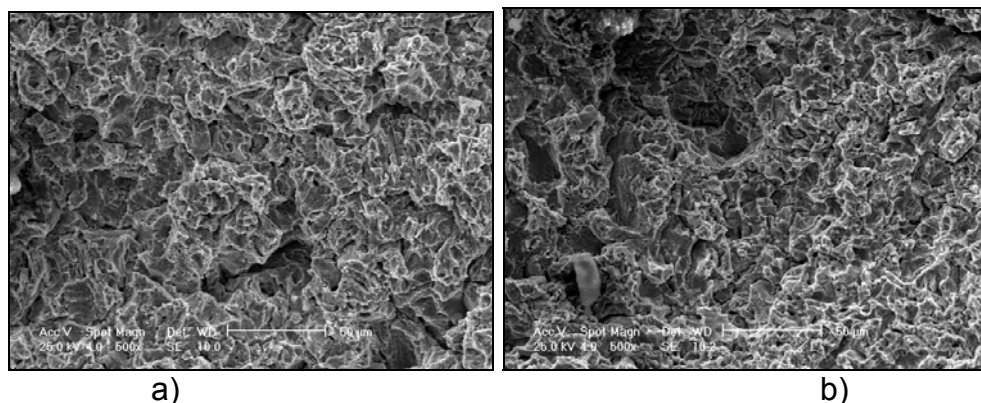


Fig. 5. SEM images (magnification 500X)
 O1 to stainless steel, stainless steel b-O2

In fig. 5.b, austenitic-ferritic stainless steel O2, there is a very fine surface cavity with: nonmetallic inclusions, cleavage surfaces highlighting the fine intergranular cracks and brittle fracture character and highlighting the cleavage planes and wave propagation breaking front. To know the causes that led to their behavior and resistance to cavitation, cavitation parents layers of eroded surfaces were subjected to Vickers microhardness measurements. Microhardness values were made at a distance of about 1-2 mm, with a measurement error of $\pm 2.3\%$. The values obtained are shown in Table 5.

Table 5. Vickers microhardness values

Stainless steel	Microhardness Vickers ($\mu\text{HV}_{0.1}$)			
	Field 1	Field 2	Field 3	Average
O1	155	162	167	161
O2	136	131	129	132

Higher microhardness value O1 steel, explain why its erosion rate stabilization MDER, figure 2, start much faster and occurs at a lower value steel O2.

CONCLUSION

1. The new stainless steels O1 and O2, with the structural constitution biphasic (austenite and ferrite), were resistances, to erosion caused by vibration cavitation, higher to standard steel OE * and can be used in casting blades and rotors of pumps and hydraulic turbines.

2. The results show that it can generate different steels, with different structure, of the martensitic structure, which are preferable for high capacity welding, as to avoid cracking and preheating.

3. The generated stainless steels are the current trend, in which the percentage of carbon is limited below 1.0%, just to avoid of the difficulties encountered at repair process by welding.

REFERENCES

- [1] BORDEAȘU, I. *Eroziunea cavitațională a materialelor*, Editura Politehnica, 2006, 208 p.
- [2] BORDEAȘU, I., MITELEA, I., (2011) Cavitation Erosion Behaviour of Stainless Steels with Constant Nickel and Variable Chromium Content, *Materials Testing-Materials and Components, Technology and Application*, 2012, volume 54, nr.1, pp.53-58
- [3] BORDEAȘU, I., MITELEA, I., POPOVICIU, M. O., CHIRITA, C., Method for classifying Stainless Steels upon Cavitation Resistance, *METAL 2011, 20th International Conference on Metallurgy and Materials*, May 18-20, 2011, Brno, Czech Republic
- [4] FRANC, J.P., MICHEL, J.M. *Fundamentals of Cavitation*, Kluwer Academic Publishers, P.O.Box, 322, 3300 AH Dordrecht, The Netherlands, 2004
- [5] POPOVICIU, M. O., BORDEAȘU, I. Considerations Regarding the Total Duration of Vibratory Cavitation Erosion Test, *Third International Symposium on Cavitation*, Grenoble, France, April 1998, pp.221-226
- [6] *** Standard Test Method for Cavitation Erosion Using Vibratory Apparatus ASTM G 32-2010.

MAINTENANCE AND TESTING OF THE HYDRAULIC SERVO VALVES

Radu RADOI¹, Ioan BALAN², Iulian DUTU³

¹ INOE 2000 - IHP, radoi.ihp@fluidas.ro

² INOE 2000 - IHP, balan.ihp@fluidas.ro

³ INOE 2000 - IHP, dutu.ihp@fluidas.ro

Abstract:

The equipment which must work at high values of speed and response frequencies and reach optimum performance need to have their hydraulic installations equipped with servo valves. The costs of production of the servo valves are very high, due to their mechanical complexity and they are not compatible at all with the contaminated fluids, cause of the small gaps between the parts in motion and of the very small apertures of nozzles. If these installations are not properly maintained servo valves can be damaged very quickly and can only be remedied in centers (laboratories) by specialized personnel. The paper presents ways of identifying a faulty servo valves, symptoms and possible causes and their testing.

Keywords: hydraulic, servovalve, testing, maintenance

1. Introduction

The equipment which must work at high values of speed and response frequencies and reach optimum performance need to have their hydraulic installations equipped with servo valves. The modern servo valves are very reliable components, due to the major improvements applied to them in the course of time. The costs of production of the servo valves are very high, due to their mechanical complexity and they are not compatible at all with the contaminated fluids, cause of the small lost motions between the parts in motion and of the very small apertures. These very performant equipment are therefore suitable for sophisticated systems and require a rigorous maintenance.

These prerequisites regarding precision and dynamics of the hydraulic drives lead to the use of hydraulic devices of control with high performances. The dynamic performances of the servo valves with direct command, are limited at 80 Hz and of those with piloting stage at about 100 Hz. Beside the influence of the hydrodynamic forces, the performances of the hydraulic devices are much influenced by the dynamics of the electromechanic actuators, which drive, directly or indirectly the slide.

The close loop drives have been utilized a lot lately. In a drive of this kind with close loop or with servo control, the servo valves are the key elements, with the greatest impact upon the static and dynamic features of the drive system.

The servo valves must provide high fluid flows and dynamic features, high rigidity of the system at load and very slight deviations of position of the operating element, from the prescribed position.

For reaching this must be accomplished the following:

- High degree of accuracy at the execution of the bushand servo valve slide, for obtaining a symmetric and linear signal flow function
- Reduction of the mass of the parts in motion
- Reduction of the interference forces which have a negative impact upon the slide dynamics friction forces, hydrostatic forces, hydrodynamic forces and impulse forces

- Reduction of power losses of the piloted servo valves and minimization of the control chambers volumes
- Improvement of the dynamics of the electromechanic convertor.

2. The description of the servo valves

Due to the afferent performances, the most widely spread servo valves are the distributors with two slides see fig.1 These type of servo valves have beside the compulsory pilot, a stage of hydraulic amplification, distributor type. The pilot which comprises the couple motor and the nozzle flap amplifier may be considered and sometimes it is even utilized as a servo valve with an amplification stage. This is a classic distributor with marks executed in a higher precision class. The diagram of this type of servo valve may be seen in fig.2

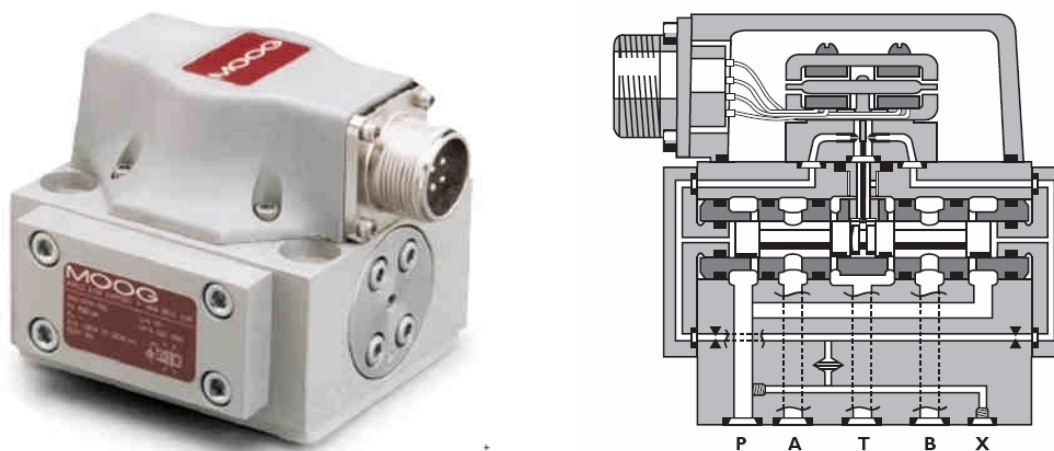


Fig. 1 Moog servo valve series G761

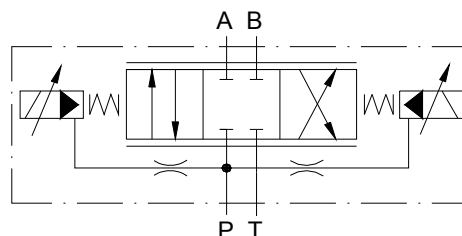


Fig. 2 2 stage servo valve scheme

The servo valves are commanded with electric signal applied to the spools of the couple motor. The two spools may be connected serially or in parallel. With a few exceptions, the servo valves use only c.c.signal.

The hydraulic installations which enclose servo valves must take into account some very strict conditions:

- The installed flow of the pump must be 10% higher than the highest flow supplied by the servo valve
- The servo valves must be protected with a filter of 5 + 15 μ m This filter is recommended to be put as an individual protection for each servo valve. It is recommended that the safety filter of the servo valve to be deprived of by pass valve
- The pressure valve which maintains pressure almost constant on the input in the valve must be chosen in such a way that for the range of the flows discharged in the basin during work the variation of the adjusted pressure to be below 10 bar
- It is recommended that the hydraulic cylinders which equip the hydraulic installation to be with bilateral rod of the same diameter. This ensures a good stability allowing also an

easier and more accurate calculation of the hydraulic system and also bring simplification of the electronic control system.

- It is recommended that servo valves to be placed as close as possible to hydraulic motors they serve. Is indicated as links of servo valve with hydraulic motor to be rigid (pipes) or not to vary their volume at pressure variations.
- It is recommended that between pumping group and servo valve be mounted a hydropneumatic accumulator whose size is determined by the pump flow and the operating mode of the system. It is necessary to provide manual controls to bring hydraulic motors in the original starting position.
- It is recommended that the hydraulic system be equipped with oil cooling - heating system to ensure a temperature of 45 to 55 °C during operation.

3. Finding faults in installations with servo valves

If it is found that the system that comprises a servo valves is not working, for testing can be replaced with another spare servo valves, and if you do not have a backup servovalve will proceed as follows:

- Shall be measured the command signal of servovalve thus checking the electronic system operation:
 - If electronic block does not give electronic signal to needed parameters search fault here and fix
 - If electronic block give control signal and if one can not vary manual the signal it must be used an external signal generator.
 - If the load does not move (at external command signal) put gauges on the supply and return ports of servo valve. If the supply pressure is good that means the pressure source is good and then continue searching fault.
- Place pressure gauges on motor ports. Vary the control signal and check output pressure at motor ports.
- If we have not a gradual increase in pressure means that the servovalve is damaged.

Faulty servovalves must be removed from a system only after the place around them it is cleaned. For servovalve removal first disconnects electrical connector, remove the screws with which it is fixed and mount the replacement servo valve whose protective cover was removed previously. Finally, the protective cover is mounted on demounted servo valve, to prevent dirt entering in the joints and losing O-rings.

To see if servovalves can be repaired these should be sent to specialized laboratories operated by highly qualified personnel .

4. Repairing servovalves

The symptoms of main defect encountered in servovalves can be:

- the servovalve give flow only one way and the electric control gives no results (nozzle clogged)
- servovalve not respond to commands (broken coil, clogged nozzles);
- Presence of flow without giving an electric command, flow which decreases at electric command in a certain sense (shifted null);
- Unequal flow at equal control level for both polarities (asymmetry)
- large hysteresis on reversing electrical control (friction between the spool and sleeve due to impurities)
- High flow at null that can not be canceled by adjutments (high wear of spool and sleeve edges)

Removal and installation of servo valves should be done only by specialized personnel and only based on accurate and complete instructions. The place where is made removal and instalation must be perfect clean. Because of the size of the nozzles and small gaps between moving parts any impurity can cause blockage of servovalve. Dismantled parts shall be placed on a non-metallic surface. On removal is well to note (mark the relative positions of the parts). Spool must be handled with care not to damage the edges. He should not be placed on hard surfaces. It is advisable to avoid removing the nozzle if it leads to change their position and if does not have the possibility of resettlement at fixed odds. If they are removed have to avoid damaging them, especially if there does not exist conditions to recalibrate them. After cleaning and repair servovalve component parts are assembled at place, then appropriate adjustments will be made and will be drawn static characteristic.

5. Testing of servovalves

Testing of servovalves is made on specialized stands. Such a stand for servo valves testing (Fig. 3) consists of: a tank on which is fixed a plate for connecting servovalve in testing circuit, a pumping group, pressure and flow transducers, a servocontroller and a computer equipped with data acquisition board.

Testing is as follows:

- 1) Check that stand and equipment fitted on it corresponds with mounting scheme;
- 2) Adjust supply pressure to servovalve at nominal value
- 3) The input current is passed several times through the circuit
- 4) The testing application is opened on the computer and then start the testing, after that the program generating the increasing steps of control signal and flow given by the servovalve is recorded and after draw the characteristic diagram
- 5) Check that the machine pressure remains relatively constant throughout the current cycle
- 6) periodic signal applied continuously allows recording characteristics during a complete cycle



Fig. 3 Servo valve mounted on stand for testing

Periodic signal during a complete cycle $\pm I_{\max}$ [mA] (maximum control current in both directions) applied to servo valve for plotting the characteristic is generated by a software application (Fig. 4). The application allows recording the data for further processing. The application generates the control signal and carries signals from the transducers through a data acquisition board.

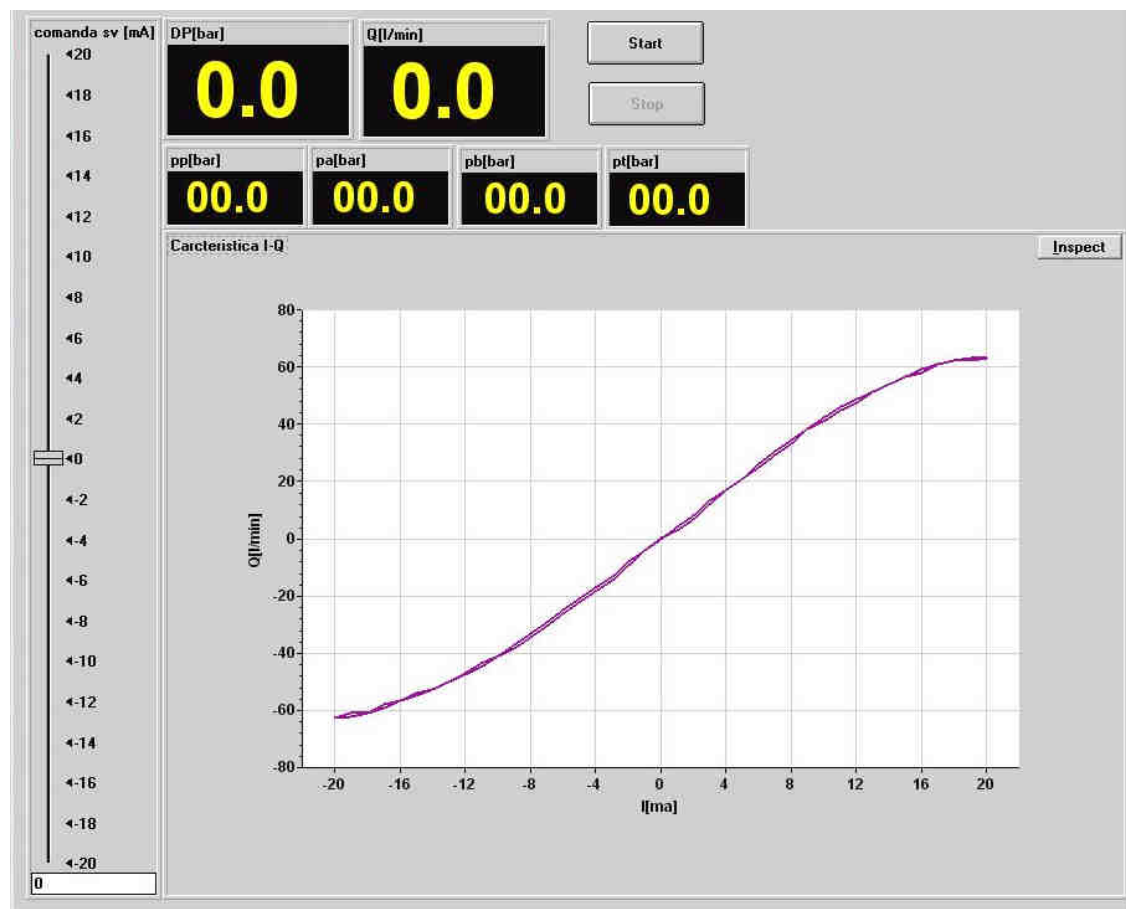


Fig. 4 Panel of the testing application made in TestPoint medium

From a recorded chart can be seen if hysteresis is large, if the parameters stipulated in the data sheet (maximum output at maximum control signal) are touched and if the chart is asymmetric or if null is shifted.

6. Terms of putting into service the installation with a new installed servo valve

Before mounting a servo valve in the system is necessary, especially in complex installations that had a very long operating since last oil change, to make a washing of a hydraulic installation. For this the servo valve is replaced with a special adapter plate for washing, on which is mounted an electrically controlled directional valve that can provide equivalent flow with that one given by the servo valve.

In some cases instead of servo valve is mounted a simple plate that directly connect the tank port with inlet pressure port. All pumps are started at low pressures (with safety valves opened, checking not to appear control signals to servo valves). Adjust safety valves at the values set by the designer.

Are given commands to the directional valve who replaced the servo valve to achieve the rated machine cycle speed of hydraulic motors. Check at the same time outward leakage appearance. After a while it stops the operation of the installation and replace the washer plate with the new servo valve. Are given to the servo valve electrical signals covering all the field of control. Give commands in automatic mode making the final adjustments at the control electronics as well as the hydraulic. It is well that all adjustments to be made at recommended hydraulic medium temperature and designer prescription which is in domain 45 to 50° C. The null of servo valve should be adjusted according to actual conditions of automatically cycle (supply pressure,

back pressure and oil temperature). Verification of correct adjustment of null is made by cutting electric connection of servo valve, in which case if the electronics is well adjusted, operated element must remain in place. After 3 hours filter cartridges are replaced with new ones.

6. Conclusions

Servo valves are high performance equipment and are suitable for installations and sophisticated systems.

Servo valves are sensitive devices and their use must meet a number of strict conditions such as:

- proper filter of oil to keep them in working order;
- respecting the installation instructions for servo valves can be achieved maximum of performance.

Repair of servo valves must be performed only by qualified personnel, otherwise these can be irreversibly affected.

REFERENCES

- [1] Cornel Velescu, Aparate si echipamente hidraulice proportionale, Mirton publishing house , Timisoara, 2003
- [2] M. Comes, P. Drumea, A. Mirea, G. Matache, Intelligent servohydraulic device for the control of the motion – 24th International Spring Seminar on Electronics Technology ISSE 2001
- [3] M. Comes, A. Drumea, A. Mirea, I Enache. , Electronic module for servohydraulic system with frequency control, MTM 2001, Romania
- [4] Dutu, R.I. Radoi, M. Blejan "Digital control module developed for a servohydraulic positioning system" Caciulata, Romania; 7-9 November, 2011, "Proceedings - HERVEX", ISSN 1454-8003; pp.381-385
- [5] http://www.moog.com/literature/ICD/G761_CDS6673_D.pdf

WHAT TO DO WITH A HYBRID DRIVE SYSTEM?

Krzysztof Kędzia

Wrocław University of Technology, Institute of Machines Design and Operation

krzysztof.kedzia@pwr.wroc.pl

Abstract: Do hybrid drive are the future? Limited resources of fossil fuels causing increasingly frequent questions about the future of propulsion systems. In this paper, on the basis of available information, was described the basic structure, types, and the potential benefits of multisources drive systems. The author's intention is to initiate a discussion which type of drive system: hydraulic, pneumatic, mechanical, electrical, is potentially the best solution to use in the future.

Keywords: *Hybrid drive system, ecology, energy, efficiency.*

1. Introduction.

Drive systems of machines and vehicles with an accumulation of energy is one of the elements of environmental technology. In a fast-changing cyclically repeated external loads of working machines and vehicles drive systems provide a reduction of primary energy consumption, and therefore exhaust gases emissions. They also allow to recuperate a kinetic or potential energy. Generally, lower energy consumption of drive systems of machines and vehicles, can be obtain by [4]:

- increasing an efficiency of drive system components,
- appropriate matching of high-efficient zones of components of powertrain,
- use of multi-source (hybrid) drive system, allowing to recuperate a kinetic or potential energy.

To design rational drive systems there should be used above listed postulates. It requires knowledge from transformation, transmission, distribution and energy recuperation field and meet several additional requirements. This applies in particular:

- Knowledge of the characteristics of the load (energetic characteristic), including flow variables (linear and angular velocity, flow rate) and effort variables (power, torque, pressure). It could be represented as: operating point, load curves, area of work or cycle work, or in the spectrum of loads.
- Knowledge of an energy characteristics (energy efficiency or losses).
- Evaluation of an energy efficiency of alternative solutions of the drive system for the same load conditions.
- Problems solving connected with structures and components selection for the drive system.
- Problems solving connected with controls issues, in particular the synthesis of control systems.

In the literature, the concept of multi-sources (or hybrid) drive systems, is known for several decades [1], [2], [3], [4]. Research and development on these issues, from economic and technological reasons, were periodic- sometimes very intensive, sometimes weak activity. They were closely related with the fuel crisis. Nowadays R&D activity in this area is more and more connected with an environmental aspects.

"Keeping up" of energy source for variable load is characteristic for classic drive systems. It is directly connected with the energy efficiency of the system, which often reaches values even below 10%. It has a significant impact on the operating costs such as: fuel and lubricants consumption, or durability of the drive system. This applies in particular to internal combustion engines.

One of the ways to solve this problem is multisources (hybrid) drive systems, characterized by the cooperation of at least two energy sources, wherein at least one of them must be the secondary source of energy.

The concept of "primary source of energy" should be understood as a source of energy with constant parameters, providing energy to the system regardless of the changes taking place in the load. This may be for example a heat engine. The "primary source of energy" is characterized by irreversible energy flow- only from source to the system.

The term "secondary source of energy" (an accumulator) means a device for accumulating potential or kinetic energy. The battery stores the surplus and / or recoverable energy. The accumulation can be realized by electrochemical, hydraulic or mechanical batteries. Secondary source of energy is characterized by reversible work.

Due to the direction of energy flow and location of the sources, there are two types of structures of hybrid systems:

- series (fig.1),
- parallel (fig.2).

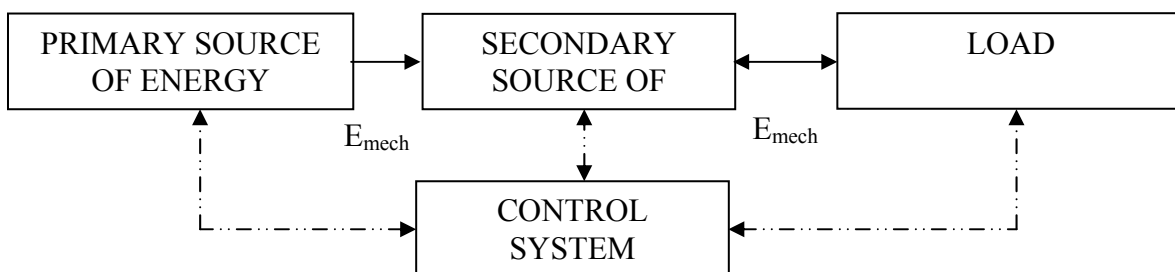


Fig. 1. Schema of series hybrid drive system.

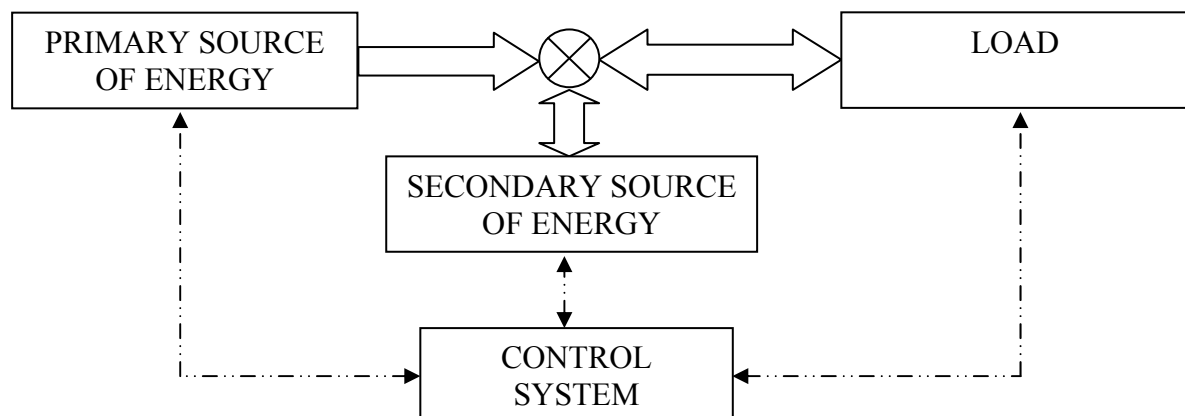


Fig. 2. Schema of parallel hybrid drive system [4].

There are many solutions of secondary sources of energy. The most widespread and historically oldest, is undoubtedly a mechanical press (serial system), in which the electric motor operates with power equal to the average power in the cycle. Increased energy demand is met from secondary sources of energy- in this case flywheel. When the press is in idling mode, flywheel gathers an energy supplied to the system by an electric motor. Other examples could be: the steam engine, compressor or IC engine, where the flywheel is used to stabilization of angular velocity [5].

Nowadays more and more companies propose a hybrid machinery and equipment of propulsion systems. Information on the details of construction and principles of their controls, is limited to the manual, because of trade secret or competition between companies. In some cases,

the construction of hybrid machines is a result of experimental tests and an engineers intuition and their experience

2. Energy sources for hybrid vehicles

There are a few power sources for hybrid vehicles [5]:

2.1. On-board or out-board rechargeable energy storage system (RESS).

A rechargeable energy storage system or RESS is a system that stores energy for delivery of power and which is rechargeable. Production storage systems use electric rechargeable traction batteries, electric double-layer capacitors or flywheel energy storage [21].

2.2. Coal, wood or other solid combustibles.

Solid fuel refers to traditional types of combustible solid fuels like firewood and coal. While these fuel types are readily available (some of them actually grow on trees), not all of them are sustainable in the long term. Coal, for example, is a fossil fuel, and its use in the production of electricity is said to make it the largest contributor to the human-made increase in CO₂ in the atmosphere. The use of coal in solid fuel heaters is, however, increasingly uncommon. Types of solid fuel:

- wood,
- charcoal,
- peat,
- coal,
- hexamine fuel tablets,
- organic pellets.

2.3. Electricity, Electromagnetic fields, Radio waves.

Electricity is the set of physical phenomena associated with the presence and flow of electric charge. Electricity gives a wide variety of well-known effects, such as lightning, static electricity, electromagnetic induction and the flow of electrical current. In addition, electricity permits the creation and reception of electromagnetic radiation such as radio waves [5].

2.4. Compressed or liquefied natural gas.

Compressed natural gas (CNG) is a fossil fuel substitute for gasoline (petrol), Diesel fuel, or propane/LPG. Although its combustion does produce greenhouse gases, it is a more environmentally clean alternative to those fuels, and it is much safer than other fuels in the event of a spill (natural gas is lighter than air, and disperses quickly when released). CNG may also be mixed with biogas, produced from landfills or wastewater, which doesn't increase the concentration of carbon in the atmosphere [22].

CNG is made by compressing natural gas (which is mainly composed of methane [CH₄]), to less than 1% of the volume it occupies at standard atmospheric pressure. It is stored and distributed in hard containers at a pressure of 200–248 bar (2900–3600 psi), usually in cylindrical or spherical shapes.

2.5. Human powered e.g. pedalling or rowing.

Human powered transport includes walking, bicycles, velomobiles, row boats, and other environmentally friendly ways of getting around. In addition to the health benefits of the exercise provided, they are far more environmentally friendly than most other options. The only downside is the speed limitations, and how far one can travel before getting exhausted [5].

2.6. Hydrogen.

A hydrogen vehicle is a vehicle that uses hydrogen as its onboard fuel for motive power. Hydrogen vehicles include hydrogen fueled space rockets, as well as automobiles and other transportation vehicles. The power plants of such vehicles convert the chemical energy of hydrogen to mechanical energy either by burning hydrogen in an internal combustion engine, or by reacting hydrogen with oxygen in a fuel cell to run electric motors. Widespread use of hydrogen for fueling transportation is a key element of a proposed hydrogen economy [11].

2.7. Petrol or Diesel fuel.

Petrol and diesel are petroleum-derived liquid mixtures used as fuels. Though both have similar base product but have different properties and usage.

Petrol is a petroleum-derived liquid mixture consisting mostly of aliphatic hydrocarbons and enhanced with aromatic hydrocarbons toluene, benzene or iso-octane to increase octane ratings, primarily used as fuel in internal combustion engines. Diesel is a specific fractional distillate of petroleum fuel oil or a washed form of vegetable oil that is used as fuel in a diesel engine invented by German engineer Rudolf Diesel [8].

2.8. Solar.

Solar energy, radiant light and heat from the sun, has been harnessed by humans since ancient times using a range of ever-evolving technologies. Solar energy technologies include solar heating, solar photovoltaics, solar thermal electricity and solar architecture, which can make considerable contributions to solving some of the most urgent problems the world now faces

The total solar energy absorbed by Earth's atmosphere, oceans and land masses is approximately 3,850,000 exajoules (EJ) per year.[6] In 2002, this was more energy in one hour than the world used in one year

2.9. Wind.

Wind is the flow of gases on a large scale. On Earth, wind consists of the bulk movement of air. In outer space, solar wind is the movement of gases or charged particles from the sun through space, while planetary wind is the outgassing of light chemical elements from a planet's atmosphere into space. Winds are commonly classified by their spatial scale, their speed, the types of forces that cause them, the regions in which they occur, and their effect.

3. Engine type.

3.1. Hybrid electric-petroleum vehicles

When the term hybrid vehicle is used, it most often refers to a Hybrid electric vehicle. These encompass such vehicles as the Saturn Vue, Toyota Prius, Toyota Camry Hybrid, Ford Escape Hybrid, Toyota Highlander Hybrid, Honda Insight, Honda Civic Hybrid, Lexus RX 400h and 450h and others. A petroleum-electric hybrid most commonly uses internal combustion engines (generally gasoline or Diesel engines, powered by a variety of fuels) and electric batteries to power the vehicle. There are many types of petroleum-electric hybrid drivetrains, from Full hybrid to Mild hybrid, which offer varying advantages and disadvantages [5].

3.2. Continuously outboard recharged electric vehicle (COREV).

Given suitable infrastructure, permissions and vehicles, BEVs can be recharged while the user drives. The BEV establishes contact with an electrified rail, plate or overhead wires on the highway via an attached conducting wheel or other similar mechanism (see Conduit current collection). The BEV's batteries are recharged by this process on the highway and can then be

used normally on other roads until the battery is discharged. Some of battery-electric locomotives used for maintenance trains on the London Underground are capable of this mode of operation. Power is picked up from the electrified rails where possible, switching to battery power where the electricity supply is disconnected.

3.3. Hybrid fuel (dual mode).

In addition to vehicles that use two or more different devices for propulsion, some also consider vehicles that use distinct energy sources or input types ("fuels") using the same engine to be hybrids, although to avoid confusion with hybrids as described above and to use correctly the terms, these are perhaps more correctly described as dual mode vehicles [5]:

- Some electric trolleybuses can switch between an on board diesel engine and overhead electrical power depending on conditions (see dual mode bus). In principle, this could be combined with a battery subsystem to create a true plug-in hybrid trolleybus, although as of 2006[update], no such design seems to have been announced.
- Flexible-fuel vehicles can use a mixture of input fuels mixed in one tank — typically gasoline and ethanol, or methanol, or biobutanol.
- Bi-fuel vehicle: Liquified petroleum gas and natural gas are very different from petroleum or diesel and cannot be used in the same tanks, so it would be impossible to build an (LPG or NG) flexible fuel system. Instead vehicles are built with two, parallel, fuel systems feeding one engine. While the duplicated tanks cost space in some applications, the increased range and flexibility where (LPG or NG) infrastructure is incomplete may be a significant incentive to purchase.
- Some vehicles have been modified to use another fuel source if it is available, such as cars modified to run on autogas (LPG) and diesels modified to run on waste vegetable oil that has not been processed into biodiesel.
- Power-assist mechanisms for bicycles and other human-powered vehicles are also included (see Motorized bicycle).

3.4 Fluid power hybrid.

Hydraulic and pneumatic hybrid vehicles use an engine to charge a pressure accumulator to drive the wheels via hydraulic or pneumatic (i.e. compressed air) drive units. In most cases the engine is detached from the drivetrain merely only to change the energy accumulator. The transmission is seamless.

3.5 Electric-human power hybrid vehicle.

Another form of hybrid vehicle are human power-electric vehicles. These include such vehicles as the Sinclair C5, Twike, electric bicycles, and electric skateboards [5].

4. Environmental issues.

4.1. Fuel consumption and emissions reductions.

Start/Stop: In the NEDC (New European driving cycle) a fuel consumption reduction of 5-8 percent can be achieved with engine stop at vehicle standstill (fig. 3) [23].

Optimised operation: Engine operation with low engine load can be substituted by electric driving. Further, the combination of combustion engine and electric machine offers the possibility to shift the engine load point

Brake energy recovery: Recovery of the brake energy results in a fuel consumption reduction of 3-10 percent in the NEDC, depending on the layout of the hybrid powertrain, the maximum power of the electric machine and the efficiencies of the powertrain components

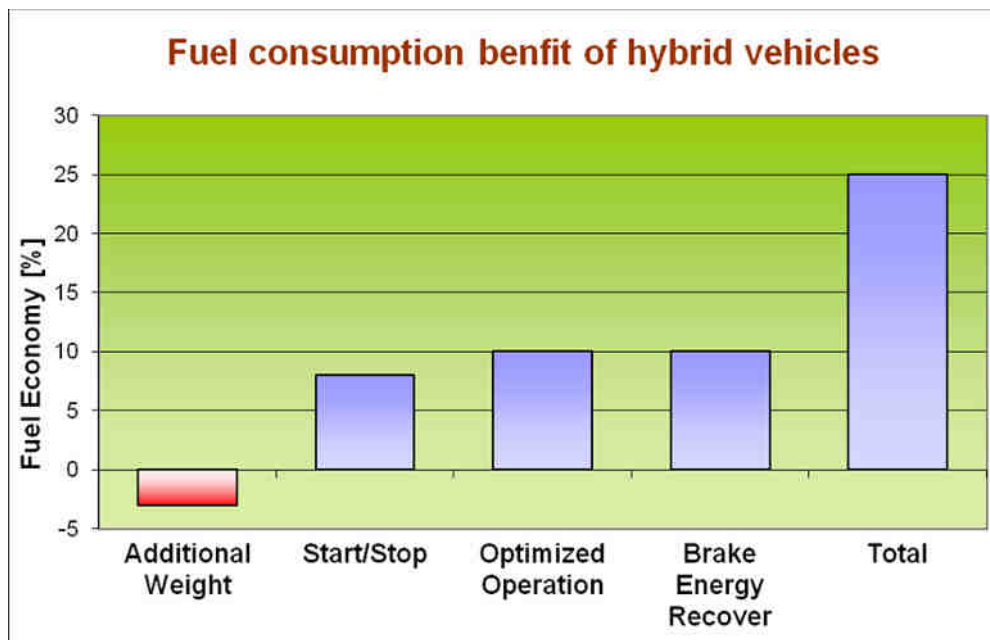


Fig.3 . Fuel consumption benefit of hybrid vehicles [23].

Figure 4 shows the simulated fuel consumption values for a conventional vehicle, the parallel hybrid and the parallel hybrid with fuel cell range extender.

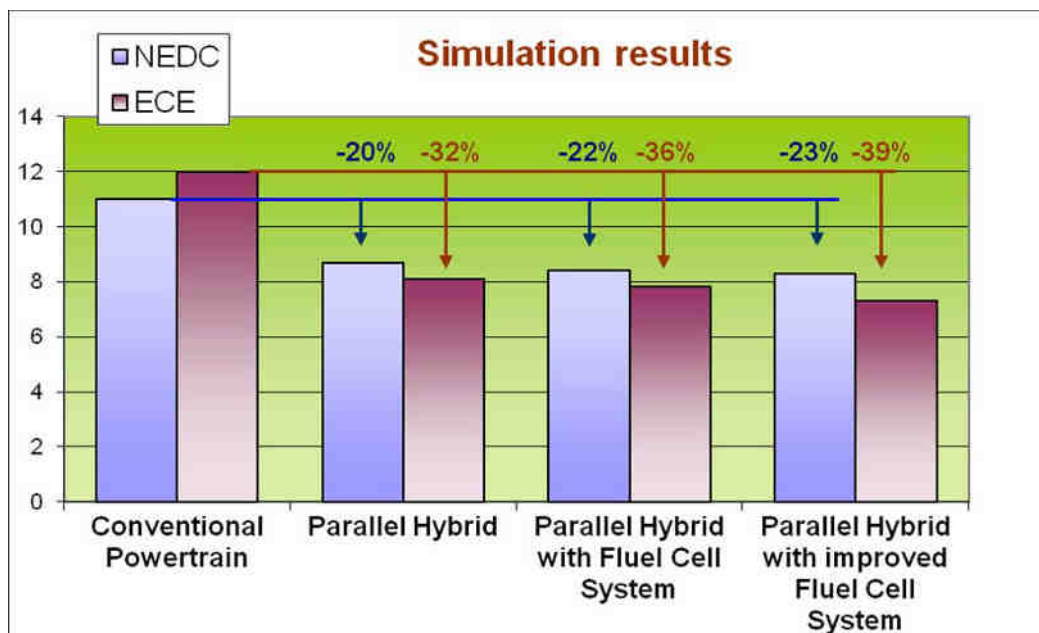


Fig. 4. Simulated fuel consumption values for a conventional vehicle, the parallel hybrid and the parallel hybrid with fuel cell range extender [23].

Hybridisation offers a big potential to reduce the fuel consumption especially in the ECE (urban part of the NEDC cycle) as all hybrid features – start/stop, electric driving and energy recovery – can be fully used.

4.2. Hybrid vehicle emissions.

Hybrid vehicle emissions today are getting close to or even lower than the recommended level set by the EPA (Environmental Protection Agency). The recommended levels they suggest for a typical passenger vehicle should be equated to 5.5 metric tons of carbon dioxide. The three most popular hybrid vehicles, Honda Civic, Honda Insight and Toyota Prius, set the standards even higher by producing 4.1, 3.5, and 3.5 tons showing a major improvement in carbon dioxide emissions. Hybrid vehicles can reduce air emissions of smog-forming pollutants by up to 90% and cut carbon dioxide emissions in half.

4.3. Environmental impact of hybrid car battery.

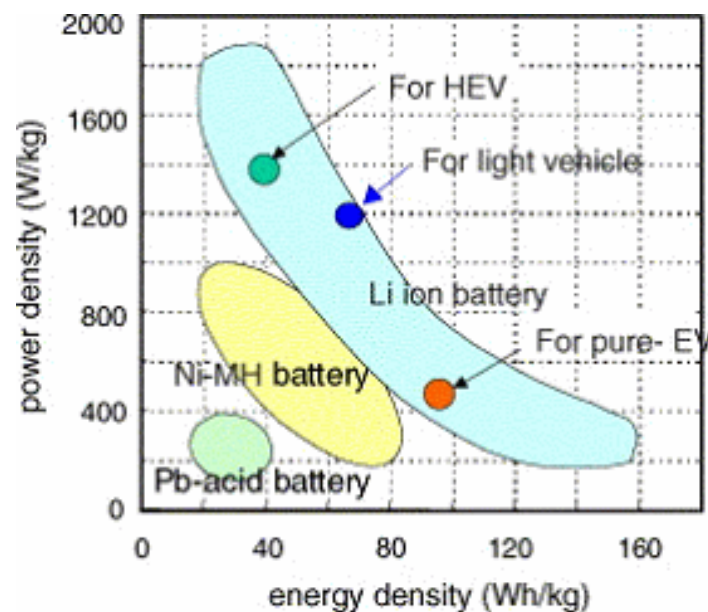


Fig. 5. Comparison of energy densities of rechargeable batteries [18].

Though hybrid cars consume less gas than conventional cars, there is still an issue regarding the environmental damage of the hybrid car battery. Today most hybrid car batteries are one of two types: 1) nickel metal hydride, or 2) lithium ion; both are regarded as more environmentally friendly than lead-based batteries which constitute the bulk of petro car starter batteries today. There are many types of batteries (fig. 5). Some are far more toxic than others. Lithium ion is the least toxic of the three mentioned above.[19]

The toxicity levels and environmental impact of nickel metal hydride batteries the type currently used in hybrids are much lower than batteries like lead acid or nickel cadmium. However, nickel-based batteries are known carcinogens, and have been shown to cause a variety of teratogenic effects.[20]

The Lithium-ion battery has attracted attention due to its potential for use in hybrid electric vehicles. Hitachi is a leader in its development. In addition to its smaller size and lighter weight, lithium-ion batteries deliver performance that helps to protect the environment with features such as improved charge efficiency without memory effect. The lithium-ion batteries are appealing because they have the highest energy density of any rechargeable batteries and can produce a voltage more than three times that of nickel-metal hydride battery cell while simultaneously storing large quantities of electricity as well. The batteries also produce higher output (boosting vehicle power), higher efficiency (avoiding wasteful use of electricity), and provides excellent durability, compared with the life of the battery being roughly equivalent to the life of the vehicle. Additionally, use of lithium-ion batteries reduces the overall weight of the vehicle and also achieves improved

fuel economy of 30% better than petro-powered vehicles with a consequent reduction in CO₂ emissions helping to prevent global warming [19].

4.4. Raw materials increasing costs.

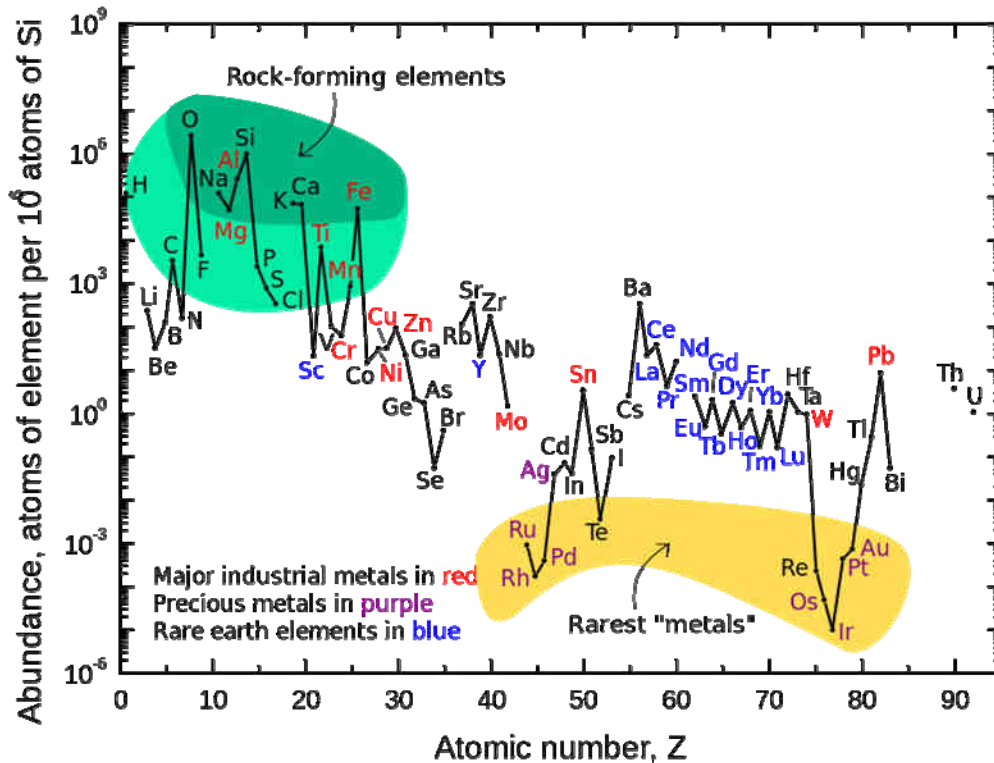


Fig. 6. Abundance of elements in the Earth crust per million of Si atoms [11], [12].

There is an impending increase in the costs of many rare materials (fig.6) used in the manufacture of hybrid cars [15]. For example, the rare earth element dysprosium is required to fabricate many of the advanced electric motors and battery systems in hybrid propulsion systems [15], [16]. Neodymium is another rare earth metal which is a crucial ingredient in high-strength magnets that are found in permanent magnet electric motors [13].

Nearly all the rare earth elements in the world come from China [14], and many analysts believe that an overall increase in Chinese electronics manufacturing will consume this entire supply by 2012 [15]. In addition, export quotas on Chinese rare earth elements have resulted in an unknown amount of supply [11], [14].

A few non-Chinese sources such as the advanced Hoidas Lake project in northern Canada as well as Mount Weld in Australia are currently under development; however, the barriers to entry are high [17] and require years to go online.

5. Conclusions.

So what we have to do? We have to plan future without oil.

With the price of crude hovering above \$140 a barrel there is significant pressure to reduce and manage our energy consumption. Goldman Sachs has predicted that we will soon hit \$200 per barrel [24].

Politicians and commentators are quick to offer solutions or attribute blame. However many of them deny the fact that in the not too distant future, supply will not be able to keep up with demand. Drilling cannot fix this and speculators are not to blame. Speculators are simply reading the markets. Making pariahs out of speculators is yet another way to avoid the reality of the energy

problems we face. And drilling for oil in Alaska or off America's shores will further degrade the environment and do nothing to reduce the price of oil [24].

Even the much maligned government of China has put energy efficiency on the top of their agenda. Within the realm of today's technology it is entirely possible to achieve a 10% reduction in energy consumption. Although inflation is a real problem, there are some upsides to increased oil prices. The high price of oil exerts pressure to reduce consumption and research alternatives [24].

Although oil is still part of the energy equation, in the future we will have a more diversified energy economy that is much less dependent on oil. If we are to be weaned off of oil we will need to focus on energy in a methodical way. From a policy point of view we need incentives and disincentives in support of efficiency and alternatives. We need national and global energy strategies [24].

REFERENCES (Arial, 11pt, Bold)

- [1] A. Szumanowski, "Hybrid electric vehicle drive design", Institute for Sustainable Technologies- NRI, ISBN 83-7204-456-2, Poland, 2006.
- [2] J.R. Cristobal Mateo, "Multi-Criteria Analysis in the Renewable Energy Industry", Springer- Verlag London Limited, 2012.
- [3] C. Cristescu, "Recuperarea energiei cinetice la franarea autovehiculelor", Editura AGIR, 2008.
- [4] K. Kędzia, "Metoda optymalizacji energetycznej i ekologicznej hydrostatycznego wieloźródłowego układu napędowego", Monography, Wrocław University of Technology, 2004.
- [5] http://en.wikipedia.org/wiki/Greenhouse_gases.
- [6] <http://www.thegreenmarketoracle.com/2011/12/ev-sales-predictions-in-us.html>.
- [7] http://en.wikipedia.org/wiki/Green_vehicle#National_and_international_promotion.
- [8] <http://www.epa.gov/oms/technology/research/how-it-works.htm>.
- [9] <http://www.epa.gov/oms/technology/research/how-it-works.htm> (2011, Richard Matthews).
- [10] http://en.wikipedia.org/wiki/Rare_earth_elements.
- [11] Lunn, J. (2006-10-03). Great western minerals. London. http://www.gwmg.ca/pdf/Insinger_Report.pdf. Retrieved 2008-03-18.
- [12] http://en.wikipedia.org/w/index.php?title=File:Elemental_abundances.svg&page=1.
- [13] Choruscars.com. (PDF) . Retrieved on 2012-04-18.
- [14] Haxel, G; J. Hedrick; J. Orris (2002). "Rare earth elements critical resources for high technology" (PDF). USGS Fact Sheet: 087-02 (Reston, VA, USA: United States Geological Survey). <http://pubs.usgs.gov/fs/2002/fs087-02/fs087-02.pdf>.
- [15] Cox, C (2008). "Rare earth innovation: the silent shift to china". Herndon, VA, USA: The Anchor House Inc. <http://theanchorhouse.com/2008/03>. Retrieved cited 2008-03-18.
- [16] G, Nishiyama. "Japan urges China to ease rare metals supply." 8 November 2007. Reuters Latest News. 10 March 2008 Reuters.com.
- [17] http://csis.org/files/publication/101005_DIIG_Current_Issues_no22_Rare_earth_elements.pdf
- [18] http://www.hitachi.com/rd/research/hrl/battery_01.html.
- [19] Environmental impact of hybrid car battery. (2008). Retrieved December 09, 2009 from Hybridcars.com.
- [20] Gelani, S; M. Morano (1980). "Congenital abnormalities in nickel poisoning in chick embryos" (PDF). Archives of Environmental Contamination and Toxicology (Newark, NJ, USA: Springer New York) 9 (1): 17–22. PMID 7369783. <http://www.springerlink.com/content/x37h8256j6g27g84/fulltext.pdf>. Retrieved 2008-12-09.
- [21] http://en.wikipedia.org/wiki/Rechargeable_energy_storage_system.
- [22] http://en.wikipedia.org/wiki/Compressed_natural_gas.
- [23] http://www.autofocusasia.com/engine_chassis_systems/hybrid_and_fuelcell.htm.
- [24] <http://www.thegreenmarketoracle.com/2011/12/ev-sales-predictions-in-us.html>.

TRIBOLOGICAL RESEARCHES REGARDING THE INCREASING OF PERFORMANCES OF THE FLUID POWER EQUIPMENTS

Ph. D. Eng. Corneliu CRISTESCU¹, Ph. D. Eng. Petrin DRUMEA¹,
Assoc. Prof. Ph.D.Eng. Constantin RANEA²

¹*Hydraulics & Pneumatics Research Institute-INOE 2000-IHP from Bucharest, ROMANIA,*

²*"POLITEHNICA" University of Bucharest, ROMANIA*

E-mail: cristescu.ihp@fluidas.ro; ihp@fluidas.ro; constantin.ranea@ancs

Abstract: The article presents a series of tribological researches regarding the increasing of the performances of fluid power equipments, developed in the **Laboratory of Tribology and Lubrication Systems**, within **Hydraulics and Pneumatics Research Institute** in Bucharest-INOE 2000-IHP, including some concrete results obtained. In particular, are presented, some researches on the tribological behavior of sealing systems of hydraulic cylinders, as well as several testing devices of some tribology couplings which are specific to hydraulic equipment.

Keywords: tribology, hydraulics, testing laboratory, testing stand, lubrication systems,

1 Introduction

Having **over 50 years** of experience in Fluid Power field, in the current research, besides the theoretical aspects needed to be clarified a series of specific aspects,, in the institute a particular attention has the experimental research, designed to confirm the theoretical research, or showing certain performance of the components or for the equipment which are investigated..

The main research directions in the activity of the institute are:

- hydrotronics, mechatronics and **tribology**;
- green energies;
- technological transfer.

Between the **10 research laboratories**, which were developed in the institute, one of the most important laboratories is **The Research Laboratory for Tribology and Lubrication Equipments**, where were developed o **series of research activities** regarding the knowing the tribological behavior of the hydraulic elements and systems, in order to optimize the energetic efficiency of all hydraulic driving systems. It is meant for research in the general field of tribology, especially for the systems and equipments centralized lubrication, that are important for the security of technological systems.

3. The main direction of the tribological research

In the **Research Laboratory for Tribology and Lubrication Equipments**, the main direction of the research activities, which are developed are:

1. The tribological research of the sealing systems from the hydraulic drive sistems, especially from the hydraulic and pneumatic cylinders;
2. The tribological investigation of the material couples with radial relative motion, from hydraulic drive systems (radial bearings, radial seals, radial joints, etc..), including hydrostatic radial bearings;
3. Tribological Research of the the material couples with relative frontal /axial motion, from the hydraulic drive systems (flat bearings, axial or frontal, front seals, etc..), Including hydrostatic thrust bearings;
4. Tribological Research of the material couples with the relative translational motion, from the hydraulic drive systems (axial couples, translational seals, and, also, the specific translational systems of the piston on cylinder;
5. Tribological research on classical, modern and modernized lubrication systems.

4. The tribological research of the sealing systems of the hydraulic cylinders

Hydraulic cylinders, which are basic components of hydraulic control and actuation systems, convert hydrostatic energy into mechanical energy, by achieving, in a certain time, a certain force, with a certain speed in a straight stroke and must ensure a proper dynamic behavior, The researches, regarding the tribological behavior of the sealing system of the hydraulic cylinders, were developed together the specialists from the *University of Poitiers, Poitiers, France*. Until now, were developed two steps:

1. Experimental research regarding experimental the **determination of frictional forces that** occur between the rods of hydraulic cylinders and their seals.;
2. Experimental research in order **to measure the friction forces which appear in the pistons seal** of the hydraulic cylinders.

4.1 Experimental researches for determining of the frictional forces from sealing of rod of hydraulic cylinders

This are presented some aspects of conducting, within INOE 2000-IHP, of experimental research on the **determination of frictional forces that** occur between the rods of hydraulic cylinders and their seals. In the first part, are presented some specific elements of the experimental stand developed and in the second part are presented some graphical results.

For experimental determination of frictional forces, occurring **between the seals and hydraulic cylinder rod**, was designed and developed a **testing stand** equipped with modern "on-line" system for measuring the evolution of the parameters of interest. The main unit of the test stand is the experimental device, which contains the investigated sealing and is mounted on the framework of the drive system Figure 1, where it can be seen both the dual sealing sleeve which contains the two gasket U shape, Figure 2, the pressure and temperature transducer, as well as the force transducer, Figure 3. A general view of the stand can seen in Figure 4, a, b.



Fig. 1: The experimental device mounted on stand.



Fig.2 The pressure and temperature transducer.



Fig. 3 The force transducer.



a): General view if the stand



b) The manual acting of the pump

Fig. 4: The general view of the testing stand

Some experimental graphical results for rod sealing

To concretize the above mentioned, below will show some examples of complex graphics obtained for **certain pressure** and **speed steps**, which will reveal some interesting and instructive points.

Thus, in Figure 5 si Figura 6, are represented the complex characteristic graphs for pressure steps values of **100 bar** and **200 bar** and theoretical **100 mm/s**).

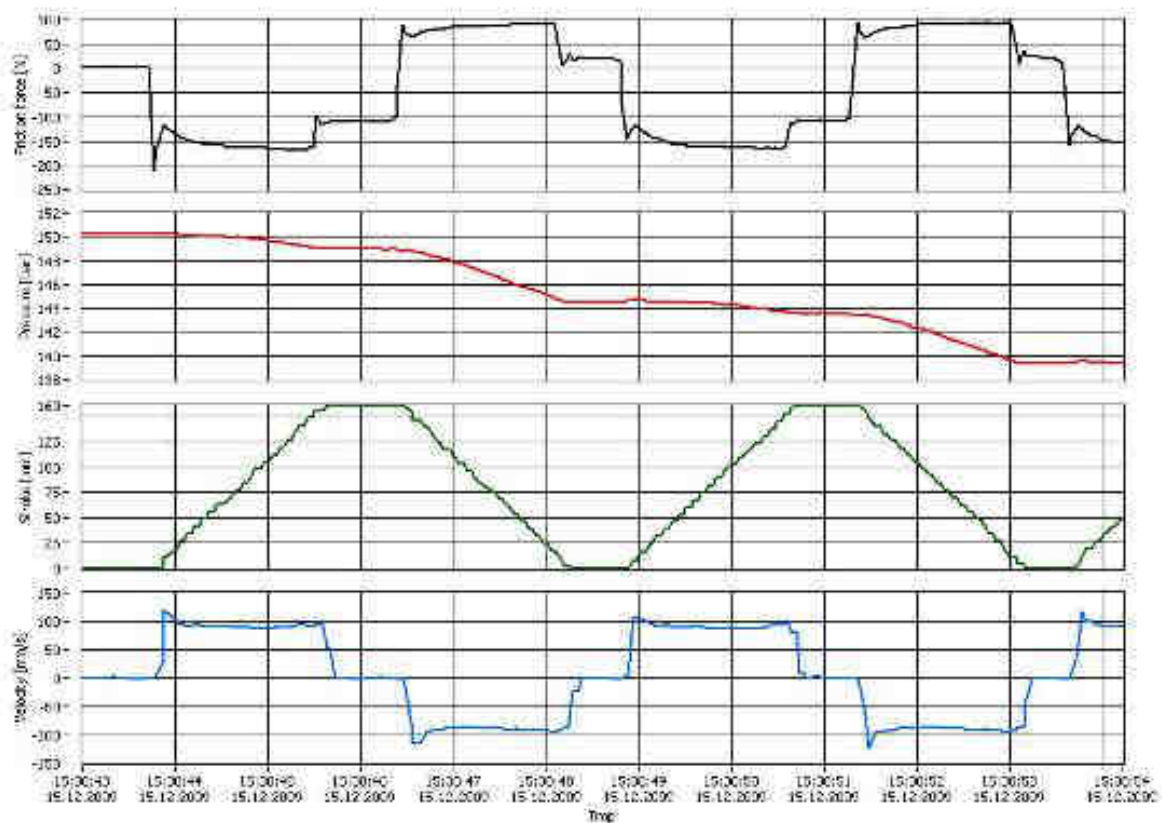


Fig. 5 The complex graphics for **rod sealing** at pressure of **100 bar**.

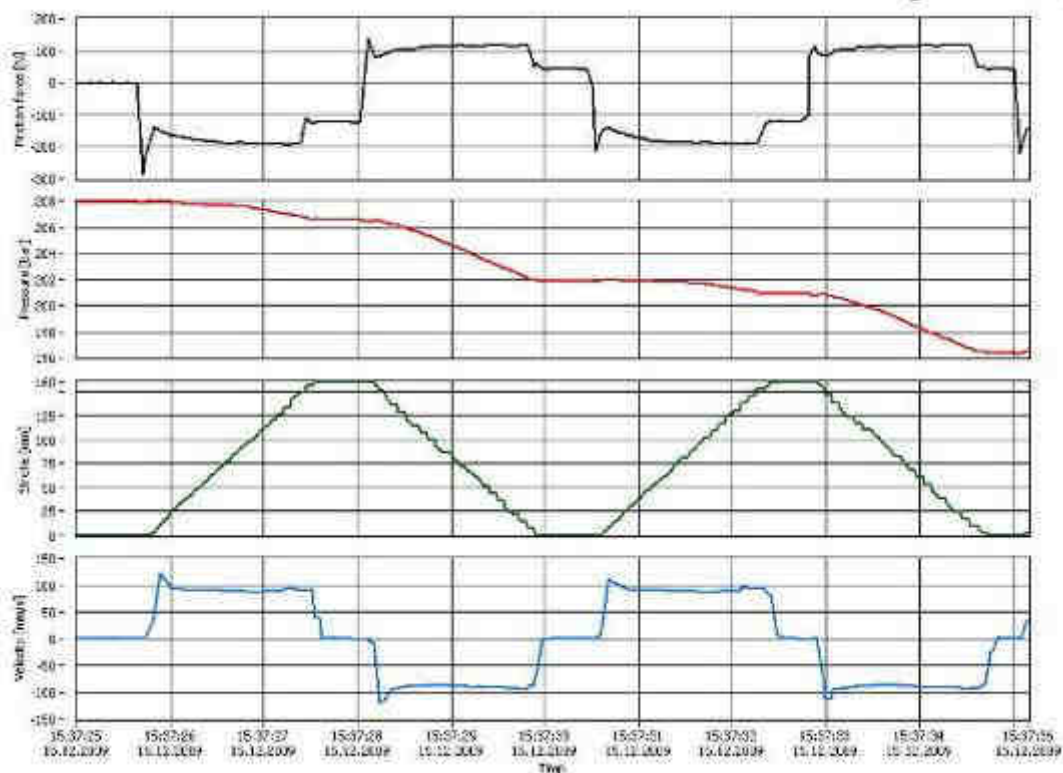


Fig. 6 The complex graphics for **rod sealing** at pressure of **200 bar**.

4.2. Experimental research for measuring the friction forces which appear in the pistons seal of the hydraulic cylinders

The mobile/dynamic translation sealing are specific to the hydraulic cylinders, Figure 7a, where realize the sealing on the piston with diameter d , being in reciprocating translation motion on the stroke, in a fluid medium with the constant viscosity η and under pressure p . In Figure 7b, d is the piston diameter, S is the stroke, v and v_r are velocities in the both senses

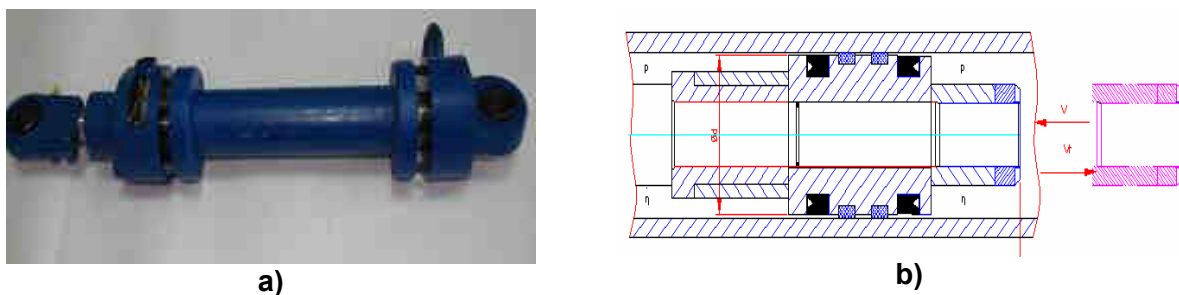


Fig. 7 Hidraulic cylinders piston sealing

For evaluating the friction forces from the **piston seal** of the hydraulic cylinders, there was **designed and developed a special experimental device**, which was conceived purposefully for working by mounting on an existing stand, which provides operational strokes for piston.

The adopted technical solution was the replacement of the piston, with one new piston double sealed, which contains two spaces where are placed 2 U seal shape type seals, fixed with the wings facing one another.

The pressure of working oil, sealed by the two gaskets tested, is created by using a hand pump, which has a pressure gauge to indicate directly the working pressure and, also, a local display pressure transducer.

The **experimental device**, presented in Figure 8, operates in vertical position and it needs the mounting of the rod of the experimental device on the mobile rod of the hydraulic cylinder from one existing Stand.. Figure 9 presents the pressure and temperature transducer and Figure 10 presents the force transducer, used to measure the friction forces.



Fig. 8: The experimental - device mounted on stand.



Fig. 9: The pressure and temperature transducer.



Fig. 10: The force transducer.

Also, the stand has others transducers as: stroke transducer, a digital thermometer for the ambient temperature and flow transducer.

By means of special electric cables, all signals provided by transducers reach the acquisition board installed on the computer, and this one, based on specialized software, allows the capture, storage and processing of data.

Some experimental graphical results for piston sealing

To concretize the above mentioned, below will show some examples of complex graphics obtained for **certain pressure** and **speed steps**, which will reveal some interesting and instructive points.

Thus, in Figure 11 si Figure 12, are represented the complex characteristic graphs for pressure steps values of **100 bar** and **200 bar** and theoretical **100 mm/s**).

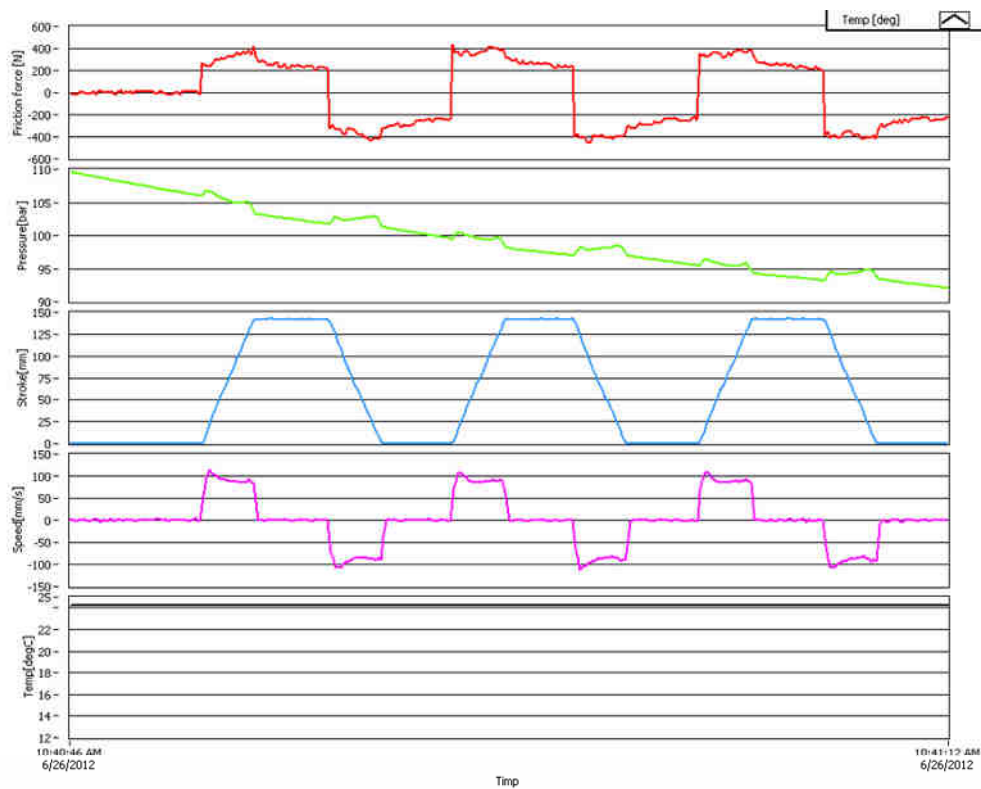


Fig. 11 The complex graphics for piston sealing at pressure of **100 bar**.

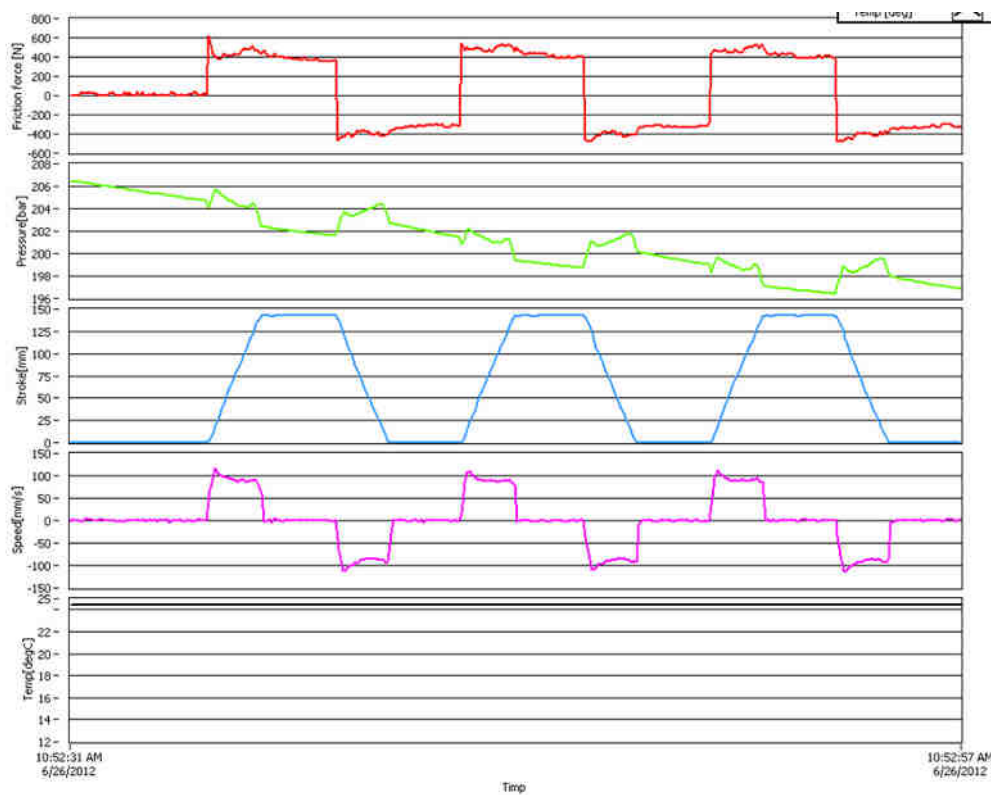


Fig. 12 The complex graphics for piston sealing at pressure of **100 bar**.

5. The testing device for radial hydrostatic bearings and radial sealing systems

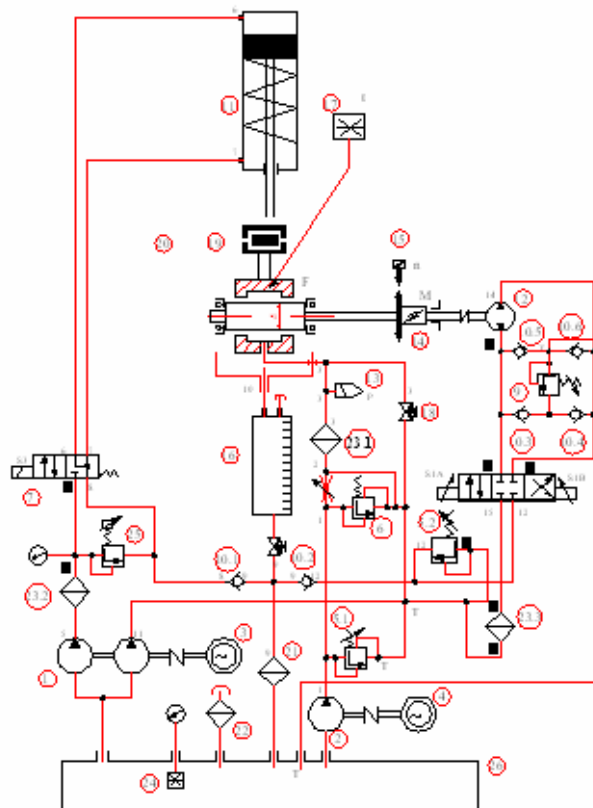
In the **Research Laboratory for Tribology and Lubrication Equipments**, there is an electro-mechanical-hydraulic testing device for radial hydrostatic bearings and radial sealing systems, which enables the development of research for industrial applications, regarding measuring of the friction couple/moment which appears in the working regimes of the machinery and equipments. This testing device is presented in the **Figures 13**, where it can see, also, the Hydraulic action scheme.



–Side view–



–Top view–



Hydraulic action scheme

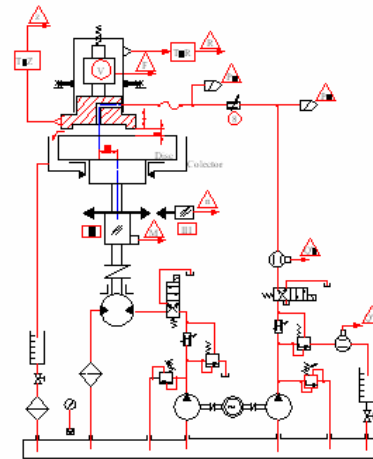
Figure 13: The testing device for radial seals and radial hydrostatic bearings

6. The testing device for frontal hydrostatic bearings and axial sealing systems,

A second device, also, an electro-mechanical-hydraulic device, which is in the Research Laboratory for Tribology and Lubrication Equipments, allows to develop the experimental researches of the axial/frontal hydrostatic bearings and frontal sealing systems, belonging from industrial applications. The testing device is presented in **Figure 14**.



The physical testing device



Hydraulic action scheme

Figure 14. The testing device for frontal seals and frontal hydrostatic bearings

7 The durability Testing of the translational seals systems from the hydraulic cylinders

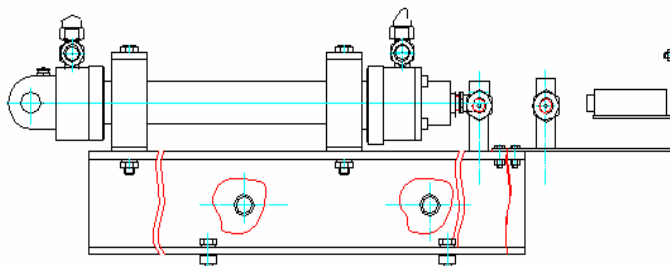
Other testing device is for durability testing for the transnational seals system from hydraulic cylinders, which is presented in the **Figure 15**.



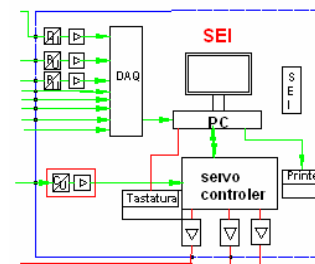
The physical testing device



The acquisition system



The design of testing device



The scheme of acquisition system

Figure 15: The testing device of seals durability

8. Classical, modern and modernized lubrication systems

In the Tribology Laboratory was **effectuated o lot of studies** regarding the basic and modern lubrication systems used in the industrial equipments, in order to create new technical solution and for improve the used now on the old machineries.

The laboratory has a **number of functional panels**, for the main systems of centralized lubrication, namely for volume dosing systems, **Figure 16**, progressive dosing systems, **Figure 17**, the lubrication systems with two lines, **Figure 18**, the recirculation system with electronic monitoring, **Figure 19**, and, also, the micro lubrication systems and spray lubrication systems..

These functional panels are used in **training activities** of our institute, which are developed with the **industrial companies, in order to transfer the basic knowledge**



Figure 16: The volumic dosing lubrication systems,



Figure 17: The progressive dosing lubrication systems



Figure 18: The lubrication systems with two lines



Figure 19: The recirculation lubrication system with electronic monitoring

These **functional panels materializing**, at small scale, **the real lubrication systems** of the machines and technological equipment from the industry, and can be used for testing for specific lubrication components, for the training activities in the lubrication field, and, also, for functional demonstrations of the main/based lubrication systems.

9. Conclusions

The paper presents a series of tribological research which have developed in Tribology and Lubrication Systems from Hydraulics & Pneumatics Research Institute-INOE 2000-IHP, regarding the increasing of the performances of the fluid power equipments.

- The paper presents, in detail, the measurement device and the stand for measuring frictional forces in rod seals and in piston seals of hydraulic cylinders and there are shown graphic examples of their variation.

- Valid measurements of frictional forces are obtained in downward stroke, due to the phenomenon of natural alignment of the piston rod and the force transducer that eliminates the occurrence of additional jamming forces.
- It is shown that the three graphs for two consecutive cycles, which are almost identical, demonstrate *repeatability* of the process.
- In the paper are presented examples of complex graphical variation, for 100 bar and 200 bar, two examples for rod friction forces and two for piston friction forces.
- The measurement system, based on advanced transducers and electronic and computerized data processing, guarantees the accuracy of measurements performed on the stand.

The paper presents different researching devices for radial and frontal hydrostatic bearings and sealing systems, and, also, some classical, modern and modernized lubrication systems

Finally, considering all the above, it can say that the **Tribology and Lubrication Systems Laboratory** from INOE 2000-IHP has an important endowment and can develop interesting research works on tribology and lubrication industrial equipments.

The development of large scale works, needs integrated research strengths, that can be achieved through cooperation between universities and institutes with expertise in the field, from different countries, which is possible only on one European research projects

REFERENCES

1. Cristescu C., Drumea P., Dumitrescu C., The theoretical evaluation and experimental measuring of the friction forces from the sealing of rod at the hydraulic cylinders, Proceedings of The 26-th international scientific conference- "65 years Faculty of Machine Technology", Technical University Sofia, 13 – 16 September 2010, Sozopol, Bulgaria, 2010, pag.491-497.
2. Cristescu, C., Drumea, P., Mathematical modeling and numerical simulation of the tribological behavior of mobile translation sealing subjected at high pressures, In: Hidraulica, Sept. 2008, no. 2, pp. 26-33 (2008).
3. Drumea P., Cristescu C., Fatu A., Hajjam M., Experimental research for measuring friction forces from rod sealing at the hydraulic cylinders, Proceedings-Abstracts of *The 11th International Conference on Tribology "ROTRIB'10"*, November 4-6 2010, Iasi, Romania, pp. 1.1.7 - 1.1.8,
4. M. Crudu, A. Fatu, M. Hajjam, C. Cristescu: "Numerical and experimental study of reciprocating rod seals including surface roughness effects /Etude numerique et experimental des effets de la rugosite sur le comportement des joints hydrauliques en translation. 11th EDF Pprime Workshop: „Behaviour of Dynamic Seals in Unexpected Operating Conditions", Futuroscope, Septembrie, 2012, Poitiers, France.
5. DRUMEA, P., CRISTESCU, C., OLIVER HEIPL. Experimental Researches for Determining the Friction Forces in the Piston Seals of the Hydraulic Cylinders /Experimentelle Untersuchungen zur Bestimmung der Reibkräfte in Kolbendichtungen von Hydraulikzylindern. In: PROCEEDINGS of The 17-th International Sealing Conference ISC-2012, 13-14 Sept. 2012, STUTTGART, Germany.
6. Calinoiu C., Senzori si traductoare (Sensors and transducers), vol. I, Technical Publishing House, Bucharest, (2009).

HYDRAULICS FOR MOBILE VEHICLES. NEW DRIVE SCHEMES

PhD stud. eng. Mihail PETRACHE¹, eng. Sava ANGHEL², eng. Alina Iolanda POPESCU²

¹SC LYRA PROD IMPEX SRL, representative of Company Poclain Hydraulics, office@lyra.ro,

²INOE 2000 – IHP, sava.ihp@fluidas.ro

²INOE 2000 – IHP, alina.ihp@fluidas.ro

Abstract:

In the article we present several new solutions of hydraulic drives for mobile vehicles from the Poclain Hydraulics. Company Poclain Hydraulics has expertise in the fields construction, agriculture, handling, industry, marines, transportation, environment.

Keywords:

hydrostatic transmissions, mobile vehicles, radial pumps, radial hydraulic motors

1. Introduction

POCLAIN HYDRAULICS has become the world leader in hydrostatic transmissions based on high performance cam-lobe radial-piston motors. This expertise has led to its expansion in fast growing niche markets, such as mobile machinery used in agriculture, construction, public works and material handling. Beyond this off-road and all-terrain vehicle market expertise, today we offer innovative solutions through hydraulic hybridations.

2. Our Hydraulic Solutions for Sustainable Mobility

2.1 What is a hydrostatic transmission?

A power transmission system that uses oil to provide torque to the wheels. It includes all the parts situated between the motor and the wheels that transfer the energy to the driving wheels.

There are several types of transmissions that ensure the drive of vehicles (table1):

- Mechanical Transmission
- Electric Transmission
- Hydrostatic Transmission

	Mechanical Power	Electronic Power	Hydraulic Power
Is transfered by :	Parts (pinions, pulleys, etc) ⇒ design constraints and wear	Electrons ⇒ design flexibility	Oil (heat-transfer fluid) ⇒ design flexibility
Is defined using:	$P = C \times W$ (Torque x Speed of Rotation)	$P = U \times I$ (Voltage x Intensity)	$P = P \times Q$ (Pressure x Flow)
Is characterised by:	A low power density	A low power density	A high power density

Table1

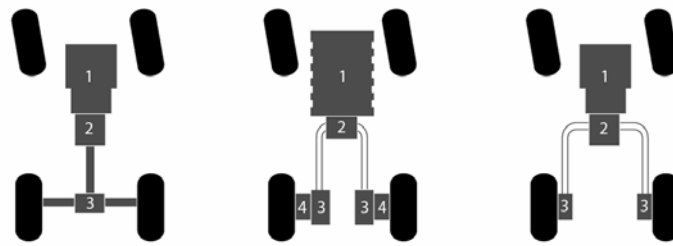


Fig.1 Looking at the vehicles (from above with the steering wheels at the top)

Mechanical Transmission	Electric Transmission	Hydraulic Transmission
1. Engine 2. Gearbox 3. Differential	1. Battery 2. Electronic 3. Electric motor 4. Reducer	1. Engine 2. Hydraulic Pump 3. Hydraulic Motor

Table 2

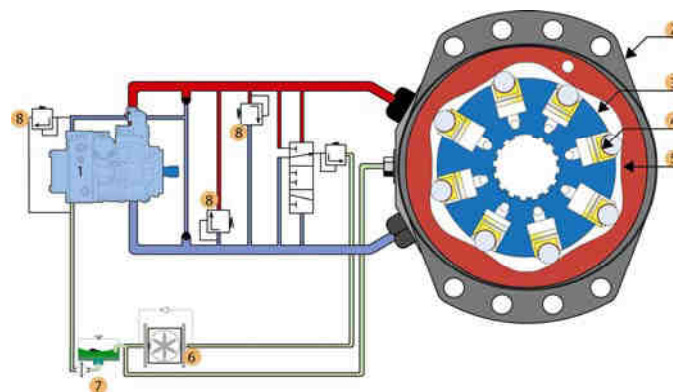


Fig. 2 Scheme of hydraulic drive in close circuit

2.2 Our technology

Components (fig.2)

The pump (1) is driven by the engine and sends oil to the hydraulic motor (2), driving the wheels of the vehicle. The purpose of this type of device is to provide unequalled torque, necessary for vehicles working in extreme conditions while offering great freedom of design.

How the hydrostatic transmission functions

The pump (1) sends the oil through a hose under high pressure P (in red). This oil is delivered to the motor (2). It is distributed into a cylinder-block (3) that contains pistons (4). Pushed by the oil, they come into contact with a cam (5) whose lobed shape forces the cylinder-block unit to rotate. This drives a shaft that transfers this rotation to a wheel, enabling movement of the machinery.

The oil is released from the motor through a hose, under lower pressure (in blue), and at a reduced temperature thanks to the exchange system integrated into the motor (in green), which diverts a portion of "hot" oil back through the oil cooler (6) and to the tank (7). If extra torque is required because of steep slopes or rough ground the fluid's pressure increases.

Valves (8) protect the circuit from pressure spikes. Flow and pressure can be controlled by the valves in the hydraulic circuit. The hydraulic fluid is the medium that transmits the power of the hydrostatic transmission.

3. "Eco-label" fluids compatibility

Poclain Hydraulics has conducted testing campaigns in its laboratories for the following two types of biodegradable oils and has validated their compatibility:

- Synthetic ester-based oils (HEES) that are biodegradable but generally of petrochemical origin;
- Food-based oils (canola or sunflower), that are both biodegradable and compatible with any accidental contact with food products.

It should be noted that an old machine can use these oils, provided some precautions are taken.

4. AddiDrive™ Assist

Overview: an additional hydrostatic transmission offering trucks and convoys better mobility in difficult driving conditions such as: mud, snow, sand, etc. This hydraulic aid, installed on the front or rear axles is an ecological alternative to full-time all-wheel drive, engaging on-demand only when needed for higher torque and improved traction control. Providing dramatically reduced weight and improved center of gravity (because the cab height is identical to a non-driven front truck axle), improvements are realized in fuel consumption and additional payload while simultaneously improving vehicle stability and safety.

4.1 The Poclain Hydraulics Technical Solution: AddiDrive™ Assist

The Proposed System (fig.3): hydraulic motors integrated into the axle

Two hydraulic motors (1) are directly integrated onto the spindle of either a steering axle or a fixed axle. They are connected by a pump (2) at the output of the gearbox power take-off (PTO) (4) and a hydraulic valve (3) and are electrically controlled from the dashboard, so you can activate this hydraulic transmission on-demand, even when the vehicle is moving.

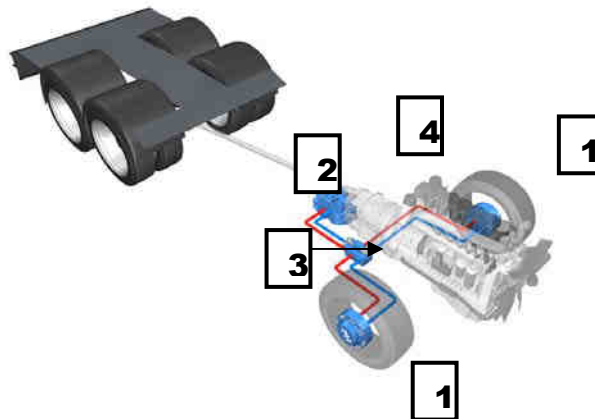


Fig. 3 Poclain Hydraulic System with AddiDrive™ Assist

1 – The Heart of the System: the MFE08 Hydraulic Motor (fig.4)

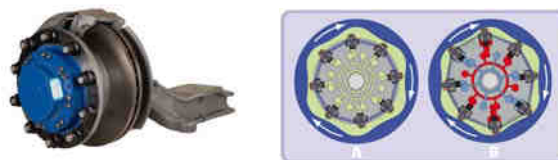


Fig.4 MFE08 Hydraulic Motor

This motor provides greater off-road capabilities thanks to its' high torque (up to 15 600 Nm per axle). In difficult road conditions, the driver shifts the transmission from mechanical to mechanical plus hydraulic transmissions at speeds up to 28 km/h. Once this speed is reached, the hydraulic motors can be freewheeled at up to 600 RPM with close to 100 percent efficiency. As the motor is highly compact, it can be inserted into the wheel of an existing axle, without modifying the chassis.

2 – A variable displacement pump, coupled through a PTO to the engine, delivering pressure up to 420 bar.

3 - A valve used to engage, disengage, and freewheel the motor

4 - The gearbox with PTO output

5 – The engine

4.2 Comparison with All Wheel Drive Vehicles (table 3)

	AddiDrive™ Assist (on tractor)	All Wheel Drive Vehicles
Performance / Consumption	Approximate mass of system (2 motors + pump+ valve) = 120 kg	Require heavier components <ul style="list-style-type: none"> • transfer case • front axle • planetary gear i.e. a total mass of 500 kg, increasing fuel consumption and decreasing payload
	The height of the vehicle is not increased (integrates into standard chassis)	Height of vehicles is increased due to front axle (+ 14 cm). Consequently, the center of gravity is higher, reducing stability and mobility
	Freewheel without mechanical friction so therefore minimal efficiency losses	Drag torque due to friction between mechanical parts: ~ 15 kW, i.e. 5 - 10 % reduction in fuel economy
	Less wear on brakes and clutch	
Safety	Control of vehicle in difficult driving conditions (such as snow covered roads)	
	Hydrostatic braking, acting as an integral retarder without using the service brakes or separate retarder	Friction braking wear

Table 3

On a trailer (fig.5):

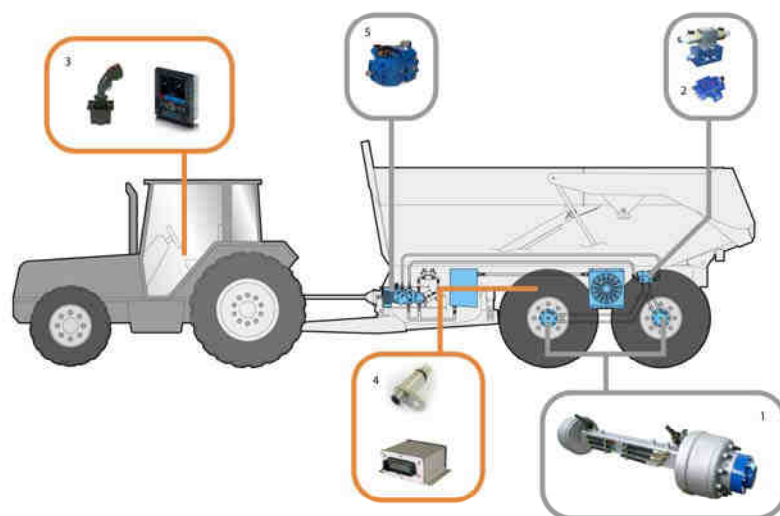


Fig. 5 Components on a trailer

1 –hydraulic motor or axle ; 2 – valves ; 3 –joystick and display ; 4 – Ecu and speed sensor ; 5 hydraulic pump.

There is no alternative technology to the hydraulic trailer assistance. Trailer assistance increases the mobility of heavy-load trailers. For example, two “8x6” trucks can carry the equivalent payload of three “6x4” trucks in off-road conditions, offering a great productivity advantage.

Results

- 5 to 10% improvement in fuel economy.
- Increases the mobility of transport vehicles which lowers the number of different types of vehicles required.

5. AddiDrive™ CreepDrive

Overview: this hybrid mechanical-hydraulic transmission is designed for vehicles that travel at normal speeds and work at low speeds. Shifting into hydraulic transmission at low revs reduces wear on clutches and brakes, limits particle emissions and lowers fuel consumption, while guaranteeing a constant speed.

5.1 The Poclain Hydraulics Technical Solution: CreepDrive™

The proposed system (fig.6): a single component enables you to shift from a mechanical to a hydraulic transmission.

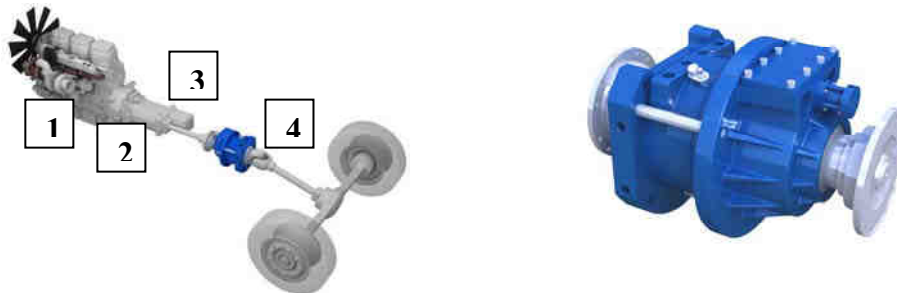


Fig. 6 Poclain Hydraulic System with CreepDrive™

- 1 – Engine
- 2 – PTO Gearbox
- 3 – Variable Displacement Pump
- 4 – CDM 222-050

At the heart of the CreepDrive™: the CM222-050 motor

The CDM 222-050 integrates into a radial piston hydraulic motor that is activated by a pneumatic control when the speed is lower than 10 km/h.

It delivers 40 kW of max. power, with a displacement of up to 1000 cc. Being compact and light-weight (124 kg), it can easily be inserted on transmission shafts.

5.2 Comparison with a Traditional Mechanical Transmission (table 4)

	CreepDrive™	Traditional Mechanical Transmissions
Pollution / Consumption	No stress on the clutch	Strong stress on the clutch at low speeds, wear and therefore the emission of fine particles (PM10) from the brakes
	Independence between the speed of the combustion engine and that of the vehicle progress lead to a reduction in consumption	Overspeeds at start-up lead to a high consumption

	Noise reduction (no combustion engine acceleration)	Noise pollution due to the increases and losses in revs
	Allows the combustion engine's performances to be optimised at high speeds, thus reducing losses and limiting consumption	The combustion engine is dimensioned to operate at both low and high speeds and thus releases more pollution at low speeds.
Safety	Hydrostatic braking (dynamic braking, based on the flow of the variable displacement pump. Motors can operate with retarders). Hard-wearing with no heat emission.	Friction braking (wear and particle emission)

Table 4

6. Conclusions

Hydraulic drive systems of mobile vehicles suggested by company Poclain Hydraulics solve practical situations with their advantages and disadvantages.

REFERENCES

- [1] Processing after "Poclain Hydraulics - Worldwide leader of hydrostatic transmissions";
- [2] P. Drumea, M. Comes, A. Mirea, M. Blejan – "Positioning systems tuning interface using proportional hydraulic drivers " – The 4TH International Symposium For Informatics And Tehnology In Electronic Modules Domain, București september 22 – 24, 1998.
- [3] P. Drumea, G. Radulescu, N. Ionita – „Implicarea actionarilor hidraulice si pneumatice in domeniile de interes ale cercetarii europene: energie, mediu, agricultura, transporturi, adderation" - International Symposium of Hydraulics, Pneumatics, Seals, Precision Mechanics, Devices and Specific Electronic Equipments, Mechatronics – HERVEX 2008, ISSN 1454-8003, pp. 1-10;
- [4] P. Drumea, T.C. Popescu, Ion Guta Dragos – "Research activities regarding energetic and functional advantages of hydraulic transmissions" - 10th International multidisciplinary scientific geoconference - SGEM 2010, June 20 – 25, 2010, Albena Resort, Bulgaria, ISSN 1314-2704;
- [5] P. Drumea, T.C. Popescu, M. Blejan, D. Rotaru – "Research activities regarding secondary and primary adjustment in fluid power system "- The 7th International Fluid Power Conference Aachen „Efficiency through Fluid Power“, Scientific Poster Session, Industrial Hydraulics, 22-24 March 2010, Aachen, Germany.

LIFTING PLATFORM WITH POTENTIAL ENERGY RECOVERY SYSTEM

PhD. Eng Catalin DUMITRESCU¹, PhD. Eng. Corneliu CRISTESCU¹,
Dipl. Eng. Florin GEORGESCU¹, Dipl. Eng. Liliana DUMITRESCU¹

¹ INOE 2000-IHP Bucuresti, e-mail: dumitrescu.ihp@fluidas.ro; cristescu.ihp@fluidas.ro

Abstract: *The article presents a technical solution for recovery of potential energy, with industrial application for electro-driven lifting platforms which are used for lifting persons with disabilities. We know that a load (weight) elevated to a certain height, involves the use of a form of energy, which in most cases is not recovered, not even partially, but it is dissipated into the environment. The basic idea of the solution presented is the recovery of potential energy from the descent load (weight), its conversion and storage, followed by its use in lifting phase of load.*

Keywords: *energy recovery, lifting platform, hydraulic system*

1. Introduction

Depending on the destination, there are several types of platform lifts.

An important category is represented by the platforms lifts typically used by people with disabilities for their access to public buildings (town halls, local councils, hospitals, police, theaters, museums, etc.), to which it relates, in particular, this article.

But there are platform lifts that are used in other areas such as construction, which also are used for various operations performed at height.

All these platforms, most hydraulic, at every stroke upward, generating energy required to perform the work needed, and then this potential energy is dissipated into the environment, usually by narrowing cross section of the liquid which such warms and requires additional energy to cool the working fluid.

Under these conditions, the efficiency of these devices is quite low.

Technical problem which arises is whether we can recover at least part of the potential energy.

But for this, need to find intelligent technical solutions with high efficiency.

That is why, in this paper, is presented a solution that can recover some of the available potential energy and to improve the energy efficiency of the platform.

2. Presentation of the existing/classic lifting platform

The existing platform lifts, code 125-0 PA, designed and executed by INOE 2000-IHP Bucharest is shown in Figure 1, which was used for implementation of the energy recovery potential, consists of:

- a) a mechanism of articulated bars, consists of two parts in the form of "X" articulate and arranged one above the other, having the upper working platform itself. Parts are metal profiles (round and square pipes etc.) welded and articulated by bolts.
- b) one hydraulic cylinder for actuating platform, code CSL 2016 (producer Hydraulics Plopeni), having the following functions:
 - output rod: platform reaches desired height or maximum allowed;
 - stationary: if the cylinder holes are hydraulic locked, thus platform is strong stationary, allowing the operator to work as long as he want;
 - rod- withdrawal: platform descends controlled.

Technical characteristics of the hydraulic cylinder are:

- hole diameter = 50.8 mm
- diameter rod = 31.75 mm
- total course = 406.4 mm
- nominal pressure = 175 bar.



Fig.1 Classical platform lift

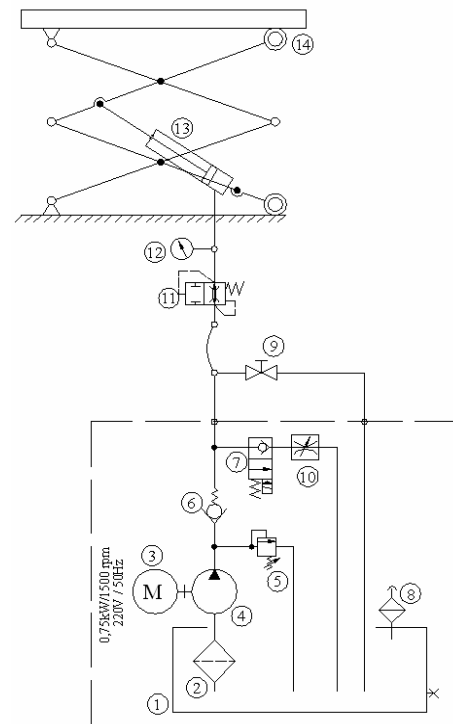


Fig. 2 Hydraulic diagram

Hydraulic drive "classical", meaning without recovery potential energy: constructive, specific construction with minimum dimensions that fit in size of platform lifts even stowed position (closed) completely. Actuated electrical elements (electric motor distributor tightly closed) uses electrical phase 220V / 50Hz ("household").

Hydraulic actuation component can be seen in Figure 2: The main components are:

- pos. 1 = oil tank. With oil volum $V_0 = 10 \text{ dm}^3$;
- pos. 2 = oil filter (strainer) mounted on pump suction;
- pos. 3 = asynchronous electric motor 220V/50Hz, $N = 0.75 \text{ kW}$, $n = 1460 \text{ rpm}$;
- pos. 4 = gear pump $V_g = 3.2 \text{ cm}^3/\text{rev}$, ensuring a flow of $4.7 \text{ dm}^3/\text{min}$, useful working pressure (producer Hesper Bucharest);
- pos. 5 = pressure valve (safety) directive, which allows a pressure of max. 100 bar;
- pos. 6 = one-way valve;
- pos. 7 = distributor tightly closed, type "cartridge", electric actuators (220V/50Hz).
 6, 7 positions have the role of lock the stationary hydraulic platform, mechanical default, in the desired position.
- pos. 8 = fill filter tank / air filter tank
- pos. 9 = valve manually operated, having the role of descent of the platform in case of failure of electric nature;
- pos. 10 = throttle, cruise control acting as the descent of the platform;
- pos. 11 = safety valve, the role of locking of the fall platform in case the breakage of pipes (pipes, hoses);
- pos. 12 = the manometer with glycerin 63, 0-250 bar.

3. Presentation of the lifting platform with energy recovery system

The lifting platform with the energy recovery system, shown in Figure 3, consists of elements existing platform, classic, which is implementing the system/method of recovery potential energy. System or hydraulic module of recovery energy completes "classic" hydraulic system in order to recovery the potential energy during descent load (weight), through its capture, storage in batteries, followed then by its reuse in phase of lifting weight.

Hydraulic energy recovery system is shown in Figure 4 and has the following composition:

- pos. 15 = transducer course;
- pos. 16 = the manometer with glycerin, 63, 0-250 bar
- pos. 17 = security block accumulator Dn 10, Pn = 400 bar (HYDAC);
- pos. 18 = accumulator with membrane $V_0 = 2.5 \text{ dm}^3$, Pn = 400 bar (HYDAC);
- pos. 19 = hydraulic block devices (HIDROSIB Sibiu);
- pos. 20 = throttle valve Dn 6, Pn = 400 bar;
- pos. 21 = flow transducer (flowmeter);
- pos. 22 = hydraulic cylinder, CH25U-63/40-350-3BM0 code, with pressure multiplier role;
- pos. 23 = one-way valve SUP6 code, 1-0, Dn 6, Pn = 315 bar (HIDROSIB Sibiu);
- pos. 24, 25, 26 = distributors tightly closed and electric drive Dn 6, Pn = 315 bar, 220V/50Hz.



Fig. 3 Lifting platform with potential energy recovery system

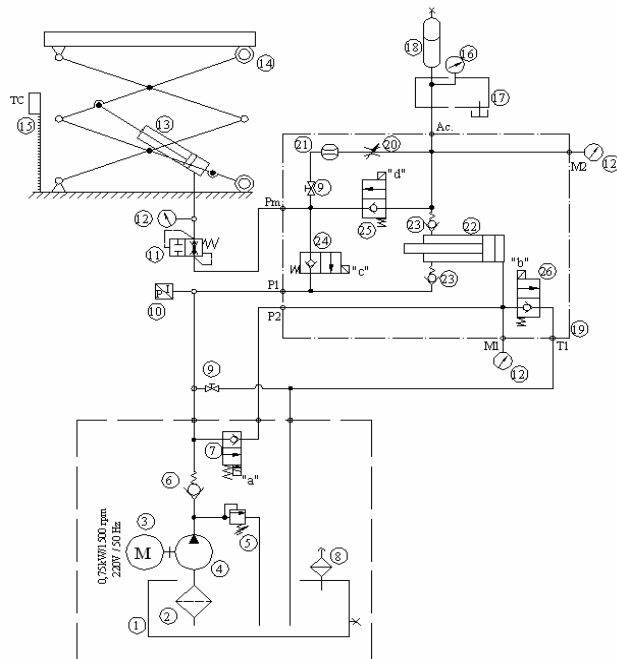


Fig.4 Hydraulic energy recovery scheme

4. Functional description platform lifts with energy recovery

The functioning of platform lifts with potential energy recovery system, is based on the potential energy storage in the descent phase of platform / load in a hydraulic accumulator with membrane and its reuse in the lifting phase.

During the descent phase, **hydraulic energy (pressure x flow)** is multiplied by a hydraulic cylinder acting as multiplier and transferred into an accumulator with membrane, it can store up to start lifting phase, after which the hydraulic energy is transmitted to the hydraulic cylinder drive platform.

Hydraulic cylinder used for energy multiplication, multiply the output pressure of 1.675 times the input pressure (if present), the multiplication of pressure depending on the size of the piston and cylinder rod.

Below are described the main phases of platform lifts drive:

A) Lifting platform:

- command to start the electric motor, Item 3 and electromagnetic drive 'b' of distributor, Item 26;
- electromagnets "a", "c" and "d" disengaged.

Driving circuit: 4-6, P1 and from P1: * 24-25-18 * PM-11-13 (hydraulic cylinder drive of the platform 13, thus lifting platform)

* 23, cylinder rod multiplier 22 is withdrawn, the liquid from piston chamber is evacuated to the tank by 26.

B) Stop (stationary platform):

Electrical drives previous are canceled, multiplier cylinder rod is withdrawn and all hydraulic circuits to the tank are closed.

The platform stationary strong in place.

C) Lowering platform:

- simultaneous are commanded electromagnetic drive "a" and "c" of distributors Item 7 and 24;
- Item 3 electric motor is not acted;
- electromagnets "b" and "d" of distributors, Item 26 and 25 are disengaged.

Driving circuit:

- under the influence of weight (load), oil hydraulic from cylinder piston chamber of the platform 13-11-Pm-24-P1-P2-7-cylinder piston of chamber multiplier 22 which multiplies the pressure, 23-18. So at the end of this phase, the platform lowers, the accumulator 18 is loaded with pressure cylinder multiplied by the multiplier 22 and the cylinder rod is out.

D) Lifting platform with energy recovered:

- the electromagnet "d" of distributor Item 25 is acted

Driving circuit:

- from the accumulator pos-18-25-PM-11-chamber piston of hydraulic cylinder of the platform, Item 13, so the platform is raised to the desired height, cylinder rod multiplier Item 22 still remains outstanding.

5. Conclusions

The authors of this work, researchers at INOE 2000-IHP Bucharest, proposed theoretically and practically through experimentation on the physical model of the idea presented, the following:

- Hydraulic design approach and rethinking the idea of energy recovery drive hydraulic (pressure x flow) from passive phase of action, its storing in active phases of work;
- reduce electricity consumption, considering increase trend of its price;
- applying on an industrial scale of those listed, considering minimal modifications of existing lifting platforms on the market.

REFERENCES

- [1] DRUMEA, P., CRISTESCU, C., LEPADATU, I., DUMITRESCU, C., DUTU, I., DUMITRESCU, L. Echipament pentru deplasarea pe verticala a persoanelor cu dizabilitati locomotorii. In: vol. Stiinta si Inginerie - Lucrarile cele de A- VI-a Conferinta Nationale multidisciplinare cu participare internationala – Profesorul Dorin Pavel-, fondatorul hidroenergeticii românești, SEBES, 2006., pp. 401 – 406, ISBN 10 973 – 8130 – 82 – 4 / ISBN 13 978 - 973 – 8130 – 82 – 1.
- [2] CRISTESCU, C.. Theoretical Research Regarding the Evolution of the Dynamic Parameters of the Vertical Elevation Equipment Used by the Persons with Locomotion Disabilities. In: journal HIDRAULICA no. 1-2 , July 2006, pp. 14-22, ISSN 1453 - 7303.
- [3] MIREA, Ad., RADULESCU, G., MATACHE, G., CRISTESCU, C., Cercetari privind recuperarea energiilor libere la autovehicule rutiere. In: Buletinul AGIR, no.4, 2006, pp. 90 – 95, Publishing House AGIR, Bucharest 2006, ISSN 1224 – 7928.
- [4] CRISTESCU, C., LEPADATU, I., DUMITRESCU, C., DUTU, I., Modern hydraulically driven accessibility means developed by INOE 2000 – IHP Bucharest. In: HIDRAULICA, no. 1-2 (20), July 2007, pp. 18 – 22, ISSN 1453 – 7303.
- [5] CRISTESCU, C., KREVEY, P., ILIE, I., BLEJAN, M., DUTU, I., DUMITRESCU, C., Mechatronics system for recovering kinetic energy of the hybrid – drive motor vehicles. In: vol: Proceedeings of The 2nd International Conference „Optimization of the Robots and Manipulators” OPTIROB 2007 – PREDEAL, Romania 24 - 27 May, pp. 113 – 116. Publishing House BREN PUBLISHING HAUSE, ISBN 978 - 973 - 648 – 656 – 2.
- [6] Virgil MARIN, Rudolf MOSCOVICI, Dumitru TENESLAV, "Hydraulic drive systems and automatic", Technical Publishing House, Bucharest 1981.

HYDRAULIC DRIVING SYSTEMS FOR MOBILE EQUIPMENTS DESTINED FOR ASPHALT POURING

Victor BalasoIU¹, Mircea Popoviciu¹, Ilare Bordeasu¹

¹Timisoara "Politehnica" University, Hydraulic Machinery Department,
e-mail: balasoIU@mec.upt.ro; balasoIU89@yahoo.com; ilarica@mec.upt.ro
Phone: 004.0256.403680; 004.0356426950; Fax 004.0256.403682

Abstract: The present paper is concerned with the problems occurring in the design and manufacturing of the mobile equipments destined for asphalt pouring. The continuous development of the civil engineering works implies a new conception of the equipments used in this branch of industrial activity. That is why, the range of the devices used in civil engineering works utilizing hydraulic actuators became in our days very large, this category of equipments becoming one of the principal users of hydraulic driving systems. After presenting some principles aspects of driving equipments for mobile devices there are presented various types of hydrostatic actuators used in mobile equipments. Analyzing the specific design problems, we insisted upon the computation of the hydraulic diagram putting in evidence some examples of hydrostatic traction in close circuit with integral hydrostatic transformation.

The main advantages of the hydraulic driving systems are: the stability of the moving velocity, rapid adjustment or inversion of the movement and the possibility to standardize both the elements and the whole system. These advantages determined the rapid extension of the hydraulic drive systems in the civil engineering plants.

Key words: Hydraulic driving systems, Civil engineering plant, Asphalt pouring equipments

1. Introduction

The continuous development of the civil engineering works implies a new conception of the equipments used in this branch of industrial activity. The introduction and the development of hydraulic actuators for the majority of the civil engineering plants, represented a qualitative jump for the improvement of these devices. The introduction of hydraulic driving for the discussed equipments must take into consideration the following characteristics:

- the dimensions and the weight must be cut to a minimum to find room in the limited dimensions of the vehicle and to maintain a reduced fuel consumption;
- the driving possibilities for pump (or pumps) are limited;
- the hydraulic installation is subjected to severe conditions from the ergonomic and maneuvering points of view as a result of both the reduced room and the multiple tasks of the driver, most of them requiring great manual dexterity;
- between the pumping, distribution and adjusting elements and those for execution, often exist relative movements and that circumstance implies the use of flexible pipes;
- the access for the repair work and correct maintenance are sometimes inauspicious and in the same time the equipment is running in an unfavorable environment (dust, mud, rain and great temperature variations); supplementary, sometime the personnel does not have adequate qualifications for the maintenance of hydraulic equipments.

Despite of those adversities, in the building of the mobile equipments there are in use a great number of hydraulic devices from both points of view as nomenclature and as manufacturing volume.

2. The hydraulic transmission in the manufacturing of the equipments for asphalt pouring

The object of the driving system is the hydraulic transmission, which consist invariably from two basic components (fig. 1): the volumetric pump 1, which transform the mechanical energy taken from the driver 2, in hydraulic energy, preponderantly potential energy (pressure) and the hydrostatic motor, which reconvert the hydraulic energy into a mechanical one but with modified parameters; this energy that is afterwards transmitted to the working mechanism 4.

Although the driving systems are con-fronted with a great variety of conditions (various technological processes, different environments and stresses) there are a lot of unique features the most important being:

- the system running is based on the same power processes;

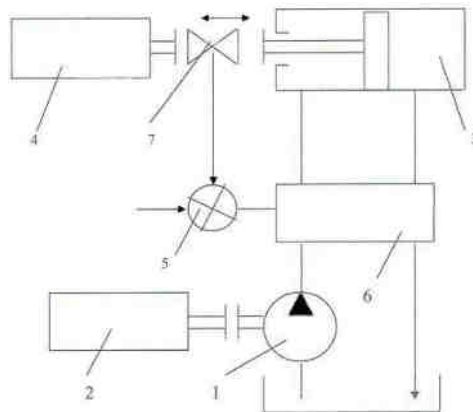


Fig. 1. The diagram of a hydraulic driving system

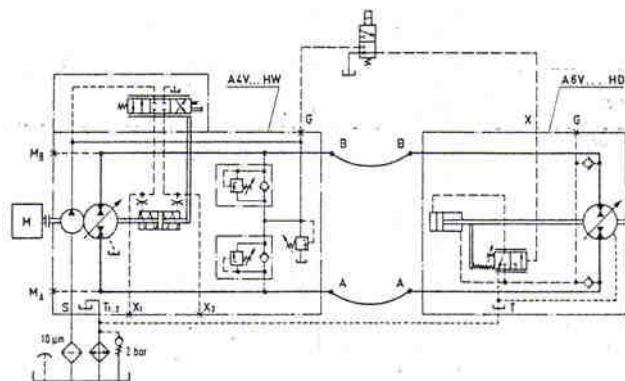


Fig. 2. The principle hydraulic diagram in close circuit

- the flow between the pump and the motor is the same; but from this point of view this systems can be divided into two great groups: with open circuit (for which the liquid is under the atmospheric pressure at the level of the oil tank) and with close circuit (for which the energy level is exchanged between the pump and the motor in a circuit without contact to the atmosphere).

For the following discussions the chosen hydraulic diagram is presented in fig. 2.

The transmission is equipped with a pump A4VG having axial pistons and inclined disks as well as a motor A6V with axial pistons and an inclined block both produced by the German business house REXROTH. The system has a mixed transmission, the primary adjustment being continuous through changing the inclination of the disk and the secondary adjustment being realized in steps, through tipping the pistons block, in two positions.

The primary adjustment is localized at the primary unit. Simply by changing the geometric volume of the primary unit (the pump) and maintaining the other parameters, there are obtained various working regimes. The secondary adjustment is localized at the level of the rotating motor and is

realized by modifying the pressure. Different working positions of the units with axial pistons, respectively the modifications their geometric volumes are obtained with the help of hydraulic *servo-flow* control valves. The protection of the mechanical elements is assured through the pressure valves included in the pump. The principal pump adjustment cylinder, in the absence of the driving pressure, maintain the pump disk –through back springs- at the angle zero, so that the pump does not deliver liquid.

In the moment of distributor commutation the cylinder tilt the disk in the commanded direction, determining a value different from zero of the geometric volume, and the pump deliver oil in the commanded direction. The motor, in the supplying moment has the maximum geometric volume and begin to rotate with the normal speed.

The presented drive system can operate both as motor and brake. For a system in close circuit the braking operation is realized in counter-flow. That means a superposition of two flows:

- the flow given by the motor, running as pump, from the beginning of the braking;
- the flow absorbed or delivered by the pump working either as motor or pump.

It is to observe three running regimes of the pump:

a. Running as a motor and maintaining the delivery direction, permitting the adjustment of the geometric volume from the maximum value to zero. The reverse flow can be considered as negative and assures a moderate braking similarly to those of the motor brake for common motor vehicle.

b. The inactive regime, with “zero” reverse flow (zero geometric volume). The pump does not deliver liquid and assure an abrupt brake closing the flow delivered by the motor, and provoking the opening of the pressure valve for the branch under pressure.

c. The pumping regime, with changing the delivery direction and permitting the adjustment of the geometric regime from zero to the maximum value. The counter flow is considered “positive” and assures a violent brake provoking overpressures controlled by the shock valves.

3. Diagram of hydraulic traction, in close circuit, with integral hydrostatic transformations. Typical examples.

3.1. Diagram with manual adjustment of the velocity, without automatic limitation of the consumed (fig.3)

The system is characterized through the manual command of the pump discharge adjustment. The command can be executed both direct, as is presented in fig. 3a and with hydraulic assistance as in fig. 3b. The moving direction of the vehicle is achieved directly by the pump adjustment device. The maximum level of the consumed power is not supervised by the hydraulic system at overloads, so there is possible the sudden shutdown of the thermal motor.

3.2. The diagram with manual adjustment of the velocity and with automatic limitation of the consumed power, through the “sliding” under load of thermal motor (fig.4)

In such a diagram the moving direction of the vehicle is selected with the directional control valve 4, with an electric command. The adjustment of the movement velocity is done by acting manual (or with a pedal) the device 3. The limitation of the consumed power till to the value momentary developed by the thermal motor is realized in this way: with the increase of the traction load, the rotation speed of the motor 1 decreases, producing the decrease of the command pump 2 discharge; this reduction has as effect –when the valve of the device 3 is maintained in the same position- the reduction of the command pressure of the pump adjusting device and implicitly the decrease of the main pump discharge.

3.3. The diagram with manual adjustment of the velocity and with automatic limitation of the consumed power, through “sliding” under load of thermal motor (fig.5).

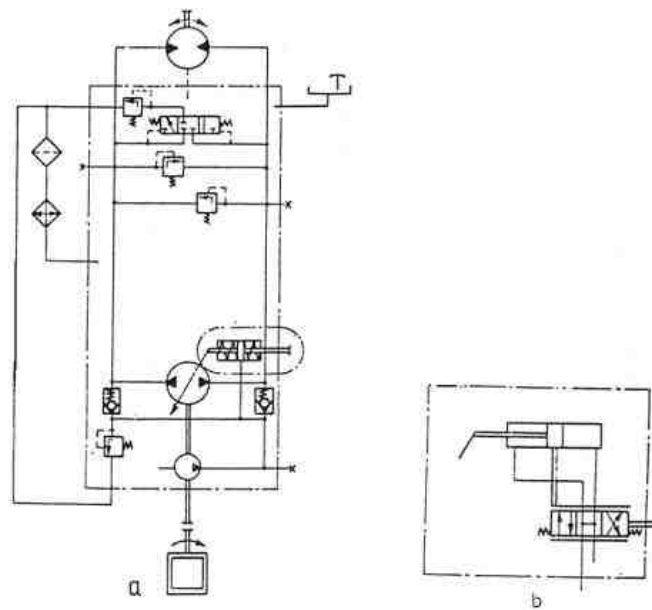


Fig. 3

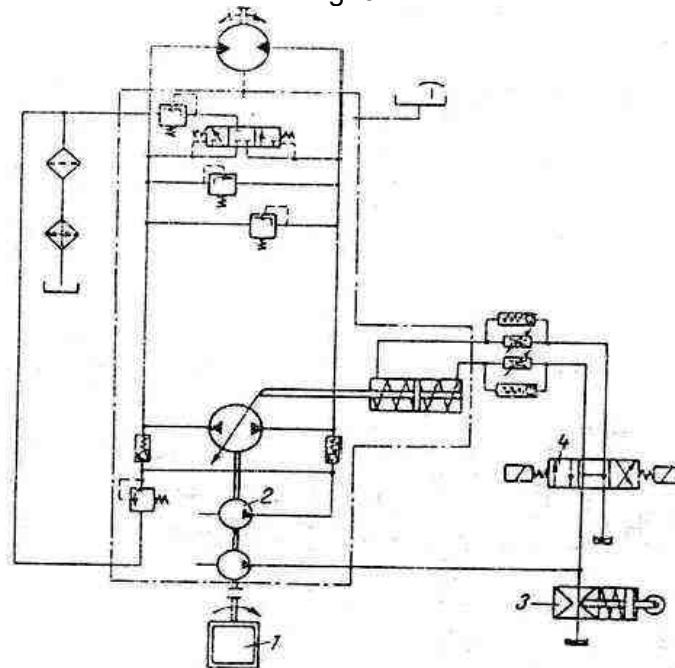


Fig. 4

For the selection of the movement direction, both the automatic adjustment of the velocity and the limitation of the consumed power is realized through devices similarly to those in fig. 4. From the presented device with valve the system in fig. 5a differs only through the elements for the manual adjustment of the velocity. The system in fig. 5.b is provided with the same device but having hydraulic piston, which annihilate the command pressure, and in the same time the flow capacity of the main pump, in the moments when the traction load exceeds the values established by the spring adjustment.

The system in fig.5.c annihilate the advance movement through the increase of the load upon an auxiliary device, hydraulic actuated by a supplementary pump driven by same thermal motor.

3.4. The diagram with manual adjustment of the velocity and the automatic limitation of the consumed power through a power valve (fig.6).

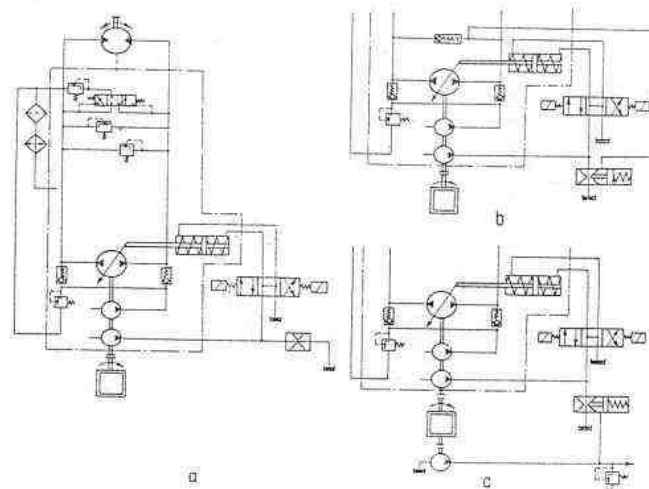


Fig.5

The tilting angle, respective the main pump 2 discharge is controlled by three variable elements: the rotational speed “n” of the thermal motor 1, automatically adjusted by the device 6; the working pressure “p” acting upon the surface “s” of the power limiting device 4 and the command pressure “p_c” acting upon the surface “S” of the command device 5.

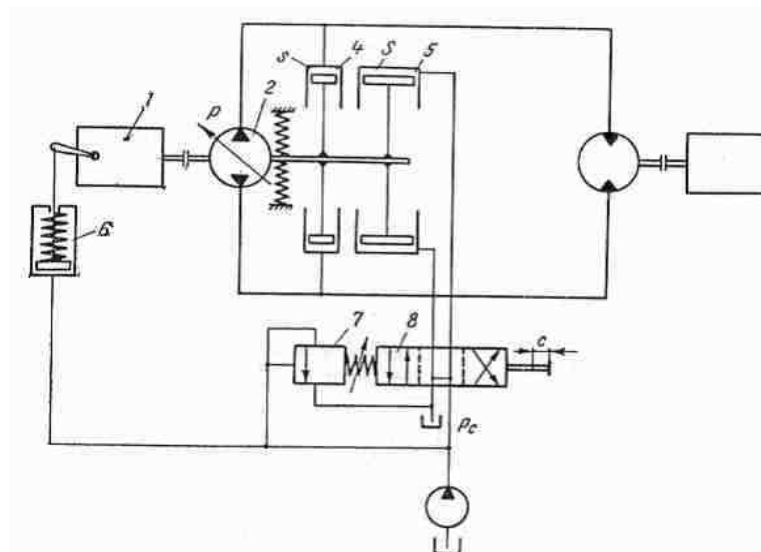


Fig. 6

As a consequence the flow capacity “Q” varies with the mentioned elements:

$$Q = K_1 n (p_s S - p_s) \quad (1.1)$$

$$P = K_2 Q p = K_1 K_2 n (p_c S - p_s) \quad (1.2)$$

From the presented relations it can be seen that -in principle- the consumed power “P” can be maintained constant, for a constant command pressure „p_c”. This pressure, which selects the maximum advance velocity, is manually commanded with the help of the flow control valve 8. At the neutral position of the flow control valve p_c=0 the vehicle is at rest. With the increase of the stroke “c” of the spool valve 8, in one or the other direction, increases also the tension in the spring, of the valve 7, respective the command pressure „p_c” and implicit the flow capacity „Q”.

3.5. Diagram with manual adjustment of the velocity, automatic limitation of the consumed power through the power valve and with mechanic command of the thermal motor rotational speed (fig.7)

The command section, which creates the command pressure " p_c ", is identical to that of the precedent case. Because the pump adjusting device needs an increased pressure, it is provided the circuit " p_a ". The command applied upon the actuating flow control valve 1 is simultaneously transmitted, on a mechanic way, at the hand lever or the pedal for the acceleration of the thermal motor.

The limitation of the consumed power is realized with the help of the power valve 3. When the pressure " p " on the working circuit overcame the value anterior adjusted with the spring of the valve 3 (respective the value that coupled at the pump maximum flow capacity attains the level of the installed power) the valve 3 opens, less or more, provoking the decrease of the command pressure " p_c " and simultaneously the valve 3 opens more or less provoking the decrease of the command pressure, the decrease of the flow capacity and in this way the vehicle velocity.

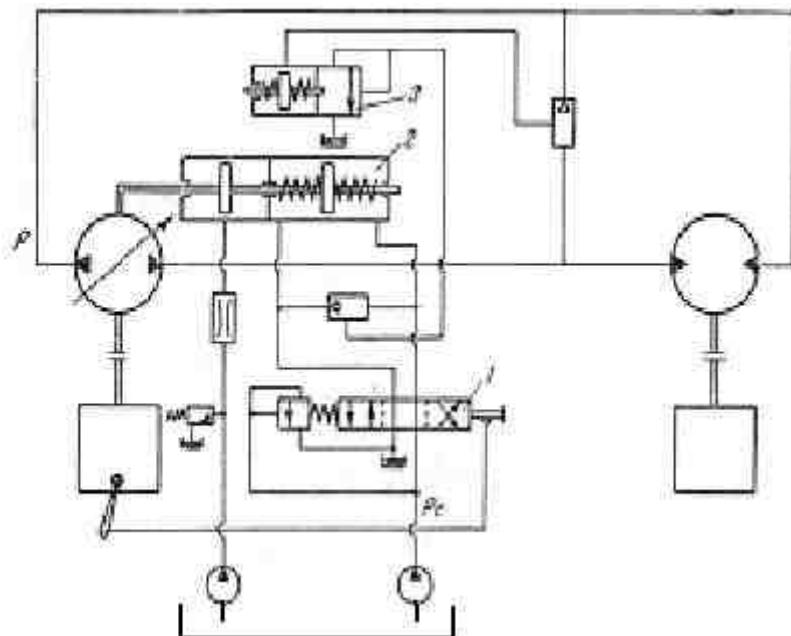


Fig. 7

3.6. Diagram with manual adjustment of the velocity, automatic limitation of the consumed power through the power valve and with hydraulic command of the thermal motor rotational speed (fig.8)

The diagram is identical with the precedent one, with a small difference, namely the device for the motor acceleration is hydraulic actuated with the help of a flow control valve 2, supplementary to those for the command of the principal pump flow capacity (flow control valve 1).

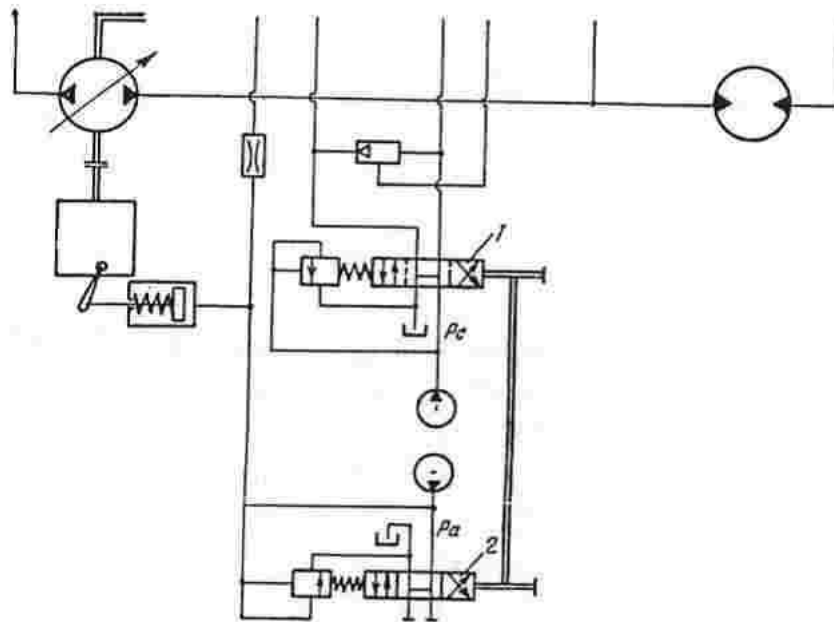


Fig. 8

It is to be mentioned that the circuit for the command of acceleration cannot be the same with those for „ p_c ” because an overloading „ p_c ” will be reduced automatically as a result of the intervention of the power valve so the rotation velocity will be also simultaneously reduced.

4. Conclusions

1. The majority of the hydrostatic traction systems included in the working devices are realized in close circuit, from strategic reasons, specific to the building of mobile devices (reduced weights and volumes).

2. Introducing hydraulic adjustable pumps and motors in the diagram (fig.2) has favorable effects concerning the elastic adaptation of the traction characteristics (force and velocity) to the terrain conditions, the thermal motor (frequently of Diesel type) remaining at a stable running point.

3. Supplementary, the system presented in fig.2 offer the possibility of continuous adjustment of the motor regime with the help of a servo commanded pump.

4. In accordance with the considered equipment, it is possible to adopt one of the presented transmission or a combination of two or more variants (fig.3... 8).

5. Pursuing the equipment evolution it can be concluded that the mechanical transmission is gradually replaced by the hydraulic transmissions, because the later present the following advantages:

- Continuous adjustment without shocks, for the whole range of rotational velocities and torques.
- High torque at the beginning of motion.
- Safe working at normal parameters to positive and negative slopes.
- Simple handling without the necessity of great efforts from the driver.
- Great efficiency and reliability.
- Easy maintenance.

In order to assure the basic functions, the presented hydraulic systems, besides the fundamental elements, are provided with some supplementary devices necessary for specific adjustments.

As a general conclusion it must be said that a severe procedure in the use of the hydraulic transmission devices must be compulsory respected.

References:

- [1] **Bălăsoiu V.**, - Echipamente hidraulice de actionare, fundamente teoretice, fiabilitate, Editura Eurostampa, Timisoara, 2001.
- [2] **Bălăsoiu V.**, Pădurean I., - Echipamente și sisteme hidraulice de actionare, Compendium, Editura Orizonturi Universitare, Timisoara, 2004
- [3] **Bălăsoiu V.**, - Cercetari teoretice si experimentale asupra sistemelor electrohidraulice tip servovalva-cilindru-sarcina, pentru module de roboti industriali, Teza de doctorat, Institutul Politehnic Timisoara, 1987.
- [4] **Călărașu D.**, - Reglarea secundara a sistemelor de actionare hidrostatica in regim de presiune cvasiconstanta, Editura MEDIATECH, 1999,
- [5] **Cristian I.**, - Servosisteme electrohidraulice analogice, Editura Universitatii Transilvania, Brasov, 2003,
- [6] **Esnault Fr.**, Beneteau P., - Hydrostatique 1, Hydrostatique, Transmission de puissance, Cours et applications, Ed. Ellipses, 1997, Paris,
- [7] **Murvy P.** - Cercetari privind comportarea transmisiilor hidrostatice pentru sistemele de propulsie in sistem de franare, Teza de doctorat, Universitatea Politehnica din Timisoara, 1998
- [8] **Oprean A.** - Actionari si automatizari hidraulice, Sisteme mecano - pneumo - electrohidraulice, Editura Tehnica, Bucuresti 1983.
- [9] **Pătruț P.**, Nicolae I., - Actionari hidraulice si automatizari, Teorie, aparate, sisteme automate si aplicatii industriale, Editura "Nausicaa" Bucuresti, 1998.
- [10] **Vasiliu N.**, Vasiliu Dana., - Actionari hidraulice si pneumatice, Vol. 1, Editura Tehnica, Bucuresti, 2005. ***
- [11] - Hydraulik Komponent.,MANNESMANN REXROTH, Lohr am Main, 1989.
- [12] *** - Components for Hydraulic Proportional and Servo Systems Electronics and accessories., MANNESMANN REXROTH. Lohr am Main. 1984.
- [13] **Vasiliu N.**, Catana Il., - Transmisii hidraulice si electrohidraulice, Reglarea masinilor hidraulice volumice, Vol II, Editura Tehnica, Bucuresti. 1997.
- [14] *** - Hydraulik Trainer , MANNESMAN REXROTH, Lohr am Main, 1986.
- [15] *** - Der Hydraulik Trainer, Band 2, Proportional -und Servoventil Technik, Mannesmann, REXROTH, GmbH, 1986

RESEARCH ON FRICTION LOSSES IN THE TENSIONING DEVICES UNDER LOAD

Andrei GRAMA¹, Constantin CHIRIȚĂ¹, Mihai AFRĂSINEI¹, Vasile DAMASCHIN¹

¹ Tehnical University "Gheorghe Asachi" from Iassy, e-mail address andreiasi79@yahoo.com

Abstract: *Determination the size of losses by friction under load tensioning devices used and their comparison with values given in the literature, the tensioning devices made by companies profile [1], [2], [3]. Friction is determined based on theoretical relationships and experimental with a specially designed stand that determines the actual power draw. Knowing that the actual value pulling force is less than the theoretical load force due to friction in the system, we obtain a relative loss through friction. Based on both research theoretical and experimental, we get conclusions on both friction losses and linearity check real force pulling.*

Keywords: *pretensioning, tensioning devices, friction losses*

1. Introduction

Determination the size of losses by friction under load tensioning devices used and their comparison with values given in the literature, the tensioning devices made by companies profile [1], [2], [3].

Friction force due to friction tensioning devices that oppose the advance piston. This force is opposite force must be added active and effective tensioning force.

2. Theoretical determination of friction single – wire tensioning devices

(Arial, 11pt, Regular) To determine by theoretical friction single - wire tensioning devices, will leave the relationship (1.1) which gives the theoretical value of load force.

$$(1.1) \quad F_{inc} = S \cdot P$$

where:

S - cylinder piston surface tension conducting effective cm²,

P - pressure hydraulic power source developed for prestressing in bar.

The actual value pulling force is less than the theoretical load force due to friction in the system and, as such, we have a relative friction loss is given by (1.2)

$$(1.2) \quad \Delta F_f = \frac{F_{inc} - F_{exp}}{F_{exp}} 100[\%]$$

where:

F_{exp} = real strength developed tensioning device measured the load at the output hydraulic pressure source work.

It is noted that in determining relative losses by friction we need the theoretical values of the loading force and the actual force values are obtained experimentally.

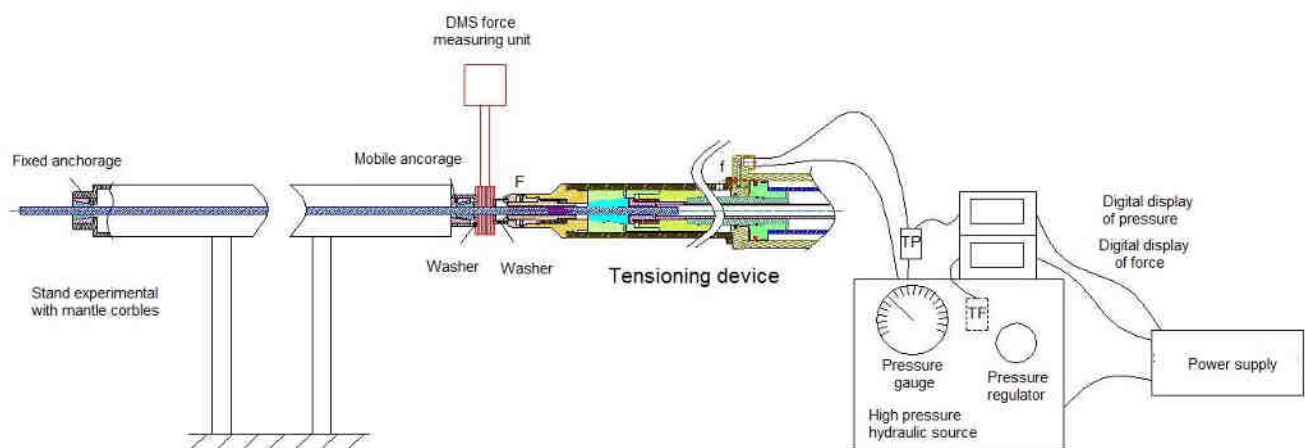
Theoretical loading force values, calculated for the period 60 bar - 390 bar, in increments of 10 to 10 bar are shown in Tab. 2.1.

Table 2.1 The theoretical values to pretensioning a strand

Force 16 [tF] Pressure 700 [bar]					
Pressure [bar]	Force [tF]	Pressure [bar]	Force [tF]	Pressure [bar]	Force [tF]
60	2,598	180	7,794	300	12,99
70	3,031	190	8,227	310	13,423
80	3,464	200	8,66	320	13,856
90	3,897	210	9,093	330	14,289
100	4,33	220	9,526	340	14,722
110	4,763	230	9,959	350	15,155
120	5,196	240	10,392	360	15,588
130	5,629	250	10,825	370	16,021
140	6,062	260	11,258	380	16,454
150	6,495	270	11,691	390	16,887
160	6,928	280	12,124		
170	7,361	290	12,557		

3. Experimental determination of pulling force at single – wire tensioning devices

Real pulling force will be determined using the stand shown in Fig. 3.1.



*Fig. 3.1. Experimental facility for determining friction from tensioner
TF - force transducer, PT - pressure transducer*

Will be testing to two tensioning devices research conducted in the Department of Hydraulic and Pneumatic Systems Engineering (DISAHP) Department of Machine Tools of Faculty of Mechanical Engineering and Management Industrial Technical University "Gheorghe Asachi" from Iassy of which can strain tendons in force for 16 tF, one with working stroke of 200mm and second 500 mm. These devices are conducting cylinder piston surface tension of: 43.3 cm².

Stand components to determine friction tensioning devices are shown in Fig. 3.1:

- High pressure hydraulic source for tension;
- Stand experimental with mantle corbles
- wire TBP 9
- DMS force measuring unit applied wire calibrating the display of force pulling on high pressure hydraulic source;
- pressure transducer 0 to 1200 bar,
- force transducer 0 to 25 tF;
- digital display of pressure;
- digital display of force;
- single –wire tensioning device
- power supply 220V, Uca.

Calibration of force transducer 0-25 tF

To measure the pulling force by pressure transducer included in high pressure hydraulic source, it is necessary to calibrate the pressure transducer in units of force

In this respect it will use a DMS force measuring unit type DMS 25, produced by Paul Maschinenfabrick calibrated and not damaged. DMS force measuring unit is installed between blocking system and the single-wire tensioning device as shown in Fig. 3.1.

It will introduce the best possible positioning two washers glued on both sides DMS force measuring unit. Will be effective tension-type TBP9 wire, by using the tensioning force of 16 tF and 200 mm stroke. Tension is achieved at working pressure hydraulic power source 100, 200, 300 and 400 bar.

Values of strength obtained DMS force measuring unit indicated by the digital display are read and note that in Tab. 3.1.

Table 3.1 The force calibrating digital display unit pressure

Working pressure [bar]	Value read from the force measuring equipment [tF] (at DMS force measuring unit)				Value read from a digital display unit pressure [tF] (at electro-hydraulic power unit)			
	1	2	3	SD	1	2	3	SD
100	4,05	4,15	4,1	4,1	3,85	4,05	3,95	3,95
200	8,25	8,5	8,35	8,37	7,95	8,15	8,25	8,12
300	12,50	12,35	12,20	12,35	12,05	12,15	12,10	12,1
400	16,25	16,50	16,35	16,37	16,05	16,30	16,25	16,2

To make the correction digital device display pressure, use the relation (3.1)

$$(3.1) \quad k = \frac{\text{average value obtained with DMS force measuring unit}}{\text{average value obtained with pressure display device}}$$

They obtained values of Tab. 3.2

Table 3.2 Values for different levels of pressure correction

Working pressure [bar]	Value read from the force measuring equipment [tF] (at DMS force measuring unit)	Value read from a digital display unit pressure [tF] (at electro-hydraulic power unit)	Digital correction value
100	4,1	3,95	1,0380
200	8,37	8,12	1,0308
300	12,35	12,1	1,0207
400	16,37	16,2	1,0105

Calculation is the standard deviation digital correction value is obtained: $k = 1.025$

We say that after correcting digital display device using the relation 3.3, the force indicated by the digital display device is less than 2.5% of DMS force measuring unit or, in other words, the strength of strand is higher by 2.5%.

Next, digital display calibrated pressure device to the value found by calculation by applying average correction factor displays program.

Repeat measurements after the above mode and obtain very similar values of pulling force on both equipment were analyzed for all measurements.

A first set of tests were performed on the tensioning device of 16 tF and 200 mm stroke work and to doing so.

For each pressure step in Tab. 2.1. were performed three sets of measurements yielding three values of pulling force. These values, together with relevant theoretical load force taken from Tab. 2.1 are shown in Tab. 3.3. Here, are numerically and arithmetic averages of sets of 3 values measured experimental force and friction losses relative to the device.

Table 3.3. Experimental results obtained for losses
tensioning device of 16 tF with stroke 200 mm

No. crt.	Pressure [bar]	F_{exp} [tF]			F_{inc} [tF]	SD F_{exp} [tF]	Relative loss in device [%]
		1	2	3			
1	60	2,4	2,56	2,61	2,52	2,598	2,87
2	70	2,83	2,79	2,68	2,77	3,031	8,72
3	80	3,25	3,27	3,26	3,26	3,464	5,89
4	90	3,67	3,7	3,71	3,69	3,897	5,23
5	100	4,06	4,04	4,12	4,07	4,33	5,93
6	110	4,52	4,53	4,61	4,55	4,763	4,40
7	120	4,9	5,03	5,03	4,99	5,196	4,03
8	130	5,42	5,33	5,43	5,39	5,629	4,19
9	140	5,82	5,84	5,82	5,83	6,062	3,88
10	150	6,21	6,24	6,28	6,24	6,495	3,87
11	160	6,57	6,56	6,6	6,58	6,928	5,07
12	170	6,97	6,96	7	6,98	7,361	5,22
13	180	7,32	7,41	7,46	7,40	7,794	5,10
14	190	7,82	8,02	8,06	7,97	8,227	3,16
15	200	8,3	8,45	8,42	8,39	8,66	3,12
16	210	8,58	8,75	8,72	8,68	9,093	4,51
17	220	9,01	9,12	9,15	9,09	9,526	4,54
18	230	9,48	9,69	9,62	9,60	9,959	3,64
19	240	9,9	10,03	10,02	9,98	10,392	3,93
20	250	10,39	10,34	10,34	10,36	10,825	4,33
21	260	10,78	10,81	10,82	10,80	11,258	4,04
22	270	11,12	11,02	11,21	11,12	11,691	4,91
23	280	11,46	11,54	11,6	11,53	12,124	4,87
24	290	11,96	12	12,02	11,99	12,557	4,49
25	300	12,34	12,52	12,65	12,50	12,99	3,75

26	310	12,75	13	13,06	12,94	13,423	3,62
27	320	13,11	13,35	13,35	13,27	13,856	4,23
28	330	13,64	13,81	13,81	13,75	14,289	3,75
29	340	14,1	14,12	14,2	14,14	14,722	3,95
30	350	14,51	14,61	14,62	14,58	15,155	3,79
31	360	14,9	15,02	15,02	14,98	15,588	3,90
32	370	15,21	15,43	15,43	15,36	16,021	4,15
33	380	15,7	15,94	15,93	15,86	16,454	3,63
34	390	16,05	16,34	16,26	16,22	16,887	3,97

From experiments with effective pull force values obtained for the single – wire tensioning device of 16tF and stroke of 200 mm, graphs were drawn based on the values of pressure, without pressure multiplier Fig. 3.2 and pressure multiplier Fig. 3.3, in order to check the linearity real force.

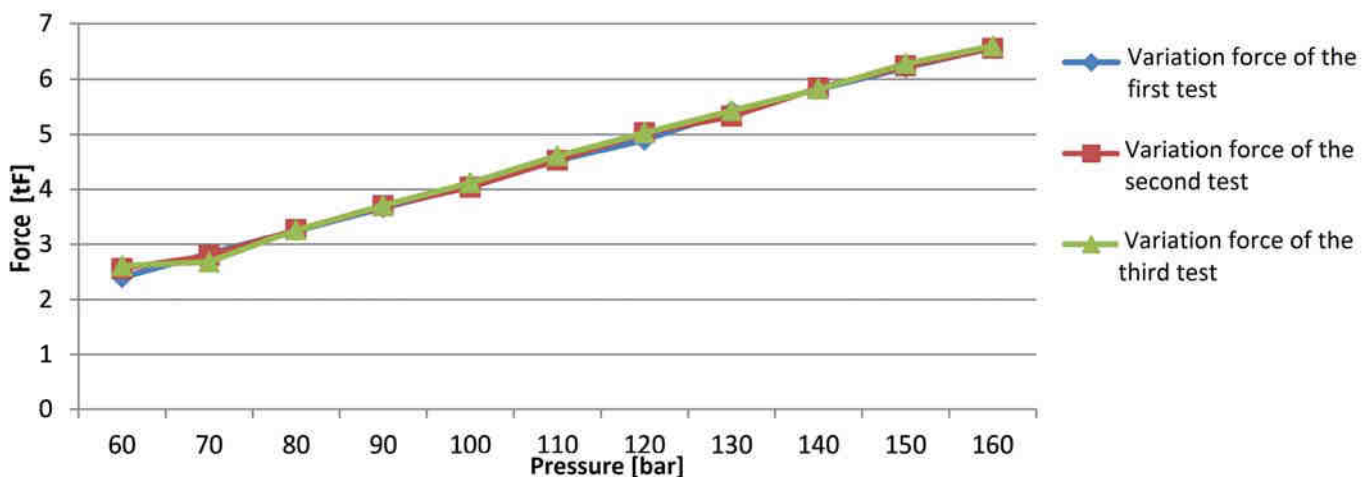


Fig. 3.2. Force at low pressure variation made with tensioning device for 16 tF with 200 mm stroke

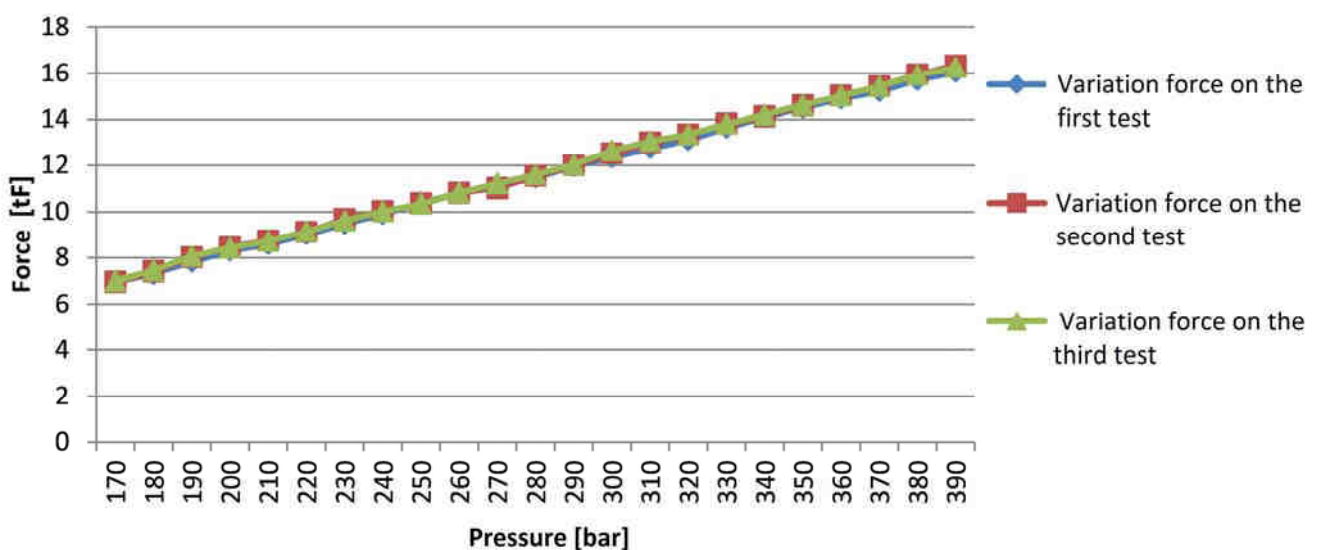


Fig. 3.3. Force at high pressure variation made with tensioning device for 16 tF with 200 mm stroke

Tests performed on the same single – wire tensioning device but with 500 mm stroke; were made using the same methodology as in the previous case, the values obtained are presented in Tab. 3.4.

Table 3.4. Experimental results obtained for losses
tensioning device of 16 tF with stroke 500 mm

No. crt.	Pressure [bar]	F_{exp} [tF]			F_{inc} [tF]	SD F_{exp} [tF]	Relative loss in device [%]
		1	2	3			
1	60	2,43	2,4	2,42	2,598	2,417	6,98
2	70	2,8	2,85	2,82	3,031	2,823	6,85
3	80	3,22	3,23	3,23	3,464	3,227	6,85
4	90	3,68	3,67	3,71	3,897	3,687	5,40
5	100	4,08	4,09	4,12	4,330	4,097	5,39
6	110	4,4	4,41	4,45	4,763	4,420	7,20
7	120	4,7	4,85	4,89	5,196	4,813	7,36
8	130	5,2	5,25	5,23	5,629	5,227	7,15
9	140	5,76	5,73	5,73	6,062	5,740	5,31
10	150	6,02	6,03	6,03	6,495	6,027	7,21
11	160	6,53	6,51	6,53	6,928	6,523	5,84
12	170	6,92	7,02	7,12	7,361	7,020	4,63
13	180	7,46	7,46	7,47	7,794	7,463	4,24
14	190	7,85	7,9	7,83	8,227	7,860	4,46
15	200	8,25	8,24	8,47	8,660	8,320	3,93
16	210	8,58	8,62	8,61	9,093	8,603	5,39
17	220	8,92	8,9	8,94	9,526	8,920	6,36
18	230	9,28	9,35	9,29	9,959	9,307	6,55
19	240	9,81	9,76	9,81	10,392	9,793	5,76
20	250	10,23	10,21	10,25	10,825	10,230	5,50
21	260	10,61	10,65	10,54	11,258	10,600	5,84
22	270	11,23	11,36	11,36	11,691	11,317	3,20
23	280	11,48	11,73	11,71	12,124	11,640	3,99
24	290	12,03	11,92	12,03	12,557	11,993	4,49
25	300	12,46	12,51	12,4	12,990	12,457	4,11
26	310	12,92	12,91	12,86	13,423	12,897	3,92
27	320	13,3	13,2	13,28	13,856	13,260	4,30
28	330	13,65	13,86	13,72	14,289	13,743	3,82
29	340	14,02	14	14,03	14,722	14,017	4,79
30	350	14,4	14,64	14,64	15,155	14,560	3,93
31	360	14,71	14,84	14,85	15,588	14,800	5,06
32	370	15,21	15,4	15,34	16,021	15,317	4,40
33	380	15,58	15,52	15,75	16,454	15,617	5,09
34	390	16,01	16,01	16,03	16,887	16,017	5,15

The effective force values obtained experimentally for pretensioning device of 16tF with stroke of 500 mm graphs were drawn based on the values of pressure, without pressure multiplier Fig. 3.4 and with pressure multiplier Fig. 3.5, in order to check the linearity real force.

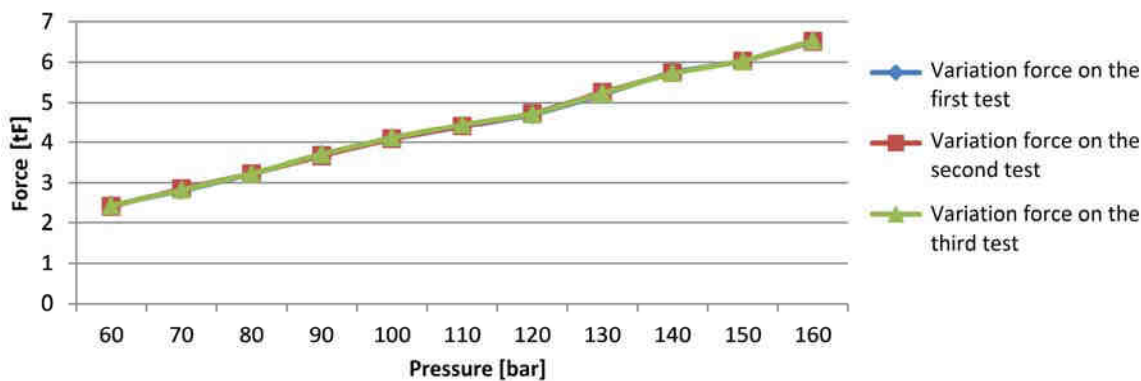


Fig. 3.4. Force at low pressure variation made with pretensioning device for 16 tF with 500 mm stroke

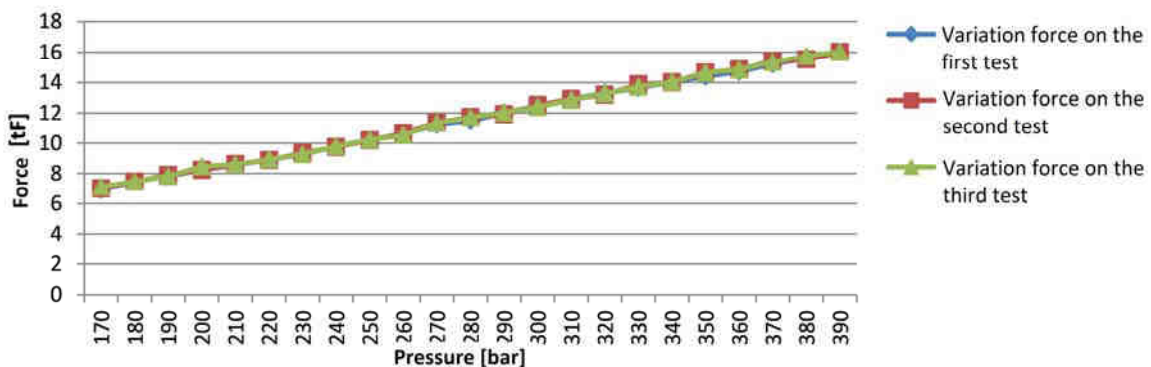


Fig. 3.5. Force at high pressure variation made with pretensioning device for 16 tF with 500 mm stroke

4. Conclusions

The data analysis presented in Tab. 3.3 and 3.4 and the graphs in Fig. 3.2. - 3.5, we draw the following conclusions:

⇒ The four graphs shown real strength is observed that the variation can be considered linear, so we can say that the real strength varies directly proportional to pressure as the force varies theoretical (equation 1.1.)

⇒ Also the tab. 3.3 and Tab. 3.4, it is observed that the relative loss of power by friction device limits vary between 3.16% and 8.72%, maximum known in the literature [1], [2], [3], pretensioning devices with similar characteristics is 10% - 15%.

⇒ The above led to the conclusion that the devices studied achieved comparable performance with devices made by other manufacturers, which validates the use of this device stand prestressed tension reinforcement.

REFERENCES

- [1] <http://www.bianchicasseforme.it>
- [2] HYDRAMOLD Contract grant no. 151, Tensrelax, Phase I Studies and experimental models "Development of a hydraulic power equipment technology, innovation, modernization of tension reinforcement for prestressed concrete structures", November 2008
- [3] Paul Maschinenfabrik GmbH&Co. KG "Operating Manual – Pump Unit – Mach. No.:07196878/2", Max-Paul-Straße 1 88525 Dürmentingen/Germany
- [4] . Chiriță, A. Grama, D. Zetu, „High Pressure Hydraulic Unit Used in Making Prestressed Reinforced Concrete Structure” Buletinul I.P. Iași, publicat de U.T. „Gheorghe Asachi”, Iași, Tomul LVI (LX), Fasc. 1, (2010), Secțiunea Construcții de mașini, pag 213-222

TRANSFER FUNCTION OF A PRESSURE TRANSDUCER WITH DRAWER

I. Nicolae¹, M. Cotrumba¹

¹Ovidius University of Constanta, Mamaia Ave., no 124, Constanta, Romania

ABSTRACT

This paper concludes that the operational principle of the pressure transducer with drawer consists in the balance of forces that indirectly measure pressure with an elastic component.

1. GENERAL CONSIDERATIONS

In many liquid controllers or automatic air-hydraulic systems, the pressure transducer is an important element. No matter the kinematic diagram, the operational principle consists in the balance of forces that indirectly measure pressure by means of an elastic standard component. In this case pressure variation will produce a variable force able to make the drawer slide.

A variant of this transducer type is represented in figure 1.

This transducer carries out a conversion from pressure variation in the drawer's sliding movement.

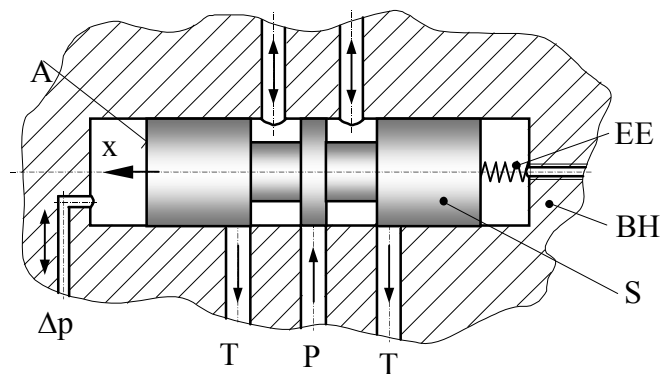


Figure 1. Pressure transducer with drawer. Legend: BH – hydraulic block; EE – elastic component; S – drawer; P – pressure source; x – drawer sliding movement; Δp – pressure variation; A – drawer area; T – tank.

2. TRANSFER FUNCTION CALCULUS

The following letter notes are used to establish the transfer function: k – spring constant [daN/cm]; Δp – applied pressure variation [daN/cm²]; A_s – drawer section area [cm²]; m_s – drawer and 1/3 of spring mass [kg]; α – viscose friction coefficient of drawer [daN·s/cm]; x – drawer sliding movement [cm]; δ – damping factor [-]; ω_n – system pulsation [1/s].

The viscose friction coefficient is influenced by liquid losses under pressure at piston level and is expressed as:

$$\alpha = R_0 \cdot A_s^2 = \frac{\nu_{oil} \cdot \rho_{oil} \cdot l_s}{\pi \cdot D_s \cdot j_s^3} \cdot A_s^2 \quad (1)$$

where: D_s – drawer diameter [cm]; j_s – drawer diameter clearance in hydraulic block [cm]; l_s – drawer length [cm]; ν_{oil} – liquid kinematic viscosity [daN/cm]; ρ_{oil} – liquid density [kg/m³].

A pressure variation is added to the equilibrium equation to get drawer's speed and acceleration.

In condition of rest an equilibrium equation at forces level is written:

$$\Delta p \cdot A_s = k \cdot x \text{ where } \Delta p = \frac{k \cdot x}{A_s} \quad (2)$$

In order that drawer can reach certain speed, additional pressure is necessary to cover viscose factor force of liquid, expressed by viscose friction coefficient:

$$\Delta p \cdot A_s = \alpha \frac{dx}{dt}; \Delta p = \frac{\alpha}{A_s} \cdot \frac{dx}{dt} \quad (3)$$

Using Newton's second law:

$$\Delta p \cdot A_s = m_s \frac{d^2x}{dt^2} \Rightarrow \Delta p = \frac{m_s}{A_s} \cdot \frac{d^2x}{dt^2} \quad (4)$$

By adding up pressure components:

$$\Delta p = \frac{k \cdot x}{A_s} + \frac{\alpha}{A_s} \cdot \frac{dx}{dt} + \frac{m_s}{A_s} \cdot \frac{d^2x}{dt^2} \quad (5)$$

Laplace function is applied and the result is:

$$\Delta p(s) \frac{k}{A_s} X(s) + \frac{\alpha}{A_s} sX(s) + \frac{m_s}{A_s} s^2(s)X \quad (6)$$

And is written as the transfer function:

$$\frac{X(s)}{\Delta p(s)} = \frac{\frac{A_s}{k}}{\frac{m_s}{k} s^2 + \left(\frac{\alpha}{k}\right)s + 1} \quad (7)$$

If we note: $\omega_n = \sqrt{\frac{k}{m_s}}$ - its own pulsation and $\delta = \frac{\alpha}{2k} \sqrt{\frac{k}{m_s}} = \frac{\alpha}{2\sqrt{k \cdot m_s}}$ - damping factor, the transfer function can be written as:

$$\frac{X(s)}{\Delta p(s)} = \frac{\frac{A_s}{k}}{\frac{m_s}{\omega_n^2} s^2 + \left(\frac{2 \cdot \delta}{\omega_n}\right)s + 1} \quad (8)$$

For studying frequency field we note $s = \omega \cdot i$ and the transfer function nominator can be expressed as:

$$\begin{aligned} \frac{1}{\omega_n^2} s^2 + \left(\frac{2 \cdot \delta}{\omega_n}\right)s + 1 &= \left(\frac{\omega}{\omega_n}\right)^2 i^2 + 2 \cdot \delta \frac{\omega}{\omega_n} i + \\ + 1 &= 1 - \left(\frac{\omega}{\omega_n}\right)^2 + 2 \cdot \delta \frac{\omega}{\omega_n} i \end{aligned} \quad (9)$$

By replacing expression 9 in 8 and rationalizing nominator, the transfer function location is expressed as:

$$LT(\omega i) = \frac{K \left[1 - \left(\frac{\omega}{\omega_n} \right)^2 \right]}{\left[1 - \left(\frac{\omega}{\omega_n} \right)^2 + \left(2 \cdot \delta \cdot \frac{\omega}{\omega_n} \right)^2 \right]} - \frac{2 \cdot \delta \cdot \left(\frac{\omega}{\omega_n} \right)}{\left[1 - \left(\frac{\omega}{\omega_n} \right)^2 + \left(2 \cdot \delta \cdot \frac{\omega}{\omega_n} \right)^2 \right]} \cdot i \quad (10)$$

To study transfer function in frequency field a Mathcad

program was written, to plot: amplitude

– frequency logistic feature (figure 2), phase - frequency logistic feature (figure 3) and the transfer function location (figure 4). The study has been simulated by varying frequency between 0 - 300 Hz, for three damping factors ($0 < \delta < 1$, $\delta = 1$, $\delta > 1$).

3. TRANSFER FUNCTION OF A PRESSURE TRANSDUCER

Notes: 1 daN = 10 N; 1 bar = 10^5 Pa

Initial data: $m_s = 0,25 \frac{\text{daN} \cdot \text{s}^2}{\text{m}}$; $\rho_{oil} = 850 \frac{\text{kg}}{\text{m}^3}$; $v_{oil} = 6 \cdot 10^{-8} \frac{\text{m}^2}{\text{s}}$; $k = 3000 \frac{\text{daN}}{\text{m}}$; $j_s = 20 \cdot 10^{-3} \text{ mm}$; $D_s = 10 \text{ mm}$; $l_s = 20 \text{ mm}$.

Solution: $A_s = \frac{\pi D_s^2}{4}$; $A_s = 7,854 \cdot 10^{-5} \text{ m}^2$ - drawer area; $\alpha = \frac{v_{oil} \cdot \rho_{oil} \cdot l_s}{\pi D_s j_s^3}$; $\alpha = 0,025 \frac{\text{daN} \cdot \text{s}}{\text{cm}}$ - viscose

friction coefficient; $\omega_n = \sqrt{\frac{k}{m_s}}$; $\omega_n = 109,545 \text{ Hz}$ - proper pulsation; $K_{am} = \frac{A_s}{k}$; $K_{am} = 0,026 \frac{\text{cm}^3}{\text{daN}}$ -

multiplication factor; $\delta = \frac{\alpha}{2\sqrt{k \cdot m_s}}$; $\delta = 0,046$ - damping factor; $i = 0 \dots 1000$; $\omega i = i \text{ Hz}$ - logarithm

frequency characteristic; $N(i, \delta) = \left[1 - \left(\frac{\omega_i}{\omega_n} \right)^2 \right]^2 + \left(2 \cdot \delta \cdot \frac{\omega_i}{\omega_n} \right)^2$ - transfer function nominator;

$LT(i, \delta) = K_{am} \cdot \frac{\left[1 - \left(\frac{\omega_i}{\omega_n} \right)^2 - 2\delta \cdot \frac{\omega_i}{\omega_n} \cdot i \right]}{N(i, \delta)}$ - transfer function location;

$Am(i, \delta) = \sqrt{\text{Re}(LT(i, \delta))^2 + \text{Im}(LT(i, \delta))^2}$ - amplitude value.

Amplitude - frequency characteristic, represented in figure 2, is expressed as:

$$A1_i = 20 \cdot \log\left(\frac{Am(i, \delta)}{K_{am}}\right)$$

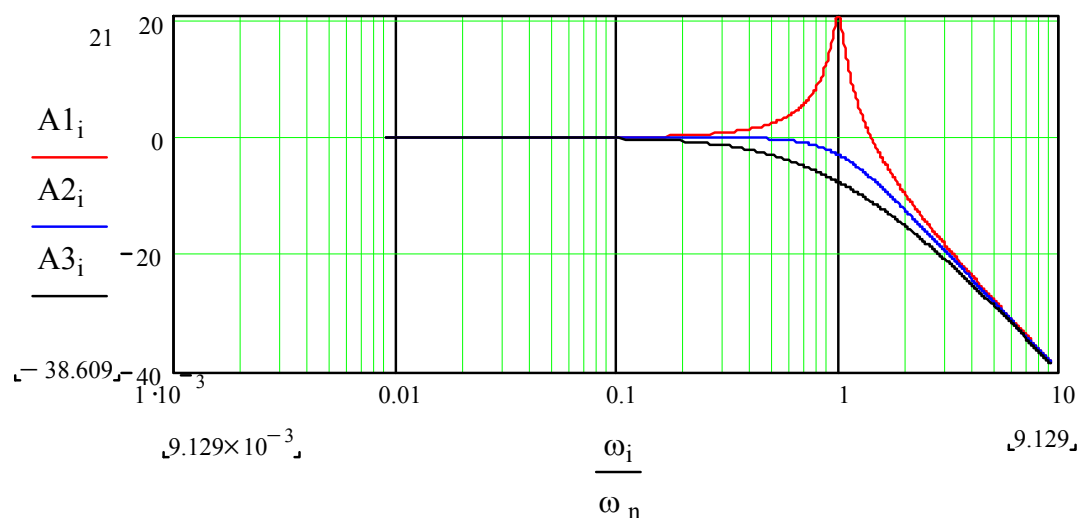


Figure 2. Amplitude – frequency logistic feature

Damping factor is given three values:

$$\delta 2 = 0,7 \quad A2_i = 20 \cdot \log\left(\frac{Am(i, \delta 2)}{K_{am}}\right)$$

$$\delta 3 = 1,2 \quad A3_i = 20 \cdot \log\left(\frac{Am(i, \delta 3)}{K_{am}}\right)$$

Damping factor is given several values:

$$\Phi(i, \delta) = -\text{atan}\left(\frac{\text{Im}(LT(i, \delta))}{\text{Re}(LT(i, \delta))}\right) \cdot \frac{1}{\text{deg}} \quad \text{- phase-frequency characteristic (represented in figure 3)}$$

$$\delta 2 = 1 \quad \delta 3 = 1,5 \quad \Phi 1i = \Phi(i, \delta) \quad \Phi 2i = \Phi(i, \delta 2) \quad \Phi 3i = \Phi(i, \delta 3).$$

Transfer location: $\delta = 0,4$ is represented in fig. 4.

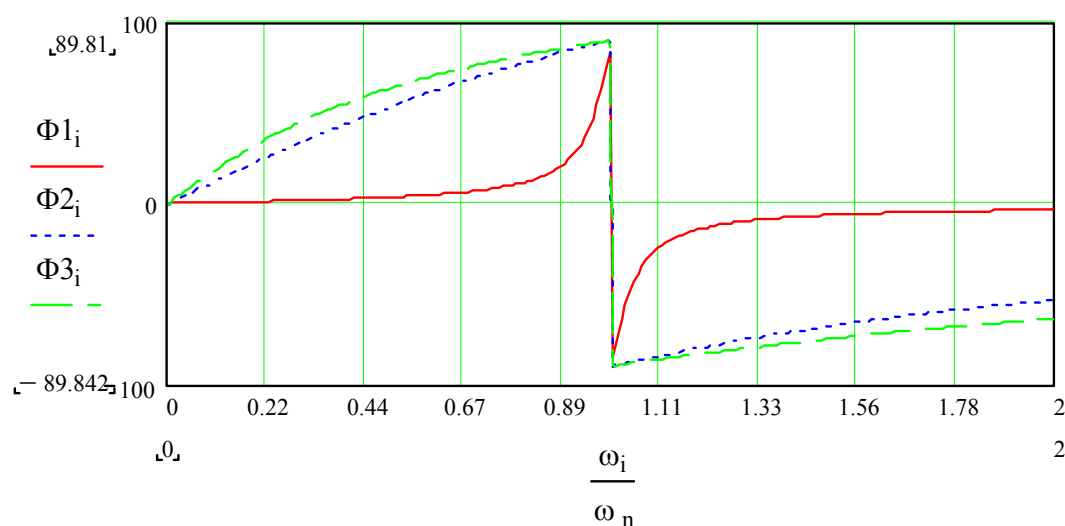


Figure 3. Phase - frequency logistic feature

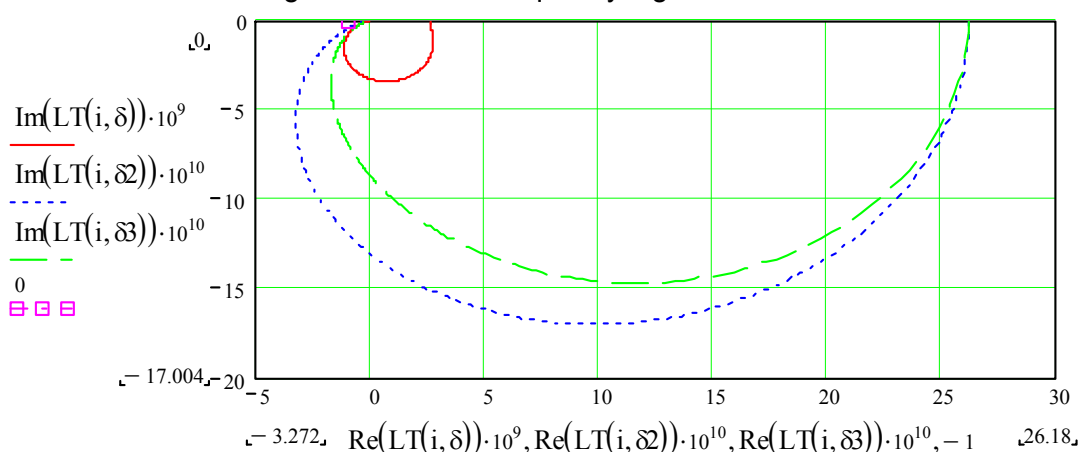


Figure 4. Transfer function location

4. CONCLUSIONS

- the system is absolutely stable when the three coefficients are positive;
- the response to stage signal is non-periodic when $\delta > 1$ and periodically damped when $0 < \delta < 1$;
- the response to frequency produces resonance when $\delta = 0,707$;
- with input frequencies of 0...300 Hz the system stays almost constant;
- frequency characteristics lead to the conclusion that this transducer acts as a low-pass filter;
- the pressure transducer is a proportional mechanic system with a second rat inertia.

5. REFERENCES

1. Ernest, E., Lewis, H. S. S.– *Sisteme hidraulice automate*, Ed. Tehnică, București, 1968;
2. Petre, P., Nicolae, I.– *Acționări hidraulice și automatizări*, Ed. Nausica, 1998.

LIFTING EQUIPMENT WITH RECOVERY SYSTEM OF POTENTIAL ENERGY

Eng. Stefan ALEXANDRESCU¹, Ph. Dr. Eng. Corneliu CRISTESCU¹,

Ph.Dr. Eng. Gheorghe SOVAIALA¹, Tech. Pr. Ioan PAVEL¹

Eng. Alexandru MARINESCU¹

¹ Hydraulics and Pneumatics Research Institute INOE 2000-IHP, Bucharest, **ROMANIA**,

E-mail: alexandrescu.ihp@fluidas.ro

Abstract: *The capture and the reuse of different forms of energy have become over the past decade a new research domain, topical, in order to save energy especially in the conditions of increases of the fuel prices. If the energy can not be defined only using a very general principle of physics, the energy transformation, ie the transition of energy from one form to another, is easily observed and measured using laboratory instruments.*

To this scope the product Lifting equipment with recovery system of potential energy, developed as a prototype as a result of a research work, aims the recovery by hydraulic way of the potential energy under latent and active form of the masses which rise and fall controlled in gravitational field.

Keywords: *energy recovery, hydraulic systems, energy saving, innovation*

1. Introduction

As is known, the energy of the moving objects is called kinetic energy and converts in gravitational potential energy if a weight is stopped at different heights. For example, a suspended weight or a quantity of liquid which is in a dam shows a form of waiting-latent potential energy. The change position of the weight by dropping in gravitational field by its height variation leads to the appearance of an active energy capable to develop an active energy of movement and thus a mechanical work. In fact, both the potential energy, as well as the kinetic energy are two forms of mechanical energy. Based on these theoretical considerations, in INOE 2000-IHP has been made a lifting equipment of some loads / weights at different heights, with hydraulic drive system used in the necessary stages of some technological assembly processes. At the descent of these loads, with a speed controlled in gravitational field, the potential energy, transformed by the system of cables and rolls into kinetic energy at drum, is converted into hydrostatic energy by an hydrostatic unit, which is stored and then reused in the lifting phases. First, it should be specified that energy recovery is not limited to use pump in some idle phases of a technological system. The equipment turn potential energy into mechanical work which then converts in a hydrostatic energy stored in a hydraulic accumulator.

As is known, the potential energy is calculated using the formula:

$$E_p = mgh = Gh,$$

in which:

E_p – is potential energy;

m - the mass object descends in gravitational field

g - acceleration of gravity;

h - the height in which is found the subject at a time;

G - raised weight then falls in gravitational field;

Actually, the loss of a weight in gravitational field with controlled speed, will generate a hydraulic energy characterized by flow and pressure. This energy, in the equipment is stored in an accumulator that load under adiabatic transformation of the gas.

2. Presentation of the lifting equipment with energy recovery

The lifting equipment with energy recovery was designed and manufactured at INOE 2000-IHP and will be tested in the next future. Constructive, the lifting equipment with energy recovery is composed of the following main parts;

- The lifting device;
- The module for recovery and reuse of energy;
- The hydraulic mobile station

2.1. The lifting device

The lifting device, figure 1 and figure 2, consists in a lattice frame movable on wheels, with the drum drive system by the axial pistons unit. It also has a system of pulleys of which one mobile to doubling the lift weight.

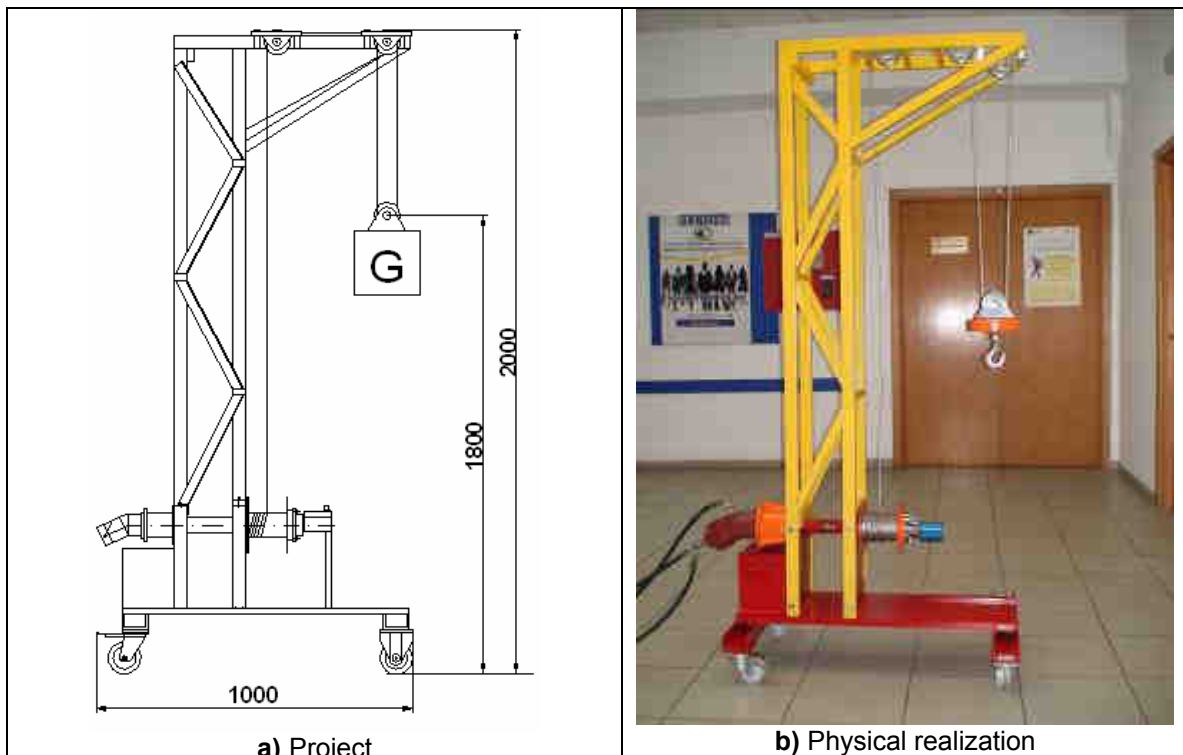
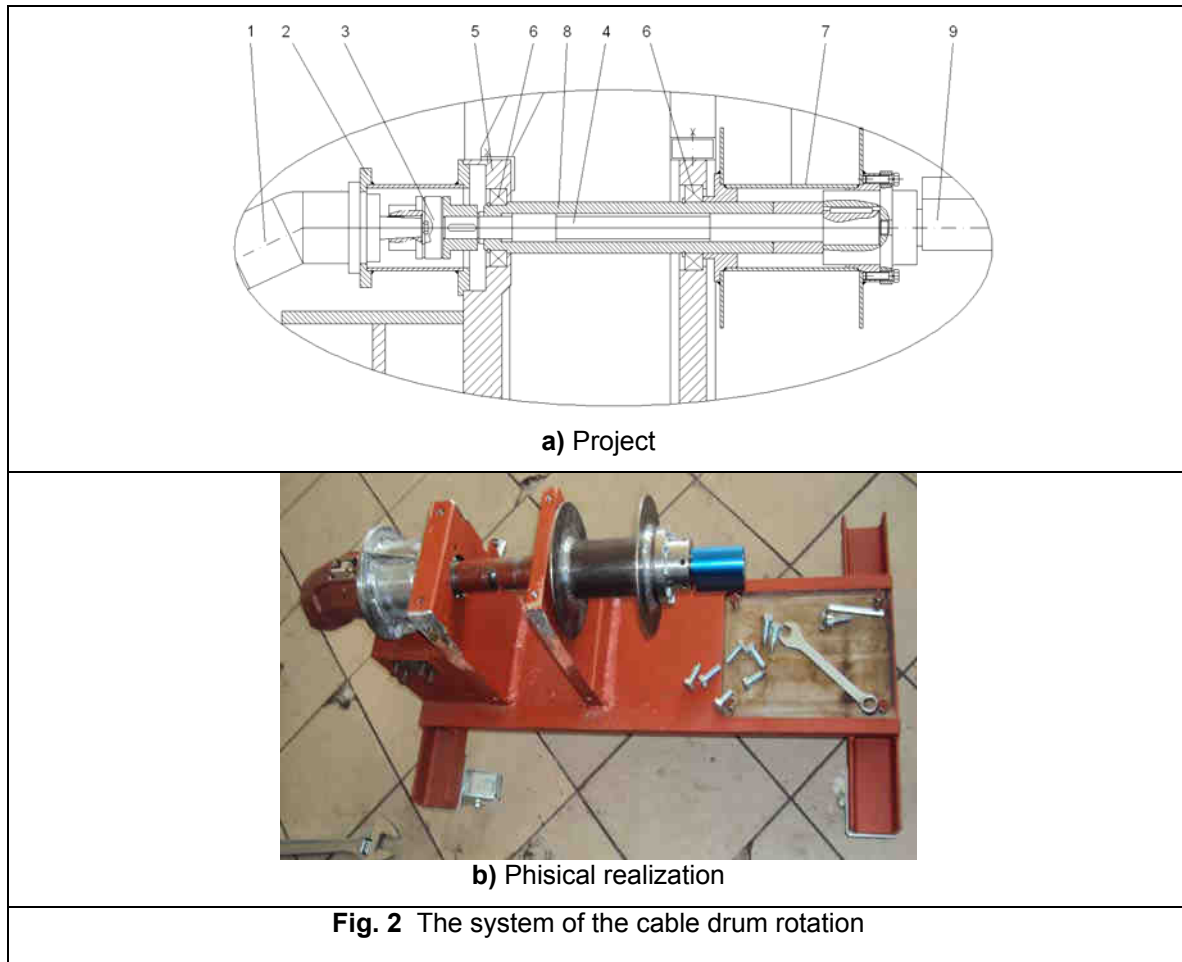


Fig. 1 The lifting device

2.1.1. The rotation system of the cable winding drum

This system, figure 2, a and b, has dual role, to ensure the weight lifting when axial piston unit has motor function and in descent phase controlled to provide hydraulic energy, having pump function. According to figure 2 a, the drum rotation system consists of: 1 - axial piston unit, 2 - connector, 3 - flexible coupling, 4 - shaft drive, 5-stand, 6-roller bearings, 7 - drum winding of the cable, 8 - shaft port-drum, 9 - torque and speed transducer



In the phase of weight lifting, the hydraulic station supply the hydraulic motor 1, which by coupling 3, train shaft 4. It is integral with the drum 7 and shaft 8, through torque and speed transducer 9 and together performs a rotational motion.

In the descent phase of weight, gravity pulls the cable drum, which train the drum 7, and through torque and speed transducer 9 and coupling 3, trains the hydraulic unit 1 which, in this phase have the pump function and converts the potential energy in hydrostatic energy, which is then stored in the hydropneumatic accumulator of the recovery module, for reuse in the next phase of lifting.

2.1.2 The carrying structure of the device

The carrying structure of the device is a metallic building as a lattice beam, capable to take the loads outcoming from the lift process. On top, the structure, is equipped with a system of pulleys, one of which is mobile pulley, allowing the lifting of a double load, relative to the effort of lifting cable drum. figure 3, a and b.



a –Side view



b –Bellow view

Fig. 3 The roller system of the lifting cable by rolls

2.2. The module for recovery and reuse of energy

At the controlled lowering weight, the torque produced by drum and the tangential force of cable train pump 1, and the potential energy is converted into hydrostatic energy and then is stored in an accumulator, being reused in the next cycle of work. As can be see in figure 4a, at descent, the accumulator load from the values pressure-volume p_1 and V_1 to pressure-volume values p_2 , V_2 , corresponding to a quantity volume ΔV . In the next phase of work, at weight lifting, in the hydraulic system adding up the pump flow q_p and accumulator flow q_2 , corresponding to quantity of oil ΔV , figure 4 b. Also when starting the pump, the pressure is p_2 ; is done an economy power and thus important electric energy, because q_p product has a lower value.

curve of the nitrogen variation from the accumulator

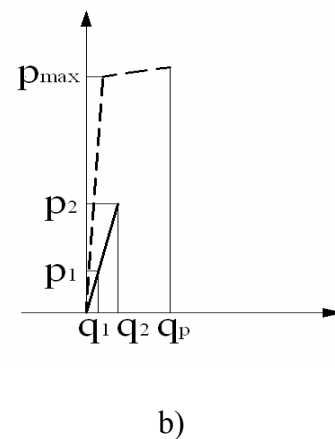
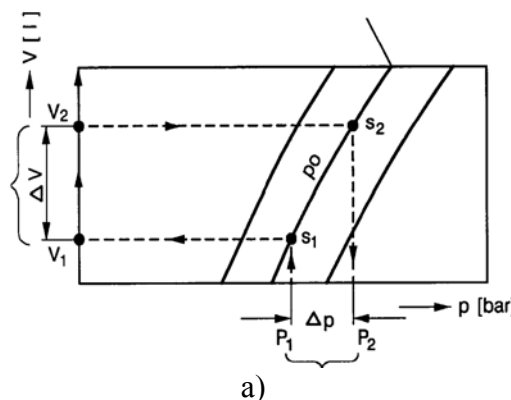


Fig.4- The chart of load and reuse of the hydraulic energy

The recovery module designed in institute, figure 5, is composed, mainly, a block with hydraulic equipments of distribution and control of pressure necessary to capture and reuse the hydraulic energy. Most appliances, are mounted on hydraulic block, physically realized by a specialized company, figure 6, but the mobile station supply too. , figure 7 and figure 8.

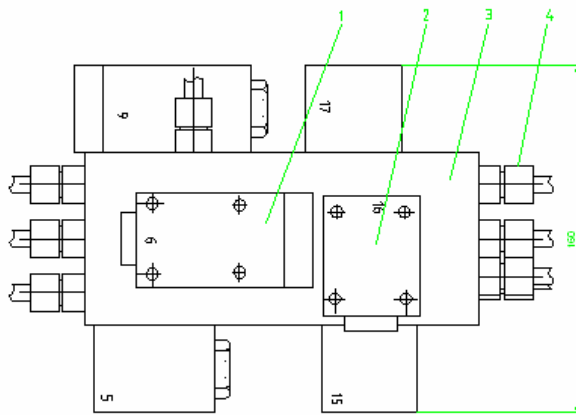


Fig. 5- Project hydraulic block

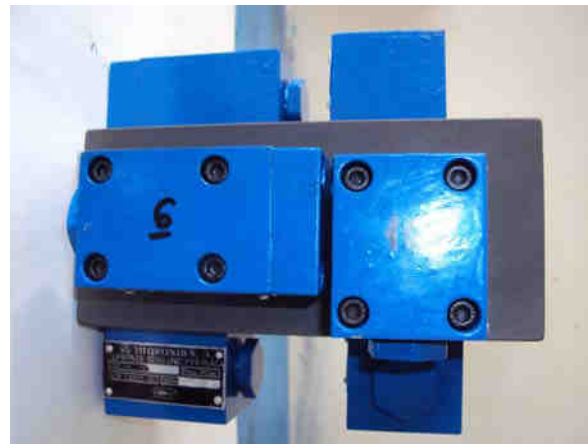


Fig. 6- Hydraulic block physically realized

2.3. Mobile hydraulic station

An important component part of lifting equipment with recovery of the potential energy is the hydraulic power station. It moves and connects with the drum rotating hydraulic system through hoses with quick couplers. As can be seen in figure 7, the station in standard construction is composed of one electric pump, a hydraulic distributor for connecting of flow, regulators etc. It also has different equipments for measure and controls: manometers, thermometer, level sensing and filters. On the prototype, the station was adapted by mounting on it the recovery module components such as: hydraulic distribution block, the hydraulic accumulator for storage the recovered energy and the distributor of connection to pumps of recovery module, as can be seen in figure 8.



Fig. 7 - The initial mobile hydraulic station

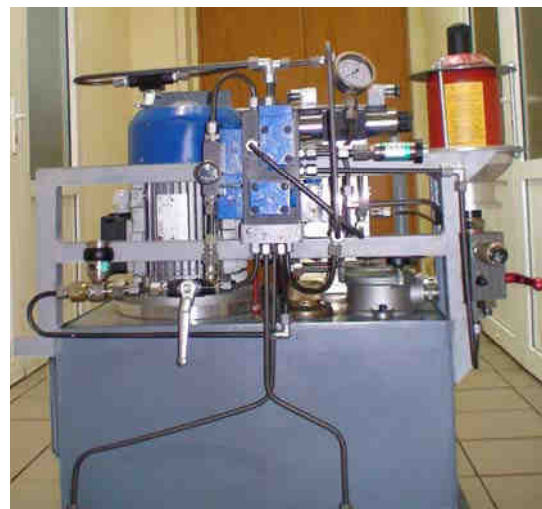


Fig. 8 - The adapted hydraulic mobile station

3. Technical characteristics of the equipment:

The lifting equipment has the following technical characteristics:

- lifting weight: max.200 kg;
- lifting height: max. 1800 mm;
- number of coils: max.15
- working pressure: max. 200 bar;
- the winding drum diameter: 76 mm
- the used axial piston unit: F110 A25 IPG - manufacturer HIDRAULICA, UMP Plopeni with the following technical characteristics:
 - displacement: 7,6 cm³
 - normal working pressure: 200 bar;
 - maximum working pressure: 350 bar;
 - maximum able torque: 70 Nm

Based on calculations with the above dates, at the operating pressure of 200 bar resulted an effective torque of winding drum of 44 Nm cable, that allows lifting of a weight of 200 kg at mobile pulley (with2-wire).

4. Operation of lifting equipment with energy recovery

To understand, in detail, the process of converting, storing and reusing of the potential energy of the lifted weight, by equipment, in figure 9 is shown the hydraulic scheme of the manufactured and designed equipment.

4.1. Control of working pressure

After starting of the electropump (hydraulic pump 1 and electric motor 2), completely close the flow regulator 14 and then adjust pressure valve 3 to 200 bar viewed by gauge 4.

4.2. Weight lifting phase, G

When working the electromagnet E1 of distributor 5, The pressure opens first the unlock check valve 12, and then check valve 13. The check valve 11 remains closed because the accumulator is empty. The flow is regulated by the flow regulator 14, and then the circuit put in movement the hydraulic motor 7, executed, thus, the lifting of the load.

4.3. Stop in phase of weight lifting at different heights

Disoperate E1 but pregnancy don't down, because the restricted sense of check valve 13 does not permit this.

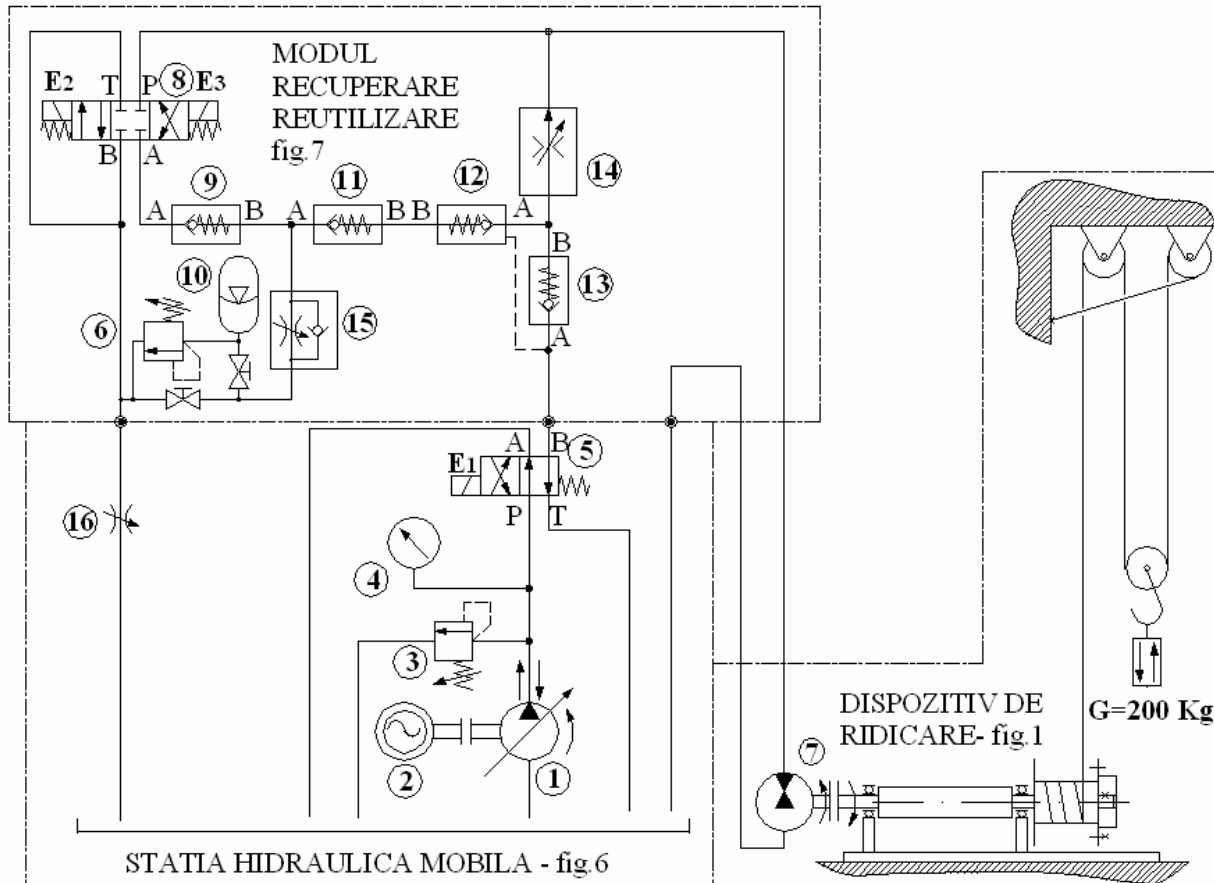


Figure 9- Hydraulic schema of the hydraulic energy recovery equipment

4.4. The recover of potential energy at downhill

Operate the electromagnet E2 of the distributor 8, the fluid flow being on path P-A opens check valve 9 and charge the accumulator until the maximum pressure of 200 bar, regulated by pressure valve 6. The accumulator 10 is loaded according to the schedule in Figure 7 in the descent weight phase. The scend speed control is realised by throttle 15, which, in reality, adjusts the charging time of the accumulator. After termination of pregnancy descent and charging the accumulator, it cancel E2 and acts E3. The scend speed adjusts by the throttle 16. without recover energy still further.

4.5. The use of stored energy at resumption of work cycle

At lifting, act E1 which open first valve 12, which discharge the accumulator, because check valve 13 has an opening pressure greater than the pressure control of valve 13. Increasing pressure pump, close valve 11 functioning, further, only pump, the electromagnets E2 and E3 being disoperates.

5. Conclusions

-The lifting equipment with potential energy recovery system, by transforming it into stored hydraulic energy, presents an innovative character applicable to lifting machines. It may be used, alone or together with other methods of potential energy recovery, for example with hydraulic cylinders or brake energy of moving vehicles.

- After testing of lifting equipment with potential energy recovery system, the solution adopted can serve as a reference model and transferred to industry at interested operators.

-The adopted energy recovery method is added to the database / technical knowledge concerning on energy recovery, along with other forms of green energy: solar, of waves, of wind, of braking, etc, according to the forecasts of energy crisis and the increase of the fuels prices.

REFERENCES

- [1] N. Vasiliu, D. Vasiliu, "Fluid Power Systems", Vol.I, Technical Publishing House, Bucharest, 2005.
- [2] C. Cristescu, P. Drumea, I. Ilie, M. Blejan, I. Dutu, Mechatronics system for recovering braking energy conceived for the medium and heavy motor vehicles, Paper Nr. F014-"ISSE 2008 31st. International Spring Seminar on Electronics Technology Reliability and Life-time Prediction", 7-11 May, 2008, BUDAPEST, HUNGARY, <http://www.isse-eu.net>, www.ett.bme.hu/isse/isse2008/
- (ISI-Thomson, UT WOS: 000272337900081)
- [3] C.Cristescu, "Recuperarea energiei cinetice la franarea autovehiculelor", Editura AGIR, Bucuresti,2008.
- [4] C.Cristescu, s.a. "Echipamente si sisteme mecatronice de recuperare a energiei de franare la autovehiculelor grele, HERVEX 2007, ISSN 1454-8003.
- [5] A.Oprean, s.a., "Actionari si automatizari hidraulice. Elemente si sisteme. Editura Tehnica, Bucurest, 1982
- [6] [http/ www.rexroth bosch group](http://www.rexrothboschgroup.com) – catalog produse.

NUMERICAL SIMULATIONS FOR A HYDRAULIC SYSTEM WITH SECONDARY CONTROL

Vasile HUIAN¹, Doru CĂLĂRAȘU¹ Constantin CHIRIȚĂ¹, Mihai AFRĂSINEI¹

¹ Universitatea Tehnică "GH. Asachi" Iași, Facultatea de Construcții de Mașini și Management Industrial
e-mail: huian.vasile@yahoo.com

Abstract: The paper presents results of research on hydraulic systems with secondary regulation in circuit with quasi constant pressure. There study presents the fundamentals that led to the development of secondary control systems. The diagram principle is presented for secondary adjustable hydraulic units in an open circuit and describes the system operation and automatic control loop. Change to the torque does not directly influence system pressure p , but through the intervention of control loop, the flow changes. This implies a control system to intervene quickly in order to change the flow. Using the Matlab Simulink programming environment we have obtained results on dynamic behavior of the systems. The presented and interpreted results pertain to system indicial responses to the stage of load variation.

Keywords: secondary control, simulation, torque, displacement, pressure

1. Introduction

Growing area of using hydraulic and automation actuators and their requirements, require adjusting the volume as an area of particular interest to researchers.[1,2,3,4,5]

Adjusting means change the capacity of hydrostatic pump-motor units, resulting in change of the ratio between the components of motion and effort in a limited area. One can change this, for a given power ratio (Q / Q_{max}) and ($\Delta P / \Delta P_{max}$) at different values V of capacity hydrostatic units [2,5].

Figure 1. presents a fundamental diagram of a system with secondary regulation. Inserting the hydropneumatic accumulator in power transmission system, imposed pressures $p_1 = p_2 = p_3$ depending on its charge status. Torque modification at the exit does not directly affect system pressure p , but by accelerating or braking at shaft, the flow changes.

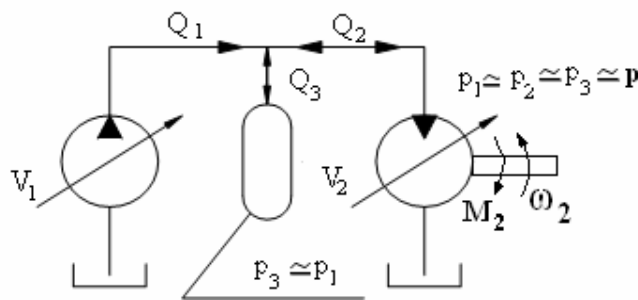


Fig.1.The fundamental diagram of a system with secondary regulation [2]

Flows Q_1 and Q_2 are decoupled through the accumulator and can take values independent of each other. The difference in flow $\Delta Q = Q_1 \pm Q_2 = Q_3$ circulates from or to the accumulator and amends its' charge state so the pressure p . [2,5]

This determines the control system to quickly intervene to alter the flow.

Torque adjustment takes place through a change in the flow, respectively by changing the hydrostatic drive unit volume. This control system is used on systems mobile equipment, systems with recovering kinetic energy during braking (automotive), aviation simulators, etc..Energy demanded is set directly on consumers, avoiding their mutual influence.

2. The structure of hydrostatic drive system with adjustable secondary drive

The fundamental diagram of a demo stand is shown in figure.2.

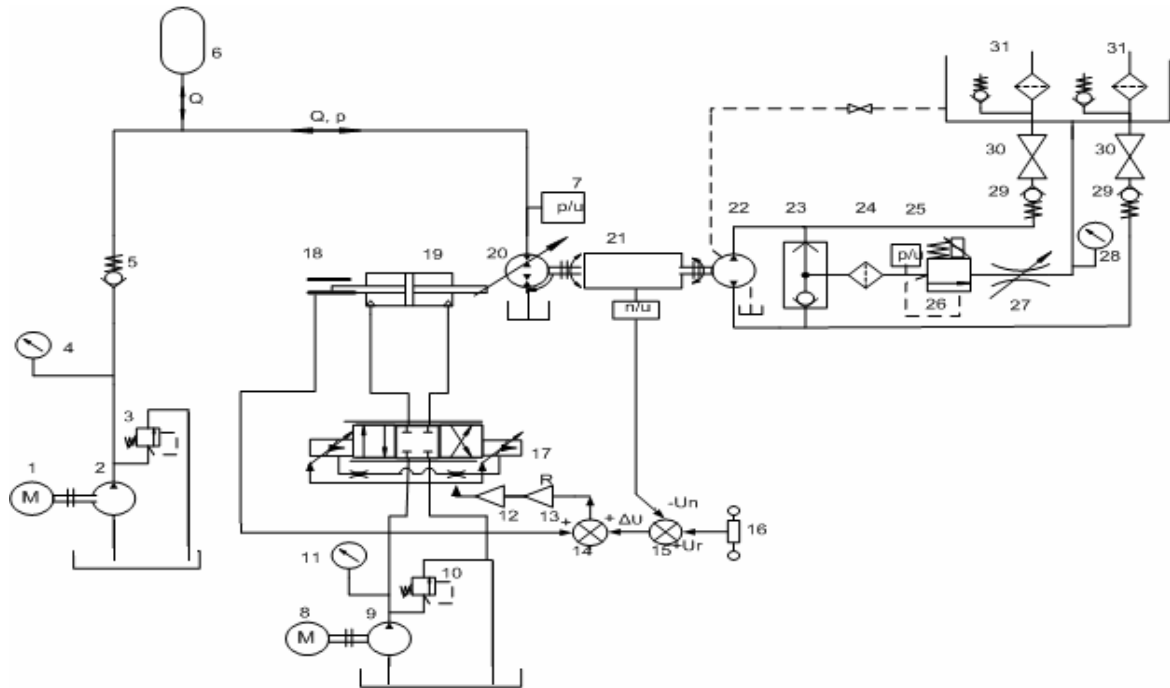


Fig.2.The fundamental diagram of the demo stand

Primary drive block contains: 2 pump with constant flow, 1 electric motor, 3 safety valve, 5 way valve, 4 pressure gauge, 6 hydropneumatic accumulator.

Secondary drive block contains: 20 hydrostatic drive pump-motor with adjustable capacity, capacity control element, namely the linear hydraulic motor 19, 10 pressure limiting valve, and the elements that make automatic control loop, respectively servo valves 17, amplifier control servo valves 13, block position signal amplification of linear motor 15, adder 14, comparator 15, transducer with digital display (pressure, flow, speed) 21, displacement transducer 18, block 16 prescribing reference size.

Block load contains: 22 pump, 23 the valve which selects the branch of high pressure fluid pump and send it to load valve 26, which regulates the pressure in the load circuit. Pressure filter 24 ensures smoothness of 10 μ m proportional valve required by the working fluid. The pressure transducer 25, 27 adjustable throttle, 28 pressure gauge, 29 way valve, 30 valve.

Second hydrostatic unit can have for a given speed n depending on the torque size M , any capacity $V \in [-V_{max}, V_{max}]$. For a working pressure $p \approx$ quasiconstant, capacity V determines the size of torque.

3. NUMERICAL SMULATION OF SYSTEM WITH HIDROSTATIC SECONDARY CONTROL

3.1 Simulation model for adjustable secondary drive system using Matlab Simulink

The simulation is appoints model validation from a real situation to understand the impact of changes in operating conditions regarding the system behavior and the effect of the introduction of various control strategies. Simulation of the structure and functioning of a set model allows all

possible states for the model and provides verification of the existence of properties set in the analysis stage.

The fact that these properties are not confirmed indicates the presence of one or more errors in the composition of system, or in determining its properties. Therefore, the final validation for obtaining operating characteristics determined by the design can be reached only by simulation results. Simulation allows experimentation with real or hypothetical situations, impossible or difficult to achieve in ongoing operation state of a system. A particular situation can be studied and the results allow comparison. In figure.3. presents the model block diagram in order to be simulated using Matlab Simulink program.

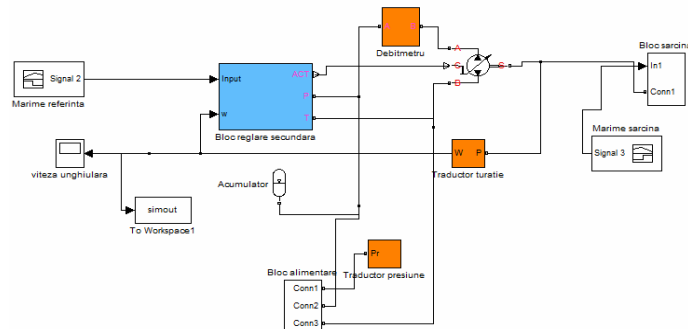


Fig.3. Block diagram used for simulation model

3.2 Influence of charging hydropneumatic accumulator pressure to system features

For simulation is imposed a constant angular velocity ω_r , by a block reference figure.4b. It is follow pressure influence of charging hydropneumatic accumulator on the indexical responses of the system. Size of disruptive signal is step type, figure.4a., inserted through a load block.

Simulations are performed for two values of the hydropneumatic accumulator pressure 56 bar and 10 bar. It shows the indexical responses of pressure, flow and speed.

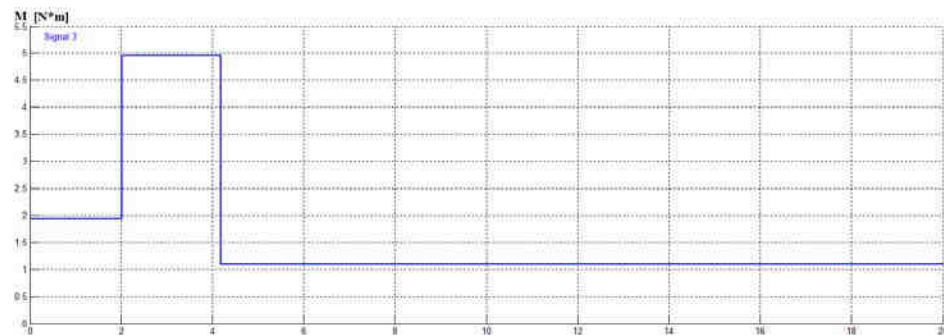


Fig.4a Load signal

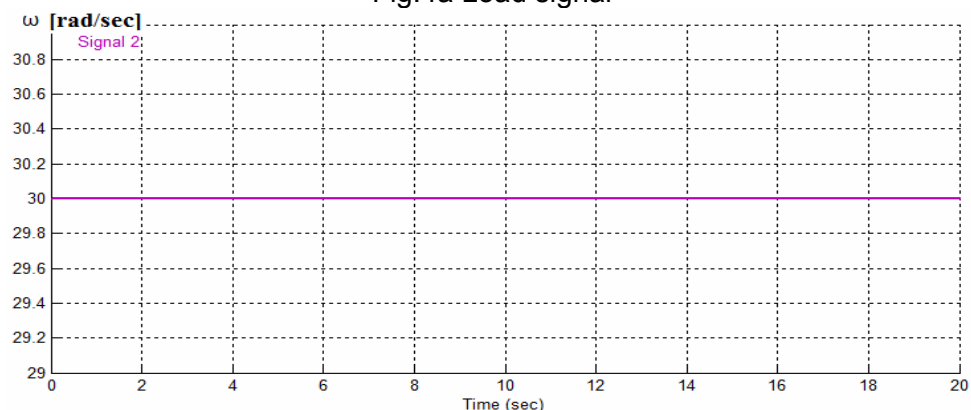


Fig.4b Reference signal

In figure.5, figure.6, and figure.7, are presented indexical responses of the system to load changes, respectively flow, speed, pressure for loading the hydropneumatical accumulator with 56 bar.

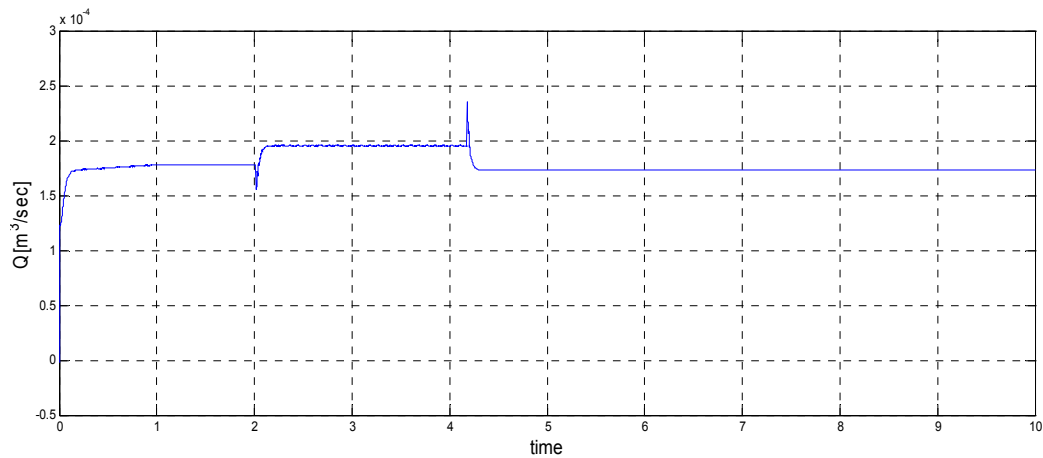
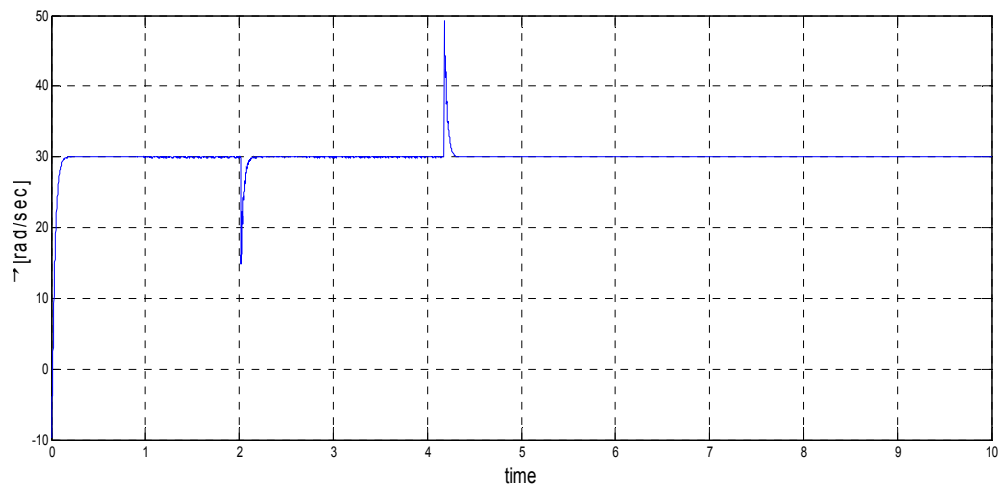
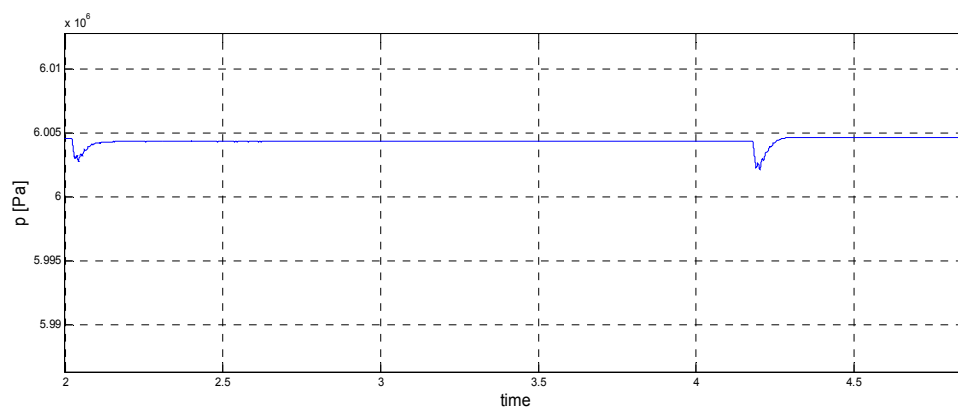


Fig.5 Indexical responses of flow at load step variation



. Fig.6 Indexical responses of rotation speed at load step variation



. Fig.7 Indexical responses of pressure at load step variation

In figure.8, figure.9, and figure.10, are presented indexical responses of the system to load changes, respectively flow, speed, pressure for loading the hydropneumatical accumulator with 10 bar.

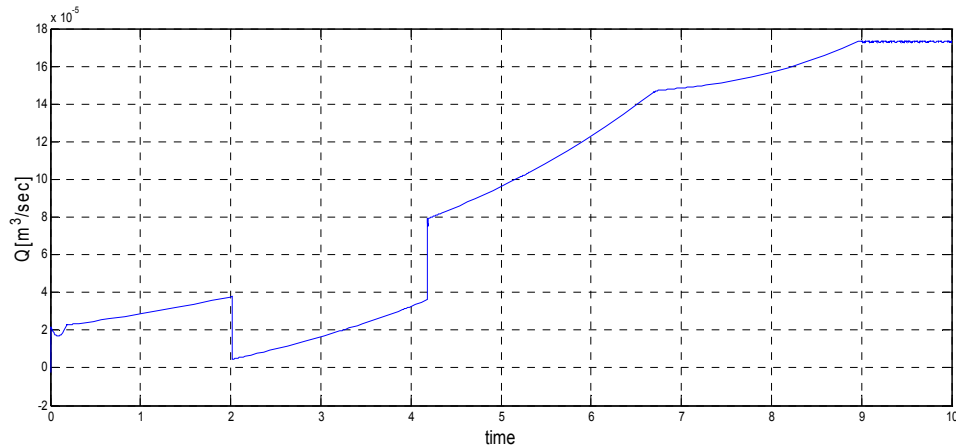


Fig.8 Indexical responses of flow at load step variation

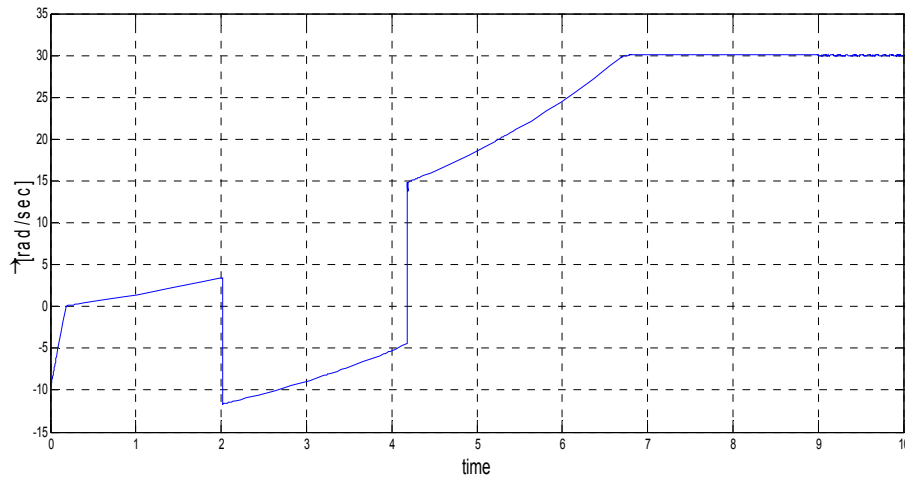


Fig.9 Indexical responses of rotation speed at load step variation

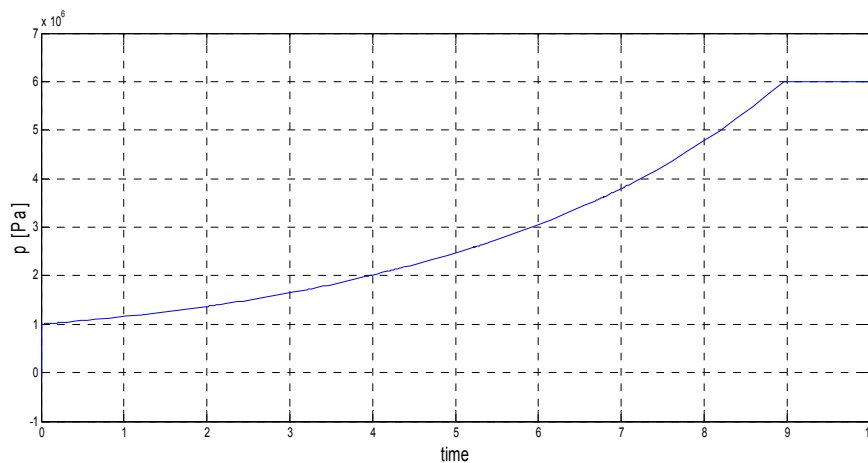


Fig.10 Indexical responses of pressure at load step variation

The analysis of the two sets of results obtained by numerical simulation are found influence of accumulator parameters on the functioning of the hydraulic system with secondary control.

Figure.8, figure.9, figure.10, shows a malfunction of the hydraulic system. Choice of accumulator suitable parameters leads to desired performance.

4. CONCLUSION

By the analysis of indexical responses shown in figure.5, figure.6, and figure.7 is found:

- automatic system is a control system which ensures that any changes in torque disturbing is followed by a transient change of the output signal.
- the system is dynamically stable.
- through automatic control system, load variation leads to changes in engine displacement and respectively flow, figure.5.
- by changing the flow speed of hydraulic motor returns to the imposed value by reference signal, figure.6.
- the system allows maintain pressure quasi constant to flow control at load variation figure.7.
- appear areas with shorter oscillation of the output value at the beginning of the transient regime. They amortized quickly for themselves.
- Choice of accumulator suitable parameters leads to desired performance.

REFERENCES

1. Biderman, Olaf ; Geerling Gerhard. Power Control Units with Secondary Controlled Hydraulic Motors-A New Concept For Application In Aircraft Hight lift Systems, Tolouse, France 1998.
2. Calarasu, D. Reglarea secundara a sistemelor de actionare hidrostatica in regim de presiune cvasiconstanta, pp.30-31, Editura MEDIA-TECH, Iasi. 1999.
3. Calarasu, D. Automatizarea sistemelor hidraulice, Editura 'Gh Asachi' Iasi 2002.
4. Dengcheng Ma. Study on Dynamic Characteristics of a Secondary Regulated Loading System. Modern Applied Science, Vol. 4, No. 11; November 2010
5. Huian Vasile, Doru Calarasu, et all ; RESULTS OBTAINED BY NUMERICAL SIMULATION FOR A HYDRAULIC SYSTEM WITH SECONDARY REGULATION The 16th International Conference, Modern Technologies, Quality and Innovation, vol 1 pg 449-452, 24-26 May, 2012 Sinaia Romania. ISSN 2069-6736

DIGITAL CONTROL MODULES FOR HYDRONIC EQUIPMENTS

Iulian DUȚU¹, Radu RĂDOI¹, Despina DUMINICĂ²

¹ Hydraulics and Pneumatics Research Institute, Bucharest, Romania, dutu.ihp@fluidas.ro

² POLITEHNICA University of Bucharest, Faculty of Mechanics and Mechatronics

Abstract: Widespread deployment of hydronic drive systems and their integration into complex manufacturing processes requires interfacing them with computer or digital systems. The integration of digital electronic technologies into hydronic equipment allow the users to measure and connect them to informatics manufacturing systems thus improving command and control performances. Overall development of microcontroller based smart systems along with the development of new types of sensors enabled the development and integration of digital measurement and control technologies in modern driving systems, even at equipment level.

Keywords: *digital, control, hydronics, modern*

1. Introduction

High precision driving and control systems are nowadays a necessity whose weight increases along with technical progress and development of new solutions for high-end technical fields such as multi-axis positioning, industrial robotics and numeric control machines and so on. Overcoming the limitations through the development of new solutions based on the use of informatics technologies and microcontroller based electronic modules started a new trend in electro-hydraulic driving systems.

The integration within driving systems' structure of electro-hydraulic equipments and actuators along with transducers and electronic digital or analog modules has increased overall flexibility thus establishing a new technological field – hydronics. Hydraulic proportional servo-equipment (which is state of the art hydronic equipment) is used widely in driving and control installations, having exceptional dynamic characteristics, flexibility, high precision and smaller sizes therefore replacing common driving and control schematics. Hence the need to control more accurate technical and functional parameters of hydronic equipment, as this will affect the functional characteristics of driving and control systems in which are integrated.

The architecture of hydronic driving and control systems integrates components and informatics technologies that facilitate the way that measurement, data acquisition and data processing are related to the physical parameters of a given system. Electronic modules and informatics technologies used along with hydronic equipment give the possibility to develop modern systems that easily adapt to variable workspace conditions and disturbances.

2. Digital modules in hydronics

Although the majority of electronic control modules and control systems available on the market include a relatively large number of analog components, the authors propose a digital electronic module based on a general purpose 8-bit microcontroller. The increased integration of electronic components has drastically reduced the size of driving and control modules therefore allowing the implementation of more functions on a single board. Digital electronic modules for hydronic equipment require increased computing power for digital control algorithms, such as PID, but also smaller dimensions in order to be integrated into the hydraulic equipment.

The digital electronic module that the authors describe is a RISC microcontroller from Microchip's 16Fxxx family. It is structured on Harvard architecture with separated buses for data and instructions, with memory paging which is a very important aspect because it is one its major disadvantages – it complicates the development of software in assembly language. The

implementation of electronic digital intelligence in industrial control systems allows also easy interconnection with computer systems, data storage or processing modules. Communication between two digital devices can be made locally – when they are in close proximity - or can be at distance by using remote data transmission through wired and optical fiber solutions (using dedicated protocols) or wireless connections such as GSM.



Figure 1 – Digital control modules available on market.

The microcontroller's structure include a set of hardware functions that facilitate the development of analog and digital applications, simplifying the interface logic, reducing energy consumption, and minimizing electromagnetic compatibility issues. The microcontroller is equipped with electrically rewritable program memory (FLASH) and allows the change of its software program without removing it from its socket in the printed circuit board (this is the ICSP facility: In-Circuit Serial Programming).

2. Hardware structure of the digital module

The authors have developed an innovative solution for one digital control module for hydronic equipment that comprises the following structural components:

- analog (4...20mA) and digital (0...5V) inputs, needed to interconnect the module with system's transducers, pressure switches, push-buttons, knobs etc;
- analog and digital outputs as control signals that drive the hydronic and auxiliary equipment;
- serial MODBUS communication;
- switching power source, input voltage must be between 10...36VDC.

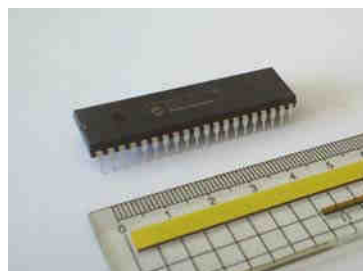
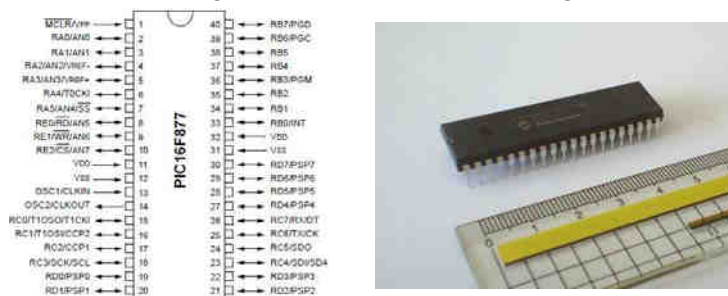


Figure 2 – Microcontroller PIC 16F877

The microcontroller given in Figure 2 has three input/output 8-bit ports, one input/output 6-bit port and one input/output 3-bit port, all software configurable. There are also available three timers, one analog-digital 10-bit converter, Capture/Compare/PWM and USART.

The digital electronic module has voltage (0...5V or 0...10V) or current (4...20mA) hardware configurable inputs.

The digital module has four (adjustable) reserved inputs as follows:

- program input;
- offset input;
- feedback input;
- feedback offset.

For future improvements, the digital module has been provided with supplementary analog inputs for voltage or current, hardware selectable.



Figure 3 – Digital control module: assembled PCB TOP view.

3. Software program of the digital module

The software program of the digital control module has a main loop, a peripheral init sequence, interrupt service routine and the digital PID control algorithm. Main loop is using a state-machine architecture which implements basic functions of the electronic module. Interrupt service routine has code sequences that implement analog-digital conversion, real-time clock and buffer management for USART receive/transmit.

The interrupt service routine accepts interrupt events from the following peripherals:

- timer circuit, used to generate a 1ms real-time clock. In the init sequence of the timer circuit this is configured to be incremented once every 200ns. The timer will generate an interrupt when the overflow event occurs (0xFFFF to 0x0000). The timer is reinitialized in the interrupt service routine;
- analog-digital convertor, configured to generate an interrupt request when the result of the current conversion is available;
- USART module, configured to generate an interrupt request when is transmitted or received a character. The end of transmission of one character starts the transmission of the next character in the reception buffer. End of reception is signalized, in MODBUS ASCII protocol, when it is received a 0xA or 0xD character code.

The interrupt request subroutine for timer overflow is:

- refreshing the real-time clock (used for process synchronizing);
- timer initialization;
- analog-digital conversion start.

The interrupt request subroutine for analog-digital convertor is

- numeric filtering of the analog input signal;
- analog input selection;
- analog-digital convertor initialization.

MODBUS ASCII communication that is implemented on the digital control module is based on a protocol that Modicon has introduced in 1979. The advantages of using MODBUS are:

- easy implementation;
- it does not need dedicated hardware circuitry;
- simple and efficient error detection mechanism;
- it is open source.

There are a few minor disadvantages of the MODBUS protocol, such as the relatively rigid structure of MASTER-SLAVE network – SLAVE equipment cannot initiate a transmission for an event – and limited communication speed at 115200 baud.

The most important parameter in the control algorithm is the loop duration, because when using floating point calculations this conducts to higher execution times. Where possible it is preferred to use floating point because of easy implementation and it can be avoided the rounding and overflow errors – associated with floating point representation.

5. Experimental rig

In order to test the digital control module capabilities there has been used an existing testing rig in the Servo-technique laboratory of Hydraulics and Pneumatics Research Institute. The hydraulic circuits of the existing testing rig need to be reconfigured in order to fit the new digital control module and hydronic equipment. The experimental model of the digital control module was included in a positioning hydronic system.

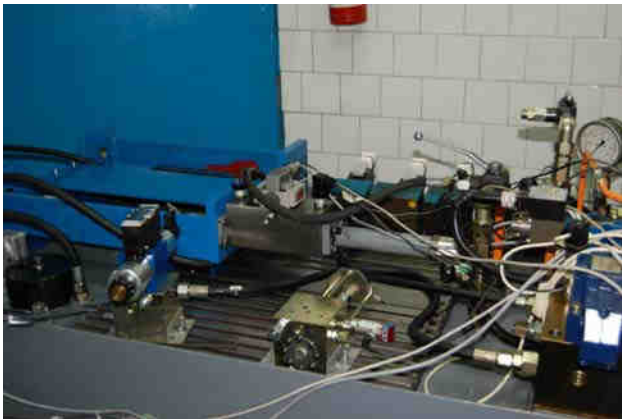


Figure 4 – Experimental hydronic testing rig: general view.

The testing rig can allow various electro-hydraulic configurations, having a high degree of flexibility. Maximum working pressure is 315 bar and maximum flow 120l/min. The structure of the testing rig comprises: hydronic equipment (a servovalve), a bilateral rod hydraulic cylinder with low friction, a stroke transducer, one hydraulic power source, DAQ system and the digital control module. It is also used a metallic adapter plate which connects the hydronic equipment to the hydraulic power source of the testing rig, tank and consumers A and B (the hydraulic cylinder and two pressure transducers). The pressure transducers are used to record the pressure on A and B circuits during experiments.

The hydronic equipment (servovalve) is driven by the digital control module that the authors propose. Choosing a certain type of hydronic equipment takes into account the general requirements for the system – such as the actuator type and its operating mode.

During experiments there has been used a DAQ system that comprises:

- electronic transducers for physical parameters of interest, such as stroke, pressure, flow, force and temperature;
- measurement amplifiers, used for interfacing the output signal of a certain transducer with the type required by the DAQ board;
- DAQ board, used for converting analog process signals into digital signals that PCs use;
- virtual instrument developed using LabView, used for data processing, filtering, storage and graphical representation of certain states or signals in the process.

The DAQ system is based on a common configuration of simultaneous parameter acquisition and has been designed after a comprehensive analysis of the parameters involved in the experimentation on the digital control module, choosing high performance devices and equipments characterized by increased robustness and dynamic characteristics.

Virtual instrument was designed to work both in static and dynamic modes having minimum user intervention. The initialization of the DAQ board, all software variables and constants along with the scaling of the DAQ channels are done by the virtual instrument. Experimental data are acquired continuously after the user presses START button available on the front panel of the virtual instrument. The data acquisition will stop automatically after acquiring several signal periods. The virtual instrument scales and filters acquired data and after that it displays it on a graph control. Data values are stored in column separated values .DAT files.

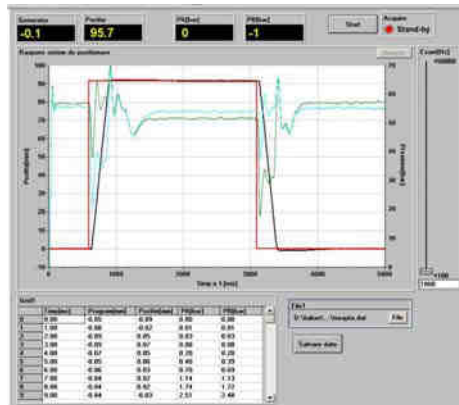


Figure 5 – Front panel of the virtual instrument

The front panel of the virtual instrument contains the following controls:

- displays for current signal values;
- control signal display (*Generator*);
- stroke transducer display (*Position*);
- pressure A value display (*PA[bar]*);
- pressure B value display (*PB[bar]*);
- acquisition *START* button;
- optical *Acquire* button;
- *Esant[Hz]* slider for modifying sampling rate.

6. Experimental results

Control signal used during experimentations as reference is given by a square wave signal generator. The reference signal is applied to the digital control module described above on a dedicated input, having a period of $T = 10s$ and an amplitude between $-10 \dots 10V$.

In the Figures below, it is given the response of the hydronic system with closed-loop digital control when varying PID regulator's gains (blue = reference; red = response).

Processing of experimental data was made using Microsoft Excel.

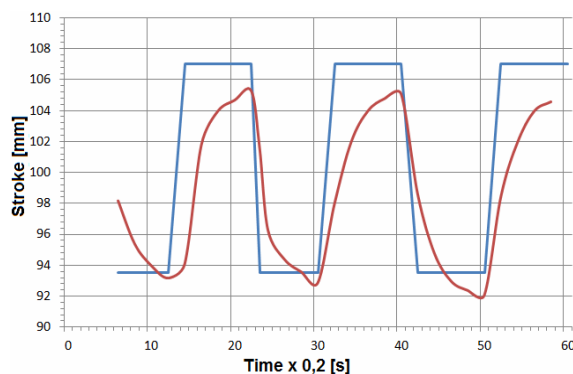


Figure 6 - Square wave response, when $P = 1$, $I = 0$, $D = 0$

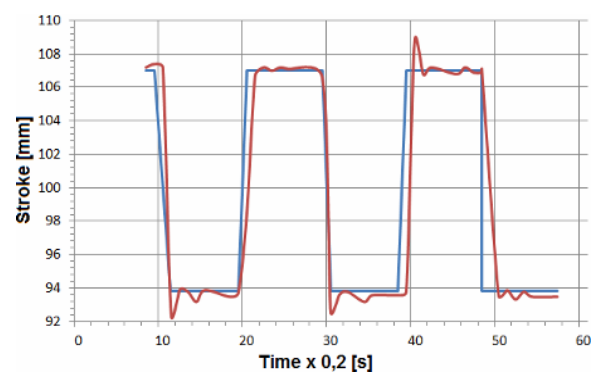


Figure 7 - Square wave response, when $P = 10$, $I = 0$, $D = 0$

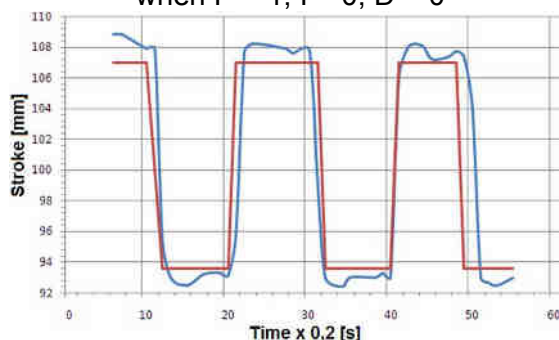


Figure 8 - Square wave response, when $P = 5$, $I = 0,001$, $D = 0$

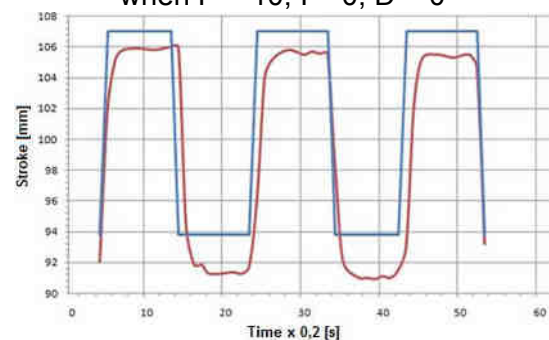


Figure 9 - Square wave response, when $P = 5$, $I = 0$, $D = 0,5$

In Figure 6, it is shown the response of the hydronic system, when $P = 1$, $I = 0$ and $D = 0$. In this case it can be seen that the system follows with low accuracy the reference signal having a low tendency of oscillation. The rising and falling edges of the response signal are heavy modified, having almost no level and high error when P gain has a low value.

In Figure 7, it is shown that when increasing the proportional gain to 10 ($P = 10$) the delay between the reference signal and response signal is reduced, but the amplitude of system's oscillations is increasing. The edges of the response signal are improved, delay time is low, but the presence of the oscillations leads to a poor system dynamic.

In Figure 8, the variation of the integrative gain, $I = 0,001$, leads to a decrease of the error. When increasing the integrative gain the error decreases or even drops to zero, having as disadvantage the appearance of some overrides on the rising edge of the response signal.

In Figure 9, the variation of the derivative gain, $D = 0,5$ has a direct influence on the waveform of the response signal – rising and falling edges are less modified, the level has small oscillation tendencies, delay time is increasing slowly. It can be noticed a heavy reduction to zero of the overriding.

7. Conclusions

Experimental behavior of the digital control module can be considered as expected. Low values of the proportional gain lead to a high stationary error; high values of the proportional gain lead to oscillations. The stationary error decreases or even drops to zero when the integrative gain has a high value, but it will appear an overriding of the response signal. A high value of the derivative gain has a negative impact on the waveform of the response signal. The hydronic system has an integrative behavior and when choosing inappropriate values for the integrative gain will result significant overrides of the response signal leading to poor positioning accuracy of the system.

As future improvements, the authors would like to reduce the size of the digital module by using SMD components and to improve the digital PID control algorithm.

REFERENCES

- [1] *L. Visioli*, Practical PID Control – (Advances in industrial control), Springer-Verlag, London UK, 2004
- [2] **Duminičă, D.**, *Avram, A., Alexandrescu, N.*, Stadiul actual în domeniul acționărilor hidronice, Simpozionul „Relansarea și creșterea competitivității sectoarelor economice din industria prelucrătoare”, București, 23-24 septembrie 2004, în volumul conferinței.
- [3] *Teodor Costinel Popescu, Iulian Duțu, Cătălin Vasiliu, Marius Mitroi*, Adjustment of conformity parameters of PID-type regulators using simulation th by AMESim, 7 International Industrial Simulation Conference 2009, ISC 2009, June 1-3, 2009, Loughborough, United Kingdom, Article Number ENER_01, pp.269-274, <http://www.eurosis.org/cms/?q=node/927> (Publication of EUROSIS-ETI).
- [4] *Marian Blejan, Iulian Duțu, Bogdan Lupu, Corneliu Cristescu*, Data Acquisition and Control Unit for Electro-Hydraulic Applications, ABSTRACT PROCEEDINGS of the 32nd International Spring Seminar on Electronics Technology-ISSE 2009, May 13-17, 2009 Brno, Czech Republic, pag. 268-269, ISBN 978-80-214-3874-3, <http://www.isse2009.org/>. (ISI-Thomson).
- [5] *Alexandrescu, N.*, "Hydronics – Angewandte Mechatronik in hydraulischen Antriebssystemen und Komponenten, 44. Internationales Wissenschaftliches Kolloquium, Ilmenau, 20-23 Septembrie 1999.
- [6] *** <http://www.microchip.com>
- [7] *** <http://www.boschrexroth.de>

INCREASING THE ENERGETIC EFFICIENCY OF PET BUNDLING PRESS USING HIDROSTATIC ENERGY RECOVERING SYSTEMS

Ionel NITA^{1a}, Corneliu CRISTESCU^{1b}, Alexandra Liana VISAN^{1c} and Alexandru MARINESCU^{1d}

¹ HYDRAULICS & PNEUMATICS RESEARCH INSTITUTE in Bucharest INOE 2000,

^ae-mail: nita.ihp@fluidas.ro; ^be-mail: cristescu.ihp@fluidas.ro; ^ce-mail: valexandra.ihp@fluidas.ro;

^de-mail: marinescu.ihp@fluidas.ro.

Abstract: Paper aims to present a simple model of energy recovery system that can be adopted and implemented on any compacting - packing press for packaging waste for the smallest to the biggest capacity performing small structural changes. The power efficiency system it was applied on a 60 kN compacting - packing hydraulic press for PET, system which was designed and manufactured by INOE 2000-IHP Bucharest in the research and development programme frame (RELANSIN and MENER). In this paper are presented the constructive and functional features of this equipment made during the optimisation process which aims to quantify the pressing and bundling process.

Keywords: power efficiency, PET bundling press, hydrostatic energy,

1. Introduction

PET bundling press used to compress industrial and alimentary packaging (bottles, containers, cans and boxes) in compact and homogeneous bulk with well-defined dimensions, which are directly influenced by press enclosure and hydraulic power system. The bunches obtained during the compacting process must meet certain criteria: easy to manipulate, to have a stable form and structure that last in time. These properties are very important during the transport and storage phase.

Therefore the hydraulic driving system must develop a compression force Fh , to compact the plastic waste and to make a uniform distribution in press working enclosure. Also the hydraulic power is influenced by the PET shape and dimensions that can be: unaltered or deformed, with or without cork, regular or irregular volumes with different stiffness. For this reason the deformation force applied Fd may vary in the technological bundling process because the compressed materials are changing the shape and the strength during the compaction process. This to make a bunch with a height H it is necessary to provide several wasted feed phases and n several pressing cycles, in which the driving system has an h active stroke.

In our case the active stroke is the pressing height/cycle and must assure the maximum stroke of the hydraulic system for which our system is designed.

Following the above conditions and observations during the bundling process must be ensured a safety pressure $p_0 = \min (1.2-1.3) \times p_d$ (where the p_d is the waste specific deformation – pressure or the waste tensile strength), that generate a hydraulic force $Fh = \min (1.2-1.3) \times Fd$. This equation can be written as $p_0 \times S_c = \min (1.2-1.3) \times p_d \times S_d$ [daN], where: S_c is the compression cylinder area and the S_d is the enclosure press surface.

From the energetic balance, the hydraulic bundling energy Eh necessary for a single compressing operation must be proportional to deformation energy that must be consumed to achieve a compact bunch, energy calculated with equation 1.

$$Eh > \min (1.2-1.3) \times Ed \quad [J]$$

[1]

The hydraulic energy necessary for the entaier process Σeh is presented in equation 2 and is corelated with the consumed energy during an entaier compressing process Σed .

$$\Sigma eh > \min (1.2-1.3) \Sigma ed \text{ [J]} \quad [2]$$

Given that bundling press function must operate to a minimum working pressure p_0 the hydraulic energy generated to the ending of active stroke will be discharge to the fluid tank and in that way a very important part of the hydraulic power is lost. Losses which can be estimated with equation 3 and 4.

$$\Delta E = E_h - E_d = (0.2 \dots 0.3) E_h \text{ [J]} \quad [3]$$

$$\Delta \Sigma e = \Sigma eh - \Sigma ed = (0.2 \dots 0.3) \Sigma eh \text{ [J]} \quad [4]$$

Implementing a mechanical-hydraulic energy recovery system on a standard press tend to reduce the hydraulic power discharge during one compression operation and to used it in the subsequent compressions or in the anther technological phase.

2. The working principle of PET bundling press with energy recovery system

The PET bundling press on which was incorporated the energy recovery system, has the following functional systems: the compacting - packing press, the hydraulic driving system SHB and the energy recovery system SREB, fig.1.

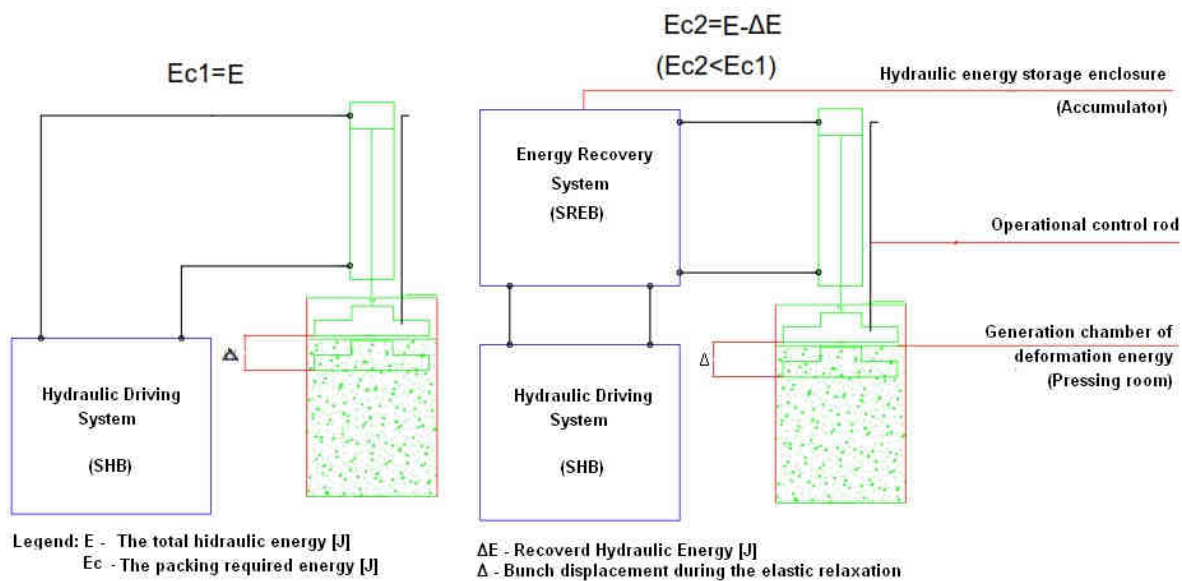


Fig.1 PET hydraulic bundling press.

The principle underlying the system operation consist using the relaxation bunch energy after there was compress the waste to freely lifting the press platen with Δ , without any energy from the press driving system. Summing the mechanical works developed during bundling process, was estimated a decrease up to 20% from the energy consumption in order to achieve a bunch in comparison with the classical solution. Energy excess is stored as a hydraulic energy (flow or pressure) in a hydraulic accumulator, from which will be supplied the next compacting operation from the bundling process until the pressure reaches the pressure p_a (pressure inside the accumulator) and only the p_i is generated by the hydraulic system (pressure needed to compact the waste in i cycle).

The functional differences between the standard press and the bundling press with energy recovery system are:

- The standard press the electric engine energy $Ec1$ is transformed in hydraulic energy used to compacting and retirement of the pressing plate.
- For the bundling press with energy recovery system, is used only a part from the electrical energy $Ec2$ which is transformed in hydraulic energy and used to the compacting operation and retirement operation will be made using the relaxation bunch energy and only if it is necessary will be used hydraulic energy. From this reason the energetic saving will be $\Delta E = Ec1 - Ec2$, where the $Ec2 = f(pa)$.

3. The estimations regarding the energy recovery system

The press on which was implement the energy recovery system was a waste hydraulic press, PCM 60-00 de 60kN, system that was designed and manufactured by INOE 2000 – IHP Bucharest. As was mentioned above a very important parameter is the shape of the waste that can be: unaltered, deformed, pre-pressed and minced. Once known what type of materials are compacted it can be estimated the charged material supplied that is $0.28 \div 0.32$ [kg/m³] and the degree of homogenization 20% \div 25%. The hydraulic working parameters are: the maximum working pressure $p_o = 110$ [bar]; the nominal working pressure $p = 80 \div 90$ [bar]; the flow rate $Q = 15$ [l/min]; the active stroke $Ka = H0$ and can have the maximum value of 750 [mm]; the maximum installed power 2.2 [kW] and presents a semi-automatic working cycle.

Other parameters that can be useful during the static and dynamic characteristics are: the elastic retirement force $Fh = 250 \div 500$ [daN], which depends on the elastic detriment degree (0.1... 0.2); the maximum hydraulic pressure losses 5 [bar]; the pressing plate inertial mass to lifting and the hydraulic resistance $Rh < Fd = (0, 1..0, 2) Fh$.

Applying the classical energy estimation methodology it can be calculated the recovered energy during the three working phases during the compacting – packing process, fig.2.

The working phases during the waste compacting – packing process are as follows.

Compaction chamber filling with raw materials, which has the volume $V = L \times B \times H0$.

The first compacting operation, it has the index 1 in the mathematical equations. During this operation are realized the next phases:

- The plateau advance phase F1, in which are monitor the following parameters:
 - advance stroke, $Ka1 = H01$ [mm], where $H01 = H0 - h1$ ($H0$ is the initial volume occupied by PET waste and $h1$ is the height of compress waste that depends on the supply pressure p and the compacted volume $V1$;
 - compacting force, $Fh1 = p \times Sc$ [daN], that depends on the cylinder active surface;
 - compacting energy, $E1 = (H0 - H01) \times Fh1 = h1 \times Fh1$ [J];

In this phase cannot be recorded any energy saving.

- Engine uncoupling phase F2, that starts in the moment in which the working pressure arrives to P and the plateau advances is stopped. In this phase the compacting waste have the tendency to decompress, case in which is create a loosening force $Fd = (0, 1..0, 2) p \times Sc$ that is generating a energy $\Delta E1 = (0, 1..0, 2) (H0 - H01) \times Fh1 = (0, 1..0, 2) h1 \times Fh1$ [J]. This energy is transformed in mechanical work to lift the pressing platen with $k1 = \Delta h1$, where $\Delta h1 < \Delta$ [mm] and in hydraulic energy that will be stored in an accumulator ($pa = f(\Delta E1, V1)$) where the $V1$ is the store oil volume $V1 = Sc \times h1$ [l];
- Withdraw of the press plate, F3. In this phase are monitor the redraw stroke, $Kr1 = H01 - k1$ [mm].

The second material compaction batch to fill the compressing chamber that must supply with materials that can have a volume $V = L \times B \times H0 - h1$.

The second cycle of compression, which is noted with index 2 and has the next phases:

- The plateau advance phase F1, that has the next parameters:

- advance stroke, $Ka2 = H01 - h2$ [mm], where $h2$ is the thickness of the second compacting layer ($h2 > h1$) and is influenced by the working pressure and the compressing material volume ($h2 = f(p, V2)$);
- compacting force, $Fh2 = (p - pa) \times Sc$ [daN];

In this phase it can be used the energy recovered from the previous operation.

- Engine uncoupling phase F2, in the moment in which the working pressure reach P and the plateau advances is stopped. In this phase the compacting waste have the tendency to decompress, case in which is create a loosening force $Fd = (0,1..0,2) p \times Sc$ that is generating a energy $\Delta E2 = (0,1..0,2) (H0 - H01) \times Fh2$ [J] [J]. This energy is transformed in mechanical work to lift the pressing platen with $k2 = \Delta h2$, where $\Delta h2 < \Delta$ [mm] and in hydraulic energy that will be stored in an accumulator ($pa = f(\Delta E2, V2)$ where the $V2$ is the store oil volume $V2 = Sc \times h2$ [l]);

The last three operations must be repeated and the estimations can be made replacing the $H0$ with $H0i - h1i + 1$, where i is the operation number ($i = 5, 6$) until the bunch high reaches H , value that in our case depends by the press capacity.

The total energy recovered is estimated is estimated with equation [5].

$$\sum \Delta E_i = (0,1..0,2) \sum (H0 - H0i) \times Fh_i [J]; (i=5..6) \quad [5]$$

The energy recovery degree G_R can be calculated with relation [6] and depends by the effective energy E .

$$G_R = (\sum \Delta E_i / E) \times 100 [\%] \quad [6]$$

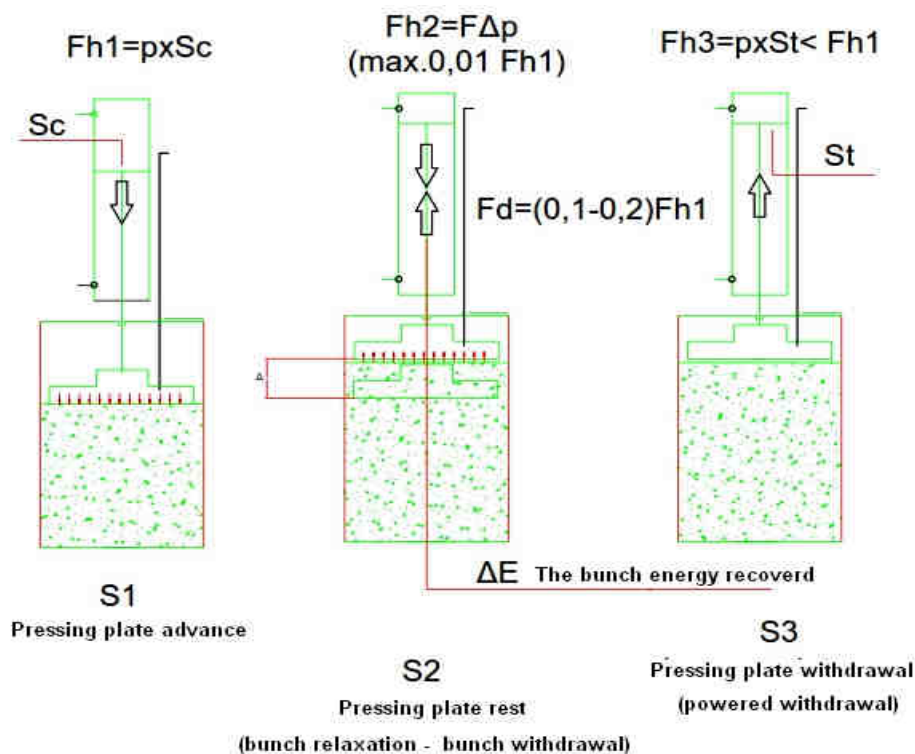


Fig.2. Working principle of waste PET press.

4. The running of pet bundling press embedded with an hydrostatic energy recovering systems

The hydraulic system is the main component of which it can be recovered an important quantity of energy. The hydraulic divining system SHB contains: an mono-phase electric engine - 1, that has the power of 2.2 kW; gear pump - 2, with a flow rate of 15 [l/min]; pressure valve set to 120 [bar]; electrical $\frac{3}{4}$ directional control valve Dn6 (24Vcc) - 4; 100 [bar] pressure switch – 5.1; hydraulic cylinder $\Phi 80/56-800$ [mm] -6; electric stroke stop -7.1 and 7.2; the displacement transducer 12; see fig. 3.

The energy recovery system SREB is made from: 80 [bar] pressure switch – 5.2; 2/4 directional control valve Dn6 with memory - 8; hydraulic accumulator for 20 [l] and 45 [bar] -9.

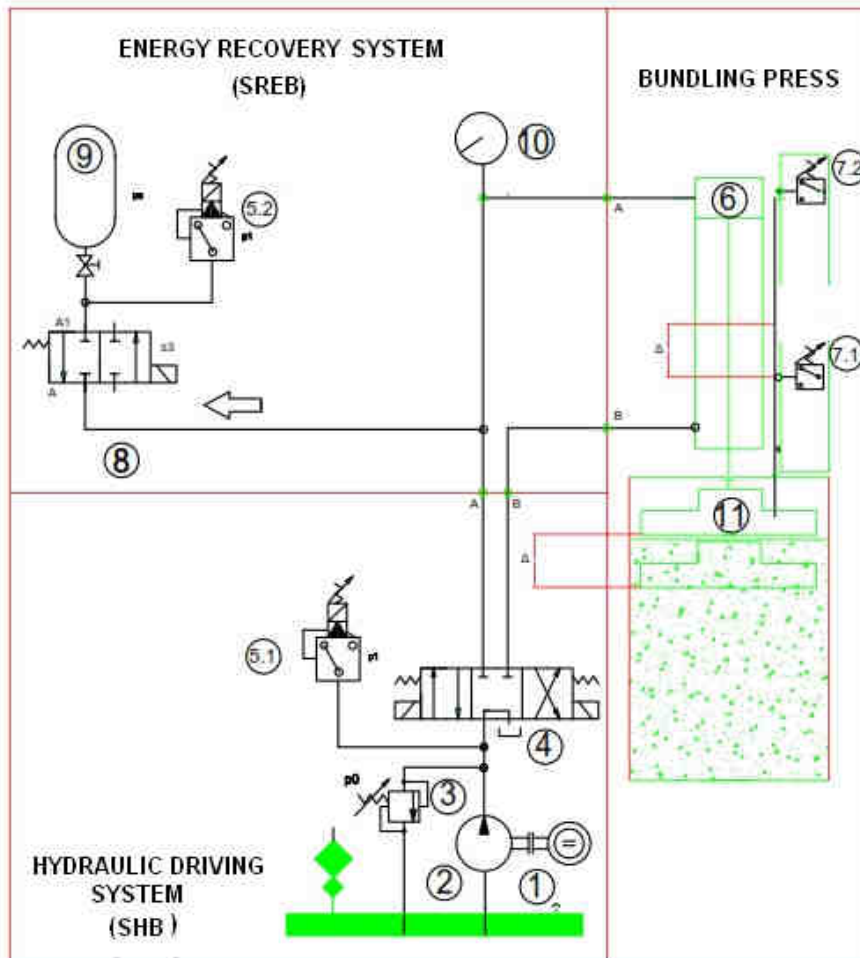


Fig.3. PET bundling press using hydrostatic energy recovering systems

The hydraulic PET bundling press on which is implemented the energy recovering systems works like this:

- Compacting process – cycle 1, consist from the next operations. Once the waste was loaded the S1 electromagnet commute the directional control valve 4 to position I. The pressure inside the hydraulic system rises and the compacting plateau 11 came down. When the hydraulic pressure arrive to p_1 the pressure switch 5.1 deactivate the S1 signal and the directional valve 4 commute to the centre position (in this case the electric stroke stop 7.1 is not active). From this moment on the directional control valve 8 switches to the chamber 33. The remanence pressure from the active cylinder chamber (preserved from previous compression or packing operations) and also the waste decompression that raise the compacting plate to the h_1 height and is generating the mechanical work and the energy $Ed = Fdxh_1$. The hydraulic accumulator 9 is supplied with oil under the pressure p_a . Once the oil pressure rises to p_a the pressure switch 5.2 commands the directional valve control to change its position. From this moment one the

directional valve 4 is commanded by the electromagnet S2 that raise the compacting plateau. Once the cylinder return to the initial position the limitation sensor 7.2 stops the plate to the upper position and the directional control valve 4 return in the centre position and the pressing cycles is changing.

- Pressing process – cycle 2. In this cycle the first two operations are the same like in the cycle 1. In this process the energy recovering systems begin to make the difference. The directional control valve 8 changes its position and the hydraulic accumulator 9 supplies the power system with the working pressure p_a and also the cylinder chamber that lower the compacting plateau 6. When the pressure reach $p_{a0} = 10-15$ [bar] switches the electromagnetic command S3 and the compacting plate stopes to last layer of waste. The manuvrs repeat from the step 3 to the end as was mentioned in cycle 1.

- The cycle 2 repeats until the waste bunch is made.

Using the PCM 60-00 press med by IHP it can me realized five until seven pressing cycles in order to manufacture a bunch.

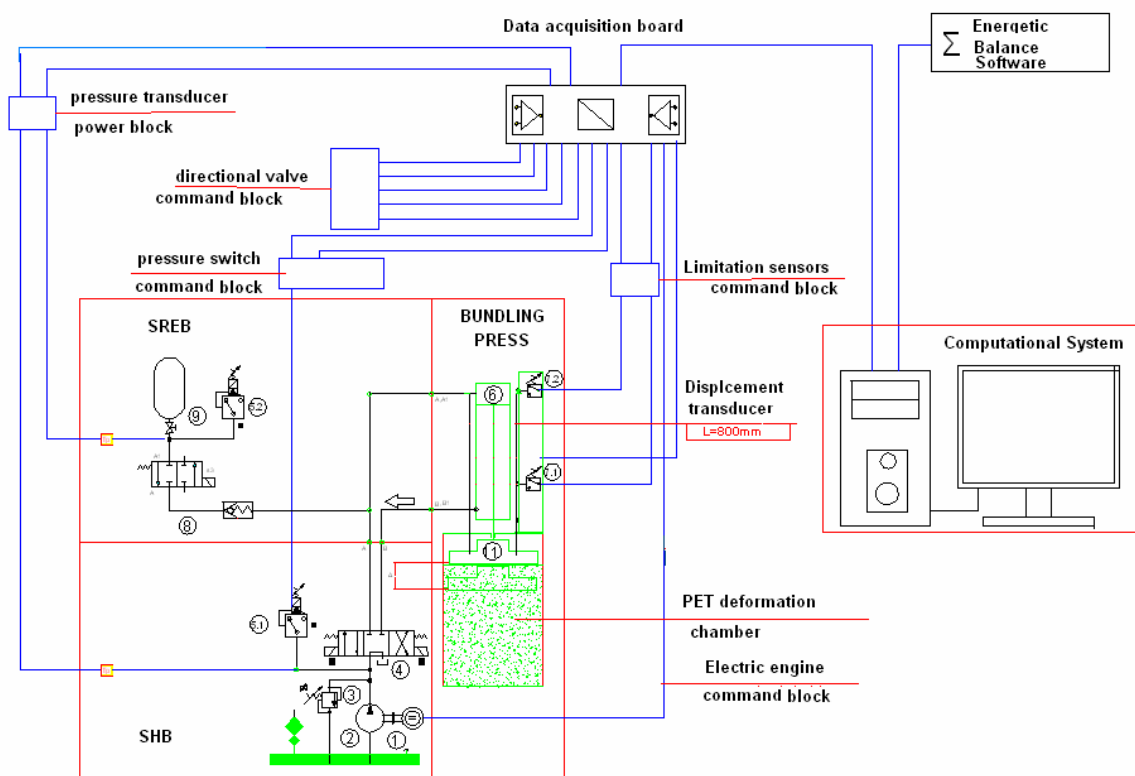


Fig.4

The command and control system is design (fig.4) to measure the energetic efficiency of the PET bundling press is made form:

- pressure transducer, $Tp1$ and $Tp2$, positioned on the main supply lain (compacting hydraulic system) and on the secondary line (the recovery system) in order to acquire the $P1$ and p_a values;
- displacement transducer TI , with measurement field of 800 [mm] that is positioned on the pressing cylinder. This transducer is used to acquire the parameters: Hi , hi , and Δi ;
- electric power sources and signal generator for: pressure transducer; pressure switches, stroke imitators, the directional control valve and the electric engine;
- data acquisition board;
- PC system and energetic balance software.

5. The energy recover methodology

The testing methodology that estimates the recovered energy is a very complex procedure that must take in to consideration all the working parameters (the press gauge – geometric parameters, the working parameters, the static and dynamic characteristics). For this reason is used an data acquisition system that is connected with an computational system. Once the system is initialized are introduced the geometric and working parameters (p , p_1 , p_a , H_0 and H_1). During the bunch compressing operations will be acquired the data transited from the displacement and pressure transducers for every phase (T_i , h_i , Δi , etc.) The intelligent system will estimate the energy saved for every compacting cycle respecting the equation 5 to the end of compacting process will be calculated the energy recovery degree 6.

With this system the hydraulic energy recovered from all the compacting phases will be stored in the hydraulic accumulator and will be used to displace the hydraulic driving system. The plateau lowering in the absence of the SREB requires to start the electric engine to power compacting system and for this reason will be made an important energy saving.

6. CONCLUSIONS

Applying the energy recovery system (SREB) on PET compacting - packing press, design by IHP Bucharest, the energy saving is 15 -20%., energy that can be used in the next compressing cycle, as was mentioned above or for other technical operations like: opening system of working enclosure, the bunch extraction, etc.

The energy recovering system presented in this paper can be implemented and adapt for any type of PET compacting - packing press from the smallest ones to the highest processing capacity. The system can be provided with an electronic command and control panel in order to monitor the energy recovered and to control the compacting process.

REFERENCES

- [1]. Karl Otto Tildmann, „Recycling betrieblicher Abfälle. Neue Techniken und Verfahren zur wirtschaftlichen Wiederverwertung industrieller Rückstände“, vol. I, II, III, 1996;
- [2]. F. Keiser, „Berechnungen an der Scheidmühle. Dechema Monographien, vol. I, 1996;
- [3]. dipl. ing. Mayerhauser, Aufbereiten von Papier – und Kunststoffabfällen (1996);
- [4]. dr. ing. R. Iatan, Cercetări privind reciclarea deșeurilor din mase plastice și hârtie, 1984;
- [5]. M. Rusu, N. Goldenberg, „Valorificarea resurselor secundare” 1984.

HYBRID SYSTEM FOR ENERGY RECOVERY AT BREAKING

Alexandru VASILE¹, Andrei DRUMEA¹, Cristina MARGHESCU¹, Paul SVASTA¹,
Andreea BRODEALA¹

¹ "Politehnica" University of Bucharest/CETTI, Splaiul Independenței, no. 313, 060042, Bucharest, Romania
andrei.drumea@cetti.ro

Abstract: Nowadays when there is great interest in reducing pollution by using renewable energy in transportation, it is important to research solutions with high energy storage efficiency for storing the energy produced by the electric motor as well as that generated by the systems that convert renewable energy.

Employing only accumulators in the automotive industry is not enough because the electric current that the accumulator absorbs has a value that is small when compared to the value of the currents that can be generated by electric motors used in a system with regenerative breaking (the electrochemical process through which charge is accumulated is limitative). In this context it is possible to use a supercapacitor-accumulator hybrid system.

The hybrid system can accumulate and generate electric charge under currents of thousand Amperes. The advantage of using this combination, Pb accumulator/supercapacitor battery (this is formed by coupling the two battery's in parallel) on an auto-vehicle is that it leads to a decrease in weight/unit of energy. Another advantage is given by the high number of charge/discharge cycles possible when using supercapacitors. They are also capable of generating power peaks.

Keywords: Automotive, EDLC, hybrid auto vehicle

1. Introduction

Electrochemical capacitors are known today through several names such as supercapacitor, ultracapacitor or EDLC - Electrochemical Double Layer Capacitor. The list of possible names is almost as long as that of producers and since the technology is still in its early stages a name to be used by all has yet to be decided.

The structure of an EDLC is that of an electrochemical capacitor with an unusually high energy density when compared to other types of capacitors, usually in the range of thousand times bigger than that of an electrochemical capacitor. As an example, a classical electrochemical capacitor will have a capacity with a value of tens of thousand of mili Farads. A supercapacitor with the same dimensions will have a capacitance value in the range of several Farads, but at a working voltage that is usually smaller, around 2,5 V. In 2010 the first supercapacitors with a value of 5000 F were introduced. The biggest energy density of a commercially available EDLC is of 30 Wh / kg [1].

The electric charge accumulated in an electrochemical double layer capacitor is stored similarly with that in a conventional electrochemical capacitor. The difference is that charge is accumulated not on the two electrodes but at the interface between the surface of the conductor and an electrolytic substance (see also Fig. 1). The charge accumulated through this mechanism will form a double charge layer, the distance between each layer being of several Angstroms.

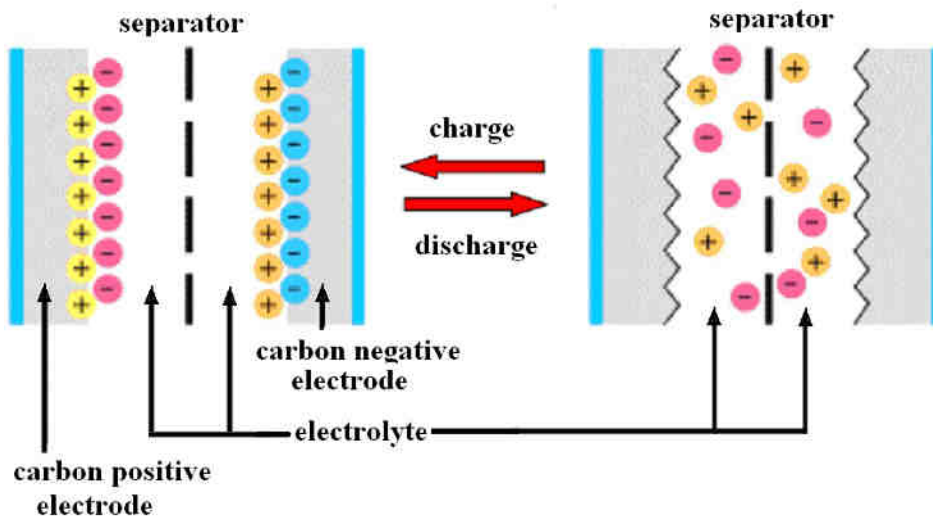


Fig. 1. Storage mechanism in electrochemical capacitors [1]

Production technologies used nowadays for manufacturing EDLC structures only allow the production of EDLCs with a high current loss. The capacitors are also highly dependent on the surrounding temperature. In Fig. 2 the variation of the voltage at the terminals of the supercapacitor at different temperatures is presented. It should be noticed that after 100 hours since charging without a load the voltage drops to almost half, the accumulated charge also drops. Temperatures over 30°C can lead to an important discharge which can be inconvenient in some applications (Fig.2) [1].

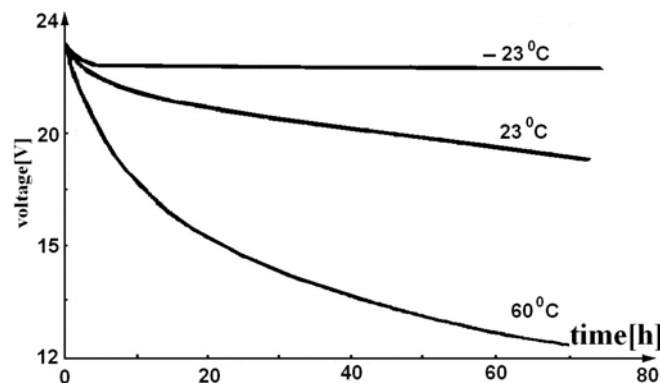


Fig.2. Voltage variation at the terminals of an EDLC in time and at different temperatures [1]

Replacing electrochemical reactions with purely electrostatic reactions is the first important difference between supercapacitors and batteries, both seen as energy storage devices. The main difference between electrochemical accumulators and supercapacitors is that the first is a real source of direct current while the supercapacitor is nothing else but a passive component that can participate at rather lengthy transitory processes (up to tens of minutes), processes that involve considerable transfer of power. An accumulator battery stores high energy/kilogram for a long time while a supercapacitor stores and can give a high energy in a short time [2, 3].

2. Restrictive technical conditions

A supercapacitor battery will not be able to store enough charge for operating modes at medium currents for longer periods. Similarly, a battery of lead accumulators should be oversized to be able to deliver the necessary energy for high current peaks operating mode. Over sizing a lead accumulator battery leads to an increase in the system mass and costs. Using a hybrid source formed from a capacitor battery and a lead accumulator battery would lead to a decrease of roughly 60% of the system weight and would also considerably reduce costs [2, 3].

By analyzing the self-discharge process for a supercapacitor it is possible to observe that as the temperature increases, the stored energy, in time, decreases significantly. By separating the two processes at low temperatures and at high temperatures employing a supercapacitor in a system, in the automotive field, will be done using electronic circuitry to separate the lead accumulator from the supercapacitor battery while the vehicle is stationary.

3. Block diagram of the hybrid system for starting the engine

The electronic circuit should discern between the moment when the system uses power from the supercapacitor and the moment when (for example) the auto vehicle is stationary. The circuit couples the EDLC battery in parallel with the lead battery (at a time t) only a few seconds (n) before the starter is operated, in order to accumulate charge. In these n seconds the supercapacitor must absorb energy from the Pb accumulator and reach peak charged state. At $t+n$ seconds the system is ready to deliver a very high current to be used by the starter. The current for the starter comes not only from the accumulator but also from the supercapacitor that is connected in parallel. This is necessary because after the vehicle was stationary for an extended period (especially if it was at high temperatures) the supercapacitor discharges unlike the accumulator which has smaller loss [2, 3].

The advantage of using an accumulator with suercapacitors on an auto vehicle is the reduction of the weight/energy unit. For example instead of a 60Ah accumulator which has a 400A short-circuit current it is possible to use a Pb accumulator of 25Ah with a 100A short-circuit current and a supercapacitor with a maximum current of 300 Ah. This way at $t+n$ the 100A current from the Pb accumulator and the 300A current that the supercapacitor can give for several seconds can be used, This is enough for starting an engine, especially a diesel one. Starting an engine usually takes about 1...3 seconds. Companies from this field can manufacture such a circuit that equalizes voltage on a supercapacitor (Fig.3) [2, 3].

When the ignition contact is operated by the driver (time t), a voltage is applied not only on the usual load but also at the terminals of the command and timing circuit, which will close the static contactor. The booting of the ECU (electronic control unit) starts and pressure starts to build up in the fuel system. After a time (n seconds) a command is sent to the ECU, the board markers are extinguished and the starter can be operated, the EDLC battery has stored enough energy to compensate the load lost during parking. When operating the starter the available current for the starter (I_o) is I_1 plus I_2 . Since I_1 is about 100A, I_2 can be, depending on EDLC type, about 300A. The total available current for operating the starter is 400A, which replaces the big accumulator short circuit current of 60...70Ah. During engine operation, the electric machine (alternator) of the vehicle, charges not only the accumulator but also the EDLC battery [2, 3].

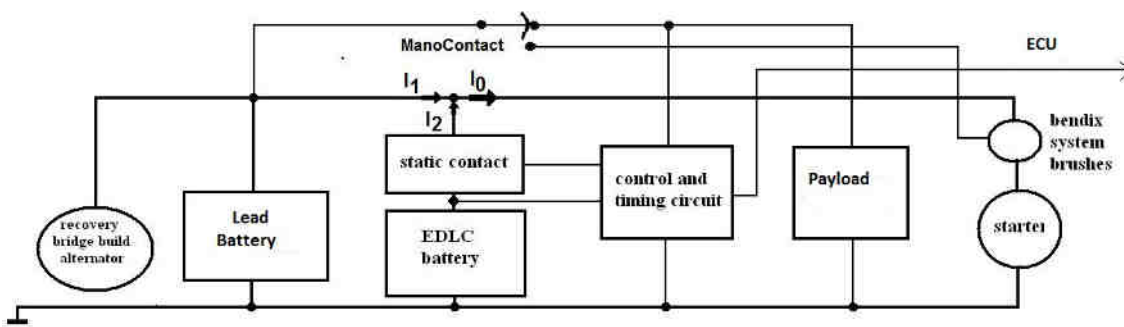


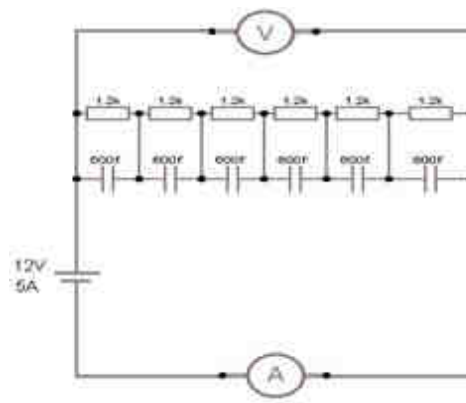
Fig. 3. Electronic command circuit for the lead battery and EDLC battery [2, 3]

At a new startup the command and timing circuit first measures the voltage on the EDLC. If the voltage is high, the EDLC has lost a small quantity of charge then the time n to starting is decreased with a time constant, constant that is deduced from the characteristic [2, 3].

We have used six 600 F supercapacitors coupled in series (Fig. 4 a) obtaining a supercapacitor battery. This was used for a series of measurements regarding the starting of a Dacia 1300 engine with a 20Ah accumulator.



a)



b)

Fig. 4. a) Battery using six 600F supercapacitors connected in series [4]

b) Resistors are connected in parallel with each series connected capacitor

When several supercapacitors are connected in series, to prevent over-charge of one of the supercapacitor, resistors are connected in parallel with each series connected capacitor (Fig.4 b). The disadvantage being that the supercapacitor discharges even when the charging system is deactivated. Using an electronic circuit can solve this problem [5].

Balancing resistors are used to maintain an even voltage at the supercapacitors terminals. When the voltage increases on a cell, part of the current will flow through the resistor thus leading to a decrease in voltage. This is true for each supercapacitor cell [5].

4. Block diagram of the electronic circuit used on a hybrid electric auto vehicle

Nowadays the difference between the energy and the power density between these components can be seen as an advantage when combining them in a power system where they can fill in each other's weaknesses. Another application is in the field of hybrid auto vehicles where breaking leads to the forming of transitory current movements and to energy requests for short periods. It is especially true since the price for a supercapacitor has reached 2 dollars for a F and is still decreasing [6].

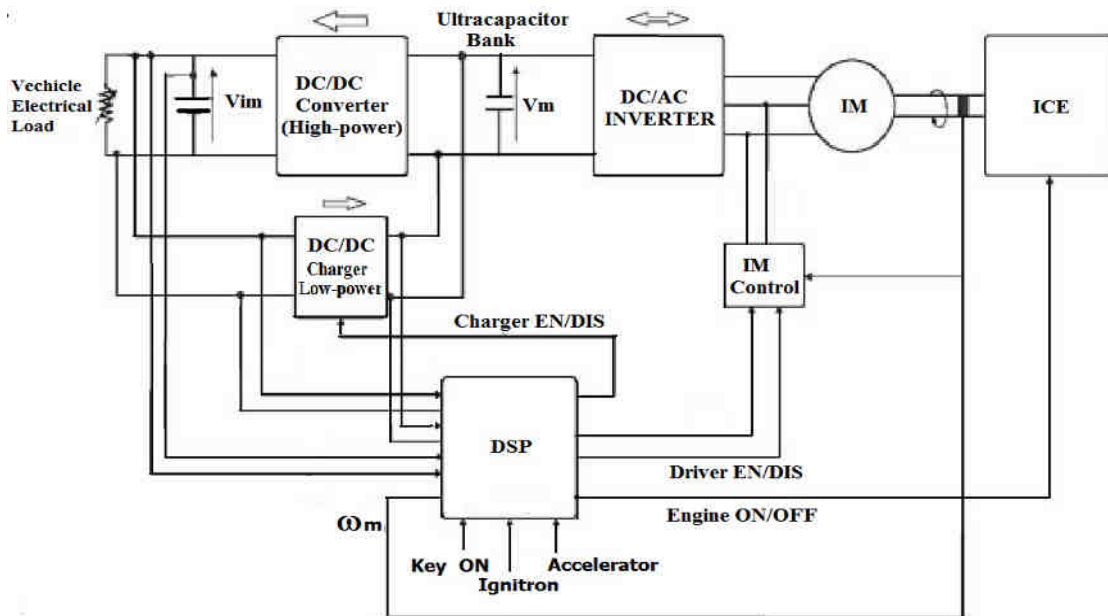


Fig. 5. Block diagram of the electronic circuit used on a hybrid electric auto vehicle [7]

The first auto vehicles to use supercapacitors as auxiliary elements were tanks with diesel engines and locomotives. Recently they have begun to raise interest in the energy field since they are able to store charge faster than conventional accumulators which recommends them for use in regenerative breaking applications.

Using exclusively electrochemical accumulators would be inefficient for passenger vehicles because of the high charging time. Supercapacitors on the other hand can charge faster than accumulators so it is possible for vehicles with frequent stops to charge rapidly. When the bus stops a captor on the top side lifts for a few meters and makes contact with a charging line. In a few seconds the hybrid batteries placed under the seats are charged. It is also possible to recover the breaking energy.

5. Conclusions

Supercapacitors, as a way to store energy have advantages and disadvantages when compared with the device most used to store energy, the accumulator. This explains the use of hybrid systems battery-supercapacitor in some applications. The field concerning the fabrication of supercapacitors still has a long way to go until these can replace accumulators.

The system that we propose that uses six supercapacitors of 600 F each is still in the development stage but the experimental results obtained and that have been presented are very promising. A supercapacitor is a good solution to use in an electric hybrid system.

The capacity of a supercapacitor used to store the deceleration energy for short periods is later transferred to the motor on commuting power categories. The advantages are a longer battery life/more charge cycles as well as complete recovery of the energy produced by the electric motor at breaking.

For hybrid auto vehicles where it is necessary to accumulate a high quantity of charge at breaking and since lead accumulators are not capable of storing high quantities of energy in a short period it is possible to use a lead accumulator and a battery of supercapacitors.

REFERENCES

- [1] P. Svasta, A. Vasile, C. Ionescu, V. Columbeanu, "Componente electronice pasive - Condensatoare - Proprietăți, Construcție, Tehnologie, Aplicații", Cavallioti Publishing House, Bucharest, 2010
- [2] A. Vasile, A. Drumea, P. Svasta, A. Brodeală, C. Ionescu, C. Marghescu „Dispozitive moderne pentru acumularea de sarcină electrică și aplicații specifice”- Hervex 2010 Hydraulics;Pneumatics;Fine mechanics Tools;Mecatronics;Sealing Systems Dedicated electronic devices and equipment, Calimănești-Caciulata 10-12 noiembrie 2010, ISSN 1454-8003, pg. 156-162
- [3] A. Brodeală, A. Vasile, P. Svasta, C. Marghescu, E. Ceuca – “Supercapacitors and Their Specific Applications in the Automotive Field” - SATEE 2010 - Smart Applications & Technologies for Electronic Engineering, Alba Iulia, 8-10 September 2010
- [4] B. Mihăilescu, A. Vasile, P. Svasta, A. Brodeală – “Start Soft Stop for Controlling a Reversible Electric Motor Used in Automotive”- 2011 IEEE 17th International Symposium for Design and Technology in Electronic Packaging (SIITME) Abstract Proceedings, Timișoara, Romania, 978-1-4577-1277-7/11, 20-23 October 2011
- [5] Andreea Brodeală, Alexandru Vasile, Paul Svasta, Bogdan Mihailescu “Storage and Usage System of Electrostatic Energy with EDLC”, 2011 IEEE 17th International Symposium for Design and Technology in Electronic Packaging (SIITME) Abstract Proceedings, Timisoara, Romania, 978-1-4577-1277-7/11, pg. 141-144, 20-23 October 2011
- [6] Richard Ball, 2006, Electronicsweekly.com, 2008-01-06,
<http://www.electronicsweekly.com/Articles/2006/03/01/37810/Supercapacitors+see+growth+as+costs+fall.ht>
- [7] Obreja Vasile, “Tehnologie pe baza de materiale nanostructurate pentru condensatori electrochimici cu strat dublu utilizabili la stocarea energiei electrice (Supercondensatori), Raport de cercetare, September 2006, program CEEX”

MOBILE SKID SIMULATOR FOR THE TRAINING OF CAR DRIVERS

Radu Iulian RADOI¹, Ioan BĂLAN¹, Marian BLEJAN¹

¹ INOE 2000 – IHP Bucuresti, radoi.ihp@fluidas.ro

Abstract: The article presents the construction of a mobile simulator for the training of car drivers. The simulator helps the car drivers to learn the skills for redressing the car if it skids. The simulator comprises a metallic frame which has set at ends four hydraulic cylinders with pivotant wheels on which is suspended the car aiming to create the conditions for car skids. The drive of the cylinders is made by means of a mini pumping group supplied with electricity from the car dashboard, the commands being given by the instructor by means of a remote control.

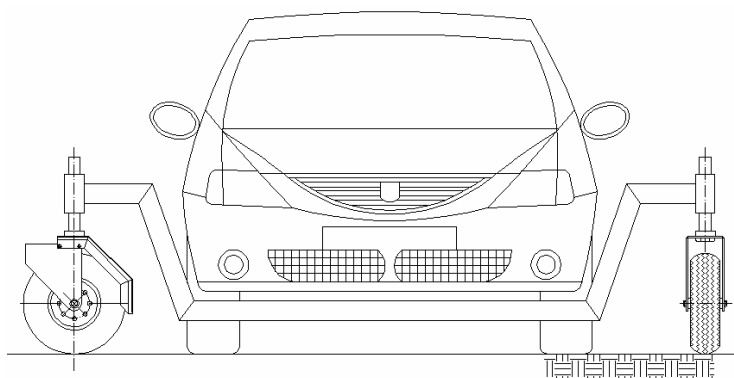
Keywords: simulator, skidcar, hydraulic, training

1. Introduction

The drivers that take driving lessons on cars equipped with mobile simulators for lateral skids, shall acquire in hours abilities and experience for various skid plays, so they will react instinctively, the risks being significantly reduced. This kind of simulator is cheaper, its maintenance and use costs being more reduced than of other simulators. We shall describe below the construction and characteristics of this type of simulator designed and realized by INOE 2000 – IHP București.

2. General Description

The general principle which stays at the base of the training activity which will be made by means of this simulator consists in a controlled suspension of the car at a 0 value – the car relies exclusively on its wheels (the pivotant wheels have no contact with the ground), until a max.value – the car wheels have no more contact with the ground (frame assembly / the car relies exclusively on the pivotant wheels. In these variable conditions of contact with the ground will be possible to reproduce the trajectories of a car which loses adherence to tread and skids under the action of the centrifugal force.



System characteristics:

Mechano hydraulic characteristics

- max.pressure: 70 bar
- max.load. 1600 daN
- time for lifting max.load/bridge: 0,8 sec.
- max.stroke of the cylinders: 130 mm

Electric characteristics

- supply voltage: 13,8 V
- power motor electropump: 150 W
- remote control communication: RS232
- nr.memories: 8 positions

Fig. 1 Overall view of the assembly

2.1 Mechanical Part

The mechanical part consists of a frame (Fig. 2) composed of front and back bunks, the longitudinal longerons which link the front and back bunks and two intermediary bunks, provided with rubber dampers on which is suspended the car from the jack's mounting points, located in the sills zone. At the ends of the front and back bunks are mounted some special hydraulic cylinders, which resist at the couple (torque) appearing in the rod not only at the axial forces. In the down ends of the cylinder rods are mounted pivotant wheels.

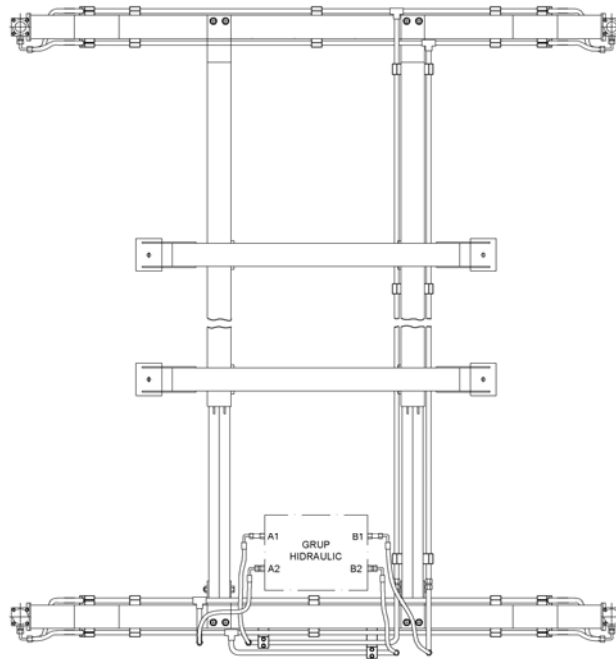


Fig. 2 The simulator frames and the pipes setting

2.2 Hydraulic Diagram

The hydraulic diagram (Fig.3) allows the drive of the 4 hydraulic cylinders (12), provided for lifting the frame, by means of some electric prompts given to the distributors (14). In the diagram were set unlockable valves (8) so that the cylinders will not go down in time cause of the losses from the hydraulic distributor, the distributor not being tightly shut. The throttle track (13) has the role of controlling the descent speed of the hydraulic cylinders. For being possible to use a low power electropump (150 W) it was provided a pneumohydraulic accumulator (9) which accumulates a volume of oil under pressure, that allows the lifting of the frame in 0,8 sec. For each bridge. The oil from the accumulator allows an integral lifting of the frame or two lifting prompts with half of the load. After the depletion of the oil from the accumulator, this is recharged by the pump(2), the monitoring of the charging degree of the accumulator, being made by means of the pressure transducer (10). The use of a higher power pump would have led to complications in what regards the supply with electricity, being required ~ 70 A at 12 V for being possible to provide the necessary flow for the lifting speed.

The resistive stroke transducers (11) have the role of measuring the cylinders stroke from each bridge. In the diagram appear a directional valve (4) which does not allow that the oil from the accumulator to discharge through the pump, a manometer(6), safety valve (5), oil filter provided with detour valve (for the case of warping) directional valve and an oil tank (3).

The pumping unit comprises almost the entire hydraulic diagram with the exception of the hydraulic cylinders. This consists of the pump with toothed wheels, the electric motor, the gripping block and a set of modular plates that contain elements of the diagram or on which are fixed the distributor and the oil filter. The pressure transducer is connected at a port corresponding to the

discharge branch from the pump at which are also connected the pneumohydraulic accumulator and the manometer. The pumping group is assembled on a support placed and anchored in the spare wheel notch. The connection of the pumping group to the installation is made with 4 hoses.

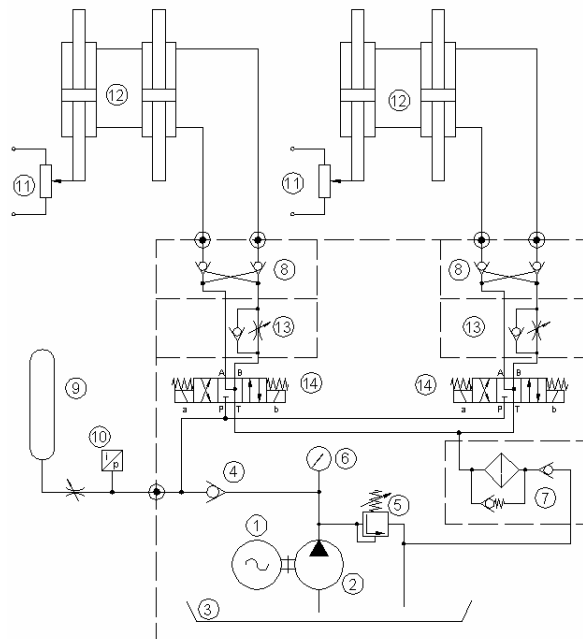


Fig. 3 Hydraulic diagram

2.3 Electronic and Electric Diagram

The diagram of the command plate (Fig. 4) has at its base a microcontroller 16F88. The diagram allows monitoring on two inputs the signals from the resistive stroke transducers and on another input of the signal from the pressure transducer.

From the 5 outputs of the microcontroller are prompted some circuits BTS436L2 which supply the power relay of the electric motor driving the pump and the electromagnets of the two distributors.

The remote control diagram has at the base the same microcontroller 16F88, which will comprise the program allowing the memorization of the settings and the command plate prompt. The diagram of the remote control allows the independent adjustment of the height on the 2 bridges, by means of 2 potentiometers and is provided with 8 buttons M1,..., M8 by means of which may be memorized values of height adjustments for both bridges. The set button performs the memorization in one of the selected locations M1,...,M8. The confirmation of the selection of a button and the condition are signalled by LEDs placed near the buttons.

Both diagrams enclose a circuit MAX232 for serial communication and a circuit LM2574 for reaching the 5 V tension required for integrated circuits.

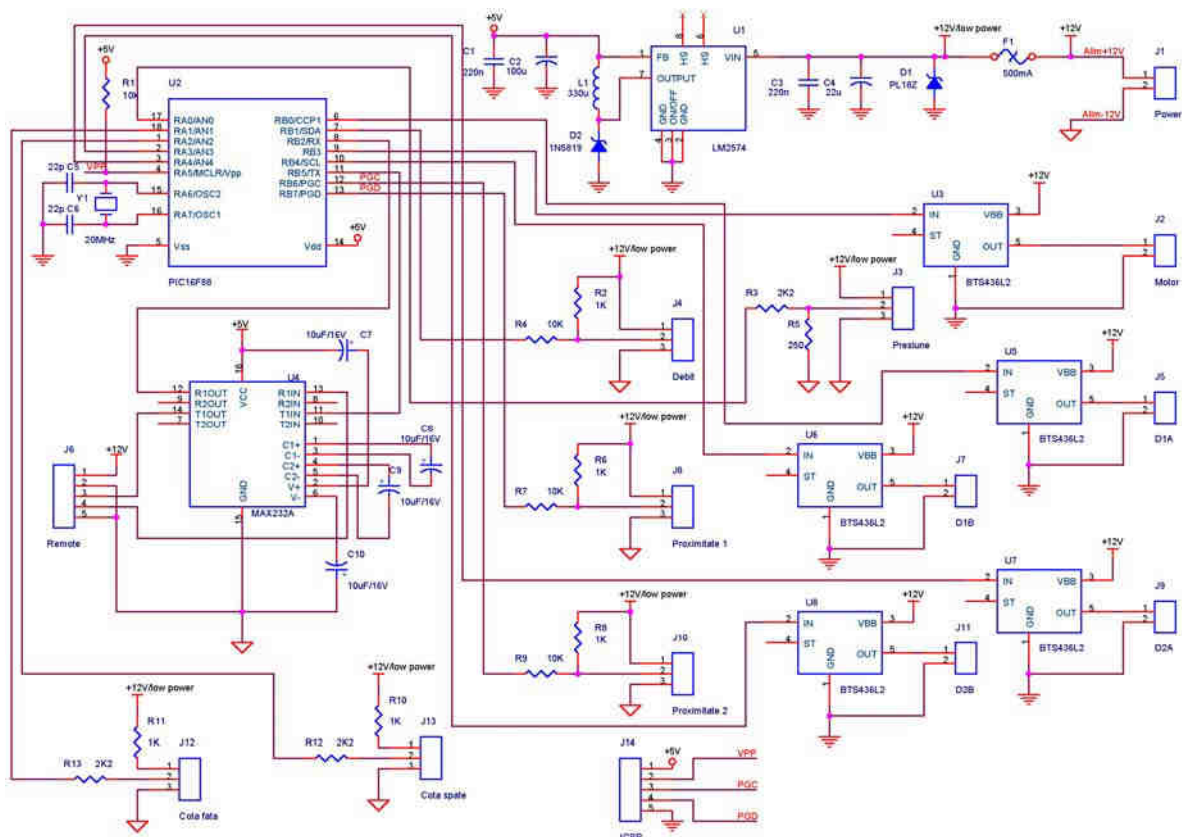


Fig. 4 The diagram of the command module

The electric installation consists of the following main components remote control, the electronic command block, pressure transducer and the electric motor of the pump provided with power relay At the electronic command block are connected, by cables all the other elements as well as the supply cable from the car dashboard. The remote control and the electronic command block are assembled in plastic boxes provided with connectors for the communication cable.

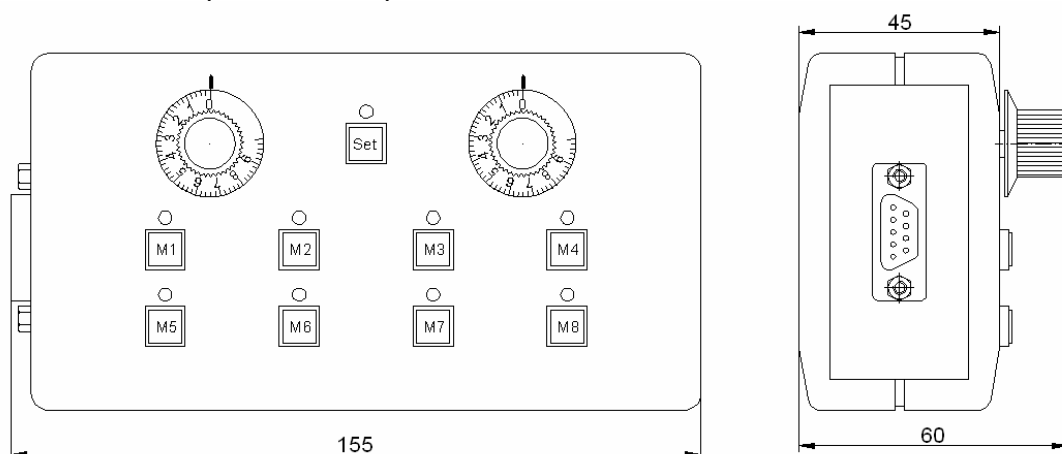


Fig. 5 The remote control of the simulator

3. Operating Mode

The system activation is made by putting under tension from a switch of the command module placed near the pumping unit from the trunk. The presence of tension is indicated by a led placed on the lead of the box in which is the command module.

The instructor has at his disposal a remote control linked by means of a cable by the box with the command module. With this remote control the instructor may adjust the height of the front and back bridges, independently, from the 2 potentiometers. The adjusted values for the front and back bridges may be memorized in 8 locations corresponding to the buttons M1,...,M8. For memorization is used the SET button. After pressing the button the LED blinks moment when the potentiometers become active being possible to change the height of the 2 bridges and if pressed one of the buttons M1...M8 the set values are memorized. The confirmation is made by being lit the LED corresponding to the pressed button. The commutation between memories is made by pressing the memory buttons the activated memory having the LED switched on. If desired a change of the memorized values the memory locations may be rewritten with new values for lifting the car body.

4. Conclusions

The use of the lateral skids simulator may reduce the number of car accidents occurring cause of bad meteorological conditions (wet roads or covered with ice and snow, the drivers acquiring abilities for reacting in an appropriate way at the occurrence of skids).

The simulator is easy to use, the instructor being able to modify the adjustment of height, increasing or decreasing the possibility of occurrence of skids. This type of simulator is cheaper, its maintenance and use costs being lower than of other types of simulators and it is very performant.

REFERENCES

- [1] N. Vasiliu, D. Vasiliu, "Fluid Power Systems", Vol.I. Technical Publishing House, Bucharest, 2005
- [2] V. Marin, R. Moscovici, D. Teneslav, "Sisteme hidraulice de reglare automată – Probleme Practice", Technical Publishing House București, 1981
- [3] G. Rădulescu, R. Rădoi, I. Duțu, Complex systems for electrohydraulic drive mechatronic, Caciulata, Romania; 7-9 November, 2009, "Proceedings - HERVEX", ISSN 1454-8003; pp.182-187
- [4] T.C. Popescu, A. Drumea and I. Dutu, "Numerical simulation and experimental identification of the laser controlled modular system purposefully created for equipping the terrace leveling installations", ISSE-2008, Budapest, Hungary; 7-11 May, 2008, "Proceedings - Reliability and Life-time Prediction", ISBN: 978-963-06-4915-5; pp.336-341
- [5] <http://www.skidcar.com/skidcar-system/mobile-driver-training.php>

THEORETICAL AND EXPERIMENTAL RESEARCH OF RECIPROCATING ROD SEALS

Monica CRUDU¹, Aurelian FATU¹, Mohamed HAJJAM¹, Corneliu CRISTESCU²

¹ University of Poitiers, Poitiers, France, mohamed.hajjam@univ-poitiers.fr

² Hydraulics and Pneumatics Research Institute - INOE2000 IHP, Bucharest, Romania, cristescu.ihp@fluidas.ro

Abstract: *In this paper a numerical model previously developed by the authors to study the sealing performances of hydraulic reciprocating seals, is extended in order to include seal roughness. The model is verified on a typical elastomeric "U" rod seal in steady state conditions. The inverse theory is applied to the dry frictionless contact pressure distribution, obtained from a FEM simulation of the rough seal assembly. Three types of roughness are generated on the surface of the seal in contact with the rod. The average roughness (R_a) of the generated seal surfaces is equal to the measured average roughness of the studied seal. The numerical results of the elastomeric rough seal sliding on a smooth rod are compared with measurements, obtained on an original experimental device. The comparison concerns the friction force, obtained for different hydraulic pressures varying from 4 MPa up to 20 MPa and for two stroke velocities. The influence the roughness geometrical distribution as well as the wave length on the seal performances is analysed. It is proved that the seal roughness has an important influence over the numerical predictions*

Keywords: *rod seal, roughness effect, inverse hydrodynamic lubrication, friction*

1. Introduction

Rod seals are the most vital components of the sealing system. Their role is to ensure the sealing of the pressurized hydraulic fluid from the environment during the reciprocating motion of the rod. The failure of this type of seal can induce the failure of the hydraulic system or can damage the environment. Modelling the behaviour of hydraulic seals has always been a challenge due to a great numbers of influence parameters such as non-linearity of seal materiel or extreme operation conditions. The main part of the existing numerical models assumes fluid film lubrication and perfectly smooth surfaces in contact. In reality, hydraulic seals deals with mixed lubrication regime and the experimental studies demonstrated that seal roughness plays an important role in the lubrication of the sealing contact [1], [2], [3].

In this paper a numerical model previously developed [5] by the authors to study the sealing performances of hydraulic reciprocating seals, is extended in order to include seal roughness effect. This is for the first time as far as the authors knows when the roughness effects are treated by an IHL approach. The influence of the roughness geometrical distribution and wave length over the sealing performances is analysed. Numerical results, in terms of friction forces, are compared with experimental ones, obtained with an original experimental device.

2. Model description

A numerical model previously developed by the authors to study the sealing performances of hydraulic reciprocating seals, is improved in order to include seal roughness. This improvement is undertaken in an original way. The inverse lubrication theory is applied to the dry frictionless contact pressure distribution, obtained from a FEM simulation of a rough seal and a smooth rod assembly. The analysis is made for the steady-state case of a reciprocating hydrogenates nitrile rubber "U" type rod seal. The geometry of the studied seal is presented in fig.1.

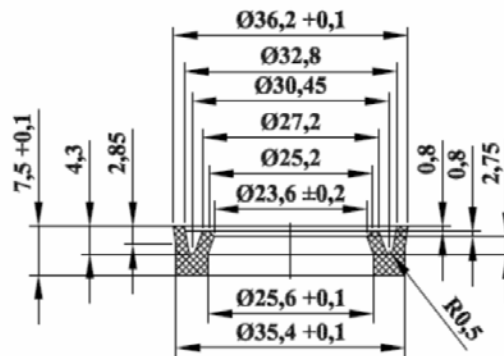


Fig.1-Test seal geometry

2.1. Simulation of the rough seal assembly

The first step in the theoretical analysis is the FEM simulation of the rough seal assembly. In order to model the seal roughness sinusoids with the same arithmetic average roughness (R_a) as the studied seal are used, the measured arithmetic average roughness of the seal being $1.54 \mu\text{m}$. (Fig.2).

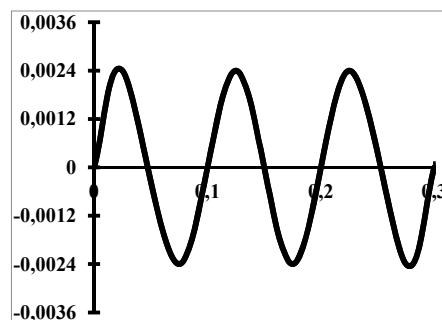


Fig.2- Seal roughness distribution

The seal material behaviour is described using Mooney-Rivlin hyperplastic model (Abaqus). More details concerning the choice of the material model are given in references [4], [5].

The seal is meshed with axial symmetrical elements and for the contact region a structured quadratic mesh of $2 \mu\text{m}$ length is used (Fig.3). The seal housing and the rod are treated like rigid parts. The seal is compressed between the rod and the seal housing and then is submitted at four different hydraulic pressures (p_{alim}), between 4MPa and 20MPa. (fig.3).

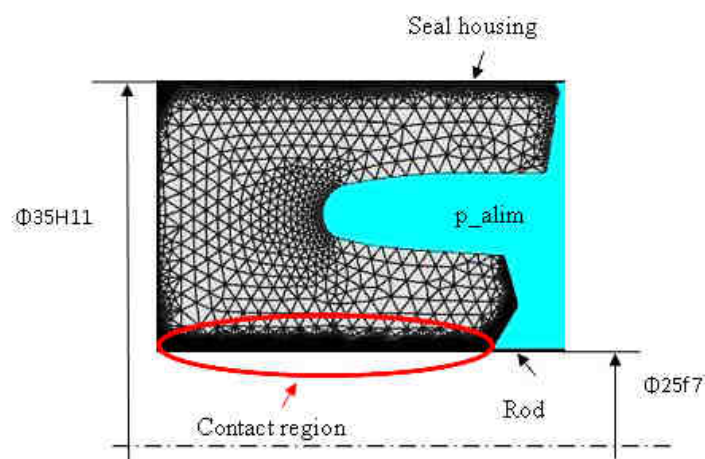


Fig.3- Test seal before assembly

2.2. IHL theory

The numerical model presented in this paper is based on the inverse hydrodynamic lubrication theory represented by the Reynolds equation.

$$\frac{\partial}{\partial x} \left(\frac{h^3}{\mu} \frac{\partial p}{\partial x} \right) = 6U \frac{\partial h}{\partial x} \quad (1)$$

Where p and h are the local pressure and film thickness in the contact, U is the net sliding velocity and μ is the lubricant pressure dependent dynamic viscosity.

The hydrodynamic pressure distribution is considered equal to the dry contact pressure obtained by FEM simulation of the rough seal assembly, because the radial charge of the seal imposed by the film in contact is negligible comparing to the deformation of the seal during assembly. Therefore, Reynolds equation is solved in the film thickness h and this is the so-called inverse hydrodynamic lubrication (IHL) theory. The authors have previously published a detailed presentation of the IHL model in references [4], [5].

3. Experimental Work

In order to validate our numerical model a comparison with experimental results, in terms of friction forces is conducted. The experimental results were obtained with an original experimental device, design and conceived by INOE 2000 IHP Bucharest (fig.4), capable of measuring the friction force between a rod and two U type seals at constant pressure, speed and temperature. A detailed description of the device is given in reference [6], [7].

The experimental device was mounted on an old stand, existing in INOE 2000-IHP, (fig.4 a and b).



(a) Overview of the test stand.



(b) Creating pressure with hand Pump.

Fig.4- The stand for experimental determination of frictional forces

The main unit of the test stand is the experimental device, which contains the investigated sealing and is mounted on the framework of the drive system Figure 5, where it can be seen both the dual sealing sleeve, Figure 6, the pressure and temperature transducer, as well as the force transducer, Figure 7.



Figure 5: The experimental device mounted on stand.



Figure 6: the pressure and temperature transducer.



Figure 7: The force transducer

The drive system has, at the bottom of the framework, a stroke transducer, shown in Figure 8, which allows measurement of the stroke, on the one hand, including measuring the actual speed of displacement of the rod through the gaskets seals, obtained by derivation of the stroke. The ambient temperature, at which experimental research is conducted, is measured by a digital thermometer, shown in Figure 9, which by its contact rod, directly indicates the instantaneous temperature of the stand. Pressure of working oil, sealed by the two gaskets tested, is created by using a hand pump, shown in Figure 10. Hand pump has a pressure gauge to indicate directly the working pressure and, also, a local display pressure transducer that allows pressure digital reading and sending signal for storage to the computer.



Figure 8: The stroke transducer.



Figure 9: The thermometer



Figure 10: The hand pump

4. Results

After the simulation of the seal assembly an initial pressure field and film thickness distribution are obtained. In fig.4 is represented the pressure field and film distribution obtained for an input pressure of 4.5 MPa. For a better comprehension of the next discussions, we will refer to the seal surface in contact with the rod considering one of the three composing parts of contact: entry region of contact, contact region and exit region of contact. (Fig.11)

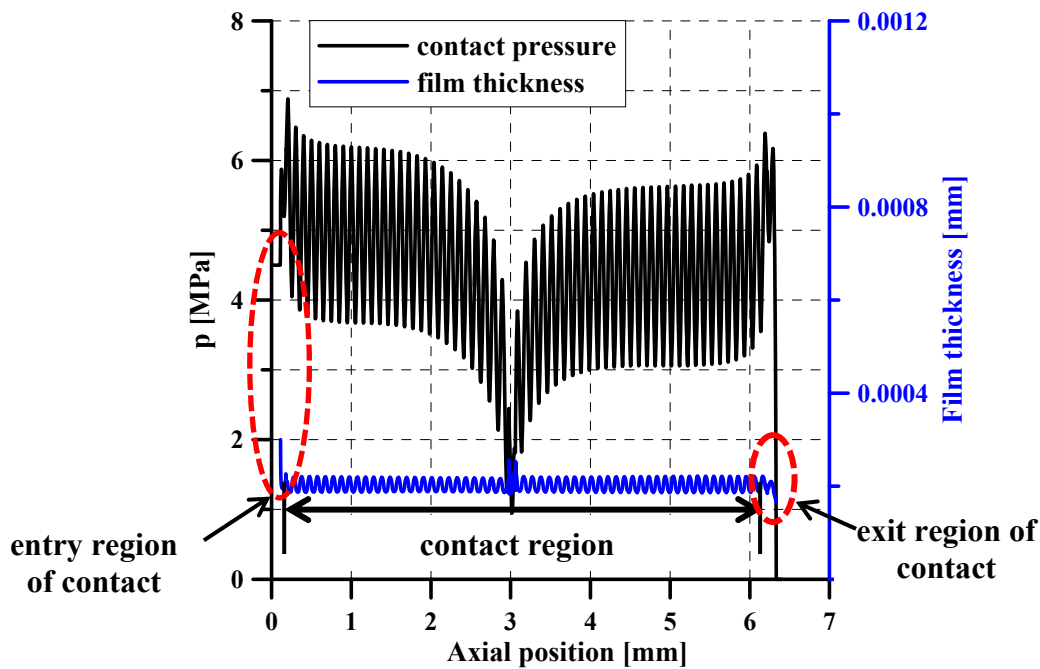


Fig.11- Contact pressure and film thickness obtained by FEM simulation

The roughness effect of the seal surface in contact with the rod over the sealing characteristics obtained with the IHL model is analysed. In a first phase the surface of the seal placed in the entry region is considered smooth.

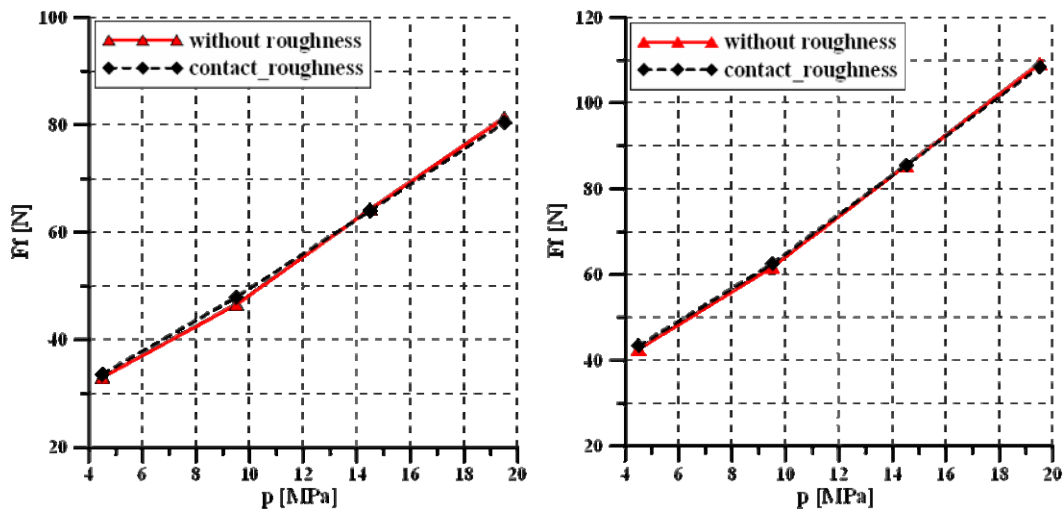


Fig.12- Friction force variation with the input pressure obtained for a smooth seal and for a rough seal when the entry region of contact is considered smooth

The characteristics of the seals obtained after the IHL calculation were equal to those obtained for a smooth seal, so in a next step we represented the roughness also in the entry region of contact. The results increased with about 10%, so a first conclusion of our analysis was that when treating the roughness effect by an IHL approach it is mandatory to consider rough also the entry region of contact. This result was kind of expected due to the fact that the quality of the IHL results strongly depends on the position of the first inflexion point, placed in the entry region in contact.

In order to see if the positioning of roughness distribution in the entry region of contact influences the calculated HD characteristics of the analysed seal, we displaced the initial roughness distribution with a quarter wave lengths. (fig.12).

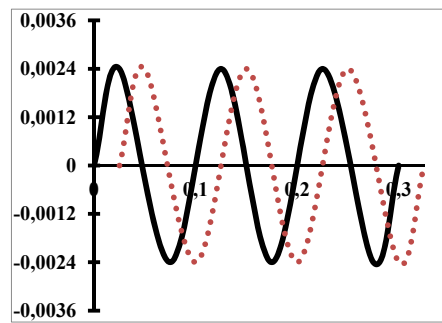


Fig.13- Initial and displaced seal roughness distribution

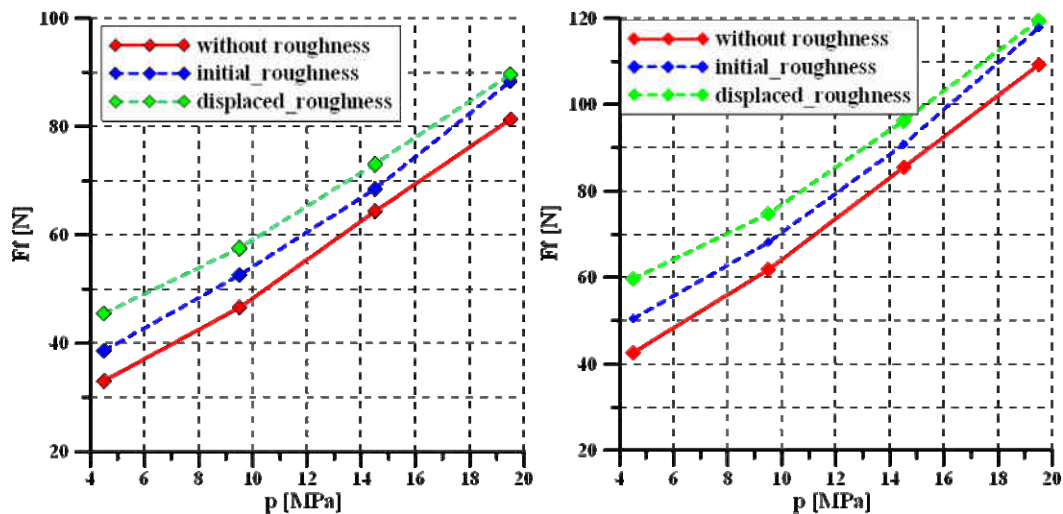


Fig.14- Friction force variation with the input pressure obtained for a smooth seal, for a rough seal and for a rough seal with a quart of wave length displaced roughness distribution

The results obtained this time increased with about 20% by comparison with the results obtained for a smooth seal. It seems like the IHL analysis is very sensitive also to the positioning of the roughness distribution in the entry region of contact.

The wave length as well as the geometrical distribution of the initial roughness of the seal surface in contact with the rod was varied in order to analyze the effect of these two parameters over the calculated HD seal characteristics. Two types of roughness were analyzed: the first type consist in sinusoids with a wavelength of 0.1 mm and three different amplitudes being: 0.0024 mm, 0.0021 mm, 0.0026 mm and the second type consists in sinusoids with a wavelength of 0.15 mm and an amplitude equal 0.0024 mm. (Fig. 15)

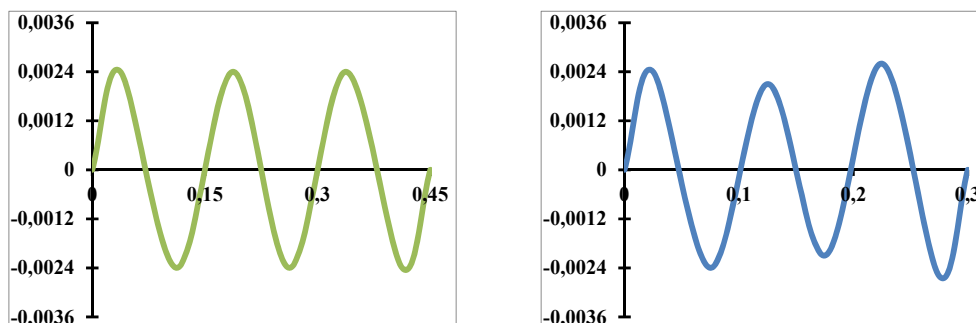


Fig.15- Analyzed seal roughness distribution

The results obtained in terms of friction forces variation with the input pressure at two reciprocated speeds are represented in fig. 16.

It seems like the geometrical distribution has an influence smaller than 2% over the calculated friction forces for the two reciprocated speeds tested. The influence of the wave length is about 5% at a reciprocated speed of 43 mm/s while at 80mm/s the effect decreases at 2 %.

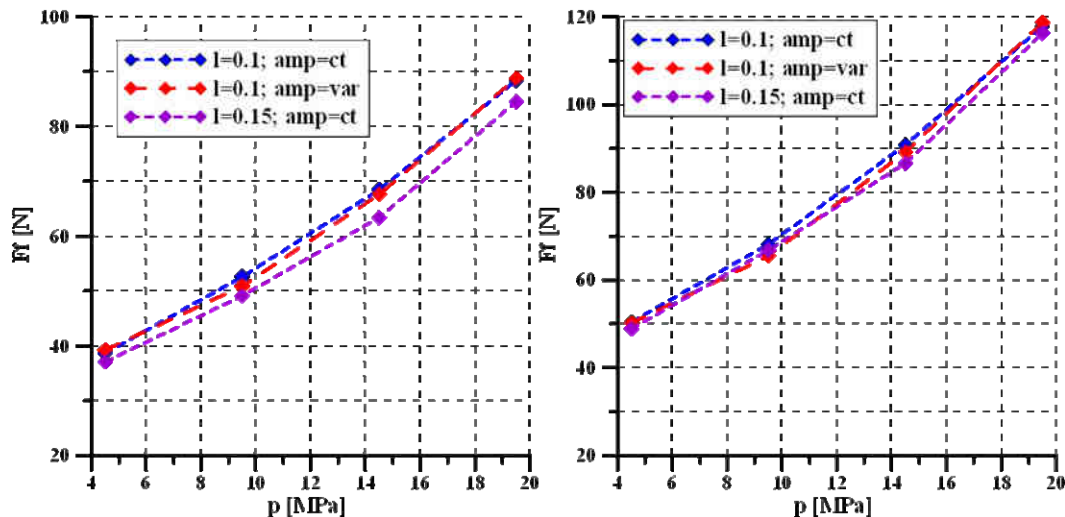


Fig.16- Friction force variation with the input pressure obtained for a rough seal with different wave lengths and geometrical distributions

After this parametrical study the results of the improved numerical model were compared with experimental results. The comparison concerns the friction forces, obtained at four hydraulic pressures varying from 4MPa up to 20 MPa and for two reciprocating speeds of 43 mm/s and 80 mm/s. This two reciprocating speeds correspond to a minimum and a maximum power flow supply of the hydraulic motor that assures the reciprocating motion of the experimental device.

In fig. 17 is represented the comparison between the experimental results and numerical ones obtained with the previously model that doesn't take into account the seal roughness effect and with the improved numerical model. As it can be easily observed the new model offers a significantly better correlation with the experimental measurement. In our situation the results obtained with the initial tested roughness distribution are in better agreement with the experimental measurements.

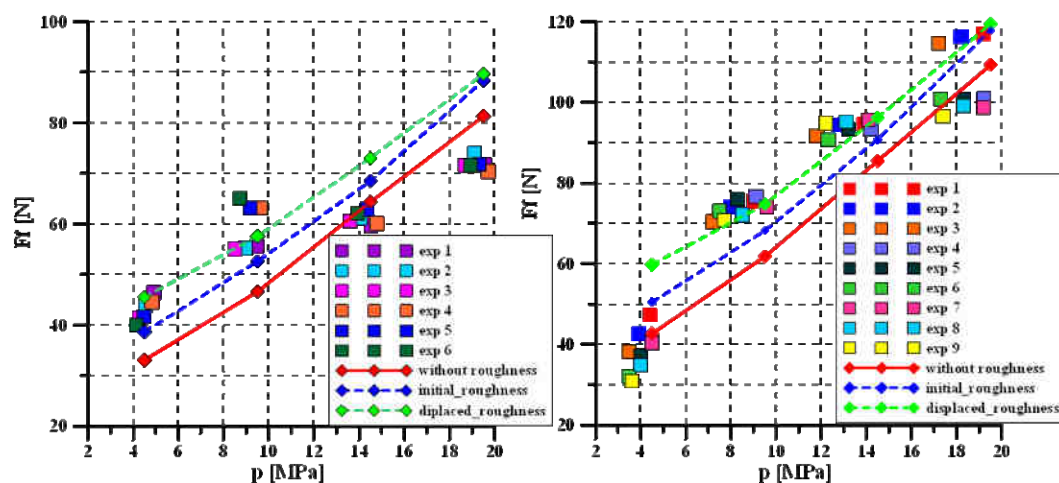


Fig.17- Comparison between the experimental results and the numerical results obtained with the previously and the improved numerical model

However it is clear that much work must be done in order to establish a precise algorithm regarding the correct determination of the seal roughness influence over the predicted HD characteristics.

5. Conclusions

A previously presented IHL model is extended in order to include seal roughness effect. Briefly the inverse lubrication theory is applied to the dry frictionless contact pressure distribution, obtained from a FEM simulation of a rough seal and a smooth rod assembly. The average roughness (R_a) of the seal surface in contact with the rod is chosen equal to the measured average roughness of the studied seal. The results obtained significantly improve the correlation with experimental measurements. The wave length and the roughness geometrical distribution don't seem to have a big influence over the numerical results. However, when the wave length of the seal roughness increases, a variation with 5% of the friction forces by comparison with those obtained for the initial analysed roughness is observed at 43 mm/s. Particular attention must be given to positioning of the roughness distribution in the entry region of contact, because it appears to have an important influence over the numerical results. This fact is not surprising given the importance of the position of the inflection point A in the entry region to the quality of the results.

Acknowledgement

The work has been funded by the Sectorial Operational Programmed Human Resources Development 2007-2013 of the Romanian Ministry of Labour, Family and Social Protection through the Financial Agreement POSDRU/88/1.5/S/61178.

The authors' are grateful to the Technical Centre for the Mechanical Industry (CETIM) – Nantes that financially supported this work.

Also, the authors' wish to thank INOE 2000 IHP, Bucharest, Romania for the support and technical assistance in performing this work.

REFERENCES

- [1] R.K Flitney and B.S. Nau: "Effects of surface finish on reciprocating seal performance", 14th International Conference on Fluid Sealing, BHR Group (1994).
- [2] F. Steep and G. Wustenhagen: "Counter surfaces of hydraulic sealing systems for heavy duty applications", 14th International Sealing Conference, VDMA (2006).
- [3] A. Raidt: "Extended approach for the classification of the quality of the sliding surface", 14th International Sealing Conference, VDMA (2006)
- [4] A. Fatu, M.Hajjam: "Numerical modelling of hydraulic seals by inverse lubrication theory", Proc. IMechE, Part J: J. Eng. Tribology, 2011.
- [5] M.Crudu, A. Fatu, S. Cananau, M.Hajjam, A. Pascu: "A numerical and experimental friction analysis of reciprocating hydraulic 'U' rod seals", Proc. IMechE, Part J: J. Eng. Tribology, 2012.
- [6] Monica CRUDU, Corneliu CRISTESCU, Sorin CANANAU, Adrian PASCU. Experimental investigation of elastomeric U rod seals friction during transient conditions. In: PROCEEDINGS of The 18-th Edition of International Saloon for Hydraulics and Pneumatics-HERVEX-2011, 9-11 November 2011, Calimanesti –Caciulata, Romania, pag. 375-380, ISSN 1454-8003.
- [7] M. Crudu, A. Fatu, M. Hajjam, C. Cristescu: "Numerical and experimental study of reciprocating rod seals including surface roughness effects /Etude numerique et experimental des effets de la rugosite sur le comportement des joints hydrauliques en translation. 11th EDF Pprime Workshop: „Behaviour of Dynamic Seals in Unexpected Operating Conditions", Futuroscope, Septembrie, 2012, Poitiers, France.

MODELING, SIMULATION, AND ENERGY EFFICIENCY MEASUREMENT OF COMPACT UTILITY LOADER HYDRAULIC SYSTEM

Shinok LEE¹, Mingi CHO², Daeyoung SHIN³, and Gangwon LEE⁴

¹Korea Institute of Industrial Technology, shinokee@kitech.re.kr

² Korea Institute of Industrial Technology, alsrl86@kitech.re.kr

³ Korea Institute of Industrial Technology, dyshin@kitech.re.kr

⁴ Korea Institute of Industrial Technology, ggang@kitech.re.kr

Abstract: Compact utility loader, also known as the mini skid-steer, belongs to smallest family of earth-moving machinery. With residential and commercial irrigation market growing, the expectations of these small machines go beyond performance. In this paper the mechanical and hydraulic system of such machine is modelled and simulated. Also energy efficiency measurement is performed on the actual machine to assess the conventional hydraulic system. The developed model can be used to suggest and simulate alternative energy saving hydraulic system which can be applied to the loader in the future.

Keywords: compact utility loader, mini track loader, hydraulic system, construction equipment, energy efficiency

1. Introduction

On recurring energy crisis and ever growing demand for fossil fuels the academia has been responding for decades by searching for alternative energy source and developing systems and parts to effectively process usable resources. The importance of efficiently converting available energy into actual work in hydraulic machinery has long been emphasized both in academia and industry. The load-sensing system and constant pressure system that industry has grown fond of, system utilizing independent metering valves [1], open circuit displacement controlled actuation [2], closed circuit displacement controlled actuation [3], and digital hydraulics [4] are various innovative efforts for minimizing avoidable losses present in the conventional but rather inefficient hydraulic systems still common in the mobile hydraulic industry.

These competing methods all have their pros and cons, but one of the biggest roadblock to commercialization of academia inspired energy saving methods seems to be the shortage of off-the-shelf items to realize such innovation. Besides some of the top-tier manufacturers who can handle the development of necessary special parts the industry will have to respond slowly for such innovations to actually sink in.

Makers of smaller machines such as compact utility loader will not be ready for advanced technology because most studies are primarily and strictly focused on application of bigger machines with bigger markets. In order to demonstrate the applicability of energy saving method it is helpful to study various range of different machines in terms of size, and this study probes into the mechanical and hydraulic system of smaller utility loader which are very similar to its bigger siblings in terms of its composition but distinguishable in its capacity and work cycle pattern.

2. Modeling and simulation of compact utility loader

The utility loader modelled in this study is Toro Dingo TX420[6] and its basic specifications are listed in table 1.1.

Table 1.1 Toro Dingo TX420 Basic Specifications

Item	Specification
Tip Capacity	671.3 kg
Speed	7.2 km/h forward 3.2 km/h reverse
Weight	909.9 kg (with bucket)
L x W x H	2.3 m x 0.86 m x 1.17 m
Gear Pump	20.8 lpm @ 3600 RPM (loader) 42.2 lpm @ 3600 RPM (auxiliary)
Loader Valve	Relief @ 165.5 bar

First step is to model the mechanical system of the loader to analyze its kinematics and dynamics. The major parts of the loader were modelled using SolidWorks 3D modelling software as shown in figure 2.1.



Figure 2.1. 3D modeling of the loader

With its dimensions and specifications known, the 3D model was then translated into MATLAB simMechanics for multi-body dynamic analysis as seen in figure 2.2. The simMechanics model can be interactively simulated with modelled hydraulic system to predict machine kinematics and dynamics, working hydraulic pressures, and hydraulic energy efficiency.

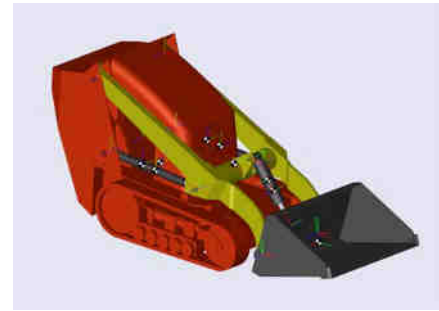
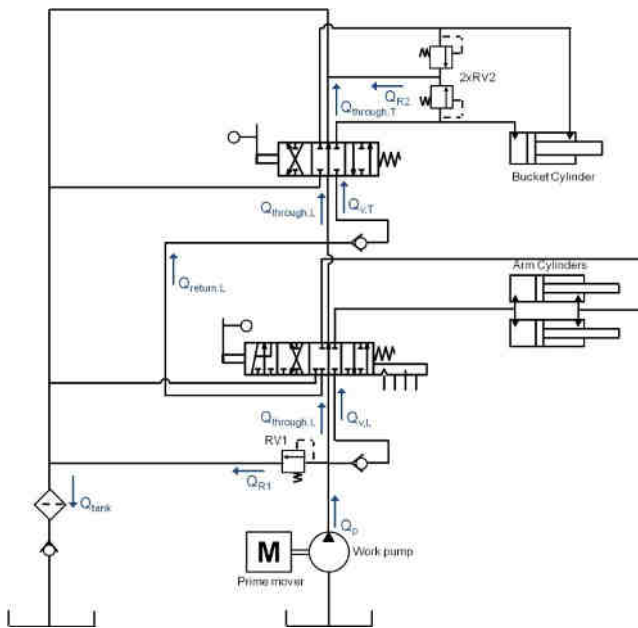


Figure 2.2. simMechanics Model of the loader

The next step is to identify and model the hydraulic system of the loader shown in figure 2.3. For simplicity the drive circuit and auxiliary circuit has been left out in the drawing. The working hydraulic system of the loader is open centre, constant flow system. There are three relief valves as safety circuitry and two directional control valves in series metering the flow into the cylinders. The working pump with 5.78 cc/rev can output flow of 20.8 l/min at 3600 RPM ideally. The pressure and the flow at each section can be described by set of well known hydraulic equations. First, the pressure at the pump outlet is described using pressure build-up equation 2.1.

$$\dot{p}_{\text{pump}} = \frac{1}{C_{H,\text{line}}} (Q_p - Q_{\text{through},L} - Q_{v,L} - Q_{R1} - Q_{\text{Leakage}}) \quad (2.1)$$

Figure 2.3. Working hydraulic circuit of the loader

The hydraulic capacitance of the line $C_{H,\text{line}}$ includes the volume of the pipeline from the pump outlet to the inlet of directional control valve. Q_p is the supply flow of the pump calculated using equation 2.2 assuming nearly constant maximum engine speed $n = 3250 \pm 50$ RPM, as read from the internal tachometer. The volumetric efficiency of the gear pump η_v was assumed to be 0.85.

$$Q_p = \eta_v n V_i \quad (2.2)$$

Flow metered by the directional control valve can be described by the valve orifice equation 2.3, which

$$Q_v = (\alpha_D \pi d) y_v \sqrt{\frac{2}{\rho} |\Delta p|} \quad (2.3)$$

is a function of valve spool position y_v controlled manually by the operator. The pressure difference Δp is difference between the pump pressure and whichever port of cylinder connected for metering in and the difference between the cylinder pressure and tank pressure for metering out. The equation 2.4 and

$$Q_{through,L} = Q_p - Q_{v,L} - Q_{R1} \quad (2.4)$$

$$Q_{through,T} = Q_{through,L} + Q_{return,L} - Q_{v,T} \quad (2.5)$$

equation 2.5 describes the hydraulic flow that passes through the directional control valves when it is not fully open. These hydraulic oil are throttled back to the tank without doing any work, but only adding heat to the system. This is major source of energy loss in such open center system without any flow control. Next, the equation (2.6) and (2.7) are the pressure build-up equation which can be

$$\dot{p}_A = \frac{1}{C_{H,A}} (Q_A - A_A \dot{x} - Q_L) \quad (2.6)$$

$$\dot{p}_B = \frac{1}{C_{H,B}} (-Q_B + A_B \dot{x} + Q_L) \quad (2.7)$$

applied to both arm cylinder and bucket cylinder respectively. Finally the hydraulic energy converted to mechanical motion is described by the equation (2.8) and figure 2.4.

$$m \ddot{x} = F_{cylinder} - F_f - F_L = (p_A A_A - p_B A_B) - c_v \dot{x} - F_L \quad (2.8)$$

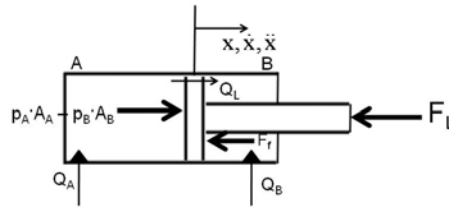


Figure 2.4. Hydraulic actuator

The linear inertia m and load force F_L are function of cylinder stroke displacement, arm angle, and bucket load weight, and these can all be calculated from multi-body dynamic analysis based on simMechanics simulation. The friction force F_f is assumed to be viscous only, neglecting coulomb and static friction which are of less magnitude. Figure 2.5 represents an example of multi-body dynamic analysis performed for simulating and measuring F_L with varying arm position.

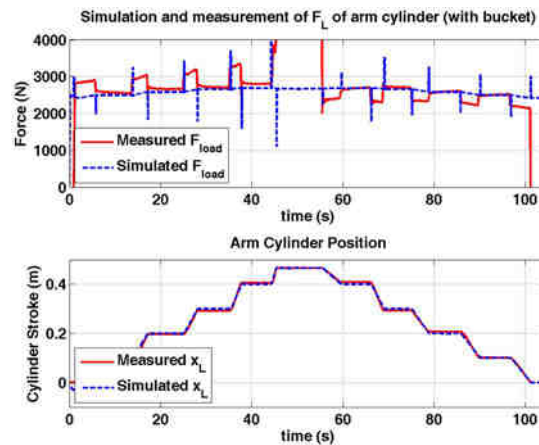


Figure 2.5. Simulation and measurement of F_L

3. Energy efficiency measurement of compact utility loader

To verify the simulation model and measure energy efficiency of the loader hydraulic system, the utility loader was equipped with pressure sensors and wire sensors as schemed in figure 3.1.

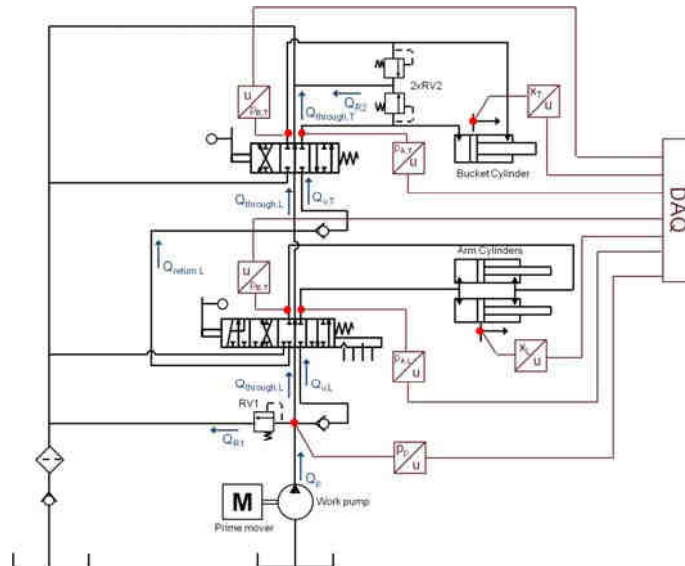


Figure 3.1. Sensors installed for energy efficiency measurement

The pressure sensors measure pressures at outlet of the work pump and at the chamber and rod side of both arm and bucket actuator. The wire sensors measure the linear displacements of the arm and bucket cylinder.

A simple work cycle was performed to assess the energy efficiency of the working loader with conventional open centre constant flow system. The proposed cycle illustrated in figure 3.2 basically starts out by machine picking up the payload comprising set of rectangular metal disks for consistently

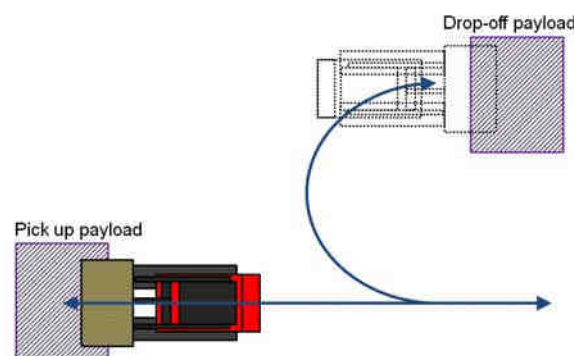


Figure 3.2. Simple work cycle for energy efficiency measurement

variable weight, and finishes by dropping off the payload five meters away from the pick-up point. In order to pick up the load the bucket must push the payload against the wall emulating digging or scooping motion to some extent. The work cycle was performed four times each with payload of 80 kg and 240 kg.

4. Measurement result and analysis

Figure 4.1 plots the cylinder stroke during one chosen cycle for example. The plot illustrates some scooping motion of the bucket and lifting and lowering of the load. Figure 4.2 then shows the pressure level of the pump, arm, and the bucket during the same cycle, and it can be seen that the load exerts highest pressure on the bucket cylinder, and the pump pressure shoots up to match the actuation pressure whenever the valve opens. Even when the valve is closed the pump pressure is maintained at about 4 bar with the engine running, constantly pumping flow back into the tank. This flow and pressure during idling is a complete energy waste present in open centre constant flow systems. During each load cycle nearly 80% of the hydraulic flow was pumped unused back into the tank. Obviously the wasted portion would increase with increased idling hour of the pump.

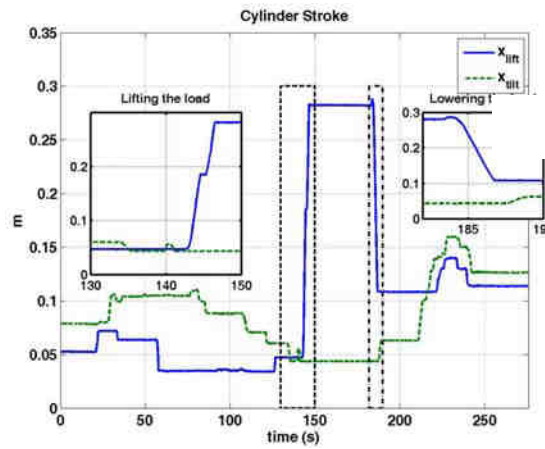


Figure 4.1. Cylinder displacement during the work cycle

$$\dot{E}_{pump} = \dot{V}_{lift,hydraulic} + \dot{V}_{tilt,hydraulic} + \dot{E}_{throttled,metered} \quad (4.1)$$

$$\dot{V}_{hydraulic} = \dot{p}_A A_A \cdot \dot{x}, \quad y_v > 0 \quad (4.2)$$

$$\dot{V}_{hydraulic} = -\dot{p}_B A_B \cdot \dot{x}, \quad y_v < 0 \quad (4.3)$$

$$\dot{E}_{throttled,metered} = (Q_p - Q_{through,T} - Q_{R1} - Q_{R2}) \Delta p_{pump} \quad (4.4)$$

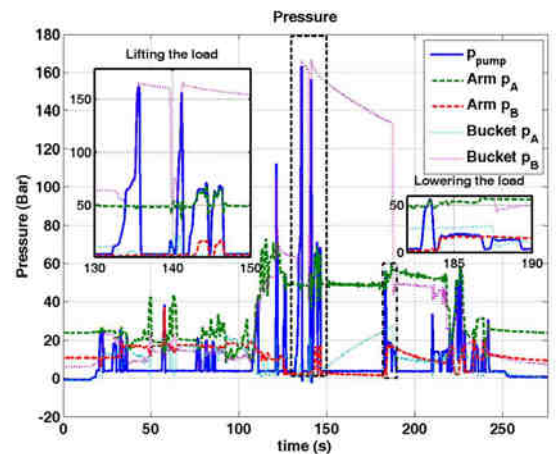


Figure 4.2 Hydraulic pressure during the work cycle

Next, with measured pressure and cylinder stroke, the power usage and energy efficiency of the hydraulic system can be calculated using equation 4.1-4.4. The equation 4.1 shows that the power of the pump is used for either delivering the hydraulic flow to each actuator or throttling and metering it back into the tank uselessly. Figure 4.3 shows that when y_v is greater than zero, equation 4.2 should be used for calculating power utilized by the pump for delivering necessary flow into the hydraulic cylinder, and 4.3 used when y_v is less than zero. The pump flow or the energy that is wasted by throttling and metering can be calculated using equation 4.4 in conjunction with the hydraulic equations described in chapter 2. The calculated power is plotted in figure 4.4. It can be seen that more energy is used to deliver flow into the pump when lifting the load than lowering the load because lifting requires overrunning the load while lowering is aided by the load. Because constant flow from the pump is metered in to the cylinders and flow from the cylinders are metered out to the tank without any recuperation or regeneration, the energy of the hydraulic pump is constantly in waste.

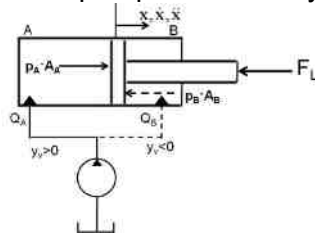


Figure 4.3. Hydraulic flow delivery

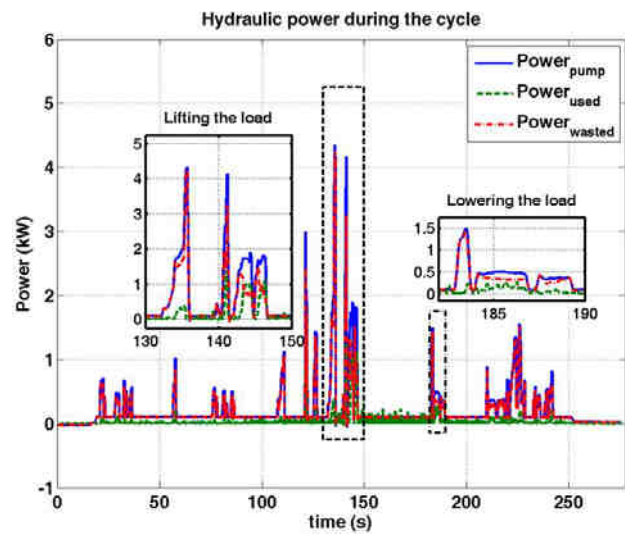


Figure 4.4. Hydraulic power during the work cycle

Further, the energy efficiency of a work cycle can be calculated by integrating calculated power over time as described by equation 4.5, which is also equivalent to equation 4.6. The energy efficiency

$$\xi_{\text{hydraulic_work}} = \frac{E_{\text{pump}} - E_{\text{throttled,metered}}}{E_{\text{pump}}} = \frac{\int_{t_{\text{cycle}}} (\dot{E}_{\text{pump}} - \dot{E}_{\text{throttled,metered}}) dt}{\int_{t_{\text{cycle}}} Q_p \Delta p_{\text{pump}} dt} \quad (4.5)$$

$$\xi_{\text{hydraulic_work}} = \frac{W_{\text{lift,hydraulic}} + W_{\text{tilt,hydraulic}}}{E_{\text{pump}}} = \frac{\int_{t_{\text{cycle}}} (\dot{W}_{\text{lift,hydraulic}} + \dot{W}_{\text{tilt,hydraulic}}) dt}{\int_{t_{\text{cycle}}} Q_p \Delta p_{\text{pump}} dt} \quad (4.6)$$

of a chosen cycle is plotted in figure 4.5.

The energy efficiency at the end of the cycle accumulates to nearly 18%.

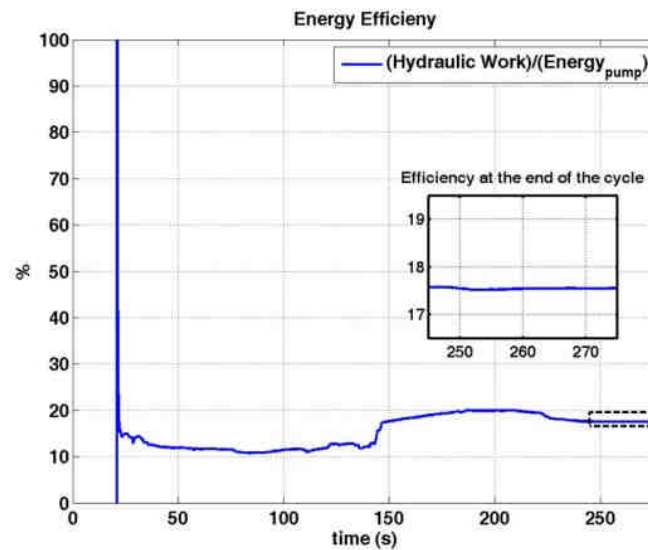


Figure 4.5. Hydraulic power during the work cycle

This means only 18% of the hydraulic power delivered from the pump was actually utilized during this particular work cycle. The work efficiency values calculated for each payload are tabulated in table 4.1

Table 4.1. Hydraulic work efficiency of work cycle with payload = 80kg, 240 kg

Hydraulic Work Efficiency (%)	Payload = 80 kg	Payload = 240 kg
Trial 1	26.83	17.55
Trial 2	31.80	22.39
Trial 3	20.92	28.67
Trial 4	21.28	27.70
Mean	25.21	24.08

The hydraulic work efficiency of this particular open centre constant flow system averages out to about 25%, spanning from 18 to 30%. The rest of the energy is wasted in throttling, metering, and compensating for pipeline losses all adding up as heat into the system. This poor usage of available energy clearly suggests that more efficient hydraulic system needs to be developed and applied to small earthmoving machines.

4. Conclusion

The mechanical and hydraulic system of compact utility loader has been modelled for simulating the dynamics of the loader and calculating energy efficiency. Also energy efficiency measurement has been performed on the actual loader with two different payloads, and the result showed that only about quarter of the pump energy was translated into actual mechanical workings. This poor hydraulic energy usage shows the necessity to supersede the conventional system for these small machines. Next step is to suggest alternative but more efficient hydraulic system, and apply it to the developed simulation model. The alternative system will need to consider the practicality for smaller system, so the system can be tested on the actual loader as soon as the simulation model demonstrate energy improvement. With the improved hydraulic

system, perhaps the engine can be replaced with an electric motor in the future, which can realize effective in-building use of the small but powerful earthmoving machines.

5. Nomenclature

Symbol	Unit	Description
p_{pump}	[Pa]	Pump outlet pressure
p_A	[Pa]	Actuator cylinder chamber side pressure
p_B	[Pa]	Actuator cylinder rod side pressure
$C_{H,line}$	[m ³ /Pa]	Hydraulic capacitance of pump outlet line
$C_{H,A}$	[m ³ /Pa]	Hydraulic capacitance of actuator cylinder chamber side
$C_{H,B}$	[m ³ /Pa]	Hydraulic capacitance of actuator cylinder rod side
$Q_{return,L}$	[m ³ /s]	Return flow of the arm cylinder
$Q_{Leakage}$	[m ³ /s]	Pump leakage
Q_L	[m ³ /s]	Internal leakage of actuator cylinder
Q_{R1}	[m ³ /s]	Flow of relief valve 1
Q_{R2}	[m ³ /s]	Flow of relief valve 2
n	RPM	Engine speed/Pump speed
V_i	cc/rev	Pump displacement
η_v	-	Volumetric efficiency of the pump
α_D	-	Coefficient of orifice equation
d	[m]	Spool diameter
y_v	[m]	Spool opening
ρ	[kg/m ³]	Fluid density
A_A, A_B	[m ²]	Actuator cylinder chamber side area, rod side area
x, \dot{x}, \ddot{x}	[m, m/s, m/s ²]	Actuator cylinder displacement, velocity, and acceleration
m	[kg]	Linear mass of actuator cylinder
c_v	[N·s/m]	Viscous friction coefficient

REFERENCES

- [1] B. Eriksson, and J. -O. Palmberg, Individual metering fluid power systems: challenges and opportunities. In Proceedings, Proceedings of the Institution of Mechanical Engineers, Part I: Journal of Systems and Control Engineering March 1, 2011 225: 196-211
- [2] K. Heybroek, Saving energy in construction machinery using displacement control hydraulics. Lic Thesis, LiU-Tryck, Linköping, Sweden, 2008
- [3] J. Zimmerman, 2008. Design and Simulation of an Energy Saving Displacement-Controlled Actuation System for a Hydraulic Excavator. M.S. Thesis. School of Mechanical Engineering, Purdue University, West Lafayette, IN, USA.
- [4] M. Linjama, Digital Fluid Power – State of the Art, The Twelfth Scandinavian International Conference on Fluid Power, May 18-20, 2011, Tampere, Finland
- [5] J. Zimmerman, M. Pelosi, C. Williamson and M. Ivantysynova. 2007. Energy Consumption of an LS Excavator Hydraulic System. 2007 ASME International Mechanical Engineering Congress and Exposition IMECE2007. Seattle, Washington, USA
- [6] Toro Dingo Tracked Models Specifications. http://www.toro.com/professional/sws/brochure/Track_specs.pdf

HYDRAULIC SCHEMES FOR IMPACT DEVICES. A CONTROL SYSTEM FOR IMPACT MECHANISMS USING A ROTATABLE DISTRIBUTION VALVE – PART1

Claudia KOZMA¹, Liviu VAIDA²

¹ Technical University of Cluj Napoca, Caudia.Kozma@termo.utcluj.ro

² Liviu.Vaida@termo.utcluj.ro

Abstract: *Different structures for impact devices are projected and each of them solves an encountered problem during drilling operation. Methods for minimizing the reciprocating frequency of the impact piston and thus the striking frequency of the dislocating tool are continuously searched. Hydraulic operating schemes are conceived on the basis of patented impact devices or accordingly to the revealed control systems. There are selected and underlined the important observations which arise from the exemplified operating principles. The examples are disposed in descending order by their publication date.*

Keywords: *impact device, percussive mechanism, rock drill, hydraulic hammer, control system, control valve, linear hydraulic motor, shock wave, stress pulse*

1. Percussion drilling operating principle

Drilling by percussion or rotary percussion refers to a mechanical process for dislocation of formations like rock, concrete and asphalt.

Drilling principle is based upon an impact mechanism which imparts shocks to a tool (a bit, a rod steel or a shank). The impact mechanism has a piston which by hitting the tool transmits energy forward to the tool. The tool transmits the shocks to the rock causing the rock to be subjected to the dislocation process.

In drilling with a top hammer, [1] the kinetic energy of the impact piston is transmitted further through a drill steel to a drill bit which is the dislocating tool. The kinetic energy is transmitted in the form of a shock wave. When the shock reaches the dislocation tool, part of the energy is transformed into work and the rest is reflected. In consequence, the dislocation tool is forced to penetrate the rock. The reflected energy returns through the drill steel.

In drilling with a down the hole hammer, [1] the energy of the impact piston is transmitted directly to the dislocation tool. It is obtained a greater performance than drilling with a top hammer.

In drilling with breaking hammers of the type usually supported by excavator arms, the energy of the impact piston is also transmitted directly to the dislocation tool. The breaking hammers of this type are also called hydraulic breakers and hydraulic attachments.

The percussion force is the parameter that has the greater influence upon the penetration rate, [1]. The percussion force and the percussions or impacts are provided by the impact mechanism which is comprised in the hammer's housing.

The shape of the transmitted shock wave depends basically on the design of the impact piston. [12]

Because the impact mechanism is basically a hydraulic linear motor, its working or drive chambers are formed between the piston and the cylinder bore.

The hydraulic impact mechanism has the most important element represented by the piston of the hydraulic linear motor. The impact piston is mounted such that it can move in a cylinder bore which is realized in the machine housing. The impact piston is exposed to alternating pressure such that a reciprocating motion of the impact piston in the cylinder bore is achieved.

As sustained in [5], the alternating pressure in the impact mechanism is most often obtained through a separate switch-over valve, normally of gate type and controlled by the position of the impact piston in the cylinder bore. The switch-over valve couples alternately to at least one of two

working chambers of the impact mechanism and supplies fluid pressure and subsequently to discharges fluid pressure.

The periodically alternating pressure arises in this manner with the periodicity that corresponds to the impact frequency of the impact mechanism. [5]

Through the reciprocating motion of the impact piston is pushed towards the dislocation tool and pulled back. Stress wave or stress pulse is generated by the forwarding piston motion.

2. Control systems of existing impact mechanism

It has been studied structures of hydraulic impact or percussion devices and their methods of generating stress pulse. Based on their description hydraulic schemes are presented further.

According to [2], the pressure fluid operated impact device comprises a separated energy charging space which can comprise one or more hydraulic accumulators, Fig.1. The energy charging space is permanently in connection with a pressure supply source. Furthermore, the energy charging space is coupled to a 4/2-ways control valve which controls pressure fluid feed to the working chamber.

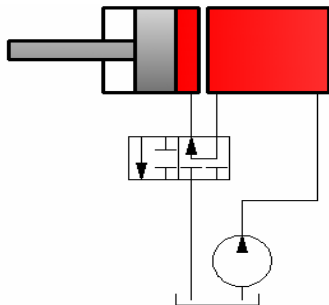


Fig.1. The hydraulic scheme of the stress pulse generating method presented through the impact device described in [2].

In one of its working position, the control valve supply pressure the drive chamber of the hydraulic motor producing a force which pushes the piston towards the tool.

In the other working position of the control valve, the fluid from the drive chamber is discharged to the tank causing the retraction of the piston.

In [3] is described a method for producing a shock wave pulse in a tool direction.

It is stated in [3] that the rock drilling efficiency is affected by the pulse energy which depends on the pulse shape. The possibility of adjusting the length of the shock wave pulse results in the possibility of modifying and decreasing rock penetration resistance during rock drilling.

According to [3], the pulse length can be controlled by regulating of one of a plurality of control parameters that effects pulse production.

In Fig.2 and Fig. 3 it can be observed a 3/2-ways control valve. The control valve periodically

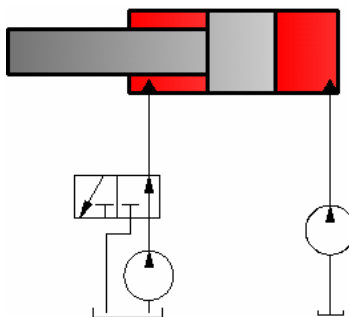


Fig.3. The hydraulic scheme of the method for generating impact pulses, [3].

transmits exit pressure from a pump to the drive chamber of the hydraulic linear motor and periodically relief the pressure of the drive chamber.

Two separated hydraulic pressure source are used, each of them feeding one of the motor working chambers.

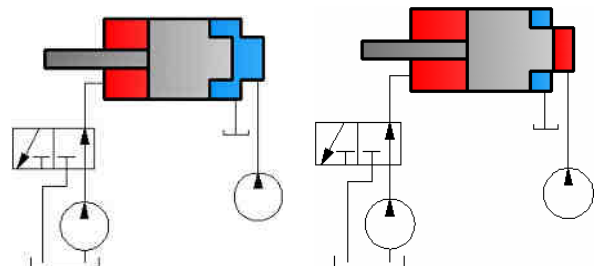


Fig.2. The hydraulic scheme of the method for generating impact pulses, [3].

The shock wave pulse is produced through a rapid relief of the fluid pressure after a certain displacement of the impulse piston relative to the impact device housing. The length of the shock wave pulse remains to depend in this case on the time passed until the control valve release the pressure from the drive chamber and the force produced to push the impact piston towards the dislocation tool.

In [4], it is presented a percussion apparatus driven by a pressurized incompressible fluid. An underlined observation is that there is never any metallic impact between the impact piston and the cylinder.

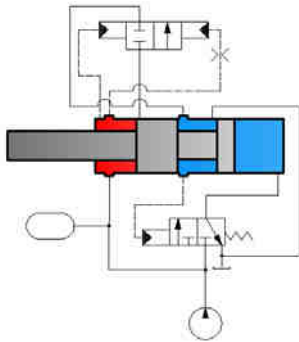


Fig.4. The hydraulic scheme of the impact hammer, [4].

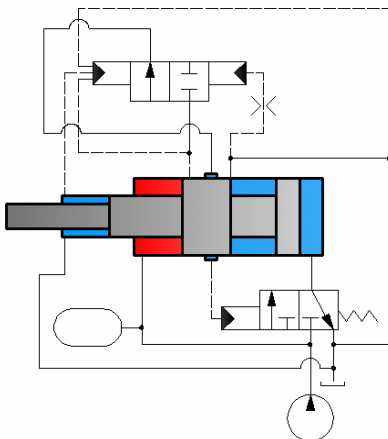


Fig.5. The hydraulic scheme of the impact hammer, [4].

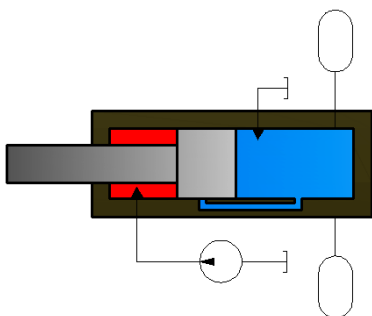


Fig.8. A pressure fluid operated percussion device of the valveless type, [5].

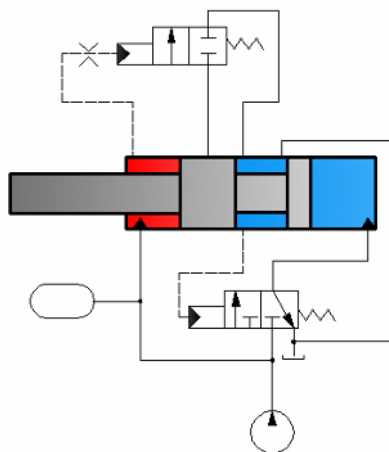


Fig.6. The hydraulic scheme of the impact hammer, [4].

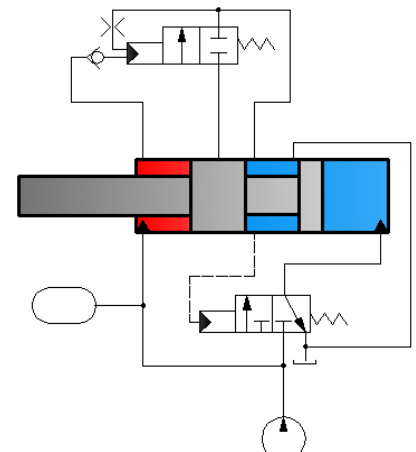


Fig.7. The hydraulic scheme of the impact hammer, [4].

These accumulators are included in order to make possible impact mechanisms that are lighter, cheaper and more sustainable from the point of view of material fatigue.

As it must be observed and taken into account, instead of having a separate switch-over valve, the impact piston in valveless hydraulic impact mechanism is caused to perform also the work of a

switch-over valve. This is possible through the piston movement during its motion which causes opening and closing for the supply and drainage of driving fluid under pressure.

The impact piston moves in the cylinder bore in a manner that provides an alternating pressure in at least one of two motor working chambers. The motor smaller working chamber is permanently fed with hydraulic pressure from a pump. Channels are arranged in the machine housing for the pressurization and drainage of the motor larger working chamber.

The invention from [6] provides a percussion device which has a good efficiency and which enables dynamic forces generated therein and drawbacks caused thereby to become significantly smaller. The stress pulse frequencies are significantly higher than existing ones.

Pressure liquid is intermittently fed to the percussion device through a 3/2-ways control valve,

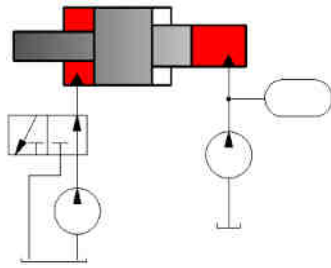


Fig.9. The actuating principle of the [6] impact device.

Fig.9, such that the pressure liquid pushes the motor piston into a predetermined backward position.

Pressure liquid is alternately and rapidly discharged from the percussion device through the 3/2-ways valve. In consequence, the pressure difference created in the hydraulic linear motor pushes the motor piston towards the tool, generating a stress pulse in the tool.

A separate pressure liquid source is in permanent connection with the larger working pressure chamber so that the piston is continuously subjected to the fed pressure towards the tool. A hydraulic accumulator is mounted for absorbing shocks and increasing the impact piston speed.

In [7] the movement of the impact or striking piston is controlled by a 4/3-ways control valve. The control valve is arranged to alternatively connect a chamber to a pressure source and to low pressure in dependence on a signal corresponding to the axial position of the percussion piston. A valve is arranged to allow adjustment of the axial position of the percussion piston at which the signal is transmitted, by opening and blocking of a connection between one or more control channels and the control valve. The length of the piston stroke is adjusted in this manner.

A more complex control and command structure for a percussion drill is revealed in [8]. It is presented in [8] an internal hydraulic damping system for reducing the power

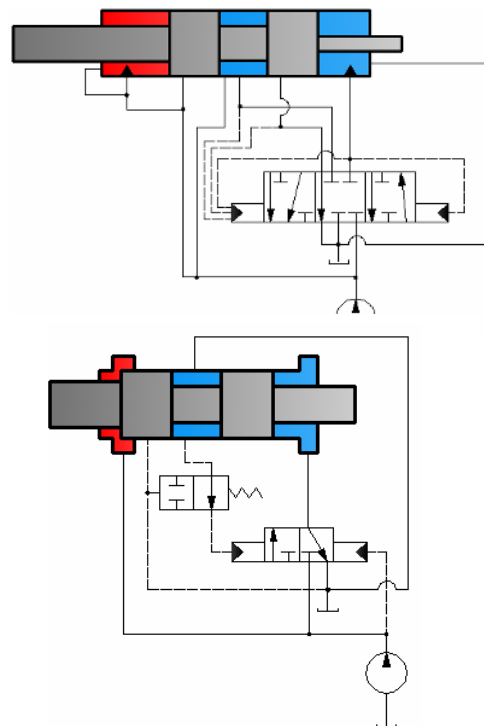


Fig.12. The operating principle of the [9] striking mechanism.

output (i.e. the velocity) of the impact piston, through mechanical alignment, exactly before the impact hits the tool or a shank or a drill steel. The smaller working chamber of the hydraulic linear motor is permanently connected to the only hydraulic pressure source of the impact mechanism, Fig. 11. A hydraulic operated control valve is in fluid communication with the piston-hammer through the motor larger drive chamber and through an intermediate annular chamber.

In [9] the operating principle comprises a shut-off valve or a stop valve and a 3/2-ways control valve.

The 3/2-ways control valve automatically stops the impact mechanism if it is exceeded a predetermined maximum value based on the working pressure, Fig.12.

For the pressure fluid operated impact device from [10], a sequence valve, a pressure hydraulic source, a 3/2-ways distribution valve are used.

According to [10], the impact piston cannot start operating until the pressure of the supplied hydraulic fluid exceeds the

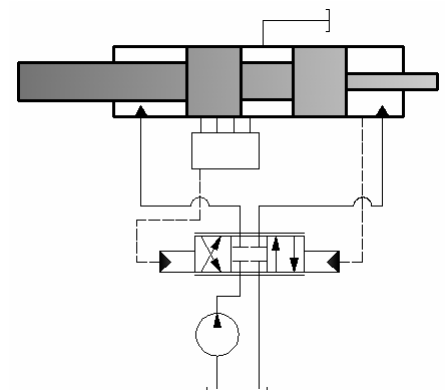


Fig.10. The actuating principle of the [7] impact device.

pre-load pressure level of the accumulator and will not continue to operate after the fluid pressure has dropped below the pre-load pressure level of the accumulator.

The sequence valve is mounted in the drain line, Fig.13, to keep up the pressure in the motor larger working chamber so that the resulting forward directed force prevents the piston from being moved backwards in the cylinder bore at pressure levels in the supply passage below the pre-load pressure level of the accumulator. In this manner, the sequence valve creates a minimum pressure level in the motor larger working chamber such that a too low feed pressure in the supply passage would not be able to accomplish reciprocation of the hammer piston.

The sequence valve is also adapted to the pre-load pressure of the accumulator in such a way that the obtained minimum pressure in the motor larger working chamber will always be high enough to prevent a supply pressure below the preload pressure of the accumulator to move the piston backwards in the cylinder bore.

The pressure accumulator is preloaded to a certain pre-load pressure level. The hydraulic accumulator increases the performance and protects the impact mechanism against damaging pressure gradients and fluid cavities during striking mechanism operation.

A different type of distribution valve, a rotatable one, is used in [11]. Methods of generating stress pulses in impact devices are presented. The underlined ideas are:

- There is not needed a reciprocating percussion piston to generate the stress pulse by means of its kinetic energy.
- No large masses are moved back and forth.
- Small dynamic forces comparatively with those resulted with the reciprocating percussion piston.
- The operation of the impact device is easy to adjust in order to achieve impact performance as desired by using the described method from [11].

The rotatable distribution valve is mounted coaxially with the tool. The rotatable distribution valve is rotated around its axis by means of a suitable rotating mechanism or rotated back and forth.

The opening of the rotatable control valve serves as pressure fluid channels, return channels or channels connected thereto.

According to [11], the supply openings of the rotatable control valve, one by one or simultaneously, allow the pressure fluid to flow to the working chamber. In the other working position of the rotatable control valve, its discharge openings located alternately with the supply openings allow, one by one or simultaneously, allow the pressure fluid to quickly flow from the working chamber.

The operating principle of the rotatable distribution valve has, as a first important result, the

generation of a stress pulse in the tool, and as a last result the ending of the generation of the stress pulse in the tool. The stress pulse is conveyed by the pressure fluid and is generated by compressing the tool through the pushed piston against it.

Another method from [11], implies that the stress pulse acts between the impact device and the tool.

Methods for controlling a pressure fluid operated percussion device with rotatable control valve can be studied also in [12, and 13]. In order to generate a stress pulse, the piston of the hydraulic linear motor presses the tool against a material to be broken. The length of the stress pulse is adjusted by adjusting the time during which pressure influences the piston.

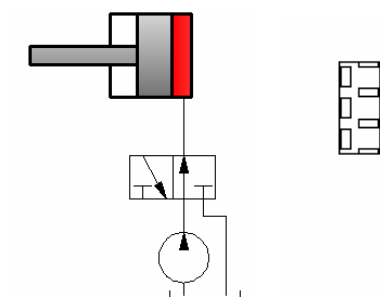


Fig.14. The operating principle of a percussion mechanism and the rotatable distribution valve, [11].

In [14], the used stress element is the liquid. The stress element energy is subjected to pressure in a one valve working position. In the other working

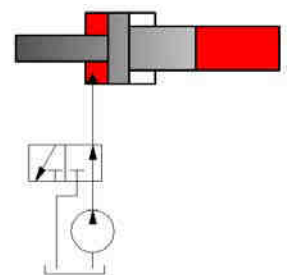


Fig.15. A control system for an impact device, [14].

position of the 3/2-ways directional control valve, the stress element energy is released abruptly and discharged as a stress pulse to the tool, Fig.15. The drill tool can be in direct or indirect contact with the stress element.

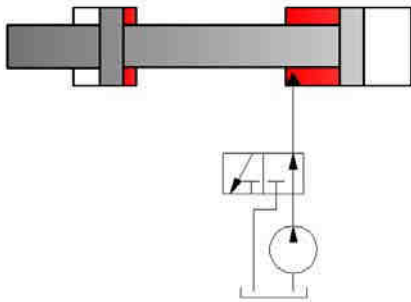


Fig.16. The operating principle of the impact device presented in [14].

Straining the impact element naturally requires energy, which is directed at the used elastic impact element either mechanically, hydraulically or hydro mechanically. Each case is described in [15] with the corresponding illustrations. The stored stress energy in the elastic impact element is

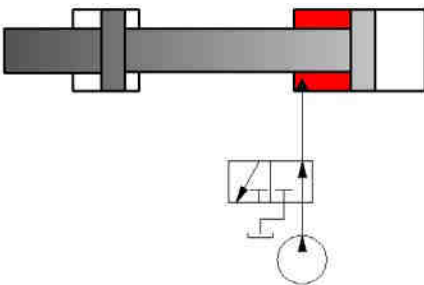


Fig.17. The operating principle of the impact device presented in [15].

discharged in the form of a stress pulse directed at the tool. As stated in [15], the mechanism subjects suddenly stress to the impact element and thereafter releases the impact element from the stress. The impact element is compressed or alternatively stretched to such an extent as to change the length of the elastic impact element compared to its rest length. This change is of the order of a millimeter: 1-2 mm. If the elastic impact mechanism is released more slowly, the strength of the stress pulse propagating to the tool can be decreased and the length of the stress pulse increased. In Fig.17, the hydraulic fluid delivered from the pump stretches the elastic impact element until the desired stress state is

obtained. The stress state arises because, as it can be observed in Fig.17, the movement of the elastic impact element is restricted or limited. To provide a stroke, this feeding with hydraulic fluid under pressure is suddenly stopped by the 3/2-ways control valve. The elastic impact element is shortened and in consequence a stress pulse is propagated in the tool.

In [16] the impact device housing comprises a reciprocating movable tubular valve mounted separately of the impact piston. Channels are provided so as to act on the end surfaces of the tubular control valve. The control system can be analyzed in Fig.18. The reference [17] gives a method for monitoring the operation of a percussion device. As it is described, from pressure pulsation, parameters depicting the operating state of the percussion device are determined. Further, on the basis of the parameters the operating state of the percussion device is determined.

Fig.19 comprises a control valve 1 of the percussion device, a pressure sensor 2, a control unit 3 and analyzing device 3.

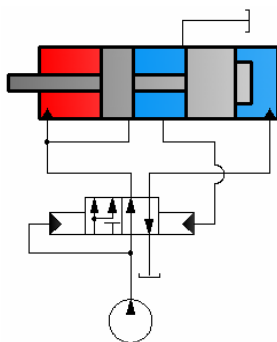


Fig.18. An operating principle of a percussion mechanism revealed in [16].

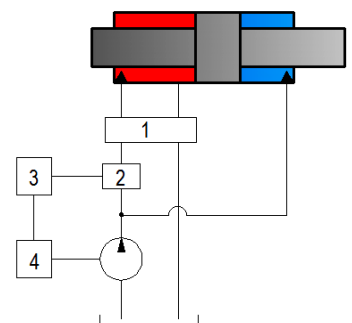


Fig.19. A schematically presented method for the operation of a percussion device, [17].

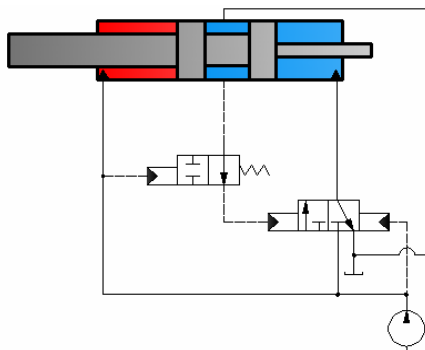


Fig.20. An operating principle of a percussion device, according to [18].

The operating state of the percussion device is conveyed from the analyzing device 3 to a control unit 4. The analyzing device and the control unit can be integrated into one device or unit.

The [18] patented document provides an automatic stopping of the hydraulic hammer if the operating pressure acting upon it reaches inadmissibly high values, Fig.20.

The 2/2-ways valve (the shut-off valve) is included for switching the working positions of the 3/2-ways control valve which controls the movement of the impact piston, Fig.20.

Instead of the pressure shut-off valve it can be used, according to [18], with a pressure-limiting valve.

Methods for controlling the operating cycle of an impact device are presented in [19, 20].

A sleeve control slide is arranged into a space formed around the percussion piston, acting as in Fig.21, like a 3/2-ways

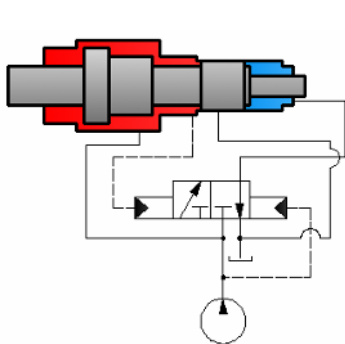


Fig.21. The operating principle of an impact device presented in [19].

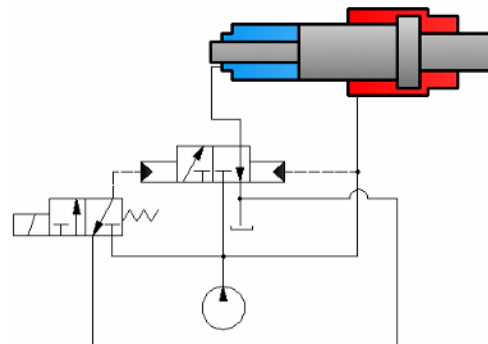


Fig.22. a) The operating principle of an impact device presented in [19] when the flow from a working chamber is discharged.

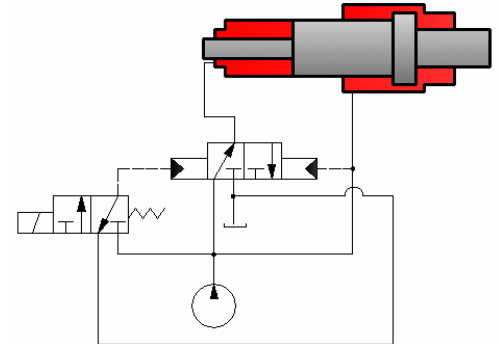


Fig.23. b) The operating principle of an impact device presented in [19] when the discharge from Fig.22 a) is interrupted.

control valve.

Changes in the travel direction of the percussion piston are controlled by means of the electrically driven 3/2-ways control valve illustrated in Fig.22 and Fig.23.

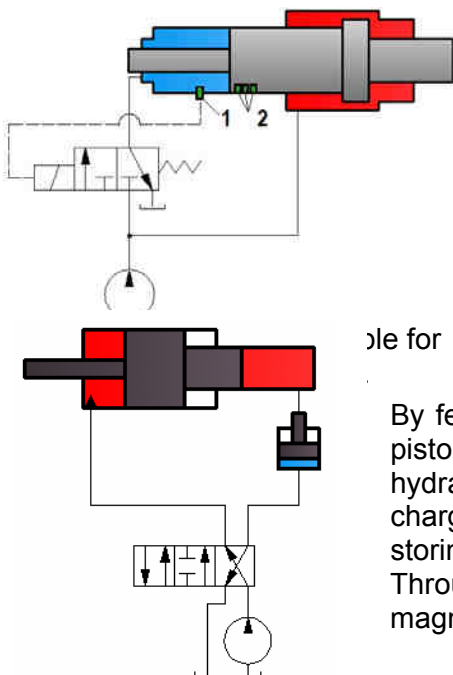


Fig.25. An operating principle for a rock drilling machine [21].

There is a sensor 1 included to detect the slots 2 made in the impact piston, when the piston passes the sensor 1, Fig.24. After the slots of the piston pass the sensor 1, the control valve switches its working positions and accordingly, the supply fluid from the pump flow through the 3/2-ways control valve.

The stress element used in [21] is again liquid and is subjected to pressure and correspondingly is released abruptly from the pressure.

It must be noticed in Fig.25 and Fig.26 the presence of a pressure intensifier piston. The machine housing can comprise one or more separate pressure intensifier pistons.

By feeding the pressure fluid to the intensifier piston, the intensifier piston is pushed towards the pre-charged working chamber of the hydraulic linear motor. As a result, the pressure from the pre-charged chamber increases and this space acts like an energy storing material. The volume in the pre-charged chamber is reduced. Through the Fig.26 and [21] it is proposed a structure by which the magnitude of a stress pulse can be raised without the pump.

After pushing the intensifier piston as desired, the pressure fluid flow is released abruptly by the 4/3-ways control valve. In consequence, the stress energy is discharged as a stress pulse to the tool in direct or indirect contact with the stress element.

In Fig. 27, according to [21], a separate piston is used to define as desired an energy storing space. The volume of the energy storing space can be modified in length by rotating a mechanical screw, as in the Fig. 26, or using other solutions to modify the position of the adjustment piston. In consequence, the volume of the energy storing space reduces or increases.

The change in the volume of the energy storing space can be used for controlling properties like the amplitude and the length of the stress wave pulse.

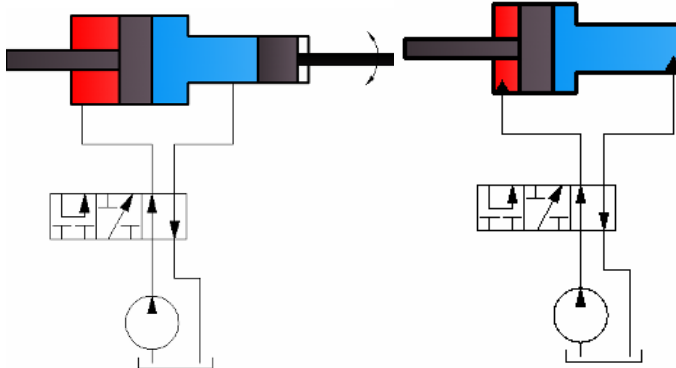


Fig.27. An operating principle for a rock drilling machine [21] with or without an adjustment piston.

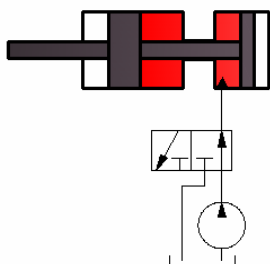


Fig.28. An operating principle for a rock drilling machine [21].

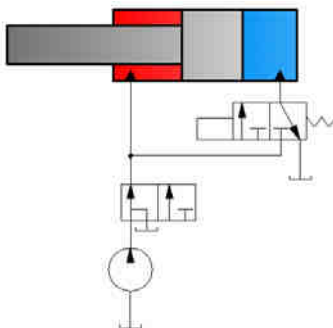


Fig.30. The operating principle of the percussion mechanism described in [23].

apparatus for percussive drilling, Fig.30 and Fig.31. The impact device acts independently of the rotation.

In Fig.28, according to [21], the stressing of the energy storing material is implemented with a two-part piston. The description of the operating principle is similar with the description yet provided through Fig. 16 and [21].

A method for controlling rock drilling on the basis of specific energy consumption, Fig. 29, is revealed in [22]. Accordingly, the specific energy of drilling is the quantity of energy used per a unit of length of the drilled hole. Not only the used impact energy, but also the energy used at least one other sub-process is taken into account when determining the specific energy. It can be moreover considered rotation energy, feeding energy and flushing energy. Drilling variables are adjusted so that the specific energy is of a predetermined size.

Sensors as flow sensors, pressure sensors, sensors to measure the volume flow produced by the pump at each time and a sensor for monitoring the penetration rate of the drilling device are included. The sensors transmit measuring data to a control device.

In [23] it is proposed and described a device for supplying hydraulic power to a rotary

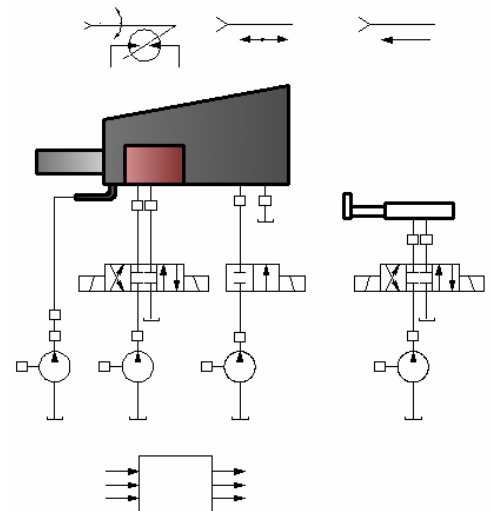


Fig.29. Method for controlling rock drilling on the basis of specific energy consumption [22]

The control system of the percussion mechanism presented in [23] is separately illustrated in Fig.30.

The supplying system for the percussion mechanism and the rotation mechanism of the impact device presented in [23] is illustrated in Fig.31.

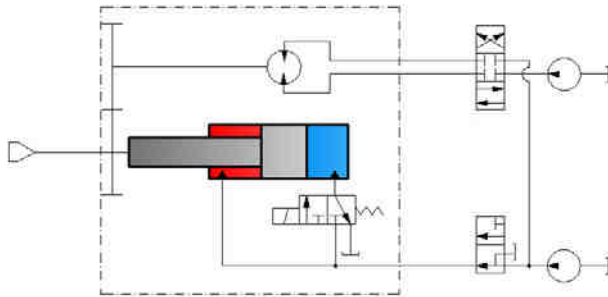


Fig.31. The operating principle of a hydraulic rotary impact device, [23].

A considerable subject is provided in [24]. Accordingly, it may be desirable to equip fluid operated impact devices with a mechanism that protects against no load strokes, particularly in the interest of avoiding undesired stress.

A control unit influences the movements of the percussion piston and is blocked by a safety element in the form of a multiple position valve actuated automatically, Fig. 32. As stated in [24], the percussion device starts up without being influenced by the safety element and is

halted if the percussion piston overshoots the extended position occurring in normal operation by a defined distance, thereby assuming a no-load-stroke position.

In [25] a method and device to determine the operating time and the operating condition of a hydraulic percussion unit is provided. A chamber which is arranged separately from the working chambers of the hydraulic linear motor is created, Fig.33. In this separate chamber a gas cushion under pressure is accommodated to support the percussion piston.

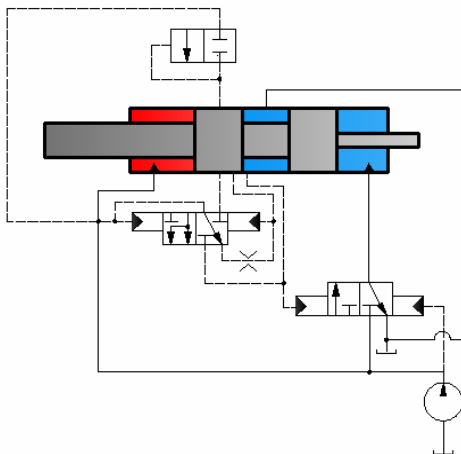


Fig.32. Method to prevent the blank firing of a percussive device [24]

Methods for minimizing blank firing or no-load strikes of a percussion device are unfolded in [26].

Even if a hammer generally operates well it can appear problems. A hammer operating with a tool not in contact with the rock (concrete or asphalt) is subjected to significant damages induced by the operation of the hammer itself. The amount of energy supplied by the high pressure hydraulic fluid which could not be transmitted forward to the rock is absorbed by the hammer. In consequence, the impact mechanism is heated or damaged.

The impact mechanism may be operated in a low frequency or in a slow mode for a selected initial period whenever the hammer is actuated. As suggested and affirmed in [26], the initial period of low frequency operation is selectable from an excavator cab by an operator by means of a hand operated control.

Accordingly, the control system provides a reduced flow of hydraulic fluid to the impact mechanism, for a selected period of time upon actuation of the hammer and then provides full hydraulic flow thus increasing the frequency of impacts to full rated values, Fig. 34, Fig. 35, Fig. 36.

A shuttle valve is provided to a variable

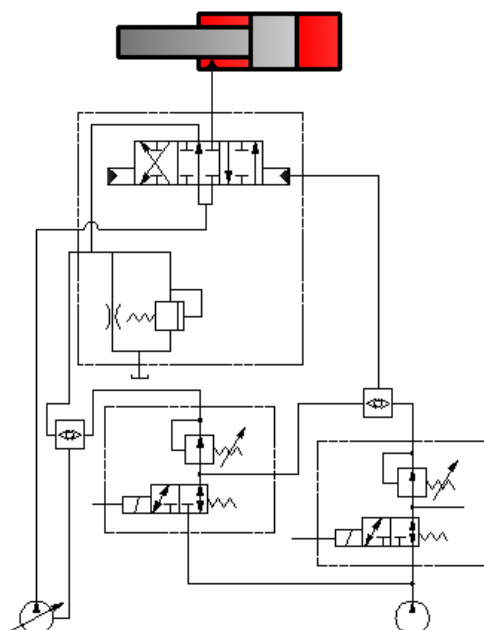


Fig.35. A control system to reduce blank firing of a percussion device,

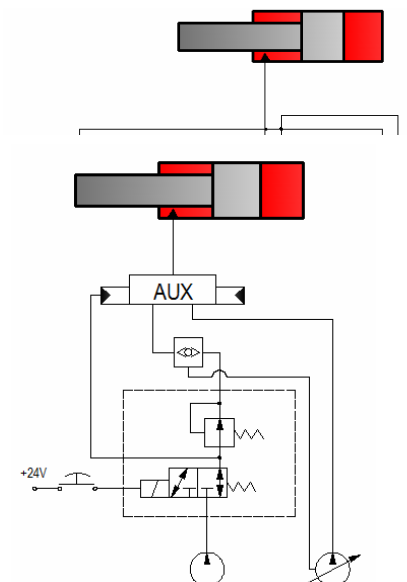


Fig.36. A control system to reduce blank firing of a percussion device, [26].

output main pump, Fig.35. The shuttle valve is further provided with two control inputs.

Generally, the auxiliary valves and pumps form part of an excavator as being commercially available products.

By means of the switch from Fig.36, the control system provides hydraulic fluid to the impact mechanism at rated flow and at rated pressure. The switch is an electrical one

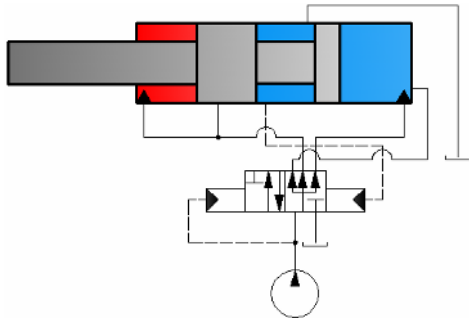


Fig.37. A control system for an impact device, [27].

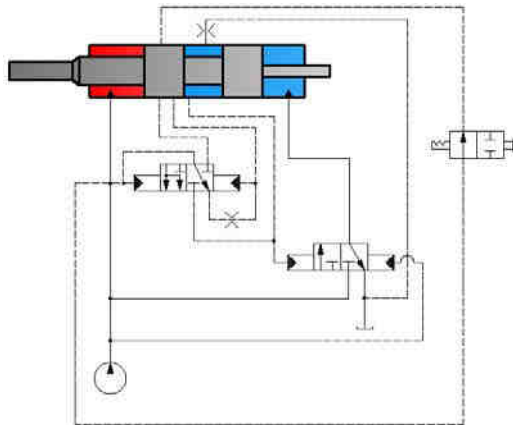


Fig.38. An operating principle of an impact mechanism according to [28].

percussion piston is shut down if it has overshoot the extended position occurring in normal operation by a predetermined distance in the work-stroke direction and reached the no-load strike position, Fig. 38. Its normal position refers to long and/or short stroke operation.

The aim of [28] is to achieve an impact device the high impact frequency substantially maintained without appearing cavitations problems.

A control system used generally by the percussion mechanism manufacturers is illustrated in Fig. 39 accordingly [29].

The hydraulic linear 3/2-ways distribution valve, Fig.38, can have variable hydraulic resistances [29] or passive (fix) hydraulic resistances with throttling valve on the discharge line [30].

Another typical operating system is conceived in [31] and comprises, Fig.40, variable and passive hydraulic resistances, a hydraulic accumulator and a 4/2-ways hydraulic linear distributor, a differential piston in the hydraulic linear motor, a constant output pump and tank.

and is positioned in the operator cab. As affirmed in [26] the switch can be a button or a lever operated by hand or foot. Accordingly, the switch is normally a momentary contact switch and it can be maintained closed to operate the impact device.

The machine housing from [27] includes the impact piston and the valve body which controls the piston movements. In order to speed up the impact piston movements there are two supply pressure lines.

Another method to treat blank firing is founded and proposed in [28]. To avoid no-load strikes, the

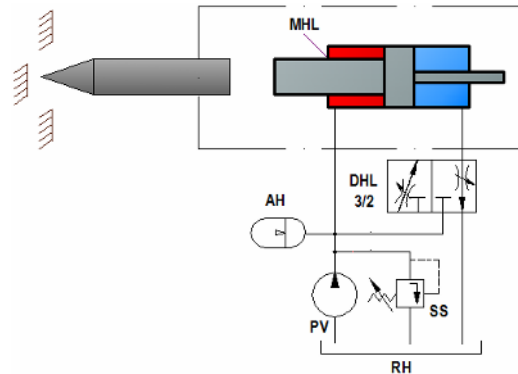


Fig.39. The typical operating system of an impact device, accordingly to [29], where:
MHL –linear hydraulic motor; 3/2 DHL – 3/2-ways hydraulic linear distributor; AH – hydraulic accumulator; PV – volumetric pump; SS – safety valve; RH –hydraulic reservoir.

REFERENCES

- [1] C.L. Jimeno, E.L. Jimeno, et al., "Drilling and Blasting of Rocks", translated by Yvonne Visser De Ramiro, ISBN 9054101997, 1995
- [2] M. Keskiniva, J. Maki, et. all., "Impact device and method for generating stress pulse therein", Assignee: Sandvik Mining and Construction Oy, Pat. No.: US 8151901 B2, 2012

- [3] G. Tuomas, "Method and device for rock drilling", Assignee: Atlas Copco Rock Drills AB, US 8151899 B2, 2012
- [4] B. Piras, "Percussion equipment driven by a pressurized incompressible fluid", Assignee: Montabert, US 8151900 B2
- [5] M. Pettersson, A. Johansson, "Hydraulic impact mechanism for use in equipment for treating rock and concrete", Applicant: Atlas Copco Rock Drills AB, Pat. No.: WO 2012/030272 A1, 2012
- [6] M. Keskiniva, J. Maki, et. all, "Pressure-fluid-operated percussion device", Assignee: Sandvik Mining and Construction OY, Pat. No.: US 7878263 B2, 2011
- [7] P. Birath, "Percussion device, drilling machine including such a percussion device and method for controlling such a percussion device", Assignee: Atlas Copco Rock Drills AB, Pat. No.: US 8069928 B2, 2011
- [8] W. N. Patterson, G. R. Patterson, "Internally dampened percussion rock drill", Pat. No.: US 8028772 B2, 2011
- [9] S. Lohmann, K. Fritz, et. all, "Hydraulic impact hammer with overpressure and piston-overtravel protection", Assignee: Atlas Copco Construction Tools GmbH, Pat. No.: US 7779930 B2, 2010
- [10] R. S. Henriksson, A. W. Lundgren, "Hydraulic impact mechanism", Assignee: Atlas Copco Construction Tools AB, Pat. No.: US 7410010 B2, 2008
- [11] E. Ahola, M. Esko, et. all., "Method for controlling pressure fluid operated percussion device, and percussion device", Assignee: Sandvik Mining and Construction Oy, Pat. No.: US 7836969 B2, 2010
- [12] M. Keskiniva, J. Maki, et. all., "Method of generating stress pulse in tool by means of pressure fluid operated impact device, and impact device", Assignee: Sandvik Mining and Construction Oy, US 7322425 B2, 2008
- [13] M. Keskiniva, J. Maki, et. all., "Impact device with a rotatable control valve", Assignee: Sandvik Mining and Construction Oy, Pat. No.: US 7290622 B2, 2007
- [14] M. Keskiniva, E. Ahola, et. all., "Percussion device with a transmission element compressing an elastic energy storing material", Assignee: Sandvik Mining and Construction Oy, Pat. No.: US 7441608 B2, 2008
- [15] M. Keskiniva, J. Maki, et. all., "Impact device", Assignee: Sandvik Tamrock Oy, US 7013996 B2, 2006
- [16] K. Andersson, "Percussion device", Assignee: Atlas Copco Rock Drills AB, US 2007/0267223 A1, 2007
- [17] M. Keskiniva, T. Kempainen, et. all., "Method and apparatus for monitoring operation of percussion device", Assignee: Sandvik Tamrock Oy, Pat. No.: US: 7051525 B2, 2006
- [18] H. J. Prokop, M. Geimer, "Hammer with high pressure shut-off", Assignee: Krupp Berco Bautechnik GmbH, US 6959967, 2005
- [19] A. Koskimaki, "Method for controlling operating cycle of impact device, and impact device", Assignee: Sandvik Tamrock Oy, Pat. No.: US 2004/0144551 A1, 2004
- [20] A. Koskimaki, "Method for controlling operating cycle of impact device, and impact device", Assignee: Sandvik Tamrock Oy, Pat. No.: US 6877569 B2, 2005
- [21] M. Keskiniva, E. Ahola, et. all, "Percussion device with a transmission element compressing an elastic energy storing material", Assignee: Sandvik Tamrock Oy, Pat. No.: US 2005/0139368 A1, 2005
- [22] V. Uitto, "Method and arrangement for controlling percussion rock drilling", Assignee: Sandvik Tamrock Oy, Pat. No.: US 2005/0006143 A1, 2005
- [23] B. Cadet, "Device for hydraulic power supply of a rotary apparatus for percussive drilling", Assignee: Montabert S.A., Pat. No.: US 6883620 B1, 2005
- [24] T. Ahr, T. Deimel, et. all, "Method and apparatus for protecting a fluid-operated percussion device against no-load strokes", Assignee: Krupp Berco Bautechnik GmbH, Pat. No.: US 6672403 B2, 2004
- [25] H. J. Prokop, M. Geimer, et. all., "Method and device for determining the operating time and the operating condition of a hydraulic percussion unit", Assignee: Krupp Berco Bautechnik GmbH, US 6510902 B1, 2003
- [26] R. A. Webel, "Slow start control for a hydraulic hammer", Assignee: NPK Construction Equipment Inc., US 6491114 B1, 2002
- [27] K. Andersson, J. Robert, "Hammer device", Assignee: Atlas Copco Rock Drills AB, US 6371222 B1, 2002
- [28] T. Deimel, M. Geimer, et. all, "Fluid operated percussion device", Assignee: Krupp Berco Bautechnik GmbH, US 6334495 B2, 2002
- [29] I.V.Mentez, „Influence of design factors on the efficiency of hydraulic hammers”, Journal of Mining Science, Vol. 39, No. 4, pp. 98-103, 2003, UDC 622.232
- [30] L.V. Gorodilov, „Calculation of the main parameters of a hydraulic percussive machine”, Journal of Mining Science, Vol. 35, No. 2, 1999
- [31] L.V. Gorodilov, „Mathematical models of hydraulic percussion systems”, Journal of Mining Science, Vol. 41, No. 5, 2005

HYDRAULIC SCHEMES FOR IMPACT DEVICES. A CONTROL SYSTEM FOR IMPACT MECHANISMS USING A ROTATABLE DISTRIBUTION VALVE – PART 2

Claudia KOZMA¹, Liviu VAIDA²

¹ Technical University of Cluj Napoca, Caudia.Kozma@termo.utcluj.ro

² Liviu.Vaida@termo.utcluj.ro

Abstract: A research on different structures regarding impact devices and the corresponding control systems can be viewed in the previous part of this article. Forward it is presented and proposed a control system and an operating principle for an impact mechanism disclosing a rotatable control valve. It is revealed also an experimental model, a 2D constructional drawing. The experimental model includes the control system.

Keywords: impact device, percussive mechanism, rock drill, hydraulic hammer, control system, control valve, linear hydraulic motor

1. A proposed control system for an impact mechanism

A proposed control system for a fluid operated impact device (hydraulic rock drill or hydraulic breaker) on the basis of a rotary valve is illustrated in Fig.1. The proposed control system is described in [1] and is to be patented [2]. A mathematical analyze of the hydraulic impact mechanism presented in Fig.1 is realized in [3]. It is underlined in [3] that the proposed control system is composed by passive hydraulic resistances. According to [3], the hydraulic linear motor used as an impact mechanism is controlled by a combination of half-bridges D+E. The passive hydraulic resistances form in a rotatable distribution valve, Fig.2.

The rotatable distribution valve has eight grooves on its cylindrical face, Fig. 1 and Fig.2. Four grooves are disposed as openings through which the C2 chamber of the hydraulic linear motor is connected to the hydraulic pressure source. Four grooves are realized alternately and through which the C2 drive chamber is connected to the tank.

The 3/2-ways rotatable distribution valve has its cylindrical spool comprised by the impact piston by means of a cylindrical bore, Fig.3. In the cylindrical bore the rotatable spool is mounted coaxially with the piston and is rotated around its axis by means of a suitable rotating mechanism. The valve sleeve or the rotatable distribution valve housing is constituted by the prominence b_p of the piston 2, Fig. 3. The spool is rotated in the piston bore through a shaft s .

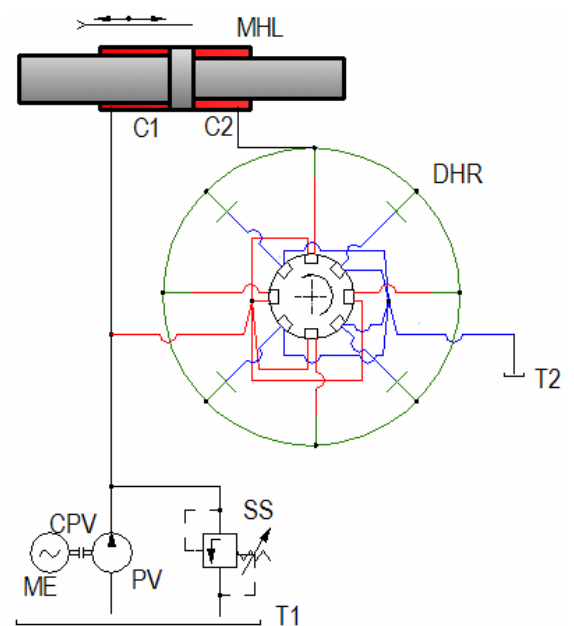


Fig.1. The hydraulic scheme of the proposed control system comprising: ME – electrical motor; CPV – pump coupling; PV – volumetric pump; SS – safety valve; T1, T2 – tank; DHR – hydraulic rotary distributor; MHL –linear hydraulic motor.

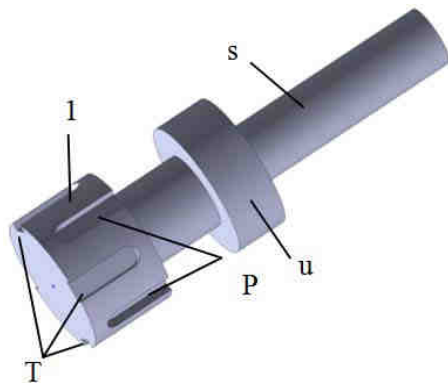


Fig.2. The rotatable spool of the distributor valve [2], where: 2 is the rotatable spool; T, the symbol for the return/discharge slots; P, the symbol for the supply slots; u is a fluid confine shoulder; s, the spool shaft imparting the rotation movement.

kinetic energy for the impact piston. Consequently, the impact piston moves towards the tool (a shank, a drill steel or a drill bit) and hits it. The collision energy is transformed in shock wave pulse and a part of it is delivered to the rock (or concrete or asphalt) and the rest returned.

The periodically alternating pressure arises in this manner with the periodicity that corresponds to the impact frequency of the impact mechanism and is directly proportional with the speed of the rotating mechanism which is provided to rotate the cylindrical spool.

The grooves of the rotatable distribution valve serve as small channels connected permanently to the pressure line, four of them, and the rest of it are permanently connected to the return line – Fig. 1 and Fig. 3.

The rotatable spool, Fig.2, presents axially grooves or slots notated with P and T to suggest the connection with the pump and with the tank.

The stress pulse is conveyed by the pressure fluid in the C2 drive chamber. The pressure fluid acts on the larger piston surface causing the piston to be pushed farther and compressing the fluid volume from the C1 working chamber. The liquid fluid is a storing energy medium. As the rotatable distribution valve continues to rotate, the hydraulic fluid from the C2 working chamber returns to the tank. By this pressure fluid discharge, the stored energy from the C1 chamber is transformed in a

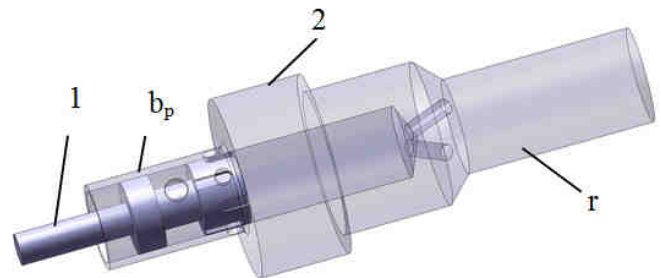


Fig.3. The rotating spool positioned in the body of a motor piston [2], where: 1 is the rotatable spool; 2 is the motor piston; r, the piston rod; b_p , the piston prominence.

2. An experimental model including the proposed control system

A next step after submission of the proposed control structure for a percussion mechanism is to design or project a physical structure for farther experiments.

In the designed structure, a linear hydraulic motor is built-up by two bodies, B1 and B2, Fig.4. The piston 2 of the linear hydraulic motor MHL delimitates two working chambers, C1 and C2, Fig.1. In Fig.4 is marked only the C2 working chamber, the position approaching to an end stroke. The rotatable spool 1 of the hydraulic distributor is, accordingly, mounted in cylindrical bore which is realized in the piston rod opposed to the rod piston denoted as r. Farther, the rotatable spool has a shaft s assembled by means of a woodruff key with the shaft of a hydraulic gear motor MRD2-212D. By rotating the rotatable spool shaft s the spool 2 changes its working positions. In a one working positions, the fluid flow transmitted through the supply line PL passes via the P slots (Fig.3) in the working chamber C2. A pressure arises and acts upon the piston surface against the pressure acting permanently in the working chamber C1. The piston surface from the working chamber C2 is larger than the piston surface from the working chamber C1, disclosing a differential linear hydraulic motor. The pressure arising in C2 chamber is greater that the corresponding one in C1 chamber and pushes the impact piston toward the tool. The tool can be a shank, a drill steel or a rod bit.

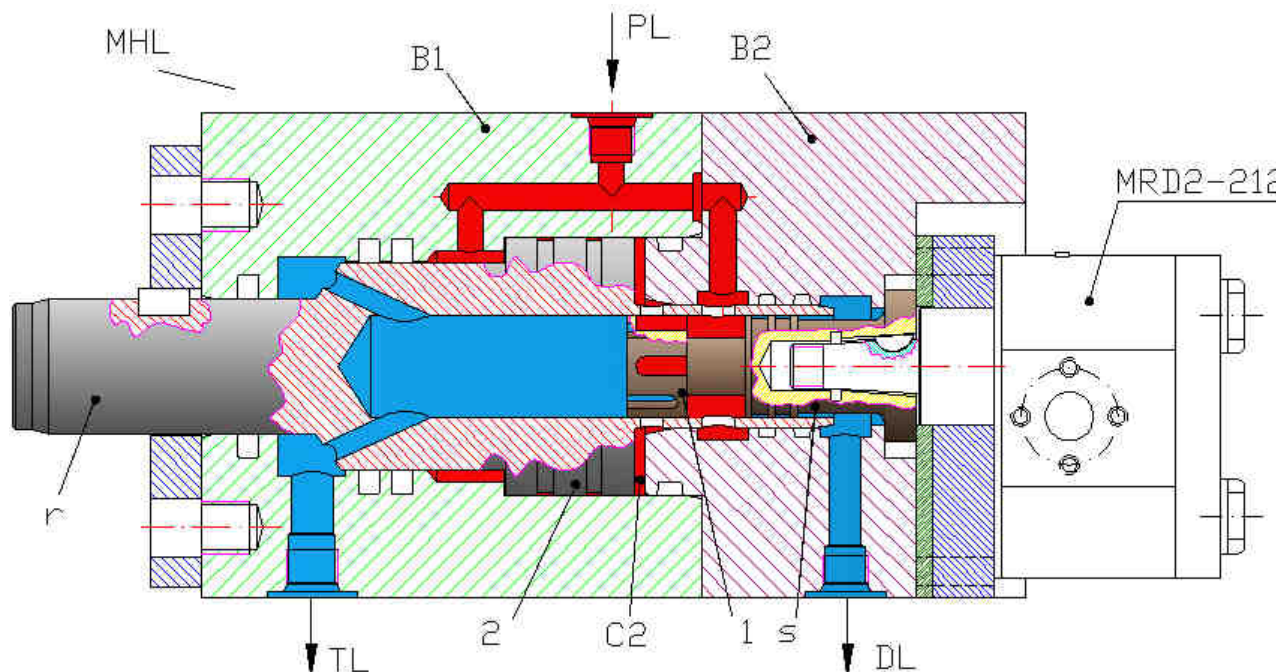


Fig.4. The conceived experimental model with the proposed control system included, where: B1 and B2 are the two bodies of the impact mechanism; P is the supply line; T is the discharge line; D is the drainage line; 1 is the rotatable distribution valve; s is the shaft of the rotatable distributor; 2 is the impact piston; r is the rod piston; MRD2-212D is the hydraulic gear motor for the rotation of the rotatable distributor shaft.

To be noticed that the fluid flow from the working chamber C1 is not sent to the tank and is directed to the working chamber C2 thus increasing the impact piston speed.

In the other working position of the 3/2-ways rotatable distributor, by means of the T slots of the rotatable spool 1, fluid flow from the C2 drive chamber is sent to the return or discharge line TL as the pressure from C1 working chamber pushes the piston back.

The return stroke is alternated continuously by the forward stroke and the length of the impact piston stroke depends on the shaft speed of the rotating mechanism MRD2.

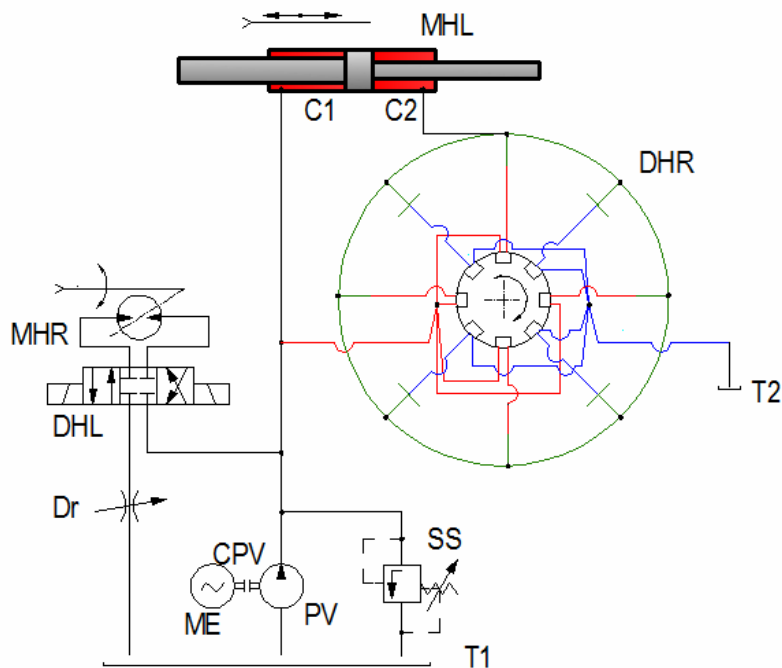
Furthermore, flanges and sealing gaskets are included in the design of the experimental model. A drainage line DL collects and directs the leakages to the hydraulic reservoir.

The energy transmitted to the tool is used in the collision of the rod bit and the rock (asphalt or concrete) to dislocate the material by repetitive strikes.

A rotatable mechanism can be used in parallel with the impact mechanism from Fig.4 to rotate the tool according to the requirements.

In the previous part of the article it is illustrated a device for supplying hydraulic power to a rotary apparatus for percussive drilling where the impact device acts independently of the rotation. The two mechanism are supplied with hydraulic pressure from two separate hydraulic pressure sources. It is known in [1] that the percussion mechanism and the rotation mechanism are supplied from the same hydraulic pressure source, are mounted in series and operate simultaneously. To supply the impact mechanism with fluid pressure, a control valve must be moved against a force spring. The percussion mechanism is blocked unless a predetermined value is exceeded. According to [1], the percussion mechanism and the rotation mechanism work „in series” permitting the work tool (the drill pipe and the bit) to rotate without necessitating to start the percussion mechanism and by varying the inlet rate of flow.

A single hydraulic pressure source (pump) simplifies the hydraulic circuits but the rotation remains completely dependent on the percussion.



In Fig.5, it is included a rotary mechanism for the rotation of the tool working completely dependent on the impact mechanism.

Farther improvements on the proposed control system conceived for a percussion mechanism can be discussed and applied regarding the previous part of this article and [1].

Fig.5. The hydraulic scheme of the proposed control system operating simultaneously with the rotation mechanism, where: MHR – hydraulic rotary motor; DHL – linear hydraulic distributor; DR – throttling valve.

REFERENCES

- [1] C. Kozma, „A constructional and functional improvement in hydraulic rotary percussive drill”, Proceedings of 2011 International Salon of Hydraulics and Pneumatics – Hervex, ISSN 1454-8003, 2011
- [2] L. Vaida, C. Kozma, *Generator hidraulic de vibrații pentru perforatoare hidraulice rotopercutante*, registered to OSIM: A/10018/2012
- [3] C. Kozma, *Mathematical modelling of a hydraulic vibro percussive system*, SIDOC Project – Doctoral students' session, 2012

STRENGTHENING SURFACE LAYERS OF COMPONENTS

Marian KRÁLIK¹

¹ Faculty of Mechanical Engineering, Slovak University of Technology in Bratislava, marian.kralik@stuba.sk

Abstract: *Ultrasonically oscillating technological tools are able to intensify and enhance the quality of material shaping and machining processes. Present paper deals with strengthening surface layers of components. Properties of surfaces can influence the workability of cyclically stressed components, such as antifriction bearings. The change in surface layers properties can be influenced also by plastic deformations that are dealt with in the paper as well. Present paper describes the background for ultrasonic hardening of surface layers – as applied at the department determination of tensions in the surface layer by means of calculations and some result of performed experiments.*

Keywords: *hardening surface layers, plastic deformations, ultrasound, simulation*

1. Introduction

One of the criteria of assessing the quality of components manufactured is the preciseness of its dimensions, geometrical preciseness and surface roughness. Increasing demands to operational properties of the product enforce monitoring and evaluating of chemical and physical changes in the surface layer of machined surfaces of components as a result of the manufacturing process. Under plastic materials machining the field of plastic deformations penetrates also into the work-piece layers that are under the cutting edge. The largest deformations arise directly at the surface and are lowering with increased depth. In a particular depth below the surface the original, not deformed structure of the material exists. Plastic deformation of metal materials is always connected with the hardness change and with occurrence of residual stresses.

2. TO PLASTIC DEFORMATION OF SURFACE LAYERS

Cold plastic deformation is the most simply way how to change mechanical properties of materials. A precondition to improving effectiveness of the process was a more detailed knowledge of the strengthening mechanism and its impact on changes in the utilizable characteristics of components with the aim to determine optimum technological conditions. That's why theoretical and experimental studies are developed and a major attention is given to improving the process and even more the control.

The plastic deformation is the most common way of a permanent change in the solid's form. Main mechanism of plastic deformation is the slip realized by slipping motion of dislocations. Reasons to the experimentally monitored complex form of the stress – deformation interdependence is to be found in the changed conditions of the motion of dislocations. Plastic deformation is connected with the significant hardening. Increase in hardening, lower yield point and hardness can be expressed by different concepts including the impact of deformation conditions (mainly the temperature, size and speed of the deformation), as well as by the interrelations between mechanical properties and structure of the material in terms of the size of the grain, density of dislocations, etc. Physical and mechanical properties of the surface machined are then different than those of the material in the whole cut through the work-piece. Its hardness is significantly higher, toughness is lower, etc. In some materials, surface hardness is 30% higher than the hardness of the basic material of the work-piece. Crystallization structure, size of the grain, chemical composition, content and impurities are main parameters determining the behaviour of deformation. Their impact can be seen in changes in microstructure, motion of dislocations and interactions between grid disturbances. Studies of deformation behaviour of the material while chip breaking are oriented on micromechanisms based on material damages due to breaking.

3. SIMULATION AND MODELLING OF THE DYNAMIC HARDENING PROCESS WITH 20 kHz VIBRATED TOOL

Surface layer hardening simulation by means of the ultrasonically wobbled tool using the combined method of final and discrete elements was applied in order to achieve, via surface treatment of machine parts, increased fatigue life by implementing pressure surface stresses. The applied combined method includes advantages of both materially and geometrically non-linear final elements methods and mutual interaction of a large number of bodies (discrete elements). It facilitates dynamic solution of tasks, i.e. propagation of stress waves and their mutual interaction. The main principle is on the Fig. 1.

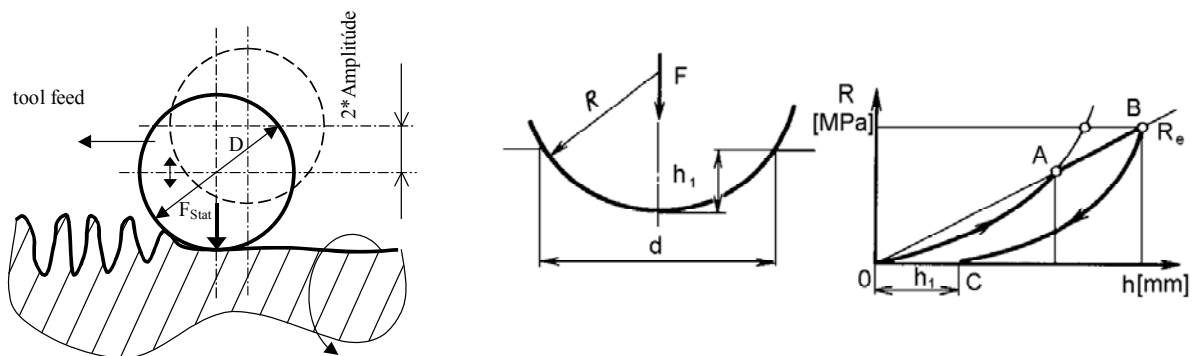


Fig. 1 Ultrasonic hardening process by surface quality enhances and surface changes on the ball incidence on the surface and the course of elastic and plastic deformation according to stress [2]

Under the hard ball incidence on the surface, while force of the ball's acting is F , according to the magnitude of F , at first an elastic deformation of the surface occurs and then a plastic one (the curve OAB at the Fig. 1).

Due to plastic deformations occurred, the relieving process proceeds along the BC curve. The residual plastic deformation is manifested by the impression dimension d that corresponds to the dimension OC. Plastic deformation below the impression is evenly distributed as if copying the ball's surface, friction not taking into account. The depth of material compression h is proportional to the depth of impression h_1 , that means $h = mh_1$. According to the conditions of the technological process coefficient $m = 2 \dots 20$. Author of the publication [3] finds out that impression diameter d and the ball's diameter D is appropriate to describe plastic deformation. Under normal conditions of shot peening the ratio d/D is in the range $0.1 - 0.2$. Similarly we can calculate the depth of the layer (h_p) affected by the plastic deformation. In practice empirical relations for particular types of material are used. For steel the $h_p \approx 1.5 d$, for aluminium alloys $h_p \approx (5.8 h D/h)$ where h is the depth of impression. The equations mentioned don't take into account friction conditions impact, assume that solid contacted are isotropic and behave according to Hook's law, the contact surface is small and a loading force acts vertically on the surface.

4. CONDITIONS AND OBJECTIVES OF EXPERIMENTAL INVESTIGATION

In the proposed simulations the following conditions were considered:

- The tool tip has a shape of a semisphere
- High-frequency tool excitation of 20 kHz
- The tool is considered to be a perfectly solid body.

Simulation computations were carried out for selected machine part and tool geometries:

- Material: bearing steel STN 14 109.6
- Modulus of elasticity E= 210 000 MPa

- | | |
|----------------------------------|-------------------------------|
| • Poisson's ratio | $\nu = 0,3$ |
| • Initial yield point | diameter 40 mm, length 230 mm |
| • Tool spherical area diameter | 8 mm |
| • Tool vibration amplitude | $A = 36 \mu\text{m}$ |
| • Tool feed | $f = 300 \text{ mm.s}^{-1}$ |
| • Coulomb's friction coefficient | $\mu = 0,7 \text{ or } 0,05$ |

For simulation of the surface layer hardening with ultrasonic vibrations instrument the combined method finite and discrete element was used. The obtained results on presented pictures show on changes in surface layer.

The objective of the performed simulation computation was:

- Determination of the residual stress in the surface layer
- Determination of local plastic areas
- Stress wave propagation in the surface layer.

5. RESULTS AND DISCUSSION

The research published by the authors in [1] was devoted to investigation of the contact surface influenced by wobbling tool after the time $t = 0.00005 \text{ s}$, $t = 0.02 \text{ s}$ and $t = 0.04 \text{ s}$ which relates, with respect to the hardening tool feed speed, to the nearly first tool contact, then contact after 6 mm and finally contact in distance of 12 mm from the first tool contact with the hardened material. Within the surface layer analysis there were made partial analyses of axial stress courses in the depth under the surface and the plastic deformation course in dependence on time. From a large number of outputs only those have been selected for this paper, which indicate the size and course of plastic deformation, specifically after the tool travelled 12 mm (Fig.2).

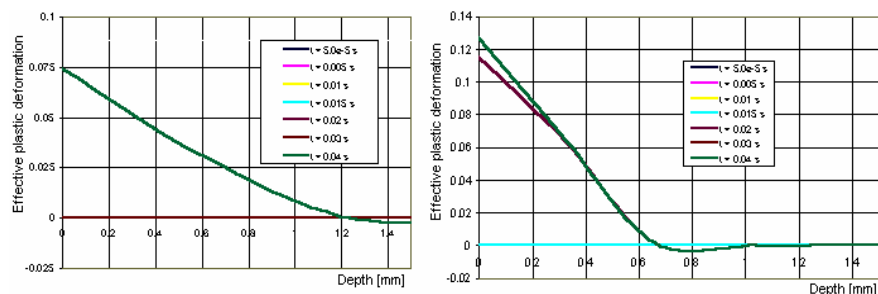
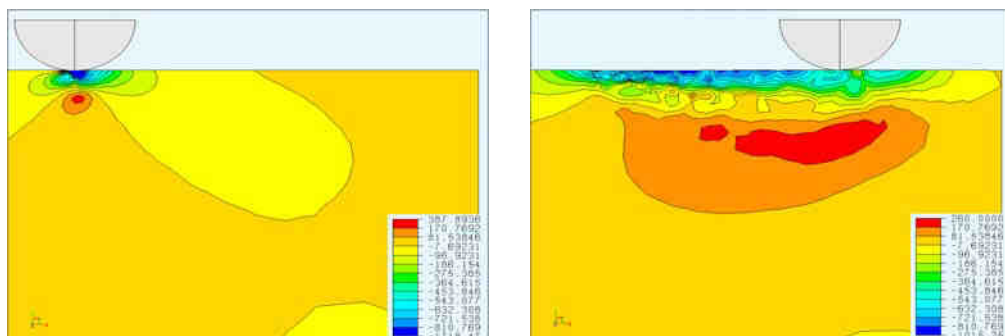


Fig.2 The course of plastic deformation in the depth at the beginning of the motion and after the tool travelled 12 mm, $D = 8 \text{ mm}$, $A = 36 \mu\text{m}$, $f = 300 \text{ mm s}^{-1}$, $\mu = 0,7$

Interesting is the course of the tool contact force on the workpiece surface. Simulation was carried out in a regime when the tool touches the surface with a zero push force (a limit state) and the double amplitude causes the below presented force course. The force, after the higher initial value, gradually stabilizes at the value of approximately 600 N. This is probably due to diminishing the area on the workpiece, which is deformed under the impressed ball influence during further



impacts (Fig. 3 and 4).

Fig.3 The material stress on the start and after 12 mm the motion, $D = 3 \text{ mm}$, $A = 36 \mu\text{m}$, $f = 300 \text{ mm s}^{-1}$, $\mu = 0,7$

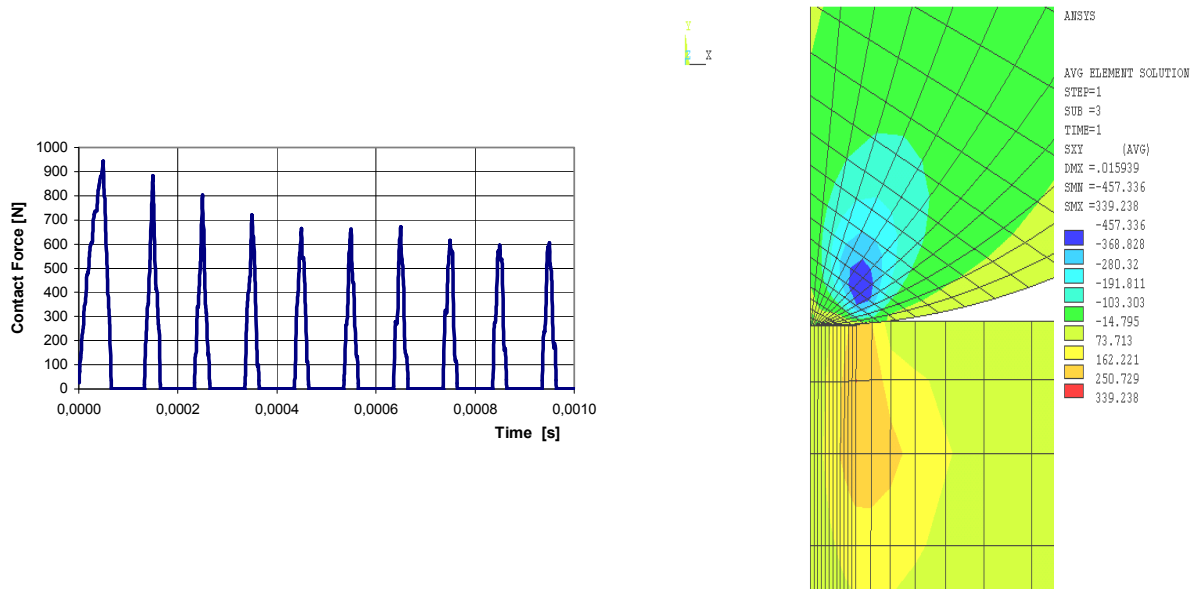


Fig. 4 Detail of the contact force course between the tool tip and workpiece (on the left) and area of the slip stresses under tool (right side)

In fig. 5 illustrative schemes of solution of tools used in ultrasonic dynamic hardening of precise surfaces of metal materials is presented.

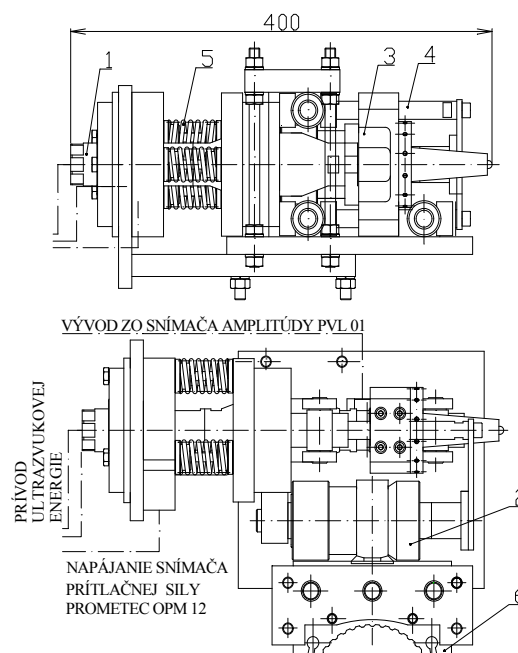


Fig. 5 General design of ultrasonic tool. 1- ultrasonic resonator, 2- leading radial tool movement, 3 - tool, 4 – leading system, 5 –pressure spring system, 6 – gripping on machine tool.

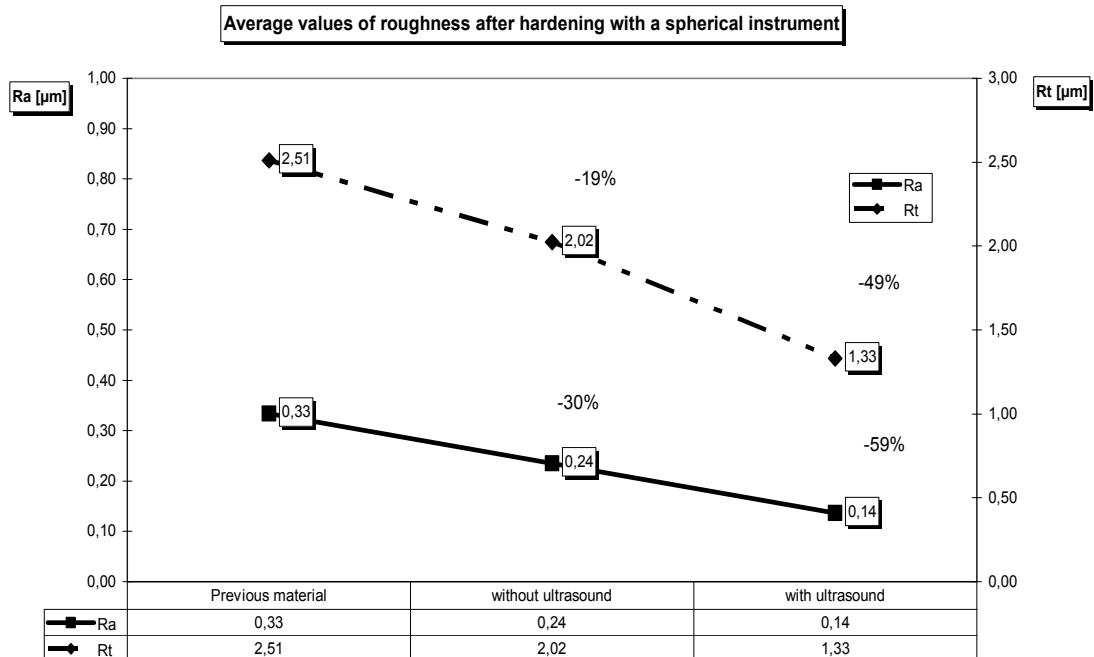


Fig.6 Average values of surface roughness Ra and Rt after hardening with spherical instrument with tool material of cemented carbide P20.

From the diagram you can see the reduction surface roughness. Using ultrasound affects the reduction of values Ra and Rt on value 50% initial roughness (Fig. 6).

On the fig. 7 is displayed the change of material ration (Abbott) curve. On the left side is material ratio (Abbott) curve before hardening (after grinding); on right side is material ratio curve after ultrasonic hardening.

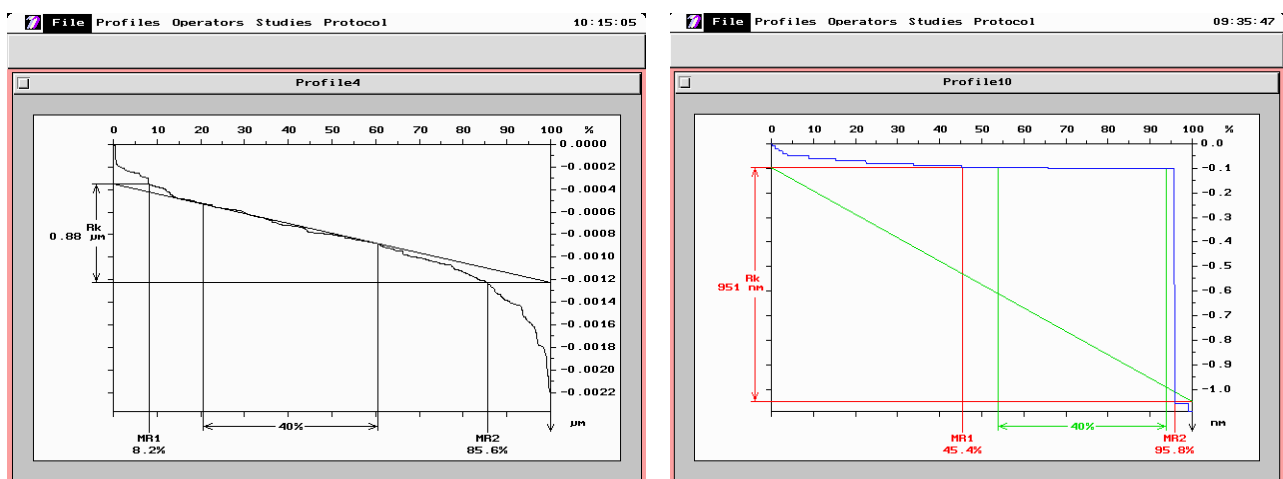


Fig. 7 Material ratio (Abbott) curve before hardening and after ultrasonic hardening according to norm STN EN ISO 13 565-2

6. Conclusions

Currently we are dealing with dynamic hardening of circular paths of antifriction bearings rings by ultrasonic methods. Performing experiments were the content of the research project VEGA 1/1056/12 that was also a background of our paper.

REFERENCES

- [1] Tolnay, M., Králik, M., Bachratý, M: Simulation and modelling of the dynamic hardening process with 20 kHz vibrated tool. In ITC 2009 : 7th International tools conference. Zlín, ČR, 3.-4.2.2009. Zlín: Univerzita Tomáše Bati ve Zlíne, 2009, ISBN 978-80-7318-794-1.
- [2] Odincov, L.G.: Upročnenije i otdelka detalej poverchnostnym plastičeskim deformirovanijem. Spravočnik. Mašinostrojenie, Moskva 1987
- [3] Tolnay, M. – Králik, M. – Élesztös, P. – Mihalčák, P. – Vlnka, J.: Simulation of dynamic hardened contact process with ultrasonic vibrated tool. In TRENDS IN THE DEVELOPMENT OF MACHINERY AND ASSOCIATED TECHNOLOGY: 7TH. Trends in the development of machinery and associated technology. TMT 2003: Proceedings. Zenica: University of Zenica, 2003, s. 533–536.

CAMIRO LONG LIFE NEW HYDRAULIC EQUIPMENT TECHNOLOGY FOR DRILLING FLUIDS AND SALT WATER INJECTION PUMPS

Miron M. PROCOP, Oana-Miruna PROCOP, Rodica PROCOP.

SC. CAMIRO ENGINEERING SRL. Constanta, 900716, 2C - 1 Decembrie 1918,

Tel: +4 0722679476; Tel/Fax: 0341-409865.

www.camiro.eu, camiro.group@gmail.com, Romania

Abstract: *The present paper describes the new technology that started the improvement of the hydraulic equipment of drilling mud pumps 2PN 1600 and 3PN 1600 type, used in drilling of oil wells on rigs in the Black Sea and onshore of salt water injection pumps 2 PN 400 mounted in OMV Petrom sites.*

Keywords: *high-pressure piston, high endurance, variable profile, balancing surface wear*

1. Introduction

As researches that are made at world scale regarding the friction and wear behavior of high performance polyimide (PI) and its composites reinforced with glass fiber add-ons, short cut carbon fiber and solid lubricants such as graphite, MoS₂ and polytetrafluoroethylene (PTFE) have evolved in two directions: under dry sliding and under water lubrication with open circuit, aiming at selecting matching materials for the pumps of pure water power transmission. The wear mechanism in the two directions regarding to compound friction and friction conditions has been comparatively analysed on scanning electron microscopic examination of the worn composite and steel counterpart surfaces.

Research revealed as the results, the incorporation of solid lubricants and carbon fiber in PI contributed to improve the friction and wear behavior considerably. PI-based composites sliding against stainless steel register higher friction coefficients and wear rates under water-lubricated condition than under dry sliding.

The difference in the wear rates of the composites becomes margined under water lubrication, owing to the boundary lubrication effect of the water absorption layer, though the transfer of PI and its composites was considerably hindered in this case. PI and its composites are characterized by plastic deformation, micro cracking, and spalling under both dry- and water-lubricated sliding.

Such plastic deformation, micro cracking, and spalling is significantly abated under water-lubricated condition. This accounted for the better friction and wear behavior of the composites under water-lubricated condition. [3], [4], [5], [6].

2. Experimental.

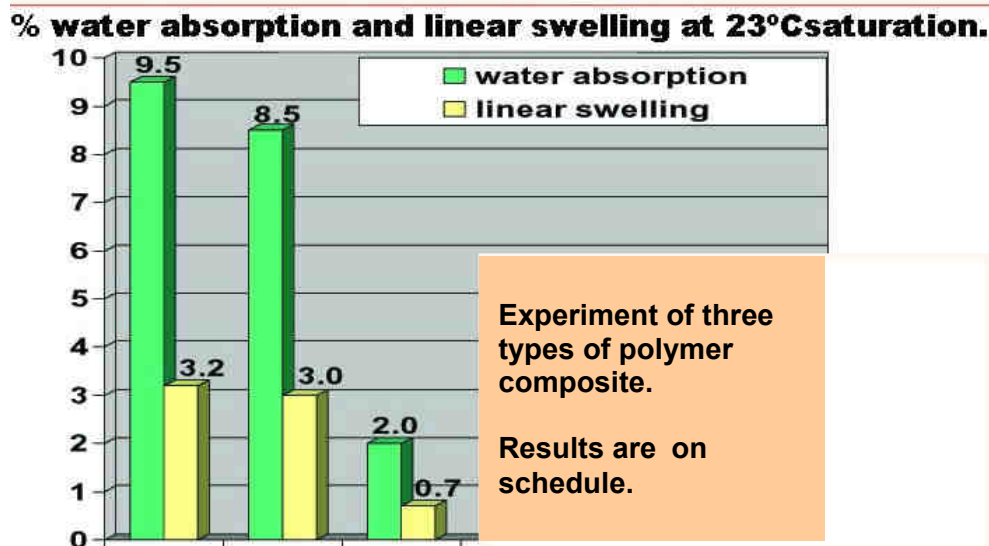
Tribological study regarding the behaviour of materials used in prior manufacturing of hydraulic-operated power cylinder and drilling pump piston as building block revealed the following aspects:

- hydraulic-operated power cylinder and drilling pump piston building block is subject to an alternate stroke wear – active process due to tough working conditions: $P_{nom} = 120\text{--}500$ bars; $R_{g.surf.} = 0,6\text{--}0,4\mu\text{m}$; $T = 60\text{--}90^\circ\text{C}$, the drill fluid is contaminated with silica microparticles.

- The design, the choice of materials, form and dimensions do not insure the tehnologic role of drilling pump piston.

The answer was choosing the right tribomaterials, that could insure the gaskets working order of piston at 500 bars, in andurance conditions, that can insure a higher working durability than the drilling time of oil well.

According to data tribo-materials behavior result



To obtain an active variable profile of the specially-designed gasket, the right trek is to adopt the tribo-materials water lubricated, that can insure the permanent seal and centering of the piston with abutting joint. Also, tribo-materials based composites sliding against stainless steel register higher friction coefficients and wear rates over water-lubricated condition than under dry sliding.[3]. The friction coefficient increases unsignificant because a 20% AquaLube water solution was used as a lubricant. The AquaLube water solution is an environment-friendly monomer with exceptional lubrication properties.



The results were obvious in the drilling well GALATA EAST FINDER WELL – A, on the SATURN jackup oil rig, on the continental plateau of Turkey, when only 6 cyliders of 6 3/4" were used and 6 pistons of 6 3/4" with active variable profile were used.

No tehnological stop due to the hydraulic equipment was registered on the entire drilling time and the cementing operations at 2500 m.

Fig. 1. Checking equipment CAMIRO LONG LIFE with variable profile.

Fig.2. The circular uniform wear of the special gaskets with variable profile. (Old and new Camiro piston for simplex and douplex pumps).



FIG.3. The new Long Life CAMIRO hydraulic equipment for mud pumps and salt water injection pumps 2 PN 400 was mounted in OMV Petrom sites.



3. Conclusions

CAMIRO high-pressure, high endurance pistons with variable profile for balancing surface wear insure under given conditions:

- Water lubrication in open circuit of working surfaces of the hydraulic equipment and wear protection of pressure-cylinder metallic surfaces;
- Pressure-cylinders are wear protected by the elements that insure the variable profile and determin the increase in there using time, drastic reduction of technological stop time, of cost in spare parts and maintenance;
- Productivity is high due to increased endurance of piston-pressure cylinder building block resulting in a controlled high-pressure seal;
- The piston maintenance service is safe, quick and ergonomic;
- Climatic and protection conditions of CAMIRO pistons have to be under strict control due to the properties of the used materials.

- Thus, the pistons have to be stored in low atmospheric humidity under 5%. In case of higher atmospheric humidity other protective measures are in order: - the gasket have to be protected by a thin layer of grease after there fabrication;
- After building-up the pistons have to be protected with grease in plastic bags.

4. Acknowledgments

The authors wish to give thanks to PETROMAR, OMV PETROM, GSP DRILLING Co. and RIG SERVICE from CONSTANTA for their given assistance in the testing of the experimental model of the new piston with variable profile for balancing surface wear of CAMIRO ENGINEERING.

REFERENCES (Arial, 11pt, Bold)

- [1] www.camiro.eu
- [2] camiro.group@gmail.com
- [3] Lorena Deleanu, Iulian Barsan: PTFE Composites and Water Lubrication Rev. Materiale Plastice, Bucuresti Romania, Chem. Abs.: MPLAAM 44 Vol.44,nr.1,martie 2007.
- [4] J.H. Jia, H.D. Zhou:A comparative investigation of the friction and wear behavior of polyimide composites under dry sliding and water –lubricated condition, State Key Laboratory of Engineering Plastic, Institute of Chemistry, Chinese Academy of Science, P.O. Box 2907, Beijing 100080, People's Republic of China - Materials Science and Engineering A Volume 356, Issues 1-2, 15 September 2003, Pages 48-53 - <http://www.sciencedirect.com>
- [5] Yu-Hsing Wang¹, J. Carlos Santamarina²: Dynamic Coupling Effects in Frictional Geomaterials — Stochastic Resonance, J. Geotech. and Geoenviron. Engrg., Volume 128, Issue 11, pp. 952-962 (November 2002);
- [6] N.L. McCooka, M.A. Hamiltona: Tribological results of PEEK nanocomposites in dry sliding against 440C in various gas environment, Department of Mechanical and Aerospace Engineering, University of Florida, Gainesville, FL 32611, United States. <http://www.sciencedirect.com>

SOME ASPECTS OF THE DRIVE WITH THE MASSES UNBALANCED VIBRATING

Stoica Dorel¹, Voicu Gheorghe², Carmen Otilia Rusanescu³

¹ University Politehnica Bucharest, Biotechnical Faculty of Engineering, dorelstc@yahoo.com

² University Politehnica Bucharest, Biotechnical Faculty of Engineering, otiliarusanescu@yahoo.com

Abstract:

Mathematical modeling of vibratory phenomena of machines with working with vibratory motion requires a number of simplifying assumptions that make the analysis result to depart more or less real phenomenon [1].

Kinematic and dynamic study of surface separation (body work) is required to estimate the interaction with the workpiece and its movement on work surface, coupled with the proper conduct of the process of separation or transport.

Keywords: sieve, generating vibrations, sizing counterweight

1. Introduction

The separation of particles through sieve openings within blocks of flat site separation is achieved by providing a relative movement (sifting) them to the filter surface. Relative displacement of particles is obtained by printing an oscillating vibrated or rotational movement block screenings. Screening machines which are made up of separate blocks with oscillating flat site can be operated with different systems or actuators such as eccentric mechanism or mechanisms such as vibration generators drive with rotating unbalanced masses [2]. These mechanisms can be swings (vertical rotation counterweights) or mechanisms vibrating electric called with (horizontally rotating counterweights).

The vibration generator used to drive the oscillating blocks are present in systems with rotating unbalanced masses, resulting in disruptive force directed (unidirectional).

Working body vibrating machine (with block site) is generally a movement of translation, linear or circular, depending on the type vibration generator.

Working oscillations vibrating body (in our case sieves) in a particular direction, are those printed material relative motion of particles per site, so important for sifting motion. Unbalanced mass vibration generators with rotating inertial forces developed with periodic variation due to eccentric rotating unbalanced masses. The weights used are volanții static unbalanced unbalanced mass at the center is not on the axis of rotation. And dynamically unbalanced flywheels are used in the centrifugal moments of inertia are different from zero or combinations of these two types of flywheels.

Absolute orientation in space and time variation character of the forces and moments developed depends on body movement to be driven and the engine that drives unbalanced masses.

They are important for particles to be separated holes and for particles larger than the openings to be transported to escape so as not to worsen the separation process. In operation, the drive of a building site separation, two vibrating with ballast can occupy one of the positions of figura.1.

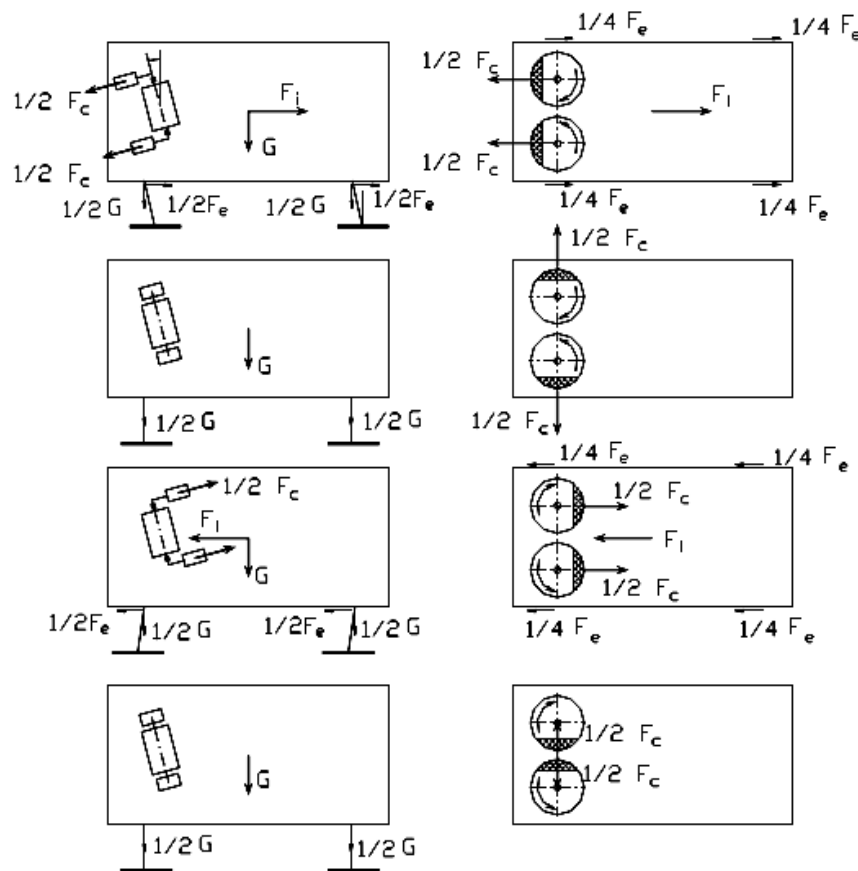


Fig.1. Pozițiile limită corespunzătoare ale mecanismului de acționare cu două generatoare de vibrații,

2. Materials and methods

Analyzing the forces acting on a system composed of two mechanisms electric vibrators and block screenings (if the axis of rotation is vertical counterweights) noted that: the center of gravity of the two vibrating counterweights (upper or lower) is always on the same level; components of inertia forces F_c , the counterweights, perpendicular to the longitudinal axis of the block with the site have the same horizontal direction and auto balance; components of inertia forces F_c , parallel to the longitudinal axis of the block with the site dynamic balancing force resistant to displacement thereof, together with the inertia of the entire system (Fig. 2).

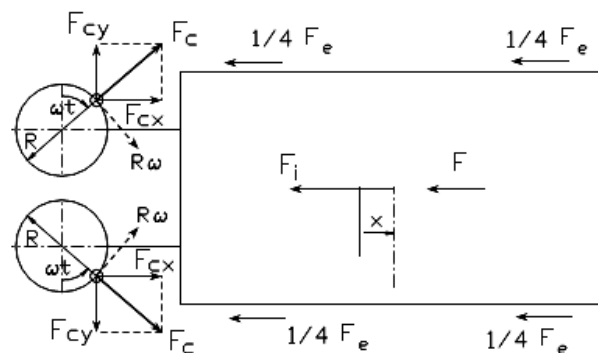


Fig.2. Forces acting on the block diagram with two generators driven site vibration (top view)[1]

3. Results and discussion

- Resistant forces moving block screenings are:
- Resistance force due to deformation of elastic support $F_e = c \cdot z \cdot x$;
- Force the block back to its original position due to removal from the position $F_r = (M + 2m)g \cdot \frac{x}{l}$;
- The force of inertia of the whole system $F_i = (M + 2m) \frac{d^2x}{dt^2}$,

where M is the mass separation block (including vibration generators without ballast mass), m - total mass of the two counterweights of a vibration generator, x is the horizontal displacement of the system, l - length brackets, c - stiffness of the elastic element, z - number of elastic support; g - acceleration of gravity.

Neglecting vertical displacement of the center of gravity, elasticity environmental support and resistance based on momentum conservation law passed by rotating counterweights two electrovibratoare, the entire system (Fig. 1), we can write the relation:

$$2m \cdot \omega R \cos(\omega t) \cdot \cos \varepsilon = (M + 2m) \cdot \frac{dx}{dt} \quad (1)$$

where:

- Dx / dt is the rate of movement of block with site horizontally;
 - $R \cos(\omega t) \cos(\varepsilon)$ is the speed of movement of the counterweights on the block;
 - R is the radius of rotation of the center of gravity of the ballast vibration generator.
- Separating the terms in equation (1) and integrating, results:

$$x = \frac{2m}{M + 2m} R \sin(\omega t) \cdot \cos \varepsilon + C_1 \quad (2)$$

With initial conditions ($x = 0$, $\omega t = 0$), introduced in equation (2), determine the constant of integration, namely $C_1 = 0$, and the final expression of the displacement x is:

$$x = \frac{2m}{M + 2m} R \cdot \sin(\omega t) \cdot \cos \varepsilon, \quad (3)$$

relationship representing variation block movement harmonic separation under the action of inertia forces of counterweights.

From equation (3) we notice that:

- For $t = 0$, move it $x = 0$;
- For $\omega t = \pi / 2$, moving block separation is $x = \frac{2Rm \cos \varepsilon}{M + 2m}$

$$\text{and amplitude is: } A = \frac{2m}{M + 2m} R \cdot \cos \varepsilon \quad (4)$$

From equation (4) it is observed that for certain values constructive known masses M and m, the variation of the angle ε determines the oscillation amplitude variation with site building. Since one vibration generator technical data are given generally centrifugal force of counterweights (F_c) and the total mass of the generator amplitude can be estimated using previous relationship according to these sizes by multiplying the resulting expression 4 is ω^2 :

$$A = \frac{2 F_c \cdot \cos \varepsilon}{M_{t,b} \cdot \omega^2} \quad (5)$$

where $M_{t,b} = M + 2m$ is the mass of block with site with two vibrating table.

Taking into account the other forces that affect motion separation block (F_r and F_e - figura.1) and neglecting the vertical movement of the block (supports with reduced length) assuming frictionless

joints system, the system design horizontal forces (Figure .1) and in terms of power system dynamic equilibrium is obtained differential equation system displacement (horizontal) [3] as follows:

$$c \cdot z \cdot x + (M + 2m)g \cdot \frac{x}{l} + (M + 2m) \cdot \frac{d^2 x}{dt^2} = 2m R \cdot \omega^2 \sin(\omega t) \cdot \cos \varepsilon \quad (6)$$

where:

- L, z is the length or number, elastic support suspending the block;
- C is the stiffness of elastic support.

Equation (6) can be arranged as

$$\frac{d^2 x}{dt^2} + \left(\frac{c \cdot z}{M + 2m} + \frac{g}{l} \right) \cdot x = \left(\frac{2m}{M + 2m} R \cdot \omega^2 \cdot \cos \varepsilon \right) \cdot \sin(\omega t) \quad (7)$$

If it is noted in brackets with constant sizes:

$$\alpha^2 = \frac{c \cdot z}{M + 2m} + \frac{g}{l}, \quad \beta = \frac{2m}{M + 2m} R \cdot \omega^2 \cdot \cos \varepsilon \quad (8)$$

then equation (7) becomes:

$$\frac{d^2 x}{dt^2} + \alpha^2 \cdot x = \beta \cdot \sin(\omega t) \quad (9)$$

which is the equation of forced vibration without damping, which is a 2nd order differential equation with constant coefficients, homogenous.

The general solution of this equation is:

$$x = C_1 \cdot \sin(\alpha t) + C_2 \cdot \cos(\alpha t) + \frac{\beta}{\alpha^2 - \omega^2} \cdot \sin(\omega t) \quad (10)$$

where C_1 and C_2 are constants of integration to be determined from initial conditions. For the simplest initial conditions assume that at $t = 0$ we have $x = 0$ and $dx / dt = 0$, that the system is at rest in the equilibrium position.

Taking into account equation (10) and the conditions, as the calculations are obtained:: $C_2=0$ și $C_1=(-\beta\alpha)/(\alpha^3-\alpha\omega^2)$

In this case, the general solution given by (10) becomes:

$$x = \frac{\beta}{\alpha^2 - \omega^2} \cdot \left[\sin(\omega t) - \frac{\omega}{\alpha} \sin(\alpha t) \right] \quad (11)$$

It is noted that the movement system is an overlap of two vibration amplitudes and pulse different vibration to pulsation α own free vibration of elastic systems and forced vibration with angular frequency ω disruptive force due counterweights.

Are preferred ω and α where pulsations and are much different, either $\omega \ll \alpha$, even $\alpha \ll \omega$ if it should be avoided and ω and α close or equal.

If frequent practice that $\alpha \ll \omega$, from equation (11) that the amplitude of vibration of the system is:

$$A = \frac{\beta}{\omega^2 - \alpha^2} \quad (12)$$

or, taking into account the notations (8), we obtain:

$$A = \frac{2mR \cos \varepsilon}{(M + 2m) - \frac{1}{\omega^2} \left[cz + \frac{(M + 2m)g}{l} \right]} \quad (13)$$

If we consider the technical data of a source of vibration (F_c , the total mass of the generator, ω) relation (13) can be put in the form:

$$A = \frac{2F_c \cdot \cos \varepsilon}{M_{t,b} \cdot \omega^2 - \left(cz + \frac{M_{t,b} \cdot g}{l} \right)} \quad (14)$$

From relations (13) and (14) we notice that in a given situation a vibrator system by M , m , c , R , ω (or F_c , M_t , b , c , ω) amplitude "A" vibration system can be adjusted by adjusting the angle of the generator assembly ε counterweight vibration [5].

If the required amplitude of the vibration, the relation (13) can size the counterweights for known values of other quantities, using the relationship:

$$m = \frac{A \left[\frac{1}{\omega^2} \left(cz + \frac{M \cdot g}{l} \right) - M \right]}{2R \cos \varepsilon + A \left(1 - \frac{g}{l \cdot \omega^2} \right)} \quad (15)$$

Relation (15) can be used to assess the design of such counterweights vibration generators proposed.

If MDG-46x24 meal machine, equipped with two vibrating type MAVAR 112-6-7 ($F_c = 7000$ N, $P = 0.4$ kW $M_t = 0.81$ Nm, $n = 1000$ rot/ min; total weight is 75 kg), knowing the mass of 437.8 kg and block the site oscillation angle $\varepsilon = 7^\circ$, we obtain the following characteristics:

a) Using relation (5) is estimated amplitude oscillations separation block as $A = 2.16$ mm ($A = 2.4$ mm for $n = 950$ rot / min). If the angle of oscillation increases to $\varepsilon = 30^\circ$, the oscillation amplitude decreases to 1.9 mm ($A = 2.1$ mm for $n = 950$ r / min).

b) If the block websites Separation of MDG-46x24 meal machine is suspended on four helical spring type elastic supports with length $l = 345$ mm and features: $D_m = 50$ mm, $d_s = 10$ mm, $n = 7$ turns, stiffness "c" a calculated support is set to $c = 111428.6$ N / m Using relation (14), the amplitude of oscillation is $A = 2.7$ mm for $A \cong \varepsilon = 7^\circ$ and 2.4 mm for $\varepsilon = 30^\circ$.

c) If you use double brackets embedded rubber ring section with $D = 62$ mm, $d = 32$ mm and $l = 90$ mm, the stiffness of a medium is $c = 88738.7$ N / m (for $E = 80$ daN / cm²), leading to an oscillation amplitude $A = 2.3$ mm for $\varepsilon = 30^\circ$.

d) If it is necessary that the amplitude of oscillation to be 3 mm, then using equation (14) to obtain the necessary centrifugal force $F_c = 9042.7$ N and if for this centrifugal force, requiring a range of ballast arrangement is obtain their mass $m = 16.5$ kg.

In Figure 3 is the variation of the vibration system using MathCAD program version 13, [4], determined by the relation 14 (fig.3.a) and the relation 14 (fig.13.b) in case F_c force centrifugal counterweights is. Length of elastic support is $l = 345$ mm M-block partition table (including vibration generators without ballast mass) $M = 437.75$ kg, m - mass of the two counterweights of a vibration generator $m = 75$ kg, stiffness of support is $c = 88738.7$ N / m, R is the radius of rotation of the center of gravity of the ballast vibration generator, $R = 0.4$ m, ω the angular velocity of the flywheel that supports unbalanced mass (time varying). SI-510 performs intensive separator separating impurities from grain mixtures for grinding, driven in oscillatory motion with two vibrating MVSI 10/200-S90 electric power 0.185 kW, weight 16.9 kg, centrifugal force $F_c = 1830$ N; torque $M_t = 1632$ Nm at $n = 1000$ rot/min.

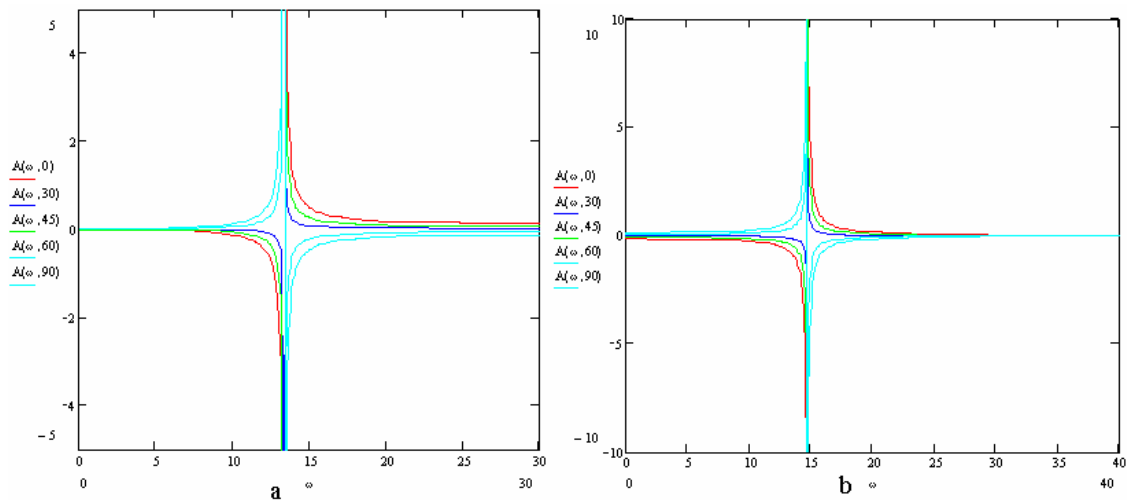


Fig.3. Variația amplitudinii vibrației pentru diferite viteze unghiulare ale volantului, [6]

Considering that the site block mass is about 120 kg ($M_{tb} \approx 154$ kg), for the brackets to the vertical angle of approximately 7° , where counterweights shaft angle from the vertical is 25° , determine the steering angle $\varepsilon = 18^\circ$ oscillation and then, using the relation (5), determine the amplitude of the oscillations block $A \approx 2,1$ mm separation as 2.1 mm ($A = 2.3$ mm for $n = 950$ rot / min).

Block screenings and intensive separator SI-510 is suspended on four rubber elastic support (40-45 Shore) with length $l = 93$ mm and annular section with $D = 82$ mm and $d = 30$ mm in the central section. Considering supports embedded simple elastic rigidity of support is $c = 32516.7$ N / m ($E = 40$ daN/cm²), leading to an oscillation amplitude $A \approx 2.3$ mm (2.5 mm) .If elastic supports are considered dual flush, then it follows an amplitude of oscillation of 3.0 mm and 3.5 mm for $n = 950$ rot / min

4. Conclusions

To estimate the centrifugal force necessary to obtain a certain movement amplitudes can use the above relations, from which it can choose accordingly, in catalogs, the most appropriate vibration generators.

Knowing the centrifugal force necessary ballast weights may be set appropriately when required radius of rotation thereof, or the radius of rotation is determined for a given mass

REFERENCES

- [1]. D. Stoica, Gh. Voicu, N. Ungureanu, P. Voicu, N. Orasanu- "Research on the working process and efficiency of a conical suspended sieve with pendulum movement", Proceedings of the 40. International Symposium on Agricultural Engineering – Actual Tasks on Agricultural Engineering (ISSN 1333–2651, ISI Proceedings) – Opatija, Croatia 21-24. february 2012, (ISI Index to Scientific and Technical Proceedings; CAB International Agricultural Engineering Abstracts; Cambridge Scientific Abstracts - InterD0k)
- [2]. Gh. Voicu, T. Căsandriu – "Analiza comparativă a modelelor matematice utilizate la descrierea procesului de separare a semințelor pe sitele sistemului de curățire de la combinele de cereale", Revista Construcția de mașini, 2004;
- [3]. Gh. Voicu, T. Căsandriu, - "Calculul sistemului de acționare a unui bloc de site cu generatoare de vibrații cu mase neechilibrate", Bucuresti 2005
- [4]. E. Schaiber, D Licsăndriu. – "MathCAD" - prezentare și probleme rezolvate, Ed. Tehnică, București, 1994
- [5]. D. Stoica – "Elemente actuale de tip vibrator la mașinile și sisteme pentru prelucrarea materialelor și a produselor agricole", Referat nr. 1 (Teza de doctorat), București , 2006
- [6]. D. Stoica – "Contribuții la studiul fenomenelor vibratorii privind utilajele din domeniul prelucrării produselor agricole" (Teza de doctorat), Bucuresti, 2011

CONSIDERATIONS ABOUT THE SELECTION OF THE HAMMER MILLS OF LOW CAPACITY

Lecturer phd.eng. Mihaela Florentina Duțu¹ Prof. phd.eng. Ladislau David¹, Prof. phd.eng. Ion Dinu¹,
lecturer phd.eng. Carmen Otilia Rusănescu¹

¹ University Politehnica of Bucharest, Biotechnique Systems Departament, e-mail:
davidmihaela@hotmail.com

Abstract: *In this paper is presented the choice of optimal structural and functional parameters of hammer mills for small farms. To do this, develop a program in Pascal with which the calculations. For inclusion in the program data is necessary to choose several types of hammer mills and criteria to be used to determine the operational utility.*

Keywords: *hammer mill, criterion, operational utility*

1. Introduction

For choosing the universal hammer mills with small capacity with constructive and functional parameters, for small farms is necessary to know the constructive characteristics of mills and valuing them. Comparison of mills is done using the STEM method and for the calculations is recommended to use the computer.

2. Calculation algorithm

For comparison, we have considered the following universal hammer mill with small capacity manufactured in the country:

- M1 - universal mill of small capacity manufactured by SC AZOMA SA
- M2 - increased capacity mill MC -0.9 manufactured by SC Agromec SA
- M3 - universal mill feed MU - 5.5 manufactured by SC AZOMA SA
- M4 - universal mill feed MU - 7.5 manufactured by SC AZOMA SA
- M5 - universal mill feed MU - 11 manufactured by SC AZOMA SA
- M6 - hammer mill MC - 1.0 manufactured by SC Tehnostar SA
- M7 - Leopard hammer mill, manufactured by Barbieri

Determining operational utility from these trailers are done with STEM method and have taken into account the following criteria:

- C1 - average working capacity (t / h);
- C2 - degree of universality;
- C3 - the number of bits per rotor (pieces);
- C4 - number of blades on the rotor (pieces);
- C5 - electric drive motor power (kW);
- C6 - hammer mill mass (kg);
- C7 - specific energy consumption (kWh / t);
- C8 - degree of universality (3 - to process grain, corn cobs and fibroaselor, 2 - for processing grain and corn cobs);
- C9 - operating mode (1 - for direct coupling of the electric motor, 2 - for coupling through an additional transmission 3 - for other drives).

Criteria C1 - C4 is recommended to have maximum value and the criteria C5 - C9 to be the minimum. The values of these criteria v_{ij} ($i = 1 \dots 9, j = 1 \dots 4$), for each hammer mills considered, or presented in Table 1

Table 1

	M1	M2	M3	M4	M5	M6	M7
C1	0,45	0,78	0,61	1,35	1,2	0,77	0,4
C2	3	2	3	3	3	2	3
C3	20	42	16	16	20	56	12
C4	0	0	2	2	2	0	3
C5	2,2	15	5,5	7,5	11	15	9
C6	53	23,5	800	800	1000	1000	83
C7	12,7	19,4	18,1	16,1	19,4	10,6	15
C8	0,3	4,79	2,37	2,37	3,33	0,7	1,07
C9	1	2	1	1	2	2	3

Using relations (1) and (2) determine the utility matrix (u_{ij}) presented in Table 2:

$$u_{ij} = \begin{cases} 1 & \text{for } v_{ijmax} \\ \frac{v_{ij} - v_{ijmin}}{v_{ijmax} - v_{ijmin}} & \\ 0 & \text{for } v_{ijmin} \end{cases} \quad (1)$$

$$u_{ij} = \begin{cases} 1 & \text{for } v_{ijmin} \\ \frac{v_{ijmax} - v_{ij}}{v_{ijmax} - v_{ijmin}} & \\ 0 & \text{for } v_{ijmax} \end{cases} \quad (2)$$

Next, rank the criteria considered their importance. Were considered as very important the criteria C1, C2, C5 and C7. Criteria were considered important are: C3, C4 and C6 and less important criteria C8 and C9.

Compare each criterion C_i ($i = 1, \dots, 9$) with all other criteria and determine important coefficients n_{ij} ($i = 1, \dots, 9, j = 1, \dots, 9, i \neq j$) which is assigns the value 1, if the criterion considered is C_n , 2 if the criterion C_m is less important than C_n , 4 where C_m is very important in relation to C_n and 0 otherwise

Table 2

	M1	M2	M3	M4	M5	M6	M7
C1	0,05	0,4	0,22	1	0,84	0,38	0
C2	1	0	1	1	1	0	1
C3	0,18	0,68	0,09	0,09	0,18	1	0
C4	0	0	0,66	0,66	0,66	0	1
C5	1	0	0,74	0,58	0,31	0	0,47
C6	1	0,82	0,28	0,28	0,09	0	0,97
C7	0,75	0,002	0,15	0,15	0	1	0,5
C8	1	0	0,54	0,54	0,32	0,91	0,83
C9	1	0,5	1	1	0,5	0,5	0

The weights for each criterion are calculated with:

$$p_i = \frac{\sum_{j=1}^{10} a_{ij}}{\sum_{i=1}^{10} \sum_{j=1}^{10} a_{ij}} \quad (3)$$

the following values:

$$p_1 = 0,19; p_2 = 0,19; p_3 = 0,07; p_4 = 0,07; p_5 = 0,19; p_6 = 0,07;$$

$$p_7 = 0,19; p_8 = 0,01; p_9 = 0,01$$

Total utility service shall be calculated by the formula:

$$U_{exp j} = \sum_{i=1}^{10} u_{ij} \cdot p_i, \quad i=1...10; j=1....5 \quad (4)$$

To hammer mills considered total operating utilities are:

$$U_1 = 0,646; U_2 = 0,187; U_3 = 0,497; U_4 = 0,661; U_5 = 0,49; U_6 = 0,352; U_7 = 0,525$$

Table 3

	C1	C2	C3	C4	C5	C6	C7	C8	C9
C1	0	1	2	2	1	2	1	4	4
C2	1	0	2	2	1	2	1	4	4
C3	0	0	0	1	0	1	0	2	2
C4	0	0	1	0	0	1	0	2	2
C5	1	1	2	2	0	2	1	4	4
C6	0	0	1	1	0	0	0	2	2
C7	1	1	2	2	1	2	0	4	4
C8	0	0	0	0	0	0	0	0	1
C9	0	0	0	0	0	0	0	1	0

3. Conclusions

Based on the presented algorithm was developed a computer program in Pascal, with which all calculations were performed. Analysis has shown that a hammer mill with a small capacity with best operational performance is M4 - universal mill feed MU -7.5 manufactured by SC AZOMA SA whose total utility service shall be $u_4 = 0,661$.

One can use M1 - small universal mill capacity manufactured by SC AZOMA SA who has the total utility operating very close $u_1 = 0,646$ and M7 - Leopard hammer mill manufactured by Barbieri with utility $u_7 = 0,525$.

Not recommended M6- hammer mill MC - 1.0 manufactured by SC Tehnostar SA who have the total utility operating $u_6 = 0,352$ and M2 - increased mill capacity MC - 0.9 manufactured by SC Agromec SA Margineni with the total utility $u_2 = 0,187$.

The method presented is an objective criterion for choosing the hammer mill with small capacity who corresponds to the greatest extent, farmer requirements.

REFERENCES

- [1] Bordânc M., Rusovici Al. – Organizarea și conducerea întreprinderilor agricole, Editura IPB, 1983, voll și II
- [2] “*** Îndrumător de utilaje agricole, Ed. Ceres, 1995

A NEW SOLUTION FOR WATER JET CUTTING MACHINE TOOL

Rareş PETRUŞ¹, Cornel CIUPAN², Emilia CIUPAN³

¹ Technical University of Cluj-Napoca, rares.petrus@muri.utcluj.ro

² Technical University of Cluj-Napoca, cornel.ciupan@muri.utcluj.ro

³ Technical University of Cluj-Napoca, emilia.ciupan@mis.utcluj.ro

Abstract: This paper presents a solution for achieving the high pressures specific to water jet cutting machines, using sonicity theory. The system consists of a generator that transmits pressure waves to a sonic amplifier that can be mounted directly in the cutting head. Based on the research carried out on an experimental model, the paper also proposes solutions to improve the system.

Keywords: water jet cutting, sonic generator, amplifier.

1. Introduction

The water jet cutting process was patented under the name “jet cutting technology at high pressure” in 1968, by Dr. Norman Franz from the McCartney-Ingersoll Rand, U.S.A. The first industrial facility to use water jet cutting was implemented in 1971. Flow Systems company from U.S.A. became world leader in this technology and its main promoter in the industrial sector.

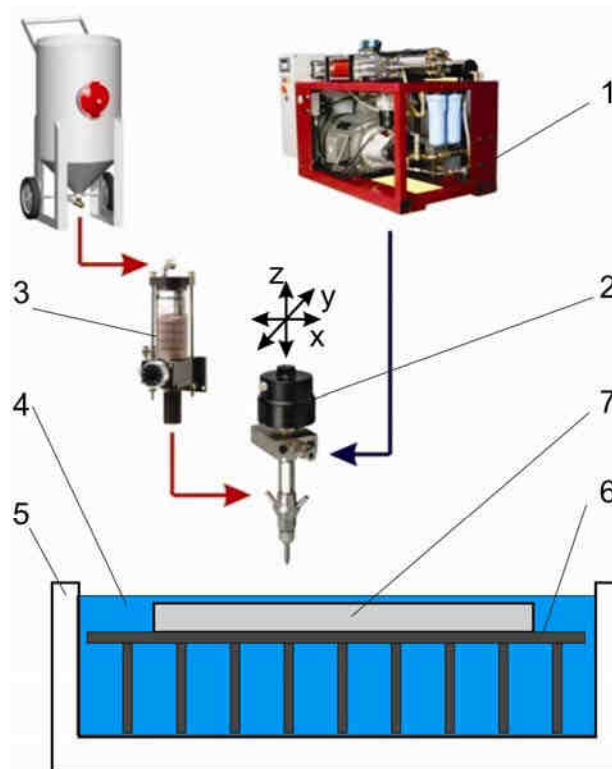


Figure 1. Block diagram of a water jet cutting machine

The first industrial applications have been made in the aviation industry (U.S.A., Canada, Japan), where jet cutting has been used for cutting materials such as plastic, composite, multilayer materials, etc. With the advent of new alloy materials and ceramics, hard and difficult to machine by conventional processes, a new technology was needed for cutting and processing.

In 1984, the Flow Systems Company produces the first water jet cutting-abrasive installation. This innovation constitutes a genuine revolution in jet cutting technology, giving it a whole new dimension. The technique enables cutting of most materials, metallic or non-metallic, special alloys, composites and ceramics. This versatility gives it a good position compared to other recent cutting technologies (ex. plasma, laser).

Abrasive water jet (AWJ) cutting processes are used mainly for cutting operations, but there are applications for operations like turning, milling, or deep drilling. It is foreseeable that AWJ processing could replace traditional cutting processing operations in some areas.

The block diagram of a water jet cutting machine is shown in figure 1. The machine consists of a pump (1), which provides water at a pressure of approx. 40 MPa to cutting head (2). In the cutting head, water is mixed with abrasive from the system (3). Part (7) is fixed on the machine table (5), on some support beams (6). Water level (4) from the water tank passes with 1-3 mm over the piece (7). Because the work piece has large dimensions, the cutting head is the mobile element and make the feed movements on the x, y, z axes.

2. Proposed solution

The Water jet machining system (Fig.2) comprises a sonic generator (GS) with the role of transforming mechanical energy produced by the engine (1) in pressure waves, that are transmitted by means of a hydraulic fluid to cutting head (CT), where it creates water working pressure. The sonic generator (GS) is engaged by a motor (1), electric or thermic, that drives a shaft (2) on which there are mounted some cams (3). The cams (3) act by means of some rollers (4) upon the pickers (5) that move through the connecting members (6) of the arcs (7), pistons (8) mounted in a body (9) of a sonic generator (GS).

Between each of the pistons (8) and the liners (10), we will introduce a low viscosity fluid (oil gas). Thus, it is formed a closed hydraulic circuit number, equal to the number of pistons (8). Oil gas, found between sonic generator (GS) and cutting head (CT), is maintained under pressure (20-70 bars), with the aid of compensating valves (SC1) and (SC2). The springs (12) push the pistons (13) and ensures minimum pressure of circuit. Through their motion, the pistons (8) create in the pipes (14) pressure waves that acts on pistons receivers (15), causing a synchronic displacement of pistons pairs (8) and (16), located on the same circuit. The pistons (16) are coupled through connecting pieces (17) with small pistons (18) of the high pressure pump (20). In their motion, small pistons (18) change the volume of the chamber (19) of the pump (20) causing suction and pressure side of the pressure water, through direction valves (20) and (21).

Cutting burst jet is formed in nozzle (23) of the cutting head. High pressure sealing elements (24) reduce flow losses in high pressure circuit. Water flow and pressure are proportional to the forming jet stroke pistons (15) and (17). To adjust these parameters, has been provided a feedback loop made up of the pressure transducer (25), the comparator (26) and actuators (27).

When between size of control "c" and size of the reaction "r" is an error "ε", caused by the change of the size or water pressure in low pressure circuit, or the nozzle wear or sealing elements, actuator (28) make a move "e" to racks (29), for each piston (8).

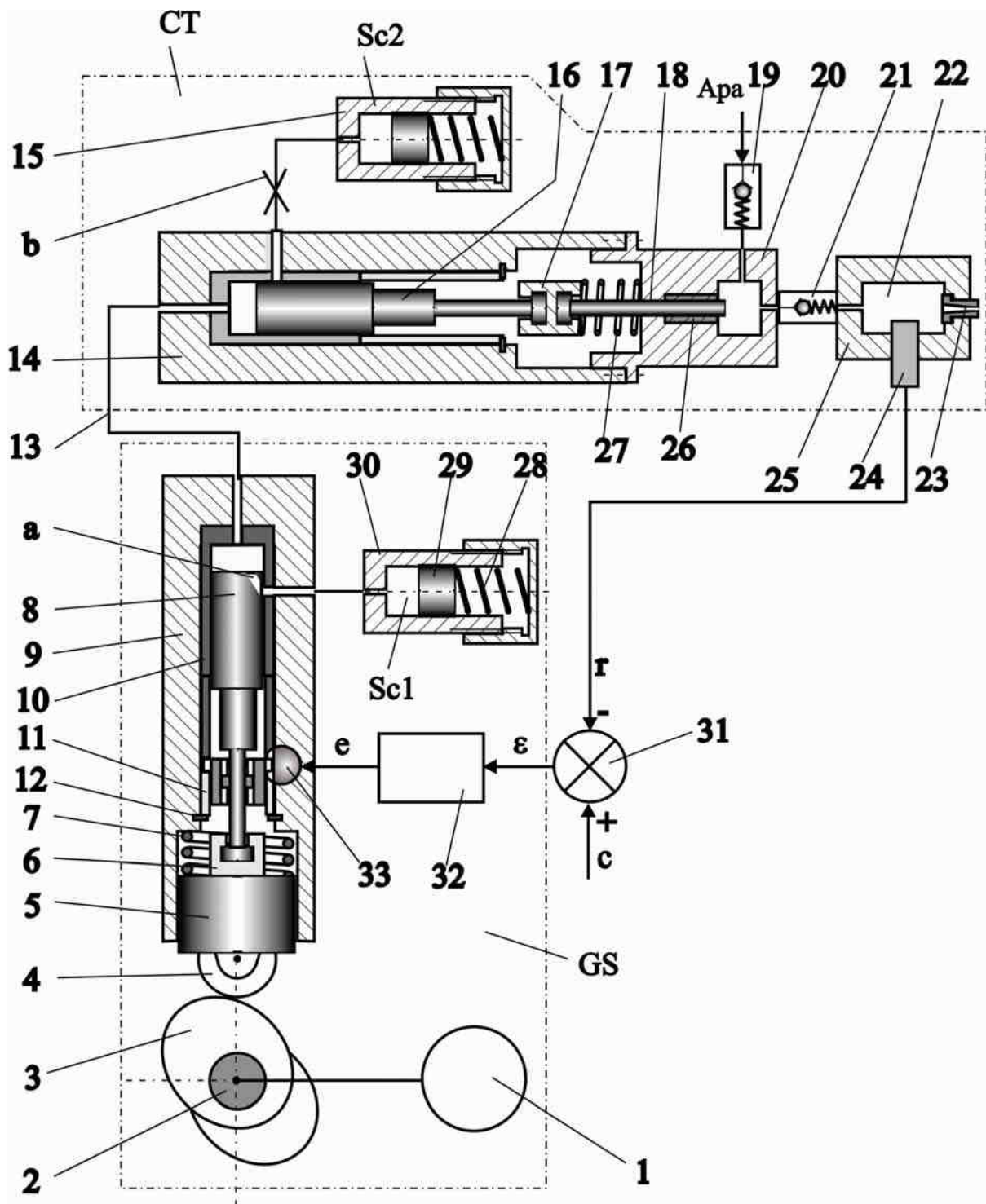


Figure 2. Water jet processing system

The racks (29) rotates the pistons (8) through the gears (30), changing the slot position "a" of each piston against the valve orifice communicating with compensation valve (Sc1). The angular position of the piston slot (12) has a direct influence on the amplitude of the pressure waves created by the sonic generator. This changes the position of the piston stroke receivers (15) and adjusts the flow, respectively, the pressure in the high pressure circuit.

The compensation valve (Sc2) is used to offset fluid losses through leaks, to mitigate reflected waves the pistons, and bleed receivers in the initial phase. Hydraulic resistance "b" located on pipe compensation valve (Sc2) serves to direct wave action pressure on receiver pistons.

On the basis scheme of figure 2 was made an experimental model. With the experimental model has been studied obtained pressure in high pressure floor. This was done by measuring the carrying capacities deformation on focusing nozzle. It was concluded that the pressure created by the high pressure floor is between 2500 and 3000 daN/cm².

3. Conclusions

From the research done, following conclusions have been drawn:

- It has been shown that the solution adopted by transmitting energy in the form of pressure waves from sonic generator to cutting head allows mounting the cutting head amplifier into the cutting head, which offers the advantages of water transport pipeline working pressure metal or Kevlar;
- It was found that water working pressure obtained at the output of the amplifier is reduced to the pressure that has been designed for installation (75%);
- In the solution designed, amplifier has very low reliability (app.10 hours).

To improve performance by increasing the operating pressure and reliability, are proposed the following changes:

- Increasing pressure wave amplitude of the sonic generator (GS);
- Increasing the amplification ratio of the cutting head;
- Developing a mathematical model to optimize installation parameters.

REFERENCES:

1. Momber A. Kovacevic R. "Principles of Abrasive Water Jet Machining", Springer, 1998
2. Ciupan, C. ş.a. "Tehnologii moderne de debitare a metalelor". Tehnică şi inginerie, Cluj-Napoca, 2001
3. Ciupan C. Morar, L. Pop A. "Innovative system with abrasive water jet". Annals of DAAAM for 2008 & Proceedings of the 19th International DAAAM Symposium, 2008
4. Pop A. "Study of Computer Control Strategy for Jet Cutting Integrated Systems", Ph.D. Thesis, Technical University of Cluj-Napoca, 2004
5. Patent RO 121987 "Water jet processing system"

RESEARCHES TO IMPROVE WORKING PROCESS OF ACTIVE WORKING PARTS, HYDRAULIC ACTUATED, FROM CONSTRUCTION OF THE EQUIPMENT "EXPLANT 500"

Constantin COTA¹, Elena Mihaela NAGY¹, Nicolae CIOICA¹

¹ National Institute of Research - Development for Machines and Installations Designed to Agriculture and Food Industry – INMA, Bucharest; inmacj@rdsmail.ro

Abstract:

The working principle of the machinery and technical equipment for extraction plants with root ball is based on penetration into the soil of the active working parts (spades), cutting the soil ball and extracting it together with the plant (tree saplings, tree, shrub), in a view to transplantation. From constructive point of view, penetration into the soil of the active working parts is ensured by means of some double acting hydraulic cylinders, the penetration force being linear and directly proportional to the pressure in the hydraulic system. From analysis of the results obtained in the tests, was noted the fact that the resistance to penetration of the soil in which we worked, determined over the depth of penetration in the soil of the active parts (spades) of the equipment increase directly proportional to the depth of penetration and inversely proportional with soil moisture.

Increasing the efficiency of the penetration force into the soil, of the active working parts (spades) is achieved by providing a hydraulic pulsating force (with shocks) through a hydraulic control and operated device, with shocks. Hydraulic operation with shocks can be used as needed,- in heavy soils with high penetration resistance

Keywords:penetration resistance, hydraulic actuating,extract of planting material.

1.Introduction

To obtain saplings of adequate quality, in terms of economical efficiency, both regarding saplings for fruit growing sector and for arranging urban green areas or forestry plantations, in nurseries a series of works are performed to maintenance the crop. An important part, in terms of energy and labor consumption, in work technologies in nurseries, it has putting out of saplings, in order to its transplantation or delivery for planting.

Preliminary researches conducted have revealed that the highest energy consumption is recorded during the penetration process of working parts into the soil, under the action of hydraulic force. In this context enroll our concerns to find ways to increase efficiency of soil penetration force of the working parts.

2. Material and method

The technical equipment, EXPLANT 500 (*fig.1*) is meant to extract dendro-horticol planting material, ornamental or fruit bearing, medium -sized and large, with root ball, from nurseries and/or forestry plantations, in order to transplant them in green areas, plantations and/or growing fields from nurseries. Also, the machine can be used to anticipated digging of holes, where follows to make transplanting, either of planting material (saplings) extracted with root ball or saplings with bare root (without soil bale).

Actuating active working parts is achieved by the machinery own hydraulic system, actuated by the tractor from the unit.

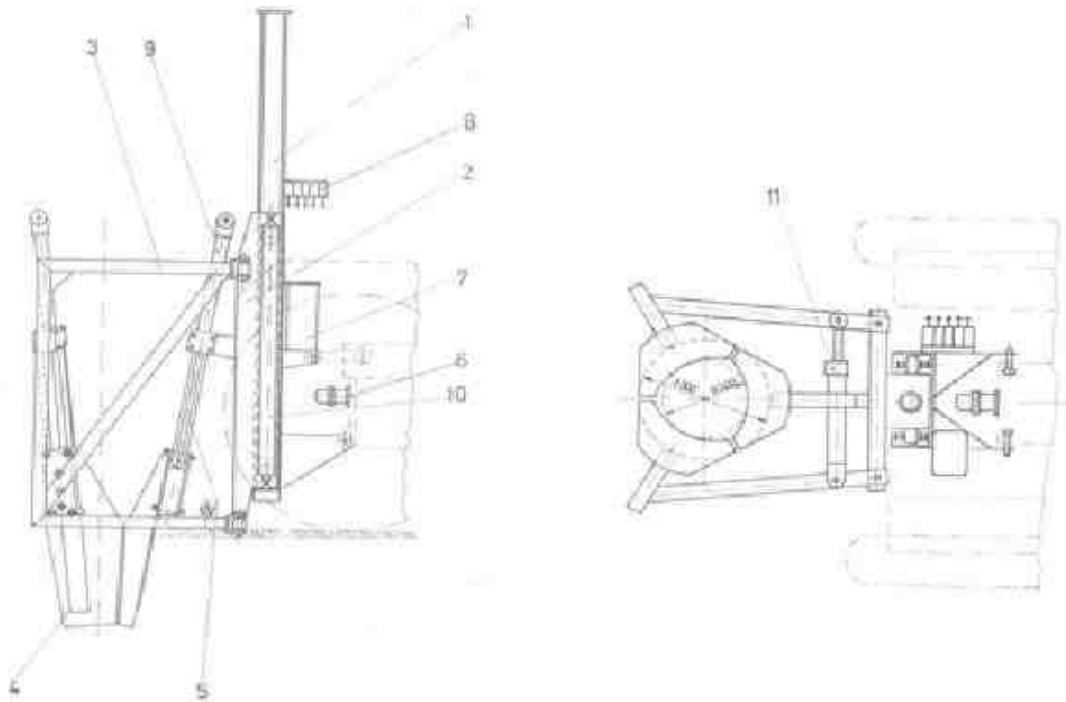


Figure1. Constructive scheme of the equipment to extract plants with root ball EXPLANT 500

The main parts of the equipment are:

The guide frame (1) is a construction of steel profiles, welded, which serves to support all the other parts of the machinery.

The sliding body (2) is a welded body provided with guide rollers that bear the entire assembly of spades and ensure its vertical movement.

Spades' support arms (3) -are in number two and provide support to the two lateral spades. The support arms are articulated on the sliding body so that to allow "opening" and "closing" the two lateral spades in order to embrace the plant to be extracted.

The spades (4) are in number three: one central and two lateral. The spades are made of steel and have a cylindrical shape with four sharp edges to cut both soil and roots of the plant to be extracted. The spades are mounted so that to go into the soil inclined (about 15°) to ensure the achievement of a truncated cone-shaped bale of soil.

Guide of spades (5) - ensure movement of the spades and their correct positioning so that the bale of soil have truncated -cone shape.

Hydraulic pump (6) is PRD-117D type, with volume of 3.25 cm³/rot, and a maximum pressure of 200 bar, ensuring actuating of all hydraulic cylinders of the machinery with a view to cut the soil and lift the plant with the root ball. Actuating the hydraulic pump is performed by the final transmission of the 45 HP tractor, being adopted an innovative technical solution that makes the object of a patent application.

Oil tank (7) is a welded construction made of iron sheet, it has a capacity of approximately 20 l and it is equipped with filtering system of the oil recirculated in the hydraulic system.

Distributor (8) is a manual distributor with 5 sectors, modular, and which ensures three positions: lifting, lowering and neutral.

Hydraulic cylinders for actuating the spades (9) are in number three, one for each spade and ensure spades' penetration into the soil. Cylinders are Ø 50x500 type, and they are equipped with the possibility of fastening on the sliding body.

Lifting hydraulic cylinder (10) provides vertical movement of the sliding body (2) achieving thus lay on the soil of the spades' assembly, and, after "cutting " the soil bale, lifting it to the desired height. A Ø63x1000 cylinder is used.

Hydraulic cylinder for actuating spades' support arms (11) is a cylinder $\varnothing 40 \times 250$ and it ensures opening and closing movement of the two lateral spades so they can be positioned around the tree to be extracted.

Working process of the equipment, (fig.2) consists of the following phases:

Phase I. With spades (4) lifted upright, with the sliding body (2) near to the ground and the spades' support arms (3) wide open, by maneuvering the tractor, the equipment is positioned near the plant to be extracted, so that the three spades to be at equal distance from stem.

Phase II. Lateral spades approaches the plant by actuating the cylinder (11) and it is commanded descending of the sliding body (2) simultaneously with actuating the cylinder (10) until the tractor is supported on the spades supports.

Phase III. Spades (4) are pushed in the soil by actuating the cylinders (9) successively, starting with the central spade, obtaining roots' cutting, and cutting lateral sides of the soil bale.

Phase IV. By actuating the cylinder (10) is ordered lifting of the sliding body (2) together with spades' assembly, and thus are performed extraction and lifting of the root ball plant above the ground. Cutting the vertical roots and cutting the lower part of the bale is achieved by pulling up.

Phase V. By wide opening of the lateral spades, with the cylinder (11), the root ball is released, and it can be putted down on the ground, in baskets for local handling or for packaging and loading in vehicles.



Figure 2. Aspects of the phases of working process during extraction of the root ball plants

Characteristics of test conditions for the EXPLANT 500 are presented in Table1.

Determination of soil resistance to penetration was made with a penetrometer Spectrum Technologies SC 900, accuracy class ± 1.25 cm and ± 103 kPa, and the soil moisture was determined with a moisture-meter Spectrum Technologies TDR 300 with accuracy class $\pm 3.0\%$

Tabel.1

Characteristics of test conditions

Characteristics	U.M	Work performed		
		Extract ornamental trees		Extract ornamental trees
Plants characteristics :				
- Species	-	Thuja	Apple+pear	-
- heigh	cm	150-200	130-160	-
- stem diameter (at 10 cm above the ground)	cm	2,5-4,0	2,0-3,0	-
- tree crown diameter	cm	120-140	80-100	-
Soil characteristics				
- soil conditions	-	Tillage	Tillage	fallow
- soil type	-	clayey-sandy	clayey	clayey
- penetration resistance :				
- 0-10 cm	kPa	1200	1300	1400
- 10-20 cm	kPa	2200	2400	2600
- 20- 30 cm	kPa	3000	3500	4000
- 30-40 cm	kPa	3800	over 4500	over 4500
- 40-50 cm	kPa	Over 4500	-	-
- soil moisture in layer :				
- 0-10 cm	%	16,2	17,6	18,7
- 10-20 cm	%	18,7	22,3	23,1
- 20- 30 cm	%	15,1	19,0	20,4
- 30-40 cm	%	12,3	14,2	16,8
- 40-50 cm	%	10,9	11,4	12,3
Land characteristics:				
- Inclination	Grade	0-3	0-3	0-4
- preliminary tillage	-	deep plowing and annual maintenace works	deep plowing and annual maintenace works	-
- height of unevenness	cm/ml	4	3	6

3. Results and discussions

From constructive point of view, penetration into the soil of the active working parts is ensured by means of some double acting hydraulic cylinders, the penetration force beeing linear and directly proportional to the pressure in the hydraulic system.

From the analysis of working conditions characteristics in testing EXPLANT 500, it is noted the fact that the penetration resistance of soil in which we worked determined over the depth of penetration into the soil of the active parts (spades) of the equipment (*fig.3 and 4*) had relatively high values, these increasing directly proportional to the depth of penetration and inversely proportional with soil moisture.

It was noted that to ensure the necessary size of the root ball is necessary increasing the penetration force of the spades into the soil. Since the maximum penetration force in soil is limited by construction of the equipment EXPLANT 500 was chosen a hidraulyc control device with hydraulic shocks that provides increased efficiency of soil penetration force by providing of a pulsating hydraulic force.

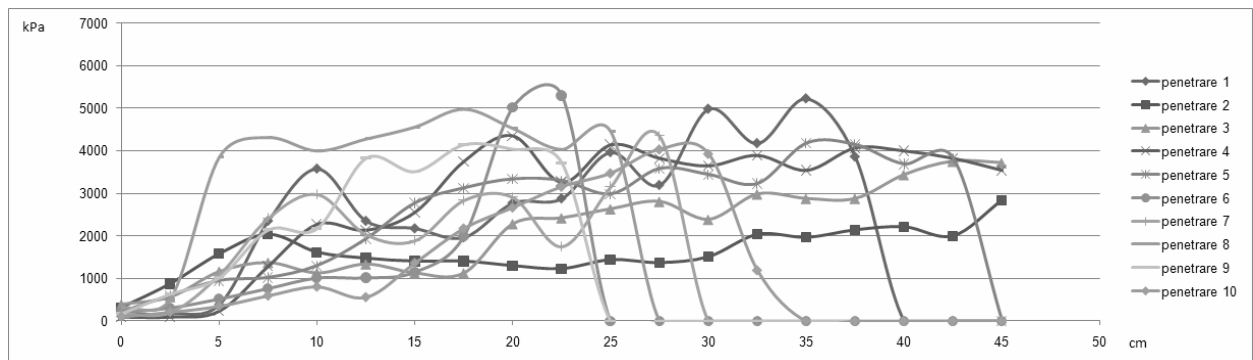


Figure 3. Variation of penetration resistance over the working depth

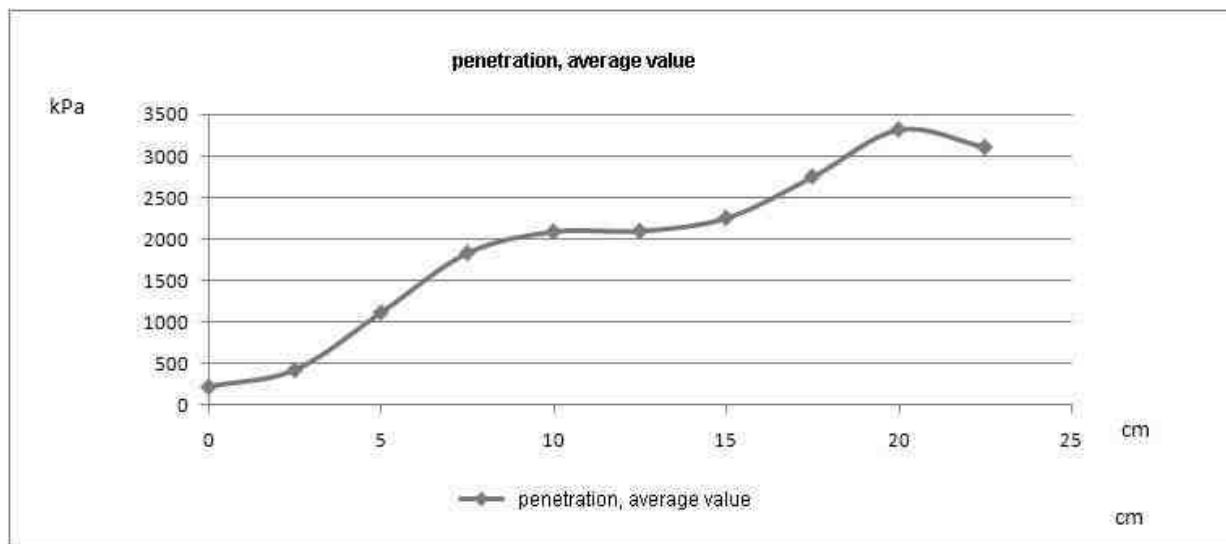


Figure 4. Variation of average resistance to penetration over working depth

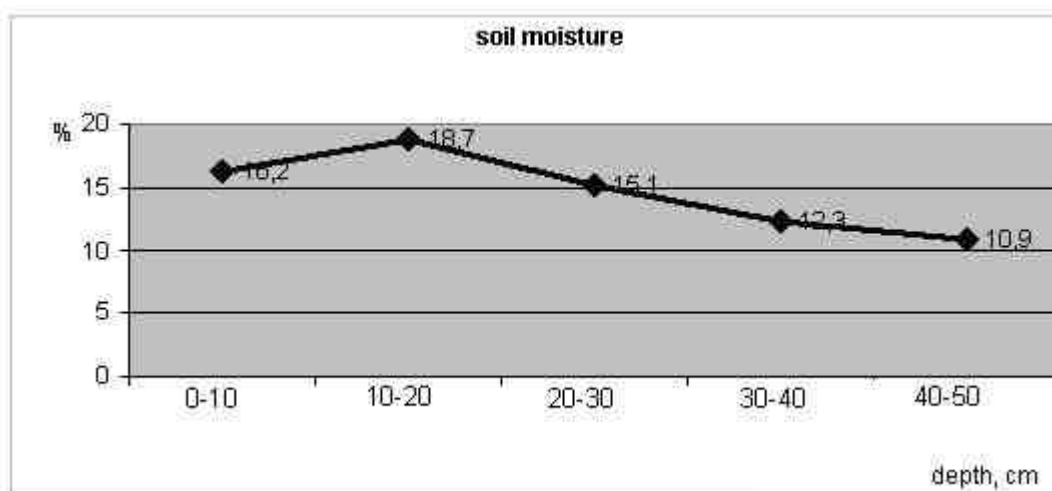


Figure 5. Variation of soil moisture over working depth

The technical solution adopted for the hydraulic control device with shocks (*fig. 6*) is characterized in that the electric hydraulic distributor, DHE, voluntarily ordered by electronic control unit, ECU, produces transformation of the linear force obtained by sending oil from reservoir R, at

the pressure provided by the P pump through the manually distributors, DHM, in a hydraulic pulsating force that through the pipes, C, and double acting hydraulic cylinder, Ch, is transmitted to the spade, S.

The hydraulic actuating with shocks can be used as needed, in heavy soils with high penetration resistance, shocks` frequency beeing adjustable through the electronic control unit.

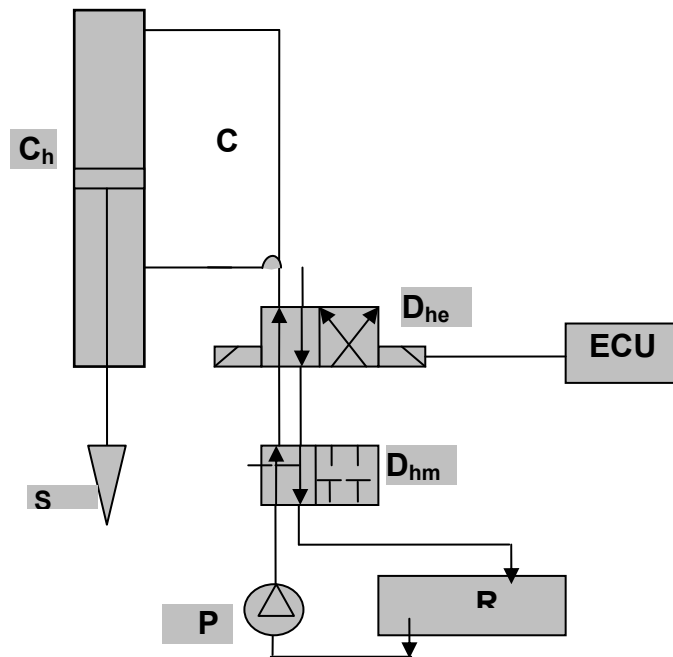


Figure 6. The scheme of the actuating and control hydraulic device, with shocks

4. Conclusions

From experiments it follows that:

- the soil resistance to penetration is directly proportional to the depth of penetration and inversely proportional to soil moisture;
- penetration force of spades into the soil, is linear and directly proportional to the pressure in the hydraulic system, which makes that, under heavy soils conditions, the spades penetration depth into the soil to be limited;
- increasing efficiency of penetration force of spades into the soil, it is made by ensuring of a pulsating hydraulic force, thus ensuring the necessary working depth.

REFERENCES

***, Contract de cercetare 15N/27.02.2009-“ Perfectionarea tehnologiei si dezvoltarea unui produs nou, competitiv, pentru mecanizarea lucrarilor in pepinierile horticole si de productie a materialului dendrologic”

THE CONTROL OF THE ABRASIVE WATER JET PROCESSING USING A NEURONAL NETWORK MODEL

Emilia CIUPAN¹, Cornel CIUPAN², Rareş PETRUŞ³

¹ Technical University of Cluj-Napoca, emilia.ciupan@mis.utcluj.ro

² Technical University of Cluj-Napoca, cornel.ciupan@muri.utcluj.ro

³ Technical University of Cluj-Napoca, rares.petrus@muri.utcluj.ro

Abstract: *The paper presents a neural model used to control an abrasive water jet process. The material features and the focus nozzle wear are considered the input parameters. The output ones are taken into account the feed rate and the abrasive consumption. A neural model with back propagation algorithm was used. The training and the validation data were calculated based on the values presented by the water jet cutting machines manufacturers.*

Keywords: *water, jet, processing, neural, network, control*

1. Tolerances with water jets cutting process

Water jets can make parts to very good tolerances. Today the modern water jet cutting machines can create parts with a tolerance of as small as 0.05 mm and usually is easier to obtain tolerances under 0.1 mm. The achieving of these tolerances requires an understanding of the factors that affect the precision of water jet machining. The positioning accuracy refers to how precisely the abrasive water jet cutting head can be positioned on the X-Y cutting table. Being able to precisely position the cutting head is an important first step to achieving high tolerances, but it's only the first step.

“Some manufacturers stretch the truth a bit when quoting tolerances or they quote the positioning accuracy of the mechanics of the machine, which does not necessarily translate into the cutting accuracy in the final parts. A machine that can position the cutting head to within 0.025 mm might still produce parts accurate to only 0.12 mm.” [4]

The precision is affected by a large number of factors. To control some of these factors is easier, than for others is very difficult. For example, the hardness of the material affects how precisely you can machine it. Harder materials typically exhibit less taper, and taper is an important factor to determining what kind of tolerances can be obtained. We can compensate the taper by adjusting the cutting speed or tilting the cutting head. As the material thickness is increased, the more difficult to control the behaviour of the jet as it exits out the bottom. This will cause blow-out in the corners, and more taper around curves. The material thickness also affects both the value and the type of taper. The taper shape depends on the thickness of materials. Thus, with increasing material thickness taper its surface changed from "V" (for material thinner than 5 mm) on the barrel surface.

Obviously, it is easier to offer the more precisely movement of the cutting head, but is very difficult to obtain parts with very tight tolerances. Therefore, mathematical models are needed to control the process parameters.

As well as another processing methods, the control of the abrasive jet process lead to the improvement of the processing quality and efficiency. The study about the influence of the process parameters [2] using an “energetic” model show that the focus nozzle diameter has a strong influence on the zone depth.

Regarding this influence the focus nozzle diameter [1] proposed the control of the standoff distance for maintaining a constant zone depth for a constant cutting speed. This control solves two important problems:

- to choose an on-line monitoring system of the nozzle wear;
- to establish a model of control which has the nozzle wear the input value and the standoff distance the output value maintaining the zone depth constant.

In the water jet machining must be programmed both feed rate and abrasive consumption. These parameters depend on the processed material features (type, thickness etc.), the surface quality to be obtained and the focus nozzle wear.

The mathematical model [1] [2] is not enough to determine the feed rate and the abrasive consumption. This is the reason why it is proposed a neural model.

2. Structure of the neural network

It is considered a neural network with back propagation learning algorithm. Figure 1 shows the network topology with two input nodes which represents the material thickness and the nozzle wear and two output nodes that represents the feed rate and the abrasive consumption.

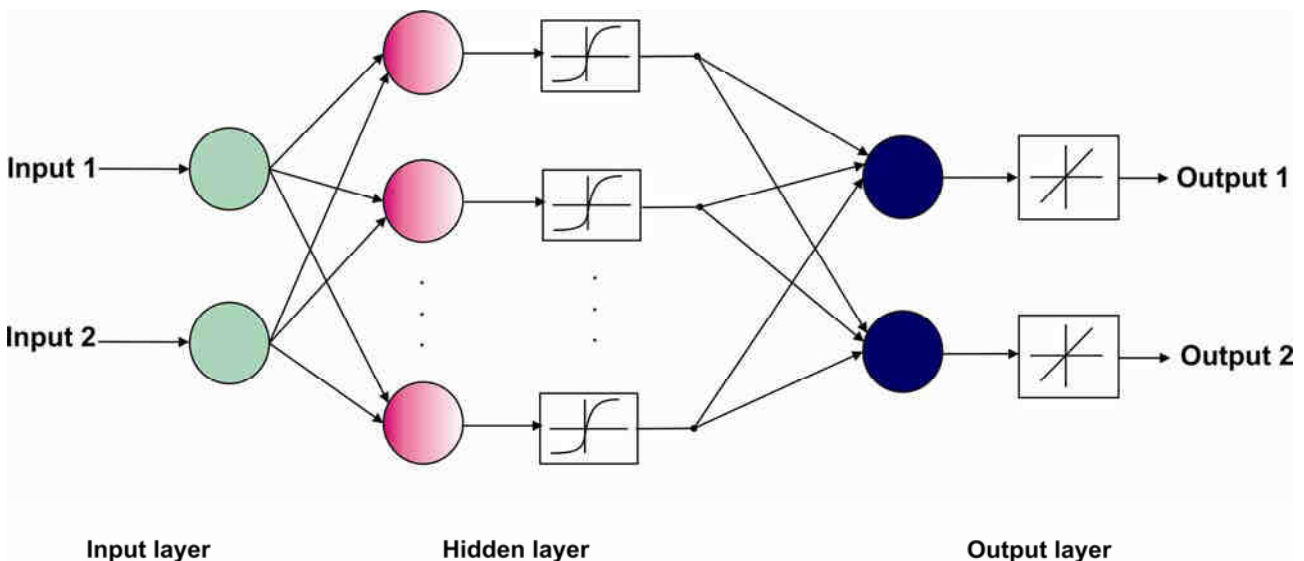


Figure 1. Neural network structure

For the hidden layer were chosen 20 neurons. The activation function for the hidden layer is the sigmoid function and pureline function for the output one.

Neural network modelling involves two phases: the training and the validation phase. The network training was accomplished using data from field literature [4]. Table 1 presents the training data set.

Table 1. Training data set

No.	Input 1	Input 2	Output 1	Output 2	No.	Input 1	Input 2	Output 1	Output 2
1	5	0	200	320	19	38.1	0.05	25.7467	355
2	5	0.025	192.275	332	20	38.1	0.1	23.4137	380
3	5	0.05	184.3	355	21	50.8	0	17.8	320
4	5	0.1	167.6	380	22	50.8	0.025	17.1125	332
5	10	0	120	320	23	50.8	0.05	16.4027	355
6	10	0.025	115.365	332	24	50.8	0.1	14.9164	380
7	10	0.05	110.58	355	25	63.5	0	12.7	320
8	10	0.1	100.56	380	26	63.5	0.025	12.2095	332
9	12.7	0	101.6	320	27	63.5	0.05	11.7031	355
10	12.7	0.025	97.6757	332	28	63.5	0.1	10.6426	380
11	12.7	0.05	93.6244	355	29	76.2	0	8.9	320
12	12.7	0.1	85.1408	380	30	76.2	0.025	8.55624	332
13	25.4	0	40.64	320	31	76.2	0.05	8.20135	355
14	25.4	0.025	39.0703	332	32	76.2	0.1	7.4582	380
15	25.4	0.05	36.0033	355	33	101.6	0	5.1	320
16	25.4	0.1	30.1707	380	34	101.6	0.025	4.90301	332
17	38.1	0	27.94	320	35	101.6	0.05	4.69965	355
18	38.1	0.025	26.8608	332	36	101.6	0.1	4.2738	380

Were chosen the process parameters for a stainless steel processing and an averaged quality processing on a machine which has the following features: 50 HP pump, one cutting head, 60000 PSI (4137 bar) 0.25 mm orifice diameter, 0.76 mm abrasive nozzle diameter.

Input 1 (figure 1) represents the material thickness and Input 2 the focus nozzle wear. The nozzle wear was considered to be 0.0025 mm/h and then, wear values corresponding to 0-10-20-40 of operating hours. Output 1 represents the material thickness and Output 2, the abrasive consumption. Abrasive consumption was determined on the principle of maintaining a constant concentration of abrasive particles in the jet section.

The model validation was done using input values shown in table 2 and denoted Input 1 and Input 2. The effective outputs were compared with the target ones. The resulted errors are presented in the two last columns of table 2.

Figure 2 illustrates the graphical representation of the target outputs and the effective ones.

Although the training data set was quite small in relation to the variation of the material thickness (5-100 mm), the neural model provides close values relative to target values for the abrasive consumption and far values, unacceptable, for feed rate. It is necessary another selection of the input data set.

This time were used 60 pairs of input-output values. The distribution of the material thickness was done by a geometric series.

Table 2. Validation data set

No.	Input 1	Input 2	Output 1 (target 1)	Output 2 (target 2)	Output 1 (effective 1)	Output 2 (effective 2)	Δ Output 1/ target 1 (%)	Δ Output 2/ target 2 (%)
1	8	0	135	320	129.10	320.001	4.37%	0.0002%
2	8	0.025	129.79	332	124.95	331.999	3.72%	0.0002%
3	8	0.05	124.40	355	120.72	354.999	2.96%	0.0002%
4	8	0.1	113.13	380	113.16	380.001	0.02%	0.0002%
5	15	0	88.9	320	83.79	320.000	5.75%	0.0001%
6	15	0.025	85.47	332	72.85	331.999	14.76%	0.0004%
7	15	0.05	81.92	355	68.40	354.999	16.50%	0.0004%
8	15	0.1	74.50	380	61.10	380.000	17.98%	0.0000%
9	30	0	38	320	30.90	320.001	18.68%	0.0003%
10	30	0.025	36.53	332	28.99	332.000	20.64%	0.0001%
11	30	0.05	35.02	355	26.65	354.999	23.90%	0.0002%
12	30	0.1	31.84	380	22.21	380.001	30.24%	0.0002%
13	60	0	15.6	320	13.33	320.001	14.55%	0.0003%
14	60	0.025	15.00	332	12.66	331.999	15.56%	0.0002%
15	60	0.05	14.38	355	11.90	354.999	17.21%	0.0002%
16	60	0.1	13.07	380	11.33	380.001	13.34%	0.0001%
17	80	0	8.6	320	8.06	320.001	6.24%	0.0003%
18	80	0.025	8.27	332	7.71	331.999	6.73%	0.0002%
19	80	0.05	7.92	355	7.25	354.999	8.55%	0.0003%
20	80	0.1	7.21	380	6.61	380.001	8.30%	0.0002%

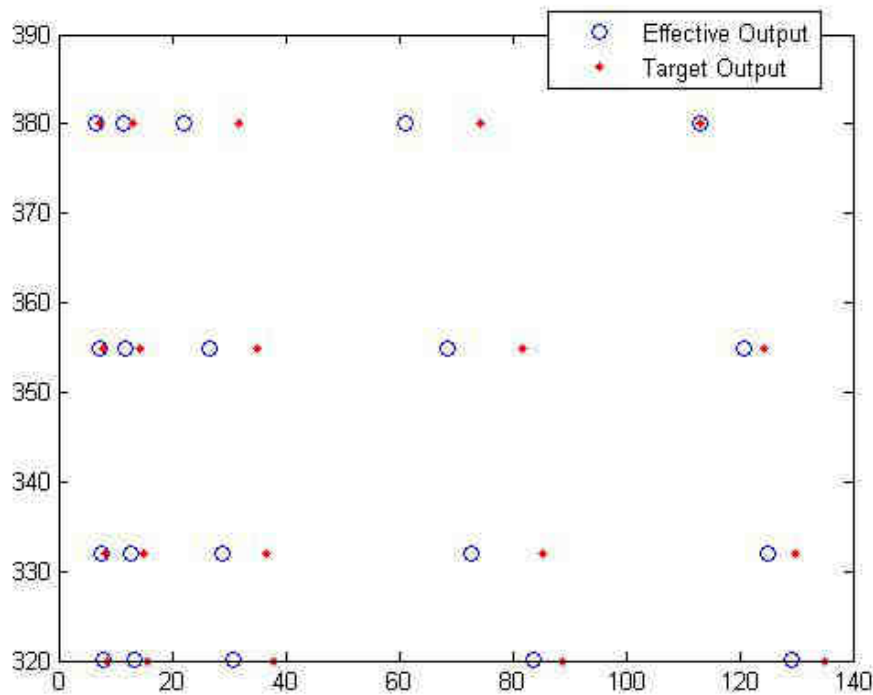


Figure 2. Representation of the target outputs – effective outputs (after the first training)

For the parameter Input 1 (thickness) were elected 15 values from 5-113 mm with ratio 1.25. For the parameter Input 2 (nozzle wear) were chosen 4 values from 0 to 0.1 mm with ratio 2. The results obtained during the validation phase are better, the error being less then 10 % (Figure 3).

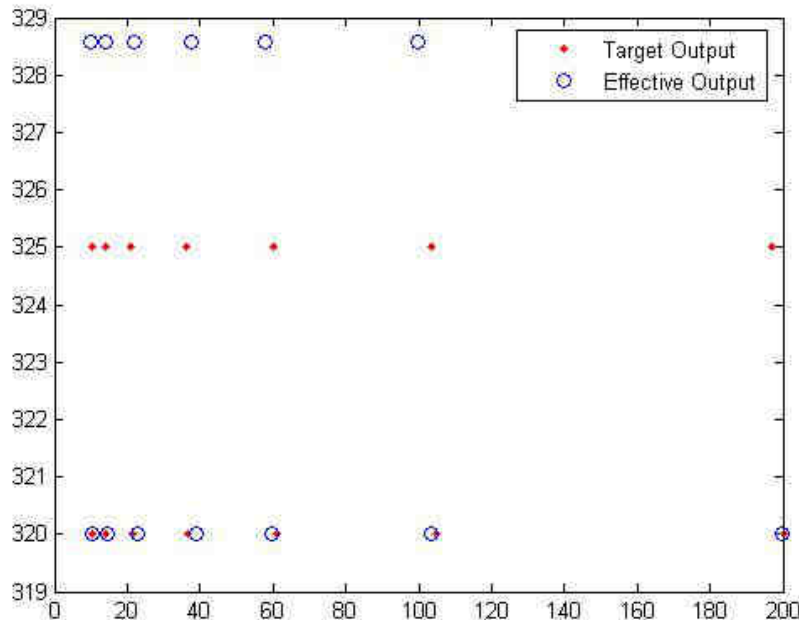


Figure 3. Representation of the target outputs – effective outputs (after the second training)

3. Conclusions

The following steps need to be taken in order to develop a neural model that accounts for all the technological parameters of a water jet cutting machine: selecting the input parameters; sorting the parameters into categories; determining the number of input variables; determining the output parameters; creating separate models for different types of machined materials; preparing the training data and the validation data; choosing the network structure and beginning training; validating the model and using it commercially.

In order to obtain an acceptable error it is necessary to train the network with a set of data as large as possible. Also it is recommended that the domain covered by training data is greater than the domain covered by normal work data.

REFERENCES

- [1] C.Ciupan, L. Morar, A. Pop, "Innovative system with abrasive water jet", Annals of DAAAM for 2008 & Proceedings of the 19th International DAAAM Symposium, B. Katalinic (eds.), ISBN 978-3-901509-68-1, Vienna, oct. 2008, DAAAM International Vienna
- [2] A. Pop, "Study of Computer Control Strategy for Jet Cutting Integrated Systems", Ph.D. Thesis, Technical University of Cluj-Napoca, 2004
- [3] A. Zilouchian, M. Jamshidi, Intelligent Control Systems Using Soft Computing Methodologies, CRC Press, 2001
- [4] <http://www.waterjets.org>

EXPERIMENTAL RESEARCH BY MEASURING THE PULLING FORCE OPERATING PRESSURE USING THE DATA ACQUISITION BOARD

Constantin CHIRIȚĂ¹, Andrei GRAMA¹ Mihai AFRĂSINEI¹, Vasile DAMASCHIN¹

¹ Tehnical University "Gheorghe Asachi" from Iassy, e-mail address andreiasi79@yahoo.com

Abstract: The purpose of this research is to highlight all the phenomena occurring in the system during a pulling cycle which allows us to intervene in order to optimize the operating parameters of the device to pull the piston race start time until when there is actual grabbing stranded and effective start pulling. By carrying out a set of experiments using data card achizition presented in this paper, we determine and conclude data position working cylinder tensioning device at the start pulling to its initial position and the efective start pulling

Keywords: pretensioning device, pressure

1. Introduction

The purpose of this research is to highlight all the phenomena occurring in the system during a pulling cycle which allows us to intervene in order to optimize the operating parameters of the device to pull the piston race start time until when there is actual grabbing stranded and efective start pulling. This allows us to determine the position of the working cylinder tensioning device when starting the drawing to its original position and the efective start pulling.

2. The stand of experimental presentation

Data acquisition will be on stand shown in Fig. 2.1,

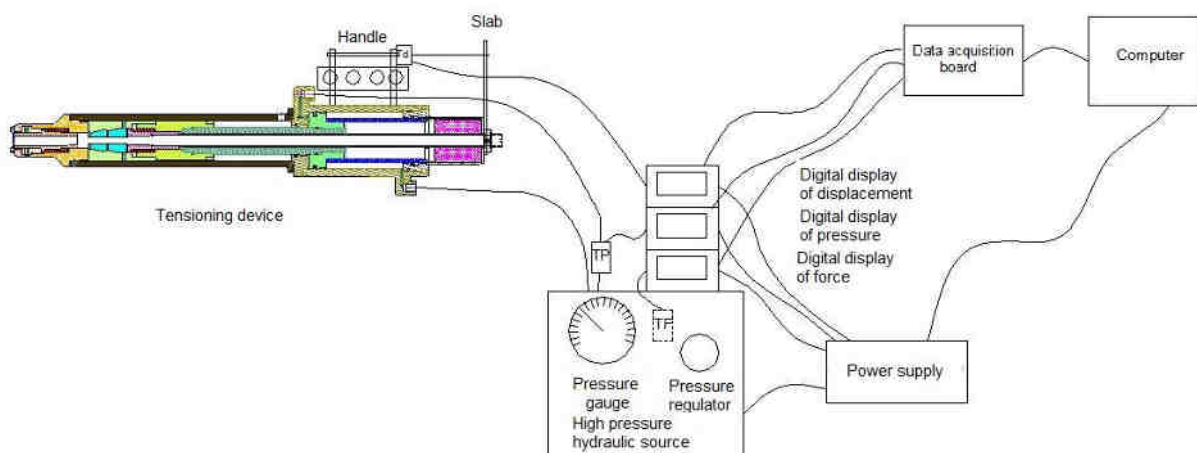


Fig. 2.1. Stand working to determine the main parameters of the single wire tensioning device with data acquisition card and a Computer (PC)

Data acquisition system include:

1. Transducers

- a. Pressure transducer 0 to 1200 bar produced by SUCO, code transducer 0620 [1]
Output signal 4-20 mA 2-wire
Input pressure from 0 to 1200 bar
Accuracy class $\pm 0.5\%$ of maximum pressure at 20 °C

- [2] b. Load transducer from 0 to 25 tF produced by Aplisens, code transducer PCE28PD
Output signal 4-20 mA 2-wire
Input pressure from 0 to 1000 bar
Accuracy class $\pm 0.2\%$
- [3] c. Displacement transducer 0 to 1000 mm produced by HYDRAMOLD code HTD 1000
Output signal 4-20 mA 2-wire
Domeniul de măsurare 0 – 1000 mm
Analog signal - quadrature pulses 0-5 V
Accuracy class $\pm 0,01\%$
- d. Digital display units HYDRAMOLD products codeHUDA -01AI [3]
Output signal 4-20 mA 2-wire
The measuring range can change depending on what you want to measure the 4 digits and three decimal opportunity
Accuracy class $\pm 0,5\%$
2. Data acquisition system include:
- Terminal block
 - Digital analog converter (DAQ)
 - Cables

Terminal block produced by National Instrument, BCS product code 68 [3]

SCB-68 terminal block is a sturdy block, shielded, terminated by a DAQ device for damping noise type with 68 pins. It includes a provisional assembly and a temperature sensor IC to compensate for the cold junction temperature measurement.

Dimensions 19,5X15,2X4,5 cm
Multifunctional accessories DAQ
Series M - 68 pin device
Noise reduction
Connect with threaded socket
Connectors 0 or 1

Digital analog converter (DAQ) is manufactured by National Instruments, NI DAQ Card product code - 6036 E. [4]

Analog input
Single output channel number 16
Number of differential channels 8
Resolution 16 bit
Transfer rate 200 kS/s
Maximum voltage 10 V
The maximum change voltage -10V, 10V
Accuracy maximum voltage variation 7,56 mV
Minimum variation voltage -50 mV, 50 mV
Accuracy minimal changes voltage 0,061 mV

Analog output
Number of channels 2

Resolution 16 bits
 Maximum voltage 10 V
 The maximum change voltage -10V, 10V
 Accuracy maximum voltage variation 2,547 mV
 Minimum variation voltage -10 V, 10 V
 Accuracy minimal changes voltage 2,547 mV
 Transfer rate 1 KS/s
 Input current 5mA one channel
 Channel intensity 10mA

Digital input / output
 Bidirectional channels 8
 Input channels 0
 Synchronization schedule
 Logic levels TTL
 Programmable input filters don't have
 Intensity to a value 24 mA
 Intensity for all values 192 mA
 Timer don't have
 Depreciation I / O don't have
 The maximum change voltage 0V, 5 V
 Minimum variation voltage 0V, 5 V

Counter (soft)
 Number of counters 2
 Maximum voltage 0V, 5 V
 Maximum frequency of the source 20 MHz
 The minimum input pulse 10 ns
 Pulse generator have
 Resolution 24 bits
 Stability in time 100 ppm
 TTL logic levels
 Dimensions: 8,56x5,4x0,5 cm

Produced by National Instrument cable, product code 68-68 SHC-EPM [4]

3. IBM PC computer system x86
4. Software
 - S. O. Microsoft Windows XP SP3 x86
 - LabView 8.5
 - LabView 8.5.1 Real Time



Fig. 2.1. Stand Overview



Fig. 2.2. Overview stand and modules for data acquisition

An important component of the experimental stand is the automatic control loop, shown in block diagram form in Fig. 2.3

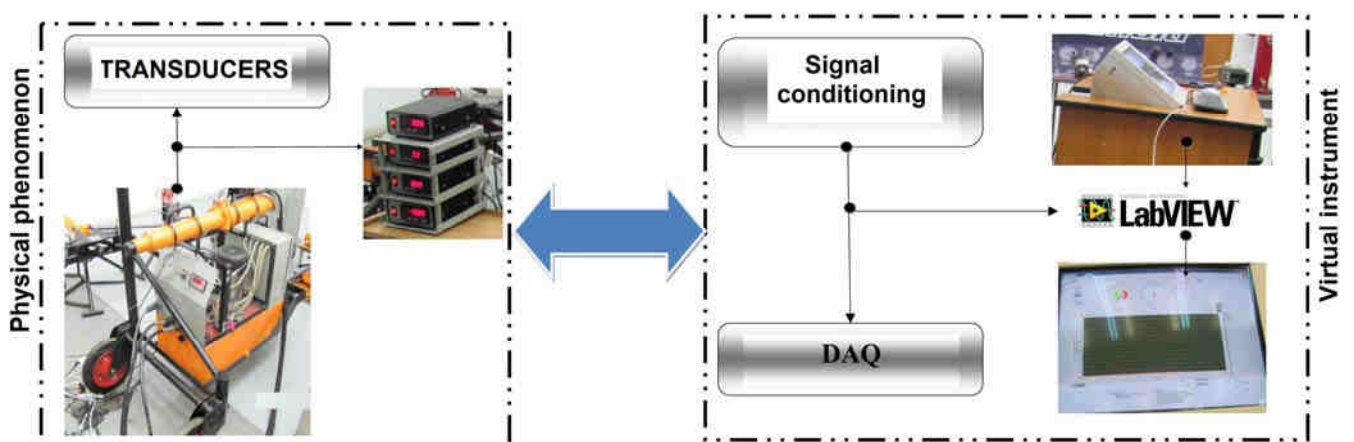


Fig. 2.3 Block diagram of the automatic control loop

Physical phenomenon and receiving transducers convert physical quantity (pressure, force, etc..) In a size other, with digital display units. Toggle between the digital signal from transducer converts the voltage signal thus obtained is proportional to the size variation monitored.

SCB-68 terminal block electrical signals generated by the transducers bring in a form that digital analog converter (DAQ) can accept. The terminal may signal amplification condition, its linearization, filtering, etc..

Acquisition board to convert electrical signals through its basic component, analog-to-digital converter. This displays a numeric value to a voltage, thus making it possible interpretareaa the computing system.

Virtual tool work bench in Fig. 3.33 comprises the hardware - digital analog converter (SCB-68 terminal block, data acquisition card NI DAQ Card - 6036 E and its relationship with cable-EPM SHC 68-68 and the software, taken in conjunction with the needs of working hydraulic stand. The resulting virtual instrument comprising: measuring instruments and controls for plant automation.

The graphical interface of this program included digital display units and signs made in a form similar graphics devices and real devices, the user manevrându also their real elements.

Virtual instruments associated hydraulic stand was developed using LabVIEW programming environment used mainly for signal acquisition and presentation graphics or table data.

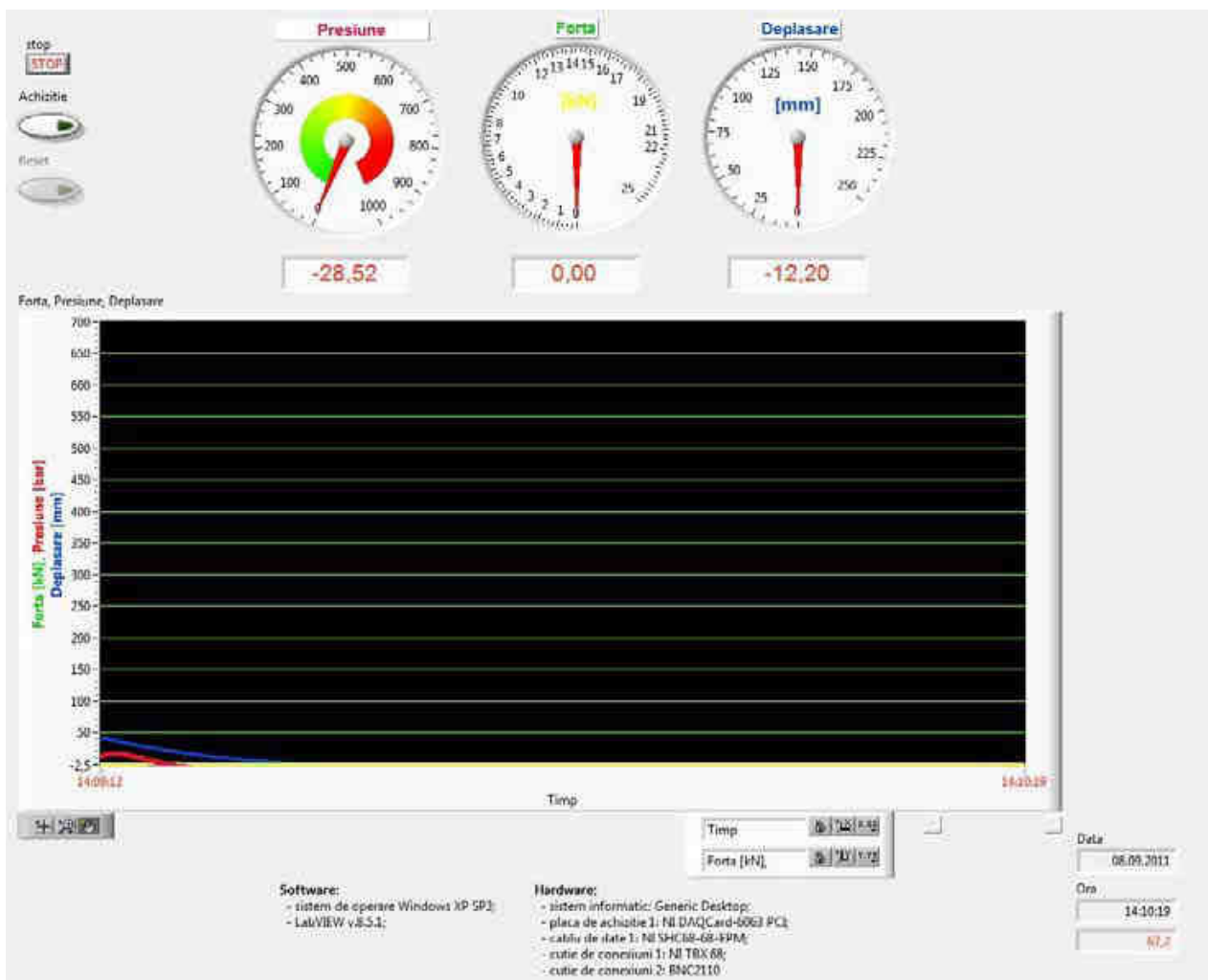


Fig. 2.4. Overview of data acquisition terminal display

Terminal shown in Fig. 3.37, includes a series of bar graphs to visualize signals scaled unit corresponding physical quantity monitored through hardware part that receives signals from transducers mounted on the equipment for tensioning in Fig. 3.33. Displays all system through introducing numeric calculation, or a virtual potentiometer, setpoint (SETPOINT) which was used in digital toggle between. Terminal panel was created using elements of display and control

procedures extracted from library LabVIEW programming environment, adapted to the experimental stand.

Data obtained during the experiment can be viewed in numerical form (right next chart Fig. 2.4) corresponding indicator as measured quantities or as window graphic created for this purpose.

3. Development program at experiments

Experiment was conducted for 16 tF tensioning device with stroke 200 mm at idle. To perform data acquisition was pursued to achieve links to all components of the stand, checking their physical and connections for data acquisition.

Purpose data acquisition is to check the seating position of a set of marten corbel from the tensioning device of 16 tF stroke of 200 mm. For this tensioning device consists of a arc positioning ferries limiting drawing as shown in Fig. 3.1.

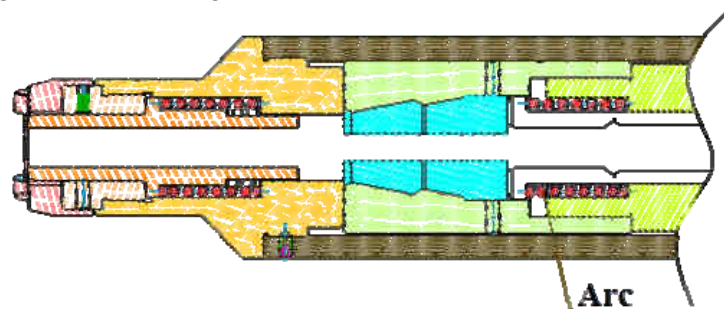


Fig. 3.1. Section tensioning device

Adjustable arc analyzed using cross pintle nut.

To obtain a satisfactory result, have made a total of three shots at full load tensioning device previously prepared.

After testing, we were unable to obtain numerical data, which were made graficele in Fig. 3.2 - 3.4, where we see how time-varying data using data acquisition board for input parameters, respectively while firing cylinder displacement and output parameters: friction and pressure working conditions listed above.

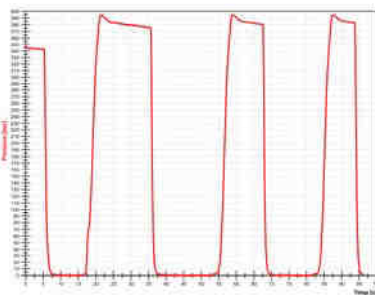


Fig. 3.2. Pressure variation over time of three races positioning spring

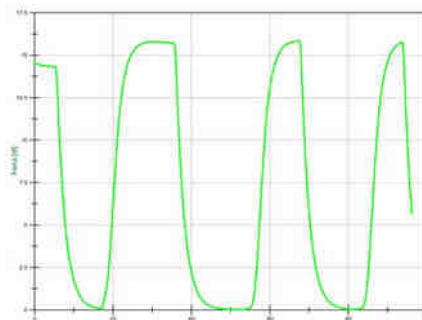


Fig. 3.3. Force variation with time for three races positioning spring

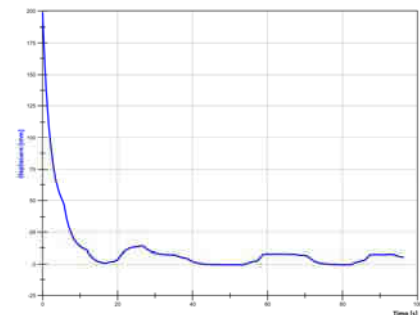


Fig. 3.4. Displacement variation with time for the first three races of positioning adjustment spring

The data provided by the data acquisition board, we can see that working pressure of working hydraulic pressure source and the force experienced by the device components from tension varies proportionally to time by law shown in Fig. 2.6 and 2.7, adjustment for the three values of initial positioning spring firing ferries, the amount of force and pressure varied in the same conditions for all three tests performed.

By analyzing data from the pressure and pulling force when the race reaches the beginning of the tensioner, and these low values of 0.7 bar, 0.15 tF respectively.

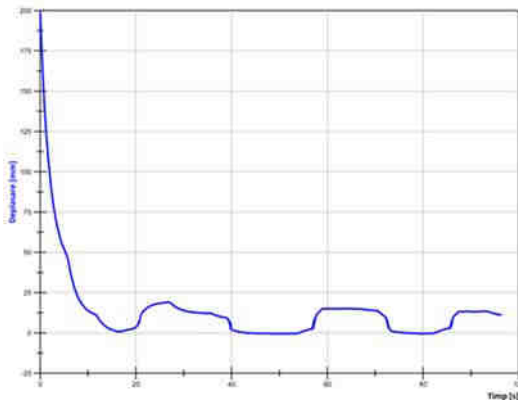


Fig. 2.9. Displacement variation over time of three races arc positioning achieved by adjusting two empty tensioning device 16tF with a 200 mm stroke, using a data acquisition board.

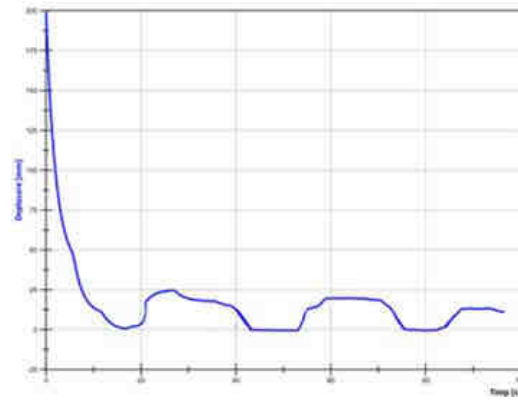


Fig. 2.10. Displacement variation over time of three races positioning spring by the third adjustment made with the tensioning device 16tF with stroke 200 mm, using a data acquisition board.

4. Conclusions

Firing cylinder displacement value varies depending on how performing positioning control spring clamp for tensioning strand. Following such an arc testing were obtained drawing cylinder displacement variations for different settings of the arc. It can be seen from data from data acquisition board that this value varies from 15 mm to 18.5 mm and then 25 mm.

To get the best possible adjustment of the spring, there will be a mechanical clamping nut with as strong transverse pin for zero value of the cylinder stroke work tensioning device and maintain for a longer period of time tensioning device in position to withdraw the original position.

REFERENCES

- [1] Suco <http://www.suco-pressureswitches.com>
- [2] Aplsens <http://www.aplsens.pl/en/produkty/pc.html>
- [3] Hydramold, <http://www.hydramold.com/produse.php?cat=SistemeMasurareDigitala>
- [4] National Instruments <http://www.ni.com/>

RISK ASSESSING WITH FMEA ANALYSIS AND FUZZY LOGIC

Despina DUMINICĂ¹, Mihai AVRAM², Iulian DUȚU³

¹ POLITEHNICA University of Bucharest, despina_duminica@yahoo.com

² POLITEHNICA University of Bucharest, mavram02@yahoo.com

³ Hydraulics and Pneumatics Research Institute, Bucharest, dutu.ihp@fluidas.ro

Abstract: *The need for failure free products occupies a privileged position among increasing customer expectations. In order to satisfy such requirements, risk analysis must be performed in the early stage of a product development. Failure mode and effect analysis is a systematic technique for identifying, prioritizing and obviating potential failure modes before they occur. Fuzzy risk priority numbers are considered a promising solution in order to give a more accurate ranking of potential risks.*

Keywords: *quality assurance, failure modes and effect analysis, fuzzy risk priority numbers*

1. Introduction

Nowadays, a company looking for competitive advantage must keep in mind that the timescale of product conception and development is shifting from the long to the shorter term – and ultimately to a near real-time response. In order to comply with increasing customer expectations, incorporating quality in products and services even from their development stages is a must.

Failure Modes and Effect Analysis (FMEA) is a methodology designed to identify potential failure modes for a product or process before they occur, to assess the risk associated with each failure mode, to rank the issues in terms of importance and to identify and carry out corrective actions to address the most serious concerns. Corrective actions include, among others, fail-safe mechanisms, redundant controls, error-handling routines, fault-tolerance, alarms and testing activities.

Two alternative approaches may be used: a functional approach or a hardware approach. The functional approach considers sub-systems in terms of their function within the system, being often applied when hardware components cannot be uniquely identified, and the hardware approach is usually adopted when components can be uniquely identified in the system.

The formal approach of FMEA analysis is documented in [1]. The method and its applications are also described in [2].

The FMECA procedure extends the FMEA analysis and consists of two parts: the first part identifies failure modes and their effects and the second part ranks failure modes according to their potential risks. The risk associated with the potential problems identified through the analysis is evaluated, generally, by two methods: risk priority numbers (RPN) and criticality analysis.

Two types of criticality analysis, quantitative and qualitative, are described in [1]. To use the quantitative criticality analysis method, the team must:

- define the reliability / unreliability for each item, at a given operating time;
- identify the portion of the item's unreliability that can be attributed to each potential failure mode;
- rate the probability of loss (or severity) that will result from each failure mode that may occur;
- calculate the criticality for each potential failure mode by obtaining the product of the three factors: Item Unreliability, Mode Ratio of Unreliability and Probability of Loss;
- calculate the criticality of each item by obtaining the sum of the criticalities for each failure mode that has been identified for the item.

To use the qualitative criticality analysis method to evaluate risk and prioritize corrective actions, the analysis team must:

- rate the severity of the potential effects of failure;
- rate the likelihood of occurrence for each potential failure mode;
- compare failure modes via a criticality matrix, which identifies severity of the horizontal axis and occurrence on the vertical axis.

Risk priority numbers are mostly used in the automotive industry [3]. A risk priority number (RPN) represents the mathematical product of the seriousness of a group of effects (severity S), the likelihood that a cause will create the failure associated with those effects (occurrence O), and an ability to detect the failure before leading to serious effects (detection D). RPNs are used to help identify the most serious risks and to place priorities when planning corrective action.

2. Typical Computation of Risk Priority Numbers

In order to perform RPN computation, Severity, Occurrence and Detection should be quantified. Different situations are rated on a scale sensible enough, according to consistent evaluation criteria. Scales from 1 to 10 or from 1 to 4 are generally used. The minimum value ("no risk") is rated with 1.

The case study consisted of the RPNs computation in order to assess and rank risks that could appear in the functioning of a water meter used in domestic applications.

The FMEA analysis was based on the causes and effects diagram presented in figure 1. The diagram pointed out the problems that could appear in the functioning of the water meter.

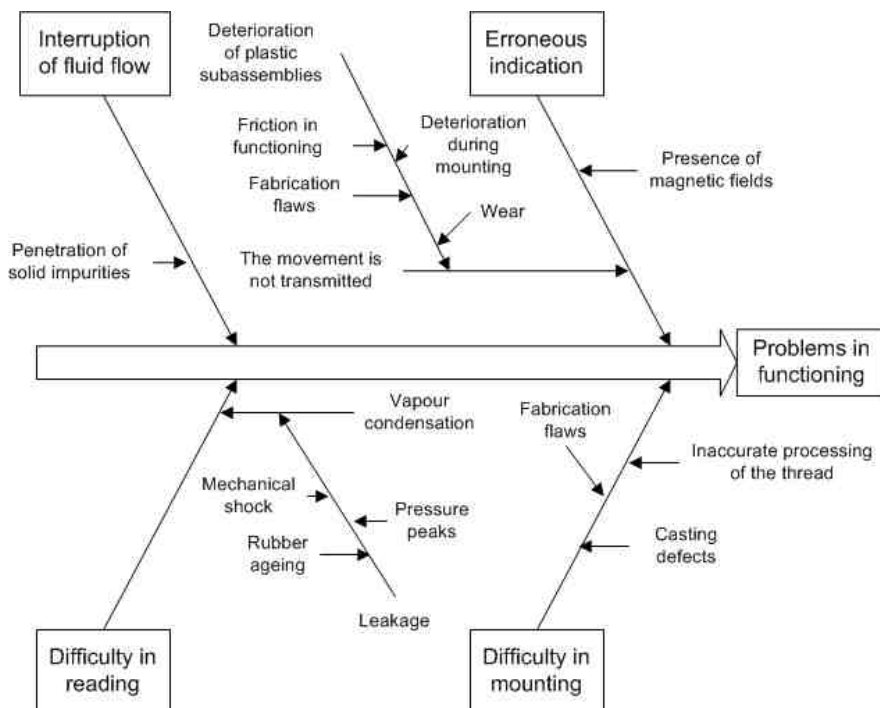


Fig. 1: Causes and effects diagram established for the water meter

Due to the fact that FMECA analysis involves a great amount of design, maintenance and cost data, the need for a database dedicated to quality problems appeared. Using this purpose-developed database, it is possible to elaborate detail and summary maintenance reports, monthly reports, reports for a specified kind of product, for a specified kind of failure mode or exception reports (for instance, the percentage of products that fail before the mean working time).

The created database allows developing a unified coding system for components, functions and their importance, failure modes, causes, effects and means of prevention. Using the database eases also the work when doing FMECA analysis, proving itself especially useful when determining RPNs.

Severity, Occurrence and Detection were rated according to Table 1 [4].

Table 1: Rating Severity, Occurrence and Detection

<i>Occurence: Failure Rates</i>	<i>Rank</i>	<i>Severity:</i>	<i>Rank</i>
Repeated failures: more than 1 in 10	10	Repairing time longer than 60 min	4
Repeated failures: under 1 in 10	9	Repairing time between 20 and 60 min	3
Repeated failures: under 1 in 50	8	Repairing time between 1 and 20 min	2
Occasional failures: under 1 in 100	7	Repairing time under 1 min	1
Occasional failures: under 1 in 200	6	<i>Likelihood of Detection by Design Control</i>	<i>Rank</i>
Occasional failures: under 1 in 500	5		
Occasional failures: under 1 in 1,000	4	No warning signs	4
Relatively few failures: under 1 in 5,000	3	Warning signs difficult to notice	3
Relatively few failures: under 1 in 10,000	2	Warning signs that could pass unnoticed	2
Failure is unlikely: under 1 in 100,000	1	Warning signs easily noticeable	1

Figure 2 presents an example of introducing service data (the same example of the water meter was considered).

The screenshot shows a software window titled "FMECA Analysis". It contains several input fields with dropdown menus. The data entered is as follows:

- Part Code:** GET2
- Failure Mode :** Wear
- Potential Effect :** Water condenses
- Potential Cause :** Rubber ageing
- Prevention Means :** Choosing of appropriate materials
- Person In Charge :** Cristescu Doina
- Occurence :** Occasional failures: under 1 in 1000
- Severity :** Repairing time between 1 and 20 min
- Detection :** Warning signs that could pass unnoticed

At the bottom, there is a status bar that says "Record: 6 of 16".

Fig. 2: Form used for introducing service data

Maintenance data allow determining the percentage of failures in meeting a requirement, fact that eases choosing the appropriate prevention means. It is possible also to estimate costs for a specified function, using the cost function matrix. Various libraries of components, associated with their costs, allow the comparison of solutions, in order to select the most appropriate one from the point of view of life cycle costing.

Synthetically, the advantages offered by the developed database are:

- computation of FMECA parameters, such as RPNs;
- correlation among functions, components and costs;
- unified framework that integrates design data for the new product and maintenance data for similar products, characteristic of concurrent engineering.

3. Fuzzy Computation of Risk Priority Numbers

However, the specific criteria generally used for describing Severity, Occurrence and Detection (such are the criteria presented in Table 1) are mostly subjective and described qualitatively in natural language, deriving from the previous experience of a group of experts or of the design team. It has also being pointed out that different score combinations of severity, occurrence and detection led to the same RPN, even when it was obvious that the gravity of the risks involved was not the same [5]. The relative significance of the three indexes is neglected, all of them being assumed to be of equal importance, when in fact the nature of a process or of a product increases often the weight of an index in regard to the other two. Consequently, some combinations of the three indexes S, O and D can hide high danger risks even if their RPN is relatively low.

Another shortcoming of the typical RPN computation method is that only a limited set of outputs from the output range can be obtained. For instance, if each of the three inputs is rated on a scale from 1 to 10, their combination leads to only 120 values from the range of $10 \times 10 \times 10 = 1000$ values. The mean of these 120 values is equal to 166, far from the middle of the interval, and the medial is equal to 105. In fact, only 6% of the obtained values situate among the middle of the interval.

To overcome the above presented weaknesses of the typical approach, fuzzy mathematics, developed for solving problems where parameter descriptions are subjective, vague and imprecise, was considered a promising tool for directly manipulating the linguistic terms used for the description of severity, occurrence and detection in order to assess risks associated to each failure mode [5-8].

The methodology of the fuzzy RPNs is based on fuzzy set theory [9, 10]. The three inputs S, O and D are fuzzified and evaluated in a fuzzy inference engine built on a consistent base of IF-THEN rules. The fuzzy output is defuzzified to get the crisp value of the RPN that will be used for a more accurate ranking of the potential risks.

The case study continued with the fuzzy computation of RPNs. Occurrence, severity and detection were rated on a scale from 1 to 10, according to Tables 2, 3 and 4. The analyzed failure modes are presented in Table 5 and the resulted RPNs are presented in Table 6. For the sake of clarity, only the first relevant 8 failure modes were preserved.

Table 2 Occurrence Rating

<i>Occurrence: Failure Rates</i>	<i>Rank</i>
Repeated failures	8, 9, 10
Occasional failures	4, 5, 6, 7
Relatively few failures	2, 3
Failure is unlikely	1

Table 3 Severity Rating

<i>Severity: MTTR (Mean Time To Repair)</i>	<i>Rank</i>
Repairing time longer than 60 min	8, 9, 10
Repairing time between 20 and 60 min	4, 5, 6, 7
Repairing time between 1 and 20 min	2, 3
Repairing time under 1 min	1

Table 4 Detection Rating

<i>Detection: Likelihood To Detect The Failure Before Serious Effects Appear</i>	<i>Rank</i>
No warning signs	8, 9, 10
Warning signs difficult to notice	4, 5, 6, 7
Warning signs that could pass unnoticed	2, 3
Warning signs easily noticeable	1

Table 5 Analyzed Failure Modes

<i>Code</i>	<i>Involved part or subassembly</i>	<i>Failure mode</i>	<i>Effect</i>	<i>Potential cause</i>	<i>Preventive action</i>
FM1	Body	Unable to mount	Replacement of the water meter	Inaccurate processing of the thread	Assurance of the quality of manufacturing
FM2	Body	Leakage	Fluid leakage	Casting defects	Assurance of the quality of casting
FM3	Body O-ring	Wear	Fluid leakage, condensation	Rubber wear	Adequate materials
FM4	Body O-ring	Wear	Fluid leakage, condensation	Deterioration during mounting	Assurance of the quality of mounting
FM5	Gear subassembly	Input loss	Erroneous indication	Friction in functioning	Adequate materials
FM6	Plastic cover	Breaking, cracking	Penetration of impurities	Mechanical shocks	Adequate materials
FM7	Plastic cover	Breaking, cracking	Penetration of impurities	Plastic ageing	Adequate materials
FM8	Indicator subassembly	Input loss	Erroneous indication	Friction in functioning	Adequate materials

Table 6 Criticality Assessment Using RPNs

<i>Code</i>	<i>Failure rates</i>	<i>O</i>	<i>MTTR (min)</i>	<i>S</i>	<i>Likelihood of non-detection (%)</i>	<i>D</i>	<i>RPN</i>	<i>Rank</i>
FM8	under 1 in 5,000	3	30	5	65	7	105	1
FM5	under 1 in 1,000	4	20	3	75	8	96	2
FM3	under 1 in 1,000	4	15	3	20	5	60	3-4
FM2	under 1 in 50,000	1	45	6	95	10	60	3-4
FM1	under 1 in 30,000	1	30	4	80	9	36	5
FM4	under 1 in 10,000	2	15	3	25	5	30	6
FM7	under 1 in 5,000	3	5	2	5	2	12	7
FM6	under 1 in 20,000	1	5	2	5	2	4	8

As mentioned above, the allocation of the scores remains subjective. It is a matter of estimating the risks involved, thus different experts can have different opinions.

The resulting hierarchy is somewhat unexpected. For instance, one would suppose that failure modes with high dissatisfaction potential (FM1, FM2, FM3) would have a higher ranking. Also, equal priorities are assigned to two very different failure modes (FM3 and FM2).

In order to obtain a risk prioritization that would reflect better the customer perception in terms of dissatisfaction, a fuzzy computation of the RPN was proposed.

The fuzzy sets corresponding to the inputs and to the outputs are presented in Table 7. Four categories were associated to each fuzzy set: VL (very low), L, (low), M (moderate) and H (high). The output of the fuzzy system, FRPN, was scaled in the range 0...1000 in order to be compatible with the previous results. Table 8 presents the inference rules adopted for this application, based on expert knowledge.

Table 7 Fuzzy sets corresponding to inputs and outputs

Name	Symbol	Type	Indicator	Unit	Min. value	Max. value	Fuzzy sets
Occurrence	O	Input	Common logarithm of failure rate	-	-6	0	VL, L, M, H
Severity	S	Input	MTTR	min	0	100	VL, L, M, H
Detection	D	Input	Likelihood of non-detection	-	0	1	VL, L, M, H
Fuzzy RPN	FRPN	Output	-	-	0	1000	VL, L, M, H

Gaussian shapes were adopted for the membership functions, because they are considered to best fit normal distributions and also allow obtaining a more smooth control surface, without sharp edges that can lead to an unpredictable behaviour of the system.

Minimum function was used in order to implement AND method and implication. Maximum function was used in order to implement OR method and aggregation. The centroid method was chosen for defuzzification.

The fuzzy logic system was simulated using MATLAB-SIMULINK. Figure 3 presents, as an example, the set of rules activated for the values corresponding to the failure mode FM1.

Table 8 The inference rules

Occurrence: VL					
		Severity			
		VL	L	M	H
Detecti on	VL	VL	VL	VL	L
	L	VL	VL	L	L
	M	VL	L	L	M
	H	L	L	M	M

Occurrence: L					
		Severity			
		VL	L	M	H
Detecti on	VL	VL	VL	L	L
	L	VL	L	L	M
	M	L	L	M	M
	H	L	M	M	H

Occurrence: M					
		Severity			
		VL	L	M	H
Detecti on	VL	VL	L	L	M
	L	L	L	M	M
	M	L	M	M	H
	H	M	M	H	H

Occurrence: H					
		Severity			
		VL	L	M	H
Detecti on	VL	L	L	M	M
	L	L	M	M	H
	M	M	M	H	H
	H	M	H	H	H

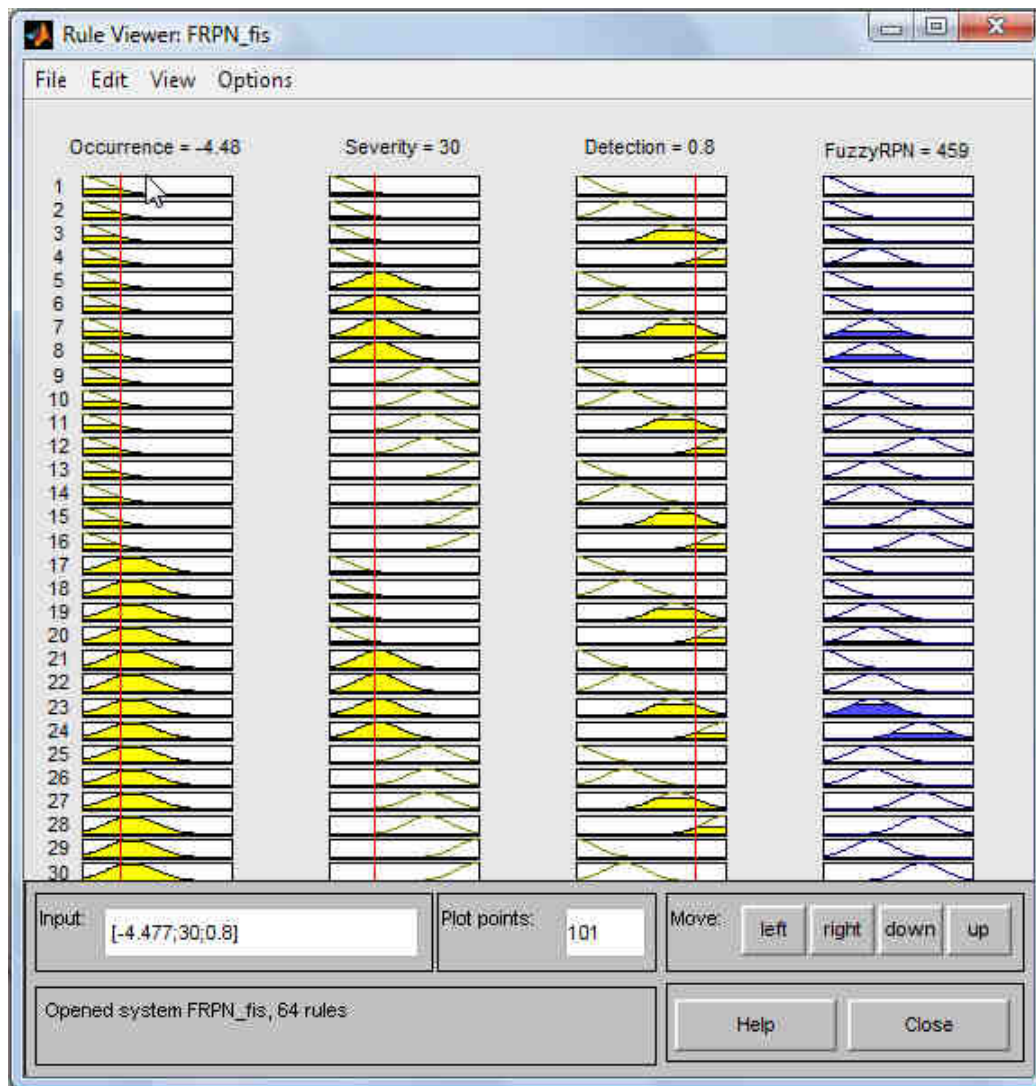


Fig. 3: Set of rules activated by the failure mode FM1

The same failure modes were analyzed, in order to compare the previous results, calculated by "classical" assessment of RPNs, with the values obtained by fuzzy computation. The defuzzification values of RPNs are presented in Table 9.

Table 9 Fuzzy computation of RPNs

Code	Involved part or subassembly	Failure mode	Fuzzy RPN	Rank	Previous rank
FM2	Body	Leakage	532.8	1	3-4
FM1	Body	Unable to mount	459	2	5
FM5	Gear subassembly	Input loss	425.6	3	2
FM8	Indicator subassembly	Input loss	374	4	1
FM3	O-Ring	Wear	289.3	5	3-4
FM4	O-Ring	Wear	202.8	6	6
FM7	Plastic cover	Breaking, cracking	192.2	7	7
FM6	Plastic cover	Breaking, cracking	169.2	8	8

It can be noticed that the results obtained by fuzzy inference provide a hierarchy of potential risks that differs from the ranking established by typical computation of the RPN, but reflect more accurately the dissatisfaction felt by the customer that faces the effects of a certain failure mode.

The fuzzy inference does not allow identical values of RPNs to appear for different sets of risk factors. In fact, two identical RPNs can be obtained only for two failure modes that feature exactly the same values of the three indexes: occurrence, severity and detection.

4. Conclusions

The results obtained by fuzzy inference provide a hierarchy of potential risks that differs from the ranking established by typical computation of the RPN, but reflect more accurately the dissatisfaction felt by the customer that faces the effects of a certain failure mode. Risk factors are evaluated in a linguistic manner, using qualifications rather than rigorous numerical values. This feature eases the manipulation of vague and imprecise information, often the case in the practice of product design. Fuzzy inference does not allow identical values of RPNs to appear for different sets of risk factors. Also, the whole range of outputs is used. The method can be extended considering even more risk factors.

REFERENCES

- [1] US-MIL-STD-1629A, "Procedures For Performing A Failure Mode Effects And Criticality Analysis", 1984
- [2] D. H. Stamatis, "Failure Mode and Effect Analysis – FMEA from Theory to Execution", ASQC Press, New York, 1995
- [3] Ford Motor Company, "Potential Failure Mode And Effect Analysis In Design And For Manufacturing And Assembly Process", Instruction Manual, 1998
- [4] H. Garin, "AMDEC/AMDE/AEEL", AFNOR, Paris, 1994
- [5] A. Pillay, J. Wang, "Modified failure mode and effects analysis using approximate reasoning", Reliability Engineering & System Safety, 2003 (79), pp.69–85
- [6] J.B. Bowles, C.E. Pelaez, "Fuzzy logic prioritization of failures in a system failure mode, effects, and criticality analysis," Reliability Engineering and System Safety, 1995, (50), pp.205-213
- [7] L.-H. Chen, W.-C. Ko, „Fuzzy linear programming models for new product using QFD with FMEA“, Applied Mathematical Modeling, 2009, (33), pp.633-647
- [8] H.T. Liu, "The extension of fuzzy QFD: From product planning to part deployment", Expert Systems with Applications: An International Journal archive, 2009, (36) pp.11131-11144
- [9] L. A. Zadeh, "Fuzzy sets", Information and Control, 1965, (8), pp.338–353
- [10] H. Bühler, "Réglage par logique floue", Presses Polytechniques et Universitaires Romandes, Lausanne, 1994.

THE STUDY OF ELASTIC-PLASTIC PROPERTIES OF THE COMPOSITE PLATING MACROINDENTATION

Vasile JAVGUREANU¹, Pavel GORDELENCO²

¹ Technical University of Moldova, v_javgureanu@yahoo.com

² Technical University of Moldova, pavel_gr@mail.utm.md

Abstract: *Determined that no recovery and dynamic hardness work expended on elastic-plastic deformation have extreme character study for the iron plating that coincide with previous recommendations for these coatings in terms of their optimal durability.*

Keywords: *elastic-plastic, properties, composite, plating, macro indentation, micro hardness.*

1. Introduction

The relevance of the study and control of physical and mechanical properties of materials at the surface and in the upper layers due to the fact that the contact interaction and contact deformation associated almost all modern methods of treatment, hardening and metal compounds, and service properties of materials under conditions of cracking, fatigue, seizure and wear. One of the methods for testing the surface properties of materials - testing micro hardness or macrohardness.

2. Overview

Development of the indentation test can be qualitatively compared to the development of the tensile test, when the transition was made from a simple tensile test for continuous registration chart stress - strain. Material test method measures the indentation several important parameters characterizing the physical - mechanical characteristics of composite electroplating, both traditional and newly produced only by these tests. Test method of elastic plastic properties of coatings based on the record of the kinetic diagram pressing a spherical diamond indenter. As a spherical diamond indenter used artificial diamond with sphere radius of 1 mm. The test is composite iron electroplating thickness of 0.5 mm, the diameter of the sample in this case is 30 mm.

Test method for macrohardness allows testing of materials for wide purposes from 1 micron or more. One cannot determine the fraction of the strength characteristics of the material, but also the elastic plastic properties of the material.

Many researchers have studied the shape of the plastically deformed zone and the nature of the deformation in the volume under the imprint [1]. The overall conclusion of this work is to ensure that the boundary of the plastically deformed zone under the imprint of diameter d is similar in shape to the part of the sphere for both metals and for polymers. This conclusion is valid also for the case of the elastic indentation of the sphere.

We studied the deformation of deep and surface layers of the material [1] under the indenter methods applied in the plane of the grid meridian section of the specimen. In fig.1 shows the deformation of the material layers deep indentation of a spherical indenter [1].

The figure shows that the maximal strain axis at a depth of indentation half the radius of the print at the point of maximum shear stress. On the surface indentation strain grows from the centre to the contour near the contour, they decrease and outside change direction. The inversion of the direction of the deformation is due to the fact that in print and at some depth below the material undergoes axial compression and broadening in the radial direction.

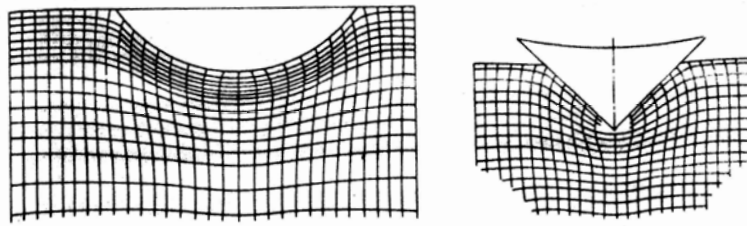


Fig. 1. Distortion rectangular grid ball indentation.

This paper presents the study of elastic-plastic properties of iron plating method indentation of a spherical indenter.

Experimentally determined elastoplastic characteristics (h_y ; h_n ; h) work expended on elastic (A_y), plastic (A_n) and the total deformation (A), unrestored (H_h) and dynamic hardness (H_d), the indentation load on spherical diamond indenter (P) volume and elastic (V_y), plastic (V_n) and total (V) of the deformed material wear iron plating obtained from the electrolyte [1, 2]. Above characteristics were determined at the facility for research in material hardness macro volume equipped with an inductive sensor and a differential amplifier to record chart pressing spherical diamond indenter and indentation recovery after unloading.

Dynamic hardness (H_d) was defined as the ratio of the total of (A) the cost of the deformation to the calculated volume of deformed material (V) and all studied galvanic iron coatings.

3. Discussion of experimental studies.

The study showed that the studied characteristic of wear-resistant iron plating varies with the condition of electrolysis (D_k , T).

With the increase in current density (D_k) from 5 to 40 A/dm² electrolysis at a constant temperature (40°C), the elastic indentation depth (h_y), and pressing the material volume elastic coating (V_y) respectively increased from 1,30 to 1,42 (m) and of $53,4 \cdot 10^{-7}$ to $63,28 \cdot 10^{-7}$ (mm³). Hardness (H_n) dynamic hardness (H_d), the load on the indenter (P) and the work spent on the elastic deformation of the coating (A_y) have extreme values. With increasing current density, table 1, (D_k) of 5 to 20 A/dm², hardness (H_h) increased from 3560 to 3920 (N/mm²), dynamic hardness (H_d) increased from 2375 to 2614 (N/mm²) load on a spherical diamond indenter from 44,7 to 49,2 (H) and the work spent on the elastic deformation of iron plating (A_y) increased from $19,36 \cdot 10^{-3}$ to $21,98 \cdot 10^{-3}$ (N•mm). With further increase of the current density (D_k) from 20 to 40 A/dm² hardness (H_h) decreased from 3920 to 3280 (N/mm²), the dynamic hardness (H_d) decreased from 2614 to 2189 (N/mm²), the load (P) decreased from 49,2 to 41,2 (H) and the work spent on the elastic deformation (A_y) coatings decreased from $21,98$ to $19,50 \cdot 10^{-3}$ (N•mm).

Table 1

Elastic properties and hardness of iron coatings

Electrolysis conditions		H_h , H/mm ² ($h=2 \mu\text{m}$)	H_d , H/mm ²	P , H	Elastic properties of iron plating		
D_k , A/dm ²	T , °C				h_y , μm	A_y , H•mm	$V_y \cdot 10^{-7}$, mm ³
5	40	3560	2375	44,7	1,30	0,01936	53,4
10	40	3760	2515	47,4	1,32	0,02086	54,68
20	40	3920	2614	49,2	1,34	0,02198	56,35
40	40	3280	2189	41,2	1,42	0,01950	63,28

Table 2

Plastic properties and hardness of iron coatings

Electrolysis conditions		Hh, H/mm ² (h=2 μm)	Hd, H/mm ²	P, H	Plastic properties of iron plating		
Дк, A/dm ²	T, °C				hn, μm	Ап, H·mm	Vn·10 ⁻⁷ , mm ³
5	40	3560	2375	44,7	0,70	0,01043	15,38
10	40	3760	2515	47,4	0,68	0,1074	14,51
20	40	3920	2614	49,2	0,66	0,1082	13,67
40	40	3280	2189	41,2	0,58	0,00797	10,56

Extreme hardness (Hh), dynamic hardness (Hd), the load on the indenter (R) and the work spent on the elastic deformation of iron plating coincide with existing guidelines for the choice of electrolysis conditions for optimum electrochemical properties of iron coatings in terms of their durability [2].

With the increase in current density (Дк), table 2, from 5 to 40 (A/dm²) at a constant temperature electrolysis (40°C) plastic indentation depth (hn) and volume plastic indentation material (Vn) are reduced, respectively, from 0.70 to 0.58 (m) and from 15,38·10⁻⁷ to 10,56·10⁻⁷ (mm³).

Table 3

General properties and hardness of iron coatings

Electrolysis conditions		Hh, H/mm ² (h=2 μm)	Hd, H/mm ²	P, H	General properties of iron plating		
Дк, A/dm ²	T, °C				h, μm	A, H·mm	V·10 ⁻⁷ , mm ³
5	40	3560	2375	44,7	2,0	0,0298	125,51
10	40	3760	2515	47,4	2,0	0,0316	125,51
20	40	3920	2614	49,2	2,0	0,0328	125,51
40	40	3280	2169	41,2	2,0	0,0275	125,51

With the increase in current density (Дк), from 5 to 20 (A/dm²) at a constant temperature electrolysis (40°C), hardness (Hh), dynamic hardness (Hd), the indentation load (P) is increased as in the previous case (table 1), and the work expended in plastic deformation of iron coatings increased from 10,43·10⁻³ to 10,82·10⁻³ (N·mm). With further increase of the current density (Дк), at a constant temperature electrolysis (40°C), 20 to 40 (A/dm²), dynamic hardness (Hd), the indentation load (P) is increased as in the previous case (table 1) and the work expended in plastic deformation of iron coatings decreased from 10,82 · 10⁻³ to 7,97·10⁻³ (N·mm).

And in this case, the extreme hardness (Hh), dynamic hardness (Hd), the indentation load (P) and the work expended in plastic deformation (AP) iron coatings coincide with existing guidelines for the choice of electrolysis conditions to obtain the best properties of iron coatings, with a point of their durability [2].

With the increase in current density (Дк), table 3, from 5 to 40 (A/dm²) at a constant temperature electrolysis (40°C), the total indentation depth (h) and total volume dent coating material (V) are constant and are equal to 2.0 (m) and 125,51·10⁻⁷ (mm³).

With the increase in current density (Дк), from 5 to 20 (A/dm²) at a constant temperature electrolysis (40°C), hardness (Hh), dynamic hardness (Hd), the indentation load (P) is increased as in the previous case (table 1.2), and the work expended on the deformation of iron coatings (A) increased by 29,8·10⁻³ to 32,8·10⁻³ (N·mm). With further increase of the current density (Дк), at a constant temperature electrolysis (40°C) 5 to 20 (A/vm²), hardness (Hh), dynamic hardness (Hd), the indentation load (P) decreased as in the previous case (table 1, 2), and the total work expended on the deformation of iron coatings decreased from 32,8·10⁻³ to 27,5·10⁻³ (N·mm).

And in this case, the extreme hardness (Hh), dynamic hardness (Hd), the indentation load (P) and the work spent on the total deformation of iron coatings (A) coincide with the current recommendations for the choice of electrolysis conditions for the production, the optimal properties of iron coatings with point of view of their wear resistance [2].

With increasing temperature electrolysis (T) to obtain the iron plating (table 4) from 20 to 60°C ($D_k=20 \text{ A/dm}^2$) elastic structure component indentation depth (h_y) decreased from 1.52 to 1.10 microns and volume print (V_y) decreased from $72,5 \cdot 10^{-7}$ to $37,98 \cdot 10^{-7} \text{ (mm}^3\text{)}$.

Table 4

Elastic properties and hardness of iron coatings

Electrolysis conditions		Hh, H/mm ² (h=2 μm)	Hd, H/mm ²	P, H	Elastic properties of iron plating		
D_k , A/dm ²	T, °C				h_y , μm	Ay, H·mm	$V_y \cdot 10^{-7}$, mm ³
20	20	2650	1780	33,5	1,52	0,01697	72,5
20	40	3920	2614	49,2	1,34	0,02198	56,35
20	60	2800	1870	35,2	1,10	0,02191	37,98

With increasing temperature electrolysis from 20 to 40°C hardness (Hh) increased from 2650 to 3920 (N/mm²), the dynamic hardness increased from 1780 to 2614 (N/mm²), the indentation load (P) increased from 33.5 to 49.2 (N), the work spent on the elastic deformation of iron coatings (Ay) increased from $16,97 \cdot 10^{-3}$ to $21,98 \cdot 10^{-3} \text{ (N} \cdot \text{mm}^3\text{)}$. With further increase of temperature electrolysis (T) from 40 to 60°C, the hardness (Hh) decreased from 3920 to 2800 (N/mm²), the dynamic hardness (Hd) decreased from 2614 to 1870 (N/mm²), the indentation load (P) decreased from 49.2 to 35.2 (H) and the work spent on the elastic deformation (Ay) iron coatings decreased from $21,98 \cdot 10^{-3}$ to $12,91 \cdot 10^{-3} \text{ (N} \cdot \text{mm}^3\text{)}$. And in this case, the extreme hardness (Hh), dynamic hardness (Hd), the indentation load (P), the work spent on the elastic deformation of iron coatings (Ay) depending on changes in temperature electrolysis (T) at a constant current density ($D_k=20 \text{ A/vm}^2$) coincide with existing guidelines for the choice of electrolysis conditions to obtain the best properties of iron coatings, in terms of their optimal wear resistance [2].

With increasing temperature electrolysis (T) to obtain iron coatings (table 5) from 20 to 60°C ($D_k=20 \text{ A/vm}^2$) increased from 2650 to 3920 (N/mm²), the dynamic hardness increased from 1780 to 2614 (H/mm²), the indentation load (P) increased from 33.5 to 49.2 (H), the work spent on the elastic deformation of iron coatings (Ay) increased from $16,97 \cdot 10^{-3}$ to $21,98 \cdot 10^{-3} \text{ (N} \cdot \text{mm}^3\text{)}$ plastic component of the indentation depth (H_p) increased from 0.48 to 0.90 (m) and volume print in plastic indentations (V_p) increased from $7,23 \cdot 10^{-7}$ to $25,42 \cdot 10^{-7} \text{ (mm}^3\text{)}$.

Table 5

Plastic properties and hardness of iron coatings

Electrolysis conditions		Hh, H/mm ² (h=2 μm)	Hd, H/mm ²	P, H	Plastic properties of iron plating		
D_k , A/dm ²	T, °C				h_y , μm	Ay, H·mm	$V_y \cdot 10^{-7}$, mm ³
20	20	2650	1780	33,5	0,48	0,00536	7,23
20	40	3920	2614	49,2	0,66	0,01082	13,67
20	60	2800	1870	35,2	0,90	0,01056	25,42

With increasing temperature from 20 to 40°C, the hardness (Hh) dynamic hardness (Hd) indentation load (P) has increased in importance as in the previous case (table 4), and the work expended in plastic deformation (Ap) iron coatings increased from $5,36 \cdot 10^{-3}$ to $10,82 \cdot 10^{-3} \text{ (N} \cdot \text{mm}^3\text{)}$. With further increase of temperature electrolysis (T) from 40 to 60°C hardness (Hh) dynamic hardness (Hd), the indentation load (P) decreased in value as in the previous case (table 4), and the work expended in plastic deformation of iron coatings (Ap) decreased from $10,82 \cdot 10^{-3}$ to $10,56 \cdot 10^{-3} \text{ (N} \cdot \text{mm}^3\text{)}$.

With increasing temperature electrolysis (T) from 20 to 60°C, on receipt of iron plating, at a constant current density ($D_k=20 \text{ A/dm}^2$) total depth of indentations (h) and volume print for elasto indentation (V) is constant and appropriate work 2.0 (m) and $125,5 \cdot 10^{-7} \text{ (mm}^3\text{)}$, table 6.

Table 6

Elastoplastic properties of iron coatings

Electrolysis conditions		Hh, H/mm ² (h=2 μm)	Hd, H/mm ²	P, H	Elastoplastic properties iron coatings		
D_k , A/dm ²	T, °C				h, μm	A, H·mm	$V \cdot 10^{-7}$, mm ³
20	20	2650	1780	33,5	2,0	0,02233	125,51
20	40	3920	2614	49,2	2,0	0,03280	125,51
20	60	2800	1870	35,2	2,0	0,02347	125,51

With increasing temperature electrolysis (T) from 20 to 40°C, at a constant current density ($D_k=20 \text{ A/dm}^2$), hardness (Hh), dynamic hardness (Hd), the indentation load (P), increasing in value as in the previous cases (table 4.5), and the work spent on the elastic-plastic deformation of iron coatings indentation increased from $22,33 \cdot 10^{-3}$ to $32,80 \cdot 10^{-3} \text{ (N} \cdot \text{mm}^3\text{)}$. With further increase of temperature electrolysis (T) from 40 to 60°C ($D_k=20 \text{ A/dm}^2$), hardness (Hh), dynamic hardness (Hd), the indentation load (P) decreased in value as the previous cases (table 4), and the work expended in plastic deformation of iron coatings decreased from $32,80 \cdot 10^{-3}$ to $23,47 \cdot 10^{-3} \text{ (N} \cdot \text{mm}^3\text{)}$.

As in the previous cases (table 4, 5) with increasing temperature electrolysis (T), hardness (Hh), dynamic hardness (Hd), the indentation load (P) and work (A) expended in elastic-plastic deformation of iron coatings is extreme.

One of the important problems predicting wear resistance of materials engineering. In this sense, the method of testing the hardness in macro volume relates to micromechanical tests to find the most reasonable approach to the characteristics of the material.

We obtained different parameters Nh, Hd, R and A have a good correlation with the intensity of wear of composite plating.

Thus, the parameters Nh, Hd, A, F can be used later to refine the description of the wear rate on these parameters is based on the concept of additive contribution causes these structural indicators [1].

The study showed that the parameters Nh, Hd, R, A, sensitive elastoplastic properties of composite plating have extreme values as the wear rate, with a change of electrolysis conditions (D_k , T) coincides with the existing recommendations on the choice of electrolysis conditions where optimal properties iron coatings in terms of their durability.

4. Conclusions

• Put the text of your conclusions here Put the text of your conclusions here• Found that the unrecovered hardness (Nh), dynamic hardness (Hd), the work expended on elastic-plastic deformation (A) have extreme character with the changing conditions of electrolysis to study iron coatings.

• Extreme values unreduced hardness (Nh), dynamic hardness (Hd), the indentation load (P), the work expended in plastic (A_p) and elastoplastic (A) deformation coincide with our earlier recommendations for iron coatings in terms of their optimal durability.

• Physical - mechanical characteristics (Nh, Hd, A, A_p , P) plating have a good correlation with the wear rate of the coatings.

• Physical - mechanical characteristics (Nh, Hd, R, A_p , A) can be used to refine the description of the wear of iron coatings.

REFERENCES

- [1] S.Bulichev, V.Alehin, "Ispitanie materialov neprerivnim vdavlivaniem indentora", Moskva, Mashinostroyeniye, 1990, 224p.
- [2] V.Gologan, V.Azhder, V.ZHavguryanu, "Povishenie dolgovechnosti detaley mashin iznosostoykimi pokritiyami", Kishinev, Izd-vo «Shtiintsa», 1979, 112p.
- [3] V.Javgureanu, V.Ajder, V.Ceban, Pavlova L., "The correlation of restored and unrestored microhardness of wearproof iron plating". Conferință științifică internațională TMCR -2003, Chișinău, 2003, pp. 412-415.
- [4] V.Javgureanu, P.Gordelenco, M.Elita, "The work of deforming wear-proof iron-nikel plating in microsqueling", The Annals of University „Dunărea de Jos” of Galați, Fascicle VIII, 2004, Tribology, Romania, pp. 65-68.
- [5] V.Javgureanu, P.Gordelenco, M. Elita, "Relationship of the restored and unrestored microhardness of the chromium coating", The Annals of University „Dunărea de Jos” of Galați, Fascicle VIII, 2004, Tribology, Romania, pp. 48-51.
- [6] V.Javgureanu, P.Gordelenco, M.Elita, "Le rapport de la microdurete restauree et non restauree des convertures de crome", Conferință Științifică Internațională TNCR, Chișinău, 2005, vol. 2, pp. 166-169.
- [7] V.Javgureanu, P.Gordelenco, "Sootnoshenie vosstanovlennoy i nevostanovlennoy mikrotverdosti hromovih pokritiy", Mezhdunarodnaya NTK „Mashinostroyeniye i Tehnosfera XXI veka”, Sevastopol', 2005.
- [8] V.Javgureanu, "Issledovanie raboti deformacii iznosostoykih gal'vanicheskikh pokritiy pri mikrovdavlivanii", Mezhdunarodnaya NTK „Novie processy i ih modeli v resurso i energosberegayuschih tehnologiyah”, Odessa, 2003, p. 7-8.

PLOTTING THE CLARIFYING CURVES AND DETERMINATION OF THE SPECIFIC AMOUNT OF SETTLED MATERIAL DURING THE INITIAL PERIOD TO SEDIMENTATION IN STATIONARY COLUMN OF AQUEOUS SUSPENSIONS OF SOLIDS

Victor Viorel SAFTA¹, Mirela DILEA¹, Gabriel Alexandru CONSTANTIN¹

¹ University Politehnica of Bucharest, Faculty of Biotechnical Systems Engineering
saftavictorviorel@yahoo.com

Abstract: *In the present paper there are presented an algorithm and a program for plotting the clarifying curves and for determination of the specific amount of settled material during the initial period based on data obtained from sedimentation experiments in stationary column of aqueous suspensions of solids particles with different concentrations. The algorithm and program have been developed for an interactive, rapid and convenient processing of the data obtained from sedimentation experiments in stationary column of aqueous suspensions of solids particles and allow obtaining with accuracy of precise and expressive graphs which characterize the behaviour of aqueous suspensions to sedimentation in stationary column.*

Sedimentation study of different aqueous suspensions of solids particles in stationary column is of great importance for experimentally determining the important parameters required to design and exploitation clarifiers and sludge thickeners from wastewater treatment plants.

Keywords: *sedimentation in stationary column of aqueous suspensions, algorithm, program, clarifying curves, specific amount of settled material during the initial period*

1. Introduction

Sedimentation is the process of separation solid particles in suspension in a liquid by gravitational settling on the enclosure's bottom where the fluid is located [1, 5, 6].

In the practice of water management, studying the phenomenon of solid particles sedimentation in water provides very important experimental data, both for the proper design and exploitation of decanted impurities separation equipment or sludge thickeners from wastewater treatment plants and for the efficient administration of natural water courses [3].

The study of solid particles sedimentation in water is done both for stationary systems (stationary columns) and for dynamical systems (currents with different flow directions).

Experimental study of sedimentation process in stationary column of different aqueous suspension of solid particles has as main result the possibility of obtaining *clarifying curves* which, besides giving a complete image about how the water is clarified during the process, allow through the various processing to obtain important characteristics parameters such as: specific amount of settled material during the initial period of process, the maximum volume of settled material, the determination of sediment compaction characteristic index of a given aqueous suspension, the time required to obtain a certain degree of sediment compacting, particles rate during sedimentation. All these parameters are very important in design and exploitation clarifiers and sludge thickeners from wastewater treatment plants.

2. Experimental study of the sedimentation of aqueous suspension of solid particles in stationary column

If in a glass tube there is introduced a certain amount of diluted suspension composed of water and solid particles and let it rest, it can be observed after a period of time the appearance of distinct areas. There are usually three zones in the sedimentation of concentrated suspensions (see Figure 1), such as: clear liquid zone at the top of the tube, a zone with water in which solids

are in the sedimentation process at the middle of the tube and a zone with concentrated sludge settled at the bottom of the column [3, 4].

These three areas are separated by two interfaces, namely clarified water – suspension interface and suspension – concentrated sludge settled interface. It is to be noted that the water with solid suspensions zone is usually vertically layered as a function of concentration of particles in suspension which is decanted.

Over time, clarified water – suspension interface descending, while suspension – concentrated sludge settled interface is lifted and at a certain moment of time these interfaces reach the same height and overlap. In this case, in column remain only two zones, namely, clarified water zone and one of concentrated sludge settled.

The point in which the two interfaces are overlapped is named **critical point** of clarification process and corresponds to maximum volume of settled material and it's a measure of its height.

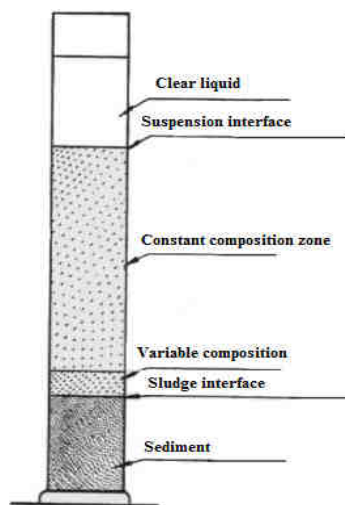


Figure1 Diluted suspension settling in the stationary column [3, 4]

If the observation is continued, it is observed that the clarified water – concentrated sludge settled interface descends very slowly (the speeds are much lower than the descend speed of clarified water – suspension interface from the first part of this process).

According to Camp and Fitch's studies [2] related to settling of various types of suspensions, they showed that the settling process can be divided into specific phases depending on the concentration and nature of solid particles (in terms of their flocculation), such as (Figure 2): type I clarification, type II clarification, mass sedimentation and sediment compaction.

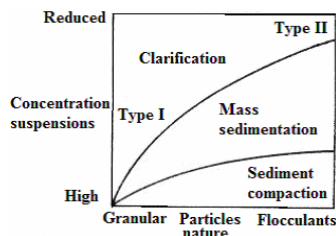


Figure 2 Decantation phase diagram [2]

Type I clarification appears in the case of pure granular particles sedimentation in dilute suspensions. In this case, the sedimentation is considered unimpeded, every particle is moving individually on its trajectory, and the characteristics of particle motion depends only the properties of liquid and solid particles. The sediment obtained is not compacted. This kind of settling can be found in practice in the case of grit chambers.

Type II clarification occurs when flocculent particles are settled in diluted suspensions. In this case, heavy particles with high sedimentation rates catching up and collide with lighter particles

with lower sedimentation rates, forming aggregates with high rate of deposition. The probability of developing aggregates increases as the depth of water layer is higher. This kind of settling can be found in the upper zone of settlers.

Mass sedimentation occurs when particles are settled in high concentration suspensions. In this case, depending of the concentration, areas with uniform composition are formed, in which all particles work collectively, resulting a deposition with a slower rate than for clarification. This kind of settling can be found in the middle zone of settlers.

Sediment compaction is an extremely slow process that involves liquid displacement from sediment layer which is compacted, so through a medium whose porosity is continuously reducing. In this case, the compaction rate decreases with time, due to increased resistance to fluid flow [3].

It should be noted that a slow stirring foster the sediment compaction process that forms on the settlers' foundation.

Experimental studies of sedimentation process in stationary column of aqueous suspension which were the basis to achieve the program and algorithm were performed on a laboratory stand composed by 5 sedimentation columns. Suspensions used were composed of water and powdered calcium carbonate with concentrations of 2%, 4%, 6%, 8% and 10%. Suspension volume in each column was 1.5 l.

It was registered the clarified water – suspension interface position at regular intervals 0.05 h (3 minutes) for 2,5 h, and then at 0,5 h (30 minutes) up to 6,5 h and after 24 h. Based on registered values, were plotted variation curves as a function of time for clarified water – suspension interface.

3. Algorithm and calculation program for plotting the clarifying curves and for determination of the specific amount of settled material during the initial period

The used algorithm for plotting the clarifying curves and for determination of the specific amount of settled material during the initial period as a function of suspensions concentration is shown in Figure 3.

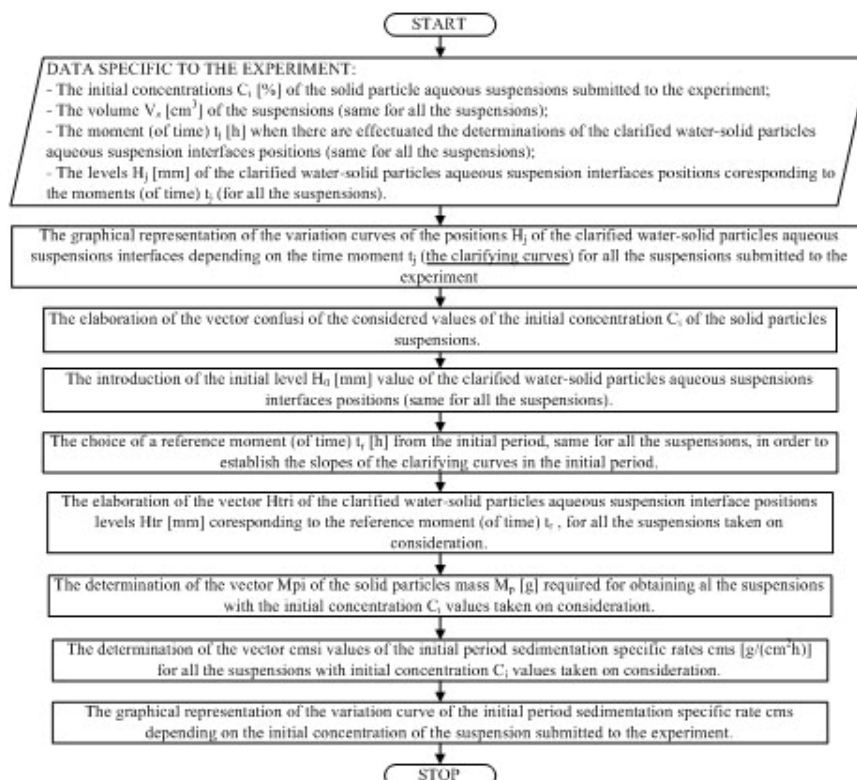


Figure 3 Structural scheme of the sequential algorithm

Based on previously presented algorithm, was developed a calculation program in MathCad programming software which is shown below.

LAYOUT PROGRAM FOR SOLID PARTICLES AQUEOUS SUSPENSIONS CLARIFYING CURVES AND FOR INITIAL PERIOD SEDIMENTATION SPECIFIC RATE VARIATION IN RELATION WITH THE CONCENTRATION OF THE SUSPENSIONS

Vs := 1500

ρ_{apa} := 1

The volumes V_s [cm³] of solid particles aqueous suspensions (calcium carbonate powder) submitted to the experiment, with initial concentration C_i [%] of 2%, 4%, 6%, 8%, 10%.

The density of water ρ_{apa} [g/cm³]

The elaboration of the input data matrix D_{ia}, D_{ib}, and D_{ic} concerning the measurements during the experiment, with i rows and j columns each, wherein:

- on the row 0 of the matrix D_{ia}, there are written the moments (of time) t_j [s] when there are effected the determinations of the clarified water-solid particles aqueous suspension interfaces position, noted as D_{ia} 0, j;
- on the row 1 of the matrix D_{ia}, there are written the levels H_j [mm] of the clarified water-solid particles aqueous suspension interface positions, for an initial concentration of the suspension C_i = 2%, noted as D_{ia} 1, j;
- on the row 0 of the matrix D_{ib}, there are written the levels H_j [mm] of the clarified water-solid particles aqueous suspension interface positions, for an initial concentration of the suspension C_i = 4%, noted as D_{ib} 0, j;
- on the row 1 of the matrix D_{ib}, there are written the levels H_j [mm] of the clarified water-solid particles aqueous suspension interface positions, for an initial concentration of the suspension C_i = 6%, noted as D_{ib} 1, j;
- on the row 0 of the matrix D_{ic}, there are written the levels H_j [mm] of the clarified water-solid particles aqueous suspension interface positions, for an initial concentration of the suspension C_i = 8%, noted as D_{ic} 0, j;
- on the row 1 of the matrix D_{ic}, there are written the levels H_j [mm] of the clarified water-solid particles aqueous suspension interface positions, for an initial concentration of the suspension C_i = 10%, noted as D_{ic} 1, j.

wherein, with j is noted the current number of the determinations effected during the experiment, which corresponds to the number of columns of the matrix D_{ia}, D_{ib}, and D_{ic}.

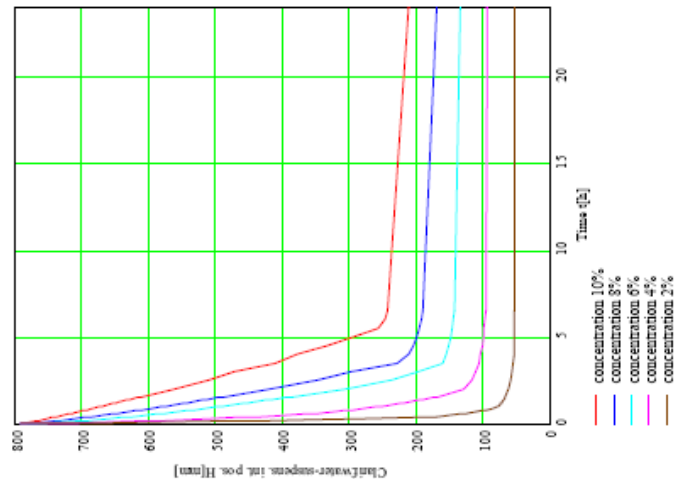
j := 0..43

D_{ia} := (0 0.05 0.1 0.15 0.2 0.25 0.3 0.35 0.4 0.45 0.5 0.55 0.6 0.65 0.7 0.75 0.8 0.85 0.9 0.95 1 1.05 1.1 1.15 1.2 1.25 1.3 1.35 1.4 1.45 1.5 1.55 2 2.5 3 3.5 4 4.5 5 5.5 6 6.5 34)

D_{ib} := (790 770 756 739 731 720 708 697 686 676 665 656 646 637 627 618 609 600 591 582 574 565 557 549 543 535 527 519 512 504 497 489 418 345 286 238 209 202 198 194 190 188 167)

D_{ic} := (790 758 732 703 690 673 656 641 628 614 601 588 576 565 554 542 531 521 510 500 490 479 469 459 452 443 433 423 415 405 395 386 305 234 195 159 154 150 147 145 143 141 132)

The graphical representation of the variation curves of the positions H_j of the clarified water-solid particles aqueous suspension interfaces depending on the moments (of time) t_j, for the suspensions with initial concentration of 2%, 4%, 6%, 8%, 10%, which are named clarifying curves.



the elaboration of the vector c_{consus_i} of the considered values of the initial concentration C_i [%] of the suspensions submitted to the experiment.

$$i = 0..5$$

$$c_{consus} \rightarrow \begin{pmatrix} 0 \\ 2 \\ 4 \\ 6 \\ 8 \\ 10 \end{pmatrix}$$

wherein, with i is noted the current number of the values of the suspensions initial concentration

The introduction of the initial level H_0 [mm] of the clarified water-solid particles aqueous suspension interfaces positions at the moment (of time) $(QD)_{i=0,0}$ (which is the same for all the suspensions regardless of concentration)

$$H_0 \rightarrow D_{i=0,0}$$

The choice of a reference moment (of time) π [h] from the initial period, more precisely from the limit of linearity of all the clarifying curves (relieved through the precedent graph), in order to establish the slopes of the clarifying curves in the initial period.

$$\pi \rightarrow D_{i=0,5}$$

The elaboration of the vector $H_{\pi i}$ of the clarified water-solid particles aqueous suspension interface positions levels H_{π} [mm] corresponding to the reference moment (of time) π , for all the suspensions with the initial concentration C_i values taken on consideration.

$$H_{\pi} \rightarrow \begin{pmatrix} 0 \\ D_{i=1,5} \\ D_{i=2,5} \\ D_{i=3,5} \\ D_{i=4,5} \\ D_{i=5,5} \end{pmatrix}$$

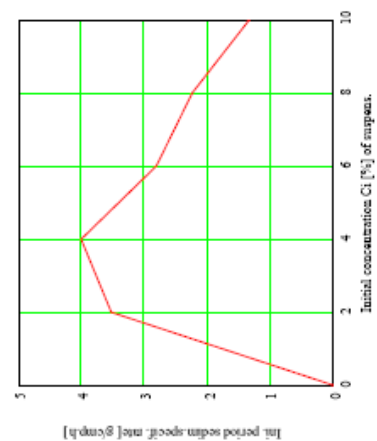
The determination of the vector $M_{\pi i}$ values of the solid particles mass M_{π} [g] required for obtaining all the suspensions with the initial concentration C_i values taken on consideration.

$$M_{\pi i} \rightarrow \frac{c_{consus_i} \cdot V_s \cdot \rho_{susp}}{100}$$

The determination of the vector c_{msi} values of the initial period sedimentation specific rates c_{ms} [g/cup.h] for all the suspensions with the initial concentration C_i values taken on consideration.

$$c_{ms_i} \rightarrow \frac{H_0 - H_{\pi i}}{10 \cdot \pi} \cdot \frac{M_{\pi i}}{V_s}$$

The graphical representation of the variation curve of the initial period sedimentation specific rate c_{ms} depending on the initial concentration of the suspension submitted to the experiment.



$$H_{\pi} \rightarrow \begin{pmatrix} 0 \\ 351 \\ 540 \\ 673 \\ 720 \\ 757 \end{pmatrix}$$

$$M_{\pi} \rightarrow \begin{pmatrix} 0 \\ 30 \\ 60 \\ 90 \\ 120 \\ 150 \end{pmatrix}$$

$$c_{ms} \rightarrow \begin{pmatrix} 0 \\ 3.512 \\ 4 \\ 2.808 \\ 2.24 \\ 1.32 \end{pmatrix}$$

4. Conclusions

In the present paper there is presented an algorithm under which was created a program for plotting the clarifying curves and for determination of the specific amount of settled material during the initial period.

The program was designed for an interactive, rapid and convenient processing of the data obtained from sedimentation experiments in stationary column of aqueous suspensions of solid particles. It should be mentioned that for this program have been used experimental data obtained from sedimentation experiments in stationary column of aqueous suspensions of calcium carbonate powder with different concentrations.

Clarifying curves obtained, drawn with high accuracy give the possibility of determination by further processing of the important parameters required to design and exploitation clarifiers and sludge thickeners from wastewater treatment plants.

Furthermore, the variation curves of the specific amount of settled material during the initial period depending on the suspension concentration offers very useful information about maximum amount, respectively the maximum volume of settled material from the sedimentation process of analyzed suspensions.

REFERENCES

- [1] E. Guazzelli, "Observation, analysis and modelling in complex fluid media - Sedimentation of small particles: how can such a simple problem be so difficult?", C. R. Mecanique, 2006, 334, pp. 539–544
- [2] J. Florea, D. Robescu "Hidrodinamica instalațiilor de transport hidropneumatic și de depoluare a apei și a aerului " Editura Didactică și Pedagogică, București, 1982
- [3] V.V. Safta, M. L. Toma, N. Ungureanu "Experimente în domeniul tratării apelor", Editura Printech, București, 2012, ISBN 978-606-521-875-8
- [4] *** "W2 Sedimentation Studies Apparatus – Instruction Manual", ARMFIELD Limited, England, UK, Issue 4, 1995
- [5] ***<http://www.iwawaterwiki.org/xwiki/bin/view/Articles/SedimentationProcesses>
- [6] ***<http://water.me.vccs.edu/courses/env110/lesson5.htm>

THE MEASUREMENT WITH PNEUMATIC TRANSDUCERS OF THE CERAMIC PRODUCTS CONTRACTION AT DRYING

Murad Erol¹, Dumitrescu Catalin², Haraga Georgeta¹, Dumitrescu Liliana²

¹. POLITEHNICA University of Bucharest, ROMANIA

². INOE 2000 –IHP, Bucharest-ROMANIA

Abstract

Drying is a very important operation within the process of manufacture of ceramic products and construction materials. A high quality drying leads to very low final losses caused by the cracks and cleaves which occur during the burning in the oven. An important parameter of the drying process is the dimensional contraction of the bodies, during drying. For the online control of the drying process and depending on the contraction evolution, it was created a pneumatic transducer, with which can be measured the linear contraction, on a witness body, with a max error of 1%. The transducer performs a conversion linear contraction pressure, due to the fact that the air pressure is not influenced by temperature and the elastic element of the pneumatic cylinder is realized from steel, with a slight variation of the elastic properties up to 150°C. The measurement pressure is linearly converted in a tension which is input signal in the PLC controlling the drying installation. In order to obtain a very low consumption of energy of the measurement system, the transducer works in a sampled operational mode, which may provide a high measurement precision.

Key words: drying, pneumatic transducer, contraction, ceramics

1. Introduction

Drying is a very important operation within the process of manufacture of ceramic products and construction materials. A high quality drying leads to very low final losses caused by the cracks and cleaves which occur during the burning in the oven

The drying time for the average size bricks are relatively high, 36-48 h. In all the drying installations it is used a drying agent obtained by mixing combustion gases and atmospheric air. The famous brands (Lingle, Ceric, Rietter, Keller, Fuschs, etc) deliver technological installations with automatic control systems, which use process models pre selected depending on the type of brick to be dried and the chemical mineralogic and physico ceramic properties of the raw clayey materials.

For optimizing the drying process it must be compensated entirely the influence of the perturbations caused by the composition and granulometry of the bodies subjected to the drying process. The online measurement of the discharged water mass and of the linear contraction of the bodies allows the achievement of high quality products, with minimum energetic consumption and an increase of the real manufacture capacity.

In fig.1 is shown the graphic of the relative variation of humidity W and contraction C of the bricks, during the the drying process



During the drying process the body contracts itself and it is measured a closeness of the anchors with ΔL . The relative contraction coefficient ε is calculated with the relation:

Due to the fact that during the drying process temperature varies between 20 up to 150 °C the anchors and the support mechanism are made of invar. The mechanical devices in use is ponderous and has no output signal for the modern automatic adjustment systems. There are also used resistive displacement transducers with temperature compensation, which are expensive and less reliable.

In figure 2 is shown the functional scheme of the pneumatic transducer for measuring the linear contraction of the bricks during the drying process and in fig.3 the functional scheme of the control block.



The absolute contraction is represented by the variation of the distance ΔL between the anchor 1 fixed on the body 2 of the transducer and anchor 3 which is fixed on the rod 4 that slides in the guide 5 on which is the pawl 6. The rod 4 is connected to the support 7 on which is jointed a lever 9 which is pushed continuously by the spring 11 to the fix contact 8 which is at 2s distance of the fix contact 10. The lever 9 is also in contact with the rod 12 of the pneumatic cylinder with simple action 13 that has a membrane 16 which presses on the rigid centre 15 that leans on the spiral spring 14. For having the center of gravity of the device between the 2 anchors, it is mounted a load 17 for balance.

For simplifying the construction it was adopted a scheme with 2 contacts K1 and K2 serially linked to R1, with signal I_{mas} in a current intensity on a single conductor connected by means of R2 at the plus of the supply voltage stabilized U_{st} . The command signal in tension U_{cd} is compared on 2 comparators C1 and C2 with two tensions $0,25 U_{st}$ at C1 and $0,75 U_{st}$ at C2. The output signals of the comparators CS for writing and CR for deleting are applied to a bistable BIST1 whose output u_1 commands the distributor D1 through which is introduced compressed air in the cylinder 13 through the pneumatic resistance RP. For discharging the air from the cylinder 13 it is commanded through the output command signals CRp and CSp the bistable BIST2 with which is commanded the distributor D2.

The measurement pressure p_{mas} is converted in tension signal with a convertor P/U from which gets out the signal U_{mas} .

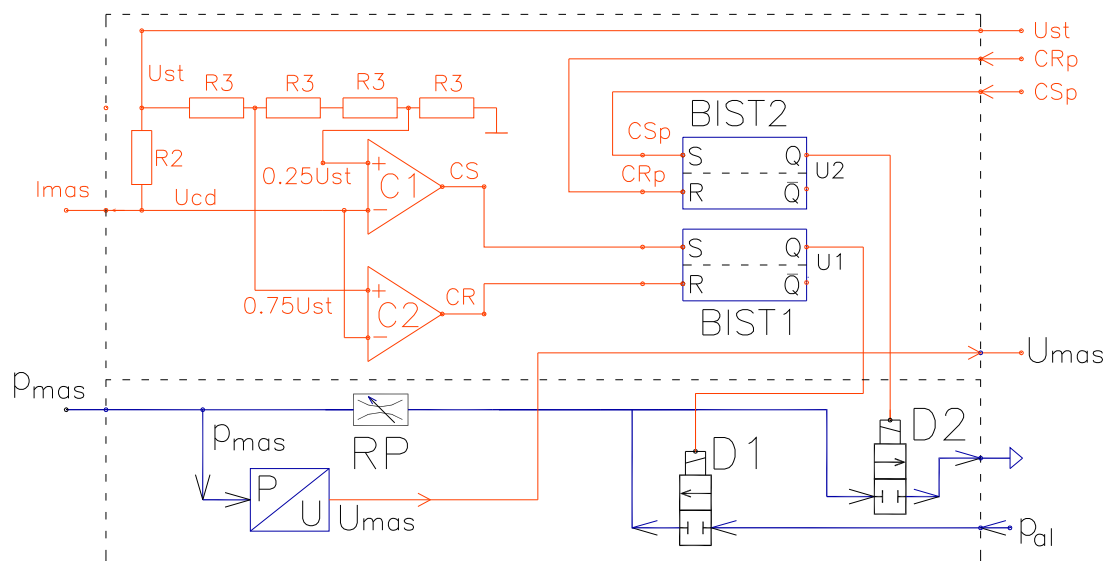


Fig. 3 The scheme of the command block

Initially in the raw brick are plunged the anchors 1 and 3 positioned at the nominal distance L_0 . If in the pneumatic cylinder 13 there is no pressure, the spring 14 retracts the rod 12 of the piston and the spring 11 presses on the comparison lever 9 that will rely on the contact K1.

When the contact K1 is shut in the command block is generated a signal $u_1=1$ of opening the distributor D1; it starts the pressure growth p_{mas} , the rigid centre 15 compresses the spring 14 and displaces the rod 12 until it reaches the lever 9 that it will rotate around the joint until it leans on the contact K2. The command block generates a shut signal $u_1=0$ for D1 and p_{mas} stabilizes at a new value p_{mas0} that is the value from which is started the measurement. From the converter p/U results U_{mas0} memorized as origin for measuring contraction.

In the drying process cause of the brick contraction the anchor 3 and rod 4 will displace towards the anchor 1, the spring 11 releases and under the action of the spring 11 the comparison lever 9 rotates itself until the contact K1 shuts. It is generated the signal CS which applied at BIST1 makes that $u_1=1$ and D1 it opens. It starts the pressure p_{mas} growth from the cylinder which leads to the compression of the spring 14 and the displacement of the rod 12 that rotates the lever 9 until

the contact K2 shuts, which leads to the generation of a signal CR which applied at BIST1 makes $u_1=0$ and shuts D1.

For a displacement with 2s between the contacts K1 and K2 the rod 12 displaces with Δh_{arc} :

$$\Delta h_{arc} = 2 \cdot s \cdot \frac{d_2}{d_1 + d_2} = \frac{2 \cdot s}{i_{pg}} \quad (2)$$

where i_{pg} is the transfer factor of the lever 9.

The variation Δp_{mas} of the measurement pressure for a sampling step is:

$$\Delta p_{mas}[i] = \frac{\Delta h_{arc} K_{arc}}{S_{mef}} = \frac{2 \cdot s}{i_{pg}} \cdot \frac{K_{arc}}{S_{mef}} \quad (3)$$

Because the value of variation $\Delta L[i]$ of the absolute contraction for sampling is:

$$\Delta L[i] = \frac{2 \cdot s}{i_{pg}} = const. \quad (4)$$

It results that:

$$\Delta p_{mas}[i] = \frac{\Delta h_{arc} K_{arc}}{S_{mef}} = \Delta L \cdot \frac{K_{arc}}{S_{mef}} = const. \quad (5)$$

If it adopts constructively the value $L_0=100\text{mm}$ and the max.contraction is $\varepsilon_{max} \leq 10\%$ it results that the max.value of the displacement to be measured is of $\Delta L_{max} = 10 \text{ mm}$.

For being efficient in controlling the drying process it is required that the device to belong to the CP1 class of precision, meaning that the sampling error $\Delta L[i]$ is:

$$\Delta L[i] = \Delta L_{max} \cdot \varepsilon_{est} = 10 \text{ mm} \cdot 0.01 = 0.1 \text{ mm}. \quad (6)$$

For $s=0,25 \text{ mm}$ it results that the transfer factor i_{pg} must have the value:

$$i_{pg} = \frac{2 \cdot s}{\Delta L[i]} = \frac{2 \cdot 0,25}{0,1} = 5 \quad (7)$$

For the measurement accuracy and for decreasing the weight of the pneumatic cylinder it is limited the total variation of the measurement pressure at $\Delta p_{max} = 0,4 \text{ bar}$, which leads to:

$$\frac{K_{arc}}{S_{mef}} = \frac{\Delta p_{max}}{\Delta L_{max}} = \frac{4000 \text{ Pa}}{0,01 \cdot m} = 4 \cdot 10^5 \frac{N/m}{m^2} \quad (8)$$

With the relation (8) may be dimensioned the pneumatic cylinder in constructive correlation with the assembly of the measurement device.

The transition from 20 to 150 °C may generate dilatations of the cylinder 13, of the rigid centre 14, as well as modifications of the elastic characteristic of the spring 14. These may influence the precision in measuring the contraction of the brick, during the drying process. The material from which will be made the cylinder, the rigid centre and the spring is superinvar type (58% Fe + 42% Ni) which has a dilatation coefficient of $\alpha_1=4 \cdot 10^{-6}$ until 300 °C and it maintains its elastic characteristic until 150 °C.

Therefore the effective average diameter of the goffered membrane will have the real value of :

$$D_{mef}(T) = D_{mef0} \cdot (1 + \alpha_1 \Delta T) \quad (9)$$

where: $\Delta T = T_{mas} - 20$ is the temperature difference

The error ε_D caused by the temperature variation will have the value:

$$\varepsilon_D = \left(\frac{D_{mef}(T)_{max}}{D_{mef0}} \right)^2 - 1 = (1 + \alpha_1 \Delta T_{max})^2 - 1 = (1 + 4E^{-6} \cdot 130)^2 - 1 = 4,027E^{-5} \quad (10)$$

From the relation (10) it results that the error ε_D caused by the thermal dilatation of the pneumatic cylinder is very low and it may be ignored in the measurement of the contraction.

3. Conclusions

For measuring an important parameter of the drying process of the raw ceramic products, the linear contraction, parameter that must be measured in an environment with a relatively high temperature 120..150 °C, it is proposed the use of an unconventional pneumatic transducer by means of which may be performed precise measurements, which has a plain structure and is much cheaper than the similar electronic variants.

The pneumatic transducer for measuring online the contraction of the raw bricks during drying has more precision at measurement, more than 1% for an initial distance between the measurement anchors of 100 mm.

It is conceived for a safe and easy use, it couples with the outside by means of a pneumatic pipe made of teflon with the diameter of 4 mm and an electric conductor of 1 mm² has at wires a PLC compatible electric signal.

Were used the concepts specific for – low cost automatisation – which led to the achievement of a plain and precise device, much more cheaper than other variants in use.

The metallic materials used for the pneumatic cylinder, spring and membrane have the dilatation coefficients very small which ensures a very slight variation of the effective average diameter of the goffered membranes below $4 \cdot 10^{-5}$, which leads to a very high measurement precision.

References

- [1]. Berling B., Heinrich B., Thrun W., Vogt W., *Kaspers/Küfner Messen- Steuern- Regeln: Elemente der Automatisierungstechnik*, Springer DE, 2005
- [2]. Douglas M. Considine, *Process/Industrial Instruments and Controls Handbook*, 4th Edition, , McGraw-Hill, 1993
- [3]. Hasatani M., Itaya Y., Muroie K., Contraction Characteristics of molded ceramics during drying, I.J. Drying Technology, Volume 11, Issue 4, 1993
- [4]. Hitoshi Takeda, *CIA - Low Cost Intelligent Automation: Produktivitätsvorteile durch Einfachautomatisierung*, Landsberg am Lech : Mi-Fachverl. Redline, 2006.
- [5]. Murad E., The measurement of the parameters of the drying process of ceramic products with unconventional pneumatic transducers, Simpozion HERVEX 2007, Călimănești, 14-16 noiembrie, 2007
- [6]. Murad E., Chercheș T., Unconventional pneumatic transducers with low energetic consumption for measuring the forces from the agricultural installations and in food industry HERVEX 2008, Călimănești 15-17 noiembrie 2008
- [7]. Murad E., Dumitrescu C., Haraga G., Dumitrescu L., *Pneumatic metering systems for amount of water extracted in convective drying processes*, International Scientific Conference Conference - DTMM, Iași, 14 -16 mai 2010
- [8]. Murad E., Dumitrescu C., Haraga G., Dumitrescu L. *Force pneumatic transducers with low energy consumption in stochastic measurement operations*; Simpozion HERVEX, 2010, Călimănești, 10-12 noiembrie 2010
- [9]. Murad E., Dumitrescu C., Haraga G., Dumitrescu L., Pneumatic transducers for measuring the speed of drying ceramic materials, SINUC 2010, Al XVI-a Simpozion National de Utilaje pentru Construcții, București, 16-17 decembrie 2010
- [10]. Radcenco V., Alexandrescu N., Ionescu E., *Calculation and design of the pneumatic elements and schemes*, Editura Tehnică, București. 1985
- [11]. * * * *Displacement Measurement, Linear and Angular*, CRC Press LLC, 1999

DIRECT / INDIRECT ADAPTIVE ROBUST CONTROL FOR LINEAR HYDRAULIC ACTUATOR

Daniel Vasile BANYAI¹, Ioan-Lucian MARCU³, Liviu Ioan VAIDA³

¹ Technical University of Cluj-Napoca, daniel.banyai@termo.utcluj.ro

² Technical University of Cluj-Napoca, lucian.marcu@termo.utcluj.ro

² Technical University of Cluj-Napoca, liviu.vaida @termo.utcluj.ro

Abstract: *The focus of the paper is on the nonlinear model based control of systems with unknown parameters and uncertain nonlinearities. The objective is to maximize the achievable performance of a controlled system and to obtain accurate parameter estimates. This is achieved by integrating the excellent output tracking performance achieved by the direct adaptive robust control with the good parameter estimation process of indirect adaptive designs. The paper contains a brief description of the nonlinear control algorithm and concludes with the results that demonstrate the high quality of the nonlinear contro versus classic control (PID).*

Keywords: *nonlinear system, nonlinear control, uncertain nonlinearities.*

1. Introduction

For many years, the research in control of hydraulic machines, was focused on linear control, this was mostly due to the simplicity and ease of implementation of these methods.

Besides the nonlinear nature of the dynamic behavior, hydraulic systems have a lot of parametric uncertainties, which are found in variations of load and variations of hydraulic parameters such as modulus of elasticity. Uncertainties related to the nonlinearities are favored by: external disturbances, leakage flow, unmatched friction, etc. For these reasons, most often for nonlinear systems best control structure is a nonlinear one.

Specialty literature offers algorithms for nonlinear control[1...7]:

- feedback linearization method, is used in many applications, requiring two controllers and an accurate modelling of the system, otherwise it becomes unstable;
- optimal control, nonlinear, which like the previous method requires accurate knowledge of the system;
- nonlinear adaptive control, first applied by Alleyen and Hedrick showed that nonlinear control strategies consider only parametric uncertainties;
- D.irect A.daptive R.obust Control, which fails to take into account the nonlinearities and uncertainties related to system parameters, characterized by excellent performance in terms of "tracking" control ;
- I.ndirect A.daptive R.obust Control, provides a good estimation of the system parameters.

In this paper is developed an algorithm for the analysis of nonlinear systems, which integrates D.A.R.C. and I.A.R.C. (D. / I.A.R.C.).

2. Mathematical model of the system

Functional diagram of the system that is intended to be controlled by two nonlinear methods is presented in Figure 1.

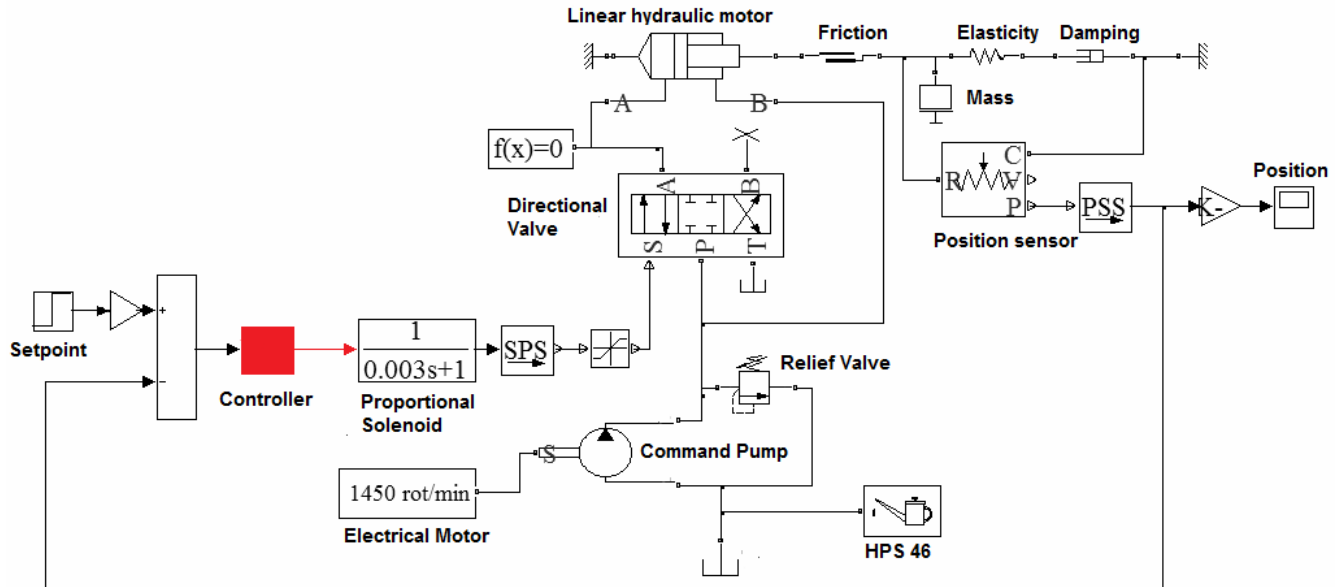


Figure 1 Functional diagram of the investigated system

Mechanical equilibrium equation of the linear motor is:

$$m_p \cdot \ddot{x}_m = A \cdot p_A - \alpha_a \cdot A \cdot p_B + F_{am} + k_m \cdot x_m - (C_3 + C_4) \cdot \dot{x}_m + \frac{m \cdot \omega^2 \cdot R^2}{a^2} \cdot x_m - \frac{\pi \cdot d^2 \cdot R}{4a} \cdot p_s + \tilde{f}(t, x_m, \dot{x}_m), \quad (1)$$

where $\tilde{f}(t, x_m, \dot{x}_m)$ is the error that incorporates external disturbances and friction forces non modelled.

the notations have the following meanings:

\dot{p}_A – the temporal derivative of the pressure function, p_A , in the large chamber of the linear hydraulic motor; \dot{p}_B – the temporal derivative of the pressure function, p_B , in the small chamber of the linear hydraulic motor; p_A – the pressure in the large chamber of the linear hydraulic motor; p_B – the pressure in the small chamber of the linear hydraulic motor; p_T – tank pressure, ($p_T=0$); p_c – the pressure between the pump and control valve; p_s – load pressure; E_U – elasticity modulus; V_A – the volume of oil under pressure p_A ; V_B – the volume of oil under pressure p_B ; V_T – (dead) volume in the supply circuit of the linear motor, (connecting pipes volume); Q_A – flow rate that enters or is discharged from the large chamber of the positioning hydraulic motor; Q_B – the flow rate that enters or is discharged from the small chamber of the positioning hydraulic motor; A – the piston area (rodless); x_m – linear position of the hydraulic motor; c_{LG} – leakage flow coefficient dependent of speed; c_{LP} – leakage flow coefficient dependent of pressure; α – piston surface ratio; α_Q – flow rate coefficient; d_v – proportional valve diameter; x_v – linear position of the proportional valve; ρ – oil density; T_v – time constant for control valve; K_v – the gain

of control valve; m_p – linear motor piston mass; F_{am} – preload force of the spring in the linear motor; k_m – spring stiffness; c_3, c_4 – viscous damping coefficient; m – piston and rod of the variable pump's, reduced mass; ω – angular velocity of the pump's piston holder; R – pump's pistons placement radius; a – tilting radius of the variable pump; d – pump's pistons diameter.

Continuity equations are:

$$Q_A = \begin{cases} k_v \cdot x_v \cdot \sqrt{p_C - p_A}, x_v \geq 0 \\ k_v \cdot x_v \cdot \sqrt{p_A}, x_v < 0 \end{cases} = g_3; \quad (2)$$

$$Q_B = \begin{cases} k_v \cdot x_v \cdot \sqrt{p_B}, x_v \geq 0 \\ k_v \cdot x_v \cdot \sqrt{p_C - p_B}, x_v < 0 \end{cases} = g_4. \quad (3)$$

The equations that show the forming of the pressure in the linear motor are:

$$\dot{x}_m = \frac{E_U}{V_T + A \cdot x_m} (Q_A - A \cdot \dot{x}_m + \tilde{Q}_A^0(p_A, p_B, p_S, p_T)); \quad (4)$$

$$\dot{x}_m = \frac{E_U}{V_T + \alpha_a \cdot A (L - x_m)} (-Q_B + \alpha_a \cdot A \cdot \dot{x}_m - \tilde{Q}_B^0(p_A, p_B, p_S, p_T)), \quad (5)$$

where $\tilde{Q}_A^0, \tilde{Q}_B^0$ is the modelling error for flow equations.

Are defined the following variables in state space:

$$x = [x_1, x_2, x_3, x_4]^T = [x_m, \dot{x}_m, p_A, p_B]^T. \quad (6)$$

Considering $x_d(t)$ the desired position of the hydraulic differential motor, it seeks to obtain an input u , so that the size of output $y=x_1$, to be as close as possible to the ordered value, despite various uncertainties of the model.

The system is subjected to parametric uncertainties due to the variation of the elasticity modulus, friction and damping, and the nominal value of the modelling errors (d, d_n).

The equations system with input size $u = x_v$ in state space becomes:

$$\left\{ \begin{array}{l} \dot{x}_1 = x_2 \\ \dot{x}_2 = \frac{1}{m_p} [x_2 \cdot A - x_4 \cdot \alpha_a \cdot A + x_1 (F_{am} + k_1) - (C_3 + C_4) \cdot x_2 - k_2 + d] \\ \dot{x}_3 = \frac{E_U}{V_A(x_1)} [-A \cdot x_2 + g_3(x_2, \text{sign}(u) \cdot u) + \tilde{Q}_A] \\ \dot{x}_4 = \frac{E_U}{V_B(x_1)} [\alpha_a \cdot A \cdot x_2 - g_4(x_4, \text{sign}(u) \cdot u) - \tilde{Q}_B] \\ d = \tilde{f}(t, x_1, x_2) \\ V_A(x_1) = V_T + A \cdot x_1 \\ V_B(x_1) = V_T + \alpha_a \cdot A (L - x_1) \end{array} \right. \quad (7)$$

For simplicity, we have considered only modulus E_u , and the nominal value of the modelling error d , d_n . With the remaining parameters can do the same, if necessary.

It defines the following set of unknown parameters:

$$\lambda = [\lambda_1, \lambda_2]^T; \quad (8)$$

$$\lambda_1 = d_n, \quad \lambda_2 = E_u. \quad (9)$$

With this system described in state space can be linearized according to λ as follows:

$$\begin{cases} \dot{x}_1 = x_2 \\ \dot{x}_2 = \frac{1}{m_f} [x_2 \cdot A - x_2 \cdot \alpha_2 \cdot A + x_1 (F_{em} + k_1) - (C_2 + C_4) \cdot x_2 - k_2 + d] + \lambda_1 + \tilde{d}(t, x_1, x_2) \\ \dot{x}_3 = \frac{\lambda_2}{V_A(x_1)} \cdot (-A \cdot x_2 + Q_A + \tilde{Q}_A) \\ \dot{x}_4 = \frac{\lambda_2}{V_B(x_1)} \cdot (\alpha_2 \cdot A \cdot x_2 - Q_B - \tilde{Q}_B) \\ \tilde{d}(t, x_1, x_2) = d - d_n \end{cases} \quad (10)$$

Uncertain parameters and uncertain nonlinearities satisfy the following:

$$\lambda \in \Omega_\theta = \{\lambda : \lambda_{\min} < \lambda < \lambda_{\max}\}; \quad (11)$$

$$|\tilde{d}(t, x_1, x_2)| \leq \delta_d \cdot (x_1, x_2, t); \quad (12)$$

$$|\tilde{Q}_i(x_3, x_4, p_C, p_T)| \leq \delta_{Q_i}(x_3, x_4, p_C, p_T); i: A, B, \quad (13)$$

where: $\delta_d, \delta_{Q_A}, \delta_{Q_B}$ - known and:

$$\lambda_{\min} = [\lambda_{1\min}, \lambda_{2\min}]^T; \quad (14)$$

$$\lambda_{\max} = [\lambda_{1\max}, \lambda_{2\max}]^T, \quad (15)$$

Are made the following notations:

$\tilde{\lambda}$ is the estimated error of λ ;

$\hat{\lambda}$ - estimation of λ .

$$\tilde{\lambda} = \hat{\lambda} - \lambda. \quad (16)$$

Define the following discontinuous projections:

$$proj_{\hat{\lambda}_i}(\bullet_i) = \begin{cases} 0, \text{daca } \hat{\lambda}_i = \lambda_{i\max} \text{ si } \bullet_i > 0; \\ 0, \text{daca } \hat{\lambda}_i = \lambda_{i\min} \text{ si } \bullet_i < 0; \\ \bullet_i \end{cases} \quad (17)$$

And the saturation function:

$$sat_{\lambda_M}(\Gamma \tau) = S_0 \Gamma \tau; \quad (18)$$

$$S_0 = \begin{cases} 1, & \text{daca } \|\Gamma \tau\| \leq \lambda_M^g; \\ \frac{\lambda_M^g}{\|\Gamma \tau\|} \text{daca } \|\Gamma \tau\| > \lambda_M^g. \end{cases} \quad (19)$$

It uses an adaptation law given by:

$$\dot{\lambda} = proj_{\lambda}^{\lambda_M^g} \left(sat_{\lambda_M^g}(\Gamma \tau) \right), \quad (20)$$

where: $\Gamma > 0$ is a diagonal matrix;

τ – adapting function;

λ_M^g – upper limit of the adaptation rate.

It is known that for $\forall \tau$ the projection used in equation (20) guarantees:

$$(P_1) \dot{\lambda} \in \bar{\Omega}_{\lambda} = \left\{ \dot{\lambda} : \lambda_{\min} \leq \dot{\lambda} \leq \lambda_{\max} \right\}; \quad (21)$$

$$(P_2) \dot{\lambda}^T \left(\Gamma^{-1} proj_{\lambda}^{\lambda_M^g} \left(\left(sat_{\lambda_M^g}(\Gamma \tau) \right) - \Gamma^{-1} sat_{\lambda_M^g}(\Gamma \tau) \right) \right) \leq 0; \quad (22)$$

$$(P_3) \left\| \dot{\lambda} \right\| \leq \lambda_M^g. \quad (23)$$

Are defined the following functions:

$$z_1 = x_1 - x_d(t); \quad (24)$$

$$z_2 = \dot{x}_1 + k_1 \cdot z_1 = x_2 - x_{2eq}. \quad (25)$$

3. Controller design

Nonlinear controller design requires three steps:

Step 1

Is chosen a virtual control law given by the relations:

$$\alpha_1(x_1, t) = \alpha_{1a} + \alpha_{1S1}; \quad (26)$$

$$\alpha_{1a} = \ddot{x}_d; \quad (27)$$

$$\alpha_{1S1} = -k_{1S1} z_1, \quad (28)$$

where k_{1S1} is gain factor of the positive feedback.

Step 2

The second equation of the system (10):

$$-\ddot{x}_2 = b_2 x_3 + \phi_2^T \lambda_C + \Delta_2; \quad (29)$$

$$b_2 = \frac{A}{m_p}; \quad (30)$$

$$\phi_2^T = [\alpha_a \cdot A (F_{am} + k_1)(C_3 + C_4) - k_2]; \quad (31)$$

$$\lambda_C = [\lambda_1 \lambda_2]. \quad (32)$$

Is chosen the adjustment law for x_3 :

$$\alpha_2(\bar{x}_2, \hat{\lambda}_C, t) = \alpha_{2a} + \alpha_{2s}; \quad (33)$$

$$\alpha_{2a1} = \frac{1}{\hat{b}_2} \left[k_{1S1} \cdot x_2 + k_{1S1} \cdot x_d + \ddot{x}_2 - \phi_2^T \hat{\lambda}_C - z_1 \right]; \quad (34)$$

$$\alpha_{2a2} = -\frac{1}{\hat{b}_2} \cdot \lambda_2. \quad (35)$$

Step 3

At this step is defined the desired position x_v of the valve, that is considered the input of the system.

$$\ddot{x}_3 = b_3 u + \phi_3^T \lambda_C; \quad (36)$$

$$u(\bar{x}_3, \hat{\theta}_C, t) = u_a + u_s; \quad (37)$$

$$F_p = \frac{d_A \cdot A}{V_A} + \frac{Q_B \cdot \alpha_a \cdot A}{V_B} = u; \quad (38)$$

$$x_v = \frac{F_p}{\frac{g_3 \cdot A \cdot k_v}{V_A} + \frac{g_4 \cdot \alpha_a \cdot A \cdot k_v}{V_B}}. \quad (39)$$

4. Results and Conclusions

The controller presented in this paper have a good potential to use it in electro-hydraulic control systems with variable displacement pumps, it can get both good dynamic behaviour and a more precise estimate of the system parameters, the performance of which are difficult to reach for a nonlinear systems with regulators and classical control strategies.

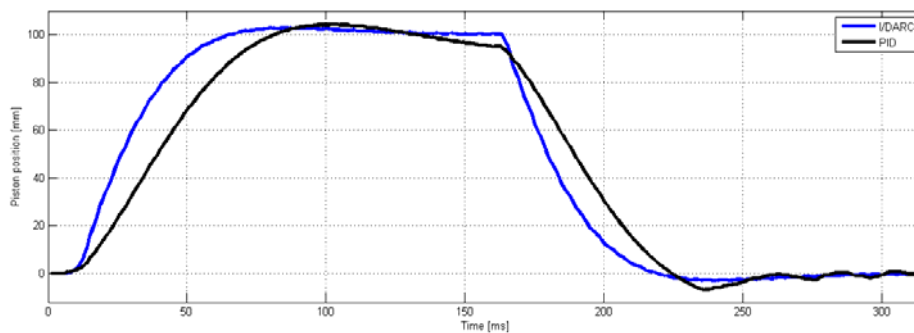


Figure 2 Dynamic behaviour of the system (Classic Control; Nonlinear Control)

REFERENCES

- [1] Virvalo T., Comparison of Tracking Controllers of Hydraulic Cylinder Drive by Simulations, Service Robotics and Mechatronics, Part 4, p. 55-60, 2010.
- [2] Wang A., Yue B., Jiang K., Lin X., Non-linear Improvement on Hydraulic Pump and Motor Models Based on Parameter Optimization Algorithms, Lecture Notes in Computer Science, Artificial Intelligence and Computational Intelligence, Vol. 6320 p. 16-23, 2010.
- [3] Wang Y., Schinkel M., Hunt K.J., PID and PID-like Controller Design by Pole Assignment within D-stable Regions, Centre for Systems and Control, Dept. of Mechanical Engineering, James Watt Building, University of Glasgow, Glasgow, G12 8QQ, 2001.
- [4] Yu H., Feng Z., Wang X., Nonlinear Control for a Class of Hydraulic Servo-System, Journal of Hejiang University Science, Nr. 5(11), p. 1413-1417, 2003.
- [5] Yao B., Bu F., Adaptive Robust Motion Control of Single-Rod Hydraulic Actuators: Theory and Experiments, IEEE/ASME Transactions on Mechatronics, Vol. 5, Nr. 1, p. 71-91, martie 2000.
- [6] Yuzev A., Partial Asymptotic Stabilization of Nonlinear Distributed Parameter Systems, Automatica, Nr. 41, p. 1-10, 2005.
- [7] Zheng D., Hoo K.A., Poovoso M.J., Finite Dimensional Modeling and Control of Distributed Parameter Systems, Proceeding of the American Control Conference, p. 4377-4382, 2002.

THE CALORIC EFFECTS IN ONE SERIAL SONIC INSTALLATION

BAL CARMEN¹, BAL NICOLAIE²

¹ Technical University of Cluj Napoca, carmen.bal@dppd.utcluj.ro

² Technical University of Cluj Napoca, nicubal@yahoo.com

Abstract: *In the last time, the development of the science and the technicians are realised the big progress and the level of the general knowledge of the persons implicated in this activity are advances and probable the knowledge of the sonicity are not brake by the wrong idea or disregarded by "incompressibility of flow"*

Sonicity is the science of transmitting mechanical energy through vibrations. Starting from the theory of the musical accords, Gogu Constantinescu found the laws for transmitting the mechanical power to the distance through oscillations that propagate in continuous environments (liquid or solid) due to their elasticity.

In the paper we make the effect of the friction in the sonic installation were the sonic flow are influence by the friction. This effect makes the growing of the temperature in the sonic resistance, same the caloric effect of the alternative current. This paper is the base of departure for the future research about the caloric effects of the sonicity theory in the practice.

Keywords: *sonic pressure, sonic flow, sonic generator, perdittance, sonic resistance, sonic capacity.*

1. Introduction

One of the fundamental problems of mechanical engineering is energy transmission (presented in different forms) at distance, where at a certain point it can be transformed into a useful mechanical work. [1].

The methods of moving the energy into liquids, used in present paper, are generally based on continuous transmission of pressure and flow, thus these produced at one end of a line can be taken at the other end, the liquid being considered incompressible. The science which is based on the application of elastic proprieties of matter at energy transmission carries the name of *sonic science* or *sonicity* [1].

Energy transmission through fluid compressibility has been approached for the first time, both theoretically and experimentally, by Gogu Constantinescu, who performed his research in the British Navy Laboratory of Coniston and developed the so-called "theory of sonicity". The great inventor has spent a considerable amount of money in order to convince the world the fluids are much more compressible than generally accepted, and that this feature is essential to vibration propagation through fluids [1].

As asserted from its very inception, sonicity is analogous to electricity and sonic transmission is similar to alternating current transmission. By considering this analogy is valid, it follows that fluid compression is equivalent to electric charge accumulation in a capacitor.

Sonic actuation permits the optimal combination between the ease of processing electric signals (of low energy) and the high-power sonic actuation, which eliminates the greatest parts in a classical hydraulic system (such as hydraulic reservoirs, control systems for pressure, flow, direction, etc), resulting in an actuation which melts the virtues of low-energy signal processing and the high-output, small-volume, economical and compact sonic actuation [2].

It should be mentioned that this approach of the problem makes the sonicity theory a particular case of power transmission through "displacement", which means the fluid, instead of flowing continuously from generator to they actuator, evolves harmonically in time at various wavelengths and frequencies [2].

In the new system, energy is transmitted from one point to another by covering distances which can be large, by applying periodical compressions which generate longitudinal vibrations in columns of solids, liquids and gases. The energy transmitted through these periodical longitudinal pressure and volume vibrations is in fact power transmission through sonic waves.

This concept enables obtaining thermal effects through fluid motion or/and synchronous, non-synchronous, single-phase actuation when using a small volume of non-polluting fluid, such as water. The effect of this solution is that one can eliminate the individual equipment for flow and pressure adjustment and control by transferring them in the modern domain of computerized electronic control.

2. The friction effects in the sonic serial installation formed by two capacity condenser and one friction resistance

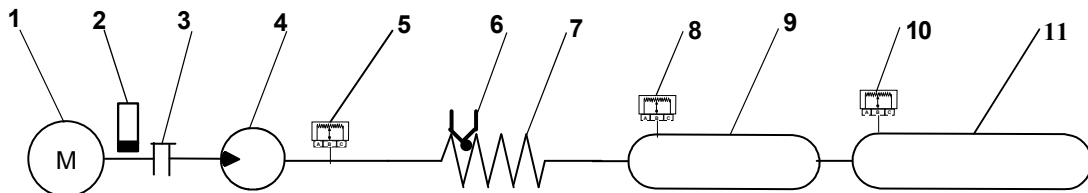


Fig. 1 The experimental sonic serial installation

1- electrical motor; - 2 – the proximity sensor; 3 – flexible coupling claw, 4 – hydraulic pump; 5, 8, 10 – pressure sensor; 6 – temperature sensor; 7 – friction resistance; 9 – small capacity cylinders; 11- big cylinder capacity

This experimental study used the installation presented in figure 1, starting from different frequencies of the drive motor acting the piston of the sonic generator. For each frequency were made three measures corresponding to a static pressure in the installation of 0 bar, 0,5 bar. [3]

In the figure 1 is presented, the installation were the small condenser are connected in

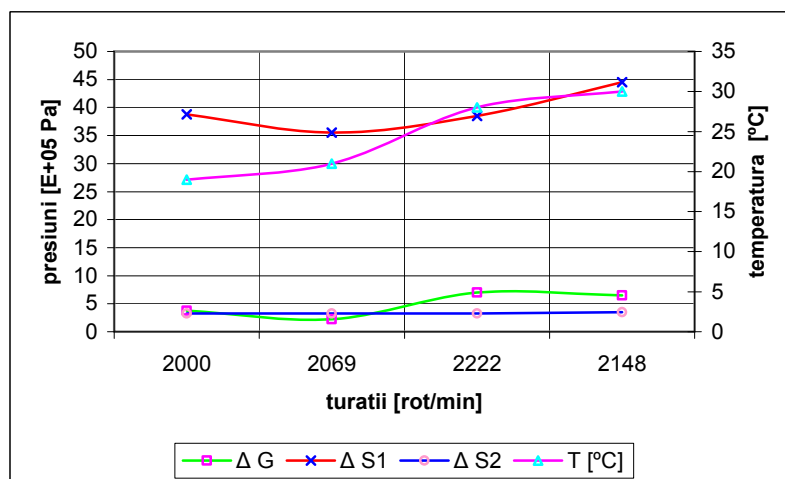


Fig.2 The diagram of variation of the pressure and the temperature function the speed to the static pressure 0 Pa

series with the friction resistance. The installation is formed by the sonic generator who is connecting by a pipe with the by two capacity condenser and one friction resistance.

The figure 2 and 3 is presented the variation in time of the diagrams of the pressure and the temperature and also the revolution speed for the static pressure of 0 E+05 Pa. Capacity pressure on the two cylinders was not modified in turn generating pressure remains constant around the 40E+05 Pa. Although the speed was very high 2200 rpm temperature failed to surpass the 30°C, there may be air in the system because after a time period is stopped the electric motor.[3]

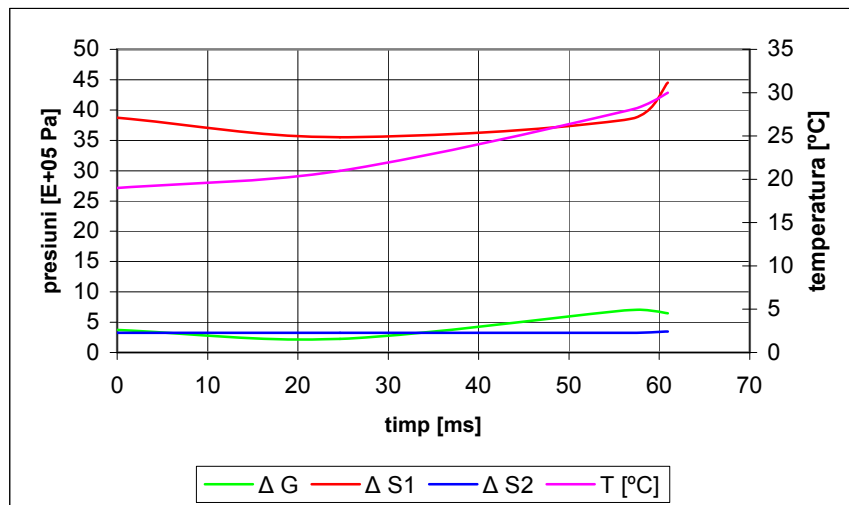


Fig. 3. The diagram of variation of the pressure and the temperature function the time to the static pressure 0 Pa

In the figure 4 and 5 is presented the variation in time of the diagrams of the pressure and the temperature and also the revolution speed for the static pressure of 0,5 E+05 Pa. In this situation it is noticed that the pressures on pressure sensors on the cylinders are constant and about equal with a pressure of approximately 50E+05 Pa.

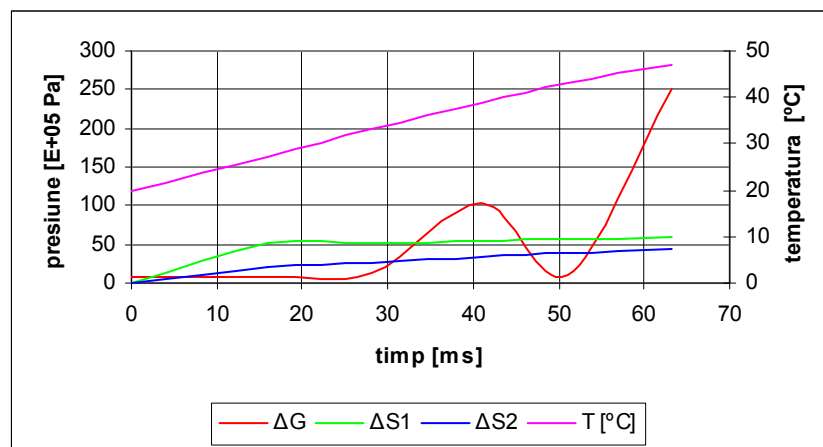


Fig. 4 The diagram of variation of the pressure and the temperature function the time to the static pressure 0,5E+05 Pa

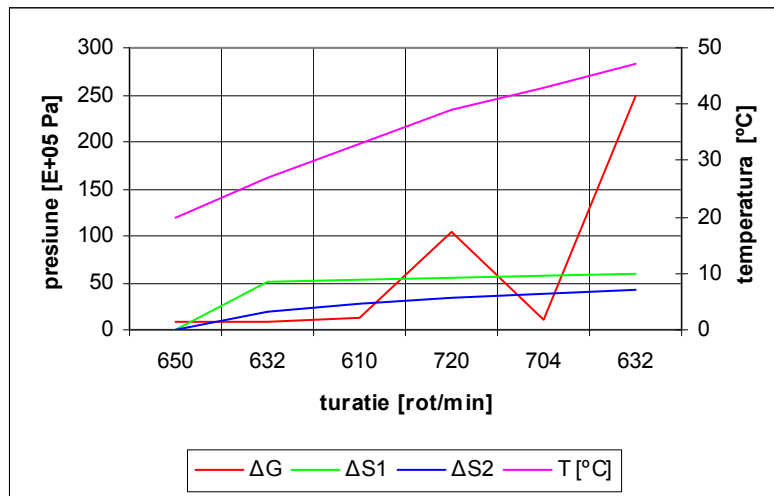


Fig. 5 The diagram of variation of the pressure and the temperature function the speed to the static pressure 0,5E+05 Pa

Pressure on the generator is oscillating, and after about 50 seconds has a jump up to 250E+05 Pa, at which point the electric engine shutdown. The temperature does not exceed 48°C to stop functioning electric engine.[3]

In 6 figures has represented the variation of pressure and temperature according to time for static pressure 2E+05 Pa. Startup speed was 1500 rpm. the pressures on those two cylinders are approximately constant and equal to 40E+05 Pa while the pressure on the generator increases continuously up to the 180E+05 Pa after a glitch with pressure and stop the engine. Maximum temperature reached is 70°C.

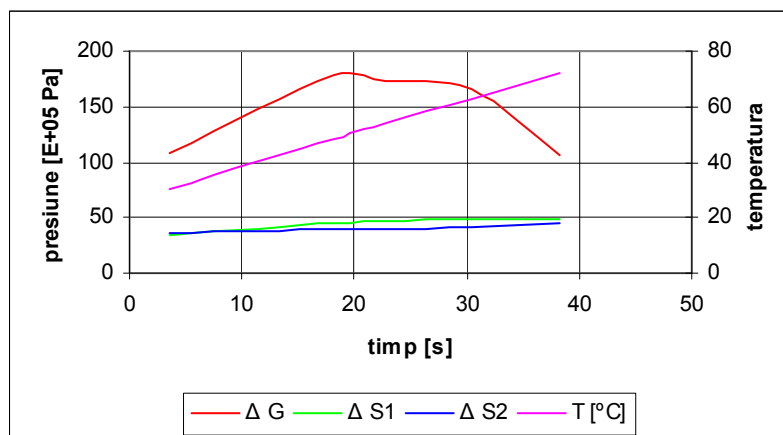


Fig. 6 The diagram of variation of the pressure and the temperature function the speed to the static pressure 0,5E+05 Pa

Experimental results achieved with other pressures and speeds were not significant they demonstrating that this constructive version of installation is not recommended.

3. Conclusions

From the analysis the diagrams to serial sonic installation can extract the following conclusions [3]:

- once with the increasing pressures in installation, there is a pronounced decrease of speed to the electric engine;
- static pressure in the installation influence increasing much faster in the pressure equipment;
- the pressure in the cylinder does not exceed 30×10^5 Pa and has almost the same amount in those two cylinders;
- because the electric motor stops after a short period of function (about 1 min) does not recommend the stand under this form manufacture.

REFERENCES

- [1]. Constantinescu, G., (1985), The theory of the sonicity, București, Editura Academiei.
- [2]. Carmen Bal, (2007), The caloric effect in the circuits by harmonic flow, Cluj Napoca, Ed. ALMA MATER, ISBN 978-973-7898-75-3.
- [3]. Carmen Bal, (2006), Research and contributions about the drive systems with the harmonic flow, the doctoral thesis Technical University of Cluj Napoca.
- [4]. Pop I. Ioan, Carmen Bal, Marcu Lucian ș.a., (2007), Sonicity applications. Experimental results. Iași, Ed. Performantica, ISBN 978-973-730-391-2.

SOME ELASTOPLASTIC DEFORMATION AND FAILURE GALVANIC ELECTROLYTIC IRON COVER

Vasile JAVGUREANU¹, Pavel GORDELENCO²

¹ Technical University of Moldova, v_javgureanu@yahoo.com

² Technical University of Moldova, pavel_gr@mail.utm.md

Abstract: *Defined physical and mechanical characteristics of wear resistance of iron coatings by measurement of hardness in the macro-volume and proved that they have a good correlation with the wear rate of the coatings. The data obtained can be used to describe the subtle intensity of wear of these coatings.*

Keywords: *elastoplastic, deformation, failure, galvanic, electrolytic, iron cover.*

1. Introduction

Electrolytic wear resistant coatings are widely used to harden and the restoration of parts of machines in the industry in order to increase their longevity. It is known that the electrodeposition conditions have a significant impact on the physical and mechanical properties of electrolytic plating. Knowledge of the physical and mechanical characteristics of the metal plating needed to make informed choices of technological conditions of deposition depending on the operating conditions of the restoration of the parts as well as for important structural calculations [1].

2. Overview

An important parameter in the study of physical and mechanical properties of wear-resistant plating is their fragility. This property plating is undesirable as fragility effect on such an important performance for abrasion [1].

Actual problems of studies of the physical and mechanical characteristics of the materials in the surface and subsurface layers due to the fact that the contact deformation associated with modern methods of treatment, hardening and metal compounds. Kinetic test hardness and micro hardness opens new possibilities for the determination of physical and mechanical properties and fracture toughness of electrolytic plating [1].

The possibility of determining the characteristics of elastic-plastic (h_y ; h_n ; h), the work required to deform (A_y ; A_n ; A), unrestored and dynamic hardness (H_h ; H_d), modulus of elasticity (E), the critical load indentation with a start brittle fracture (P_{kp}) ratio preventing recovery and dynamic hardness to elastic modulus (H_h/E ; H_d/E), yield strength (G_t), the true ultimate strength (Se), ultimate strength (O_v), yield strength (O_{az}), impact resistance (An), the degree of deformation in the contact area (Ψ).

The work carried out some of the features of large elastic-plastic deformation and fracture of iron electrolytic coatings obtained from electrolyte 1, sbr.59 [1]. The samples used rollers with diameter 30 mm, coating thickness of 0.5 mm and a length of 100 mm, which were treated with optimal conditions of grinding. Physical and mechanical properties were determined at the facility for research in material hardness macro volume equipped with an inductive sensor and the differential amplifier to record chart indentation of a spherical indenter and indentation recovery after unloading.

Dynamic hardness (H_d) was defined as the ratio of the total of the cost of the elastic-plastic deformation to volume deformable material (v) in all studied galvanic iron coatings.

3. Discussion of experimental studies

The research showed that studied the physical and mechanical characteristics of wear-resistant iron coatings vary with the conditions of electrolysis (tables 1-2).

With the increase in current density (Δk) from 5 to 40 A/m² at a constant temperature electrolysis (40°), the critical load indentation (P_c) and the elastic modulus of coatings (E) decreased respectively from 200 to 130⁴ and 1.95×10^4 to 1.6×10^4 (H/mm²). The work expended on elastic (A_y), plastic (A_n), elastoplastic (A) indentation hardness unreduced (H_h), dynamic hardness (H_d), the indentation load (P), the ratio H_h/E have extreme values (table 1).

Table 1

Physical and mechanical properties of iron coatings ($n = 1m$).

Electrolysis conditions		Work expended on the deformation of surfaces			$H_h, H/mm^2$ ($hr=2\mu m$)	H_d/Hm^2	P, H	P_c, H	$E \cdot 10^4$ H/mm ²	H_h/E	H_d/E
$\Delta k,$ A/dm ²	$T,$ °C	$A_y,$ H/mm	$A_n,$ H*mm	$A,$ H*mm							
5	40	0,01936	0,01043	0,0298	3560	2375	44,7	200	1,95	0,1826	0,1218
10	40	0,02086	0,01074	0,0310	3760	2515	47,4	170	1,85	0,2032	0,1359
20	40	0,02198	0,01082	0,0328	3920	2614	49,2	150	1,75	0,2240	0,1494
40	40	0,01950	0,00797	0,0275	3280	2189	41,2	130	1,60	0,2050	0,1368

Physical and mechanical properties of iron coatings (table 1) were determined for the same indentation depth ($H=2\mu m$) by a known procedure [1].

Studies have shown that an increase in current density from 5 to 20 (A/dm²) at constant temperature electrolysis (40°C), the work spent on the elastic deformation increased from $19,36 \cdot 10^{-3}$ to $21,98 \cdot 10^{-3}$ (N/mm²), work spent on plastic deformation increased from $10,43 \cdot 10^{-3}$ to $10,82 \cdot 10^{-3}$ (N/mm), the total work spent on elastic-plastic deformation of the coating increased $29,8 \cdot 10^{-3}$ to $32,8 \cdot 10^{-3}$ (N/mm). With further increase of the current density from 20 to 40 (A/dm²) at constant temperature electrolysis (40°C), the work spent on the elastic deformation increased from $21,98 \cdot 10^{-3}$ to $19,5 \cdot 10^{-3}$ (N/mm), the work expended in plastic deformation decreased from $10,82 \cdot 10^{-3}$ to $7,97 \cdot 10^{-3}$ (N/mm²), the total work spent on the elastic-plastic deformation of the coating decreased $32,8 \cdot 10^{-3}$ to $27,5 \cdot 10^{-3}$ (N/mm). From the results of the study show that the work spent on the elastic (A_y), plastic (A_n) and the elastic-plastic deformation (A) iron coatings, at constant temperature electrolysis are extreme.

The character changes unreduced hardness (H_h), dynamic hardness (H_d) and a spherical indenter load indentation to a depth $2\mu m$ with increasing current density from 5 to 40 (A/dm²), at a constant temperature electrolysis (40°C) are also extreme. With the increase in current density from 5 to 20 (A/dm²) unreduced hardness (H_h) increased from 3560 to 3920 (H/mm²), dynamic hardness (H_d) increased from 2375 to 2614 (H/mm²), and the indentation load (P) increased from 44.7 to 49.2 (H). With further increase of the current density (CD), at a constant temperature electrolysis (40°C) 20 to 40 (H/mm²) unreduced hardness (H_h) decreased from 3920 to 3280 (H/mm²), dynamic hardness (H_d) decreased from 2611 up to 2189 (H/mm²) and the indentation load was reduced from 49.2 to 41.2 (H) (table 1).

With increasing temperature electrolysis (T , table 2), at a constant current density ($\Delta k=20$ A/dm²), from 20 to 60°C, the critical load indentation, characterizing start brittle material, and the elastic modulus of coatings increased accordingly from 105 to 210 (H) and from 1.3×10^4 to 2.1×10^4 (N/mm²).

Nature of the change of the cost of the elastic (A_y), plastic (A_n), elastic-plastic deformation of iron coatings with temperature electrolysis of 20 to 60°C, at a constant current density ($\Delta k=20$ A/dm²) is also extreme. With increasing temperature electrolysis of 20 to 40°C, at a constant

current density ($\Delta k=20 \text{ A/dm}^2$), the work expended on elastic (A_y), plastic (A_n) and elastic-plastic deformation (A) increased respectively from 16.97×10^{-3} to $21.98 \times 10^{-3} \text{ (N}\cdot\text{mm)}$, from 5.36×10^{-3} to $10.82 \times 10^{-3} \text{ (N}\cdot\text{mm)}$ and from 22.33×10^{-3} to $32.8 \times 10^{-3} \text{ (N}\cdot\text{mm)}$. With further increase of the temperature (T) at a constant current density ($\Delta k=20 \text{ A/dm}^2$), the work spent on the elastic (A_y), plastic (A_n) and elastic-plastic indentation iron coatings decreased, respectively, from 21.98×10^{-3} to $12.91 \times 10^{-3} \text{ (N}\cdot\text{mm)}$, from 10.82×10^{-3} to $10.56 \times 10^{-3} \text{ (N}\cdot\text{mm)}$ and from 32.8×10^{-3} to $10.56 \times 10^{-3} \text{ (N}\cdot\text{mm)}$.

Table 2

Physical and mechanical properties of iron coatings (e-t 1)

Electrolysis conditions		Work expended on the deformation of surfaces			H_h , H/mm^2 ($h=2\mu\text{m}$)	$H_d H_m^2$	P, H	$P_{0.2}, H$	$E_{10(4)}$ H/mm^2	H_h/E	H_d/E
Δk , A/dm^2	T , $^\circ\text{C}$	A_y , $\text{H}\cdot\text{mm}$	A_n , $\text{H}\cdot\text{mm}$	A , $\text{H}\cdot\text{mm}$							
20	20	0,01697	0,00536	0,02233	2650	1780	33,5	105	1,3	0,2038	0,1369
20	40	0,2198	0,1082	0,0328	3920	2614	49,2	150	1,75	0,2240	0,1494
20	60	0,1291	0,1056	0,0235	2800	1870	35,2	210	2,1	0,1333	0,089

The character changes unreduced hardness (N_h), dynamic hardness (H_d) and load the indentation of a spherical indenter at a depth of 2 m, with increasing temperature electrolysis from 20 to 60°C , at a constant current density ($\Delta k=20 \text{ A/dm}^2$) are also extreme. With increasing temperature electrolysis (T) from 20 to 40°C , at a constant current density ($\Delta k=20 \text{ A/dm}^2$), unreduced hardness (H_h) increased from 2650 to 3920 (N/mm^2), dynamic hardness (H_d) increased from 1780 to 2614 (N/mm^2), and the indentation load (P) increased from 33.5 to 49.2 (H).

With further increase of temperature from 40 to 60°C , at a constant current density ($\Delta k=20 \text{ A/dm}^2$), unreduced hardness decreased from 3920 to 2800 (N/mm^2), dynamic hardness decreased from 2614 to 1870 (N/mm^2), and the load indentation decreased from 49.2 to 35.2 (H).

Much attention in the study of physical and mechanical properties of wear-resistant plating on defining their fragility. The fragility of the coating has a significant influence of the conditions of electrode position. With the increase of their stiffness (increased current density, the decrease of temperature electrolysis) is significantly increased [1]. The electrolyte composition may have different influence on the considered properties of the coatings.

It was proved that the method of measuring the hardness of iron coatings with different loads on a spherical indenter, with initial loads (up to P_{cr}) unreduced hardness ($H_n=P/\pi Dh$) is a constant value [1]. With further increase of the load (more P_{cr}), this value rises sharply, indicating that the departure from the mechanical similarity. On the given pattern is significantly affected by the conditions of electrolysis. With increasing current density, the initial violation of the laws occurs at lower loads on the spherical indenter.

The study features an elastic (h_y) and plastic (h_n) strain bodily galvanic coatings obtained after processing the indentation diagrams showed that the responsibility for the results is the change in the nature of the elastic deformation, depending on the load conditions. Regardless of the production of coatings with an increase in the load on the spherical indenter elastic component (h_y) strain coating first increases sharply (to P_{cr}), and then it rises slightly (after P_{cr}).

This proved that the main reason causing the violation of the law of the mechanical similarity, due to the onset of brittle fracture of iron plating.

Comparing the values of the critical load indentation of a spherical indenter with their values determined by observations of the formation of ring cracks around the indentation imprint, we can say that the beginning of the destruction of iron coatings can be determined much more accurately by examining the indentation depth of the indenter and the load (P_{cr}), as to form ring crack growth is possible initial cracks and the formation of new, behind which is difficult to observe. Critical stress (H_{hcr}) can be taken as a criterion for evaluating the tendency to brittle fracture surfaces.

Study of the effect of current density (Δk) and the temperature electrolysis (T) on the propensity of iron coatings to brittle fracture showed that with increasing current density from 5 to 40 (A/dm²) at a constant temperature electrolysis (40°C) the critical load indentation of a spherical indenter is reduced from 200 to 130 (H), indicating that the increased susceptibility of iron coatings to brittle fracture. With increasing temperature electrolysis of 20 to 60°C at a constant current density ($\Delta k=20$ A/dm²) critical load indentation of a spherical indenter is increased from 105 to 210 (H), indicating a decline in iron coatings propensity to brittle fracture.

One of the current problems is the prediction of durability engineering materials. In this sense, the method of testing the hardness refers to the micromechanical test method allows for the most reasonable approach to the evaluation of the characteristics of the material.

The obtained dimensional parameters H_n , P_{cr} , P , H_d , E and dimensionless H_h/E and H_d/E have a good correlation with the wear rate of wear-resistant iron coatings. Ratio H_h/E , H_d/E sensitive elastic-plastic properties of iron coatings accurately describe the process of wear.

Thus, the parameters H_h , H_d , H_h/E and H_d/E can be used in the future to refine the description of the wear surfaces. The choice depends on the wear rate of these parameters is based on the provision of additivity contributions of these structural parameters.

The results showed that the ratio of H_h/E and H_d/E sensitive elastic-plastic properties of iron coatings are extreme values as previously discussed options (A_y , A_n , A , H_h , H_d , P) with a change of electrolysis conditions (Δk , T), which coincide with existing guidelines for the choice of electrolysis conditions for optimum coating properties in terms of their durability.

With the increase in current density (Δk) from 5 to 20 (A/dm²), at a constant temperature electrolysis (40°C), the ratio (table 1) H_h/E and H_d/E increases, respectively, from $18,26 \times 10^{-3}$ to $22,40 \times 10^{-3}$ and from $12,18 \times 10^{-3}$ to $14,94 \times 10^{-3}$. With further increase of the current density (Δk) 20 to 40 (A/dm²), at a constant temperature electrolysis (40°C) ratio H_h/E and H_d/E reduced accordingly from $22,40 \times 10^{-3}$ to $20,50 \times 10^{-3}$ and from $14,94 \times 10^{-3}$ to $13,68 \times 10^{-3}$.

With increasing temperature electrolysis (T), from 20 to 40°C at a constant current density (20A/dm²) ratio H_h/E and H_d/E increases, respectively, from $13,69 \times 10^{-3}$ to $14,94 \times 10^{-3}$. With further increase of temperature electrolysis (T) from 40 to 60°C, the ratio H_h/E and H_d/E decreased respectively from $22,40 \times 10^{-3}$ to $13,33 \times 10^{-3}$, at a constant current density ($\Delta k=20$ A/dm²).

4. Conclusions

- Experimentally that unreduced hardness (H_h), dynamic hardness (H_d), the work spent on the elastic (A_y), plastic (A_r), elastic-plastic deformation, the load on a spherical indenter (with $h=2\mu m$) ratio H_h/E , H_d/E have extreme character with the changing conditions of electrolysis (Δk , T) for the studied iron coatings.
- Extreme values unreduced hardness (H_h), dynamic hardness (H_d), the work spent on the elastic (A_y), plastic (A_n), elastoplastic, deformation (A), the load on a spherical indenter (P) ratio H_h/E , H_d/E coincide with our earlier recommendations for iron plating coverage in terms of ensuring their optimum durability.
- The method of measuring hardness in macro volume can reasonably determine the physical and mechanical characteristics (H_h , H_d) (A_y , A_n , A, P, H_h/E , H_d/E) iron wear-resistant plating.
- Physical and mechanical properties (A_n , H_d , A_y , A, P, H_h/E , H_d/E) wear resistant plating have good correlations with the intensity of wear of these coatings.
- Physical and mechanical properties (H_h , H_d , A_y , A_n , A, H_h/E , H_d/E) can be used to refine the description of the wear iron coatings.

REFERENCES

- [1] S.Bulichev, V.Alehin, "Ispitanie materialov neprerivnim vdavlivaniem indentora", Moskva, Mashinostroenie, 1990, 224p.
- [2] V.Gologan, V.Azhder, V.ZHavguryanu, "Povishenie dolgovechnosti detaley mashin iznosostoykimi pokritiyami", Kishinev, Izd-vo «Shtiintsa», 1979, 112p.

- [3] V.Javgureanu, V.Ajder, V.Ceban, Pavlova L., "The correlation of restored and unrestored microhardness of wearproof iron plating". Conferință științifică internațională TMCR -2003, Chișinău, 2003, pp. 412-415.
- [4] V.Javgureanu, P.Gordelenco, M.Elita, "The work of deforming wear-proof iron-nikel plating in microsqueling", The Annals of University „Dunărea de Jos” of Galați, Fascicle VIII, 2004, Tribology, Romania, pp. 65-68.
- [5] V.Javgureanu, P.Gordelenco, M. Elita, "Relationship of the restored and unrestored microhardness of the chromium coating", The Annals of University „Dunărea de Jos” of Galați, Fascicle VIII, 2004, Tribology, Romania, pp. 48-51.
- [6] V.Javgureanu, P.Gordelenco, M.Elita, "Le rapport de la microdurete restauree et non restauree des convertures de crome", Conferință Științifică Internațională TNCR, Chișinău, 2005, vol. 2, pp. 166-169.
- [7] V.Javgureanu, P.Gordelenco, "Sootnoshenie vosstanovlennoy i nevostanovlennoy mikrotverdosti hromovih pokritiy", Mezhdunarodnaya NTK „Mashinostroenie i Tehnosfera XXI veka”, Sevastopol', 2005.
- [8] V.Javgureanu, "Issledovanie raboti deformacii iznosostoykih gal'vanicheskikh pokritiy pri mikrovdavlivanii", Mezhdunarodnaya NTK „Novie processy i ih modeli v resurso i energosberegayuschih tehnologiyah", Odessa, 2003, p. 7-8.

DESIGN OF THE SYSTEM DRIVE TO THE PNEUMO-VEHICLE WITH PNEUMATIC LINEAR ENGINE IN 2 CYLINDERS

Constantin BUNGĂU¹, Tudor MITRAN¹, Tiberiu VESSELENYI¹, Dan CRĂCIUN¹

¹ University of Oradea, bungau@uoradea.ro

Abstract: The paper aims to present the design of a pneumatically drive with applied thematic for an vehicles structure with unconventional propulsion. The general development of these drive was imposed by constructive and safety limitations.

Keywords: pneumatic, linear engine, vehicle.

1. Introduction

The interest of the development of propulsion systems that should comply with the severe environment regulations determines the work in new alternative directions to the classical propulsion systems [2], [3], [6], [7] and [11].

One of the proposed solutions is presented in this paper.

The solution is based on an auctioning system using as “fuel” compressed air. Similar researches were developed in [1], [4], [5], [7], [8], [9] and [10].

2. The design of the pneumatic auctioning system for the pneumo-vehicle

The calculus has started from the initial data: maximum working pressure $p=10$ bar, compressed air tank of 10 l at 200 bar.

The engine design is presented in figure 1.

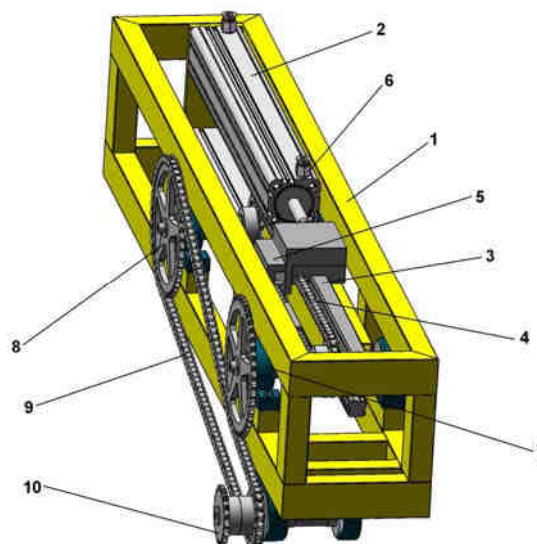


Figure 1. The vehicle's pneumatic engine

It includes the figure 1 made with rectangular profile aluminum welded in protective environment. The two cylinders 2 are mounted on the frame. The shafts have at one end a chain wheel 8. Each shaft has two bearings 7. The rectilinear movement is ensured by the guidance system 3. The transmission consists of the wheels 8 and 10 and the chain 9.

The engine has two Rexroth pneumatic cylinders and the air flow is command by two valves mounted on one cylinder. The air flow in the second cylinder is regulated from an IndraControl L10.1 CML10.1-NN-210-NB-NNNN-NW PLC produced by Bosch Rexroth based on the information coming from the first cylinder.

The cylinders inner diameter is of 50 mm and the stroke is of 320 mm. The cylinder capacity of the engine will be:

$$V_t = 4 \cdot \left[\frac{\pi}{4} \cdot (5^2 \cdot 32 - 1,6^2 \cdot 32) \right] = 2256 \text{ cm}^3 \quad [1]$$

Both cylinders are auctioning on two chain pinion (1 and 2), linked together with a chain, and rotating in opposite senses. At each stroke one of the cylinders is pushing and the other one is pulling one of the chain pinions and at the following stroke the cylinders are auctioning on the other chain pinion. Each of this chain pinions are mounted at one end of a shaft and there is another chain pinion at the other end (3 and 4, see figure8).

By using a chain the opposite movement of the chain pinions 3 and 4 can be transformed so that the chain pinion 5 (linked with the driving wheel) should rotate in one sense. The pneumatic scheme for the engine is presented in figure 2.

The valves are controlled by the PLC unit.

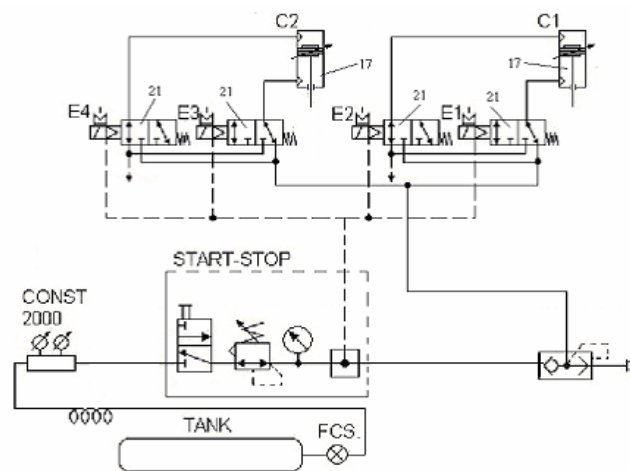


Figure 2. Pneumatic design

The components used in pneumatic scheme are presented in table 1.

Table 1

No.	Denomination	Pieces
1.	Stud fitting	10
2.	Elbow fitting	8
3.	Shut-off valve	2
4.	Pressure Regulator	1
5.	Block assembly kit	1
6.	Mounting Bracket	6
7.	Distributor	1
8.	Quick exhaust valve	2
9.	Silencers	2
10.	Y fitting	8
11.	Push-in fitting	10
12.	Fine setting valve	1
13.	Lock nut	1
14.	Pressure piece	1
15.	Cover for stroke limitation	1
16.	Compressed air tubing	12 m
17.	Pneumatic cylinder	2
21.	Valve	4

The pneumatic command system parts are presented in table 2

Table 2

No.	Denomination	Pieces
1.	PLC	1
2.	Plug pack	1
3.	Firmware CF card	1
4.	Software DVD SWA-IWORKS-IL	1
5.	Software SVL-IWORKS-IL	1
6.	16 Digit IN, R-IB IL 24 DI 16-PAC	1
7.	16 Digit OUT, R-IB IL 24 DO 16-PAC	1

3. The structural design of the vehicle (engine assembly, framework and transmission

The main dimensions of the vehicle are (see fig. 3):

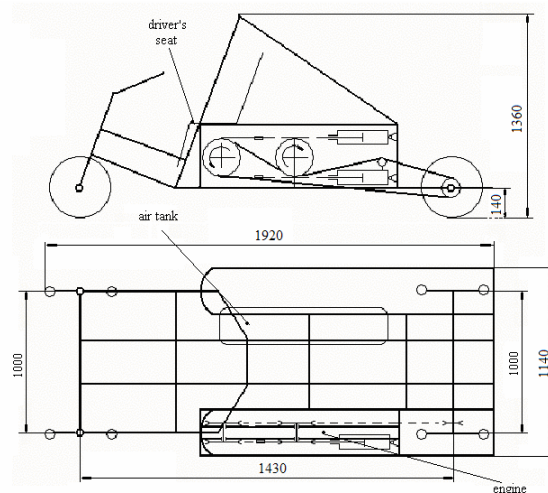


Figure3. The main dimensions

- total length: 1920 mm
- width: 1140 mm
- height: 1360 mm
- wheel base: 1430 mm
- front wheel track: 1000 mm
- rear wheel track: 1000 mm
- clearance between the bottom of the vehicle and the ground surface: 140 mm

The driver's seat is situated in the front part of the vehicle, the air tank and the engine are under it in the right side and left side respectively (see fig. 1 and fig. 3)

The vehicle's center of gravity was calculated according with figure 4

$G_a = 140$ kg – the total mass of the vehicle (with driver)

$G_1 = 50$ kg – the mass on the front wheel axle

$G_2 = 90$ kg – the mass on the rear wheel axle

b – the distance between the rear wheel axle and the center of gravity

a – the distance between the front wheel axle and the center of gravity

$$b = L \cdot \frac{G_2}{G_a} = 1430 \cdot \frac{90}{140} = 920 \text{ mm}$$

$$a = L - b = 1430 - 920 = 510 \text{ mm}$$

$G'_1=40$ kg – the mass on the front wheel axle on a platform inclined at 15°

$G'_2=100$ kg – the mass on the rear wheel axle on a plan inclined at 15°

$r=250$ mm – the wheel's radius

h_g – the height of the center of gravity

$$h_g = \left(\frac{G'_2}{G_a} \cdot L - a \right) \cdot \operatorname{ctg} \alpha + r = \left(\frac{100}{140} \cdot 1430 - 920 \right) \cdot \operatorname{ctg} 15 + 250 = 628 \text{ mm} \quad [2]$$

$$\alpha_r < \operatorname{arctg} \frac{b}{h_g} = \operatorname{arctg} \frac{510}{628} \cong 39^\circ \quad [3]$$

The condition for longitudinal stability at overturning on a horizontal road is:

$$v_a < \sqrt{\frac{26 \cdot b \cdot G_a}{2 \cdot h_g \cdot k \cdot A + \rho \cdot C_z \cdot A \cdot b}} \text{ [km/h]} \quad [4]$$

v_a [km/h] – the vehicle's speed

$k=0,062$ – vehicle's frontal aerodynamic coefficient

$A=0,7$ m² – vehicle's transversal section area

$\rho=1,21$ kg/m³ – air density

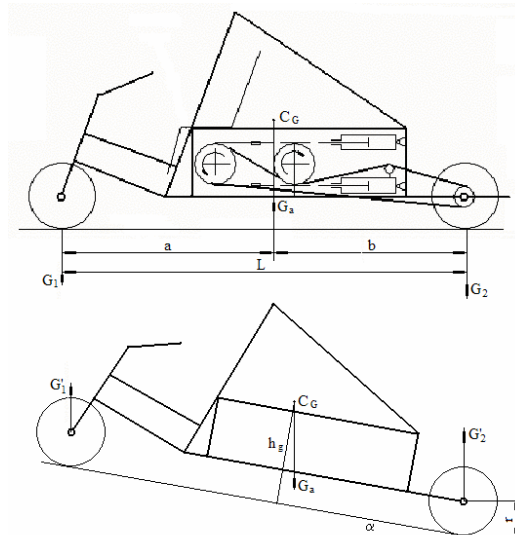


Figure 4 The position of the center of gravity

$C_z=0,45$ – the portance coefficient

$$v_a < \sqrt{\frac{26 \cdot 0,51 \cdot 140}{2 \cdot 0,628 \cdot 0,062 \cdot 0,7 + 1,21 \cdot 0,45 \cdot 0,7 \cdot 0,51}} = 86 \text{ km/h} \quad [5]$$

The condition for transversal stability at overturning on a horizontal road is:

$$v_{ar} \leq 7,97 \sqrt{\frac{R \cdot E}{h_g}} \text{ [km/h]} \quad [6]$$

$R=8$ m – the curve's radius

$E=1000$ mm – the wheel track

$$v_{ar} \leq 7,97 \sqrt{\frac{8 \cdot 1}{0,628}} = 28,5 \text{ km/h} \quad [7]$$

The minimum curve's radius that the vehicle can take without a transversal overturning at 40 km/h is:

$$R_{\max} = \frac{v_{ar}^2 \cdot h_g}{7,97^2 \cdot E} \text{ [m]} \quad [8]$$

$$R_{\max} = \frac{40^2 \cdot 0,628}{7,97^2 \cdot 1} = 15,8 \text{ m}$$

The condition for stability at transversal wheel slide at a curve radius of 8 m is:

$$v_{ar} \leq 711,3 \sqrt{\phi_y \cdot R} \text{ [Km/h]} \quad [9]$$

$\phi_y=0,2$ the adherence coefficient on transversal direction

$$v_{ar} \leq 711,3 \sqrt{0,2 \cdot 8} = 14,3 \text{ km / h}$$

The vehicle has a "car" character because the driver's seat is inside.

The chassis is made with aluminum rectangular box section bars. The bars are welded. As seen in figure 5, it's a classical rectangular construction with 4 side-members and several cross-members. Above the driver's seat is a safety tube welded on the chassis and fastened with two supplementary bars. The safety tube has a diameter of 25 mm with a wall thickness of 2,5 mm. The frame width at the driver's shoulders is 770 mm.

A headrest is mounted in the back of the driver's seat.

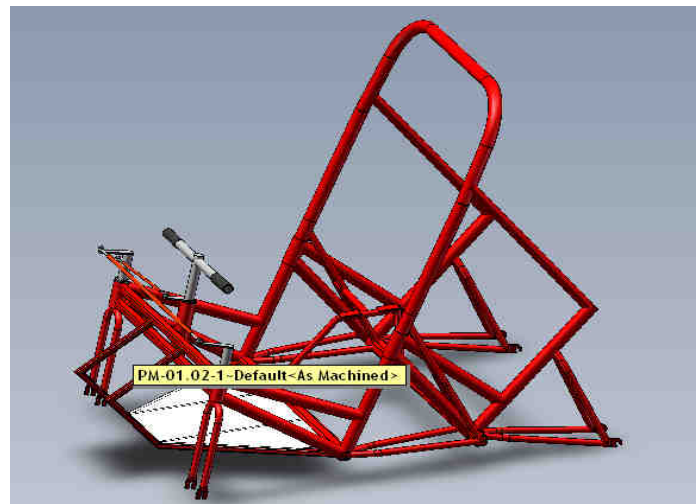


Figure 5. The general layout of the framework

The engine and the air bottle are placed under the driver's seat and separated of it with an aluminum sheet.

The estimated loads are shown in figure 6.

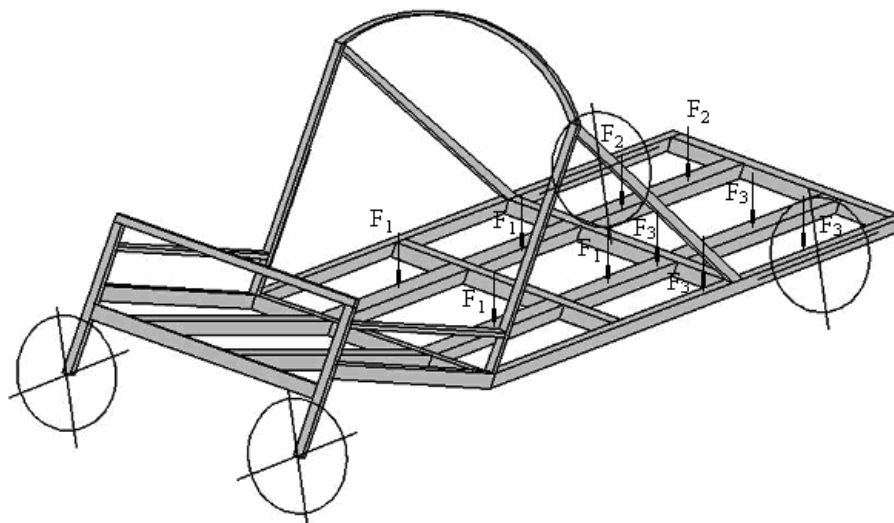


Figure 6 . The forces on the framework

$$F_1 = G_1/4 = 200 \text{ N}$$

where $G_1 \approx 800 \text{ N}$ is the estimated weight of the driver and the seat

$$F_2 = G_2/2 = 60 \text{ N}$$

where $G_2 \approx 120 \text{ N}$ is the estimated weight of the air tank

$$F_3 = G_3/4 = 70 \text{ N}$$

where $G_3 \approx 280 \text{ N}$ is the estimated weight of the motor

4. Conclusions

Based on the conception presented in this paper, a pneumo-vehicle was realized in the laboratories of the University from Oradea. The vehicle is presented in figure 7.



Figure 7. The construction of the pneumo-vehicle

The driver's seat is situated in front of the vehicle.

The pneumo-vehicle has 4 wheels (two in front for steering and two in the rear).

The vehicle framework is realized with aluminum bars welded together. The engine has two pneumatic cylinders which are operated by 2 valves. Using a chain transmission, the torque is transmitted to one of the rear wheels.

Aluminum was chosen in order to reduce the vehicle mass. The linear engine should produce a constant torque.

REFERENCES

- [1] Louis Arnoux "PEAK OIL, _CLIMATE CHANGE_ & ALL THAT JAZZ" IT MDI, *Energy Limited*, 2008
- [2] <http://www.commoditiesrecoverycorp.com/electricmotors.htm>
- [3] <http://www.evworks.com.au/tech/>
- [4] <http://www.forbes.com/forbes/2008/0505/058.html>
- [5] <http://www.greencar.com/articles/trends-air-powered-cars.php>
- [6] <http://greencar.md/automobile-electrice/>
- [7] <http://www.renewablepowernews.com/archives/1497>
- [8] <http://www.research.com/negre/negre.htm>
- [9] <http://spectrum.ieee.org/energy/environment/deflating-the-air-car/0>
- [10] http://www.thefuture.net.nz/mdi_tech.htm
- [11] <http://worldwide.espacenet.com/publicationDetails/description>

NOTES ON THE ENERGETIC TRANSFER IN HYDROSTATIC SYSTEMS

Eugen DOBÂNDĂ¹

¹ Universitatea POLITEHNICA din Timișoara, Facultatea de Mecanică, eugendobanda@yahoo.com

Abstract: *The paper intent to present a new way to consider the energy transfer through the elements of a hydrostatic system, by taking into account different ways of the inputs and outputs values in each particular element.*

Keywords: *hydrostatic system, energy transfer, efficiency*

1. Introduction

Generally, a simple hydrostatic system is composed by a motor (which generate stereo-mechanic energy), a hydrostatic generator (which generate hydraulic energy), control equipments, and hydraulic motors (which convert the hydraulic energy into stereo-mechanic energy). The fluxes of energy through the system define the working regimes and the efficiency of the system.

2. General review

Let it be considered a simple hydrostatic system through which will be analysed the transfer of the energy. In order to realize that purpose, first let us take the basic elements of the considered system and analyse the way that the energetic transfer is realized.

Each element will be considered as an informatics quadripol, and has characteristic energy values as follows:

- a.) the fix displacement pump has flow and pressure as input and output values and the rotational speed of the electric motor as parameter,
- b.) the cylinder (linear motor) has the flow, pressure, force (to the stroke), and the displacement of the stroke as inputs and outputs values,
- c.) the fix displacement [rotational] motor has pressure, flow, rotational speed and momentum as inputs and outputs values, and the return pressure (the tank pressure) as parameter,
- d.) the directional control valve has flow and pressure as inputs and outputs values,
- e.) the flow control valve has flow and pressure as input and output values and the opening gap as parameter,
- f.) the pressure relief valve has pressure and flow as inputs and outputs values, and the return pressure (the tank pressure) and the displacement of the command spring as parameters.

In figures 1 to 3 there are presented the system and his main working positions.

3. The characteristics of the elements of the system, in “classical” approach

According to [6], [1], and [7], in “classical” description, the elements of the analysed system are considered as follows:

- a.) the fix displacement pump has as input values the pressure, the output value the flow, and as parameter, the rotational speed of the electrical motor, as shown in figure 4,
- b.) the cylinder has the flow and the force on the rod as input values and the speed on the rod, the pressure as outputs values and the return pressure (the pressure in the tank) as parameter, as shown in figure 5,
- c.) the fix displacement (rotational) motor has the flow and the momentum on the shaft as inputs, the pressure and the rotational speed of the shaft as outputs values and the return pressure (the pressure in the tank) as parameter, as shown in figure 6,
- d.) the directional control valve has the flow an the pressure as inputs values, and also the pressure as outputs values, as shown in figure 7,

- e.) the pressure relief vane has the flow and the pressure as input values, the pressure as output values and the return pressure (the pressure in the tank) and the displacement of the element which define the opening, as shown in figure 8.

In all the cases, the geometry of each element is considered, also, as parametric condition. Combining the elements and representing the energy fluxes, there is obtaining the chain presented in figure 9.

4. The new considerations of the elements of the system

In our appreciation, the elements presented above, transfer in a better way the energy if the input and output values are reconsidered, as follows:

- a.) the fix displacement pump has the rotational speed of the electrical motor as input value and the pressure and the flow as output values, as shown in figure 10,
- b.) the cylinder has the flow and the pressure as input values, the speed and the force on the rod, the as outputs values and the return pressure (the pressure in the tank) as parameter, as shown in figure 11,
- c.) the fix displacement (rotational) motor has the flow and the pressure as input values, the and the momentum and shaft rotational speed of the shaft as output values and the return pressure (the pressure in the tank) as parameter, as shown in figure 12.

In all the cases, the geometry of each element is considered, also, as parametric condition. Combining the elements and representing the energy fluxes, there is obtaining the chain presented in figure 13.

5. Conclusions

There were presented two ways of considering the energetic transfer through the elements of a hydrostatic system.

The differences consist in the reconsideration of the input and the output values, obtaining, in the new way of description a better way of representing the transfer of the energy.

Also, as reveal the figure 13, by compared with figure 9, the flux of energy in the new description is more direct then in the "classical" one.

More, in "classical" way to consider the energy transfer, the mathematical model of the elements of the system, in his ensemble, present transcendental equations. But, the new description, considering the same set of equations, result the equations can be resolved in a direct mode, with a minimum effort.

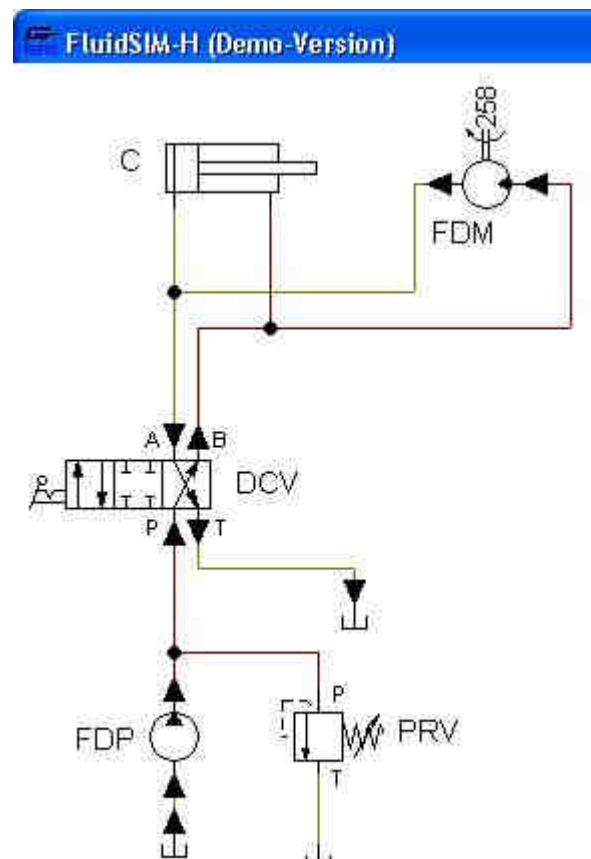
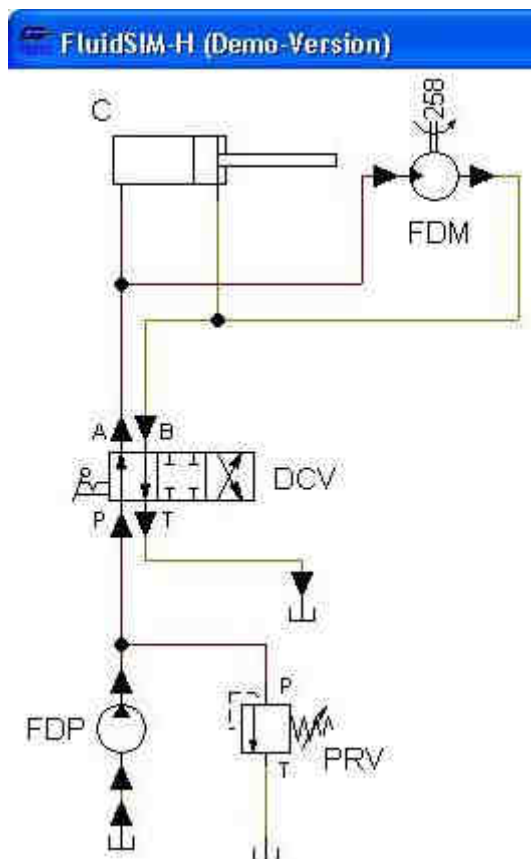
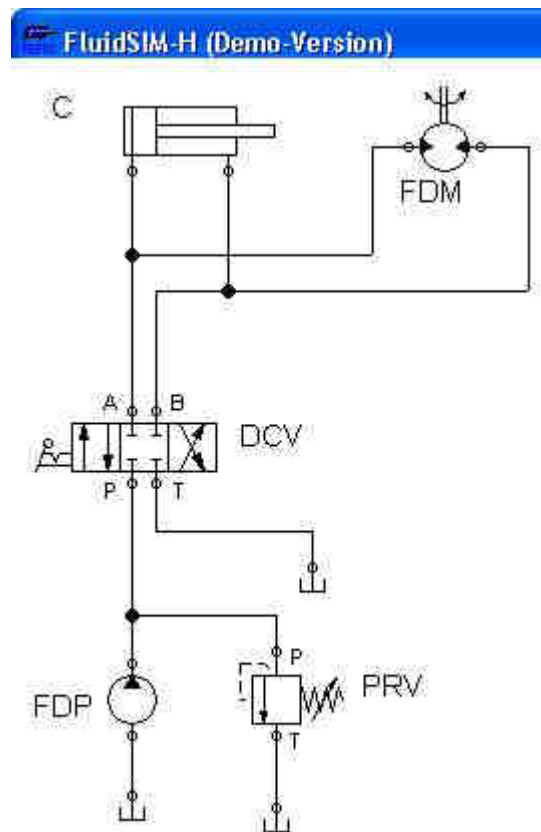


Figure 2. The analysed system; position A

Figure 3. The analysed system; position B

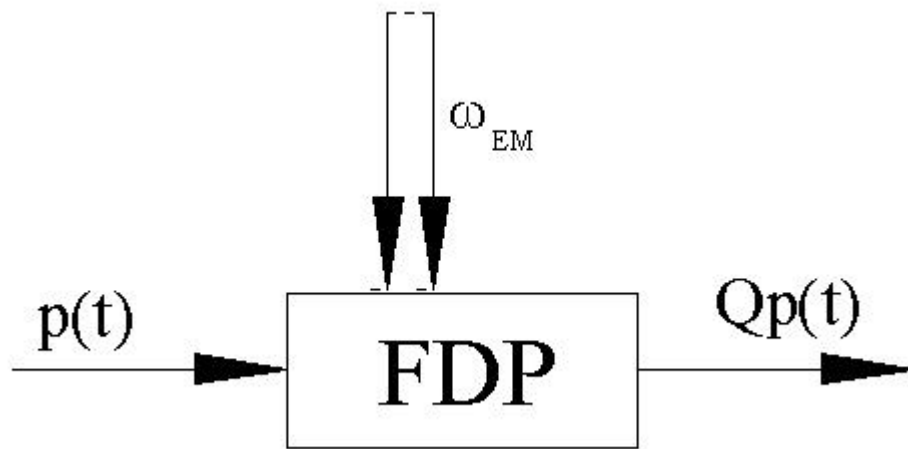


Figure 4. The fix displacement pump, in "classic" description

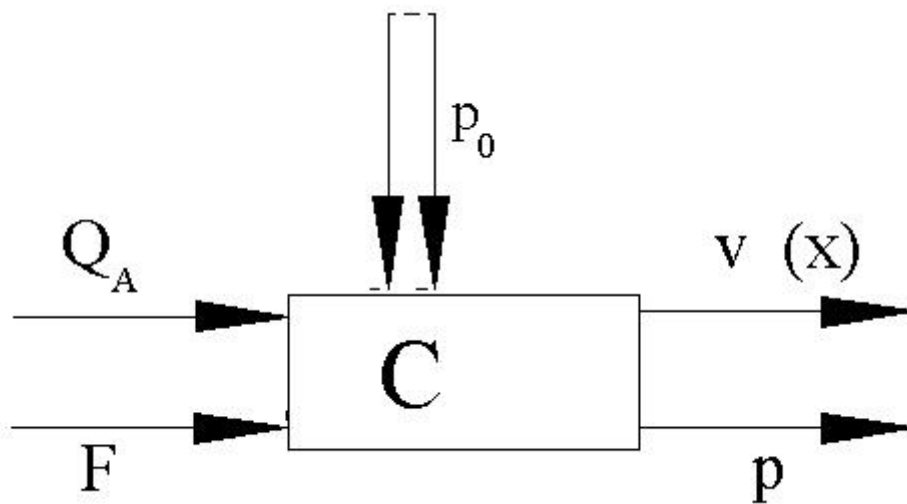


Figure 5. The cylinder, in "classic" description

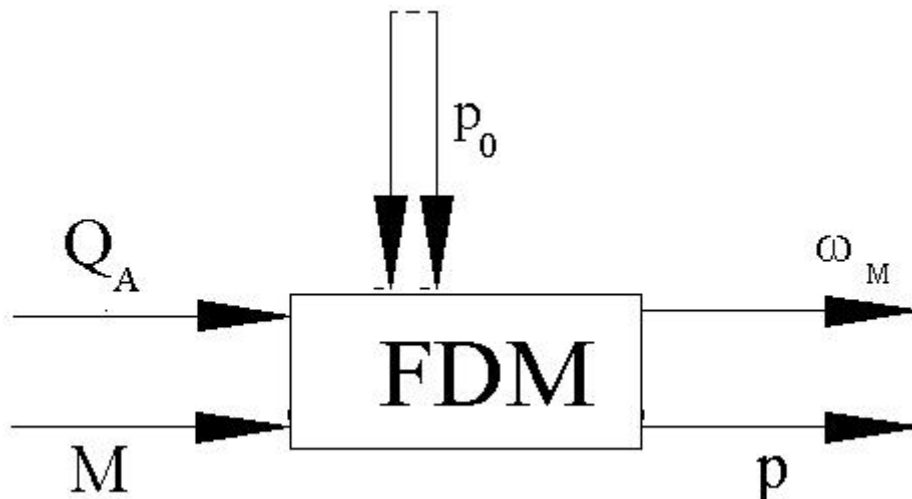


Figure 6. The motor, in "classic" description

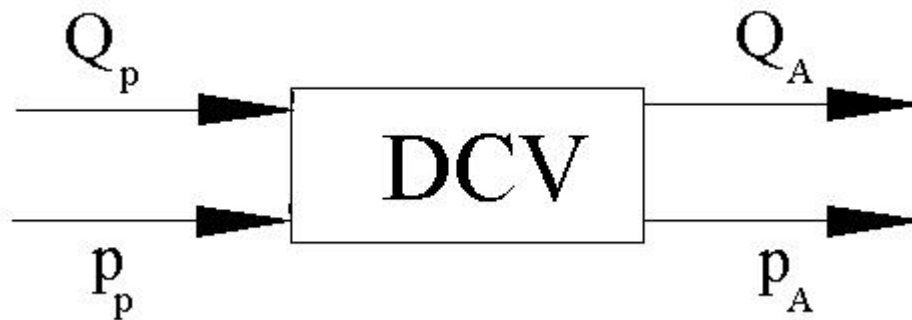


Figure 7. The directional control valve

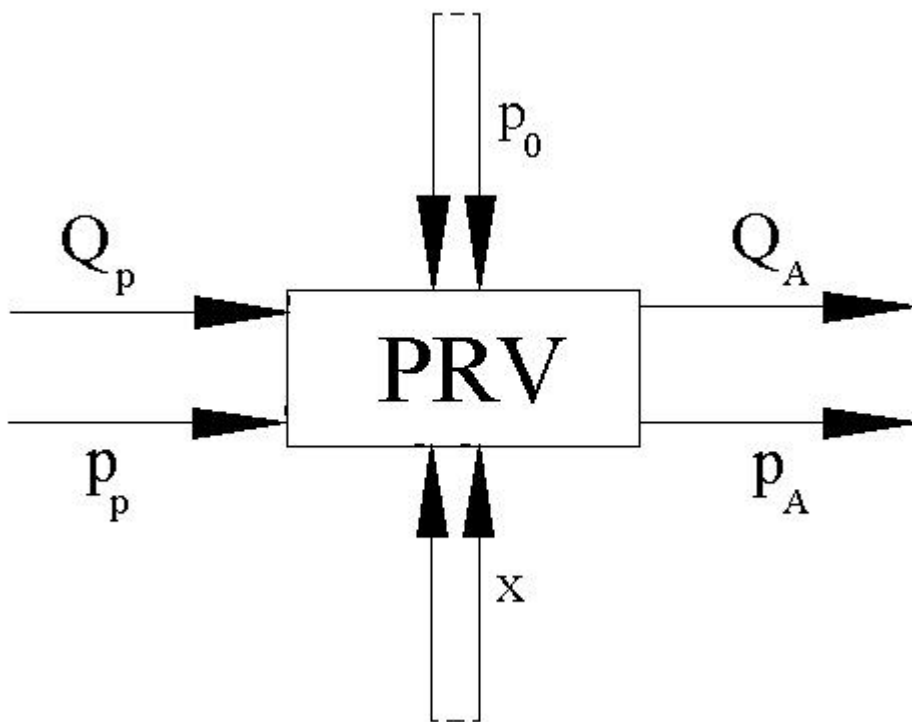


Figure 8. The pressure relief valve



Figure 10. The fix displacement pump, in new description

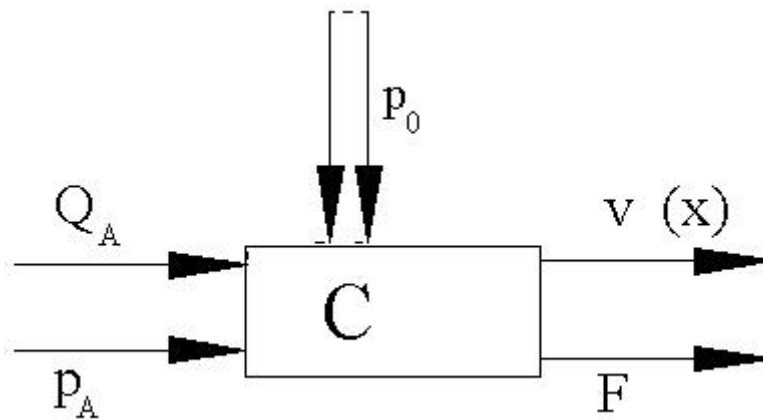


Figure 11. The cylinder, in new description

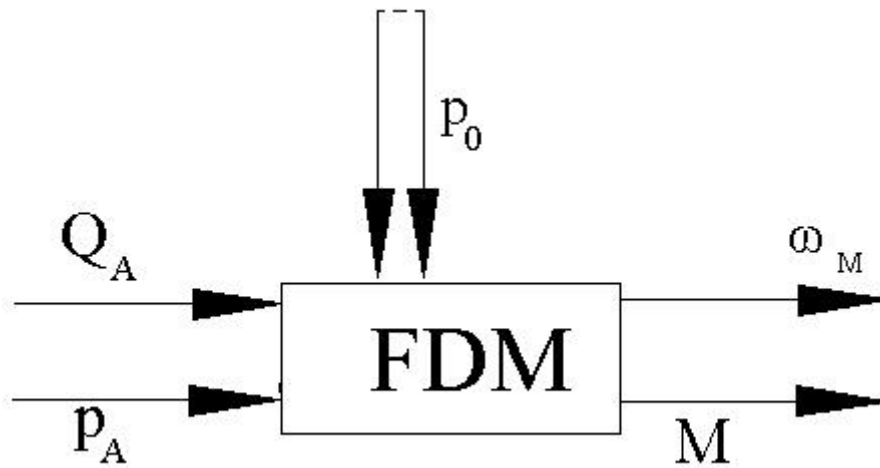


Figure 12. The motor, in new description

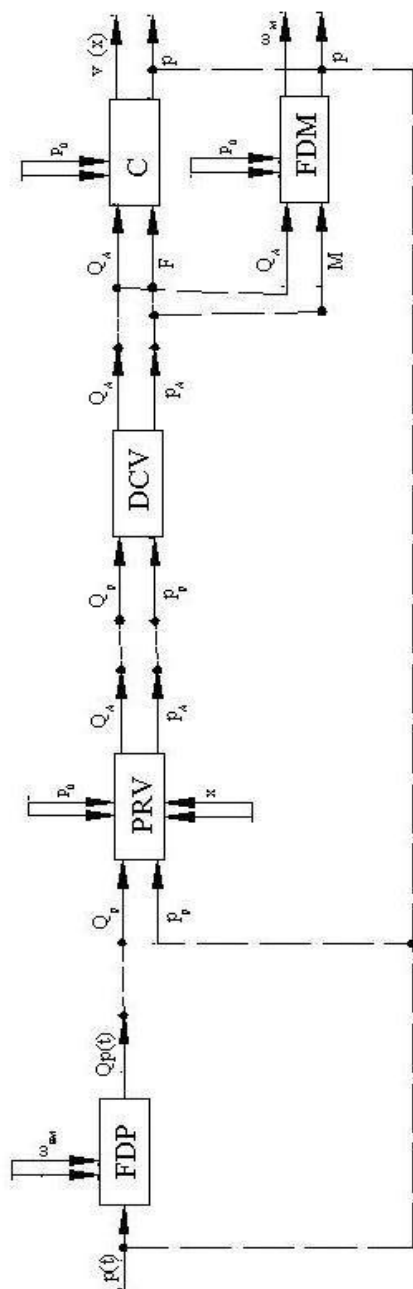


Figure 9. The system, according , to the "classic" description

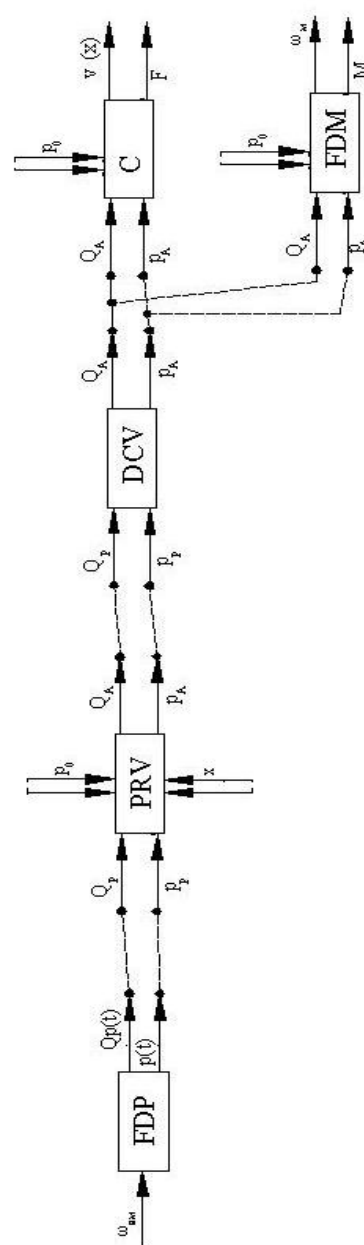


Figure 13. The system, according , to the new description

REFERENCES

- [1] V. Bălăsoiu, ș.a. "Echipamente și sisteme hidraulice de acționare și automatizare. Mașini volumice" vol. 1, Editura Orizonturi Universitare, Timișoara, 2007
- [2] V. Bălăsoiu, ș.a. "Echipamente și sisteme hidraulice de acționare și automatizare. Aparatură hidraulică" vol. 2, Editura Orizonturi Universitare, Timișoara, 2008
- [3] M. Bărglăzan, "Reglarea și automatizarea sistemelor hidraulice", Institutul Politehnic "Traian Vuia", Timișoara, 1979
- [4] C. Buda, "Elemente de reglaj și automatizare", Editura Didactică și Pedagogică, București, 1975
- [5] V. Marin, A. Marin, "Sisteme hidraulice automate. Construcție, reglare, exploatare", Editura Tehnică, București, 1987
- [6] A. Oprean, ș.a., "Acționări și automatizări hidraulice", Editura Tehnică, București, 1989
- [7] N. Vasiliu, ș.a. "Acționări hidraulice și pneumatice", vol. 1, Editura Tehnică, București, 2005
- [8] <http://www.festo.com>

EXPERIMENTAL RESEARCH TO VALIDATE SIMULATION MODEL OF HYDRAULIC MOTOR HYDRAULIC TRANSMISSION FOR LOW POWER WIND TURBINES

Constantin CHIRIȚĂ I¹, Mihai AFRĂSINEI², Vasile DAMASCHIN¹, Andrei GRAMA¹

¹ Tehnical University "Gheorghe Asachi" from Iassy, e-mail automecanica_iasi@yahoo.com

Abstract: To validate the accuracy of the results obtained by numerical simulation model, experimental investigations aim to determine the step responses of the transmission to change the input parameters (speed of the turbine shaft and load shaft hydraulic motor). To this end, Adaptive hydraulic transmission system was materialized on experimental stand. This stand is made study dynamic behavior of the system under real conditions. *Experimental procedure is done basically by the same way as in the experiment by numerical simulation.*

Keywords: hydraulic transmission, pumps with variable flow rate, wind turbine

1. Introduction

Experimental procedure is done basically by the same way as in the experiment by numerical simulation.

Designed experimental bench work were introduced two modules (Figure 1) and filtering module and a module for open circuit. Filtration module fitted with electric pump 5 is designed to filter oil returning to the tank from the pump off and drain pump. Open circuit module is provided additionally to enable bench and other elements of the composition of hydraulic transmission. In experimental work, this module is not used for research purposes pursued.

2. Presentation the stand of experimental

Overview, experimental stand components are shown in Figure 2.2, where the observed location of the stand closed circuit module being visible double pump 12, the turbine rotor simulation module 13 and pump control mechanism. On the left side of the figure is shown the load module. Location of various hydraulic components would be tested experimentally is the mass M T channel, the module is powered by a constant flow pump 6 (Figure 2.1), driven by an asynchronous electric motor 3.

Specifications:

Load Module	maximum flow rate:	20 l/min
	maximum pressure:	300 bar
Closed loop mode:	variable work flow rate:	0...27 l/min
	maximum pressure:	300 bar
Open circuit mode:	nominal flow rate:	40 l/min
	maximum pressure:	150 bar
Filtering module:	nominal flow rate:	11 l/min
	maximum pressure:	10 bar

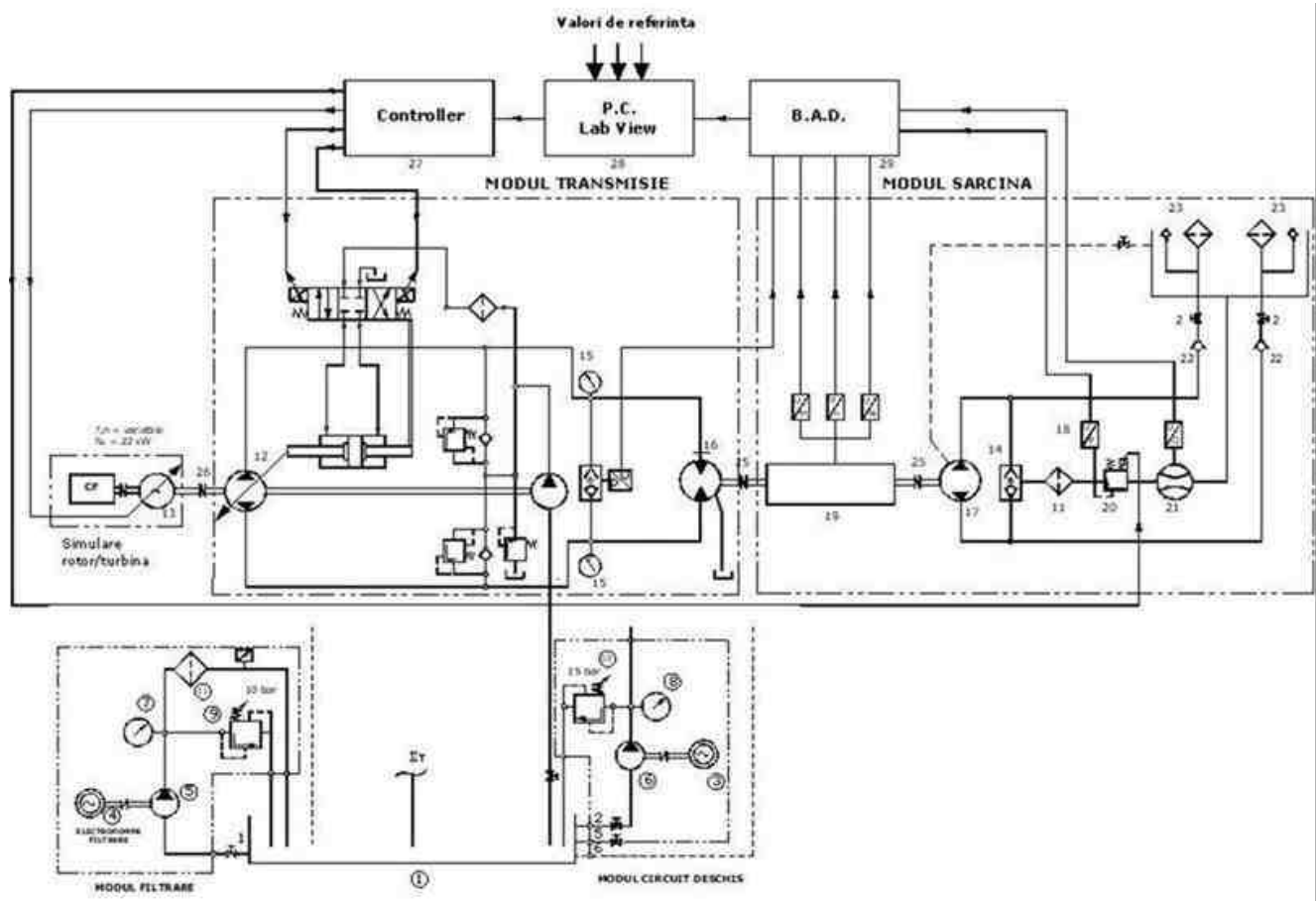


Fig. 2.1. Experimental stand hydraulic transmission scheme automotive proposed adaptive

Structural elements of the hydraulic system names are set out below:

- | | |
|--------------------------------------|---|
| 1 Check valve | 13 Principal tank |
| 2 Pressure gauge Ø100, 0-400 bar | 14 Ball valve |
| 3 Axial piston unit | 15 Three-phase asynchronous electric motor, 11 kW, 1440 rot/min |
| 4 Axial piston unit | 16 Three-phase asynchronous electric motor, 0.75 kW, 1440 rot/min |
| 5 Pressure transducer | 17 Gear pump |
| 6 Transducer speed, torque and power | 18 Vane pump $V_g = 27.4 \text{ cmc/rot}$ |
| 7 Proportional pressure valve | 19 Pressure gauge Ø100, 0-25 bar |
| 8 Flow rate transducer | 20 Pressure gauge Ø100, 0-400 bar |
| 9 One-way valve | 21 Piloted valve pressure |
| 10 Suction filter (strainer) | 22 Piloted valve pressure pilotată |
| 11 Tank load mode | 23 Pressure filter |
| 12 Coupling type SINGLE FLEX | 24 Axial piston pump in closed circuit |

The data acquisition and control include the following:

1. Transducers (sensors)
 - a. Pressure transducer output signal unified
pressure input 0-400 bar out 4-20 mA

- accuracy class $\pm 0.25\%$ BFSL
 b. Flow rate transducer with signal output in unified
 flow rate input 10-318 l/min out 4-20mA
 working pressure 0-400 bar
 accuracy class $\pm 0.25\%$ BFSO
 c. inductive speed sensor
 speed input 0-3000 rpm out 4-20mA
 accuracy class $\pm 0.15\%$ BFSO

2. *Distribution system National Instruments Compact FieldPoint*

a. Controller cFP 2020

CPU Clock	75 MHz
System Memory	32 MB
Flash	512 Mb
Ethernet	1
RS232	3
RS485	1
Operating system	LabVIEW Real Time

b. Analog modul cFP AIO 600

Analog input

Channels	4
Mesh resolution	12 bits
Sampling frequency	1.7 kS/s (1.7 kHz)
Input	4 mA , 20 mA
Sensitivity	3.91 μ A

Analog output

Channels	4
Mesh resolution	12 bits
Output	4 mA , 20 mA
Sensitivity	3.91 μ A
Output frequency	1.7 kS/s (1.7 kHz)

3. *Acquisition board NI DAQ DAQCard-6036E*

Analog input

Channels	16
Mesh resolution	16 bits
Sampling frequency	200 kS/s
Input	10 V
Sensitivity	4.26 mV

Analog output

Channels	2
Mesh resolution	16 bits
Output	10 V
Sensitivity	2.547 mV
Output frequency	1 kS/s

4. *Computing system type IBM PC x86*

5. *Software*

S.O Microsoft Windows XP SP 3
 x86 LabView 8.5
 LabView 8.5.1 Real Time

Note

System control and data acquisition was detailed only for functions that have been used in experimental research.

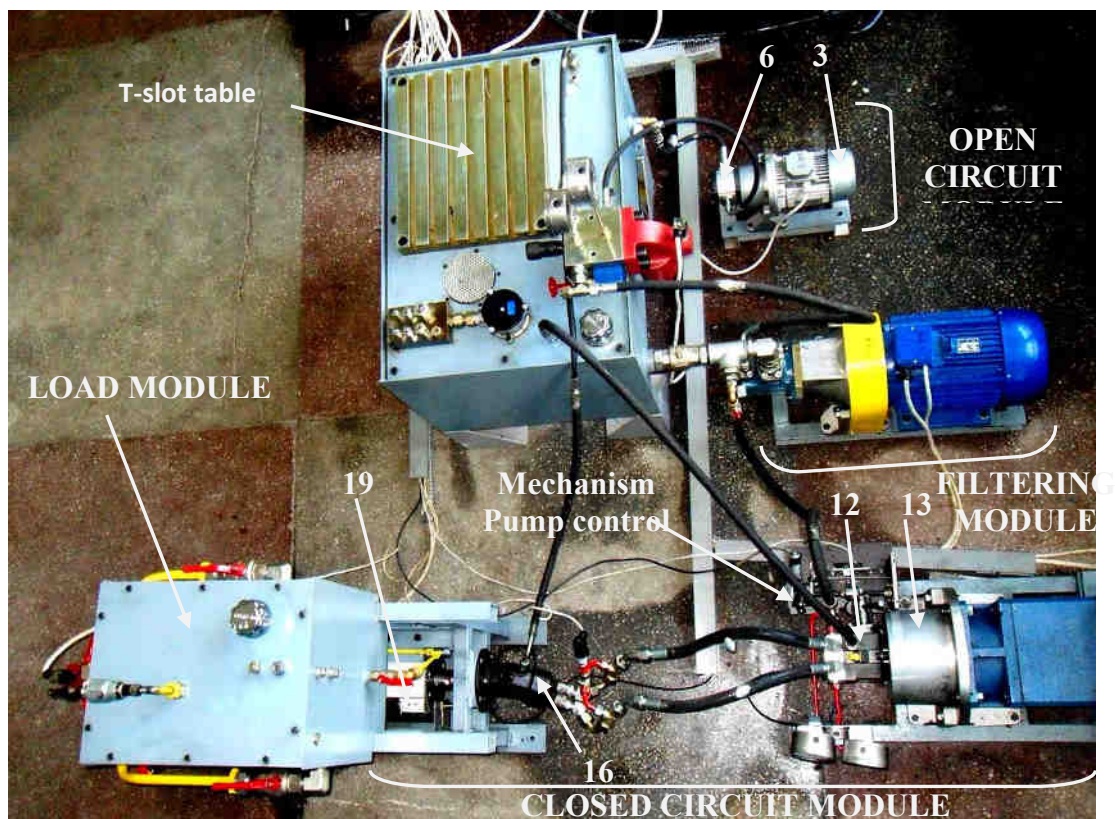


Fig. 2.2 Overview top of the stand

An important component of the experimental stand is the automatic control loop presented as a block diagram in Figure 2.3.

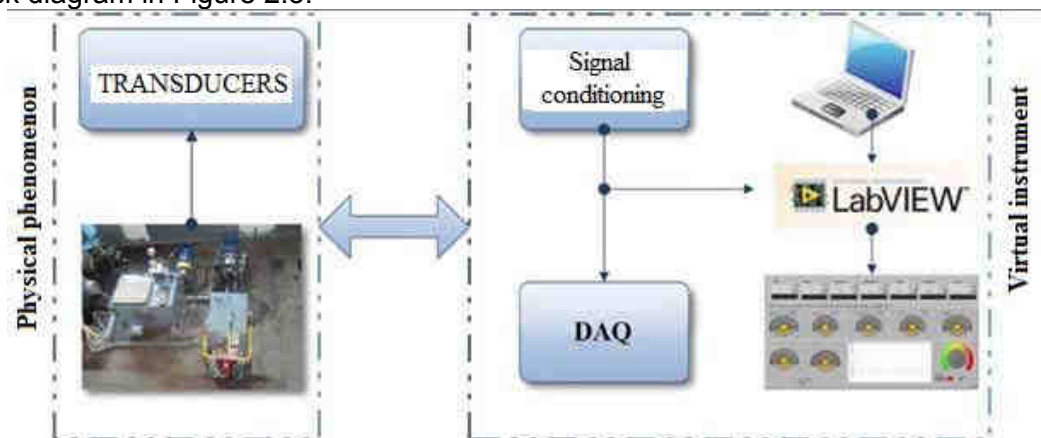


Fig. 2.3 Block diagram of the automatic control loop

Physical phenomenon and receiving transducers convert physical quantity (pressure, flow rate, etc..) In a size other mainly in voltage, the resulting signal is proportional to the size variation monitored.

Conditioning modules provide electrical signals generated by the transducers in a form that acquisition DAQ board can accept. Examples of signal conditioning is amplification, linearization, filtering, isolation, etc..

Acquisition board to convert electrical signals through its basic component, analog-to-digital converter. It attaches a numerical value to a voltage, thus making it possible to interpret the computing system.

Virtual tool work bench consists of the hardware - digital analog converter (Compact FieldPoint distribution system [1] and data acquisition board NiDAQ [2]) and the software taken in

conjunction with the needs of working hydraulic stand. The resulting virtual instrument comprises measuring devices and controls for plant automation. The graphical interface of this program included controls and indicators made in a form similar graphics devices and real devices, the user manevrându also their real elements.

Virtual instrumentation associated hydraulic stand was developed using LabVIEW graphical programming environment [3], used mainly for signal acquisition, measurement and analysis graphical or tabular presentation of data.

The front panel, shown in Figure 2.4, comprises a series of bar graphs to visualize signals scaled unit corresponding physical quantity monitored through hardware part that receives signals from transducers mounted hydraulic bench. Also through the front panel numeric input, or through a virtual potentiometer, setpoint (SETPOINT) control system. The front panel was created using display elements and control procedures extracted from library LabVIEW programming environment and a range of filtering procedures and interpretation of signals [4], adapted to the experimental stand.



Fig.2.4 Front panel [4]



3. Development program at experiments

This work was repeated four reference speed rotary motor shaft (500, 600, 700, 800 r / min) and were extracted step responses of automatic scheme to these values. Picture experimental values for this series of experiments is presented in Table 3.1.

No. crt.	Pressure charging circuit [bar]	Pressure variation in load circuit [bar]	Speed hydraulic motor [rpm]	Variation of rotor speed [rpm]
1	50	-	500	50
2				100
3				150
4			600	50
5				100
6				150
7				700

8				100
9				150
10				50
11			800	100
12				150
13				50
14			500	100
15				150
16				50
17			600	100
18	75	-		150
19				50
20			700	100
21				150
22				50
23			800	100
24				150
25				50
26			500	100
27				150
28				50
29			600	100
30	100	-		150
31				50
32			700	100
33				150
34				50
35			800	100
36				150

4. Experimental results for a series of research at constant load hydraulic motor shaft

For each group in a series of studies with values given in Table 5.1 was done as follows:

- Fix loading pressure pump load the value $\Delta p = 50$ bar;
- Bring the hydraulic motor shaft speed to the reference value, the switching frequency converter;
- Enter the reference value calculation system using virtual potentiometer;
- Change Δn turbine rotor speed = 50 rev / min;
- For each of these groups attempt to extract step responses of the system of the computing system.

In this way are obtained step responses of the system shown in Figure 4.1

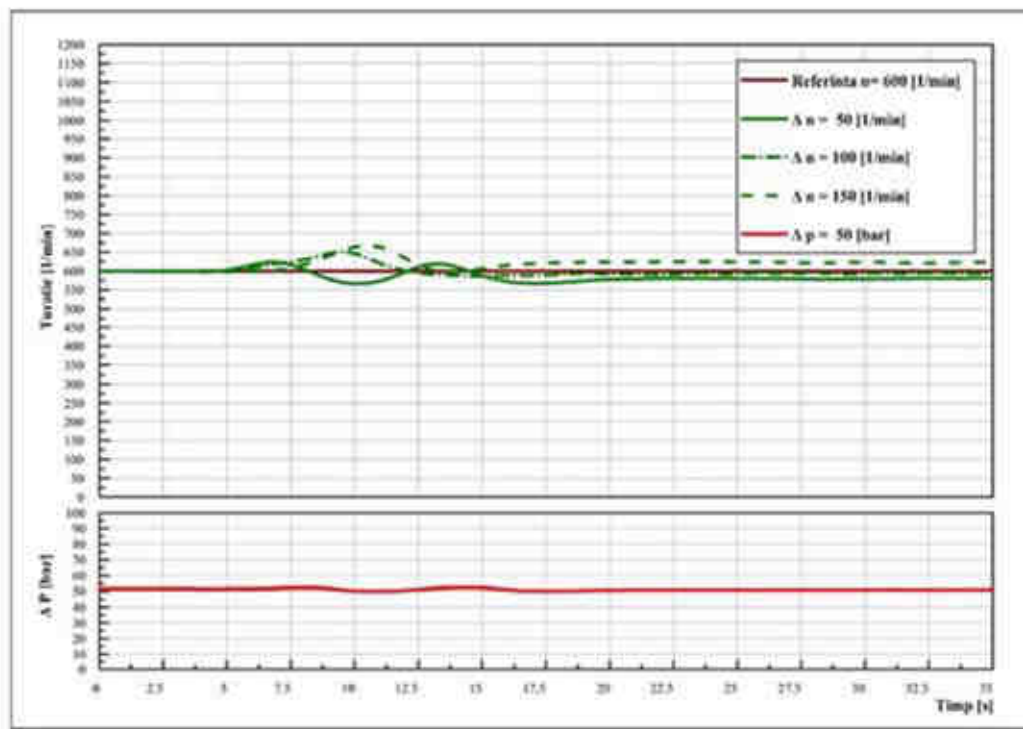


Fig. 4.1. Step responses superimposed $n_{ref} = 600$ rpm, $\Delta p = \text{constant} = 50$ bar and $\Delta n = 50, 100, 150$ rpm

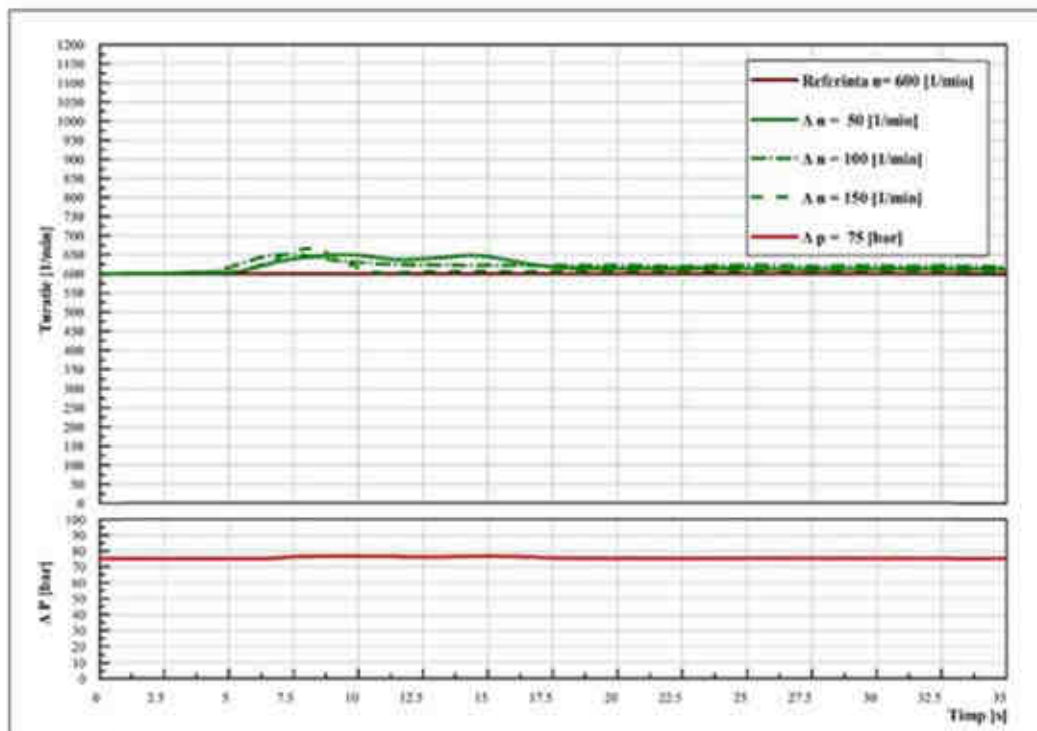


Fig.4.2. Step responses superimposed $n_{ref} = 600$ rpm, $\Delta p = \text{constant} = 75$ bar and $\Delta n = 50, 100, 150$ rpm

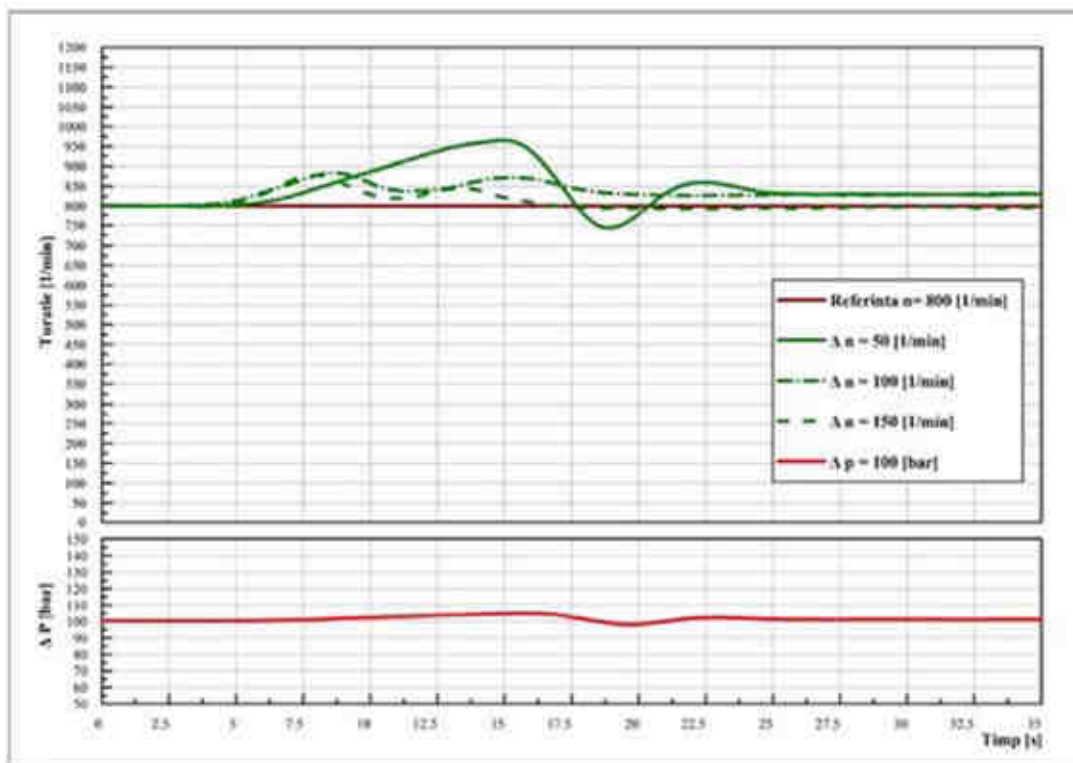


Fig. 5.18 Responses indexical overlapping $n_{ref} = 800$ rpm, $\Delta p = \text{constant} = 100$ bar and $\Delta n = 50, 100, 150$ rpm

4. Conclusions

The analysis of experimental results obtained in the two series of tests, the following conclusions were drawn:

Step response obtained by experimental testing is characterized by a transient period longer than responses obtained by numerical simulation, this is because, if the numerical simulation, can be effectively applied in step variation, while the research conducted on the experimental stand, variable speed turbine rotor (the first series of tests) or load variation in shaft hydraulic motors (from the second series of tests) can not be achieved only uphill due to the fact that variations are obtained by manual handling of potentiometers;

Adjustment errors are inevitable due to the existence of mechanism games pitch wheel pump and the possible delays that may occur in electronic data processing chain and the precision of the transducers used;

Finally, it can be concluded that the new Adaptive hydraulic system behaves under realistic conditions (wind velocity and variation of load to the motor shaft generator) as a dynamically stable system

REFERENCES

- [1] <http://sine.ni.com/nips/cds/view/p/lang/en/nid/11572>
- [2] <http://sine.ni.com/nips/cds/view/p/lang/en/nid/11914>
- [3] <http://www.ni.com/labview/>
- [4] Afrăsinei M., Damaschin V. ©D.I.S.A.H.P. – www.disahp.net

CERCETĂRI ȘI TEHNOLOGII PENTRU REDUCEREA CONSUMULUI DE CARBURANT AL AUTOVEHICULELOR DE TRANSPORT MARFĂ ȘI PERSOANE

Drd .ing. ZORIN BERCEA¹ și prof. dr. ing LIVIU VAIDA²

^{1,2} Universitatea Tehnică din Cluj Napoca, Facultatea de Mecanică, Departamentul de Inginerie Mecanică, Cluj-Napoca, România

¹ e-mail: Vasile.Bercea@termo.utcluj.ro;

² e-mail: Liviu.Vaida@termo.utcluj.ro

Abstract: *Poluarea mediului prin emisiile de gaze de evacuare ale motoarelor termice care propulsează autovehiculele și reducerea continuă a resurselor de combustibili fosili pentru producerea carburanților sunt de multă vreme probleme centrale ale politicilor naționale ale statelor Uniunii Europene, dar și ale organismelor de conducere comunitare. În condițiile în care autovehiculele cu tracțiune electrică au utilizări limitate, iar autovehiculele hibride (care sunt propulsate în principal tot de motoare termice) sunt fabricate în principal cu destinația de autoturisme, se impun măsuri eficiente pentru reducerea consumului de carburant al motoarelor termice care propulsează majoritatea autovehiculelor de transport marfă și persoane. În cele ce urmează, se continuă un alt articol al autorilor ^[1] în care au fost analizați principalii factori care influențează consumul de carburant al autovehiculelor având aceste destinații. Se prezintă cercetări, direcții de proiectare și tehnologii care determină pe de-o parte reducerea sarcinii rezistive pe care trebuie să o învingă motorul, păstrând capacitatea de transport a autovehiculului pe care îl propulsează, iar pe de alta, creșterea randamentului acestor propulsoare și în consecință, reducerea consumului de carburant.*

Keywords: *autovehicule, factor de încărcare, rezistența aerodinamică, rezistența la rulare, randamentul motoarelor cu ardere internă.*

1. Introducere

Cu câteva excepții notabile, proporțiile emisiilor totale de gaze cu efect de seră (excluzând exploatarea terenurilor și silvicultura) emise de fiecare dintre principalele categorii de surse în UE-27 s-au schimbat foarte puțin între 1990 și 2009. Principalele schimbări au fost reducerile din industriile prelucrătoare și din construcții (de la 14,8% la 11,5%) și din sectorul proceselor industriale (de la 8,3% la 7%), precum și, în special, creșterea de la 13,8% la 20,2% din transporturi. Schimbările proporțiilor emise de alte categorii au fost minore. Intensitatea GES a consumului de energie s-a diminuat moderat, între 2000 și 2009, cu toate că într-un ritm mai lent decât în anii 1990. Trecerea la combustibilii cu un conținut mai redus de carbon este principala cauză a acestei reduceri^[3].

Între 2001 și 2010, temperatura medie la suprafața planetei a fost cu 0,46°C mai mare decât media din anii 1961-1990, ceea ce face din acest deceniu cea mai călduroasă perioadă înregistrată vreodată. Astfel, se continuă tendința evolutivă a temperaturii, întrucât anii 2000 au fost mai călduroși decât anii 1990, care au fost, la rândul lor, mai călduroși decât anii 1980 și deceniile anterioare^[3].

Între anii 2000 și 2009, ponderea modală a transportului rutier intern de mărfuri din UE a crescut la 77,5%, odată cu scăderea ușoară a ponderii transportului feroviar și a transportului pe căi navigabile interioare, în cursul aceleiași perioade. Aceste schimbări au fost însoțite de creșterea performanței transporturilor (tone-km) între anii 2000 și 2007, iar din 2008 aceasta a început să se alinieze creșterii economice mai reduse, determinate de criza economică. Cercetările efectuate în ultimele decenii de marii producători de autovehicule, dar și de diverse organizații naționale și internaționale au început să devină tot mai coerente, cu o viziune de ansamblu asupra tuturor factorilor tehnici, organizatorici și umani care determină sau influențează consumul specific de carburanți în transporturile auto.

Principalii factori care influențează semnificativ consumul specific de carburant [$l/(t \cdot km)$ sau $l/(1000 t \cdot km)$] în transporturile auto sunt analizați în ^{[1],[2]} și evident în unele dintre lucrările menționate în bibliografiile care au stat la baza elaborării acestora. Aceștia sunt:

- influența sarcinii utile: 15-30%, cu posibilități de reducere a consumului de carburanți de cca. 15%;
- rezistența aerodinamică: consumă peste 50% din puterea efectivă livrată de motor, cu posibilități de reducere a consumului de carburanți de până la 10%;
- rezistența la rulare a anvelopelor consumă cca. 32% din puterea efectivă a motorului, iar prin utilizarea unor anvelope și a unor presiuni de aer adecvate, se poate reduce consumul de carburant cu cca. 5-7%.
- randamentul efectiv al motoarelor cu ardere internă pentru autovehicule nu depășesc 40% (motoarele Diesel), iar perspectivele de creștere ale acestora sunt limitate: cca. 15%.

Având ca bază concluziile articolului^[1], se vor analiza în cele ce urmează strategii, cercetări și tehnologii care permit reducerea consumului specific de carburant în transporturile auto, în condițiile asigurării siguranței circulației, cu limitele impuse de căile de rulare și de viaducte.

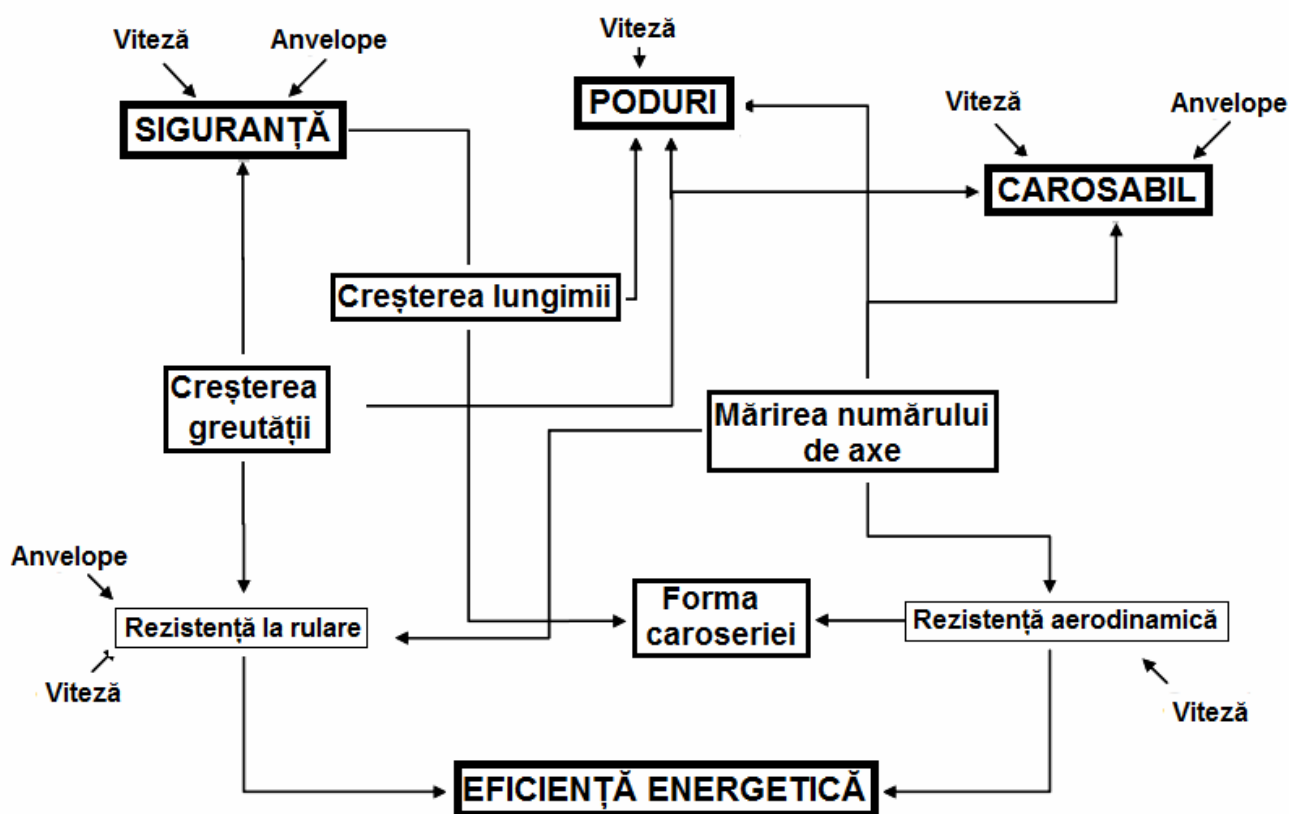


Figura 1: Schema efectelor asociate autovehiculelor grele de transport privind consumul de carburanți, infrastructura și siguranța circulației ^[2]

2. Mărirea capacității totale de încărcare

Așa cum s-a arătat în articolul ^[1] cercetările efectuate demonstrează în general scăderea consumului specific de carburant raportat odată cu creșterea masei totale a vehiculului, pe distanțe lungi, complet încărcat. Astfel în 2008, Institutul de Cercetare American în Transporturi (ATRI) a actualizat un studiu anterior realizat în 2004 cu privire la avantajele creșterii mării (lungimii) și greutateii autocamioanelor în ceea ce privește economia de combustibil și emisiile de gaze ^[4]. Șase combinații de autovehicule (spre exemplu, tractor plus remorcă) au fost analizate în acest studiu: două autocamioane uzuale: tractorul + semiremorcă cu 5 axe și autocamionul + remorca - DBL și

patru autocamioane grele (aşa-numite "vehicule mai mari de productivitate" :HPV); a se vedea figura 2.

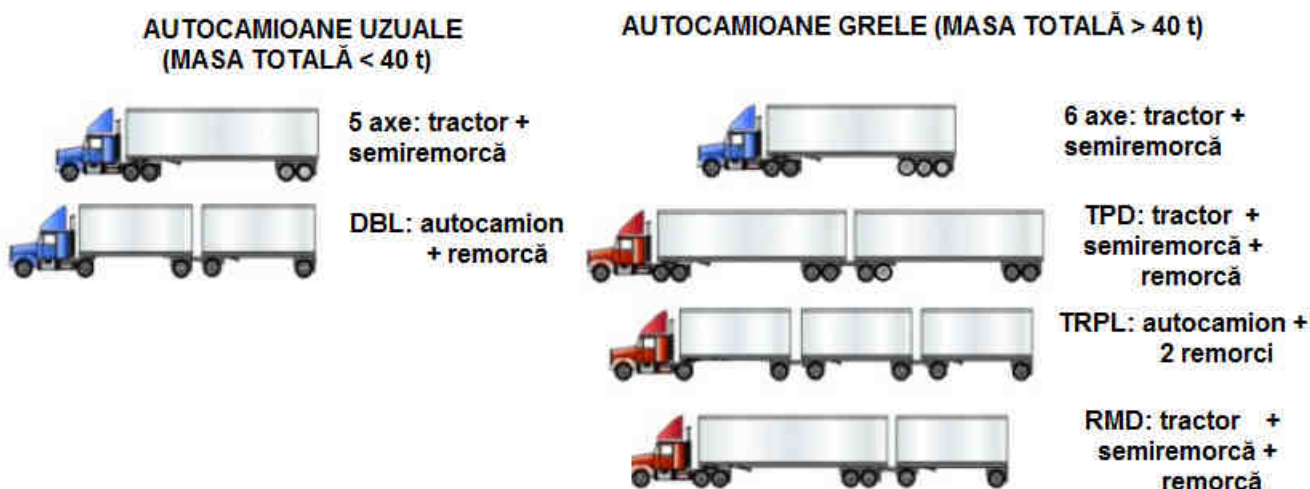


Figura 2: Configurații de autocamioane luate în considerare în studiul de ATRI^[4]

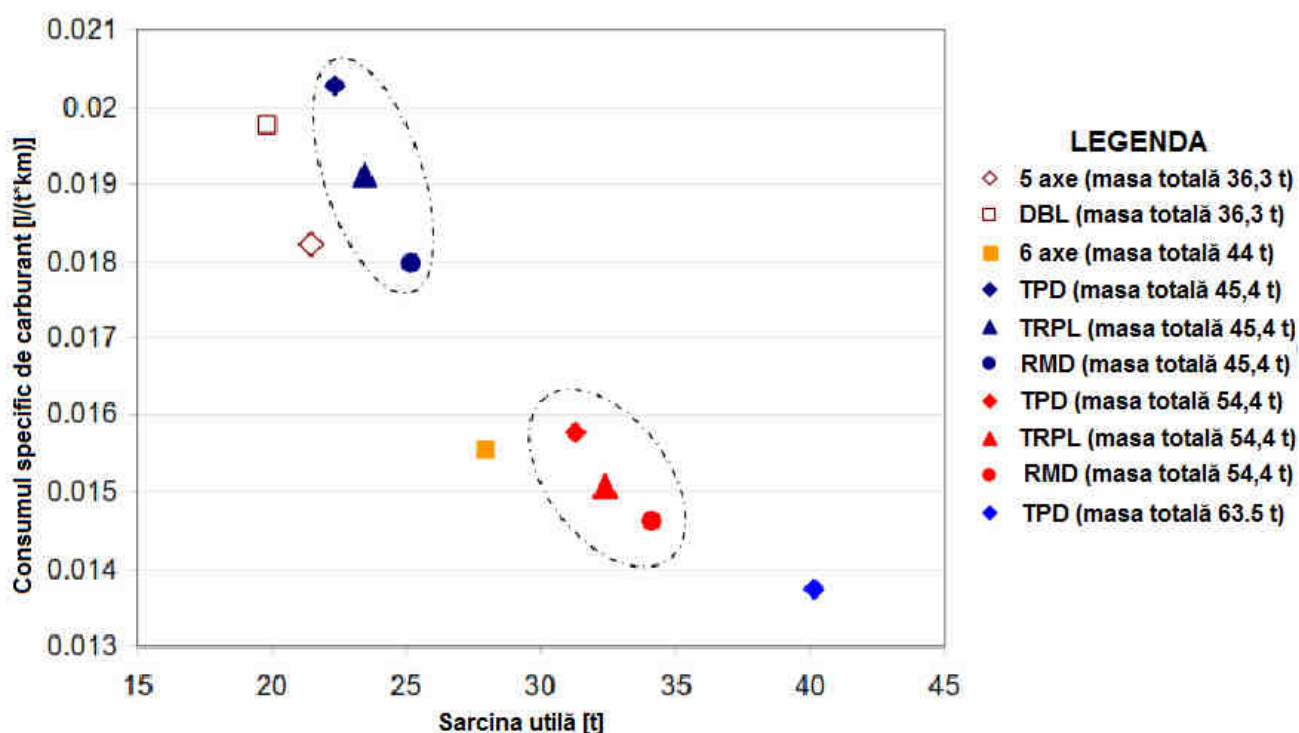


Figura 3: Consumul specific de carburant în raport cu sarcina utilă pentru autocamioanele studiate în^[4]

În această diagramă pot fi evidențiate două grupuri de autocamioane (în roșu și albastru), alcătuite din configurațiile de vehicule TPD, TRPL și RMD, cu o masă maximă autorizată de 45,4 tone (în albastru), respective 54,4 tone (în roșu). În ambele cazuri, configurația TPD prezintă consumul specific cel mai mare datorită masei proprii mai mari (tara) și a măririi motorului. Cu toate acestea configurația TPD devine mai eficientă dacă sarcina utilă ajunge la capacitate maximă. Se poate concluziona că:

- primul grup (în albastru) arată că diferențele între consumurile specifice ale RMD, comparativ cu 5-axe sunt mici (1% economii de energie pentru RMD), iar TPD ar consuma cu 10% mai mult. Aceasta se datorează masei proprii (tara) mai mari: remorcă suplimentară, a creșterii numărului de

axe, dimensiunea mai mare a motorului, etc), combinate cu un coeficient de încărcare (vezi ^[1]) mai redus.

- al doilea grup (în roșu) prezintă câștiguri de eficiență de 25% și respectiv 15% pentru RMD și TPD, comparativ cu autovehiculul de referință (5-axe). Configurația TPD poate reduce consumul specific de carburant cu 33% comparativ cu 5-axe, când autocamionul este complet încărcat ^[4]. Cu toate acestea, trebuie remarcat faptul că aceasta este o reducere potențială maximă, fără luarea în considerare a impactului introducerii acestor autocamioane grele în flota europeană, necesitând evaluarea efectelor asupra mediului și a unor efecte economice care ar putea compensa (sau nu) acest avantaj. La o primă analiză se poate aștepta la reducerea poluării mediului, pentru că două astfel de autovehicule cu masa totală de cca. 60 t ar putea înlocui trei autovehicule standard (autotractor cu semiremorcă, sau autocamion cu remorcă de 40 t)

3. Micșorarea rezistenței aerodinamice

Figura 4 oferă o vedere simplificată a surselor de rezistență aerodinamică ale autovehiculelor de transport marfă de mare tonaj. Comparativ cu un autotractor cu o semiremorcă standard, care are de obicei un punct de discontinuitate, un vehicul combinat va avea două puncte de discontinuitate, adică una între cabină și semiremorca celălaltă între semiremorci și remorca suplimentară (a se vedea Figura 4). De asemenea vor fi generate zonele de turbulențe (fluxul de aer turbulent) și de frecare suplimentare (marcate cu roșu) care vor crește coeficientul de rezistență aerodinamică ^[6].

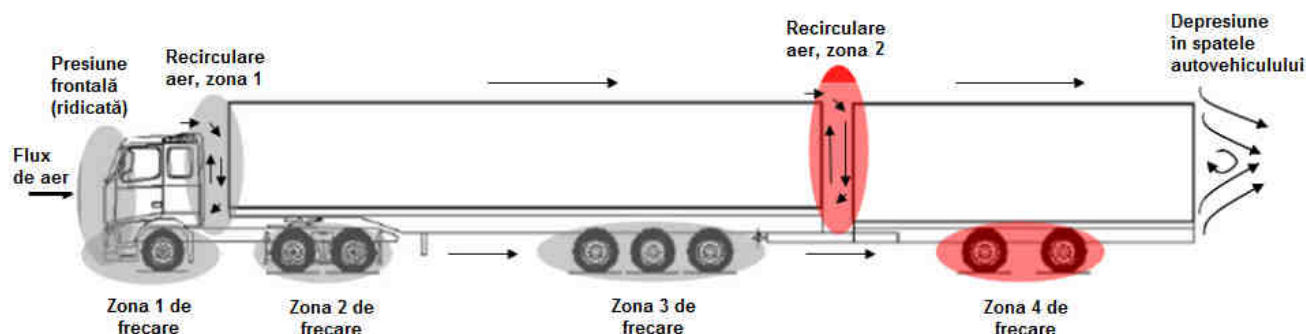


Figura 4: Prezentarea simplificată a surselor de generare a rezistenței aerodinamice ^[6]

Așa cum s-a arătat în ^{[1],[2]} cercetările efectuate în ultimele decenii au dus la reducerea coeficientului aerodinamic (vezi ^[1]) al autovehiculelor de transport marfă de mare tonaj în jurul valorii de 0,6 ^{[1],[2]} și poate fi redus chiar până la 0,45 ^[5] prin utilizarea unor dispozitive și reproiectarea caroseriilor ^[2], existând un mare potențialul de reducere a consumului de carburant și a emisiilor de CO².

Câteva exemple sunt prezentate în continuare:

- Pentru tractor, aerodinamica poate fi îmbunătățită prin utilizarea învelișului aerodinamic/deflectoare (acoperiș și lateral) sau cu o cabină prelungitoare (ajută la reducerea decalajului dintre tractor și remorcă). În general, economiile potențiale de la aerodinamica tractorului sunt de aproximativ 4-6%, aproximativ echivalente cu cele posibile de la remorcă. Acest lucru ar reduce mai mult de 10% din combustibil ^[2].

- Pentru remorcă, aerodinamica poate fi îmbunătățită prin adăugarea de diferite tipuri de dispozitive, cum ar fi învelișul aerodinamic burtă sau praguri ^[5]. În "HDEnergy" ^[7], s-a estimat că "schimbarea tipului de remorcă (de la 4 - la 5 axe) și prin adăugarea unui deflector de aer pentru autotractor, economia de carburant pentru un vehicul la o viteză de 80 km/h poate fi de aproximativ 10%" ^[7].

4. Micșorarea rezistenței la rulare

Așa cum s-a prezentat în ^[1], rezistența la rulare a pneurilor autovehiculelor este produsă de frecările de carosabil și din interiorul acestora (frecări între straturi sau interne, din material), depinzând de calitatea produsului, crescând cu partea din greutatea totală preluată de anvelopă și

scăzând cu creșterea presiunii aerului din acestea. Reducerea semnificativă a rezistenței la rulare poate fi obținută prin controlul presiunii în pneuri și prin utilizarea unor pneuri mai eficiente energetic. În medie, în general, se presupune că o reducere de 10% din rezistența la rulare conduce la o reducere de 2-3% a consumului de carburant. Se vor prezenta în cele ce urmează unele tehnologii de micșorare a rezistenței la rulare a pneurilor. Este important să se țină cont de faptul că pneurile mai eficiente energetic vor reduce consumul de energie, dar pot accentua uzura căii de rulare. De asemenea, pneurile umflate peste presiunea normală indicată de furnizor poate ajuta la reducerea consumului de combustibil, dar pot afecta siguranța circulației și mării uzura autovehiculului și a căii de rulare ^[2].

-Sistemele de monitorizare a presiunii pneurilor (TPMS): utilizate pentru autovehicule pentru pasageri, folosirea TPMS pentru autocamioane este un foarte eficient mod pentru reducerea consumului de carburant și al emisiilor de CO² în paralel cu îmbunătățirea siguranței circulației. Se estimează că în UE anvelopele în funcțiune sunt sub-umflate cu 0,2 până la 0,4 bari, în medie, pentru autoturisme și 0,5 bari pentru camioane^[8]. Există pe piață mai multe tipuri de sisteme automate de monitorizare a presiunii din pneuri care pot fi instalate pe autocamioane și pot monitoriza și pneurile de pe remorcă. Deoarece aceste dispozitive sunt destul de complexe (și relativ costisitoare) și rata de penetrare pe piață este încă foarte limitată și încă nu sunt obligatorii în UE ^[2].

- Pneuri cu rezistență joasă la rulare (LRRT): încorporarea de siliciu în compoziția benzii de rulare a anvelopei poate duce la o reducere a rezistența la rulare de până la 20%, ceea ce ar putea economisi până la 5% din carburant. La nivel global, utilizarea de pneuri LRR poate reduce consumul de carburant cu aproximativ 2-5%, în funcție de condițiile de conducere ^[2]. Se estimează că, dacă toate pneurile unui autocamion sunt înlocuite cu cele de tip LRR, s-ar reduce consumul de carburant cu aproximativ 6-7% în transportul de marfuri^[9]. Pneurile LRR nu prezintă efecte adverse asupra siguranței (frânarea umedă este chiar îmbunătățită) și pot avea o durată de viață mărită^[2].

-Înlocuirea pneurilor duble pe axele motoare cu pneuri late, care sunt mai ușoare, au o rezistență mai scăzută la rulare, sunt mult mai "stabile" și mai ușor de întreținut, reducându-se și costurile de reparații. În funcție de producătorul de pneuri, acestea pot reduce consumul de carburant cu 2-5% comparativ cu pneurile duble^[10]. Trebuie menționat faptul că utilizarea de bază a pneurilor late necesită echiparea autocamioanelor cu (the Tyre Pressure Monitoring System –TPMS) și sisteme (the Electronic Stability Control systems – ESC) ^[2]. Mai mult decât atât, economii importante pot fi obținute în cazul în care sunt montate pe jante din aluminiu (aproximativ 90 kg per osie). Pneurile late vor contribui la îmbunătățirea eficienței energetice a autocamioanelor, dar acestea pot duce la efecte adverse de uzură a drumului, din cauza presiunii mai mari a acestora și a zonei de contact mai reduse ^{[11],[12]}.

5. Creșterea randamentului motoarelor cu ardere internă

Motoarele cu ardere internă utilizate în prezent pentru propulsarea autocamioanelor, autotractoarelor, autobuzelor și autocarelor sunt în UE preponderent de tip Diesel, pentru randamentul lor superior celor pe benzină (40% față de 35%) și pentru prețul mai redus al motorinei ^{[1],[2],[13-18]}.

Cercetarea bibliografică demonstrează că este foarte dificil de obținut în viitorul apropiat creșteri importante ale randamentelor directe ale motoarelor termice utilizate în prezent în transporturile auto de mărfuri și persoane. O direcție importantă de dezvoltare a cercetărilor este creșterea randamentului general al acestor categorii de motoare prin recuperarea exergiei pierdute prin gazele evacuate, lichidul de răcire și uleiul de ungere ^[14], cu până la 15% ^{[19],[20]}.

Se prezintă în continuare câteva dintre cercetările efectuate în diverse state, pentru recuperarea exergiei pierdute a motoarelor cu ardere internă și conversia acesteia în lucru mecanic util.

5.1. Sistemul turbocompound mecanic

Un motor turbocompound este un motor cu piston, care folosește o turbină de recuperare a energiei din gazele de eșapament. Turbina B acționează turbocompresorul de aer proaspăt A, dar este și conectată mecanic printr-un reductor de turație și un ambreiaj, la arborele cotit D. Turbina crește puterea motorului fără mărirea consumului de carburant, pentru că este o turbină de viteză (care utilizează în principal energia cinetică a gazelor de eșapament) reducând astfel consumul specific de combustibil. Utilizate mai întâi în aviație și în marină, fiind instalate pe motoare Diesel jumelate în doi timpi, ulterior aa fost încorporate de unii producători de autocamioane grele propulsate de motoare Diesel. Exemplele includ Detroit Diesel DD15, Scania DTC11 și VOLVO D12 500TC^{[21],[22],[23]}.

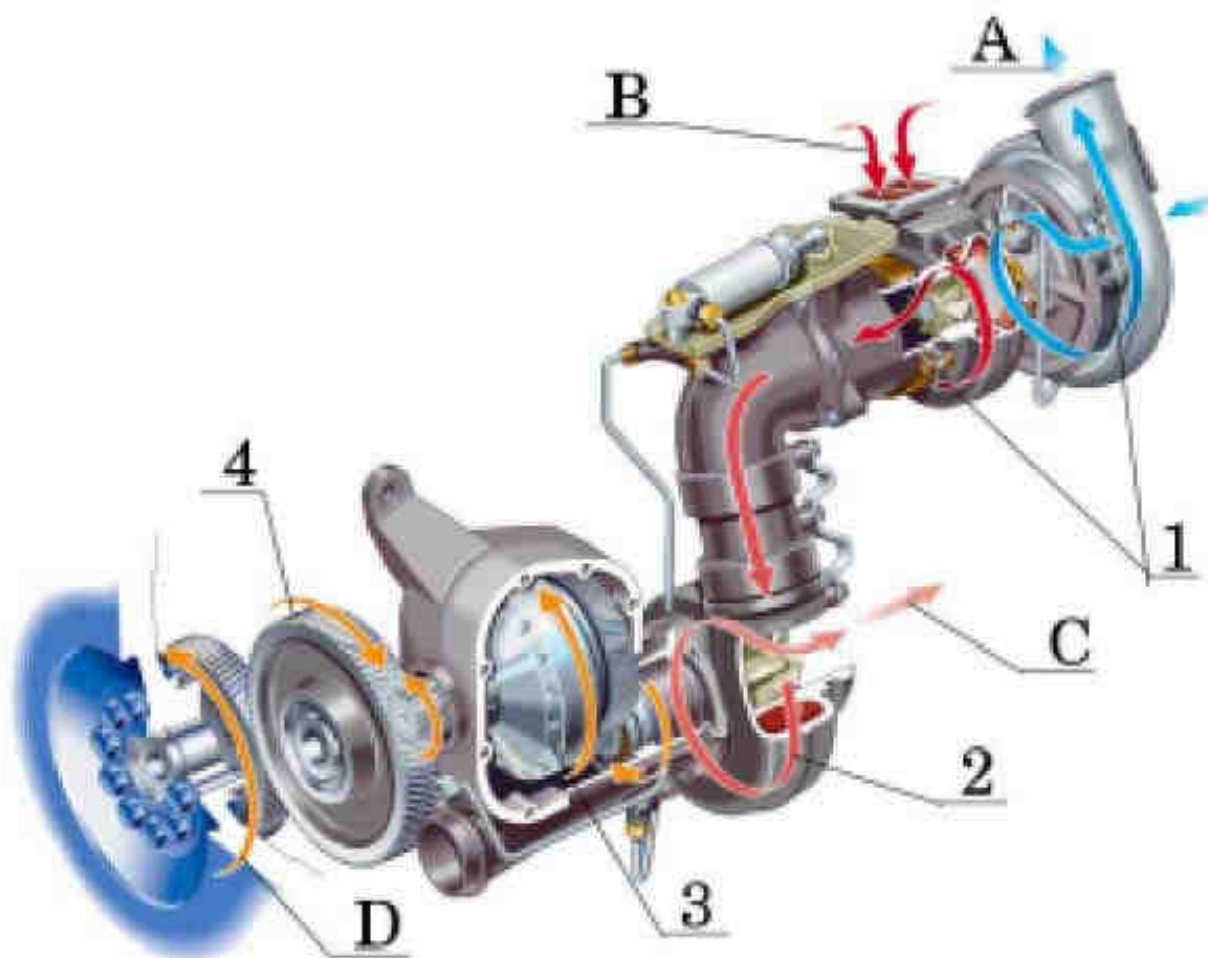


Figura 5. Sistemul turbocompound de pe motorul Scania DTC 11, echipat cu sistem turbocompound:
1- turbo-compresor, 2- turbină de putere, 3-ambreiaj hidraulic, 4-angrenaj arbore cotit. ^[23]

Acest sistem de recuperare a energiei gazelor evacuate poate aduce o creștere a randamentului efectiv de 5 până la 10% pentru modelul de pe motorul Scania DTC 11 sau de cca. 3% - modelul instalat pe motorul Volvo D12 500 TC ^{[21],[22],[23]}.

5.2. Sistemul turbocompound electric

Acest sistem utilizează o turbină de recuperare a energiei din gazele de eșapament, care în acest caz acționează atât turbocompresorul de aer proaspăt, dar și un generator electric. A fost utilizat

de producătorii de motoare mari, pe tractoare grele, utilaje sau autocamioane grele cu transmisii electrice sau hidralice, cum sunt John Deere, Caterpillar, etc.^{[24],[25]}. Vezi Figura 6:

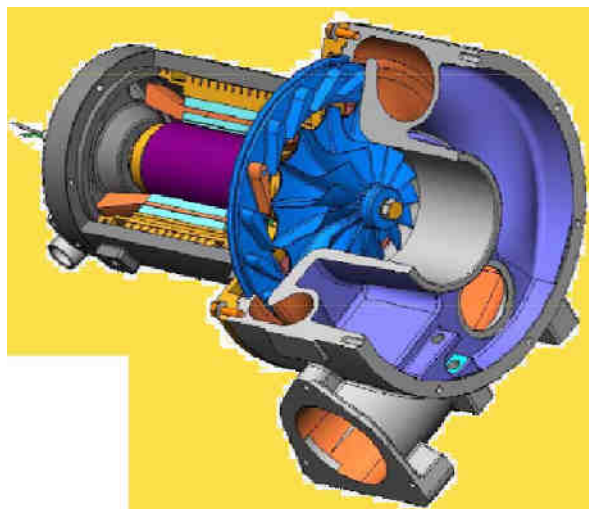
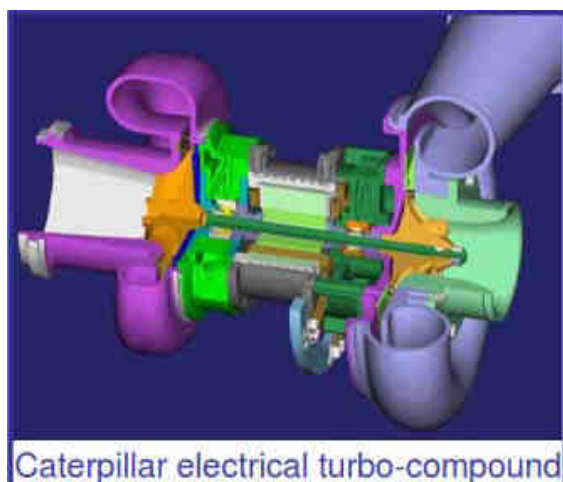


Fig. 6.a) John Deere: Electric Turbo Compounding^[24]; b) Caterpillar electrical turbo-compound^[25]

Măsurătorile efectuate pe bancul de test demonstrează că se obține o creștere generală a randamentului efectiv prin utilizarea energiei electrice produse de către turbogenerator în instalațiile de forță ale utilajelor de la 3 la 5%^{[24],[25]} și în anumite condiții de funcționare de până la 10%^[22].

5.3. Sistemul turbo-generator TIGERS

Inginerii britanici au dezvoltat un mecanism simplu pentru recuperarea energiei din gazele evacuate care ar putea reduce consumul de combustibil al vehiculului cu până la 10%. TIGERS (Turbo-generator Integrated Gas Energy Recovery System) recuperează o parte din energia gazelor evacuate pentru a antrena un mic generator electric care alimentează cu energie electrică sistemul electric auto^[26] (vezi figura 7)

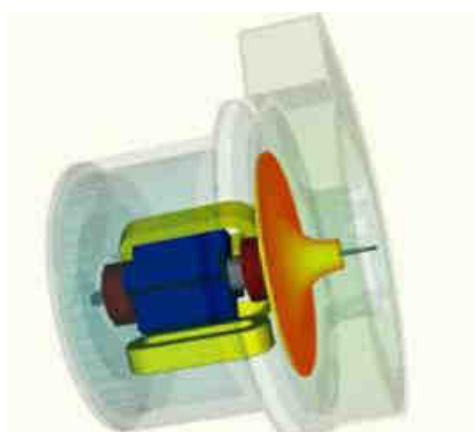
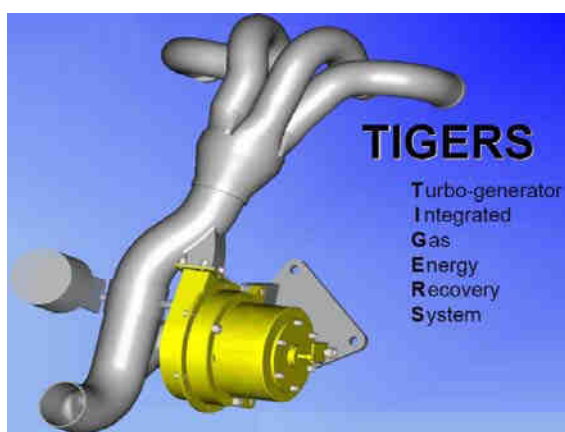


Fig. 7. Sistemul TIGERS creat de TIGERS Group (un grup de cercetători britanici)^[26]

Prin utilizarea acestui sistem se poate asigura creșterea randamentului general al motorului și consumul de combustibil poate fi redus între 5% și 10%. Într-o mașină hibrid-electrică sistemul TIGERS ar putea alimenta direct bateria pentru a crește raza de acțiune a vehiculului^[26].

5.4. Tehnologia “heat2power”

Sistemul "Heat2power" se bazează pe utilizarea unui motor termic suplimentar cu piston, cu unul sau mai mulți cilindri, funcționând cu fluid de lucru aer cald, instalat pe motorul cu ardere internă a cărui căldură o recuperează și o transformă în lucru mecanic util și cu care se conectează prin intermediul unui ambreiaj sau o curea de transmisie.

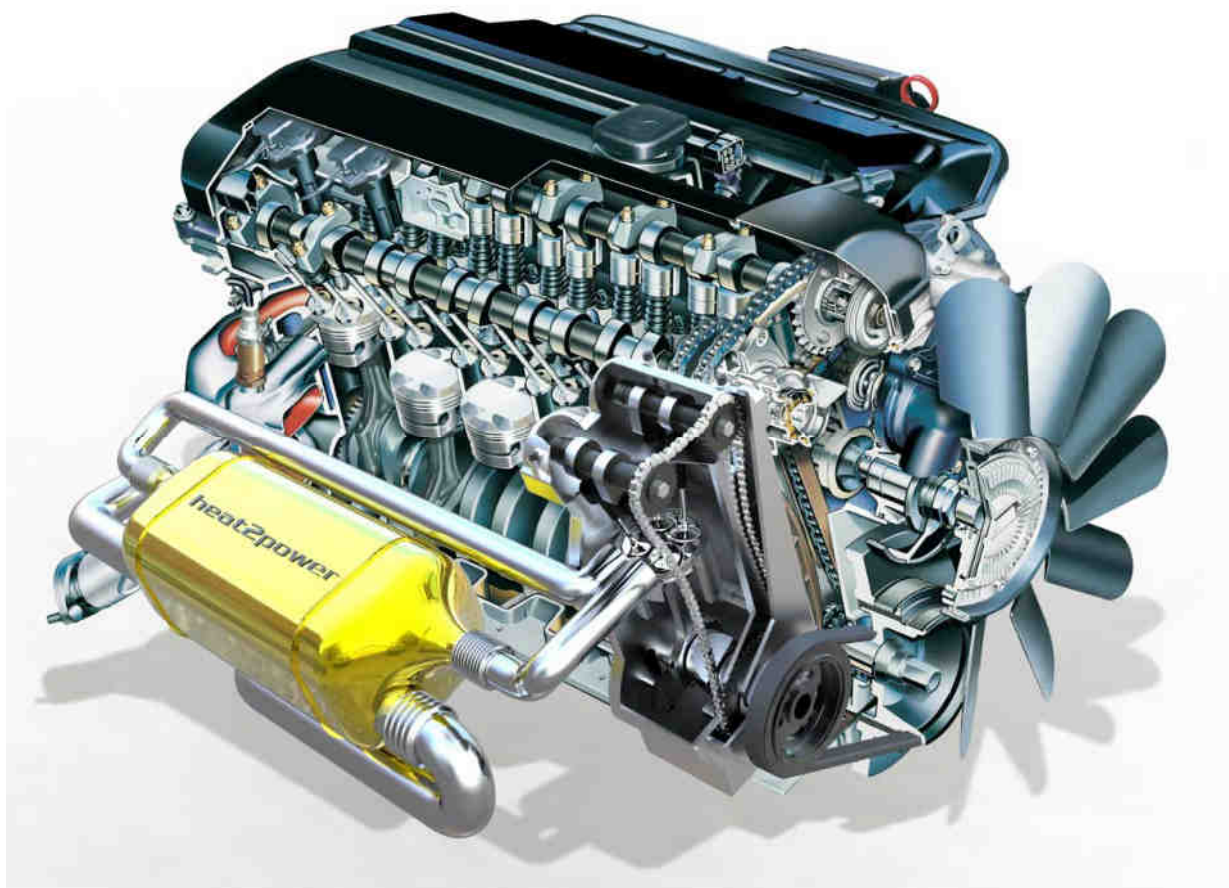


Fig. 8. Modulul "Heat2power" montat pe un motor existent ^[22]

În sistem se introduce căldura recuperată din gazele evacuate ale motorului cu ardere internă prin circuitul primar al unui schimbător de căldură gaz-gaz cu temperature de funcționare ridicată (de până la 950°C). Circuitul secundar este un circuit închis, umplut cu aer comprimat, care după ce este încălzit în schimbător intră în cilindrul motorului cu aer prin supapele de admisie, se produce detenta aerului care determină mișcarea pistonului. După terminarea cursei pistonului, aerul care a intrat în cilindru cu o temperatură între 600-950 °C, este evacuat din cilindru prin supapele de evacuare la o temperatură joasă de cca. 250-300 °C, răcit și recirculat. Practic este vorba de un ciclu termodinamic motor (cu piston) cu sursa de căldură externă motorului. Cercetătorii și producătorii sistemului spun că acesta poate recupera între 18-35 % din căldura pierdută și se poate asigura o economie de combustibil de min. 15% ^[22].

5.5. Turbosteamer

Un turbosteamer este un termen folosit de BMW pentru a descrie un ciclu motor combinat. Acesta folosește un motor termic pentru a converti energia termică a pierderilor de căldură de la un motor cu ardere internă în putere suplimentară pentru vehicul. Dispozitivul turbosteamer utilizează căldura gazelor evacuate și a sistemului de răcire pentru a transforma un lichid (poate fi apa) în vapori, care parcurg ciclul motor Rankine și produc un lucru mecanic util care este transmis la arborele cotit.

Reducerea consumului de combustibil al motorului complet echipat anunțat de BMW este de până la 17%.^{[27],[28]}

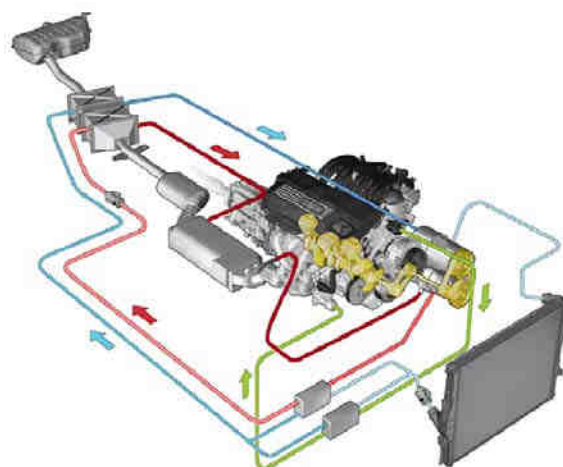


Fig. 9. Turbosteamer BMW, funcționând după ciclul Rankine^{[27],[28]}

5.6. Utilizarea ciclului Kalina pentru recuperarea exergiei pierdute

În^{[14],[20]} au fost analizate bilanțurile energetice și exergetice ale unui motor Diesel VW 1,9 TDI, cu un randament efectiv de până la 40% și a fost determinat totalul fluxurilor de energie termică recuperabilă E_Q din pierderile de căldură prin gazele evacuate, lichidul de răcire și uleiul de ungere, raportat la fluxul termic echivalent lucrului mecanic efectiv Q_e :

$$E_Q = 32,41 \% Q_e \quad (1) \quad [14],[20]$$

Pentru transformarea acestei energii termice în lucru mecanic util, este necesară utilizarea unui ciclu termodinamic motor, care să poată funcționa cu surse de căldură cu temperaturi reduse și medii. A fost analizată varianta ciclului Kalina, care utilizează ca agent termic un amestec organic de amoniac și apă, cu un interval al temperaturilor de fierbere mai mic decât temperatura de fierbere a apei^[20]. Schema prezentată în Figura 13 pentru recuperarea exergiei pierdute și conversia acesteia în energie electric, a preluat elemente ale schemei centralei electrice geotermale de la HÚSAVIK^[20].

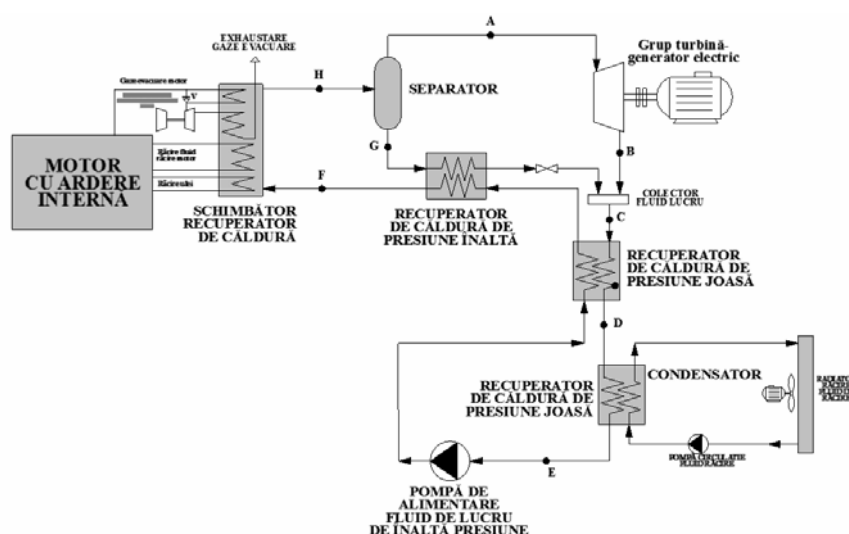


Figura 10. Schemă de utilizare a ciclului Kalina, pentru recuperarea exergiei pierdute de la un motor termic și conversia acesteia în energie electrică (scăderea consumului efectiv cu cca. 15%)^[20].

6. Instruirea specifică a conducătorilor auto

Este cunoscut faptul că "Eco-Driving" este o modalitate eficientă de a economisi carburantul. Scopul instruirii este de a îmbunătăți informarea șoferilor și cunoașterea problemelor legate de mediu, învățarea tehnicilor de deplasare, de control al vitezei, de reducere a mersului în gol, conducere mai lină și de a frâna utilizând frâna de motor, montarea corectă a dispozitivele aerodinamice, verificarea stării pneurilor, etc Chiar dacă mai multe studii arată potențialele economii de combustibil de până la 20%, SmartWay EPA a raportat o reducere potențială reală de cca. 4%^[10].

7. Concluzii

1. Încărcarea autovehiculelor la o capacitate cât mai apropiată de cea nominală și utilizarea în transporturile pe autostradă a autovehiculelor combinate grele cu masa totală de cca. 60 t utilizate la un factor de încărcare de peste 77%, permite reducerea consumului specific de carburant cu 15-25%.
2. Reproiectarea caroseriilor autovehiculelor și remorcilor și utilizarea de elemente și accesorii care reduc rezistența aerodinamică la înaintare determină scăderea puterii efective necesare livrate de motor și reducerea consumul de carburant cu până la 10%.
3. Micșorarea rezistenței la înaintare prin rulare a pneurilor prin utilizarea Sistemelor de monitorizare a presiunii pneurilor (TPMS), a pneurilor cu rezistență joasă la rulare (LRRT), înlocuirea pneurilor duble cu pneuri late, permite reducerea consumului de carburant cu cca. 5-7%.
4. Creșterea randamentelor generale ale motoarelor termice care propulsează autovehiculele prin recuperarea exergiei pierdute și transformarea acesteia în lucru mecanic util, cu permite reducerea consumului de carburant cu cca. 15%.
5. Instruirea specifică a conducătorilor auto pentru conducerea autovehiculelor de transport marfă și persoane, permite reducerea consumului de carburant cu cca. 4% și prelungirea duratelor de viață ale pneurilor și autovehiculelor.

References

- [1] Bercea, Z., Vaida, L. Factori care influențează semnificativ consumul de carburant al autovehiculelor, Proceedings of 2012 International Salon of Hydraulics and Pneumatics – HERVEX, 7 - 9 November, Calimanesti-Caciulata, Romania, 2012.
- [2] Guillaume Leduc, Longer and Heavier Vehicles: An overview of technical aspects, European Commission, Joint Research Centre, Institute for Prospective Technological Studies, Luxembourg: Office for Official Publications of the European Communities, 2009.
- [3] Sustainable development in the European Union - 2009 monitoring report of the EU sustainable development strategy, Office for Official Publications of the European Communities, ISBN 978-92-79-12695-6, Luxembourg, 2009.
- [4] Energy and Emissions Impacts of Operating Higher Productivity Vehicles– Update 2008, The American Transportation Research Institute (ATRI) and Its Western Highway Institute, in Cooperation with Cummins Inc., March 2008.
- [5] Ogburn, M., J., and Ramroth, L., A., Truck Efficiency and GHG Reduction Opportunities in the Canadian Fleet, Rocky Mountain Institute, 2007.
- [6] Aurell, J., Wadman, T., Vehicle combinations based on the modular concept, Committee 54: Vehicles and Transports, Report 1/2007.
- [7] Fuel savings for heavy-duty vehicles "HDEnergy", Summary Report 2003 – 2005, Ed. Nils - Olof Nylund, VTT, 2006.
- [8] Onoda, T., Gueret, T., Fuel Efficient Road Vehicle Non-Engine Components, Potential Savings and Policy Recommendations, IEA Information Paper in support of the G8 plan of action, October 2007.
- [9] Larsson, S., Data and Indicators for Road Freight Transport, presentation at the IEA/International Transport Forum Workshop on "New Energy Indicators for Transport: The Way Forward", Paris, 28-29 January 2008.
- [10] U.S. Environmental Protection Agency, SmartWay Transport Partnership programme (EPA, 2004).

- [11] Al-Qadi, I., L., Impact of Wide-Base Tyres on Pavement and Trucking Operation, presentation at the International Workshop on the Use of Wide-Base Tires, October 2007.
- [12] Effects of Wide Single Tyres and Dual Tyres, COST 334 final report, November 2001. <http://www.rws.nl/rws/dww/home/cost334tyres/chapter4.pdf>.
- [13] Burnete, N., s.a., Motoare Diesel și biocombustibili pentru transportul urban, Editura Mediamira, Cluj-Napoca, 2008.
- [14] Bercea V.Z., Raport de cercetare: "Stadiul actual al cercetărilor privind creșterea randamentului motoarelor cu ardere internă", Școala Doctorală a U.T.C.N., 2012.
- [15] Bătagă, N., Burnete, N., Căzilă Aurica, Rus, I., Sopa, S., Teborean, I., Motoare cu ardere internă, Editura didactică și pedagogică, București, 1995;
- [16] Grünwald, B., Teoria, calculul și construcția motoarelor pentru autovehicule rutiere, Editura didactică și pedagogică, București, 1980.
- [17] ***http://www.volkswagen.ro/despre_volkswagen/inovatii/motoare/fsi/fsi/.
- [18] ***http://www.volkswagen.ro/despre_volkswagen/inovatii/motoare/tsi/tsi/.
- [19] Bercea, V.Z., Vaida, L., Determination of exergy loss for Diesel engine, Proceedings of 2011 International Salon of Hydraulics and Pneumatics – HERVEX, 9-11.11.2011, Calimanesti-Caciulata, Romania, pag. 117-124.
- [20] Bercea, V.Z., Utilizarea ciclului Kalina pentru creșterea randamentului global de funcționare a motoarelor cu ardere internă, Sesiunea de comunicări științifice a studenților Facultății de Mecanică, Cluj-Napoca, 20 mai 2011.
- [21] "Turbocompounding the Wright Way", by Tom Fey, Journal of the Aircraft Engine Historical Society Volume 5, Number 2.
- [22] *** <http://www.heat2power.net/en>.
- [23] ***Bronisaw Sendyka, Jacek Soczówka: RECOVERY OF EXHAUST GASES ENERGY BY MEANS OF TURBOCOMPOUND, prin <http://www.heat2power.net/en>.
- [24] ***http://www1.eere.energy.gov/vehiclesandfuels/pdfs/deer_2006/session6/2006_deer_vuk.pdf.
- [25] ***http://www1.eere.energy.gov/vehiclesandfuels/pdfs/deer_2004/session4/2004_deer_hopmann.pdf.
- [26] ***http://www.greencarcongress.com/2005/09/tigers_exhaust_.html.
- [27] ***http://www.motortrend.com/features/editorial/112_0606_technologue_hybrid_qa/viewall.html.
- [28] ***<https://www.press.bmwgroup.com/pressclub/p/pcgl/pressDetail.html?outputChannelId=6&id=T0119738EN>

EXPERIMENTAL RESEARCH TO VALIDATE SIMULATION MODEL OF CONSTANT SPEED AT LOW POWER AXIS WIND TURBINE

Mihai AFRĂSINEI¹, Constantin CHIRIȚĂ², Vasile DAMASCHIN¹, Andrei GRAMA¹

¹ Tehnical University "Gheorghe Asachi" from Iassy, e-mail address automecanica_iasi@yahoo.com

Abstract: To validate the accuracy of the results obtained by numerical simulation model, experimental investigations aim to determine the step responses of the transmission to change the input parameters (speed of the turbine shaft and load shaft hydraulic motor). To this end, Adaptive hydraulic transmission system was materialized on experimental stand. This stand is made study dynamic behavior of the system under real conditions. *Experimental procedure is done basically by the same way as in the experiment by numerical simulation.*

Keywords: hydraulic transmission, pumps with variable flow rate, wind turbine

1. Introduction

Experimental procedure is done basically by the same way as in the experiment by numerical simulation.

Designed experimental bench work were introduced two modules (Figure 1) and filtering module and a module for open circuit. Filtration module fitted with electric pump 5 is designed to filter oil returning to the tank from the pump off and drain pump. Open circuit module is provided additionally to enable bench and other elements of the composition of hydraulic transmission. In experimental work, this module is not used for research purposes pursued.

2. Presentation the stand of experimental

Overview, experimental stand components are shown in Figure 2.2, where the observed location of the stand closed circuit module being visible double pump 12, the turbine rotor simulation module 13 and pump control mechanism. On the left side of the figure is shown the load module. Location of various hydraulic components would be tested experimentally is the mass M T channel, the module is powered by a constant flow pump 6 (Figure 2.1), driven by an asynchronous electric motor 3.

Specifications:

Load Module	maximum flow rate:	20 l/min
	maximum pressure:	300 bar
Closed loop mode:	variable work flow rate:	0...27 l/min
	maximum pressure:	300 bar
Open circuit mode:	nominal flow rate:	40 l/min
	maximum pressure:	150 bar
Filtering module:	nominal flow rate:	11 l/min
	maximum pressure:	10 bar

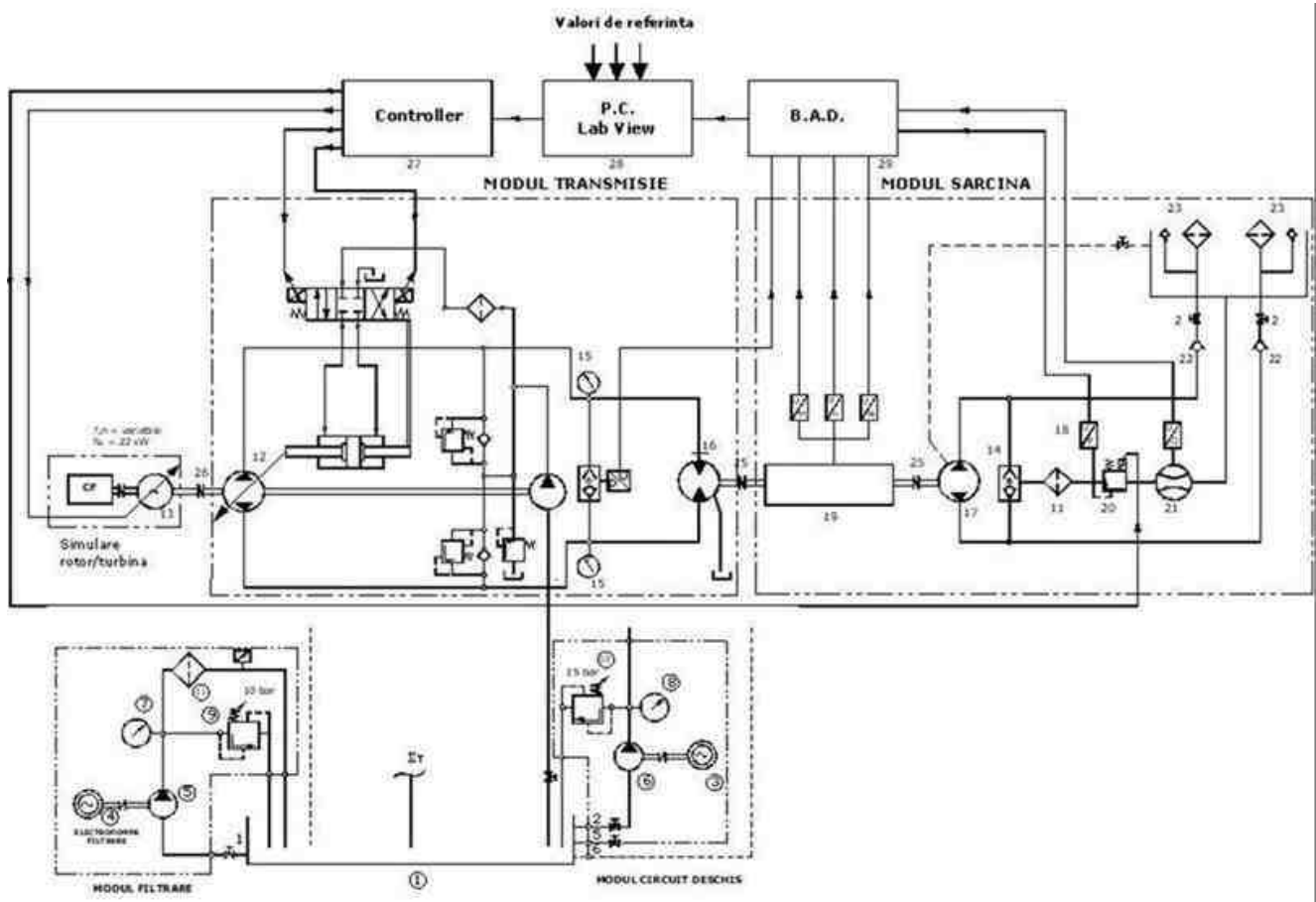


Fig. 2.1. Experimental stand hydraulic transmission scheme automotive proposed adaptive

Structural elements of the hydraulic system names are set out below:

- | | |
|--------------------------------------|---|
| 1 Check valve | 13 Principal tank |
| 2 Pressure gauge Ø100, 0-400 bar | 14 Ball valve |
| 3 Axial piston unit | 15 Three-phase asynchronous electric motor, 11 kW, 1440 rot/min |
| 4 Axial piston unit | 16 Three-phase asynchronous electric motor, 0.75 kW, 1440 rot/min |
| 5 Pressure transducer | 17 Gear pump |
| 6 Transducer speed, torque and power | 18 Vane pump $V_g = 27.4 \text{ cmc/rot}$ |
| 7 Proportional pressure valve | 19 Pressure gauge Ø100, 0-25 bar |
| 8 Flow rate transducer | 20 Pressure gauge Ø100, 0-400 bar |
| 9 One-way valve | 21 Piloted valve pressure |
| 10 Suction filter (strainer) | 22 Piloted valve pressure pilotată |
| 11 Tank load mode | 23 Pressure filter |
| 12 Coupling type SINGLE FLEX | 24 Axial piston pump in closed circuit |

The data acquisition and control include the following:

1. Transducers (sensors)
 - a. Pressure transducer output signal unified
pressure input 0-400 bar out 4-20 mA

- accuracy class $\pm 0.25\%$ BFSL
 b. Flow rate transducer with signal output in unified
 flow rate input 10-318 l/min out 4-20mA
 working pressure 0-400 bar
 accuracy class $\pm 0.25\%$ BFSO
 c. inductive speed sensor
 speed input 0-3000 rpm out 4-20mA
 accuracy class $\pm 0.15\%$ BFSO

2. *Distribution system National Instruments Compact FieldPoint*

a. Controller cFP 2020

CPU Clock	75 MHz
System Memory	32 MB
Flash	512 Mb
Ethernet	1
RS232	3
RS485	1
Operating system	LabVIEW Real Time

b. Analog modul cFP AIO 600

Analog input

Channels	4
Mesh resolution	12 bits
Sampling frequency	1.7 kS/s (1.7 kHz)
Input	4 mA , 20 mA
Sensitivity	3.91 μ A

Analog output

Channels	4
Mesh resolution	12 bits
Output	4 mA , 20 mA
Sensitivity	3.91 μ A
Output frequency	1.7 kS/s (1.7 kHz)

3. *Acquisition board NI DAQ DAQCard-6036E*

Analog input

Channels	16
Mesh resolution	16 bits
Sampling frequency	200 kS/s
Input	10 V
Sensitivity	4.26 mV

Analog output

Channels	2
Mesh resolution	16 bits
Output	10 V
Sensitivity	2.547 mV
Output frequency	1 kS/s

4. *Computing system type IBM PC x86*

5. *Software*

S.O Microsoft Windows XP SP 3
 x86 LabView 8.5
 LabView 8.5.1 Real Time

Note

System control and data acquisition was detailed only for functions that have been used in experimental research.

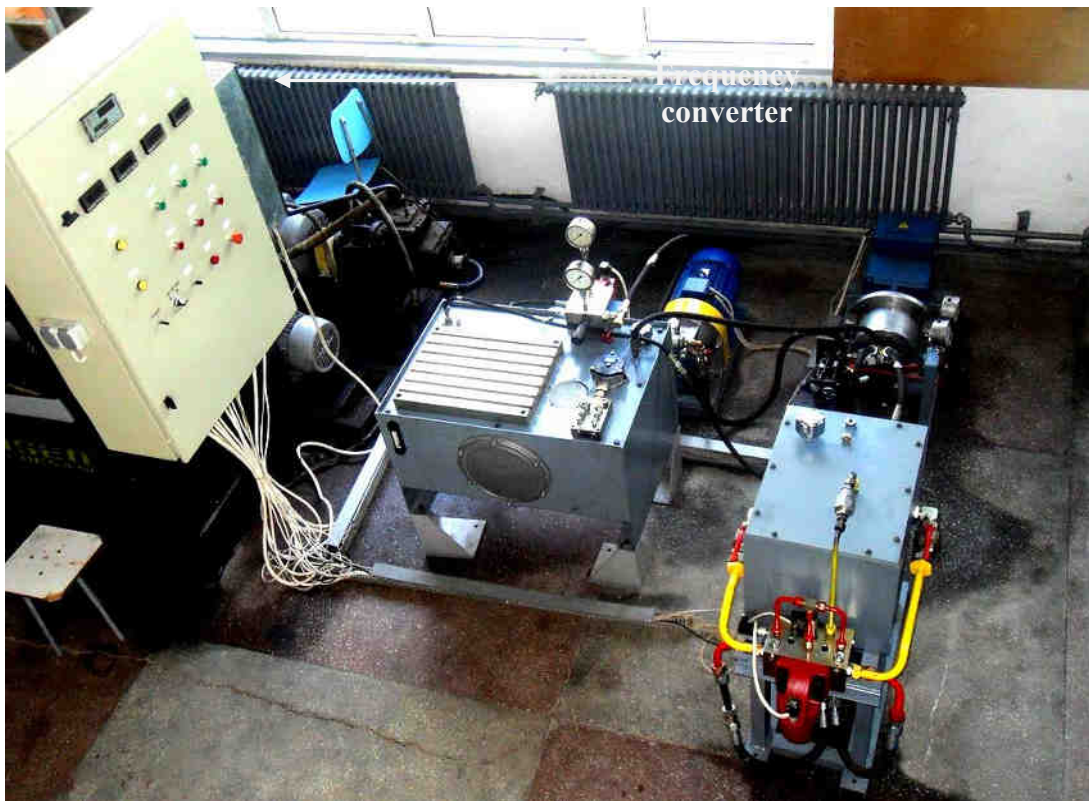


Fig. 2.2 Overview top of the stand

An important component of the experimental stand is the automatic control loop presented as a block diagram in Figure 2.3.

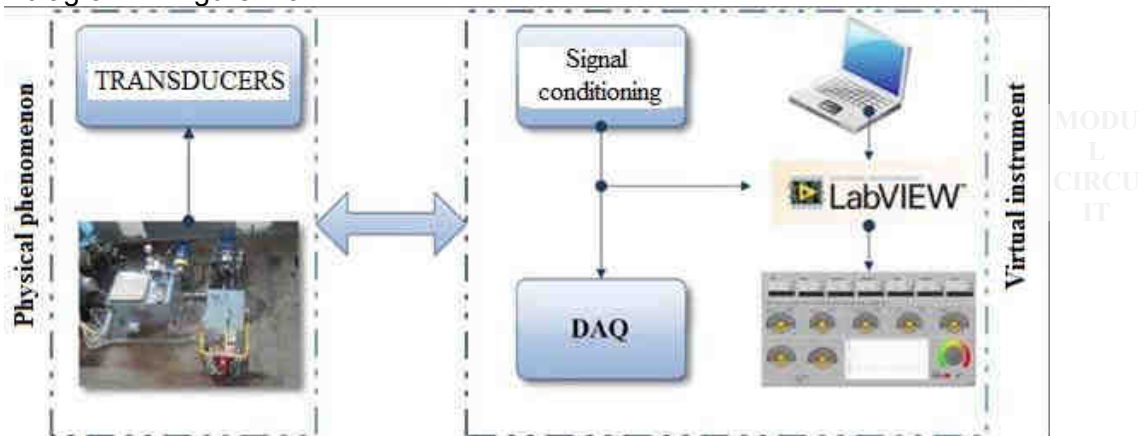


Fig. 2.3 Block diagram of the automatic control loop

Physical phenomenon and receiving transducers convert physical quantity (pressure, flow rate, etc..) In a size other mainly in voltage, the resulting signal is proportional to the size variation monitored.

Conditioning modules provide electrical signals generated by the transducers in a form that acquisition DAQ board can accept. Examples of signal conditioning is amplification, linearization, filtering, isolation, etc..

Acquisition board to convert electrical signals through its basic component, analog-to-digital converter. It attaches a numerical value to a voltage, thus making it possible to interpret the computing system.

Virtual tool work bench consists of the hardware - digital analog converter (Compact FieldPoint distribution system [1] and data acquisition board NiDAQ [2]) and the software taken in conjunction with the needs of working hydraulic stand. The resulting virtual instrument comprises measuring devices and controls for plant automation. The graphical interface of this program

included controls and indicators made in a form similar graphics devices and real devices, the user manevrându also their real elements.

Virtual instrumentation associated hydraulic stand was developed using LabVIEW graphical programming environment [3], used mainly for signal acquisition, measurement and analysis graphical or tabular presentation of data.

The front panel, shown in Figure 2.4, comprises a series of bar graphs to visualize signals scaled unit corresponding physical quantity monitored through hardware part that receives signals from transducers mounted hydraulic bench. Also through the front panel numeric input, or through a virtual potentiometer, setpoint (SETPOINT) control system. The front panel was created using display elements and control procedures extracted from library LabVIEW programming environment and a range of filtering procedures and interpretation of signals [4], adapted to the experimental stand.



Fig.2.4 Front panel [4]

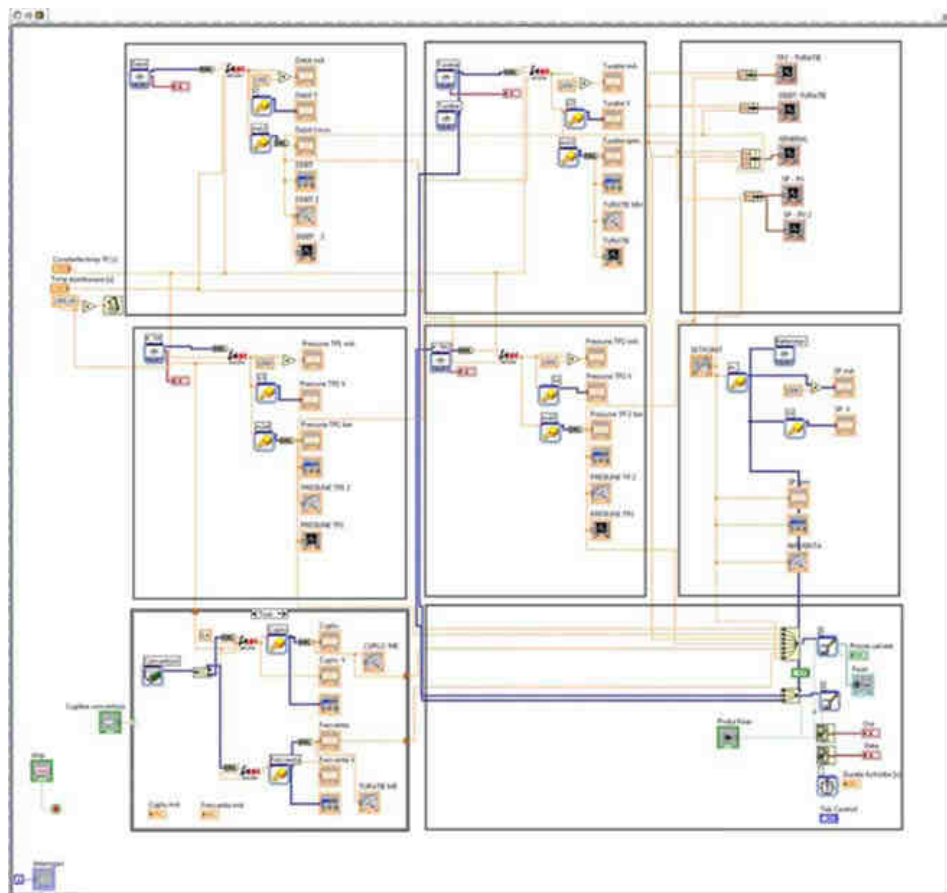


Fig.2.5 Virtual instruments - Block diagram [4]

Data obtained during the experiment can be viewed in numerical form (the top - Figure 2.5), as appropriate indicators measured quantities or as my graphic window created for this purpose.

3. Development program at experiments

Experiments were performed considering constant speed rotary hydraulic motor shaft were extracted and step responses of the system for three load levels ($\Delta p = 50, 75, 100$ bar). Experimental tests in this case were considered five values of the reference speed rotary motor shaft ($n = 500, 600, 700, 800, 1000$ rev / min). Array values for this series of experiments is presented in Table 3.1.

Table 3.1

No. crt.	Speed hydraulic motor [1/min]	Pressure variation charging circuit [bar]
1	500	50
2		75
3		100
4	600	50
5		75
6		100

7	700	50
8		75
9		100
10	800	50
11		75
12		100
13	1000	50
14		75
15		100

4. Experimental results for a series of research at constant speed turbine shaft

For each group in a series of studies with values given in Table 3.1 was done as follows:

- Turbine rotor speed is fixed at a constant value;
- Enter the reference value calculation system using virtual potentiometer;
- Modify charging circuit pressure $\Delta p = 50$ bar;
- For each of these groups attempt to extract step responses of the system of the computing system.

In this way are obtained step responses of the system shown in Figure 4.1

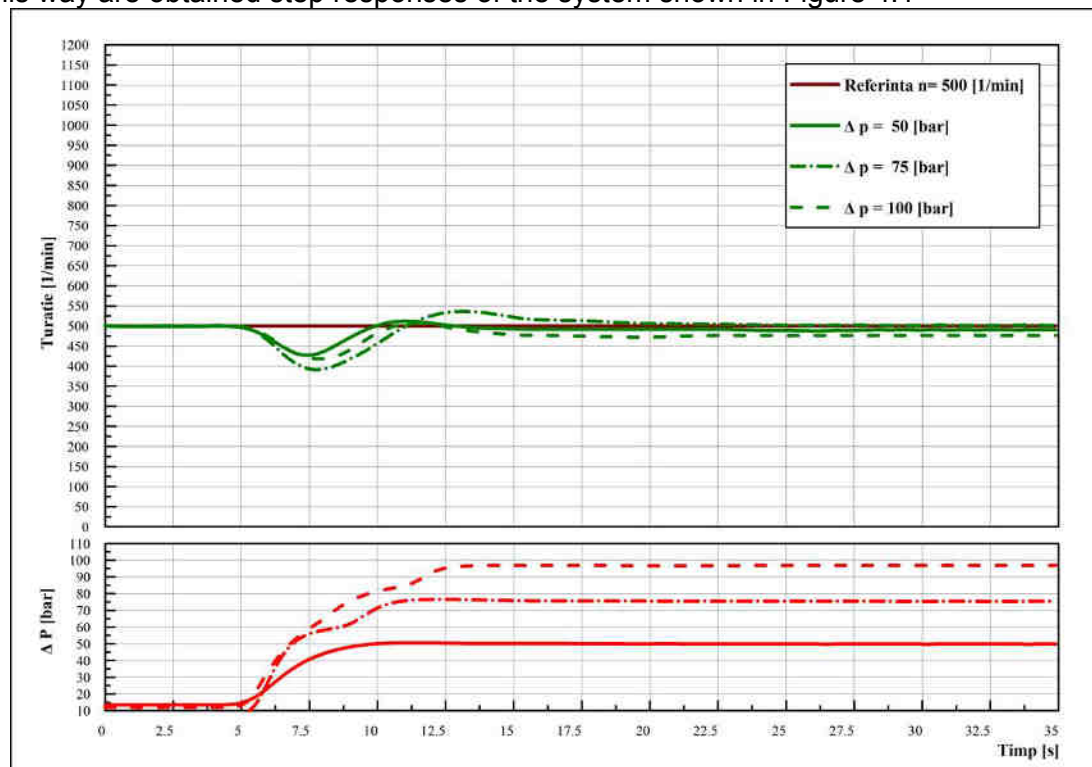


Fig. 4.1 Step response of the system to $n_{ref} = 500$ rpm and $\Delta n = \text{constant}$

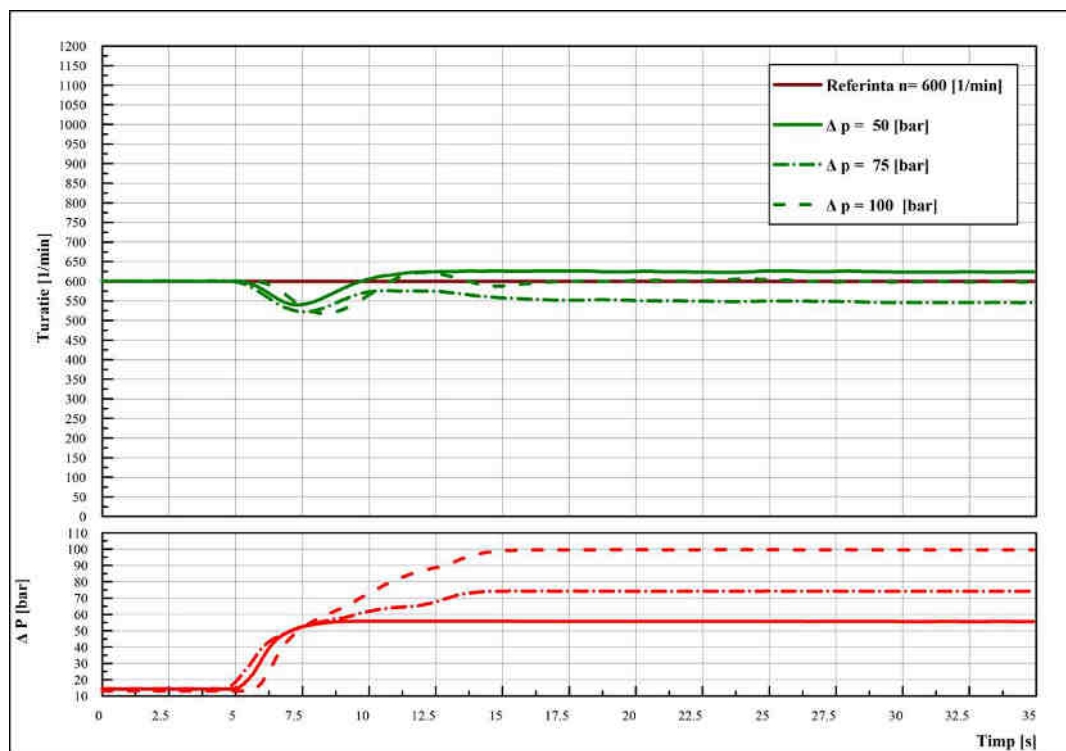


Fig. 4.2 Responses indexical ref overlapped $n = 600$ rpm, $\Delta n = \text{constant}$ and $\Delta p = 50, 75, 100$ bar

5. Conclusions

The analysis of experimental results obtained in the two series of tests, the following conclusions were drawn:

Step response obtained by experimental testing is characterized by a transient period longer than responses obtained by numerical simulation, this is because, if the numerical simulation, can be effectively applied in step variation, while the research conducted on the experimental stand, variable speed turbine rotor (the first series of tests) or load variation in shaft hydraulic motors (from the second series of tests) can not be achieved only uphill due to the fact that variations are obtained by manual handling of potentiometers;

Adjustment errors are inevitable due to the existence of mechanism games pitch wheel pump and the possible delays that may occur in electronic data processing chain and the precision of the transducers used;

Finally, it can be concluded that the new Adaptive hydraulic system behaves under realistic conditions (wind velocity and variation of load to the motor shaft generator) as a dynamically stable system

REFERENCES

- [1] <http://sine.ni.com/nips/cds/view/p/lang/en/nid/11572>
- [2] <http://sine.ni.com/nips/cds/view/p/lang/en/nid/11914>
- [3] <http://www.ni.com/labview/>
- [4] Afrăsinei M., Damaschin V. ©D.I.S.A.H.P. – www.disahp.net

STATE OF THE ART BIOMASS COMBINED HEAT AND POWER TECHNOLOGY

Curac IOAN¹, Craciun BOGDAN IONUT², Creta IOAN³

¹ Technical University Of Cluj Napoca, Department of Electrical Machines and Drives,
curac.ioan.jr@gmail.com

² Aalborg University Department of Energy Technology, bic@et.aau.dk

³ Technical University Of Cluj Napoca, Department of Mechanical Engineering,
cretaioan@gmail.com

Abstract: *In the last decades, renewable energy sources gained a lot of attention since the technologies involved overcome the challenges regarding the cost and their integration into the grid. By definition, Cogeneration is on-site generation and utilization of energy in different forms simultaneously by utilizing fuel energy at optimum efficiency in a cost-effective and environmentally responsible way. Cogeneration systems are of several types and almost all types primarily generate electricity along with making the best practical use of the heat, which is an inevitable by-product. Aim of this paper is to present an overview of biomass combined power technologies and their capabilities to sustain a system of distributed renewable energy..*

Keywords: CHP, Cogeneration, Renewable energy, Biomass

1. Introduction

Regarding environmental benefits biomass has a special appeal in this regard, as it makes no net contribution to carbon dioxide emission to the atmosphere. Regulations for making biomass economically viable are in place in many countries. For example, if biomass replaces fossil fuel in a plant, that plant earns credits for CO₂ reduction equivalent to what the fossil fuel was emitting. These credits can be sold on the market for additional revenue in countries where such trades are in practice.[6]

Green certificates are a comparatively new, advanced version of tradable quotas. In spite of its recent use, the model has gained popularity in many EU member countries since its introduction in the Netherlands at the end of the 1980s. Like traditional quotas, the model obliges a group (again producers, but more commonly consumers or distributors) to hold a certain share of their overall electricity sales/consumption in 'green' electricity in a certain time period (usually one year). In a tradable quota-model they would prove the fulfillment of their obligation by showing that they have bought the respective amount of electricity generated by renewables (contract certificate).[7]

Romania has established a market for green certificates operated by Operator of Energy Market (OPCOM) coupled with a system of mandatory quotas for suppliers. The producers of green energy receive from the TSP certificates for each 1 MWh of energy produced from green sources. The eligible sources of energy are wind, biomass, solar, geothermal, and micro-hydro power plants with an installed capacity of 10 MW or less that are either new or modernized since 2004. Suppliers have to fulfill a mandatory quota determined by National Agency of Regulation In Energy (ANRE). The green certificates are traded either bilaterally or on the green certificates market organized monthly by OPCOM. There is a minimum and a maximum price at which the green certificates can be transacted, determined by ANRE. In 2005 the minimum price was 24 euro/ MWh and 42 euro/MWh. [8]

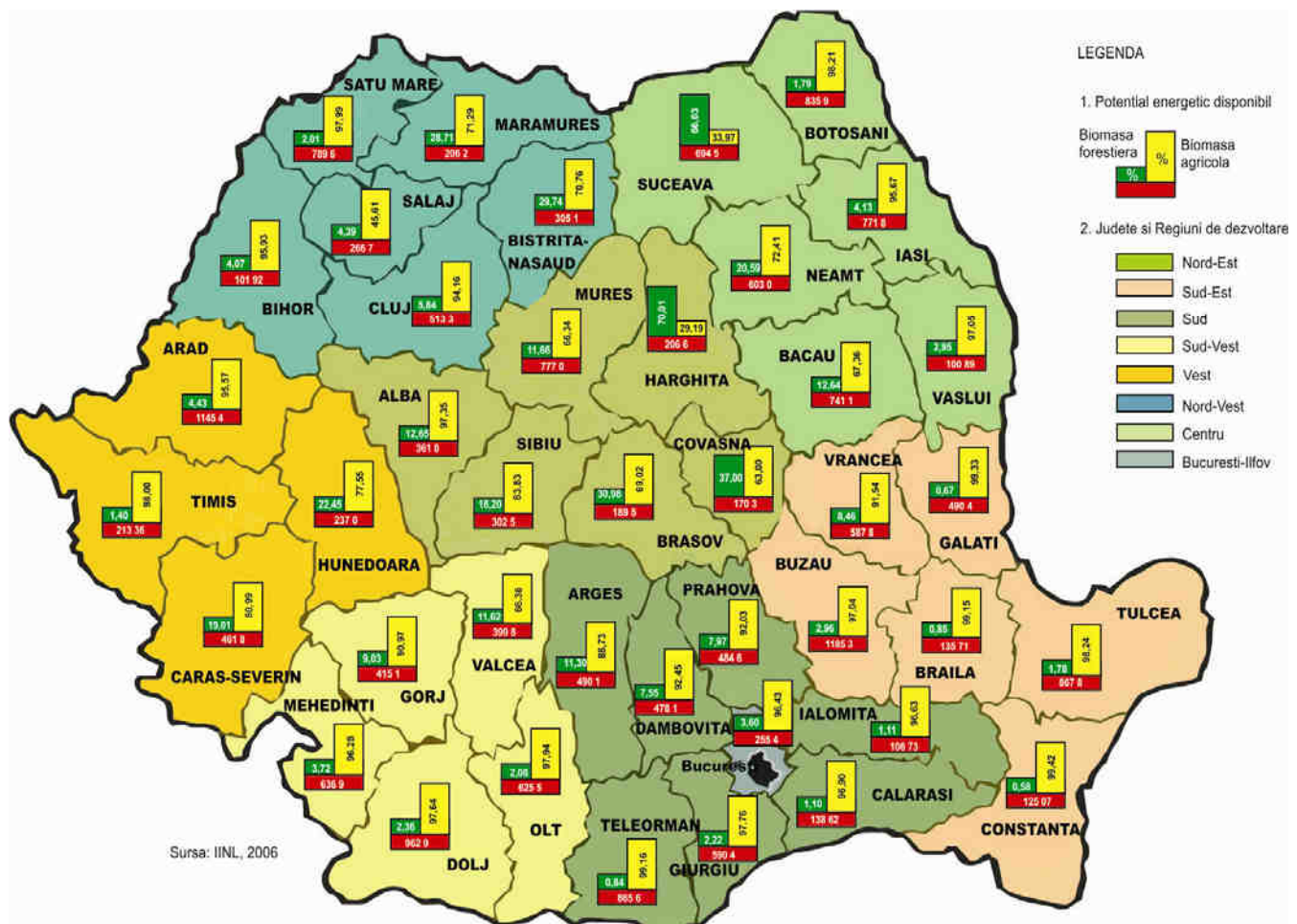


Figure 1. Biomass energetic potential in Romania

Governments strive to achieve ambitious targets of incorporating considerable amounts of distributed renewable generation (DRG) and combined heat and power (CHP) in response to the climate change challenge and the need to enhance fuel diversity [1]

Further improvements in the modulating capability of control approach may be realized if prime movers capable of rapid start-up, shut-down and cycling can be developed. The control of micro-CHP systems in this manner offers a mechanism for managing the load at distribution transformers.[2]

Cogeneration can be defined as the simultaneous production of electric power and useful heat from the burning of a single fuel. This technique of combined heat and power production has been applied successfully in industrial and tertiary sectors; the energy resources are used more efficiently, which creates opportunities for reductions in both purchased energy costs and in environmental impact. [3]

2. CLASIFICATION OF COMBINED HEAT AND POWER SYSTEMS

The two most usual forms of energy results from this process are mechanical and thermal energy. Mechanical energy is usually used to drive an electric generator. This is why the following definition, even though restrictive, often appears in the literature:

Cogeneration is the combined production of electrical (or mechanical) and useful thermal energy from the same primary energy source.[4]

Basic concepts of CHP are direct and indirect fired and presented in figure 2 and 3

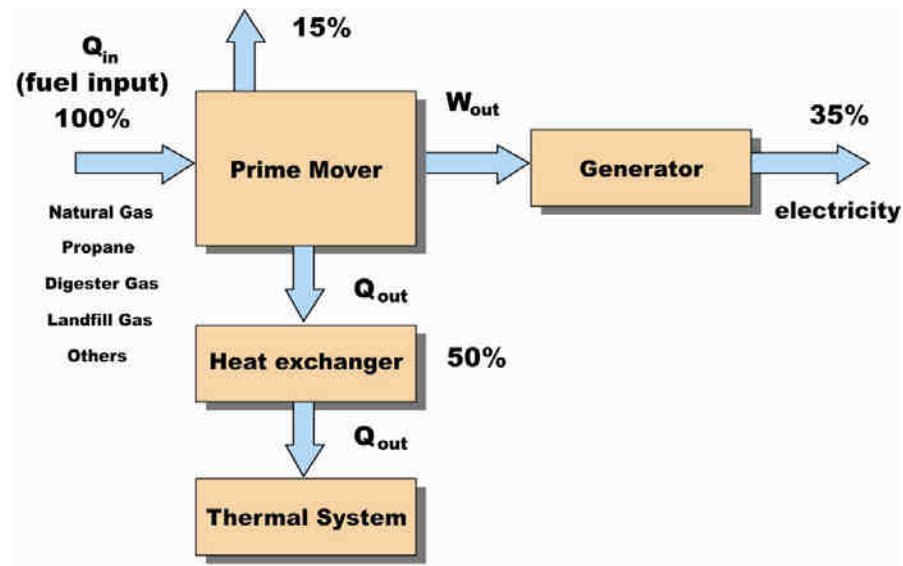


Figure 2. Combined Heat and Power Diagram – Direct Fired

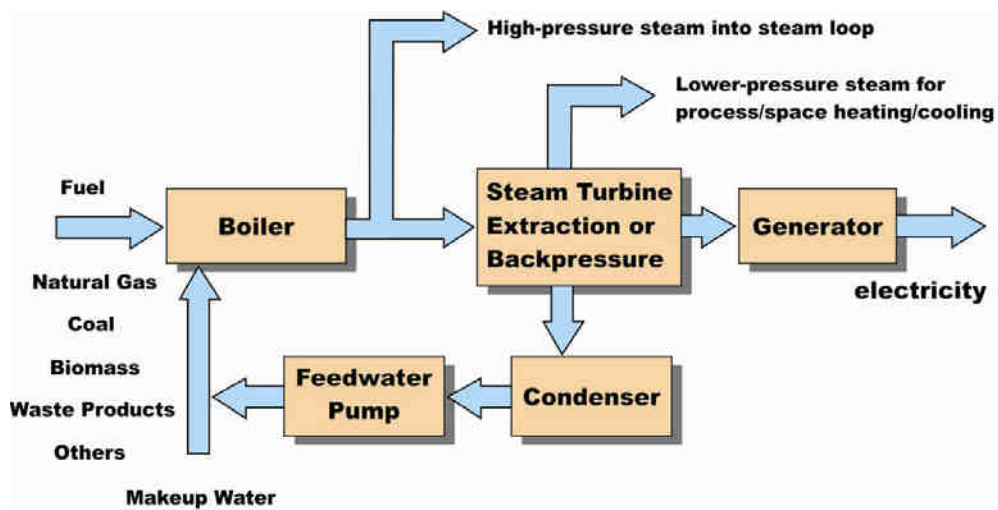


Figure 3. Combined Heat and Power Diagram – Indirect Fired

2.1 CLASIFICATION OF COMBINED HEAT AND POWER SYSTEMS FOR WOOD WASTE

Waste wood biomass conversion uses basic two categories of technologies, one is thermochemical that use high temperatures to convert feedstock to energy. However, the technologies have potential to produce electricity, heat, bio products, and fuels. The other technology is biochemical and use biological agents to convert biomass feedstock to clean energy. Also this technology have the potential to produce electricity, heat, bio products, and fuels. [9]

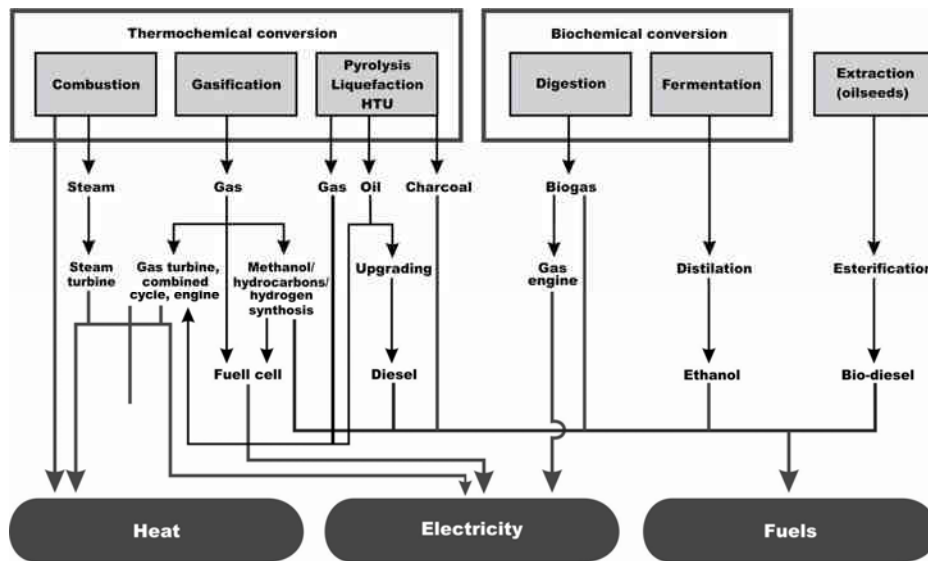


Figure 4- Main conversion options for biomass to secondary energy carriers [10]

2.2 Thermochemical conversion: Direct Combustion-Boilers

Direct combustion involves the oxidation of biomass with excess air, giving hot flue gases that produce steam in the heat exchange sections of boilers. The steam is used to produce electricity in a Rankine cycle. In an electricity-only process, all of the steam is condensed in the turbine cycle, while in CHP a portion of the steam is extracted to provide process heat. [9]

Table 1 identifies the major biomass conversion technologies and associated prime mover technologies for CHP applications. The commercial status of each technology for biomass applications is described.[11]

Direct Combustion - Boilers			
Fixed bed boilers (stocker)	Commercial technology - Stoker boilers have long been a standard technology for biomass as well as coal, and are offered by a number of manufactures.	Steam turbine	Commercial technology
Fluidized bed boilers	Commercial technology - Until recently fluidized bed boiler use has been more widespread in Europe than the United States. Fluidized bed boilers are a newer technology, but are commercially available through a number of manufacturers, many of whom are European-based.		
Cofiring	Commercial technology - Cofiring biomass with coal has been successful in a wide range of boiler types including cyclone, stoker, pulverized coal, and bubbling and circulating fluidized bed boilers.		
Modular* direct combustion technology	Commercial technology - Small boiler systems commercially available for space heating. A small number of demonstration projects in CHP configuration.	Small steam turbine	Commercial technology
		Organic Rankine cycle	Emerging technology - Some "commercial" products available.
		"Entropic" cycle	Research and development (R&D) status
		Hot air turbine	R&D status

*Small, packaged, pre-engineered systems (smaller than 5 MW).

2.3 Thermochemical conversion: Gasification

Since there is an interaction of air or oxygen and biomass in the gasifier, they are classified according to the way air or oxygen is introduced in it. There are three types of gasifiers; Downdraft, Updraft and Cross draft. As the classification implies updraft gasifier has air passing through the biomass from bottom and the combustible gases come out from the top of the gasifier. Similarly in the downdraft gasifier the air is passed from the tubers in the downdraft direction. The choice of one type of gasifier over other is dictated by the fuel, its final available form, its size, moisture content and ash content [12]

Energy Conversion Technology	Conversion Technology Commercialization Status	Integrated CHP Technology (Prime Mover)	Prime Mover Commercialization Status
Gasification			
Fixed bed gasifiers	Emerging technology - The actual number of biomass gasification systems in operation worldwide is unknown, but is estimated to be below 25.	Gas turbines - simple cycle	Prime movers have been commercially proven with natural gas and some medium heating value biogas.
Fluidized bed gasifiers	A review of gasifier manufacturers in Europe, USA, and Canada identified 50 manufacturers offering commercial gasification plants from which 75 percent of the designs were fixed bed; 20 percent of the designs were fluidized bed systems.	Gas turbines - combined cycle	Operation on low heating value biogas and the effects of impurities on prime mover reliability and longevity need to be demonstrated.
		Large internal combustion (IC) engines	
Modular* gasification technology	Emerging technology - A small number of demonstration projects supported with research, design, and development funding.	IC engine	Commercial technology - But operation on very low heating value biogas needs to be demonstrated
		Microturbine	Commercial introduction
		Fuel cell	
		Stirling engine	Emerging technology
Modular* hybrid gasification/combustion	Emerging technology - Limited commercial demonstration.	Small steam turbine	Commercial technology - But integrated system emerging.

*Small, packaged, pre-engineered systems (smaller than 5 MW).

Table 2.[13]

2.Fixed bed combustion boilers

For use of solid refuse, wood, and biomass fuels, boiler component design varies considerably from traditional fossil fuel units, but is generally more similar to systems designed for coal than for gas or oil. Similar to coal units, they are larger, more costly, and more maintenance intensive than standard gas or oil burning units [14].

Grate furnaces: There are various grate furnace technologies available: fixed grates, moving grates, travelling grates, rotating grates and vibrating grates. All of these technologies have specific advantages and disadvantages, depending on fuel properties, so careful selection and planning is necessary. That means they are appropriate for biomass fuels with high moisture content, varying particle sizes (with a downward limitation concerning the amount of fine particles in the fuel mixture) and high ash content. [15]

In a study made by [17] we can observe operational efficiencies (Figure 5) for 13 grate fired biomass CHP systems compared to the size of the plant shown as the annual production of electricity and heat.

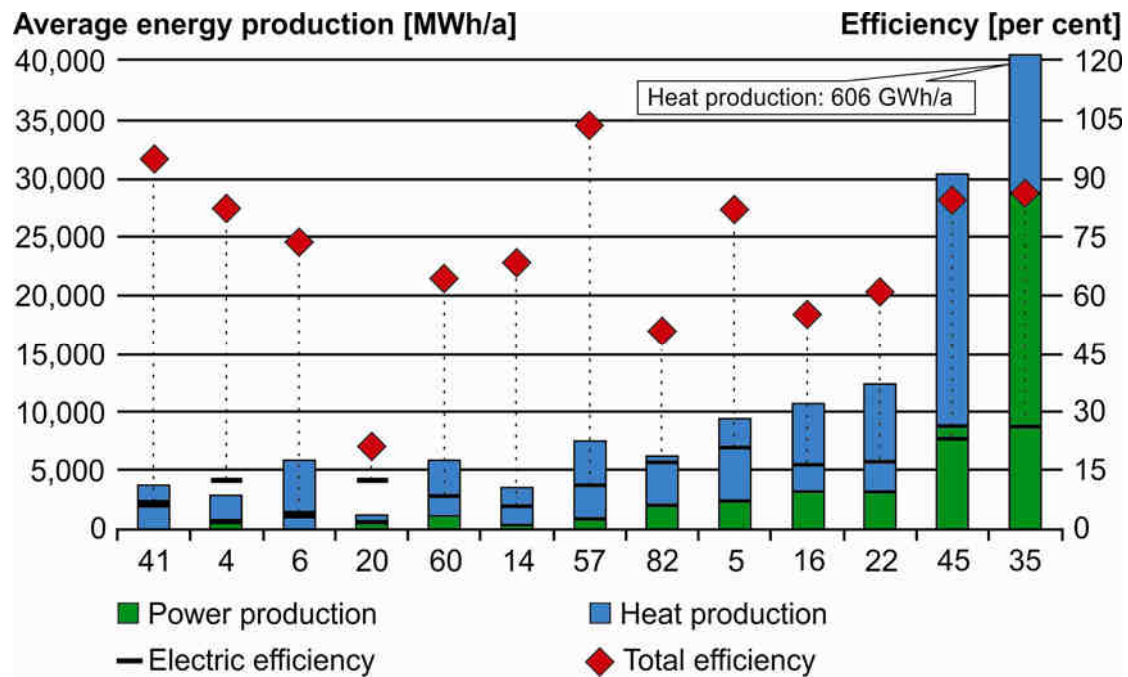


Figure 5

Based on the flow directions of fuel and the flue gas, there are three systems of operation for grate combustion plants[15]

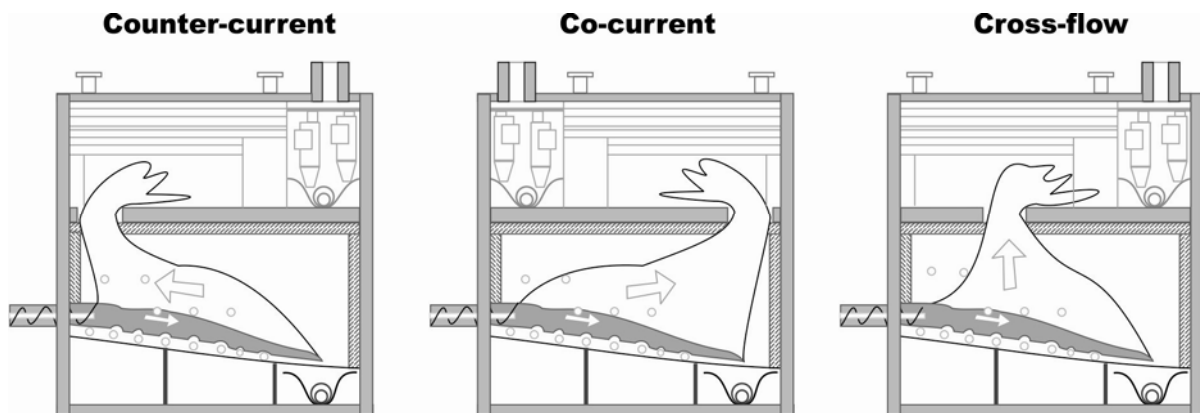


Figure 6

Counter-current combustion is most suitable for fuels with low heating values (wet bark, woodchips or sawdust). Due to the fact that the hot flue gas passes over the fresh and wet biomass fuel entering the furnace, drying and water vapor transport from the fuel bed is increased by convection (in addition to the dominating radiant heat transfer to the fuel surface).[15]

Conclusions In a country like Romania with high potential of biomass production, CHP technologies can sustain economic and technical development of distributed renewable energy generation .

REFERENCES

- [1] J.A. Pecas Lopes,, N. Hatziaargyriou, J. Mutale, P. Djapic, N. Jenkins “ Integrating distributed generation into electric power systems:A review of drivers, challenges and opportunities, *Electric Power Systems Research* 77 (2007) 1189–1203 9 October 2006,
- [2] A.D. Peacock, M. Newborough, Controlling micro-CHP systems to modulate electrical load profiles, *ELSEVIER, Energy* 32 (2007) 1093–1103, Received 1 May 2006
- [3] Bretton DJ (1997)-Cogeneration in the new deregulated energy environment. Thesis, Georgia Institute of Technology
- [4] The European Educational Tool on Cogeneration, Second Edition, December 2001
- [5] Prabir Basu, Biomass Gasification and Pyrolysis Practical Design and Theory
- [6] Viviana Cigolotti-Biomass and Wastes Sustainable Resources, Chapter 2
- [7] Marc Ringel, Fostering the use of renewable energies in the European Union: the race between feed-in tariffs and green certificates, *ELSEVIER, Renewable Energy* 31 (2006) 1–17
- [8] Oana Diaconu, Gheorghe Oprescu, Russell Pittman, Electricity reform in Romania, *ELSEVIER, Utilities Policy* 17 (2009) 114–124
- [9] Biomass Conversion Emerging technologies Feedstocks and Products, EPA/600/R-07/144
- [10] R. Saidur,, E.A. Abdelaziz, A. Demirbas, M.S. Hossain, S. Mekhilef- A review on biomass as a fuel for boilers, Elsevier, *Renewable and Sustainable Energy Reviews*15 (2011) 2262–2289
- [11] U.S. Environmental Protection Agency Combined Heat and Power Partnership- Biomass Combined Heat and Power Catalog of Technologies
- [12] Anil K. Rajvanshi, BIOMASS GASIFICATION
- [13] U.S. Environmental Protection Agency Combined Heat and Power Partnership- Biomass Combined Heat and Power Catalog of Technologies
- [14] Neil Petchers, Combined Heating, Cooling & Power Handbook:Technologies & Applications
- [15] The Handbook of Biomass Combustion and Co-firing
- [16] FALLOT, A. and GIRARD, P. (2005) ‘Spatial assessment of biomass potentials for energy scenarios’, in *Proceedings of the 14th European Biomass Conference & Exhibition*, October 2005, Paris, France, ETA-Renewable Energies, Italy, pp104–107
- [17] Andres Evald, Janet Witt, Performance comparison and recommendation for future CHP systems utilizing biomass fuels

FACTORI CARE INFLUENȚEAZĂ SEMNIFICATIV CONSUMUL DE CARBURANȚI ÎN TRANSPORTUL AUTO

Drd .ing. ZORIN BERCEA¹ și prof. dr. ing LIVIU VAIDA²

^{1,2} Universitatea Tehnică din Cluj Napoca, Facultatea de Mecanică, Departamentul de Inginerie Mecanică, Cluj-Napoca, România

¹ e-mail: Vasile.Bercea@termo.utcluj.ro;

² e-mail: Liviu.Vaida@termo.utcluj.ro

Abstract: Transporturile auto reprezintă un domeniu major al economiilor statelor europene care poate influența serios creșterea economică prin costurile tot mai ridicate ale energiei în general și al carburanților în special, dar și una din cauzele importante ale poluării mediului prin emisiile de gaze arse. În articol se prezintă modul de utilizare a energiei produse prin arderea combustibilului în motoarele termice care propulsează majoritatea autovehiculelor și a puterii efective produse la arborele cotit pentru asigurarea deplasării pe drumurile publice și principalii factori care influențează semnificativ consumul de carburanți în transporturile auto. În concluziile referatului se prezintă estimativ potențialul de reducere al consumului de carburant în perspectivă pentru principalii factori analizați, prin adoptarea unor strategii și direcții de cercetare tehnologică și de proiectare în industria autovehiculelor de transport marfă și persoane.

Keywords: motoare termice, autovehicule, rezistența aerodinamică, rezistența la rulare.

1. Introducere

Transporturile de mărfuri și persoane în general reprezintă un domeniu fundamental al economiilor statelor europene și evident și al țării noastre, cu un impact major asupra dezvoltării statelor, dar și generatoare de emisii poluante, afectând mediul înconjurător. Deși au o pondere de numai. 6% din produsul intern brut (PIB) și din forța de muncă în Uniunea Europeană, reprezintă 40% din investițiile statelor membre și 30% din consumul de energie din UE, utilizând în proporție de 98% combustibili minerali și generând 28% din emisiile de CO₂ ^[1]. PROTOCOLUL DE LA KYOTO la CONVENȚIA-CADRU A NAȚIUNILOR UNITE asupra schimbărilor climatice, adoptat la Kyoto la 11 decembrie 1997 prevede ca totalul emisiilor antropice de gaze cu efect de seră, exprimate în bioxid de carbon echivalent, să nu depășească cantitățile atribuite fiecărei țări și reducerea emisiilor globale de astfel de gaze cu cel puțin 5% față de nivelul anului 1990, în perioada de angajare 2008-2012. Se mai prevede mărirea eficienței energetice în sectoarele semnificative ale economiilor naționale și cercetarea, promovarea, valorificarea și folosirea crescândă a formelor noi de energie regenerabilă, a tehnologiilor noi, avansate, favorabile protecției mediului^[2]. Parlamentul European prezintă în rezoluția sa din 15 martie 2012: “ Îndeplinirea obiectivului de creștere cu 20 % a eficienței energetice ar permite UE să își reducă emisiile interne de CO₂ cu 25 % sau mai mult până în 2020 și că această reducere ar continua să fie rentabilă în vederea atingerii obiectivului pe termen lung de reducere până în 2050 a emisiilor de gaze cu efect de seră cu 80-95 % față de nivelurile din 1990...^[3]” .

Reducerea consumului de carburant și scăderea emisiilor de gaze cu efect de seră generate în domeniul transporturilor, în principal de procesele de combustie în motoarele termice care propulsează autovehiculele, presupune identificarea tuturor factorilor de influență prin studii amănunțite efectuate asupra componentelor și elementelor acestui domeniu complex. Au fost efectuate cercetări comandate de Comisia Europeană^[4], de diverse organizații internaționale și naționale din Uniunea Europeană ^{[6]...[20]} în care se analizează factorii care influențează consumul specific de carburanți și modul de utilizare a energiei produse prin arderea combustibilului de către motoarele termice pentru asigurarea deplasării pe drumurile publice ale autovehiculelor.

În [4], studiu efectuat pentru Comisia Europeană, printre altele se prezintă modul de utilizare a energiei produse prin arderea combustibilului în motoarele termice și a puterii efective produse la

arborele cotit, pentru asigurarea deplasării pe drumurile publice. Sinteza este prezentată în Figura 1. Astfel:

- pierderile în transmisie consumă 2% din Q și 6% din Pe;
- sistemele auxiliare consumă 4% din Q și 9% din Pe;
- rezistența aerodinamică consumă 21% din Q și 53% din Pe;
- rezistența la rulare consumă 13% din Q și 32% din Pe;.^[4]

După cum rezultă din Figura 1, randamentul mediu efectiv al motoarelor cu ardere internă este de cca. 40%, valoare confirmată și de cercetările prezentate în ^[5].

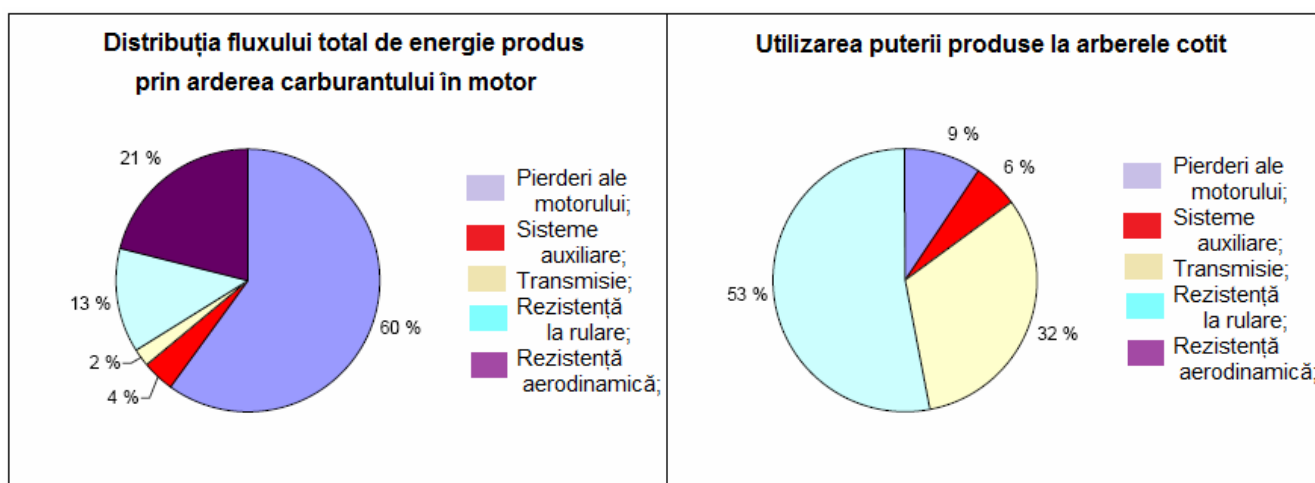


Fig. 1: Utilizarea energiei produse prin arderea carburantului și a puterii motoarelor termice ^{[4],[6]}

2. Factori de influență a consumurilor specifice de carburanți în transporturile auto

2.1 Influența sarcinii utile

Pentru a înțelege corect importanța acestui factor, trebuie arătat că în transporturile de mărfuri, încărcătura, care este de fapt sarcina utilă este deplasată de un autovehicul care are carburant, piese de schimb, etc., conduse de conducătorii auto și în care se pot afla și alte persoane care însoțesc transportul. Masa totală a autovehiculului în deplasare $M(\alpha)$ se compune din masa proprie (tara) autovehiculului (M_0), în general specificată de producător și un procent din sarcina utilă a autovehiculului (exprimată ca diferență între masa maximă a autovehiculului complet încărcat și masa proprie—tara autovehiculului) denumit coeficientul de încărcare (α):

$$M(\alpha) = M_0 + \alpha(M_{\max} - M_0) \text{ [to]} \quad (1) \quad [4]$$

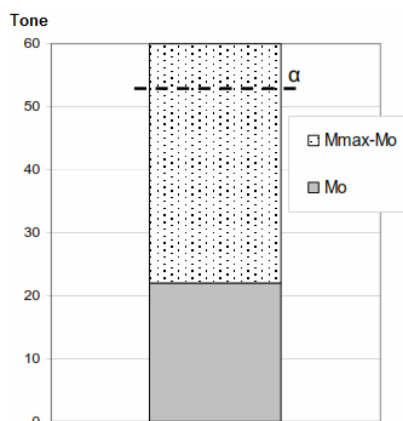


Fig. 2. Compunerea masei totale a autovehiculului ^[4]

Factorul de încărcare este definit ca raportul dintre sarcina medie de încărcare și capacitatea totală de încărcare și este determinat de modul de exploatare al autovehiculului ^[4]. Se observă că spre deosebire de coeficientul de încărcare care se referă la o situație anume, factorul de încărcare este un coeficient sintetic și se referă la activitatea unui sau a tuturor autocamioanelor unei companii într-un interval de timp. Statistic factorul de încărcare este definit ca raportul dintre numărul de tone-km efectuați și numărul de vehicul-km ale unei companii. De aceea la folosirea termenului, trebuiesc precizate condițiile de utilizare.

În cazul în care problema este analizată în termeni de combustibil consumat pe distanța parcursă (de exemplu, pe litru/100 km), cel mai mic consum de combustibil și emisiile cele mai scăzute le vor avea autovehiculele cu masa proprie cea mai mică. Astfel în ^[6] se analizează diferențele de consum de carburant între diverse combinații de autocamioane-remorcă pe șosea și autostradă pentru factori de încărcare diferiți. Consumul/100km pentru un autovehicul cu masa de 60 t s-a dovedit a fi în jurul valorilor de 30, 40 și 50 l/100km, respectiv, pentru 0% sarcină, 50% sarcină și 100% sarcină (a se vedea Figura 3). În aceleași condiții, un autocamion cu semiremorcă de 42 t consumă, respectiv 22, 30 și 35 l/100 km. În medie, consumul de energie crește liniar cu masa încărcăturii ^[7].

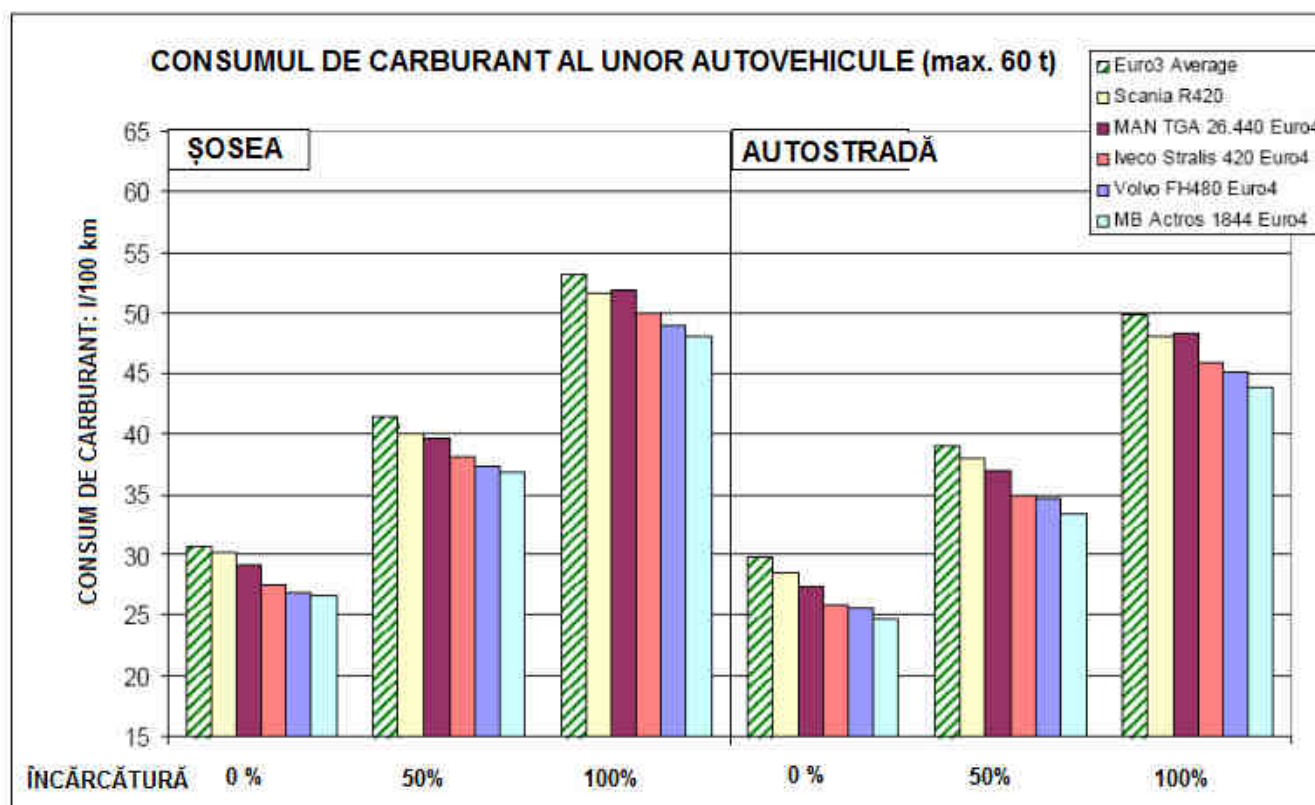


Fig. 3. Influența sarcinii utile asupra consumului de carburant ^[6]

Figura 4 arată scăderea consumului specific de carburant odată cu creșterea masei totale a autovehiculului. Este raportat că un autovehicul combinat cu masa totală de 60 t ar reduce consumul specific de combustibil cu aproximativ 15% comparativ cu un autocamion cu semiremorcă de 40 t. În cadrul unui studiu pilot care să permită autocamioanelor de mare tonaj să fie utilizate de către patru companii din Olanda (2000-2003), s-a ajuns la concluzia că, dacă sunt complet încărcate, se poate realiza o scădere a combustibilului specific consumat per tonă-km cu până la 30% ^[9].

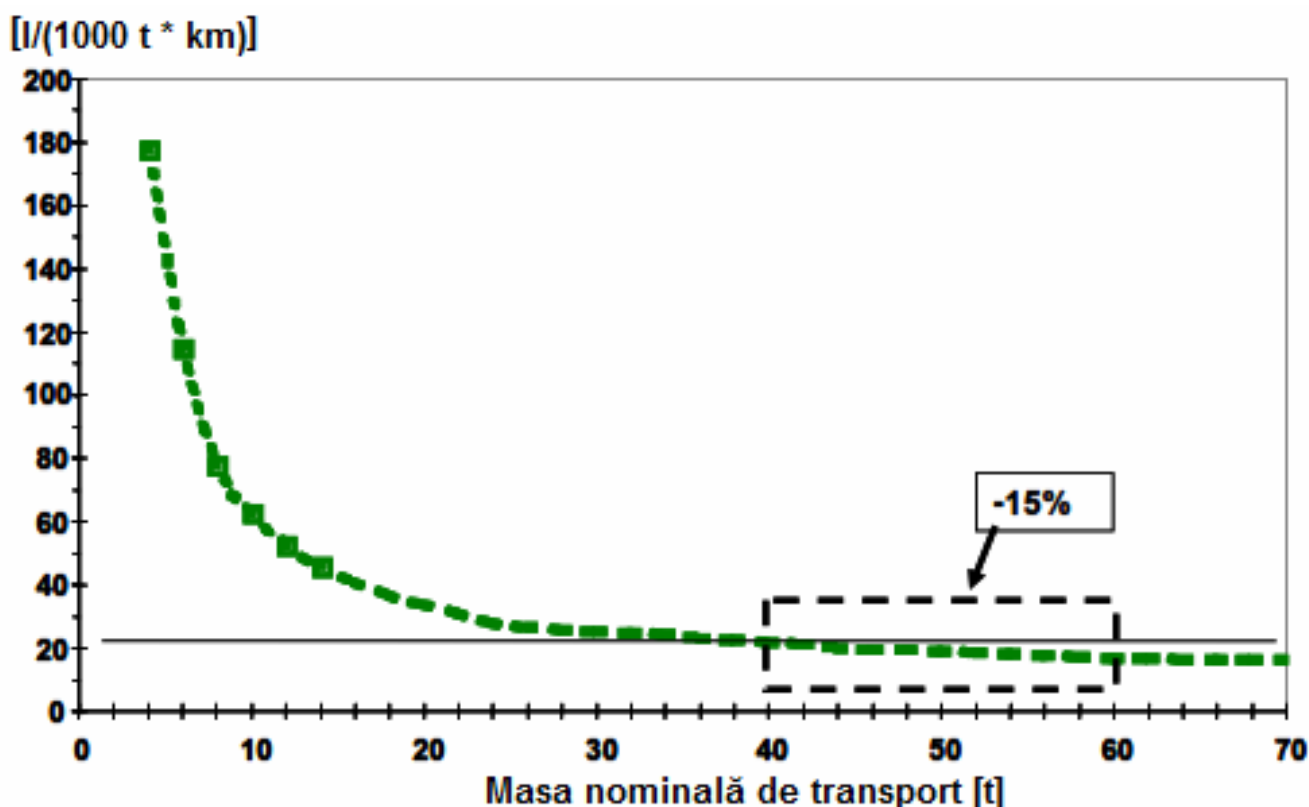


Fig. 4. Consum specific de combustibil combinat vs masa totală a autovehiculului;
 Sursa: Administrația Drumurilor suedeze^[8]

Potrivit studiului^[10], un autovehicul de 60 t ar trebui să fie încărcat cu cel puțin 77% din capacitatea maximă de încărcare, astfel încât consumul specific de combustibil (în acest caz, exprimată în litri pe t-km), poate fi comparabil cu un autovehicul de cca. 40 t. Dacă cele două autovehicule de 60 t și 40 t sunt încărcate la sarcină maximă, consumul de combustibil (l/t-km) al celui de 60 t este cu 15-30% mai mic^[9]. Aceasta este o reducere potențială maximă, fără luarea în considerare a impactului de introducere a unor autovehicule cu asemenea gabarite în flota europeană și fără evaluarea de mediu și a unor efecte economice care ar putea compensa (sau nu) acest avantaj^[10].

2.2. Rezistența la înaintare

La viteză constantă și pe drum orizontal, puterea necesară pentru a menține această viteză poate fi exprimată prin:

$$P = \eta P_{\text{motor}} = \frac{1}{2} \rho_a C_d A V^3 + mg C_r V \quad (2) \quad [4]$$

unde: P_{motor} [W] este puterea necesară menținerii vitezei constant;
 ρ_a este densitatea aerului ($\sim 1,2 \text{ kg/m}^3$);

η este randamentul transmisiei;
 C_d este coeficientul de înaintare aerodinamic ($0,6 \div 1$);

A aria frontală [m^2] ($8 \div 12 \text{ m}^2$);

V [m/s] viteza vehiculului (nu și viteza vântului);

m [kg] este masa vehiculului;

g [m/s^2] este accelerația gravitațională ($\sim 9,81$);

m/s^2);

C_r este coeficientul de rezistență la rostogolire (rulare) și depinde de tipul anvelopelor, de presiunea în anvelope, de modelul de suprafață a acestora, de viteza de deplasare și se determină experimental^[4].

Pentru drumuri în pantă, care fac unghiul α cu orizontala, ecuația 2 devine:

$$P = \eta P_{\text{motor}} = \frac{1}{2} \rho_a C_d A V^3 + mg V (C_r + \sin \alpha) \quad (3) \quad [4]$$

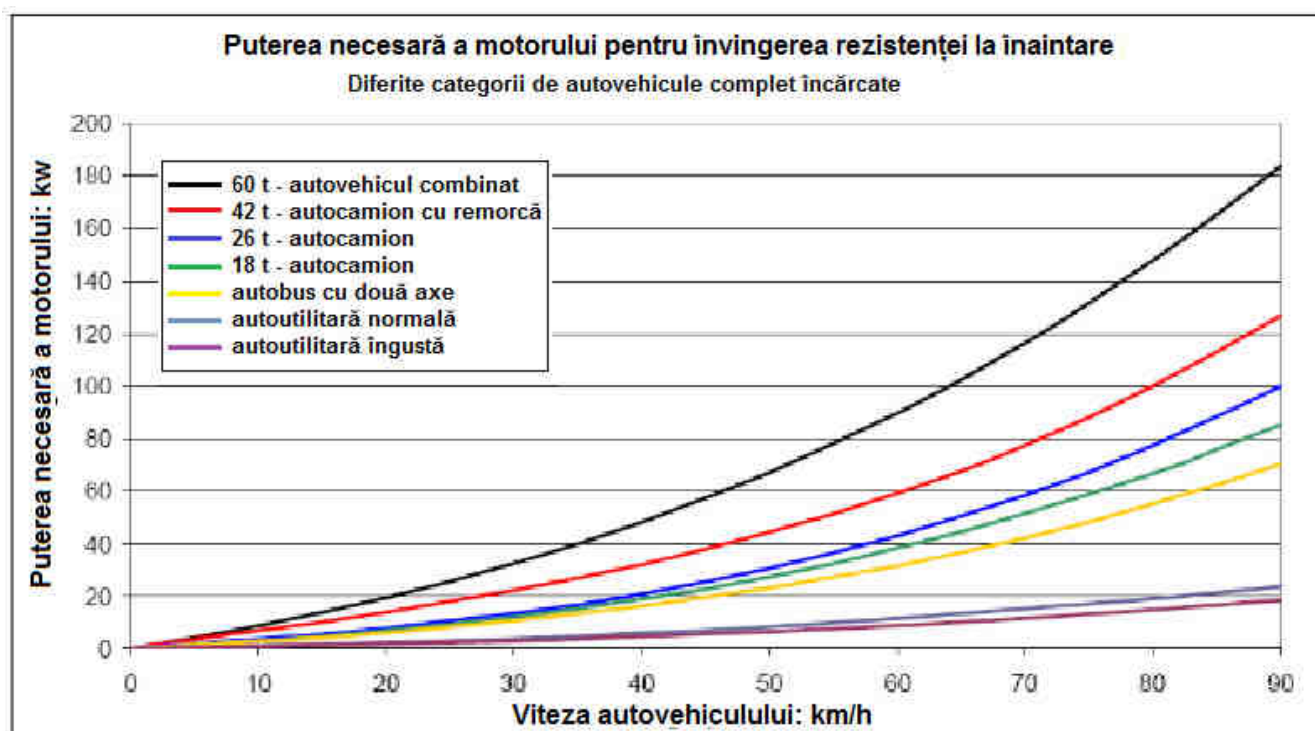


Fig. 5: Puterea necesară învingerii rezistenței globale la înaintare în raport de viteza autovehiculului. Sursa: ^[11]

Rezistențele aerodinamice și de rulare pentru cerințele de putere efectivă ale motorului depind în mare măsură de viteza vehiculului. Figura 5 arată influența vitezei asupra rezistenței la înaintare globală pentru configurații de vehicule diferite.

Așa cum era de așteptat autovehiculul combinat de 60 t prezintă o rezistență aerodinamică mult mai mare decât autocamioanele convenționale. La nivel global, se estimează că, la o viteză de peste 70 km/h, domină rezistența aerodinamică asupra rezistenței la rulare, ceea ce nu mai este cazul la viteze mai mici, când rezistența la rulare necesită o cotă mai mare de putere. Pe autostradă, învingerea rezistenței aerodinamice necesită două treimi din puterea produsă de motor ^[4].

2.3. Rezistența aerodinamică

În ecuațiile (2) și (3), puterea utilizată pentru învingerea rezistenței aerodinamice este exprimată cantitativ de expresia: $\frac{\rho_a}{2} C_d A V^3$. Dacă presupunem că autocamioane cu semiremorcă și autocamioane combinate (cu remorcă) rulează cu aceeași viteză, coeficientul aerodinamic C_d va fi principalul parametru fizic luat în considerare pentru a le putea compara. În general rezistența aerodinamică este cauzată în principal de diferența de presiune creată în timpul deplasării, între părțile din față și din spate ale autovehiculului și de fluxul de aer turbulent din jurul acestuia; celelalte surse provin din frecarea aerului care trece peste sau pe sub corpul acestuia (spre exemplu, numărul de axe, sub caroserie), precum și din fluxul de aer dintre autovehicul și remorcă sau alte componente. Ca un indiciu brut al ordinului său de mărime, raportul final al proiectului COST 346 din 2005 ^[12] a raportat o serie de coeficienți aerodinamici pentru diferite tipuri de autocamioane cu semiremorcă sau cu remorcă(i) și s-a constatat că acești coeficienți pot varia între 0,5 – 0,9 (Figura 6).

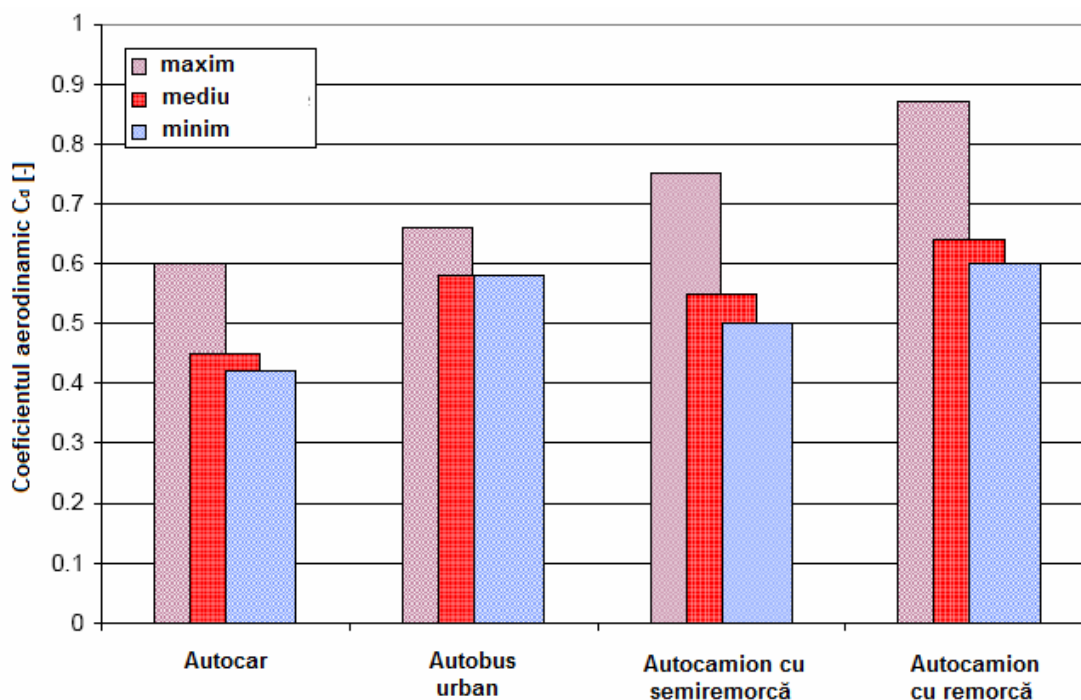


Fig. 6: Coeficienți aerodinamici pentru diferite categorii de autovehicule ^[12]

În prezent, media coeficienților aerodinamici ai autovehiculelor este în jurul valorii de 0,6 (a se vedea figura 6), ca urmare a îmbunătățirilor efectuate de către producători în ultimele decenii. Cercetătorii studiază în continuare posibilitatea reducerii rezistenței aerodinamice și propun diverse soluții tehnice pentru reducerea coeficientului de rezistență aerodinamică ^{[11], [12], [13], [14]} de la 0,6 la 0,45, prin utilizarea dispozitivelor de curent “add-on”, deflectoare, prelungirea cabinelor, utilizarea unor noi tipuri de remorci, închiderea spațiilor dintre autotractor și acestea, etc, existând un mare potențialul de a reduce consumul de carburant (mai mult de 10%) și emisiile de CO².

2.4. Rezistența la rulare a pneurilor

În ecuațiile (2) și (3), puterea propulsorului utilizată pentru învingerea rezistenței la rulare este exprimată cantitativ de termenul: mgC_rV . Spre deosebire de îmbunătățirile aerodinamice care ameliorează în principal eficiența energetică a autovehiculului prin modificări ale formei sale, reducerea rezistenței la rulare a pneurilor este mult mai complexă. În ceea ce privește studiile de specialitate, există o literatură destul de limitată care să ofere o analiză cuprinzătoare a rezistenței la rulare a pneurilor pentru diferite tipuri de autovehicule (a se vedea spre exemplu ^[12] în care se prezintă coeficienții de rezistență la rulare determinați pentru diferite tipuri de autovehicule și pneuri).

Într-adevăr, reducerea rezistenței la rulare a pneurilor înseamnă fie să acționezi asupra masei vehiculului și/sau asupra pneurilor prin micșorarea coeficientului de rezistență la rulare a pneurilor. Rezistența la rulare a pneurilor autovehiculelor este generată de frecările dintre pneuri și carosabil, dintre acestea și jante și din interiorul acestora (frecări între straturi sau interne, din material). Aceasta se produce sub acțiunea fracțiunii din masa autovehiculului preluată de acea axă și este influențată de elasticitatea și calitatea materialului din anvelope și de presiunea aerului din acestea. Există, prin urmare, un compromis care trebuie atins între eficiență, siguranța rutieră și uzură.

Este important să se țină cont de faptul că pneurile mai eficiente energetic vor reduce consumul de energie, dar pot produce efecte adverse asupra siguranței și uzura căii de rulare. De asemenea, pneurile umflate peste presiunea normală indicată de furnizor poate ajuta la reducerea consumului de combustibil, dar în detrimentul uzurii autovehiculului și a căii de rulare ^[4].

Aceste influențe sunt ilustrate în Figura 7. În medie, în general, se presupune că o reducere de 10% din rezistența la rulare conduce la o reducere de 2-3% a consumului de carburant. În literatura de specialitate sunt descrise unele măsuri eficiente disponibile^[13], cum ar fi: sistemele de monitorizare a presiunii pneurilor (TPMS)^{[14],[15]}; anvelope cu rezistență joasă la rulare (LRRT)^[16], înlocuirea pe axe motoare a anvelopelor duble cu pneuri late^{[17],[18],[19]}, sisteme de control (the Electronic Stability Control systems–ESC)^[20].

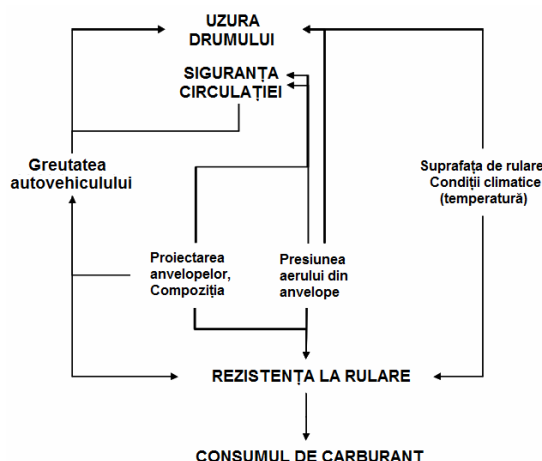


Figura 7: Vizualizare schematică a efectelor anvelopelor în consumul de carburant, siguranța circulației și uzura drumului^[4]

2.5. Randamentul motoarelor cu ardere internă

Transformarea de către motoarele cu ardere internă a energiei chimice a combustibilului, prin arderea acestuia, în lucru mecanic disponibil la arborele cotit este însoțită de o serie de pierderi, reflectate în bilanțurile energetice ale acestora, determinate prin calcul sau experimental^{[1],[5],[25],[26]}. Cercetarea bibliografică, dar și măsurătorile efectuate în Laboratorul de Motoare Termice al Facultății de Mecanică a UTC-N^[27], demonstrează că motoarele cu aprindere prin comprimare, comparate cu motoarele cu aprindere prin scânteie, au în general randamente efective superioare și consumuri specifice efective de combustibil mai mici. Cauzele sunt, în principal: raportul de comprimare mai mare, temperatură de ardere mai redusă a motorinii care arde la presiune constantă la o temperatură mai scăzută decât benzina și cu pierderi mai mici. Randamentele efective realizate de motoarele Diesel performante sunt în jur de 40%^{[1],[4],[5],[25],[26],[27]}. Pe cale de consecință, autocamioanele pentru transporturile de mărfuri auto au fost echipate cu propulsoare de tip Diesel, iar motoarele cu aprindere prin scânteie pentru avantajele pe care le au (puteri efective volumice mari, posibilitatea schimbării foarte rapide a sarcinii, a puterii efective livrate, a turației, etc.) sunt utilizate mai mult pentru autoturisme. De remarcat că și aceste motoare datorită în special tehnologiilor de injecție directă a benzinei în cilindru și a turbosupraalimentării au permis creșterea randamentului până la 35%^[21,22,23,24].

3. Concluzii

1. Sarcina utilă și factorul de încărcare al autovehiculelor influențează consumul de carburant/to-km cu cca. 15-30%, fiind mai economice autovehiculele cu capacități mari de încărcare utilizate la un factor de încărcare de peste 77%, situație în care consumul de carburant se poate reduce cu 15%.
2. Rezistența la înaintare aerodinamică necesită peste 50% din puterea efectivă livrată de motor, iar prin optimizarea proiectării autovehiculelor și a remorcilor, consumul de carburant poate fi redus cu până la 10%.
3. Rezistența la înaintare prin rulare a pneurilor necesită cca. 32% din puterea efectivă a motorului, iar prin utilizarea unor pneuri cu rezistență joasă la rulare și a unor presiuni de aer adecvate, se poate reduce consumul de carburant cu cca. 5-7%.

4. Randamentele efective ale motoarelor care propulsează autovehiculele, nu depășesc 35% (motoarele cu aprindere prin scânteie), respectiv 40% (motoarele Diesel), iar perspectivele de creștere ale randamentelor sunt limitate: cca. 5%, respectiv până la cca. 45% pentru motoarele Diesel ^[27].

References

- [1] Burnete, N., s.a., Motoare Diesel și biocombustibili pentru transportul urban, Editura Mediamira, Cluj-Napoca, 2008.
- [2] PROTOCOLUL DE LA KYOTO LA CONVENTIA-CADRU A NATIUNILOR UNITE ASUPRA SCHIMBARILOR CLIMATICE, 11 Decembrie 1997.
- [3] European Parliament resolution of 15 March 2012 on a Roadmap for moving to a competitive low carbon economy in 2050 (2011/2095(INI)), Strasbourg.
- [4] Guillaume Leduc, Longer and Heavier Vehicles: An overview of technical aspects, European Commission, Joint Research Centre, Institute for Prospective Technological Studies, Luxembourg: Office for Official Publications of the European Communities, 2009.
- [5] Bercea V.Z., Raport de cercetare: "Stadiul actual al cercetărilor privind creșterea randamentului motoarelor cu ardere internă", Școala Doctorală a U.T.C.N., 2012.
- [6] Heavy-Duty Vehicles: Safety, Environmental Impacts and New Technology "RASTU", Annual Report 2007, Ed. Nils-Olof Nylund, VTT, 2008.
- [7] EcoTransIT: Ecological Transport Information Tool, Environmental Methodology and Data, update 2008, IFEU, July 2008.
- [8] Hedberg, S., Monitoring of weights and dimensions of loading units in intermodal transport. The modular concept in practice: Experiences made in Sweden, Swedish Road Administration, presentation at the UNECE WP 24, 2008.
- [9] Inzet van langere en/of zwaardere vrachtauto's in het intermodal vervoer in Nederland: Effecten op de uitstoot van CO₂ en NO_x, 2000 (in Dutch).
- [10] Longer and Heavier on German Roads. Do Megatrucks Contribute Towards Sustainable Transports. Umweltbundesamt (UBA), August 2007.
- [11] Fuel savings for heavy-duty vehicles "HDEnergy", Summary Report 2003 – 2005, Ed. Nils - Olof Nylund, VTT, 2006.
- [12] Energy and Fuel Consumption from Heavy Duty Vehicles, COST 346, Final Report, 2005.
- [13] Ogburn, M., J., and Ramroth, L., A., Truck Efficiency and GHG Reduction Opportunities in the Canadian Fleet, Rocky Mountain Institute, 2007.
- [14] Onoda, T., Gueret, T., Fuel Efficient Road Vehicle Non-Engine Components, Potential Savings and Policy Recommendations, IEA Information Paper in support of the G8 plan of action, October 2007.
- [15] Stock, K., Tire Pressure Monitoring Systems, presentation at the IEA workshop, Improving the On-Road Performance of Motor Vehicles, Paris, Nov. 2005.
- [16] Larsson, S., Data and Indicators for Road Freight Transport, presentation at the IEA/International Transport Forum Workshop on "New Energy Indicators for Transport: The Way Forward", Paris, 28-29 January 2008.
- [17] U.S. Environmental Protection Agency, SmartWay Transport Partnership programme (EPA, 2004).
- [18] Al-Qadi, I., L., Impact of Wide-Base Tyres on Pavement and Trucking Operation, presentation at the International Workshop on the Use of Wide-Base Tires, October 2007.
- [19] Effects of Wide Single Tyres and Dual Tyres, COST 334 final report, November 2001. <http://www.rws.nl/rws/dww/home/cost334tyres/chapter4.pdf>.
- [20] [EC, 2008b] Proposal for a Regulation of the European Parliament and of the Council concerning type-approval requirements for the general safety of motor vehicles. Impact Assessment. SEC(2008) 1908, May 2008.
- [21] Hardenberg, Horst O., The Middle Ages of the Internal combustion Engine, Society of Automotive Engineers (SAE), 1999.
- [22] ***http://www.volkswagen.ro/despre_volkswagen/inovatii/motoare/fsi/fsi/.
- [23] ***http://www.volkswagen.ro/despre_volkswagen/inovatii/motoare/tsi/tsi/.
- [24] *** <http://www.treehugger.com/cars/5-technologies-that-make-internal-combustion-engines-better.html>.
- [25] Bătagă, N., Burnete, N., Căzilă Aurica, Rus, I., Sopa, S., Teborean, I., Motoare cu ardere internă, Editura didactică și pedagogică, București, 1995;
- [26] Grünwald, B., Teoria, calculul și construcția motoarelor pentru autovehicule rutiere, Editura didactică și pedagogică, București, 1980.
- [27] Bercea, V.Z., Vaida, L., Determination of exergy loss for Diesel engine, Proceedings of 2011 International Salon of Hydraulics and Pneumatics – HERVEX, 9-11.11.2011, Calimanesti-Caciulata, Romania, pag. 117-124

INFLUENCE OF CRIMPING ANGLE ON HEAT TRANSFER FOR HEAT EXCHANGERS

Oana GIURGIU¹, Dan OPRUTA², Angela PLESA³

¹ Technical University of Cluj Napoca, Department of Mechanical Engineering, Oana.Giurgiu@termo.utcluj.ro

² e-mail: Dan.Opruta@termo.utcluj.ro

³ e-mail: Angela.Plesa@termo.utcluj.ro

Abstract: Optimization of plate heat exchangers using CFD numerical method type (Computational Fluid Dynamics) allows us to study the flow phenomenon without them actually being realized. Comparatively, in this paper are presented the results from the simulation for two virtual models of plate heat exchangers. Plate geometry differs through the angle of corrugation β . It was also studied the phenomenon of heat transfer on the primary circuit (hot water).

Keywords: heat flow, plate geometry, corrugation angle.

1. Introduction

This study aims to analyze the flow phenomenon and its effects on overall heat transfer coefficient and heat flux for two different geometric patterns plate heat exchangers.

For this purpose, two virtual plate models were designed using different values for corrugation angle $\beta = 30^\circ$ and 45° . Comparative, were analyzed the results of numerical simulation type CFD of the two geometries.

Varying mass flow of working agent have been studied the effects of plate geometry on both the overall heat transfer coefficient and the heat flow.

Characteristic size of a heat exchanger is given by the thermal load Q , which is the heat flow exchanged between the two agents:

$$Q = k \cdot A \cdot \Delta T \quad (1)$$

Where k is the overall heat transfer coefficient, A - heat transfer area and ΔT - is the difference between the temperature of the two fluids.

Enhancement of heat transfer can be achieved by modifying separately or simultaneously these three factors: k , A and ΔT in equation (1). Typically, increasing the value of ΔT is not considered as a good method to enhance heat exchange due to high thermodynamic losses (exergy) produced by heat transfer at large differences of temperature. Another method of increasing the heat exchange is increasing k (Relations 2).

$$k = \frac{1}{\frac{1}{\alpha_1} + R_p + R_d + \frac{1}{\alpha_2}}, [W / m^2 K] \quad (2)$$

This can be achieved by minimizing thermal resistance (R_p and R_d), eliminating the resistances introduced by deposits on heat exchange surfaces and choosing materials for plates with thermal conductivity and a thickness as small as possible. The thermal resistance of the wall represents a small part of the overall heat transfer coefficient, which is why must be operated on the two heat convection coefficients. The value of k is always less than the lowest value of the coefficients α_1 and α_2 that is why the increase of k is significantly influenced only by increasing the lowest coefficient of convection.

The easiest way to enhance heat transfer process is to increase the heat transfer surface. Plate heat exchangers allows increases or decreases of the heat exchange surface A , according to the needs by adding or removing plates especially to those with plates and gaskets. Through this, need to be studied two important aspects: increasing the heat transfer area and create turbulence on heat flow circuits [1].

Plate geometry must be designed in such a way as to enhance turbulent flow of fluid through channels formed between two adjacent plates because turbulence leads to increased heat transfer which is reflected in overall heat transfer coefficient characterizing the device. It is known that wavy plate of the heat exchangers increase the heat transfer area and create turbulence in the flow, leading to increased heat transfer [2]. Heat transfer characteristics are related to hydraulic diameter, heat transfer surface, number of channels and especially the corrugation angle β of the wavy channel. This last factor (β), that characterizes the plate geometry, influences the flow regime by creating vortices and vortex areas [3].

2. CFD analysis

Numerical analysis of the two models was performed using Fluent software. This software allows us to use several models of turbulence. For this study it was used ($k - \omega$) SST turbulence model, because for this type of geometry it is important that both, near walls and center areas to be modeled in detail. This model is a complex one, a combination of other two models ($k - \omega$) and ($k - \epsilon$), and has a function that activates model ($k - \omega$) in the near wall areas and ($k - \epsilon$) model for central areas, thus permitting benefiting from the advantages of the two models into one.

Geometric patterns analyzed (Figure 1) were created in Solid Works and imported into Fluent where it was created mesh geometry. To mesh a 3D domain are usually used: tetrahedrons, hexahedron, triangular prisms, quadrilateral pyramids or irregular polyhedral, [4, 5].

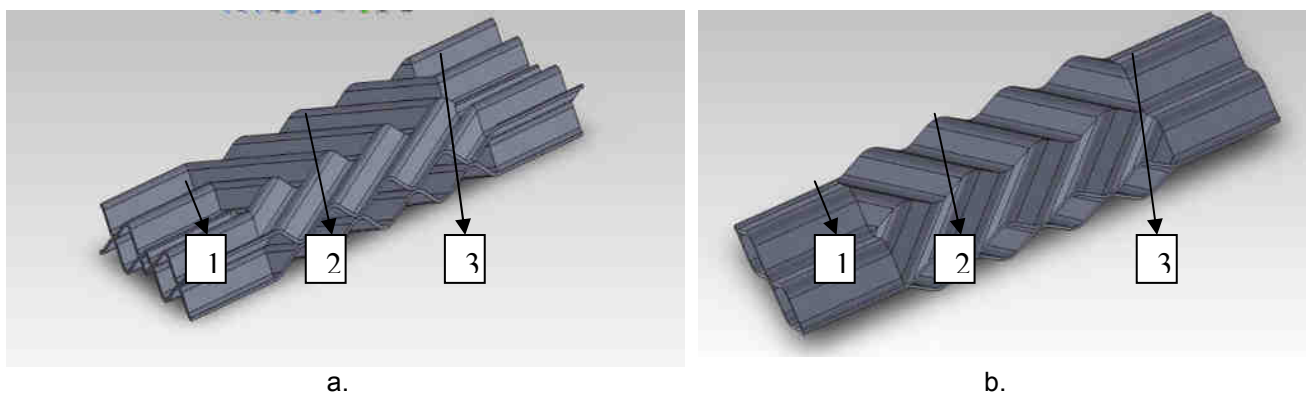


Figure. 1 Geometrics models
a. $\beta = 30^\circ$, b. $\beta = 45^\circ$

Based on these considerations the mesh (Figure 2) of the two models was realized with tetrahedral elements, approximately 13.8 million, being thin in entry (marked with number 1 in Figure 1) and exit areas (zone 3 in Figure 1) and dense heat transfer area, marked with 2 in the same figure.

Imposed boundary conditions were the same for both models studied. The primary fluid temperature was imposed at 80°C and the secondary agent (the cold) at 20°C . To simplify the model was considered that the hot fluid crosses the space formed between the two plates and the plates have the cold fluid temperature.

Fluent solver gives us more options for interpolation schemes of "upwind". In this study we used a "2nd order upwind" to solve the system of five equations. Regarding the accuracy of the results, it was imposed a criterion of convergence for all residual variables 10^{-4} , [6].

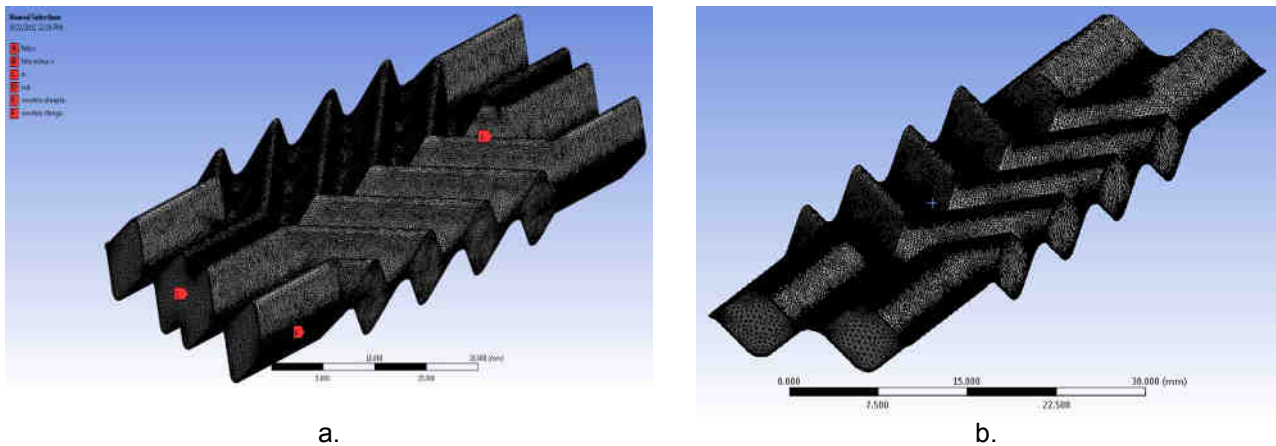


Figure. 2 Mesh
a. $\beta = 30^\circ$, b. $\beta = 45^\circ$

3. CFD Results

The results of this study suggest that fluid flow is mainly oriented in the interior of the wavy areas and it follows them (Figure 3). Note that the central layer in the fluid follows the length of the wavy channel formed between the two plates. Layers of fluid near the wall plate follows the wavy channel in the direction of the crimping angle β , then intersect and mix with remaining fluid. It can be seen that in the wavy areas turbulences occurs and the flow is more pronounced in there, and is reflected in increased heat transfer.

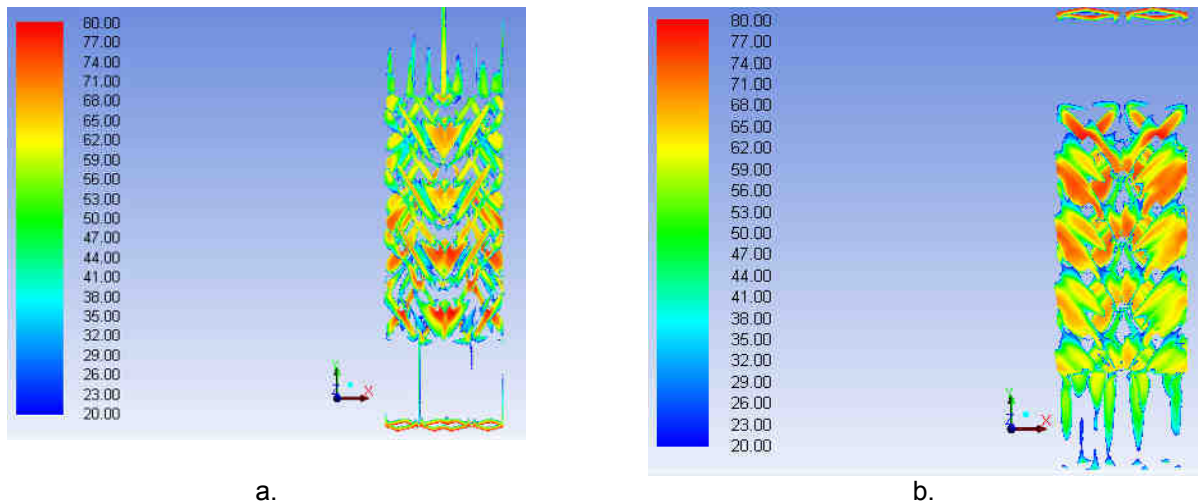


Figure. 3 Vorticity iso-surface colored by temperature
a. $\beta = 30^\circ$, b. $\beta = 45^\circ$

Figure 4 shows the effect of mass flow and crimping angle on the overall heat transfer coefficient k . According to the chart, for each model analyzed, there is a proportional increase of overall heat transfer coefficient with the increase of mass flow. The geometric model with the lowest crimping angle, subject the working fluid to more abrupt changes. This is causing modifications in velocity and in the direction of flow, thus increasing the contact time of the fluid with the plate, leading to increasing heat transfer.

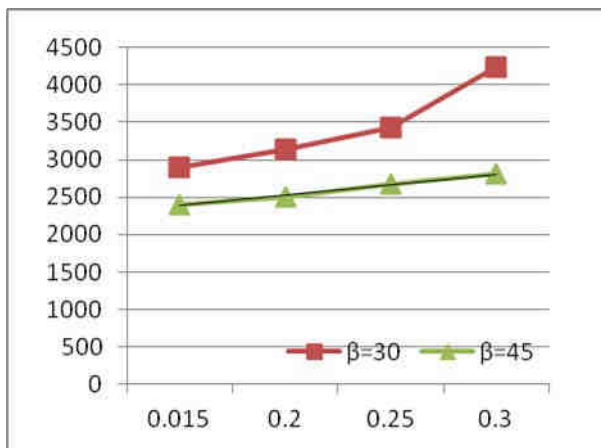


Figure. 4 Heat transfer coefficient versus mass flow rate

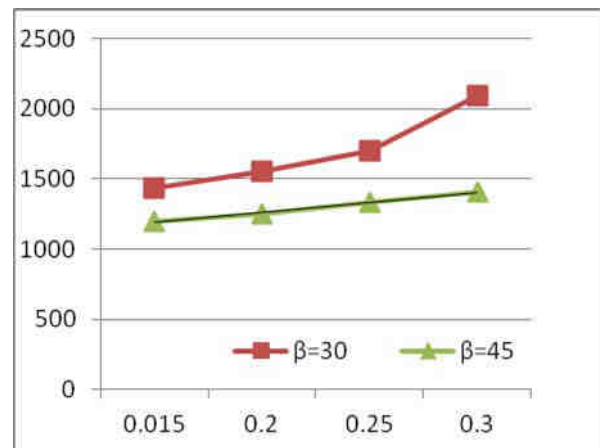


Figure. 5 Heat flow versus mass flow rate

Figure 5 shows the effect of mass flow and crimping angle on the heat flow. From the heat flow equation (Equation 1) result that it depends on the overall heat transfer coefficient, heat exchange surface and the difference of temperature between inlet and outlet. Thus heat flow follows the same trend of increase with increasing flow. This chart also shows that geometry with the lowest crimping angle has the best results.

5. Conclusions

This paper presents a numerical study CFD type over the plate of heat exchangers. For this study were designed two models of plates with 30 and 45 degrees value of corrugation angle. Overall heat transfer coefficient has a tendency to increase with increasing mass flow. In terms of heat transfer is recommended to use geometries with a small value for corrugated angle, because the heat transfer is more intense. This is due to changes that appear in agent flow velocity which leads to turbulence formations.

Acknowledgment:

This paper was supported by the project "Improvement of the doctoral studies quality in engineering science for development of the knowledge based society-QDOC" contract no. POSDRU/107/1.5/S/78534, project co-funded by the European Social Fund through the Sectorial Operational Program Human Resources 2007-2013.

REFERENCES

- [1] A. Plesa, C. F. Grieb, M. Nagi, „Utilaje termice. Schimbatoare de caldura cu placi” Vol.1, Ed. Mediamira, 2008
- [2] T.A. Rush, T.A. Newell, A.M. Jacobi, An experimental study of flow and heat transfer in sinusoidal wavy passages, Int. J. Heat Mass Transfer 42 (1999) 1545–1553.
- [3] Jialing Zhu, Wei Zhang “Optimization design of plate heat exchangers (PHE) for geothermal district heating systems” vol. 33, pg. 337-347, 2004
- [4] R. Resiga “Complemente de mecanica fluidelor si tehnici de solutionare numerica”, Ed. Orizonturi Universitare, Timisoara, 1999
- [5] Shan-Fu Shen, Wagdi G. Habashi, Local linearization of the finite element method and its applications to compressible flows, International Journal for Numerical Methods in Engineering, vol. 10, iss. 3, pp. 565–577, 1976
- [6] Salim M. Salim, and S.C. Cheah, „Wall y+ Strategy for Dealing with Wall-bounded Turbulent Flows”, Proceedings of the International MultiConference of Engineers and Computer Scientists 2009 Vol II IMECS 2009, March 18 - 20, 2009, Hong Kong

SOLAR POWER INSTALLATION HOT WATER TO HOUSING FAMILY TYPE

Carmen Otilia Rusănescu¹, Adriana Gruia², Mihaela-Florentina Duțu³, Stoica Dorel⁴

¹ University Politehnica Bucharest, Biotechnical Faculty of Engineering, otiliarusanescu@yahoo.com

⁴ University Politehnica Bucharest, Biotechnical Faculty of Engineering, dorelstc@yahoo.com

Abstract: *In this paper, we present a solar thermal system for hot water supply of family housing to be functional and to exploit solar heat all year round: in summer for hot water and cold season contributes to heating the water in the storage tank. For this purpose we chose a storage tank with two coil type heat exchanger (exchanger for solar circuit and the other for connecting to a boiler) and a 2 kW electric resistance (to heat water in the boiler when any of the two sources is not available). We determined the average monthly temperatures accumulated water storage tank in summer.*

Keywords: *solar system, solar heat, solar collector field*

1. Introduction

This paper is part of the new technological approach that takes account of capitalization "clean sources" which provide effective protection of the environment. Solar energy is available worldwide. Solar energy is the only form of clean energy that does not create harmful by products, as in classical and nuclear fuels, solar energy does heat release in other forms of energy, but heat transport from the place of capture to the user. The traditional system for domestic hot water production, harnessing, always use a collector containing heat (liquid or gaseous working fluid) with or without accumulation system.

The principle of operation of these facilities is relatively simple and is based on the conversions of solar radiation into heat energy used to heat domestic water. Installation of solar energy conversion into heat is the main equipment solar collectors that convert solar radiant energy into thermal energy, solar heat storage devices, network transmission and distribution pipelines solar heat to consumers and automation elements whole process of production, storage, transport and distribution of solar heat. Typical, application systems for producing solar water heating provides hot water supply temperature of 45 °C in summer. In March-April and September-October the system can take only part of the thermal load required to produce hot water.

In practice it was found that the production of hot water at a temperature of 45 °C, considering the cold water temperature of 10 °C, 35 °C water temperature must be raised. Under these conditions the collector absorbing surface must reach a temperature of 50-70°C to transfer heat to the heat and domestic hot water then an acceptable efficiency.

Systems for domestic hot water still running and in winter, because they can provide even sunny winter days the amount of heat to be transferred to the domestic hot water.

All the practice has been established that a person consumes 50 liters per day hot water. This requires an area of 1,5 m² of collector covering domestic hot water needs a rate of 90-100%.

Average solar radiation is considered 1000 kW/m² per year.

Depending on the size of the solar hot water preparation and constructive solution adopted to obtain 300-500 kW/m² per year.

2. Materials and methods

When choosing a solar system for hot water, you first need to set the preferred temperature hot water usage and quantity and distribution needs throughout the day. Temperature of hot water use

in most practical installations in operation temperature is 45°C. Hot water needs, depend on the attitudes and habits of consumers and the characteristics and specific features of each application. The study concerns a family home consists of four that has a fuel consumption of 50 liters / person / day, so the solar system will need to produce 200 liters of hot water daily.

Distribution of daily consumption of hot water, over 24 hours is considered statistically consistent with values determined by measurements.

On this basis we determined that the volume of storage tank which should cover domestic hot water scarcity at peak hours, you must be at least 120 liters. Therefore we chose a boiler with a capacity of 200 liters.

Cold water temperature used in hot water take into account the value of 10°C. Hot water will be prepared so that the user can reach a temperature of 45°C. To ensure that temperature is required at the point of storage temperature is higher, setting the value of 45°C Achieved by means of mixing valve placed on the grid, leaving the boiler. Typically, the point of storage is practiced temperature 60°C [1], which provides safe disinfection of hot water from Legionella bacteria.

In terms of health it is recommended that the hot water system to intervene household disinfectant at least once a year by raising water temperatures above 60°C stored for a period of time.

- The solar system object of this study will be operational throughout the year, in summer for hot water and cold season to contribute to preheat cold water in the boiler, following the rise in temperature of water use by at 45°C is achieved by heating boiler (gas and condensation) or a 2-kW electric resistance heater mounted.

For this purpose choose a bivalent boiler with two coils and electrical resistance of 2 kW.

Basic options for choosing solar thermal system for domestic hot water is to optimize the investment and operating costs. For this purpose we adopted the solution of solar thermal energy recovery throughout the year.

For this purpose we analyzed three offers of technically all three offerings using the same schematic structure of the solar system, all using vacuum tube panels, constructive solutions are relatively similar, which makes choosing the lowest bid price, respectively HELIS solar system. It provides heating to 200 liters of water at $t_0 = 10^\circ\text{C}$ (cold temperature) to $t_{\text{acm}} = 45^\circ\text{C}$ (temperature hot water consumption).

3. Results and discussion

- The amount of solar heat (Q_n) for heating water volume of 200 l is given by:

$$Q_n = m_a \cdot c_a \cdot \Delta t \quad (1)$$

- m_a - mass of water in kg corresponding to a volume of 200 l ($m_a = 200$ kg);
- c_a = specific heat of water ($c_a = 4,173 \cdot 10^3$ J/kg·°C);
- Δt = temperature difference in °C ($\Delta t = 35^\circ\text{C}$ C).

- The area calculated as required solar collector:

$$S_{\text{col}} = \frac{Q_n}{\eta_{\text{col}} \cdot G_{\beta \text{ med}}} \quad (2)$$

- η_{col} - collector efficiency HELIS ($\eta_{\text{col}} = 0,83$ %);

- $G_{\beta \text{ med}}$ - global radiation on collector plane averaged from March to October;
 $G_{\beta \text{ med}} = 16,6$ MJ/m²·zi.

$$S_{\text{col}} = \frac{29,21}{0,83 \cdot 16,6} = 2,12 \text{ m}^2.$$

- Actually used a solar collector area of supply is 3.7 m² favorable situation because it has reserves to compensate for the heat losses along the primary circuit and the heat exchanger S_1 . Theoretical explanations:

Solar circuit heat transfer in the boiler is achieved by S_1 which is heated in the heat exchanger fluid. Solar system with heat exchanger circuit S_1 form a closed system in which the movement is made by heating liquid.

The process can take place so that natural circulation and forced circulation as (solar circuit pump that increases the productivity of exchange). Heat load of the heat exchanger is determined from the heat balance equation [3]:

$$\dot{Q} = G_1 \cdot c_1 \cdot \Delta t_1 = \frac{1}{\eta_{sc}} \cdot G_2 \cdot c_2 \cdot \Delta t_2$$

where: \dot{Q} [W] is the flow of heat from the solar circuit;

G_1, G_2 [kg/h] is the mass flow of liquids;

c_1, c_2 [J/kg·°C] is the specific heat of liquids

The heat transfer due to a temperature difference occurs by conduction and radiation through the surface S_1 by the equation:

$$\dot{Q} = k \cdot S \cdot \Delta t_{med} \text{ [W]}$$

where k is the overall heat exchange coefficient [W/m²·°C]

To simplify assessment levels recorded in stored water temperature in the boiler use:

- The relationship of heat quantity:

$$Q_a = m_a \cdot c_a \cdot \Delta t$$

where: Q_a [J] is the amount of heat (thermal energy) received water from the boiler during the exchange, which is equal to the change in internal energy.

- expression exchanger efficiency:

$$Q_a = \eta_{sc} \cdot Q_d \text{ [2]}$$

where: Q_d [J] is the amount of heat absorbed by the solar collector heat solar heating cycle.

- Heat quantity Q_d :

$$Q_d = S_{col} \cdot \eta_{col} \cdot G_{\beta med} \quad (3)$$

- The amount of heat Q_a :

$$Q_a = \eta_{sc} \cdot Q_d$$

- The relationship determine the amount of heat stored in the boiler water temperature t_{sb} :

$$Q_a = m_a \cdot c_a \cdot (t_{sb} - t_0) \quad (4)$$

$$t_{sb} = t_0 + \frac{Q_a}{m_a \cdot c_a} \text{ °C} \quad (5)$$

$$t_{sb} = 10 + \frac{45,88 \cdot 10^6}{200 \cdot 4,173 \cdot 10^3} = 64,97 \text{ °C}$$

This temperature is the average temperature of the water stored in the tank during the hot season.

- To determine the monthly average temperatures during each month of the hot season, from relations (3) and (4) calculate the amount of heat taken from the water heater:

$$Q_a = \eta_{sc} \cdot Q_d = G_{\beta med} \cdot \eta_{sc} \cdot \eta_{col} \cdot S_{col}$$

$$Q_a = G_{\beta med} \cdot 0,9 \cdot 0,83 \cdot 3,7 = 2,76 \cdot G_{\beta med}$$

The value of q is introduced in relation (5) becomes:

$$t_{sb} = t_0 + \frac{2,76 \cdot G_{\beta med}}{m_a \cdot c_a}$$

Table 1 Monthly average temperatures in the months of March to October


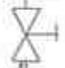



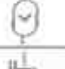








$t_{sbIII} \text{ °C}$	$t_{sbIV} \text{ °C}$	$t_{sbV} \text{ °C}$	$t_{sbVI} \text{ °C}$	$t_{sbVII} \text{ °C}$	$t_{sbVIII} \text{ °C}$	$t_{sbIX} \text{ °C}$	$t_{sbX} \text{ °C}$
47,91	60,82	68,31	75,44	73,92	72,50	66,40	42,97

Level during April-September temperatures of over 60°C will ensure sterilization of water stored in the tank against Legionella bacteria.

Hot water temperature of 45°C will ensure the automatic mixing valve is placed at the exit of the boiler. The calculated values for cylinder temperature which explains the company MEGASUN as typical boiler cold water temperature = 10°C, cylinder temperature = 60°C and hot water temperature prepared by mixing = 45°C. Heater coil is calculated so that the solar circuit is circulated heat with temperatures between 55°C and 80°C.

Schematic structure of the solar system HELIS

Solar system presented consists primarily of the following components:

	solar collector field		filling valve drain
	shut off valves		heating cooling equipment off the cycle primary
	retaining flap		expansion box
	temperature sensors		air vent
	pump		thermostatic mixing valve
	safety valve		coil heat exchanger
	flow sensors		panel

Conclusions:

In this paper, we chose a solar thermal system for hot water supply of family housing to be functional and to exploit solar heat all year round: in summer for hot water and cold season contribute to the heating of water in the storage tank.

For this purpose we chose a storage tank (tank) with two coil type heat exchanger (exchanger for solar circuit and the other for connecting to a boiler) and a 2 kW electric resistance (to heat water in the boiler when any of the two sources is not available).

To purchase equipment solar system components we considered that most companies that have manufacturing and marketing concern such facilities supplied equipment packages and electronic components integrated for different types of applications that use solar thermal. As a result, the three bids considered that the technically used the same schematic structure of the solar thermal system we chose the one with the lowest price.

We determined the average monthly temperatures accumulated water storage tank in summer. Especially solar panel scheme used HEAT-PIPE Helis presents a major advantage to be taken into account in that outside a maximum efficiency of 80% has the advantage that installs with simple installation procedures. It is worth noting that the entire solar installation can be installed and functionally tested prior to actually mount the solar collector vacuum tubes. They can be mounted at the end of trial operations of the solar system in a very short and very simple installation procedure

References

- [1] www.megasun.com - solar thermal
- [2] Răducanu P. Technical Thermodynamics, Bren Publishing House, Bucharest, 2010
- [3] Kicighin M.A., Kostenko G.N. - Heat exchangers and vaporizing facilities, Technical Publishing House, Bucharest, 1958

STUDY ON THE WORKING PRINCIPLE OF A HYDRAULIC ENERGY DISSIPATION DEVICE

Gavril AXINTI, Florin NEDELCUȚ, Fănel ȘCHEAUA

“Dunărea de Jos” Galați University, Mechanical Engineering Faculty Brăila, MECMET Research Center,
gaxinti@ugal.ro ; florin.nedelcut@ugal.ro ; fanel.scheaua@ugal.ro

Abstract: *This study presents an innovative solution of a hydraulic damping system that can perform a certain level of seismic energy dissipation, adequate for man-made structures. The system is represented by an adaptive isolation system, expected to improve the behavior of certain structures during seismic actions. The proposed system consists of a hydraulic damper, where the viscous damping device is represented by a cylinder with piston and piston rod, filled with a viscous fluid, fluid which can be mineral oil or silicone oil. The seismic driven translational motion of the piston rod together with the piston is forcing the viscous fluid to circulate inside the cylinder through a certain number of orifices bored in the piston. A CFD analysis was performed using a simplified model of hydraulic dissipation device, with the purpose to highlight the fluid particles motion inside the device when connected to the mobile part of the structure driven by seismic movements. The proposed system is therefore capable of simultaneously limiting the response of both base isolation system and superstructure, for a large variety of seismic ground motions.*

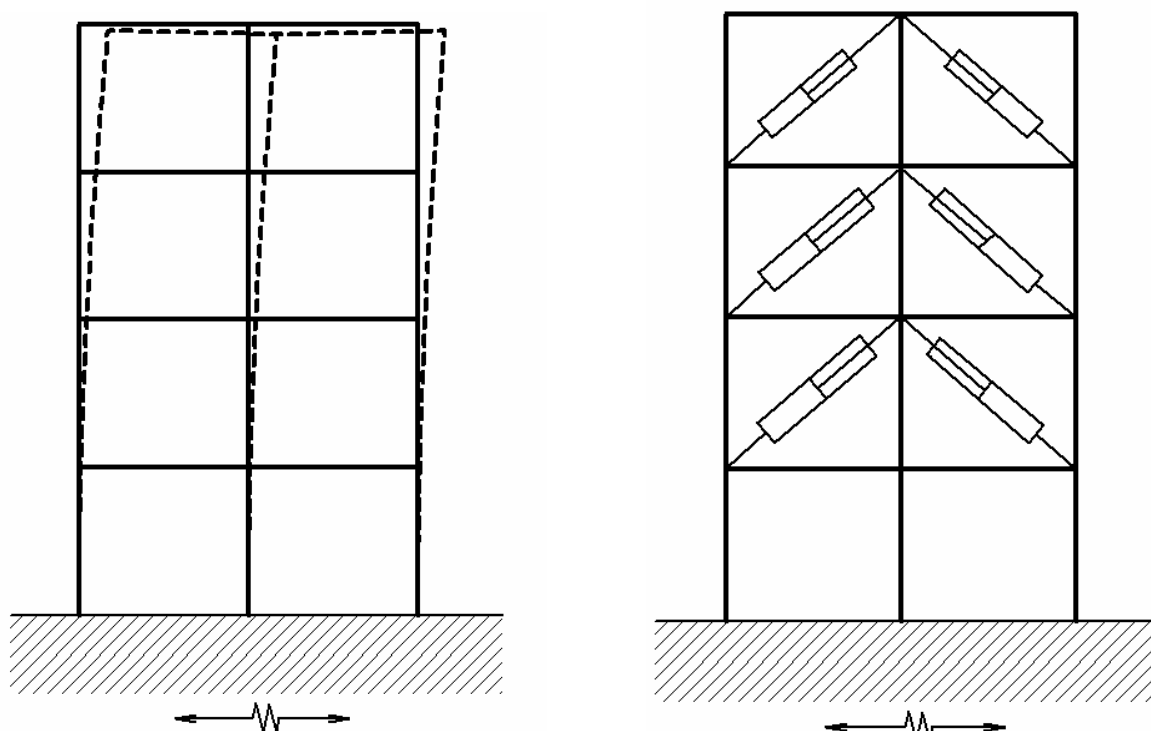
Keywords: *seismic energy dissipation, hydraulic device, viscous fluid, CFD, piston*

1. Introduction

Seismic action represents a dynamic action, variable in time, having the effect of uncontrolled ground motion. Basic characteristic of seismic action effects on building structures is the presence of inertial forces. Structural safety was the main concern of designers and builders of all time. To protect a structure against seismic action can be used some isolation systems that can modify structure behavior during seismic events. Such devices installed inside the building structural frames or between superstructure and foundation can provide a certain degree of limitation of the movements within structure due to occurrence of an earthquake, thereby maintaining the structure stable. A hydraulic device that can achieve seismic energy dissipation is analyzed in terms of working principle during this study.

2. State of art of a hydraulic seismic energy dissipation system

A conventional structure experiences deformations within each level of the structure and amplified accelerations at upper levels. In contrast, isolated structures experience smaller deformations, while the accelerations are relatively uniform over the height. A hydraulic system can perform a limitation of structural movements during ground motions caused by an earthquake and the different constructive solutions that were used so far proved the utility of getting a higher structural stability during high intensity seismic movements. This feature is attained especially because these devices are working as dumpers mainly to axial motion components and are inducing a delay of a quarter of period of the seismic oscillations.



a) non – isolated structure

b) structure with hidraulic systems

Fig. 1 Structural frame model subjected by a seismic action

The isolation system consists of a combination between a certain numbers of hydraulic dissipation devices named otherwise fluid viscous dampers. Usually, the hydraulic dissipation device is placed between structural frames therefore are limiting the lateral movements and avoiding their shearing effects. Consequently, a hydraulic dissipation device converts the mechanical energy into caloric energy (heat), transmitted to the external environment trough cylinder walls. The hydraulic damping device acts as a seismic energy dissipation device combined with a lateral (horizontal) displacement restraint. It is mainly composed of a cylinder with piston and piston rod, filled with a viscous fluid, fluid which can be mineral oil or silicone oil. The seismic driven translational motion of the piston rod together with the piston is forcing the viscous fluid to circulate inside the cylinder through a certain number of orifices bored in the piston. According [2], a common feature of several of the seismic records, especially for sites located near the epicentral region of the earthquake, is a long-period velocity pulse of very large amplitude, so the horizontal speed typically for this range of earthquake is of at least 1 m/s.

3. Simplified hydraulic device model

A hydraulic dissipation device system consists of a cylinder with piston filled with fluid inside that can be mineral or silicone oil. In the piston head are made a number of orifices which allow a translational motion for the piston inside the cylinder by forcing the fluid through a certain number of small diameter orifices.

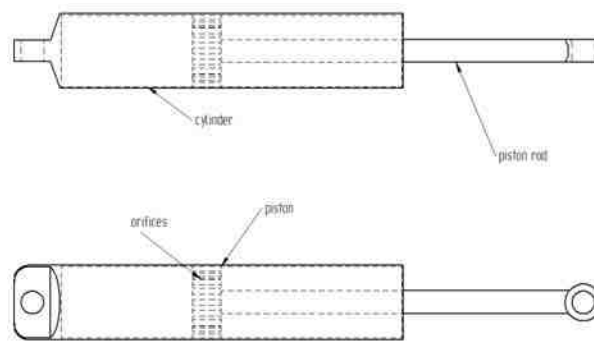


Fig. 2 Hydraulic dissipation device model

In the occurrence of an earthquake hydraulic system become operational by repeated compression-tension translational motions. Because of the working fluid properties in terms of viscosity and internal friction at the fluid particles level occurring inside the cylinder, the device responds with a resistance to piston movement. This resistance force take over and passively consumes a part of seismic energy transmitted by earthquake to structure thus improving the structure response during seismic action.

Also, the inclusion of the hydraulic device into the structure is altering the seismic induced movements, inducing a delay of a quarter of period. The simplified 3D model of seismic energy dissipation device was studied with a CFD software, in order to observe the fluid dynamics.

4. Results

The purpose of this study was to highlight the fluid particles motion inside the cylinder when connected with the mobile part of the structure, driven by seismic movements so we made a CFD analysis with the help of AnSYS Flowizard software. The 3D model of the hydraulic dissipation device was a simplified one, according the practical requirements of the study. The fluid taken into consideration for the CFD study was a high-viscosity silicone-oil type, with a viscosity of $29.1 \text{ kgm}^{-1} \cdot \text{s}^{-1}$ and a density of 970.0 kg/m^3 [1].

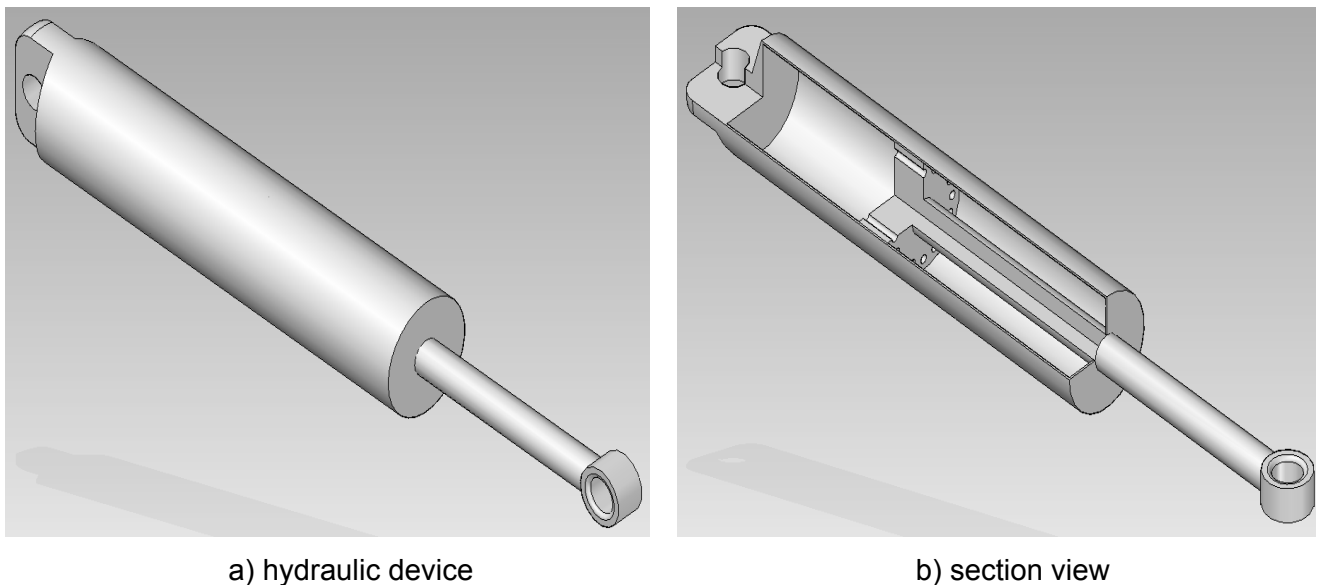


Fig. 3 Hydraulic device 3D assembly

The fluid material properties in terms of density, viscosity, specific heat and thermal conductivity are important because the dissipation of the energy and load during the device operation is based mainly on these properties. The input information for the material properties

used in hydraulic device operation of the regions properties for both fluid region and internal solid model are declared in *Table 1* and *Table 2*.

Table 1

Fluid region physical properties				
<i>Fluid</i>	<i>Viscosity (kg/m.s)</i>	<i>Specific Heat (J/kg.K)</i>	<i>Thermal Conductivity (W/m.K)</i>	<i>Density (kg/m³)</i>
silicone-oil	29.1	1601	0.159	970

Table 2

Solid regions physical properties			
<i>Solid (Cylinder, piston, rod)</i>	<i>Specific Heat (J/kg.K)</i>	<i>Thermal Conductivity (W/m.K)</i>	<i>Density (kg/m³)</i>
steel	502.48	16.27	8030

The mesh of the 3D hydraulic device model had 176024 tetrahedral cells.

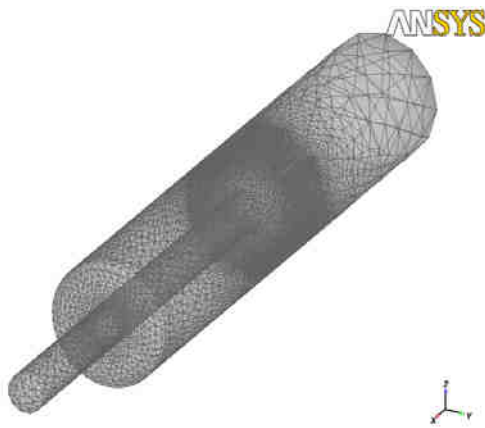


Fig. 4 The 3D mesh



Fig. 5 Assembly active regions

We focused on calculating the axial force developed inside the cylinder when seismic movements at a certain speed drive the piston and piston rod. They were declared three different values for piston velocity inside the cylinder thus achieving three different values for the axial force acting on the piston coupled with the rod. The next figure (Fig. 6) presents the diagram of the axial force when the axial speed covers a certain speed range, corresponding to some usual seismic frequencies for buildings and structures.

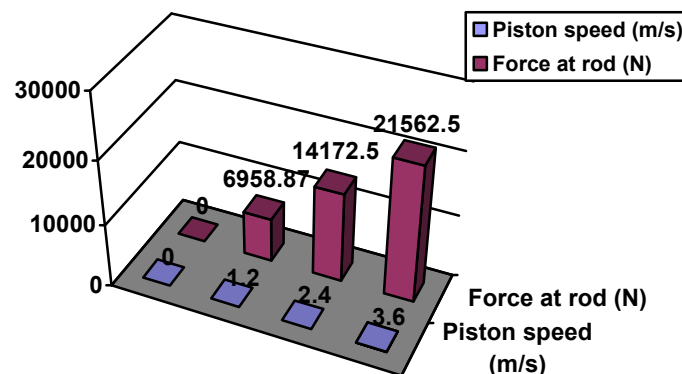


Fig. 6 Axial forces at a corresponding piston speed

Table 3

Axial forces at a corresponding piston speed				
Piston speed (m/s)	0	1.2	2.4	3.6
Force at rod (N)	0	6958.87	14172.5	21562.5

Force diagram shows that higher the axial speed is (corresponding to different frequencies), higher the forces induced into the hydraulic device are. Also, we found that, for axial speed up to 4 m/s, this dependency is quasi linear.

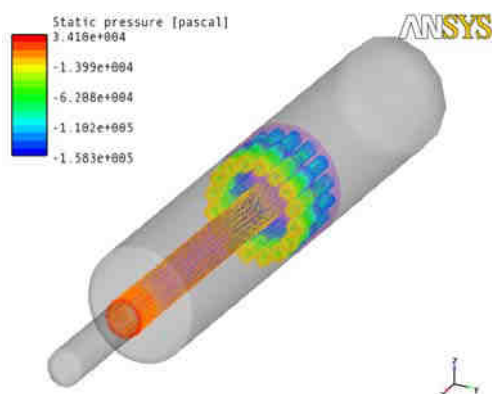


Fig. 7 Static pressure distribution for 1.2 m/s piston and rod speed

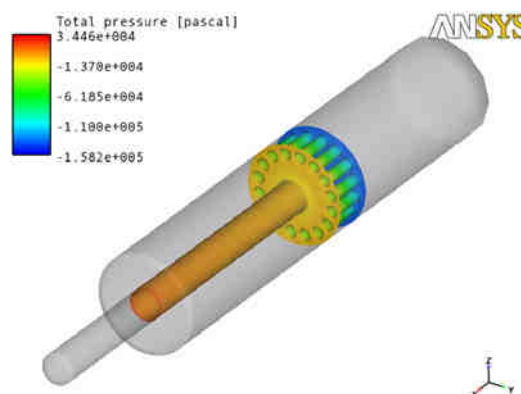


Fig. 8 Total pressure distribution for 1.2 m/s piston and rod speed

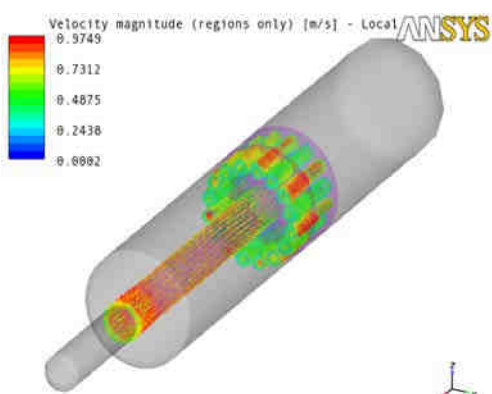


Fig. 9 Velocity magnitude distribution of the fluid for 1.2 m/s piston and rod speed

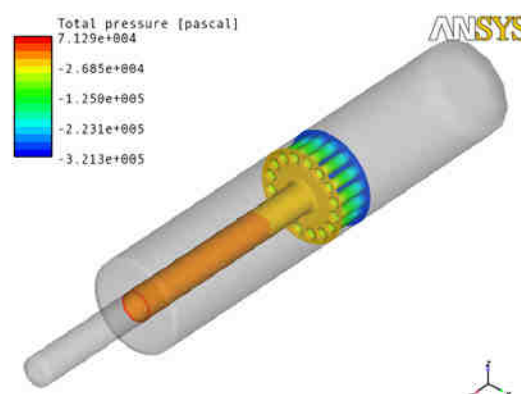


Fig. 10 Total pressure distribution for 2.4 m/s piston and rod speed

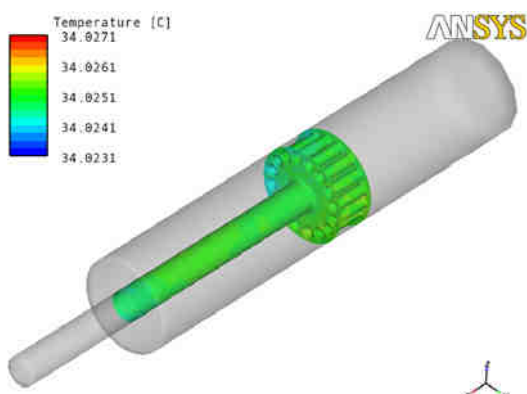


Fig. 11 Temperature distribution for 1.2 m/s piston and rod speed

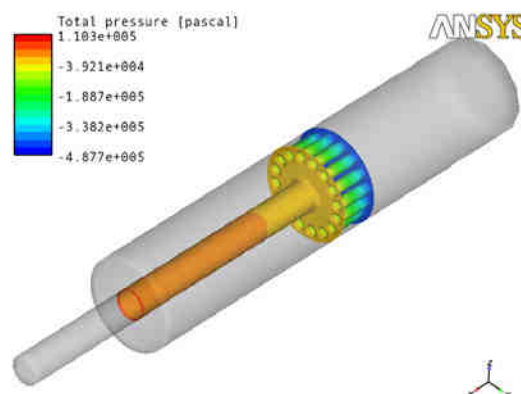


Fig. 12 Total pressure distribution for 3.6 m/s piston and rod speed

The temperature was almost constant for the speed range studied, with values of 34-35°C. Initially, we estimated that when the speed will increase, the high viscosity of the silicone-oil will produce more and more heat, through internal friction, but the study showed it to remain almost constant. We may explain this discrepancy by taking into consideration the low Re number of the fluid flow, with values up to 80; i.e. in the laminar range, where also the friction losses are smaller than in the turbulent range.

5. Conclusions

A limitation of seismic hazard of exposed structures is the main concern of structural designers. In order to achieve a certain level of limitation are used seismic energy dissipation systems that are embedded in structural resistance frames. Their action improves the structure behavior during a seismic action through a dissipative function. This is usually achieved by transforming a certain amount of seismic mechanical energy into another energy form, namely heat energy. The heat is released due to friction occurring inside the fluid, at the molecular level.

An optimal solution is represented by hydraulic seismic energy dissipation devices. Such devices can be used to limit successfully the amount of energy introduced into the structure by the earthquake. The proposed system is therefore capable of simultaneously limiting the response of superstructure, also limiting the load, for a large variety of seismic ground motions.

Hydraulic device dissipative capabilities are determined by working fluid properties as by the size, form and dimensions of the orifices made in the piston head.

Also, the capacity to face higher seismic frequencies oscillations is proportional up to a limit due to the mechanical resilience of the materials of cylinder, piston and rod.

REFERENCES

- [1] <http://www.clearcoproducts.com/pdf/high-viscosity/NP-PSF-30000cSt-60000cSt.pdf>.
- [2] J. X., Zhao, *Response of seismically isolated buildings with buffers subjected to near-source ground motions and possible alternative isolation systems*, Bulletin of the New Zealand Society for Earthquake Engineering, Vol. 37, No. 3, September 2004, pp. 111-133
- [3] G., Axinti, A. S., Axinti, *Acționări hidraulice și pneumatice*, Vol III, Editura "Tehnica-Info" Chișinău 2009
- [4] Hauk, N., *The influence of kinematic of mechanisms drive with hydraulic cylinders about the output of the system*, Al VIII-lea Simpozion Internațional de Teoria Mașinilor și Mecanismelor - SYROM, București 2001
- [5] Scheaua F., Nedelcuț F., *Study on a seismic isolation method suitable for an architectural monument*, The Annals of "Dunărea de Jos" University of Galati, Fascicle XIV Mechanical Engineering, ISSN 1224-5615, pp. 65-70, 2012

HEAT GENERATORS WITH TLUD GASIFIER FOR GENERATING ENERGY FROM BIOMASS WITH A NEGATIVE BALANCE OF CO₂

Erol MURAD¹, Florian DRAGOMIR²

¹ Univ. POLITEHNICA București, e-mail address erolmurad@yahoo.com

² PROMECO SD.SRL

Abstract: *This paper presents heat generators for thermal energy production from local biomass or pellets with a negative or neutral balance of CO₂. It is used biomass gasification process, type Top-Lit Up-Draft (abbreviated TLUD) because it is easy to operate, simple construction, and it produces CO and PM emissions under existing rules. TLUD heat generators can be used for heating greenhouses, dryers, production facilities, housing, hot air, hot water, steam. From a batch of biomass results among others, biochar in a rate of 10-15% can be used as valuable agricultural amendment for soil carbon sequestration from the atmosphere. TLUD generators can be used as thermal energy sources for micro cogeneration with low percentage by electricity (<8%) for agriculture - greenhouses and dryers - and isolated areas.*

Keywords: *biomass, gasification, biochar, TLUD, carbon balance*

1. Introduction

Currently, due to the continuous global warming it become more and more important the problem of reducing the CO₂ concentration in the atmosphere. Biomass was and is a renewable source of thermal energy, which can be easily converted into mechanical energy and electricity. Burning wood and vegetal biomass, was and is still used as a way of generating thermal energy with efficiency and high emissions of CO and solid particles (PM) in the atmosphere.

Thermo-chemical gasification of biomass, a process known and used for over 130 years, converts biomass into a combustible gas with high energy conversion efficiency and low emissions of solid particles. The gas produced can burn efficiently and cleanly.

Installations for gasification are relatively complex, large-sized and using generator gas called gasogen in internal combustion engines, requires cooling and filtering operations with equipments which greatly increase the cost of the installation.

These aspects have influenced the increased use of more external combustion steam cycles, conventional or organic Rankine for producing electricity in cogeneration mode, even if these devices are more expensive than internal combustion engines. Direct burning of gasogen doesn't requires cooling and filtering, which substantially reduces the cost of energy installations.

For small thermal power it has been designed a new type of process for micro-gasification of biomass, Reed 1985, called Top Lit Up-Draft Abbreviated TLUD. This process works with fixed bed biomass and is a combination of the classical type co-current (downdraft) and counter-current (updraft) and is characterized by an extremely low emission of solid particles and high tolerance to the type biomass used.

A TLUD generator can be coupled directly with a gas burner, resulting a thermal energy generator, hereinafter referred TLUD. It is characterized by simplicity design, small size, high functional stability, high efficiency conversion of biomass into thermal energy and with very low concentrations of CO and PM in the flue gas [1,2,4,14,15,17].

TLUD generators are used in many thermal applications from cooking stoves from 1 to 3 kW for small industrial installations with thermal power of 30-60 kW.

Because they are very tolerant to the type of biomass used TLUD generators can be widely used as thermal energy sources, clean and green in isolated areas where local biomass is abundant and easily harvested and chopped at a very low cost on average € 40 / t [5, 6,7,10].

2. Micro-gasification process TLUD

Figure 1 presents a functional diagram of micro-gasification process TLUD. Biomass layer is introduced into the reactor and is based on a grid through which, from bottom to top, passes air flow for gasification. Priming gasification process is done by ignition the top layer of biomass in the reactor, front biomass burning down continuous by consuming it. Due to the heat radiated from the combustion front biomass is heated, dried and then enters in a fast pyrolysis process that releases volatiles which burn, understoichiometric with air gasification. From the combustion of volatiles results: CO, CO₂, H₂, H₂O, CH₄ and heavy hydrocarbons called tars. Biomass, ash-free and moisture-free, contains on average 75% volatile and 25% fixed carbon. Fixed carbon do not enter in the pyrolysis and remains in the incandescent coal layer ($\approx 700^{\circ}\text{C}$) through which pass the products resulted from fast pyrolysis. They come in reduction reactions, mainly $\text{C} + \text{CO}_2 \Rightarrow 2\text{CO}$ and $\text{C} + \text{H}_2\text{O} \Rightarrow \text{CO} + \text{H}_2$, resulting in a fuel gas, hereinafter gasogen, which has an average composition: CO - 15%; H₂ - 12%; CH₄ - 2 \approx 3 and 2% \approx 3% tars, and an average temperature of 500°C . [2,3,17].

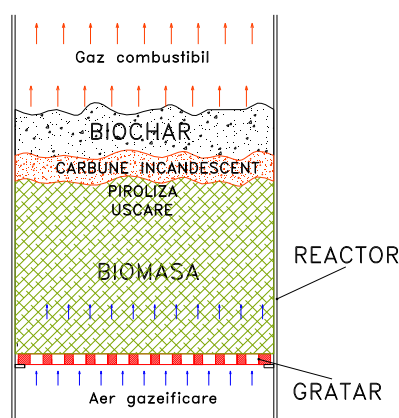


Fig.1 Micro-gasification process TLUD

When the combustion front reached the grate, all volatiles from biomass were gasified, as a part of the carbon fixed, on the grill remains about 10 to 20% hot charcoal, which is called in the scientific literature the term **biochar**.

This phase of converting biomass into fuel gas is called gasification incandescent layer.

The proportion of biochar, in which is incorporated most of the ash from biomass, depends both on the fixed carbon from the biomass and maintained the reaction temperature to reduce carbon (reaction Boudouard), a high temperature ensures reduction of more carbon. Thus in a well insulated ceramic reactor, proportion of biochar is on average $\leq 10\%$. If continuous air supply for gasification remains an incandescent layer of coal from which it results mainly CO and less CO₂ that going over hot coal reacts enters in the reduction reaction $\text{C} + \text{CO}_2 \Rightarrow 2\text{CO}$. This second phase is called coal gasification; thermal power produced is about 25% of that produced in the incandescent layer phase.

From the experiments performed it was found that the biomass consumed during pyrolysis is gasified with an energy conversion efficiency high η_{conv} 93-95%. Gasification of the biochar is performed with a energy conversion efficiency of 85-90%, lower than the first phase due to thermal losses caused by very high temperature of the resulted gasogen $\approx 1000^{\circ}\text{C}$. [2,12,13,16,17].

3. TLUD heat generators

Functional diagram of a TLUD generator with coupled burner is shown in Figure 2. The micro-gasification process is supplied with air from a variable speed ventilator. Biomass is introduced into the reactor and is based on a grid through which, from bottom to top, passes the air for gasification. Initialization process is done from the free upper layer biomass.

Thermal energy is obtained by burning hot gasogen, resulted during pyrolysis, it is mixed with preheated combustion air introduced into the combustion zone through holes located at the top of the reactor. Mixture with high turbulence burns with flame at the upper mouth of the generator with high temperature 900-1000°C. To adjust the heating power necessary it is varied the air flow D_{ag} for gasification and D_{ard} for combustion through two flaps, coupled mechanically or by varying ventilator speed. TLUD process is with fixed bed of biomass and therefore the generator operates in batch mode to recharging.

Gasification is made with a low intensity, with reduced specific consumptions 100-150 kg_{bm}/m²h leading to reduced specific powers from reactor 250 to 350 kW/m². The slow process maintains superficial speed of the produced gasogen to very low values $v_{sup} \leq 0.06$ m/s which ensures reduction of free ash for concentrations M2.5 at the exit of the burner up to 5 mg / MJ_{bm}, worth at least five times lower than current standards required for solid fuel heat generators. Since it is ensured a very good mixing of gasogen with combustion air, for an optimal excess 1.4 -1.5 in flue gas CO concentration is below 2% or 0.8 g / MJ_{bm}, value below current imposed rules. This makes the heat generator TLUD to be the least polluting production systems comparing it others thermal energy solid fuel.

This type of heat generator was developed and used in stoves to prepare food in isolated areas, working very well with a wide variety of local biomass. A notable example is the energy and environmental performance by portable stove produced by Philips, in which the ventilator is powered by electricity produced by a heat-generator with semiconductors mounted under grill, being a typical heat generator with energy independence.

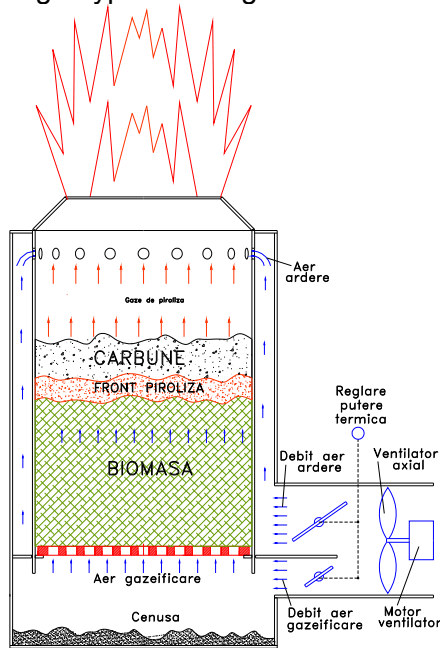


Fig. 2 Functional scheme of TLUD generator with burner coupled

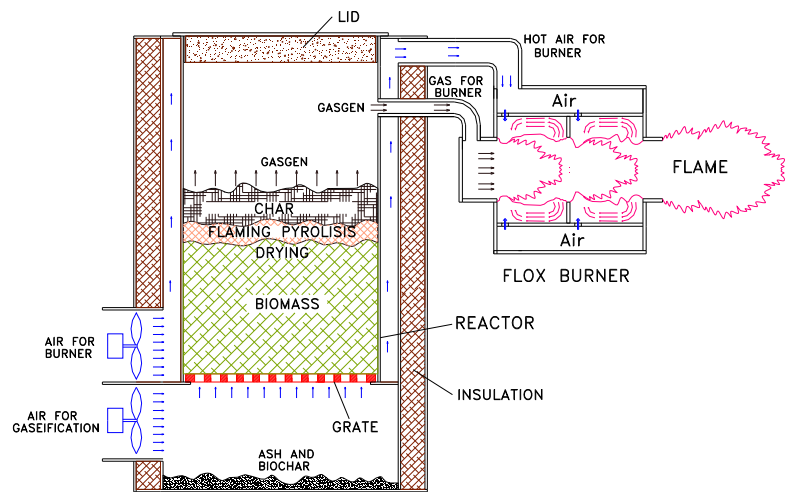


Fig. 3 Functional diagram of TLUD generator with FLOX burner

Figure 3 shows a functional diagram of a generator TLUD whose gasogen's burner is separated by the gasogen. Gasogen is a fuel gas with low caloric value and for an efficient combustion it uses specialized burners type FLOX.

To achieve thermal performance and functional requirements imposed by current industrial consumers of thermal energy, TLUD heat generator can be equipped with an automatic driving device oriented PLC. In Figure 4 is shown a block diagram of a heat generator TLUD for use in greenhouses and convective dryers. [7.10]

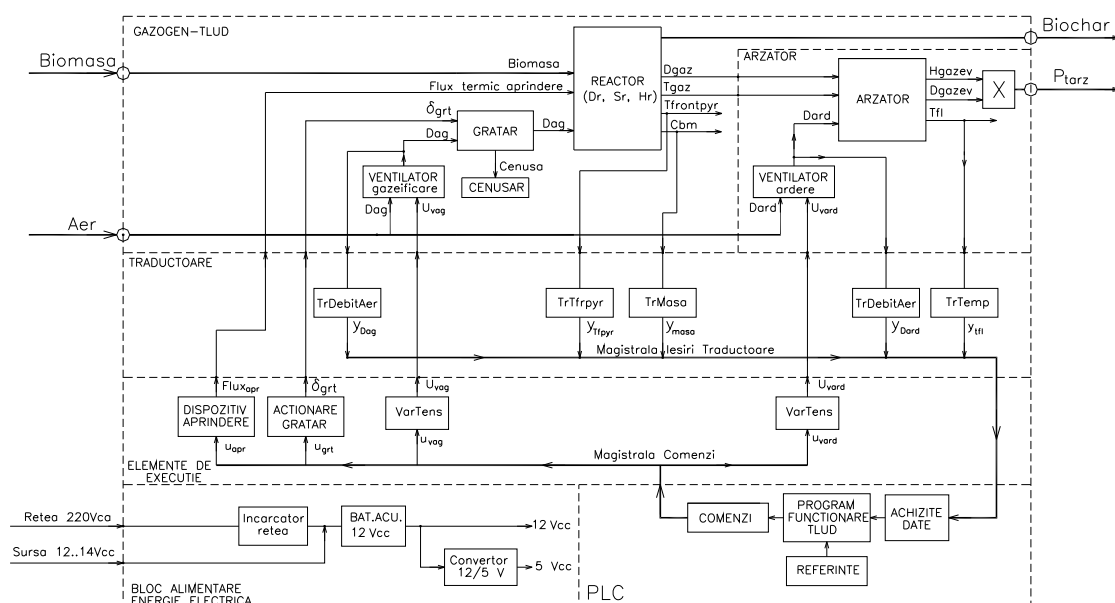


Fig. 4. Block diagram of a heat generator, TLUD

In the generator TLUD enters biomass, air for gasification and combustion and electricity. Consumed energy is at most 0.3% of the heat produced, aspect which recommends the use of TLUD thermal generators in isolated areas.

The main features from TLUD heat generator are: thermal power P_{tarz} and mass M_{bch} of biochar. Periodically must be downloaded the ash which on average represents 0.2% of the used biomass. The difference between mineral is incorporated into biochar.

Figure 5 presents a cooking stove type Oorja-Plus 20kW and Figure 6 presents an TLUD experimental generator with nominal power 30 kW. In Figures 7 and 8 are presented generators type TLUD Oorja-Jumbo (India) from 15 to 60 kW which operates with pellets from vegetal agricultural residues and are designed for food preparation and other thermal applications. [2]



Fig.5 Oorja - Plus



Fig.6 The generator GAZMER -TLUD by 30 kW



Fig.7 Oorja-Jumbo-K15



Fig.8 Oorja-Jumbo-K60



Fig.9 Battery generator TLUD 2x15 kW for bakeries



Fig.10 Battery generator TLUD 2x60 kW with burner for a convective dryer

In Figures 9 and 10 are presented generator batteries TLUD for use in bakeries and convective dryers; facilities designed, developed and conducted by Professor Alexis Belonio from the Philippines. [1]

4. TLUD Features

Biomass used in micro-gasification process TLUD separates energy and mass into two parts: part from biomass, which is completely converted into gasogen, and biochar remaining after gasification phase in incandescent layer. For example in Table 1 are presented chemical compositions and lower calorific values of biomass derived from the apple tree felling, the biochar and the part of biomass integral gasified. The ash from biomass remains in biochar and the water is part of gasified biomass.[8,9,11]

It appears that if the thermal energy production the biochar is not gaseified, it can be used only 78% from the potential energy of biomass loaded in the reactor. This is essential in choosing the operating mode of the generator TLUD: with or without biochar gasification. The two operating modes involve different materials and constructive solutions; the biochar gasification takes place at high temperatures at which must resist both reactor and grill.

Another aspect is the utilization rate of energy biomass. When the biochar has use value, both economically and environmentally, it is recommended operation mode with the production of

biochar. If it is necessary to fully utilize the available resources of energy, the biochar will be gasified, but TLUD generator will cost more or will wear out more faster.

Table 1 Properties of biomass from trimming apple trees

Size	UM	Biomass chopped	Biochar	Biomass gasified
<i>Relative mass</i>	%	100.00	15.00	85.00
Carbon	%	43.11	73.60	36.78
Oxygen	%	35.57	10.80	39.94
Hydrogen	%	5.12	2.20	5.63
Ash	%	1.20	8.00	0.00
Water	%	15.00	0.00	17.65
P.C.I.	MJ/kg	15.30	22.40	14.05
Rate of energy use	%	100	21.96	78.04

Table 2 presents the main functional characteristics of thermal generators TLUD.

Table 2 Characteristics and operating performance thermal generators TLUD

Characteristic	UM	Chopped apple-trees		Pellets	
		with biochar	without biochar	with biochar	without biochar
Density layer	$\text{kg}_{\text{bm}}/\text{m}^3$	300.00	300.00	600.00	600.00
Specific nominal consumption	$\text{kg}_{\text{bm}}/\text{m}^2\text{h}$	100.00	100.00	100.00	100.00
Ratio biochar	$\text{kg}_{\text{bch}}/\text{kg}_{\text{bm}}$	0.15	0.00	0.10	0.00
Average C content in biochar	-	0.74	0.74	0.80	0.80
P.C.I. biomass	$\text{MJ}/\text{kg}_{\text{bm}}$	15.30	15.30	16.50	16.50
P.C.I. biochar	$\text{MJ}/\text{kg}_{\text{bch}}$	22.40	22.40	24.50	24.50
P.C.I. gasified biomass	$\text{MJ}/\text{kg}_{\text{bm}g}$	14.05	15.30	15.61	16.50
Utilization rate of energy from biomass	-	0.78	1.00	0.85	1.00
Nominal energy efficiency	-	0.93	0.93	0.93	0.93
Useful specific energy	$\text{kWh}/\text{kg}_{\text{bm}}$	3.09	3.96	3.63	4.27
Specific thermal power	kW/m^2	308.78	308.78	363.35	363.35
Useful energy density	MWh/m^3	0.93	1.19	2.18	2.56
Specific emission of CO	$\text{kg}/\text{m}_2\text{h}$	5.56	5.56	6.54	6.54
Specific emissions of $\text{PM}_{2.5}$	$\text{g}/\text{m}_2\text{h}$	4.45	4.45	5.23	5.23
CO2 balance retained in the soil	$\text{kg}/\text{m}^3_{\text{bm}}$	-121.44	0.00	-176.00	0.00

Were analyzed using the operating modes with and without biochar for two types of biomass:

- Biomass from trimming apple trees (Table 1) - for example with the exact values,
- Woody biomass pellets with 8% humidity and average features.

We used the same specific biomass consumption times $C_{\text{bmh}} = 100 \text{ kg}_{\text{bm}}/\text{m}^2\text{h}$ to make a comparison of performance.

Energy efficiency in nominal mode is the product energy conversion efficiency $\eta_{\text{conv}} = 0.95$ with combustion efficiency $\eta_{\text{ard}} = 0.98$. It is a maximum value but feasible and further used to highlight maximum performance.

It appears that specific useful power output has values from 300 to 360 kW/m^2 , very low values are about 1% of the outbreaks of biomass combustion, which gives to TLUD functionally operating safety and high durability.

A specific feature of TLUD is useful energy density of reactor volume ρ_{enr} , with values from 0.93 to 2.56 MWh/m^3 , parameter is useful energy stored in biomass in the reactor. It is clear

advantage of using a biomass compacted to achieve a longer duration of operation without recharging, but with much higher costs.

The performances of TLUD ecological thermal generators are given by:

- CO emission relative to the reactor section, with the average of $6 \text{ kg.CO}_2/\text{m}^2\text{h}$, which corresponds to a $2\% \text{ CO} / (\text{CO} + \text{CO}_2)$ from the flue gases;
- Specific emissions of PM which is very low, between 4.4 and $5.3 \text{ g/m}^2\text{h}$ practically smokeless conversion of biomass into heat;
- Specific CO_2 balance corresponding biochar is incorporated as an amendment to agricultural soils, with huge values between -120 and $-180 \text{ kg.CO}_2/\text{m}^3_{\text{bm}}$ or $-400 \text{ kg.CO}_2/\text{t}_{\text{bm}}$ in regimes with biochar and obviously zero when produced biochar is gasified in the second phase.

Energy and economic difference between the two operating regimes is highlighted by the - useful energy produced from biomass - which without biochar procedure has the value 1 when is achieved with 28% more thermal energy than the first phase. If it passes the gasification phase of biochar finally get a neutral CO_2 balance.

In Table 3 are presented constructive dates, functional and economic for a TLUD generator with a reactor of 1 m perimeter they can get a heat output of 30 kW. The data in the table can be used both for comparison TLUD generators and initial calculation.

Table 3 TLUD thermal generator with burner coupled

Characteristic	UM	Minced apple-trees		Pellets	
		with biochar	without biochar	with biochar	without biochar
Diameter reactor	m	0.317	0.317	0.317	0.317
Reactor section	m^2	0.079	0.079	0.079	0.079
Nominal hourly consumption	$\text{kg}_{\text{bm}}/\text{h}$	7.892	7.892	7.892	7.892
Nominal power	kW	24.370	31.228	28.677	33.677
PM emission	g/h	0.351	0.450	0.413	0.485
CO emission	g/h	0.439	0.562	0.516	0.606
Biochar produced	$\text{kg}_{\text{bch}}/\text{h}$	1.184	0.000	0.789	0.000
CO_2 balance	kg/h	-3.195	0.000	-2.315	0.000
Price biomass processed locally	€/t	40.00	40.00	160.00	160.00
Price biomass purchased	€/t	80.00	80.00	160.00	160.00
Fuel cost from BM-local	€/kWh	0.013	0.010	0.044	0.037
Energy cost from BM purchased	€/kWh	0.026	0.020	0.044	0.037
Relative costs BM-local	%	100	78	340	289
Relative costs BM-purchased	%	200	156	340	289

An economic assessment of the costs of production by thermal energy with TLUD generators shows that the possibility of using local available biomass under normal circumstances, shredded and dried at the place of use, lead to fuel costs 2 times lower than for biomass minced bought and 3.7 times lower than for pellets.

5. Conclusions

1. The generator with micro-gasification process TLUD can use a wide variety of biomass to produce thermal energy for high energy conversion efficiency and very low emissions. Is a fixed bed process, which operates in charge mode and requires no mixing. It is much cheaper than other biomass burners, easy to maintain and with high reliability.

2. TLUD generator is the only producer of both energy and biochar which has great value in use both as agricultural amendment and for carbon sequestration in soil with a negative balance up to $-400 \text{ kg.CO}_2/\text{t}_{\text{bm}}$.

3. Use of cheap and available local biomass provides very low cost for thermal energy produced, about $13 \text{ €} / \text{MWh}$, 3.7 times cheaper than the use of pellets.

4. Adjusting thermal power of generator TLUD in range 50-100% is made through ventilators speed variation; the generator is very easy controlled from the level of operator up to automatic driving controller to a PLC.

5. TLUD generator consume electricity which is up 0.3% of the thermal energy produced, being a perfect user for external combustion cogeneration plants used in achieving energy independence.

6. This paper provides an introduction to aspects of the operation and use of thermal generators TLUD with primary data for initial calculations.

REFERENCES

- [1] (Belonio Alexis, *Rice husk gas stove handbook*, College of Agriculture, Central Philippine University, 2005
- [2] Mukunda H., ș.a, *Gasifier stoves – science, technology and field outreach*, CURRENT SCIENCE, vol. 98, no. 5, 10 march 2010
- [3] Murad Erol, *Optimisation of biomass gasification load regime*, International Conference ENERGIE - MEDIU CIEM 2005, UPB, București oct. 2005
- [4] Murad E., Safta V. V., Haraga G., *Biomass regenerating source of thermal energy for drying installations*, Conferința ISIRB, Hunedoara aprilie 2009
- [5] Murad E., Seiculescu M., Sima C., Haraga G., *Utilizarea potențialului energetic al corzilor de viță*, Conferința de Comunicări Științifice, INCVV Valea Călugărească, 10 iunie 2010
- [6] Murad E., Crăciunescu A., Haraga G., Panțiru A., *Instalații de uscare convectivă cu independență energetică bazată pe biomasă și panouri fotovoltaice*, Simpozion HERVEX 2010, Călimănești, 10-12 noiembrie 2010;
- [7] Murad E., Maican E., Biriș Ș.S., Vlăduț V., *Heating greenhouses with TLUD biomass energy modules*, 3rd International Conference „Research People and Actual Tasks on Multidisciplinary Sciences” 8–10 June 2011, Lozenec, Bulgaria
- [8] Murad E., Culamet A., Zamfiroiu G., *Biochar- Economically and ecologically efficient technology for carbon fixing*, Simpozion HERVEX 2011, 9-11 noiembrie Călimănești, ISSN 1454-8003
- [9] Murad E., Ciubucă A., Aylin C., Radu M., *Biochar-ul produs din coarde de viță amendament ecologic pentru viticultură*, Sesiunea Științifică a ICDVV Valea Călugărească, 12 iunie 2012
- [10] Murad E., Vintilă M., Crăciunescu A., *Uscătoare cu impact ecologic redus pentru zone montane*, Sesiunea de comunicări științifice – ICEDIMPH-HORTING, 20 septembrie 2012
- [11] Murad E., Achim Ghe., Rusănescu C., *Valorificarea energetică și ecologică a biomasei tăierilor din livezi*, Sesiunea de comunicări științifice – ICEDIMPH-HORTING, 20 septembrie 2012
- [12] Porteiro, J., Patino D., s.a., *Experimental analysis of the inition front propagation of several biomass fuels in fixed-bed combustor*, FUEL 89, 2010, pag. 26-35
- [13] Reed T.B., Das A., *Handbook of Biomass Downdraft Gasifier Engine Systems*, U.S Department of Energy, Colorado, 1988
- [14] Reed T.B., Walt R., Ellis S., Das A., Deutche S., *Superficial velocity - the key to downdraft gasification*, 4th Biomass Conference of the Americas, Oakland, CA, 29 aug. 1999
- [15] Reed T.B., Anselmo E., Kricher K, *Testing and Modeling the Wood-gas Turbo Stove*, Conference: Progress în Thermochemical Biomass Conversion, Tyrol, Austria, sept. 2000
- [16] aastamoinen J.J., Taipale R., Horttanainen M., Sarkomaa P., *Propagation of the Ignition Front in Beds of Wood Particles*, COMBUSTION AND FLAME 123:214–226 (2000), Elsevier Science Inc.
- [17] Varunkunar S., *Packed bed gasification-combustion in biomass domestic stove and combustion systems*, Teza de doctorat, Department of Aerospace Engineering Indian Institute of Science, Bangalore, India, feb. 2012

PNEUMATIC MEASURING OF THE BIOMASS CONSUMPTION FOR TLUD GENERATOR

Erol MURAD¹, Cătălin DUMITRESCU², Georgeta HARAGA¹, Liliana DUMITRESCU²

¹ Universitatea POLITEHNICA din București, e-mail address: erolmurad@yahoo.com

² INOE 2000 – IHP, e-mail address: dumitrescu.ihp@fluidas.ro

Abstract: *Efficient management of energy production from biomass with thermal generators and generators TLUD requires continuous measurements of biomass consumption correlated with input parameters which is air flow for gasification. As an alternative to electronic measuring systems, which in the exploitation conditions for gasogen are more expensive than the usual ones, it is analyzed the use of pneumatic force sensors at which the measured pressure is not sensitive to temperature variations.*

Measurement of biomass is performed online with a pneumatic force transducer working under sampled measurements. Measurement structure presented has very low energy consumption, specific to the technical systems with energy independence and low cost automation. The measurement system is connected to PLC for automatic driving of thermal system. Adjusting performances of the thermal generator operating mode and energy consumption for force transducer were determined by simulation experiments conducted with a simulation model and a numerical simulation program, developed in the simulation environment MEDSIMFP10. Simulation experiments confirmed low pneumatic energy consumption and a better measurement accuracy.

Keywords: *pneumatic transducer, power, biomass, TLUD, energy consumption, low cost*

1. Introduction

The production of energy from biomass is an ecological and economical method which is in competition with other sources: solar thermal and photovoltaic, wind energy, hydro or geothermal. The main advantage of biomass is that it can be produced energy with it when, where and in the necessary amounts.

At present, in parallel with up-draft and down-draft gasification systems, are developed systems based on the TLUD process that is easy to use and stable in operation; the system has the advantage of being cheap and recently revealed that produces an unconverted carbon quota called biochar, which if is introduced in soil represents a great soil amendment and contributes to the increase of land fertility and through carbon sequestration in soil relatively large periods of time contributes directly to the reduction of the CO₂ in the atmosphere. A TLUD thermal generator consists of a generator with TLUD process of micro-gasification of biomass which produces fuel gas which is combusted in a burner directly coupled to the generator. [2,8,9]. The automatic management of thermal power generation process requires the measurement of biomass C_{bm} consumption (kg_{·bm}/s) and air flow D_{ag} for gasification (kg_{·aer}/s). TLUD thermal modules require very little electricity to operate, maximum 0.3% of rated thermal power, TLUD being the thermal energy source suitable for installations with energy independence used in agriculture and isolated areas. [1,3,7,8]

This paper presents and analyzes the operation and performances of a measurement scheme online for the weight of a TLUD generator that uses a pneumatic force transducer working under sampled mode. The solution presented is characterized by very low energy consumption, low price and a measurement error $\leq 2\%$. The measurement system is connected to the PLC dedicated to automatic management of thermal system.

2. Thermal generator with TLUD gasogen

An ecological and economical alternative for biomass gasification is the process of micro-gasification TLUD (Top-Lit Up-Draft), designed by Thomas Reed in 1985. In this TLUD process

biomass layer is fixed in the reactor and the oxidation and pyrolysis front continuously descends consuming biomass, features that ensure safe operation and controllers. Operation is in batches with acceptable variation thermal load from 50 to 100%. In Figure 1 is a functional schematic diagram for a thermal module TLUD and in Figure 2 a thermal module GAZMER FORTE-30. [8]

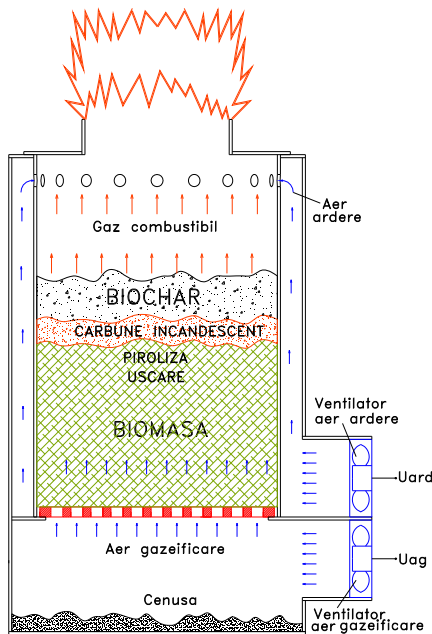


Fig. 1 Schematic functional of a thermal module TLUD



Fig. 2 Thermal module TLUD by 30 kW

G_{MGB} weight thermal module is the weight of the generator and burner G_G and the weight of the biomass and biochar G_{bm} from reactor:

$$G_{MGB} = G_G + G_{bm} = g \cdot (M_G + M_{bm}) \quad (1)$$

CG_G center of gravity is fixed as position but the center of gravity CG_{bm} volume of biomass is offset horizontally by $\pm e_{bm}$ (figure 3); therefore the center of gravity position CG_{MGB} thermal module is between CG_G and CG_{bm} shifted horizontally by $\pm e_{MGB}$ (m). It follows that there is an eccentricity between CG_G and horizontal positions CG_{bm} . Calibration of the weighing system is done with G_G value which is known. When biomass is loaded, thermal module center of gravity moves in CG_{MGB} which is offset from the CG_G with e_{MGB} that will have a value of:

$$e_{MGB} = e_{bm} \frac{G_{bm}}{G_G + G_{bm}} \quad (2)$$

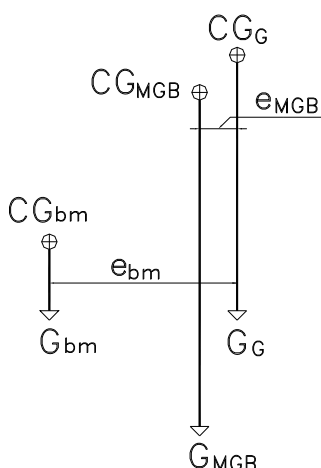


Fig. 3 Diagram of positions for centers of gravity

) value decreases during operation due to biomass consumption and weight reduction G_{bm} . This function will affect measurement accuracy.

of the gasification process, about 3 -10 min, after that the pneumatic sensor doesn't be need to supplied with compressed air. Reading the transducer output voltage y_G is realized in PLC with a frequency ≥ 10 Hz.

For measurement of biomass consumption, the gasogen 1 is positioned on a support 2 which is leaned on two ball bearings 3 and on another support 4 type knife-wedge, on the lever of weighing 5 which has one end resting on base and the other end resting on the pneumatic force transducer 6 which is connected to the interface block 7 through which the compressed air supply to pressure p_{ai} and measuring signal exits Y_G . Vertical center of gravity CG_{MGB} is at the distance L_1 from supports 3. The distance between 3 and 4 supports is L_2 . The measured force F_{mas} applied to the transducer has the value:

$$F_{mas} = (G_G + G_{bm}) \cdot \frac{L_3 \cdot L_1}{L_4 \cdot L_2} = (M_G + M_{bm}) \cdot K_F = F_{masG} + F_{masbm} \quad (3)$$

where: M_G and M_{bm} – weight of gasogen and biomass (kg);

K_F - transfer factor of the weighing machine (s/m²);

F_{masG} – the component due to gasogen (N);

F_{masbm} – the component due to biomass (N);

Biomass consumption dM_{bm} / dt (kg/s) in the variant of sampled reading with Δt will be:

$$\frac{\Delta M_{bm}}{\Delta t} = \frac{1}{K_F} \cdot \frac{\Delta F_{mas}}{\Delta t} \quad (4)$$

Electrical output interface has the value y_G (V):

$$y_G = F_{mas} \cdot K_{TR} \quad (5)$$

Where: K_{TR} is transfer factor of force transducer (V/N).

The measured biomass consumption $C_{bm\ mas}$ (kg/s) is calculated using:

$$C_{bm\ mas} = \frac{\Delta M_{bm}}{\Delta t} = \frac{1}{K_F \cdot K_{TR}} \cdot \frac{\Delta y_G}{\Delta t} \quad (6)$$

At calibration:

$$\text{when : } G_{bm} = 0 \text{ results } L_1 = L_{1ini} = \text{const.} \quad (7)$$

Because there is an eccentricity $\pm e_{MGB}$ between CG_G and horizontal positions CG_{MGB} , in this case transfer factor K_{Fbm} for biomass will have a value of:

$$K_{Fbm} = (L_{1ini} \pm e_{MGB}) \cdot \frac{L_3}{L_4 \cdot L_2} = (1 \pm \varepsilon_{MGB}) \cdot \frac{L_{1ini} \cdot L_3}{L_4 \cdot L_2} = K_F \cdot (1 \pm \varepsilon_{MGB}) \quad (8)$$

where ε_{MGB} is the relative eccentricity:

$$\varepsilon_{MGB} = \frac{e_{MGB}}{L_{1ini}} = \frac{e_{bm}}{L_{1ini}} \cdot \frac{G_{bm}}{G_G + G_{bm}} \quad (9)$$

Considering that $e_{bm}/L_{1ini} \leq 0.1$ and $G_{BM} \leq 0.25 G_G$ it results:

$$\varepsilon_{MGB} \leq 0.1 \cdot \frac{0.25 G_G}{G_G + 0.25 G_{bm}} = 0.02 = 2\% \quad (10)$$

Measured biomass consumption $C_{bm\ mas}$ is:

$$C_{bm\ mas} = \frac{\Delta M_{bm\ mas}}{\Delta t} = \frac{1}{K_{Fbm} \cdot K_{TR}} \cdot \frac{\Delta y_G}{\Delta t} = \frac{1}{(1 \pm \varepsilon_{MGB}) K_F \cdot K_{TR}} \cdot \frac{\Delta y_G}{\Delta t} = \frac{1}{(1 \pm \varepsilon_{MGB})} C_{bm} \quad (11)$$

It follows that the actual consumption of biomass C_{bm} is:

$$C_{bm} = C_{bm\ mas} \cdot (1 \pm \varepsilon_{MGB}) \quad (12)$$

Considering that at the start of the gasification process, the maximum value for $\varepsilon_{MGB} \leq 0.02$, or 2%, and decreases continuously at the end of the process, it can be accepted that it is possible

to use efficiently for calculating primary energy consumption and optimal management of thermal generator. An important index in generator TLUD is the ratio of air flow D_{ag} and mass flow of gasified biomass C_{bm} ; this report is noted with A/F and has an average value of 1.5. A/F will be estimated in the field (1.428; 1.579) as acceptable because the stoichiometric air flow that is specific real gasified biomass varies in the exploitation by $\pm 10\%$, much more than the measurement error of biomass consumption. To validate the proposed solution was made a simulation program for thermal generator GAZMER FORTE - 30 with weight $M_G = 85$ kg and a maximum load of pellets $M_{bm0} = 40$ kg. It used a pneumatic force transducer with nominal size measurement $F_{masn} = 50$ N and $K_{TR} = 0.06$ (V/N). That mechanical balance factor transfer value must $K_F > 24.50$ and was chosen constructive $K_F = 25.00$. To ensure the best possible measurement accuracy has been chosen a pneumatic capacity $V_{ad} = 500$ cm³, leading to mitigate errors due to imperfections valve-ball settlement.

5. The results of simulated experiments

From the simulation it results that the maximum acceleration lifting the nozzle is only 97.5 mm/s² and maximum lift $h_{max} = 0.272$ mm. It appears that the movement period of the nozzle is up to 4 s, and then measuring chamber pressure remains constant and proportional to the force measured $F_{mas}(t)$. The relocation of nozzle on the ball is made damped at a zero speed virtually, which doesn't produce shocks in operation and deformation in the contact area nozzle-ball, ensuring high durability for the transducer. Distributor DP is open only 2 s and it is consumed in the startup sequence measuring only 2.257 Ncm³ air.

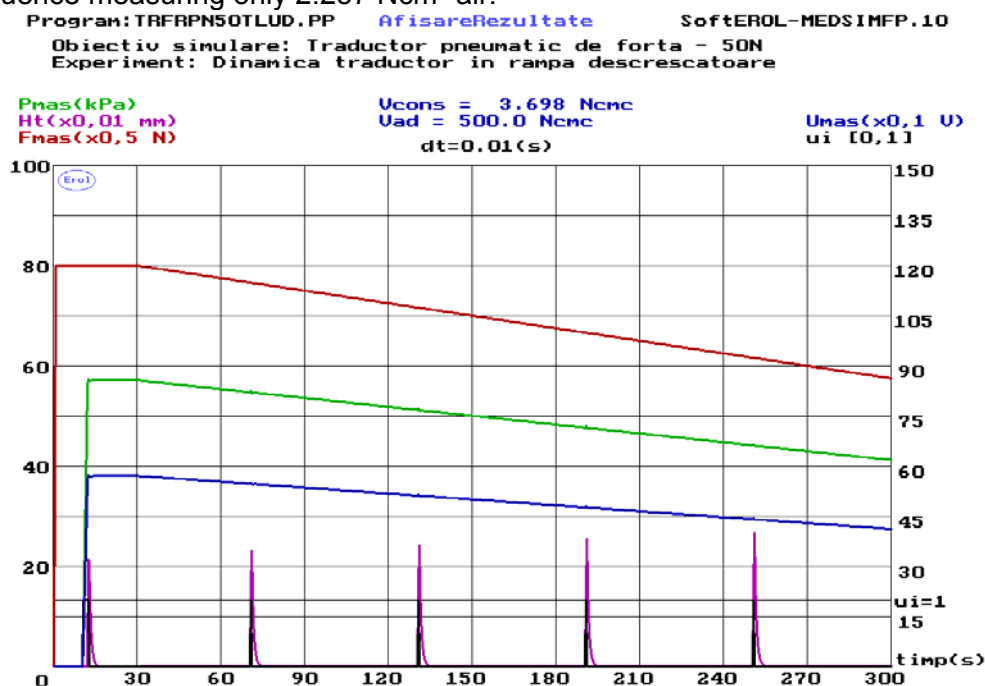


Fig. 7 Experiment measuring the consumption of biomass $dM_{bm}(t)/dt < 0$

In Figure 6 is presented a simulated experiment when the weight of biomass decreases continuously and slowly.

Assuming that between two commands for opening distributor DP, pressure can greatly decrease due to leaks and wear, air consumption per hour would be up to 135.42 Ncm³/h, which is a very small volume. For example, in continuous operation for 24 hours would consume 3.25 Ndm³ air, which would require a tank by 2 dm³ which is loaded once a day at 3 bar.

6. Conclusions

It was designed a measuring biomass consumption device for gasogen TLUD in which has been used a pneumatic force transducer designed especially for processes with slow variation measured force, something typical for biomass consumption in TLUD.

To simplify and cheapen constructive solution it was used a single force transducer; the software calibration makes all calibration operations on each recharge of batches of biomass, which provides a maximum error of 2%.

It results from simulation experiments that a transducer with full scale 50 N can operate continuously 24 hours supplied from a 2 liter reservoir loaded to 3 bar once a day.

The measurement system presented operates with very low pneumatic energy consumption, is simple, cheap, durable, and lightweight gauge.

REFERENCES

- [1]. Adams S., Meyer G., Fitzgerald J., 2008. *Biomass Heating in the Commercial Greenhouse*. University of Nebraska, Biological Sciences Engineering, 2008
- [2]. Mukunda H. s., ş.a, 2010. *Gasifier stoves – science, technology and field outreach*, CURRENT SCIENCE, vol. 98, no. 5, 10 march 2010
- [3]. Murad E., Chercheş T., *Traductoare pneumatice neconvenţionale cu consum redus de energie pentru măsurarea forţelor din instalaţii agricole şi în industria alimentară*, HERVEX 2008, Călimăneşti 15-17 noiembrie 2008
- [4]. Murad E., Maican E., Marin A., Dumitrescu C., *Dinamica traductoarelor pneumatice cu consum redus de energie pentru măsurarea forţelor în procese lente*, HERVEX 2008, Călimăneşti 18-20 noiembrie 2009
- [5]. Murad E., Dumitrescu C., Haraga G., Dumitrescu L., *Pneumatic metering systems for amount of water extracted in convectiv drying processes*, International Scientific Conference Conference - DTMM, Iaşi, 14 -16 mai 2010
- [6]. Murad E., Dumitrescu C., Haraga G., Dumitrescu L., *Traductoare pneumatice pentru masurarea vitezei de uscare a materialelor ceramice*, SINUC 2010, Al XVI-a Simpozion National de Utilaje pentru Construcţii, Bucureşti, 16-17 decembrie 2010
- [7]. Murad E., Maican E., Biriş S.S., Vlăduţ V., *Heating greenhouses with TLUD biomass energy modules*, 3rd International Conference „Research People and Actual Tasks on Multidisciplinary Sciences” 8–10 June 2011, Lozenec, Bulgaria
- [8]. Murad E., Dragomir F., *Generatoare termice cu gazogen TLUD pentru producerea din biomasă a energiei cu un bilanţ negativ de CO₂*, HERVEX 2012, Călimăneşti 7-9 noiembrie 2012
- [9]. Varunkunar S., (2012) Packed bed gasification-combustion in biomass domestic stove and combustion systems, Teza de doctorat, Department of Aerospace Engineering Indian Institute of Science, Bangalore, India, feb. 2012

MONITORING OF ENVIRONMENTAL FACTORS AT VEGETABLE OILS PRODUCING UNITS

Ass.Prof.phd.eng.Gabriela SIMION¹, eng.Alina COLAN¹, lect. phd.eng.MihaelaFlorentina DUTU¹

¹ University Politehnica of Bucharest, Biotechnique Systems Departament, e-mail: gacsimion@gmail.com

Abstract: *The activity in vegetable oil producing is necessary to be monitored and controlled in order to see its impact on environmental factors. The main sources of pollutants in the production activities of vegetable oils are industrial and domestic wastewater, the combustion gases resulting from thermo power plant, dust in the processing of raw materials, waste resulting from the technological process.*

Keywords: *environment factors, monitoring, vegetable oils, pollutants, waste water.*

1. Introduction

For environment factors monitoring ,a permanent supervision is necessary .Emitted pollutants for each factor of the environment (water, air, soil) are compared to the limits and threshold values, laid down by the legislation in the field of environmental protection. In oil industry , there are monitored parameters as energy consumption, water consumption,the volume of waste water,the level of emissions to water and air,the amount of solid waste resulting,consumption of dangerous substances.[4]

2. Technology Flow in Vegetable Oils Industry and Monitored Factors

- Oilseeds processing:
 - husking and grinding;
 - pressing - hot pressing
 - cold pressing
 - extraction with solvents
 - Refining crude oil:
 - Neutralization and tooth whitening
 - Vinterization
 - Deodorization
 - Final filtration and bottling of the refined oil
 - Splitting soap stock from refining and producing fatty acids.[5]

The monitoring objectives are the basis for determing what parameters will be measured.In technological processes for vegetable oil production, the objectives that may specify concentration of material in suspension in waste water , energy consumption , pollutants in air emissions.Knowing what to measure , another important questions is „When and how frequently should be measurements be taken?”.Samples are collected from different levels of vegetable oil production and there are estimated mean and maximum concentration during the year.[4]



Fig.1 Technological Process Flow for Vegetable Oil

The vegetable oil processing include preparation of raw materials including husking, cleaning, crushing and conditioning. The extraction process is mechanical, after boiling the liquid oil is skimmed, pressed and filtered. Residues are conditioned(generally dried) and are reprocessed to yield by-products such as animal feed.Crude oil refining includes degumming, neutralization, bleaching, deodorization and further refining.

A good monitoring system includes data relating to operating conditions, analytical methods for sampling and measurements. For data acquisition some tests are necessary and measurement pH meter - for measuring the pH of wastewater,Turbidimeter for measuring the turbidity particulate astewater.equipments as Gas Analyzer used to measure emissions ,Portable Monitor for measuring waste. Measurements in the case of air emissions will be made annually, and in case of wastewater, the analyses will be periodically repeated at 6 months.

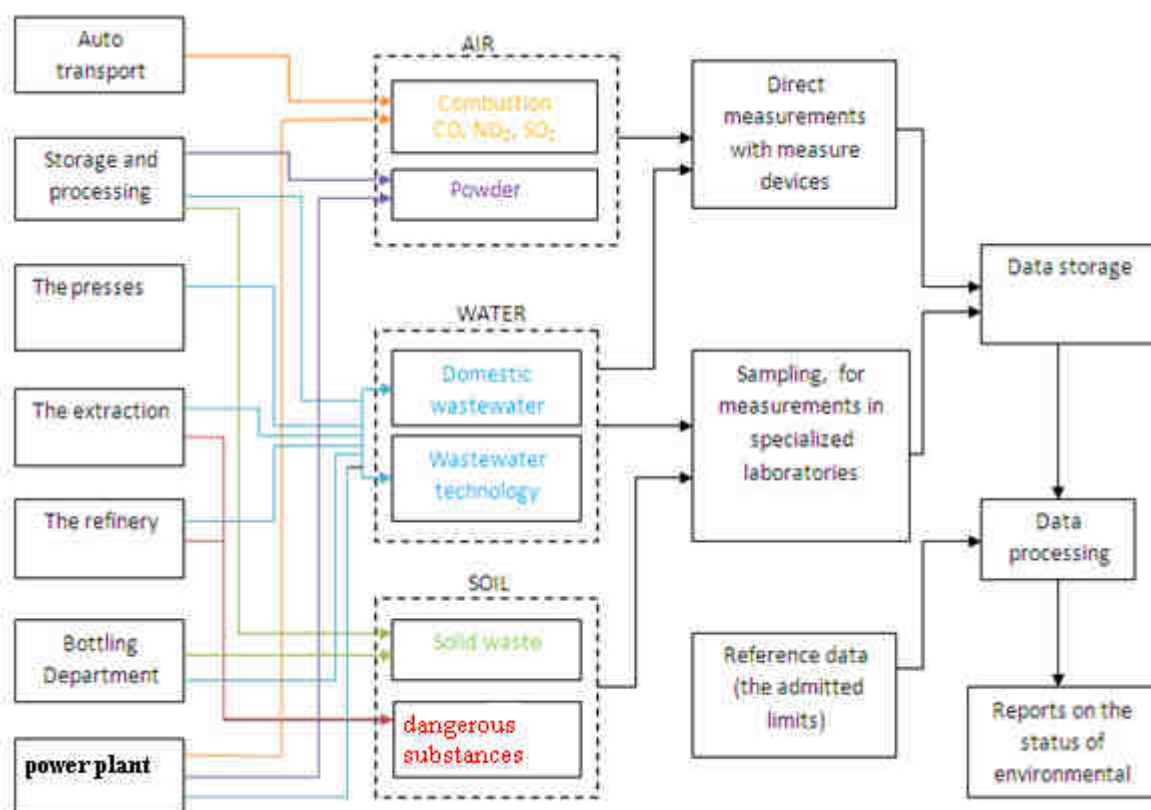


Figure 2. Monitoring of Environment Factors For Vegetable Oil Production Levels

3.The emission of pollutants into waters

As a result of conducting commercial activity within the company result the following types of wastewater:

- wastewater technology
- domestic wastewater
- cooling waters

For water pollution is watching the indicators:

- Biochemical oxygen consumption
- Materials in suspension
- Extractable substances

Table 1

source of pollution	total water consumption [m ³ /year]	CBO5 [Kg/year]	Materials in suspension [Kg/year]	Extractable substances [Kg/year]
Department presses	14.488	289	320	122
Mining Department	608.090	4.692	12.138	8.251
refinery Department	188.262	1.908	22.027	4.423
bottling Department	72.013	2.118	4.337	2.824
permissible limits [mg/l]	-	300	350	500

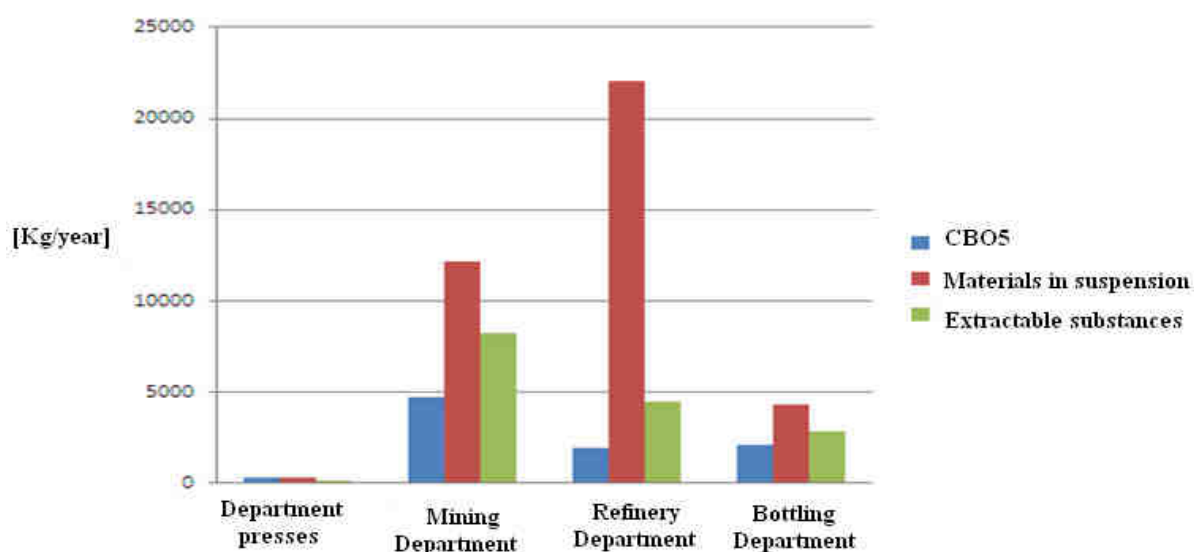


Figure 3. Indicators of Wastewater Pollutants Chart within the Production Sections

4.The emission of pollutants into the air

The sources of pollution of the environment factor "air" within the unit are:

- burnt gases discharged from thermo power plant
- burnt gases discharged from the exhaust pipes of cars and locomotives in operation equipment
- the gases of the extraction of oil from the broken
- dusts resulting from the operation of cleaning of raw material

Burnt gases discharged from thermo power plant:

a) fuel used – methane gas

The amount of fuel used annual is 5.998.130 m³

Table 2

type of pollutant	concentrations and mass flows determined			maximum allowable concentration
	mg/Nm ³	kg/h	kg/ year	mg/Nm ³
particulate matter	1	0.106	839.5	5
CO	6	0.634	5.021.28	100
NO2	265	28.002	221.760.00	350
SO2	—	—	—	35

b) fuel used - peel of seeds

The amount of fuel used annual is 12.784.4 t

Table3

type of pollutant	concentrations and mass flows determined			maximum allowable concentration
	mg/Nm ³	kg/h	kg/ year	mg/Nm ³
particulate matter	2.50	0.123	974.2	5
CO	91.00	4.488	35.544,9	250
NO ₂	293.50	14.475	114.642	500
SO ₂	17.85	0.880	6.969,6	2.000

Burnt gases discharged as a result of the operation of auto. The amount of fuel used annual:

- 51.194 l gasoline;
- 124.030 l diesel.

Pollutants discharged in are the following:

Table 4

FUEL	M.U.	CO	NO ₂	VOC	particulate matter	SO ₂	CO ₂
GASOLINE	kg/1.0001	74	25	44.3	-	-	2.300
DIESEL	kg/1.000 1	11	25	4.45	1.56	3.24	2.800

5. Establishment of waste

In the wake of technological process result the following scrap:

- Peel of sunflower seeds, 12.784.4 t/year, used as fuel in the thermo power plant. After burning operation resulting the ashes - 1.151 t/year

Other types of waste products are given in table 5.

Table 5

The waste type	Amount [Kg/year]
mucilages	258.580
residual mud	132.617
shards of glass	105.400
scrap iron	152.690

bronze	43
cast iron	10.950
copper	258

Conclusions:

Pollution prevention practices in vegetable oil industry focus on reducing production energy losses, fat concentration and material in suspension from waste waters and gas pollutants emission in the air. These demands will lead to compliance with emissions requirements. For this is important to monitor key production parameters, design and operate the production system to achieve recommended wastewater loads, recirculate cooling waters, collect wastes for use in by-products or as fuel.

REFERENCES

- [1] G. Simion "Environment Factors Monitoring and Control ", *Matrix Edition*, Bucharest, 2012
- [2] "Vegetable Oil Processing", Pollution Prevention and Abatement Handbook WORLD BANK GROUP July 1998 pages 430-432
- [3] - [http://www.ifc.org/ifcext/enviro.nsf/Content/Environmental Guidelines](http://www.ifc.org/ifcext/enviro.nsf/Content/Environmental%20Guidelines)
- [4] Report on the study of environmental impact assessment "Extraction factory of vegetable oils" Timisoara, elaborated by S.C. Tellus Adviser S.R.L. 2009
- [5] <http://extractive.wikispaces.com/file/view/Fabricarea+uleiului+de+floarea-soarelui.pdf>

EXPERIMENTAL RESEARCH TO VALIDATE THE SIMULATION MODEL HYDRAULIC TRANSMISSION FOR WIND TURBINES SMALL ADAPTIVE PRESSURE CONTROL ON CALCULATION ERRORS

Vasile DAMASCHIN¹, Mihai AFRĂSINEI¹, Constantin CHIRIȚĂ¹, Andrei GRAMA¹

¹ Tehnical University "Gheorghe Asachi" from Iassy, e-mail address automecanica_iasi@yahoo.com

Abstract: To validate the accuracy of the results obtained by numerical simulation model, experimental investigations aim to determine the step responses of the transmission to change the input parameters (speed of the turbine shaft and load shaft hydraulic motor). To this end, Adaptive hydraulic transmission system was materialized on experimental stand. This stand is made study dynamic behavior of the system under real conditions. *Experimental procedure is done basically by the same way as in the experiment by numerical simulation.*

Keywords: hydraulic transmission, pumps with variable flow rate, wind turbine

1. Introduction

Experimental procedure is done basically by the same way as in the experiment by numerical simulation.

Designed experimental bench work were introduced two modules (Figure 2.1) and filtering module and a module for open circuit. Filtration module fitted with electric pump 5 is designed to filter oil returning to the tank from the pump off and drain pump. Open circuit module is provided additionally to enable bench and other elements of the composition of hydraulic transmission. In experimental work, this module is not used for research purposes pursued.

2. Presentation the stand of experimental

Overview, experimental stand components are shown in Figure 2.2, where the observed location of the stand closed circuit module being visible double pump 12, the turbine rotor simulation module 13 and pump control mechanism. On the left side of the figure is shown the load module. Location of various hydraulic components would be tested experimentally is the mass M T channel, the module is powered by a constant flow pump 6 (Figure 2.1), driven by an asynchronous electric motor 3.

Specifications:

Load Module	maximum flow rate:	20 l/min
	maximum pressure:	300 bar
Closed loop mode:	variable work flow rate:	0...27 l/min
	maximum pressure:	300 bar
Open circuit mode:	nominal flow rate:	40 l/min
	maximum pressure:	150 bar
Filtering module:	nominal flow rate:	11 l/min
	maximum pressure:	10 bar

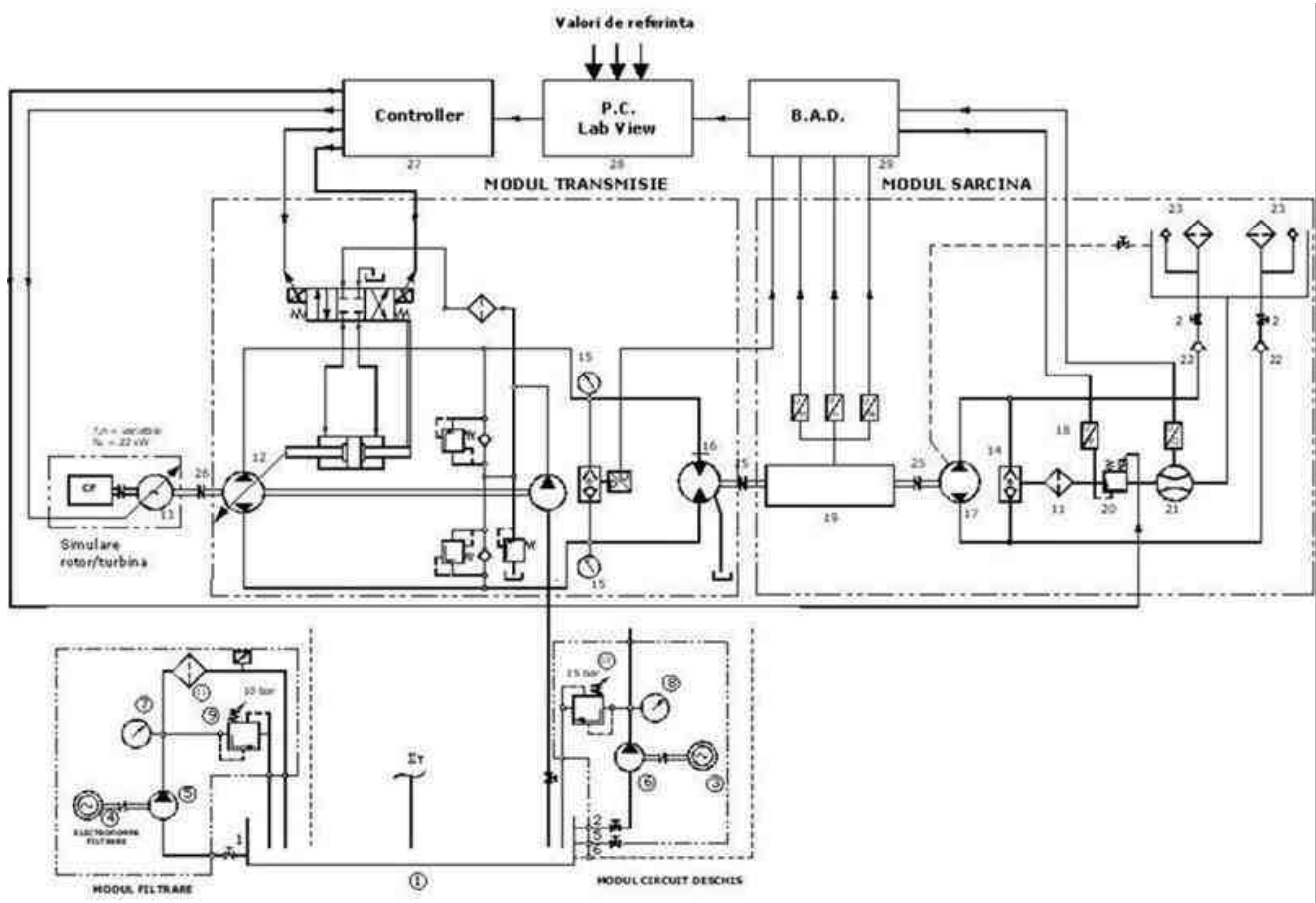


Fig. 2.1. Experimental stand hydraulic transmission scheme automotive proposed adaptive

Structural elements of the hydraulic system names are set out below:

- | | |
|--------------------------------------|---|
| 1 Check valve | 13 Principal tank |
| 2 Pressure gauge Ø100, 0-400 bar | 14 Ball valve |
| 3 Axial piston unit | 15 Three-phase asynchronous electric motor, 11 kW, 1440 rot/min |
| 4 Axial piston unit | 16 Three-phase asynchronous electric motor, 0.75 kW, 1440 rot/min |
| 5 Pressure transducer | 17 Gear pump |
| 6 Transducer speed, torque and power | 18 Vane pump $V_g = 27.4 \text{ cmc/rot}$ |
| 7 Proportional pressure valve | 19 Pressure gauge Ø100, 0-25 bar |
| 8 Flow rate transducer | 20 Pressure gauge Ø100, 0-400 bar |
| 9 One-way valve | 21 Piloted valve pressure |
| 10 Suction filter (strainer) | 22 Piloted valve pressure pilotată |
| 11 Tank load mode | 23 Pressure filter |
| 12 Coupling type SINGLE FLEX | 24 Axial piston pump in closed circuit |

The data acquisition and control include the following:

1. Transducers (sensors)
 - a. Pressure transducer output signal unified
pressure input 0-400 bar out 4-20 mA

accuracy class $\pm 0.25\%$ BFSL

b. Flow rate transducer with signal output in unified
flow rate input 10-318 l/min out 4-20mA

working pressure 0-400 bar
accuracy class $\pm 0.25\%$ BFSO

c. inductive speed sensor
speed input 0-3000 rpm out 4-20mA
accuracy class $\pm 0.15\%$ BFSO

2. *Distribution system National Instruments Compact FieldPoint*

a. Controller cFP 2020

CPU Clock	75 MHz
System Memory	32 MB
Flash	512 Mb
Ethernet	1
RS232	3
RS485	1
Operating system	LabVIEW Real Time

b. Analog modul cFP AIO 600

Analog input

Channels	4
Mesh resolution	12 bits
Sampling frequency	1.7 kS/s (1.7 kHz)
Input	4 mA , 20 mA
Sensitivity	3.91 μ A

Analog output

Channels	4
Mesh resolution	12 bits
Output	4 mA , 20 mA
Sensitivity	3.91 μ A
Output frequency	1.7 kS/s (1.7 kHz)

3. *Acquisition board NI DAQ DAQCard-6036E*

Analog input

Channels	16
Mesh resolution	16 bits
Sampling frequency	200 kS/s
Input	10 V
Sensitivity	4.26 mV

Analog output

Channels	2
Mesh resolution	16 bits
Output	10 V
Sensitivity	2.547 mV
Output frequency	1 kS/s

4. *Computing system type IBM PC x86*

5. *Software*

S.O Microsoft Windows XP SP 3
x86 LabView 8.5
LabView 8.5.1 Real Time

Note

System control and data acquisition was detailed only for functions that have been used in experimental research.

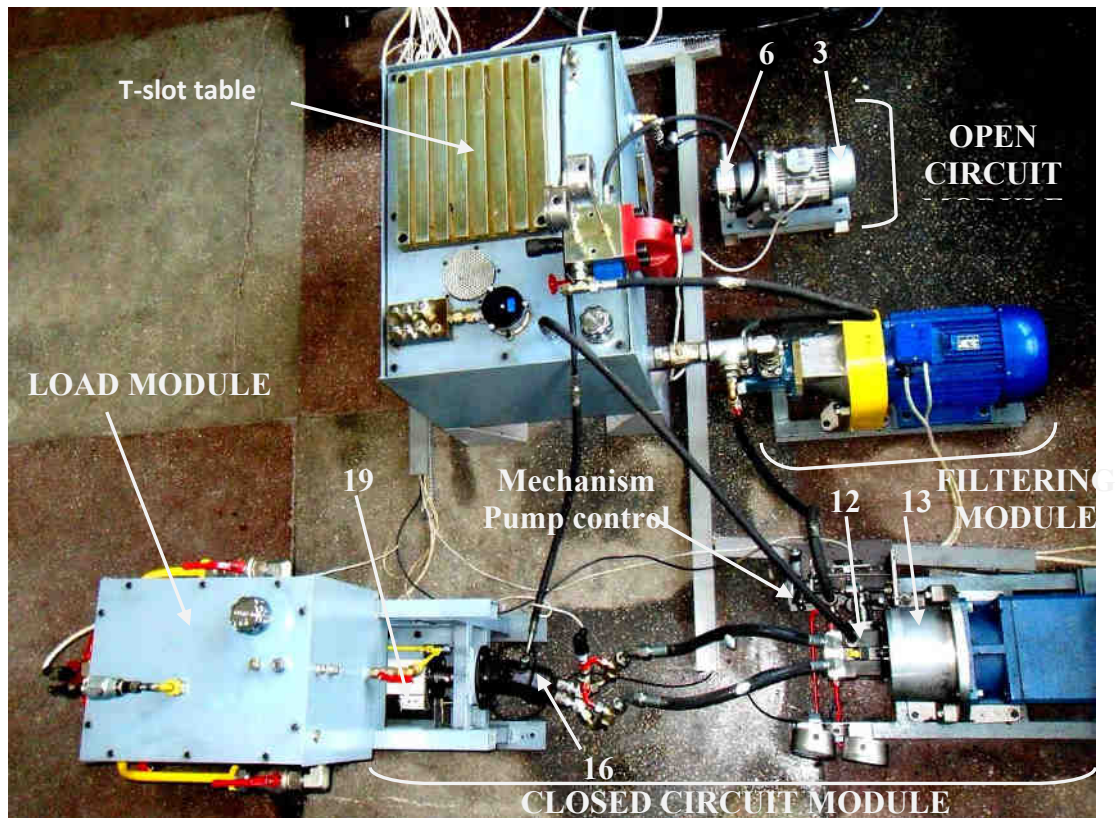


Fig. 2.2 Overview top of the stand

An important component of the experimental stand is the automatic control loop presented as a block diagram in Figure 2.3.

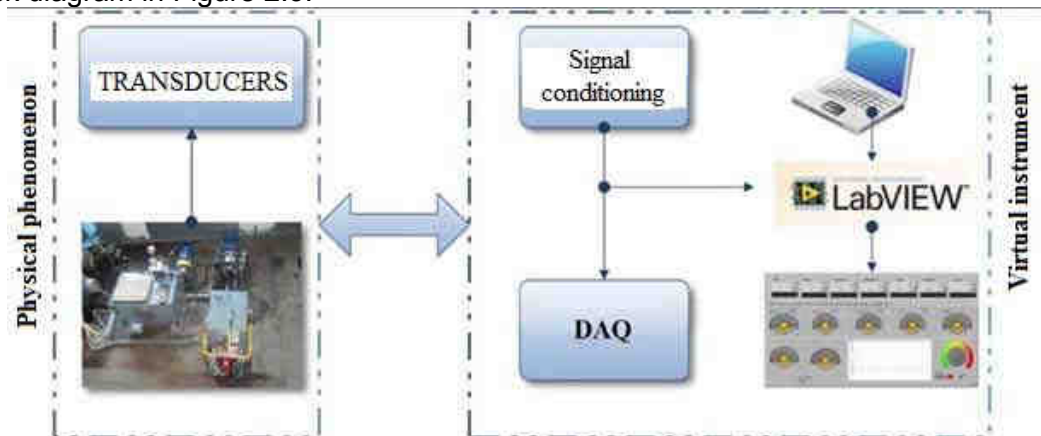


Fig. 2.3 Block diagram of the automatic control loop

Physical phenomenon and receiving transducers convert physical quantity (pressure, flow rate, etc..) In a size other mainly in voltage, the resulting signal is proportional to the size variation monitored.

Conditioning modules provide electrical signals generated by the transducers in a form that acquisition DAQ board can accept. Examples of signal conditioning is amplification, linearization, filtering, isolation, etc..

Acquisition board to convert electrical signals through its basic component, analog-to-digital converter. It attaches a numerical value to a voltage, thus making it possible to interpret the computing system.

Virtual tool work bench consists of the hardware - digital analog converter (Compact FieldPoint distribution system [1] and data acquisition board NiDAQ [2]) and the software taken in

conjunction with the needs of working hydraulic stand. The resulting virtual instrument comprises measuring devices and controls for plant automation. The graphical interface of this program included controls and indicators made in a form similar graphics devices and real devices, the user manevrându also their real elements.

Virtual instrumentation associated hydraulic stand was developed using LabVIEW graphical programming environment [3], used mainly for signal acquisition, measurement and analysis graphical or tabular presentation of data.

The front panel, shown in Figure 2.4, comprises a series of bar graphs to visualize signals scaled unit corresponding physical quantity monitored through hardware part that receives signals from transducers mounted hydraulic bench. Also through the front panel numeric input, or through a virtual potentiometer, setpoint (SETPOINT) control system. The front panel was created using display elements and control procedures extracted from library LabVIEW programming environment and a range of filtering procedures and interpretation of signals [4], adapted to the experimental stand.



Fig.2.4 Front panel [4]

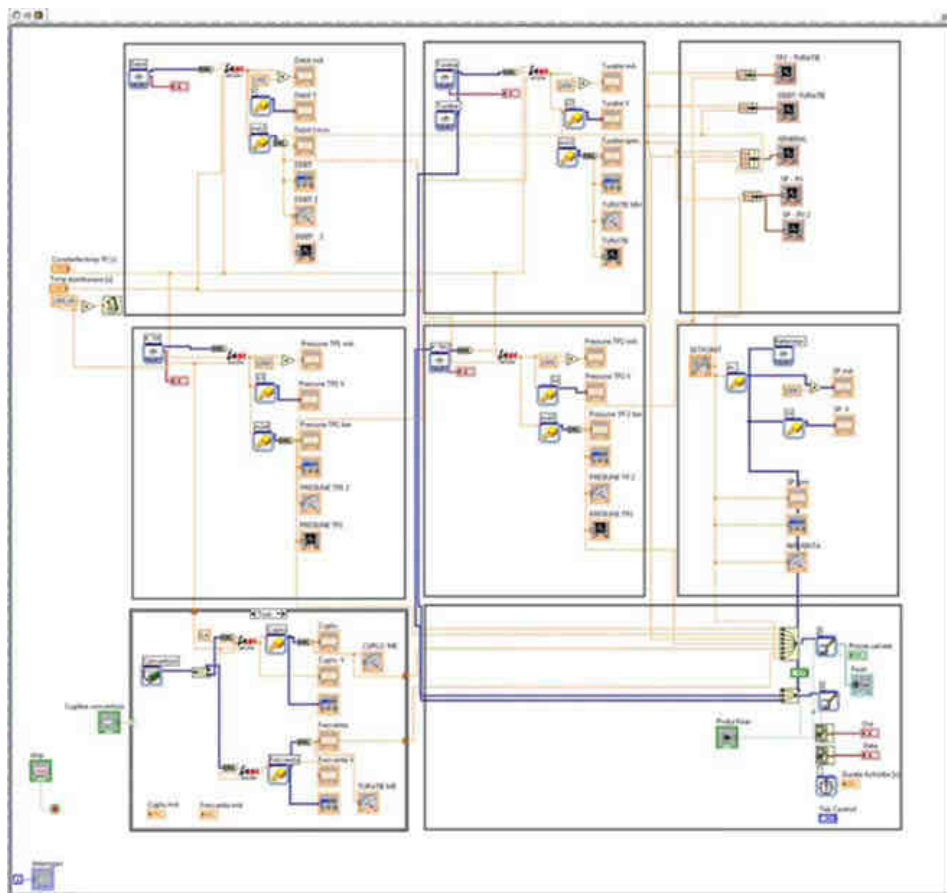


Fig.2.5 Virtual instruments - Block diagram [4]

Data obtained during the experiment can be viewed in numerical form (the top - Figure 2.5), as appropriate indicators measured quantities or as my graphic window created for this purpose.

3. The adjustment calculation errors

From the answers provided in Ch.4, in which, after the transitional regime, the engine speed practical it overlaps the speed of reference, in the case of real system response system is achieved with some deviation from the reference value, even in the period of stabilization in running through the adjusting system.

For calculating the steady adjusting errors using a spreadsheet program MS Excel. The manner to achieve the calculation example is presented graphically on the methodology used (Figure 5.23), which emphasize the area transient (A, B) and stationary zone (C):

► The area of transient - A, B - represents the period from the disruptive element up to stabilize the value of the reference system of the motor. Transitional regime ends when the response (spindle engine speed hydraulic motors) falls within a limit (non-standard) $\pm 1 \dots \pm 5\%$ from the reference value. In practice, the transitional regime cease when the answer can no longer exceed the limits for hysteresis.

A - natural response of the system to perturbation, B - Override.

► The stationary regime - C - represents the hydraulic motors spindle speed constant and the disruptive factor influence came to an end. The static scheme reported in tests on hydraulic stand is nonlinear, fits within the hysteresis of $\pm 1 \dots \pm 5\%$ compared to the reference value.

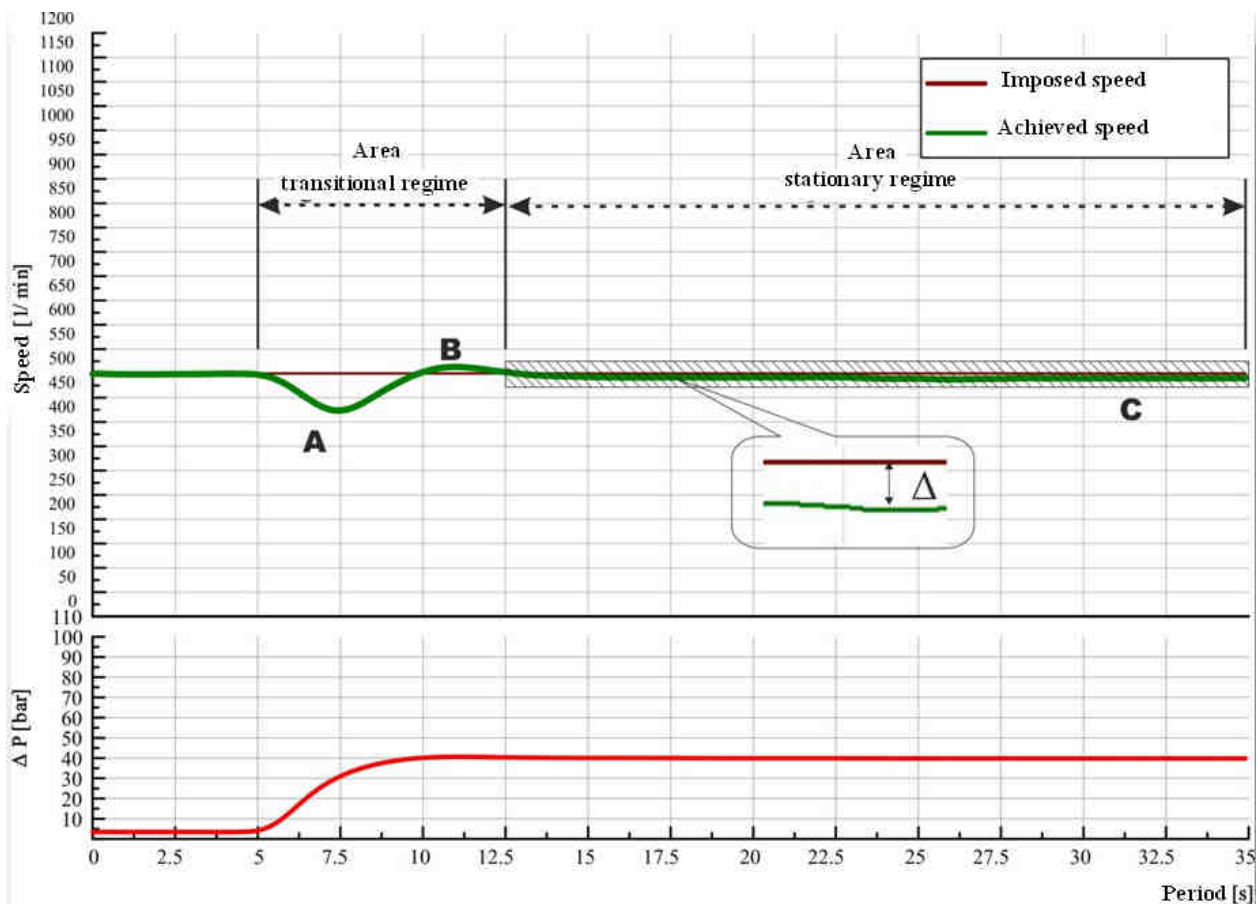


Fig. 3.1 Graphical illustration of the methodology for calculating the absolute errors, relative concerned

- Calculate the absolute error adjusting defined as the difference between the reference module and hydraulic motors spindle speed value in static (enforced speed – the speed achieved);
- Calculate the relative error of adjusting, which is the ratio of the absolute error and the reference value as a percentage; $\Delta x_e = \frac{|n_{ref} - n|}{n_{ref}} * 100$;
- Both absolute error and relative error of were calculated for each numeric value in the range of stationary regime, the final value of the arithmetic mean of them.

This manner of calculation was repeated for each actual step responses obtained from experimental tests, the first series of tests (constant load, variable speed) and the tests of the second series (constant input speed and variable load to shaft of the hydraulic motors). The results of this calculation for the first series of tests are shown in tabel 3.1

Table 3.1

No. crt.	Pressure loading circuit [bar]	Hydraulic engine speed [rev/min]	Change in turbine rotor revolutions [rev/min]	Absolute error Δ [l/min]	Relative error $\Delta x\%$
1	50	500	50	2.38	0.47
2			100	24.78	4.96
3			150	13.36	2.47
4		600	50	20.04	3.34
5			100	7.19	1.20
6			150	22.84	3.81
7		700	50	3.77	0.53
8			100	14.87	2.12
9			150	3.61	0.52
10		800	50	5.57	0.69
11			100	52.87	6.61
12			150	12.14	1.52
13	75	500	50	25.83	4.77
14			100	5.80	1.16
15			150	11.56	2.31
16		600	50	12.21	20.4
17			100	20.79	3.47
18			150	7.04	1.17
19		700	50	15.68	2.24
20			100	10.57	1.51
21			150	5.05	0.72
22		800	50	8.86	1.11
23			100	27.80	3.48
24			150	37.54	4.69
25	100	500	50	9.31	1.86
26			100	15.14	3.03
27			150	5.47	1.09
28		600	50	15.02	2.50
29			100	21.36	3.56
30			150	8.43	1.40
31		700	50	40.88	5.84
32			100	10.50	1.50
33			150	6.67	0.95
34		800	50	29.55	3.69
35			100	28.56	3.57
36			150	4.51	0.56

The figures for the second series of tests are presented in Table 3.2

Tabel 3.2

No. crt	Hydraulic engine Speed [rev/min]	Pressure variation loading circuit [bar]	Absolute error Δ [l/min]	Relative error Δx_e %
1	500	50	9.52	1.90
2		75	2.67	0.53
3		100	24.32	4.86
4	600	50	24.77	4.13
5		75	50.98	8.50
6		100	0.40	0.07
7	700	50	4.15	0.59
8		75	11.15	1.59
9		100	34.32	4.90
10	800	50	35.28	4.41
11		75	5.16	0.64
12		100	22.85	2.86
13	1000	50	41.52	4.15
14		75	27.60	2.76
15		100	15.12	1.51

4. Conclusions

After analyzing the experimental results obtained from both series of tests, the following conclusions were drawn:

Step responses achieved experimental resulting with an error of setting higher or lower than the reference speed, in order to evaluate the error at steady speed, calculations were conducted in the previous subchapter are presented both in Tables 3.1 and 3.2

From the analysis of the values of the two tables is found that the relative error of Δx_e [%] of adjustment does not exceed the permissible limits in the literature ($\pm 1 \dots \pm 5\%$). In our case, the maximum relative error of is $\Delta x_e = 4.96\%$, obtained at constant load test at 50 bar and reference speed 500 rev / min (Table 3.1).

Adjustment errors are inevitable due to the existence game pitch drive mechanism of the pump, as well as any delays that may occur in electronic data processing chain and the precision of the transducers used;

REFERENCES

- [1] <http://sine.ni.com/nips/cds/view/p/lang/en/nid/11572>
- [2] <http://sine.ni.com/nips/cds/view/p/lang/en/nid/11914>
- [3] <http://www.ni.com/labview/>
- [4] Afrăsinei M., Damaschin V. ©D.I.S.A.H.P. – www.disahp.net

CONSIDERATIONS FOR OPTIMIZING THE CROPS IN AGRICULTURAL FARMS FROM THE MARKET ECONOMY IN ROMANIA

Lect. phd.ec.Oana David¹, Prof.phd.eng. Ladislau David²,
lect. phd.eng.Mihaela Florentina Duțu²

1 University Politehnica of Bucharest, Department of Economics, e-mail:davidoana@hotmail.com

2 University Politehnica of Bucharest, Biotechnology Systems Departament, e-mail:
davidmihaela@hotmail.com

Abstract: After 1989, due to land restitution to former owners, have appeared in the farming sector holding a number of farms of different sizes, some small, others formed by association of several owners in an attempt to achieve some farms that can be exploited as effectively. Because today the majority of agricultural land is in private ownership and agricultural production is insufficient, resorting to imports, the paper presents a model for optimizing the agricultural production on these farms.

Keywords: farms, market economy, agricultural land

1. Introduction

The Romanian Revolution of December 1989 marked deeply the Romanian rural area. In a very short time there were essential changes in land ownership, is radically changing social and economic organization of agriculture, its settlement

In post-revolutionary period there were dramatic changes in terms of agricultural holdings. Disappeared completely socialist agricultural enterprises (state and cooperative) their place being taken by new types of associative or corporate holdings.

Following the transformations that have occurred in recent years, the Romanian agriculture has suffered the impact of quantitative and qualitative changes in the fields of law, legal, economic and social with adverse effects in the short term.[1]

The paper aims to present a model for optimizing the agricultural production in these new types of holdings which were established in the Romanian economy

2. Calculation algorithm

To substantiate the structure of vegetable crops on a vegetable farm we use an economic and mathematical model of linear programming. The developed model should ensure the production established and use of more complete the resources.[2]

The objective function, called optimization criterion of the model is represented by the total profit maximizing farm. The objective function is:

$$y = a_0 + a_1x_1 + a_2x_2 + a_3x_3 \quad (1)$$

where:

- a_0, a_1, a_2, a_3 -are, in this case, the average profits for different cultures;
- x_1, x_2, x_3 - are, area cultivated with different crops.

You can use several optimization criteria, but never simultaneously.

The restrictions model ensures the established production and the complete use of resources. To be optimized the restrictions model are determined so as to ensure a maximum functionality of each of them, namely:

- be fully arable cultivation;
- crop rotation restrictions;

- use of labor at full capacity;
- ensure delivery of contracted products;
- cost per hectare is dimensioned so as to not exceed the available resources.

The restrictions are:

$$x_1 \leq x_{1max}; \quad x_1 \geq x_{1min}$$

$$x_2 \leq x_{2max};$$

$$x_2 \geq x_{2min}$$

(2)

$$x_3 \leq x_{3max}; \quad x_3 \geq x_{3min}$$

$$b_{1i}x_1 + b_{2i}x_2 + b_{3i}x_3 \leq d_i \quad i = 1, 2, \dots, n_1$$

(3)

$$b_{1i}x_1 + b_{2i}x_2 + b_{3i}x_3 \leq d_i, \quad i = n_1 + 1, \dots, n_1 + n_2$$

where:

- b_{1i}, b_{2i}, b_{3i} are the labor is needed per hectare for different crops (for $i = 1, 2, \dots, n_1$) expressed in man-days /ha and average yields per hectare for each crop and $i = n_1 + 1, \dots, n_1 + n_2$

Determining the optimal value of the objective function in the presence of restrictions is done using the primal simplex algorithm. For this, objective function and the system of equations that define the restrictions will be written in tabular form:

Tabel 1

		j	1	2	3	4	5	6	7	8	9
i			x_1	x_2	x_3	x_4	x_5	x_6	x_7	x_8	x_9
1	x_4	C_{11}	D_{11}	D_{12}	D_{13}	D_{14}	D_{15}	D_{16}	D_{17}	D_{18}	D_{19}
2	x_5	C_{21}	D_{21}	D_{22}	D_{23}	D_{24}	D_{25}	D_{26}	D_{27}	D_{28}	D_{29}
3	x_6	C_{31}	D_{31}	D_{32}	D_{33}	D_{34}	D_{35}	D_{36}	D_{37}	D_{38}	D_{39}
4	x_7	C_{41}	D_{41}	D_{42}	D_{43}	D_{44}	D_{45}	D_{46}	D_{47}	D_{48}	D_{49}
5	x_8	C_{51}	D_{51}	D_{52}	D_{53}	D_{54}	D_{55}	D_{56}	D_{57}	D_{58}	D_{59}
6	x_9	C_{61}	D_{61}	D_{62}	D_{63}	D_{64}	D_{65}	D_{66}	D_{67}	D_{68}	D_{69}
	Y	E_0	E_1	E_2	E_3	E_4	E_5	E_6	E_7	E_8	E_9

Table elements are calculated by relations:

$$C_{i1} = d_i, \quad i = 1, 2, \dots, n_1 + n_2$$

$$D_{ij} = b_{ij}, \quad i = 1, 2, \dots, n_1; j = 1, 2, \dots, m (m - 3)$$

$$D_{ij} = b_{ij}, \quad i = 1, 2, \dots, n_1 + n_2; j = 1, 2, \dots, m$$

$$D_{ij} = 1, \quad i = j - m; j = m + 1, \dots, m + n_1$$

$$D_{ij} = 0, \quad j = m + n_1 + 1, \dots, m + n_1 + n_2$$

$$E_0 = a_0$$

$$E_i = a_i, \quad i = 1, 2, \dots, m$$

For calculating the maximum value:

$$E_0 = -a_0$$

$$E_i = -a_i, \quad i = 1, 2, \dots, m$$

(4)

(5)

If all coefficients of the last row of the table are positive ($E_i > 0$) to obtain the optimal solution [3]. If there are negative coefficients do iterations. Interchange column (p_1) is determined from the condition:

$$| - E_i | = \max, \quad i = 1, 2, \dots, m \quad (6)$$

Interchange Line (q_1) is determined from the condition:

$$\frac{C_{i1}}{D_{i,p_1}} = \min, \quad i = 1, 2, \dots, n_1 + n_2; D_{i,p_1} > 0 \quad (7)$$

At the intersection of column p_1 and of line q_1 is pivotal element D_{q_1,p_1} .

Next, calculate the following elements for the following table corresponding to the next point (k). For this the coefficients of line pivot q_1 fall to pivot D_{q_1,p_1} .

$$C_{q_1 1}^{(k)} = \frac{C_{q_1 1}^{(k-1)}}{D_{q_1 p_1}^{(k-1)}} \quad (8)$$

$$D_{q_1 j}^{(k)} = \frac{D_{q_1 j}^{(k-1)}}{D_{q_1 p_1}^{(k-1)}}, \quad j = 1, 2, \dots, m, \quad j \neq p_1 \quad (9)$$

$$D_{q_1 j}^{(k)} = \frac{1}{D_{q_1 p_1}^{(k-1)}}, \quad j = p_1 \quad (10)$$

Other elements of the table for the point test (k) is calculated from the table elements for tested point ($k-1$) with the relationship:

$$C_{q_1 1}^{(k)} = \frac{C_{q_1 1}^{(k-1)}}{D_{q_1 p_1}^{(k-1)}} \quad (11)$$

$$D_{q_1 j}^{(k)} = \frac{D_{q_1 n+q_1}^{(k-1)}}{D_{jp_1}^{(k-1)}}, \quad j = 1, 2, \dots, m, \quad j = p_1$$

$$D_{q_1 j}^{(k)} = \frac{D_{q_1 j}^{(k-1)}}{D_{jp_1}^{(k-1)}}, \quad j = 1, 2, \dots, m, \quad j \neq p_1$$

$$E_0^{(k)} = E_0^{(k-1)} - C_{q_1 1}^{(k-1)} * D_{m+1,p_1}$$

$$C_{i1}^{(k)} = C_{i1}^{(k-1)} - C_{q_1 1}^{(k-1)} * D_{i,p_1} \quad i = 1, 2, \dots, m, \quad i \neq q_1$$

$$D_{ij}^{(k)} = D_{ij}^{(k-1)} - D_{q_1 j}^{(k-1)} * D_{j,p_1}^{(k-1)}, \quad i = 1, 2, \dots, m, \quad j = 1, 2, \dots, m, \quad i \neq q_1$$

$$E_j^{(k)} = E_j^{(k-1)} - D_{q_1 j}^{(k-1)} * D_{m+1,p_1}^{(k-1)}, \quad j = 1, 2, \dots, m, \quad j \neq q_1$$

$$E_j^{(k)} = -D_{q_1 j}^{(k-1)} * D_{m+1,p_1}^{(k-1)}, \quad j = 1, 2, \dots, m, \quad j = q_1$$

Changes, among them, the positions of the x_{p_1} and x_{q_1} variables. Check if the coefficients of the last row of the table are positive [4]. If the condition is met it displays the function value:

- maximum value is $y = E_0$;
- the minimum value is $y = -E_0$.

Values of the independent variables are the values of the coefficients C_{ij} .

3. Conclusions

Based on the presented algorithm was developed a computer program in Pascal, with which all calculations were performed.

We considered a farm of 1,500 hectares total area, occupied by three crops: corn, wheat and barley. It was followed the optimization for the areas under these crops. Average profits for corn are $a_1 = 13,3$ thousands ron/ha, for wheat, $a_1 = 17,1$ thousands ron/ha, for barley and $a_1 = 3,5$ thousands ron/ha.

$$y = 13,3x_1 + 17,1x_2 + 3,5x_3 \quad (12)$$

Rotation restrictions are:

$$\begin{aligned} x_1 &\leq 937 & x_2 &\leq 932 \\ x_3 &\leq 1509 & x_3 &\geq 100 \end{aligned} \quad (13)$$

Labor consumption per hectare is $b_1 = 13,3$ man-days/ha for maize, $b_2 = 2,5$ man-days/ha for growing wheat and $b_3 = 2,5$ man-days/ha culture barley. The average yields per hectare are considered: $b_4 = 5,85$ t/ha for maize, $b_5 = 3,8$ t/ha for wheat and $b_6 = 3,9$ t/ha for barley crop. Restrictions on labor utilization and ensuring delivery of contracted goods production (firm contracts being 6.400t) are:

$$\begin{aligned} 13,3x_1 + 2,5x_2 + 2,5x_3 &\leq 10.217 \\ 13,5x_1 + 2,5x_2 + 2,5x_3 &\geq 12.217 \\ 5,85x_1 + 3,8x_2 + 3,9x_3 &\geq 6.400 \end{aligned} \quad (14)$$

After calculations we obtain the following results:

- area occupied by the three crops considered is: 600 ha corn (40% of total area), 800 ha of wheat (53.3% of total area) and 100 ha barley (6.7% of the area);
- total production that can be obtained is: 6938 tons of which 3,510 tons of corn, 3,038 tons of wheat and 390 tons of barley;
- use of manpower needed to get the total production is 10,249 man-days to 8100 man-days for corn, wheat 1944 man-days and 250 man-days for barley;
- total production profit made in the circumstances, is 22,01 million ron distributed as follows: 7,97 million ron for corn, 13,7 million ron for wheat and 0,35 million ton for barley.

References

1. Alexandri C., Food security and balance in Romania, Publisher GEEA, Bucharest, 2001;
2. Iosif Gh.N., Resources and market food products, Publisher Tribuna Economica, Bucharest, 1998;
3. Lapusan Al., Agrarian structure, Publisher Banea Press, Bucharest, 2002;
4. Zahiu I., Agricultural economics and organization units, Publisher ASE, Bucharest, 1993.

BIODEGRADABLE OILS – METHODS FOR DETERMINING THE PERFORMANCES OF BIODEGRADABLE OILS

eng. Alina Iolanda POPESCU¹, eng. Sava ANGHEL¹, PhD stud. eng. Mihail PETRACHE²,
PhD stud. eng. Adrian Georgian PANȚIRU¹, eng. Alexandru MARINESCU¹

¹INOE 2000 – IHP, alina.ihp@fluidas.ro ; sava.ihp@fluidas.ro; pantiru.ihp@fluidas.ro ;
marinescu.ihp@fluidas.ro

²SC LYRA PROD IMPEX SRL, office@lyra.ro

Abstract:

The article deals with the biodegradable liquids used in hydraulic drive systems of the machines that work in natural environment from agriculture, forestry or navy. Are presented biodegradable liquids with their interaction in the way in which are illustrated in the scientific literature. The authors describe methods of determination of the biodegradable liquids performances using a stand of comparative testing.

Keywords:

hydraulic drive fluid, biodegradability, testing stand, gear pumps

1. Introduction

Classical liquids used in hydraulic drive systems have harmful effect on the environment. In order to protect nature in U.E. were introduced very harsh rules regarding the environment protection. Thus, began to use in hydraulic drive systems of equipment from agriculture, forestry, navy, liquids with neutral properties on the environment and which degrade in time - biodegradable.

Biodegradation is the process by which organic substances are broken down by the enzymes produced by living organisms. Organic material can be degraded aerobically, with oxygen or anaerobically, without oxygen. A term related to biodegradation is biomineralisation, in which organic matter is converted into minerals (Diaz, 2008). By definition, biodegradation is the chemical transformation of a substance caused by organisms or their enzymes. There are two major types of biodegradation – Primary Biodegradation, which refers to the modification of a substance by microorganisms such that a change is caused in some specific measurable property of the substance (US Army Corps of Engineers, 1999). When the term primary biodegradation is used it refers to Aluyor et al. 545 minimal transformation that alters the physical characteristics of a compound while leaving the molecule largely intact. Intermediary metabolites produced may however be more toxic than the original substrate (wiserenewables. com, 2006). Thus mineralization is the true aim. When this happens it is referred to as Ultimate or Complete Biodegradation; which is the degradation achieved when a substance is totally utilized by microorganisms resulting in the production of carbon dioxide, methane, water, mineral salts, and new microbial cellular constituents (US Army Corps of Engineers, 1999).

Manufacturers and blenders of biodegradable oils promote these for use based on the importance of biodegradability and no toxicity. But performance issues - like oxidation stability, antiwear protection, hydrolytic stability, viscosity- temperature properties and cost factors - are usually presented only wherever these features provide an advantage to the particular manufacturer.

2. Types of biodegradable liquids

2.1 Vegetable oils include corn, soybean, rapeseed (canola), sunflower, peanut, olive oil and others. In their natural form, these oils consist primarily of triglyceride molecular structures (figure 1) and as such they have performance limitations, most notably, poor thermal, hydrolytic and oxidation stability. For example, most natural vegetable oils cannot withstand reservoir temperatures greater than 80°C.

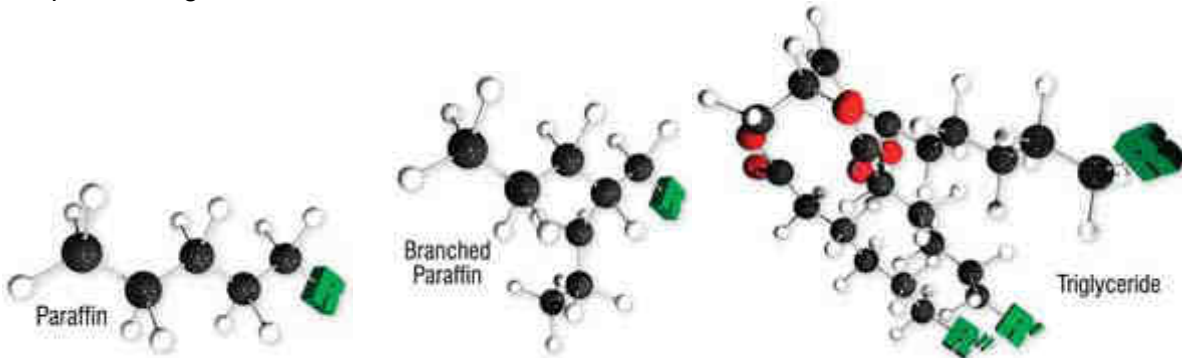


Fig.1 Triglyceride structure

In addition, water, even in small amounts of a few hundred parts per million, is the natural enemy of vegetable oils and can cause serious foaming and degradation problems. In general, these oils also exhibit low cold-flow abilities. On the other hand, most of these natural oils have good lubricating qualities due to their polar nature. This provides good metalwetting attraction and also makes them good solvents for helping keep dirt and debris off metal surfaces. Their molecular structure provides for a high natural viscosity and viscosity index. Genetic modifications have also overcome much of the thermal and oxidative stability problems, particularly with soybean and canola oils. Hydraulic oils for use in mobile equipment can be made from a blend of synthetic diester and canola (rapeseed) oil to deliver excellent temperature viscosity properties and good oxidation stability - even in the colder operating conditions found in Northern climates.

Vegetable Oils are well-suited for use in low to medium pressure hydraulic systems, or lightly loaded gear drives where the operating temperature does not normally exceed 60°C (140°F) and where there is little chance of water ingress or high contamination. Where the threat of contamination exists, filters must be inspected more frequently, due to the lower filterability of these fluids. Gear boxes and hydraulic systems should be thoroughly flushed to remove debris, sludge and silt prior to the application of vegetable-base lubricants to avoid any unnecessary incompatibility potential. There may also be some negative reaction to sealing materials such as neoprene and nitrile.

2.2 Synthetic oils are briefly described below.

2.2.1 Polyalphaolefins (PAOs) exhibit excellent low-temperature properties, but tend to shrink rubber seal materials. PAOs are finding increased use as hydraulic and engine oils, particularly in cold-climate applications and where hydraulic pressures are high. These oils are also finding selected use as gear lubricants due to their ability to provide lower operating temperatures and their lower coefficient of friction, both of which help reduce wear. These products are generally compatible with mineral oils and as a result, there is no requirement for extensive flushing prior to conversion unless required by the manufacturer. PAOs have a negative effect on certain sealing materials causing shrinkage so initial leakage may be a problem.

2.2.2 Diesters have good antioxidation characteristics and seal swell properties. They are excellent lubricants for compressors and turbines. Diester fluids may have a negative effect on certain varnish or paint surfaces, due to their exceptional solvency and detergency, so it would be wise to

remove the paint from any internal contact surfaces such as the e, so initial leakage may be a problem. In addition, these fluids can negatively affect sealing materials, and fluorocarbon seals should be considered for these applications.

2.2.3 Polyalkylene Glycols (also known as Polyglycols) PAGs can be both water soluble (ethyleneoxide) and water insoluble (propylene oxide). One disadvantage of PAGs is their tendency to emulsify water in certain equipment, such as gear boxes, which will cause foaming, sludge and corrosion. A major disadvantage of both PAOs and PAGs is their poor solubility with regard to additives. Today, some manufacturers are blending diesters with PAOs to form base oils which are biodegradable, have good solubility, resist oxidation and have good temperature viscosity characteristics. Others are blending synthetic diesters with canola to provide similar results. Polyglycols (PAGs) can be either polyethylene or polypropylene oxide-based, with water solubility differing according to type. Polyethylene-based PAGs are highly water soluble, are poorly miscible with mineral oils and are very polar. As a result, thorough flushing of the system should be carried out prior to the conversion from mineral oil-based products. Their water solubility helps to provide biodegradability, but also provides a disadvantage in lubricant applications, because free water contamination tends to occur quickly.

A most important consideration that is also frequently ignored is whether or not the new biodegradable fluid is compatible with mineral oil. If it is not, serious problems may result if all of the old mineral oil is not thoroughly flushed from the system before the new fluid is installed. Symptoms of a poor or incomplete conversion to biodegradable fluids include severe foaming, leaking seals, plugged filters, higher-than-normal wear on some components (such as hydraulic pump), and increased operating temperatures.

Additionally, the high specific gravity of biodegradable fluids tends to elevate solid particle contaminant retention (that is particles are less prone to settle). To offset this threat, the filtration systems should be modified or upgraded to ensure that bearing surfaces are not exposed to high contaminant levels. Three-micron filters installed in a side-stream are beneficial in controlling contamination in hydraulic applications. Operating temperatures must be controlled in order to avoid excessive and unnecessary evaporation of these water miscible fluids. The recommended operating temperature should be kept within a range of about 50 °C to 60 °C (122 °F to 140 °F). Another consideration when using biodegradable water-based and water soluble fluids in a hydraulic application is cavitation damage to pressure relief valves which may be required to remain in the discharge or open position for long periods. Vapor phase cavitation can cause erosion of the valve seat due to high vapor pressure, which can lead to premature relief valve failure. Proper valve selection prior to conversion should be considered.

Generally speaking, biodegradable oils should be maintained and monitored during use just like mineral-base oils. They must be kept cool, clean and dry (water-free) and their condition should be monitored on a regularly scheduled basis using readily available oil analysis techniques.

3. Method for monitoring and determining the performance of hydraulic drive fluids

In patent application with number A / 00242 - 04.04.2007 is suggested a determining method of hydraulic drive fluids performance using a testing stand, shown in **Fig.2**.

Alternative to endurance test stand consists of double divided tank **1**, on whose upper lid is secured the electric motor **2** with double shaft, that can simultaneously engage two hydrostatic pumps **3.1** and **3.2**, the **3.1** pump rotating transducer of moment and rotation speed, **4**, through time, and **3.2** pump rotating transducer of moment, **5**, through time.

On outlet circuit of **3.1** pump are installed pressure valve **6.1** and pressure transducer **7.1** and on outlet circuit of **3.2** pump are found mounted pressure valve **6.2** and pressure transducer **7.2**.

On return circuit of pressure valve **6.1** is found flow transducer **8.1**, and on valve return **6.2** is found mounted flow transducer **8.2**.

3.1 suction pump is connected to **a** section of reservoir **1** and **3.2** suction pump is connected to **b** section of reservoir **1**.

Outlet circuit from flow transducer **8.1**, returns in reservoir **1**, in **a** section and outlet circuit from flow transducer **8.2**, returns in reservoir **1**, in **b** section.

Connection between hydraulic equipments previously described are made through some pipes and linkages.

For a good using of the stand should exist the condition that **3.1** and **3.2** pumps to be indidentically from constructive and dimensional point of view.

The way of functional of the stand is the following:

Fill **a** section with mineral oil (hydraulic oil with spread domain of use) and fill **b** section and with vegetable (biodegradable) oil.

Starts the electric engine **2**, which is the moment when **3.1** pump sucks the mineral oil from **a** section and escapes it through the pressure valve **6.1** and flow transducer **8.1**, back into the reservoir **1**, in the same **a** section; simultaneously **3.2** pump sucks the vegetable oil from **b** section and escapes it through the pressure valve **6.2** and flow transducer **8.2**, back into the reservoir, in the same **b** section.

Adjusts **6.1** and **6.2** valves at the same value of the discharge pressure, which is usually the testing pressure.

If engages the electrical connections of moment and rotation speed transducer **4**, of moment transducer **5**, of pressure transducers **7.1** and **7.2** and of flow transducers **8.1** and **8.2**, with one acquisition board and a system of computing, that are not on the figure, can measure the driving times, pumps rotation speed, discharge pressure and performed flow; As it is known that: the moment multiplied with rotation speed and divided at a constant is equal with the consumed power, and the pressure multiplied with the flow and divided at another constant is equal with the usable hydraulic power, can be determined and compared the yields of the same pumps, which function with different oils at the beginning of the tests, during the tests and at the end of endurance.

Also, through regular monitoring of the pumps yield, can find running time, then pumps are out of use (when is found that the useful power falls below acceptable percentage from consumed power).

Main advantages of the invention are:

- can test simultaneously at endurance two hydrostatic pumps, but which circulate different liquids, as type and as viscosity, which do not mix with each other;
- can permanent measure basic parameters in „on line” system , for the entire period of endurance;
- directly determines the influence of the use of inadequate oils on durability of hydrostatic pumps.

4. Conclusions

By performing stand was created a device by which we can determine performances of biodegradable hydraulic drive fluids.

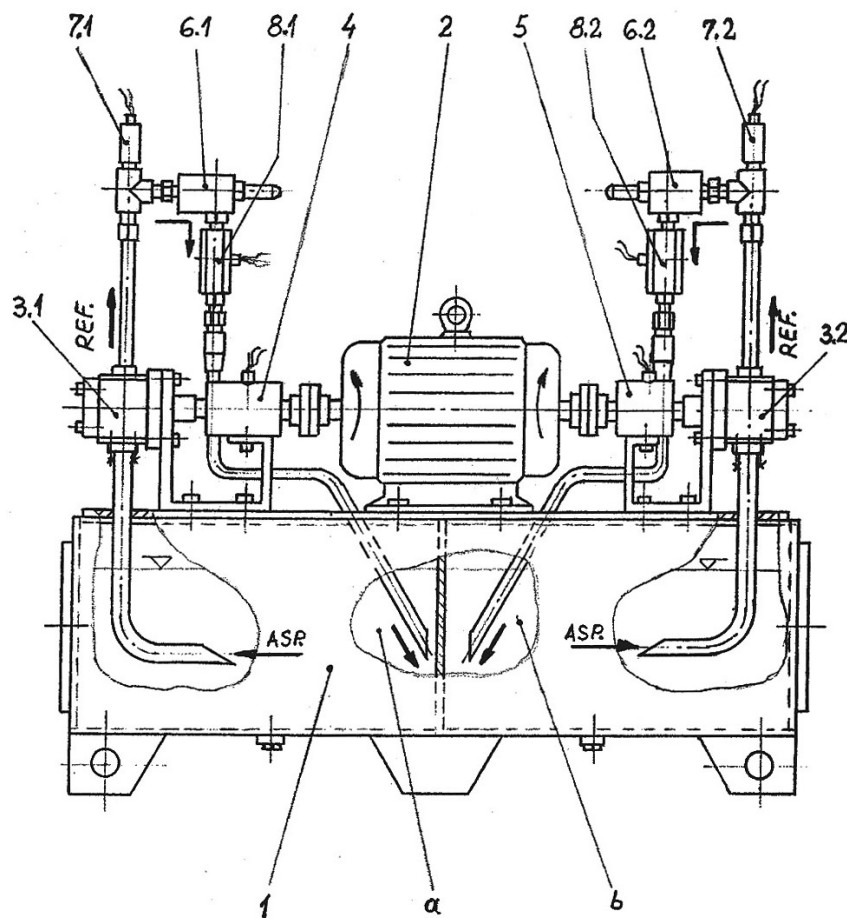


Fig.2 Stand for determining the performance of biodegradable oils

REFERENCES

- [1] Lloyd Leugner, Maintenance Technology International, Inc.; "Biodegradable Oils - How to Apply and Maintain"; This article originally appeared in "Lubes'N'Greases", June 1998;
- [2] N. Ioniță, C. Dumitrescu, L. Dumitrescu, "Stand de testare comparativă la durabilitate a pompelor hidrostactice rotative", Patent application, no A / 00242 -04.04.2007;
- [3] D. Klamann, "Lubricants and Related Products ", Germany: Verlag Chemie. pp. 107-113, 121, 325-326;
- [4] L. Leugner, "The Practical Handbook of Machinery Lubrication", 2nd Edition, Canada: Maintenance Technology International, Inc. pp. 75-76, 144, 149;
- [5] P. Drumea, M. Comes, A. Mirea, M. Blejan – "Positioning systems tuning interface using proportional hydraulic drivers" – The 4th International Symposium For Informatics And Tehnology In Electronic Modules Domain, Bucharest, September 22 – 24, 1998;
- [6] C. Cristescu, P. Drumea, C. Dumitrescu - "The testing system of the pumps with gear wheels for determining the volumetric efficiency"; In Proceedings of 2010 - IEEE , International Conference on Automation, Quality and Testing, Robotics AQTR 2010 - THETA 17th edition - May 28-30 2010, Cluj-Napoca, Romania , pp. 195- 199, ISBN 978-1-4244-6722-4, IEEE Catalog Number CFP10AQT-PRT.

HYDRAULIC INSTALLATION WITH ENERGETIC AUTONOMY FOR LAKES AERATION

Adrian CIOCANEA¹, Sanda BUDEA¹

¹University Politehnica of Bucharest, Department of Hydraulics and Hydraulic Machinery, email:
adrian.ciocanea@upb.ro; sanda.budea@upb.ro

Abstract: *The paper is presenting a hydraulic installation aimed to improve the water quality contained in lakes, basins, reservoirs or rivers with slow motion. The proposed installation could be also used in early stages of wastewater treatment facilities. One presents the aeration process provided by the proposed installation and the advantages of such method in reducing the level of lakes eutrophication. Also, there are presented the experimental results concerning energetic characteristics of the installation in order to be powered by solar PV panels for 24 hour operation.*

Keywords: *water quality, water aeration, eutrophication.*

1. Introduction

Water resources are the subject of increasing anthropogenic pollution from industrial or domestic sources. There are over 80,000 known natural chemicals obtained by industrial processes that can create billions of effects by combining them. Water quality, determined by analyzing the organoleptical, physical, chemical, biological and bacteriological characteristics may degrade due to different types of pollution: pollution with fertilizers, bacterial, or chemical asphyxiation. The forms of pollution can occur separately or together - the most frequent case. One such case is that of eutrophication, natural evolutive process that can be enhanced by human intervention. When the metabolic chain breaks in closed water basins bottom accumulation deposits representing secondary source of biogenic elements arises. Enrichment of water by nutrients, mainly nitrogen and phosphorus, lead to flourishing algae, excessive growth of aquatic macrophytes, a high turbidity, leak of oxygen in bottom waters of the lake and, in some cases, induce a disagreeable water's smell and taste.

Once the eutrophication occurred, either from natural or artificial causes, water quality decline from ultraoligotrophic, oligotrophic and mesotrophic basin, to eutrophic and hipereutrophic. Final stage resulting in aging and lake disappearance by swamp transformation. The environmental element to quantify the degree of eutrophication of a lake is the algal biomass, eco-physiological indicator directly dependent of the lake's state. Blue-green algae - also known as the cianophite, or cianoprocariote cyanobacteria, algae- are the most common in the lake waters.

In order to preserve water quality relevant parameters must be monitored. The main physico-chemical and biological analyzes currently made are related to: indicators of the oxygen (O_2 dissolved, CCO-Mn, CCO-Cr, CBO 5); indicators of nutrients regime (ammonium, nitrites, nitrates, phosphates); indicators biocenosis planktonic (phytoplankton, zooplankton) physico-chemical and bacteriological aids (pH, CO_2 , alkalinity, Mn, Fe, total coliforms bacilli, etc.). These indicators can take values within certain limits, and accordingly lake will be considered into the categories: oligotrophic lakes, mesotrophic or eutrophic as shown in Table 1.

Table no.1

	oligotrophic lakes	mesotrophic lakes	eutrophic lakes
Saturation degree in oxygen O ₂ (%)	minim 70	40 – 70	sub 40
Total nitrogen N (mg/dm ³)	maxim 0,3	maxim	minim 1,5
Total Phosphorus P (mg/dm ³)	maxim 0,03	maxim 0,1	minim 0,15
phytoplankton biomass (mg/dm ³)	< 10	10 (incl) -20 (excl)	minim 20

The surface of the lakes in Romania – including all the categories and anthropogenic rivers - is estimated at 2,600 km², about 11% of the country area. During the years the quality of many lakes was monitored, and also of the groundwater - polluted with nutrients - from Bucharest and surrounding areas. It was found that many of monitored lakes (Lake Snagov, Morii Lake, Park Carol Lake and Park Tineretului Lake etc.) have serious problems due to high concentrations of nitrogen and phosphorus and large quantities of sulfur.

2. Aeration process and methods to improve water quality

The aeration process of the lake is necessary during the periods of the year in which the exchange of water and matter between hipolimnion and epilimnion is in standstill - the hot season. During this period, phosphorus, nitrogen and their compounds complex nutrients, that cause reactions in the aquifer environment, develop blue-green algae, in lakes that presents the ratio N / P low. An increase in temperature or excess nutrients can lead to bloom of algal and plant growth, resulting an increase in dissolved oxygen concentration. When the algae decompose, the dissolved oxygen decreases. Relationship between water temperature and O₂ concentration is illustrated in fig.1 a.

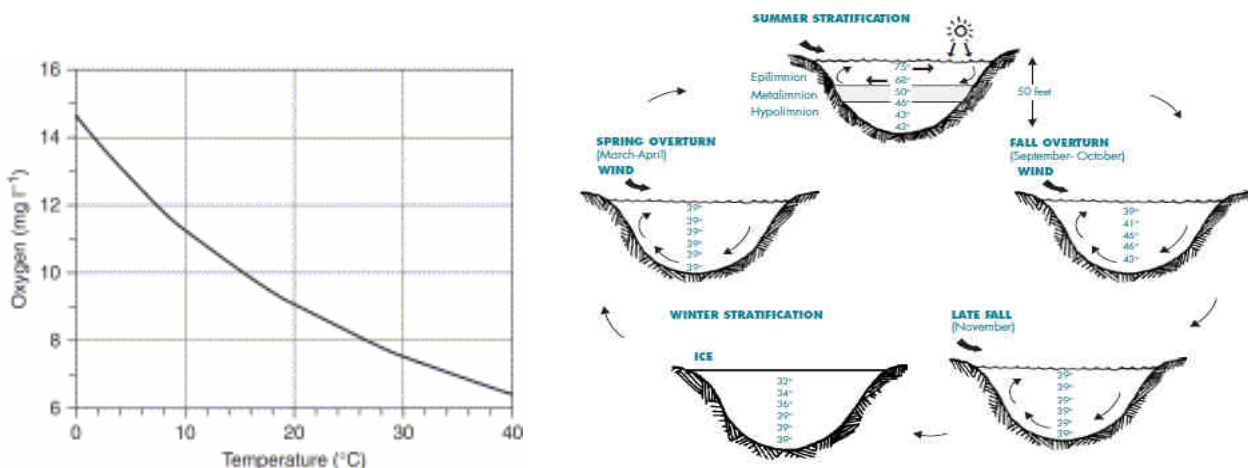


Fig. 1 a. Relationship between water temperature and O₂ concentration (at saturation) under normal air pressure for pure water. b.turnover phenomenon [16]

Taking into account that aquatic life is significantly influenced by stratification and by layers inversion (turnover phenomenon mentioned above) - Figure 1 b, the methods of water quality improvement must keep as possible the stability of the aquifer natural environment. From this point of view, global motion induced by the proposed installation, prevents that phosphorus and nitrogen to become source for blue-green algae bloom, which create toxic conditions for aquatic life.

By submerged installation is realised the water mixture that allows to nutrients to enter in the food chain of the lake, so phosphorus and nitrogen level is no longer a problem, becoming productive lake.

Biodiversity is reinvigorated, water becomes clean, the dissolved oxygen increase, pH values decrease and also the chlorophyll. Regarding the rate of growth of the fish, this can reach approx. 15-20 times higher than in the previous case to place the hydraulic installation.

Methods to reduce the eutrophication of lakes and improve the water quality are varied: chemical methods (precipitation of nutrients, dredging of the anoxic sludge from the lake bottom or his inactivation), biological methods (mowing and removal of algal vegetation and even fish, application of toxic substances - herbicide, algicides, pesticides, direct manipulation of the food chain and ecological balance through the introduction of allochthonous species etc.) and mechanical aeration methods. In case of mechanical methods, studies in this field [1], [2], [3], [4], [5], [6], [7] shows that refreshing the water's surface improves up to 7 times the transfer of gas into and from its volume, compared to the water surface without motion. Thus a better oxygen absorption and elimination of methane or ammonia occurs.

This paper presents a mechanical installation for water aeration, working in two versions, first with axial impeller, second with two cross / frontal impellers, the last one is the subject of a patent (OSIM A00706/8.10.2012) [15]. The aeration methods – the mechanical mixing, the oxygen injection, the air injection - are closer than the natural biochemical processes, without interfering with negative uncontrollable effects on aquatic ecosystems.

Aeration can be done through: pneumatic oxygenation equipment with porous diffusers, mechanical aeration equipment to ensure continuous recirculation of a quantity of water (aeration brushes, mechanical surface aerators with slow impeller and axial impeller, etc.) and mixed equipment [8], [9], [10], [11].

Proposed installation in this paper fulfill in good condition hypolimnetic aeration requirements: keep stratification, and water temperature to the hypolimnion level does not rise significantly, increase oxygen levels in the hypolimnion, decreases levels of iron, manganese, hydrogen sulfide and methane, not significantly affected zooplankton populations, does not change the level of chlorophyll, increases the fish population in cold waters. This article analyzes the performance of a hydrodynamic hypolimnetic aeration installation, whose main feature is a continuous operation regime, adapted to the aquatic ecosystem in which it is placed.

3. Hydraulic installation for water aeration

Proposed aeration installation is floating, mobile, energetic autonomous and it is a hydraulic machinery with an essential hydraulic element (the impeller) axial - figure no. 2 a - or cross/transversal impeller- figure no. 2 b - modified to operate at lower rotational speeds in order do not disturb the balance of aquatic microsystem between its layers, providing exogenous water oxygen (atmospheric oxygen dissolved to 50 mg oxygen/l/m²).

Hydraulic machine is immersed in lakes (for axial impeller) or is in deep layers (for transversal impeller) operating as drowning and therefore requiring low power consumption, as a result, hydraulic head will be about 5-20 mm water column. On the other hand, imposing the condition that the flow velocity be reduced so as not to disturb the balance of aquatic microsystem, the rate flow of hydraulic machine is also reduced.

In such condition result that the necessary power to drive the hydraulic machine will be also reduced, under about 100 W, considering also the efficiency of the installation. Taking account of the reduced consumption of energy, the mechanical installation for water aeration has the advantage of power supply from renewable sources, in this case from photovoltaic panels.

The installation is realised in order to minimize the possible degree of turbulence mixing of water's surface, while re-circulating water from deep layers.

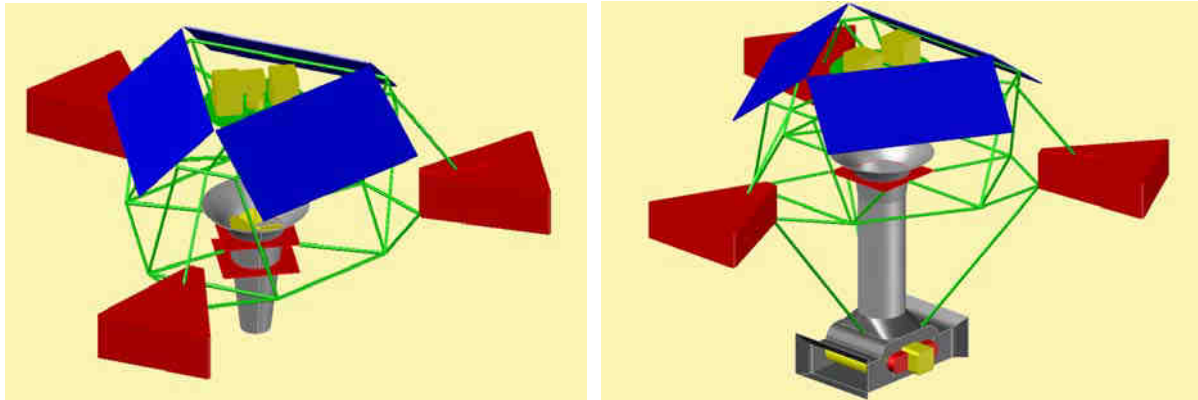


Fig. 2 Hydraulic installation for water aeration

a. Axial impeller placed under water surface; b. Transversal impeller placed near the bottom of the water

Water flow that passes directly through the installation induces a secondary flow approx. 2-2.5 times higher in the rest of the basin. In the circulation, changing the shape of the free surface by waves of the wind does not affect the flow induced by the installation, because the regime is almost laminar.

The installation presented in this article was designed and manufactured in Renewable Energy Laboratory of the Power Engineering Faculty of UPB - Hydraulics, Hydraulic Machinery and Environmental Engineering Department. Constructive solution with axial impeller with diameter of 350 mm, was tested in order to determine the total energy balance for sizing photovoltaic solar panels used for power supply.

The hydraulic machine is rotated with low rotational speed, about 60-70 rot/min by an electric drive brushless, low power about 100 W, placed directly on the impeller shaft and connected to a battery of accumulators.

The hydraulic flow is about 250-300 l / min. The installation is electronically controlled so that the rotation speed of the electric motor to be constant and batteries are protected from overload. Also, the installation operation is monitored by GPS, the system sending SMS reports on relevant parameters - rotation speed, battery status, etc.. The installation was sized to be possible to store energy in batteries, to ensure its continuous operation day / night during in the warm season.

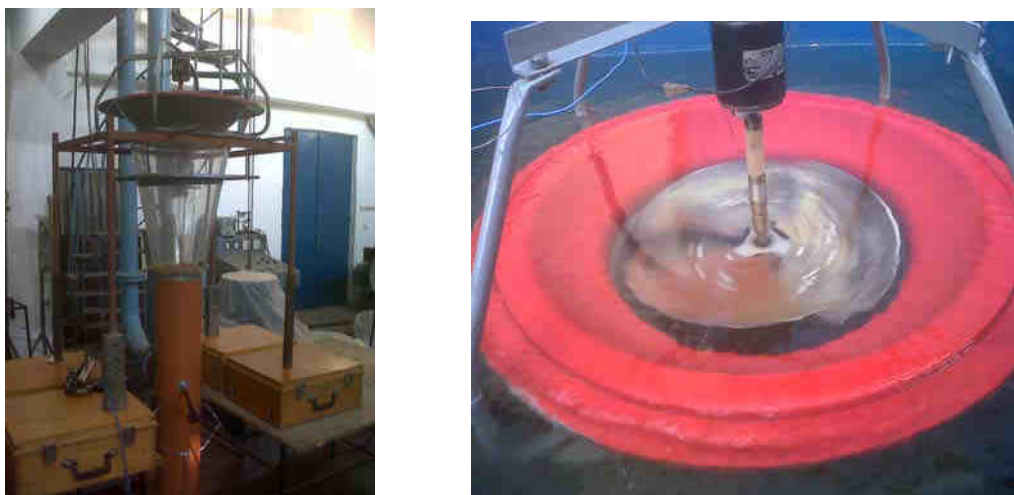


Fig. 3. The hydraulic machine tested - version with axial impeller

a. hydraulic machine tested in air b. hydraulic machine tested in water

In figure 3 a.b. is presented the hydraulic machine in version with axial impeller, equipping some similar installations [16].

For the version with axial impeller was designed and tested many models of impellers, with two or three blades and different inclination angles of them. The installation was preliminary tested both in air, also in water, in a basin with variable level. Were drawn characteristic curves $H(Q)$, $P(Q)$ and $P(n)$ like presenting in figure 4 a.b. The flow rate Q was determinate using a hydrometer mills movements, and the head H was measured on the diffuser circumference, previously marked.

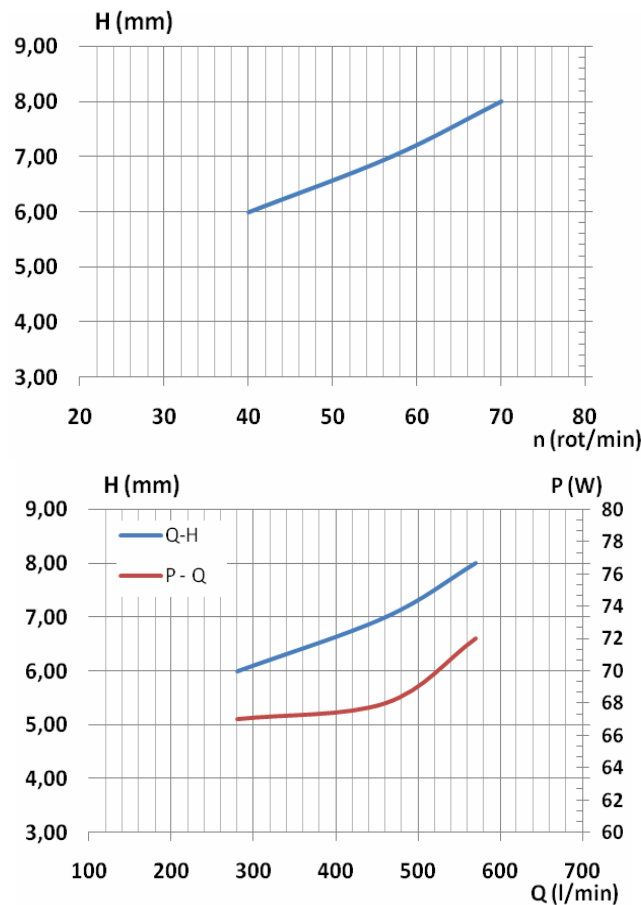


Fig. 4 Characteristic curves for hydraulic machine with axial impeller

The experimental results illustrated that for selected dimension of the installation $D_{rotor} = 350$ mm, $D_{confuzor} = 700$ mm – the necessary power supply was $P_a = 70$ W corresponding to a rotational speed of $n = 70$ rot/min for a water rate flow of $Q = 270$ l/min.

The hydraulic installation for the renaturation of the water, presented in this paper, will be tested „in situ”, location is set on one of the branches pond in Pipera, to verify operating efficiency in real conditions for an operating cycle of an year.

Preliminary results expected are in Figure 5 a, b before and after placing the installation, after a short period of its operation.



Fig. 5 Lake state before and after the placement of the installation

Analysis the efficiency of the installation follows to confirm the aquifer environmental effects such as increasing the level of dissolved oxygen in the hipolimnionului, maintaining as much as possible the stratification and the temperature, iron, manganese, hydrogen sulfide and methane levels tend to decline, zooplankton populations remain generally unaffected, the chlorophyll does not change, fish population in cold waters increases.

5. Conclusion

Article present a mechanical hydraulic installation for water's aeration designed, manufactured and tested under laboratory conditions in University Politehnica of BucharestHydraulics, Hydraulic Machinery and Environmental Engineering Department. Preliminary results made possible the impeller selection, the most appropriate in terms of hydraulic parameters and energy. These operating characteristics allowed to select the photovoltaic panels that acts to the motor drive and to determinate the re-circulating water volume and implicit estimate of the water aerated surfaces. Future experiments "in situ" will be dedicated especially to the aquifer environmental influences, monitoring especially the pH levels, the concentration of dissolved oxygen, and the concentration of phosphorus and nitrogen.

Acknowledgment

This work has been perfected with contract Checks of Innovation No. 119 CI /2012, contract surveyed by UEFISCDI.

REFERENCES

- [1] S. Stoianovici, D. Robescu – Procedures and mechanical equipment for wastewater treatment, Ed. Tehnica, 1982.
- [2] Byron Shaw, Christine Mechenich, and Lowell Klessig, Understanding lake data (G3582).
- [3] N.C. Boelee, H. Temmink, M. Janssen, C.J.N. Buisman, R.H. Wijffels - Nitrogen and phosphorus removal from municipal wastewater effluent using microalgal biofilms, Water Research, Vol. 45, Issue 18, 2011, pag 5925-5922.
- [4] Bei Wang, Christopher Q. Lan - Biomass production and nitrogen and phosphorus removal by the green algae *Neochloris oleoabundans* in simulated wastewater and secondary municipal wastewater effluent, Bioresource Technology, Volume 102, Issue 10, May 2011, pag 5639-5644.
- [5] E.E. Prepas, T. Charette - Worldwide Eutrophication of Water Bodies: Causes, Concerns, Controls, Volume 9, Pages 311-331, www.sciencedirect.com/science/article/pii/B0080437516091696
- [6] J M Malmaeus, L Håkanson – Development of a lake eutrophication model, Ecological Modelling (2004), Volume: 171, Issue: 1-2, Pag. 35-63.
- [7] VH Smith, G.D. Tilman, JC NeKola - Eutrophication: impact of excess nutrient inputs on freshwater, marine and terrestrial ecosystems, Environmental Pollution, Vol.100 Issues 1-3, 1999, pag. 179-196.

- [8] Neelam Verma - Restoration of urban lakes through aeration, International Journal of Applied Environmental Sciences, March, 2008
- [9] Davut Hanbay, Ahmet Baylar, Murat Batan - Prediction of aeration efficiency on stepped cascades by using least square, support vector machines Expert Systems with Applications 36 (2009), pag. 4248–4252
- [10] Robert B. Banks, Liqa Raschid-Sally, Chongrak Polprasert - Mechanical Mixing and Surface Reaeration, Journal of environmental Engineering, Vol. 109, no.1, 1093, pag. 232-241
- [11] Claude E Boyd - Pond water aeration systems, Aquacultural Engineering, Vol. 18, issue 1, 1998, pag. 9-40.
- [12] Yang-Cheng Shih, Hung-Chi Hou b, Hsueh-Cheng Chiang - On similitude of the cross flow fan in a split-type air-conditioner, Applied Thermal Engineering 28 (2008) pag.1853–1864 .
- [13] Sanda Budea, Cornelia Chiuideu – Approach about the efficient use of solar energy in Romanian's climatic conditions, FOREN 2010, 14-17 iunie, Neptun.
- [14] Sanda Budea, Adrian Ciocanea - A qualitative analyse of flow spectrum through work machines with lateral chanell using numerical methods, (pag. 142-149 vol 2), OPROTEH 2007, Bacau 1-3 noiembrie 2007. ISSN 1224-7480.
- [15] Adrian Ciocanea, Sanda Budea – Instalatie pentru aerarea apei din lacuri, rezervoare si rauri avand viteze reduse de curgere, brevet de inventie OSIM A00706/8.10.2012.
- [16] www.solarbee.com/technology
- [17] www.thepowmill-mattawafish.blogspot.com

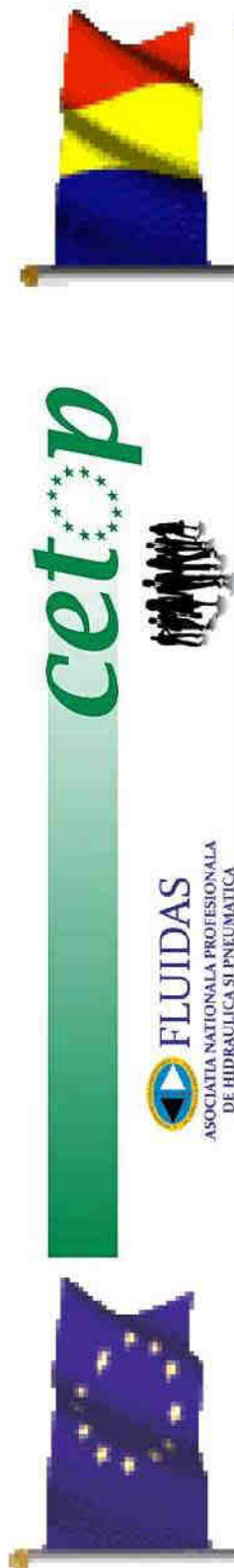


EDUCATION & QUALIFICATIONS IN FLUID POWER



*Chaired by John R Savage -
Vice President CETOP Education
Chairman BFPA Education & Training (UK)
Director National Fluid Power Centre (UK)*





CETOP- Education Recommendations.

- Produced in the late 90s by the CETOP EDUCATION COMMITTEE

PURPOSE-

- To establish an industry standard for education and training aligned to those involved in the maintenance of fluid power systems.

CETOP Education Recommendations are not a training course

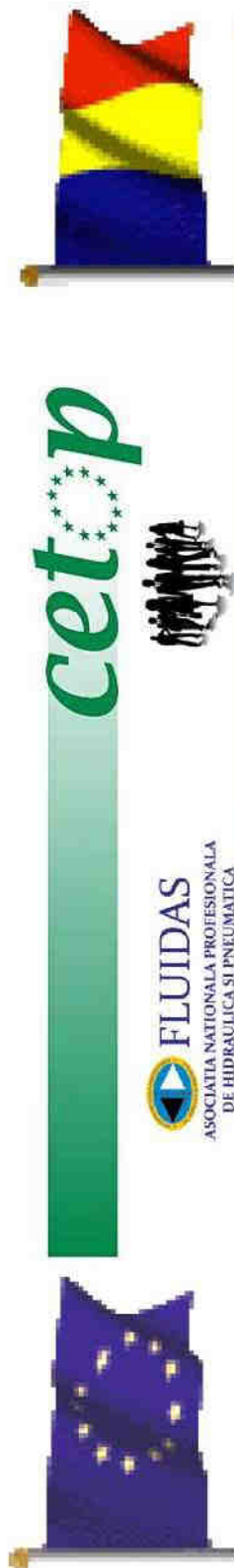
- They outline the recommended knowledge and skills as a minimum requirement placing the emphasis upon COMPETENCE during the assessment process

CETOP Education Recommendations are sector specific.

- They can be adapted to meet any sector where fluid power is in uses



Education & Qualifications in Fluid Power



CETOP- Education Recommendations

It was decided that these recommendations would be aimed at 3 specific vocational levels

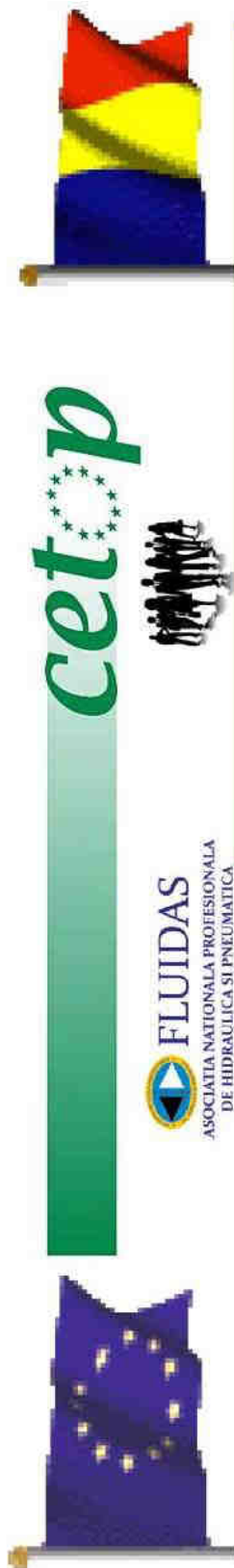
LEVEL 1. Related to first line maintenance/working to instructions and often supervision, basic understanding only. **Function**

LEVEL 2. Performs a variety of activities, requiring technical understanding and the ability to make a positive response to deviation (maintenance team member) **Function/Operation**

LEVEL 3. Involved in a broad and often complex range of activities. Responsible for quality of work undertaken and outcomes
Function/Operation/Application/Control



Education & Qualifications in Fluid Power



CETOP- Education Recommendations
Were designed to be easily implemented by Education and Training Establishments

CETOP- Education Recommendations
Should be fully understood by National Trade Associations and promoted accordingly

National Trade Associations and members
should collaborate with education and training establishments and help them to better understand the aims of the CETOP EDUCATION RECOMMENDATIONS.



Education & Qualifications in Fluid Power



What do I need to do to meet the CETOP EDUCATION RECOMMENDATIONS?

Many education and training establishments already deliver courses involving fluid power

Step 1- Introduce the CETOP Education

Recommendations and explain the purpose

Step2- Refer to their course syllabi and cross reference with the CETOP Education recommendations

YOU MAY WELL BE SURPRISED AT THE AMOUNT OF COMMON SUBJECTS EXIST.

Step 3- Look at the depth of content and begin to align these with the specific LEVEL



Education & Qualifications in Fluid Power



Knowledge Based Subjects at LEVEL 1:

- Fundamental Principles
- Hydraulic System Construction and Symbols
- Operation of Major Components
- Hydraulic Fluid and Characteristics
- Contamination Control
- First Line Management
- Maintenance Procedures

Knowledge Based Subjects at LEVEL 2: (INDUSTRIAL)

- Fundamental Principles
- Hydraulic System Components
- Pumps and Associated Control Systems
- Hydraulic Actuators
- Circuitry and Control Features
- Hydraulic Fluids
- Contamination Control
- Reservoirs and Auxiliary Equipment
- Maintenance, Monitoring and Fault Finding Procedures

HEALTH and SAFETY is a CORE SUBJECT and is applied at every level

Education & Qualifications in Fluid Power



cetop



FLUIDAS
ASOCIATIA NATIONALA PROFESIONALA
DE HIDRAULICA SI PNEUMATICA

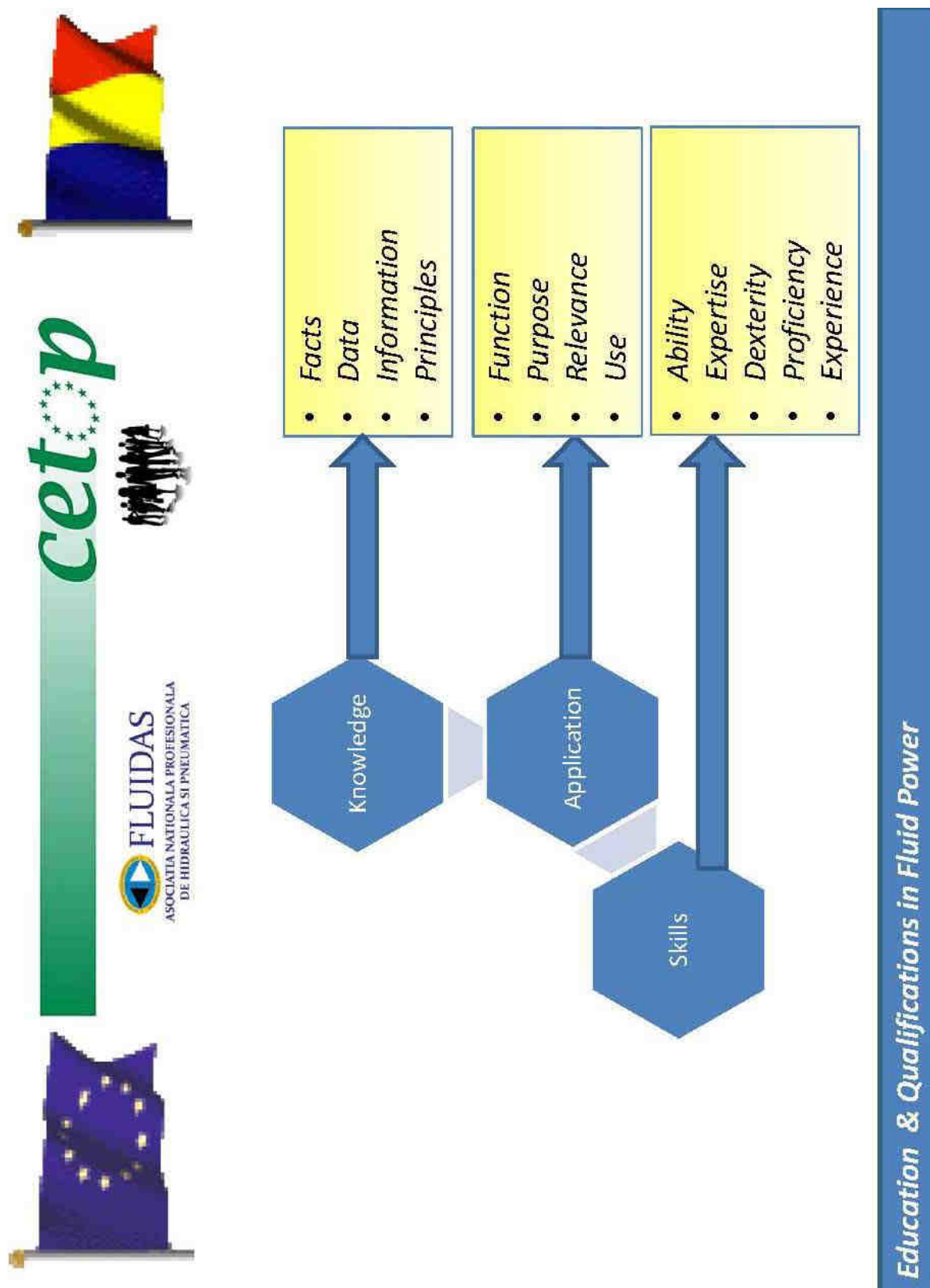


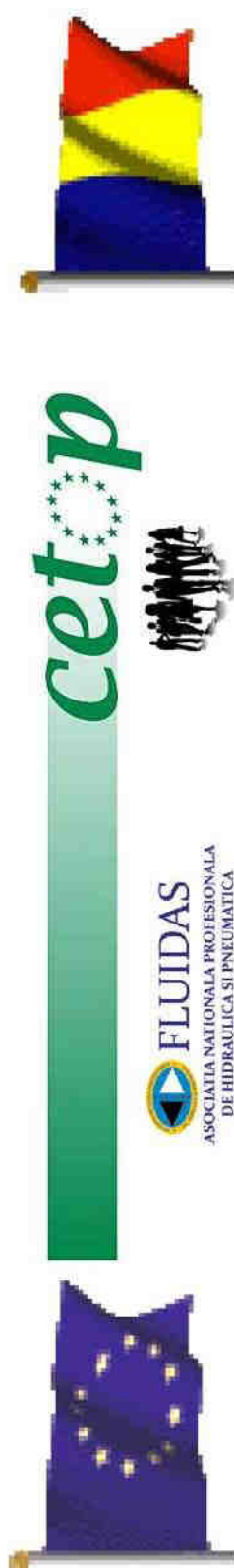
Knowledge Based Subjects at LEVEL 3: (INDUSTRIAL)

- Application of Fundamental Principles
- Hydraulic System Components
- Valve Mounting Styles/Configurations
- Slip-in Logic Cartridge Valves
- Fundamental Electrical Principles
- Electrical/ Electronic Components
- Proportional Valve Technology
- Pumps and Associated Controls
- Hydraulic Actuators (Motors/Cylinders)
- Closed-Loop Hydrostatic Transmissions
- Reservoirs, Conditioning and Auxiliary Components
- Pipes and Hoses- Installation and Commissioning Procedures
- Contamination Control
- Circuitry and Control Features(Recognition and use of hydraulic and electrical symbols)
- Installation and Commissioning Procedures
- Maintenance, Monitoring and Fault Finding Procedures

HEALTH and SAFETY is a CORE SUBJECT and is applied at every level

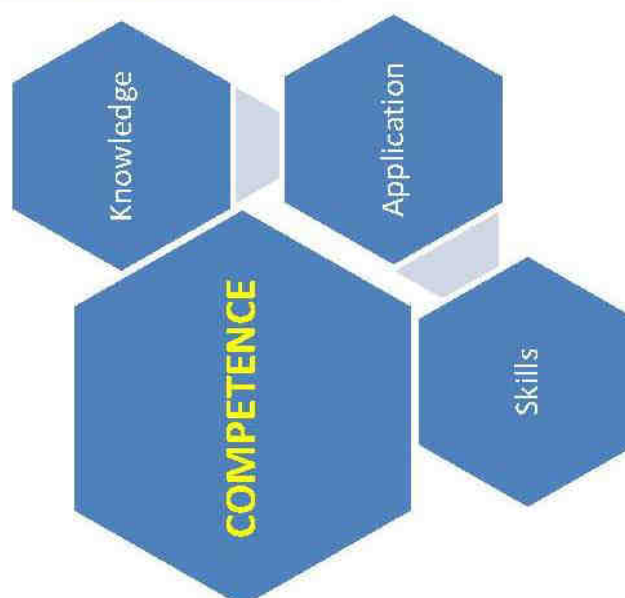
Education & Qualifications in Fluid Power



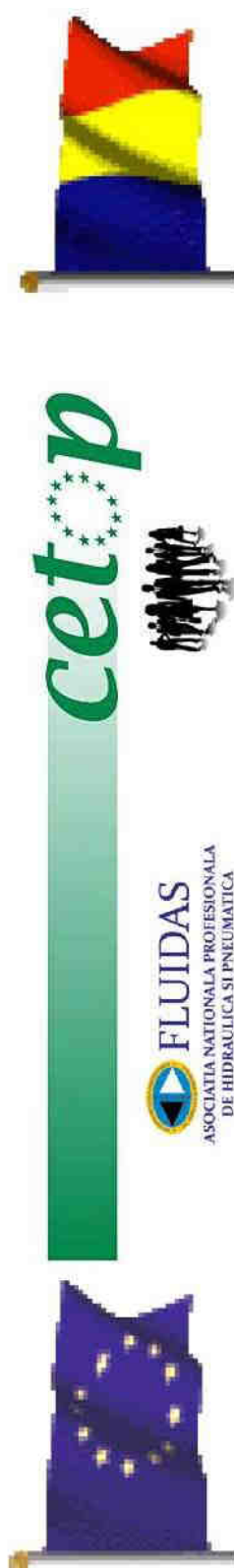


*From the very start -
CETOP EDUCATION RECOMMENDATIONS would
combine **education** with **training**, enabling
maintenance staff to combine both **knowledge**
and **skills** to perform their work based tasks*

*This combination of knowledge and skills would
be addressed by the term "**COMPETENCE**"*



Education & Qualifications in Fluid Power



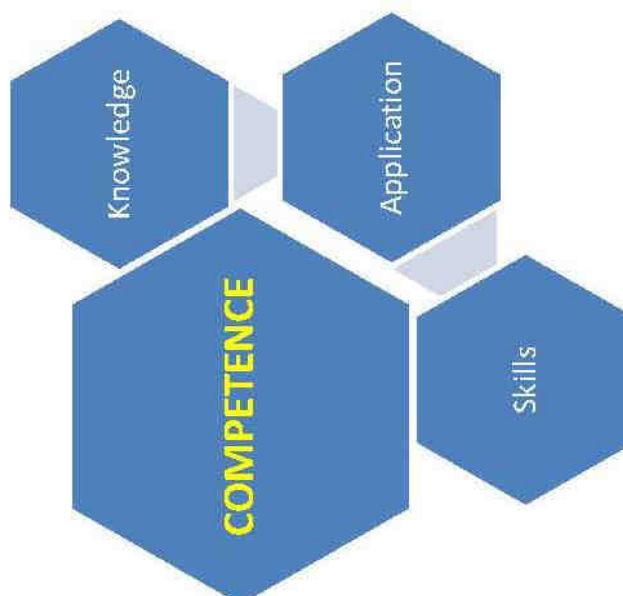
*From this point onwards
CETOP Education Recommendations would lead
to a QUALIFICATION STRUCTURE consisting of:*

1. Knowledge Based Assessment

This taking the form of a WRITTEN EXAMINATION

2. Practical Task Assessment

*This taking the form of a "one to one" assessment
in carrying out a particular range of tasks*

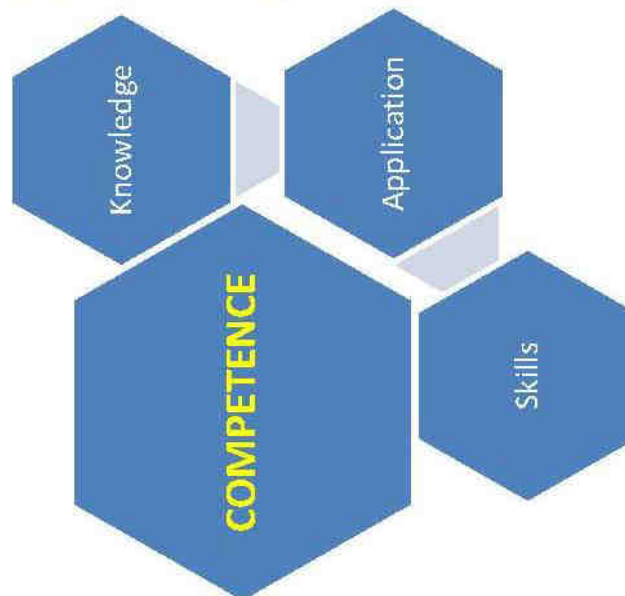


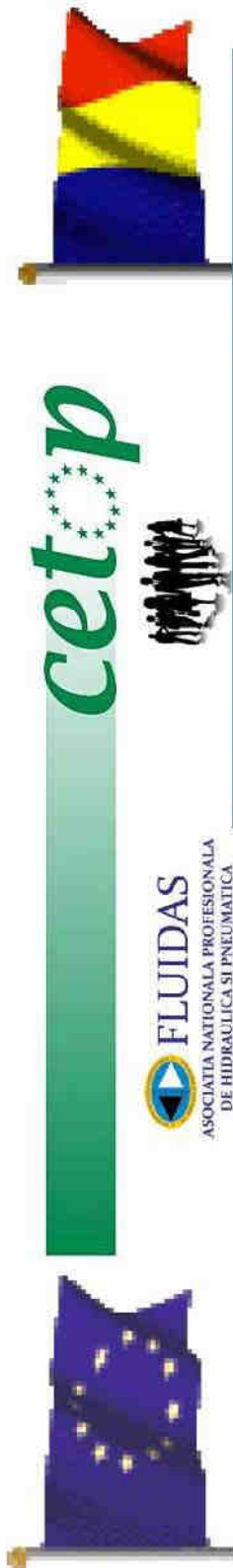


*Within the CETOP Education Recommendations this part of the qualification is covered by what are termed **ASSESSED ABILITY**.*

*Each **ASSESSED ABILITY** was carefully chosen by the CETOP Education Working Group to meet both the level and skills of maintenance staff.*

*Each **ASSESSED ABILITY** was then supported by the **EVIDENCE REQUIRED** to address competence in carryout a particular task*





To effectively practice the **ASSESSED ABILITY** and be **ASSESSED** would require access to an extensive range of equipment as well as having highly knowledgeable practically trained **TRAINING ENGINEERS/ASSESSORS**



Education & Qualifications in Fluid Power



cetop



FLUIDAS
 ASOCIATIA NATIONALA PROFESIONALA
 DE HIDRAULICA SI PNEUMATICA



Let us assume that the TASK on this occasion is to assemble a hydraulic system and commission to carryout a particular function.



Inline with the TASK the **ASSESSED ABILITIES** would include:

- Interpreting the electro-hydraulic circuit diagram
- Assembling the electro-hydraulic system involving on-off and proportional control from given information and commissioning accordingly
- Carryout effective fault diagnosis and rectify

For each of these, there is a list of **EVIDENCE** required

The **ASSESSOR** using a **CHECKLIST** approach, whilst **observing** the candidate in action and asking key questions and obtaining progressive feedback will **PASS** or **FAIL** the candidate on meeting or not meeting the required **PERFORMANCE CRITERIA**.

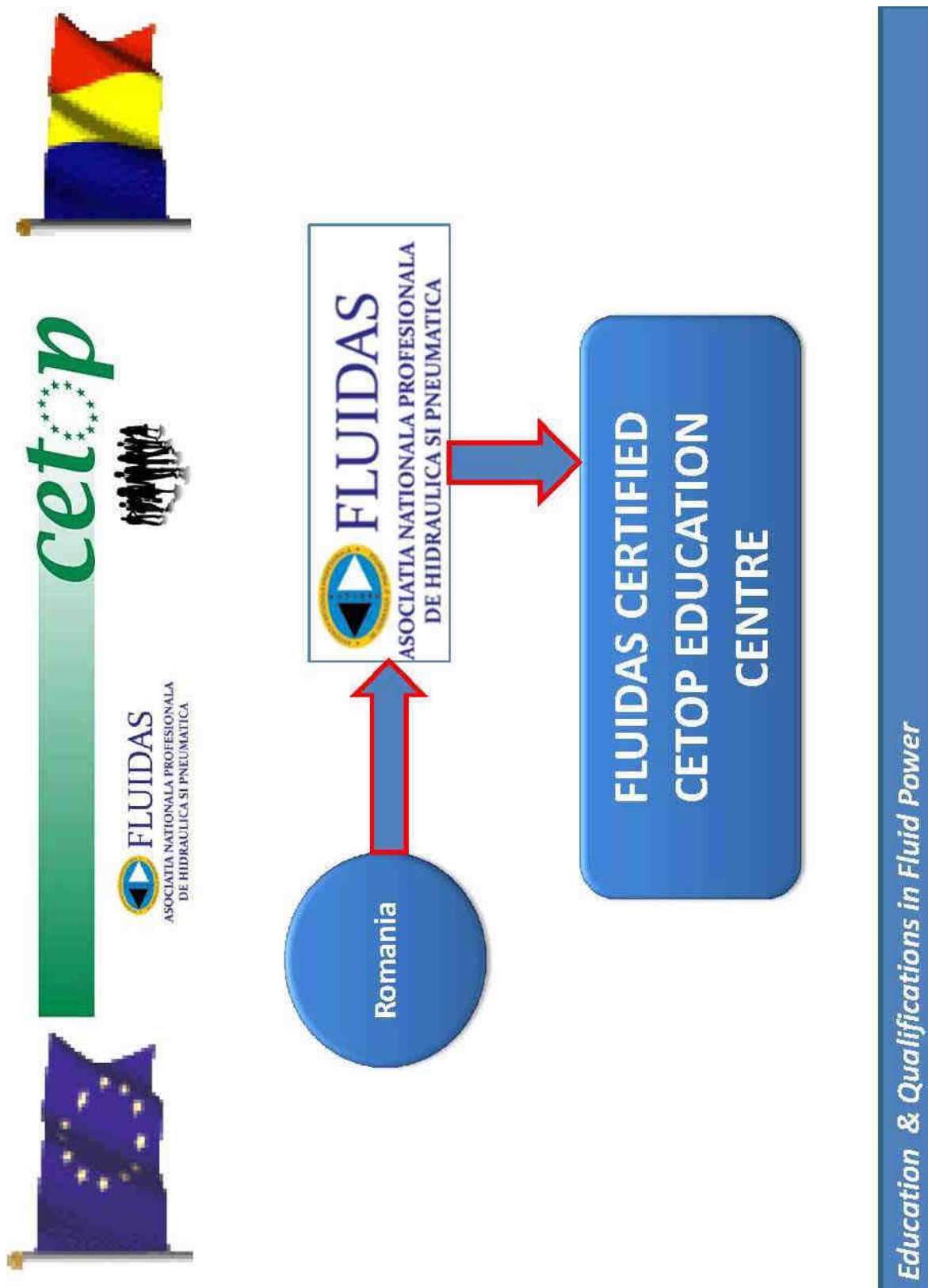
Education & Qualifications in Fluid Power

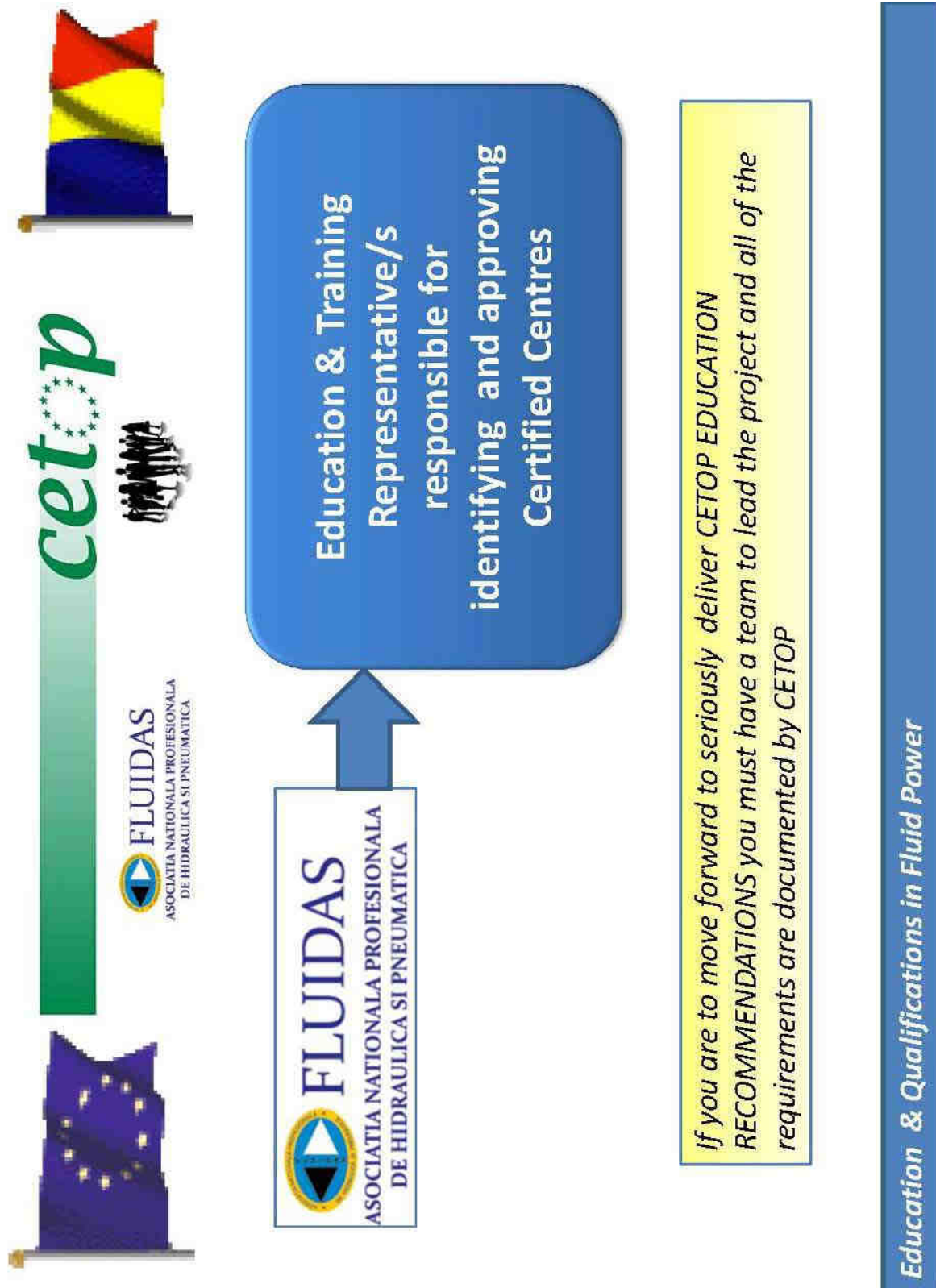


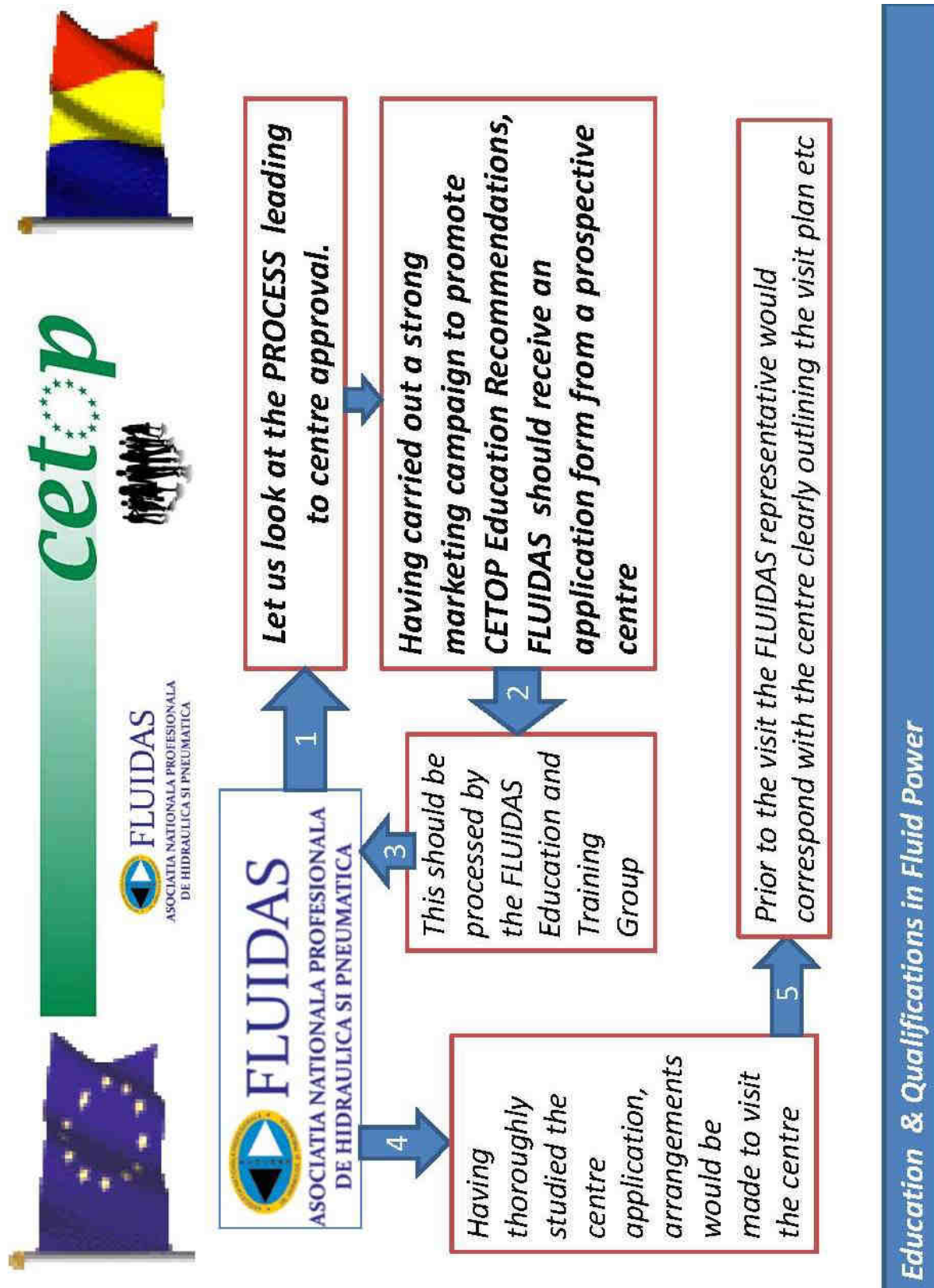
**The NATIONAL FLUID POWER CENTRE
 is a BFPA certified CETOP Education Centre**

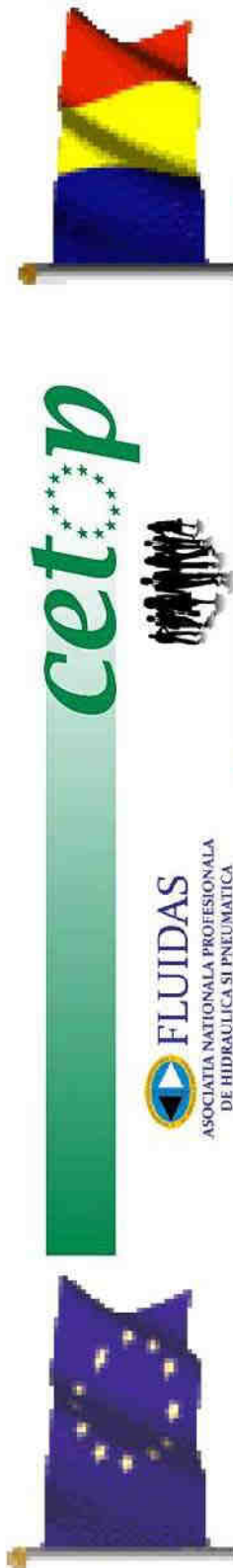
*This means that a representative
 from the BFPA has visited to NFPC following
 the NFPCs application for approval.*

- The BFPA representative following the
 CETOP APPROVED CENTRE GUIDELINE
 Reviewing:
- Accommodation/Facilities
 - Practical Equipment
 - Delivery and Management Team
 - Scheme Administration
 - Health and Safety/Hygiene
 - Equal Opportunities Policy







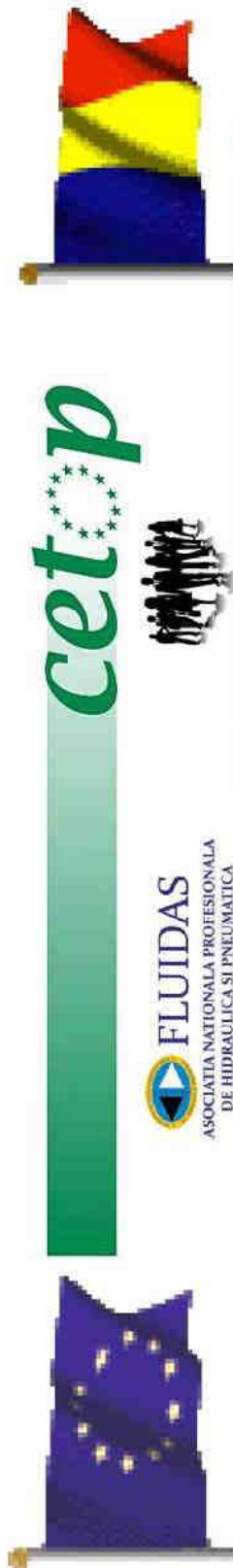


*During the planned Approval Visit
FLUIDAS would look at:*

- *the capability of the staff together with their experience and qualifications*
- *the suitability and adequacy of the training rooms and practical facilities.*
- *the infrastructure of the organisation in respect to management capability and health and safety issues*



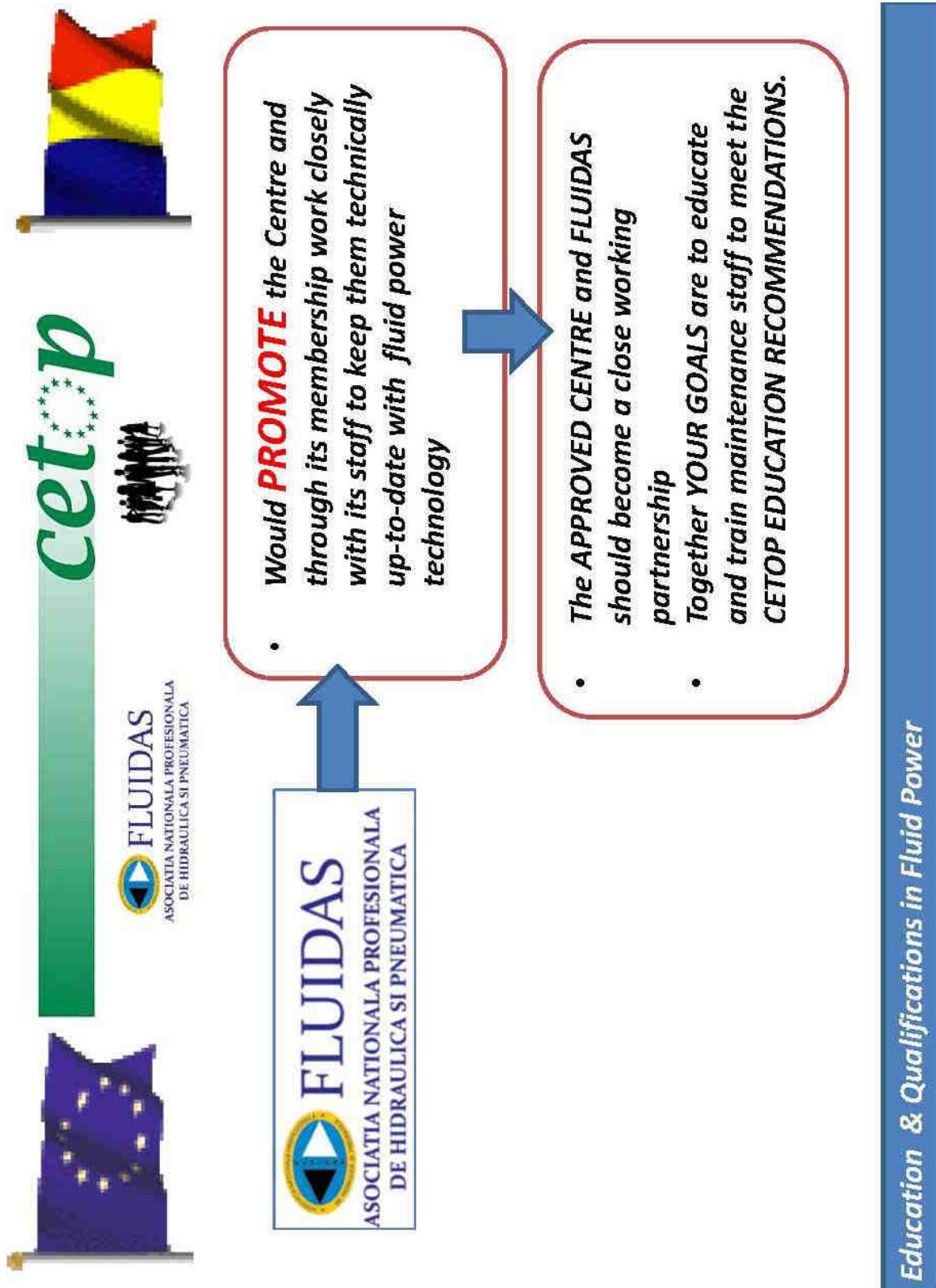
Education & Qualifications in Fluid Power

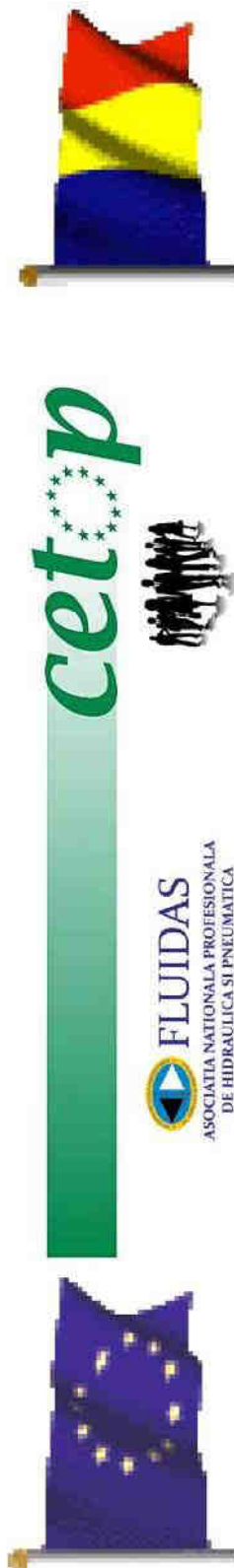


Should such a centre fail to meet the approval criteria FLUIDAS would make the necessary recommendations for improvements and an agreed time scale would normally be established before a 2nd approval visit is set up .

LETS US ASSUME THE CENTRE MEETS THE APPROVAL CRITERIA.
FLUIDAS applies to CETOP for that centre to receive its certificate as a CETOP CERTIFIED EDUCATION CENTRE relating to the level/s for which it has applied.

Education & Qualifications in Fluid Power





FLUIDAS
ASOCIATIA NATIONALA PROFESIONALA
DE HIDRAULICA SI PNEUMATICA



Is there a particular model way in which to deliver CETOP Education Recommendations?

ANSWER- NO.

CETOP Education Recommendations outline a minimum level of knowledge and skills to be achieved

THEY ARE A DESTINATION
The route or journey or period of time is totally flexible.

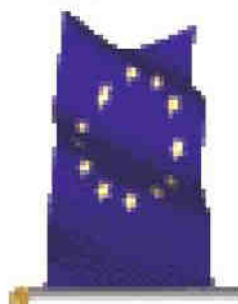
Education & Qualifications in Fluid Power



cetop



FLUIDAS
ASOCIATIA NATIONALA PROFESIONALA
DE HIDRAULICA SI PNEUMATICA



FLUIDAS
ASOCIATIA NATIONALA PROFESIONALA
DE HIDRAULICA SI PNEUMATICA



LET US NOW TALK
LET US NOW AGREE TO MOVE THINGS FORWARD
LET US NOW CREATE POSITIVE ACTIONS

Education & Qualifications in Fluid Power



**New SMC didactic
equipments - support for
performance in education**

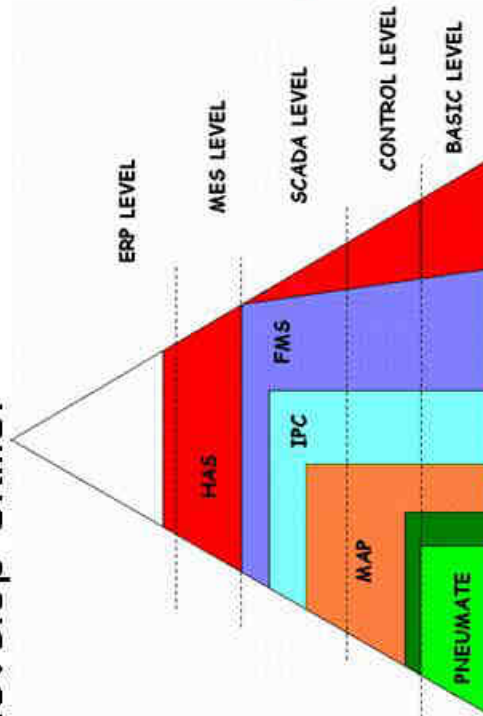
Prof. dr. ing. **Valeriu Banu** – Director Tehnic
Ing. **Dragos Gheorghe** - Industrial Project Manager

WHAT MAKES THE DIFFERENCE ?




THE PHILOSOPHY

- We conceive the didactic equipment as an integration of technologies duly organized to develop skills.




- As these tools must provide a solution to industrial needs, they have to reproduce as maximum, the industrial processes of the modern industry.


...& what is new?




PNEUMATE




PNEUTRAINER




VAC-200




AUTOSIM




MAP-200




AUTOMATE-200




HAS-200




FMS-200

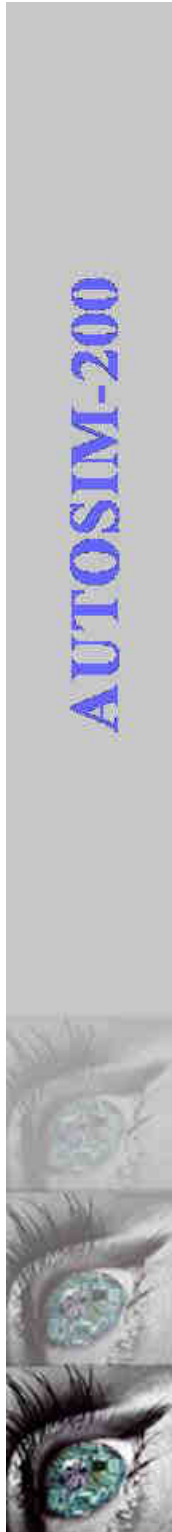


IPC-200



MAS-200



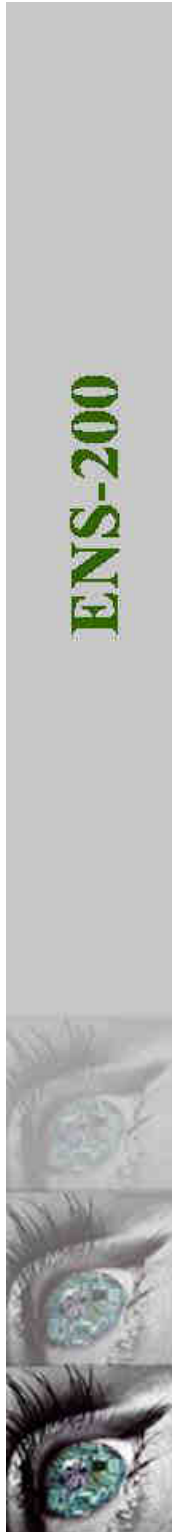


Automation simulator



- New features:
- 3D model simulation.
- Communication with real equipment.
- ...





Energy saving trainer



A real way to introduce the “green” approach into the manufacturing/engineering programs.

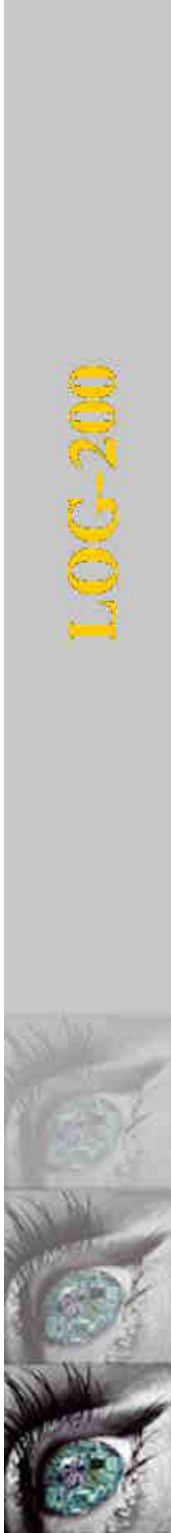




Hydraulics/ electrohydraulics

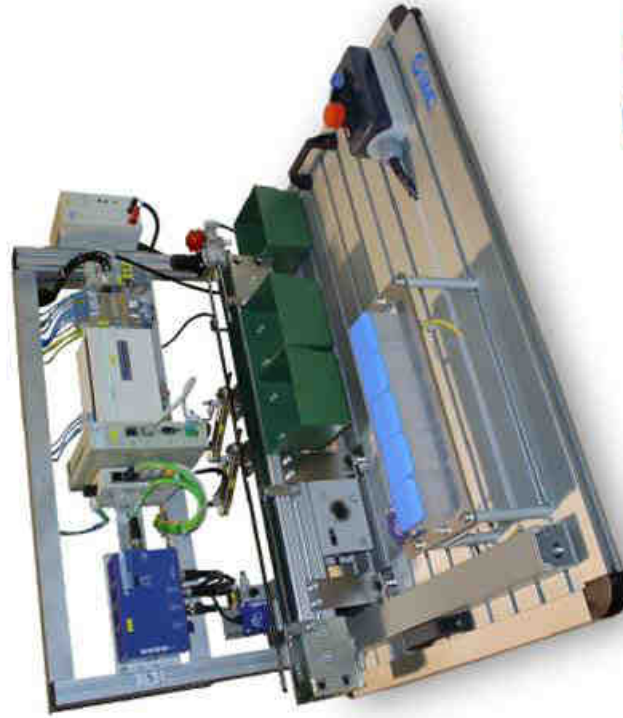
- Standard compositions:
 - Hydraulics level I.
 - Hydraulics level II.
 - Electrohydraulics.
 - Proportional hydraulics level I.
 - Applications in proportional hydraulics level II.
- Transparent hydraulics.

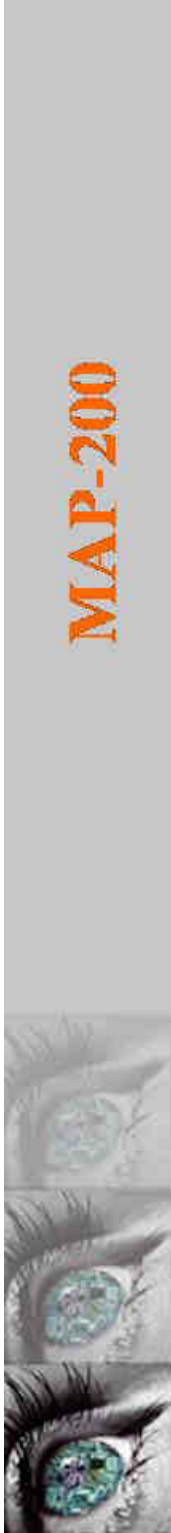




RFID logistics trainer

- Logistics application context.
- RFID technology included.
- PLC controlled
- Object traceability via web page.



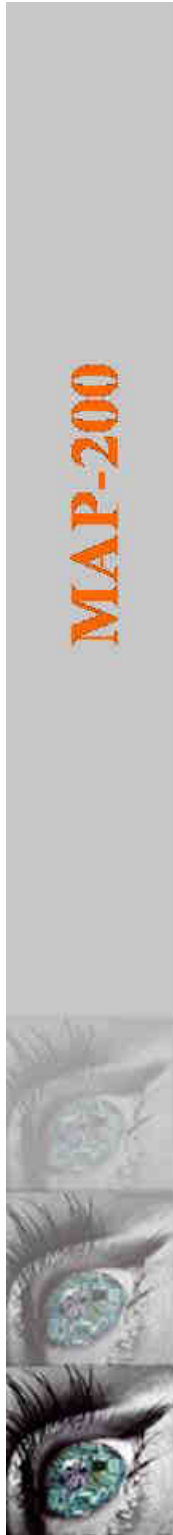


Handling systems:

MAP-206: Handling device using electric actuators:

- Only electrical actuators.
- HMI with built-in PLC.
- X-Y servo-controlled axis.
- Z axis: electrical cylinder.



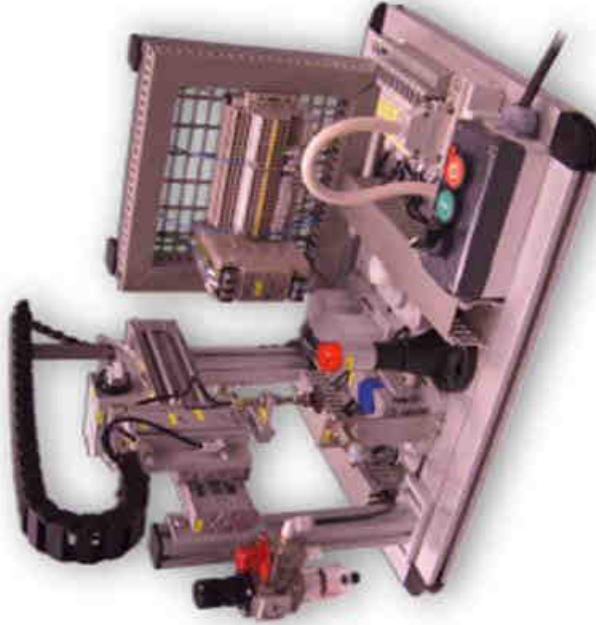
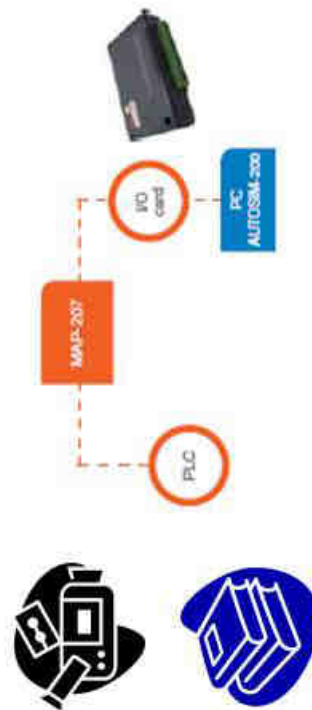


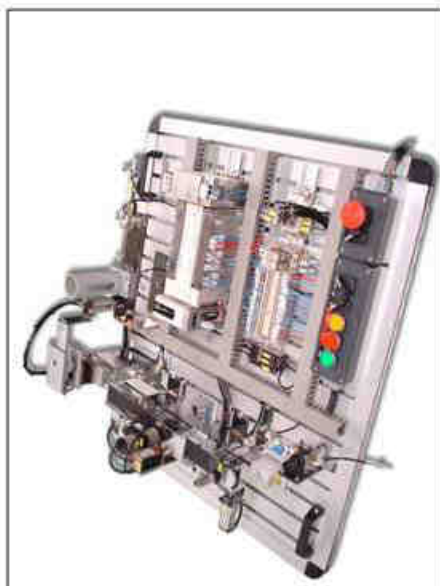
MAP-200

Handling systems:

MAP-207: Handling device allowing parts classification:

- Up to 6 different parts:
- 3 diameters.
- 2 materials.
- PLC \ I/O card + Autosim control.



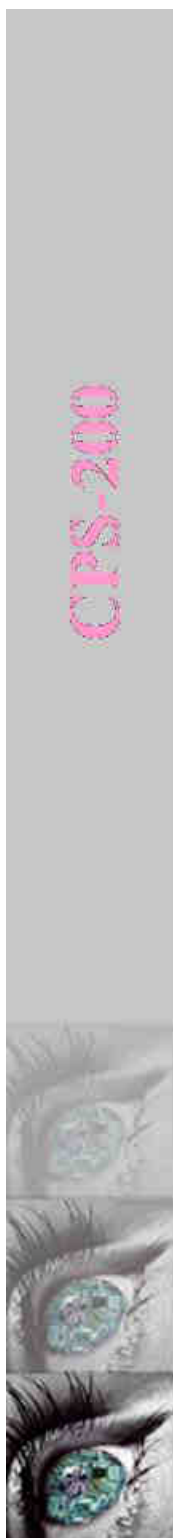


Compact version

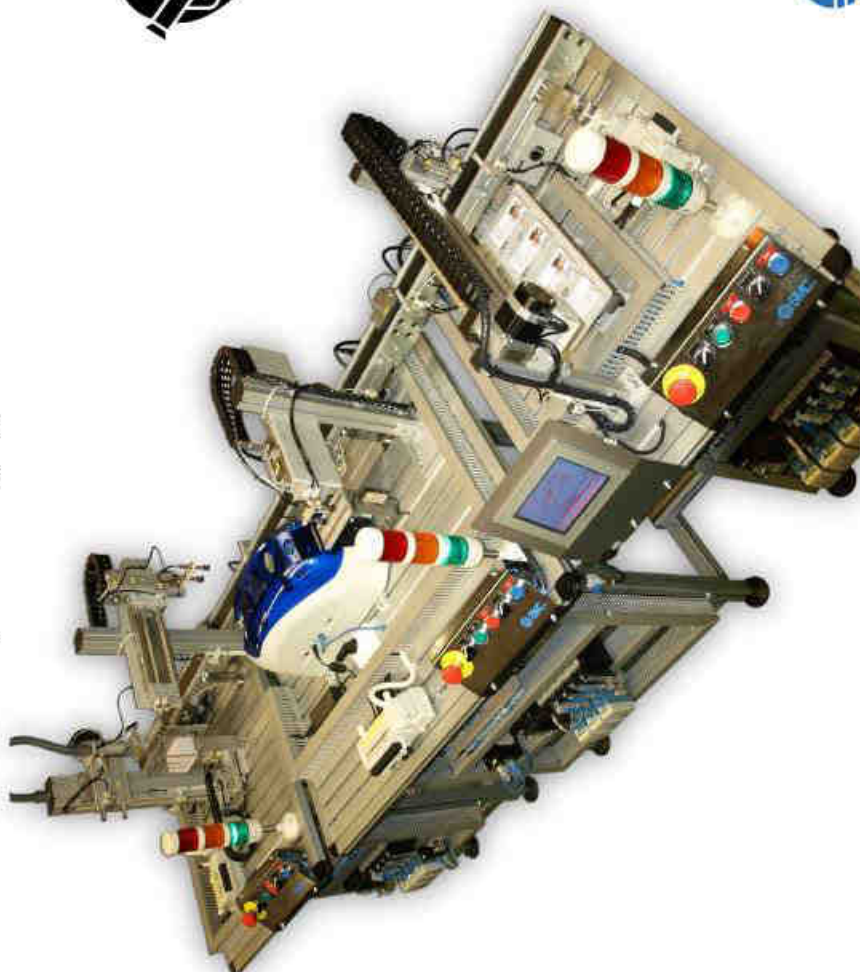


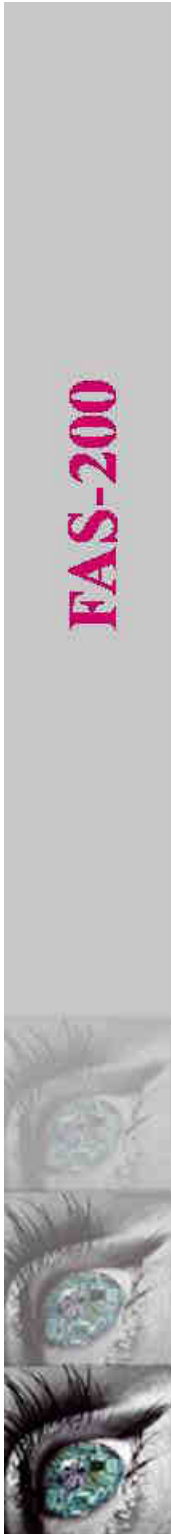
**Version with rollig frame
and folding control panel**



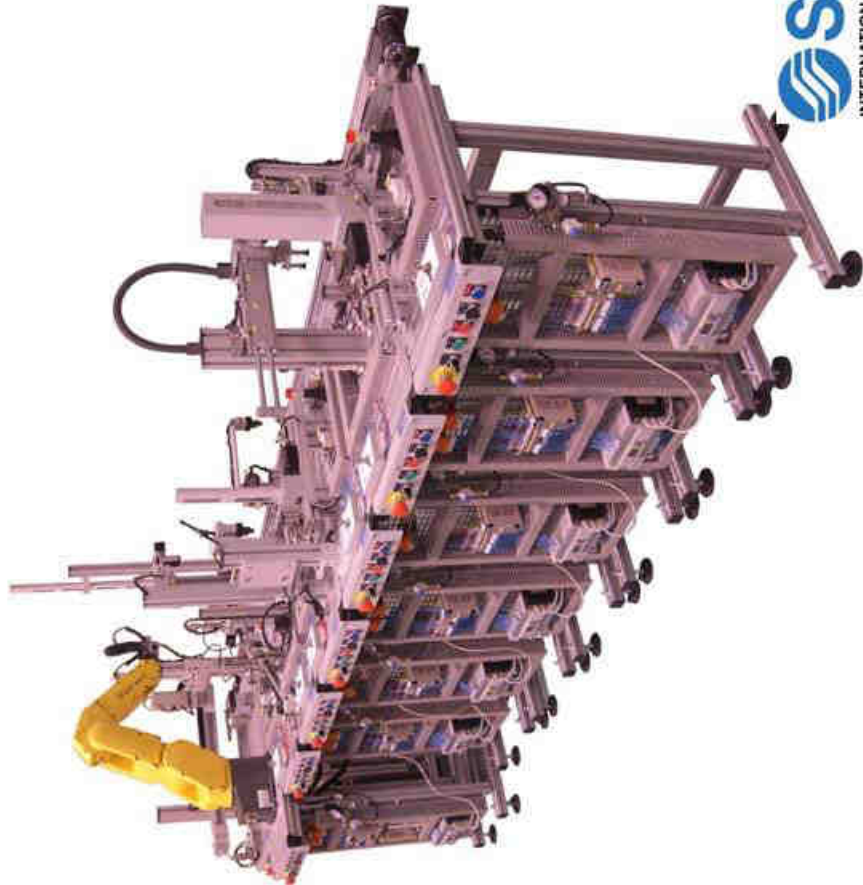


Cards printing system:



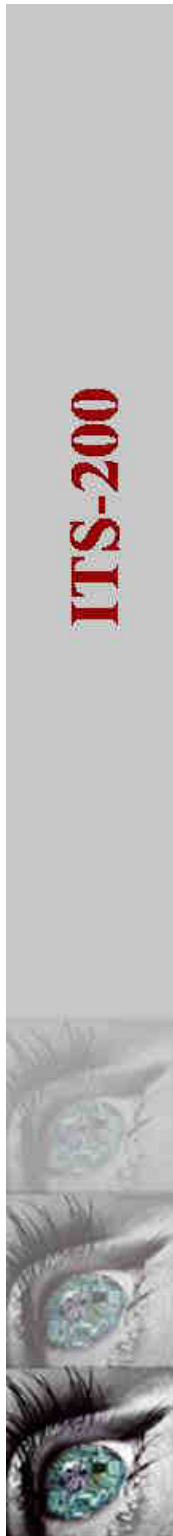


Flexible Assembly System



- Up to 18 stations.
- Multiple configurations.
- Breakdown box.
- PLC controlled.
- SCADA application.

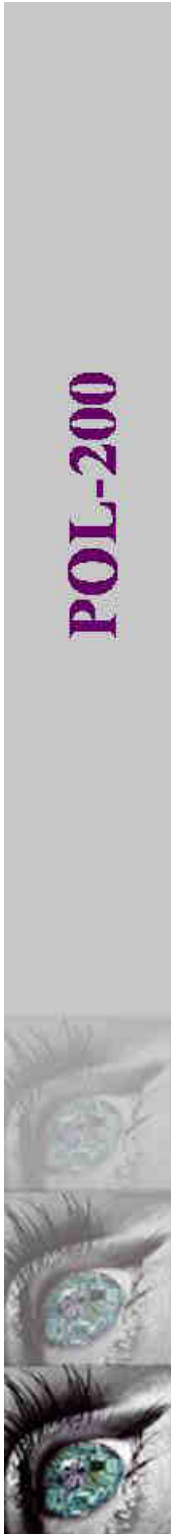




Innovative training system:

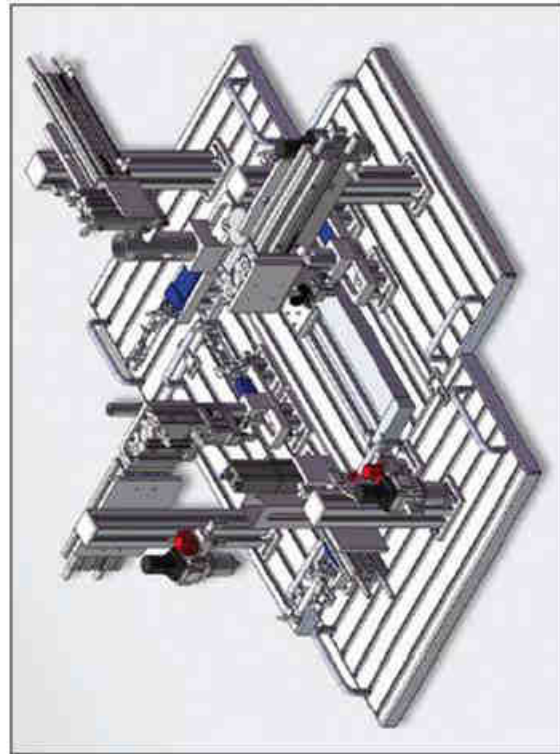
- State-of-the-art in:
- Sensors.
- Servo-drives.
- RFID.
- AC/DC motors.
- Closed loop system.





Polymechanics and automation:

- Project based product:
 - Machining, assembly, wiring and programming
 - Up to 5 stations.
 - POL-201 official platform in Spainskills 2011.

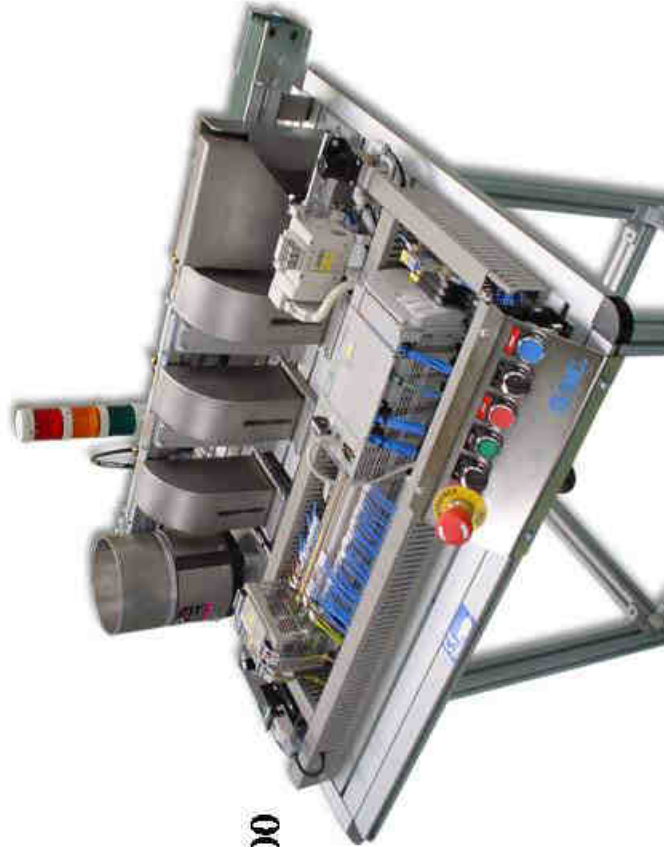




Others: HAS-212

HAS-212 – Recycling station:

- HAS-212 classifies the mixed raw material.
- Vibrating container.
- Two conveyor belt.
- Ready to be added in HAS-200 systems.





E-learning: 10 courses package covering the fundamentals of automation. Ready during 2012.



Chapter 3 Pneumatic Actuators

Pneumatic actuators are pressurized air to move mechanical components.

They are used in applications such as machine loading and unloading, material handling, product assembly, welding, packing, testing and quality control.

Course Menu:

- 1 180 Skills
- 2 Intro to Pneumatics
- 3 Pneumatic Actuators
- 4 Pascal's Law
- 5 Ohm's Law
- 6 Multimeters
- 7 Additional 180 Works

SMC INTERNATIONAL TRAINING

SMC-100 Introduction to Pneumatics

Copyright © 2008 SMC Airtech, Ltd.



NEW INSTRUMENT FOR LUBRICANTS BEHAVIOR EDUCATION AND TRAINING

Alexandru RĂDULESCU¹, Irina RĂDULESCU²

¹ University POLITEHNICA Bucharest, e-mail: varrav2000@yahoo.com

² S.C. ICTCM S.A. Bucharest, e-mail: irena_sandu@yahoo.com

Abstract: *The paper presents a wear degree and durability modeling and simulation tool for oils, by developing a fast diagnostic device for liquid lubricants, with minimum investment, with a high precision degree and easy to use. Significant benefits are made by the proposed procedure: the small amount of lubricant required for a determination, the short time measurement and the possibility of adapting the method according to concrete conditions. This is used as a method of educating and training students and specialists in the lubricating process.*

Keywords: *informatic integrated tool, wear, durability, lubricant*

1. Introduction

Considering lubricants as lifeblood of industrial machinery, their role is to protect critical components and to help promote enhanced operation, just as blood supports health in the human body, [1]. That is why it is important to collect valuable insights about industrial equipment using oil analyses. Checking the lubricant by oil analysis is useful to help evaluate the condition of internal hardware equipment, as well as the in-service lubricant, in order to obtain information for extending the useful lives of both. It is vital to identify early warning signs (contamination, increasing wear metals) for minimizing unscheduled maintenance.

If lubricants degradation is a quantified process, information about physical characteristics and chemical composition changes are important. These are caused by internal and external factors and by the severity of operating conditions. Lubricants degradation factors over time is due to mechanical loads, operating temperature and contamination. It is a progressive process, being more intense as the service conditions are more severe. Some of the most important factors involved in determining of the lubricants degradation and their disuse [1], [2] are: the contamination with different impurities or chemical agents, during the usage, transport or storage, the mechanical effects of thermal overstressing, the possibility of increased aeration and water penetration into the oil, in bigger quantity.

The shortened lubricant use is the consequence of reported changes that is sometimes associated with the equipment safety endangering [3]. The problem of a long use of industrial lubricants is transposed over the existence of a life cycle, which is economically satisfactory. Also it has good effects the proper lubricants choice, suitable for the production equipment that implies reduced life cycle costs. Identifying the degradation causes is possible with a careful laboratory control made by specialized personnel, involving determinations of specific parameters, typical tests on laboratory stands, by using standardized methods. The interests of specialists regarding the assessment of the lubricating environment efficacy led to the development of laboratory methodologies to simulate real conditions, which are specific to machinery exploitation, [5].

2. International and national good practice stories

Important to note that, at international level, main directions are orientated to the preventive maintainability domain, for applying into any closed lubrication system. Methods known from applicative researches must be mentioned: the method of the intersection curve of acidity with the curve of alkalinity, which is used for alkaline oil (especially when it is used a fuel with sulphur), the microscopic oil analysis, the method of oil spot. Some examples from industrial domain are the German MAN firm, which uses the basicity analysis method for Mobil class oils, for the oil lifetime

determination for engines trucks, the firm Mercedes from Germany, which uses insoluble impurity in oil, with microscopic tests for class Shell oils, (the changing moment indicators are the number and the size of particles in suspension).

BOGE Compressors Ltd. From United Kingdom can yield up to 5% energy savings by using its special lubricants (S46 Screw Lube mineral oil, SYPREM 8000 S), which extend maintenance life to 40.000 hours. The importance of using the adequate lubricant and the oil changing moment at the proper mileage can improve engine reliability and has the potential to reduce nationwide waste and recycled oil by 325 million gallons annually, [6], and [7].

An example of the introduction of science in the service of creating sustainable solutions is DuPont Company, which is operating in over 70 countries, offering a wide range of innovative products and services in various fields: agriculture, nutrition, electronics, communications, safety and protection, construction transport, electrical appliances. Over 20 years the department of lubricants - DuPont™ Krytox offered performance for mechanical systems: turbines, gearboxes, dampers, valves, fittings and other components. The specific technology "Krytox lubricants" provides the best performance for equipment and the lowest life cycle cost for lubricants by:

- a longer lubrication time: By using the products offered by the company it is reduced the amount of lubricant needed 10 times or more, thereby reducing costs and re-lubrication frequency. "Krytox lubricants" can extend the duration of the weekly lubrication every year;
- reduced wear: "Krytox lubricants" can reduce the wear of bearings and gears, and ensure functioning under extreme temperatures (225°F - 750°F) and chemical products, thus reducing maintenance efforts and having a significant possibility of failure for the components;
- chemical compatibility and safety for the environment: "Krytox lubricants" provides chemical products, that are biological and ecological inert, silicone-free, contain no hazardous materials or chlorine. Also, working with less lubricant is thus reducing waste lubricant [4].

Experience shows that achieving a long life cycle works by reconditioning services lubricants in 3 directions: removing contaminants, "refreshing" the additives system and / or rebuilding additives system. Considering the national level, there were made used oil changing moment evaluations at ROMAN firm on Lubriffin oils (Romania). There is applied the oil spot method, which analyse the aspect of the spot made on a filter paper; another method applied on Lubriffin oils, in ROMAN firm, is represented by the photoelectric method, which allows the establishment of used oil changing moment, according to the quantity of oil impurities.

Researches made by "POLITEHNICA" University from Bucharest and "GHEORGHE ASACHI" Technical University from Iași followed the determination of the rheological properties of the mixture oil - polymers, emphasizing their non-Newtonian thixotropic character. Same educational level, "TRANSILVANIA" University from Brașov obtained interesting results in management of lubricants solid residues, by using the ferografic analysis of used oils. Also lubricants properties and durability researches were made in Romanian manufacturing bearing firms: RULMENTUL Brașov, TIMKEN Ploiești or Koyo Alexandria.

The industrial laboratories offered the opportunity to make physical-chemical standard tests and tribological ones (Timken stand, Amsler stand, etc). The information obtained by analyzing these methods give important data from performing laboratories, at high technical level, but it involves special attention from the technical staff, a good practice experience and high level practitioners, [8].

3. Practical issues concerning the industrial lubricants longer use

The problem of industrial lubricants longer use is reflected into the economically satisfactory life cycle existence. The right choosing of lubricants has effects in longer use of production equipment and life cycle costs. By lubricants selection for existing equipment within a factory it must consider a number of factors:

- the frequency of lubrication: considering the use of lubricants, power generating equipment may require frequent re-lubrication, which may have an impact on production and can be expensive over time.
- extreme production environment: high temperatures and concentrated chemicals can cause lubricant breakdown, by compromising performance and leading to a maintenance extra effort.

- safety and environmental issues: Some lubricants contain chemical volatile organic materials or chlorinated materials that can be hazardous to the environment and employees. Frequent re-lubrication can increase the exposure of employees to hazardous areas with high temperatures.

It is necessary to follow a certain protocol to ensure the accuracy and correct information from lubricant analysis results. For taking a representative sample must always use a clean, dry, dust free area until the sample is taken. Also, specialist must draw samples when equipment is at its normal operating temperature and while the machine is running, if it can be done safely. Otherwise, it is recommended to draw samples as soon as possible after the equipment has been shutdown.

Properly location consists in taking samples downstream of the filters, the critical lubrication points. Also, it must avoid sampling from reservoirs, where unrepresentative samples may be produced by possible stratification and sediment and distorting results. For some cases (gearboxes) where the equipment doesn't have a circulating system, samples must be taken from the gearbox bath or sump, several inches deep from the bottom of the bath, to avoid accidentally including the insoluble layer, that has appropriately settled to the bottom.

Considering viscosity as the most critical parameter for most applications, researches showed that it can change over time or more quickly in equipment that sees extreme temperatures or high pressures or high speeds. That is important always monitor lubricant viscosity closely, to ensure that it is within the targeted viscosity range, thus minimizing wear between critical equipment components. If the viscosity changes by $\pm 15\%$ of its original value, it must monitor the oil more frequently. Equipment can perform normally if the lubricant is outside of this range, but it should be watched more closely as this usually indicates changes are needed. All equipment applications have stated recommended operating temperatures and recommended lubricants that meet that condition. If oil temperatures significantly vary (particularly trending higher) it is recommended to re-review the ISO grade of the oil to ensure that an appropriate film thickness is being provided to insure efficient wear-free performance.

Tracking equipment health also implies monitoring wear metals. As equipment ages, components start to wear; it is important to monitor the degree of wear to permit scheduling routine, planned repairs rather than waiting for unplanned equipment shutdown. Common wear metals to be monitored for various systems include:

- Hydraulics: copper, iron, lead (aluminum, tin, chromium less common)
- Compressors: iron, copper, lead (tin, aluminum, nickel less common)
- Gearboxes: iron, copper, aluminum (lead, tin, chromium less common).

Iron and copper are used in nearly every piece of equipment, so monitor their presence closely for almost all machine types. Another common cause for equipment shutdowns is contamination that is present in different forms: dirt, dust, water. Most airborne contaminants show up in an oil analysis as silicon. The most effective way to extend equipment and lubricant life is to implement a comprehensive lubricant analysis program. It will help identify early warning signs of contamination and minimize unscheduled maintenance, [9].

4. Global performance passport of the lubricants

For obtaining the integrated informatic device there were used advanced technologies, which are present in the four working component modules, in order to realize the lubricants behavior modeling and simulation. Their core functions are described here:

1. The theoretical module role is to analyze the phenomena which are based the lubricant film extrusion process. Also it generates theoretical curves specific to the interstitial fluid flow, which are necessary for the experimental results correlation and interpretation, [7].

2. The rheological experimental module is a modern one, containing an original measurement device, which is coupled with a data acquisition and data processing system. By using a small amount of lubricant for the diagnose (100 ml) and two semi - coupling, it is registered the time variation function lubricant pressure and thickness. It is important to work with qualified staff or to educate students and specialists to work with the three pressure transducers and one proximity sensor, while the oil film is expelled under the wight of the upper coupling (figure 1). Squeeze-film

curve is recorded as the „fingerprint” of the used lubricant, that depends on many factors, including the lubricant wear degree, [4].

COMPLEX MONITORING INSTRUMENT

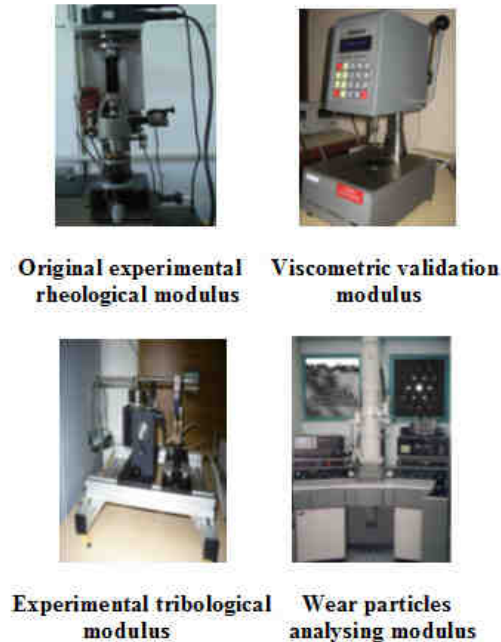


Figure 1. Complex monitoring instrument, [10], [11], [12], [13]

3. Considering the viscometric validation module, this one is based on a PHYSICA rheometer and it is composed of a mechanical unit and an electronic one. The components of mechanical unit are represented by the measurement system, thermostat installation, training system and additional installations. The electronic unit is composed of a transfer system for the measured parameters, the data processing system and the central control and command unit. The module role is to validate the experimental results which are supplied by the experimental rheological module and to establish the necessary correlations [5], [6].

4. The spectrometric analysis module is based on the use of transmission electron microscopy by obtaining information concerning the wear particles which can be identified in samples of worn off lubricants. By comparing two microscopic structures of the same lubricant (Figure 2), in various stages of use, it may reveal the wear particles, their shape and their size [8].

Among the advanced technologies used in education and training for lubrication processes a special one is represented by the LabVIEW software - Laboratory Virtual Instrument Engineering Workbench, a graphical programming environment developed by National Instruments Corporation. The software is useful in data acquisition, processing and presentation, also for control and industrial process control, for the systems dynamic behavior analysis.

5. The new instrument for lubricants behavior education & training results and conclusions

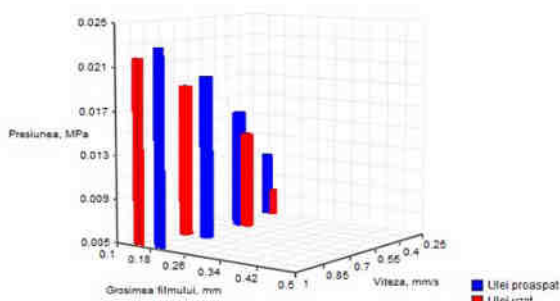
The core of this global methodology for the study of industrial lubricants behavior is represented by a complex monitoring tool, composed by four experimental modules: rheological, viscometric, tribological and a module concerning structural analysis. The original rheological experimental module has a measuring device mounted on a Weissenberg rheogoniometer and a data acquisition and processing system, [10]. A small amount of lubricant is used for diagnose and the temporal variation of lubricant film thickness is recorded, by using a proximity sensor, while the oil film is expelled with constant speed. The recorded information is the squeeze-film curve, the "fingerprint" of the worn-out lubricant.

The viscometric module based on a Brookfield viscometer validates the experimental results provided by the rheological experimental module and establishes the necessary correlations, [11]. The tribological experimental module consists in a friction torque pin – disk tribometer, having the role to determine the friction coefficient variation due to contact pressure and sliding speed, for lubricants with varying wear degrees, in terms of the same friction torque use, [13].

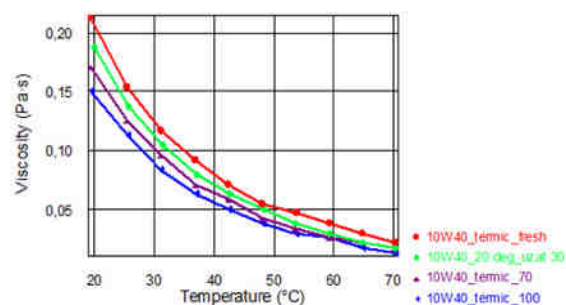
The wear particles analysis module is based on the transmission electronic microscopy, obtaining information on the wear particles from worn lubricants samples. The principle is to compare two microscopically structures of the same lubricant, in various decay stages, revealing the wear particles, their shape and their concentration, by using the JEOL Japan - JEM - 200 CX transmission electron microscope, [12].

The four modules and the related global methodology represent a new, modern instrument for lubricants behavior Education & Training, by assessing and quantifying the industrial lubricants life cycle aims. Finally, the achievement of a global lubricants performance passport is a complete characterization of the lubricants behavior, which is studied during their life cycle, in terms of rheological, tribological, viscometric and microscopically point of view. Important issues are solved due to this instrument:

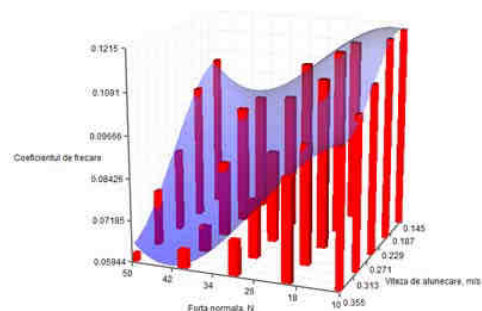
- the global rheological lubricant feature is expressed by the maximum pressure of fresh and worn lubricating film and it is obtained with the original rheological experimental module;
- the reference rheological lubricant feature is obtained with the viscometer validation module and it is expressed by the variation of viscosity by the temperature, according to various lubricant wear stages;
- the tribological lubricant feature is obtained with the tribological experimental module, which is expressed by the friction coefficient variation according to the normal pressing force and the sliding speed, both for fresh and worn lubricant;
- the structural (microscopic) lubricant feature is obtained with the wear particles analysis module and it is done by the solid particles type, which are identified in the fresh and worn lubricant, [14].



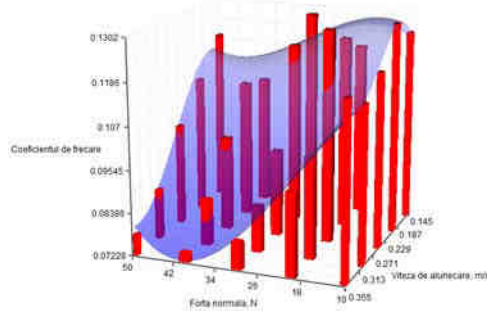
a) Lubricant Global Rheological Characteristic



b) Lubricant Reference Rheological Characteristic



c) Lubricant Tribological Characteristic (Fresh)



d) Lubricant Tribological Characteristic (Used)

Figure 2. Example of the Global Lubricant Performance Passport (10W40 oil)

6. Conclusions

The global performance lubricants passport represents a complete characterization of studied lubricants behavior, during their life time. Each lubricant has a specific rheological, tribological and structural behavior, which requires continuous monitoring of these properties, all the use period, from fresh stage till its complete depletion.

The utility of this instrument is reflected on the issues that may be solved: the assessment of the lifetime reserve, function specific use conditions (load, speed, temperature, etc.), reducing costs operations, (with initial investment for the preliminary experimental tests conduct), good and available information about lubricants behavior for industry, educational and training domains. It is necessary to notify that the achievement of a global performance lubricant passport should be correlated with the determination of economic profitability threshold for the investment made by a potential user.

This paper proposed a framework for developing a practical methodology for testing lubricants, by using global performance lubricants passport model, it will minimize equipment downtime, permitting more efficient maintenance scheduling, protect warranty claims and increase equipment resale value.

REFERENCES

- [1] L.R. Rudnick, Lubricant Additives Chemistry And Applications, The Energy Institute The Pennsylvania State University, Pennsylvania, U.S.A., 2003
- [2] I. I. Stefanescu, M. Ripa, L. Deleanu, Lubrifiere si materiale de ungere, (Lubrication and lubricants), Ed. AIUS Craiova, 2005
- [3] N. Olaru, Tribologie. Elemente de bază asupra frecării, uzării și ungerii, (Tribology. Basic elements on the friction, wear and lubrication), Universitatea Tehnică „Gh. Asachi” Iași, 1995
- [4] http://www2.dupont.com/Lubricants/en_US/uses_apps/industries/power_gen.html
- [5] H. Kaleli, Evaluation of additive's layer formation in engine crankcase oil using two different types of tribological test rigs, Industrial Lubrication and Tribology, Vol. 56, No. 3, 2004, pp. 158-170
- [6] R. D. Youngk, Automobile engine reliability, maintainability and oil maintenance, Reliability and Maintainability Symposium, Proceedings. Annual Volume, Issue , 2000
- [7] J. D. Summers-Smith, A Tribology Casebook – A Lifetime in Tribology. Mechanical Engineering & Bury St. Edmunds Publications, London, Great Britain, 1997
- [8] J. R. Sieber, S.G. Salmon, Elemental analysis of lubricating oils and greases, Lubrication, Vol. 80, No.1, 1994, pp. 83-89
- [9] <http://www.plantservices.com/articles/2008/094.html?page=2>
- [10] J. F. Hutton, On using the Weissenberg rheogoniometer to measure normal stresses in lubricating greases as examples of materials which have a yield stress, RHEOLOGICA ACTA, Vol. 14, No. 11, 1975, pp. 979 – 992
- [11] Brookfield Viscometers, rheometers and texture analyzers for viscosity measurement and control and tensile testing. <http://www.brookfieldengineering.com/>
- [12] M. Kubozoe, S. Okamura, H. Akahori, An Experiment with the Spot Scan TEM Technique, Journal of Electron Microscopy, Vol. 28, No. 4, 1979, pp. 263 – 275
- [13] Lubricant Testing Products, <http://www.dasolit.com>
- [14] Radulescu Irina, Teza de doctorat: “Cercetări experimentale privind monitorizarea lubrifianților industriali pe durata lor de viață” („Experimental researches concerning the industrial lubricants monitoring during their lifetime”), Bucuresti, 2010

RELAȚII PUBLICE ȘI COMUNICARE ÎN FOLOSUL ACTIVITĂȚILOR DE CERCETARE-DEZVOLTARE-INOVAR

Ing. Radu Jecu – Centrul de Informare Tehnologică - CENTIREM

Institutul de Cercetare – Dezvoltare pentru Metale și Resurse Radioactive - ICPMRR București

REZUMAT

Prezenta comunicare constituie un avertisment succint în vederea reconsiderării rolului preocupărilor pe linie de relații publice și comunicare în folosul activităților de cercetare-dezvoltare-inovare. Recunoașterea utilității comunicării științei în cadrul Strategiei Naționale pentru Cercetare-Dezvoltare-Inovare pentru perioada 2007-2013 nu a fost urmată de implementarea consecventă prin Programele Planului Național de Cercetare, Dezvoltare și Inovare II. Criza a condus astfel la amânarea șansei ameliorării situației din sistemul cercetare-dezvoltare-inovare din perspectiva relațiilor publice și comunicării, prin rezultate specifice.

ABSTRACT

This paper is a warning in order to revalue the attention for public relations and communication in the research-development-innovation field. The recognition of the need of science communication by the National Research-Development-Innovation Strategy for 2007-2013 was not followed by consequent implementation in the projects competitions of the Programs of The Second National Research-Development-Innovation Plan. The crisis lead to the adjournment of the improvement of the public relations and communications problems Romanian research-development-innovation system

Strategia Națională pentru Cercetare-Dezvoltare-Inovare pentru perioada 2007-2013, aprobată prin *Hotărârea Guvernului nr. 217/ 2007*

1. în Capitolul 3, subcapitolul Creșterea capacității instituționale specifică între “Obiectivele strategice ale sistemului de cercetare-dezvoltare-inovare” (pag. 19) menționează:

Consolidarea rolului științei în societate prin comunicarea științei, promovarea eticii și egalității de șanse în cercetare, dezvoltarea de interfețe dedicate dialogului știință-societate.

2. în Capitolul 4 “Cercetarea exploratorie și de frontieră” (pag. 21) se arată că: “având în vedere importanța cercetării fundamentale pentru dezvoltarea cunoașterii și formarea resursei umane înalt calificate, *accentul va fi pus pe excelență, pe interdisciplinaritate și vizibilitate internațională.*”

3. în Capitolul 6 “Inovarea” (pag. 33) specifică:

Inovarea este practic un rezultat pentru care cercetarea poate fi una dintre surse, alături de alți factori precum experiența, comunicarea, marketingul etc.

Aceste referințe demonstrează că, în momentul elaborării Strategiei, Autoritatea Națională pentru Cercetarea Științifică avea o viziune conformă politicilor europene în domeniu, rolul activităților de relații publice și comunicare în dezvoltarea științei fiind evidențiat în document.

Planul Național de Cercetare, Dezvoltare și Inovare II pentru perioada 2007-2013, aprobat prin *Hotărârea Guvernului nr. 475/ 2007*, principalul instrument prin care Autoritatea Națională pentru Cercetare Științifică implementează Strategia Națională pentru Cercetare-Dezvoltare-Inovare, este structurat în 4 programe: RESURSE UMANE, IDEI, PARTENERIATE, PARTENERIATE, INOVARE, CAPACITĂȚI. În pachetele de informații, prevederile privind comunicarea științei se rezumă la eligibilitatea cheltuielilor pentru diseminarea rezultatelor științifice realizate prin proiecte. exceptând programul CAPACITĂȚI, Modulul II despre care vom mai aminti. De asemenea, în Programul IDEI, la proiectele de tip Workshop Exploratoriu și Școală de Studii

Avansate și în Programul INOVARE, la proiectele de tip Cecuri pentru Inovare, mai puțin complexe și cu finanțare redusă, diseminarea nu este expres menționată ca activitate eligibilă.

Conform Planul Național de Cercetare, Dezvoltare și Inovare II (Programul PARTENERIATE, Subprogram "Proiecte Colaborative de Cercetare Aplicativă", pag. 72) organizația de cercetare este "entitate, spre exemplu o universitate sau un institut de cercetare, indiferent de statutul său legal (de drept public sau privat) sau modalitățile de finanțare, *al cărei scop principal* este de a conduce activități de cercetare fundamentală, cercetare industrială sau dezvoltare experimentală **și de a disemina rezultatele sale prin activități de educație, publicare sau transfer tehnologic**".

În absența indicațiilor din pachetele de informații, în majoritatea covârșitoare a cazurilor, organizațiile de cercetare rezumă activitățile de comunicare a științei la diseminarea rezultatelor proiectelor la nivelul publicării în reviste de specialitate și participări la manifestări (mese rotunde, workshopuri, simpozioane naționale / internaționale, târguri naționale / internaționale). Acest tip de diseminare este însă specific cerințelor cercetării fundamentale care, fiind orientată spre dobândirea de cunoștințe științifice noi, precum și spre formularea și verificarea de noi ipoteze și teorii, fără a avea scop industrial sau comercial, necesită comunicare cu precădere în interiorul comunității științifice respective. Pe de altă parte, menționăm că recente prevederi elaborate de UEFISCDI referitoare la conducătorii de proiecte și organizațiile eligibile constrâng oarecum spre astfel de activități indiferent de tipul organizației de cercetare participante la competițiile de proiecte.

Diseminarea rezultatelor cercetării aplicative este restrânsă la acest nivel deși aceasta (cercetarea aplicativă) este orientată spre largirea cunoștințelor, cu scopul de a utiliza aceste cunoștințe pentru dezvoltarea de noi produse, procese sau servicii ori pentru a îmbunătăți semnificativ produsele, procesele sau serviciile existente. Comunicarea nu se extinde spre potențiali beneficiari sau entități interesate / comunități afectate de rezultatele posibilei aplicări a proiectului iar proiectele care vizează o comunitate nu sunt suficient discutate cu reprezentanții acesteia, nici la nivel de autorități, nici la nivel de masă.

Carențele menționate mai sus provin din mai multe cauze, între care cea majoră este obișnuința de decenii a organizațiilor de cercetare de a comunica numai în interiorul propriei comunități științifice **care a condus la lipsa preocupărilor în domeniul relațiilor publice și comunicării**. Prin Programul CAPACITĂȚI, Modulul II s-a căutat ameliorarea situației în această zonă a activităților organizațiilor de cercetare din sectorul public. Programul în sine a fost creat "pentru a permite cercetătorilor să lucreze utilizând aparatură performantă, să beneficieze de un management adecvat și să mențină o relație permanentă cu nevoile socio-economice" (Planul Național de Cercetare, Dezvoltare și Inovare II, pag. 9). Subcapitolul dedicat Modulului II al acestui program conține mențiuni care implică o dezvoltare a comunicării și implicării strategiilor de relații publice. Modulul II a fost destinat exclusiv proiectelor suport care vizează ca obiective orientarea spre piață a cercetării-dezvoltării-inovării și promovarea și întărirea rolului științei în societate prin activități ca: servicii, diseminare de informații, manifestări, acțiuni promoționale pentru cunoașterea rezultatelor, imagine, studii prospective. Criza economico-financiară a determinat restrângerea fondurilor și restrângerea activităților la nivelul celor de foresight, amânând astfel șansa ameliorării situației din sistemul cercetare-dezvoltare-inovare din perspectiva relațiilor publice și comunicării, prin rezultate specifice.

În contextul economic românesc, date fiind condițiile globale actuale, dar și de perspectivă, ieșirea din criză presupune – între multe altele – **fluidizarea comunicării** între mediul științific și cel economic și de afaceri, între comunitatea științifică și societate.

După anul 2000, în țara noastră a început să se dezvolte infrastructura de inovare și transfer tehnologic. **Rețeaua Națională de Inovare și Transfer Tehnologic (ReNITT)** integrează principalii actori din domeniul transferului de cunoștințe și tehnologie la nivel național (54 de entități între care: 20 centre de informare tehnologică, 14 centre de transfer tehnologic, 16 incubatoare tehnologice și de afaceri, 4 parcuri științifice și tehnologice) fiind prezentă în toate regiunile de dezvoltare ale țării, cu precădere pe lângă organizații de cercetare.

La nivelul entităților de transfer tehnologic și inovare sunt prevăzute a se desfășura și activități de comunicare a științei:

- creșterea vizibilității organizațiilor de cercetare – dezvoltare;
- creșterea gradului de valorificare a rezultatelor cercetării;
- îmbunătățirea relațiilor între unitățile de cercetare – dezvoltare și agenții economici și respectiv, între unitățile de cercetare – dezvoltare și societate.

Abordarea acestora din perspectiva relațiilor publice și comunicării reclamă apariția unei noi specializări/ocupații interdisciplinare - **comunicatorii de știință** - care s-ar putea implica în:

- promovarea imaginii organizațiilor de cercetare – dezvoltare oferind informații structurate conform solicitărilor mediilor interesate;
- prezentarea rezultatelor activităților de cercetare – dezvoltare în cadrul unor manifestări și evenimente stimulând încheierea de noi contacte și parteneriate;
- facilitarea comunicării cu autoritățile, agenții economici, organizațiile neguvernamentale, informarea societății în probleme legate de activitatea de cercetare-dezvoltare.

Totodată, feed-back-ul activității comunicatorilor de știință poate constitui o sursă de informații extrem de utilă atât pentru unitățile de cercetare-dezvoltare, cât și pentru entitățile de inovare și transfer tehnologic în sensul unei mai juste și rapide corelări a activității lor cu problemele concrete și imediate ale economiei și cu așteptările societății.

Credem că sunt suficiente aceste motive pentru a sublinia necesitatea integrării comunicatorilor de știință în entitățile de transfer tehnologic.

Menționăm că, spre deosebire de relaționiști/specialiști în relații publice – al căror principal rol este comunicarea cu mass-media, comunicatorii de știință se adresează autorităților, agenților economici, organizațiilor neguvernamentale, comunității.

În loc de concluzii, propuneri:

1. Redeschiderea competiției de proiecte în cadrul Modulului II din Programul Capacități.
2. Inserarea în pachetele de informații ale viitoarelor competiții naționale de proiecte de cercetare-dezvoltare-inovare de prevederi referitoare la:
 - diseminarea adecvată a rezultatelor științifice obținute;
 - consultarea autorităților, respectiv populației în legătură cu obiectivele și, respectiv, riscurile proiectelor.
3. Formarea de comunicatori de știință.

STOCK EXCHANGE OF NEW INVENTIONS

Petrin DRUMEA¹, Niculae IONIȚĂ¹, Costinel POPESCU¹, Cătălin DUMITRESCU¹

¹ INOE 2000 - IHP, e-mail dumitrescu.ihp@fluidas.ro

Abstract: This paper aims to present some of the inventions which were patented in recent years by the Institute of Hydraulics and Pneumatics in Bucharest, as a result of research work carried out in specific areas of its activity.

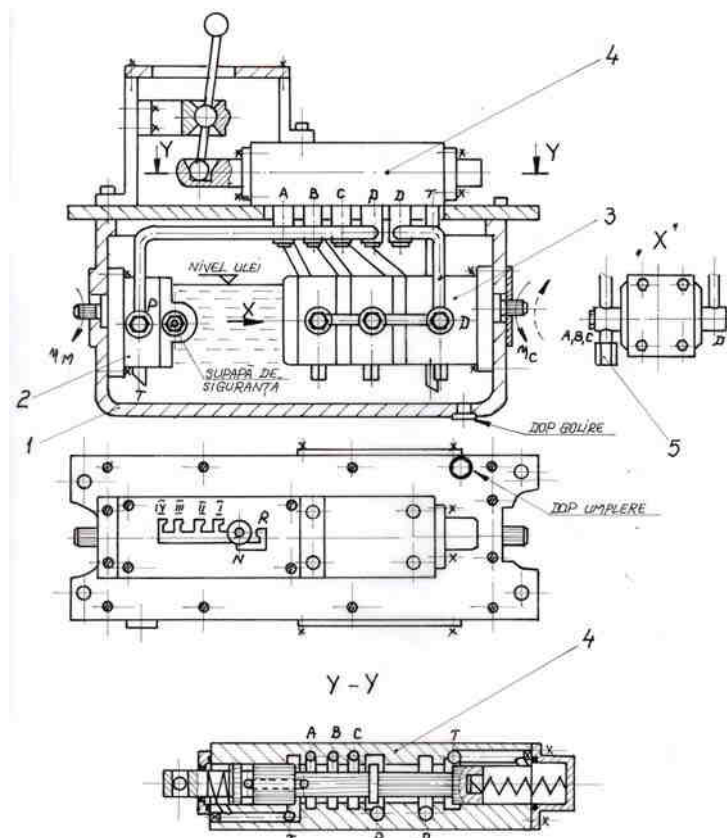
Keywords: hydraulic, energy recovery, energy unconventional, medical devices.

1. HYDRAULIC

„Hydraulic gearbox” – patent no. 122974/2010

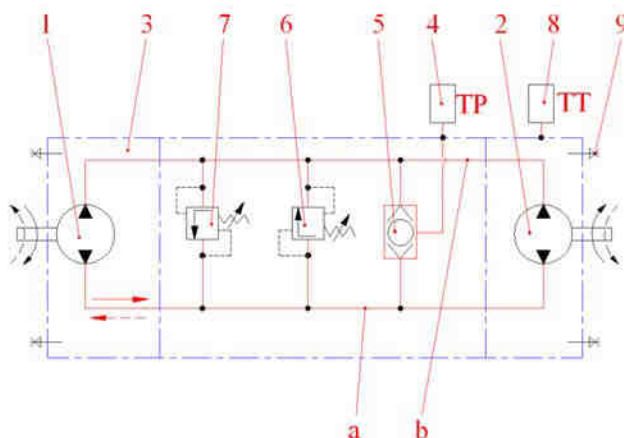
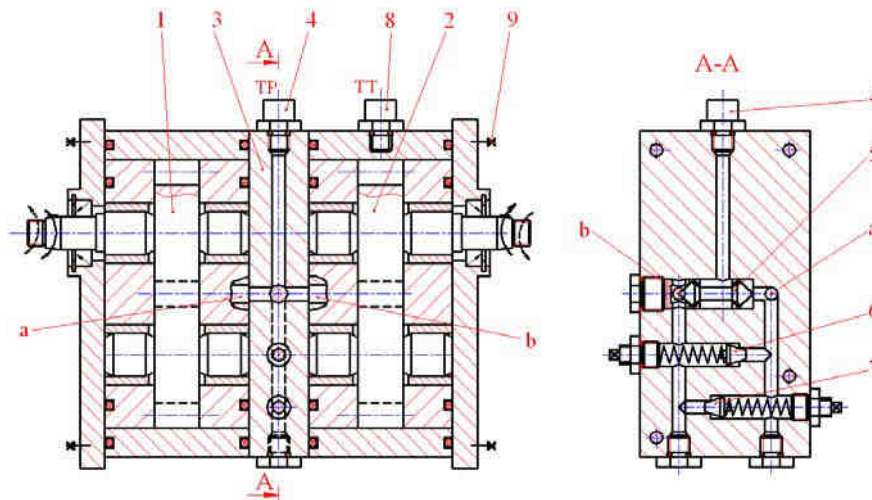
The invention relates to a hydraulic gearbox, designed coaching system of a car driving vehicles or plant.

Gearbox according to the invention comprises a steps hydraulic transmission, which has a housing (1) filled with oil to a manageable level, the gear pump (2) is arranged in it, that acts a hydraulic gear motor (3), consisting of three distinct sections, through a hydraulically distributor (4) that, depending on the position chosen field, acts the engine (3) the connections between hydraulic equipment being made by some pipe and some connectors which contains on the supply circuits of the hydraulic motor (3) some valves (5.1), (5.2) and (5.3) which aspires oil if the distributor (4) is closed.



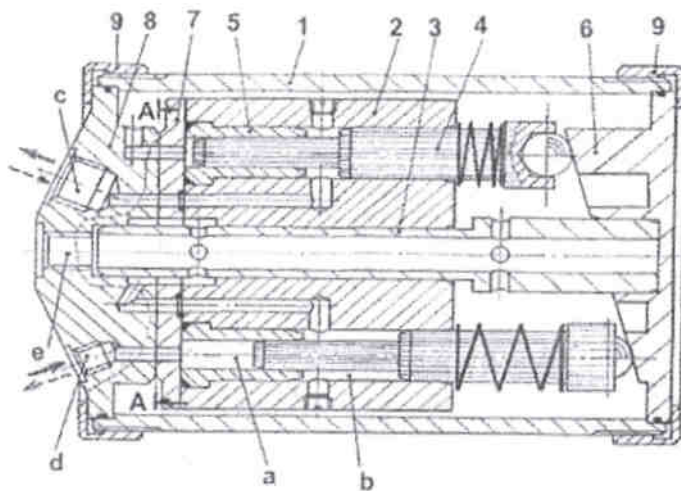
„Device for measuring torque and speed (RPM)” – patent no. 122931/2010

The invention relates to a hydraulic device for torque and speed used in laboratory for testing rotating machines. The device according to the invention consists of a reversible gear pump (1), coupled to a hydraulic reversible gear motor (2), supplying it through a connection plate (3), which contains a pressure transducer (4) that receives information from both hydraulic circuits, through a selection valve (5), overload protection circuits or lock and by two pressure limitation valves (6) and (7) arranged in the connection plate (3), in the motor housing (2) is arranged, in the vicinity of the gear output, a magnetic speed transducer (8).



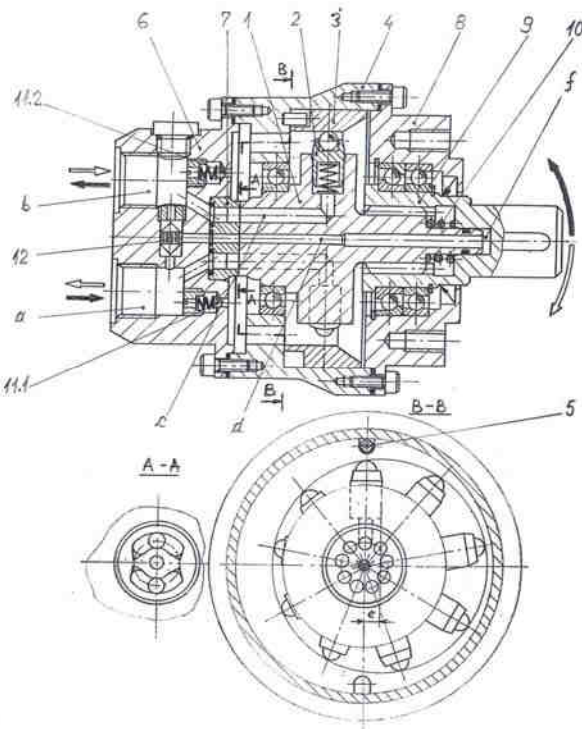
„Rotary hydraulic equipment” – patent no. 123329/2011

The invention relates to a flow or pressure multiplier, for hydraulic actuation. Multiplier, according to the invention, comprises a tubular housing (1), in which is placed a rotor (2), arranged on a tubular shaft (3), in which is placed an odd number of axial pistons (4), which together with some separation bushes (5), forming two compression chambers (a and b) whose different volume determines a ratio multiplier, the axial pistons (4) leaning through some springs and some balls, on a tilted disc (6), the rotor (2) being closed with a distribution disc (7), that connects hydraulic lines, through two holes, with a supply cover (8), which frontal rests on it and has some hydraulic connections holes (c, d and e) and semicircular slits (f, g, h and i).



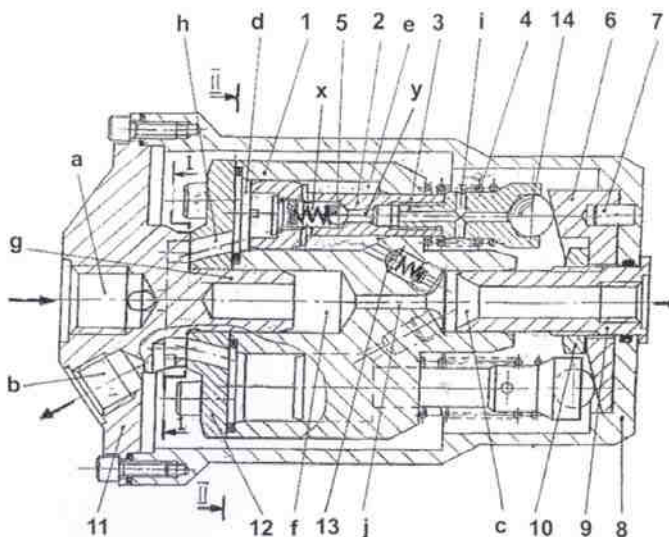
„Rotary hydraulic machine” – patent no. 123433/2012

The invention relates to a rotary hydraulic unit that can work as a pump or motor in open circuit or closed circuit in any hydraulic actuator, having the possibility to change the direction of rotation of the drive shaft. Unit according to the invention consists of a rotor (1) in which can slide on radial direction, some pistons (2) in odd numbers, which are in contact with a running path (3) with eccentric circular seat, fixed in a outer housing (4) closed the rear, with a hydraulic connection cover (6) provided with some holes (a and b) outer through a distribution plate (7) with two semicircular slits are connecting with the piston compression chambers (2) through ducts (c) applied to the rotor (1), and in front with a lid fixing (8) where there is a splined shaft (9) coupled to the rotor (1), pressed on the distribution board (7) by a spring helical (10), for use both as a pump and the rotary hydraulic motor.



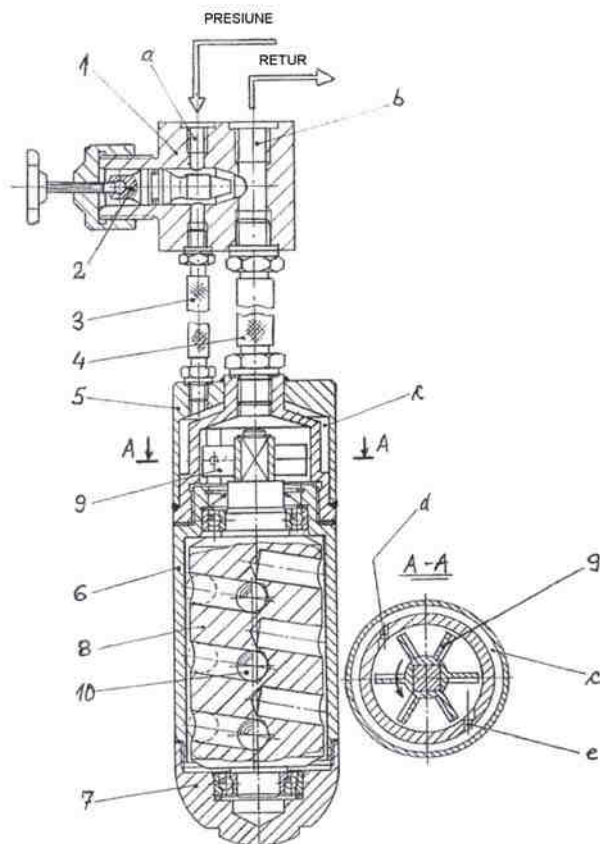
„Rotary hydraulic transformer” – patent no. 123434/2012

The invention relates to a rotary hydraulic multiplier equipped with axial pistons, which multiplies pressure in continuous flow used in hydraulic. Multiplier, according to the invention consists of a rotor (1) in which are placed some pistons (2) whose number is odd, screwing, each, to support heads (3), pushed through ball, by springs (4) of the titled disc (6) positioned with screw (7) in a circular housing (8) rotor (1) is fixed in part on a high pressure output connection (9), mounted in the housing (8) by a nut (10), and, on the other hand, on a central axis of a supply cover (11), equipped with an low pressure orifice (a), a return orifice (b) and two symmetrical semicircular slits (a.1 and b.1) in contact with some routing holes, practiced in a distribution cover (12), which closes tightly rotor (1).



„Cylinder hydraulic vibrators for concrete” – nr. brevet 126576/2012

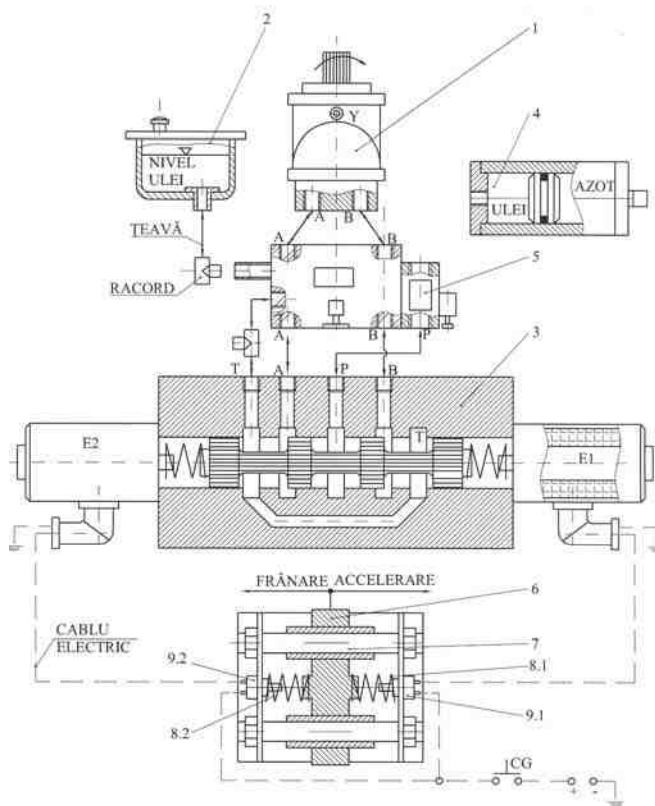
The invention relates to a vibrating cylindrical tank, hydraulic and manual handling that can be used for internal vibrating of concrete molded into the construction works. Vibrating cylinder according to the invention comprises a power connector (1), in which there is a control valve (2) of the fluid flow sent through a hose (3) and returned through another hose (4) to and from an operating head (5), screwed to a cylindrical housing (6), closed with a cover bearing (7), in which there is a rotor (8), dynamically balanced, with radial cylindrical channels placed inclined, they find themselves on one side of the rotor (8) sliding balls (10) the rotating is achieved by a turbine (9), which may turn idle at low speed and may vary up to full speed centrifugal force, by running the ball (10), on the cylindrical housing (6), for discharging by tasks of a rotor bearings (8).



2. ENERGY RECOVERY

„Hydraulic for recovery braking energy” – patent no. 122959/2010

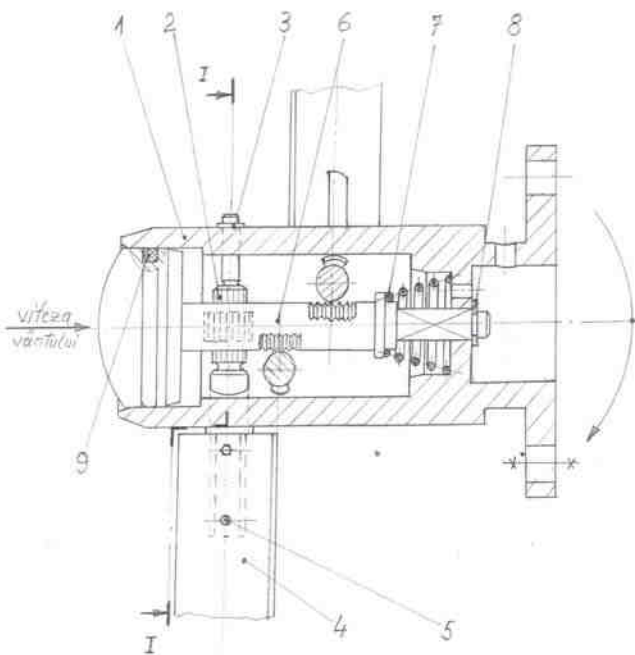
The invention relates to a hydraulic system, for recovery, storage and reuse braking energy to a road vehicle in order to save fuel. System according to the invention consists of a hydraulic unit (1) having an axial pistons with fixed displacement which receives rotation from an outlet gearbox drive a car, a oil compensation tank (2) of which the hydraulic unit (1) aspires working fluid, a electrically operated distributor (3) that connects hydraulic unit (1) and storage battery (4) of recovery energy, a block (5) with protection and hydraulic valves and inertial control device, consisting of an inertial disc (6) some guides (7), some helical springs (8.1 and 8.2) and some electrical switches (9.1 and 9.2).



3. UNCONVENTIONAL ENERGY

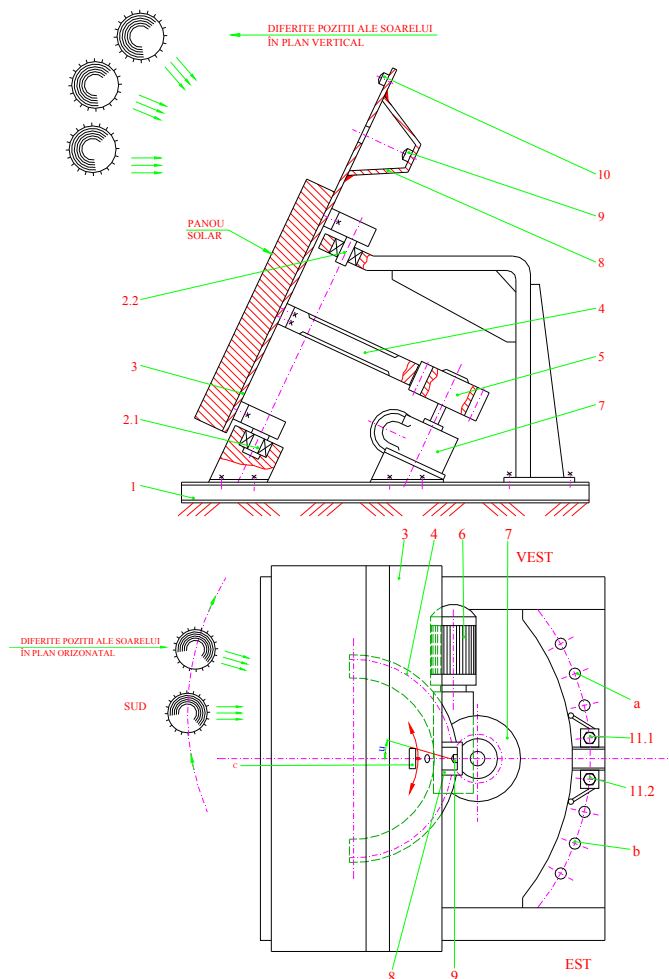
„Wind turbine” – patent no. 127087/2012

The invention relates to a horizontal axis turbine with three pallets that can capture wind energy to turn it into rotary motion, which can be used for either driving various machines, such as power generators, mills and pumps water. Wind turbine according to the invention consists a drive head (1) with hexagonal shape, finished with a drive flange, in which are fixed the three axes serrated (2), radial unbalanced position, equally spaced, but placed in different transverse planes, secured with washers (3), which are attached by one of the pallets (4), fixed with screws (5), that have from the mounting an angle of 45° to the plane of rotation, which can be changed by rotating the toothed axes (2) to a maximum of 90° , driven by a multiple rack with piston (6), ensured by the snap ring (8) and sealed with gasket (9), pressed against a conical spring (7), by the dynamic pressure of the wind, so that, between two acceptable speed limits of the wind, the turbine maintains a constant speed and when exceed maximum safety speed of the wind, the turbine must to stop.



„Device for automatic orientation of a solar collector ” – nr. brevet 126700/2012

The invention relates to a mechanism by which it can be automatically oriented to the sun a capture sunlight solar panel, photovoltaic or hot water throughout the day. The mechanism according to the invention is composed of a metal frame (1), fixed horizontally on the ground or on the roof of a house, which has two slide bearings (2.1) and (2.2) aligned by an tilted axis at an angle of 55° to the horizontal, around which rotate a panel (3), driven by a gear composed of crown (4), pinion (5), worm gear (7), driven by an DC electromotor (6), which is controlled by a photocell (9) located in a black box (8) which is illuminated by the sun through a directional slit only if another photocell (10) senses that the sun is in the sky, the angle of rotation from east to west is determined by two limiters of courses (11.1) and (11.2), adjustable for position, depending on the season.



4. MEDICAL EQUIPMENT

„Electropneumatic device for perfusion” – patent no. 122709/2009

The invention relates to an electropneumatic device for perfusion for medical interventions, using the infusion set equipped with a liquid bag, which can be programmed and it maintains stable the dose throughout the infusion period, whether the intervention is in hospital or rescue. The device according to the invention consists a body (1), sealed with a cover (2), provided with a slot in which is placed the bag infusion set, subjected to air pressure made by a proportional controller (3) coupled to a pressurized chamber own device, protected by a safety valve (4) which can be powered by an electrocompressor (5), on-off by a pressure sensor (6), or from an external source through a valve (7). The device can be programmed an infused liquid dosage and can maintain constant throughout the period of time required, because it has a flowmeter with magnetic resonance (8), which together with an electronic block (9), powered by an electric battery (10), can adjust the control current that is applied the proportional controller (3), corresponding to a pressure of pressing need and keep it constant.

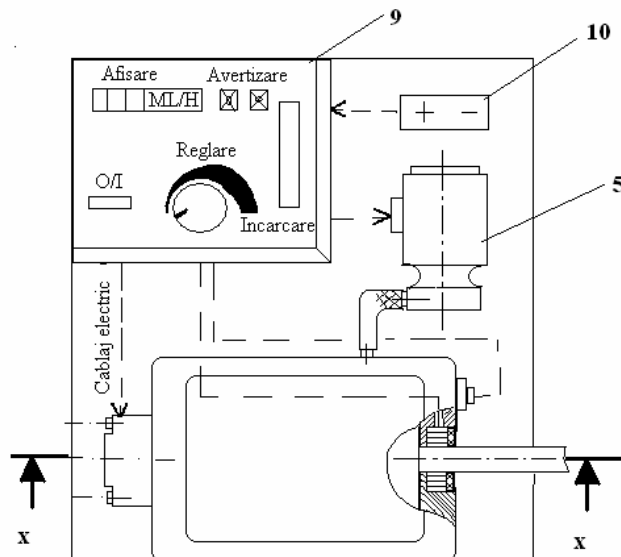
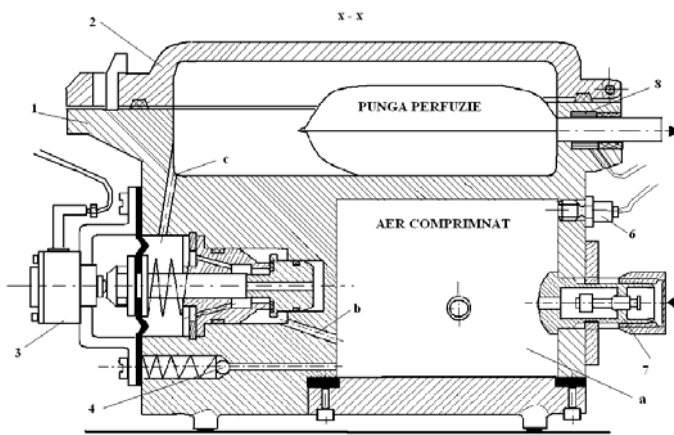


Fig. 1.



EDUCATION IN DEVELOPMENT OF ELECTRONIC MODULES USING FREE AND OPEN SOURCE SOFTWARE TOOLS

Andrei DRUMEA¹, Alexandru VASILE¹

¹ "Politehnica" University Bucharest, 313 Spl. Independentei, 060042 Bucharest, andrei.drumea@cetti.ro

Abstract: An important topic in electronics education is the design and development of electronic modules with emphasis on embedded systems, complex activity that combines hardware and software design. Hardware development chain consists of analog and digital design, schematics capture and circuit simulation, printed circuit board design and generation of manufacturing information. Software development requires tools like code editor, compiler and debugger, usually grouped together in an Integrated Development Environment (IDE). Some key aspects of educational software are accessibility, simplicity, quality of documentation and lower cost for a working licence. Unfortunately, typical commercial software is expensive and too complex so, for educational purposes, free and/or open source software can be a better option. Present paper analyses some free and open source software tools for electronic modules development: gEDA, Eagle Light edition and KiCad for schematics capture and printed circuit design, LTSpiceIV and Ngspice for circuit simulation, and Code::Blocks and Eclipse for software development for embedded systems.

Keywords: electronic modules, CAD, education, open source

1. Introduction

Education in the field of mechatronics includes electronics courses, usually related to embedded systems development. This topic covers many important areas like software development, analog and digital circuits design and simulation, CAD/CAM activities like printed circuit board design and preparing for manufacturing; all these activities require software tools coupled in a chain (fig.1).

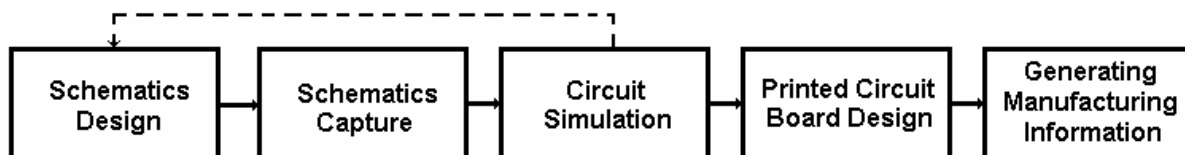


Fig.1 Typical hardware development tool chain

CAD/CAM software can be proprietary, with higher or lower license costs, or free/open source software, usually developed by academia or enthusiasts/hobbyists. In last years, a lot of proprietary software for electronics evolved into complex packages, hard to manage and too complicated to use in education environment where focus is on solving simple problems and explain principles. Free and open source software, on the other side, is developed with these aspects in mind, and in last years it reached a performance level almost similar with commercial software. Free software is released as binary (already compiled code, ready for run) and as source code (that must be compiled first by the user) and this means that source code is always available for improvements for free and open source software. A quote from GNU General Public License, version 3, 29 June 2007, developed by Free Software Foundation Inc., describes the essence of free software ([3]): "When we speak of free software, we are referring to freedom, not price. Our General Public Licenses are designed to make sure that you have the freedom to distribute copies of free software (and charge for them if you wish), that you receive source code or can get it if you want it, that you can change the software or use pieces of it in new free programs, and that you know you can do these things."

2. Tools for hardware design of electronic modules

CAD software for electronic modules design consists, at least, in schematic capture program and printed circuit board (PCB) layout editor. Extra modules, like circuit simulator and Gerber viewer program for preparing manufacturing files, can be available.

Commercial software for electronic design is represented by tools like Mentor Graphics, Cadence with Orcad ([1]) and Allegro suites, Altium Designer or EAGLE.

Among these programs, an interesting option is freeware version of EAGLE (Easily Applicable Graphical Layout Editor) ([8]), that combines all features of commercial version (same simplicity and productivity, access to all component libraries and ability to run ULPs- user language programs to automate some tasks) . The limits of freeware version are acceptable for education – schematic must fit on one A4 page, printed circuit board design with no more than 2 layers and 80x100mm board size, but student projects usually fit in these limits. A GPS module board ([2]) was easily developed within these constraints.

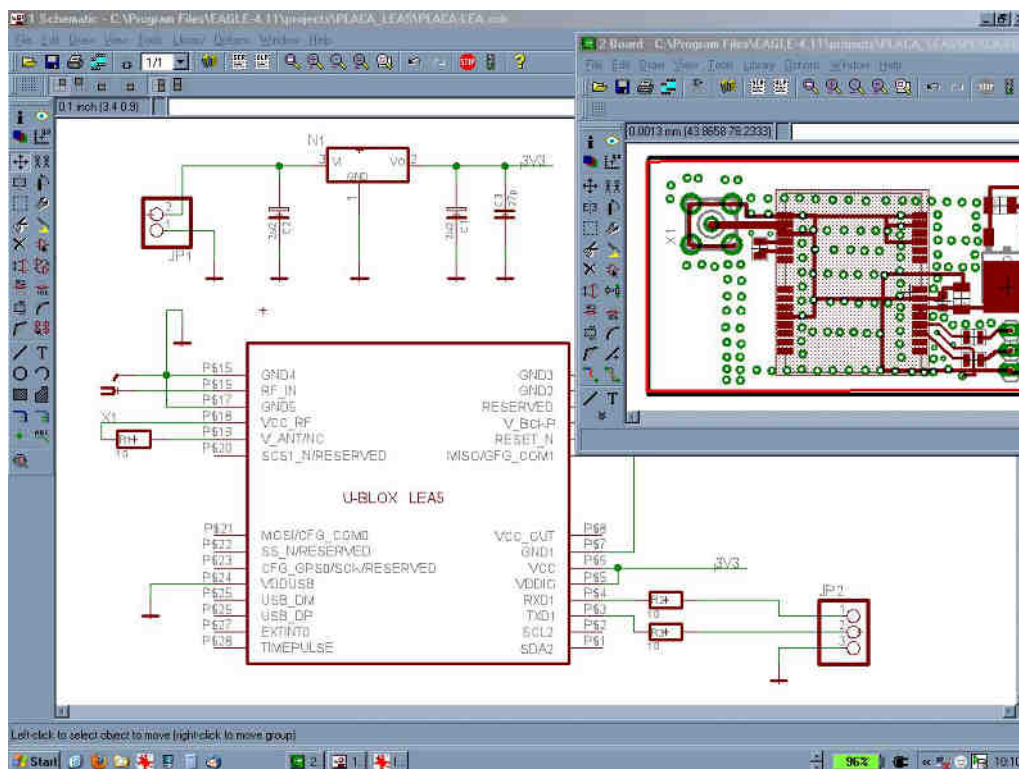


Fig.2 Schematic capture and layout design in EAGLE framework

Unfortunately EAGLE package offers no circuit simulation tool. An excellent option is to use another free program, LTSpiceIV, from semiconductor vendor Linear Technology. The program has a powerful SPICE engine (Simulation Program with Integrated Circuit Emphasis, de facto standard in electronic circuit simulation) and offers modern device models; it is obviously biased on Linear Technology components but extra devices can be added into the libraries. Other advantages are frequent updates and releases and a large and internet-active user base. Its installation is small and the program is able to use multi-core processors for faster simulations. In some simple examples of circuits, the program performs much better and reaches convergence without any tweaks compared to commercial Spice implementations. In figure 3 is shown the simulation of an astable circuit with LTSpiceIV program.

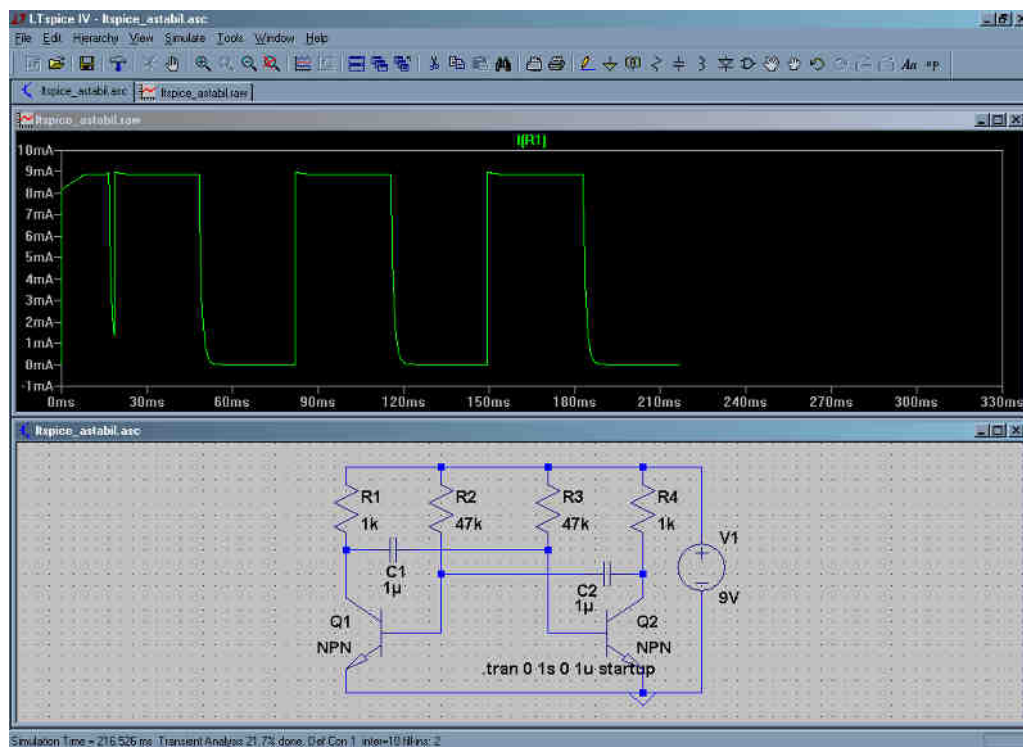


Fig.3 Simulation of a simple circuit using LTSpiceIV

Another software tool for electronics design is KiCad. It consists of Eeschema schematic editor (fig.4), PCBnew board editor, Gerber viewer (fig.5) and library management tools. It is open source program, so free to use and all sources available (Eagle and LTSpiceIV sources are not available). Its interface is not as efficient as Eagle, but is intuitive and easy to learn.

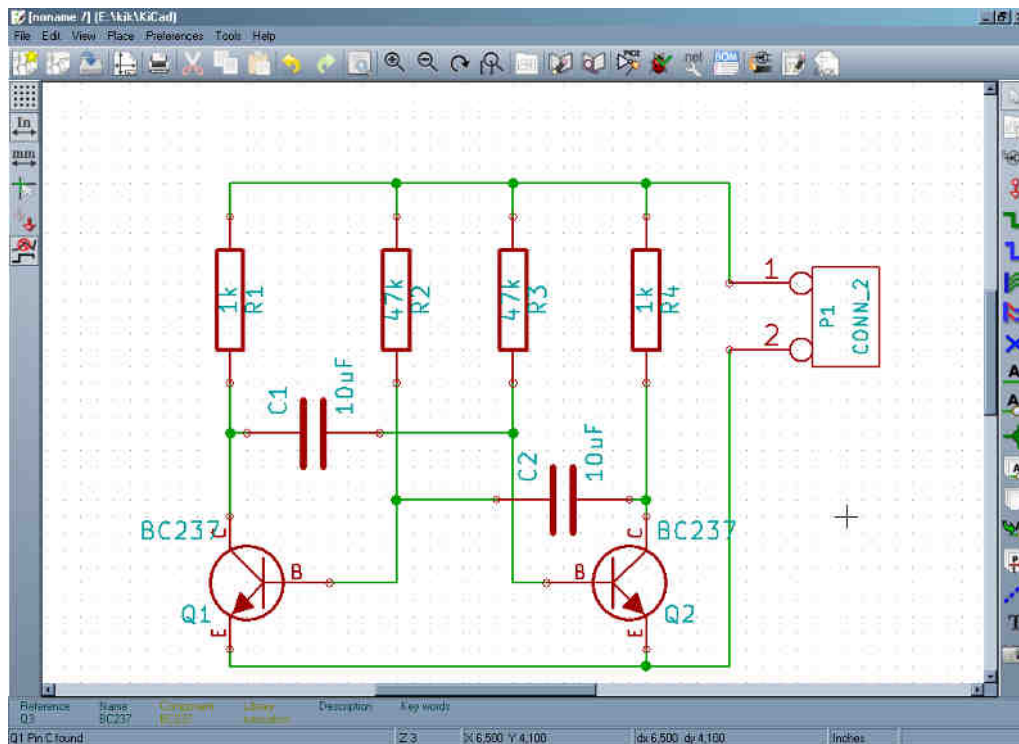


Fig.4 Schematic capture in KiCad framework

The board editor can process boards with maximum 16 electrical layers and 12 technical layers (like solder mask, silkscreen) and has a large component database.

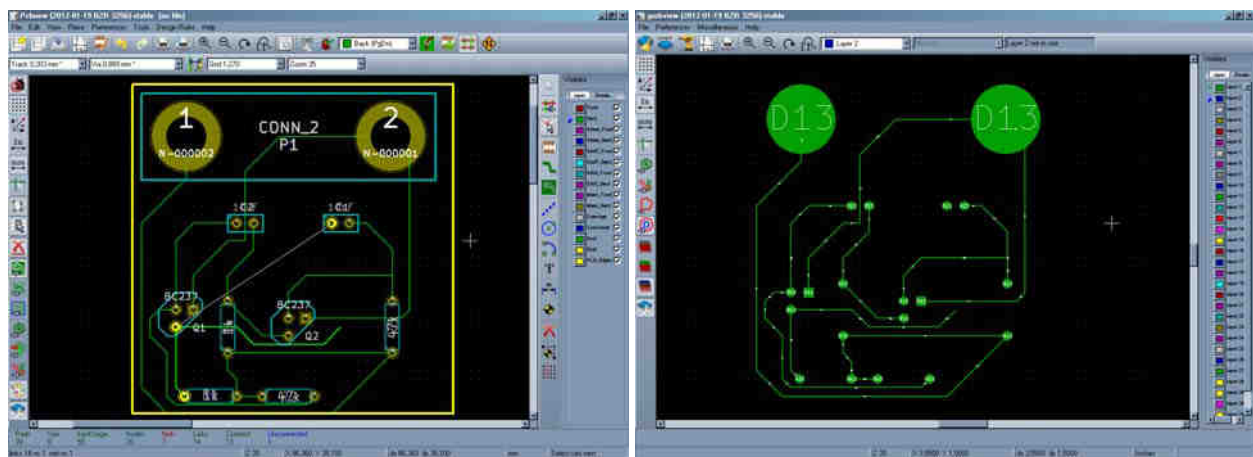


Fig.5 Layout editor and Gerber viewer in KiCad framework

Another powerful CAD suite for electronics is gEDA (GPL EDA), also open source and with large user database ([6]). It consists of gschem schematic capture, pcb board editor, Gerber viewer and integrates also other open source tools like spice. gEDA suite is developed especially for GNU/Linux open source operating systems. In figure 6 is shown a simple connector design with gschem and gerbv performed by Peter Clifton ([4]).

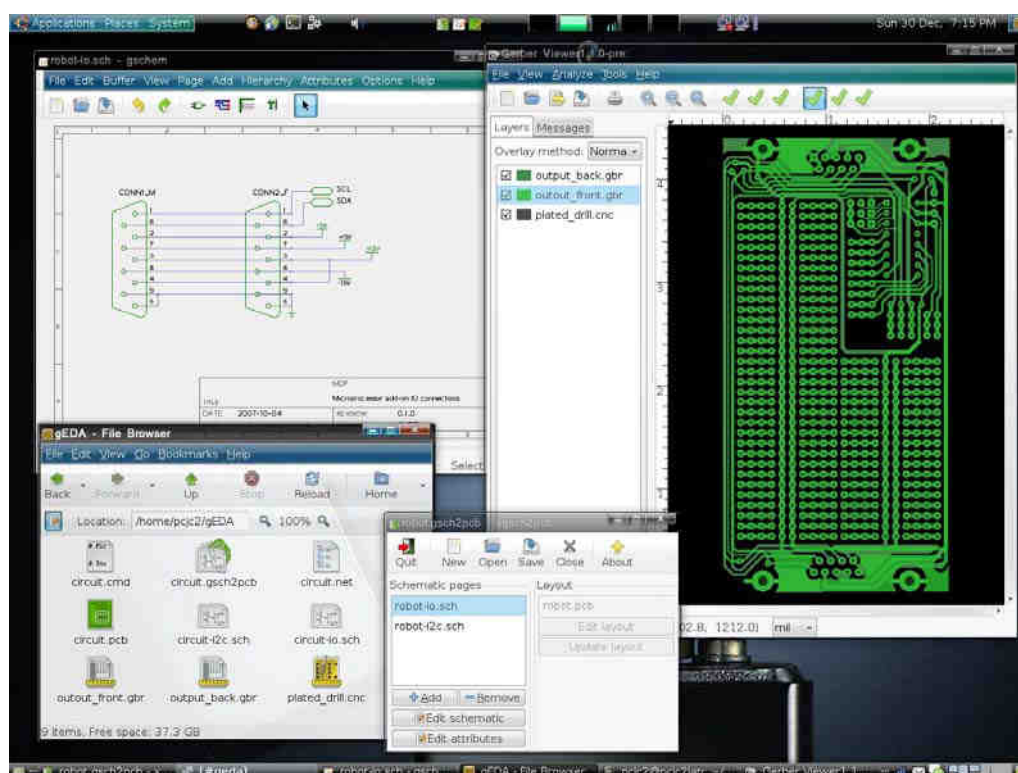


Fig.6 Schematics capture and Gerber viewer in gEDA framework

Board editor is also very powerful and with large component libraries. Lots of electronics projects on Internet are developed using gEDA tools. In fig. 7 is shown such a project, a lightning detector board developed by Kai-Martin Knaak ([4]).

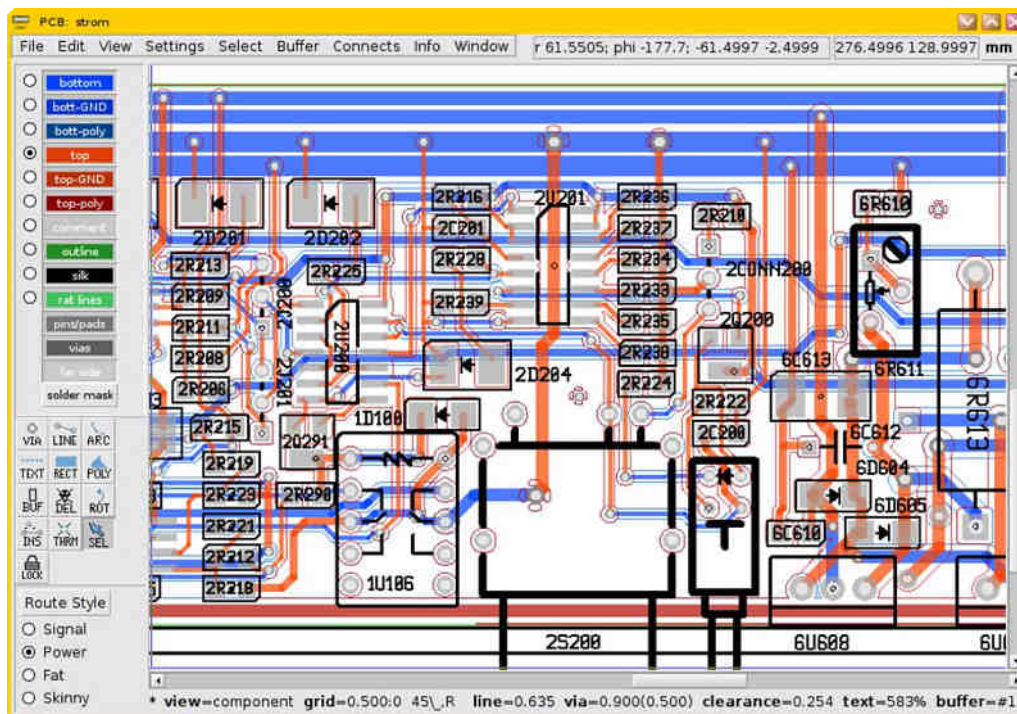


Fig.7 Layout editor in gEDA framework

3. Free and open source tools for software development for embedded systems

Embedded systems development usually requires C code editor, compiler, debugger and programmer. The large availability of open source GNU C Compiler for almost all existing processors made it a good choice in embedded system design. Its only disadvantage is the lack of a user friendly integrated development environment (IDE). Fortunately, in the last years 2 solutions occurred – Eclipse framework, a Java based IDE, very complex and powerful, but hard to manage and with large resource requirements, and Code::Blocks.

Code::Blocks is an open source IDE designed to be very extensible and fully configurable that runs on slow machines and has a consistent look, feel and operation across platforms ([5]). It can be extended with plugins so any extra functions can be implemented using another plugin. For instance, compiling and debugging for different processors or microcontrollers like Intel MCS51, Atmel AVR, Texas Instruments MSP430, ARM, MIPS, PowerPC processors or even Windows, Mac OS X or Android applications.

For a complete embedded systems development framework, user must provide for Code::Blocks the required (cross) compiler and debugger and to make some small configurations. After these steps, development process runs smoothly and can be more productive than commercial solutions. For example, for MSP430 microcontrollers, Code::Blocks IDE, mspgcc C compiler and mspdebug debugger offer an open source alternative more productive than chip manufacturer solutions and without any limitations in code size.

In figure 8 is shown a small C program for MSP430 microcontroller edited and compiled using Code::Blocks framework.

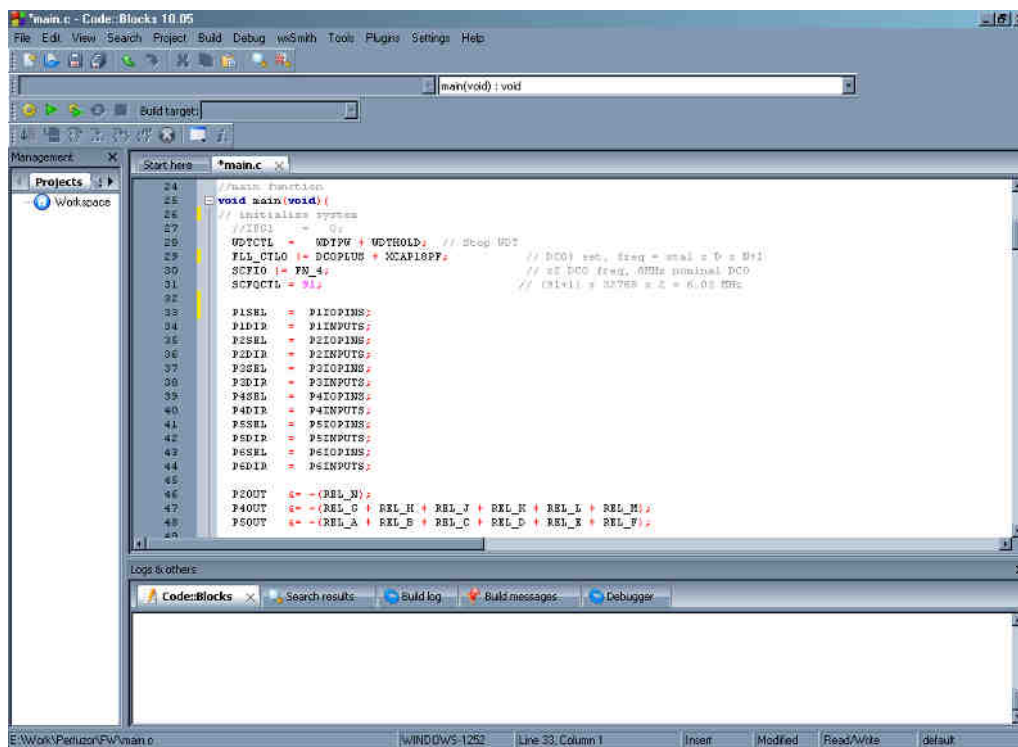


Fig.8 Code::Blocks editor with C program for MSP430 microcontroller

4. Conclusions

Education in electronics, especially in embedded system design, can be performed using only free and open source software tools. The quality of these products greatly improved in the last years and reached almost the same level with commercial software, but their inherent

REFERENCES

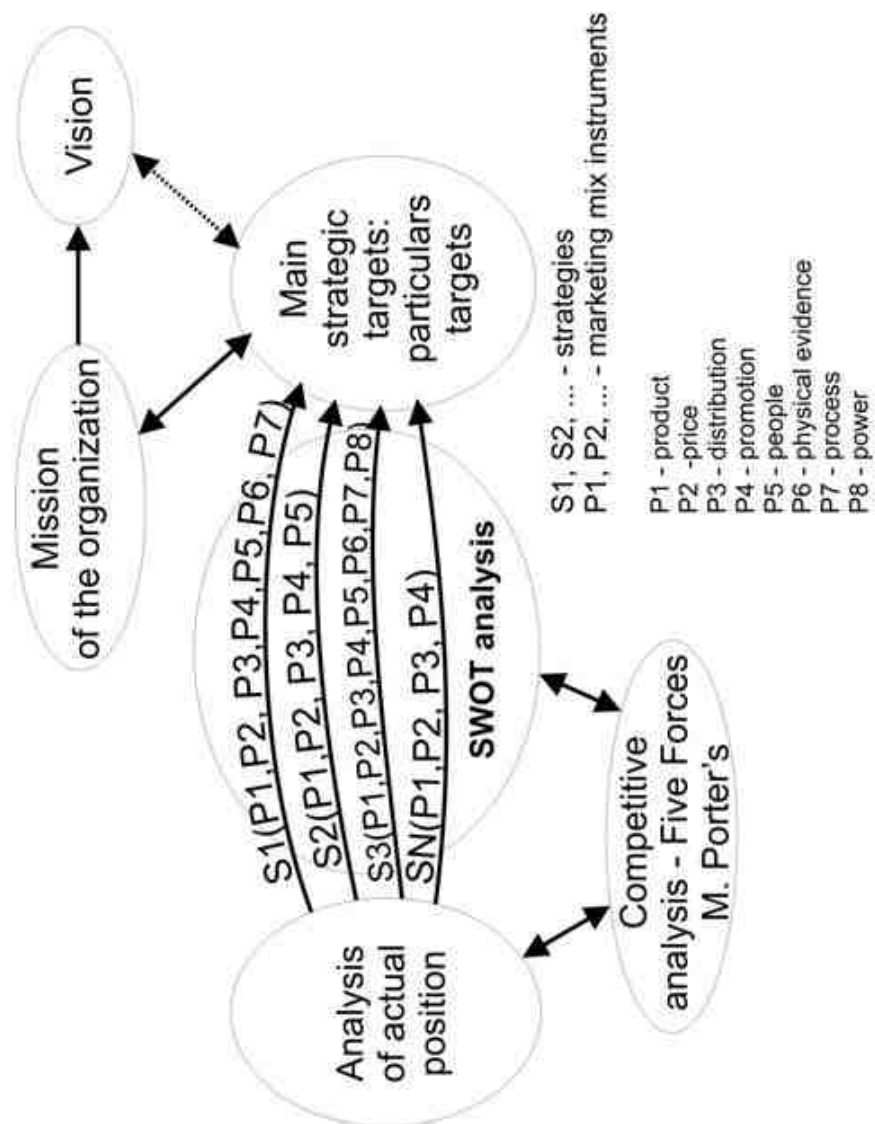
- [1] K. Mitzner, "Complete PCB design using OrCad capture and layout", Newnes, Burlington MA, USA, 2007
- [2] A.Drumea, N.Irimie, R.Bunea and Al.Vasile, "Communication Module for Laser Rangefinder with Integrated Positioning System", SIITME-2009, Gyula, Hungary; 17-20 September, 2009, ISBN: 978-1-4244-5132-6; pp.301-304
- [3] <http://www.gnu.org/licenses/gpl.html>
- [4] <http://en.wikipedia.org/wiki/GEDA>
- [5] <http://www.codeblocks.org/>
- [6] <http://www.geda-project.org/>
- [7] <http://www.kicad-pcb.org>
- [8] www.cadsoft.de

Elements of strategy and innovation policies in the field of fluid power – introduction

Henryk Chrostowski – Wrocław University of
Technology, Institute of Machine Design and
Operation, Corporation of Hydraulic and Pneumatic
Drive and Control

Zygmunt Popczyk - Wrocław University of
Technology, Institute of Machine Design and
Operation

Strategy - idea



HERVEX 2012

Selected macroeconomic data of the selected countries in 2010 - I

Country	Population (million)	GDP per inhabitant (in current pricing, thousands of USD)	Expenses in the R&D area related to GDP, %	R&D employees per 1,000 employed	Expenses per R&D one employed (in thousands of USD)*
Germany	81,644	40,479	2,78	7,7	147,146
Poland	38,187	12,289	0,68	3,9	42,866
Romania	21,444	7,573	0,57	2,1	60,339
UK	62,227	36,158	1,85	8,0	113,353
Slovakia	5,431	16,078	0,49	5,6	36,100
Czech Republic	10,526	18,256	1,53	5,6	74,160
Russia	141,892	10,429	1,24	6,4	39,444

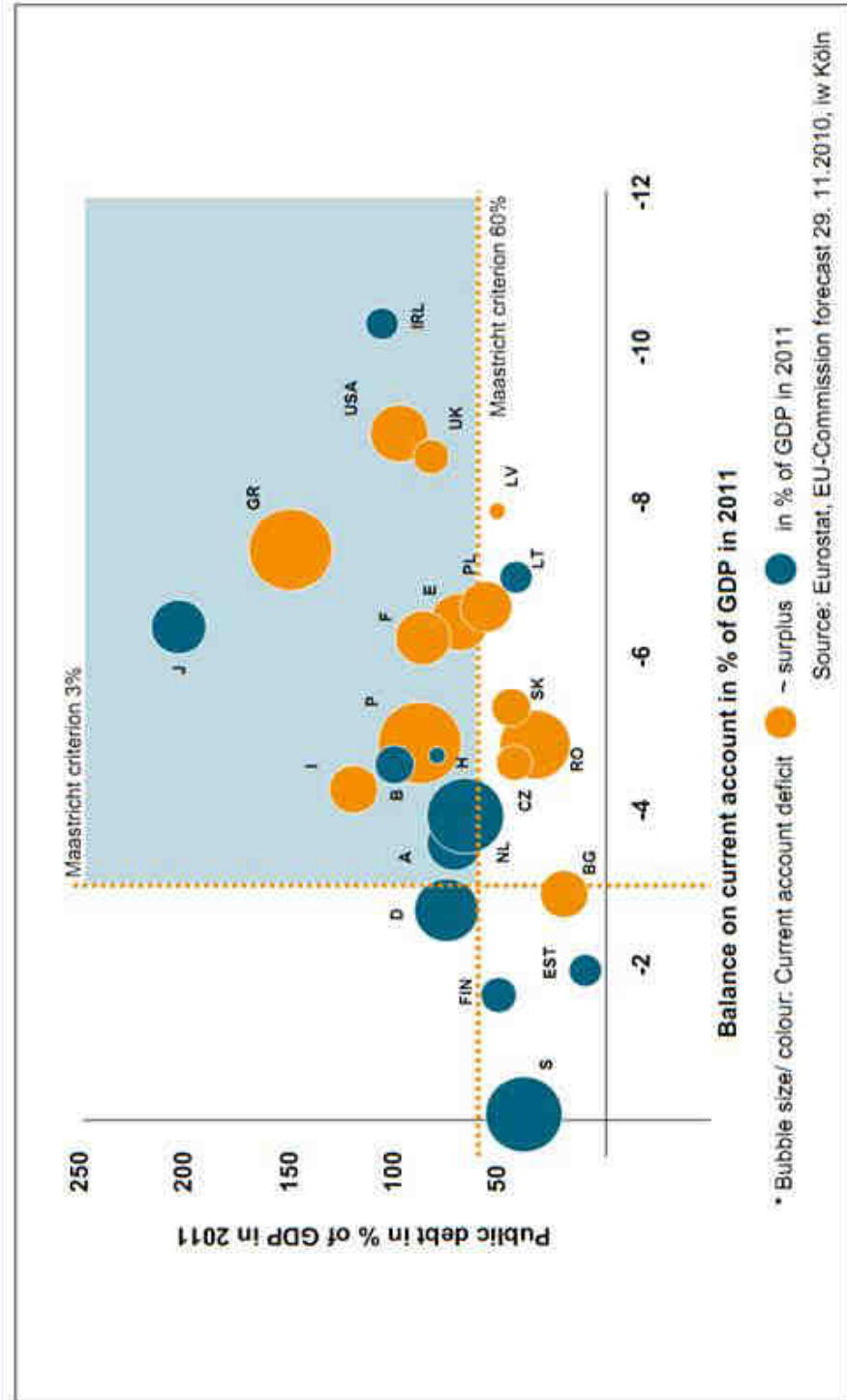
HERVEX 2012

3

Selected macroeconomic data of the selected countries in 2010 - II

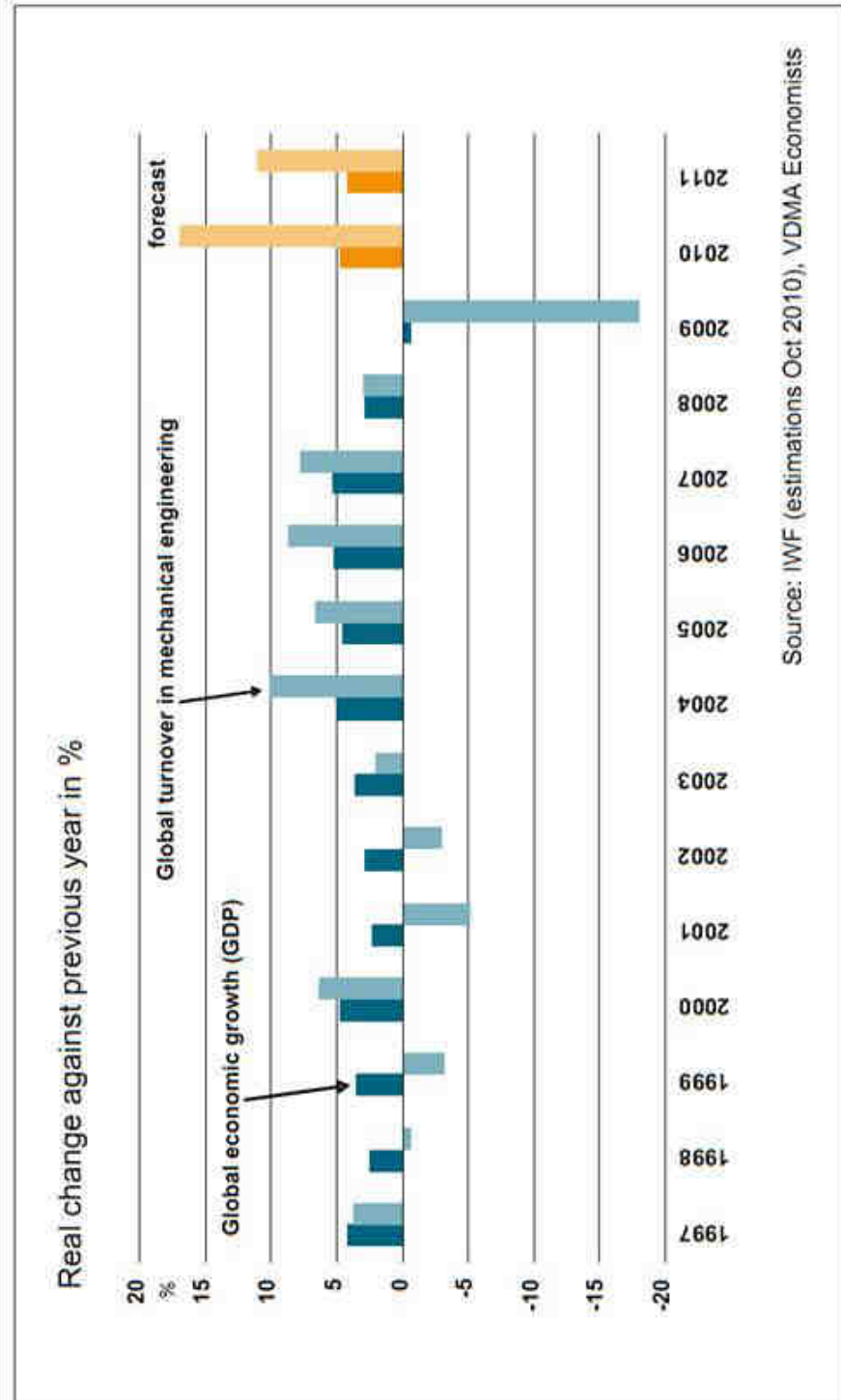
Country	Exports		Students	
	per capita in USD	in % of the world	per 10 thousand population	of which foreign students in % total students
Czech Rep.	12 554	0,9	407	7,3
Germany	15 572	9,0	282 *	11,1 *
Poland	4 184	1,1	564	0,8
Romania	2 302	0,3	521	0,9
Russia	2 803	2,8	675	1,4
Slovakia	11 912	0,5	439	2,7
UK	6 592	2,9	397	15,3
* data 2003/04				

Public debt and balance on current account



International Fluid Power Summit meeting, 5 April 2011 in Hanover, Germany
 Chart 2 • April 2011
 HERVEX 2012

Global economic growth and global turnover in mechanical engineering



International Fluid Power Summit, 20110405, Dr. Ralph Wiechers/VDMA

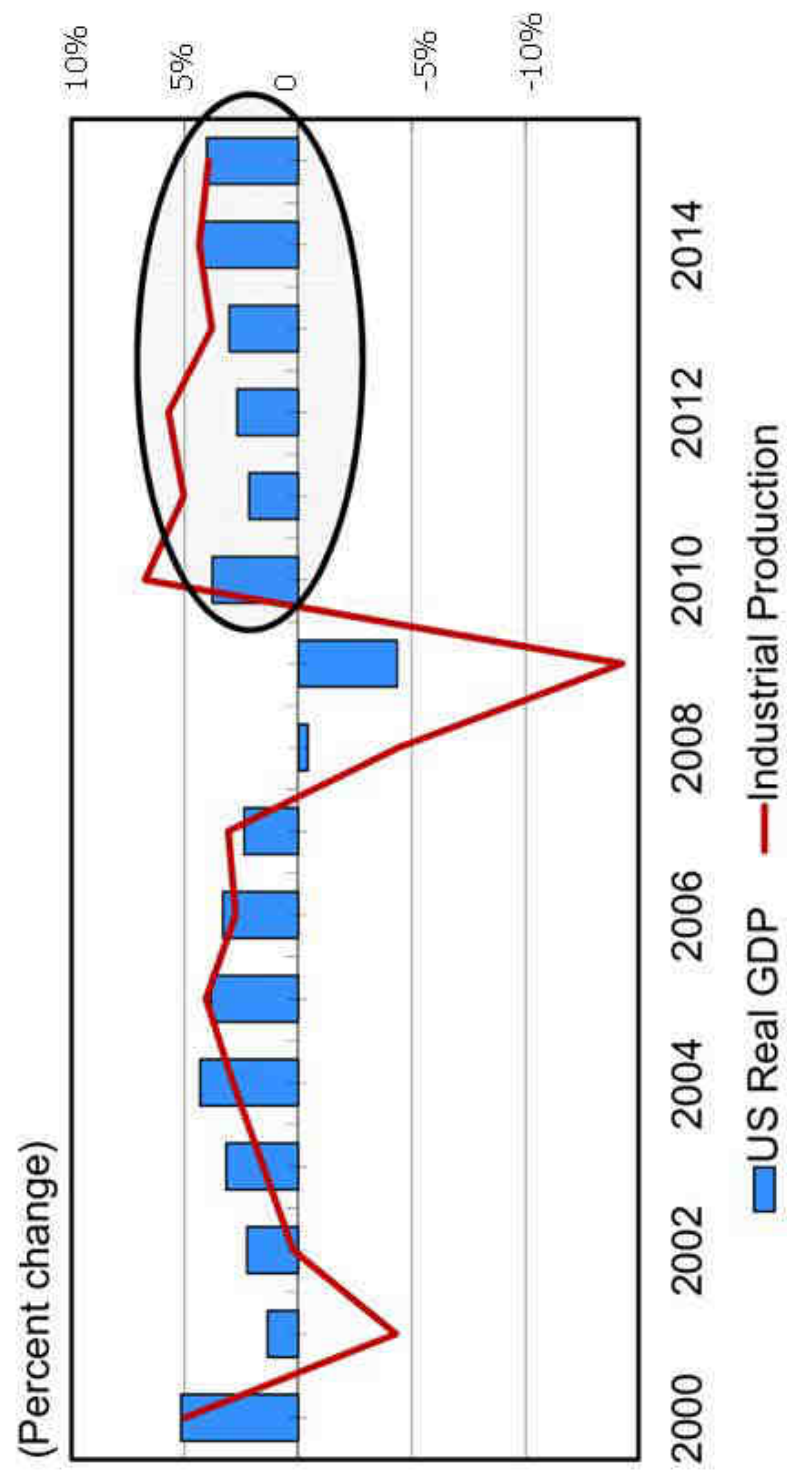
HERVEX 2012

Page 4 • 07.04.2011

6

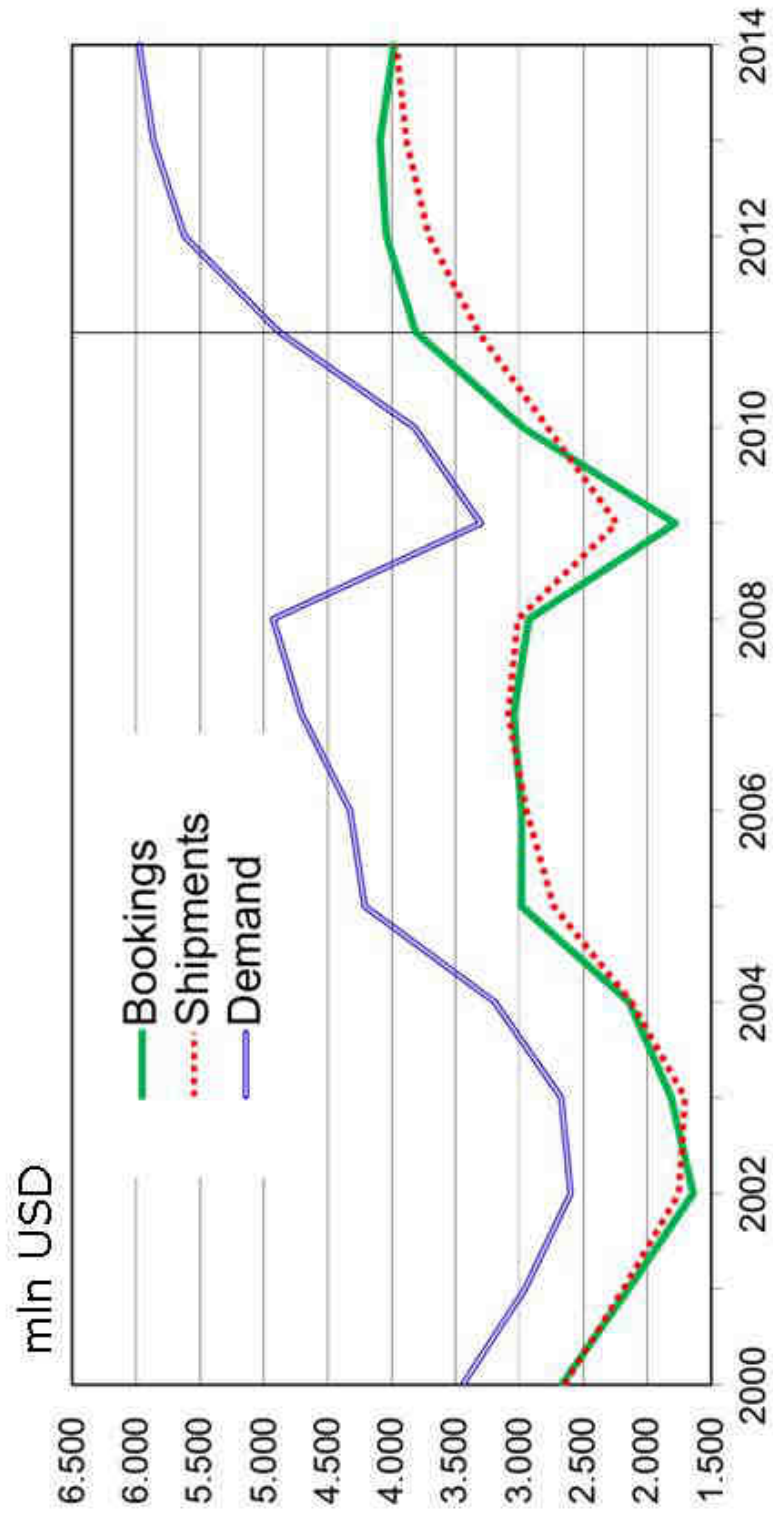
Real GDP and Industrial Production Growth in USA

Good News for Gear Market



HERVEX 2012

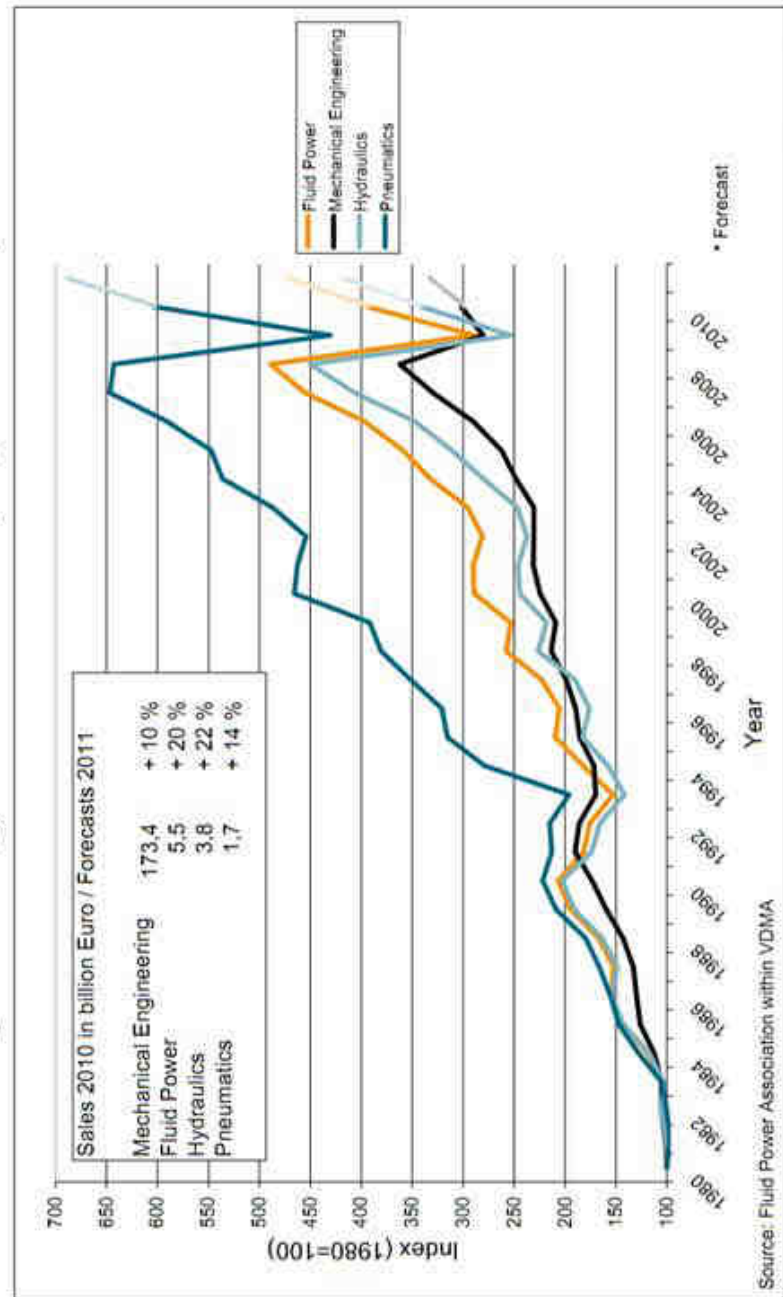
US Gear Booking&Shipments



HERVEX 2012

Sales development 1980-2011 in Germany

Mechanical Engineering/Fluid Power/Hydraulics/Pneumatics



Source: Fluid Power Association within VDMA

International Fluid Power Summit meeting, 5 April 2011 in Hanover, Germany

HERVEX 2012

Chart 8 • April 2011

Orders in machinery industry in Germany

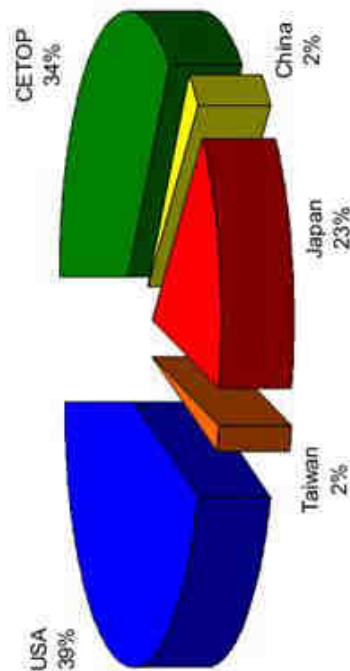
Sector	2008 do 2007	2009 do 2008	2010 do 2009	2011 do 2010
Construction equipment	-35	-64	+59	+55
Building materials machine	+3	-52	+43	+55
Minig machines	+17	-49	+48	+10
Hydraulic	-23	-74	+137	+58

10

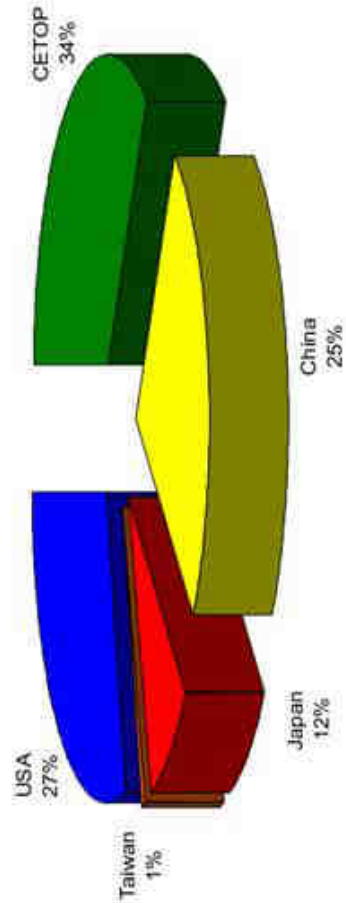
HERVEX 2012

Development of the Fluid Power Market and it's major shareholders

2000 FLUID POWER SHARES
 National Home Sales

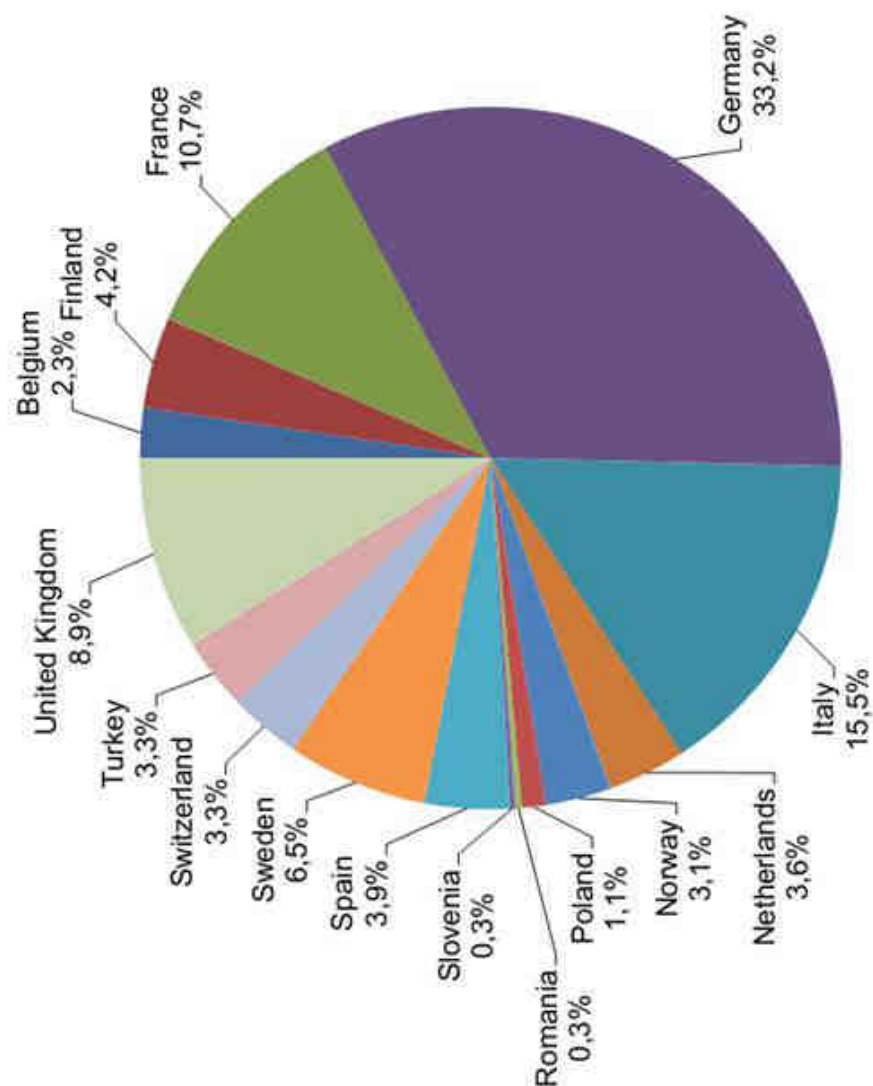


2011 FLUID POWER SHARES
 National Home Sales



HERVEX 2012

Home market Fluid Power (Estimated): 12.0 billion Euro – CETOP 2011



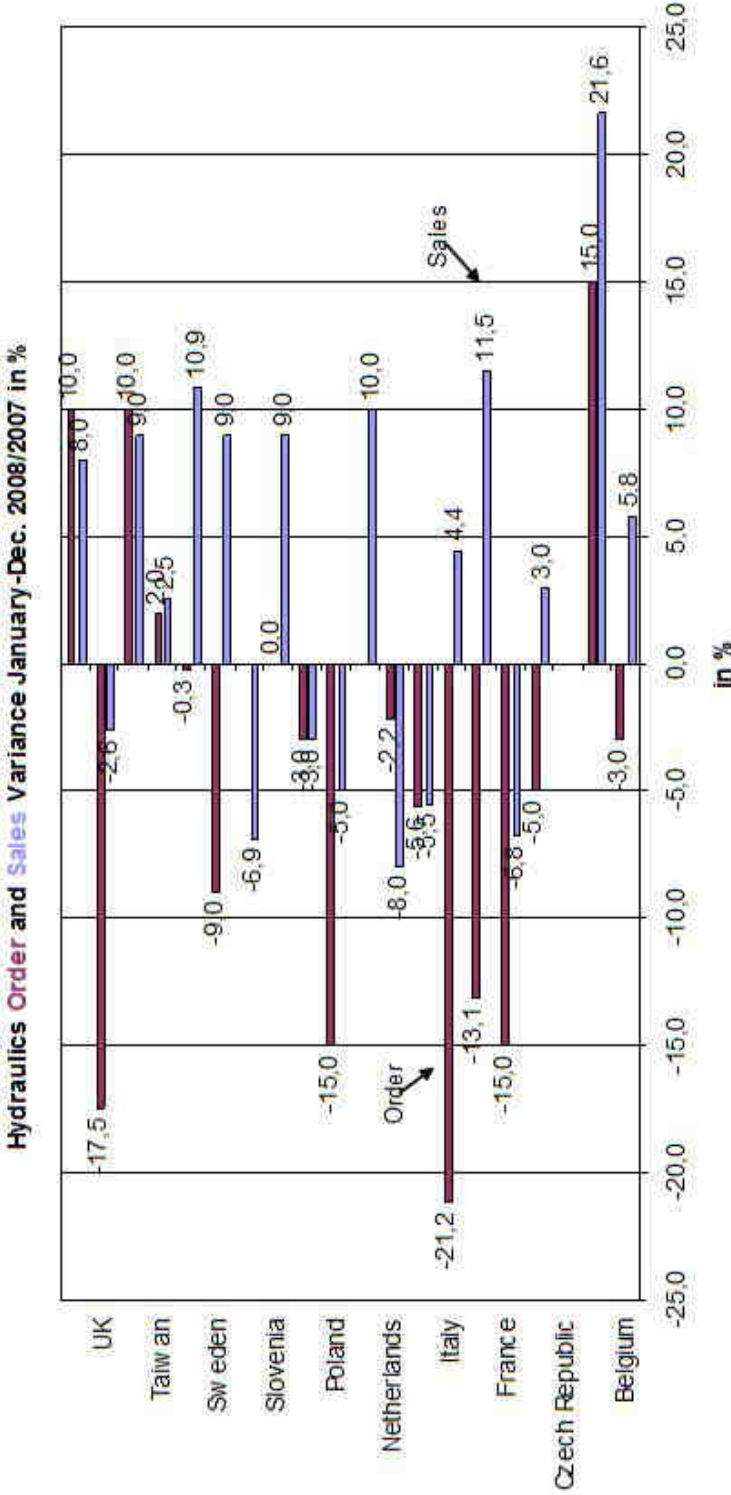
HERVEX 2012

12

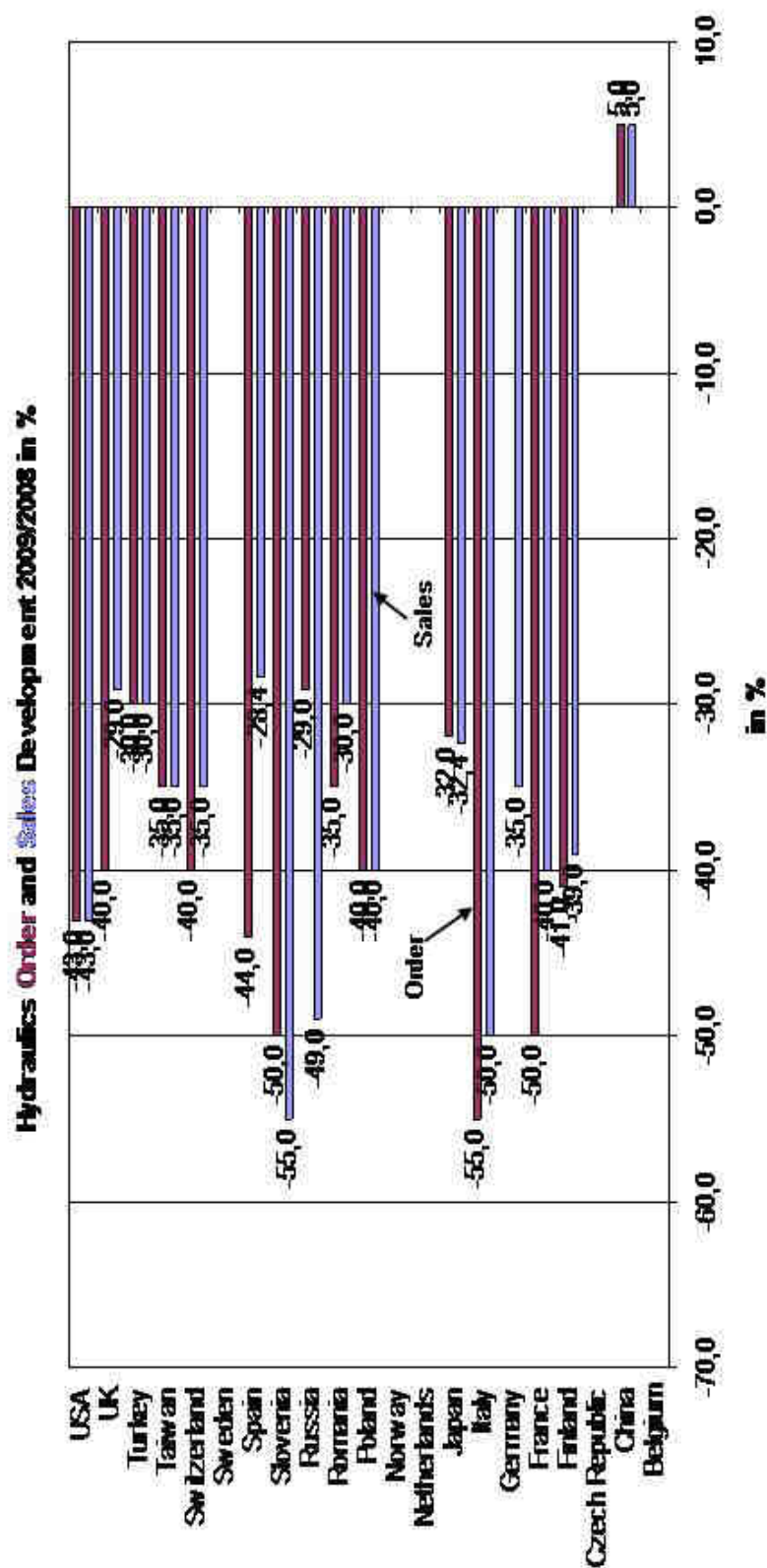
Sales and orders for hydraulics products

January-December 2008 vs 2007, domestic markets, %

RECESSION

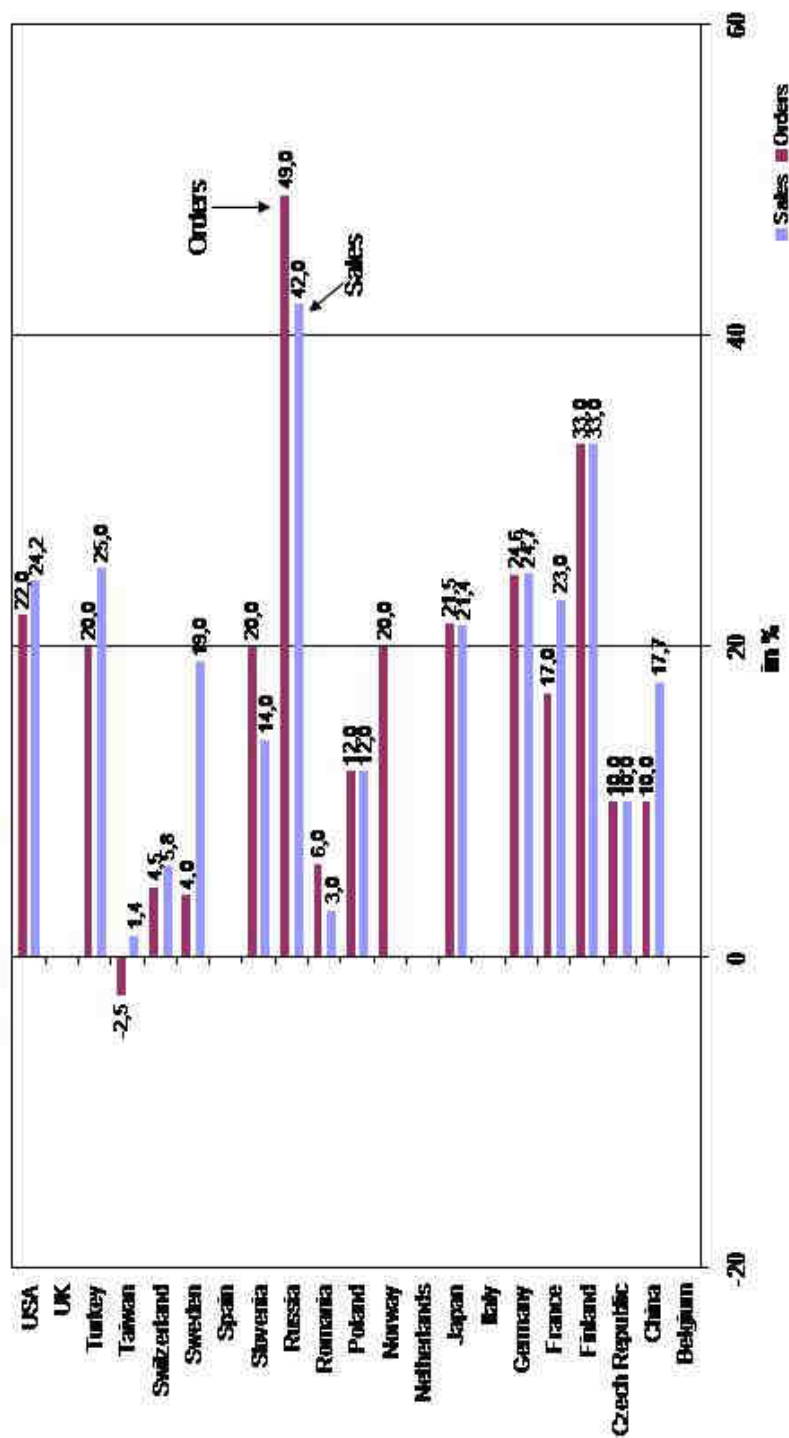


Sales and orders for hydraulics products 2009 vs 2008, domestic markets, % CRISIS



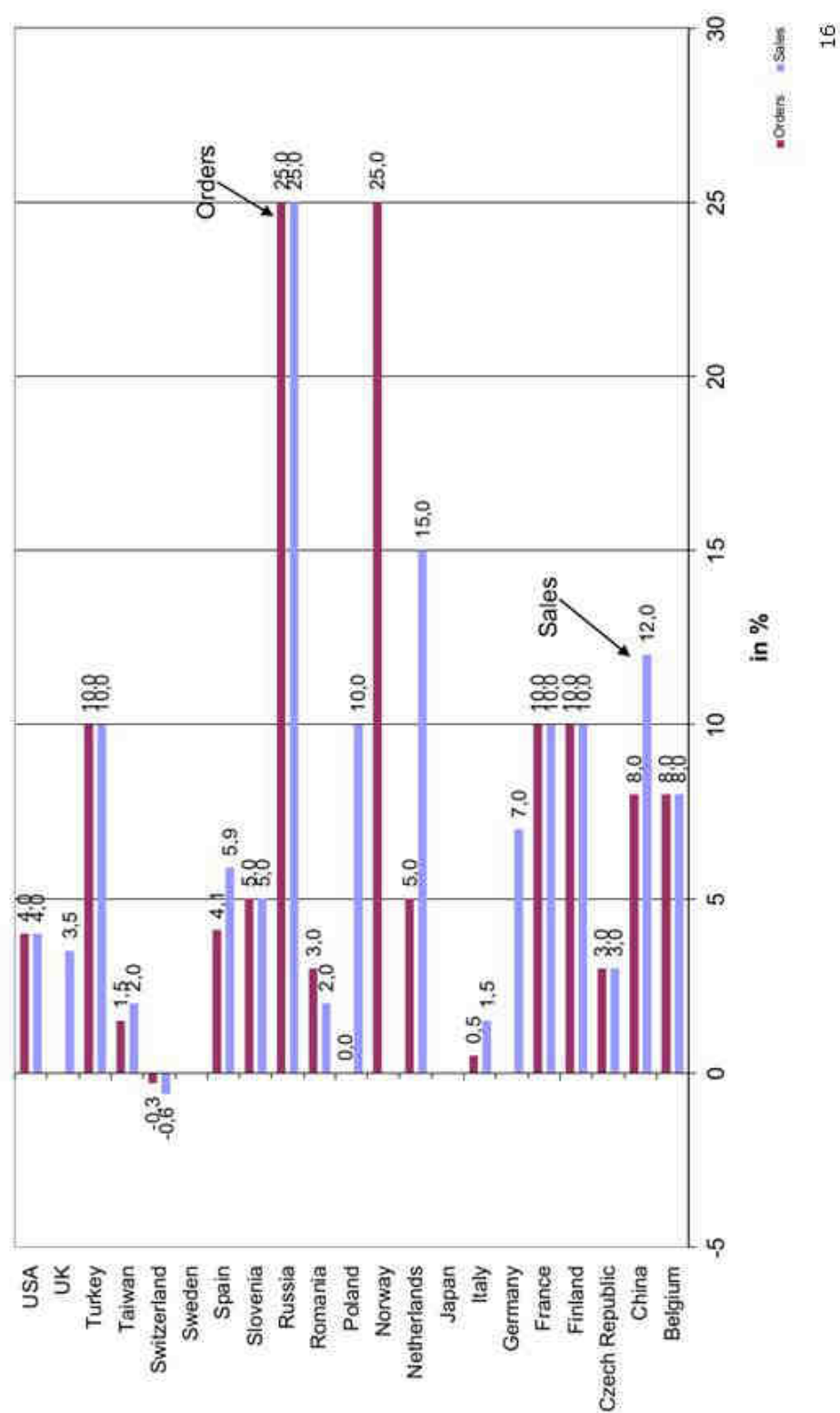
Sales and orders for hydraulics products 2011 vs 2010 domestic markets, % DEVELOPMENT

Hydraulics Orders and Sales Changes Jan.-Dec. 2011/Jan.-Dec. 2010 in %



HERVEX 2012

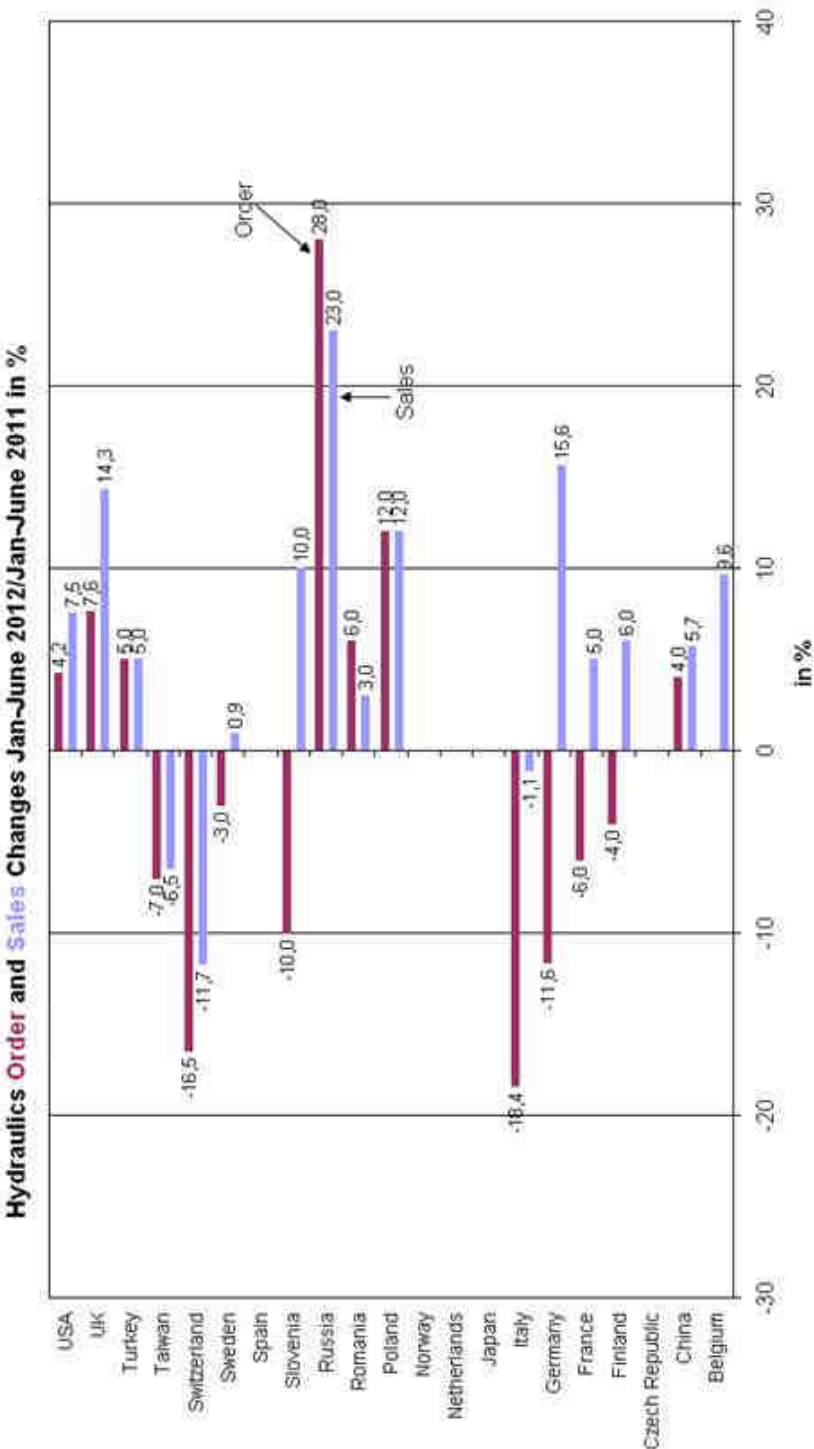
Sales and orders for hydraulics forecast 2012 vs 2011 (December 2010)



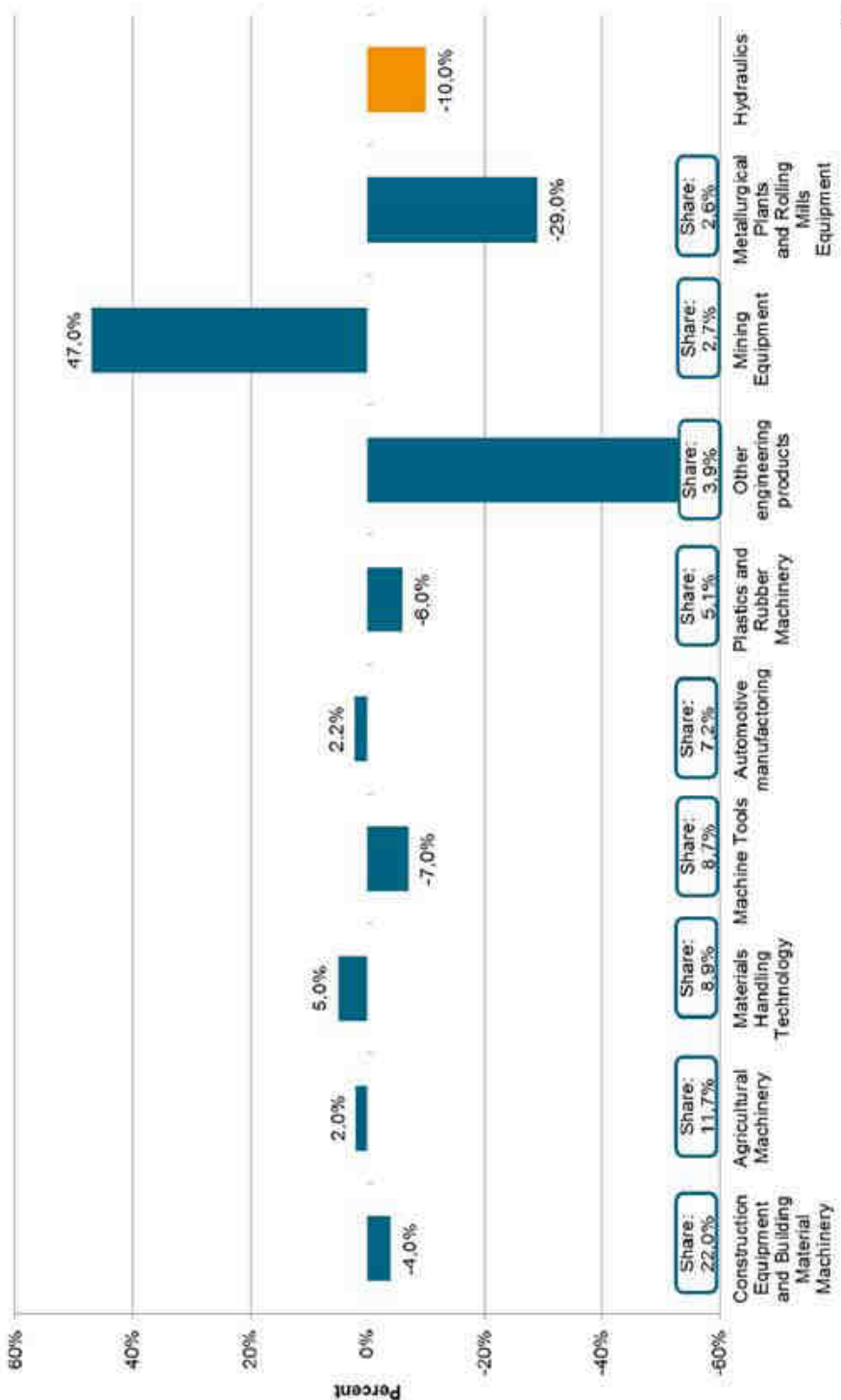
Sales and orders for hydraulics products

January-June 2012 vs 2011, domestic markets, %

RECESSION

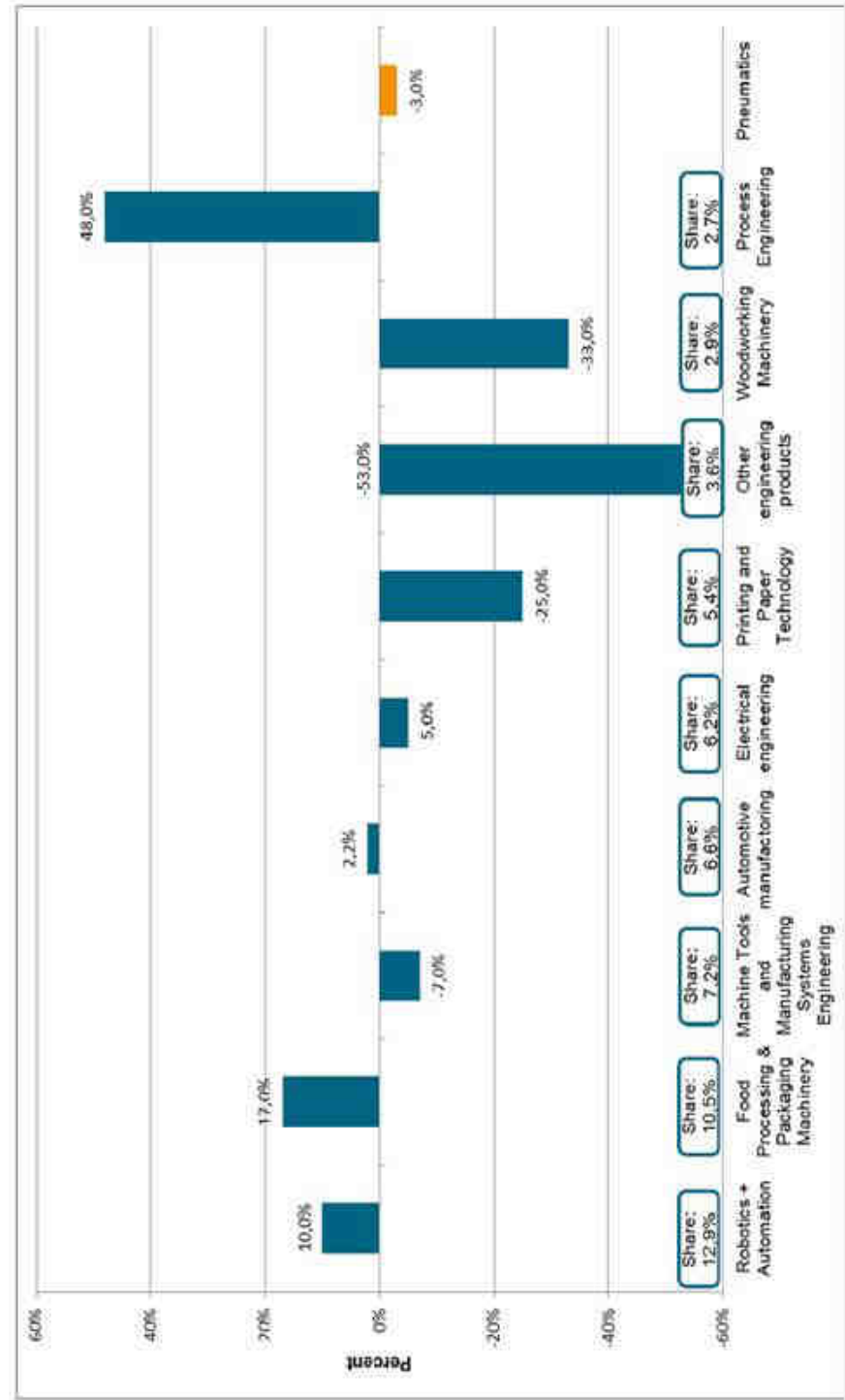


Rates of change Jan-Mar 2012/Jan-Mar 2011
and hydraulics customer groups shares in turnover in Germany

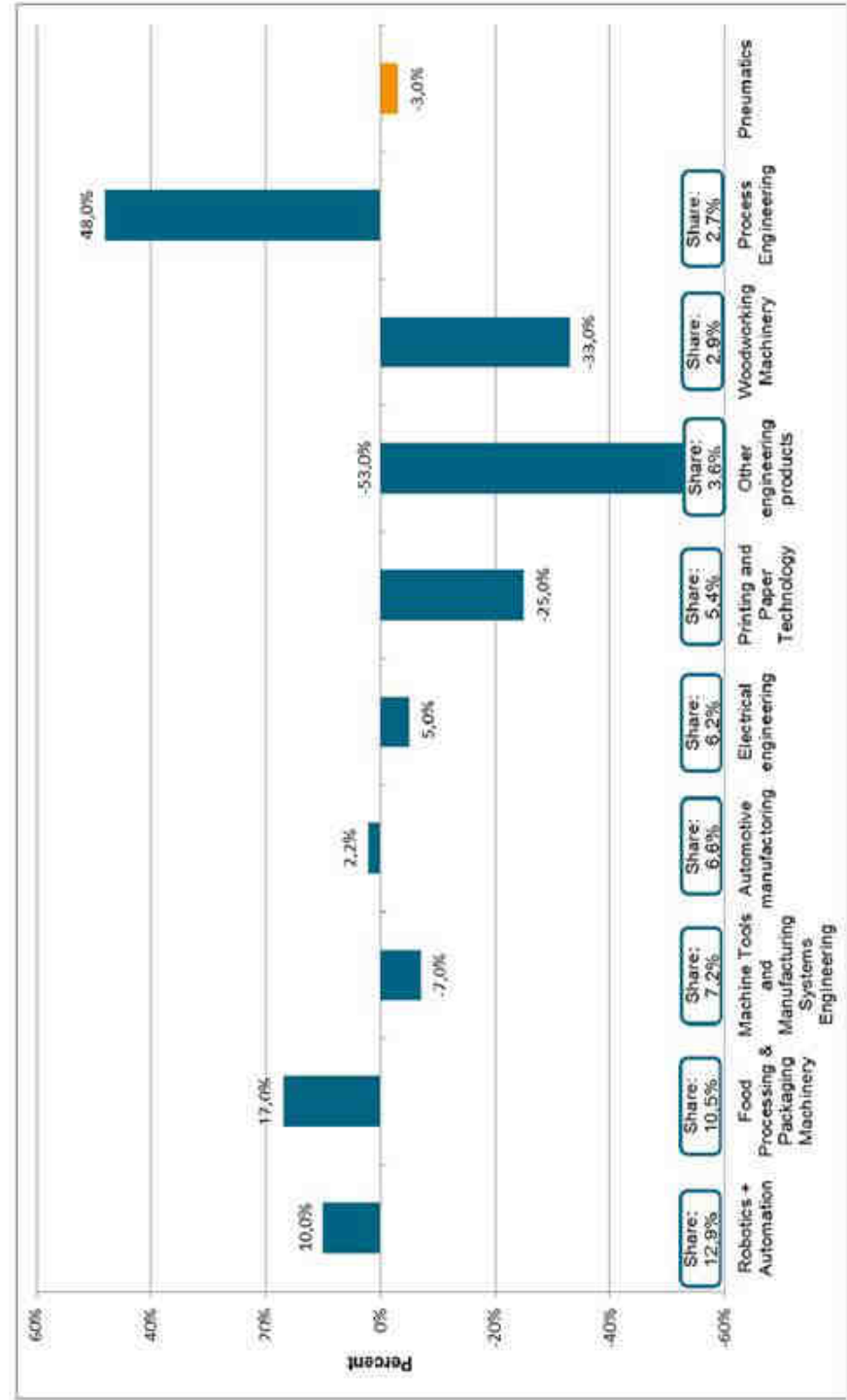


HERVEX 2012

Rates of change Jan-Mar 2012/Jan-Mar 2011 and pneumatics customer groups shares in turnover in Germany



Rates of change Jan-Mar 2012/Jan-Mar 2011 and pneumatics customer groups shares in turnover in Germany



Lesson from a crisis

Mechanical engineering predominantly proactive

Defensive strategy (15.1%*) <ul style="list-style-type: none"> ● <i>Reduce risk (22%)</i> <ul style="list-style-type: none"> ○ Install early warning system ○ Improve risk management ○ Reduce dependency on new business ● <i>Reduce speed of growth (9%)</i> <ul style="list-style-type: none"> ○ Reduce capacities ○ Slower speed of investment ○ More cautious growth <p>* Share of replies received from major mechanical engineering companies (turnover > 10 mio.Euro), category "very important"</p>	Buffer strategy (31.8%*) <ul style="list-style-type: none"> ● <i>Increase flexibility of (43%)</i> <ul style="list-style-type: none"> ○ Capacity utilisation ○ Fixed costs ○ Working time ● <i>Improve financial precautions (28%)</i> <ul style="list-style-type: none"> ○ Improve liquidity management ○ Use alternative sources of financing ○ Build up financial resources ○ Concentrate on profitable products 	Offensive strategy (41.8%*) <ul style="list-style-type: none"> ● <i>Strengthen innovative power (56%)</i> <ul style="list-style-type: none"> ○ Develop new products ○ Improve processes ○ Use new technologies ● <i>HR development measures (31%)</i> <ul style="list-style-type: none"> ○ Improve competencies ○ Employee retention strategies <p>source: <i>Lehren einer Krise – Die Sicht des Maschinenbaus</i> (Lessons from a crisis), Empirical study of IW Köln Consult GmbH in cooperation with the Institute of the German Economy commissioned by IMPULS – Stiftung für den Maschinenbau, den Anlagenbau und die Informationstechnik, Dezember 2010</p>
--	---	---

HERVEX 2012

21

Energy efficiency: main target of European



- International
 - World Climate Conference (Copenhagen 2009 and currently Durban 2011), Kyoto Protocol
- EU
 - "Magic formula 3x20"
 - 20% saving of energy
 - 20% reduction of CO₂ emission
 - 20% renewable energies until 2020
- National
 - Adaption of European requirements
 - Special programmes of the policy with regard to energy and climate
 - Energy efficiency is a focal point of activity of the policy
- Consequences
 - Support programmes (e.g. German Framework Programme 2007-2013: 3,5 bn. EURO are related to R&D in modern energy technologies)
 - Technical Regulations (e.g. ErP Energy related Products Directive)
 - Market pressure (product labelling, e.g. A++)

Energy policy

- 20-20-20 targets until 2020
 - Reduction of greenhouse gas emissions by 20%
 - Increase of energy efficiency by 20%
 - Share of renewable energies 20%
- Action plan energy efficiency (8 March 2011)
 - energy audits for big companies
 - Intensive use of ecodesign directive
 - Financial measures for energy efficiency investments
- Roadmap resource efficiency (June 2011)
 - Ban of certain materials through ecodesign directive
 - Information obligation for manufactures
 - Recycling certificates

The ecodesign directive – the all purpose tool

- Framework Directive for the setting of ecodesign requirements for energy related products
 - Intention: cover all environmental aspects of a product
 - Practice: used to regulate energy efficiency of products
- First wave: Consumer and mass products
 - Light bulbs, washing machines, pumps, etc...
- Second wave: Capital and industrial goods
 - Industrial furnaces, machine tools, etc...
- Third wave: Industrial systems?

Roadmap to a resource efficient Europe



- **New requirements for capital goods?**
 - Introduction of minimum recycled material rates, durability and reusability criteria
 - Extensions of producer responsibility for key products
 - Information duties (complete declaration of materials etc.)
 - Recycling certificates (Model: Emission trade system), indicators, benchmarks
 - Decoupling growth from resource use
- **Possible instrument: ErP Directive!**

Market outlook potential of some lead markets

	Global market 2007	Increase 2007-2020
Energy efficiency	538 bn. Euro	1030 bn. Euro
Sustainable water management	361 bn. Euro	805 bn. Euro
Sustainable mobility	200 bn. Euro	300 bn. Euro
Energy production	155 bn. Euro	615 bn. Euro
Natural resources & efficiency of material	94 bn. Euro	335 bn. Euro
Circular flow management, waste material, recycling	35 bn. Euro	53 bn. Euro
		6.5% increase p.a. since Fukushima higher

Source: Roland Berger Strategy Consultants, 2009

HERVEX 2012

26

SWOT - Strengths of German machinery industry

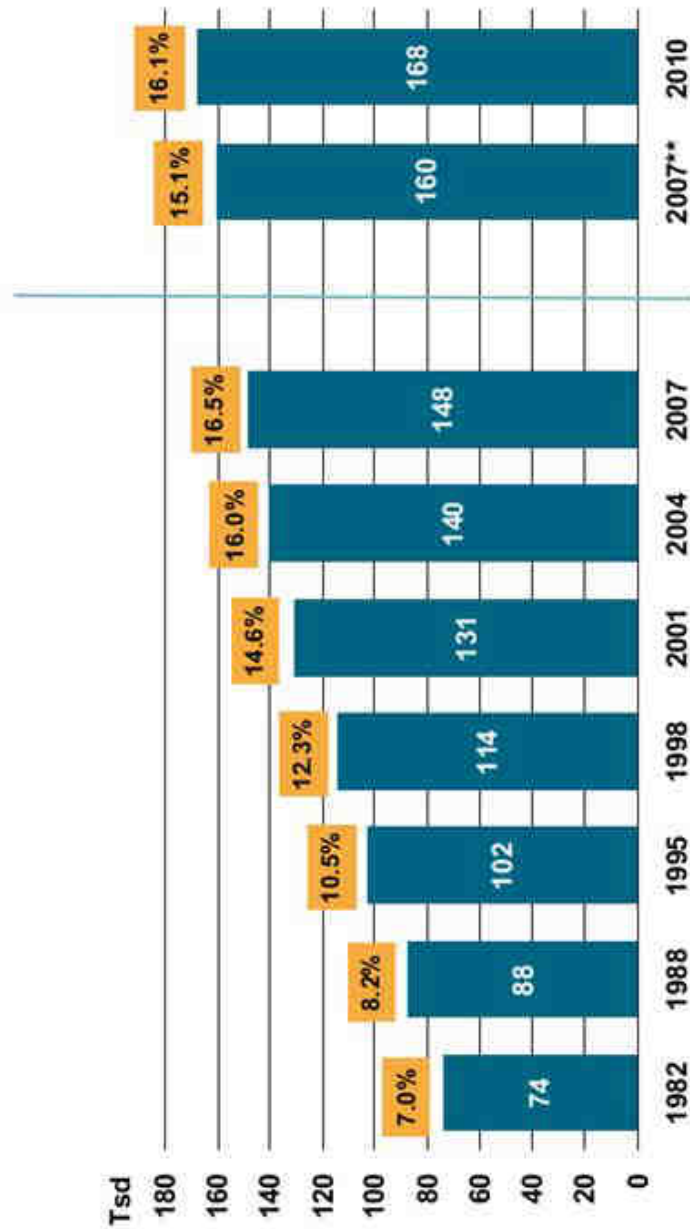
- Innovation
 - ~ 4% R & D ratio (in % of production 2010)
 - 50% of the engineers work in R & D and Design
 - e.g. in Germany, the machinery industry is the most important employer for engineers
- Quality
 - High quality of products
 - High quality of processes
- Flexibility
 - Product design
 - Time to market
 - Production capacity (e.g. German "Kurzarbeit")
- Productivity
 - Driven by Know-how, not by quantities
 - Mass markets: through global direct investment, German quality merges with local production

Activities of the Fluid Power Association and the Fluid Power Fund

- Together with member companies, initiator of the creation and establishment of a foundation professorship in Karlsruhe
- Ideal platform for information events, conferences and colloquiums, such as
 - International Fluid Power Conference, IFK – spring 2014 in Aachen
 - International Sealing Conference, ISC – 13th/14th September 2012 in Stuttgart
 - Mobilhydraulik-Kolloquium, - 27th/28th September 2012 in Karlsruhe
 - Conference on „Hybridantriebe für Mobile Antriebsmaschinen“ - 19th/20th February 2013 in Karlsruhe
 - Transfer event for cluster projects, for example, "More Reliable Mechatronic Systems" and "TEAM - Development of Technologies for Energy-Saving Drives for Mobile Machines"
- Platform for and initiator of education and training initiatives
- Direct and indirect support of students and scientific institute staff
- Joint research projects with the Fluid Power Research Fund

Engineers in the ME Industry 2010: Companies again create more jobs

In thousand and as a percent of employment*



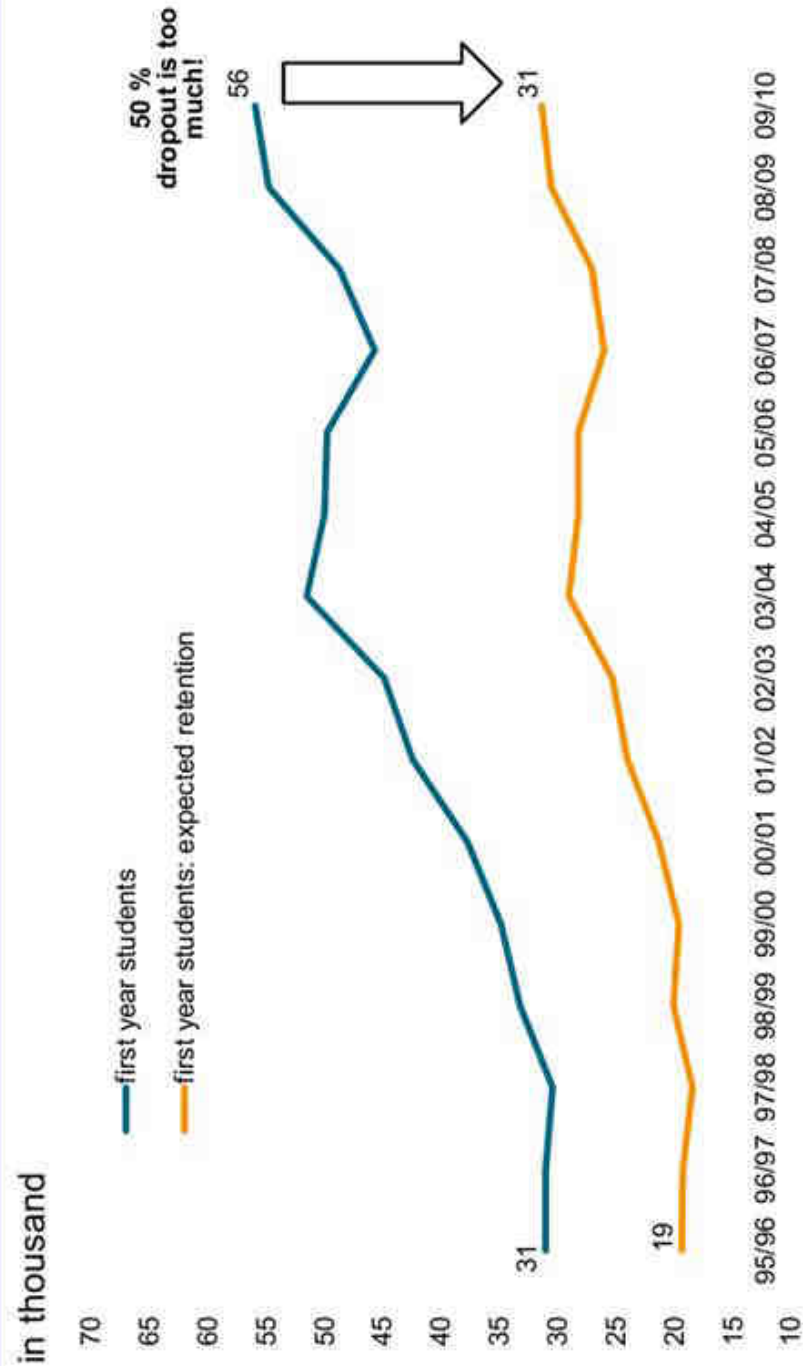
* in companies with 20 and more employees

** due to methodical changes not comparable to earlier years

Source: VDMA Engineer Surveys

HERVEX 2012

First year students in mechanical and electrical engineering*: how many will stay the course?



* without students in Master- and PhD-programmes

Source: Statistical Office, HIS

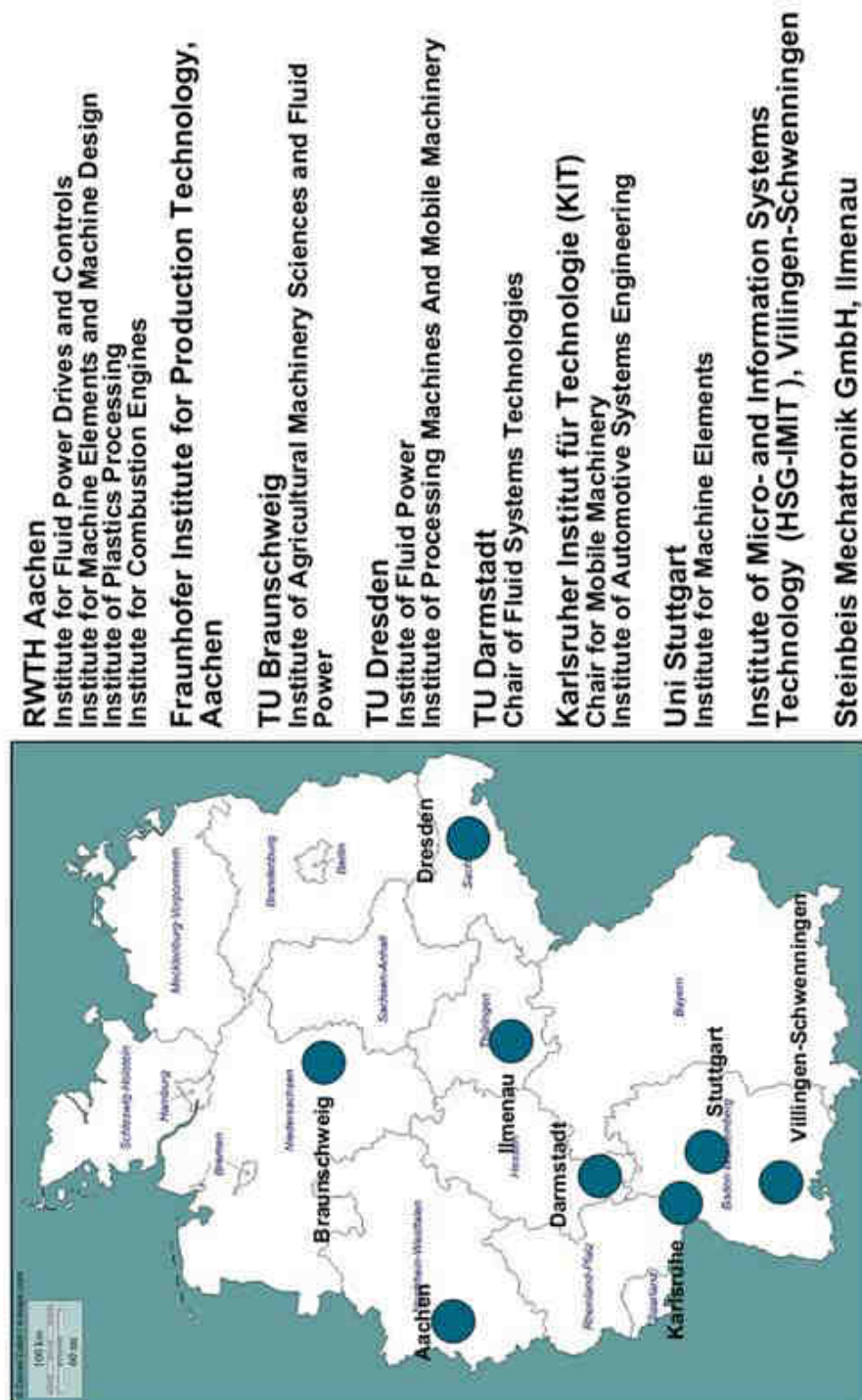
HERVEX 2012

30

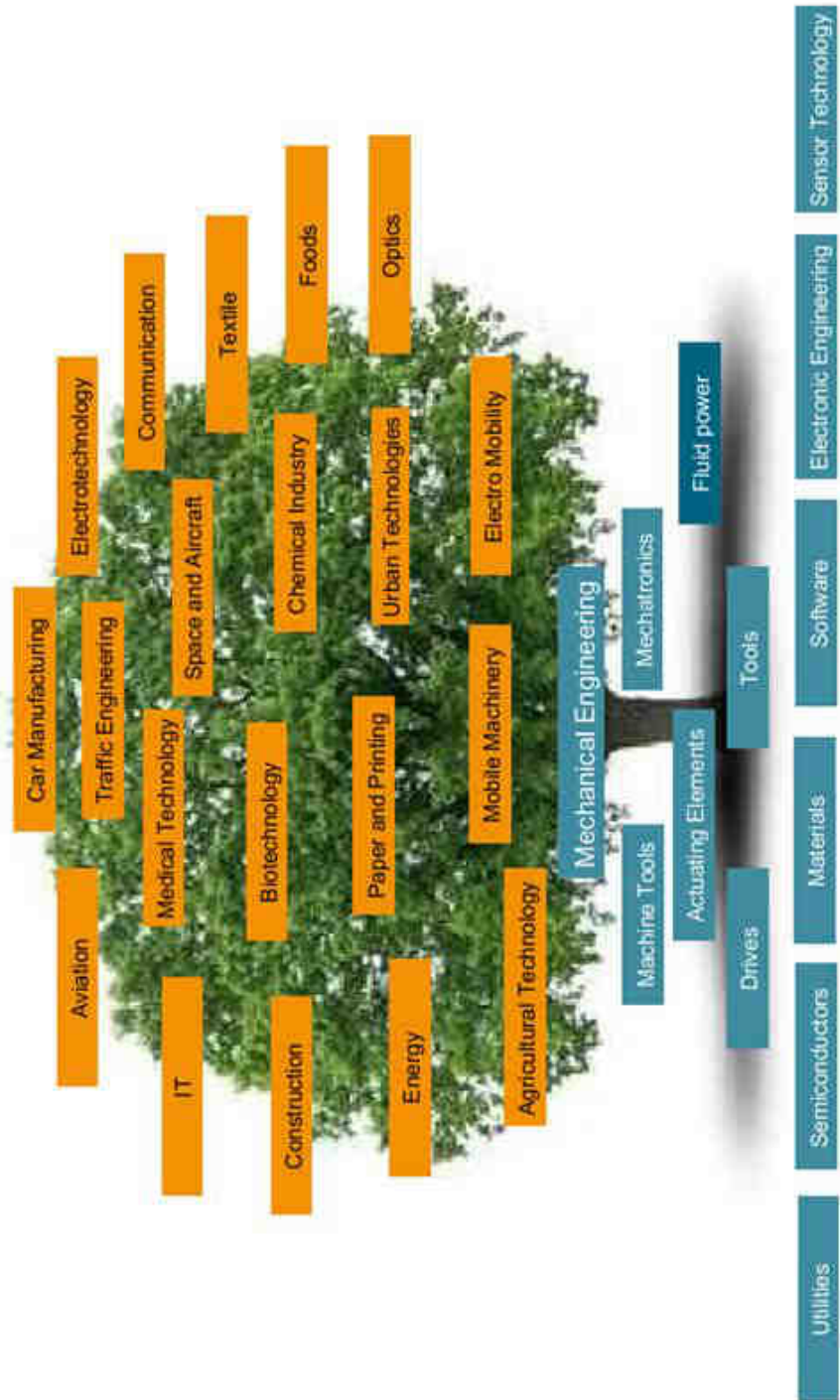
Main topics Fluid Power Research Fund

- Fluid power in competition with alternative drive technologies
- Development methodology and simulation
- Energy efficiency and sustainability
- Intelligence, integration and miniaturization
- New materials and actuator principles
- Safety

Most important research centers of the Fluid Power Research Fund



Right in the middle of the innovation net: Machinery and plant industry – The enabling industry



HERVEX 2012

33



www.hervex.eu